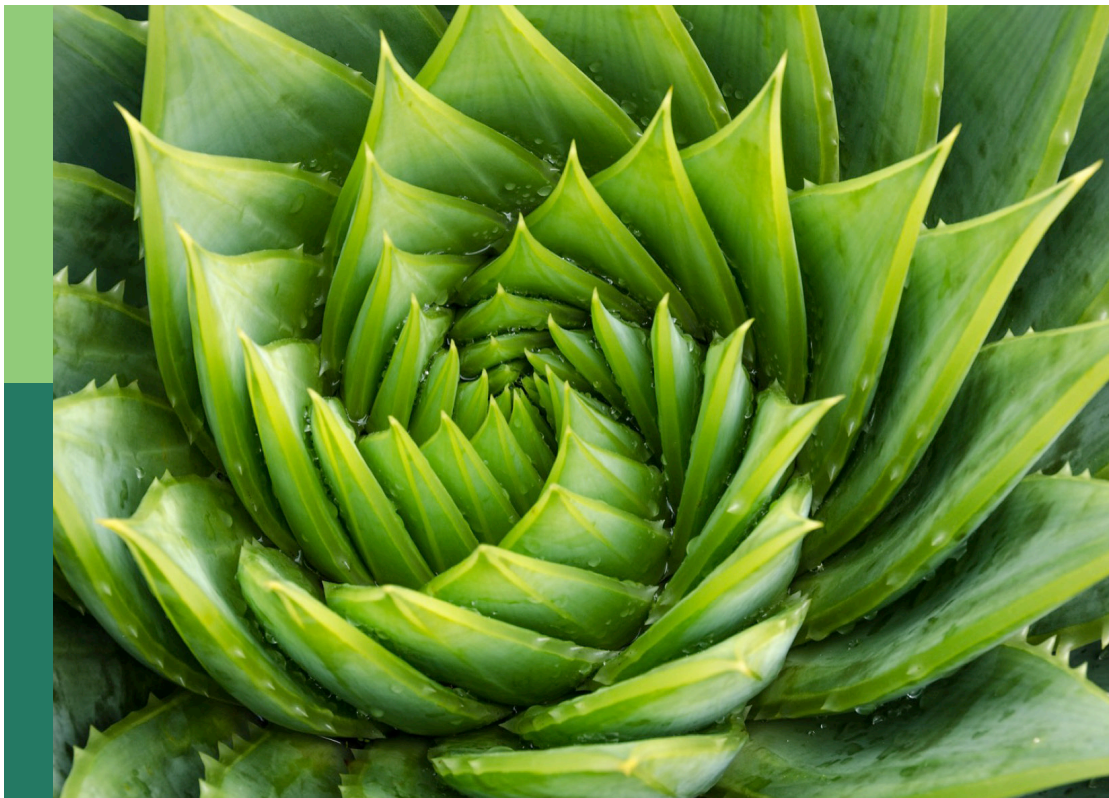
frontiers | Research Topics

Insights in plant biotechnology: 2021

Edited by
James Lloyd, Jens Kossmann, Peng Zhang, Ralf Alexander Wilhelm and Manoj K. Sharma

Published in
Frontiers in Plant Science



FRONTIERS EBOOK COPYRIGHT STATEMENT

The copyright in the text of individual articles in this ebook is the property of their respective authors or their respective institutions or funders. The copyright in graphics and images within each article may be subject to copyright of other parties. In both cases this is subject to a license granted to Frontiers.

The compilation of articles constituting this ebook is the property of Frontiers.

Each article within this ebook, and the ebook itself, are published under the most recent version of the Creative Commons CC-BY licence. The version current at the date of publication of this ebook is CC-BY 4.0. If the CC-BY licence is updated, the licence granted by Frontiers is automatically updated to the new version.

When exercising any right under the CC-BY licence, Frontiers must be attributed as the original publisher of the article or ebook, as applicable.

Authors have the responsibility of ensuring that any graphics or other materials which are the property of others may be included in the CC-BY licence, but this should be checked before relying on the CC-BY licence to reproduce those materials. Any copyright notices relating to those materials must be complied with.

Copyright and source acknowledgement notices may not be removed and must be displayed in any copy, derivative work or partial copy which includes the elements in question.

All copyright, and all rights therein, are protected by national and international copyright laws. The above represents a summary only. For further information please read Frontiers' Conditions for Website Use and Copyright Statement, and the applicable CC-BY licence.

ISSN 1664-8714
ISBN 978-2-83251-658-4
DOI 10.3389/978-2-83251-658-4

About Frontiers

Frontiers is more than just an open access publisher of scholarly articles: it is a pioneering approach to the world of academia, radically improving the way scholarly research is managed. The grand vision of Frontiers is a world where all people have an equal opportunity to seek, share and generate knowledge. Frontiers provides immediate and permanent online open access to all its publications, but this alone is not enough to realize our grand goals.

Frontiers journal series

The Frontiers journal series is a multi-tier and interdisciplinary set of open-access, online journals, promising a paradigm shift from the current review, selection and dissemination processes in academic publishing. All Frontiers journals are driven by researchers for researchers; therefore, they constitute a service to the scholarly community. At the same time, the *Frontiers journal series* operates on a revolutionary invention, the tiered publishing system, initially addressing specific communities of scholars, and gradually climbing up to broader public understanding, thus serving the interests of the lay society, too.

Dedication to quality

Each Frontiers article is a landmark of the highest quality, thanks to genuinely collaborative interactions between authors and review editors, who include some of the world's best academicians. Research must be certified by peers before entering a stream of knowledge that may eventually reach the public - and shape society; therefore, Frontiers only applies the most rigorous and unbiased reviews. Frontiers revolutionizes research publishing by freely delivering the most outstanding research, evaluated with no bias from both the academic and social point of view. By applying the most advanced information technologies, Frontiers is catapulting scholarly publishing into a new generation.

What are Frontiers Research Topics?

Frontiers Research Topics are very popular trademarks of the *Frontiers journals series*: they are collections of at least ten articles, all centered on a particular subject. With their unique mix of varied contributions from Original Research to Review Articles, Frontiers Research Topics unify the most influential researchers, the latest key findings and historical advances in a hot research area.

Find out more on how to host your own Frontiers Research Topic or contribute to one as an author by contacting the Frontiers editorial office: frontiersin.org/about/contact

Insights in plant biotechnology: 2021

Topic editors

James Lloyd — Stellenbosch University, South Africa
Jens Kossmann — Stellenbosch University, South Africa
Peng Zhang — Center for Excellence in Molecular Plant Sciences, Chinese Academy of Sciences (CAS), China
Ralf Alexander Wilhelm — Institute for Biosafety in Plant Biotechnology, Federal Research Centre for Cultivated Plants, Julius Kühn-Institute, Germany
Manoj K. Sharma — Jawaharlal Nehru University, India

Citation

Lloyd, J., Kossmann, J., Zhang, P., Wilhelm, R. A., Sharma, M. K., eds. (2023). *Insights in plant biotechnology: 2021*. Lausanne: Frontiers Media SA.
doi: 10.3389/978-2-83251-658-4

Table of contents

06 Editorial: Insights in plant biotechnology: 2021
James R. Lloyd, Ralf Wilhelm, Manoj K. Sharma, Jens Kossmann and Peng Zhang

09 Genome-Wide Association Study of Phytic Acid in Wheat Grain Unravels Markers for Improving Biofortification
Zhengyu Wen, Philomin Juliana, Harshaant S. Dhugga, Mario Pacheco, Ulises I. Martínez, Agustin Aguilar, Maria I. Ibba, Velu Govindan, Ravi P. Singh and Kanwarpal S. Dhugga

18 Haplotype Analysis of Chloroplast Genomes for Jujube Breeding
Guanglong Hu, Yang Wu, Chaojun Guo, Dongye Lu, Ningguang Dong, Bo Chen, Yanjie Qiao, Yuping Zhang and Qinghua Pan

30 Salt Stress Alleviation in *Triticum aestivum* Through Primary and Secondary Metabolites Modulation by *Aspergillus terreus* BTK-1
Muhammad Ikram Khan, Niaz Ali, Gul Jan, Muhammad Hamayun, Farzana Gul Jan, Amjad Iqbal, Anwar Hussain and In-Jung Lee

43 Physiological and Molecular Changes in Cherry Red Tobacco in Response to Iron Deficiency Stress
Fei Liu, Yihan Zhang, Xiaojun Pu, Nan Cai, Xueyi Sui, Zed Rengel, Qi Chen and Zhongbang Song

53 CRISPR/Cas9 and Nanotechnology Pertinence in Agricultural Crop Refinement
Banavath Jayanna Naik, Ganesh Shimoga, Seong-Cheol Kim, Mekapogu Manjulatha, Chinreddy Subramanyam Reddy, Ramasubba Reddy Palem, Manu Kumar, Sang-Youn Kim and Soo-Hong Lee

76 A Multi-Omics Approach for Rapid Identification of Large Genomic Lesions at the *Wheat Dense Spike* (*wds*) Locus
Zhenyu Wang, Shu Tao, Shaoshuai Liu, Meiling Jia, Dada Cui, Guoliang Sun, Zhongyin Deng, Fang Wang, Xingchen Kong, Mingxue Fu, Yuqing Che, Ruyi Liao, Tao Li, Shuaifeng Geng, Long Mao and Aili Li

87 Biotechnological Road Map for Innovative Weed Management
Albert Chern Sun Wong, Karen Massel, Yasmine Lam, Jessica Hintzsche and Bhagirath Singh Chauhan

101 A Walk Through the Maze of Secondary Metabolism in Orchids: A Transcriptomic Approach
Devina Ghai, Arshpreet Kaur, Parvinderdeep S. Kahlon, Sandip V. Pawar and Jaspreet K. Sembi

117 Heat Stress-Mediated Constraints in Maize (*Zea mays*) Production: Challenges and Solutions
Ahmed H. El-Sappah, Shabir A. Rather, Shabir Hussain Wani, Ahmed S. Elrys, Muhammad Bilal, Qiulan Huang, Zahoor Ahmad Dar, Mohamed M. A. Elashtokhy, Nourhan Soaud, Monika Koul, Reyazul Rouf Mir, Kuan Yan, Jia Li, Khaled A. El-Tarabily and Manzar Abbas

140 Glyco-Engineering Plants to Produce Helminth Glycoproteins as Prospective Biopharmaceuticals: Recent Advances, Challenges and Future Prospects
Alex van der Kaaij, Kim van Noort, Pieter Nibbering, Ruud H. P. Wilbers and Arjen Schots

152 Molecular Determinants of *in vitro* Plant Regeneration: Prospects for Enhanced Manipulation of Lettuce (*Lactuca sativa* L.)
Tawni Bull and Richard Michelmore

169 Successful Production and Ligninolytic Activity of a Bacterial Laccase, Lac51, Made in *Nicotiana benthamiana via* Transient Expression
André van Eerde, Anikó Várnai, Yanliang Wang, Lisa Paruch, John-Kristian Jameson, Fen Qiao, Hans Geir Eiken, Hang Su, Vincent G. H. Eijsink and Jihong Liu Clarke

179 Eradication of *Potato Virus S, Potato Virus A,* and *Potato Virus M* From Infected *in vitro*-Grown Potato Shoots Using *in vitro* Therapies
Jean Carlos Bettoni, Liya Mathew, Ranjith Pathirana, Claudia Wiedow, Donald A. Hunter, Andrew McLachlan, Subuhi Khan, Joe Tang and Jayanthi Nadarajan

195 Genomics-Assisted Improvement of Super High-Yield Hybrid Rice Variety "Super 1000" for Resistance to Bacterial Blight and Blast Diseases
Zhizhou He, Yeyun Xin, Chunlian Wang, Hanshu Yang, Zhi Xu, Jihua Cheng, Zhouwei Li, Changrong Ye, Hexing Yin, Zhenyu Xie, Nan Jiang, Jing Huang, Jinhua Xiao, Bingchuan Tian, Yan Liang, Kaijun Zhao and Junhua Peng

211 Clustered Regularly Interspaced Short Palindromic Repeats-Associated Protein System for Resistance Against Plant Viruses: Applications and Perspectives
Fredy D. A. Silva and Elizabeth P. B. Fontes

218 Gene Editing to Accelerate Crop Breeding
Kanwarpal S. Dhugga

224 Production of Recombinant Active Human TGFβ1 in *Nicotiana benthamiana*
Aditya Prakash Soni, Juhee Lee, Kunyoo Shin, Hisashi Koiwa and Inhwan Hwang

237 Nested miRNA Secondary Structure Is a Unique Determinant of miR159 Efficacy in *Arabidopsis*
Muhammad Imran, Tengfei Liu, Zheng Wang, Min Wang, Shulin Liu, Xinyan Gao, Anning Wang, Songfeng Liu, Zhixi Tian and Min Zhang

250 Identification of Reference Genes for Reverse Transcription-Quantitative PCR Analysis of Ginger Under Abiotic Stress and for Postharvest Biology Studies
Gang Li, Jiawei Ma, Junliang Yin, Fengling Guo, Keyong Xi, Peihua Yang, Xiaodong Cai, Qie Jia, Lu Li, Yiqing Liu and Yongxing Zhu

262 Differential Gene Expression and Withanolides Biosynthesis During *in vitro* and *ex vitro* Growth of *Withania somnifera* (L.) Dunal
Sachin Ashok Thorat, Arya Kaniyassery, Poornima Poojari, Melissa Rangel, Shashikala Tantry, Kodsara Ramachandra Kiran, Manjunath B. Joshi, Padmalatha S. Rai, Anna-Maria Botha and Annamalai Muthusamy

275 Pan-genome analysis of three main Chinese chestnut varieties
Guanglong Hu, Lili Cheng, Yunhe Cheng, Weitao Mao, Yanjie Qiao and Yanping Lan

frontiers | Frontiers in Plant Science

TYPE Editorial
PUBLISHED 30 January 2023
DOI 10.3389/fpls.2023.1147930

Check for updates

OPEN ACCESS

EDITED AND REVIEWED BY
Francesco Sestili,
University of Tuscia, Italy

*CORRESPONDENCE
James R. Lloyd
lloyd@sun.ac.za

SPECIALTY SECTION
This article was submitted to Plant Biotechnology, a section of the journal Frontiers in Plant Science

RECEIVED 19 January 2023
ACCEPTED 19 January 2023
PUBLISHED 30 January 2023

CITATION
Lloyd JR, Wilhelm R, Sharma MK, Kossmann J and Zhang P (2023) Editorial: Insights in plant biotechnology: 2021. *Front. Plant Sci.* 14:1147930. doi: 10.3389/fpls.2023.1147930

COPYRIGHT
© 2023 Lloyd, Wilhelm, Sharma, Kossmann and Zhang. This is an open-access article distributed under the terms of the Creative Commons Attribution License (CC BY). The use, distribution or reproduction in other forums is permitted, provided the original author(s) and the copyright owner(s) are credited and that the original publication in this journal is cited, in accordance with accepted academic practice. No use, distribution or reproduction is permitted which does not comply with these terms.

Editorial: Insights in plant biotechnology: 2021

James R. Lloyd[1]*, Ralf Wilhelm[2], Manoj K. Sharma[3], Jens Kossmann[1] and Peng Zhang[4]

[1]Institute for Plant Biotechnology, Department of Genetics, Stellenbosch University, Stellenbosch, South Africa, [2]Institute for Biosafety in Plant Biotechnology, Julius Kühn-Institute - Federal Research Centre for Cultivated Plants, Quedlinburg, Germany, [3]Crop Genetics and Informatics Group, School of Biotechnology, Jawaharlal Nehru University, New Delhi, India, [4]CAS Center for Excellence in Molecular Plant Sciences, Chinese Academy of Sciences, Shanghai, China

KEYWORDS

abiotic and biotic stresses, plant biotechnology and breeding, pharmaceuticals, recombinant protein, genome edited crops

Editorial on the Research Topic
Insights in plant biotechnology: 2021

The Plant Biotechnology section at Frontiers in Plant Science mainly publishes applied studies examining how plants can be improved using modern genetic techniques (Lloyd and Kossmann, 2021). This Research Topic was designed to allow editors from the section to highlight some of their own plant biotechnological work. There are many aspects of crops where this is needed - for example improving yields under changing climatic conditions will be crucial to help feed the growing world population - meaning that plant biotechnology is essential for food security. Plants are also good sources of pharmaceutically active compounds and can also be genetically manipulated to make them useful platforms for producing pharmaceutical proteins. Such plants where increased amounts of pharmaceuticals can be isolated, will help many medical treatments by reducing costs. Genetic manipulation of plants underlies much plant biotechnology and this can range from traditional plant breeding, through to transgenic and genome editing technologies. Understanding and improving the uses of these technologies will allow plant biotechnologists to improve plants in a more efficient manner. This Research Topic was designed to examine a wide range of different plant biotechnological issues, from understanding and overcoming abiotic stress tolerance, to manipulating specialized metabolism and the development of genome editing techniques.

One major aspect of plant biotechnology that will need much effort is to overcome different abiotic stresses as climate change is already affecting crop yields through increasing these types of stresses (Ray et al., 2019) and will likely only be worsened by future climate change. Khan et al. examined this by testing how wheat can grow better under salt stress when exposed to an endophytic fungus. They showed that this interaction leads to alterations in primary and secondary metabolites through hormonal regulation that help overcome saline stress. The work highlights the potential of including plant-endophyte interactions when considering biotechnological means to improve plant stress tolerance. Iron deficiency or uptake efficiency can also be a considerable limit on plant growth and resilience. Liu et al. identified a tobacco mutant that grows better with little iron. They characterized it further phenotypically and employed transcriptome analyses showing differences in gene expression related to molecular and physiological changes. RT-qPCR-based gene expression studies heavily depend on the availability of appropriate reference genes. Li et al. identified a set of

reference genes in ginger, suitable for studying abiotic stress responses and postharvest biology studies. Finally, El-Sappah et al. reviewed various aspects of heat stress that affect maize production and suggest crop management and molecular breeding approaches to mitigate the effects.

Crop losses due to biotic stresses can be devastating and two papers were published examining these. In one study Bettoni et al. use *in vitro* techniques and combined chemical and thermal treatments to eliminate multiple viruses from potato plants to allow the production of virus-free plants. This procedure can play an important role in production of virus-free potato plants for farmers and can significantly improve the production of good quality potatoes. He et al. utilized genomics approaches to help in speed breeding an already high-yielding rice variety to incorporate resistance to two different bacterial diseases. This variety will be important for farmers through producing higher yields with reduced need for application of antibacterial chemicals. Although microbial infections are important, many crop losses are caused by weeds (Oerke, 2006) and Wong et al. provide a review on concepts how biotechnology (including gene drives) might serve weed management in the future.

Many compounds with pharmaceutical properties are found in plants. Further, understanding and manipulating specialized metabolism is a good way to identify and produce new drugs. A survey of orchid secondary metabolism was undertaken by Ghai et al. (2022) and utilized high throughput transcriptomics data to elucidate the role of potential candidates in secondary metabolite biosynthesis. Their findings may help in identifying interesting new compounds useful for drug development and the enzymes that synthesize them. Thorat et al. examined growth conditions that influenced accumulation of pharmaceutically important withanolides compounds in *Withania somnifera*. Using a transcriptomic approach they identified genes which are differentially expressed. Their findings could potentially be used to establish tools for rapid *in vitro* multiplication of *Withania* sp. and increase withanolides accumulation in this plant. *In vitro* cultivation and regeneration of plants is a key step for the biotechnological interventions in crops. Bull and Michelmore summarizes the current knowledge on molecular determinants of *de novo* organogenesis and somatic embryogenesis.

Plants can also be used to manufacture recombinant proteins (molecular farming), some of which can be used as pharmaceuticals or therapeutics. Such plant-based systems can have some advantages over production of the same proteins in microbes or mammalian cell cultures. One of these advantages is the easier production of heterologous glycoproteins. van der Kaaij et al. examined how this is advantageous to produce helminth glycoproteins with unusual glycan structures in plants, which can be used to treat autoimmune diseases. Two papers also reported on the production of active recombinant proteins in the forms of human transcriptional growth factor β1 (Soni et al.) or a bacterial laccase (van Eerde et al.). These proteins have pharmaceutical or biotechnological applications respectively and their production in plants should help reduce their cost.

Although modern biotechnological techniques, such as genome editing, offer novel and complementary options, traditional genetics are still crucial in improving crops. Coupled with genomic techniques this becomes increasingly important in identifying the genetic basis of traits and speed breeding these into elite varieties. Hu et al. describe the sequencing of three Chinese chestnut varieties and generation of a pangenome that will be incredibly useful for breeding efforts. Two other studies used genomic techniques: Wang et al. identify loci involved in wheat spike production through exome capture sequencing and RNAseq analysis. Similarly, Wen et al. performed a genome wide association study to improve biofortification by identifying genetic markers associated with lower phytate content in wheat grains. This will help increase availability of iron and zinc and improve the nutritional value of the grain. Finally, haplotype analysis of jujube chloroplasts was described, where they used information for 65 chloroplast genomes and will be useful for phylogenetic studies and breeding efforts in this plant (Hu et al.).

The importance of genome editing techniques in improving crop plants is broadly emphasized and a number of reviews on this subject were published. Dhugga highlighted that such techniques can speed up production of improved elite varieties with only 2-3 generations needed for variety development rather than the 5-6 that are currently required. Naik et al. examined potential interrelations between genome editing and nanotechnology for plant improvement, while Silva and Fontes examined how genome editing, especially using the CRISPR/Cas-system could help develop broad range viral resistance in plants. Despite the growing importance of genome editing for introducing mutations into plant genomes, post-transcriptional gene silencing can still play an important role in both gene function discovery and crop improvement. Imran et al. examined how nested secondary structure of miR159 influences silencing in *Arabidopsis thaliana*.

Perspective

This Research Topic scratches the surface of several aspects of plant biotechnology ranging from applied demonstrations of biotechnological solutions to problems, to descriptions of new technologies that will become increasingly important. Plant biotechnology is a broad topic which overlaps many different scientific fields. We hope that this contributes to helping the plant science community in understanding some aspects of applied plant science, how they are currently used and how they will be utilized in the future by plant biotechnologists.

Author contributions

JRL wrote the first draft of the manuscript and all authors contributed to, and approved the final version.

Conflict of interest

The authors declare that the research was conducted in the absence of any commercial or financial relationships that could be construed as a potential conflict of interest.

Publisher's note

All claims expressed in this article are solely those of the authors and do not necessarily represent those of their affiliated organizations, or those of the publisher, the editors and the reviewers. Any product that may be evaluated in this article, or claim that may be made by its manufacturer, is not guaranteed or endorsed by the publisher.

References

Lloyd, J., and Kossmann, J. (2021). Improving crops for a changing world. *Front. Plant Sci.* 12, 728328. doi: 10.3389/fpls.2021.728328

Oerke, E. C. (2006). Crop losses to pests. *J. Agric. Sci.* 144, 31–43. doi: 10.1017/S0021859605005708

Ray, D. K., West, P. C., Clark, M., Gerber, J. S., Prishchepov, A. V., and Chatterjee, S. (2019). Climate change has likely already affected global food production. *PLos One* 14, e0217148. doi: 10.1371/journal.pone.0217148

frontiers in Plant Science

ORIGINAL RESEARCH
published: 15 February 2022
doi: 10.3389/fpls.2022.830147

Genome-Wide Association Study of Phytic Acid in Wheat Grain Unravels Markers for Improving Biofortification

*Zhengyu Wen, Philomin Juliana, Harshaant S. Dhugga, Mario Pacheco, Ulises I. Martínez, Agustin Aguilar, Maria I. Ibba, Velu Govindan, Ravi P. Singh and Kanwarpal S. Dhugga**

International Maize and Wheat Improvement Center (CIMMYT), El Batan, Mexico

Biofortification of cereal grains offers a lasting solution to combat micronutrient deficiency in developing countries where it poses developmental risks to children. Breeding efforts thus far have been directed toward increasing the grain concentrations of iron (Fe) and zinc (Zn) ions. Phytic acid (PA) chelates these metal ions, reducing their bioavailability in the digestive tract. We present a high-throughput assay for quantification of PA and its application in screening a breeding population. After extraction in 96-well megatiter plates, PA content was determined from the phosphate released after treatment with a commercially available phytase enzyme. In a set of 330 breeding lines of wheat grown in the field over 3 years as part of a HarvestPlus breeding program for high grain Fe and Zn, our assay unraveled variation for PA that ranged from 0.90 to 1.72% with a mean of 1.24%. PA content was not associated with grain yield. High yielding lines were further screened for low molar PA/Fe and PA/Zn ratios for increased metal ion bioavailability, demonstrating the utility of our assay. Genome-wide association study revealed 21 genetic associations, six of which were consistent across years. Five of these associations mapped to chromosomes 1A, 2A, 2D, 5A, and 7D. Additivity over four of these haplotypes accounted for an ∼10% reduction in PA. Our study demonstrates it is possible to scale up assays to directly select for low grain PA in forward breeding programs.

Keywords: biofortification, grain nutrition, iron, zinc, phytic acid, GWAS

OPEN ACCESS

Edited by:
Francesco Sestili, University of Tuscia, Italy

Reviewed by:
Rupesh Kailasrao Deshmukh, National Agri-Food Biotechnology Institute, India
Parveen Chhuneja, Punjab Agricultural University, India

***Correspondence:**
Kanwarpal S. Dhugga
K.DHUGGA@cgiar.org

Specialty section:
This article was submitted to Plant Biotechnology, a section of the journal Frontiers in Plant Science

Received: *06 December 2021*
Accepted: *10 January 2022*
Published: *15 February 2022*

Citation:
Wen Z, Juliana P, Dhugga HS, Pacheco M, Martínez UI, Aguilar A, Ibba MI, Govindan V, Singh RP and Dhugga KS (2022) Genome-Wide Association Study of Phytic Acid in Wheat Grain Unravels Markers for Improving Biofortification. Front. Plant Sci. 13:830147. doi: 10.3389/fpls.2022.830147

INTRODUCTION

Biofortification of cereal grains is an effective route to mitigate malnourishment of underprivileged populations in developing countries (Nestel et al., 2006; Bouis and Saltzman, 2017). Most breeding efforts toward this goal have been focused on increasing the concentrations of micronutrients like iron (Fe) and zinc (Zn) in the grain (Velu et al., 2016, 2018; Cu et al., 2020). Yet, the bioavailability of these ions is known to be reduced by phytic acid (PA), which also accumulates in the grain (Turnlund et al., 1984; Hallberg et al., 1989; Roohani et al., 2013). Once chelated by PA, these metal micronutrient ions pass through the digestive tract without being absorbed (Roohani et al., 2013).

Antinutritional effects of PA have been studied in both humans and model animals. Addition of PA at a PA/Zn molar ratio of 15:1 to a formulated diet caused a 50% reduction in Zn absorption in a group of young men (Turnlund et al., 1984). Another study reported a decrease of 82% in Fe absorption upon dietary PA supplementation at a PA/Fe molar ratio of ∼5:1 (Hallberg et al., 1989). Although it is difficult to determine the lowest limit of a healthy dietary PA/Zn or PA/Fe ratio, mainly because of the interference from other dietary components, it is well documented that the negative effect of PA on the absorption of micronutrient ions is significant (Yu et al., 2010). In developing countries, where cereals serve as staple food, higher dietary PA poses an even greater threat to micronutrient sufficiency than in developed countries (Ma et al., 2007; Al Hasan et al., 2016). Excreted PA from monogastric livestock pollutes the environment. Because monogastric animals (poultry and swine) cannot metabolize PA, excreted PA in the feces contributes to freshwater eutrophication (Brinch-Pedersen et al., 2002). Breeding for low PA crop varieties offers durable solution to these concerns.

Grains from low phytic acid (*lpa*) mutants contain significantly lower PA than the wildtype in maize (Raboy et al., 2000; Shi et al., 2003; Shi et al., 2005). Nutritional benefits of *lpa* were demonstrated in an animal experiment where rats fed with *lpa* maize meal absorbed twice the Zn as compared to those fed normal meal (Lonnerdal et al., 2011). But undesirable pleiotropic effects, for example, reduced seed germination and low grain yield, associated with the *lpa* mutant have limited its breeding application (Raboy et al., 2000; Pilu et al., 2005). Alternatively, a number of transgenic approaches silencing different steps of the PA biosynthetic pathway resulted in lower grain PA content (Kuwano et al., 2006; Shi et al., 2007; Ali et al., 2013). However, consumer opposition to genetically modified crops makes it an uphill task for these products to be made available for the target geographies, particularly when stewardship remains a concern (Wulff and Dhugga, 2018). It is desirable, thus, to explore genetic determinants of seed PA concentration, so that its content in the grain could be reduced within the constraints of natural variation by forward breeding.

Recently, a genome-wide association study (GWAS) was reported on exploring the genetics of the PA content in the rice grain (Perera et al., 2019). With only 69 accessions and inconsistent planting conditions (field and glasshouse), the results were inconclusive. Clearly, the throughput of PA quantification has been an impediment in studying the genetics of its accumulation in the grain (Schlemmer et al., 2009; Sivakumaran and Kothalawala, 2018).

Currently, there are several PA quantification methods available (Gao et al., 2007; Sivakumaran and Kothalawala, 2018). A commonly used method involves forming a complex of PA in the extracted sample with ferric salts, centrifugation to remove the precipitate, and then measuring residual ferric in the supernatant colorimetrically after mixing with sulfosalicylic acid, which forms a colored complex with ferric ions (Gao et al., 2007). Alternatively, the precipitate can be resuspended and further analyzed to directly measure PA. Other methods involve high performance liquid chromatography, ion exchange chromatography, or ^{31}P nuclear magnetic resonance. These low throughput methods are not suitable for screening large breeding populations.

In this report we present an enzyme-base colorimetric method for high-throughput PA quantification. We used this method to measure the grain PA content of more than 300 field-grown wheat lines over 3 years. GWAS revealed several markers significantly associated with the PA content. Selection for as few as two of these markers could significantly reduce the grain PA content. Our study paves the way to breed for low grain PA by direct forward selection in breeding populations, at least in the later stages of a breeding program.

RESULTS AND DISCUSSION

Development of High-Throughput Assay for Phytic Acid Quantification

We used a commercially available phytase, an enzyme that cleaves phosphate groups from PA, to develop a high-throughput assay for PA determination. Phosphate release peaked at a phytase concentration of 0.75 mg/ml (**Figure 1A**). At 55°C, maximal amount of phosphate was released after 30 min of incubation (**Figure 1B**). No more than 52% of the total expected phosphate could be released regardless of the initial amount of PA in the reaction, the incubation time and the amount of enzyme used (**Figure 1B** and **Supplementary Figure 1**). Absorbance (OD_{700}) was linear over a range of 0–210 μM (R^2 = 1), which is equivalent to 0–16.8 nmol or 0–11 μg PA in each 100 μl reaction (80 μl PA standard + 20 μl phytase, **Figure 1C**). Despite minor variation for the background phosphate and the phytase protein in different batches of the commercial enzyme, no differences in enzyme activity were observed as long as the protein concentration was adjusted to 0.75 mg/ml in the reaction (**Supplementary Figure 2**). The phytase solution was stable for up to 6 weeks at 4°C after the initial preparation (**Supplementary Figure 3**).

We did not detect any additional release of phosphate by alkaline phosphatase after the phytase treatment (**Supplementary Figure 4**). In contrast, McKie and McCleary (2016) reported sequential hydrolysis using phytase and then alkaline phosphatase released all the phosphate from PA. Phytase from wheat bran used in our assay is classified as a 4-phytase (1D-numbering system, enzyme commission number 3.1.3.26), which first hydrolyzes the phosphate group at the D-4 position of the *myo*-inositol ring, resulting in *myo*-inositol 1,2,3,5,6-pentakisphosphate (Konietzny and Greiner, 2002). Then, a series of lower *myo*-inositol phosphates are produced, with *myo*-inositol triphosphate as the main product, which is in accordance with the 50% PA hydrolysis rate we observed (Tomlinson and Ballou, 1962). However, lower *myo*-inositol phosphates with three or fewer phosphate residues cannot be hydrolyzed by most plant alkaline phosphatases (Konietzny and Greiner, 2002). Alkaline phosphatase used in our study from calf intestine (enzyme commission number 3.1.3.1) is capable of hydrolyzing *myo*-inositol monophosphate (*m*IMP). However,

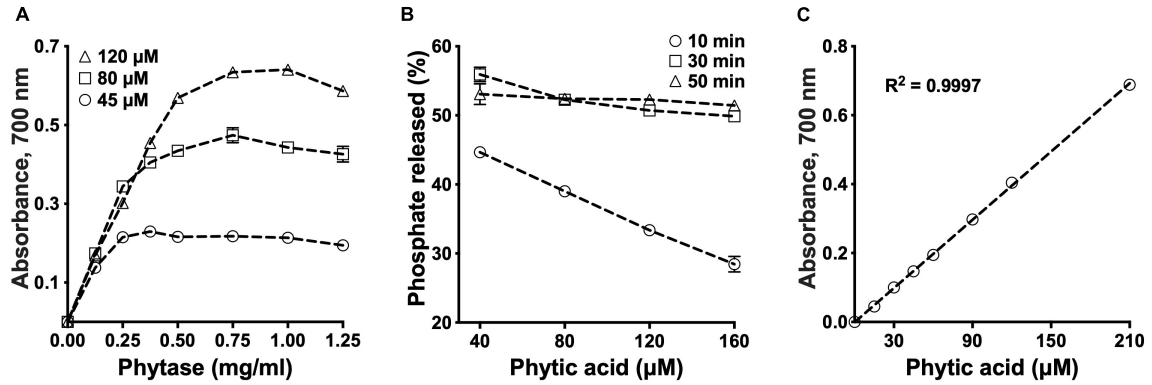


FIGURE 1 | Standardization of phytic acid (PA) hydrolysis conditions. Optimization of the phytase concentration in PA hydrolysis **(A)**. PA was treated with phytase in a series of concentrations for 30 min at 55°C. Optimization of the reaction time for PA hydrolysis **(B)**. PA was treated with 0.75 mg/ml phytase at 55°C. PA standard curve **(C)**. All values are means over two replications.

given the extremely low, if any, occurrence of *m*IMP in the PA hydrolysis products after phytase treatment, further release of phosphate was unlikely (Tomlinson and Ballou, 1962). In addition, phosphate, produced during each step of PA hydrolysis (averaged at 0.2 mM in our experiment) can strongly inhibit alkaline phosphatase (K_i = 0.03 mM) (Kaufman and Kleinberg, 1975). Unlike the wheat bran phytase we used in our study, other phytases, for example fungal phytases, can cleave a larger number of phosphate groups from the PA (Rao et al., 2009). The difference between our results and those of McKie and McCleary (2016) could possibly be attributed to the different phytases used in each study. As long as the phytase enzyme consistently cleaves the same number of phosphate groups from PA in different samples, PA quantification would be consistent.

Free phosphate concentration in wheat seed extracts was negligible as compared to that released by phytase hydrolysis (**Supplementary Figure 5A**). A comparison of the PA content measured from 330 wheat lines with or without correcting for free phosphate suggested that it was unnecessary to measure the background phosphate for GWAS (**Supplementary Figure 5B**), which would help reduce the number of assays by half.

A single-enzyme based, high-throughput assay we report here is reliable in quantifying grain PA content (see **Supplementary Figure 6**. Schematic Diagram of High-throughput Phytic Acid Quantification Method). We compared our method with a commercially available, low-throughput assay and obtained similar results (R^2 = 0.97, **Supplementary Figure 7**; McKie and McCleary, 2016).

Variation for Phytic Acid in Wheat Genotypes

We measured grain PA in the wheat lines from the HarvestPlus Association Mapping (HPAM) population grown at CIMMYT over 3 years (Velu et al., 2016, 2018). The PA content ranged from 1.06 to 1.72% (w/w) in 2014–2015, from 0.95 to 1.51% in 2015–2016 and from 0.90 to 1.35% in 2016–2017 (**Supplementary Figure 8**). The mean PA content was highest in the 2014–2015 season and lowest in the 2016–2017 season, indicating a role of environmental factors in PA accumulation (**Figure 2A**). Zinc content also followed the same pattern as PA but iron content exhibited an opposite pattern. Whereas it is difficult to pinpoint the environmental factors underlying the observed variation (**Supplementary Figure 9**), the data suggest that divalent cations, at least iron and zinc together, maintain a homeostatic molar concentration in the grain in fluctuating environments (**Figure 2B**).

The HPAM panel used in our study was previously used in the CIMMYT biofortification breeding program, the aim of which was to breed lines with increased grain Fe and Zn contents (Velu et al., 2016, 2018). Several biofortified varieties have been released from this program in India (WB-02, PBW01Zn, and HUW711), Pakistan (Zincol-16 and Akbar-19), Bangladesh (BARI-Gom 33) and Nepal (Zinc Gahun 1, Zinc Gahun 2, Bheri-Ganga, Himganga, and Khumal-Shakti) (Singh et al., 2017). However, as important factors in determining the bioavailability of Fe and Zn, the molar ratios of PA to Fe and Zn were not available at the time these selections were made. As a result, some of the released varieties with higher grain Fe and Zn did not have an optimal PA/Zn or PA/Fe molar ratios (**Figure 2C**).

Plotting of standardized variables of PA/Fe and PA/Zn ratios against grain yield allowed identification of high yielding lines with relatively low grain PA (**Figure 3**). A lack of correlation (R^2 = 0.01) between these two traits makes it possible to advance the recombinants with high yield and low grain PA. Varieties in the bottom-right quadrant (shaded area) should be prioritized during selection for their high bioavailability of Zn and Fe and grain yield. Among the five released breeding lines, only two met these criteria (**Figure 3**, green diamond). As other agronomic traits must be considered before varietal release, and the grain yield data used for this analysis were from small plots, our assay could be deployed later in the breeding cycle to advance those lines that have desired combinations of high grain metal ions and low PA.

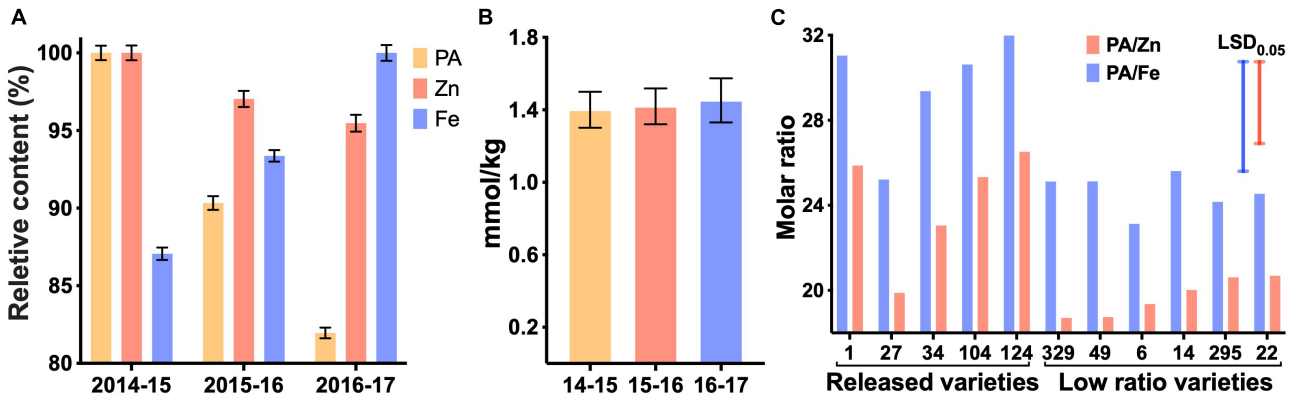


FIGURE 2 | Variations for phytic acid (PA), Fe and Zn over three growing seasons **(A,B)** and selected lines differing for PA to Fe and Zn molar ratios **(C)**. Numbers on the *X*-axis refer to years 2014–2017. Relative values of PA, Zn, and Fe **(A)**. Maximum concentrations were 1.72% for PA in 2014–2015, 38.1 mg/kg for Fe in 2016–2017 and 52.7 mg/kg for Zn in 2014–2015. Total metal ion concentration in each growing season **(B)**. Only the released wheat varieties and selected varieties with low PA/Zn and PA/Fe were plotted **(C)**. Blue and red bars represent the least significant difference. Numbers on the *X*-axis correspond to the breeding lines.

Genome-Wide Association Study for Phytic Acid Content

Genome-wide association study for PA content was performed using the mixed linear model with the PA content evaluations in all 3 years and the best linear unbiased estimates (BLUEs) obtained from the two evaluations (2015–2016 and 2016–2017, **Figure 4**). The *p*-values for the significance of marker-trait associations, the additive effect of the markers on the PA content and the percentage variation in PA content explained by the markers are shown in **Supplementary Table 1**. In the 2015–2016 dataset, 23 markers were significantly associated with PA content at a *p*-value threshold of 0.001 (**Figure 4A** and **Supplementary Table 1**). Among those, the most significant marker, wsnp_BE444579B_Ta_2_1 on chromosome 3B (physical location unaligned in Refseq v1.0), followed by the marker IACX8282 on chromosome 5AL were also significant after Bonferroni correction (α level of 0.20). In addition, BS00009885_51 on chromosome 1AS, four markers on chromosome 1AL between base pair positions 529666321 and 530236376, RAC875_rep_c109215_398 on chromosome 1BL, eight markers on chromosome 1DL between 430565264 and 433276844 bps, RFL_Contig3550_457 on chromosome 2A, BS00069899_51 on chromosome 2DS, Ku_c69970_624 on chromosome 3AL, RAC875_c39141_55 on chromosome 5BL, IAAV5761 on chromosome 6AL, RAC875_c82406_177 on chromosome 6DS and BobWhite_c34689_116 on chromosome 7DL were also associated with PA content in the 2015–2016 dataset.

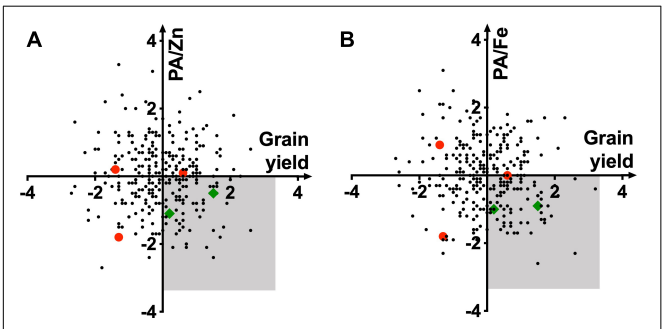


FIGURE 3 | Relationship of standardized PA/Zn **(A)** and PA/Fe **(B)** molar ratios with grain yield. Quadrangles representing wheat lines with high bioavailability of Zn and Fe and high grain yield are shaded in gray. Red dots and green diamonds represent wheat lines released as commercial varieties. PA, Fe, Zn, and yield data were averaged over 2015–2016 and 2016–2017 seasons.

In the 2016–2017 dataset, 20 markers were significantly associated with PA content (**Figure 4B** and **Supplementary Table 1**). Among them, the most significant markers were BobWhite_c34689_116 on chromosome 7DL, RFL_Contig3550_457 on chromosome 2A and BS00009885_51 on chromosome 1A. Furthermore, BS00048118_51 on chromosome 1AS, BS00071630_51 and Tdurum_contig48302_532 on chromosome 2AS, RAC875_rep_c109207_706 on chromosome 2BS, BS00069899_51 on chromosome 2DS, wsnp_BE444579B_Ta_2_1 on chromosome 3B (physical location unaligned in Refseq v1.0), Excalibur_rep_c70578_299 on chromosome 4AL, BS00063809_51 on chromosome 4BS, IACX8282 on chromosome 5AL, four markers on chromosome 5DL between 543272435 and 548368912 bps and three markers on chromosome 6AS including RFL_Contig2815_1135, Kukri_c10226_1815, and BobWhite_c23888_124 were also significantly associated with the PA content in the 2016–2017 dataset. No significant associations that were consistent with the 2015–2017 data sets were found in the 2014–2015 data set. It is possible that the environmental conditions that led to high grain PA in that year also contributed to the noise level, masking the genetic signal (**Supplementary Figure 9**).

In the dataset with the BLUEs obtained from the two evaluations, 17 markers were significantly associated with PA content (**Figure 4C** and **Supplementary Table 1**), among which wsnp_BE444579B_Ta_2_1on

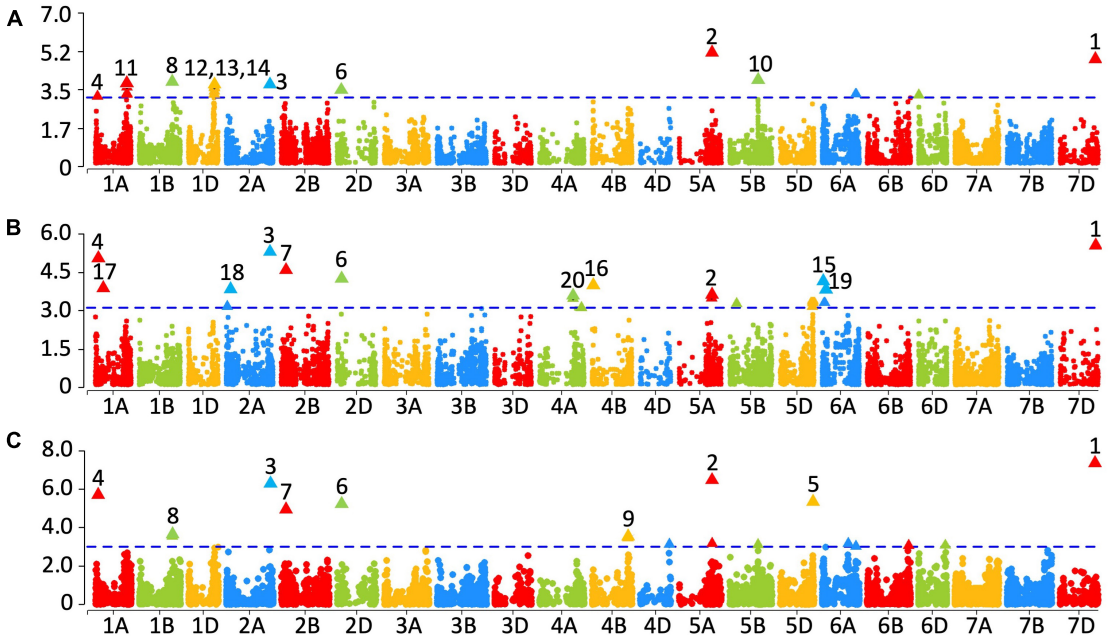


FIGURE 4 | Markers significantly associated with grain phytic acid from year 2015–2016 **(A)**, 2016–2017 **(B)** and averaged over two years **(C)**. The $-\log_{10}$ *p*-values are shown on the *y*-axis. Markers that were significant at a *p*-value of 0.001 are numbered: (1) BobWhite_c34689_116, (2) IACX8282, (3) RFL_Contig3550_457, (4) BS00009885_51, (5) Excalibur_c48387_58, (6) BS00069899_51, (7) RAC875_rep_c109207_706, (8) RAC875_rep_c109215_398, (9) Kukri_c9545_864, (10) RAC875_c39141_55, (11) Excalibur_c1236_444, (12) Ra_c15730_3403, (13) Excalibur_c16570_925, (14) D_GDS7LZN02GSCOW_131, (15) RFL_Contig2815_1135, (16) BS00063809_51, 17) BS00048118_51, (18) Tdurum_contig48302_532, (19) BobWhite_c23888_124, (20) and Excalibur_rep_c70578_299.

chromosome 3B (physical location unaligned in Refseq v1.0), BobWhite_c34689_116 on chromosome 7DL, IACX8282 on chromosome 5AL, RFL_Contig3550_457 on chromosome 2A, BS00009885_51 on chromosome 1A, Excalibur_c48387_58 on chromosome 5DL, BS00069899_51 on chromosome 2DS and RAC875_rep_c109207_706 on chromosome 2BS were also significant. In addition, RAC875_rep_c109215_398 on chromosome 1BL, IAAV2328 on chromosome 5AL, Kukri_c9545_864 on chromosome 4BL, IACX11246 on chromosome 4DL, IAAV2328 on chromosome 5AL, RAC875_c39141_55 on chromosome 5BL, Kukri_c1281_515 and IAAV5761 on chromosome 6AL, BS00067417_51 on chromosome 6BL, BS00109999_51 on chromosome 6DL and Kukri_c35508_426 on chromosome 7D were also significantly associated with PA content in the BLUEs dataset.

Overall, six consistent and significant associations for the PA content across two of the 3 years were obtained (**Figure 5** and **Supplementary Table 2**). Significant phenotypic variation in PA content could be attributed to the alleles at these six markers (**Figure 5**). Of the 330 lines, 296 had the allelic fingerprints (increasing allele, decreasing allele, and heterozygote) of these six markers (**Supplementary Figure 10**). Approximately half the lines, 153, had no favorable allele (less PA), 104 lines had 1–5, and 39 lines had all six 6 favorable alleles (**Supplementary Table 2**). The effect of four of the six favorable alleles on grain PA was additive, showing a reduction from 1.21% with no favorable allele down to 1.13% (**Figure 6**), which could potentially increase the bioavailability of Fe and Zn by ∼7%. These results highlight the value of PA assays in lowering its content through forward selection.

Genes within 1 Mbp upstream and downstream of the six markers are listed in **Supplementary Table 3**. An ABC-2 type transporter gene (TraesCS5A01G344500) on chromosome 5A, which is located ∼0.42 Mbp from marker IACX8282, presents a candidate for genetic manipulation. A similar gene has been previously shown to control the PA level in the maize grain and soybean seed (Shi et al., 2007). Silencing this gene specifically in the embryo caused a 75% reduction in the seed PA content without any noticeable pleiotropic effects (Shi et al., 2007). Two other genes (TraesCS7D01G454300 and TraesCS7D01G454500) annotated as dolichyl-diphosphooligosaccharide-protein glycosyltransferase were respectively located 1.3 and 130 Kbp distal to marker BobWhite_c34689_116 on chromosome 7D. These genes were upregulated in low PA soybean mutants, suggesting their possible role in PA formation (Yuan et al., 2017). All these genes can be silenced by gene editing. Knocking out the ABC transporter gene in particular might lead to a greater reduction in grain PA than the allelic variant in our study with the assumption that the desirable allelic variant has reduced function.

The value of our assay in screening breeding populations for improved biofortification can be judged from a reevaluation of the original selections that were made based only on high grain mineral ion concentrations (Velu et al., 2016, 2018). Fewer than

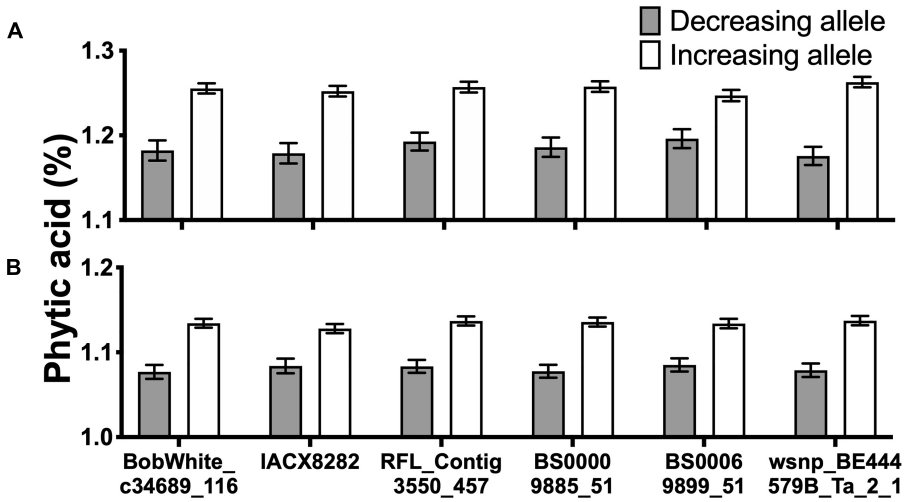


FIGURE 5 | Grain phytic acid (PA) content in the presence or absence of desirable alleles. Six markers consistently associated with grain PA content in year 2015–2016 **(A)** and 2016–2017 **(B)**. All values are means over the respective number of lines for each allele.

1/3rd of the 330 lines contained four or more desirable alleles for low grain PA (**Figure 6**), the frequency that is also reflected in the commercial varieties that have been released in different countries (**Figure 2C**). Only one of the five released varieties had desirable PA to mineral ion ratios (**Figure 2C**). In the future, aside from their usefulness in direct selection for low grain PA, the desirable haplotypes could be used to prescreen the parental lines to set up crosses in the breeding programs targeted toward improving grain biofortification (**Figures 4–6**).

We have presented a high-throughput, reliable and easy-to-use PA quantification method that is scalable for phenotyping large breeding populations. Markers identified in our wheat grain PA GWAS could assist in screening late-stage breeding populations for the identification of low grain PA wheat varieties. Further, our method is widely applicable to other crops.

EXPERIMENTAL PROCEDURES

Wheat Population and Field Experiment

The HarvestPlus Association Mapping (HPAM) panel consisted of 330 wheat lines from CIMMYT's biofortification breeding program. This genetically diverse panel could be divided into five sub-populations that were derived from: (1) landraces; (2) *Triticum durum*-based synthetic hexaploid derivatives; (3) *Triticum dicoccon*-based synthetic hexaploid derivatives; (4) *Triticum spelta* derivatives; and (5) CIMMYT's pre-breeding derivatives of diverse progenitors including *Triticum polonicum* (Velu et al., 2018). The panel was grown in a randomized complete block design in two replications with a plot size of 2 m^2 at CIMMYT's experimental station in Ciudad Obregon, Sonora, Mexico (27°24′N, 109°56′W) during three successive crop seasons (2014–15, 2015–16, and 2016–17). Trials were irrigated five times throughout the crop cycle and fertilized at a rate of 200:50 (N:P) $kg.ha^{-1}$, of which 50:50 was applied in pre-sowing and 150:00 at tillering stage. Diseases and pests were controlled chemically, whereas weeds were controlled manually and chemically according to CIMMYT's standard protocols. Zinc was applied at a rate of 25 $kg.ha^{-1}$ as $ZnSO_4.7H_2O$ over three crop cycles to reduce soil heterogeneity for this micronutrient. Soil analysis of the experimental area showed an average Zn concentration of 1.2 ppm at soil depth of 0–30 cm, and 0.86 ppm at a soil depth of 30–60 cm. The average Fe concentration in the soil was 5.0 and 6.1 ppm, at 0–30 and 30–60 cm soil depth, respectively. Rest of the details were as previously reported (Cu et al., 2020).

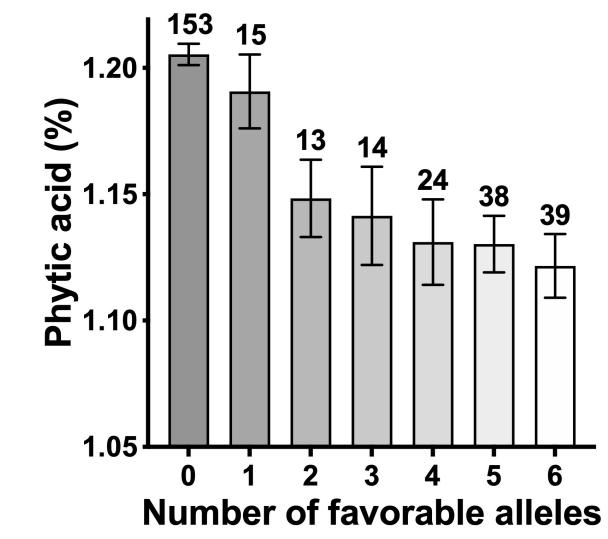


FIGURE 6 | Phytic acid content in wheat lines as a function of number of favorable alleles. The number of lines in each group are shown on top of respective bars.

Wheat head samples were collected from five plants per genotype in each plot at physiological maturity in each of the seasons. All samples were oven dried at 40°C for 4 days, threshed, grain separated and subjected to subsequent analyses. Iron and zinc were determined as previously described (Cu et al., 2020).

Phytic Acid Extraction From Wheat Seeds

Wheat grains (10 grains per line) were dried at 60°C for 3 days and ground using a GenoGrinder (model 2010, SPEX Sample Prep, United States) with small grinding vial set (6751, SPEX Sample Prep) for 15 s four times at 1750 rpm. Fifty mg of each flour sample were weighted into individual microtiter tube in a 96-tube rack format, 600 μl of 0.6 M HCl added using a Liquidator96 96-well pipettor (LIQ-96-200, METTLER TOLEDO, United States). After sealing the tubes, PA was extracted at room temperature on a shaker at 150 rpm overnight. The sample racks were centrifuged at 4800 g for 10 min in a Megafuge 40R centrifuge (Thermo Scientific, United States, rotor 75003607), followed by transferring 50 μl supernatant into new microtiter tubes. The clear PA extracts were neutralized by mixing with 50 μl 0.6 M NaOH and then diluted with 900 μl 0.2 M sodium acetate (NaOAc), pH 5.5.

Phytase Working Solution

Phytase (P1259, Sigma-Aldrich, United States) was dissolved in 0.2 M NaOAc, pH 5.5, to give a concentration of 10 mg/ml. Actual phytase concentration was quantified using a bicinchoninic acid protein determination kit (BCA1 and B9643, Sigma-Aldrich, United States) and a microplate reader (FLUOstar Omega, BMG Labtech, Germany). The phytase working solution was prepared by adjusting the actual phytase concentration to 4 mg/ml using the NaOAc buffer.

Phytic Acid and Phosphate Standards

Phytic Acid solution (593648, Sigma-Aldrich, United States) was used to prepare a series of PA standard solutions in the NaOAc buffer. Phosphate standards were prepared by dissolving KH_2PO_4 in the NaOAc buffer.

Phytic Acid Hydrolysis and Quantification

High-throughput assays were performed essentially as described for other traits previously (Silva et al., 2017, 2018). PA in 80 μl diluted extract (and PA standards and phosphate standards) was hydrolyzed by mixing with 20 μl phytase working solution and incubated at 55°C for 30 min. Then each reaction was mixed with the 100 μl color reagent and incubated at 37°C for 30 min. The color reagent is consisted of the four solutions in a ration of A:B:C:D = 1:1:1:2 (A. 2.5% (w/w) $(NH_4)_2MoO_4$, B. 3 M H_2SO_4, C. 10% (w/w) ascorbic acid and D. H_2O). Then the reactions were centrifuged at 4700 rpm for 10 min. 100 μl supernatant of each reaction was transferred to a 96-well plate and absorbance was measured at a wavelength of 700 nm. The wavelength was determined by scanning through the absorbance of phosphate standards.

Genotyping Data, Population Structure, and Kinship Analysis

The 330 lines in the HPAM panel were genotyped using the Illumina iSelect 90 K Infinitum single nucleotide polymorphism array. Quality control of the genotyping data was done by filtering markers with greater than 70% missing data, less than 5% minor allele frequency and greater than 10% heterozygosity. We then obtained the physical positions of the markers in the reference genome of wheat (Refseq v1.0) available at https://triticeaetoolbox.org/wheat/maps (Appels et al., 2018). Plot of SNP densities in different chromosomes or the number of SNPs within a 10 Mb window revealed moderate to good coverage in the telomeric regions, and a relatively lower coverage in the centromeric regions (**Supplementary Figure 11**). The highest number of markers were in the B genome (4,323 markers, 42.6%), followed by the A genome (4,038 markers, 39.8%) and the D genome (1,797 markers, 17.7%).

Population structure of the lines in the panel was done using the principal component analysis in TASSEL (Trait Analysis by aSSociation Evolution and Linkage) version 5. Moderate population structure was observed and the first two principal components explained 10.9 and 7.2% of the variation, respectively (**Supplementary Figure 12**). In addition, we also obtained the kinship between the lines using the centered identity-by-state method in TASSEL version 5 (Endelman and Jannink, 2012). Several lines formed clusters with a relationship of 0.4–0.6, while only a few lines had a relationship of over 0.7 (**Supplementary Figure 13**).

Genome-Wide Association Mapping and Allelic Fingerprinting

We performed genome-wide association mapping for PA content in TASSEL version 5 with the mixed linear model and used the optimum level of compression and the "population parameters previously determined" options (Yu et al., 2006; Zhang et al., 2010). The first two principal components that accounted for the population structure were used as fixed effects and the kinship matrix among the lines was used as the random effect in the mixed linear model (Price et al., 2006). We obtained the marker *p*-values, additive effects and percentage variation explained by each marker and then plotted the Manhattan plots with the - $\log_{10}$ *p*-values of the markers using the "R" package CMplot (Lilin-Yin, 2018). To declare significance of the markers, we used a *p*-value threshold of 0.001 and also corrected for multiple testing using the Bonferroni method at an α level of 0.20. The markers that were consistently associated with PA content in the two evaluations were then identified and the alleles associated with increasing and decreasing the PA content at these markers were fingerprinted in all the lines. We then determined the relationships between the number of PA favorable alleles (PA decreasing alleles) at the consistent markers and the PA content and visualized them using box plots, created using the R package, "ggplot2" (Ginestet, 2011). Finally, we also obtained the genes that were 100 Mb upstream and downstream of the consistently significant markers using Jbrowse

available at https://wheat-urgi.versailles.inra.fr/Tools/JBrowse and explored the genes in the interval to identify potential PA-associated candidate genes.

DATA AVAILABILITY STATEMENT

The datasets presented in this study can be found in the **Supplementary Material**.

AUTHOR CONTRIBUTIONS

ZW, HSD, and KSD developed and refined the assay. ZW oversaw screening of the grain samples. MP, UIM, and AA carried out the assays in the population and MII compared different methods. VG and RPS conducted the field experiments and provided the grain samples. PJ carried out GWAS analysis. ZW and KSD wrote and revised the manuscript. All authors contributed to the article and approved the submitted version.

FUNDING

This work was supported by the CGIAR Research Program on Wheat (WHEAT), HarvestPlus, Bill & Melinda Gates Foundation, and Foreign Commonwealth and Development Office of the United Kingdom.

SUPPLEMENTARY MATERIAL

The Supplementary Material for this article can be found online at: https://www.frontiersin.org/articles/10.3389/fpls.2022.830147/full#supplementary-material

REFERENCES

Al Hasan, S. M., Hassan, M., Saha, S., Islam, M., Billah, M., and Islam, S. (2016). Dietary phytate intake inhibits the bioavailability of iron and calcium in the diets of pregnant women in rural Bangladesh: a cross-sectional study. *BMC Nutr.* 2:24.

Ali, N., Paul, S., Gayen, D., Sarkar, S. N., Datta, K., and Datta, S. K. (2013). Development of low phytate rice by RNAi mediated seed-specific silencing of inositol 1,3,4,5,6-pentakisphosphate 2-kinase gene (IPK1). *PLoS One* 8:e68161. doi: 10.1371/journal.pone.0068161

Appels, R., Eversole, K., Stein, N., Feuillet, C., Keller, B., Rogers, J., et al. (2018). Shifting the limits in wheat research and breeding using a fully annotated reference genome. *Science* 361:eaar7191. doi: 10.1126/science.aar7191

Bouis, H. E., and Saltzman, A. (2017). Improving nutrition through biofortification: a review of evidence from HarvestPlus, 2003 through 2016. *Glob. Food Sec.* 12, 49–58. doi: 10.1016/j.gfs.2017.01.009

Brinch-Pedersen, H., Sorensen, L. D., and Holm, P. B. (2002). Engineering crop plants: getting a handle on phosphate. *Trends Plant Sci.* 7, 118–125. doi: 10.1016/s1360-1385(01)02222-1

Cu, S. T., Guild, G., Nicolson, A., Velu, G., Singh, R., and Stangoulis, J. (2020). Genetic dissection of zinc, iron, copper, manganese and phosphorus in wheat (*Triticum aestivum* L.) grain and rachis at two developmental stages. *Plant Sci.* 291:110338. doi: 10.1016/j.plantsci.2019.110338

Endelman, J. B., and Jannink, J. L. (2012). Shrinkage estimation of the realized relationship matrix. *G3* 2, 1405–1413. doi: 10.1534/g3.112.004259

Gao, Y., Shang, C., Maroof, M. A. S., Biyashev, R. M., Grabau, E. A., Kwanyuen, P., et al. (2007). A modified colorimetric method for phytic acid analysis in soybean. *Crop Sci.* 47, 1797–1803. doi: 10.2135/cropsci2007.03.0122

Ginestet, C. (2011). ggplot2: Elegant graphics for data analysis. *J. R. Stat. Soc. Series* 174, 245–245. doi: 10.1111/j.1467-985x.2010.00676_9.x

Hallberg, L., Brune, M., and Rossander, L. (1989). Iron absorption in man: ascorbic acid and dose-dependent inhibition by phytate. *Am. J. Clin. Nutr.* 49, 140–144. doi: 10.1093/ajcn/49.1.140

Kaufman, H. W., and Kleinberg, I. (1975). Hydrolysis of phytate and its inositol phosphate intermediates by an acid and an alkaline phosphatase. *Arch. Oral. Biol.* 20, 157–160. doi: 10.1016/0003-9969(75)90002-3

Konietzny, U., and Greiner, R. (2002). Molecular and catalytic properties of phytate-degrading enzymes (phytases). *Int. J. food Sci. Technol.* 37, 791–812. doi: 10.1371/journal.pone.0094403

Kuwano, M., Ohyama, A., Tanaka, Y., Mimura, T., Takaiwa, F., and Yoshida, K. T. (2006). Molecular breeding for transgenic rice with low-phytic-acid phenotype through manipulating myo-inositol 3-phosphate synthase gene. *Mol. Breed.* 18, 263–272. doi: 10.1007/s11032-006-9038-x

Lilin-Yin (2018). *Package 'CMplot' Version 3.4.0.*

Lonnerdal, B., Mendoza, C., Brown, K. H., Rutger, J. N., and Raboy, V. (2011). Zinc absorption from low phytic acid genotypes of maize (*Zea mays* L.), barley (*Hordeum vulgare* L.), and rice (*Oryza sativa* L.) assessed in a suckling rat pup model. *J. Agric. Food Chem.* 59, 4755–4762. doi: 10.1021/jf1043663

Ma, G., Li, Y., Jin, Y., Zhai, F., Kok, F. J., and Yang, X. (2007). Phytate intake and molar ratios of phytate to zinc, iron and calcium in the diets of people in China. *Eur. J. Clin. Nutr.* 61, 368–374. doi: 10.1038/sj.ejcn.1602513

McKie, V. A., and McCleary, B. V. (2016). A novel and rapid colorimetric method for measuring total phosphorus and phytic acid in foods and animal feeds. *J. AOAC Int.* 99, 738–743. doi: 10.5740/jaoacint.16-0029

Nestel, P., Bouis, H. E., Meenakshi, J. V., and Pfeiffer, W. (2006). Biofortification of staple food crops. *J. Nutr.* 136, 1064–1067.

Perera, I., Fukushima, A., Arai, M., Yamada, K., Nagasaka, S., Seneweera, S., et al. (2019). Identification of low phytic acid and high Zn bioavailable rice (Oryza sativa L.) from 69 accessions of the world rice core collection. *J. Cereal Sci.* 85, 206–213. doi: 10.1016/j.jcs.2018.12.010

Pilu, R., Landoni, M., Cassani, E., Doria, E., and Nielsen, E. (2005). The maize lpa241 mutation causes a remarkable variability of expression and some pleiotropic effects. *Crop Sci.* 45, 2096–2105. doi: 10.2135/cropsci2004.0651

Price, A. L., Patterson, N. J., Plenge, R. M., Weinblatt, M. E., Shadick, N. A., and Reich, D. (2006). Principal components analysis corrects for stratification in genome-wide association studies. *Nat. Genet.* 38, 904–909. doi: 10.1038/ng1847

Raboy, V., Gerbasi, P. F., Young, K. A., Stoneberg, S. D., Pickett, S. G., Bauman, A. T., et al. (2000). Origin and seed phenotype of maize low phytic acid 1-1 and low phytic acid 2-1. *Plant Physiol.* 124, 355–368. doi: 10.1104/pp.124.1.355

Rao, D. E. C. S., Rao, K. V., Reddy, T. P., and Reddy, V. D. (2009). Molecular characterization, physicochemical properties, known and potential applications of phytases: an overview. *Crit. Rev. Biotechnol.* 29, 182–198. doi: 10.1080/07388550902919571

Roohani, N., Hurrell, R., Kelishadi, R., and Schulin, R. (2013). Zinc and its importance for human health: an integrative review. *J. Res. Med. Sci.* 18, 144–157.

Schlemmer, U., Frolich, W., Prieto, R. M., and Grases, F. (2009). Phytate in foods and significance for humans: food sources, intake, processing, bioavailability, protective role and analysis. *Mol. Nutr. Food Res.* 53, S330–S375. doi: 10.1002/mnfr.200900099

Shi, J. R., Wang, H. Y., Schellin, K., Li, B. L., Faller, M., Stoop, J. M., et al. (2007). Embryo-specific silencing of a transporter reduces phytic acid content of maize and soybean seeds. *Nat. Biotechnol.* 25, 930–937. doi: 10.1038/nbt1322

Shi, J., Wang, H., Hazebroek, J., Ertl, D. S., and Harp, T. (2005). The maize low-phytic acid 3 encodes a myo-inositol kinase that plays a role in phytic acid biosynthesis in developing seeds. *Plant J.* 42, 708–719. doi: 10.1111/j.1365-313X.2005.02412.x

Shi, J., Wang, H., Wu, Y., Hazebroek, J., Meeley, R. B., and Ertl, D. S. (2003). The maize low-phytic acid mutant lpa2 is caused by mutation in an inositol phosphate kinase gene. *Plant Physiol.* 131, 507–515. doi: 10.1104/pp.014258

Silva, I. T., Abbaraju, H. K. R., Fallis, L. P., Liu, H. J., Lee, M., and Dhugga, K. S. (2017). Biochemical and genetic analyses of N metabolism in maize testcross seedlings: 1. Leaves. *Theor. Appl. Genet.* 130, 1453–1466. doi: 10.1007/s00122-017-2900-x

Silva, I. T., Abbaraju, H. K. R., Fallis, L. P., Liu, H. J., Lee, M., and Dhugga, K. S. (2018). Biochemical and genetic analyses of N metabolism in maize testcross seedlings: 2. Roots. *Theor. Appl. Genet.* 131, 1191–1205. doi: 10.1007/s00122-018-3071-0

Singh, R., Govindan, V., Andersson, M. S., Bouis, H., and Jamora, N. (2017). *Zinc-Biofortified Wheat: Harnessing Genetic Diversity for Improved Nutritional Quality*. Bonn: Global Crop Diversity Trust.

Sivakumaran, K., and Kothalawala, S. (2018). An overview of the analytical methods for food phytates. *Int. J. Chem. Stud.* 6, 2016–2020.

Tomlinson, R. V., and Ballou, C. E. (1962). Myoinositol polyphosphate intermediates in the dephosphorylation of phytic acid by phytase. *Biochemistry* 1, 166–171. doi: 10.1021/bi00907a025

Turnlund, J. R., King, J. C., Keyes, W. R., Gong, B., and Michel, M. C. (1984). A stable isotope study of zinc absorption in young men: effects of phytate and alpha-cellulose. *Am. J. Clin. Nutr.* 40, 1071–1077. doi: 10.1093/ajcn/40.5.1071

Velu, G., Crossa, J., Singh, R. P., Hao, Y. F., Dreisigacker, S., Perez-Rodriguez, P., et al. (2016). Genomic prediction for grain zinc and iron concentrations in spring wheat. *Theor. Appl. Genet.* 129, 1595–1605. doi: 10.1007/s00122-016-2726-y

Velu, G., Singh, R. P., Crespo-Herrera, L., Juliana, P., Dreisigacker, S., Valluru, R., et al. (2018). Genetic dissection of grain zinc concentration in spring wheat for mainstreaming biofortification in CIMMYT wheat breeding. *Sci. Rep.* 8:13526. doi: 10.1038/s41598-018-31951-z

Wulff, B. B. H., and Dhugga, K. S. (2018). Wheat-the cereal abandoned by GM Genetic modification of wheat for disease resistance could help stabilize food production. *Science* 361, 451–452.

Yu, J. M., Pressoir, G., Briggs, W. H., Bi, I. V., Yamasaki, M., Doebley, J. F., et al. (2006). A unified mixed-model method for association mapping that accounts for multiple levels of relatedness. *Nat. Genet.* 38, 203–208. doi: 10.1038/ng1702

Yu, Y., Lu, L., Wang, R. L., Xi, L., Luo, X. G., and Liu, B. (2010). Effects of zinc source and phytate on zinc absorption by in situ ligated intestinal loops of broilers. *Poult Sci.* 89, 2157–2165. doi: 10.3382/ps.2009-00486

Yuan, F. J., Yu, X. M., Dong, D. K., Yang, Q. H., Fu, X. J., Zhu, S. L., et al. (2017). Whole genome-wide transcript profiling to identify differentially expressed genes associated with seed field emergence in two soybean low phytate mutants. *Bmc Plant Biol.* 17:16. doi: 10.1186/s12870-016-0953-7

Zhang, Z. W., Ersoz, E., Lai, C. Q., Todhunter, R. J., Tiwari, H. K., Gore, M. A., et al. (2010). Mixed linear model approach adapted for genome-wide association studies. *Nat. Genet.* 42, 355–U118. doi: 10.1038/ng.546

Conflict of Interest: The authors declare that the research was conducted in the absence of any commercial or financial relationships that could be construed as a potential conflict of interest.

Publisher's Note: All claims expressed in this article are solely those of the authors and do not necessarily represent those of their affiliated organizations, or those of the publisher, the editors and the reviewers. Any product that may be evaluated in this article, or claim that may be made by its manufacturer, is not guaranteed or endorsed by the publisher.

Copyright © 2022 Wen, Juliana, Dhugga, Pacheco, Martínez, Aguilar, Ibba, Govindan, Singh and Dhugga. This is an open-access article distributed under the terms of the Creative Commons Attribution License (CC BY). The use, distribution or reproduction in other forums is permitted, provided the original author(s) and the copyright owner(s) are credited and that the original publication in this journal is cited, in accordance with accepted academic practice. No use, distribution or reproduction is permitted which does not comply with these terms.

frontiers in Plant Science

ORIGINAL RESEARCH
published: 10 March 2022
doi: 10.3389/fpls.2022.841767

Haplotype Analysis of Chloroplast Genomes for Jujube Breeding

Guanglong Hu†, Yang Wu†, Chaojun Guo†, Dongye Lu, Ningguang Dong, Bo Chen, Yanjie Qiao, Yuping Zhang and Qinghua Pan**

Key Laboratory of Biology and Genetic Improvement of Horticultural Crops (North China), Ministry of Agriculture, Beijing Engineering Research Center for Deciduous Fruit Trees, Institute of Forestry and Pomology, Beijing Academy of Agriculture and Forestry Sciences, Beijing, China

Jujube (family Rhamnaceae) is an important economic fruit tree in China. In this study, we reported 26 chloroplast (cp) sequences of jujube using Illumina paired-end sequencing. The sequence length of cp genome was 161, 367–161, 849 bp, which was composed of a large single-copy region (89053–89437 bp) and a small single-copy region (19356–19362 bp) separated by a pair of reverse repeat regions (26478–26533 bp). Each cp genome encodes the same 130 genes, including 112 unique genes, being quite conserved in genome structure and gene sequence. A total of 118 single base substitutions (SNPs) and 130 InDels were detected in 65 jujube accessions. Phylogenetic and haplotype network construction methods were used to analyze the origin and evolution of jujube and its sour-tasting relatives. We detected 32 effective haplotypes, consisting of 20 unique jujube haplotypes and 9 unique sour–jujube haplotypes. Compared with sour–jujube, jujube showed greater haplotype diversity at the chloroplast DNA level. To cultivate crisp and sweet fruit varieties featuring strong resistance, by combining the characteristics of sour-jujube and cultivated jujube, three hybrid combinations were suggested for reciprocal crosses: "Dongzao" × "Jingzao39," "Dongzao" × "Jingzao60," "Dongzao" × "Jingzao28." This study provides the basis for jujube species' identification and breeding, and lays the foundation for future research.

Keywords: *Ziziphus jujuba*, chloroplast genome, genomic structure, phylogenetic analysis, evolutionary relationship, breeding strategy

OPEN ACCESS

Edited by:
Peng Zhang,
Center for Excellence in Molecular Plant Sciences (CAS), China

Reviewed by:
Xiaoxuan Tian,
Tianjin University of Traditional Chinese Medicine, China
Abdullah,
Quaid-i-Azam University, Pakistan

****Correspondence:***
Yuping Zhang
zhyptt@163.com
Qinghua Pan
qinghua_pan@sina.com

†These authors have contributed equally to this work

Specialty section:
This article was submitted to Plant Biotechnology, a section of the journal Frontiers in Plant Science

Received: *22 December 2021*
Accepted: *11 February 2022*
Published: *10 March 2022*

Citation:
Hu G, Wu Y, Guo C, Lu D, Dong N, Chen B, Qiao Y, Zhang Y and Pan Q (2022) Haplotype Analysis of Chloroplast Genomes for Jujube Breeding. Front. Plant Sci. 13:841767. doi: 10.3389/fpls.2022.841767

INTRODUCTION

Jujube (*Ziziphus jujuba* Mill.) is woody plant native to China, distributed throughout the country, that has been cultivated thousands of years there, and is now also grown across Asia, Europe, and the Americas (Guo et al., 2011). Jujube fruit is sweet and rich in vitamin C. Accordingly, Chinese jujube has important economic value as a food and a resource for the production of medicines and other health-promoting products (Shan et al., 2019; Rashwan et al., 2020; Sabri et al., 2021). Although there are extremely rich germplasm resources for jujube, the lack of improved varieties remains a limiting factor for its industrial development (Chang, 2018; Liu P. et al., 2020).

There are 700 jujube varieties and 30 sour-jujube varieties included in *Chinese fruit trees record–Chinese jujube* (Qu and Wang, 2013). Among them, 261 are suitable fresh-eating varieties, 224 are dried-fruit varieties, 159 are concurrent varieties and 56 candied date varieties. However, none of these varieties were obtained through cross breeding, having instead been selected from local

varieties through long-term natural variation. So far, few novel varieties have been successfully bred through cross breeding. The breeding structure of jujube in China is characterized by disequilibrium. Among the existing production area and yield of jujube, about 80% of each is used for dried fruit ("dates") and processing, with less than 20% of each used for fresh-fruit consumption. Special processing of certain varieties still lacks research and development. The degradation of local traditional jujube varieties is serious, leading to uneven quality and poor resistance against disease (Wang et al., 2012).

Both objective and subjective factors currently hinder the development of jujube hybrid breeding programs. *Objective factors*: First, jujube flowers are small, generally 5–7 mm in diameter, which makes it difficult for anthers and stamens to be manually peeled off; hence, both emasculation and artificial pollination are challenging. Second, the fruit-setting rate of jujube trees is very low, with a blooming period of 2 months in which flowers are abundant. The buds, flowers and fruits coexist during this blooming period. The nutritional competition among these parts is fierce, resulting in less effective flowers, a short effective pollination period, and serious flower and fruit drops. Accordingly, the natural fruit-setting rate of jujube is 1–2%, and likewise low for artificial hybridization. Third, jujube's embryo abortion rate is high, and its kernel rate is low. Embryo abortion is prevalent in many varieties of jujube; this causes fruit drop, while late embryo abortion leads to no seed kernel formed, a crucial factor affecting artificial hybrid breeding. *Subjective factors*: Breeders tend to be bound by traditional concepts of hybrid breeding. At its core, artificial hybridization is the artificial selection of parents. Artificial emasculation, fertilization, and bagging are the breeding methods used for hybrid offspring, which ignores an in-depth understanding of the nature of hybrid breeding, impeding innovation, which seriously hinders the advancement of jujube hybrid breeding programs (Li and Wei, 2013; Wang et al., 2016).

Furthermore, systematic records during the breeding or vegetative propagation of jujube hybrids and/or clones are scarce. Additionally, for those breeding activities whose priority registration is that of new high-performing clones, it is absolutely essential have clear, unequivocal species identification.

There are two main ways to study biological evolution: (1) classical taxonomy based on apparent traits, and (2) biochemical and molecular analyses. Morphological markers are appearance traits that exhibit clear genetic polymorphisms (Li et al., 2015). Li et al. (2015) proposed an adaptive relationship exists between jujube leaf veins and temperature and precipitation, and argued that leaf vein characteristics could be used as a key feature to distinguish varieties and determine their patterns of introduction into different regions. However, quantitative traits are susceptible to external factors, and so they cannot fully convey the genetic variation harbored within a species. Molecular marker technology has since become the main method by which analyze genetic diversity, and now widely used in jujube genetic diversity research. In this respect, simple sequence repeat (SSR) markers have the advantages of stability, repeatability, and co-dominance. An example of their use is the work by Zhang et al. (2013), who used five pairs of SSR primers to analyze the genetic diversity and population structure of 50 different jujube samples collected along the Yellow River in Shaanxi Province.

For a long time, the taxonomic status of jujube and sour-jujube has been controversial (Li et al., 2018; Wang et al., 2019; Liu M. et al., 2020). To address these questions, many studies have been carried using molecular markers to analyze the nuclear genome, including those focusing on the haplotype composition, genetic diversity, and geographical origin of jujube (Liu et al., 2014; Shen et al., 2020; Song et al., 2021). Notably, chloroplast microsatellite markers were used to analyze cytoplasmic inheritance. For example, using chloroplast SSR technology (Yang, 2014) found that jujube and sour -jujube shared multiple haplotypes, with no significant genetic differentiation between these two populations, which suggests the evolution of sour-jujube into jujube occurred *via* multiple paths. Shen (2016) used nuclear and chloroplast SSR markers to comprehensively analyze polymorphism information, uncovering rich genetic diversity in Chinese jujube that was greater in sour-jujube than jujube at the nucleoplasm level. Yet, relatively few studies have conducted detailed genetic analyses of jujube vis-à-vis sour-jujube. Here, we present the complete and annotated DNA sequences for the chloroplast genomes of *Ziziphus jujuba* (jujube) and *Z. jujuba* var. *spinosa* (sour-jujube).

Chloroplast is one pigment body in algae and green plants, being a semiautonomous organelle in which photosynthesis occurs in plant cells. It has its own independent genome that encoded a series of specific proteins, and contains independent genetic materials and systems. Further, the chloroplast is also involved in the biosynthesis of fatty acids, vitamins, pigments, and amino acids, and thus critical for developmental processes that include these compounds (Prabhudas et al., 2016).

The chloroplast genome is a circular DNA molecule in angiosperms that has a typical tetragonal structure and consists of two inverted repeats (IR), a short single copy sequence (SSC), and a long single-copy sequence (LSC). Changes in the size of the chloroplast genome during evolution are mainly due to the extension, reduction, or loss of the IR regions and changes in the length of intergenic regions. The chloroplast genome is small in size, ranging from 120 to 217 kb. Compared with the nuclear and mitochondrial genomes, the chloroplast genome is more conserved in both its gene content and physical structure (Raubeson and Jansen, 2005). The nucleotide mutation rate of chloroplast genes is moderate, being higher than that of mitochondrial genes but lower than that of nuclear genes (Dong et al., 2020). Evolutionary events, such as gene mutation, duplication, loss, and rearrangement, have been detected in chloroplast genomes (Dong et al., 2013; Choi et al., 2016). The chloroplast genome is haploid, non-recombining, and maternally inherited, rendering it an ideal model for evolutionary and comparative genomic research (Birky, 2001; Wu and Ge, 2012). At a higher classification level, the comparative analysis of chloroplast genomes is proving useful for phylogenetic studies (Abdullah et al., 2020, 2021) and understanding genome

evolution as related to changes in genome size, gene and intron loss, and nucleotide substitution (Ahmed et al., 2020; Lee et al., 2021). Comparative studies on chloroplast genomes have been conducted on multiple focus species (Young et al., 2011), genera (Greiner et al., 2008), and families of plants (Daniell et al., 2006).

Chloroplast genomes are reconstructed in phylogeny and DNA barcoding studies, and can be used to investigate the geographical origins of some important domesticated crops. However, there are relatively few studies that examine the genetic relationships of intraspecific varieties for breeding strategy (Daniell et al., 2016).

This study had four objectives: (1) To study the global structure of the chloroplast genome in jujube; (2) To analyze the polymorphism of nucleotide sequences and variation in repeat sequences among jujube chloroplast genomes; (3) To construct a haplotype network using these chloroplast genome sequences, to explore the phylogenetic relationships between jujube and sour-jujube; (4) To select parents for hybrid combinations of fresh-fruit jujube varieties. Our results will be useful for the identification of jujube cultivars, for determining their origins, for genetic breeding improvement and plant protection, and for conducting further evolutionary studies.

MATERIALS AND METHODS

Plant Material Collection and DNA Extraction

We sequenced 26 jujube accessions in this study. All the sampled plants were cultured in the germplasm resources nursery of Institute of Forestry and Pomology, Beijing Academy of Agriculture and Forestry Sciences, Beijing, China. The plants were identified by Professor Qinghua Pan.

The specimens were stored in Key Laboratory of Biology and Genetic Improvement of Horticultural Crops (North China), Ministry of Agriculture. Each fresh leaf was immediately dried and stored with silica gel before its DNA extraction. Total DNA was extracted from 26 leaf samples using a modified CTAB protocol (Li J. et al., 2013). The high-quality total DNA samples were then stored at -80°C until their use.

Including the other 39 data downloaded from the Sequence Read Archive database (NCBI), a complete sample list can be found in **Supplementary Table 1**. All of 65 materials, corresponding to 52 cultivated jujube and 13 wild sour-jujube, were included in the analyses below.

DNA Fragmentation, Library Preparation, and High-Throughput Sequencing

Total DNA was fragmented by ultrasonication, and 350 bp DNA fragments were recovered by gel cutting. Libraries with an average length of 350 bp were constructed using the Nextera XT DNA Library Preparation Kit (Illumina, San Diego, CA, United States). Sequencing was performed on the HiSeq X Ten PE150 platform (Illumina).

Data Assembly

The raw data obtained from high-throughput sequencing were subjected to quality control procedures, by using Trimmomatic v0.36 (Bolger et al., 2014), after which SPAdes v3.10 was used for the *de novo* data assembly (Bankevich et al., 2012). The BLAST program was used to select chloroplast genome contigs from the assembled data (Altschul et al., 1997). Next, the chloroplast genome contigs were assembled using Sequencher 4.10.[1] Published original second-generation sequencing raw data were downloaded from the Sequence Read Archive (SRA) database (refer to **Supplementary Tables 1**, **2**) and chloroplast genome assembly was performed.

Chloroplast Genome Annotation

Annotations was performed using the Plann script (Huang and Cronk, 2015), with the published chloroplast genome of *Z. jujuba* (GenBank number KX266829) serving as the reference sequence. Some unsuccessfully annotated or incorrectly annotated genes were manually added using Sequin software.

Analysis of Variation Within Species

The chloroplast genome sequences of all jujube materials were assembled and aligned using MAFFT v7 software (Katoh and Standley, 2013). Informative sites and variable sites in the whole chloroplast genome, IRs, LSC, and SSC regions were counted by MEGA V7.0 for the comparison and alignment of sequence matrices (Sudhir et al., 2016). The nucleotide diversity, number of haplotypes, and haplotype diversity of the sequences were calculated using DnaSP V6 (Rozas et al., 2017). The orientation of single base substitutions (SNPs) and insertions/deletions (InDels) in each chloroplast genome is based on RBZ12. InDels were classified as described elsewhere (Dong et al., 2020).

Phylogenetic Analysis

The chloroplast genomes of jujube and sour-jujube were compared to determine their phylogenetic relationships using the maximum likelihood method (ML). The ensuing ML trees were analyzed using RAxML v.8.2 software (Alexandros, 2014) with the evolution model set to "GTR-GAMMA." A heuristic search was used to find the best tree, for which the support rate of each node was determined *via* 500 rounds of fast self-expansion analysis.

Haplotype Network Construction

The haplotypes of the chloroplast genomes were calculated using DnaSP v6 software, and PopART software was used to build the TCS network diagram (Leigh and Bryant, 2015).

Phenotyping

Phenotypic traits of the jujube breeding materials were tested here according to China national industry standard test guide LY/T2190-2013 (Li X. et al., 2013). Their fruit quality indexes were also tested according to the national standard by Pony Testing International Group.[2]

[1] https://www.genecodes.com/

[2] http://zx.ponytest.net.cn/

RESULTS

Chloroplast Genome Size

The chloroplast genome sizes of the 65 jujube materials analyzed in this study are shown in **Supplementary Table 3**. A genome's total sequence length ranged from 161,367 to 161,849 bp. The size of the LSC region was 89,053 to 89,437 bp and that of the SSC region was 19,356 to 19,362 bp, while that of the IR (A/B) regions was 26,478 to 26,533 bp (**Figure 1**). Overall, the GC content of the chloroplast genomic sequences was consistent, at 36.7–36.8%, while that of the LSC, SSC, and IR (A/B) regions respectively were 34.5–34.6, 30.9, and 42.6% (**Supplementary Table 3**). Thus, the sequence lengths of the 65 chloroplast genomes were very similar, and their GC content almost the same. These chloroplast genome sequences have been added to the SRA under accession number (**Supplementary Table 3**).

A total of 130 genes were encoded in the chloroplast genome of jujube, including 112 unique genes. There were 18 genes in the IR region. Among the 112 unique genes, 76 were protein-coding genes, 4 were ribosomal RNA (rRNA) genes, and 30 were transfer RNA (tRNA) genes. Among the annotated genes, 17 contained introns, including 15 with a single intron (nine protein coding genes and six tRNA genes), and two having two introns each (*clpP* and *ycf3*). Among the 18 duplicated genes, there were seven protein-coding genes, seven tRNA genes, and four rRNA genes. The LSC region contained 60 protein-coding genes and 22 tRNA genes, while the SSC region had 12 protein-coding genes and one tRNA gene. Protein-coding genes in the chloroplast genome included nine encoding large ribosomal proteins (*rpl2, 14, 16, 20, 22, 23, 32, 33, 36*); 12 encoding small ribosomal proteins (*rps2, 3, 4, 7, 8, 11, 12, 14, 15, 16, 18, 19*); six encoding photosystem I components (*psaA, B, C, I, J, ycf4*), 15 encoding photosystem II components, and six encoding ATP synthase and electron transport chain components (*atpA, B, E, F, H, I*) (**Table 1**, **Figure 1**). The exons at the 5′ end of rps12 were positioned in the LSC region, and the repeat exons at the 3′ end were located in the IR region. Sequence analyses revealed that 45.66% of the chloroplast genome sequence encoded proteins, with another 1.73 and 5.60% that encoded tRNAs and rRNAs, respectively. The remaining 47.01% of the chloroplast genome consisted of introns, intergenic spacers, and pseudogenes.

Chloroplast Genome Variability Analysis

Chloroplast genome variability was analyzed by detecting SNPs and InDels, which arise *via* translocation, inversion, and tandem duplication.

Number and Pattern of Single Base Substitution Mutations

We distinguished 118 SNPs: 85 in the LSC, 4 in the IRs, and 29 in the SSC (**Supplementary Table 4**). Of all the SNPs, 69 were in intergenic spacer regions, 37 in exon regions, and 12 in intron regions. ycf1 had the highest number of SNPs (7), followed by atpF (5). A total of 45 transitions (Ts) and 73 transversions (Tv) were detected, and their Tv-to-Ts ratio was 1:0.6, which indicating a bias toward transitions. The most frequently occurring SNP mutations were those of C to T and G to A; by contrast, mutations from C to G and from G to C were the least frequent.

Number and Pattern of InDel Mutations

We detected 47 non-repeat InDels, two being in the IRs (*trnR, trnR-rrn5*) and 45 in the LSC (**Supplementary Table 5**). We found 36 gene spacers in one exon (*accD*) and eight introns (*atpF 1, ycf 32, trnL 5*). Most of these non-repeat InDels (85.1%) were 1–24 bp in length. We distinguished 22 repeat InDels, among which two were in the IRs (*ycf2-trnL, trnL-ycf2*) and 20 in the LSC. Nineteen gene spacers were identified in one exon (*trnL-ycf2*) and two introns (*ycf3*). Most of the repeat InDels (81.1%) were 1–17 bp in length. We found 61 SSR InDels: four in the IRs (*rps19-rpl2, rrn5-trnR, rpl2-rps19, trnR-rrn5*), 48 in the LSC, and nine in the SSC. Pattern diagram of SNP and distribution diagram of non-repeat indel and repeat indel were showed (**Supplementary Table 5** and **Figures 2**, **3**).

Phylogenetic and Haplotype Network Construction

Phylogenetic and haplotype network construction methods were used to analyze the origin and evolution of jujube and its sour-jujube. As **Figures 4**, **5** show, and as conveyed in **Supplementary Table 6**, we detected 32 effective haplotypes, consisting of 20 unique jujube haplotypes and 9 unique sour-jujube haplotypes.

DISCUSSION

Chloroplast Genome Variability

Chloroplast genome variability was analyzed by detecting SNPs and InDels, which arise *via* translocation, inversion, and tandem duplication. The nucleotide mutation rate of chloroplast genes is moderate (Dong et al., 2020), and the evolutionary events have been detected in chloroplast genomes (Dong et al., 2013; Choi et al., 2016). Comparative studies on chloroplast genomes have been conducted on multiple focus species (Young et al., 2011), genera (Greiner et al., 2008), and families of plants (Abdullah et al., 2020, 2021; Ahmed et al., 2020; Lee et al., 2021), but, there are relatively few reports about chloroplast genome variability of intraspecific varieties (Daniell et al., 2016; Nock et al., 2019; Park et al., 2020).

In this study, We distinguished 118 SNPs, 47 non-repeat InDels, 22 repeat InDels and 61 SSR InDels among 65 jujube chloroplast genomes. Therefore, the genetic diversity of jujube chloroplast genome is higher compared with other species (Nock et al., 2019), suggesting that chloroplast genome sequences are indeed very well suited for the differentiation of jujube varieties.

Evolutionary Relationship Between Jujube and Sour-Jujube

The chloroplast genome is haploid, non-recombining, and maternally inherited, rendering it an ideal model for evolutionary and comparative genomic research (Birky, 2001; Wu and Ge, 2012). In other research, such analyses have revealed copy number variations and rearrangements that were useful for

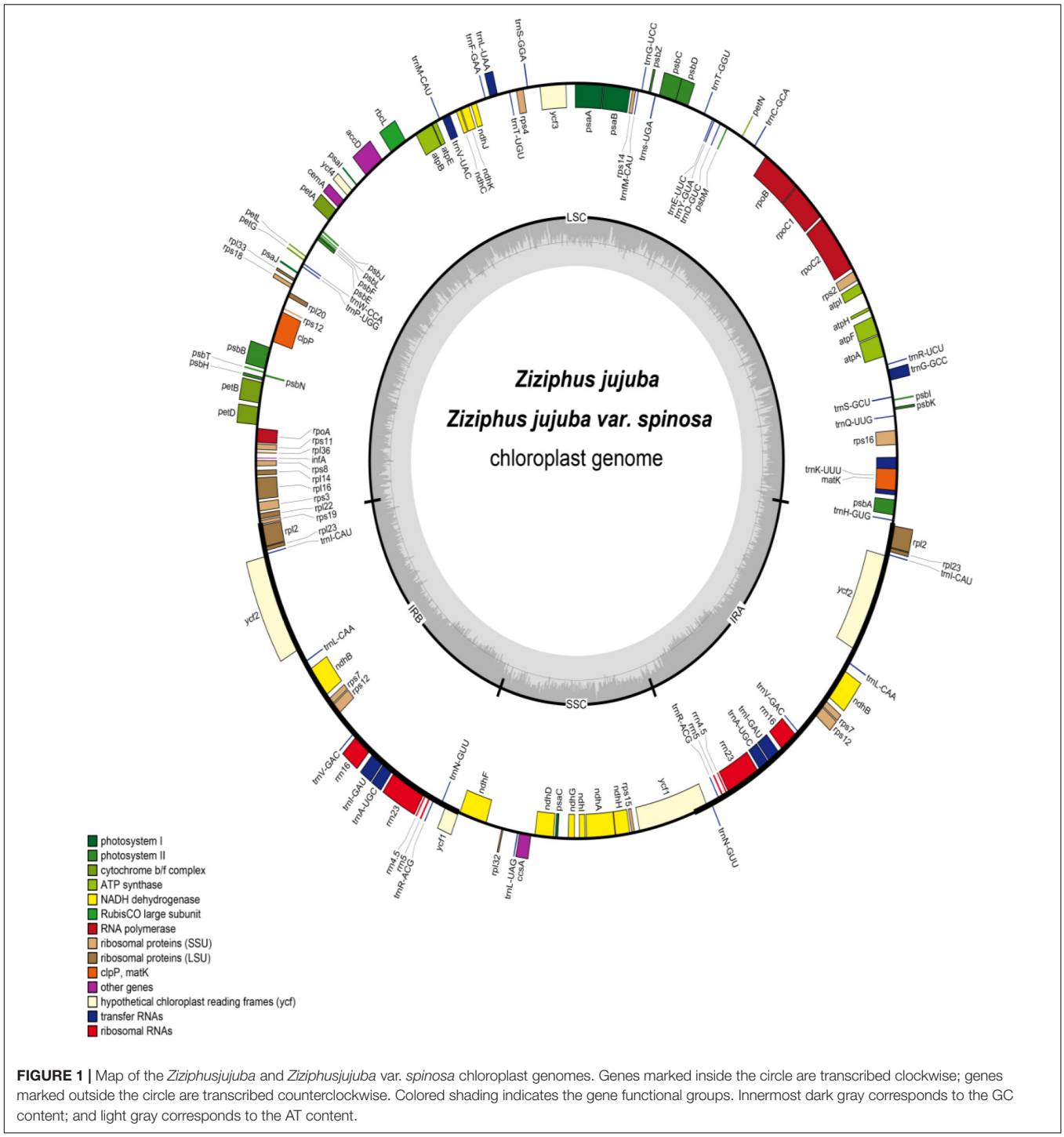


FIGURE 1 | Map of the *Ziziphusjujuba* and *Ziziphusjujuba* var. *spinosa* chloroplast genomes. Genes marked inside the circle are transcribed clockwise; genes marked outside the circle are transcribed counterclockwise. Colored shading indicates the gene functional groups. Innermost dark gray corresponds to the GC content; and light gray corresponds to the AT content.

phylogenetic reconstruction, DNA barcoding (Hollingsworth et al., 2011), and the investigation of geographical origins of some important crops (Delplancke et al., 2013).

Although individual gene segments on the chloroplast genome are already used for species differentiation in barcoding studies on plants, little is known about the usefulness of the entire chloroplast genome for intraspecies differentiation in general and for differentiation between modern varieties in particular. Results from the literature as well as from our own work suggest that chloroplast genome sequences are indeed very well suited for the differentiation of old varieties. On the other hand, they are less or not suitable for the genetic differentiation of modern cultivars, as they are often too closely related (Teske et al., 2020).

1. Because the chloroplast is highly conserved, the rate of mutation and generation of novel haplotypes occurs

TABLE 1 | Genes in the jujube chloroplast genome.

Gene product	Gene product name	Gene name
1	Photosystem I	psaA, B, C, I, J, ycf4
2	Photosystem II	psbA, B, C, D, E, F, H, I, J, K, L, M, N, T, Z
3	Cytochrome b6/f	petA, B[a], D[a], G, L, N
4	ATP synthase	atpA, B, E, F[a], H, I
5	Rubisco	rbcL
6	NADH oxidoreductase	ndhA[a], B[a, c], C, D, E, F, G, H, I, J, K
7	Ribosomal proteins (LSU)	rpl2[a,c,] 14, 16[a], 20, 22, 23[c], 32, 33, 36
8	Ribosomal proteins (SSU)	rps2, 3, 4, 7[c], 8, 11, 12[a,c,d], 14, 15, 16[a], 18, 19[c]
9	RNA polymerase	rpoA, rpoB, rpoC1[a], rpoC2
10	Other proteins	accd, ccsa, cemA, clpP[b], matK
11	Proteins of unknown function	ycf2[c], 3[b], ycf15[c], infA[e], ycf1[e]
12	Ribosomal RNAs	rrn4.5[c], 5[c], 16[c], 23[c]
13	Transfer RNAs	trnH(GUG), K(UUU)[a], Q(UUG), S(GCU), G(UCC)[a], R(UCU), C(GCA), D(GUC), Y(GUA), E(UUC), T(GGU), S(UGA), G(GCC), fM(CAU), S(GGA), T(UGU), L(UAA)[a], F(GAA), V(UAC)[a], M(CAU), W(CCA), P(UGG), I(CAU)[c], L(CAA)[c], V(GAC)[c], I(GAU)[a,c], A(UGC)[a,c,] R(ACG)[c], N(GUU)[c], L(UAG)

[a]*Gene containing a single intron;*
[b]*Gene containing two introns;*
[c]*Two gene copies in the irs;*
[d]*Gene divided into two independent transcription units;*
[e]*Pseudogene.*

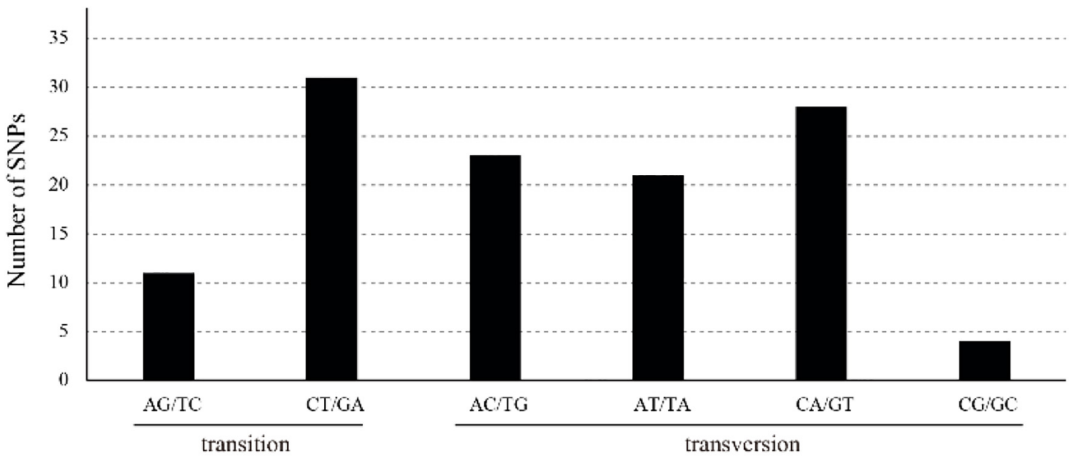


FIGURE 2 | Pattern diagram of single base substitution (SNP) in *Z. jujuba* chloroplast genomes.

over thousands of years, resulting in a lower number of discoverable haplotypes, even over large sample areas (Cruzan and Hendrickson, 2020). In this study, We detected 32 effective haplotypes, resulting in a higher number of discoverable haplotypes, consisting of 20 unique jujube haplotypes and 9 unique sour-jujube haplotypes. Among them, 3 sour-jujube and 20 jujube were haplotype-2, one sour-jujube and one jujube were haplotype-19, 4 sour-jujube and 5 jujube were haplotype-25. Compared with sour-jujube, jujube displayed greater haplotype diversity at the chloroplast DNA level. Haplotype-18 ("Xingtaizao5"), 29 ("Qingjianzao"), and 30 ("Suanzao") are transitional types between jujube and sour-jujube. In this study, the chloroplast genome was used to standardize the phylogenetic position of jujube germplasms (**Figure 5**).

For the phylogenetic analysis of chloroplast genomes, ML and BI methods were implemented; both gave a near identical topological structure, with most nodes in either phylogenetic tree having high bootstrap support values.

2. Our chloroplast haplotype analysis revealed the germplasms of jujube can be clearly divided into two groups (**Figure 4**), sour-jujube (complex A) and jujube group (complex B). Although some varieties were named sour-jujube (suanzao, in Chinese), the maternal source was not sour-jujube and vice versa.

3. The study of human surnames is of great significance (Murci et al., 2001; Cláudia et al., 2021). Human surnames are basically determined by Y chromosome information.

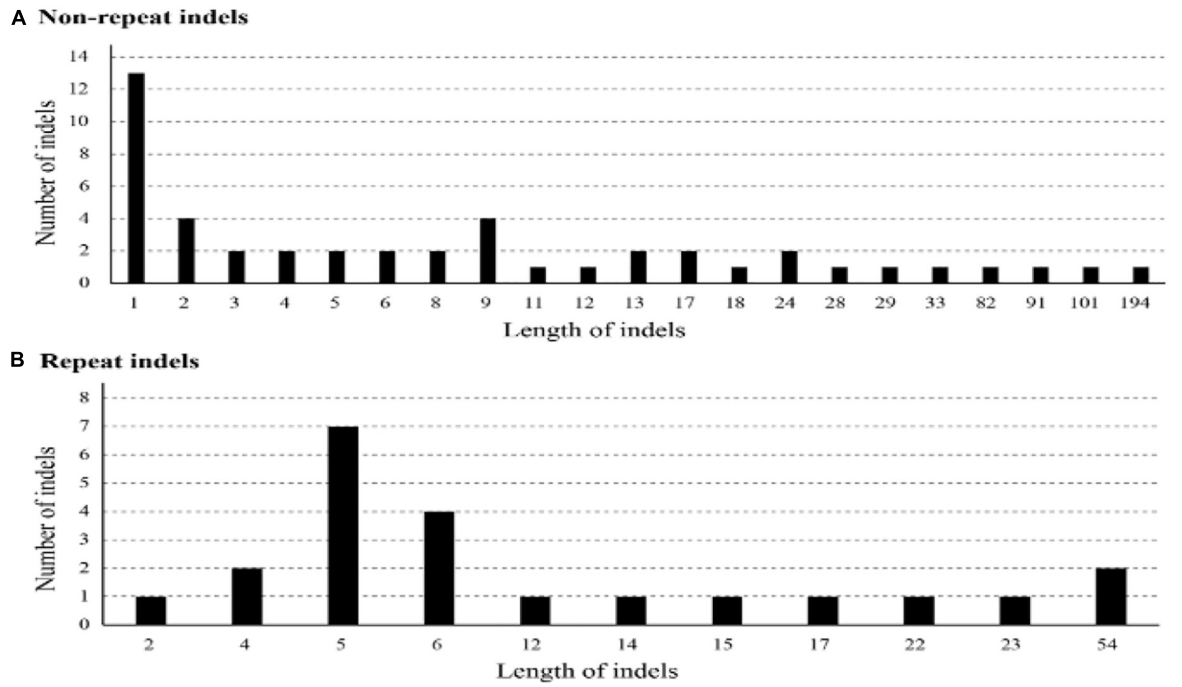


FIGURE 3 | Number of non-repeat InDels **(A)** and repeat InDels **(B)** of each length in *Z. jujuba* chloroplast genome.

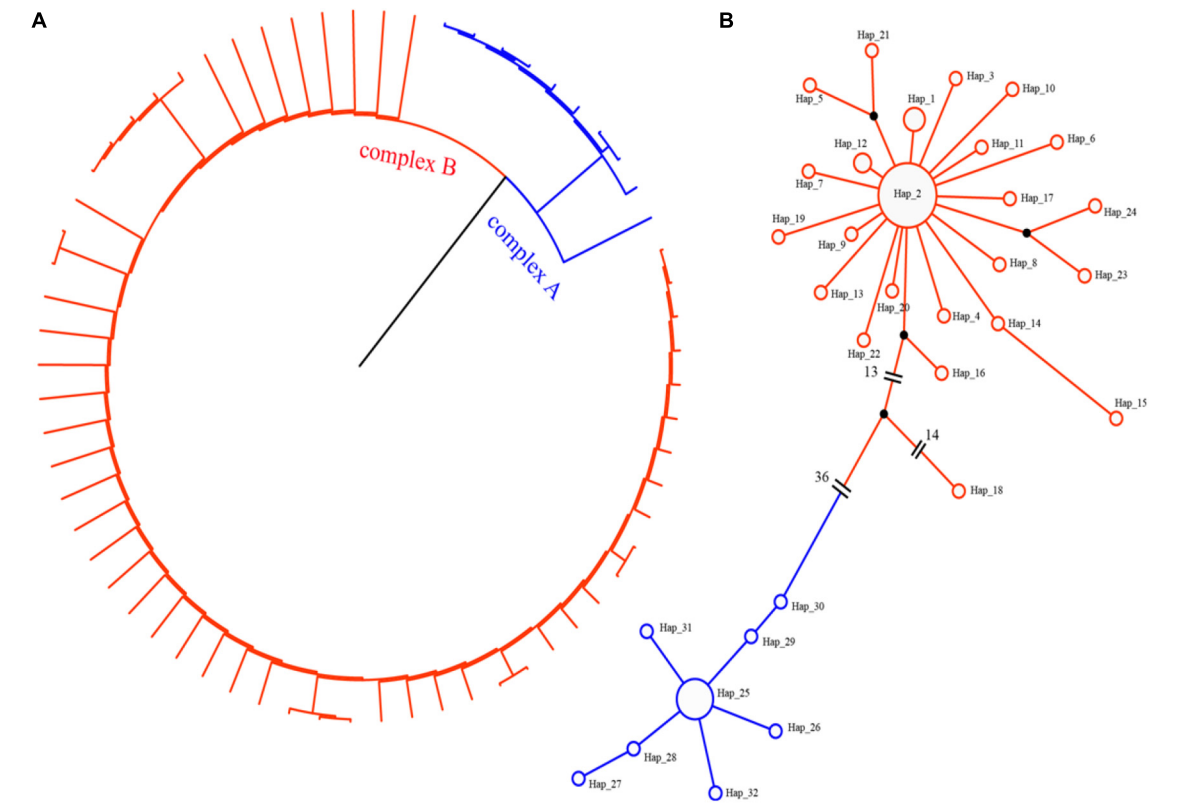


FIGURE 4 | Haplotype network diagram and phylogenetic tree. **(A)** Phylogenetic tree. **(B)** Haplotype network diagram. Circles denote haplotypes. Circle size corresponds to the proportion of a specific haplotype out of 65 samples; red represents the jujube group, while blue represents sour-jujube group.

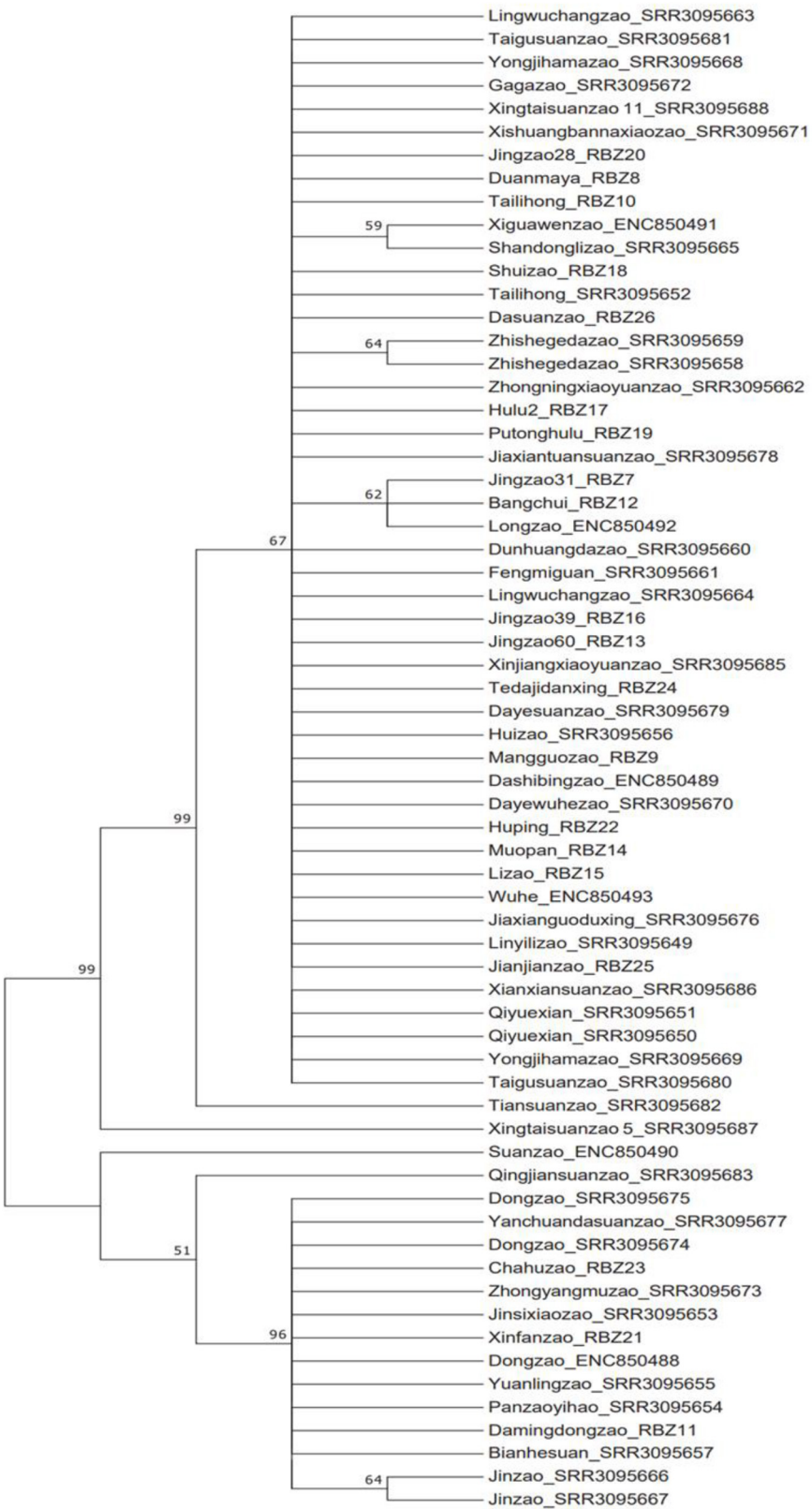


FIGURE 5 | Phylogenetic tree of 65 jujube plastomes based on whole chloroplast genome sequences with maximum likelihood and Bayesian inference. Numbers near the nodes are values for bootstrap support.

Especially, Chinese people have strict paternal surnames, which basically correspond to Y chromosome one by one (Chen et al., 2019; Zeng et al., 2019). Similarly, we used chloroplast genomic study to find the maternal surname for each jujube germplasm.

Hybrid Breeding Strategy and Parents Selection Suggestion

Hybrid breeding is the most effective and conventional method used to breed fruit tree. Through sexual hybridization, separation and recombination of parental genetic material, and innovative genetic variation, hybrid breeding of fruit trees applies knowledge of plant genetic laws to cultivate new varieties with superior or comprehensive sought-after traits of parents. Further, it can use additive and non-additive genetic effects of the parents to maintain the genetic characteristics of hybrid types *via* asexual reproduction.

Advances in plant genome biology have inspired innovative approaches to expedite the progress of assembling desirable phenotypes in crop breeding programs. A set of haplotype-defining markers can provide crop breeders with an increased opportunity to attain optimized genetic combinations for improved plant performance (Bevan et al., 2017). In this respect, useful haplotypes were discovered for future breeding in rice (Abbai et al., 2019) and pigeonpea *Cajanus cajan* (Sinha et al., 2020). There is a need to track the inheritance patterns of haplotypes in crop breeding pedigrees. This is pivotal for assembling new genomic combinations because it helps to identify optimal parents for crosses that contain the desired combinations of traits or features (Varshney et al., 2021). Here, our analysis of chloroplast haplotypes from 65 jujube plastomes indicates that the varieties of jujube can be robustly separated into two groups. The haplotype map (**Figure 4**) provides us with a breeding navigation map which can help us make hybridization strategies according to the distance of kinship. Compared with selecting parents from single subpopulations, selecting parents from these two subpopulations can significantly broaden and augment the genetic diversity of the hybrid offspring.

The variety structure of jujube in China is still dominated by cultivars for making dry fruit products. Yet, cultivars bearing fruit for fresh consumption are gaining more and more recognition in the marketplace because of their rich nutritional components; not surprising, their planting coverage is also expanding rapidly. Fresh-consumption varieties of jujube are mainly late-maturing varieties, such as "Dongzao" and "Lizao," and there is dearth of high-quality, medium and early maturing varieties. "Dongzao," mainly distributed in the provinces of Shandong, Hebei and Shaanxi, is presently the largest fresh-consumption jujube variety in China. But this variety is beset by several limitations, under normal cultivation conditions, the northernmost line of cultivation is in Tianjin and Baoding (Hebei Province). The germination rate of "Dongzao" is low, and so is its fruit-setting rate is also low, though this can be increased by spraying the plants with gibberellin. The fruit-setting rate is low in the north, and the risk of frost is greater north of Beijing (Wang et al., 2012; Shi et al., 2020). Jingzao series varieties are bred by Institute of Forestry and Pomology, Beijing Academy of Agriculture and Forestry Sciences, and are deemed suitable for planting in northern China and western China, having the advantages of producing large-sized fruit, in high yields, at early maturity (Qinghua et al., 2011). According to the haplotype map (**Figure 4**) and mounting demand for jujube's fresh fruits for eating and their breeding in northern China, we propose the following hybrid design.

Hybrid design (Phenotypic traits and the fruit quality indexes of breeding materials were obtained according to China's national standard).

1. "Dongzao" × "Jingzao39"(reciprocal cross)

   "Dongzao" Jujube features: The fruit is round, medium or large, normal fruit weight < 20 g, pulp is sweet, crisp, and good tasting; low natural fruit-setting rate and low fruit cracking rate; fruit matures in early and middle October. Each fruit has a total soluble sugar content of 22.2%, soluble solid content of 34.1%, titratable acid content of 0.43%, and vitamin C content of 352 mg/100 g.

   "Jingzao39" features: Fruit is egg-shaped; normal fruit weight > 25 g, sour and sweet pulp, crisp, and good tasting, high natural fruit-setting rate, high fruit-cracking rate, fruit matures in mid and late September. Its total soluble sugar content is 21.7%, soluble solid content is 25.4%, titratable acid content is 0.36%, and the vitamin C content is 253 mg/100 g.

   Hope to obtain: high natural fruit-setting rate, larger fruit than "Dongzao," sour and sweet taste (i.e., sweeter than "Jingzao39"), low or non-cracking fruit rate, maturation at the end of September and in early October, and stronger resistance to diseases and insects.

2. "Dongzao" × "Jingzao60" (reciprocal cross)

   "Jingzao60" features: Egg shape, fruit size > 25 g, slightly smaller than Beijing jujube 39. The pulp tastes sour and sweet, crisp, good taste, high natural fruit setting rate, fruit cracking rate is lower than "Jingzao39," mature in mid and late September. The total soluble sugar content was 18.6%, the soluble solid content was 26.1%, the titratable acid content was 0.56%, and vitamin C content is 324 mg/100 g.

   Hope to obtain: high natural fruit-setting rate, larger fruit than "Dongzao," sour and sweet taste (i.e., sweeter than"Jingzao60"), low or non-cracking fruit rate, maturation in the end of September and in early October, and stronger resistance to disease and insect.

3. "Dongzao" × "Jingzao28"(reciprocal cross)

   "Jingzao28" features: Fuit has an apple-like shape, with a size > 25 g; sour and sweet pulp, crisp, good tasting, high natural fruit-setting rate and high fruit-cracking rate, but both lower than "Jingzao39," matures in mid and late September. Its total soluble sugar content is 21.6%, soluble solid content is 28.4%, titratable acid content is 0.41%, and vitamin C content is 275 mg/100 g.

   Hope to obtain: high natural fruit-setting rate, larger fruit size than "Dongzao," sour and sweet taste (i.e., sweeter than "Jingzao28"), low or non-cracking fruit rate, maturation at the end of September and in early October, and stronger resistance to disease and insect.

From a genomic point of view, the maternal lines of "Jingzao39," "Jingzao60,"and "Jingzao28" were all derived from jujube group. Furthermore, "Jingzao39," "Jingzao60," and "Jingzao28" all had the same haplotype-2, which was the largest haplotype we identified. The "Dongzao" maternal line from sour-jujube group, has haplotype-25, this being the largest sour-jujube haplotype. Hybridization of sour-jujube and jujube is beneficial to inheriting the complementary advantages the parents offer for breeding commercial jujube.

CONCLUSION

In this paper, we reported on 65 chloroplast genomes of jujube, including 26 chloroplast genomes sequenced in this study, and compared with other reported materials. The 65 jujube chloroplast genomes' structure and gene content are similar, and highly conserved. In addition, variability of chloroplast genome (SNPs and InDels) was also analyzed. A haplotype network diagram was constructed; and a phylogenetic analysis was carried out.

Genetic relationships among jujube germplasms was revealed, which provides a timely basis for the selection of excellent cultivars. Three hybrid combinations were selected for reciprocal crosses: "Dongzao" × "Jingzao39," "Dongzao" × "Jingzao60," "Dongzao" × "Jingzao28." The chloroplast genome results also verified the rationality of hybrid combinations. Overall, this study provides chloroplast genome sequences for further research on the identification and phylogeny of *Ziziphus jujuba*, and should help to enhance our overall understanding of the domestication history of *Z. jujuba* varieties.

DATA AVAILABILITY STATEMENT

The datasets presented in this study can be found in online repositories. The names of the repository/repositories and accession number(s) can be found in the article/ **Supplementary Material**.

AUTHOR CONTRIBUTIONS

GH conducted the experiments, analyzed the data, and prepared the manuscript. YW analyzed the data. CG, DL, ND, BC, YQ, YZ, and QP performed the collection and processing of samples and analyzed the data. YZ and QP coordinated the experiments. All authors have read and agreed to the final version of the manuscript.

FUNDING

This work was financially supported by the Special Fund for the Construction of Scientific and Technological Innovation Capability (Grant Nos. KJCX20220101 and KJCX20210114), the Key Research and Design Program of Hebei Province (Grant No. 20326807D), and the Presidential Foundation of Institute of Forestry and Pomology (Grant No. LGY202003).

SUPPLEMENTARY MATERIAL

The Supplementary Material for this article can be found online at: https://www.frontiersin.org/articles/10.3389/fpls.2022.841767/full#supplementary-material

REFERENCES

Abbai, R., Singh, V. K., Nachimuthu, V. V., Sinha, P., Selvaraj, R., Vipparla, A. K., et al. (2019). Haplotype analysis of key genes governing grain yield and quality traits across 3K RG panel reveals scope for the development of tailor-made rice with enhanced genetic gains. *Plant Biotechnol. J.* 17, 1612–1622. doi: 10.1111/pbi.13087

Abdullah, Mehmood, F., Shahzadi, I., Ali, Z., Islam, M., Naeem, M., et al. (2021). Correlations among oligonucleotide repeats, nucleotide substitutions, and insertion-deletion mutations in chloroplast genomes of plant family Malvaceae. *J. Syst. Evol.* 59, 388–402.

Abdullah, Mehmood, F., Shahzadi, I., Waseem, S., Mirza, B., Ahmed, I., et al. (2020). Chloroplast genome of Hibiscus rosa-sinensis (Malvaceae): comparative analyses and identification of mutational hotspots. *Genomics* 112, 581–591. doi: 10.1016/j.ygeno.2019.04.010

Ahmed, I., Lockhart, P. J., Agoo, E. M. G., Naing, K. W., Nguyen, D. V., Medhi, D. K., et al. (2020). Evolutionary origins of taro (*Colocasia esculenta*) in Southeast Asia. *Ecol. Evol.* 10, 13530–13543. doi: 10.1002/ece3.6958

Alexandros, S. (2014). RAxML version 8: a tool for phylogenetic analysis and post-analysis of large phylogenies. *Bioinformatics* 30, 1312–1313. doi: 10.1093/bioinformatics/btu033

Altschul, S. F., Madden, T. L., Schffer, A. A., Zhang, J., Zhang, Z., Webb, M., et al. (1997). Gapped BLAST and PSI-BLAST: a new generation of protein database search programs. *Nucleic Acids Res.* 25:3389. doi: 10.1093/nar/25.17.3389

Bankevich, A., Nurk, S., Antipov, D., Gurevich, A. A., Dvorkin, M., Kulikov, A. S., et al. (2012). SPAdes: a new genome assembly algorithm and its applications to single-cell sequencing. *J. Comput. Biol.* 19, 455–477. doi: 10.1089/cmb.2012.0021

Bevan, M. W., Uauy, C., Wulff, B. B. H., Zhou, J., Krasileva, K., and Clark, M. D. (2017). Genomic innovation for crop improvement. *Nature* 543, 346–354. doi: 10.1038/nature22011

Birky, C. W. (2001). The inheritance of genes in mitochondria and chloroplasts: laws. *Mech. Models Annu. Rev. Genet.* 35, 125–148. doi: 10.1146/annurev.genet.35.102401.090231

Bolger, A. M., Lohse, M., and Usadel, B. (2014). Trimmomatic: a flexible trimmer for Illumina sequence data. *Bioinformatics* 30, 2114–2120. doi: 10.1093/bioinformatics/btu170

Chang, J. (2018). *aStudies on Genetic Diversity of Ziziphus Acidojujuba Germplasm Resources in Chaoyang Region of Western Liaoning*. [master's thesis]. Shenyang: Shenyang Agricultural University.

Chen, J., Chen, L., Liu, Y., Li, X., Yuan, Y., and Wang, Y. (2019). An index of Chinese surname distribution and its implications for population dynamics. *Am. J. Phys. Anthropol.* 169, 608–618. doi: 10.1002/ajpa.23863

Choi, K. S., Chung, M. G., and Park, S. (2016). The complete chloroplast genome sequences of three Veroniceae species (Plantaginaceae): comparative analysis and highly divergent regions. *Front. Plant Sci.* 7:355. doi: 10.3389/fpls.2016.00355

Cláudia, G., Sara, P., María, L. A., and Eduardo, A. (2021). Genealogy: the tree where history meets genetics. *Genealogy* 5:98.

Cruzan, M. B., and Hendrickson, E. C. (2020). Landscape genetics of plants: challenges and opportunities. *Plant Commun.* 1:100100. doi: 10.1016/j.xplc.2020.100100

Daniell, H., Lee, S. B., Grevich, J., Saski, C., Quesada-Vargas, T., Guda, C., et al. (2006). Complete chloroplast genome sequences of *Solanum bulbocastanum*, *Solanum lycopersicum* and comparative analyses with other *Solanaceae genomes*. *Theor. Appl. Genet.* 112, 1503–1518. doi: 10.1007/s00122-006-0254-x

Daniell, H., Lin, C.-S., Yu, M., and Chang, W.-J. (2016). Chloroplast genomes: diversity, evolution, and applications in genetic engineering. *Genome Biol.* 17:134. doi: 10.1186/s13059-016-1004-2

Delplancke, M., Alvarez, N., Benoit, L., Espindola, A., Joly, H. I., Neuenschwander, S., et al. (2013). Evolutionary history of almond tree domestication in the Mediterranean basin. *Mol. Ecol.* 22, 1092–1104. doi: 10.1111/mec.12129

Dong, W., Xu, C., Wen, J., and Zhou, S. (2020). Evolutionary directions of single nucleotide substitutions and structural mutations in the chloroplast genomes of the family Calycanthaceae. *BMC Evol. Biol.* 20:96. doi: 10.1186/s12862-020-01661-0

Dong, W. P., Xu, C., Cheng, T., Lin, K., and Zhou, S. L. (2013). Sequencing angiosperm plastid genomes made easy: a complete set of universal primers and a case study on the phylogeny of saxifragales. *Genome Biol. Evol.* 5, 989–997. doi: 10.1093/gbe/evt063

Greiner, S., Wang, X., Herrmann, R. G., Rauwolf, U., Mayer, K., Haberer, G., et al. (2008). The complete nucleotide sequences of the 5 genetically distinct plastid genomes of *Oenothera*, subsection *Oenothera*: II. A microevolutionary view using bioinformatics and formal genetic data. *Mol. Biol. Evol.* 25, 2019–2030. doi: 10.1093/molbev/msn149

Guo, S., Duan, J., Tang, Y., Qian, Y., Zhao, J., Qian, D., et al. (2011). Simultaneous qualitative and quantitative analysis of triterpenic acids, saponins and flavonoids in the leaves of two *Ziziphus* species by HPLC–PDA–MS/ELSD. *J. Pharm. Biomed. Analysis* 56, 264–270. doi: 10.1016/j.jpba.2011.05.025

Hollingsworth, P. M., Graham, S. W., and Little, D. P. (2011). Choosing and using a plant DNA barcode. *PLoS One* 6:e19254. doi: 10.1371/journal.pone.0019254

Huang, D. I., and Cronk, Q. C. (2015). Plann: a command-line application for annotating plastome sequences. *Appl. Plant Sci.* 3:1500026. doi: 10.3732/apps.1500026

Huang, J., Zhang, C. M., Zhao, X., Fei, Z. J., Wan, K. K., Zhang, Z., et al. (2016). The jujube genome provides insights into genome evolution and the domestication of sweetness/acidity taste in fruit trees. *PLoS Genet.* 12:e1006433. doi: 10.1371/journal.pgen.1006433

Katoh, K., and Standley, D. M. (2013). MAFFT multiple sequence alignment software version 7: improvements in performance and usability. *Mol. Biol. Evol.* 30, 772–780. doi: 10.1093/molbev/mst010

Lee, C., Choi, I.-S., Cardoso, D., de Lima, H. C., de Queiroz, L. P., Wojciechowski, M. F., et al. (2021). The chicken or the egg? Plastome evolution and an independent loss of the inverted repeat in papilionoid legumes. *Plant J.* 107, 861–875. doi: 10.1111/tpj.15351

Leigh, J. W., and Bryant, D. (2015). Popart : full-feature software for haplotype network construction. *Methods Ecol. Evol.* 6, 1110–1116. doi: 10.1111/2041-210x.12410

Li, B., and Wei, T. (2013). Advances in jujube breeding technology. *Ningxia Acad. Agric. For. Sci.* 54, 27–53.

Li, J., Wang, S., Yu, J., Wang, L., and Zhao, S. (2013). A modified CTAB protocol for plant DNA extraction. *Chinese Bull. Bot.* 48, 72–78. doi: 10.3724/sp.j.1259.2013.00072

Li, S., Guo, M., Fu, P., Liu, H., and Zhao, X. (2018). Genetic diversity and population structure of Chinese jujube (*Ziziphus jujuba* Mill.) and sour jujube (*Ziziphus acidojujuba* Mill.) using inter-simple sequence repeat (ISSR) markers. *Mol. Plant Breed.* 6:e27088v1.

Li, X., Huang, J., Gao, W., Wang, C., and Zhao, S. (2013). *Test Guideline for Distinctness, Uniformity and Stability-Chinese jujube(Zizyphus jujuba Mill.)*. LY/T 2190-2013. Xianyang: Northwest A & F University.

Li, X., Li, Y., Zhang, Z., and Li, X. (2015). Influences of environmental factors on leaf morphology of Chinese jujubes. *PLoS One* 10:e0127825. doi: 10.1371/journal.pone.0127825

Liu, M., Wang, J., Wang, L., Liu, P., Zhao, J., Zhao, Z., et al. (2020). The historical and current research progress on jujube-a superfruit for the future. *Hortic. Res.* 7:119. doi: 10.1038/s41438-020-00346-5

Liu, M., Zhao, J., Cai, Q., Liu, G., Wang, J., Zhao, Z., et al. (2014). The complex jujube genome provides insights into fruit tree biology. *Nat. Commun.* 5:5315. doi: 10.1038/ncomms6315

Liu, P., Wang, J. R., Liu, M. J., Zhao, Z. H., and Liu, Z. G. (2020). Advances and achievements on Chinese jujube breeding in China. *Acta Hortic.* 1287, 219–229.

Murci, L. S. Q., Krausz, C., and McElreavey, K. (2001). The human Y chromosome: function, evolution and disease. *For. Sci. Int.* 118, 169–181. doi: 10.1016/s0379-0738(01)00387-5

Nock, C. J., Hardner, C. M., Montenegro, J. D., Termizi, A. A. A., Hayashi, S., Playford, J., et al. (2019). Wild origins of macadamia domestication identified through intraspecific chloroplast genome sequencing. *Front. Plant Sci.* 10:334. doi: 10.3389/fpls.2019.00334

Park, J., Xi, H., and Kim, Y. (2020). The complete chloroplast genome of *Arabidopsis thaliana* isolated in Korea (Brassicaceae): an investigation of intraspecific variations of the chloroplast genome of korean *A. thaliana*. *Int. J. Genomics* 2020:3236461. doi: 10.1155/2020/3236461

Prabhudas, S. K., Prayaga, S., Madasamy, P., and Natarajan, P. (2016). Shallow whole genome sequencing for the assembly of complete chloroplast genome sequence of *Arachis hypogaea* L. *Front. Plant Sci.* 7:1106. doi: 10.3389/fpls.2016.01106

Qinghua, P., YuPing, Z., Jin, B., Wanmei, J., and Shaoning, L. (2011). A new fresh consuming jujube cultivar 'Jingzao60'. *Acta Hortic. Sin.* 38, 2227–2228.

Qu, Z., and Wang, Y. (2013). *Chinese Fruit Trees Record–Chinese jujube*. Beijing: China Forestry Publishing House.

Rashwan, A. K., Karim, N., Shishir, M. R. I., Bao, T., Lu, Y., and Chen, W. (2020). Jujube fruit: a potential nutritious fruit for the development of functional food products. *J. Funct. Foods* 75:104205. doi: 10.1016/j.jff.2020.104205

Raubeson, L., and Jansen, R. (2005). "Chloroplast genomes of plants," in *Plant Diversity and Evolution: Genotypic and Phenotypic Variation in Higher Plants*, ed. R. J. Henry (Wallingford: CABI).

Rozas, J., Ferrer-Mata, A., Sanchez-DelBarrio, J. C., Guirao-Rico, S., Librado, P., Ramos-Onsins, S. E., et al. (2017). DnaSP 6: DNA sequence polymorphism analysis of large data sets. *Mol. Biol. Evol.* 34, 3299–3302. doi: 10.1093/molbev/msx248

Sabri, S. M., Takruri, H. R., and Al Ismail, K. M. (2021). Nutrient composition, antioxidant activities and anti-inflammatory effect of Jujube fruit: a general review. *J. Pharm. Nutr. Sci.* 11, 164–174.

Shan, S. H., Xie, Y., Zhao, H. L., Niu, J. P., Zhang, S., Zhang, X. L., et al. (2019). Bound polyphenol extracted from jujube pulp triggers mitochondria-mediated apoptosis and cell cycle arrest of HepG2 cell *in vitro* and *in vivo*. *J. Funct. Foods* 53, 187–196.

Shen, H. (2016). *Genetic Diversity of Chinese Jujube Based on Nuclear SSR and Chloroplast SSR Markers*. [master's thesis]. Xianyang: Northwest A&F University.

Shen, J., Sun, Z., Hou, S., Liu, R., Wang, Y., and Guo, P. (2020). Assessment of genetic diversity in *Ziziphus jujube* Mill. Cultivars derived from northern China using inter-simple sequence repeat markers. *Crop Sci.* 60, 320–329. doi: 10.1002/csc2.20080

Shi, W., Zhao, Y., Ma, L., and Hao, B. (2020). Effect of fruit cracking on good fruit rate of Linyi winter jujube. *J. Fruit Tree Resour.* 1, 19–22.

Sinha, P., Singh, V. K., Saxena, R. K., Khan, A. W., Abbai, R., Chitikineni, A., et al. (2020). Superior haplotypes for haplotype-based breeding for drought tolerance in pigeonpea (*Cajanus cajan* L.). *Plant Biotechnol. J.* 18, 2482–2490. doi: 10.1111/pbi.13422

Song, L., Cao, B., Zhang, Y., Meinhardt, W. L., and Zhang, D. (2021). Mining single nucleotide polymorphism (SNP) markers for accurate genotype identification and diversity analysis of chinese jujube (*Ziziphus jujuba* Mill.) Germplasm. *Agronomy* 11, 2303–2303. doi: 10.3390/agronomy11112303

Sudhir, K., Glen, S., and Koichiro, T. (2016). MEGA7: molecular evolutionary genetics analysis version 7.0 for bigger datasets. *Mol. Biol. Evol.* 33, 1870–1874. doi: 10.1093/molbev/msw054

Teske, D., Peters, A., Moellers, A., and Fischer, M. (2020). Genomic profiling: the strengths and limitations of chloroplast genome-based plant variety authentication. *J. Agric. Food Chem.* 68, 14323–14333. doi: 10.1021/acs.jafc.0c03001

Varshney, R. K., Bohra, A., Yu, J., Graner, A., Zhang, Q., and Sorrells, M. E. (2021). Designing future crops: genomics-assisted breeding comes of age. *Trends Plant Sci.* 26, 631–649. doi: 10.1016/j.tplants.2021.03.010

Wang, D., Xiong, R., Wu, C., and Gao, J. (2016). Jujube breeding research. *J. Tarim Univ.* 28, 109–118.

Wang, J., Ge, W., and Ma, L. (2012). Analysis on restricting factors of date industry development in North China. *Anhui Agric. Sci.* 40, 2411–2413. doi: 10.1002/14651858.CD011160.pub2

Wang, L., Luo, Z., Liu, Z., Zhao, J., Deng, W., Wei, H., et al. (2019). Genome size variation within species of chinese jujube (*Ziziphus jujuba* Mill.) and its wild ancestor sour jujube (*Z. acidojujuba* Cheng et Liu). *Forests* 10:460.

Wu, Z., and Ge, S. (2012). The phylogeny of the BEP clade in grasses revisited: evidence from the whole-genome sequences of chloroplasts. *Mol. Phylogenet. Evol.* 62, 573–578. doi: 10.1016/j.ympev.2011.10.019

Yang, X. (2014). *Development of Chloroplast SSR Markers and Studies on Genetic Diversity of Ziziphus Jujube*. [master's thesis]. Xianyang: Northwest A&F University.

Young, H. A., Lanzatella, C. L., Sarath, G., and Tobias, C. M. (2011). Chloroplast genome variation in upland and lowland switchgrass. *PLoS One* 6:e23980. doi: 10.1371/journal.pone.0023980

Zeng, Z., Tian, J., Jiang, C., Ye, W., Liu, K., and Li, Y. (2019). Inferring the history of surname Ye based on Y chromosome high-resolution genotyping and sequencing data. *J. Hum. Genet.* 64, 703–709.

Zhang, C., Yin, X., Li, X., Huang, J., Wang, C., and Lian, C. (2013). Genetic diveersity of sour jujube along the Yellow Rive. *J. Northwest A F Univ.* 41, 107–119.

Conflict of Interest: The authors declare that the research was conducted in the absence of any commercial or financial relationships that could be construed as a potential conflict of interest.

Publisher's Note: All claims expressed in this article are solely those of the authors and do not necessarily represent those of their affiliated organizations, or those of the publisher, the editors and the reviewers. Any product that may be evaluated in this article, or claim that may be made by its manufacturer, is not guaranteed or endorsed by the publisher.

Copyright © 2022 Hu, Wu, Guo, Lu, Dong, Chen, Qiao, Zhang and Pan. This is an open-access article distributed under the terms of the Creative Commons Attribution License (CC BY). The use, distribution or reproduction in other forums is permitted, provided the original author(s) and the copyright owner(s) are credited and that the original publication in this journal is cited, in accordance with accepted academic practice. No use, distribution or reproduction is permitted which does not comply with these terms.

frontiers in Plant Science

ORIGINAL RESEARCH
published: 10 March 2022
doi: 10.3389/fpls.2022.779623

Salt Stress Alleviation in *Triticum aestivum* Through Primary and Secondary Metabolites Modulation by *Aspergillus terreus* BTK-1

Muhammad Ikram Khan[1], Niaz Ali[1], Gul Jan[2], Muhammad Hamayun[2], Farzana Gul Jan[2], Amjad Iqbal[3], Anwar Hussain[2] and In-Jung Lee[4]**

[1] Department of Botany, Hazara University, Mansehra, Pakistan, [2] Department of Botany, Abdul Wali Khan University, Mardan, Pakistan, [3] Department of Food Science & Technology, Abdul Wali Khan University, Mardan, Pakistan, [4] School of Applied Biosciences, Kyungpook National University, Daegu, South Korea

OPEN ACCESS

Edited by:
Peng Zhang, Center for Excellence in Molecular Plant Sciences (CAS), China

Reviewed by:
Oksana Sytar, Taras Shevchenko National University of Kyiv, Ukraine
Dilfuza Egamberdieva, Leibniz Centre for Agricultural Landscape Research (ZALF), Germany

***Correspondence:**
In-Jung Lee
ijlee@knu.ac.kr
Amjad Iqbal
amjadiqbal@awkum.edu.pk

Specialty section:
This article was submitted to Plant Biotechnology, a section of the journal Frontiers in Plant Science

Received: *19 September 2021*
Accepted: *17 January 2022*
Published: *10 March 2022*

Citation:
Khan MI, Ali N, Jan G, Hamayun M, Jan FG, Iqbal A, Hussain A and Lee I-J (2022) Salt Stress Alleviation in Triticum aestivum Through Primary and Secondary Metabolites Modulation by Aspergillus terreus BTK-1. Front. Plant Sci. 13:779623. doi: 10.3389/fpls.2022.779623

We report the growth promoting potential in wheat under saline conditions by an endophytic fungus *Aspergillus terreus* BTK-1. The isolated BTK-1 from the root of *Chenopodium album* was identified as *Aspergillus terreus* through 18S rDNA sequence analysis. BTK-1 secreted indole acetic acid (IAA), exhibited 1- aminocyclopropane-1-carboxylate deaminase (ACC) and siderophores activity, and solubilized phosphate. Wheat seedlings were exposed to a saline environment (0, 60, 120, and 180 mM) with or without BKT-1 inoculation. Seedlings inoculated with BTK-1 showed higher concentrations of IAA and gibberellins, whereas they showed low concentrations of abscisic acid compared to the BTK-1 non-inoculated plants. Also, BTK-1 inoculated wheat plants revealed significantly (P = 0.05) longer shoots and roots, biomass, and chlorophyll contents. On the contrary, plants without BTK-1 inoculation indicated significantly (P = 0.05) low amounts of carbohydrates, phenolics, prolines, potassium, magnesium, and calcium, with high amounts of Na and malonaldehyde under salt stress. Likewise, BTK-1 inoculated wheat plants showed high activity of reduced glutathione, and low activity of ascorbate, catalase, and peroxidase under salt stress. The mitigation of salinity stress by BTK-1 inoculated wheat plants suggested its use as a bio-stimulator in salt affected soils.

Keywords: endophytes, *Aspergillus terreus* BTK-1, phytohormones, salt stress, molecular identification

INTRODUCTION

Environmental stresses are among the most limiting factors globally for agricultural productivity and threat for crop yield (Muhammad et al., 2018, 2019; Ismail et al., 2021). Saline soils are one of the major issues to achieve sustainable agriculture. The effect of salinity is more severe in arid and semiarid regions owing to low rainfall, temperature, water quality, high evapotranspiration, and poor soil management practices (Shrivastava and Kumar, 2015). Soil salinity is known to inhibit plant growth (Hamayun et al., 2015, 2017). In the current scenario, scientists around the planet are working on cheap and quick methods to enhance agricultural productivity and sustainability (Mbarki et al., 2018; Moghimi et al., 2018; Del Buono, 2021). In this regard, the use of beneficial microbial symbionts is an alternative way to improve agricultural

productivity and sustainability under salt stress (Khushdil et al., 2019; Nusrat et al., 2019).

Plant–microbe interactions are thought to be a viable way to improve agricultural productivity and functioning of successful agricultural system. Plants contain a relatively diverse population of endophytes, which spend time in host tissues without producing disease (Bibi et al., 2018; Bilal et al., 2018; Ali et al., 2019). Such plant growth promoting (PGP) microbes are attaining great focus among plant biologists (Gul Jan et al., 2019; Jan et al., 2019; Kang et al., 2019; Qadir et al., 2020; Raid et al., 2021). Endophytic fungi, in fact, secured remarkable interest in the scientific community due to its symbiotic alliance with crop species (Ismail et al., 2018, 2019, 2020a,b,c, 2021). Endophytes help in plant fitness through fair distribution of growth-promoting hormones and nutrients, bring physical change in soil, and help in combating environmental stresses (Mehmood et al., 2019a,b). They produce an array of bioactive compounds that can be termed as plant growth-promoters (Kang et al., 2019). They have the ability to fetch nutrients, such as sulfur, potassium, calcium, phosphorus, and magnesium, from the soil to support host plant growth (Bilal et al., 2018; Kang et al., 2019). Endophytes produce siderophores and exhibit 1-aminocyclopropane- 1-carboxylate deaminase activity to scavenge ferric iron, fix nitrogen, and solubilize inorganic phosphate (Muhammad et al., 2018, 2019). Phytohormones produced by endophytes (for example auxins) can greatly influence metabolism, reproduction, and overall growth and help the host plant species exposed to various environmental stresses (Hamayun et al., 2017; Ismail et al., 2021; Raid et al., 2021). Certainly, it would not be an exaggeration to say that the endophytic association could recover plant health under biotic and abiotic stresses (Hamayun et al., 2017; Afridi et al., 2019; Muhammad et al., 2019; Ismail et al., 2021). Globally, wheat is considered as one of the most important cash crops. The non-uniform and rigorous use of chemical fertilizers to achieve high yields may lead to inconsistent supply of nutrients and low soil fertility. The raise in food demand at a steady rate requires a cheap and rigorous method to achieve high yields. Therefore, the current study was designed to evaluate the phytostimulatory characteristics and salt stress tolerance of a novel endophytic fungal isolate BTK-1 of *A. terreus*.

MATERIALS AND METHODS

Study Area

Soil and plant samples were collected from the Kohat district that occupies the central part of Khyber Pakhtunkhwa (KPK). The Kohat district lies between 982429 m north latitude and 1057680 m east longitude.

Soil Analysis

Soil samples were collected from the sampling sites (0–15 cm depth) with the help of a stainless-steel auger. The soil samples were dried in shade and then crushed, followed by sieving through 2 mm sieve. The resultant samples were stored in plastic bags till further physicochemical analysis. Textural classes were determined by the Bouyoucos method according to the USDA textural triangle (Bouyoucos, 1936). The electrical conductivity (EC) of the soil was determined at 25°C using an electrical conductivity meter (HM EC-3M). Soil pH was determined by using a Jenway pH meter (Model-3510). Lime contents of the soil were determined by EDTA titration method. The sodium concentration was extracted with 1 M ammonium acetate (NH_4OAc) solution and estimated by a flame photometer (Jenway, PFP7/C) as described by Heald (1965).

Plant Material and Isolation of Endophytic Fungi

Chenopodium album L. were collected from saline area of Kohat District Pakistan, and processed within 48 h of collection in the laboratory. Surface sterilization was carried out by the method of Muhammad et al. (2019). The root section of *C. album* was cut and washed in running tap water to remove soil and then soaked for 5 min in distilled water containing 4–5 drops of tween20. The soil-free soaked root samples were cut into pieces (0.5 cm) and surface sterilized by dipping it for 30 s in a solution containing 70% ethanol and 1% perchloric acid. The ethanol and perchloric traces were removed by rinsing the root segments with autoclaved distilled water (ddH_2O). Sterilized root segments (5 segments per plate) were placed on Hagem medium (0.5% glucose, 0.05% KH_2PO_4, 0.05% $MgSO_4{\cdot}7H_2O$, 0.05% NH_4Cl, 0.1% $FeCl_3$, 80 ppm streptomycin, and 1.5% agar; pH 5.6 $\pm$ 0.2) to isolate endophytic fungi. The plates were properly sealed and incubated at 27°C for 7 days. Intact surface sterilized roots were also processed in a similar way as root segments to check for any contamination by exogenous microbes. After 1 week of incubation, fungal hyphae were developed from the root segments. Individual colonies were collected and re-cultured on potato dextrose agar (PDA) media plates (potato infusion: 200 g, dextrose: 20 g, agar: 20 g, distilled water: 1 L). The PDA plates were incubated for a week at 25°C and this step was repeated till individual colonies were obtained. The fungal isolates were then enriched in flasks containing Czapek culture broth (1% peptone, 1% glucose, 0.05% $MgSO_4{\cdot}7H_2O$, 0.05% KCl, 0.001% $FeSO_4{\cdot}7H_2O$; pH 7.3 $\pm$ 0.2). The flasks were incubated in a shaking incubator for 7 days at 120 rpm and 30°C. The culture filtrate (CF) was harvested after centrifugation for 15 min at 4°C and 4,000 $\times$ *g*. The harvested pellets and supernatants were lyophilized (ISE Bondiro Freeze Dryer) at –70°C before further analysis.

Screening of the Isolated Endophytes for Plant Growth Promotion

Indole acetic acid deficient maize mutant was initially used to screen the isolated fungal endophytes for phytostimulation and IAA production. The isolates were cultured in Czapek broth and incubated in shaking incubator for 7 days at 120 rpm and 27°C. Fungal mycelia (pellets) and culture filtrates (supernatant) were separated from each other after centrifugation (10,000 rpm) of the Czapek broth for 15 min at 4°C. The pellets (fungal biomass) were lyophilized and kept for the identification of potent fungal isolate(s), while the supernatants were used in

maize growth promotion assays. IAA deficient maize seeds were surface sterilized as mentioned earlier and allowed to germinate in Petri plates containing moistened filter paper. The uniformly germinated seedlings were picked and grown in 0.8% water-agar medium under axenic conditions in growth chamber (photoperiod of 14 h light and 10 h dark; light intensity 1000 $\mu mm^{-2}s^{-2}$ Natrium lamps and relative humidity 60–70%). The fungal supernatant (10 mL) was sprayed at two-leaf stage on the apices of seedlings. Seedlings treated with distilled water were used as negative control. The seedlings from each treatment were harvested after 1-week of fungal supernatant application and evaluated for different growth parameters.

Estimation of Indole Acetic Acid Produced by the Endophytic Fungal Isolate

High performance liquid chromatography (HPLC) chromatograph was used for the analysis of IAA in the supernatant of the potent fungal isolate. The fungal supernatant (20 µl) was loaded on a 5 µm reverse phase column (µBondapak C18, 250 mm × 4 mm) with the help of an HPLC micro – syringe. The sample was fractioned under isocratic conditions with methanol and water (80:20 v/v) as a mobile phase, at a flow rate of 1.0 ml/min. Eluates were detected by a differential ultraviolet detector at 254 nm. Pure IAA was used as a standard to quantify IAA in the fungal supernatant.

Halotolerance Assay

The endophytic fungal isolate was enriched in the flasks containing Czapek broth media supplemented with various concentrations of salt (NaCl 50–500 mM). The flasks were transferred to the shaking incubator operated at 27°C and 120 rpm for 1 week. After incubation fungal mycelia from a broth media were filtered and fresh and dry weights were recorded.

Plant Growth Promoting Assay

Phosphate Solubilization

Phosphate solubilization potential of the selected endophyte was detected on Pikovskaya's (PVK) agar media by the method of Wahyudi et al. (2011). The PVK agar media was autoclaved and transferred to the plates. Fresh culture of the selected fungal stain was inoculated in the center of the plate under sterile conditions. The plates were incubated at 28 ± 2°C for 3 days; clear halo zones around the fungal colonies were recorded.

A disk (4 mm diameter) from fresh fungal culture was transferred to the Pikovskaya broth media in a 250 ml conical flask. The inoculated flasks were incubated at 30°C and 120 rpm for 15 days in a shaking incubator along with control (Un-inoculated flasks). After incubation, the contents of the flask was filtered (Whatman No. 42), and phosphate solubilization was estimated by the method used by Jackson (2005).

Siderophore Assay

The siderophore assay was performed on chrome azurol S agar media by following the modified protocol of Schwyn and Neilands (1987). The media was prepared by dissolving 60.5 mg of CAS in 50 ml distilled water, following the addition of 10 ml iron (III) solution (1 mM $FeCl_3.6H_2O$, 10 mM HCl) with persistent stirring. To this, 72.9 mg of hexadecyl tri methyl ammonium bromide (HDTMA) was added to the mixture and then topped with 40 ml of water. The contents were then autoclaved at 121°C for 15 min. After sterilization the media was added to the basal media [succinic acid 0.5%, K_2HPO_4 0.4%, $(NH_4)_2SO_4.7H_2O$, agar 2% at pH 5.3 ± 2], and gently mixed till the appearance was of a blue color. After the development of a blue color the media was transferred to the Petri plates. The fresh fungal culture was inoculated on Chrome azurol S agar media and incubated at 27°C for a week. The zone diameter was determined by the change in color from blue to purple, dark purplish red, or yellowish orange around the fungal colonies.

Analysis of the 1-Aminocyclopropane-1-Carboxylate Deaminase Activity

1-Aminocyclopropane-1-carboxylate deaminase (ACC) enzyme assay was performed by using the protocol of Penrose and Glick (2003). Liquid Dworkin and Foster mineral medium (Dworkin and Foster, 1958) was prepared (3.0 mM ACC), and then the fresh fungal culture was added to the medium and incubated at 30°C and 200 rpm for 48 h to determine the ACC deaminase production. The supernatant from the culture medium was collected at 12, 24, 36, and 48 h. The amount of α- ketobutyrate in medium was measured at 540 nm absorbance along with standard α- ketobutyrate (Sigma-Aldrich Co., Rockville, MD, United States) ranging between 0.1 and 1.0 µM. The ACC deaminase activity was expressed as the amount of α- ketobutyrate produced per mg of protein per hour.

DNA Extraction and Fungal Isolate Identification

Genomic DNA isolation and PCR were performed according to an established protocol of Khan et al. (2008). Selected endophytic fungal isolate was identified by amplifying their ITS region of 18 S rDNA with universal primers, NS1 5′ (GTA GTC ATA TGC TTG TCT C) 3′ and NS24 5′ (AAA CCT TGT TAC GAC TTT TA) 3′. The BLAST search program[1] was used to compare the sequence homology of the nucleotide of the 18S region of fungi. The closely related sequences obtained were aligned through CLUSTAL W using MEGA version 4 software (Tamura et al., 2004), and the maximum parsimony tree was constructed using the same software. The bootstrap replications (1,000) were used as a statistical support for the nodes in the phylogenetic tree.

Wheat-Endophytes Interaction Under Salt Stress

Seeds of wheat variety Bhakkar-2000 (KJ672075) were obtained from the National Agricultural Research Center (NARC), Islamabad. Healthy seeds were sterilized (70% ethanol and 1% perchloric acid), germinated in petri plates, and incubated at 28°C for 24 h. To study the microbe's interaction in wheat

[1] http://www.ncbi.nlm.nih.gov/

plants under salt stress, uniformly germinated seedlings were transferred from petri plates to autoclaved pots containing 3 kg soil. The examined composition of the soil was sand (54%), silt (44%), and clay (1.6%) with water holding capacity of 220 ml water/Kg soil (± 3.5), pH (6.8), soil texture (loamy sand), lime (2.5%), and soil organic matter (1.6%). The experiment was performed in triplicate; each replicate contained 10 pots and each pot consisted of six seedlings (total = 6 × 10 × 3 = 180 seedlings per treatment). The seeds treated with non-inoculated media were used as a control. The pots were kept in a greenhouse (30°C, 80% humidity, light/dark 14 h/10 h). To prepare inoculum of the selected fungal isolate, mycelium was harvested by centrifugation at 5000 × *g* and 4°C for 15 min from 7-day-old fungal culture. To each pot, 50 mg of crushed fungal mycelium was added and the pots were kept in a controlled environment to acclimatize the fungal isolate. The treatments were divided in to four:

T1 = Control = 0 mM NaCl (No NaCl).
T2 = 60 mM NaCl (low NaCl concentration).
T3 = 120 mM NaCl (Moderate NaCl concentration).
T4 = 180 mM NaCl (High NaCl concentration).

Salt treatments were applied after 3 weeks of germination. Seedlings from salt treatments were watered with 100 ml salt solution at 12 h intervals for the next 7 days and seedlings from the control treatment were watered with distilled water.

Analysis of Plant Growth Attributes

Randomly, 10 plants from each treatment were selected and leaves and roots were detached and kept separately. Root segments were carefully washed, scanned, and analyzed with WinRHIZO software (Ver 5.0, Regent Instruments Inc., Qubec, Canada) to determine root length, diameter, root surface area, and average root volume. The stomatal conductance and net photosynthetic rate were measured with a photosynthesis system (Li-6400, Li-COR Inc., Lincolin, NE, United States) in three plants per treatment. The stomatal conductance and net photosynthetic rate were measured under 1500 mmol/ms^2 light intensity, 65% relative humidity, 32–62°C leaf temperature, and CO_2 concentrations at 9:30–11:00 AM. Leaf area of mature leaves was measured with laser meter (CI-203 model, United States). The selected shoot and roots were washed with deionized water and dried at 70°C for 48 h to determine dry weight.

Biochemical Attributes

Estimation of Chlorophyll and Carotenoid Content

To determine chlorophyll and carotenoids contents, segments (0.8-cm diameter) from fully expanded leaves were cut out in the form of disks. The leaf disks were mixed with 2 mL of acetone (80%) and washed twice with a further 2 mL of acetone. The absorbance of the extracts was measured using a spectrophotometer (UV-1700 Pharma Spec; UV-VIS; Shimadzu Japan) at 480, 645, and 663 nm. The contents of Chl *a*, Chl *b*, and carotenoids in the extracts were determined by using MacKinney equations (Mackinney, 1941).

Proline Estimation

Proline content was observed according to the method of Bates et al. (1973). The collected fresh healthy mature leaves were washed properly with distilled water. The clean samples (200 mg) were crushed in 3% sulfo salicylic acid and centrifuged for 5 min at 13,000 rpm. The supernatant (2 ml) was collected and mixed with glacial acetic acid (2 ml) + acid ninhydrin (2 ml). The mixture was boiled in a water bath at 100°C for 1 h and then immersed immediately in ice to stop the reaction. Toluene (1 ml) was added to the reaction mixture and the mixture was shaken for 20–30 s. The absorbance of the mixture was measured by spectrophotometer at 520 nm.

Estimation of Total Phenolics

Phenolic content was estimated by the method of Malik and Singh (1980). Fresh leaves of wheat plants were collected and air dried in shade at ambient temperature. The dried leaves (200 mg) were ground into powder and mixed with methanol (1 ml) in eppendorf tube. The contents of the tube were kept for 4 h before 6 min of centrifugation at 5000 rpm. The supernatant (methanol extract 0.5 ml) was collected in fresh tubes and mixed with 2.5 ml of 10% FC reagent. The resultant mixture was retained for 5 min before mixing with 2.5 ml distilled water + 2.5 ml sodium hydrogen carbonate (7.5% $NaHCO_3$). After complete mixing the contents were kept for 1 h in the dark. The absorbance was measured at 650 nm after appearance of a blue color. The 10% FC reagent was used as blank. The total phenolic contents in the sample were measured from the calibration plot and expressed as mg galic acid equivalent of phenol/g of sample.

Total Carbohydrate Contents Estimation

The carbohydrate contents in wheat plants were observed following the protocols of Hedge and Hofreiter (1962). Healthy mature leaves from treatment plants were collected and dried. The dried plant material (200 mg) was taken in test tube, to which 10 ml water was added and boiled in a water bath for 1 h. The extract (1 ml) from the test tubes was mixed with 3 mL of 3% antheron reagent and kept on a water bath operated at 100°C for 30 min. The final absorbance was measured at 630 nm.

Malonaldehyde Determination

Malonaldehyde (MDA) was determined by following the method of Hodges et al. (1999). Fresh leaf samples (0.2 g) were homogenized in 10 ml of 10% trichloroacetic acid. The homogenate was centrifuged at 12000 rpm for 10 min and the supernatant was carefully pipetted in to a new tube. Thiobarbituric acid (2 ml of 0.6%) was added to the supernatant (2 ml) and the mixture was incubated in a water bath for 15 min at 100°C. The mixture was cooled and centrifuged at 12,000 rpm for 10 min. The absorbance of the supernatant was calculated at 532, 600, and 450 nm.

Estimation of Enzymatic Activities

The fresh healthy leaves of experimental wheat plants were collected and homogenized in extraction buffer (5 mL) containing 50 mm sodium phosphate (pH 7.8). The sample was centrifuged and the supernatant was applied to measure the activities of catalase following the methods of Aebi (1984). GSH activity was determined by the method of Carlberg and Mannervik (1975). The activity of ascorbate

peroxidase was measured according to the method of Nakano and Asada (1981).

Determination of Phytohormones

Plant hormones [gibberellins (GAs), abscisic acid (ABA), and IAA] extraction and purification in different treatments were quantified on HPLC by the method of Kettner and Dörffling (1995). The samples were passed through Millipore filter (0.45 μ) and were analyzed on HPLC (Agilent 1100) equipped with variable UV detector and C18 column (39 × 300mm) (BondaPack Porasil C18, 37/50 μm, Waters, Eschborn, BRD). Methanol and water in the ratio of (30:70; v/v) were used as mobile phase @ 1500 μl/min with a run time of 20 min/sample. The plant hormones were identified on the basis of retention time. IAA and GA were eluted at 280 and 254 nm wavelengths, respectively. For ABA the samples were injected onto a C18 column and eluted with a linear gradient of methanol (30–70%), containing 0.01% acetic acid, at a flow rate of 0.8 ml min^{-1}.

Minerals Analysis

The concentration of ions (Ca, Mg, K, Na) were quantified in dried ground plant samples. Approximately, 0.5 g of ground dried plant materials were put in digesting tubes, to which was added 3 mL perchlorate acid and 10 mL of concentrated nitric acid. The samples were then soaked for 12 h and burned at 300°C for 3 h. The residue was transferred to a 50-mL volumetric flask and had 50 mL distilled water added. The ion contents was then measured using an atomic absorption spectrophotometer (TAS-986; PERSEE Ltd., Beijing, China) (Ashraf and Orooj, 2006).

Statistical Analysis

Different treatments were compared by one way ANOVA at $P = 0.05$, followed by Tukey's multiple comparison tests by Graph Prism 5 software. The BLAST search program (see footnote 1) was used to compare the sequence homology of the nucleotide of the 18S ITS region and were aligned through CLUSTAL W using MEGA version 4 software.

RESULTS

Physiochemical Properties of the Soil

Soils were collected from the Kohat district of Khyber Pakhtunkhwa (KPK) Pakistan, from two depths (0–20 and 20–40 cm) for physico chemical analysis. Sand content of the surface soil (0–20 cm) ranged 2.01–76%, while at subsurface (20–40 cm) it was 12.4–80%. Silt content at depth 0–20 cm ranged from 10.7 to 70%, while at depth of 20–40 cm, it was 5–55%. Clay content at soil surface was 11–58.6%, while at subsurface clay contents varied from 1.9 to 69.8% (**Table 1**). Soil pH ranged from 7.1 to 7.9 in a soil depth from 0 to 20 cm, while at subsoil, the pH varied from 7.1 to 8.0. Electrical conductivity of the soil surface ranged from 2.8 to 18.2%, while at sub surface it varied from 4.4 to 17.1%. Lime content of the surface soil ranged from 1.87 to 30.1%, while at subsurface it was 2.7–38.09%. Lime contents ranged from slightly calcareous to strongly calcareous in both depths (**Table 1**).

Screening Bioassay for Fungal Isolates

A total of 10 fungal endophytes was isolated from the roots of *C. album* plants. The fungal isolates were identified on the basis of macroscopic characteristics (such as shape, colony height, growth rate and microscopic characteristics aerial hyphae, surface texture, base color, and margin). Morphological analysis showed that out of total isolated endophytes only five isolates were different. Culture filtrates (CF) of identified fungal isolates were tested on IAA mutant (dwarf cultivar) maize seedlings to identify the potent growth stimulatory and phytohormones producing fungi. The growth traits of mutant maize seedlings were recorded after 1 week of culture inoculation. Among the endophytic fungal isolates, BTK-1 enhanced shoot and root growth, chlorophyll content, and fresh biomas of IAA dwarf maize seedlings compared to the control seedlings. Other tested isolates showed less improvement in shoot growth, fresh weight, and chlorophyll content of mutant maize seedlings. Based on significant ($P = 0.05$) growth promoting potential, the endophytic fungal isolate BTK-1 was selected for identification and further analysis.

Salt Resistance by BTK-1

The results revealed that BTK-1 has resisted the salt stress up to 300 mM NaCL (**Figure 1A**). However, further increase in salt concentration resulted in growth reduction of endophytic fungal isolate BTK-1 as compared to the control. Increase in salt concentration negatively affected the fresh weight and dry weight of the BTK-1. At 500 mM NaCl in culture media, a clear decline was observed in both fresh (65%) and dry weights (60%) of endophytic fungal isolate BTK-1 compared to the control media. Minimal inhibitory concentration of NaCl was around 300 mM that reduced approximately 10% of the fresh and dry weight of endophytic fungal isolate BTK-1 (**Figure 1A**).

Determination of IAA in the Culture Filtrates of BTK-1

Different concentrations of IAA (35–40 μg/ml) in different media with or without tryptophan were observed (**Figure 1B**). IAA production was most abundant in culture filtrates with different concentrations of tryptophan. The quantity of IAA in the culture filtrates of endophytic fungal isolate BTK-1 was highest (40 μg/ml), when the media was supplemented with 1000 μg tryptophan (**Figure 1B**).

Estimation of Phosphate Solubilization, Siderophore, and 1-Aminocyclopropane-1-Carboxylate Deaminase

The endophytic fungal isolate BTK-1 actively solubilized phosphate on exposure to PVK agar medium (**Figure 2**). The phosphate content of the BTK-1 CF were initially increased and then decreased during the incubation period (5–15 days). The amount of P content on 5th day of incubation was

TABLE 1 | Physio-chemical properties of Kohat district KPK Pakistan.

Soil texture	Depth [cm]	Range	%	Soil nature	Depth [cm]	Range	%
Sand	0–20	Min	2.01%	Soil pH	0–20	Min	7.1
		Max	76.0%			Max	7.9
	20–40	Min	12.4%		20–40	Min	7.1
		Max	80.0%			Max	8.0
Silt	0–20	Min	8.45%	Electrical conductivity (μs/cm)	0–20	Min	2.8
		Max	83.0%			Max	18.2
	20–40	Min	6.00%		20–40	Min	34.7
		Max	60.0%			Max	31.7
Clay	0–20	Min	1.00%	Lime content (%)	0–20	Min	11.9
		Max	8.60%			Max	30.1
	20–40	Min	9.00%		20–40	Min	38.1
		Max	9.80%			Max	72.7

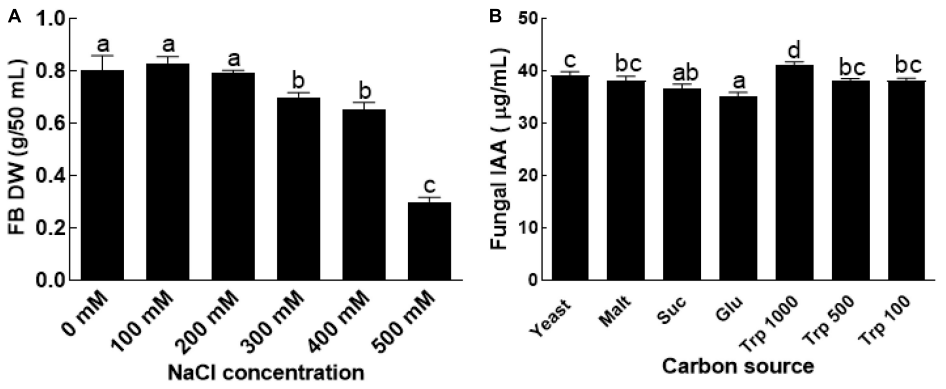


FIGURE 1 | Salt tolerance ability and IAA production by endophytic fungal isolate BTK-1. **(A)** Represents salt resistance assay of endophytic fungal isolate BTK-1 cultivated under various concentrations of NaCl; **(B)** represents production of IAA by CGF-11 on media supplemented with different nutrient sources; Suc, sucrose; Glu, glucose; Trp, tryptophan; FB, fungal biomass; DW, dry weight. Means followed by different letters are significantly different at $P \leq 0.05$. Each bar shows ± SE of means.

440 μg/ml of CF, which increased to 517 μg/ml of CF on 10th day and then decreased to 217 μg/ml of CF on 15th day of incubation (**Figure 2A**). Furthermore, the endophytic fungal isolate BTK-1 also exhibited siderophore activity (**Figure 2B**). Clear yellow halozones around the BTK-1 colonies were observed. Also, ACC deaminase activity was recorded for the endophytic fungal isolate BTK-1 that ranged from 0.7 to 0.9 μM α-ketobutyrate/mg/h during the incubation time (**Figure 2C**).

Identification of Endophytic Fungal Isolate BTK-1

The lyophilized culture of the endophytic fungal isolate BTK-1 was amplified by PCR and identified through phylogenetic analysis of the 18S rDNA sequence. Based upon BLAST results, a sequence of 18S rDNA of endophytic fungal isolate BTK-1 showed maximum homology (98%) with *Aspergillus terreus*. To confirm the identity of the endophytic fungal isolate, phylogenetic consensus tree was constructed by using maximum parsimony (MP) method in MEGA 7 package (**Figure 3**). The sequence of BTK-1 was submitted to GenBank under accession No MF678562.

Effect of BTK-1 on Wheat Growth Under Salt Stress

Wheat seedlings grown in pots inoculated with BTK-1 mycelium showed a significant (P = 0.05) improvement in shoot and root lengths and weights compared to the non-inoculated wheat plants under normal as well as salt stress (**Figure 4**). Shoot lengths of BKT-1 associated wheat plants under salt stress (60, 120, 180 mM NaCl) were significantly (P = 0.05) improved compared to the BKT-1 non-associated wheat plants (**Figure 4A**). Similarly, root length (**Figure 4B**), shoot dry weight (**Figure 4C**), and root dry weight (**Figure 4D**) of BKT-1 associated wheat plants exposed to salt stress (60, 120, 180 mM NaCl) improved significantly (P = 0.05) compared to the BKT-1 non-associated wheat plants. The amounts of photosynthetic pigments (chlorophyll *a,b*/carotenoids) improved significantly (P = 0.05) in fungus-inoculated wheat plants as compared to the non-associated plants under normal as well as saline conditions (**Figure 5**).

Effect of BTK-1 on Wheat Biochemical Attributes Under Salt Stress

Under salt stress conditions (60, 120, 180 mM NaCl), proline and phenolic contents of the BTK-1 associated wheat plants were

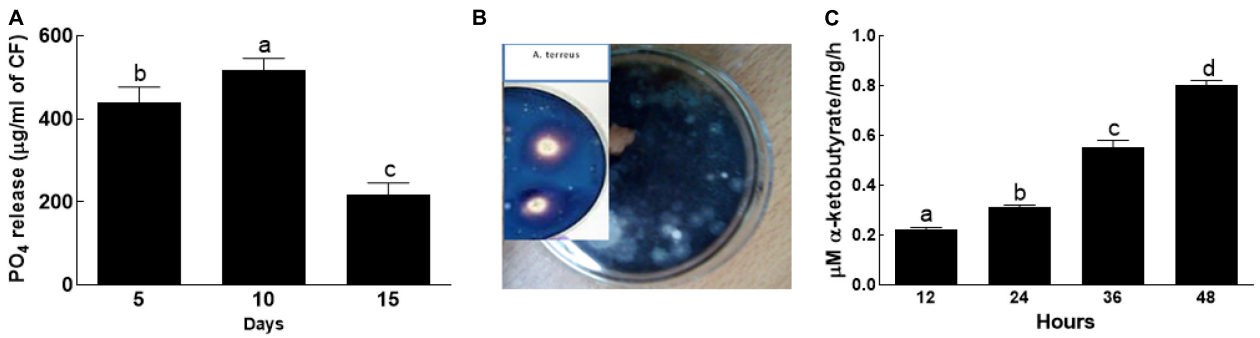


FIGURE 2 | Phosphate solubalization, siderophore, and ACC activities of endophytic fungal isolate BTK-1. **(A)** Phosphate solubalization; **(B)** siderophore; **(C)** 1-aminocyclopropane-1-carboxylate (ACC) activity of BTK-1. Means followed by different letters are significantly different at $P \leq 0.05$. Each bar shows ± SE of means.

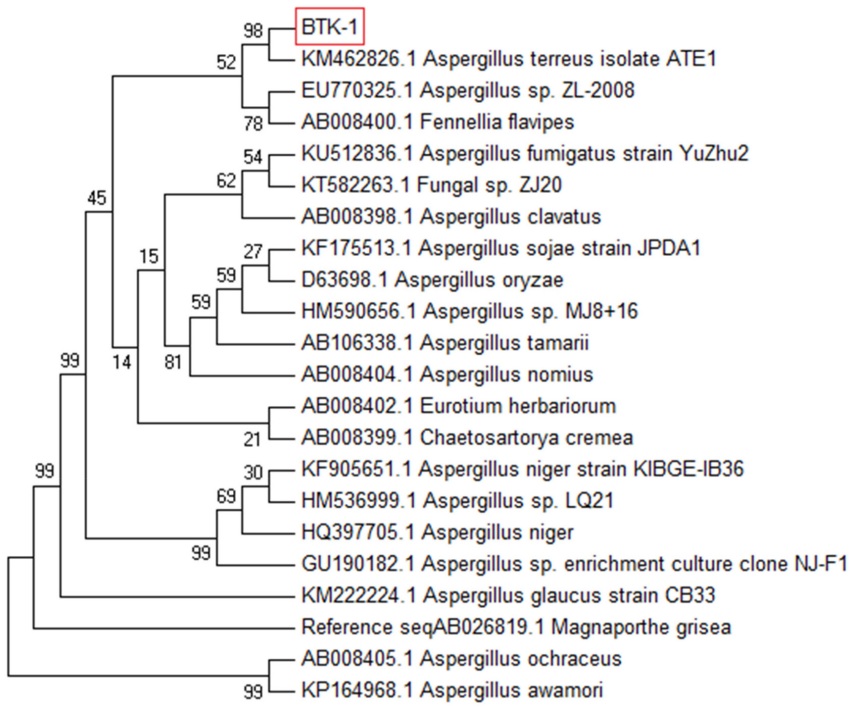


FIGURE 3 | Multiple sequence alignment file of 18S ribosomal DNA region.

significantly (P = 0.05) high compared to the non-associated plants (**Figure 6**). The biosynthesis of proline and phenolic contents were gradually increased with an increase in salt concentration. Similarly, salt stress (60, 120, 180 mM NaCl) also inhibited the production of total carbohydrate contents in BTK-1 non-inoculated wheat plants compared to the BTK-1 inoculated plants (**Figure 7A**). Moreover, total carbohydrate contents were same in BTK-1 inoculated and non-inoculated wheat plants under normal condition (0 mM NaCl stress). On a general basis, treating wheat plants with different concentrations of NaCl (60, 120, and 180 mM) hindered the production of total carbohydrate contents in wheat plants (**Figure 7A**). The data regarding MDA content revealed a significantly (P = 0.05) low amount in BKT-1 associated wheat plants under salinity (60, 120, 180 mM) stress compared to the non-associated plants (**Figure 7B**).

Effect of BTK-1 on Wheat Enzymatic Activities Under Salt Stress

Under normal growth conditions (0 mM NaCl stress), BTK-1 association with the wheat plants exhibited no effect on the activities of reduced glutathione (GSH), ascorbate, and peroxidase (**Figure 8**). However, under NaCl stress wheat plants inoculated with BTK-1 had significantly (P = 0.05) higher reduced glutathione (GSH), while the activities of peroxidase, ascorbate, and catalase were significantly (P = 0.05) reduced compared to the BTK-1 non-inoculated plants (**Figure 8**).

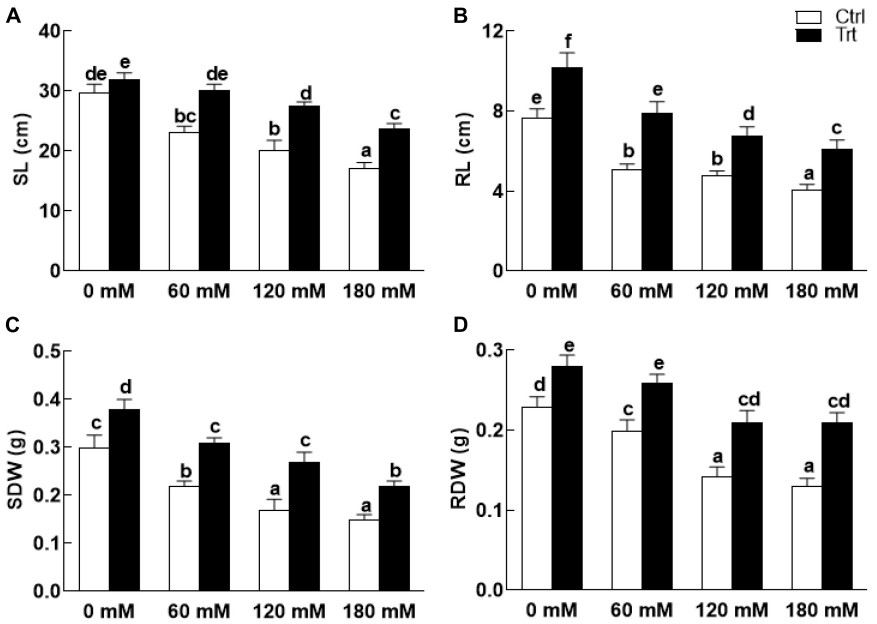


FIGURE 4 | Effect of endophytic fungal isolate BTK-1 on growth parameters of wheat plants under salt stress. Salt stress was given after 3 weeks of seed germination. **(A)** Represents shoot length (SL); **(B)** represents root length (RL); **(C)** represent shoots dry weight (SDW); **(D)** represent roots dry weight (RDW); Ctrl, control plants; Trt, BTK-1 inoculated plants; Means followed by different letters are significantly different at $P \leq 0.05$. Each bar shows ± SE of means.

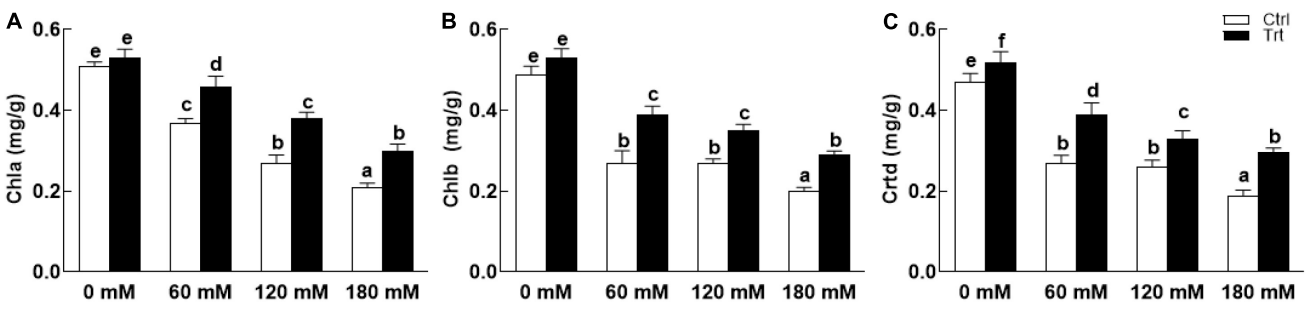


FIGURE 5 | Effect of endophytic fungal isolate BTK-1 on chlorophylls and carotenoids contents of wheat plants under salt stress. Salt stress was given after 3 weeks of seed germination. **(A)** Represents chlorophyll *a* (Chla) contents; **(B)** represents chlorophyll *b* (Chlb) contents; **(C)** represents carotenoid contents; Ctrl, control plants; Trt, BTK-1 inoculated plants; Means followed by different letters are significantly different at $P \leq 0.05$. Each bar shows ± SE of means.

Effect of BTK-1 on Wheat Endogenous Indole Acetic Acid, Gibberellins, and Abscisic Acid Under Salt Stress

The results revealed that BTK-1 inoculated wheat plants and non-inoculated plants significantly (P = 0.05) differed in phytohormones (IAA, GAs, and ABA) contents under normal (0 mM NaCl stress) as well as salt stress (60, 120, and 180 mM) conditions. BTK-1 associated wheat plants exposed to various salt concentrations (60, 120, and 180 mM) showed significantly (P = 0.05) high contents of IAA compared to the non-inoculated plants (**Figure 9A**). Similarly, upon exposure to NaCl stress (60, 120, and 180 mM), a significant (P = 0.05) increase in GA contents were found in BTK-1 inoculated wheat plants as compared to non-inoculated plants (**Figure 9B**). An opposite trend was noticed for ABA contents in wheat plants exposed to salt stress (**Figure 9C**). The ABA contents were significantly (0.05) low in BTK-1 associated wheat plants compared to the non-inoculated plants under normal (0 mM NaCl stress) as well as salt stress conditions (**Figure 9C**).

Effect of BTK-1 on Wheat Mineral Contents Under Salt Stress

The data recorded for nutrients analysis of wheat plants (with or without fungal inoculation) showed higher levels of K^+ ions under normal condition (0 mM NaCl stress). However, after exposure to salinity, the levels of K^+ in BTK-1 non-inoculated wheat plants was significantly lower compared to the BTK-1 inoculated wheat plants (**Figure 10A**). On the contrary, significantly (P = 0.05) high Na^+ ions were observed in BTK-1 non-inoculated wheat plants compared to the BTK-1 inoculated

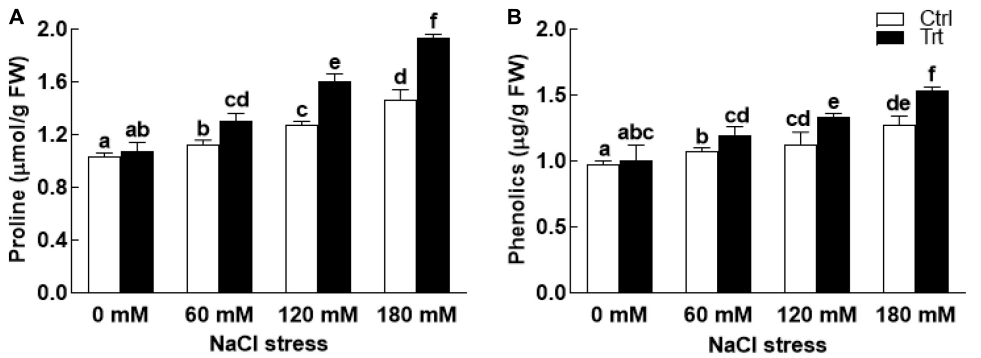


FIGURE 6 | Effect of endophytic fungal isolate BTK-1 on proline and phenolic contents of wheat plants under salinity stress. Salt stress was given after 3 weeks of seed germination. **(A)** Represents proline contents; **(B)** represents phenolic contents; Ctrl, control plants; Trt, BTK-1 inoculated plants; Means followed by different letters are significantly different at $P \leq 0.05$. Each bar shows ± SE of means.

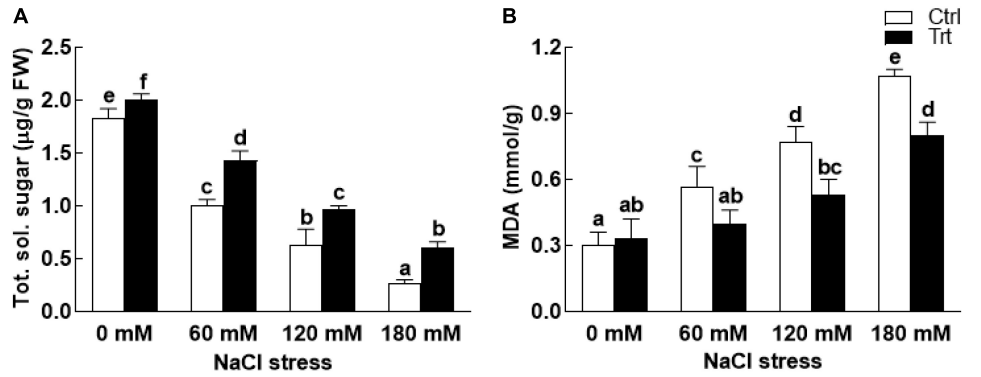


FIGURE 7 | Effect of endophytic fungal isolate BTK-1 on total sugars and MDA contents of wheat plants under salt stress. Salt stress was given after 3 weeks of seed germination. **(A)** Represents total soluble sugars (Tot. sol. Sugar); **(B)** represents malondialdehyde (MDA) content; Ctrl, control plants; Trt, BTK-1 inoculated plants; means followed by different letters are significantly different at $P \leq 0.05$. Each bar shows ± SE of means.

plants exposed to various concentrations (60, 120, and 180 mM) of NaCl (**Figure 10B**). Moreover, salt treatments (60, 120, and 180 mM) showed significant ($P = 0.05$) declination in Mg^{2+} and Ca^{2+} ions in BTK-1 non-inoculated wheat plants compared to the BTK-1 inoculated plants (**Figures 10C,D**).

DISCUSSION

In connection with the prior investigation, the current research was designed to isolate and screen endophytic fungi for polyphasic potential in order to boost wheat growth. The fungal isolates were screened for hormonal analysis and plant growth properties in order to discover potent isolate(s) (Gul Jan et al., 2019; Ismail et al., 2021). In screening bioassays, maize (IAA mutant and wild maize) seedlings were grown in hydroponic medium containing culture filtrates of isolated endophytic fungus under sterilized conditions. After a week, the best maize mutant growth promoting and IAA producing endophytic fungal isolate BTK-1 was selected and utilized in further experiments. The IAA producing endophytes with an active role in plant growth has been demonstrated by various scientists in recent times (Muhammad et al., 2018, 2019; Mehmood et al., 2019a). In fact, some of the discovered endophytes have shown the ability to secrete higher amounts of IAA, which is one of the important factors that is required by the plants to grow normally under stress conditions (Muhammad et al., 2018, 2019; Mehmood et al., 2019a). The presence of IAA in the CF of isolated BTK-1 suggests that the interaction of this endophytic fungus with wheat plants has stimulated the host growth through IAA secretion under salt stress. Several fungal endophytes, like *Aspergillus flavus*, *Paecilomyces formosus*, *Aspergillus niger*, *Penicillium funiculosum*, *Penicillium corylophilum*, and *Fusarium oxysporum* have been reported for their plant growth promotion and IAA production (Deng and Cao, 2017). Muhammad et al. (2018) reported that *Penicillium roqueforti* have the capacity to produce IAA and help the host plant species under stressful conditions.

Plants, although they are generally regarded as self-sufficient entities, are in reality associated with diverse microbial communities that confer multiple benefits under stress (Ismail et al., 2021). More recently, the role of symbiotic endophytes has been acknowledged by scientists for their role in plant resistance against stress conditions (Hamayun et al., 2017; Bibi et al., 2018). Similarly, reports are available on the role of plant

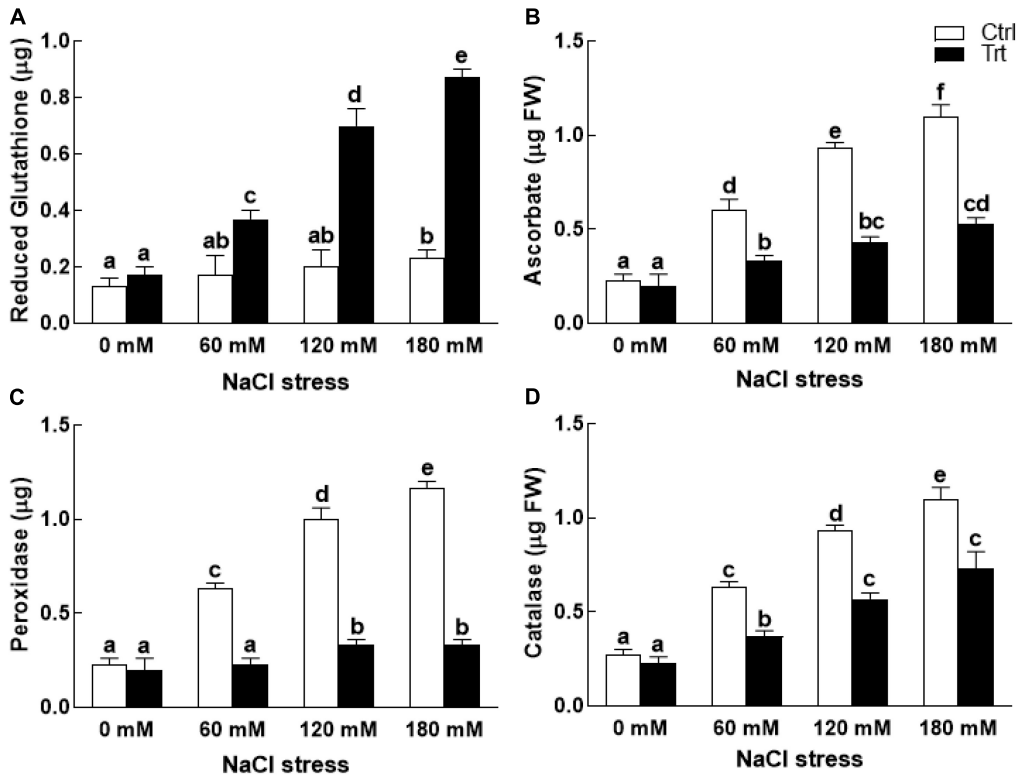


FIGURE 8 | Effect of endophytic fungal isolate BTK-1 on the enzymatic activity of wheat plants under salt stress. Salt stress was given after 3 weeks of seed germination. **(A)** Represents reduced glutathione activity; **(B)** represents ascorbate activity; **(C)** represents peroxidase activity; **(D)** represents catalase activity; Ctrl, control plants; Trt, BTK-1 inoculated plants; Means followed by different letters are significantly different at $P \leq 0.05$. Each bar shows ± SE of means.

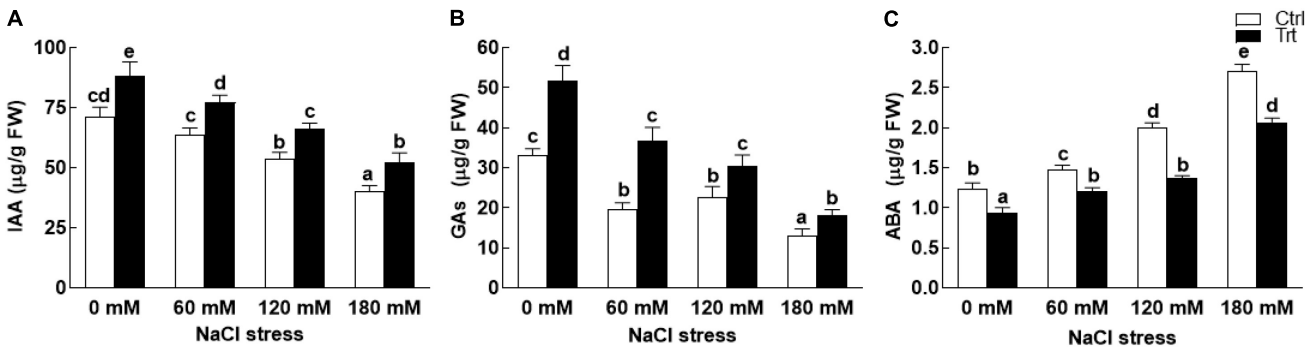


FIGURE 9 | Effect of endophytic fungal isolate BTK-1 on phytohormones of wheat plants under salt stress. Salt stress was given after 3 weeks of seed germination. **(A)** Represents IAA content; **(B)** represents GAs content; **(C)** represents ABA content; IAA, indole acetic acid; GAs, gibberellins; ABA, abscisic acid; Ctrl, control plants; Trt, BTK-1 inoculated plants; Means followed by different letters are significantly different at $P \leq 0.05$. Each bar shows ± SE of means.

growth promoting endophytes (fungi and bacteria) that increase host plants fitness by mitigating the impacts of abiotic stresses (Hamayun et al., 2017; Bibi et al., 2018). Numerous reports on endophytes suggested that fungal interaction can enhance plants growth under stress situations (Ismail et al., 2021; Raid et al., 2021). In addition to phytoharmones, biofertilization ability of endophytic fungi ensure availability of essential nutrients to host plants (Raid et al., 2021). Colonization potential of endophytes and mechanisms such as phosphate solubilization and siderophores production are very important for the host plant growth under stress (Muhammad et al., 2018, 2019). The current study also rectifies the plant growth promoting properties of the endophytic fungal isolate BTK-1. The inoculation of wheat plants with BTK-1 considerably enhanced wheat growth and helped in relieving induced salt stress (Muhammad et al., 2018; Mehmood et al., 2019a). The occurrence of inoculated endophytic fungal isolate BTK-1 inside cortical region of wheat plant roots and their successful re-isolation further strengthens

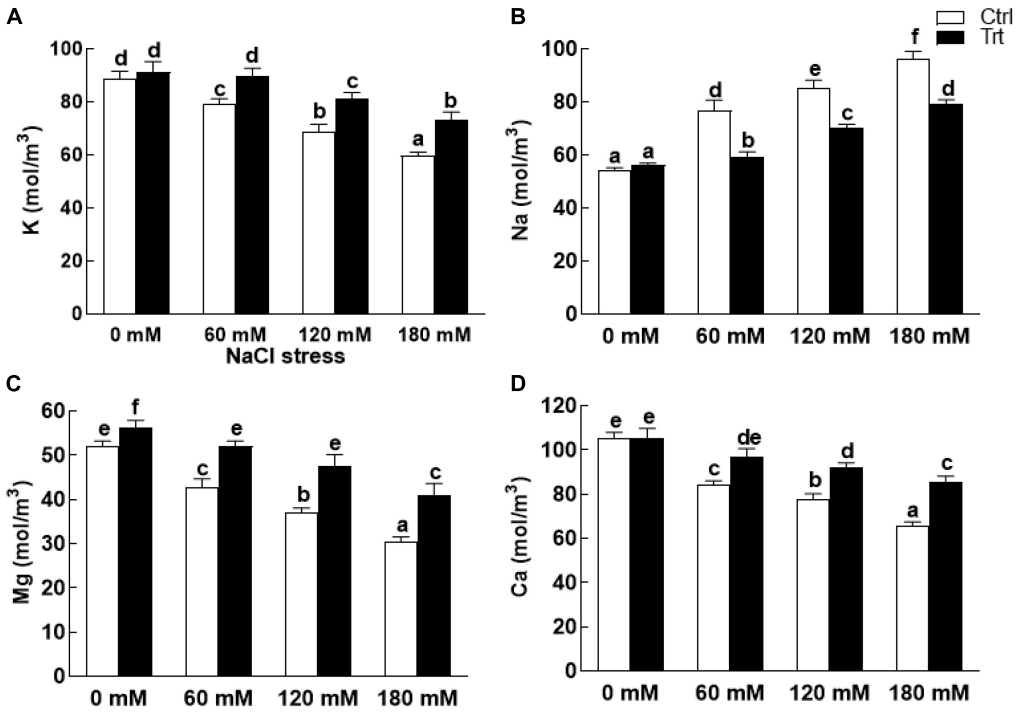


FIGURE 10 | Nutrient quantification of endophytic fungal isolate BTK-1 inoculated and non-inoculated wheat plants under salt stress. Salt stress was given after 3 weeks of seed germination. **(A)** Represents K^+ concentration; **(B)** represents Na^+ concentration; **(C)** represents Mg^+ concentration; **(D)** represents Ca^+ concentration; K^+, potassium; Na^+, sodium; Mg^+, magnesium; Ca^+, calcium; Ctrl, control plants; Trt, BTK-1 inoculated plants; Means followed by different letters are significantly different at $P \leq 0.05$. Each bar shows ± SE of means.

the active role of BTK-1. Likewise, the antioxidant scavengers can augment membrane firmness and can protect plant species against ROS attack (Ismail et al., 2021). The ROS scavenging activity can be assessed through the production of MDA, which is the lipid breakdown product under stress situations (Ismail et al., 2021). The MDA content reflects the ROS production in plant tissues during stress and is responsible for the instability of cellular membrane. From the results, we observed low levels of MDA content in fungus inoculated wheat plants that might have boosted the membrane thermo stability under induced salinity.

Osmo-protectants (proline) aggregation offer avoidance of osmotic imbalances in plants under stress circumstances (Ismail et al., 2020c, 2021). Correspondingly, nitrogen uptake by plants regulates the uptake of sodium ions that can lead to maintenance of chlorophyll and ionic stability under saline conditions (Gupta and Huang, 2014). In the current study, substantial accumulation of proline was observed in BTK-1 treated wheat plants grown under induced salinity, which signifies a decline in ionic influx and protects host plants from ionic imbalance (Gupta and Huang, 2014). Sodium and chloride ion toxicity can generate ROS, which can cause destruction in cellular functioning (Gupta and Huang, 2014). On the contrary, aggregation of antioxidants inside plant species can extend greater resistance to oxidative damage (Gharsallah et al., 2016). In the present work, we observed greater activities of antioxidant enzymes (CAT, APX, SOD, and GSH) in BTK-1 inoculated wheat plants, suggesting high oxidative stability under salt stress. Several studies reported the increased antioxidant potential of plant species associated with fungal endophytes under stress conditions (Jan et al., 2019; Muhammad et al., 2019; Ismail et al., 2021). In addition, plant hormones can secure plants and intercept stress injury through various mechanisms (Ismail et al., 2021). It is well-known that ABA levels under stress conditions increase in plants. However, our result showed low levels of ABA in BTK-1 inoculated wheat plants exposed to salt stress. Similarly, Ismail et al. (2020b) also reported low content of ABA in soybean plants associated with endophytic fungi under heat stress. However, the influence of fungi may vary among the species and its interaction with plant species as well (Ahmad et al., 2010; Ismail et al., 2018, 2019, 2020a,b,c, 2021). IAA is also extensively recognized due to its active role in plant growth and developmental processes (Kumar et al., 2017). In the current study, we observed significantly high levels of IAA in endophyte treated wheat plants that might be responsible for normal plant growth under salt stress.

CONCLUSION

BTK-1 inoculation and its symbiotic-interaction with wheat plants have promoted the growth and strengthened the host plants against the adverse effects of salinity. BTK-1 as an endophyte has secreted phytoharmones, including IAA and GA, inside the host plant that improved the productivity and quality of economically important wheat crop under stress conditions.

DATA AVAILABILITY STATEMENT

The datasets presented in this article are not readily available because all the data included in the manuscript. Requests to access the datasets should be directed to AI, amjadiqbal@awkum.edu.pk.

AUTHOR CONTRIBUTIONS

MK, GJ, and FJ designed and performed all the experiments. AI and AH analyzed the data and wrote the manuscript. AI, AH, and MH designed the experiments. AI, NA, and MH edited the manuscript. NA, GJ, MH, and I-JL supervised the project. MH and I-JL arranged the resources for the work. I-JL financed the project. All the authors contributed to the article and approved the submitted version.

FUNDING

This research was supported by Korea Basic Science Institute (National research Facilites and Equipment center) grant funded by the Ministry of Education (2021R1A6C101A416).

REFERENCES

Aebi, H. (1984). [13] Catalase in vitro. *Methods Enzymol.* 105, 121–126. doi: 10.1016/s0076-6879(84)05016-3

Afridi, S. G., Islam, N., Shams, D. F., Shams, S., Khan, A., Shah, M., et al. (2019). Assessment of air pollution tolerance of selected trees and crop species using biochemical and physiological analyses. *Fresenius Environ. Bull.* 28, 4805–4810.

Ahmad, N., Hamayun, M., Khan, S. A., Khan, A. L., Lee, I.-J., and Shin, D.-H. (2010). Gibberellin-producing endophytic fungi isolated from Monochoria vaginalis. *J. Microbiol. Biotechnol.* 20, 1744–1749.

Ali, S., Khan, S. A., Hamayun, M., Iqbal, A., Khan, A. L., Hussain, A., et al. (2019). Endophytic fungi from Caralluma acutangula can secrete plant growth promoting enzymes. *Fresenius Environ. Bull.* 28, 2688–2696.

Ashraf, M., and Orooj, A. (2006). Salt stress effects on growth, ion accumulation and seed oil concentration in an arid zone traditional medicinal plant ajwain (*Trachyspermum ammi* [L.] Sprague). *J. Arid Environ.* 64, 209–220.

Bates, L., Waldren, R., and Teare, I. (1973). Rapid determination of free proline for water-stress studies. *Plant Soil* 39, 205–207. doi: 10.1007/bf00018060

Bibi, S., Hussain, A., Hamayun, M., Rahman, H., Iqbal, A., Shah, M., et al. (2018). Bioremediation of hexavalent chromium by endophytic fungi; safe and improved production of *Lactuca sativa* L. *Chemosphere* 211, 653–663. doi: 10.1016/j.chemosphere.2018.07.197

Bilal, L., Asaf, S., Hamayun, M., Gul, H., Iqbal, A., Ullah, I., et al. (2018). Plant growth promoting endophytic fungi *Asprgillus fumigatus* TS1 and *Fusarium proliferatum* BRL1 produce gibberellins and regulates plant endogenous hormones. *Symbiosis* 76, 117–127. doi: 10.1007/s13199-018-0545-4

Bouyoucos, G. J. (1936). Directions for making mechanical analyses of soils by the hydrometer method. *Soil Sci.* 42, 225–230.

Carlberg, I., and Mannervik, B. (1975). Purification and characterization of the flavoenzyme glutathione reductase from rat liver. *J. Biol. Chem.* 250, 5475–5480.

Del Buono, D. (2021). Can biostimulants be used to mitigate the effect of anthropogenic climate change on agriculture? It is time to respond. *Sci. Total Environ.* 751:141763. doi: 10.1016/j.scitotenv.2020.141763

Deng, Z., and Cao, L. (2017). Fungal endophytes and their interactions with plants in phytoremediation: a review. *Chemosphere* 168, 1100–1106. doi: 10.1016/j.chemosphere.2016.10.097

Dworkin, M., and Foster, J. (1958). Experiments with some microorganisms which utilize ethane and hydrogen. *J. Bacteriol.* 75:592. doi: 10.1128/jb.75.5.592-603.1958

Gharsallah, C., Fakhfakh, H., Grubb, D., and Gorsane, F. (2016). Effect of salt stress on ion concentration, proline content, antioxidant enzyme activities and gene expression in tomato cultivars. *AoB Plants* 8:lw055. doi: 10.1093/aobpla/plw055

Gul Jan, F., Hamayun, M., Hussain, A., Iqbal, A., Jan, G., Khan, S. A., et al. (2019). A promising growth promoting *Meyerozyma caribbica* from *Solanum xanthocarpum* alleviated stress in maize plants. *Biosci. Rep.* 39, 1–15. doi: 10.1042/BSR20190290

Gupta, B., and Huang, B. (2014). Mechanism of salinity tolerance in plants: physiological, biochemical, and molecular characterization. *Int. J. Genomics* 2014:701596. doi: 10.1155/2014/701596

Hamayun, M., Hussain, A., Khan, S. A., Irshad, M., Khan, A. L., Waqas, M., et al. (2015). Kinetin modulates physio-hormonal attributes and isoflavone contents of Soybean grown under salinity stress. *Front. Plant Sci.* 6:377. doi: 10.3389/fpls.2015.00377

Hamayun, M., Hussain, A., Khan, S. A., Kim, H.-Y., Khan, A. L., Waqas, M., et al. (2017). Gibberellins producing endophytic fungus *Porostereum spadiceum* AGH786 rescues growth of salt affected soybean. *Front. Microbiol.* 8:686. doi: 10.3389/fmicb.2017.00686

Heald, W. R. (1965). "Calcium and magnesium," in *Methods of Soil Analysis: Part 2 Chemical and Microbiological Properties*, ed C. A. Black (Madison, WI: American Society of Agronomy) Vol. 9, 999–1010.

Hedge, J., and Hofreiter, B. (1962). *Methods in Carbohydrate Chemistry*, Vol. 17. New York, NY: Academic Press, 420.

Hodges, D. M., Delong, J. M., Forney, C. F., and Prange, R. K. (1999). Improving the thiobarbituric acid-reactive-substances assay for estimating lipid peroxidation in plant tissues containing anthocyanin and other interfering compounds. *Planta* 207, 604–611. doi: 10.1007/s00425-017-2699-3

Ismail, Anwar, H., Mehmood, A., Qadir, M., Husna, Iqbal, A., et al. (2020a). Thermal stress alleviating potential of endophytic fungus *Rhizopus oryzae* inoculated to sunflower (*Helianthus annuus* L.) and soybean (*Glycine max* L.). *Pak. J. Bot.* 52:5.

Ismail, Hamayun, M., Hussain, A., Afzal Khan, S., Iqbal, A., and Lee, I.-J. (2020b). An endophytic fungus *Aspergillus violaceofuscus* can be used as heat stress adaptive tool for *Glycine max* L. and *Helianthus annuus* L. *J. Appl. Bot. Food Qual.* 93, 112–120.

Ismail, Muhammad, H., Anwar, H., Amjad, I., Sumera, A. K., and In-Jung, L. (2020c). *Aspergillus niger* boosted heat stress tolerance in sunflower and soybean via regulating their metabolic and antioxidant system. *J. Plant Interact.* 15, 223–232.

Ismail, Hamayun, M., Hussain, A., Afzal Khan, S., Iqbal, A., and Lee, I.-J. (2019). *Aspergillus flavus* promoted the growth of soybean and sunflower seedlings at elevated temperature. *BioMed Res. Int.* 2019, 1–13. doi: 10.1155/2019/1295457

Ismail, Hamayun, M., Hussain, A., Iqbal, A., Khan, S. A., and Lee, I.-J. (2018). Endophytic fungus *Aspergillus japonicus* mediates host plant growth under normal and heat stress conditions. *BioMed Res. Int.* 2018:7696831. doi: 10.1155/2018/7696831

Ismail, Muhammad, H., Hussain, A., Iqbal, A., Khan, S. A., Khan, M. A., et al. (2021). An endophytic fungus *Gliocladium cibotii* regulates metabolic and antioxidant system of *Glycine max* and *Helianthus annuus* under heat stress. *Polish J. Environ. Stud.* 30, 1–10. doi: 10.15625/2615-9023/15888

Jackson, M. L. (2005). *Soil Chemical Analysis: Advanced Course*. Madison, WI: UW-Madison Libraries Parallel Press.

Jan, F. G., Hamayun, M., Hussain, A., Jan, G., Iqbal, A., Khan, A., et al. (2019). An endophytic isolate of the fungus *Yarrowia lipolytica* produces metabolites that ameliorate the negative impact of salt stress on the physiology of maize. *BMC Microbiol.* 19:3. doi: 10.1186/s12866-018-1374-6

Kang, S.-M., Hamayun, M., Khan, M. A., Iqbal, A., and Lee, I.-J. (2019). *Bacillus subtilis* JW1 enhances plant growth and nutrient uptake of Chinese cabbage through gibberellins secretion. *J. Appl. Bot. Food Qual.* 92, 172–178.

Kettner, J., and Dörffling, K. (1995). Biosynthesis and metabolism of abscisic acid in tomato leaves infected with *Botrytis cinerea*. *Planta* 196, 627–634.

Khan, S. A., Hamayun, M., Yoon, H., Kim, H.-Y., Suh, S.-J., Hwang, S.-K., et al. (2008). Plant growth promotion and *Penicillium citrinum*. *BMC Microbiol.* 8:231. doi: 10.1186/1471-2180-8-231

Khushdil, F., Jan, F. G., Jan, G., Hamayun, M., Iqbal, A., Hussain, A., et al. (2019). Salt stress alleviation in *Pennisetum glaucum* through secondary metabolites modulation by *Aspergillus terreus*. *Plant Physiol. Biochem.* 144, 127–134. doi: 10.1016/j.plaphy.2019.09.038

Kumar, K., Manigundan, K., and Amaresan, N. (2017). Influence of salt tolerant *Trichoderma spp.* on growth of maize (*Zea mays*) under different salinity conditions. *J. Basic Microbiol.* 57, 141–150. doi: 10.1002/jobm.201600369

Mackinney, G. (1941). Absorption of light by chlorophyll solutions. *J. Biol. Chem.* 140, 315–322.

Malik, M., and Singh, D. (1980). Analysis of finite magnetohydrodynamic journal bearings. *Wear* 64, 273–280. doi: 10.1016/0043-1648(80)90133-7

Mbarki, S., Sytar, O., Zivcak, M., Abdelly, C., Cerda, A., and Brestic, M. (2018). Anthocyanins of coloured wheat genotypes in specific response to salt stress. *Molecules* 23:1518. doi: 10.3390/molecules23071518

Mehmood, A., Hussain, A., Irshad, M., Hamayun, M., Iqbal, A., and Khan, N. (2019a). In vitro production of IAA by endophytic fungus *Aspergillus awamori* and its growth promoting activities in *Zea mays*. *Symbiosis* 77, 225–235.

Mehmood, A., Hussain, A., Irshad, M., Hamayun, M., Iqbal, A., Rahman, H., et al. (2019b). Cinnamic acid as an inhibitor of growth, flavonoids exudation and endophytic fungus colonization in maize root. *Plant Physiol. Biochem.* 135, 61–68. doi: 10.1016/j.plaphy.2018.11.029

Moghimi, A., Yang, C., Miller, M. E., Kianian, S. F., and Marchetto, P. M. (2018). A novel approach to assess salt stress tolerance in wheat using hyperspectral imaging. *Front. Plant Sci.* 9:1182. doi: 10.3389/fpls.2018.01182

Muhammad, I., Ali, N., Jan, G., Jan, F. G., Rahman, I. U., Iqbal, A., et al. (2018). IAA producing fungal endophyte *Penicillium roqueforti* Thom., enhances stress tolerance and nutrients uptake in wheat plants grown on heavy metal contaminated soils. *PLoS One* 13:e0208150. doi: 10.1371/journal.pone.0208150

Muhammad, I., Niaz, A., Gul, J., Amjad, I., Muhammad, H., Farzana, G. J., et al. (2019). *Trichoderma reesei* improved the nutrition status of wheat crop under salt stress. *J. Plant Interact.* 14, 590–602.

Nakano, Y., and Asada, K. (1981). Hydrogen peroxide is scavenged by ascorbate-specific peroxidase in spinach chloroplasts. *Plant Cell Physiol.* 22, 867–880.

Nusrat, B., Gul, J., Farzana, G. J., Muhammad, H., Amjad, I., Anwar, H., et al. (2019). *Cochliobolus sp.* acts as a biochemical modulator to alleviate salinity stress in okra plants. *Plant Physiol. Biochem.* 139, 459–469. doi: 10.1016/j.plaphy.2019.04.019

Penrose, D. M., and Glick, B. R. (2003). Methods for isolating and characterizing ACC deaminase-containing plant growth-promoting rhizobacteria. *Physiol. Plantarum* 118, 10–15. doi: 10.1034/j.1399-3054.2003.00086.x

Qadir, M., Hussain, A., Hamayun, M., Shah, M., Iqbal, A., and Murad, W. (2020). Phytohormones producing rhizobacterium alleviates chromium toxicity in *Helianthus annuus* L. by reducing chromate uptake and strengthening antioxidant system. *Chemosphere* 258:127386. doi: 10.1016/j.chemosphere.2020.127386

Raid, A., Humaira, G., Muhammad, H., Mamoona, R., Amjad, I., Mohib, S., et al. (2021). *Aspergillus awamori* ameliorates the physicochemical characteristics and mineral profile of mung bean under salt stress. *Chem. Biol. Technol. Agric.* 8, 1–13.

Schwyn, B., and Neilands, J. (1987). Universal chemical assay for the detection and determination of siderophores. *Analytical Biochem.* 160, 47–56. doi: 10.1016/0003-2697(87)90612-9

Shrivastava, P., and Kumar, R. (2015). Soil salinity: a serious environmental issue and plant growth promoting bacteria as one of the tools for its alleviation. *Saudi J. Biol. Sci.* 22, 123–131. doi: 10.1016/j.sjbs.2014.12.001

Tamura, K., Nei, M., and Kumar, S. (2004). Prospects for inferring very large phylogenies by using the neighbor-joining method. *Proc. Natl. Acad. Sci. U.S.A.* 101, 11030–11035. doi: 10.1073/pnas.0404206101

Wahyudi, A. T., Astuti, R. P., Widyawati, A., Mery, A., and Nawangsih, A. A. (2011). Characterization of *Bacillus sp.* strains isolated from rhizosphere of soybean plants for their use as potential plant growth for promoting rhizobacteria. *J. Microbiol. Antimicrobials* 3, 34–40.

Conflict of Interest: The authors declare that the research was conducted in the absence of any commercial or financial relationships that could be construed as a potential conflict of interest.

Publisher's Note: All claims expressed in this article are solely those of the authors and do not necessarily represent those of their affiliated organizations, or those of the publisher, the editors and the reviewers. Any product that may be evaluated in this article, or claim that may be made by its manufacturer, is not guaranteed or endorsed by the publisher.

Copyright © 2022 Khan, Ali, Jan, Hamayun, Jan, Iqbal, Hussain and Lee. This is an open-access article distributed under the terms of the Creative Commons Attribution License (CC BY). The use, distribution or reproduction in other forums is permitted, provided the original author(s) and the copyright owner(s) are credited and that the original publication in this journal is cited, in accordance with accepted academic practice. No use, distribution or reproduction is permitted which does not comply with these terms.

frontiers in Plant Science

ORIGINAL RESEARCH
published: 22 March 2022
doi: 10.3389/fpls.2022.861081

Physiological and Molecular Changes in Cherry Red Tobacco in Response to Iron Deficiency Stress

Fei Liu[1,2†], Yihan Zhang[1†], Xiaojun Pu[2], Nan Cai[2], Xueyi Sui[1], Zed Rengel[3,4], Qi Chen[2] and Zhongbang Song[1]*

[1] Yunnan Academy of Tobacco Agricultural Sciences, Kunming, China, [2] Faculty of Life Science and Technology, Kunming University of Science and Technology, Kunming, China, [3] UWA School of Agriculture and Environment, The University of Western Australia, Perth, WA, Australia, [4] Institute for Adriatic Crops and Karst Reclamation, Split, Croatia

The genotype CR60 is a spontaneous Cherry Red variant (containing granular red dapples on flue-cured leaves) of the Yunyan 87 (Y87) tobacco; it accumulates higher concentration of iron (Fe) in leaves than Y87, but the physiological differences between them remain largely unknown. We investigated the physiological and molecular mechanisms of CR60 in response to Fe deficiency under hydroponic conditions. Our results showed no significant phenotypic difference between Y87 and CR60 at optimal (40 μM) and high Fe (160 and 320 μM) concentrations. By contrast, CR60 exhibited higher tolerance to Fe deficiency (0 μM) than Y87, as shown by higher concentrations of chlorophyll in CR60 leaves after 21-day Fe-deficiency stress. Transcriptome profiling coupled with RT-PCR analyses found that the expression of *IRT1* and several genes associated with chlorophyll biosynthesis and photosynthesis (e.g., *PRO*, *GSA*, *FD1*, *PsbO,* and *PC*) was higher in CR60 than Y87. These results indicated that CR60 maintains sufficient Fe uptake, chlorophyll biosynthesis and photosynthetic rate when subjected to Fe starvation.

Keywords: tobacco, Cherry Red, chlorophyll, iron deficiency, transcriptome

OPEN ACCESS

Edited by:
Jian Li Yang,
Zhejiang University, China

Reviewed by:
Nannan Li,
Southwest University, China
Wei Wei Chen,
Hangzhou Normal University, China

***Correspondence:**
Zhongbang Song
zbsoon@vip.163.com

† These authors have contributed equally to this work

Specialty section:
This article was submitted to Plant Biotechnology, a section of the journal Frontiers in Plant Science

Received: *24 January 2022*
Accepted: *22 February 2022*
Published: *22 March 2022*

Citation:
Liu F, Zhang Y, Pu X, Cai N, Sui X, Rengel Z, Chen Q and Song Z (2022) Physiological and Molecular Changes in Cherry Red Tobacco in Response to Iron Deficiency Stress. Front. Plant Sci. 13:861081. doi: 10.3389/fpls.2022.861081

INTRODUCTION

Iron (Fe) is an essential plant micronutrient. The main valence forms are Fe (II) and Fe (III) (Ilbert and Bonnefoy, 2013). Although the total iron concentration in soils is high, it exists mostly in the oxidized Fe (III) form in aerated soils; this form is not directly plant-available (Guerinot and Yi, 1994; Briat et al., 2015). Plants have evolved two different molecular strategies to obtain sufficient Fe from the rhizosphere to adapt to the low-Fe environments. Dicots and non-graminaceous monocots have evolved different Fe uptake mechanisms (strategy I) (Romheld and Marschner, 1986; Hell and Stephan, 2003; Kobayashi and Nishizawa, 2012) compared with graminaceous plants (strategy II) (Romheld and Marschner, 1986; Connorton et al., 2017). Strategy I plants (such as tobacco) secrete phenolic compounds *via* phenolics efflux transporters and pump H^+ out into the rhizosphere *via* the plasma membrane H^+-ATPase, thus increasing iron solubility by chelation and contributing to Fe^{3+} reduction *via* acidification (Kim and Guerinot, 2007). Upon transfer of the dissolved Fe^{3+} from the rhizosphere to the root surface, ferric chelate reductase (FRO) reduces it to Fe^{2+} (Robinson et al., 1999), and then Fe^{2+} is absorbed into root cells by high-affinity iron-regulated transporters (IRTs) (Eide et al., 1996; Vert et al., 2002; Brumbarova et al., 2015).

Cellular iron combines with various organic substances as a structural/functional component, such as in cytochromes, catalase, peroxidases, heme, ferredoxin, and iron-sulfur clusters (Balk and Schaedler, 2014; Vigani and Murgia, 2018); these compounds are essential in chlorophyll synthesis, oxygen transport, redox reactions, nitrogen assimilation, photosynthesis, and electron transport in plants (Balk and Schaedler, 2014). For example, heme, cytochrome, iron-sulfur clusters, and ferredoxin are key components of the photosynthesis system and contribute to the photosynthetic and respiratory electron transport chains (Sousa et al., 2018; Kroh and Pilon, 2020). Therefore, iron deficiency not only leads to the inhibition of chlorophyll synthesis and diminished photosynthetic efficiency (Nelson and Ben-Shem, 2004; Msilini et al., 2011), but also results in the interruption of the respiratory electron transport in plant mitochondria and tricarboxylic acid cycle metabolism, hampering plant growth (Fernie et al., 2004).

Flue-cured leaves from common commercial tobacco [e.g., Yunyan87 (Y87)] usually display yellow appearance. However, a type of spontaneous variant that originated from flue-cured varieties has a reddish hue in flue-cured leaves and has historically been referred to as Cherry Red tobacco (Wada, 1956; Hall et al., 1965). It is reported that Cherry red leaves contain high levels of nornicotine as the principal alkaloid, whereas nicotine is the principal alkaloid in common tobacco with flue-cured yellow leaves (Wada, 1956; Hall et al., 1965). Compared with the common tobacco, high concentrations of nornicotine in the Cherry Red tobacco leaves are associated with a strong expression of nicotine *N*-demethylase gene *CYP82E4*, which plays a key role in nicotine to nornicotine conversion (Siminszky et al., 2005). Nornicotine was suggested to be a substrate reacting with *o*-quinones (produced by oxidation of chlorogenic acid and caffeic acid by polyphenol oxidase) to generate red color (570 nm wavelength) in Cherry Red tobacco (Weeks et al., 1993).

During several years of field observations, we identified a spontaneous Cherry Red variant (CR60) that originated from flue-cured cultivar Yunyan87 (Y87). In CR60, the *CYP82E4* expression was activated by an unknown mechanism, resulting in significantly increased accumulation of nornicotine in leaves (Song et al., 2021), similarly to the previous report (Siminszky et al., 2005). However, apart from *CYP82E4* expression and correspondingly high levels of nornicotine, the growth characteristics and physiological/molecular properties of CR60 are largely unknown.

In this study, we found that CR60 accumulates higher concentrations of iron in comparison with Y87 under field conditions, implying the difference in iron uptake and transport between the two genotypes. Therefore, we further analyzed the physiological and molecular changes in CR60 and Y87 exposed to different concentrations of iron under hydroponic conditions. The results showed that CR60 exhibited higher iron deficiency tolerance than Y87, which might be attributed to higher expression of several genes associated with iron uptake, chlorophyll biosynthesis and electron transport chain in the photosynthetic system of CR60.

MATERIALS AND METHODS

Plant Growth and Treatment

Seeds of CR60 and Y87 were germinated in a mixture (vermiculite:perlite:peat soil = 1:1:1, v:v:v) at 22°C under cool white light (100 μmol m^{-2} s^{-1}) with the 12-h-light/12-h-dark cycle. Ten days after germination, the seedlings were transferred to pots containing 1 L of 1/2-strength Hoagland nutrient solution (pH 6.0) with 40 μM Fe (III)-EDTA. After 3 days of recovery growth, the seedlings were transferred to fresh 1/2-strength Hoagland nutrient solution (pH 6.0) with different treatment concentrations of Fe (III)-EDTA (0, 40, 160, and 320 μM). The nutrient solutions were replaced every 2 days.

Measurement of Chlorophyll Contents

Chlorophyll was extracted from the first fully extended mature leaves (0.1 g) using dimethyl sulfoxide (DMSO, 1.5 mL) at 65°C under dark. Then, 8 mL acetone was added and mixed thoroughly. After centrifugation at 12,000 *g* at 4°C for 20 min, the supernatant was used for measurement of chlorophylls *a* and *b* using a spectrophotometer at 663 and 646 nm, respectively. The concentrations of chlorophylls *a* and *b* and total chlorophyll were calculated as described elsewhere (Hiscox and Israelstam, 1980; Lichtenthaler and Buschmann, 2001).

Total RNA Isolation, Library Construction and RNA Sequencing

Total RNA was isolated from the first fully expanded apical leaves of tobacco using the Trizol Reagent (Invitrogen, United States). A total amount of 1 μg RNA per sample was used as input material for the RNA-Seq sample preparations. Sequencing libraries were generated using a NEBNext® Ultra™ RNA Library Prep Kit for Illumina (NEB, United States) following the manufacturer's instructions. The mRNA was purified from total RNA using poly-T oligo-attached magnetic beads. Fragmentation was carried out using divalent cations under elevated temperature in the NEBNext First Strand Synthesis Reaction Buffer (5X). The first strand of cDNA was synthesized using the fragmented mRNA as a template and random oligonucleotides as primers in a M-MuLV reverse transcriptase system, followed by the degradation of the RNA strand by RNase H. The second strand of cDNA was synthesized using dNTPs in a DNA polymerase I system. The purified double-stranded cDNA was end repaired and A-tailed, sequencing adaptors were ligated, and approximately 200 bp of cDNA was screened with AMPure XP beads (Beckman Coulter, Beverly, MA, United States). After PCR amplification, the PCR products were purified with AMPure XP beads, and the library was obtained. Library quality was assessed on an Agilent Bioanalyzer 2,100 system. Twelve libraries named Y87_0 and CR60_0 (0 μM Fe) and Y87_40 and CR60_40 (40 μM Fe), each in three biological replicates (A, B, and C), were constructed. The libraries were then sequenced on an Illumina Novaseq platform, and 150 bp paired-end reads were generated. The experiments were conducted three times. The RNA sequence dataset is available in the repository of NCBI Sequence Read

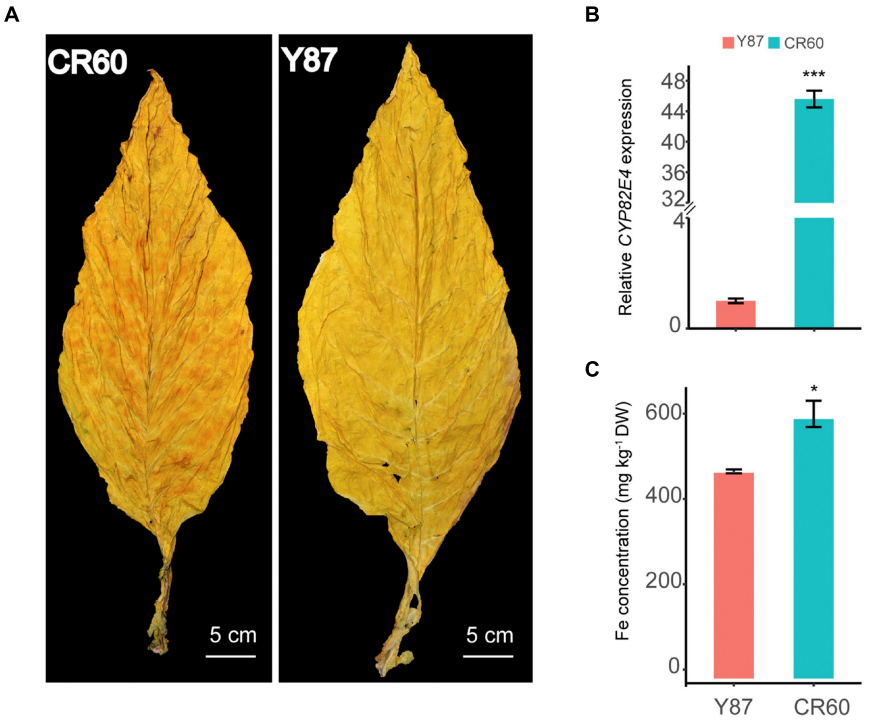


FIGURE 1 | Differential appearance of flue-cured leaves **(A)**, expression of *CYP82E4* gene **(B)** and Fe concentrations **(C)** in leaves of CR60 and Y87. The plants were cultivated in an experimental field located at the Yanhe Research Farm of Yunnan Academy of Tobacco Agricultural Sciences, Yunan Province, China (N24.14, E102.30, altitude 1,680 m). For panel **(A)** the matured leaves were harvested and flue-cured following local agricultural practices. For panel **(B)**, leaves at stalk position #10 (from top to bottom) of 2-month-old plants were harvested for RNA isolation. For panel **(C)** the 5th to 10th (from top to bottom) leaves were flue-cured and mixed for ICP-MS analysis. Three biological replicates were analyzed. Values are means ± SD ($n = 3$). Asterisks indicate significant differences between the CR60 and Y87 plants (*$P < 0.05$ and ***$p < 0.001$) as determined by the Student's *t*-test.

Archive (SRA) with the GeneBank accession No.: PRJNA807089 (https://www.ncbi.nlm.nih.gov/sra/?term=PRJNA807089).

Bioinformatic Analysis

High-quality clean reads were obtained by removing the adaptor sequences, unclear "N" nucleotides and low-quality sequences from raw reads. HISAT2 (v2.0.5) software was used to establish the index of the tobacco reference genome and align the clean reads to the tobacco reference genome (Mortazavi et al., 2008).

The featureCounts (v1.5.0-p3) was used to count the reads numbers mapped to each gene (Liao et al., 2014). The gene expression levels were represented by the expected number of Fragments Per Kilobase of transcript sequence per Million base pairs sequenced (FPKM), which was calculated on the length of the gene and the reads count mapped to this gene. Differential expression analyses were performed using the DESeq2 R package (v1.16.1). Genes with an adjusted *P*-value < 0.05 and $|\log2(\text{FoldChange})| > 0$ were considered to be differentially expressed. The Padj values were adjusted using the Benjamini and Hochberg method for controlling the false discovery rate (FDR). Gene Ontology (GO) and KEGG enrichment analysis of differentially expressed genes was implemented by the clusterProfiler and ggplot2 R packages (v3.4.4). The GO and KEGG terms with corrected *P*-value < 0.05 were considered significantly enriched in differentially expressed genes.

Reverse Transcription-Polymerase Chain Reaction Analysis

Total RNA was extracted using RNAiso Plus (Takara, Da Lian, China) according to the manufacturer's instructions. Reverse transcription was performed using a PrimeScript RT reagent kit with gDNA eraser (Takara) following the manufacturer's instructions. Quantitative PCR reactions were performed in 20 μL reaction volumes using a SYBR Premix EX Taq II Kit (Takara) according to the manufacturer's instructions. The primers used in this study are listed in **Supplementary Table 1**.

RESULTS

CR60 Leaves Accumulate High Concentrations of Iron

Granular red dapples were observed on leaves of CR60, but not in Y87 after curing (**Figure 1A**). Additionally, the expression of *CYP82E4*, a key gene involved in the conversion of nicotine to nornicotine (Siminszky et al., 2005), was significantly higher in CR60 than Y87 (**Figure 1B**). In field conditions, CR60 and Y87

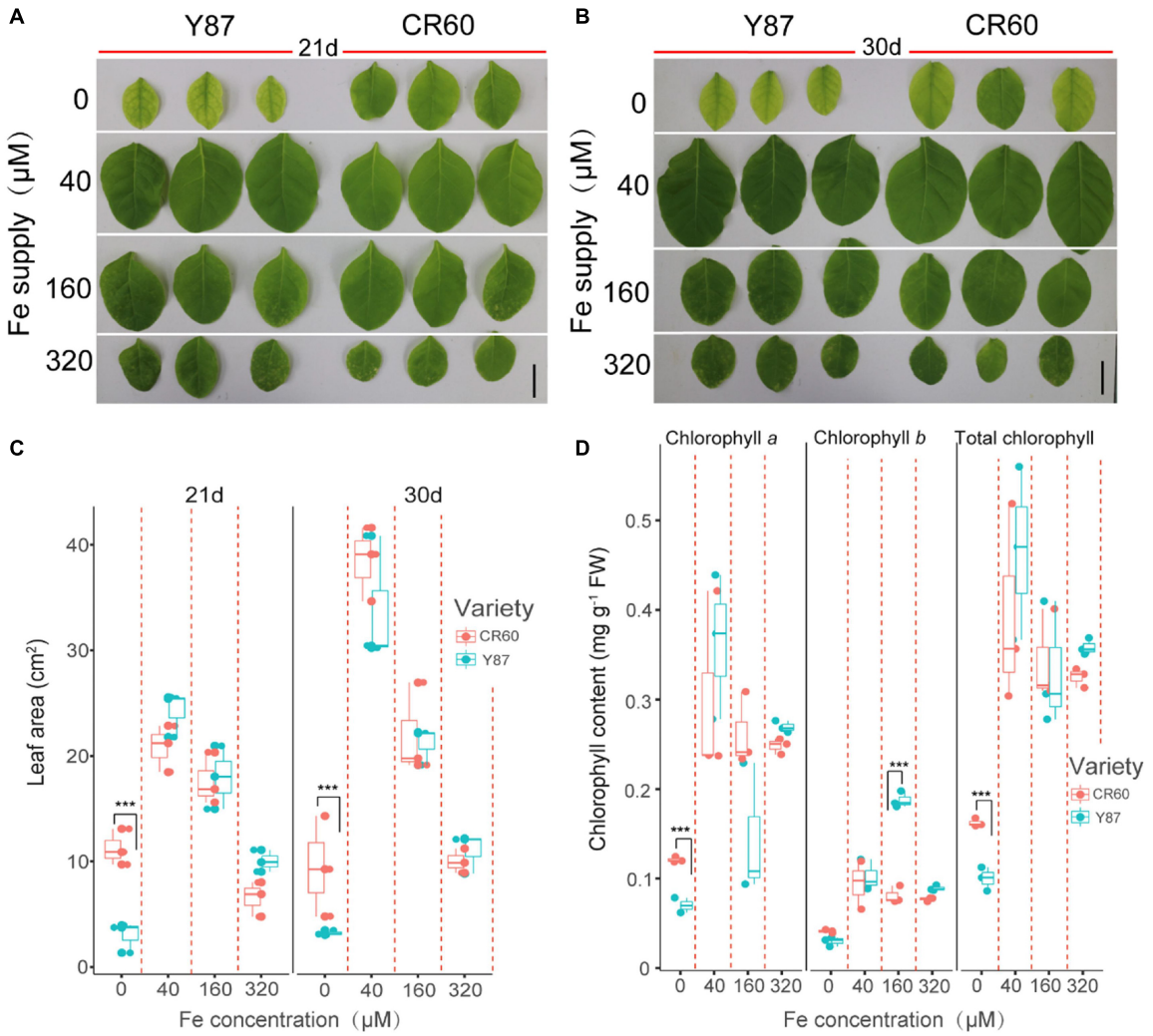


FIGURE 2 | CR60 had higher iron deficiency tolerance than Y87. Images **(A,B)**, leaf area **(C)** and chlorophyll concentrations **(D)** of the first fully expanded apical leaves of CR60 and Y87 after growing at different nutrient solution concentrations of iron (0, 40, 160, and 320 μM) for 21 and 30 days. The experiment was conducted at least three times and showed similar results. For panels **(C,D)** data were collected from plants grown at differential iron supply for 21 days and were expressed as means ± SD (n = 3). Asterisks indicate statistically significant differences between CR60 and Y87 (***$p < 0.001$) as determined by the Student's t-test.

did not show obvious differences in plant height, root length, leaf number, and biomass (data not shown); however, higher concentrations of iron were recorded in CR60 leaves compared with Y87 (**Figure 1C**).

CR60 Showed Higher Iron Deficiency Tolerance Than Y87

We then examined the physiological responses of CR60 and Y87 to differential supply of iron under hydroponic conditions. High solution concentrations of iron (160 and 320 μM) inhibited leaf growth of CR60 and Y87, but there were no significant differences between these two genotypes (**Figures 2A–C**). By contrast, the first fully expanded apical leaves of Y87 exhibited obvious interveinal chlorosis after stressed by iron deficiency for 21 and 30 days, whereas CR60 plants developed larger leaf area and greener first expanded leaves than Y87 under the same stress (**Figures 2A–C**). In accordance with these observations, concentrations of chlorophyll *a* and the total chlorophyll in the first fully expanded apical leaves of CR60 were, respectively, 42 and 44% higher than those in Y87 after the plants were stressed by iron deficiency for 21 days (**Figure 2D**).

Differentially Expressed Genes Analysis of CR60 and Y87 Between Optimal and Deficient Iron Supply

Given the different changes in the first fully expanded leaves between CR60 and Y87 under iron deficiency conditions, we performed RNA sequencing (RNA-seq) to compare the transcriptome changes in the two genotypes under optimal and iron deficiency conditions. Iron deficiency treatment

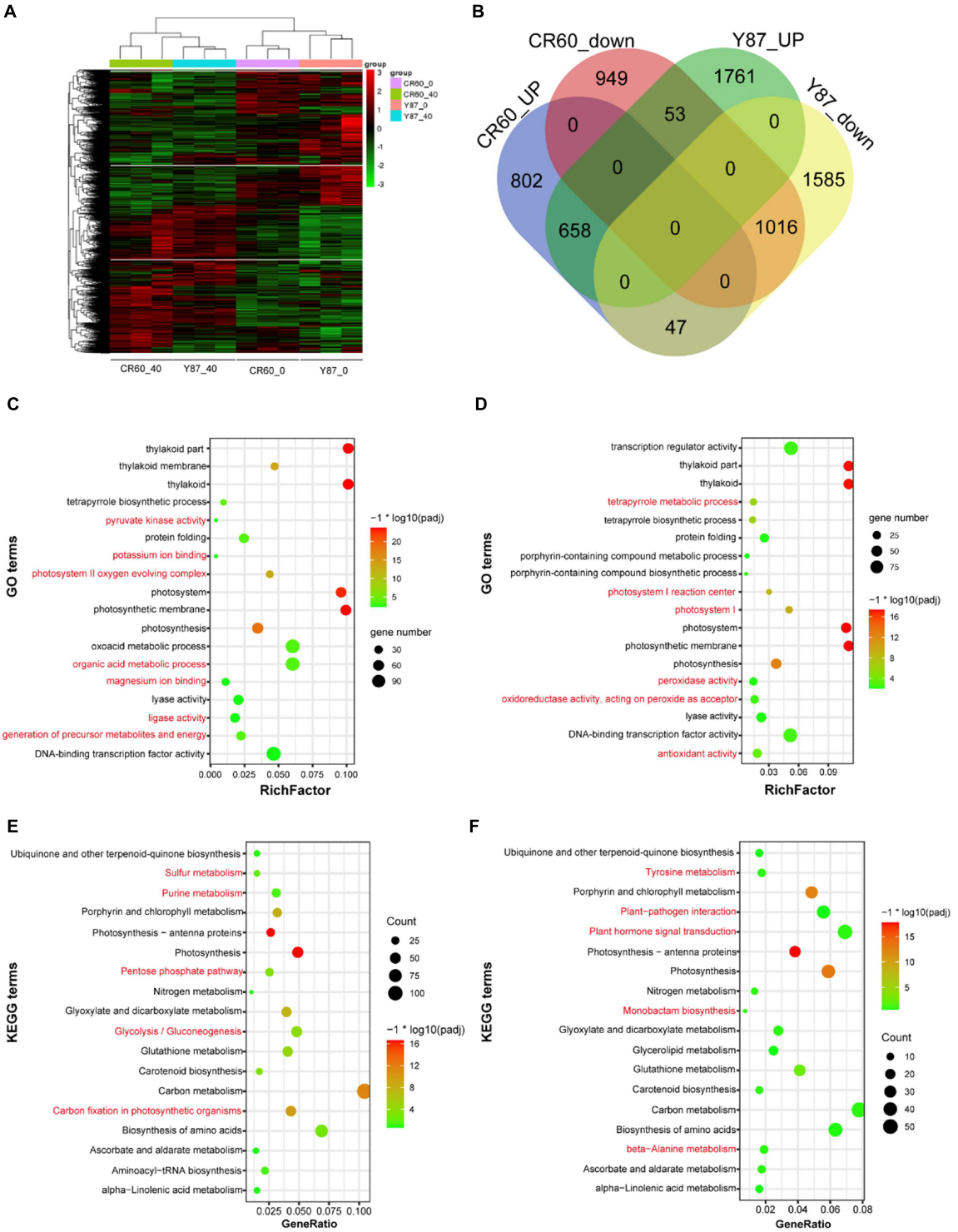


FIGURE 3 | Transcriptome profiling of CR60 and Y87 in response to iron deficiency. **(A)** Hierarchical cluster analysis of differentially expressed genes (DEGs) of CR60 and Y87 under optimal and iron deficiency conditions (n = 3). **(B)** Venn diagram showing upregulated and downregulated DEGs in CR60 and Y87 stressed by iron deficiency for 21 days compared with plants grown under optimal conditions (n = 3). The GO (Gene Ontology) enrichments of DGEs in Y87 **(C)** and CR60 **(D)**. The KEGG (Kyoto Encyclopedia of Genes and Genomes) enrichments of DGEs in Y87 **(E)** and CR60 **(F)**. Plants were grown hydroponically in 1/2 Hoagland nutrient solutions containing 0 or 40 μM Fe (III)-EDTA for 21 days. The first fully expanded apical leaves were harvested for RNA isolation and RNAseq analysis (n = 3).

triggered extensive transcriptome changes in both CR60 and Y87 (**Figure 3A**). Compared with plants grown under optimal conditions [40 μM Fe (III)-EDTA], iron deficiency [0 μM Fe (III)-EDTA] upregulated 1,507 (43%) and 2,472 (48%) differentially expressed genes (DEGs) in CR60 and Y87, respectively, whereas 2018 (57%) and 2648 (52%) DGEs were downregulated, respectively (**Figure 3B**). The DGEs showed similar patterns in both CR60 and Y87, and were highly related to photosynthesis, chlorophyll metabolism, carbon metabolism, plant hormone signaling, and peroxidase and oxidoreductase activity (**Figures 3C–F** and **Supplementary Tables 2–5**).

Iron Starvation Regulated Gene Expression Differently in CR60 and Y87

Under optimal growth conditions [40 μM Fe (III)-EDTA], 1,712 differentially expressed genes (DEGs) were identified in CR60 in comparison with Y87, out of which 1,192 (69.6%) were upregulated and 520 (30.4%) were downregulated (**Figure 4A**). These DEGs were involved mostly in plant pathogen interaction, MAPK signaling, endocytosis, sugar metabolism, and plant hormone signaling (**Figure 4B**). Under Fe deficiency conditions, 902 (52.4%) upregulated DEGs and 820 (47.6%) downregulated DEGs were found in CR60 in comparison with Y87 (**Figure 4A**). The DEGs upregulated by iron deficiency were enriched predominantly in photosynthesis (numbers of KEGG terms increased from three to 57), photosynthetic antenna proteins, carbon metabolism, starch and sucrose metabolism, glyoxylate and dicarboxylate metabolism, and purine metabolism (**Figure 4C**).

Expression Profiles of Genes Associated With Iron Uptake and Homeostasis

The expression of *IRT1* (a high-affinity Fe^{2+}-transporter) and *NRAMP3* (natural resistance-associated macrophage protein 3) was induced, but *Fer1* (ferritin 1, coding for Fe storage protein) was downregulated by Fe deficiency in leaves and roots of Y87 and CR60 (**Figures 5A,B**). The upregulation of *FRO2* (a ferric-chelate reductase) and *FRO8* in roots or *NRAMP1* in leaves of Y87 and CR60 was observed. Although the expression of *IRT1* in leaves did not show significant difference between Y87 and CR60 under normal growth conditions, its expression was significantly higher in CR60 roots than Y87 roots under Fe deficiency conditions (**Figures 5A,B**). Additionally, *Fer1* showed higher expression in CR60 than Y87 leaves at optimal Fe concentration (**Figures 5A,B**).

Expression Profiles of Genes Associated With Chlorophyll Biosynthesis and Photosynthesis

Several genes encoding key enzymes involved in chlorophyll metabolism, including *NYC1* (chlorophyll *b* reductase) and *POR* (protochlorophyllide oxidoreductase) were reduced slightly by iron deficiency, and the relative expression of these two genes was higher in CR60 than Y87 (**Figure 6A**). The expression of *COX15* (cytochrome c oxidase assembly protein) was higher in CR60 than Y87 under optimal growth conditions; by contrast, *COX15* was decreased by Fe deficiency in CR60, but increased in Y87. Additionally, the expression of *GSA* (glutamate 1-semialdehyde aminotransferase) in leaves was higher in CR60 than Y87 under both optimal and Fe deficiency conditions.

The expression of several genes associated with photosystems I and II and the electron transport chain was also analyzed (**Figure 6B**). The expression of *PsbO* (encoding the photosystem II manganese-stabilizing protein), *PC* (encoding plastocyanin),

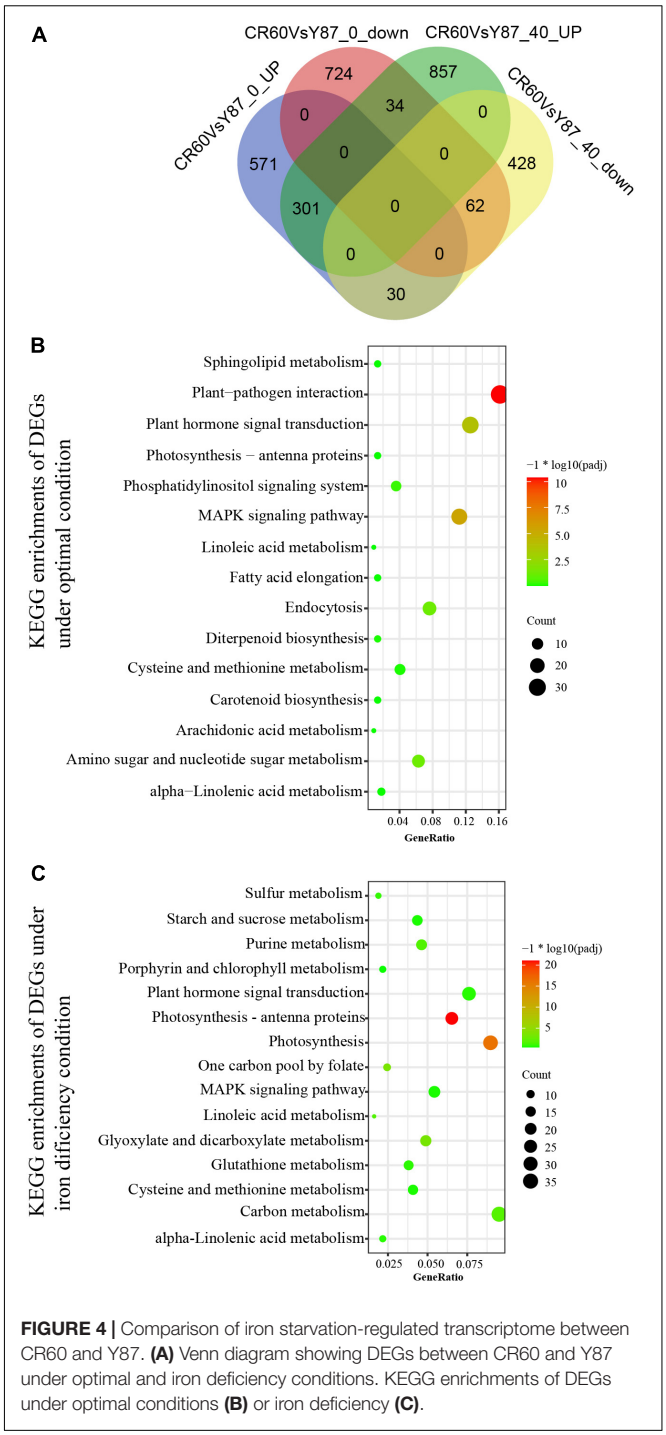


FIGURE 4 | Comparison of iron starvation-regulated transcriptome between CR60 and Y87. **(A)** Venn diagram showing DEGs between CR60 and Y87 under optimal and iron deficiency conditions. KEGG enrichments of DEGs under optimal conditions **(B)** or iron deficiency **(C)**.

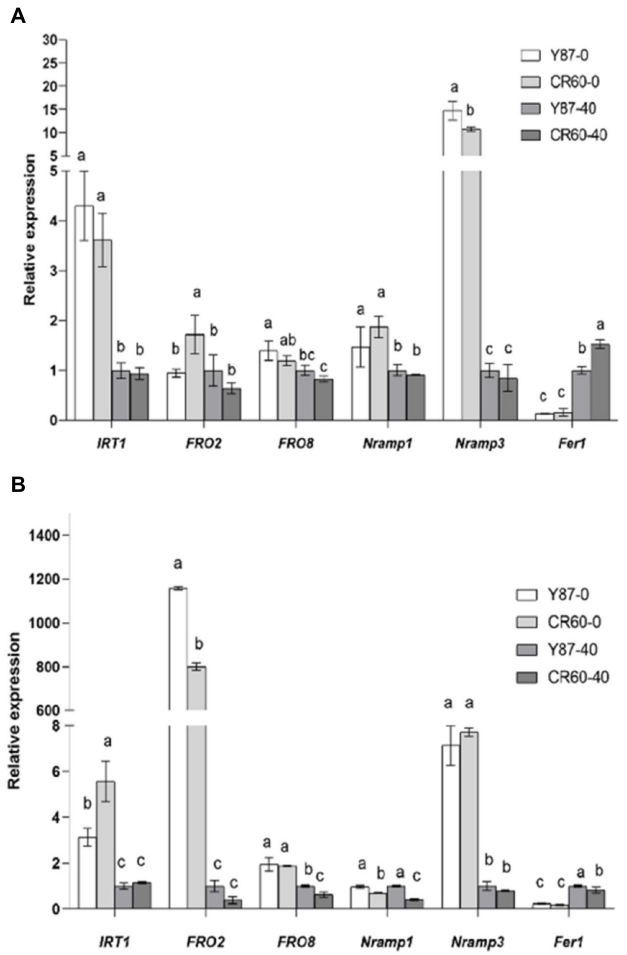


FIGURE 5 | Relative expression of genes associated with iron uptake and homeostasis in leaves **(A)** and roots **(B)** of Y87 and CR60. The plants were grown in 1/2 Hoagland nutrient solutions containing 0 or 40 μM Fe (III)-EDTA for 21 days. The first fully expanded apical leaves or whole roots were harvested for RNA isolation and RT-PCR analysis. The data are expressed as means ± SD (n = 6). Different letters indicate significant differences at $P < 0.05$ (Student's t-test).

PsaE (encoding photosystem I reaction center subunit IV), and *FD1* (encoding ferredoxin 1) was decreased by Fe deficiency in Y87 leaves, whereas the expression of these genes (*PsbO*, *PC*, and *PsaE*) was unaffected in CR60 under Fe deficiency. The expression of *ATPase subunit II* was significantly increased by Fe deficiency in CR60. Additionally, the expression of *PsbO*, *PC*, *FD1*, *ATPase subunit II*, and *ATPase subunit alpha* (*ATP1A1*) was higher in CR60 than Y87 under Fe deficiency (**Figure 6B**).

DISCUSSION

As a micronutrient, iron plays an irreplaceable role in regulating plant growth and metabolism (Kobayashi and Nishizawa, 2012). Iron is involved in chlorophyll synthesis and serves as a cofactor in numerous enzymes (Balk and Schaedler, 2014; Kroh and Pilon, 2020). It has long been known that the photosynthetic capacity of higher plants is affected by iron deficiency. The primary response associated with the insufficient availability of iron is the loss of chlorophyll and interveinal chlorosis of young leaves (Miller et al., 2008). In this work, we found that the first fully expanded apical leaves of Y87 exhibited an obvious interveinal chlorosis after 21 days of iron deficiency treatments; by contrast, CR60 remained green and contained high concentrations of chlorophyll, indicating that CR60 is more tolerant to iron deficiency stress than Y87 (**Figure 2**). A comparative transcriptome analysis between CR60 and Y87 further showed that the differences in chlorophyll synthesis and photosynthesis might be responsible for their phenotypic differences (**Figures 3C–F**, **4B,C**).

Iron uptake and translocation are tightly regulated by its transport- and homeostasis-related genes in plants. In strategy I plants (e.g., tobacco), ferric-chelate reductase (FCR) catalyzes the reduction of Fe^{3+} to Fe^{2+}, which is then assimilated into root cells *via* the high-affinity metal transporter IRT1 (iron-regulated transporter 1) (Eide et al., 1996; Robinson et al., 1999; Vert et al., 2002; Santi and Schmidt, 2009). NRAMP3 is a vacuolar metal transporter involved in homeostasis and transport of divalent metals (e.g., Fe^{2+}, Mn^{2+} and Cd^{2+}) (Thomine et al., 2003). Additionally, ferritin localized in plastids of plant leaves is an iron storage protein, and the expression of *ferritin 1* (*Fer1*) is induced by iron application in arabidopsis (Ravet et al., 2009). In this study, we found that the expression of *FRO2* and *FRO8*, two genes encoding ferric-chelate reductase, were induced in roots of both genotypes by Fe deficiency (**Figure 5B**). Additionally, *IRT1* and *NRAMP3* were also upregulated by Fe starvation in both leaves and roots of the two genotypes, whereas the expression of *IRT1* was higher in roots of CR60 than Y87 (**Figure 5B**). Iron deficit reduced the expression of *Fer1* in leaves of both CR60 and Y87, but no significant difference was found between the two genotypes (**Figure 5A**). These results indicate CR60 and Y87 share similar responses regarding Fe^{3+} reduction and iron storage under iron deficiency. The higher leaf accumulation of Fe in CR60 than Y87 (**Figure 1B**) might be attributed to higher expression of *IRT1* in roots of CR60 than Y87 during Fe starvation (**Figure 5B**), which contributed to greater tolerance to iron deficiency stress in CR60 compared with Y87. In tomato plants, iron affects the expression of *SlIRT1 via* modulation of the DNA methylation of its promoter (Chen et al., 2022). Therefore, investigating whether epigenetic modulation is also involved in iron-mediated changes in the expression of these genes in tobacco is warranted.

Iron is required not only for chlorophyll biosynthesis and the maintenance of chloroplast structure and function, but also serves as an important component of cytochromes in the electron transport chain. Approximately 80% of iron is located in photosynthesizing cells and is directly required for the structural and functional integrity of thylakoid membrane and the biosynthesis of chlorophyll (Li et al., 2021). Visible chlorosis (a decrease in chlorophyll concentration) was found in Y87 leaves stressed by Fe deficiency for 21 days (**Figures 2A,D**), indicating that Fe starvation affected the

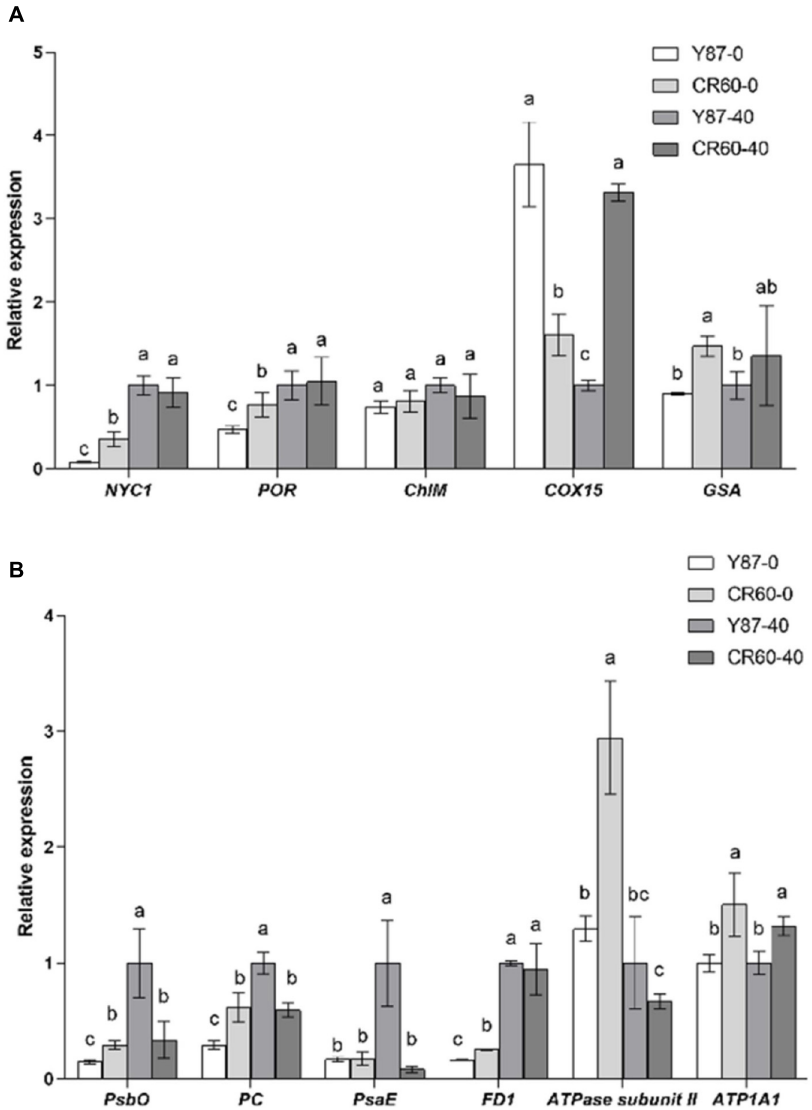


FIGURE 6 | Expression of genes associated with chlorophyll synthesis **(A)** and photosynthesis **(B)** in the first fully expanded apical leaves of Y87 and CR60. The plants were grown in 1/2 Hoagland nutrient solutions containing 0 or 40 μM Fe (III)-EDTA for 21 days. The data are expressed as means ± SD (n = 3). Different letters indicate significant differences at $P < 0.05$ (Student's t-test).

biosynthesis of chlorophyll. In contrast, CR60 developed larger leaf area, remained greener and contained higher chlorophyll concentrations than Y87 after 21 days of Fe deficiency (**Figures 2B–D**). Congruent with these observations, our transcriptome and RT-PCR results showed that a large number of genes associated with photosynthesis, PS-I/II and chlorophyll metabolism were regulated by Fe deficiency (**Figures 3**, **4**, **6** and **Supplementary Tables 2–5**). More specifically, the expression of *NYC1*, *PRO*, and *GSA*, key genes involved in the biosynthesis of chlorophyll and heme, was significantly higher in CR60 than Y87 under iron deficiency stress (**Figure 6A**), which was in accordance with higher chlorophyll concentrations measured in CR60 than Y87 (**Figure 2D**). Although iron starvation decreased the expression of *PsbO*, *PC,* and *FD1* (all associated with the electron transfer chain in the photosynthetic system), the relative expression of these genes was significantly higher in CR60 than Y87 (**Figure 6B**). Additionally, the *ATPase subunit II* expression was induced by iron deficiency and was higher in CR60 than Y87. These results suggested that CR60 maintained greater chlorophyll biosynthesis and had higher photosynthetic rate under Fe starvation than Y87.

CONCLUSION

The CR60 showed higher tolerance to iron deficiency than Y87, as shown by significant differences in leaf growth and chlorophyll

concentrations after 21 days of iron deficiency. The expression of *IRT1* and several genes associated with chlorophyll biosynthesis (e.g., *NYC1*, *PRO*, and *GSA*) and the electron transport chain in photosynthesis (e.g., *PsbO*, *PC*, *FD1*, *ATPase subunit II*, and *ATP1A1*) was higher in CR60 than Y87, which could at least partially explain greater tolerance to Fe starvation in CR60 than Y87. Furthermore, our preliminary data showed that the concentrations of iron in CR60 leaves was correlated positively with the development of granular red dapples, indicating iron might be also related to the formation of Cherry Red leaves. Therefore, whether and how iron regulates the formation of Cherry Red tobacco are questions worth investigating in the future studies.

DATA AVAILABILITY STATEMENT

The data presented in the study are deposited in the National Center for Biotechnology Information (NCBI) Sequence Read Archive (SRA), accession number PRJNA807089.

AUTHOR CONTRIBUTIONS

ZS conceived this study, analyzed the data, and wrote and revised the manuscript. FL and YZ performed the experiments, analyzed the data, and wrote the manuscript. XP, NC, and XS analyzed the data and revised the manuscript. ZR and QC analyzed the data, interpreted the results, and revised the manuscript. All authors contributed to the article and approved the submitted version.

FUNDING

This work was supported by the Yunnan Academy of Tobacco Agricultural Sciences (Grant No. YNTC-2020530000241002).

SUPPLEMENTARY MATERIAL

The Supplementary Material for this article can be found online at: https://www.frontiersin.org/articles/10.3389/fpls.2022.861081/full#supplementary-material

Supplementary Table 1 | Primers used in this study.

Supplementary Table 2 | List of GO terms of CR60 under iron deficiency conditions.

Supplementary Table 3 | List of GO terms of Y87 under iron deficiency conditions.

Supplementary Table 4 | List of KEGG terms of CR60 under iron deficiency conditions.

Supplementary Table 5 | List of KEGG terms of Y87 under iron deficiency conditions.

REFERENCES

Balk, J., and Schaedler, T. A. (2014). Iron cofactor assembly in plants. *Annu. Rev. Plant Biol.* 65, 125–153. doi: 10.1146/annurev-arplant-050213-035759

Briat, J. F., Dubos, C., and Gaymard, F. (2015). Iron nutrition, biomass production, and plant product quality. *Trends Plant Sci.* 20, 33–40. doi: 10.1016/j.tplants.2014.07.005

Brumbarova, T., Bauer, P., and Ivanov, R. (2015). Molecular mechanisms governing Arabidopsis iron uptake. *Trends Plant Sci.* 20, 124–133. doi: 10.1016/j.tplants.2014.11.004

Chen, W. W., Zhu, H. H., Wang, J. Y., Han, G. H., Huang, R. N., Hong, Y. G., et al. (2022). Comparative physiological and transcriptomic analyses reveal altered Fe-deficiency fesponses in tomato epimutant colorless non-ripening. *Front. Plant Sci.* 12:796893. doi: 10.3389/fpls.2021.796893

Connorton, J. M., Balk, J., and Rodriguez-Celma, J. (2017). Iron homeostasis in plants - a brief overview. *Metallomics* 9, 813–823. doi: 10.1039/c7mt00136c

Eide, D., Broderius, M., Fett, J., and Guerinot, M. L. (1996). A novel iron-regulated metal transporter from plants identified by functional expression in yeast. *Proc. Natl. Acad. Sci. U. S. A.* 93, 5624–5628. doi: 10.1073/pnas.93.11.5624

Fernie, A. R., Carrari, F., and Sweetlove, L. J. (2004). Respiratory metabolism: glycolysis, the TCA cycle and mitochondrial electron transport. *Curr. Opin. Plant Biol.* 7, 254–261. doi: 10.1016/j.pbi.2004.03.007

Guerinot, M. L., and Yi, Y. (1994). Iron: nutritious, noxious, and not readily available. *Plant Physiol.* 104, 815–820. doi: 10.1104/pp.104.3.815

Hall, J. L., Weybrew, J. A., and Mann, T. J. (1965). Conversion of nicotine to nornicotine in grafts between cherry-red tobacco and related materials. *Plant Physiol.* 40, 45–48. doi: 10.1104/pp.40.1.45

Hell, R., and Stephan, U. W. (2003). Iron uptake, trafficking and homeostasis in plants. *Planta* 216, 541–551. doi: 10.1007/s00425-002-0920-4

Hiscox, J., and Israelstam, G. (1980). Erratum: a method for the extraction of chlorophyll from leaf tissue without maceration. *Can. J. Bot.* 58, 403–403. doi: 10.1139/b80-044

Ilbert, M., and Bonnefoy, V. (2013). Insight into the evolution of the iron oxidation pathways. *Biochim. Biophys. Acta* 1827, 161–175. doi: 10.1016/j.bbabio.2012.10.001

Kim, S. A., and Guerinot, M. L. (2007). Mining Iron: iron uptake and transport in plants. *FEBS Lett.* 581, 2273–2280. doi: 10.1016/j.febslet.2007.04.043

Kobayashi, T., and Nishizawa, N. K. (2012). Iron uptake, translocation, and regulation in higher plants. *Annu. Rev. Plant Biol.* 63, 131–152. doi: 10.1146/annurev-arplant-042811-105522

Kroh, G. E., and Pilon, M. (2020). Regulation of iron homeostasis and use in chloroplasts. *Int. J. Mol. Sci.* 21:3395. doi: 10.3390/ijms21093395

Li, J., Cao, X., Jia, X., Liu, L., Cao, H., Qin, W., et al. (2021). Iron deficiency leads to chlorosis through impacting chlorophyll synthesis and nitrogen metabolism in *Areca catechu* L. *Front. Plant Sci.* 12:710093. doi: 10.3389/fpls.2021.710093

Liao, Y., Smyth, G. K., and Shi, W. (2014). Feature counts: an efficient general purpose program for assigning sequence reads to genomic features. *Bioinformatics* 30, 923–930. doi: 10.1093/bioinformatics/btt656

Lichtenthaler, H. K., and Buschmann, C. (2001). Chlorophylls and carotenoids: measurement and characterization by UV-VIS spectroscopy. *Curr. Protoc. Food Anal. Chem.* 1, F4.3.1–F4.3.8. doi: 10.1002/0471142913.faf0403s01

Miller, G. W., Pushnik, J. C., and Welkie, G. W. (2008). Iron chlorosis, a world wide problem, the relation of chlorophyll biosynthesis to iron. *J. Plant Nutr.* 7, 1–22. doi: 10.1080/01904168409363172

Mortazavi, A., Williams, B. A., McCue, K., Schaeffer, L., and Wold, B. (2008). Mapping and quantifying mammalian transcriptomes by RNA-Seq. *Nat. Methods* 5, 621–628. doi: 10.1038/nmeth.1226

Msilini, N., Zaghdoudi, M., Govindachary, S., Lachaal, M., Ouerghi, Z., and Carpentier, R. (2011). Inhibition of photosynthetic oxygen evolution and electron transfer from the quinone acceptor QA- to QB by iron deficiency. *Photosynth. Res.* 107, 247–256. doi: 10.1007/s11120-011-9628-2

Nelson, N., and Ben-Shem, A. (2004). The complex architecture of oxygenic photosynthesis. *Nat. Rev. Mol. Cell Biol.* 5, 971–982. doi: 10.1038/nrm1525

Ravet, K., Touraine, B., Boucherez, J., Briat, J. F., Gaymard, F., and Cellier, F. (2009). Ferritins control interaction between iron homeostasis and oxidative

stress in Arabidopsis. *Plant J.* 57, 400–412. doi: 10.1111/j.1365-313X.2008.03698.x

Robinson, N. J., Procter, C. M., Connolly, E. L., and Guerinot, M. L. (1999). A ferric-chelate reductase for iron uptake from soils. *Nature* 397, 694–697. doi: 10.1038/17800

Romheld, V., and Marschner, H. (1986). Evidence for a specific uptake system for iron phytosiderophores in roots of grasses. *Plant Physiol.* 80, 175–180. doi: 10.1104/pp.80.1.175

Santi, S., and Schmidt, W. (2009). Dissecting iron deficiency-induced proton extrusion in Arabidopsis roots. *New Phytol.* 183, 1072–1084. doi: 10.1111/j.1469-8137.2009.02908.x

Siminszky, B., Gavilano, L., Bowen, S. W., and Dewey, R. E. (2005). Conversion of nicotine to nornicotine in *Nicotiana tabacum* is mediated by CYP82E4, a cytochrome P450 monooxygenase. *Proc. Natl. Acad. Sci. U. S. A.* 102, 14919–14924. doi: 10.1073/pnas.0506581102

Song, Z., Sui, X., Zhang, Y., Wang, Y., Zhao, G., Li, Y., et al. (2021). The *CYP82E4* expression pattern and nicotine conversion rate in Cherry-red tobacco. *Acta Tabacaria Sin.* 27, 75–79. doi: 10.16472/j.chinatobacco.2021.019

Sousa, J. S., D'Imprima, E., and Vonck, J. (2018). Mitochondrial respiratory chain complexes. *Subcell Biochem.* 87, 167–227. doi: 10.1007/978-981-10-7757-9_7

Thomine, S., Lelievre, F., Debarbieux, E., Schroeder, J. I., and Barbier-Brygoo, H. (2003). AtNRAMP3, a multispecific vacuolar metal transporter involved in plant responses to iron deficiency. *Plant J.* 34, 685–695. doi: 10.1046/j.1365-313x.2003.01760.x

Vert, G., Grotz, N., Dedaldechamp, F., Gaymard, F., Guerinot, M. L., Briat, J. F., et al. (2002). IRT1, an Arabidopsis transporter essential for iron uptake from the soil and for plant growth. *Plant Cell* 14, 1223–1233. doi: 10.1105/tpc.001388

Vigani, G., and Murgia, I. (2018). Iron-Requiring enzymes in the spotlight of oxygen. *Trends Plant Sci.* 23, 874–882. doi: 10.1016/j.tplants.2018.07.005

Wada, E. (1956). Conversion of nicotine to nornicotine in Cherry Red tobacco during flue-curing. *Arch. Biochem. Biophys.* 62, 471–475. doi: 10.1016/0003-9861(56)90145-x

Weeks, W. W., Campos, M. P., and Moldoveanu, S. (1993). Biochemical and model chemical reactions for the basis of red pigment in flue-cured tobacco. *J. Agric. Food Chem.* 41, 1321–1328. doi: 10.1021/jf00032a030

Conflict of Interest: The authors declare that the research was conducted in the absence of any commercial or financial relationships that could be construed as a potential conflict of interest.

Publisher's Note: All claims expressed in this article are solely those of the authors and do not necessarily represent those of their affiliated organizations, or those of the publisher, the editors and the reviewers. Any product that may be evaluated in this article, or claim that may be made by its manufacturer, is not guaranteed or endorsed by the publisher.

Copyright © 2022 Liu, Zhang, Pu, Cai, Sui, Rengel, Chen and Song. This is an open-access article distributed under the terms of the Creative Commons Attribution License (CC BY). The use, distribution or reproduction in other forums is permitted, provided the original author(s) and the copyright owner(s) are credited and that the original publication in this journal is cited, in accordance with accepted academic practice. No use, distribution or reproduction is permitted which does not comply with these terms.

frontiers | Frontiers in Plant Science

REVIEW
published: 08 April 2022
doi: 10.3389/fpls.2022.843575

CRISPR/Cas9 and Nanotechnology Pertinence in Agricultural Crop Refinement

Banavath Jayanna Naik[1], Ganesh Shimoga[2], Seong-Cheol Kim[1], Mekapogu Manjulatha[3], Chinreddy Subramanyam Reddy[4], Ramasubba Reddy Palem[5], Manu Kumar[6], Sang-Youn Kim[2] and Soo-Hong Lee[5]**

[1] Research Institute of Climate Change and Agriculture, National Institute of Horticultural and Herbal Science, Rural Development Administration (RDA), Jeju, South Korea, [2] Interaction Laboratory, Future Convergence Engineering, Advanced Technology Research Center, Korea University of Technology and Education, Cheonan-si, South Korea, [3] Floriculture Research Division, RDA, Wanju-gun, South Korea, [4] CSSR and SRRM degree and PG College, Kadapa, India, [5] Department of Medical Biotechnology, Dongguk University, Seoul, South Korea, [6] Department of Life Science, College of Life Science and Biotechnology, Dongguk University, Seoul, South Korea

OPEN ACCESS

Edited by:
Ahmad M. Alqudah, Aarhus University, Denmark

Reviewed by:
Asad Riaz, Zhejiang University, China
Hikmet Budak, Montana Bioagriculture, Inc., United States

***Correspondence:**
Sang-Youn Kim
sykim@koreatech.ac.kr
Soo-Hong Lee
soohong@dongguk.edu

Specialty section:
This article was submitted to Plant Biotechnology, a section of the journal Frontiers in Plant Science

Received: *26 December 2021*
Accepted: *07 February 2022*
Published: *08 April 2022*

Citation:
Naik BJ, Shimoga G, Kim S-C, Manjulatha M, Subramanyam Reddy C, Palem RR, Kumar M, Kim S-Y and Lee S-H (2022) CRISPR/Cas9 and Nanotechnology Pertinence in Agricultural Crop Refinement. Front. Plant Sci. 13:843575. doi: 10.3389/fpls.2022.843575

The CRISPR/Cas9 (Clustered Regularly Interspaced Short Palindromic Repeats/CRISPR-associated protein 9) method is a versatile technique that can be applied in crop refinement. Currently, the main reasons for declining agricultural yield are global warming, low rainfall, biotic and abiotic stresses, in addition to soil fertility issues caused by the use of harmful chemicals as fertilizers/additives. The declining yields can lead to inadequate supply of nutritional food as per global demand. Grains and horticultural crops including fruits, vegetables, and ornamental plants are crucial in sustaining human life. Genomic editing using CRISPR/Cas9 and nanotechnology has numerous advantages in crop development. Improving crop production using transgenic-free CRISPR/Cas9 technology and produced fertilizers, pesticides, and boosters for plants by adopting nanotechnology-based protocols can essentially overcome the universal food scarcity. This review briefly gives an overview on the potential applications of CRISPR/Cas9 and nanotechnology-based methods in developing the cultivation of major agricultural crops. In addition, the limitations and major challenges of genome editing in grains, vegetables, and fruits have been discussed in detail by emphasizing its applications in crop refinement strategy.

Keywords: Cas9, biotic and abiotic stress, horticultural crops, nutritional value, nanoparticles, nano-fertilizers, Cas9 activators

INTRODUCTION

In agroecology, the integrated approach in production of crops and conceptual marketing management draws holistic economic concern. As reported by "Food and Agriculture Organization" (FAO, 2017), the crop failure be falls mainly due to biotic and abiotic factors, significantly influencing the economic values of crops (Gautam and Kumar, 2020). Environmental and climate changes, causing frequent flood, droughts, temperature variations, higher soil salinity, use of harmful chemicals as additives/fertilizers, pathogen triggered diseases, deteriorate the plant health and affects directly to the crop quality and yield (Bing, 2020). Typically, breeders follow

customary methods along with marker-assisted selection to introduce new traits in plants. Some chemical compounds and irradiation techniques are also employed to attain desirable traits; however, they often lead to random mutations in crop genomes.

The customary methods have certain drawbacks such as non-specificity and the generation of mutations with abundance of nucleotides (Mao et al., 2019). Natural chemical compounds from plant source that are essential to the pharmaceutical industry can only be acquired in limited quantity from normal plants compared to genomically edited plants. Moreover, the rational methods are time-consuming; consequently, breeders are unable to grow plants with desired trait in deadline. Supplying sufficient food and other plant-based chemical constituents to ever-growing population is challenging; and quite perplexing topic in near future. The CRISPR/Cas9 genome editing (GE) with nanotechnology-based protocols can potentially challenge these obstacles.

The targeted genomic engineering can be extremely beneficial to agriculture. If the function of a specific gene is known, it can be over expressed or suppressed to obtain the desired trait. Eventually, the crops that are capable of withstanding biotic and abiotic stresses can be easily developed using CRISPR/Ca9 and nanotechnology. Similarly, undesired genes can also be silenced by using these technologies, which would allow expression of only the desirable traits to eventually obtain higher yield. It will be an extremely difficult task to improve crop refinement without genomic engineering. Conventional breeding programs would require longer duration to introduce new quality-related traits or disease-tolerance traits. Therefore, genomic engineering is a striking technology for the future development of agricultural crops with nutrition. Nanotechnology-based protocols has new sets of advanced applications in agriculture and biomedicine; typically, the nano-sized particles are used to deliver the task obtain desirable results in crop development. Coalescing biotechnology and nanotechnology approaches, including GE, have more benefits than customary breeding to improve the development of food crops, which can naturally overcome biotic and abiotic stress along with enhancing the yield. This brief review mainly focuses the importance of genomic engineering in agriculture, and the progress in developing mutant plants using sequence-specific nucleases (SSNs). Furthermore, the procreation of genomically edited crops are already developed in agricultural biotechnology, the main objective, limitations and prospective challenges of GE are highlighted including the role of nanotechnology-based methods in crop refinement.

GENERATING MUTANT PLANTS USING SEQUENCE SPECIFIC NUCLEASES

Sequence specific nucleases are mainly used for precise gene editing in plants and animals. It can create mutations at desired loci in multiple genes *via* addition, deletion, and alternation of sequences (Songstad et al., 2017). To generate the mutant plants, firstly SSNs requires to be articulated in cells; subsequently, recognizing a specific DNA sequence to make the double stranded break. We can classify the SSNs into four major classes, namely (i) CRISPR-Cas9, (ii) Zinc finger nucleases (ZFN), (iii) Meganucleases, and (iv) Transcription activator-like effector nucleases (TALENs). These methods can be effectively utilized for the GE technique. CRISPR-Cas9 is derived from the adaptive immune systems of bacteria; in this mechanism, abounding components come into play to perform the GE. Zinc finger nucleases (ZFNs) are the enzymes that have been characterized 77 candidate two-finger modules (Urnov et al., 2005; Miller et al., 2007). Meganucleases are the microbial enzymes (Smith et al., 2006) that can 76 distinguish and more than 14 nucleotides for cleavage. TALENs have been developed by combining the *Fok*I nuclease domain with TALE proteins of *Xanthomonas* (Christian et al., 2010). CRISPR/Cas9 is one among the four classes of SSNs that can be used for GE (Songstad et al., 2017). GE technologies by adopting CRISPR/Cas9 methodology was investigated in 1987 and its functional application in human cell was reconnoitered in 2013 (Mali et al., 2013). Hsu et al. (2014) discussed the detailed challenges and its future prospective. Consequently, the GE technology was successfully implemented in crop refinement of soybean plant (Cai et al., 2015). Once the SSNs construct is incorporated into the plant genome, they are expressed at a distal site, while the remaining construct is removed by crossing the plant to obtain a mutated plant with no transgene. For GE with the CRISPR/Cas9 system, it is essential to deliver sgRNA and Cas9 proteins into the target cells. Expression vectors or microinjected RNA/mRNA (for Cas9) are usually used to express the sgRNA and Cas9 protein in the plant cells. The CRISPR/CAS9 technology has been performed in plant cells by using electroporation, *Agrobacterium*-mediated transformation, shotgun methodologies, and polyethylene glycol-mediated routes (Jiang et al., 2013; Li et al., 2013; Mao et al., 2013; Nekrasov et al., 2013; Shan et al., 2013). The double stranded break can be fixed either by homology directed repair (HDR) or non-homologous end joining (NHEJ) (Hsu et al., 2014). Recently, RNA viruses have been used to deliver hairpin RNAs for gene silencing, which is another reported technique to incorporate SSNs into the plant cells (Lacomme, 2015). Before the integration into plant's genomic DNA, SSNs are transiently expressed from viral vectors into mRNAs and its respective proteins. The ability to modify the genes to modulate specific traits and homologous recombination (HR) allows plant to metabolize in a manner that develops their resistance to biotic and abiotic stresses. Plants synthesized by fast-growing genome engineering, generally exhibit higher crop yields because of its higher ability for photosynthesis. Precise altering the DNA sequence is extremely important to comprehend the achievable challenges insynthetic biology (Abdallah et al., 2014; Carroll, 2014).

Components and CRISPR/Cas9 Mechanism

The guide RNA (gRNA) sequence comprising of twenty nucleotides that are essential to balance to the target DNA and the details of sgRNAs designing is well explained by Hussain et al. (2018). Similarly, the protein Cas9 has the catalytic activity and having the capability to cut the double standard DNA. When Cas9 and gRNA are combined to form a complex, cas9

immediately cuts the double-stranded DNA (Tang et al., 2019), and so forth the total gene sequence will be altered and specific protein synthesis will not befall by translation. There are two major pathways to repair the broken double-stranded DNA i.e., Non-homologous end joining (NHEJ) pathway and HDR (El-Mounadi et al., 2020).

Non-homologs End Joining Pathway

The lost DNA part cannot be recollected in this NHEJ pathway. In this repair pathway, the dimeric protein complex (Ku) binds at the end of the broken DNA and later to DNA protein kinase catalytic subunits (DNA-PKCs). Artemis proteins are also come in to play and bind at the DNA terminal to make a complex; allowing phosphorylation and eventually the synthesis of DNA begin. This double-stranded DNA converted to blunt-ended double-stranded DNA by catalytic DNA ligase reaction, forming covalent linkage of phosphodiesters (Gomez et al., 2017). This repair system allows insertions or deletions of nucleotide bases that occur during a process (Bernheim et al., 2017; Tang et al., 2019).

Homology Directed Repair Pathway

The HDR pathway use the autologous donor DNA sequences from sister chromatids or foreign DNA to create precise insertion and substitution between DNA double-strand break (DSB) sites for further alterations. Considerable research has been done previously on proteins involved in the HDR pathway, MRE11-Rad50-Nbs1 (MRN) complex binds at the 5′ end of the DSBs and forms the 3′ overhangs. Later the replication protein A (RPA) binds to the single-strand DNA to prevent the nuclease activity. RAD-51 protein involves in search of homologous DNA and eventually the invasion occurs to complete the homologs-directed repair (Tang et al., 2019). El-Mounadi et al. (2020) explained the CRISPR/Cas9 mechanism system was depicted in **Figure 1**.

IMPORTANCE OF GENOMIC ENGINEERING IN AGRICULTURE

Transgenesis profoundly involving genetic addition without changing the genetic pool to create specific traits for agricultural/agroeconomical benefits. In the present scenario, providing food security to a mounting populace is one of the major challenges in this modern world. Thenceforth, the food fructification needs to be increased over 80–90%. Furthermore, the food production is declining every year due to extreme weather conditions, climate change, global warming, farmland availability, and cumulative biotic and abiotic problems. To overcome these challenging obstacles, gene modification technique in food crops will be the superlative method to achieve the targeted tasks (FAO, 2017). The gene knockout step is a critical stage and it directly influence the phenotype. Wada et al. (2020) demonstrated genomic manipulation without the introduction of DSBs. In this modular approach, a dead Cas9 variant (dCas9) binds to the target sequence; however, it does not cleave the double-stranded DNA (Qi et al., 2013; Wang et al., 2016a; Adli, 2018). Generating gene knockouts using SSNs facilitates genetic analyses and the study of important gene functions, which will eventually help with crop improvement. The first mutation generated using SSNs were of the IPK1 gene in maize, which is catalyzed in the last step during phytate biosynthesis (Liang et al., 2014). Knocking out this gene helps in removing unwanted metabolites; eventually contributing to the accumulation of valuable biosynthetic intermediates. Prime editing is another significant approach for genomic manipulation that has been indicated in mammalian and yeast cells (Anzalone et al., 2019). Certain crops such as grains, vegetables, and fruits are vitally important to maintain global food securities and sustainable system.

Homologous recombination is a challenging process wherein chromosome can chasm by the nuclease that must be coordinated with the distribution of the DNA repair template. Initially, HR in plants was confirmed by the incorporation of marker genes at detailed chromosomal sites. Targeted transgene insertion into the euchromatin should provide promising results in plants with high transgene expression; therefore, it is a great improvement over the integration by the traditional Transgenesis (Neelendra et al., 2018). Moreover, the insertion of multiple genes at the same site will facilitate their transfer to a single mendelian locus, when the plant is crossed. Further efforts are required to familiarize plentiful genes into the germplasm by breeding. Targeted gene inclusion through HR using different SSNs has been verified in tobacco, maize, and rice (Abdallah et al., 2014; Wang et al., 2016b). In order to develop new plant varieties, some techniques have been used that are controlled by process-based regulatory frameworks. Most of the farmers, globally aim to cultivate crops that are tolerant to drought, high salinity, and diseases, with appreciable yield. Therefore, the researchers in agriculture domain are actively looking for transgenic technology and CRISPR/CAS9 to achieve targeted tasks. Guidelines and process-based regulations have been formulated and implemented by the United Nations Food and Agricultural Organization adopted by European and South American countries (FAO, 2017).

Applications of Clustered Regularly Interspaced Short Palindromic Repeats to Develop Cereal Crops

Globally, there is a renowned demand for Basmati rice because of its fragrance, long grains, and flavor texture. However, due to bacterial blight caused by *Xanthomonas oryzae* pv. *oryzae* (Xoo), the yield and rice quality will be deprived from its authentic taste. By CRISPR/Cas9 GE technique, the genes namely OsSWEET11, OsSWEET13, and OsSWEET14 could be possibly edited to overcome the bacterial blight disease (Zafar et al., 2020). New Japonica rice is another prominent Asian rice variety, developed by editing Ehd1 (Early heading date 1) gene *via agrobacterium* mediated transformation. The mutated rice varieties exhibited prolonged basic vegetative growth (BVG) period at latitudes (Wu et al., 2020). It was documented that, *OsBADH2 (betaine aldehyde dehydrogenase*) *gene was modified to develop the* fragrance in non-aromatic rice *grains for better marketing* (Ashokkumar et al., 2020). Two endogenous genes, namely *TaWaxy* and *TaMTL*, were

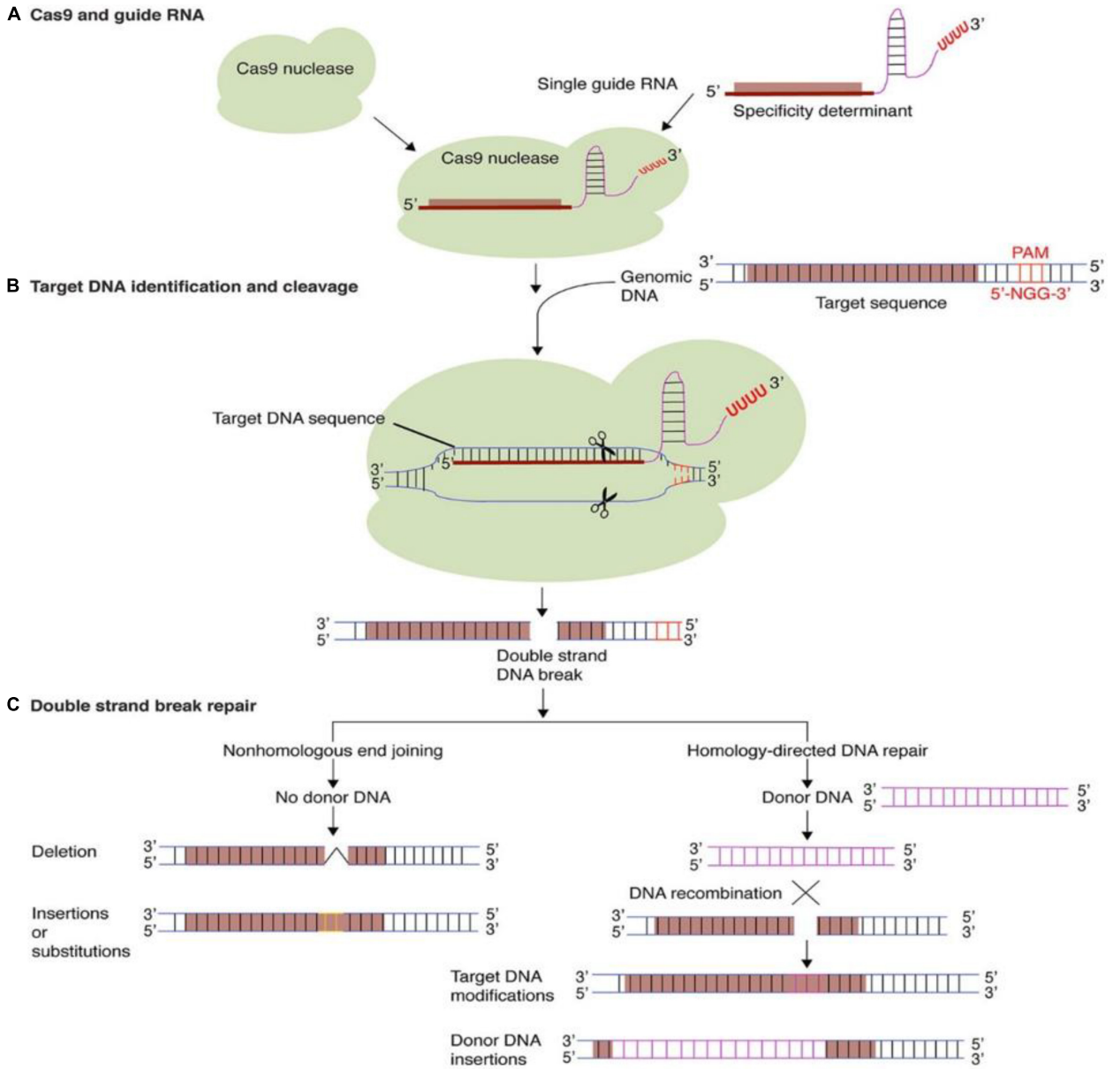


FIGURE 1 | Targeted genome editing *via* CRISPR-Cas9. **(A)** The CRISPR-Cas9 system comprises of a Cas9 protein and guide RNA. Guide RNAs regulate the target DNA specificity by sequence complementarity. **(B)** gRNA and Cas9 protein form a binary complex that specifically cleaves target DNA creating a double-strand DNA break. **(C)** Cellular DNA repair mechanisms: non-homologous end joining (NHEJ) and homology-directed repair (HDR), repairs the double strand DNA break. In the process, short insertions, deletions, nucleotide substitutions, or gene insertion may occur. Reproduced with permission from El-Mounadi et al. (2020) Frontiers.

edited by using three different promotors (*OsU6a, TaU3,* and *TaU6*) for the development of haploid plants in wheat crops. Among these three promotors, *TaU3 showed better results* (Liu et al., 2020). TaPDS gene was edited in wheat by using Cas9 and Cpf1 (AsCpf1 and LbCpf1) nucleases in wheat (Kim et al., 2021). Lipoxygenases genes (GmLox1, GmLox2, and GmLox3) were edited by using CRISPR/Cas9 to afford lipoxygenase-free new mutant lines in soybean crop, so that it can be useful for human consumption with upsurge amount of protein for health benefits (Wang et al., 2020). Aside from maize, wheat, and rice, the fourth most highly consumable crop in the world is barley. The two mutated genes, HvHPT and HvHGGT in barley are mainly accountable for the dwindled grain size to weight ratios. Furthermore, these mutated barley lines showed reduced amount of tocotrienols assayed by HPLC (Zeng et al., 2020). Groundnut is the sixth most significant oil-seed crop in the world; this legume crop fixes the nitrogen *via* symbiotic relationship with rhizobia. In this process NFR (Nod Factor Receptor) play a major role in nitrogen fixation cycle. Thence, AhNFR1 and AhNFR5 genes were mutated by CRISPR/Cas9 to proliferate the root

nodules *via* hairy root transformation system (Shu et al., 2020). CAD (cinnamyl alcohol dehydrogenase) and PDS (phytoene desaturase) genes were edited by CRISPR/Cas9 in sorghum *via* Biolistic bombardment resulted in enhanced biosynthesis of carotenoid and chlorophylls (Liu et al., 2019). SiMTL gene, which is orthologous to the maize *MATRILINEAL*/*NOT-LIKE-DAD*/*PHOSPHOLIPASE A* (*MTL*/*NLD*/*ZmPLA*) gene is edited by CRISPER/Cas9 with OsU3 promotor *via Agrobacterium* for the haploid induction in foxtail millet (Cheng et al., 2021). Please see **Supplementary Table S1** (Fauser et al., 2014; Sugano et al., 2014; Baltes et al., 2015; Li et al., 2015, Li et al., 2016, 2018b,f; Li J. et al., 2017; Michno et al., 2015; Tsai and Xue, 2015; Xie et al., 2015; Zhou et al., 2015, 2016; Zhou X. et al., 2018; Baek et al., 2016; Duan et al., 2016; Feng et al., 2016; Gao et al., 2016, 2017; Iqbal et al., 2016; Osakabe et al., 2016; Pan L. et al., 2016; Pioneer, 2016; Pyott et al., 2016; Qi et al., 2016; Waltz, 2016; Watanabe et al., 2016; Zhang Y. et al., 2016; Zhao et al., 2016; Zhu et al., 2016; Chen et al., 2017; Kapusi et al., 2017; Mercx et al., 2017; Ordon et al., 2017; Wang et al., 2017b,c; Yang et al., 2017c; Che et al., 2018; Pankaj et al., 2018). For brief listing of prime cereal/food crop genes along with its specific functions modified *via* CRISPR/Cas9 system.

Applications of Clustered Regularly Interspaced Short Palindromic Repeats to Develop Fruits/Vegetable Crops

Trans-Acting Small-interfering locus 4 (TAS4) and MYBA7 (Transcription factor) genes are edited by CRISPR/Cas9 *via* Agrobacterium to enhance the biotic and abiotic tolerance in grapes. These genes showed pronounced tolerance against the bacterium *Xylella fastidiosa* and *Grapevine Red Blotch* Virus (GRBV) causes Red Blotch Disease (Sunitha and Rock, 2020). Citrus canker is a dangerous disease caused by the bacterium *Xanthomonas axonopodis*. It is threatening to citrus family crops worldwide. The CsWRKY22 gene was edited by CRISPR/Cas9 with AtU6-1 promotor *via* Agrobacterium methodology to produce the Canker disease-free citrus in Wanjincheng orange plants. PDS (phytoene desaturase) gene was mutated for the development of Albino phenotype and carotenoid biosynthesis in banana crop (Otang Ntui et al., 2020). *Fusarium oxysporum* is a dangerous pathogen for watermelon. The editing of Clpsk1 gene that encode Phytosulfokine (PSK) precursor could be conferred to enhance resistance of *Fusarium oxysporum* to watermelon, the gene was efficiently edited by CRISPR/Cas9 system *via* Agrobacterium method to produce the *Fusarium oxysporum* resistant watermelons in appreciable yield (Zhang et al., 2020).

SlJAZ2 is a major co-receptor of coronatine (COR) in the stomatal guard cells of tomato fruit. This gene was edited for the development of bacterial speck disease resistance *via* Agrobacterium (Ortigosa et al., 2019). Broomrapes (*Phelipanche aegyptiaca* and *Orobanche* spp.), a kind of plant parasite can cause severe damage to the tomato plants. Thus, the CCD8 (Carotenoid Cleavage Dioxygenase 8) gene was edited to afford the *Phelipanche aegyptiaca* parasite resistant tomatoes (Bari et al., 2019). SlMlo1 and SlPelo genes were altered by CRISPR/Cas9 in tomato for resistant to yellow leaf curl virus and powdery mildew. These gene modifications successfully develop the pathogen-resistant tomatoes (Pramanik et al., 2021). Steroidal glycoalkaloids (SGAs) are plant secondary plant metabolites, better known for their toxic effects in humans and animals. High SGAs content can severely damage the potato quality. To diminish the SGAs content to optimum levels, StSSR2 (Sterol side chain reductase 2) gene, a key enzyme for the biosynthesis of SGAs was edited (Zheng et al., 2021). BoaCRTISO gene of Chinese kale was altered to increase the Carotenoid biosynthesis and the observed mutation rate was 81.25% (Sun B. et al., 2020). CsCRUC (*Camelina sativa* CRUCIFERIN C) gene encodes the seed proteins in *Camelina sativa* and this gene was edited by CRISPR/Cas9 to enhance the seed storage protein and enriched saturated fatty acids contents (Lyzenga et al., 2019). Powdery mildew is typically observed destructive disease that affect the leaves of wheat crop. This fungal leaf ailment can severely damage up to 40% of the crop under optimum ecological conditions (Gil-Humanes and Voytas, 2014). Thenceforth to overcome this problem MLO (MILDEW-RESISTANCE LOCUS) genes were modified in bread wheat (Wang et al., 2014). Assuredly, the bread wheat verities showed effective tolerance to powdery mildew. Bacterial blight disease is one of the most destructive afflictions, caused by *Xanthomonas oryzae* that can severely devastate for nutritional crop growth. In rice crops, the bacterial blight disease resistance was significantly improved by incorporating OsSWEET11, OsSWEET13, and OsSWEET14 genes (Zafar et al., 2020). To control the weed growth, the herbicide-resistant crops were instigated by OsPDS, OsPMS3, OsEPSPS genes (Zhang et al., 2014). The amylose content in rice endosperm was increased by the waxy (Wx) gene (Yunyan et al., 2019), thereby enhancing the grain number by OsSPL16 gene (Usman et al., 2021). Tiller-spreading phenotype of rice plants were improved by LAZY1 (LA1) gene (Miao et al., 2013). OsRR22 gene encodes 696-amino acid B-type response transcription factor that is intricate in cytokinin-signal transduction and metabolism, its loss of function suggestively upsurges the salt tolerance (Zhang A. et al., 2019) and the drought tolerance by OsNAC14 gene has been successfully developed CRISPR/Cas9 technique. For brief listing of prime fruits genes (see **Table 1**) and vegetable genes (see **Supplementary Table S2**; Ron et al., 2014; Butler et al., 2015; Ito et al., 2015; Lawrenson et al., 2015; Woo et al., 2015; Pan C. et al., 2016; Thomazella et al., 2016; Xu et al., 2016; Hayut et al., 2017; Hu et al., 2017; Klap et al., 2017; Koseoglou, 2017; Lang et al., 2017; Nonaka et al., 2017; Roldan et al., 2017; Soyk et al., 2017; Ueta et al., 2017; Yang et al., 2017b; Ye et al., 2017; Yu et al., 2017; Zhou et al., 2017) along with its specific functions modified *via* CRISPR/Cas9 system.

Applications of Clustered Regularly Interspaced Short Palindromic Repeats to Develop Ornamental Crops

Ornamental plants usually grown for decoration aspirations and are often associated with commercial orientations in

TABLE 1 | Partial list of genes of fruit crops and its specific functions modified *via* CRISPR/Cas9 system.

S. No	Crop name	Gene name	Function	References
1	Grape	*VvPDS*	Carotenoid biosynthesis and albino phenotype	Nakajima et al., 2017
2		*IdnDH (L-I donate dehydrogenase)*	Promotes tartaric acid accumulation	Ren et al., 2016
3		*VvWRKY52*	Resistance to necrotrophic fungal pathogen Botrytis cinerea	Wang et al., 2018a
4		*ALS1*	Motifs characteristic of a cell surface protein to enhance the adherence to epithelial cells	Osakabe et al., 2018
5		*CsLOB1*Promoter	Enhanced resistance to citrus canker	Jia et al., 2016
6		*TAS4b* and *MYBA*	Biotic and abiotic stress tolerance	Sunitha and Rock, 2020.
7		*MLO-7*	Increased resistance to fire blight disease	Malnoy et al., 2016
8	Citrus	*PDS and Cs2g12470*	Albino phenotype	Jia et al., 2017; Zhu et al., 2019
9		*CsLOB1*	Resistance to canker disease	Peng et al., 2017; Jia et al., 2019
10		*CsWRKY22*	Resistance to canker disease	Wang et al., 2019b
11		*DMR6*	Huanglongbing (HLB) tolerant	Zhang et al., 2018c
12	Sweet Orange	*CsPDS*	Carotenoid Biosynthesis	Jia and Wang, 2014
13	Apple	*ALS1*	Encodes cell surface protein to enhance the adherence to epithelial cells	Osakabe et al., 2018
14		*DIPM-1, 2,* and *4*	Increased resistance to fire blight disease	Malnoy et al., 2016
15	Apple and Pear	*MdPDS* and *Md TFL1*	Early flowering phenotype	Charrier et al., 2019
16	Straw berry	*AP3 (APETALA3)*	Control of flower development	Martín Pizarro et al., 2019
17		*FvARF8 and FveTAA*	Auxin biosynthesis	Zhou J. et al., 2018
18		*PDS*	Albino phenotype	Wilson et al., 2019
19	Kiwi	*AcCEN4* and *AcCEN*	Rapid terminal flower and fruit development	Varkonyi-Gasic et al., 2018
20		*PDS*	Carotenoid biosynthesis and albino phenotype	Wang et al., 2018b
21	Banana	eBSV	Resistance to banana streak virus	Tripathi et al., 2019
22		*PDS*	Carotenoid biosynthesis and albino phenotype	Kaur et al., 2018; Otang Ntui et al., 2020
23		*MaGA20ox2*	Regulates semi-dwarf	Shao et al., 2019
24	Watermelon	*ALS*	Conferring herbicide resistance	Tian et al., 2018
25		*ClPDS*	Carotenoid biosynthesis	Tian et al., 2017
26		*ClPSK1*	Resistance to *Fusarium oxysporum*	Zhang et al., 2020
27	Papaya	*alEPIC8*	Resistance to *Phytophthora palmivora*	Gumtow et al., 2018

agroecological farming practices. These attractive flowering plants are customarily utilized in extracting perfumes and opens a profitable platform in fragrance market. Ornamental plants also a play a vital economic role in farming economy and sustainable agricultural business. Marigold flower and its extracts are used in poultry industry as feed additive, in order to enhance the quality of egg production and enticing yolk color. PhNR (Petunia Nitrate Reductase) gene was modified to check the nitrogen uptake and nitrate metabolism in petunia plants. Mutated plants showed better nitrogen uptake efficiency (Subburaj et al., 2016). *CiPDS (*chicory *phytoene desaturase)* gene was edited by under U6 promotor *via* Agrobacterium mediated and protoplast transfection methods. Among these two methods, Agrobacterium mediated route showed 31.25% transformation efficiency in chicory and the mutated chicory plants showed better Albino phenotype content (Bernard et al., 2019). MADS genes (MADS, MADS44, MADS36, and MADS8) from flowering plant of the orchid genus Phalaenopsis was using CRISPR/Cas9 for floral initiation and flower development (Tong et al., 2020). *Lilium* spp. is a genus of more than 100 species of flowering plants emergent from bulbs. To intensify the beauty and color shades, LpPDS gene was edited by CRISPR/Cas9 (Yan et al., 2019), to enforce to bloom attractive pale yellow to albino–green color shades. **Table 2** gives the concise listing of prime genes of fruits and its specific functions modified *via* CRISPR/Cas9 system.

IMPORTANT CONSIDERATIONS FOR CRISPR/Cas9 GENOME EDITING

Genomic engineering has been encountered broad range of applications to introduce targeted alterations of the plant's genome to acquire desired function (Hsu et al., 2014). The NmeCas9 (*Neisseria meningitidis*) recognizes an 8-mer PAM (5′-NNNNGATT) sequence hence it can progress the target particularity, whereas SaCas9 recognizes a 6-mer PAM sequence (5′-NNGRRT) (Xing et al., 2014; Ma et al., 2015). This technique involves introducing mutations, and harnessing transgene supplementation for gene therapy and livestock improvement.

TABLE 2 | Partial list of genes of ornamental plants and its specific functions modified *via* CRISPR/Cas9 system.

S. No	Crop name	Gene name	Function	Reference
1	Petunia	*PhPDS (Phytoene Desaturase)*	Albino phenotype	Zhang B. et al., 2016
2		*PhNR (Nitrate reductase)*	Nitrogen uptake and nitrate metabolism	Subburaj et al., 2016
3		*PhACO1, 3,* and *4*	Flower longevity and the reduction in ethylene production	Xu et al., 2020
4		*PiSSK1*	S-RNase-based self-incompatibility mechanism	Sun and Kao, 2018
5	Japanese morning glory	*InDFR-B*	Floral color change	Watanabe et al., 2017
6		*InCCD4 (Carotenoid Cleavage Dioxygenase)*	Carotenoid accumulation and floral color change	Watanabe et al., 2018
7		*EPH1*	Delays petal senescence	Shibuya et al., 2018
8	Chicory	*CiPDS*	Display an albino phenotype	Bernard et al., 2019
9	*Chrysanthemum morifolium*	*CpYGFP(Yellowish-green Fluorescent)*	Disruption of fluorescence protein	Kaboshi et al., 2017
10	*Lilium pumilum*	*LpPDS*	Display an albino phenotype	Yan et al., 2019
11	*Phalaenopsis equestris*	*MADS, MADS44, MADS36,* and *MADS8*	Flower initiation and development	Tong et al., 2020
12	Wishbone Flower	*F3H (Flavanone 3-hydroxylase)*	Flavonoid biosynthesis and initiating catalysis of the 3-hydroxylation of (2S)-flavanones	Nishihara et al., 2018
13	*Camelina sativa*	*FAD2*	Enhancement of fatty acids, especially linoleic acid	Jiang et al., 2017
14	*Lotus japonicus*	*SYMRK, LjLb1, LjLb2,* and *LjLb3*	Efficient inactivation of symbiotic nitrogen fixation	Wang et al., 2016c
15	*Dendrobium officinale*	*C3H, CCR, 4CL, C4H, and IRX*	Reduced lignocellulose biosynthesis	Kui et al., 2017
16	Easter lily (*Lilium longiflorum*)	*LlPDS*	Pale yellow and albino–green chimeric mutants	Yan et al., 2019
17	*T. fournieri*	*TfRAD1*	Diverse pigmentation patterns and petal shape regulations	Su et al., 2017
18	Red sage	*SmCPS1*	Tanshinone biosynthesis	Li B. et al., 2017

CMV (Califlower mosaic Virus), AtUBO (Arabidopsis UBO) OsUBO (Oriza sativa UBO), LTR (Long terminal Repeat), OsnoRNA U3 (*Oriza sativa* snoRNA U3), AtU6 (Arabidopsis U6), OsUBI (*Oriza sativa* Ubiquitin), ZmUBI (*Zea mays* UBI), cauliflower mosaic virus 35S promoters have been used to promote Cas9 expression in plants and, more than 30 empty gRNA backbones in binary vectors was supplied by Addgene (Belhaj et al., 2013; Feng et al., 2013; Mao et al., 2013; Nekrasov et al., 2013; Upadhyay et al., 2013; Xie and Yang, 2013). Tissue specific promoters can also be used in CRISPR/Cas9 technology to edit genomes; for instance, Wang et al. (2015) used the promoter of the egg cell-specific EC1.2 gene, to initiative of Cas9. The germ line-specific SPOROCYTELESS and embryo-specific promotor DD45 (Mao et al., 2016). The promotor AtDMC1 involved in meiotic recombination (Xu et al., 2018). The pLAT52-GT for Pollen tissues (Mao et al., 2016), and pDD45-GT for egg cell-early embryo tissues (Mao et al., 2016), INCURVATA2 for dividing tissue-targeted site-directed mutagenesis (Hyun et al., 2015), and the YAO promoter for cell-division specific tissues (Yan et al., 2015). In order to knock out the expressions of multiple genes cassettes can be inserted into one plasmid, thereby guiding the Cas9 to different targets (Xing et al., 2014; Ma et al., 2015; Oz et al., 2021). Although this GE technology has key advantages, there are some negative shades involving ethical issues concerning to the disruption of ecological balance (Tavakoli et al., 2021). To overcome this, different methods including nanotechnology-based methods are being implemented to insert or silence the genes in plant cells (Nadakuduti and Enciso-Rodríguez, 2021).

EMPHASIS OF CRISPR-CAS9 IN NUTRITION AND HEALTHCARE

Despite animal-based food consumption, the global ecosystem mainly be contingent to the agro-based crops including herbivorous animals. In concern to this, extensive research findings are mainly focusing on developing nutritional cereal/vegetables/fruits/nuts (FAO, 2017). Cultivating nutritional crops mainly depends on the nature and the fertility of the soil. Sources of soil nutrients are not same and is mainly depending on the presence of organic matter. In order to overcome this nutrient deficiency, CRISPR/Cas9 technology is extremely useful to grow cereal/vegetables/fruits/nuts with high nutritional values. Recently, genomic engineering utilizes TALENs, Cas9, dCas9, and Cre inserting into the cells. The use of these proteins in human cell lines have also been verified *in vitro* and *in vivo* (Zuris et al., 2015). HR (Sun et al., 2016) mediates the modifications made by the engineered nucleases.

To date, plentiful of food-based crops have been modified to obtain good nutritional values in vegetables and fruits (Kathleen, 2015). Varieties of fruits comprised of different nutrients and biologically active compounds that are necessary in daily healthy diet. Recently, Dalla et al. (2019), Wan et al. (2021), and Xu et al. (2021) have discussed the importance of gene editing in fruits and vegetables to get nutritional rich cereal/vegetables/fruits/nuts, which are beneficial to maintain good health.

Genome-wide association studies (GWAS) have been employed to identify specific locations in the genome that can anchorage polygenic diseases such as Alzheimer's, diabetes, autism, and schizophrenia. This technique is crucial in biomedical field to treat various diseases, including the removal of HIV genome (Ebina et al., 2013; Liao et al., 2015; Kaminski et al., 2017). The *ex vivo* and *in vivo* GE of neurons, immune cells, and endothelial cells has been successfully reported in mice (Platt et al., 2014), which are challenging to modify the sensitive cells and its effective editing. Researchers have introduced resistance against malaria by editing the DNA in *Anopheles mosquitoes* (Gantz et al., 2015; Hammond et al., 2016; Macias et al., 2020). Cancer therapy strategies have also been conducted in biomedical field to treat cancerous cell lines (Yao et al., 2015; Khan et al., 2016; Yang H. et al., 2019). Furthermore, AIDS research is still ongoing to engraft Cas9-modified CCR5-human hematopoietic stem cells and progenitor cells (Mandal et al., 2014). GE techniques are gaining its impact in promising therapeutics in regenerative medicine. The primary route for disease treatment is direct GE in tissues; some reports have documents the correction of monogenic recessive genetic disorders, such as Duchenne muscular dystrophy (Ousterout et al., 2015), hemophilia (Park et al., 2016) cystic fibrosis (Schwank et al., 2013), and sickle cell anemia (Sun and Zhao, 2014). The Cas9 system has exhibited its efficacy in therapies through the insertion of SSNs into microbial populations using phages and conjugative plasmids (Citorik et al., 2014).

DEVELOPMENTS AND POSSIBILITIES FOR GENOMIC ENGINEERING IN AGRICULTURE

The comprehensive study on rice (Shan et al., 2013), sorghum (Jiang et al., 2013), tobacco (Li et al., 2013), wheat (Wang et al., 2014), tomato (Brooks et al., 2014), maize (Liang et al., 2014), sweet orange (Jia and Wang, 2014), and Arabidopsis (Li et al., 2013), stretches the vast knowledge of specific gene handling and editing. Before SSNs, RNAi technology was used to study the gene function by knocking down the targeted genes, which was not as advantageous as SSNs. Certain characteristics discussed below encompasses the examples for certain horticultural and ornamental plants using the CRISPR system. The color and weight/size ratio of tomato fruit could be developed by the editing of PL and TBG4 genes (Wang et al., 2019a). The SlNPR1 and SlCBF1 genes corresponding to drought and cold tolerance can also be modified (Li et al., 2018b; Li R. et al., 2019) and the fruit ripening transcription factor RIN (Ripening Inhibitor) could be edited, so that the tomato with desired characteristics will be maintained. Albino phenotype and flowering characters could be modified in cabbage using FRI and PDS gene editing (Murovec et al., 2018). In addition, the biosynthesis of Carotenoid pigment can be enhanced in wild cabbage with BoaCRTISO (Carotenoid isomerase) gene editing (Sun B. et al., 2020). By editing DcF3H and DcPDS, DcMYB113 genes, the accumulation of acylated anthocyanins can be enriched in the roots of carrot to afford pigmented purple carrots (Chodacka et al., 2018; Xu et al., 2019). Cucumber mosaic virus (CMV-Z1) and Zucchini yellow mosaic virus (ZYMV) are two major rapidly affecting pathogens, which can severely damage the crop. To overcome this, the pathogenic resistance can be developed/enhanced by editing elF4EF gene (Chandrasekaran et al., 2016). Drought tolerance in an important commercial crop, hot pepper (*Capsicum annuum* L. syn. chilli) was developed by editing NAC72 gene (Joshi, 2019). Furthermore, to enhance the flower longevity of attractive petunia flowers can be edited using PhACO1, 3, and 4 gene (Xu et al., 2020). The color and the Carotenoid accumulation of Japanese morning glory flower can be edited by altering its related gene InCCD4 (Carotenoid Cleavage Dioxygenase) (Watanabe et al., 2018). Compatibly, the flavonoid biosynthesis could be enriched in Wishbone flower by editing F3H (Flavanone 3- hydroxylase) gene (Nishihara et al., 2018). Moreover, the AhFAD2A and AhFAD2B genes encoding fatty acid desaturases in groundnut have been reported to be edited (Yuan et al., 2019). The TYLCV-IR (Intergenic regions) gene has been modified to overcome the multiple viral diseases in *Nicotiana benthamiana.* After gene modification plant exhibited resistance to *geminiviridaevirus*, *begomovirus*, *curtovirus*, *becurtovirus*, *eragrovirus*, *Turncurtovirus,* and *Topocuvirus* (Ali et al., 2015a,b). The resistance against *Phytophthora tropicalis* in cacao has been overcome by altering the TcNPR3 gene (Fister et al., 2018). Giovannini et al., 2021 have identified the desirable phenotypic characters in ornamental flowers, including flowering induction, floral meristem initiation and organ development, as well as color, fragrance, and shelf life. Flower longevity has been induced in petunia by altering a group of Petunia hybrid 1-aminocyclopropane-1-carboxylate oxidase (PhACO, PhACO1, PhACO3, and PhACO4) genes (Xu et al., 2020). Canker and huanglongbing diseases are the major factors in reducing the productivity of citrus plants; this problem was overcome by modifying the CsLOB1, CsWRKY22, and DMR6 genes by CRISPR/Cas9 system (Peng et al., 2017; Zhang et al., 2018c; Wang et al., 2019b). Selectable marker gene (SMG) systems are critical and play a major role in the identification of transgenic crops. Nowadays, the scientists are considering the SMGs that can affect human and animal health. The gene transferred plants (GMP: Genetically Modified Plants) usually contain the antibiotic resistant gene, so that GM plants should survive and regenerate under antibiotic medium. Whereas, the non-gene transformed plants will not rejuvenate, eventually die under toxic proximity. Although antibiotics have positive health and life prospective in human/animal health, the negative impacts of antibiotic associated diarrhea and pseudomembranous colitis will

proliferate the possibilities of subsequent diseases. By consuming those GMP (Fruits and vegetables) for prolonged usage can severely affect the human/animal health (Breyer et al., 2014). Thus, it is imperative to eliminate SMGs from transgenic crops by using CRISPR technology (Yau and Stewart, 2013). Arndell et al. (2019) edited the biosynthesis of 5-enolpyruvylshikimate-3-phosphate synthase (EPSPS) for the functional confirmation of EPSPS gene in wheat using CRISPR/Cas9. The soybean storage protein genes were also been edited successfully to observe the efficacy of CRISPR/Cas9 technique using Agrobacterium rhizogenes-mediated hairy root transformation method (Li C. et al., 2019). Acetolactate synthase (ALS) participates in amino acid biosynthesis; this amino acid is targeted by numerous herbicides. These two plant enzymes(EPSPS, ALS, ACCase), and BFP genes, confer herbicide tolerance in plants (Voytas and Gao, 2014; Sauer et al., 2016; Li et al., 2018e). Hybrid paddy are susceptible to bentazon and sulfonylureas and the BEL gene has been mutated using radiation. In the production of hybrid rice, these mutants can be used to prevent contamination in hybrid seed lots (Cantos et al., 2014). Here, the BEL gene was edited using CRISPR-Cas9 technology, and transformed into rice through *A. tumefaciens* (Xu et al., 2014). Nutrient values have also been increased in vegetables and fruits by knocking out genes using the CRISPR-Cas9 system. Visually attractive flowers possess pleasant aroma because of the presence of anthocyanin, whose expression is regulated by the MYB-bHLH-WD (MBW) complex (Albert et al., 2014; Lloyd et al., 2017). Gibberellin (GA) determines plant height and strigolactone (SL) affects branching of the shoot branching, both of which can be modulated by modifying the biosynthesis or signal transduction of GA and/or SL (D'Halluin et al., 2008).

Unwanted metabolites usually have negative impacts on the crop yield and its quality; the accumulation of these undesired metabolites can be avoided by using GE. Cyanide intoxication, ataxia or partial paralysis, and goiters are caused by cyanide, which is present in cassava (Padmaja, 1995). Glucosinolates, which produced by mustard and cabbage, also possess a high toxic content, were edited (Hannoufa et al., 2014). FAD2 and FAD3 genes produce high oleic acid and low linolenic acid in soybean; however, soybean oil allows the accumulation of monounsaturated fats and reduces the linolenic acid in the seeds (Pham et al., 2012). AtPDS3, AtFLS2, AtADH, AtFT, AtSPL4, and AtBRI1 genes are targeted in Arabidopsis with mutation rates (MRs) from 1.1 to as high as 84.8% in the first generation (Li et al., 2013). The OsPDS and OsBADH2 genes have been knocked out with MRs of 9.4 and 7.1% (Hinge et al., 2015). The DsRED2, DD20, and DD43 genes have been targeted in sorghum with MRs of 33, 59, and 76%, respectively. Similarly, the ZmIPK (13.1%), LIG1, MS26, MS45, and ALS1 genes have been edited in maize with MRs lower than 5% (Liang et al., 2014; Svitashev et al., 2015). TaMLO-A, TaMLO-B, and TaMLO-Dare three homeo alleles that confer powdery mildew resistance and have been edited with the same moderate MR of 5.6% (Wang et al., 2014). In BRI1, JAZ1, and GAI genes mutation frequencies of 26–84% have been observed (Feng et al., 2013). NtPDS and NtPDR6 have been mutated with MRs of 81.8 and 87.5%, respectively (Gao et al., 2015). The squamosa promoter binding protein-like 4 and Flowering Locus T (FT) have been mutated with an MR of 90%, which caused it to exhibit late flowering (Hyun et al., 2015).

Ma et al. (2015), have reported genome modifications at 46 target sites with an average of 85.4% mutations in monocot and dicot plants using either golden gate ligation or Gibson assembly. Using the sgRNA single, double and triple mutants have also been generated for CDKA2, CDKB1, and CDKB2 in rice (Endo et al., 2015). Dort et al. (2020) discussed forest pathosystems; some disease problems were solved using the CRISPR/Cas9 system. Zhang et al. (2014), have also reported mutations in young seedling albino (OsYSA) and OsROC5 genes with MRs of 65–66.7%. Similarly, Wang et al. (2016b), have edited the OsERF922 gene that encodes ERF transcription factors to develop resistance to rice blast disease. Transgenic poplar plants have been modified and phenotypically results revealed an MR of 51% (Fan et al., 2015). El-Mounadi et al. (2020) explained biosafety of genomically edited plants and the applications of CRISPR/CAS9 technology to enhance yield, quality, and nutritional values. The crops and seeds developed using CRISPR/Cas9 technology for cereals, vegetables, ornamental, and fruits plants are shown in **Tables 1**, **2** and **Supplementary Tables S1**, **S2**. Some multinational companies (DuPont, Monsanto, and BASF) had obtained licenses to develop new crops using CRISPR technology (Khurana and Rajarshi kumar, 2019). The sequential steps for CRISPR/Cas9 genetic transformation in plants was sketched in **Figure 2** (Manghwar et al., 2019).

ROLE OF NANOTECHNOLOGY IN CROP REFINEMENT

Nanotechnology plays a prominent role in biological, medicinal, and pharmaceuticals including plant science. Increasing resilience to biotic and abiotic stress and improving the yield/quality of the crops *via* gene editing, nanotechnology shares its connotation with CRISPR/Cas9. Nano-fertilizers (Subramanian et al., 2015; Thul and Saragani, 2015) are used in horticultural plants, including vegetables and fruits, and implemented in food crops to enhance the growth, germination rate, and genetic manipulations (Lee et al., 2010; Sheykhbaglou et al., 2010; Dimkpa et al., 2012; Shang et al., 2019; Mittal et al., 2020; Aqsa et al., 2021; Rana et al., 2021). Similarly, plant growth, nutrient uptake from roots, flowering; have also been developed by metal and carbon based nanoparticles (Aqsa et al., 2021). Photosynthesis is an energy conversion process in plants, transforming light energy into chemical energy; however, it does not occur effectively under cloudy conditions and in sun-drenched plants during the rainy season. Consequently, cell mechanisms possibly down regulated. The gold nanoparticles could be beneficial to enhance the light-harvesting capacity, thereby promoting highly excited electron transfer in the chloroplast (So et al., 2015). Environmental factors (abiotic stress) cause biochemical and physiological changes in plants and these are more susceptible to stress. Even in stressful conditions, the use of metallic nanoparticles can increase the anti-oxidative enzyme levels in plants (Mittal et al., 2020; Zhao et al., 2020;

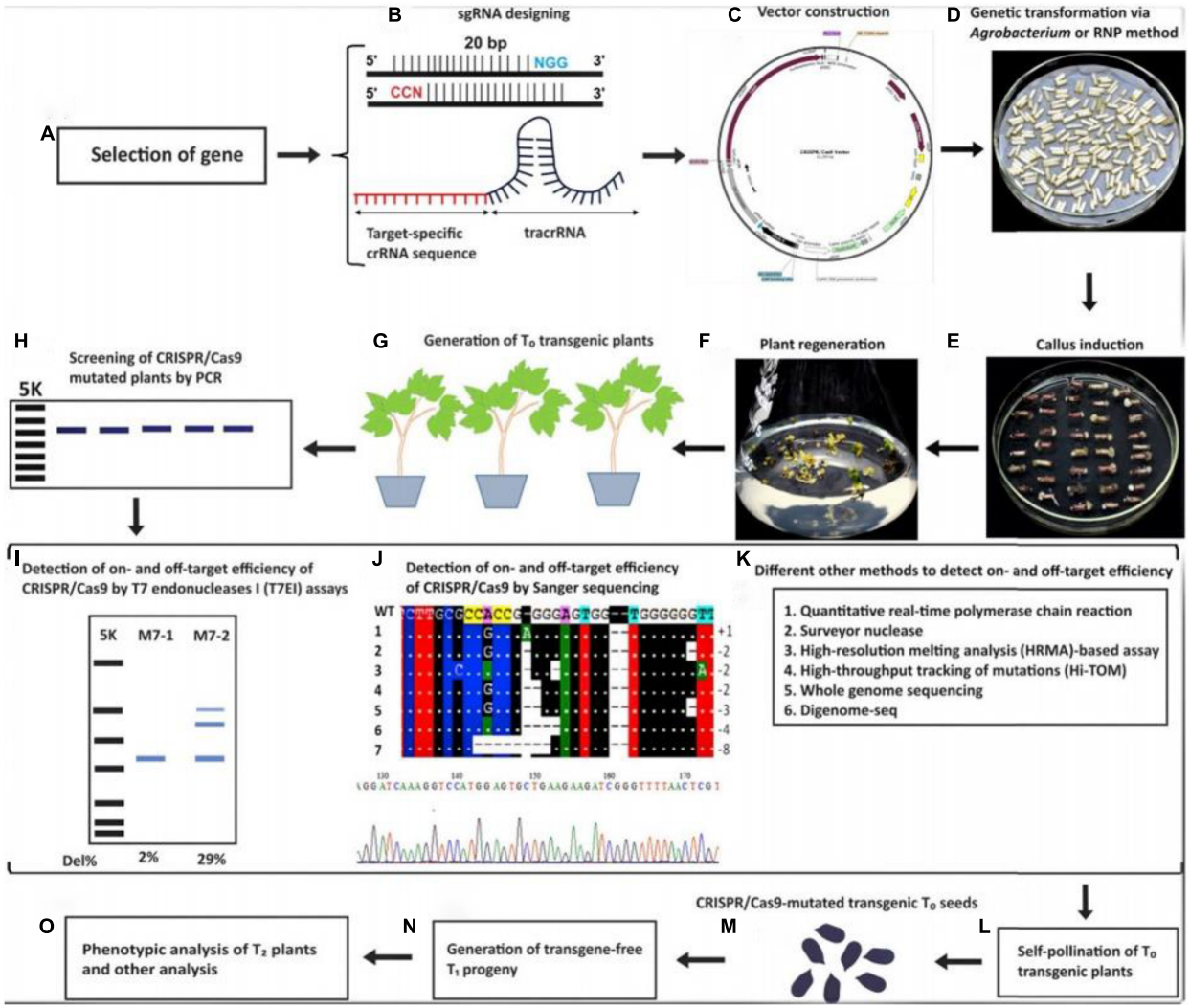


FIGURE 2 | Schematic illustration of the steps involved in CRISPR/Cas9 Genetic Transformation; **(A)** Specific gene selection, **(B)** sgRNA designing for the specific gene, **(C)** vector construction, **(D)** transformation of the CRISPR/Cas9 system *via Agrobacterium*, **(E)** callus induction from agrobacterium infected explants, **(F)** plant regeneration from callus, **(G)** T_0 CRISPR/Cas9 mutated transgenic plants, **(H)** screening of transgenic plants by PCR, **(I)** identification of mutated plants by T7E1, **(J)** detection of transgenics by sanger sequencing, **(K)** various techniques to detect transgenic plants, **(L)** self-pollination of T_0 transgenic plants for generation of homozygous T1 plants, **(M)** mutated T_0 seeds, **(N)** Generation of transgene- free T_1 progeny, **(O)** Phenotypic analysis of T_1 plants. Reproduced with permission from Manghwar et al. (2019) CellPress.

Wu and Li, 2021) and reduce the reactive oxygen species (ROS) levels in the mitochondria and chloroplasts to protect the plant (Sun L. et al., 2020; Sun et al., 2021). However, the use of these nanoparticle fertilizers in crop fields not only increase the soil fertility, but also greatly influence the water resource contamination (Naderi and Abedi, 2012; Mittal et al., 2020). Fertilizers containing microorganisms are labeled as biofertilizers, which can activate the plant system and improve the nutrient uptake from soil (Manikandan and Subramanian, 2016). Nano-fertilizers have the similar benefits like biofertilizers (Elias et al., 2019). Moreover, metallic nanoparticles have anti-pathogenic, antifungal, and antibacterial properties (Kah and Hofmann, 2014; Servin et al., 2015), so that they can survive under pathogenic bout under the soil. Brief explanation of using metallic nanoparticles in farming and its benefit in sustainable agriculture is explained in **Figure 3** (Mittal et al., 2020).

ROLE OF NANOPARTICLE-BASED GENETIC MODIFICATION OF CROPS

Nanoparticles acts as a carrier to deliver the necessary materials into plant cells, animal cells, and specific organs for cancer therapy, genetic disease treatment, and to obtain desirable traits in plants (Peng et al., 2019). Lv et al. (2020) and Ahmar et al. (2021) explained the method in which the gene transformation is performed using nanoparticles. Various types of nanoparticles have been used to deliver genetic

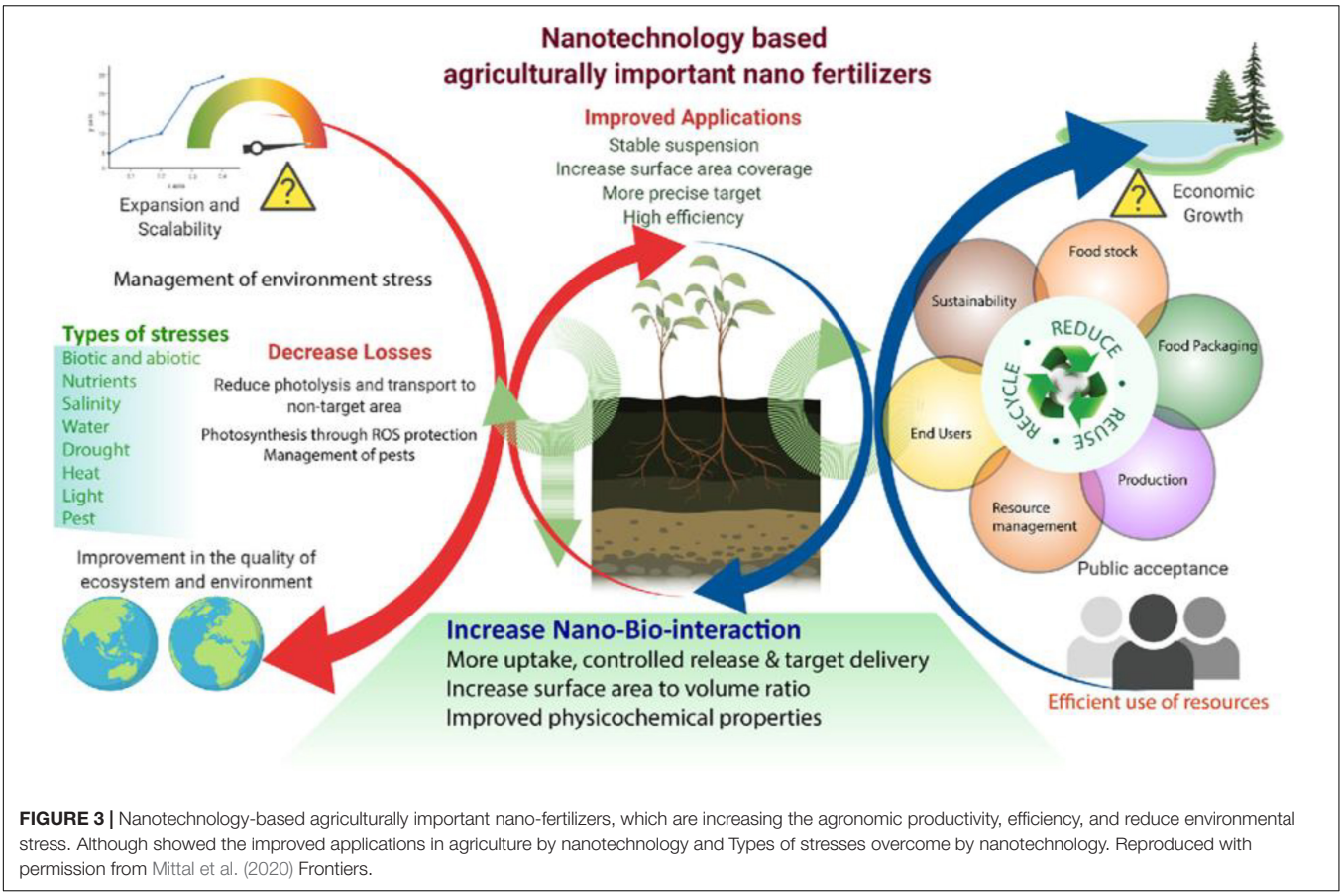


FIGURE 3 | Nanotechnology-based agriculturally important nano-fertilizers, which are increasing the agronomic productivity, efficiency, and reduce environmental stress. Although showed the improved applications in agriculture by nanotechnology and Types of stresses overcome by nanotechnology. Reproduced with permission from Mittal et al. (2020) Frontiers.

material into the plant cells through different platforms. These reports have also detailed the merits and demerits of utilizing nanoparticles in gene transfer methods. Typically, the mesoporous silica nanoparticles, carbon nanotubes, gold, and magnetic nanoparticles have been used to deliver plasmid DNA, double-stranded RNA, and siRNA into plant protoplasts or other intact cell lines (Al-Babili and Bouwmeester, 2015; Yao et al., 2016; Peng et al., 2019; Huan et al., 2020; Tsveta et al., 2021). However, Lv et al. (2020) have demonstrated the gene silencing and gene editing in plants with the use of nanoparticles; magnetic nanoparticle-based pollen transformation was used to achieve the task. In this approach, the vector-magnetic nanoparticle complex has been associated with the pollen that is dropped onto the stigma of desired plant flowers. Finally, plants produce the desired seeds by transferring the vector-magnetic nanoparticle complex into the flower stigma. Later, these flowers are modified into fruits, and the seeds were screened on antibiotic plates. The speed breeding protocol was used to obtain T0, T1, and T2 generations of transgenic plants; this breeding program is inexpensive for editing plant genomes and is employed for various *Brassica* species (Ahmar et al., 2021). Similarly, dsRNA has been loaded into the layered double hydroxide (LDH) clay nanosheets that are non-degradable, non-toxic, and resistant to easy wash. Furthermore, when these nanoparticle-dsRNA complexes are sprayed onto the plant leaves, they immediately attach to the leaf surface and are absorbed by plant viruses to induce RNAi, eventually degrading the targeted plant pathogens or endogenous mRNA can be minimized/eliminated (Lv et al., 2020). Similarly, gene editing has also been demonstrated with small NPs-CRISPR/Cas9 vector complex that was microinjected into the leaves or any other plant parts, which can be proliferated further by tissue culture or other ease protocols (Lv et al., 2020; Duan et al., 2021). Carbon dots-siRNA complex has been used to silence the GFP in tobacco and tomato plants (Schwartz et al., 2020). Demirer et al. (2021) recently demonstrated genome editing in plants using the CRISPR/Cas9 system along with nanoparticles and explained the regeneration, and phenotypic/metabolic changes of genomically edited crops. The methods in which gene expression, silencing, editing, and other applications involving nanoparticles can account for the crop refinement and are briefly explained in the **Figure 4** (Peng et al., 2019).

APPLICATIONS AND LIMITATIONS OF CRISPR/Cas9 AND NANOTECHNOLOGY SYSTEMS IN MODERN BIOLOGY

The CRISPR/Cas9 and nanotechnology aspects were successfully implemented so that relevant solicitations in plant biotechnology,

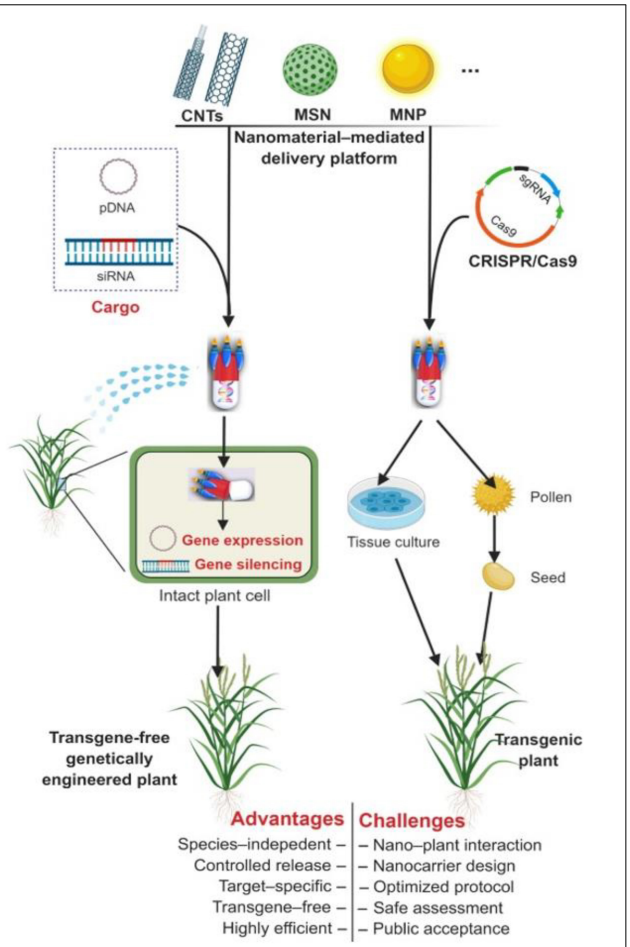


FIGURE 4 | Nanomaterial-mediated plant genetic engineering. Functionalized nanomaterials can provide a delivery platform that is capable of traversing barriers (e.g., multilayered cell walls) to deliver exogenous plasmid DNA (pDNA) and siRNA into intact plant cells. CNTs, carbon nanotubes; MSN, mesoporous silica nanoparticles; MNP, magnet nanoparticles. Reproduced with permission from Peng et al. (2019) CellPress.

food industry, livestock improvement can be achieved (Islam et al., 2020). Biofuel production (Javed et al., 2019), and rectifications of genetic and metabolic diseases can be done by controlling bacterial and viral diseases (Robert et al., 2017; Zafar et al., 2020), controlling bacterial and viral diseases (Zafar et al., 2020).

(1) This GE technology has been used to treat hematologic diseases, infectious diseases, and malignant tumors *via* gene therapy.
(2) Gene pyramids and gene knockouts can be created by inserting foreign genes through this approach.
(3) Repression/activation of gene expression.
(4) Delivery of proteins to genomic loci.
(5) Gene expression can be regulated with this technology. It also plays a major role in the progress of new mutant diversities to help the breeders.
(6) Gene silencing is an important aspect in the crop improvement program based on CRISPR intrusion (CRISPRi) (Larson et al., 2013; Qi et al., 2013).
(7) It is a promising technique to study the new gene's function.
(8) Plants that are lenient to biotic and abiotic stresses, as well as herbicides, can be easily developed.
(9) Researchers are already using this technology in gene therapy (Qian et al., 2019; Li et al., 2020).
(10) Currently, nanotechnology is being used to prepare nano-fertilizers, nano-pesticides, and to enhancing the abiotic stress tolerance, thereby protecting the crops.
(11) Different types of NPs have also been used for the transformation, editing, and silencing of genes to improve crop yield and quality.

CRISPR/Cas9 technology is among the best and most cost-effective methods for genomic editing in plants. However, some of its limitations are mentioned below.

(1) Genomic editing is inefficient and slow by the presence of larger protein sizes. Therefore, protein size should be small to ensure speedy and efficient genomic editing.
(2) It contains limited number of PAM sites at limited loci.
(3) CRISPR/CAS9 can introduce multiple random mutations, as well as mutations at unspecific loci.
(4) It has low HDR efficiency.
(5) It exhibits low efficiency against viruses.
(6) It has become difficult to commercialize transgenic crops developed using CRISPR/Cas9 technology in many countries because different countries have different rules and regulations.
(7) In backward and developing countries, there is a lack of proper understanding of pesticides, fertilizers, and other products developed by nanotechnology; therefore, it is impossible to grow better crops.

Challenges

At present, this technology is helping researchers in agriculture and breeders in developing crops that can overcome biotic and abiotic stress, with high nutritional values, and optimal yield parameters, thereby providing adequate food grains, vegetables, and fruits to current world population. Even with the availability of all types of biotechnological and bioinformatics tools, there are enduring challenges in developing genetically modified plants using the CRISPR system. Owing to unavailability of complete genome sequence information and the large genome size of some tropical, medicinally valuable crops, and fruits, some studies have been unable to edit genes to obtain desirable traits (Sanskriti et al., 2019; Zhou et al., 2019; Yang, 2020). Therefore, the biological pathways of genes and their interactions with environmental factors are still unknown (Haque et al., 2018). In order to discover new traits in tropical and other crops, one must be well-versed in the functions and regulatory elements of each gene. Moreover, in some crops, the transformation efficiency is extremely low; therefore, it takes a long time for the regeneration of explants, which is very difficult in

some crops (Altpeter et al., 2016; Sanskriti et al., 2019). However, genetically modified crops require extensive field trials (Syed et al., 2020). Of all the challenges facing in the development of genetically modified plants, lack of proper public acceptance has become the biggest challenge (Yang, 2020), and believing to be accepted in forthcoming decades (Chao et al., 2021).

CONCLUSION AND FUTURE PERSPECTIVE

Scientists and plant breeding researchers are working to develop high yielding and biotic/abiotic stress resistant variety. CRISPR/Cas9 GE in consolidation with nanotechnology have emerged as an important platform to improve the quality and desirable quality of agricultural crops with appreciable yield. These technologies are significantly susceptible and open new prospects in plant genetics. The nutritional values and quality of health prospects of plants and human could be enriched with broad spectrum of applications including in biomedical domain. The imminent fertility and diminishing useful prokaryotic microorganism issues in soil are delicate issues in addition to biotic problems. Relapsing the aforesaid issues could be feasible using CRISPR/Cas9 GE and nanotechnology aspects, it will be challenging and greatly influence to the crop refinement. Skillful editing of genetic sequence of plant genome could progressively improve the agronomic traits, photosynthetic capacity, and nutritional values. Furthermore, biotic and abiotic stress-induced issues in plants could be configured and minimized. The methodologies can also be diversified to characterize the individual gene functions, thereby improving the genomic sequences of agricultural crops to produce exceptional yield. These findings could point new strategies in agroecology facilitating the sustainable production of nutritional quality food to satisfy the increasing demand of ever-growing population.

CRISPR/Cas9 and nanoparticle complex system is an advanced innovative technique in agricultural crop development/refinement. Thus far, CRISPR system in connotation with nanotechnology has been used to improve the quality and yield of many valuable crops for future benefits. Using nanoparticle based fertilizers/additives; extinct nutrients could be regained, ensuring that the soil nutrients could be maintained. The green, non-toxic nanoparticles is a sagacious approach to increase micro and macronutrient levels in the soil for healthy growth of crops. Chemically derived nanoparticle usage should be eliminated; these can harm not only the crops but also to the environment. Zinc oxide-based nanocomposites and nano-fertilizers have shown appreciable results in crop growth; maintaining the soil salinity and fertility with robust yield. The green protocols to develop Zinc oxide-based green nanocomposites draws the attention of agro-scientific community and it should be given prime importance, so that toxic free effective nano-priming techniques can reduce the soil contamination and improves the seed quality. Metal organic frameworks (MOF) have been recently investigated as delivery systems for CRISPR/Cas9. Non-toxic and eco-friendly MOF 3-dimentional structures with biopolymer conjugates are potentially promising. Furthermore, CRISPR/Cas9-associated nanoparticle complex has been successfully utilized for transformation, silencing, and modification of genes to overcome the existing and expected critical biotic and abiotic issues, thereby producing nutritional-rich crops. This technology can be used to alter the metabolic pathways in plants to obtain desired high-quality secondary metabolites for future usage. Recently, revolutionary changes in this crop refinement program witnessed auspicious results. Nod factors have been shown to increase nitrogen efficiency in legume crops using CRISPR/Cas9 system with nano-technological contrivance. Modifying the Nod signaling pathway in cereal crops should eliminates the use of toxic inorganic fertilizers. The transformation efficiency by *Agrobacterium tumefaciens* is quite low in some specified plant tissues. Hence, an alternative bacterial system to gene transfer is necessary for ease genome editing in all crops by adopting CRISPR/Cas9-Nanotechnology system. Furthermore, the development of tissue culture free delivery protocols involving direct genomic editing in germplasms and meristematic cells of plants, can yield propitious results. To date, numerous crops have been developed with this combined CRISPR/Cas9-Nanoparticle complex system. It is advisable to framework on the products already developed by this method and ensure their recurrent use in agricultural locales. Extensive studies are recommended to elucidate the complete interactions (plant cell mechanisms) of nanoparticles/nanocomposites in all types of crops. We strongly believe that the products developed by conjoining these technologies will beneficially assist the agro-based researchers to bloom their ideas for innovative crop development/refinement.

AUTHOR CONTRIBUTIONS

BN planned the manuscript outline, wrote the draft, and prepared the tables. GS contributed in writing, reshaping/editing the manuscript and modifying the tables. GS, S-CK, MM, CS, RP, and MK proofread the manuscript. S-YK acquired the funding. S-YK and S-HL supervised the study and revised the manuscript. All the authors reviewed and approved the final version of the manuscript.

FUNDING

This work was supported by the Institute of Information and Communications Technology Planning and Evaluation (IITP) grant, funded by the Korea Government (MSIT) (No. 2020-0-00594, Morphable Haptic Controller for Manipulating VR·AR Contents). Priority Research Centers Program through the National Research Foundation of Korea (NRF) funded by the Ministry of Education (NRF-2018R1A6A1A03025526) also supported this work.

ACKNOWLEDGMENTS

The authors acknowledge Cooperative Equipment Center at KoreaTech for formal discussions. The authors are gratified to KoreaTech for providing the research opportunity/facilities.

SUPPLEMENTARY MATERIAL

The Supplementary Material for this article can be found online at: https://www.frontiersin.org/articles/10.3389/fpls.2022.843575/full#supplementary-material

REFERENCES

Abdallah, N. A., Prakash, C. S., and Hughen, A. G. (2014). Genome editing for crop improvement: challenges and opportunities. *GM Crops Food* 6, 183–205. doi: 10.1080/21645698.2015.1129937

Abe, K., Araki, E., Suzuki, Y., Toki, S., and Saika, H. (2018). Production of high oleic/low linoleic rice by genome editing. *Plant Physiol. Biochem.* 131, 58–62. doi: 10.1016/j.plaphy.2018.04.033

Adli, M. (2018). The CRISPR tool kit for genome editing and beyond. *Nat. Commun.* 9:1911. doi: 10.1038/s41467-018-04252-2

Ahmar, S., Mahmood, T., Fiaz, S., Poblet, F., Shafique, M. S., Chattha, M. S., et al. (2021). Advantage of nanotechnology-based genome editing system and its application in crop improvement. *Front. Plant Sci.* 12:663849.

Al Amin, N., Ahmad, N., Wu, N., Pu, X., Ma, T., Du, Y., et al. (2019). CRISPR-Cas9 mediated targeted disruption of FAD2-2 microsomal omega-6 desaturase in soybean (*Glycine max*.L). *BMC Biotechnol.* 19:501.

Al-Babili, S., and Bouwmeester, H. J. (2015). Strigolactones,a novel carotenoid-derived plant hormone. *Annu. Rev. Plant Biol.* 66, 161–186. doi: 10.1146/annurev-arplant-043014-114759

Albert, N. W., Davies, K. M., Lewis, D. H., Zhang, H., Montefiori, C., Boase, M. R., et al. (2014). A conserved network of transcriptional activators and repressors regulates anthocyanin pigmentation in eudicots. *Plant Cell* 26, 962–980. doi: 10.1105/tpc.113.122069

Ali, Z., Abul Faraj, A., Idris, A., Ali, S., Tashkandi, M., and Mahfouz, M. M. (2015a). CRISPR/Cas9-mediated viral interference in plants. *Genome Biol.* 16, 238–249. doi: 10.1186/s13059-015-0799-6

Ali, Z., Abul-faraj, A., Piatek, M., and Mahfouz, M. M. (2015b). Activity and specificity of TRV-mediated gene editing in plants. *Plant Signal. Behav.* 10:1044191. doi: 10.1080/15592324.2015.1044191

Altpeter, F., Springer, N. M., Bartler, L. E., Blechl, A. E., Brutnell, T. P., Citovsky, V., et al. (2016). Advancing crop transformation in the era of genome editing. *Plant Cell* 28, 1510–1520. doi: 10.1105/tpc.16.00196

Andersson, M., Turesson, H., Olsson, N., Sofie, F. A., Ohlsson, P., Gonzalez, M. N., et al. (2018). Genome editing in potato *via* CRISPR-Cas9 ribo nucleoprotein delivary. *Physiol. Plant.* 164, 378–384. doi: 10.1111/ppl.12731

Anzalone, A. V., Randolph, P. B., Davis, J. R., Sousa, A. A., Koblan, L. W., Levy, J. M., et al. (2019). Search-and-replace genome editing without double-strand breaks or donor DNA. *Nature* 576, 149–157. doi: 10.1038/s41586-019-1711-4

Aqsa, S., Tahira, Shaheera, Q., and Waqas, M. B. (2021). Applications of nanobiotechnology in plant sciences. *BJSTR* 35, 27236–27240. doi: 10.26717/BJSTR.2021.35.005632

Arndell, T., Sharma, N., Langridge, P., Baumann, U., Watson-Haigh, N. S., and Whitford, R. (2019). gRNA validation for wheat genome editing with the CRISPR-Cas9 system. *BMC Biotechnol.* 30:71. doi: 10.1186/s12896-019-0565-z

Ashokkumar, S., Jaganathan, D., Ramanathan, V., Rahman, H., Palaniswamy, R., Kambale, R., et al. (2020). Creation of novel alleles of fragrance gene OsBADH2 in rice through CRISPR/Cas9 mediated gene editing. *PLoS One* 15:e0237018. doi: 10.1371/journal.pone.0237018

Baek, K., Kim, D. H., Jeong, J., Sim, S. J., Melis, A., Kim, J. S., et al. (2016). DNA-freetwo-gene knockout in *Chlamydomonas reinhardtii via* CRISPR-Cas9 ribonucleo proteins. *Sci. Rep.* 6:30620. doi: 10.1038/srep30620

Baltes, N. J., Hummel, A. W., Konecna, E., Cegan, R., Bruns, A. N., Bisaro, D. M., et al. (2015). Conferring resistance to geminiviruses with the CRISPR–Cas prokaryotic immune system. *Nat. Plants* 1:15145. doi: 10.1039/nplants.2015.145

Bao, A., Chen, H., Chen, L., Chen, S., Hao, Q., Guo, W., et al. (2019). CRISPR/Cas9-mediated targeted mutagenesis of GmSPL9 genes alters plant architecture in soybean. *BMC Plant Biol.* 19:131. doi: 10.1186/s12870-019-1746-6

Bari, V. K., Nassar, J. A., Kheredin, S. M., Gal-On, A., Ron, M., Britt, A., et al. (2019). CRISPR/Cas9- mediated mutagenesis of CAROTENOID CLEAVAGE DIOXYGENASE 8 in tomato provides resistance against the parasitic weed Phelipanche aegyptiaca. *Sci. Rep.* 9:11438. doi: 10.1038/s41598-019-47893-z

Belhaj, K., Chaparro-Garcia, A., Kamoun, S., and Nekrasov, V. (2013). Plant genome editing made easy: targeted mutagenesis in model and crop plants using the CRISPR/Cas system. *Plant Methods* 9, 1–10. doi: 10.1186/1746-4811-9-39

Bernard, G., Gagneul, D., Alves Dos Santos, H., Etienne, A., Hilbert, J. L., and Rambaud, C. (2019). Efficient genome editing using CRISPR/Cas9 technology in chicory. *Int. J. Mol. Sci.* 20:1155. doi: 10.3390/ijms20051155

Bernheim, A., Calvo-Villamanan, A., Basier, C., Cui, L., Rocha, E. P. C., and Touchon, M. (2017). Inhibitions of NHEJ repair by type II-A CRISPR-Cas systems in bacteria. *Nat. Commun.* 8, 1–9. doi: 10.1038/s41467-017-02350-1

Bertier, L. D., Ron, M., Huo, H., Bradford, K. J., Britt, A. B., and Michelmore, R. W. (2018). High-resolution analysis of the efficiency, heritability, and editing outcomes of CRISPR/Cas9-induced modifications of NCED4 in lettuce (*Lactuca sativa*). *G3 Genes Genomes Genet.* 8, 1513–1521. doi: 10.1534/g3.117.300396

Bing, Y. (2020). Grand challenges in genome editing in plants. *Front. Genome Ed.* 2:2.

Bo, W., Zhaohui, Z., Huanhuan, Z., Xia, W., Binglin, L., Lijia, Y., et al. (2019). Targeted mutagenesis of NAC transcription factor gene, OsNAC041, leading to salt sensitivity in rice. *Rice Sci.* 26, 98–108. doi: 10.1016/j.rsci.2018.12.005

Breitler, J. C., Dechamp, E., Campa, C., Rodrigues, L. A. Z., Guyot, R., Marraccini, P., et al. (2018). CRISPR/Cas9-mediated efficient targeted mutagenesis has the potential to accelerate the domestication of *Coffea canephora*. *PCTOC* 134, 383–394. doi: 10.1007/s11240-018-1429-2

Breyer, D., Kopertekh, L., and Reheul, D. (2014). Alternatives to antibiotic resistance marker genes for *in vitro* selection of genetically modified plants – Scientific developments, current use, operational access, and biosafety considerations. *Crit. Rev. Plant Sci.* 33, 286–330. doi: 10.1080/07352689.2013.870422

Brooks, C., Nekrasov, V., Lippman, Z. B., and Van Eck, J. (2014). Efficient gene editing in tomato in the first generation using the clustered regularly interspaced short palindromic repeats/CRISPR-associated9 system. *Plant Physiol.* 166, 1292–1297. doi: 10.1104/pp.114.247577

Butler, N. M., Atkins, P. A., Voytas, D. F., and Douches, D. S. (2015). Generation and inheritance of targeted mutations in potato (*Solanum tuberosum* L.) using the CRISPR/Cas system. *PLoS One* 10:e0144591. doi: 10.1371/journal.pone.0144591

Cai, Y., Chen, L., Liu, X., Guo, C., Sun, S., Wu, C., et al. (2018). CRISPR/Cas9-mediated targeted mutagenesis of GmFT2a delays flowering time in soya bean. *Plant Biotechnol. J.* 16, 176–185. doi: 10.1111/pbi.12758

Cai, Y., Chen, L., Liu, X., Sun, S., Wu, C., Jiang, B., et al. (2015). CRISPR/Cas9-mediated genome editing in soybean hairy roots. *PLoS One* 10:e0136064. doi: 10.1371/journal.pone.0136064

Cantos, C., Francisco, P., Trijatmiko, K. R., Slamet-Loedin, I., and Chadha-Mohanty, P. K. (2014). Identification of "safe harbor" loci in indica rice genome by harnessing the property of zinc-finger nucleases to induce DNA damage and repair. *Front. Plant Sci.* 5:302. doi: 10.3389/fpls.2014.00302

Carroll, D. (2014). Genome engineering with targetable nucleases. *Annu. Rev. Biochem.* 83, 409–439. doi: 10.1146/annurev-biochem-060713-035418

Caterina, D., Adriana, L. S., and Giovanni, G. (2018). CRISPR/Cas9 editing of carotenoid genes in tomato. *Transgenic Res.* 27, 367–378. doi: 10.1007/s11248-018-0079-9

Chandrasekaran, J., Brumin, M., Wolf, D., Leibman, D., Klap, C., Pearlsman, M., et al. (2016). Development of broad virus resistance in non-transgenic cucumber using CRISPR/Cas9 technology. *Mol. Plant Pathol.* 17, 1140–1153. doi: 10.1111/mpp.12375

Chao, L., and Baohong, Z. (2019). Genome editing in cotton using CRISPR/Cas9 system. *Methods Mol. Biol.* 1902, 95–104. doi: 10.1007/978-1-4939-8952-2_8

Chao, L., Eleanor, B., Hikmet, B., and Baohong, Z. (2021). CRISPR/Cas: a nobel prize award-winning precise genome editing technology for gene therapy and crop improvement. *J. Zhejiang. Univ. Sci. B* 22, 253–284. doi: 10.1631/jzus.B2100009

Chao, L., Mengyu, H., Wenxiang, W., Hui, W., Fan, C., Wen, C., et al. (2018). An efficient CRISPR/Cas9 platform for rapidly generating simultaneous mutagenesis of multiple gene homoeologs in allotetraploid oilseed rape. *Front. Plant Sci.* 9:442. doi: 10.3389/fpls.2018.00442

Chao, S., Cai, Y., Feng, B., Jiao, G., Sheng, Z., Luo, L., et al. (2019). Editing of rice Isoamylase gene ISA1 provides insights in to its function in starch formation. *Rice Sci.* 26, 77–87. doi: 10.1016/j.rsci.2018.07.001

Charrier, A., Vergne, E., Dousset, N. J. P., Richer, A., Petiteau, A., and Chevreau, E. (2019). Efficient targeted mutagenesis in apple and first time edition of pear using the CRISPR-Cas9 system. *Front. Plant Sci.* 10:40. doi: 10.3389/fpls.2019.00040

Che, P., Anand, A., Wu, E., Sander, D., Simon, M., Zhu, W., et al. (2018). Developing a flexible, high efficiency *Agrobacterium*-mediated sorghum transformation system with broad application. *Plant Biotechnol. J.* 16, 1388–1395. doi: 10.1111/pbi.12879

Chen, R., Xu, Q., Liu, Y., Zhang, J., Ren, D., Wang, G., et al. (2018). Generation of transgene-free maize male sterile lines using the CRISPR/Cas9 system. *Front. Plant Sci.* 9:1180. doi: 10.3389/fpls.2018.01180

Chen, X., Lum, X., Shu, N., Wang, S., Wang, J., and Wang, D. (2017). Targeted mutagenesis in cotton (*Gossypium hirsutum* L.) using the CRISPR/Cas9 system. *Sci. Rep.* 7, 44304–44311. doi: 10.1038/srep44304

Chen, Y., Zhu, A., Xue, P., Wen, X., Cao, Y., Wang, B., et al. (2020). Effects of GS3 and GL3.1 for grain size editing by CRISPR/Cas9 in rice. *Rice Sci.* 27, 405–413. doi: 10.1016/j.rsci.2019.12.010

Cheng, Q., Dong, L., Su, T., Li, T., Gan, Z., Nan, H., et al. (2019). CRISPR/Cas9-mediated targeted mutagenesis of GmLHY genes alters plant height and internode length in soybean. *BMC Plant Biol.* 19:562. doi: 10.1186/s12870-019-2145-8

Cheng, Z., Sun, Y., Yang, S., Zhi, H., Yin, T., Ma, X., et al. (2021). Establishing In planta haploid inducer line by edited SiMTL in foxtail millet (Setaria italic). *Plant Biotechnol. J.* 19, 1089–1091. doi: 10.1111/pbi.13584

Chodacka, M. K., Oleszkiewicz, T., Lowder, L. G., Qi, Y., and Baranski, R. (2018). Efficient CRISPR/Cas9-based genome editing in carrot cells. *Plant Cell Rep.* 37, 575–586. doi: 10.1007/s00299-018-2252-2

Christian, M., Cermak, T., Doyle, E. L., Schmidt, C., Zhang, F., Hummel, A., et al. (2010). Targeting DNA double-strand breaks with TAL effector nucleases. *Genetics* 186, 757–761. doi: 10.1534/genetics.110.120717

Citorik, R. J., Mimee, M., and Lu, T. K. (2014). Sequence-specific antimicrobials using efficiently delivered RNA-guided nucleases. *Nat. Biotechnol.* 32, 1141–1145. doi: 10.1038/nbt.3011

Curtin, S. J., Xiong, Y., Michno, J. M., Campbell, B. W., Stec, A. O., Cermák, T., et al. (2018). CRISPR/Cas9 and TALENs generate heritable mutations for genes involved in small RNA processing of *Glycine max* and *Medicago truncatula*. *Plant Biotechnol. J.* 16, 1125–1137. doi: 10.1111/pbi.12857

Dalla, C. L. E., Mahmoud, L., Moraes, T. S., Mou, Z., Grosser, J. W., and Dutt, M. (2019). Development of improved fruit, vegetable, and ornamental crops using the CRISPR/Cas9 genome editing technique. *Plants* 8:601. doi: 10.3390/plants8120601

Demirer, G. S., Silva, T. N., Jackson, C. T., Thomas, J. B., Ehrhardt, D., Rhee, S. Y., et al. (2021). Nanotechnology to advance CRISPR–Cas genetic engineering of plants. *Nat. Nanotechnol.* 16, 243–250. doi: 10.1038/s41565-021-00854-y

Deng, L. (2018). Efficient generation of pink-fruited tomatoes using CRISPR/ Cas9 system. *J. Genet. Genome* 45, 51–54. doi: 10.1016/j.jgg.2017.10.002

D'Halluin, K., Vanderstraeten, C., Stals, E., Cornelissen, M., and Ruiter, R. (2008). Homologous recombination: a basis for targeted genome optimization in crop species such as maize. *Plant Biotechnol. J.* 6, 93–102. doi: 10.1111/J.1467-7652.2007.0035.X

Dimkpa, C. O., McLean, J. E., Latta, D. E., Manangón, E., and Britt, D. W. (2012). CuO and ZnO nanoparticles: phytotoxicity, metal speciation, and induction of oxidative stress in sand-grown wheat. *J. Nanopart Res.* 14, 1–15. doi: 10.1007/s11051-012-1125-9

Dort, E. N., Tanguay, P., and Hamelin, R. C. (2020). CRISPR/Cas9 gene editing: an unexplored frontier for forest pathology. *Front. Plant Sci.* 11:1126. doi: 10.3389/fpls.2020.01126

Duan, L., Ouyang, K., Xu, X., Xu, L., Wen, C., Zhou, X., et al. (2021). Nanoparticle delivery of CRISPR/ Cas9 for genome editing. *Front. Genet.* 12:673286. doi: 10.3389/fgene.2021.673286

Duan, Y. B., Li, J., Qin, R. Y., Xu, R. F., Li, H., Yang, Y. C., et al. (2016). Identification of a regulatory element responsible for salt induction of rice OsRAV2 through ex situ and insitu promoter analysis. *Plant Mol. Biol.* 90, 49–62. doi: 10.1007/s11103-015-0393-z

Ebina, H., Misawa, N., Kanemura, Y., and Koyanagi, Y. (2013). Harnessing the CRISPR/Cas9 system to disrupt latent HIV-1 provirus. *Sci. Rep.* 3:2510. doi: 10.1038/srep02510

Elias, E. E., Ifeyinwa, M. U., Damian, C. O., and Olubukola, O. B. (2019). The role of nanotechnology in the fortification of plant nutrients and improvement of crop production. *Appl. Sci.* 9, 1–32. doi: 10.3390/app9030499

El-Mounadi, K., Morales-Floriano, M. L., and Garcia-Ruiz, H. (2020). Principles, applications, and biosafety of plant genome editing using CRISPR-Cas9. *Front. Plant Sci.* 11:56. doi: 10.3389/fpls.2020.00056

Endo, M., Mikami, M., and Toki, S. (2015). Multigene knockout utilizing off-target mutations of the CRISPR/Cas9 system in rice. *Plant Cell Physiol.* 56, 41–47.

Fan, D., Liu, T., Li, C., Jiao, B., Li, S., Hou, Y., et al. (2015). Efficient CRISPR/Cas9-mediated targeted mutagenesis in *Populus* in the first generation. *Sci. Rep.* 5, 12217–12223. doi: 10.1038/srep12217

FAO (2017). *The Future of Food and Agriculture – Trends and Challenges*. Rome: FAO.

Fauser, F., Schiml, S., and Puchta, H. (2014). Both CRISPR/Cas based nucleases and nickases can be used efficiently for genome engineering in *Arabidopsisthaliana*. *Plant J.* 79, 348–359. doi: 10.1111/tpj.12554

Feng, C., Su, H., Bai, H., Wang, R., Liu, Y., Guo, X., et al. (2018). High efficiency genome editing using a dmc1 promoter controlled CRISPR/Cas9 system in maize. *Plant Biotechnol. J.* 16, 1848–1857. doi: 10.1111/pbi.12920

Feng, C., Yuan, J., Wang, R., Liu, Y., Birchler, J. A., and Han, F. (2016). Efficient targeted genome modification in maize using CRISPR/Cas9 system. *J. Genet. Genomics* 43, 37–43. doi: 10.1016/j.jgg.2015.10.002

Feng, Z., Zhang, B., Ding, W., Liu, X., Yang, D. L., Wei, P., et al. (2013). Efficient genome editing in plants using a CRISPR/Cas system. *Cell Res.* 23, 1229–1232. doi: 10.1038/cr.2013.114

Ferrara, M., Haidukowski, M., Logrieco, A., Leslie, J., and Mule, G. (2019). A CRISPR-Cas9 system for genome editing of *Fusarium proliferatum*. *Sci. Rep.* 9:19836. doi: 10.1038/s41598-019-56270-9

Fister, A. S., Landherr, L., Maximova, S. N., and Guiltinan, M. J. (2018). Transient expression of CRISPR/Cas9 machinery targeting TcNPR3 enhances defense response in *Theobroma cacao*. *Front. Plant Sci.* 9:268. doi: 10.3389/fpls.2018.00268

Gantz, V. M., Jasinskiene, N., Tatarenkova, O., Fazekas, A., Macias, V. M., Bier, E., et al. (2015). Highly efficient Cas9-mediated gene drives for population modification of the malaria vector mosquito *Anopheles stephensi*. *PNAS* 112, 6736–6743. doi: 10.1073/pnas.1521077112

Gao, J., Wang, G., Ma, S., Xie, X., Wu, X., and Xia, Q. (2015). CRISPR/Cas9-mediated targeted mutagenesis in *Nicotiana tabacum*. *Plant Mol. Biol.* 87, 99–110. doi: 10.1007/s11103-014-0263-0

Gao, W., Long, L., Tian, X., Xu, F., Liu, J., Singh, P. K., et al. (2017). Genome editing in cotton with the CRISPR/Cas9 system. *Front. Plant Sci.* 8:1364. doi: 10.3389/fpls.2017.01364

Gao, X., Chen, J., Dai, X., Zhang, D., and Zhao, Y. (2016). An effective strategy for reliably isolating heritable and Cas9-Free *Arabidopsis mutants* generated by CRISPR/Cas9-mediated genome editing. *Plant Physiol.* 171, 1794–1800. doi: 10.1104/pp.16.00663

Gasparis, S., Kała, M., Przyborowski, M., Łyżnik, L. A., Orczyk, W., and Nadolska-Orczyk, A. A. (2018). Simple and efficient CRISPR/Cas9 platform for induction of single and multiple, heritable mutations in barley (*Hordeum vulgare* L.). *Plant Methods* 14:111. doi: 10.1186/s13007-018-0382-8

Gautam, K., and Kumar, S. (2020). "Techniques for the detection, identification, and diagnosis of agricultural pathogens and diseases," in *Natural Remedies for Pest, Disease and Weed Control*, eds C. Egbuna and B. Sawicka (Cambridge, MA: Academic Press), 135–142.

Gil-Humanes, J., and Voytas, D. F. (2014). Wheat rescued from fungal disease. *Nat. Biotechnol.* 32, 886–887. doi: 10.1038/nbt.3013

Giovannini, A., Laura, M., Nesi, B., Savona, M., and Cardi, T. (2021). Genes and genome editing tools for breeding desirable phenotypes in ornamentals. *Plant Cell Rep.* 40, 461–478. doi: 10.1007/s00299-020-02632-x

Gomez, M. A., Lin, Z. D., Moll, T., Luebbert, C., Chauhan, R. D., Vijayaraghavan, A., et al. (2017). Simultaneous CRISPR/Cas9-mediated editing of cassava EIF4E isoforms NCBP-1 and NCBP-2 confers elevated resistance to cassava brown streak disease. *bioRxiv* [Preprint]. doi: 10.1111/pbi.12987

Gumtow, R., Wu, D., Uchida, J., and Tian, M. (2018). A Phytophthora palmivora extracellular cystatin-like protease inhibitor targets papain to contribute to virulence on papaya. *Mol. Plant Microbe Interact.* 31, 363–373. doi: 10.1094/MPMI-06-17-0131-FI

Hammond, A., Galizi, R., Kyrou, K., Simoni, A., Siniscalchi, C., Katsanos, D., et al. (2016). A CRISPR-Cas9 gene drive system targeting female reproduction in the malaria mosquito vector *Anopheles gambiae*. *Nat. Biotechnol.* 34, 78–83. doi: 10.1038/nbt.3439

Hannoufa, A., Pillai, B. V. S., and Chellamma, S. (2014). Genetic enhancement of *Brassica napus* seed quality. *Transgenic Res.* 23, 39–52. doi: 10.1007/s11248-013-9742-3

Haque, E., Taniguchi, H., Hassan, M. M., Bhowmik, P., Karim, M. R., Smiech, M., et al. (2018). Application of CRISPR/Cas9 genome editing technology for the improvement of crops cultivated in tropical climates: recent progress, prospects, and challenges. *Front. Plant Sci.* 9:617. doi: 10.3389/fpls.2018.00617

Hayut, F. S., Melamed Bessudo, C., and Levy, A. A. (2017). Targeted recombination between homologous chromosomes for precise breeding in tomato. *Nat. Commun.* 8:15605. doi: 10.1038/ncomms15605

Hinge, V., Patil, H., and Nadaf, A. (2015). Comparative characterization of aroma volatiles and related gene expression analysis at vegetative and mature stages in basmati and non-basmati rice (*Oryza sativa* L.) cultivars. *Appl. Biochem. Biotechnol.* 178, 619–639. doi: 10.1007/s12010-015-1898-2

Howells, R. M., Craze, M., Bowden, S., and Wallington, E. (2018). Efficient generation of stable, heritable gene edits in wheat using CRISPR/Cas9. *BMC Plant Biol.* 18:6088. doi: 10.1186/s12870-018-1433-z

Hsu, P. D., Lander, E. S., and Zhang, F. (2014). Development and applications of CRISPR-Cas9 for genome engineering. *Cell* 157, 1262–1278.

Hu, B., Li, D., Liu, X., Qi, J., Gao, D., Zhao, S., et al. (2017). Engineering non-transgenic gynoecious cucumber using an improved transformation protocol and optimized CRISPR/Cas9 system. *Plant Mol. Biol.* 10, 1575–1578. doi: 10.1016/j.molp.2017.09.005

Hu, J., Israeli, A., Ori, N., and Sun, T. (2018). The interaction between DELLA and ARF/IAA mediates crosstalk between gibberellin and auxin signaling to control fruit initiation in tomato. *Plant Cell* 30, 1710–1728. doi: 10.1105/tpc.18.00363

Hu, N., Xian, Z., Li, N., Liu, Y., Huang, W., Yan, F., et al. (2019). Rapid and user-friendly open-source CRISPR/Cas9 system for single- or multi-site editing of tomato genome. *Hortic. Res.* 6:7. doi: 10.1038/s41438-018-0082-6

Huan, Z., Honglu, Z., Gozde, S. D., Eduardo, G. G., Chunhai, F., and Markita, P. L. (2020). Engineering DNA nanostructures for SiRNA delivary in plants. *Nat. Protoc.* 15, 3064–3087. doi: 10.1038/s41596-020-0370-0

Huang, L., Zhang, R., Huang, G., Li, H., Melaku, G., Zhang, S., et al. (2018). Developing superior alleles of yield genes in rice by artificial mutagenesis using the CRISPR/Cas9 system. *J. Crop Prod.* 6, 475–481. doi: 10.1016/j.cj.2018.05.005

Huang, X. Z., Zeng, X. F., Li, J. R., and Zhao, D. (2017). Construction and analysis of tify1a and tify1b mutants in rice (Oryza sativa) based on CRISPR/Cas9 technology. *J. Agric. Biotechnol.* 25, 1003–1012.

Hummel, A. W., Chauhan, R. D., Cermak, T., Mutka, A. M., Vijayaraghavan, A., and Boyher, A. (2018). Allele exchange at the EPSPS locus confers glyphosate tolerance in cassava. *Plant Biotechnol. J.* 16, 1275–1282. doi: 10.1111/pbi.12868

Hussain, B., Lucas, S. T., and Budak, H. (2018). CRISPR/Cas9 in plants: at play in the genome and at work for crop improvement. *Brief Funct. Genomics* 17, 319–328. doi: 10.1093/bfgp/ely016

Hyun, Y., Kim, J., Cho, S. W., Choi, Y., Kim, J. S., and Coupland, G. (2015). Site-directed mutagenesis in *Arabidopsis thaliana* using dividing tissue-targeted RGEN of the CRISPR/Cas system to generate heritable null alleles. *Planta* 241, 271–284. doi: 10.1007/s00425-014-2180-5

Iqbal, Z., Sattar, M. N., and Shafiq, M. (2016). CRISPR/Cas9: a tool to circumscribe cotton leaf curl disease. *Front. Plant Sci.* 7:475. doi: 10.3389/fpls.2016.00475

Islam, M. D. A., Rony, S. A., Rahman, M. B., Cinar, M. U., Villena, J., Uddin, M. J., et al. (2020). Improvement of disease resistance in livestock: application of immuno genomics and CRISPR/Cas9 technology. *Animals* 10, 1–20. doi: 10.3390/ani10122236

Ito, Y., Nishizawa-Yokoi, A., Endo, M., Mikami, M., and Toki, S. (2015). CRISPR/Cas9-mediated mutagenesis of the RIN locus that regulates tomato fruit ripening. *Biochem. Biophys. Res. Commun.* 467, 76–82. doi: 10.1016/j.bbrc.2015.09.117

Javed, R. M., Noman, M., Shahid, M., Ahmed, T., Khurshid, M., Rashid, M. H., et al. (2019). Current situation of biofuel production and its enhancement by CRISPR/Cas9 –mediated genome engineering of microbial cells. *Microbiol. Res.* 219, 1–11. doi: 10.1016/j.micres.2018.10.010

Jia, H., Orbovic, V., Jones, J. B., and Wang, N. (2016). Modification of the PthA4 effector binding elements in type I CsLOB1 promoter using Cas9/sgRNA to produce transgenic Duncan grapefruit alleviating XccΔpthA4:dCsLOB1.3 infection. *Plant Biotechnol. J.* 14, 1291–1301. doi: 10.1111/pbi.12495

Jia, H., and Wang, N. (2014). Targeted genome editing of sweet orange using Cas9/sg RNA. *PLoS One* 9:e0093806. doi: 10.1371/journal.pone.0093806

Jia, H., Xu, J., Orbovic, V., Zhang, Y., and Wang, N. (2017). Editing citrus genome *via* SaCas9/sgRNA system. *Front. Plant Sci.* 8:2135. doi: 10.3389/fpls.2017.02135

Jia, H., Zhang, Y., Orbovic, V., Xu, J., White, F. F., Jones, J. B., et al. (2019). Genome editing of the disease susceptibility gene CsLOB1 in citrus confers resistance to citrus canker. *Plant Biotechnol. J.* 15, 817–823. doi: 10.1111/pbi.12677

Jiang, W., Zhou, H., Bi, H., Fromm, M., Yang, B., and Weeks, D. P. (2013). Demonstration of CRISPR/Cas9/sgRNA-mediated targeted gene modification in Arabidopsis, tobacco, sorghum and rice. *Nucleic Acids Res.* 41, 188–188. doi: 10.1093/nar/gkt780

Jiang, W. Z., Henry, I. M., Lynagh, P. G., Comai, L., Cahoon, E. B., and Weeks, D. P. (2017). Significant enhancement of fatty acid composition in seeds of the allohexaploid, Camelina sativa, using CRISPR/Cas9 gene editing. *Plant Biotechnol. J.* 15, 648–657. doi: 10.1111/pbi.12663

Jie, J., Zhang, C., Sun, Z., Wang, L., Duanmu, D., and Fan, Q. (2019). Genome editing in cowpea *Vigna unguiculata* using CRISPR-Cas9. *Int. J. Mol. Sci.* 20:2471. doi: 10.3390/ijms20102471

Joshi, R. K. (2019). Genome editing in chili pepper using a CRISPR/Cas9 Cytidine base editing system. *Asian J. Plant Sci. Res.* 9:445.

Kaboshi, M., Aida, R., and Sasaki, K. (2017). Generation of gene-edited *Chrysanthemum morifolium* using multi-copy transgenes as targets and markers. *Plant Cell Physiol.* 58, 216–226. doi: 10.1093/pcp/pcw222

Kah, M., and Hofmann, T. J. E. I. (2014). Nanopesticide research: current trends and future priorities. *Environ. Int.* 63, 224–235. doi: 10.1016/j.envint.2013.11.015

Kaminski, R., Chen, Y., Fischer, T., Tedaldi, E., Napoli, A., Zhang, Y., et al. (2017). Elimination of HIV-1 genomes from human T-lymphoid cells by CRISPR/Cas9 gene editing. *Sci. Rep.* 6, 1–15. doi: 10.1038/srep22555

Kanazashi, Y., Hirose, A., Takahashi, I., Mikami, M., Endo, M., Hirose, S., et al. (2018). Simultaneous site directed mutagenesis of duplicated loci in soybean using a single guide RNA. *Plant Cell Rep.* 37, 553–563. doi: 10.1007/s00299-018-2251-3

Kapusi, E., Corcuera-Gómez, M., Melnik, S., and Stoger, E. (2017). Heritable genomic fragment deletions and small indels in the putative ENGase gene induced by CRISPR/Cas9 in barley. *Front. Plant Sci.* 8:540. doi: 10.3389/fpls.2017.00540

Kathleen, L. H. (2015). Nutritionally enhanced food crops; progress and perspectives. *Int. J. Mol. Sci.* 16, 3895–3914. doi: 10.3390/ijms16023895

Kaur, N., Alok, A., Shivani Kaur, N., Pandey, P., Awasthi, P., and Tiwari, S. (2018). CRISPR/Cas9-mediated efficient editing in phytoene desaturase (PDS) demonstrates precise manipulation in banana cv. Rasthali genome. *Funct. Integr. Genomics* 18, 89–99. doi: 10.1007/s10142-017-0577-5

Khan, F. A., Pandupuspitasari, N. S., Chun-Jie, H., Ao, Z., Jamal, M., Zohaib, A., et al. (2016). CRISPR/Cas9 therapeutics: a cure for cancer and other genetic diseases. *Oncotarget* 7:52541. doi: 10.18632/oncotarget.9646

Khromov, A. V., Gushchin, V. A., Timerbaev, V. I, Kalinina, N. O., Taliansky, M. E., and Makarov, V. V. (2018). Guide RNA design for CRISPR/Cas9 mediated potato genome editing. *Dokl. Biophys. Mol. Biol.* 479, 90–94. doi: 10.1134/S1607672918020084

Khurana, S. M. P., and Rajarshi kumar, G. (2019). *Plant Biotechnology: Progress in Genomic Era*. Berlin: Springer Nature Singapore Pte Ltd.

Kim, D., Hager, M., Brant, E., and Budak, H. (2021). Efficient genome editing in wheat using Cas9 and Cpf1 (AsCpf1 and LbCpf1) nucleases. *Funct. Integr. Genomics* 21, 355–366. doi: 10.1007/s10142-021-00782-z

Kim, D., Kim, D., Alptekin, B., and Budak, H. (2018). CRISPR/Cas9 genome editing in wheat. *Funct. Integr. Genomics* 18, 31–41. doi: 10.1007/s10142-017-0572-x

Kis, A., Hamar, É, Tholt, G., Bán, R., and Havelda, Z. (2019). Creating highly efficient resistance against wheat dwarf virus in barley by employing CRISPR/Cas9 system. *Plant Biotechnol. J.* 17, 1004–1006. doi: 10.1111/pbi.13077

Klap, C., Yeshayahou, E., Bolger, A. M., Arazi, T., Gupta, S. K., Shabtai, S., et al. (2017). Tomato facultative parthenocarpy results from SlAGAMOUS-LIKE 6 loss of function. *Plant Biotechnol. J.* 15, 634–647. doi: 10.1111/pbi.12662

Koseoglou, E. (2017). *The Study of SlPMR4 CRISPR/Cas9-Mediated Tomato Allelic Series for Resistance Against Powdery Mildew*. Wageningen: Wageningen University.

Kui, L., Chen, H., Zhang, W., He, S., Xiong, Z., Zhang, Y., et al. (2017). Building a genetic manipulation toolbox for orchid biology: identification of constitutive promoters and application of CRISPR/Cas9 in the orchid *Dendrobiumofficinale*. *Front. Plant Sci.* 7:2036. doi: 10.3389/fpls.2016.02036

Kumar, N., Galli, M., Ordon, J., Stuttmann, J., Kogel, K. H., and Imani, J. (2018). Further analysis of barley MORC1 using a highly efficient RNA-guided Cas9 gene-editing system. *Plant Biotechnol. J.* 16, 1892–1903.

Kusano, H., Ohnuma, M., Mutsuro-Aoki, H., Asahi, T., Ichinosawa, D., Onodera, H., et al. (2018). Establishment of a modified CRISPR/Cas9 system with increased mutagenesis frequency using the translational enhancer dMac3 and multiple guide RNAs in potato. *Sci. Rep.* 8:13753. doi: 10.1038/s41598-018-32049-2

Lacomme, C. (2015). Strategies for altering plant traits using virus-induced gene silencing technologies. *Methods Mol. Biol.* 1287, 25–41. doi: 10.1007/978-1-4939-2453-0_2

Lang, Z., Wang, Y., Tang, K., Tang, D., Datsenka, T., Cheng, J., et al. (2017). Critical roles of DNA demethylation in the activation of ripening-induced genes and inhibition of ripening-repressed genes in tomato fruit. *Proc. Natl. Acad. Sci. U.S.A.* 114, 4511–4519. doi: 10.1073/pnas.1705233114

Larson, M. H., Gilbert, L. A., Wang, X., Lim, W. A., Weissman, J. S., and Qi, L. S. (2013). CRISPR interference (CRISPRi) for sequence-specific control of gene expression. *Nat. Protoc.* 8, 2180–2196. doi: 10.1038/nprot.2013.132

Lawrenson, T., and Harwood, W. A. (2019). Creating targeted gene knockouts in barley using CRISPR/Cas9. *Methods Mol. Biol.* 1900, 217–232. doi: 10.1007/978-1-4939-8944-7_14

Lawrenson, T., Shorinola, O., Stacey, N., Li, C., Østergaard, L., Patron, N., et al. (2015). Induction of targeted, heritable mutations in barley and Brassica oleracea using RNA-guided Cas9 nuclease. *Genome Biol.* 16, 258–271. doi: 10.1186/s13059-015-0826-7

Lee, C. W., Mahendra, S., Zodrow, K., Li, D., and Tsai, Y. C. (2010). Developmental phytotoxicity of metal oxide nanoparticles to Arabidopsis thaliana. *Environ. Toxicol. Chem.* 29, 669–675. doi: 10.1002/etc.58

Lemmon, Z. H. (2018). Rapid improvement of domestication traits in an orphan crop by genome editing. *Nat. Plants* 4, 766–770. doi: 10.1038/s41477-018-0259-x

Li, M., Li, X., Zhou, Z., Wu, P., Fang, M., and Pan, X. (2016). Reassessment of the four yield-related genes Gn1a, DEP1, GS3, and IPA1 in rice using a CRISPR/Cas9 system. *Front. Plant Sci.* 7:377. doi: 10.3389/fpls.2016.00377

Li, B., Cui, G., Shen, G., Zhan, Z., Huang, L., and Chen, J. (2017). Targeted mutagenesis in the medicinal plant *Salvia miltiorrhiza*. *Sci. Rep.* 7:43320. doi: 10.1038/srep43320

Li, J., Zhang, H., Si, X., Tian, Y., Chen, K., and Liu, J. (2017). Generation of thermosensitive male-sterile maize by targeted knockout of the ZmTMS5 gene. *JGG* 44, 465–468. doi: 10.1016/j.jgg.2017.02.002

Li, H., Yang, Y., Hong, W., Huang, M., Wu, M., and Zhao, X. (2020). Applications of genome editing technology in the targeted therapy of human diseases: mechanisms, advances and prospects. *Signal Transduct. Target. Ther.* 5:1. doi: 10.1038/s41392-019-0089-y

Li, J. F., Norville, J. E., Aach, J., McCormack, M., Zhang, D., and Bush, J. (2013). Multiplex and homologous recombination-mediated genome editing in *Arabidopsis* and *Nicotiana benthamiana* using guide RNA and Cas9. *Nat. Biotechnol.* 31, 688–691. doi: 10.1038/nbt.2654

Li, R., Li, R., Li, X., Fu, D., Zhu, B., Tian, H., et al. (2018a). Multiplexed CRISPR/Cas9-mediated metabolic engineering of γ- aminobutyric acid levels in *Solanum lycopersicum*. *Plant Biotechnol. J.* 16, 415–427. doi: 10.1111/pbi.12781

Li, R., Zhang, L., Wang, L., Chen, L., Zhao, R., Sheng, J., et al. (2018b). Reduction of tomato-plant chilling tolerance by CRISPR-Cas9-mediated SlCBF1 mutagenesis. *J. Agric. Food Chem.* 66, 9042–9051. doi: 10.1021/acs.jafc.8b02177

Li, R., Zhu, D. F. B., Luo, Y., and Hu, H. (2018c). CRISPR/Cas9-mediated mutagenesis of lncRNA1459 alters tomato fruit ripening. *Plant J.* 4, 513–524. doi: 10.1111/tpj.13872

Li, X., Wang, Y., Chen, S., Tian, H., Fu, D., Zhu, B., et al. (2018d). Lycopene is enriched in tomato fruit by CRISPR/Cas9-mediated multiplex genome editing. *Front. Plant Sci.* 9:559. doi: 10.3389/fpls.2018.00559

Li, C., Zong, Y., Wang, Y., Jin, S., Zhang, D., Song, Q., et al. (2018e). Expanded base editing in rice and wheat using a Cas9-adenosine deaminase fusion. *Genome Biol.* 19:59. doi: 10.1186/s13059-018-1443-z

Li, A., Jia, S., Yobi, A., Ge, Z., Sato, S. J., Zhang, C., et al. (2018f). Editing of an alpha-kafirin gene family increases, digestibility and protein quality in sorghum. *Plant Physiol.* 177, 1425–1438. doi: 10.1104/pp.18.00200

Li, T., Yang, X., Yu, Y., Si, X., Zhai, X., Zhang, H., et al. (2018g). Domestication of wild tomato is accelerated by genome editing. *Nat. Biotechnol.* 36, 1160–1163. doi: 10.1038/nbt.4273

Li, C., Nguyen, V., Liu, J., Fu, W., Chen, C., Yu, K., et al. (2019). Mutagenesis of seed storage protein genes in Soybean using CRISPR/Cas9. *BMC Res. Notes* 12:176. doi: 10.1186/s13104-019-4207-2

Li, R., Liu, C., Zhao, R., Wang, L., Chen, L., Yu, W., et al. (2019). CRISPR/Cas9-Mediated SlNPR1 mutagenesis reduces tomato plant drought tolerance. *BMC Plant Biol.* 19:38. doi: 10.1186/s12870-018-1627-4

Li, Z. S., Liu, Z. B., Xing, A. Q., Moon, B. P., Koellhoffer, J. P., and Huang, L. X. (2015). Cas9-guide RNA directed genome editing in soybean. *Plant Physiol.* 169, 960–970. doi: 10.1104/pp.15.00783

Liang, Z., Zhang, K., Chen, K., and Gao, C. (2014). Targeted mutagenesis in *Zea mays* using TALENs and the CRISPR/Cas system. *J. Genet. Genomics* 41, 63–68. doi: 10.1016/j.jgg.2013.12.001

Liao, H. K., Gu, Y., Diaz, A., Marlett, J., Takahashi, Y., Li, M., et al. (2015). Use of the CRISPR/Cas9 system as an intracellular defense against HIV-1 infection in human cells. *Nat. Commun.* 6, 1–10. doi: 10.1038/ncomms7413

Liu, G., Li, J., and Godwin, I. D. (2019). Genome editing by CRISPR/Cas9 in sorghum through biolistic bombardment. *Methods Mol. Biol.* 1931, 169–183. doi: 10.1007/978-1-4939-9039-9_12

Liu, H., Wang, K., Jia, Z., Gong, Q., Lin, Z., Du, L., et al. (2020). Efficient induction of haploid plants in wheat by editing of TaMTL using an optimized *Agrobacterium*-mediated CRISPR System. *J. Exp. Bot.* 71, 1337–1349. doi: 10.1093/jxb/erz529

Lloyd, A., Brockman, A., Aguirre, L., Campbell, A., Bean, A., Cantero, A., et al. (2017). Advances in the MYB–bHLH–WD repeat (MBW) pigment regulatory model: addition of a WRKY factor and co-option of an anthocyanin MYB for betalain regulation. *Plant Cell Physiol.* 58, 1431–1441. doi: 10.1093/pcp/pcx075

Lou, D., Wang, H., and Yu, D. (2018). The sucrose non-fermenting-1-related protein kinases SAPK1 and SAPK2 function collaboratively as positive regulators of salt stress tolerance in rice. *BMC Plant Biol.* 18:203. doi: 10.1186/s12870-018-1408-0

Lv, Z., Jiang, R., Chen, J., and Chen, W. (2020). Nanoparticle-mediated gene transformation strategies for plant genetic engineering. *Plant J.* 104, 880–891. doi: 10.1111/tpj.14973

Lyzenga, W. J., Harrington, M., Bekkaoui, D., Wigness, M., Dwayne, D., Hegedus, D. D., et al. (2019). CRISPR/Cas9 editing of three CRUCIFERIN C homoeologues alters the seed protein profile in *Camelina sativa*. *BMC Plant Biol.* 19:292. doi: 10.1186/s12870-019-1873-0

Ma, C., Liu, M., Li, Q., Si, J., Ren, X., and Song, H. (2019a). Efficient BoPDS gene editing in cabbage by the CRISPR/Cas9 System. *Hortic. Plant J.* 5, 164–169. doi: 10.1016/j.hpj.2019.04.001

Ma, C., Zhu, C., Zheng, M., Liu, M., Zhang, D., Liu, B., et al. (2019b). CRISPR/Cas9-mediated multiple gene editing in Brassica oleracea var. capitata using the endogenous tRNA-processing system. *Hortic. Res.* 6:20. doi: 10.1038/s41438-018-0107-1

Ma, X., Zhang, Q., Zhu, Q., Liu, W., Chen, Y., Qiu, R., et al. (2015). A robust CRISPR/Cas9 system for convenient, high-efficiency multiplex genome editing in monocot and dicot plants. *Mol. Plant.* 8, 1274–1284. doi: 10.1016/j.molp.2015.04.007

Macias, V. M., McKeand, S., Rodriguez, D. C., Hughes, G. L., Fazekas, A., Pujhari, S., et al. (2020). Cas9-Mediated gene-editing in the malaria mosquito *Anopheles stephensi* by remot control. *G3 Genes Genomes Genetics* 10, 1353–1360. doi: 10.1534/g3.120.401133

Macovei, A., Sevilla, N. R., Cantos, C., Jonson, G. B., Loedin, I. S., Čermák, T., et al. (2018). Novel alleles of rice eIF4G generated by CRISPR/Cas9-targeted mutagenesis confer resistance to Rice tungro spherical virus. *Plant Biotechnol. J.* 16, 1918–1927. doi: 10.1111/pbi.12927

Maioli, A., Gianoglio, S., Moglia, A., Acquadro, A., Valentino, D., Milani, A. M., et al. (2020). Simultaneous CRISPR/Cas9 editing of three PPO genes reduces fruit flesh browning in *Solanum melongena* L. *Front. Plant Sci.* 11:607161. doi: 10.3389/fpls.2020.607161

Mali, P., Aach, J., Stranges, P. B., Esvelt, K. M., Moosburner, M., Kosuri, S., et al. (2013). CAS9 transcriptional activators for target specificity screening and paired nickases for cooperative genome engineering. *Nat. Biotechnol.* 31, 833–838. doi: 10.1038/nbt.2675

Malnoy, M., Viola, R., Jung, M. H., Koo, O. J., Kim, S., Kim, J. S., et al. (2016). DNA-free genetically edited grapevine and apple protoplast using CRISPR/Cas9 ribonucleo proteins. *Front. Plant Sci.* 7:1904. doi: 10.3389/fpls.2016.01904

Mandal, P. K., Ferreira, L. M., Collins, R., Meissner, T. B., Boutwell, C. L., Friesen, M., et al. (2014). Efficient ablation of genes in human hematopoietic stem and effector cells using CRISPR/Cas9. *Cell Stem Cell* 15, 643–652. doi: 10.1016/j.stem.2014.10.004

Manghwar, H., Lindsey, K., Zhang, X., and Jin, S. (2019). CRISPR/Cas system: recent advances and future prospects for genome editing. *Trends Plant Sci.* 24, 1102–1125. doi: 10.1016/j.tplants.2019.09.006

Manikandan, A., and Subramanian, K. (2016). Evaluation of zeolite based nitrogen nano-fertilizers on maize growth, yield and quality on inceptisols and alfisols. I. *J. Plant Soil Sci.* 9, 1–9. doi: 10.9734/IJPSS/2016/22103

Mao, X., Zheng, Y., Xiao, K., Wei, Y., Zhu, Y., Cai, Q., et al. (2018). OsPRX2 contributes to stomatal closure and improves potassium deficiency tolerance in rice. *Biochem. Biophys. Res. Commun.* 495, 461–467. doi: 10.1016/j.bbrc.2017

Mao, Y., Botella, J. R., Liu, Y., and Zhu, J. K. (2019). Gene editing in plants: progress and challenges. *Natl. Sci. Rev.* 6, 421–437. doi: 10.1093/nsr/nwz005

Mao, Y., Zhang, H., Xu, N., Zhang, B., Gou, F., and Zhu, J. K. (2013). Application of the CRISPR–Cas system for efficient genome engineering in plants. *Mol. Plant.* 6, 2008–2011. doi: 10.1093/mp/sst121

Mao, Y., Zhang, Z., Feng, Z., Wei, P., Zhang, H., Botella, J. R., et al. (2016). Development of germline specific CRISPR Cas9 systems to improve the production of heritable gene modifications in *Arabidopsis*. *Plant Biotechnol. J.* 14, 519–532. doi: 10.1111/pbi.12468

Martín Pizarro, C., Triviño, J. C., and Posé, D. (2019). Functional analysis of the TM6 MADS-box gene in the octoploid strawberry by CRISPR/Cas9-directed mutagenesis. *J. Exp. Bot.* 70, 885–895. doi: 10.1093/jxb/ery400

Mercx, S., Smargiasso, N., Chaumont, F., Pauw, E. D., Boutry, M., and Navarre, C. (2017). Inactivation of the b (1, 2)- xylosyltransferase and the a (1, 3)-fucosyltransferase genes in *Nicotiana tabacum* BY-2 cells by a multiplex CRISPR/Cas9 strategy results in glycoproteins without plant-specific glycans. *Front. Plant Sci.* 8:403. doi: 10.3389/fpls.2017.00403

Miao, J., Guo, D., Zhang, J., Huang, Q., Qin, G., Zhang, X., et al. (2013). Targeted mutagenesis in rice using CRISPR-Cas system. *Cell Res.* 23, 1233–1236. doi: 10.1038/cr.2013.123

Michno, J. M., Wang, X., Liu, J., Curtin, S. J., Kono, T. J., and Stupar, R. M. (2015). CRISPR/Cas mutagenesis of soybean and *Medicago truncatula* using a new web-tool and a modified Cas9 enzyme. *GM Crops Food* 6, 243–252. doi: 10.1080/21645698.2015.1106063

Miller, J. C., Holmes, M. C., Wang, J., Guschin, D. Y., Lee, Y. L., Rupniewski, I., et al. (2007). An improved zinc-finger nuclease architecture for highly specific genome editing. *Nat. Biotechnol.* 25, 778–785. doi: 10.1038/nbt1319

Mittal, D., Kaur, G., Singh, P., Yadav, K., and Ali, S. A. (2020). Nanoparticle-based sustainable agriculture and food science: recent advances and future outlook. *Front. Nanotechnol.* 2:579954. doi: 10.3389/fnano.2020.579954

Murovec, J., Gucek, K., Bohanec, B., Avbelj, M., and Jerala, R. (2018). DNA-free genome editing of *Brassica oleracea* and *B. Rapa* protoplasts using CRISPR-Cas9 ribonucleoprotein complexes. *Front. Plant Sci.* 9:1594. doi: 10.3389/fpls.2018.01594

Nadakuduti, S. S., and Enciso-Rodríguez, F. (2021). Advances in genome editing with CRISPR systems and transformation technologies for plant DNA Manipulation. *Front. Plant Sci.* 11:637159. doi: 10.3389/fpls.2020.637159

Naderi, M. R., and Abedi, A. (2012). Application of nanotechnology in agriculture and refinement of environmental pollutants. *J. Nanotechnol.* 11, 18–26. doi: 10.4236/snl.2013.33008

Nakajima, I., Ban, Y., Azuma, A., Onoue, N., Moriguchi, T., Yamamoto, T., et al. (2017). CRISPR/Cas9- mediated targeted mutagenesis in grape. *PLoS One* 12:e0177966. doi: 10.1371/journal.pone

Nakayasu, M., Akiyama, R., Lee, H. J., Osakabe, K., Osakabe, Y., Watanabe, B., et al. (2018). Generation of solanine-free hairy roots of potato by CRISPR/Cas9 mediated genome editing of the St16DOX gene. *Plant Physiol. Biochem.* 131, 70–77. doi: 10.1016/j.plaphy.2018

Neelendra, K., Galli, M., Ordon, J., Stuttmann, J., Kogel, K. H., and Imani, J. (2018). Further analysis of barley MORC1 using a highly efficient RNA-guided Cas9 gene-editing system. *Plant Biotechnol. J.* 16, 1892–1903. doi: 10.1111/pbi.12924

Nekrasov, V., Staskawicz, B., Weigel, D., Jones, J. D., and Kamoun, S. (2013). Targeted mutagenesis in the model plant Nicotiana benthamiana using Cas9 RNA-guided endonuclease. *Nat. Biotechnol.* 31, 691–693. doi: 10.1038/nbt.2655

Nekrasov, V., Wang, C., Win, J., Lanz, C., Weigel, D., and Kamoun, S. (2017). Rapid generation of a transgene-free powdery mildew resistant tomato by genome deletion. *Sci. Rep.* 7, 482–486. doi: 10.1038/s41598-017-00578-x

Nishihara, M., Higuchi, A., Watanabe, A., and Tasaki, K. (2018). Application of the CRISPR/Cas9 system for modification of flower color in *Torenia fournieri*. *BMC Plant Biol.* 18:331. doi: 10.1186/s12870-018-1539-3

Nonaka, S., Arai, C., Takayama, M., Matsukura, C., and Ezura, H. (2017). Efficient increase of ɣ-aminobutyric acid (GABA) content in tomato fruits by targeted mutagenesis. *Sci. Rep.* 7:7057. doi: 10.1038/s41598-017-06400-y

Ordon, J., Gantner, J., Kemna, J., Schwalgun, L., Reschke, M., Streubel, J., et al. (2017). Generation of chromosomal deletions in dicotyledonous plants employing a user-friendly genome editing tool kit. *Plant J.* 89, 155–168. doi: 10.1111/tpj.13319

Ortigosa, A., Gimenez-Ibanez, S., Leonhardt, N., and Solano, R. (2019). Design of a bacterial speck resistant tomato by CRISPR/Cas9-mediated editing of SlJAZ2. *Plant Biotechnol. J.* 17, 665–673. doi: 10.1111/pbi.13006

Osakabe, Y., Liang, Z., Ren, C., Nishitani, C., Osakabe, K., Wada, M., et al. (2018). CRISPR–Cas9-mediated genome editing in apple and grapevine. *Nat. Protoc.* 13:2844. doi: 10.1038/s41596-018-0067-9

Osakabe, Y., Watanabe, T., Sugano, S. S., Ueta, R., Ishihara, R., Shinozaki, K., et al. (2016). Optimization of CRISPR/Cas9 genome editing to modify abiotic stress responses in plants. *Sci. Rep.* 6:26685. doi: 10.1038/srep26685

Otang Ntui, V., Tripathi, J., and Tripathi, L. (2020). Robust CRISPR/Cas9 mediated genome editing tool for banana and plantain (*Musa* spp.). *Curr. Plant Biol.* 21:100128. doi: 10.1016/j.cpb.2019.100128

Ousterout, D. G., Kabadi, A. M., Thakore, P. I., Majoros, W. H., Reddy, T. E., and Gersbach, C. A. (2015). Multiplex CRISPR/Cas9-based genome editing for correction of dystrophin mutations that cause Duchenne muscular dystrophy. *Nat. Commun.* 6:6244. doi: 10.1038/ncomms7244

Oz, M. T., Altpeter, A., Karan, R., Merotto, A., and Altpeter, F. (2021). CRISPR/Cas9-mediated multi-allelic gene targeting in sugarcane confers herbicide tolerance. *Front. Genome Ed.* 3:673566. doi: 10.3389/fgeed.2021.673566

Padmaja, G. (1995). Cyanide detoxification in cassava for food and feed uses. *Crit. Rev. Food Sci. Nutr.* 35, 299–339. doi: 10.1080/10408399509527703

Pan, C., Ye, L., Qin, L., Liu, X., He, Y., Wang, J., et al. (2016). CRISPR/Cas9-mediated efficient and heritable targeted mutagenesis in tomato plants in the first and later generations. *Sci. Rep.* 6:24765. doi: 10.1038/srep24765

Pan, L., Yan, J. L., Feng, J. Z., Gui, Z. Z., Xiao, Y. J., Hui, M. Y., et al. (2016). The *Arabidopsis* UDP-glycosyltransferasesUGT79B2 and UGT79B3, contribute

to cold, salt and drought stress tolerance *via* modulating anthocyanin accumulation. *Plant J.* 89, 85–103. doi: 10.1111/tpj.13324

Pankaj, B., Ellison, E., Polley, B., Bollina, V., Kulkarni, M., Ghanbarnia, K., et al. (2018). Targeted mutagenesis in wheat microspores using CRISPR/Cas9. *Sci. Rep.* 8:6502. doi: 10.1038/s41598-018-24690-8v

Park, C. Y., Lee, D. R., Sung, J. J., and Kim, D. W. (2016). Genome-editing technologies for gene correction of hemophilia. *Hum. Genet.* 15, 977–981. doi: 10.1007/s00439-016-1699-x

Peng, A., Chen, S., Lei, T., Xu, L., He, Y., Wu, L., et al. (2017). Engineering canker resistant plants through CRISPR/Cas9 targeted editing of the susceptibility gene CsLOB 1 promoter in citrus. *Plant Biotechnol. J.* 15, 1509–1519. doi: 10.1111/pbi.12733

Peng, W., Fang-Jie, Z., and Peter, M. K. (2019). Engineering crops without genome integration using nanotechnology. *Trends Plant Sci.* 24, 574–577.

Pham, A. T., Shannon, J. G., and Bilyeu, K. D. (2012). Combinations of mutant FAD2 and FAD3 genes to produce high oleic acid and low linolenic acid soybean oil. *Theor. Appl. Genet.* 125, 503–515. doi: 10.1007/s00122-012-1849-z

Pioneer (2016). *DuPont Announces Intentions to Commercialize First CRISPR-Cas Product*. Available online at: https://www.prweb.com/releases/dupont-pioneer-seed/crispr-cas-corn/prweb13349828.htm (accessed April 18, 2016).

Platt, R. J., Chen, S., Zhou, Y., Yim, M. J., Swiech, L., Kempton, H. R., et al. (2014). CRISPR-Cas9 knockin mice for genome editing and cancer modeling. *Cell* 159, 440–455. doi: 10.1016/j.cell.2014.09.014

Pramanik, D., Shelake, R. M., Park, J., Kim, M. J., Hwang, I., Park, I., et al. (2021). CRISPR/Cas9-mediated generation of pathogen-resistant tomato against tomato yellow leaf curl virus and powdery mildew. *Int. J. Mol. Sci.* 22:1878. doi: 10.3390/ijms22041878

Prihatna, C., Barbetti, M. J., and Barker, S. J. (2018). A novel tomato *Fusarium* wilt tolerance gene. *Front. Microbiol.* 9:1226. doi: 10.3389/fmicb.2018.01226

Pyott, D. E., Sheehan, E., and Molnar, A. (2016). Engineering of CRISPR/ Cas9-mediated potyvirus resistance in transgene-free *Arabidopsis* plants. *Mol. Plant Pathol.* 17, 1276–1288. doi: 10.1111/mpp.12417

Qi, L. S., Larson, M. H., Gilbert, L. A., Doudna, J. A., Weissman, J. S., Arkin, A. P., et al. (2013). Repurposing CRISPR as an RNA-guided platform for sequence-specific control of gene expression. *Cell* 152, 1173–1183.

Qi, W., Zhu, T., Tian, Z., Li, C., Zhang, W., and Song, R. (2016). High-efficiency CRISPR/Cas9 multiplex gene editing using the glycine tRNAprocessing system-based strategy in maize. *BMC Biotechnol.* 16:58.

Qian, L., Zhou, Q., Qingnan, W., Ting, X., Yang, Y., and Zhiyao, H. (2019). Applications of genome editing technology in animal disease modeling and gene therapy. *Comput. Struct. Biotechnol. J.* 17, 689–698. doi: 10.1016/j.csbj.2019.05.006

Raitskin, O., Schudoma, C., West, A., and Patron, N. J. (2019). Comparison of efficiency and specificity of CRISPR-associated (Cas) nucleases in plants: An expanded toolkit for precision genome engineering. *PLoS One* 14:e0211598. doi: 10.1371/journal.pone.0211598

Rana, R. A., Siddiqui, M. N., Skalicky, M., Brestic, M., Hossain, A., Kayesh, E., et al. (2021). Prospects of nanotechnology in improving the productivity and quality of horticultural crops. *Horticulturae* 7:332. doi: 10.3390/horticulturae7100332

Ren, C., Liu, X., Zhang, Z., Wang, Y., Duan, W., Li, S., et al. (2016). CRISPR/Cas9-mediated efficient targeted mutagenesis in Chardonnay (*Vitisvinifera* L.). *Sci. Rep.* 6:32289. doi: 10.1038/srep32289

Robert, F., Huang, S., and Pelletier, J. (2017). CRISPR / Cas9 editing to facilitate and expand drug discovery. *Curr. Gene Ther.* 17, 275–285. doi: 10.2174/1566523217666171121164615

Rodriguez-Leal, D., Lemmon, Z. H., Man, J., Bartlett, M. E., and Lippman, Z. B. (2017). Engineering quantitative trait variation for crop improvement by genome editing. *Cell* 171, 470–480. doi: 10.1016/j.cell.2017.08.030

Roldan, M. V. G., Perilleux, C., Morin, H., Huerga-Fernandez, S., Latrasse, D., Benhamed, M., et al. (2017). Natural and induced loss of function mutations in SlMBP21 MADS-box gene led to jointless-2 phenotype in tomato. *Sci. Rep.* 7:4402. doi: 10.1038/s41598-017-04556-1

Ron, M., Kajala, K., Pauluzzi, G., Wang, D., Reynoso, M. A., Zumstein, K., et al. (2014). Hairy root transformation using *Agrobacterium rhizogenes* as a tool for exploring cell type-specific gene expression and function using tomato as a model. *Plant Physiol.* 166, 455–469. doi: 10.1104/pp.114.239392

Sadanandom, A., Srivastava, A. K., and Zhang, C. (2019). Targeted mutagenesis of the SUMO protease, overly tolerant to salt1 in rice through CRISPR/Cas9-mediated genome editing reveals a major role of this SUMO protease in salt tolerance. *BioRxiv* [Preprint]. doi: 10.1101/555706

Sánchez-León, S., Gil-Humanes, J., Ozuna, C. V., Giménez, M. J., Sousa, C., Voytas, D. F., et al. (2018). Low-gluten, nontransgenic wheat engineered with CRISPR/Cas9. *Plant Biotechnol. J.* 16, 902–910. doi: 10.1111/pbi.12837

Sanskriti, V., Surbhi, K., Virender, K., Gunvant, B. P., Trupti, J., Humira, S., et al. (2019). Genome editing in Plants: exploration of technological advancements and challenges. *Cells* 8:1386. doi: 10.3390/cells8111386

Sauer, N. J., Narváez-Vásquez, J., Mozoruk, J., Miller, R. B., Warburg, Z. J., and Woodward, M. J. (2016). Oligonucleotide-mediated genome editing provides precision and function to engineered nucleases and antibiotics in plants. *Plant Physiol.* 170, 1917–1928. doi: 10.1104/pp.15.01696

Schwank, G., Koo, B. K., Sasselli, V., Dekkers, J. F., Heo, I., and Demircan, T. (2013). Functional repair of CFTR by CRISPR/Cas9 in intestinal stem cell organoids of cystic fibrosis patients. *Cell Stem Cell* 13, 653–658. doi: 10.1016/j.stem.2013.11.002

Schwartz, S. H., Hendrix, B., Hoffer, P., Sanders, R. A., and Zheng, W. (2020). Carbon dots for efficient sirna delivery and gene silencing in plants. *Plant Physiol.* 184, 647–657. doi: 10.1104/pp.20.00733

Servin, A., Elmer, W., Mukherjee, A., Torre Roche, R. D. L., and Hamdi, H. (2015). A review of the use of engineered nanomaterials to suppress plant disease and enhance crop yield. *J. Nanopart Res.* 17, 1–21. doi: 10.1007/s11051-015-2907-7

Shan, Q., Wang, Y., Li, J., Zhang, Y., Chen, K., Liang, Z., et al. (2013). Targeted genome modification of crop plants using a CRISPR-Cas system. *Nat. Biotechnol.* 31, 686–688. doi: 10.1038/nbt.2650

Shang, Y., Hasan, M. K., Ahammed, G. J., Li, M., Yin, H., and Zhou, J. (2019). Applications of nanotechnology in plant growth and crop protection: a review. *Molecules* 24:2558. doi: 10.3390/molecules24142558

Shao, X., Wu, S., Dou, T., Zhu, H., Hu, C., Huo, H., et al. (2019). Using CRISPR/Cas9 genome editing system to create MaGA20ox2 gene-modified semi-dwarf banana. *Plant Biotechnol. J.* 18, 17–19. doi: 10.1111/pbi.13216

Shen, C., Que, Z., Xia, Y., Tang, N., Li, D., He, R., et al. (2017). Knock out of the annexin gene OsAnn3 *via* CRISPR/Cas9-mediated genome editing decreased cold tolerance in rice. *J. Plant Biol.* 60, 539–547. doi: 10.1007/s12374-016-0400-1

Sheykhbaglou, R., Sedghi, M., Shishevan, M. T., and Sharifi, R. S. (2010). Effects of nano-iron oxide particles on agronomic traits of soybean. *Not. Sci. Biol.* 2, 112–113. doi: 10.15835/nsb224667

Shi, J., Gao, H., Wang, H., Lafitte, H. R., Archibald, R. L., and Yang, M. (2017). ARGOS8 variants generated by CRISPR-Cas9 improve maize grain yield under field drought stress conditions. *Plant Biotechnol. J.* 15, 207–216. doi: 10.1111/pbi.12603

Shibuya, K., Watanabe, K., and Ono, M. (2018). CRISP/Cas9-mediated mutagenesis of the EPHEMERAL1 locus that regulates petal senescence in Japanese morning glory. *Plant Physiol.* 131, 53–57. doi: 10.1016/j.plaphy.2018.04.036

Shim, J. S., Oh, N., Chung, P. J., Kim, Y. S., Choi, Y. D., and Kim, J. K. (2018). Over expression of OsNAC14 improves drought tolerance in rice. *Front. Plant Sci.* 9:310. doi: 10.3389/fpls.2018.00310

Shu, H., Luo, Z., Peng, Z., and Wang, J. (2020). The application of CRISPR/Cas9 in hair roots to explore the functions of AhNFR1 and AhNFR5 genes during peanut nodulation. *BMC Plant Biol.* 20:417. doi: 10.1186/s12870-020-02614-x

Singh, M., Kumar, M., Albertsen, M. C., Young, J. K., and Cigan, A. M. (2018). Concurrent modifications in the three homeologs of Ms45 gene with CRISPR-Cas9 lead to rapid generation of male sterile bread wheat (*Triticum aaestivum*, L.). *Plant Mol. Biol.* 97, 371–383. doi: 10.1007/s11103-018-0749-2

Smith, J., Grizot, S., Arnould, S., Duclert, A., Epinat, J. C., Chames, P., et al. (2006). A combinatorial approach to create artificial homing endonucleases cleaving chosen sequences. *Nucleic Acids Res.* 34, 149–149. doi: 10.1093/nar/gkl720

So, M. C., Wiederrecht, G. P., Mondloch, J. E., Hupp, J. T., and Farha, O. K. (2015). Metal-organic framework materials for light-harvesting and energy transfer. *Chem. Comm.* 51, 3501–3510. doi: 10.1039/c4cc09596k

Songstad, D. D., Petolino, J. F., Voytas, D. F., and Reichert, N. A. (2017). Genome editing of plants. *Crit. Rev. Plant Sci.* 36, 1–23. doi: 10.1080/07352689.2017.1281663

Soyk, S., Muller, N. A., Park, S. J., Schmalenbach, I., Jiang, K., Hayama, R., et al. (2017). Variation in the flowering gene SELF PRUNING 5G promotes day-neutrality and early yield in tomato. *Nat. Genet.* 49, 162–168. doi: 10.1038/ng.3733

Stajic, E., Kiełkowska, A., Murovec, J., and Bohanec, B. (2019). Deep sequencing analysis of CRISPR/Cas9 induced mutations by two delivery methods in target model genes and the CENH3 region of red cabbage (*Brassica oleracea* var. capitata f. rubra). *PCTOC* 139, 227–235. doi: 10.1007/s11240-019-01665-9

Su, S., Xiao, W., Guo, W., Yao, X., Xiao, J., Ye, Z., et al. (2017). The CYCLOIDEA-RADIALIS module regulates petal shape and pigmentation, leading to bilateral corolla symmetry in *Torenia fournieri* (Linderniaceae). *New Phytol.* 215, 1582–1593. doi: 10.1111/nph.14673

Subburaj, S., Chung, S. J., Lee, C., Ryu, S. M., Kim, D. H., Kim, J. S., et al. (2016). Site-directed mutagenesis in *Petunia hybrida* protoplast system using direct delivery of purified recombinant Cas9 ribonucleo proteins. *Plant Cell Rep.* 35, 1535–1544. doi: 10.1007/s00299-016-1937-7

Subramanian, K. S., Manikandan, A., Thirunavukkarasu, M., and Rahale, C. S. (2015). "Nano-fertilizers for balanced crop nutrition," in *Nanotechnologies in Food and Agriculture*, eds M. Rai, C. Ribeiro, L. Mattoso, and N. Duran (Cham: Springer), 69–80. doi: 10.1007/s00210-021-02057-7

Sugano, S. S., Shirakawa, M., Takagi, J., Mastuda, Y., Shimada, T., Nishimura, I. H., et al. (2014). CRISPR/Cas9-Mediated targeted mutagenesis in Liverwort *Marchantia polymorpha* L. *Plant Cell Physiol.* 55, 475–481. doi: 10.1093/pcp/pcu014

Sun, B., Jiang, M., Zheng, H., Jian, Y., Huang, W. L., Yuan, Q., et al. (2020). Color-related chlorophyll and carotenoid concentrations of Chinese kale can be altered through CRISPR/Cas9 targeted editing of the carotenoid isomerase gene BoaCRTISO. *Hortic. Res.* 7:161. doi: 10.1038/s41438-020-00379-w

Sun, L., Song, F., Guo, J., Zhu, X., Liu, S., Liu, F., et al. (2020). Nano-ZnO-induced drought tolerance is associated with melatonin synthesis and metabolism in maize. *Int. J. Mol. Sci.* 21, 1–18. doi: 10.3390/ijms21030782

Sun, B., Zheng, A., Jiang, M., Xue, S., Yuan, Q., Jiang, L., et al. (2018). CRISPR/Cas9-mediated mutagenesis of homologous genes in Chinese kale. *Sci. Rep.* 8:16786. doi: 10.1038/s41598-018-34884-9

Sun, L., and Kao, T. H. (2018). CRISPR/Cas9-mediated knockout of PiSSK1 reveals essential role of S-locus F-box protein-containing SCF complexes in recognition of non-self S-RNases during cross-compatible pollination in self-incompatible *Petunia inflata*. *Plant Reprod.* 31, 129–143. doi: 10.1007/s00497-017-0314-1

Sun, L., Song, F., Zhu, X., Liu, S., Liu, F., Wang, Y., et al. (2021). Nano-ZnO alleviates drought stress *via* modulating the plant water use and carbohydrate metabolism in maize. *Arch. Agro. Soil Sci.* 67, 245–259. doi: 10.1080/03650340.2020.1723003

Sun, N., and Zhao, H. (2014). Seamless correction of the sickle cell disease mutation of the HBB gene in human induced pluripotent stem cells using TALENs. *Biotechnol. Bioeng.* 111, 1048–1053. doi: 10.1002/bit.25018

Sun, Y., Jiao, G., Liu, Z., Zhang, X., Li, J., Guo, X., et al. (2017). Generation of high-amylose rice through CRISPR/Cas9-mediated targeted mutagenesis of starch branching enzymes. *Front. Plant Sci.* 8:298. doi: 10.3389/fpls.2017.00298

Sun, Y., Li, J., and Xia, L. (2016). Precise genome modification *via* sequence-specific nucleases-mediated gene targeting for crop improvement. *Front. Plant Sci.* 7:1928. doi: 10.3389/fpls.2016.01928

Sunitha, S., and Rock, C. D. (2020). CRISPR/Cas9-mediated targeted mutagenesis of TAS4 and MYBA7 loci in grapevine rootstock 101-14. *Transgenic Res.* 29, 355–367. doi: 10.1007/s11248-020-00196-w

Svitashev, S., Young, J. K., Schwartz, C., Gao, H., Falco, S. C., and Cigan, A. M. (2015). Targeted mutagenesis, precise gene editing, and site-specific gene insertion in maize using Cas9 and guide RNA. *Plant Physiol.* 169, 931–945. doi: 10.1104/pp.15.00793

Syed, S. A. Z., Ahmad, M., Herve, V., and Magdy, M. M. (2020). Engineering crops of the future: CRISPR approaches to develop climate-resilient and disease-resistant plants. *Genome Biol.* 21:289. doi: 10.1186/s13059-020-02204-y

Tang, L., Mao, B., Li, Y., Ly, Q., Zhang, L., Chen, C., et al. (2017). Knockout of OsNramp5 using the CRISPR/Cas9 system produces low Cd-accumulating indica rice without compromising yield. *Sci. Rep.* 7:14438. doi: 10.1038/s41598-017-14832-9

Tang, X. D., Gao, F., Liu, M. J., Fan, Q. L., Chen, D. K., and Ma, W. T. (2019). Methods for enhancing clustered regularly interspaced short palindromic repeats/Cas9-mediated homology-directed repair efficiency. *Front. Genet.* 10:551. doi: 10.3389/fgene.2019.00551

Tashkandi, M., Ali, Z., Aljedaani, F., Shami, A., and Mahfouz, M. M. (2018). Engineering resistance against Tomato yellow leaf curl virus *via* the CRISPR/Cas9 system in tomato. *Plant Signal. Behav.* 13:1525996. doi: 10.1080/15592324.2018

Tavakoli, K., Pour-Aboughadareh, A., Kianersi, F., Poczai, P., Etminan, A., and Shooshtari, L. (2021). Applications of CRISPR-Cas9 as an advanced genome editing system in life sciences. *BioTech* 10:14. doi: 10.3390/biotech10030014

Thomazella, D. P. T., Brail, Q., Dahlbeck, D., and Staskawicz, B. (2016). CRISPR-Cas9 mediated mutagenesis of a DMR6 ortholog in tomato confers broad-spectrum disease resistance. *BioRxiv* [Preprint]. doi: 10.1101/064824

Thul, S. T., and Saragani, B. K. (2015). "Implications of nanotechnology on plant productivity and its rhizospheric environment," in *Nanotechnology and Plants: Nanoparticles and Their Impact On Plants*, eds M. H. Siddiqui, M. H. Al-Whaibi, and M. Firoz (Cham: Springer), 37–53.

Tian, S., Jiang, L., Cui, X., Zhang, J., Guo, S., Li, M., et al. (2018). Engineering herbicide-resistant watermelon variety through CRISPR/Cas9-mediated base-editing. *Plant Cell Rep.* 37, 1353–1356. doi: 10.1007/s00299-018-2299-0

Tian, S., Jiang, L., Gao, Q., Zhang, J., Zong, M., Zhang, H., et al. (2017). Efficient CRISPR/Cas9-based gene knockout in watermelon. *Plant Cell Rep.* 36, 399–406. doi: 10.1007/s00299-016-2089-5

Tomlinson, L., Yang, Y., Emenecker, R., Smoker, M., Taylor, J., Perkins, S., et al. (2019). Using CRISPR/Cas9 genome editing in tomato to create a gibberellin-responsive dominant dwarf DELLA allele. *Plant Biotechnol. J.* 17, 132–140. doi: 10.1111/pbi.12952

Tong, C. G., Wu, F. H., Yuan, Y. H., Chen, Y. R., and Lin, C. S. (2020). High-efficiency CRISPR/Cas-based editing of *Phalaenopsis* orchid MADS genes. *Plant Biotechnol. J.* 18, 889–891. doi: 10.1111/pbi.13264

Tripathi, J. N., Ntui, V. O., Ron, M., Muiruri, S. K., Britt, A., and Tripathi, L. (2019). CRISPR/Cas9 editing of endogenous banana streak virus in the B genome of Musa spp. overcomes a major challenge in banana breeding. *Commun. Biol.* 2, 1–11. doi: 10.1038/s42003-019-0288-7

Tsai, C. J., and Xue, L. J. (2015). CRISPRing into the woods. *GM Crops Food* 6, 206–215. doi: 10.1080/21645698.2015

Tsveta, T., Lidia, S., Lora, T., Atanas, A., and Ivelin, P. (2021). DNA-free gene editing in plants: a brief overview. *Biotechnol. Biotechnol. Equip.* 35, 131–138. doi: 10.1080/13102818.2020.1858159

Tuncel, A., Corbin, K. R., Ahn-Jarvis, J., Harris, S., Hawkins, E., Smedley, M. A., et al. (2019). Cas9-mediated mutagenesis of potato starch-branching enzymes generates a range of tuber starch phenotypes. *Plant Biotechnol. J.* 17, 2259–2271. doi: 10.1111/pbi.13137

Ueta, R., Abe, C., Watanabe, T., Sugano, S. S., Ishihara, R., Ezura, H., et al. (2017). Rapid breeding of parthenocarpic tomato plants using CRISPR/Cas9. *Sci. Rep.* 7:507. doi: 10.1038/s41598-017-00501-4

Upadhyay, S. K., Kumar, J., Alok, A., and Tuli, R. (2013). RNA-guided genome editing for target gene mutations in wheat. *G3 Genes Genomes Genet.* 3, 2233–2238. doi: 10.1534/g3.113.008847

Urnov, F. D., Miller, J. C., Lee, Y. L., Beausejour, C. M., Rock, J. M., Augustus, S., et al. (2005). Highly efficient endogenous human gene correction using designed zinc-finger nucleases. *Nature* 435, 646–651. doi: 10.1038/nature03556

Usman, B., Nawaz, G., Zhao, N., Liao, S., Qin, B., Liu, F., et al. (2021). Programmed editing of rice (*Oryza sativa* L.) OsSPL16 gene using CRISPR/Cas9 improves grain yield by modulating the expression of pyruvate enzymes and cell cycle proteins. *Int. J. Mol. Sci.* 22:249. doi: 10.3390/ijms22010249

Varkonyi-Gasic, E., Wang, T. C., Jeon, S., Drummond, R. S. M., Gleave, A. P., and Allan, A. C. (2018). Mutagenesis of kiwifruit CENTRORADIALIS-like genes transforms a climbing woody perennial with long juvenility and axillary flowering into a compact plant with rapid terminal flowering. *Plant Biotechnol. J.* 17, 869–880. doi: 10.1111/pbi.13021

Veillet, F., Perrot, L., Chauvin, L., Kermarrec, M. P., Guyon-Debast, A., Chauvin, J. E., et al. (2019). Transgene-free genome editing in tomato and potato plants using *Agrobacterium*-mediated delivery of a CRISPR/Cas9 cytidine base editor. *Int. J. Mol. Sci.* 20:402. doi: 10.3390/ijms20020402

Voytas, D. F., and Gao, C. (2014). Precision genome engineering and agriculture: opportunities and regulatory challenges. *PLoS Biol.* 12:e1001877. doi: 10.1371/journal.pbio.1001877

Wada, N., Ueta, R., Osakabe, Y., and Osakabe, K. (2020). Precision genome editing in plants: state-of-the-art in CRISPR/Cas9-based genome engineering. *BMC Plant Biol.* 20:234. doi: 10.1186/s12870-020-02385-5

Waltz, E. (2016). Gene-edited CRISPR mushroom escapes US regulation. *Nature* 532:293. doi: 10.1038/nature.2016.19754

Wan, L., Wang, Z., Tang, M., Hong, D., Sun, Y., Ren, J., et al. (2021). CRISPR-Cas9 gene editing for fruit and vegetable crops: strategies and prospects. *Horticulturae* 7:193. doi: 10.3390/horticulturae7070193

Wang, D., Samsulrizal, N. H., Yan, C., Allcock, N. S., Craigon, J., Ulate, B. B., et al. (2019a). Characterization of CRISPR mutants targeting genes modulating pectin degradation in ripening tomato. *Plant Physiol.* 179, 544–557. doi: 10.1104/pp.18.01187

Wang, L., Chen, S., Peng, A., Xie, Z., He, Y., and Zou, X. (2019b). CRISPR/Cas9-mediated editing of CsWRKY22 reduces susceptibility to *Xanthomonas citri* subsp. citri in wanjincheng orange (*Citrus sinensis* (L.) Osbeck). *Plant Biotechnol. Rep.* 13, 501–510. doi: 10.1007/s11816-019-00556-x

Wang, R., da Rocha Tavano, E. C., Lammers, M., Martinelli, A. P., Angenent, G. C., and de Maagd, R. A. (2019c). Re-evaluation of transcription factor function in tomato fruit development and ripening with CRISPR/Cas9-mutagenesis. *Sci. Rep.* 9:1696. doi: 10.1038/s41598-018-38170-6

Wang, H., Wu, Y., Zhang, Y., Yang, J., Fan, W., Zhang, H., et al. (2019d). CRISPR/Cas9-based mutagenesis of starch biosynthetic genes in sweet potato (Ipomoea Batatas) for the improvement of starch quality. *Int. J. Mol. Sci.* 20:4702. doi: 10.3390/ijms20194702

Wang, B., Zhu, L., Zhao, B., Zhao, Y., Xie, Y., Zheng, Z., et al. (2019e). Development of a haploid- inducer mediated genome editing system for accelerating maize breeding. *Mol. Plant* 12, 597–602. doi: 10.1016/j.molp.2019.03.006

Wang, H., La Russa, M., and Qi, L. S. (2016a). CRISPR/Cas9 in genome editing and beyond. *Annu. Rev. Biochem.* 85, 227–264. doi: 10.1146/annurev-biochem-060815-014607

Wang, F., Wang, C., Liu, P., Lei, C., Hao, W., and Gao, Y. (2016b). Enhanced rice blast resistance by CRISPR/Cas9-targeted mutagenesis of the ERF transcription factor gene OsERF922. *PLoS One* 11:e0154027. doi: 10.1371/journal.pone.0154027

Wang, L., Wang, L., Tan, Q., Fan, Q., Zhu, H., and Hong, Z. (2016c). Efficient inactivation of symbiotic nitrogen fixation related genes in *Lotus japonicas* using CRISPR-Cas9. *Front. Plant Sci.* 7:1333. doi: 10.3389/fpls.2016.01333

Wang, J., Kuang, H., Zhang, Z., Yang, Y., Yan, L., Zhang, M., et al. (2020). Generation of seed lipoxigenase free soyabean using CRISPR-Cas9. *Crop J.* 8, 432–439. doi: 10.1016/j.cj.2019.08.008

Wang, L., Chen, L., Li, R., Zhao, R., Yang, M., Sheng, J., et al. (2017a). Reduced drought tolerance by CRISPR/Cas9-mediated SlMAPK3 mutagenesis in tomato plants. *J. Agric. Food Chem.* 65, 8674–8682. doi: 10.1021/acs.jafc.7b02745

Wang, P., Zhang, J., Sun, L., Ma, Y., Xu, J., Liang, S., et al. (2017b). High efficient multisites genome editing in allotetraploid cotton (*Gossypium hirsutum*) using CRISPR/Cas9 system. *Plant Biotechnol. J.* 16, 137–150. doi: 10.1111/pbi.12755

Wang, Y., Meng, Z., Liang, C., Meng, Z., Wang, Y., Sun, G., et al. (2017c). Increased lateral root formation by CRISPR/Cas9 mediated editing of arginase genes in cotton. *Sci. China Life Sci.* 60, 524–527. doi: 10.1007/s11427-017-9031-y

Wang, X., Tu, M., Wang, D., Liu, J., Li, Y., Li, Z., et al. (2018a). CRISPR/Cas9-mediated efficient targeted mutagenesis in grape in the first generation. *Plant Biotechnol. J.* 16, 844–855. doi: 10.1111/pbi.12832

Wang, Z., Wang, S., Li, D., Zhang, Q., Li, L., Zhong, C., et al. (2018b). Optimized paired-sgRNA/Cas9 cloning and expression cassette triggers high-efficiency multiplex genome editing in kiwifruit. *Plant Biotechnol. J.* 16, 1424–1433. doi: 10.1111/pbi.12884

Wang, T., Deng, Z., Zhang, X., Wang, H., Wang, Y., Liu, X., et al. (2018c). Tomato DCL2b is required for the biosynthesis of 22-nt small RNAs, the resulting secondary siRNAs, and the host defense against ToMV. *Hortic. Res.* 5:62. doi: 10.1038/s41438-018-0073-7

Wang, Y., Cheng, X., Shan, Q., Zhang, Y., Liu, J., Gao, C., et al. (2014). Simultaneous editing of three homoeoalleles in hexaploid bread wheat confers heritable resistance to powdery mildew. *Nat. Biotechnol.* 32, 947–951. doi: 10.1038/nbt.2969

Wang, Z. P., Xing, H. L., Dong, L., Zhang, H. Y., Han, C. Y., Wang, X. C., et al. (2015). Egg cell-specific promoter-controlled CRISPR/Cas9 efficiently generates homozygous mutants for multiple target genes in *Arabidopsis* in a single generation. *Genome Biol.* 16:144. doi: 10.1186/s13059-015-0715-0

Watanabe, K., Breier, U., Hensel, G., Kumlehn, J., Schubert, I., and Reiss, B. (2016). Stable gene replacement in barley by targeted double-strand breaks induction. *J. Exp. Bot.* 67, 1433–1445. doi: 10.1093/jxb/erv537

Watanabe, K., Kobayashi, A., Endo, M., Sage-Ono, M., Toki, S., and Ono, M. (2017). CRISPR/Cas9- mediated mutagenesis of the dihydroflavonol-4-reductase-B (DFR-B) locus in the Japanese morning glory Ipomoea (*Pharbitis*) nil. *Sci. Rep.* 7:10028. doi: 10.1038/s41598-017-10715-1

Watanabe, K., Oda-Yamamizo, C., Sage-Ono, K., Ohmiya, A., and Ono, M. (2018). Alteration of flower colour in Ipomoeanil through CRISPR/Cas9-mediated mutagenesis of carotenoid cleavage dioxygenase 4. *Transgenic Res.* 27, 25–38. doi: 10.1007/s11248-017-0051-0

Wilson, F. M., Harrison, K., Armitage, A. D., Simkin, A. J., and Harrison, R. J. (2019). CRISPR/Cas9-mediated mutagenesis of phytoene desaturase in diploid and octoploid strawberry. *Plant Methods* 15:45. doi: 10.1186/s13007-019-0428-6

Woo, J. W., Kim, J., Kwon, S., Corvalán, C., Cho, S. W., Kim, H., et al. (2015). DNA-free genome editing in plants with preassembled CRISPR-Cas9 ribonucleoproteins. *Nat. Biotechnol.* 33, 1162–1164. doi: 10.1038/nbt.3389

Wu, H., and Li, Z. (2021). Recent advances in nano-enabled agriculture for improving plant performance. *Crop J.* 10, 1–12. doi: 10.1016/j.cj.2021.06.002

Wu, M. J., Liu, H. Q., Lin, Y., Chen, J., Fu, Y., Luo, J., et al. (2020). In-frame and frame-shift editing of the *Ehd1* gene to develop *Japonica* rice with prolonged basic vegetative growth periods. *Front. Plant Sci.* 11:307. doi: 10.3389/fpls.2020.00307

Xie, K., Minkenberg, B., and Yang, Y. (2015). Boosting CRISPR/Cas9 multiplex editing capability with the endogenous tRNA-processing system. *PNAS* 112, 3570–3575. doi: 10.1073/pnas.1420294112

Xie, K., and Yang, Y. (2013). RNA-guided genome editing in plants using a CRISPR–Cas system. *Mol. Plant* 6, 1975–1983. doi: 10.1093/mp/sst119

Xing, H. L., Dong, L., Wang, Z. P., Zhang, H. Y., Han, C. Y., Liu, B., et al. (2014). A CRISPR/Cas9 tool kit for multiplex genome editing in plants. *BMC Plant Biol.* 14:327. doi: 10.1186/s12870-014-0327-y

Xiong, X., Liu, W., Jiang, J., Xu, L., Huang, L., and Cao, J. (2019). Efficient genome editing of *Brassica campestris* based on the CRISPR/Cas9 system. *Mol. Genet. Genom.* 294, 1251–1261. doi: 10.1007/s00438-019-01564-w

Xu, C., Park, S. J., Van Eck, J., and Lippman, Z. B. (2016). Control of inflorescence architecture in tomato by BTB/POZ transcriptional regulators. *Genet. Dev.* 30, 2048–2061. doi: 10.1101/gad.288415.116

Xu, J., Kang, B. C., Naing, A. H., Bae, S. J., Kim, J. S., Kim, H., et al. (2020). CRISPR/Cas9 mediated editing of 1aminocyclopropane1carboxylate oxidase1 enhances Petunia flower longevity. *Plant Biotechnol. J.* 18, 287–297. doi: 10.1111/pbi.13197

Xu, P., Su, H., Chen, W., and Lu, P. (2018). The application of a meiocyte-specific CRISPR/Cas9 (MSC) system and a suicide-MSC system in generating inheritable and stable mutations in *Arabidopsis*. *Front. Plant Sci.* 13:1007. doi: 10.3389/fpls.2018.01007

Xu, R., Li, H., Qin, R., Wang, L., Li, L., Wei, P., et al. (2014). Gene targeting using the *Agrobacterium tumefaciens*-mediated CRISPR-Cas system in rice. *Rice* 7:5. doi: 10.1186/s12284-014-0005-6

Xu, X., Yuan, Y., Feng, B., and Deng, W. (2021). CRISPR/Cas9-mediated gene-editing technology in fruit quality improvement. *Food Qual. Saf.* 4, 159–166. doi: 10.1093/fqsafe/fyaa028

Xu, Z. S., Feng, K., and Xiong, A. S. (2019). CRISPR/Cas9-mediated multiply targeted mutagenesis in orange and purple carrot plants. *Mol. Biotechnol.* 61, 191–199. doi: 10.1007/s12033-018-00150-6

Yan, L., Wei, S., Wu, Y., Li, H., Yang, W., and Xie, Q. (2015). High-efficiency genome editing in *Arabidopsis* using YAO promoter-driven CRISPR/Cas9 system. *Mol. Plant* 12, 1820–1823. doi: 10.1016/j.molp.2015.10.004

Yan, R., Wang, Z., Ren, Y., Li, H., Liu, N., and Sun, H. (2019). Establishment of efficient genetic transformation systems and application of CRISPR/Cas9 genome editing technology in *Lilium pumilum* DC. Fisch. and *Lilium longiflorum* white heaven. *Int. J. Mol. Sci.* 20:2920. doi: 10.3390/ijms20122920

Yang, B. (2020). Grand challenges in genome editing in plants. *Front. Genome Ed.* 2:2.

Yang, H., Bailey, P., and Pilarsky, C. (2019). CRISPR Cas9 in pancreatic cancer research. *Front. Cell Dev. Biol.* 7:239. doi: 10.3389/fcell.2019.00239

Yang, Y., Tang, K., Datsenka, T. U., Liu, W., Lv, S., Lang, Z., et al. (2019). Critical function of DNA methyltransferase 1 in tomato development and regulation of the DNA methylome and transcriptome. *J. Integr. Plant Biol.* 61, 1224–1242. doi: 10.1111/jipb.12778

Yang, X., Chen, L., He, J., and Yu, W. (2017a). Knocking out of carotenoid catabolic genes in rice fails to boost carotenoid accumulation, but reveals a mutation in strigolactone biosynthesis. *Plant Cell Rep.* 36, 1533–1545. doi: 10.1007/s00299-017-2172-6

Yang, Y., Zhu, G., Li, R., Yan, S., Fu, D., Zhu, B., et al. (2017b). The RNA editing factor SlORRM4 is required for normal fruit ripening in tomato. *Plant Physiol.* 175, 1690–1702. doi: 10.1104/pp.17.01265

Yang, H., Wu, J. J., Tang, T., Liu, K. D., and Dai, C. (2017c). CRISPR/Cas9-mediated genome editing efficiently creates specific mutations at multiple loci using one sgRNA in *Brassica napus*. *Sci. Rep.* 7:7489. doi: 10.1038/s41598-017-07871-9

Yao, L., Zhang, Y., Liu, C., Liu, Y., Wang, Y., and Liang, D. (2018). OsMATL mutation induces haploid seed formation in indica rice. *Nat. Plants* 4, 530–533. doi: 10.1038/s41477-018-0193-y

Yao, N., Camacho, T. A., Chukmaitov, A. S., Fleming, S. T., and Anderson, R. T. (2015). Diabetes management before and after cancer diagnosis: missed opportunity. *Ann. Transl. Med.* 3, 1–10. doi: 10.3978/j.issn.2305-5839.2015.03.52

Yao, R., Ming, Z., Yan, L., Li, S., Wang, F., Ma, S., et al. (2016). DWARF 14 is a non-canonical hormone receptor for strigolactone. *Nature* 536, 469–473. doi: 10.1038/nature19073

Yau, Y. Y., and Stewart, C. N. (2013). Less is more: strategies to remove marker genes from transgenic plants. *BMC Biotechnol.* 13:36. doi: 10.1186/1472-6750-13-36

Ye, J., Wang, X., Hu, T., Zhang, F., Wang, B., Li, C., et al. (2017). An in Del in the promoter of Al-activated malate transporter9 selected during tomato domestication determines fruit malate contents and Aluminum tolerance. *Plant Cell* 29, 2249–2268. doi: 10.1105/tpc.17.00211

Yin, Y., Qin, K., Song, X., Zhang, Q., Zhou, Y., Xia, X., et al. (2018). BZR1 transcription factor regulates heat stress tolerance through FERONIA receptor-like kinase-mediated reactive oxygen species signaling in tomato. *Plant Cell Physiol.* 59, 2239–2254. doi: 10.1093/pcp/pcy146

Yu, Q. H., Wang, B., Li, N., Tang, Y., Yang, S., Yang, T., et al. (2017). CRISPR/Cas9-induced targeted mutagenesis and gene replacement to generate long-shelf life tomato lines. *Sci. Rep.* 7:11874. doi: 10.1038/s41598-017-12262-1

Yuan, M., Zhu, J., Gong, L., He, L., Lee, C., Han, S., et al. (2019). Mutagenesis of FAD2 genes in peanut with CRISPR/Cas9 based gene editing. *BMC Biotechnol.* 19:24. doi: 10.1186/s12896-019-0516-8

Yunyan, F., Jie, Y., Fangquan, W., Fangquan, F., Wenqi, L., Jun, W., et al. (2019). Production of two elite glutinous rice varieties by editing wx gene. *Rice Sci.* 26, 118–124. doi: 10.1016/j.rsci.2018.04.007

Yuste-Lisbona, F. J., Fernandez-Lozano, A., Pineda, B., Bretones, S., Ortiz-Atienza, A., Garcia-Sogo, B., et al. (2020). ENO regulates tomato fruit size through the floral meristem development network. *PNAS* 117, 8187–8195. doi: 10.1073/pnas.1913688117

Zafar, K., Khan, M. Z., Amin, I., Mukhtar, Z., Yasmin, S., Arif, M., et al. (2020). Precise CRISPR-Cas9 mediated genome editing in super sasmati rice for resistance against bacterial blight by targeting the major susceptibility gene. *Front. Plant Sci.* 11:575. doi: 10.3389/fpls.2020.00575

Zeng, Z., Han, N., Liu, C., Buerte, B., Zhou, C., Chen, J., et al. (2020). Functional dissection of HGGT and HPT barley vitamin E biosynthesis *via* CRISPR/Cas9-enabled genome editing. *Ann. Bot.* 126, 929–942. doi: 10.1093/aob/mcaa115

Zhang, A., Liu, Y., Wang, F., Li, T., Chen, Z., Kong, D., et al. (2019). Enhanced rice salinity tolerance *via* CRISPR/Cas9-targeted mutagenesis of the OsRR22 gene. *Mol. Breed.* 39:47. doi: 10.1007/s11032-019-0954-y

Zhang, Z., Hua, L., Gupta, A., Tricoli, D., Edwards, K. J., Yang, B., et al. (2019). Development of an *Agrobacterium*-delivered CRISPR/Cas9 system for wheat genome editing. *Plant Biotechnol. J.* 17, 1623–1635. doi: 10.1111/pbi.13088

Zhang, B., Yang, X., and Yang, C. (2016). Exploiting the CRISPR/Cas9 system for targeted genome mutagenesis in petunia. *Sci. Rep.* 6:20315. doi: 10.1038/srep20315

Zhang, Y., Liang, Z., Zong, Y., Wang, Y., Liu, J., Chen, K., et al. (2016). Efficient and transgene-free genome editing in wheat through transient expression of CRISPR/Cas9 DNA or RNA. *Nat. Commun.* 7:12617. doi: 10.1038/ncomms12617

Zhang, H., Zhang, J., Wei, P., Zhang, B., Gou, F., Feng, Z., et al. (2014). The CRISPR/C as9 system produces specific and homozygous targeted gene editing in rice in one generation. *Plant Biotechnol. J.* 12, 797–807. doi: 10.1111/pbi.12200

Zhang, Y., Bai, Y., Wu, G., Zou, S., Chen, Y., Gao, C., et al. (2017). Simultaneous modification of three homoeologs of TaEDR1 by genome editing enhances powdery mildew resistance in wheat. *Plant J.* 91:714. doi: 10.1111/tpj.13599

Zhang, M., Cao, Y., Wang, Z., Wang, Z. Q., Shi, J., Liang, X., et al. (2018a). A retrotransposon in an HKT1 family sodium transporter causes variation of leaf Na+exclusion and salt tolerance in maize. *New Phytol.* 217, 1161–1176. doi: 10.1111/nph.14882

Zhang, S., Shi, Q., Duan, Y., Hall, D., Gupta, G., and Stover, E. (2018b). "Regulation of citrus DMR6 *via* RNA interference and CRISPR/Cas9-mediated gene editing to improve Huanglongbing tolerance," in *Proceedings of the Biotechnology and Genetic Enginneering-Odd*, Fort Pierce, FL.

Zhang, Z., Ge, X., Luo, X., Wang, P., Fan, Q., Hu, G., et al. (2018c). Simultaneous editing of two copies of Gh14-3-3d confers enhanced transgene-clean plant defense against *Verticillium dahliae* in allotetraploid upland cotton. *Front. Plant Sci.* 9:842. doi: 10.3389/fpls.2018.00842

Zhang, M., Liu, Q., Yang, X., Xu, J., Liu, G., Yao, X., et al. (2020). CRISPR/Cas9-mediated mutagenesis of Clpsk1 in watermelon to confer resistance to *Fusarium oxysporum* f.sp. niveum. *Plant Cell Rep.* 39, 589–595. doi: 10.1007/s00299-020-02516-0

Zhang, S. (2018). Knockout of SlMAPK3 reduced disease resistance to *Botrytis cinerea* in tomato plants. *J. Agric. Food Chem.* 66, 8949–8956. doi: 10.1021/acs.jafc.8b02191

Zhao, D. S., Li, Q. F., Zhang, C. Q., Zhang, C., Yang, Q. Q., Pan, L. X., et al. (2018). GS9 acts as a transcriptional activator to regulate rice grain shape and appearance quality. *Nat. Commun.* 9:1240. doi: 10.1038/s41467-018-03616-y

Zhao, L., Lu, L., Wang, A., Zhang, H., and Huang, M. (2020). Nano-biotechnology in agriculture: use of nanomaterials to promote plant growth and stress tolerance. *J. Agric. Food Chem.* 68, 1935–1947. doi: 10.1021/acs.jafc.9b06615

Zhao, Y., Zhang, C., Liu, W., Gao, W., Liu, C., Song, G., et al. (2016). An alternative strategy for targeted gene replacement in plants using a dual-sgRNA/Cas9 design. *Sci. Rep.* 6:23890. doi: 10.1038/srep23890

Zheng, Z., Ye, G., Zhou, Y., Pu, X., Su, W., and Wang, J. (2021). Editing sterol side chain reductase 2 gene (StSSR2) *via* CRISPR/Cas9 reduces the total steroidal glycoalkaloids in potato. *Agriculture* 14, 401–413. doi: 10.1080/26895293.2021.1925358

Zhou, H., He, M., Li, J., Chen, L., Huang, Z., Zheng, S., et al. (2016). Development of commercial thermo sensitive genic male sterile rice accelerates hybrid rice breeding usingthe CRISPR/Cas9-mediated TMS5 editing system. *Sci. Rep.* 6:37395. doi: 10.1038/srep37395

Zhou, J., Li, D., Wang, G., Wang, F., Kunjal, M., Joldersma, D., et al. (2019). Application and future perspective of CRISPR/Cas9 genome editing in fruit crops. *J. Integr. Plant Biol.* 62, 269–286. doi: 10.1111/jipb.1279

Zhou, J., Wang, G., and Liu, Z. (2018). Efficient genome editing of wild strawberry genes, vector development and validation. *Plant Biotechnol. J.* 16, 1868–1877. doi: 10.1111/pbi.12922

Zhou, X., Liao, H., Chern, M., Yin, J., Chen, Y., Wang, J., et al. (2018). Loss of function of a rice TPR-domain RNA-binding protein confers broad-spectrum disease resistance. *Proc. Natl. Acad. Sci. U.S.A.* 115, 3174–3179. doi: 10.1073/pnas.1705927115

Zhou, X., Jacobs, T. B., Xue, L. J., Harding, S. A., and Tsai, C. J. (2015). Exploiting SNPs for biallelic CRISPR mutations in the out crossing woody perennial Populus reveals 4-coumarate CoA ligase specificity and redundancy. *New Phytol.* 208, 298–301. doi: 10.1111/nph.13470

Zhou, X., Zha, M., Li, L., Imran, M., and Zhang, C. (2017). StMYB44 negatively regulates phosphate transport by suppressing expression of PHOSPHATE1 in potato. *J. Exp. Bot.* 68, 1265–1281. doi: 10.1093/jxb/erx026

Zhu, C., Zheng, X., Huang, Y., Ye, J., Chen, P., Zhang, C., et al. (2019). Genome sequencing and CRISPR/Cas9 gene editing of an early flowering Mini-Citrus (*Fortunella hindsii*). *Plant Biotechnol. J.* 17, 2199–2210. doi: 10.1111/pbi.13132

Zhu, J., Song, N., Sun, S., Yang, W., Zhao, H., Song, W., et al. (2016). Efficiency and inheritance of targeted mutagenesis in maize using CRISPR-Cas9. *JGG* 43, 25–36. doi: 10.1016/j.jgg.2015.10.006

Zsogon, A., Čermák, T., and Naves, E. R. (2018). De novo domestication of wild tomato using genome editing. *Nat. Biotechnol.* 36, 1211–1216. doi: 10.1038/nbt.4272

Zuo, Y., Feng, F., Qi, W., and Song, R. (2019). Dek42 encodes an RNA-binding protein that affects alternative Pre-MRNA splicing and maize kernel development. *J. Integr. Plant Biol.* 61, 728–748. doi: 10.1111/jipb.12798

Zuris, J. A., Thompson, D. B., Shu, Y., Guilinger, J. P., Bessen, J. L., Hu, J. H., et al. (2015). Cationic lipid-mediated delivery of proteins enables efficient protein-based genome editing *in vitro and in vivo*. *Nat. Biotechnol.* 33, 73–80. doi: 10.1038/nbt.3081

Conflict of Interest: The authors declare that the research was conducted in the absence of any commercial or financial relationships that could be construed as a potential conflict of interest.

Publisher's Note: All claims expressed in this article are solely those of the authors and do not necessarily represent those of their affiliated organizations, or those of the publisher, the editors and the reviewers. Any product that may be evaluated in this article, or claim that may be made by its manufacturer, is not guaranteed or endorsed by the publisher.

Copyright © 2022 Naik, Shimoga, Kim, Manjulatha, Subramanyam Reddy, Palem, Kumar, Kim and Lee. This is an open-access article distributed under the terms of the Creative Commons Attribution License (CC BY). The use, distribution or reproduction in other forums is permitted, provided the original author(s) and the copyright owner(s) are credited and that the original publication in this journal is cited, in accordance with accepted academic practice. No use, distribution or reproduction is permitted which does not comply with these terms.

frontiers | Frontiers in Plant Science

ORIGINAL RESEARCH
published: 13 April 2022
doi: 10.3389/fpls.2022.850302

A Multi-Omics Approach for Rapid Identification of Large Genomic Lesions at the *Wheat Dense Spike* (*wds*) Locus

Zhenyu Wang[1†], Shu Tao[1†], Shaoshuai Liu[1†], Meiling Jia[1†], Dada Cui[1], Guoliang Sun[1], Zhongyin Deng[1], Fang Wang[1], Xingchen Kong[1], Mingxue Fu[1], Yuqing Che[1], Ruyi Liao[1], Tao Li[2], Shuaifeng Geng[1], Long Mao[1]* and Aili Li[1]**

[1] National Key Facility for Crop Gene Resources and Genetic Improvement, Institute of Crop Science, Chinese Academy of Agricultural Sciences, Beijing, China, [2] College of Agriculture, Yangzhou University, Yangzhou, China

OPEN ACCESS

Edited by:
Junhua Peng,
Huazhi Rice Bio-Tech Co., Ltd., China

Reviewed by:
Jian Ma,
Sichuan Agricultural University, China
Xiaoli Jin,
Zhejiang University, China
Anna-Maria Botha-Oberholster,
Stellenbosch University, South Africa

***Correspondence:**
Shuaifeng Geng
gengshuaifeng@caas.cn
Long Mao
malong@caas.cn
orcid.org/0000-0002-3377-4040
Aili Li
liaili@caas.cn
orcid.org/0000-0001-9004-192X

[†] These authors have contributed equally to this work

Specialty section:
This article was submitted to Plant Biotechnology, a section of the journal Frontiers in Plant Science

Received: 07 January 2022
Accepted: 23 March 2022
Published: 13 April 2022

Citation:
Wang Z, Tao S, Liu S, Jia M, Cui D, Sun G, Deng Z, Wang F, Kong X, Fu M, Che Y, Liao R, Li T, Geng S, Mao L and Li A (2022) A Multi-Omics Approach for Rapid Identification of Large Genomic Lesions at the Wheat Dense Spike (wds) Locus. Front. Plant Sci. 13:850302. doi: 10.3389/fpls.2022.850302

Optimal spike architecture provides a favorable structure for grain development and yield improvement. However, the number of genes cloned to underlie wheat spike architecture is extremely limited. Here, we obtained a wheat dense spike mutant (*wds*) induced by ^{60}Co treatment of a common wheat landrace Huangfangzhu that exhibited significantly reduced spike and grain lengths. The shortened spike length was caused by longitudinal reduction in number and length of rachis cells. We adopted a multi-omics approach to identify the genomic locus underlying the *wds* mutant. We performed Exome Capture Sequencing (ECS) and identified two large deletion segments, named 6BL.1 at 334.8∼424.3 Mb and 6BL.2, 579.4∼717.8 Mb in the *wds* mutant. RNA-seq analysis confirmed that genes located in these regions lost their RNA expression. We then found that the 6BL.2 locus was overlapping with a known spike length QTL, qSL6B.2. Totally, 499 genes were located within the deleted region and two of them were found to be positively correlated with long spike accessions but not the ones with short spike. One of them, *TraesCS6B01G334600*, a well-matched homolog of the rice *OsBUL1* gene that works in the Brassinosteroids (BR) pathway, was identified to be involved in cell size and number regulation. Further transcriptome analysis of young spikes showed that hormone-related genes were enriched among differentially expressed genes, supporting *TraesCS6B01G334600* as a candidate gene. Our work provides a strategy to rapid locate genetic loci with large genomic lesions in wheat and useful resources for future wheat study.

Keywords: wheat, dense spike, RNA-seq, exome capture sequencing, *TaBUL1*

INTRODUCTION

Spike morphology is a complex multi-component trait determined by a series of related traits such as spike length, spikelet number, and spikelet density (Zhou et al., 2017). Spike length directly affects spikelet per spike and grains per spike, and hence final grain yield. Therefore, the identification of genes controlling spike-related traits is necessary to elucidate the genetic basis of wheat yield (Deng et al., 2017). Phytohormones are among the major factors that regulate spike morphogenesis

(Barazesh and McSteen, 2008; McSteen, 2009). Brassinosteroids (BRs), gibberellins (GAs), and ethylene (ETH) are actively involved in panicle development and seed set, whereas auxins and strigolactones (SLs) inhibit axillary bud growth and impact effective panicle numbers (McSteen, 2009; Shimizu-Sato et al., 2009; Dun et al., 2012). Cytokinins (CKs), auxins, and jasmonic acid (JA) are also involved in meristem fate determination. An intricate network of hormonal pathways regulate panicle development and modulate spike/panicle architecture (Zhang and Yuan, 2014).

Transcription factors also play important roles in spike morphology (Bommert and Whipple, 2018; Wang et al., 2021). In rice, the *LARGE2-APO1/APO2* module controls panicle size and grain number and is a promising target for yield improvement (Huang et al., 2021). In barley, *HvMADS1* was found to be responsible for maintaining the unbranched spike architecture at relatively high temperatures (Li et al., 2021a), while the *AP2L-5* like proteins are evolutionarily conserved in grasses and able to promote inflorescence meristem activity and to restrict floret number per spikelet (Zhong et al., 2021). In wheat, the domestication gene *Q* participated in spike length and morphology (Faris et al., 2003; Sormacheva et al., 2015). The wheat *TEOSINTE BRANCHED1* (*TB1*) homolog also affects inflorescence architecture and development (Dixon et al., 2018). Recently, the AP2 transcription factor *WFZP* was reported to directly activate *VERNALIZATION1* (*VRN1*) and wheat *HOMEOBOX4* (*TaHOX4*) to regulate spikelet initiation and development (Li et al., 2021b). More importantly, *WFZP-D* was found to be a favorable gene for high-yield crop breeding (Du et al., 2021). In spite of this, research concerning wheat spike development is still quite limited and more genes should be exploited. More recently, Pang et al. (2020) conducted a large-scale genome-wide association study (GWAS) using a panel of 768 wheat cultivars, 327,609 single-nucleotide polymorphisms (SNPs) were generated by genotyping-by-sequencing and 395 quantitative trait loci (QTLs) were detected related to 12 traits in 7 environments, of which 26 QTLs were involved in spike length. These QTLs provided a basis for further discovery of spike architecture determining genes.

The availability of the high-quality reference genome of wheat allows the application of multiple genomics tools to expedite the identification of novel genes that affect important agronomic traits. Exome capture sequencing (ECS), which captures the coding regions of the genome, is suitable for the wheat genome due to its large size (He et al., 2019; Dong et al., 2020). A genomic locus was identified on chromosome arm 4BS using this method to be associated with plant height (Mo et al., 2018). Here, through identifying a dense spike mutant *wds* that was derived from ^{60}Co treatment, we present a combinatorial approach that can locate candidate genes in a rapid way. Firstly, ECS identified two large deletion segments which were further confirmed by RNA-seq analysis. Then, based on known QTLs for wheat spike length, a candidate deletion region was isolated. In the end, combining correlation analysis of expression levels with long and short spike accessions, a gene whose expression level positively correlated with spike length was identified as a candidate for *wds*. The work provides an example of rapid identification of a large mutant locus and possible underlying genes.

MATERIALS AND METHODS

Plant Materials

Common wheat landrace Huangfangzhu (HFZ or WT) and its ^{60}Co induced wheat dense spike (*wds*) mutant (M5 lines) were kindly provided by Dr. Tao Li, Yangzhou University. Plants were grown at the field of Dongpu Experimental Station in Beijing (39.97°N, 116.34°E). Twenty wheat varieties from Chinese wheat mini-core collection, of which 10 varieties carried longer spikes and 10 varieties had shorter spikes. They were used for the association analysis of candidate gene expression levels relative to spike length traits (Wang et al., 2012). These wheat accessions were kindly provided by Dr. Xueyong Zhang, Institute of Crop Science, Chinese Academy of Agricultural Sciences, Beijing, China.

Morphological and Cellular Analysis

Three spikes per plant of a minimum of 10 lines of WT and the mutant were selected for phenotyping. The middle section of spikes at W8.5 (Waddington stage 8.5) stage was collected for cytological observations. Sections of 8 μm were prepared longitudinally along the spike axis by using Leica Ultracut rotary microtome. The number of rachis cells was counted by selecting all cells from one node and cell lengths were measured by selecting the similar regions on the rachis of the mutant and WT spikes. The WSEEN Grain Test System (WSeen)[1] was used to measure grain length, grain width, and thousand-grain weight.

Exome Capture Sequencing

Genomic DNA was isolated from wheat leaves of HFZ and *wds* (M5 lines) using the CTAB method (Rogers and Bendich, 1985). The quality and quantity of the DNA was verified using 1.0% agarose gels and a NanoDrop 2000 spectrophotometer. ECS was performed using a standard protocol on libraries generated from 500 ng genomic DNA for all individuals. The libraries were constructed according to the manufacturer's specifications (Illumina) and sequenced using the Illumina HiSeq X-ten platform to generate 150-bp paired-end reads. To avoid artificial bias, we removed following types of reads: (i) reads with $\geq$ 10% unidentified nucleotides (N); (ii) reads with $>$ 10 nt aligned to the adaptor, with $\leq$ 10% mismatches allowed; (iii) reads with $>$ 50% bases having phred quality $<$ 5. High-quality reads. These reads were subsequently aligned to the genome of the IWGSC RefSeq v1.0 reference genome with the BWA software with the command "mem -t 10 -k 32 –M" (Li and Durbin, 2009). After alignment, improperly aligned unique paired-end reads (including secondary hits reads) were filtered out using samtools software with the command "samtools view -@ 10 -h -q 10 -f 2 -F 256" (Li et al., 2009). Consequently, SNP calling was performed using the Genome Analysis Toolkit (GATK, version v4.1) by the HaplotypeCaller method (McKenna et al., 2010).

[1] http://www.wseen.com/

RNA-Seq Analysis

Total RNA was isolated from young spikes using TRIzol reagent (Invitrogen) at three key stages of HFZ and *wds*, W4, W6, and W8.5 of the Waddington scale with three biological replicates. For the long and short spike pools, ten accessions with the long spike in length distribution of a natural population (Guo et al., 2018a) were selected as members of "long spike pool" and 10 accessions with shorter spikes were selected as members of the "short spike pool." Total RNA was isolated from young spikes at the W5.5 stage. Sequencing was performed on the Illumina HiSeq 2000 platform. An average of 15.5 Gb 150-bp pair-end clean reads were generated for each sample after filtering to remove low quality reads. Clean reads were aligned to the IWGSC RefSeq v1.0 reference genome using HISAT2 (v 2.1.0) with the command "hisat2 -p 8 –rna-strandness RF" (Kim et al., 2019). The unique and high quality mapped reads were retained for subsequent analysis by screening the flags "NH:i:1" and "quality value > 60" in aligned bam file. HTSeq was used to calculate read numbers mapped to the gene models (Anders et al., 2015). Read counts were then normalized into FPKM (Fragments Per Kilobase of transcript per Million mapped reads) to acquire relative expression levels using home-made Perl scripts. In the subsequent analysis, samples with very poor repeatability ($r^2 < 0.90$) were removed in analysis.

Differential expression analysis was performed using limma R packages (Ritchie et al., 2015). In the process of limma analysis, RNA-seq reads with high quality were converted to the log-scale and empirically estimated for mean-variance relationship. The mean-variance trend was converted by the voom function into precision weights, which were incorporated into the analysis of log-transformed RNA-seq counts using the same linear modeling commands (Ritchie et al., 2015). Empirical Bayes moderated t-statistics and their associated *p*-values were generally used to evaluate the significance of the observed expression levels. After Benjamini-Hochberg's adjustment, expressed genes with *p*-value < 0.05 were treated as differential expression genes.

Statistical Analysis

Statistical analysis of mutant and HFZ lines was carried out *via* an independent Student's *t*-test. The correlation coefficient between gene expression and spike length was calculated using the R function "cor()" based on Pearson's method. The phenotypic data of grain length, grain width, and thousand-grain weight were obtained in multiple times/environments.

RESULTS

Morphological Observation of the *wds* Mutant

The *wds* mutant line at its M5 generation had significantly shorter spikes compared to the WT plants (41.4 vs. 95.5 mm, $p < 0.01$), only 56.7% of that of the WT (**Figures 1A–C**). The number of rachis internode representing spikelet number per spike was reduced from 23 in WT to 21 in the mutant ($p < 0.01$) (**Figures 1B,D**), with the average length of spike rachis internodes being reduced 47.5% from 4.15 to 1.97 mm (**Figure 1E**). On the other hand, grain length was reduced by 8.5% or 0.62 mm relative to WT (**Figures 1F,H**). However, the *wds* mutant exhibited increased grain width, while its thousand grain weight decreased relative to the WT (**Figures 1G,I,J**). The plant height of *wds* was also reduced by 20.8% (26.7 cm, $p < 0.01$) relative to WT (**Figure 1K**). Thus, the *wds* mutant showed systematic longitudinally shortened phenotypes, with shortened plant height, spike length, and grain length.

To gain insight into the causes of short spike length, we sectioned the rachis at W8.5 (Waddington staging) for microscopic observation and found that the length of mutant cells was reduced by 46.2% at the top and 34.9% at the bottom regions of the rachis (**Figures 2a–d,e**). In addition, cell width was observed to be reduced, but were mostly restricted to the upper part of the rachis (**Figure 2f**). Meanwhile, the number of rachis cells was significantly decreased, from 295.7 to 213.18 ($p < 0.01$) in *wds* (**Figure 2g**). Further comparison of longitudinal and transverse sections showed that the number of mutant rachis cells significantly decreased, from 18.6 ± 1.9 to 8.2 ± 0.8, in longitudinal sections, while increased from 16.3 ± 1.3 to 26.2 ± 2.2 in transverse sections ($p < 0.01$) (**Figure 2h**), suggesting that the re-organization of rachis cells in the internode may contribute to the altered mutant phenotypes. These data demonstrated that the shortened rachis was caused by the reduced length and number of rachis cells in the longitudinal direction.

Identification of Two Major Deletions on Chromosome 6BL in *wds*

In order to probe the mutation loci in *wds*, ECS was performed using the first-generation wheat exome capture probes—which collectively represented 110 Mb of low copy number regions across the wheat genome (Jordan et al., 2015). Reads obtained were mapped to the IWGSC wheat genome assembly RefSeq v1.0 (Lang et al., 2018), yielding a total of 329.9 million mapping reads with an average of 98.9% mapping ratio for the two lines (**Supplementary Table 1**). By analyzing the dataset using the Genome Analysis Toolkit (GATK) pipeline, we identified a total of 2,024,173 SNPs and 185,396 short insertions and deletions (INDELs) (**Supplementary Table 2**). Surprisingly, two large segment deletions were observed on the long arm of chromosome 6B and were named 6BL.1 (334.8∼424.3 Mb) carrying 113 genes and 6BL.2 (579.4∼717.8 Mb) carrying 499 genes (**Figure 3A** and **Supplementary Table 3**).

To check whether these genes were lost as a result of segment deletion in *wds*, we further performed transcriptome analysis of the mutant line and the wild type. To cover more genes, we isolated RNA from spikes at three stages W4, W6, and W8.5 which represented the time points at the appearance of stamen primordium stage, the stylar canal of ovules with a narrow opening stage, and the formation of stigmatic branches stage, respectively (Zheng et al., 2016). These stages also corresponded to the times of pre-, middle-, and post-spike elongation (**Figures 5A–C**). An average of 15.5 Gigabyte (Gb) 150-bp pair-end clean reads were obtained for each sample using Illumina

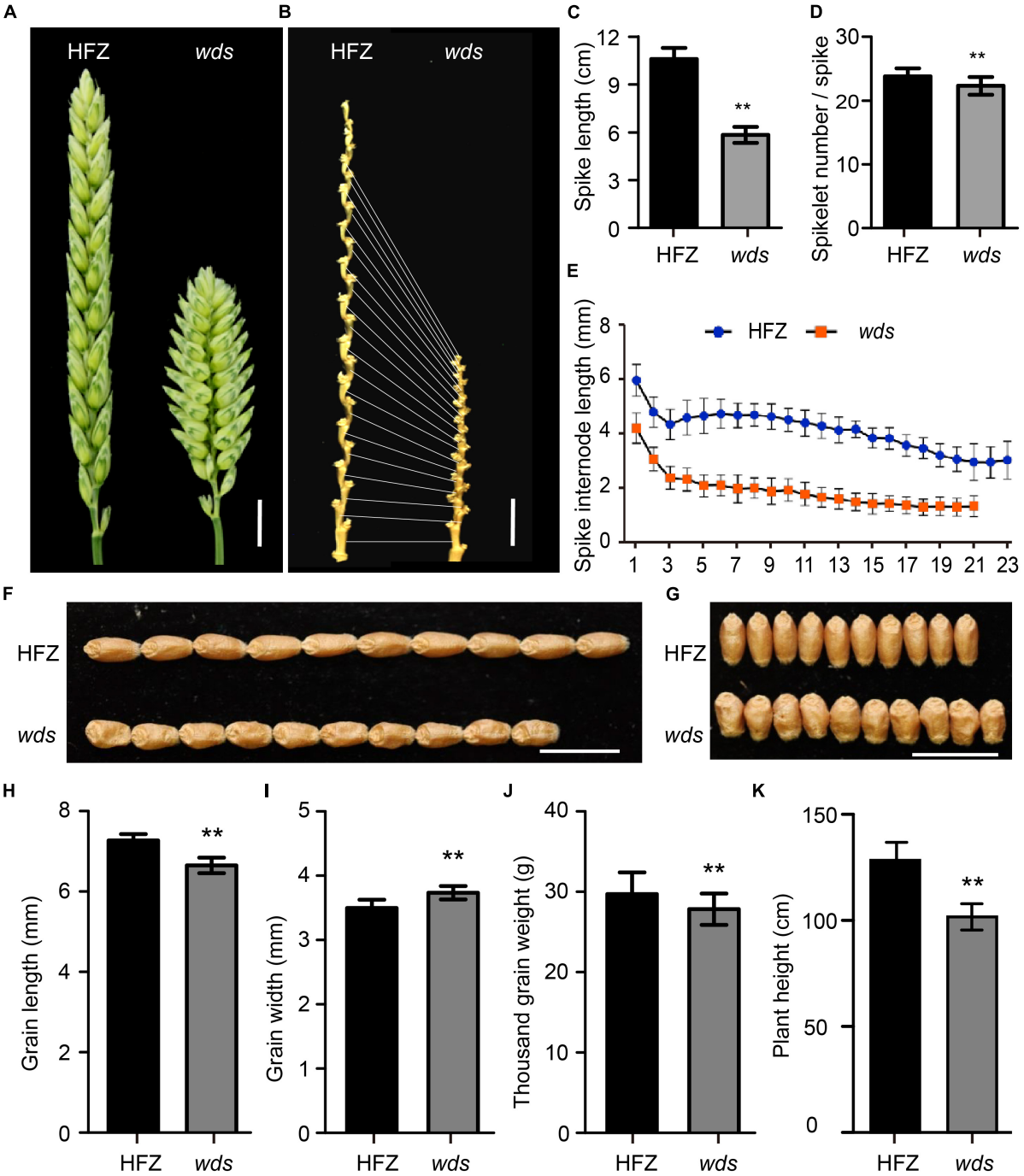


FIGURE 1 | Morphology of the *wds* mutant. **(A)** The dense spike of the mutant. Scale bar = 1 cm. **(B)** Spike internode morphology. Scale bar = 1 cm. **(C,D)** Statistical analysis of spike length **(C)** and spikelet number per spike **(D)** of HFZ and *wds*. **(E)** Statistical analysis of spike internode length in HFZ and *wds*. **(F,G)** Comparison of grain length **(F)** and grain width **(G)** between HFZ and *wds*. **(H–K)** Statistical analysis of grain length **(H)**, grain width **(I)**, thousand grain weight **(J)**, and plant height **(K)** of HFZ and *wds*. n = 50. Significance was measured using Student's *t*-test, $^{**}p < 0.01$.

HiSeq 2000 platform (**Supplementary Table 4**). After data filtering, clean reads were mapped to the IWGSC wheat genome reference annotation (v1.0), yielding an average of 97.49% overall alignment rate and 90.08% of them were uniquely mapped to the wheat genome (**Supplementary Table 5**). Expression levels were obtained by mapping reads to the gene model and were converted to FPMK. Gene expression correlation analysis showed high coefficients among replications, more than 0.98 (**Supplementary Table 6**). Principal component analysis (PCA) confirmed the quality of the replications (**Supplementary Figure 1**). In line

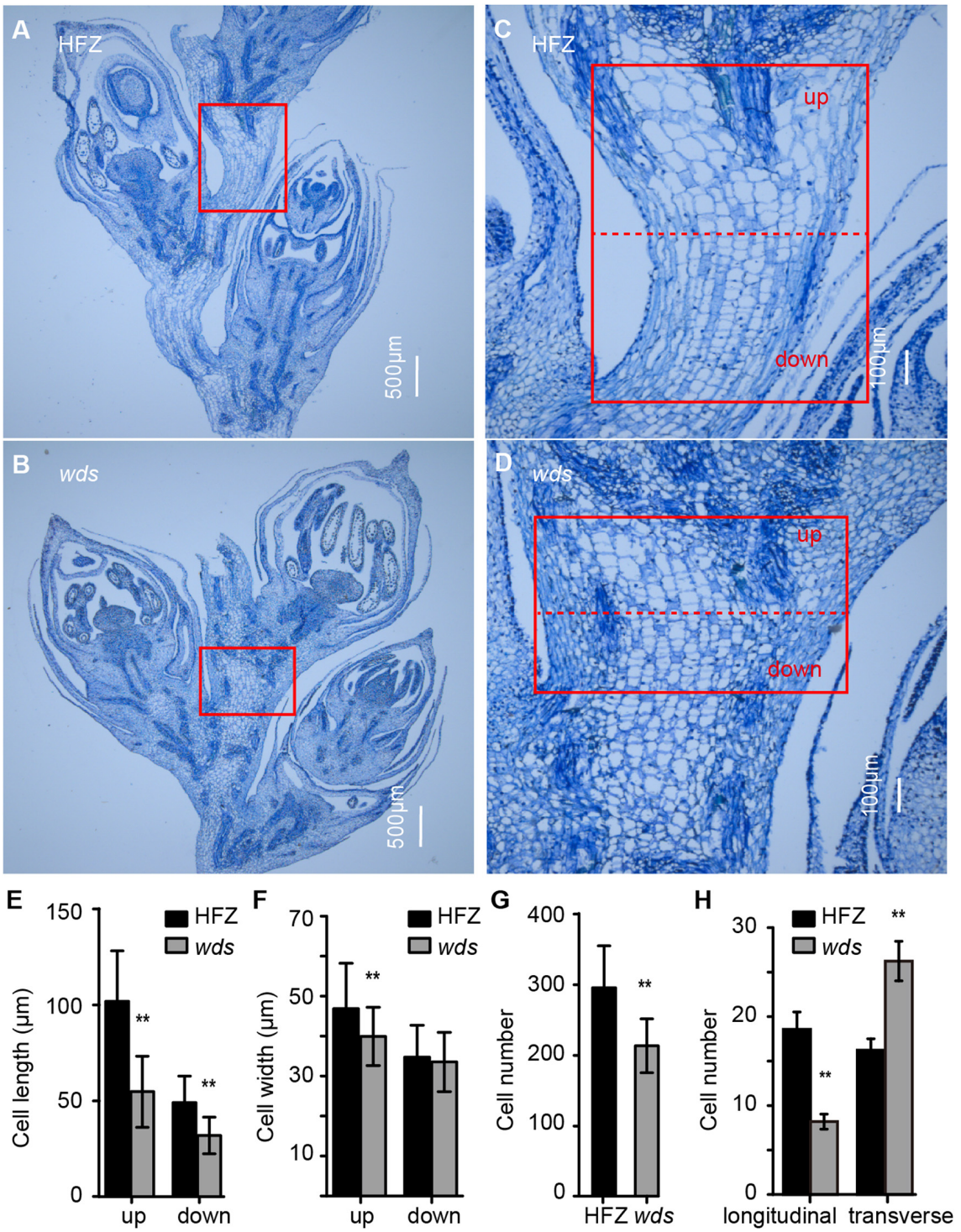


FIGURE 2 | Cytological observations of rachis cells. **(A–D)** Magnified views of rachis cells in HFZ (up) and *wds* (down) in the longitudinal direction. **(A,B)** Scale bar = 500 μm. **(C,D)** Scale bar = 100 μm. **(E–H)** Statistical analysis of cell length, cell width, cell number and the number of cells in longitudinal and transverse directions. Significance was measured using Student's *t*-test, $^{**}p < 0.01$.

with the ECS result, there was only 0.45 and 0.9% sequencing coverage within the 6BL.1 and 6BL.2 regions in *wds*, which may be caused by mismatching, while the average coverage was 13.2 and 15.1% in the corresponding genomic regions in WT, confirming that these genes were indeed lost in *wds* (**Figures 3B,C**).

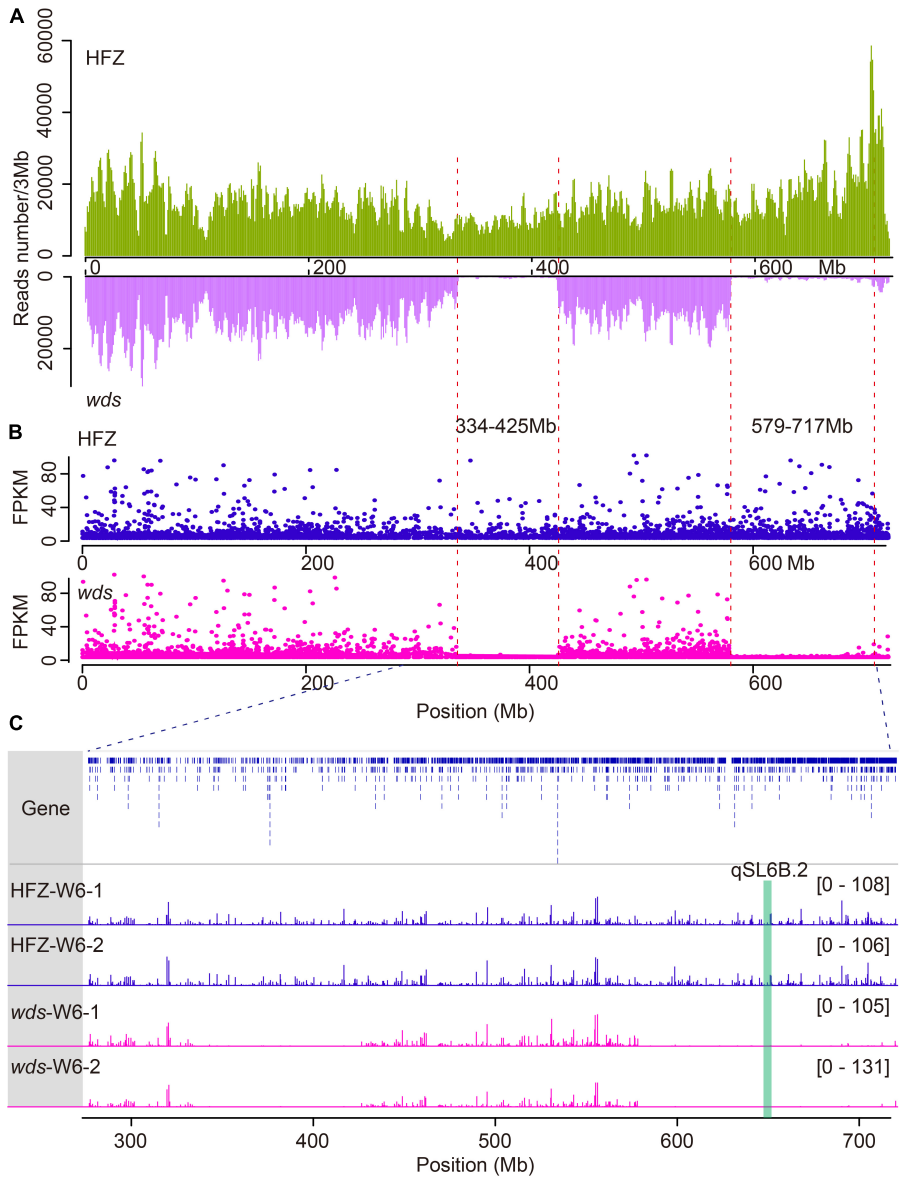


FIGURE 3 | Comparison of genes expression and reads coverage within deleted regions in WT and *wds*. **(A)** Reads mapping depth of ECS reads on chromosome 6B. The horizontal axis (X-axis) corresponds to the length of the chromosome and the Y axis indicates reads mapping depth. **(B)** Gene expression levels in FPKM on Chr6B. **(C)** Reads coverage within deleted regions.

Identification of a Candidate Gene in the Interval of 6BL.2

To check whether the two deleted segments were responsible for the mutant phenotype, we mapped two deleted segments with existing spike length QTLs on chromosome 6B and found that the 6BL.2 locus overlapped with QTL for spike length located at 643.8–644.2 Mb (p = 9.25E-06) as reported by a previous study (Pang et al., 2020), suggesting that a possible candidate gene may be located in this region.

We then screened the 499 genes at 6BL.2 by studying expressed genes (401) with FPKM > 1 in at least one sample (**Supplementary Table 7**). *K*-means clustering divided these genes into four subclusters according to their expression patterns over the developmental course (**Figure 4A**). We paid special attention to subcluster 2 (containing 25 genes) because gene expression levels in this cluster were continuously increased that was consistent with spike development in WT, but not in *wds* (**Figure 4A**).

We then examined the expression patterns of these 25 genes for their association with spike length by using spike length pools composed of long- and short-spike accessions respectively. As shown in **Figure 4**, 10 accessions with the long spike in length distribution of a natural population (Guo et al., 2018a) were selected as members of "long spike pool" and 10 accessions with

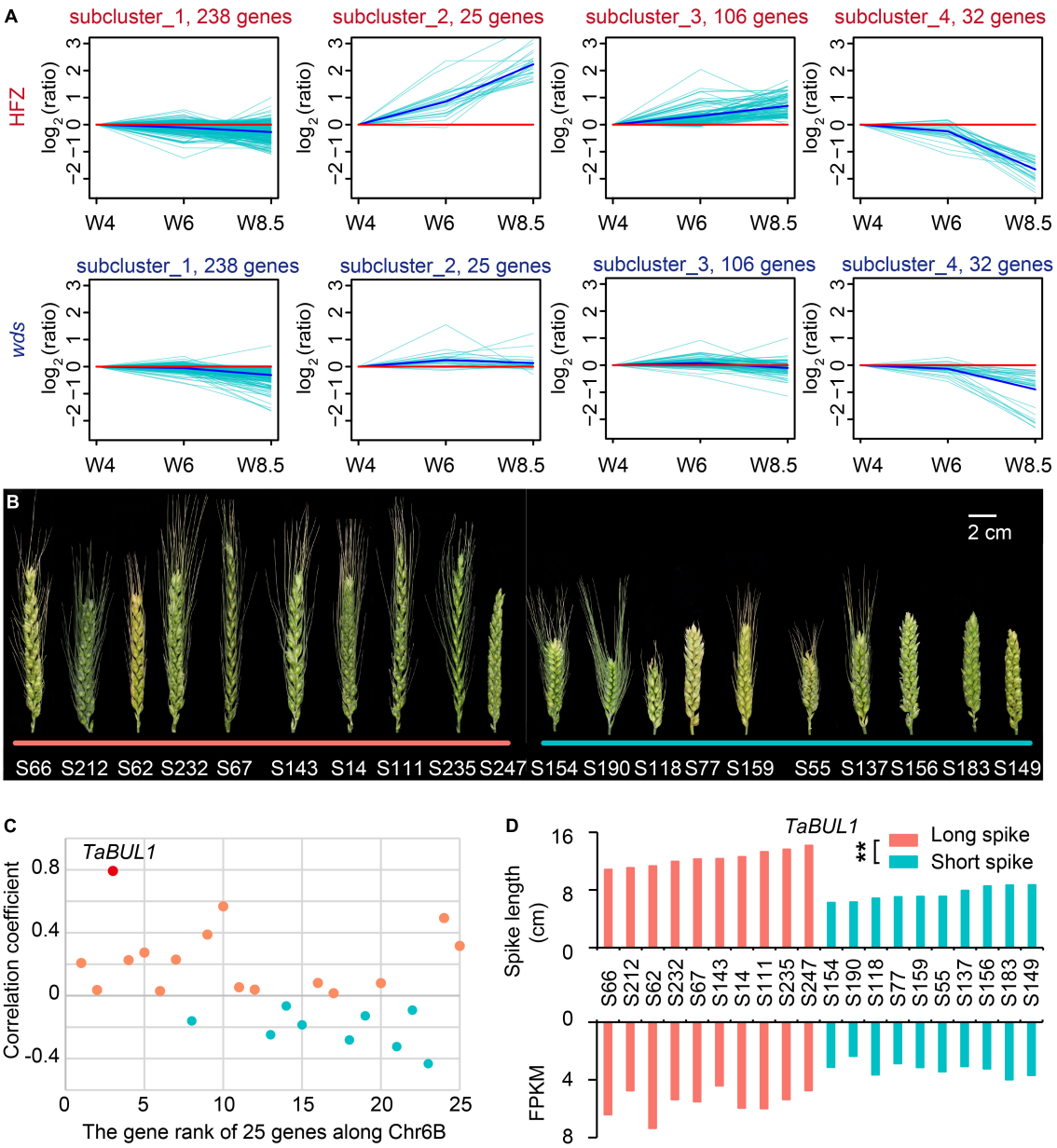


FIGURE 4 | Characterization of candidate loci based on spike length pools. **(A)** Gene expression patterns on chromosome 6B in HFZ and *wds*. **(B)** Selected varieties for spike length pools. The left 10 accessions from the long spike pool and the right 10 from the short spike pool. Scale bar = 2 cm. **(C)** The correlation coefficient of the expression levels of 25 expressed genes with spike length using spike length pools. **(D)** Significant correlation between spike lengths and expression levels of *TaBUL1* in varieties of the two spike length pools. *p*-value was determined by Student's *t*-test. $^{**}p < 0.01$.

short spike in length distribution were selected as members of "short spike pool" (**Figure 4B**). Total RNA was isolated from spikes of these accessions at stage W5.5 and was used for sequencing and transcriptome analysis. Among the above 25 genes, there were only two genes whose expression level was not only significantly positively correlated with phenotype ($p < 0.01$), but also had correlation coefficient greater than 0.5 (**Figure 4C** and **Supplementary Table 8**). One of the two genes, *TraesCS6B01G334600*, was found to have the highest correlation between its RNA expression level and spike length with a 0.79 correlation coefficient ($p < 0.01$) (**Figure 4C**). Annotation showed that the gene, named *TaBUL1-6B*, was orthologous gene of the rice *OsBUL1* (*BRASSINOSTEROID UPREGULATED 1-LIKE1*) gene (**Supplementary Figure 3**). In addition to the orthologs of *OsBUL1* on homoeologous group (HG) 6 (*TraesCS6A01G306200*, *TaBUL1-6A*; *TraesCS6B01G334600*, *TaBUL1-6B*; *TraesCS6D01G285300*, *TaBUL1-6D*), *TaBUL1* indeed has paralog genes on HG 7 (*TraesCS7A01G185300*, *TaBUL1-7A*; *TraesCS7B01G090500*, *TaBUL1-7B*; *TraesCS7D01G187000*, *TaBUL1-7D*)

(**Supplementary Figure 3** and **Supplementary Table 9**). The expression patterns of *TaBUL1* on HG 6 (*TaBUL1-6A, TaBUL1-6B, TaBUL1-6D*) were obviously different from the ones on HG7 (*TaBUL1-7A, TaBUL1-7B, TaBUL1-7D*). From W4 to W6, *TaBUL1* on HG7 (7A, 7B, 7D) were nearly not expressed, while the ones on chromosome 6 were expressed up to about 10 FPKM, indicating the obvious subfunctionalization of these two group genes (**Supplementary Figure 4A**).

As for the three homoeologus genes *TaBUL1* (6A, 6B, 6D), *TaBUL1-6B* has one different amino acid in the conserved domain bHLH from the other two (**Supplementary Figure 4B**), suggesting the function of *TaBUL1-6B* on deletion region might be different from *TaBUL1-6A* and *TaBUL1-6D*. In addition, the *wds* mutant showed smaller spikelet and produced smaller grains relative to WT, similar to phenotypes of the *OsBUL1* mutant. More importantly, the expression level of *TaBUL1-6B* in long spike extreme pool was significantly higher ($p < 0.0001$) than that in short spike extreme pool materials (**Figure 4D**), while expression of *TaBUL1-6B* was barely detectable in the *wds* mutant. Thus, we deduced that *TaBUL1-6B* may be a candidate gene responsible for the altered phenotype of the *wds* mutant.

Transcriptome Alteration Caused by the *wds* Mutation

To study genome-wide gene expression changes in the *wds* mutant, we analyzed RNA-seq data from spikes at W4, W6, and W8.5 of the WT and the mutant (**Figures 5A–C**). Cluster pedigree analysis showed highly correlated gene expression levels among replications (**Supplementary Figure 2**). A total of 2,726 (W4), 1,779 (W6), and 2,607 (W8.5) genes were significantly up-regulated (p-value < 0.05) and 1,599 (W4), 1,630 (W6), and 2,389 (W8.5) genes were significantly down-regulated (p-value < 0.05) in the indicated stages in the *wds* mutant (**Figure 5D** and **Supplementary Tables 10, 11**). Of these, 457 up-regulated genes and 1,225 down-regulated genes were shared at three developmental stages, whereas others were stage-specific (**Figures 5E,F**).

Gene Ontology (GO) analysis revealed three most enriched GO terms at W4, i.e., the JA-mediated signaling pathway (GO: 2000022, $p = 4.04e\text{-}17$), the SA-mediated signaling pathway (GO: 0046244: $p = 6.68e\text{-}13$), and the phenol-contained compound catabolic pathway (GO: 0019336, $p = 1.35e\text{-}11$) (**Figure 5G** and **Supplementary Table 12**). JA-mediated signaling pathway (GO: 2000022) was also enriched at W6 ($p = 1.6e\text{-}13$) where the other two most enriched GO terms were photosynthesis pathway (GO: 0009765, $p = 2.54e\text{-}4$) and sporopollenin biosynthetic pathway (GO: 0080110, $p = 2.54e\text{-}4$) (**Figure 5G** and **Supplementary Table 13**). Interestingly, at W8.5, genes mostly enriched were those related to ethanol (GO: 0045471, $p = 1.03e\text{-}25$), response to copper ion (GO: 0046688, $p = 1.12e\text{-}20$), and response to arsenic-containing substance (GO: 0046685, $p = 1.20e\text{-}11$) (**Figure 5G** and **Supplementary Table 14**), indicating that genes for spike development were mainly functional at early stages.

Further examination of known hormone-related genes affected by the *wds* mutation showed that most hormonal genes, such as GA, ETH, JA, SL, and auxin related genes, except those related to SA, were significantly altered in the mutant (**Figure 5H**). Of note, *TraesCS5B01G153200*, a homolog of *D53*, a governing gene of spike length in the regulation of spike architecture, was continuously down-regulated over the three stages. Besides, all three homoeologs of the rice *OsEATB* gene (*TraesCS5A01G238400*, *TraesCS5B01G236900*, *TraesCS5D01G24530*), which encodes an ERF protein and is involved in the crosstalk between ETH and GA to reduce rice plant height and panicle length at the maturity stage, were up-regulated at the stage of W4 in *wds*. Taken together, the *wds* mutant seemed to affect the complex hormone regulatory network through the BR pathway, probably *via TaBUL1*, making it the most possible candidate gene for the dense spike phenotype.

DISCUSSION

A Multi-Omics Approach to Rapidly Locate a Candidate Causal Locus in a Mutant

Improving spike morphology is an effective strategy to increase grain yield (Guo et al., 2018b). This can be achieved by modifying spike length, spikelet number per spike, and the number of florets per spikelet. The discovery of functional genes underlying agronomic traits is of great importance for wheat improvement. Recently, an effective method, termed bulked segregant exome capture sequencing (BSE-Seq) was reported for identifying causal mutations or candidate genes which integrated the newly designed wheat exome capture panel, bulked segregant pools sequencing, and a robust algorithm varBScore (Dong et al., 2020). BSE-Seq was used to identify a wheat yellow leaf mutant gene, *ygl1*, using an ethyl methanesulfonate (EMS) mutant population which was found to encode a magnesium- chelatase subunit chlI (Dong et al., 2020). In this work, we combined ECS, RNA-seq, and association analysis with extreme trait pools to rapidly characterize a spike mutant *wds* that showed dense and short spikes. ECS identified two large deletion segments which were confirmed by RNA-seq. Assisted with gene expression data, we found the second deletion segment overlapped with a reported spike length QTL and identified a possible candidate gene based on its expression pattern and information from the model plant. We showed that in the case of large deletion, RNA-seq helps to rapidly detect potential loci and genes based on their expression levels. It may serve as the first step for gene cloning with unknown genetic lesions before investing unnecessary effort.

Phytohormones and Spike Morphology Development

Phytohormones are small regulatory molecules that form a regulatory network in coordinating various developmental aspects of yield-related traits and therefore control the yield potential of crops (Zhang and Yuan, 2014). Phytohormones are also extensively involved in shoot branching (tillering), panicle branching, panicle length, and seed set percentage (Santner et al., 2009). JA plays a key role in spikelet morphogenesis,

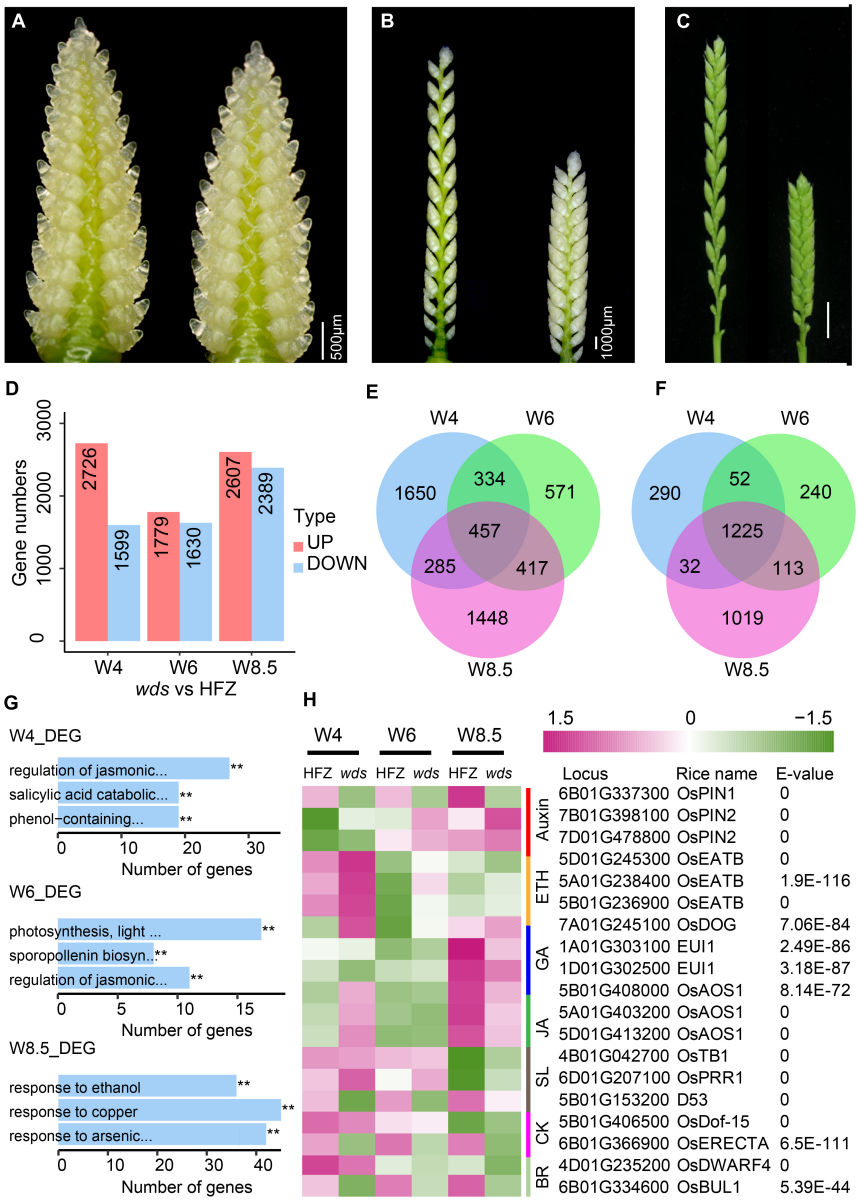


FIGURE 5 | Differentially expressed genes (DEGs) between HFZ and *wds* spikes. **(A–C)** Stages of spikes used for RNA-seq analysis. **(A)** W4, **(B)** W6, and **(C)** W8.5. Scale bar = 500 μm **(A)**, Scale bar = 1000 μm **(B)**, Scale bar = 1 cm **(C)**. **(D)** Numbers of DEGs at stages W4, W6, W8.5. Red color, up-regulated; green color, down-regulated. Venn diagrams of up-regulated **(E)** and down-regulated **(F)** DEGs at W4, W6, and W8.5. **(G)** The top three most significantly enriched GO terms at the three developmental stages. **(H)** Heatmap of expression dynamics of known hormone-related genes. On the right are RefseqV1.0 gene annotation and similarity (blast *E*-values) of the genes with rice homologs.

deciding floral organ identity and floral organ number along with the E-class gene, *OsMADS1* for floral meristem determinacy in spikelet development (Cai et al., 2014). Our transcriptome analysis showed the GO term for JA-mediated signaling pathway genes were enriched at both W4 and W6 stages, suggesting that JA signaling pathway was affected in the *wds* mutant. On the other hand, ETH also plays a role in the regulation of panicle architecture, controlling grain size and grain filling rate (Yin et al., 2017). At W8.5, in addition to three significantly enriched GO terms mentioned above, one GO term, response to ETH stimulus, is highly enriched (GO:0009727, p = 2.61e-6) (**Supplementary Table 11**). This shift from the JA pathway to the ETH pathway may imply that the *wds* mutant has a phasing effect on spike development. Most importantly, the candidate gene identified from the locus 6BL.2 was a BR-related gene, providing additional evidence that dense spike phenotype is related to hormones. In rice, *SMALL GRAIN 11* (*SMG11*), a novel allele of *DWARF2* (*D2*) encoding a cytochrome P450 (CYP90D2), is involved in BR biosynthesis. The morphological traits of *smg11*, including erect, shorter, and denser panicles at the mature stage,

exhibit decreased length of rachis and more but smaller grains, suggesting that BR plays a role in deciding cell division and elongation. Mutation of BR-related genes disrupts regular cell division and elongation, resulting in a short spike phenotype (Fang et al., 2016). In our study, microscopic observations showed significantly decreased length of rachis cells and the increased number of transverse rachis cells in the *wds* mutant, consistent with the function of BR in regulating plant cell elongation and division. These data supported the hypothesis that a gene associated with BR was responsible for the phenotypic alteration. Further experiments should be carried out *via* gene editing strategy to confirm its function.

The Candidate Gene May Have Pleiotropic Effects

In addition to spike length, the *wds* mutant also showed a clear reduction in plant height, indicating its nature as a pleiotropic gene. In rice, the *Ghd7* gene (*Grain number*, *plant height*, *and heading date7*), for example, encodes a CCT (CONSTANS, CONSTANS-LIKE, and TIMING OF CHLOROPHYLL A/B BINDING1) domain protein which is involved in the rice flowering pathway but also contributes to rice yield potential (Xue et al., 2008). In rice, *OsBUL1* was involved in the regulation of cell size development and the mutation of *OsBUL1* reduced plant height by making internode cells shorter (Jang et al., 2017). Similarly, *OsBUL1* was also involved in controlling plant height, spike length, and grain length (Heang and Sassa, 2012). We showed here that the wheat *TaBUL1* may also serve as a pleiotropic gene and be responsible for multiple traits in wheat. *TaBUL1-6B* was located in one of the two large deletion segments that overlapped with a known spike length QTL. RNA-seq analysis supported its function as a major regulator for spike development in wheat. The gene may be valuable in breeding for yield improvement.

CONCLUSION

With a high-quality wheat genome sequence available, a number of techniques that were once only available for model plants can be applied to the genetic cloning agriculturally important genes of this polyploid species. This work not only provides a strategy for rapidly locating large lesions in wheat using multiple genomic methodologies, but also provides valuable resources for wheat research, including ECS data, transcriptome data and extreme pool data of critical stages of spike development.

DATA AVAILABILITY STATEMENT

The ECS and RNA-seq data have been submitted to NCBI under the project numbers PRJNA792309 and PRJNA803598.

AUTHOR CONTRIBUTIONS

AL, LM, and SG designed the project. MJ, ST, SL, DC, and GS performed laboratory experiments. TL, ZD, FW, XK, and SG aided in experiments. ZW, MF, YC, and RL performed data analysis. ZW and SL drafted the manuscript. AL and LM revised the manuscript. All authors have read and approved the manuscript.

FUNDING

This work was supported by the National Natural Science Foundation of China (#31971930 to AL), the Hebei Natural Science Foundation (C2021205013), and the Agricultural Science and Technology Innovation Program (CAAS-ZDRW202002 and CAAS-ZDRW202201).

ACKNOWLEDGMENTS

We thank Chenyang Hao and Xueyong Zhang for providing wheat materials for association study.

SUPPLEMENTARY MATERIAL

The Supplementary Material for this article can be found online at: https://www.frontiersin.org/articles/10.3389/fpls.2022.850302/full#supplementary-material

Supplementary Figure 1 | Principal component analysis (PCA) of RNA-seq samples, showing good replication quality.

Supplementary Figure 2 | Cluster dendrogram analysis of RNA-seq samples.

Supplementary Figure 3 | The phylogeny of wheat *BUL* genes.

Supplementary Figure 4 | Expression and protein sequence characterization of *TaBUL1* gene. **(A)** The expression of *TaBUL1* in HFZ and *wds*. **(B)** The multiple sequence alignment among TaBUL1 protein sequences.

REFERENCES

Anders, S., Pyl, P. T., and Huber, W. (2015). HTSeq—a Python framework to work with high-throughput sequencing data. *Bioinformatics* 31, 166–169. doi: 10.1093/bioinformatics/btu638

Barazesh, S., and McSteen, P. (2008). Hormonal control of grass inflorescence development. *Trends Plant Sci.* 13, 656–662. doi: 10.1016/j.tplants.2008.09.007

Bommert, P., and Whipple, C. (2018). Grass inflorescence architecture and meristem determinacy. *Semin. Cell Dev. Biol.* 79, 37–47. doi: 10.1016/j.semcdb.2017.10.004

Cai, Q., Yuan, Z., Chen, M., Yin, C., Luo, Z., Zhao, X., et al. (2014). Jasmonic acid regulates spikelet development in rice. *Nat. Commun.* 5:3476.

Deng, Z., Cui, Y., Han, Q., Fang, W., Li, J., and Tian, J. (2017). Discovery of consistent QTLs of wheat spike-related traits under nitrogen treatment at different development stages. *Front. Plant Sci.* 8:2120. doi: 10.3389/fpls.2017.02120

Dixon, L. E., Greenwood, J. R., Bencivenga, S., Zhang, P., Cockram, J., Mellers, G., et al. (2018). TEOSINTE BRANCHED1 regulates inflorescence architecture and development in bread wheat (*Triticum aestivum*). *Plant Cell* 30, 563–581. doi: 10.1105/tpc.17.00961

Dong, C., Zhang, L., Chen, Z., Xia, C., Gu, Y., Wang, J., et al. (2020). Combining a new exome capture panel with an effective varbscore algorithm accelerates BSA-based gene cloning in wheat. *Front. Plant Sci.* 11:1249. doi: 10.3389/fpls.2020.01249

Du, D., Zhang, D., Yuan, J., Feng, M., Li, Z., Wang, Z., et al. (2021). FRIZZY PANICLE defines a regulatory hub for simultaneously controlling spikelet formation and awn elongation in bread wheat. *New Phytol.* 231, 814–833. doi: 10.1111/nph.17388

Dun, E. A., De Saint Germain, A., Rameau, C., and Beveridge, C. A. (2012). Antagonistic action of strigolactone and cytokinin in bud outgrowth control. *Plant physiol.* 158, 487–498. doi: 10.1104/pp.111.186783

Fang, N., Xu, R., Huang, L., Zhang, B., Duan, P., Li, N., et al. (2016). SMALL GRAIN 11 controls grain size, grain number and grain yield in rice. *Rice* 9:64. doi: 10.1186/s12284-016-0136-z

Faris, J. D., Fellers, J. P., Brooks, S. A., and Gill, B. S. (2003). A bacterial artificial chromosome contig spanning the major domestication locus Q in wheat and identification of a candidate gene. *Genetics* 164, 311–321. doi: 10.1093/genetics/164.1.311

Guo, J., Shi, W., Zhang, Z., Cheng, J., Sun, D., Yu, J., et al. (2018a). Association of yield-related traits in founder genotypes and derivatives of common wheat (*Triticum aestivum* L.). *BMC Plant Biol.* 18:38. doi: 10.1186/s12870-018-1234-4

Guo, Z., Zhao, Y., Röder, M. S., Reif, J. C., Ganal, M. W., Chen, D., et al. (2018b). Manipulation and prediction of spike morphology traits for the improvement of grain yield in wheat. *Sci. Rep.* 8:14435. doi: 10.1038/s41598-018-31977-3

He, F., Pasam, R., Shi, F., Kant, S., Keeble-Gagnere, G., Kay, P., et al. (2019). Exome sequencing highlights the role of wild-relative introgression in shaping the adaptive landscape of the wheat genome. *Nat. Genet.* 51, 896–904. doi: 10.1038/s41588-019-0382-2

Heang, D., and Sassa, H. (2012). An atypical bHLH protein encoded by positive regulator of grain length 2 is involved in controlling grain length and weight of rice through interaction with a typical bHLH protein APG. *Breed Sci.* 62, 133–141. doi: 10.1270/jsbbs.62.133

Huang, L., Hua, K., Xu, R., Zeng, D., Wang, R., Dong, G., et al. (2021). The LARGE2-APO1/APO2 regulatory module controls panicle size and grain number in rice. *Plant Cell* 33, 1212–1228. doi: 10.1093/plcell/koab041

Jang, S., An, G., and Li, H. Y. (2017). rice leaf angle and grain size are affected by the OsBUL1 transcriptional activator complex. *Plant Physiol.* 173, 688–702. doi: 10.1104/pp.16.01653

Jordan, K. W., Wang, S., Lun, Y., Gardiner, L. J., Maclachlan, R., Hucl, P., et al. (2015). A haplotype map of allohexaploid wheat reveals distinct patterns of selection on homoeologous genomes. *Genome Biol.* 16:48. doi: 10.1186/s13059-015-0606-4

Kim, D., Paggi, J. M., Park, C., Bennett, C., and Salzberg, S. L. (2019). Graph-based genome alignment and genotyping with HISAT2 and HISAT-genotype. *Nat Biotechnol.* 37, 907–915. doi: 10.1038/s41587-019-0201-4

Lang, D., Appels, R., Rigault, P., Kanyuka, K., Twardziok, S., Melonek, J., et al. (2018). Shifting the limits in wheat research and breeding using a fully annotated reference genome. *Science* 361, eaar7191. doi: 10.1126/science.aar7191

Li, H., and Durbin, R. (2009). Fast and accurate short read alignment with Burrows-Wheeler transform. *Bioinformatics* 25, 1754–1760.

Li, H., Handsaker, B., Wysoker, A., Fennell, T., Ruan, J., Homer, N., et al. (2009). The sequence alignment/map format and SAMtools. *Bioinformatics* 25, 2078–2079. doi: 10.1093/bioinformatics/btp352

Li, G., Kuijer, H. N. J., Yang, X., Liu, H., Shen, C., Shi, J., et al. (2021a). MADS1 maintains barley spike morphology at high ambient temperatures. *Nat. Plants* 7, 1093–1107. doi: 10.1038/s41477-021-00957-3

Li, Y., Li, L., Zhao, M., Guo, L., Guo, X., Zhao, D., et al. (2021b). Wheat Frizzy Panicle activates vernalization1-a and homeobox4-a to regulate spike development in wheat. *Plant Biotechnol. J.* 19, 1141–1154. doi: 10.1111/pbi.13535

McKenna, A., Hanna, M., Banks, E., Sivachenko, A., Cibulskis, K., Kernytsky, A., et al. (2010). The genome analysis toolkit: a mapreduce framework for analyzing next-generation DNA sequencing data. *Genome Res.* 20, 1297–1303. doi: 10.1101/gr.107524.110

McSteen, P. (2009). Hormonal regulation of branching in grasses. *Plant Physiol.* 149, 46–55. doi: 10.1104/pp.108.129056

Mo, Y., Howell, T., Vasquez-Gross, H., De Haro, L. A., Dubcovsky, J., and Pearce, S. (2018). Mapping causal mutations by exome sequencing in a wheat TILLING population: a tall mutant case study. *Mol. Genet. Genom.* 293, 463–477. doi: 10.1007/s00438-017-1401-6

Pang, Y., Liu, C., Wang, D., St. Amand, P., Bernardo, A., Li, W., et al. (2020). High-resolution genome-wide association study identifies genomic regions and candidate genes for important agronomic traits in wheat. *Mol. Plant* 13, 1311–1327. doi: 10.1016/j.molp.2020.07.008

Ritchie, M. E., Phipson, B., Wu, D., Hu, Y., Law, C. W., Shi, W., et al. (2015). limma powers differential expression analyses for RNA-sequencing and microarray studies. *Nucleic Acids Res.* 43:e47. doi: 10.1093/nar/gkv007

Rogers, S. O., and Bendich, A. J. (1985). Extraction of DNA from milligram amounts of fresh, herbarium and mummified plant tissues. *Plant Mol. Biol.* 5, 69–76. doi: 10.1007/BF00020088

Santner, A., Calderon-Villalobos, L. I., and Estelle, M. (2009). Plant hormones are versatile chemical regulators of plant growth. *Nat. Chem. Biol.* 5, 301–307. doi: 10.1038/nchembio.165

Shimizu-Sato, S., Tanaka, M., and Mori, H. (2009). Auxin-cytokinin interactions in the control of shoot branching. *Plant Mol. Biol.* 69, 429–435. doi: 10.1007/s11103-008-9416-3

Sormacheva, I., Golovnina, K., Vavilova, V., Kosuge, K., Watanabe, N., Blinov, A., et al. (2015). Q gene variability in wheat species with different spike morphology. *Genet. Resour. Crop Evol.* 62, 837–852. doi: 10.1186/s12870-020-02536-8

Wang, C., Yang, X., and Li, G. (2021). Molecular insights into inflorescence meristem specification for yield potential in cereal crops. *Int. J. Mol. Sci.* 22:3508. doi: 10.3390/ijms22073508

Wang, L., Ge, H., Hao, C., Dong, Y., and Zhang, X. (2012). Identifying loci influencing 1,000-kernel weight in wheat by microsatellite screening for evidence of selection during breeding. *PLoS One* 7:e29432. doi: 10.1371/journal.pone.0029432

Xue, W., Xing, Y., Weng, X., Zhao, Y., Tang, W., Wang, L., et al. (2008). Natural variation in Ghd7 is an important regulator of heading date and yield potential in rice. *Nat. Genet.* 40, 761–767. doi: 10.1038/ng.143

Yin, C.-C., Zhao, H., Ma, B., Chen, S.-Y., and Zhang, J.-S. (2017). Diverse roles of ethylene in regulating agronomic traits in rice. *Front. Plant Sci.* 8:1676. doi: 10.3389/fpls.2017.01676

Zhang, D., and Yuan, Z. (2014). Molecular control of grass inflorescence development. *Annu. Rev. Plant Biol.* 65, 553–578. doi: 10.1146/annurev-arplant-050213-040104

Zheng, C., Zhu, Y., Wang, C., and Guo, T. (2016). Wheat grain yield increase in response to pre-anthesis foliar application of 6-benzylaminopurine is dependent on floret development. *PLoS One* 11:e0156627. doi: 10.1371/journal.pone.0156627

Zhong, J., Van Esse, G. W., Bi, X., Lan, T., Walla, A., Sang, Q., et al. (2021). INTERMEDIUM-M encodes an ⁢em>HvAP2L-H5⁢/em> ortholog and is required for inflorescence indeterminacy and spikelet determinacy in barley. *Proc. Natl. Acad. Sci. U.S.A* 118:e2011779118.

Zhou, Y., Conway, B., Miller, D., Marshall, D., Cooper, A., Murphy, P., et al. (2017). Quantitative trait loci mapping for spike characteristics in hexaploid wheat. *Plant Genome* 10, 1–15. doi: 10.3835/plantgenome2016.10.0101

Conflict of Interest: The authors declare that the research was conducted in the absence of any commercial or financial relationships that could be construed as a potential conflict of interest.

Publisher's Note: All claims expressed in this article are solely those of the authors and do not necessarily represent those of their affiliated organizations, or those of the publisher, the editors and the reviewers. Any product that may be evaluated in this article, or claim that may be made by its manufacturer, is not guaranteed or endorsed by the publisher.

Copyright © 2022 Wang, Tao, Liu, Jia, Cui, Sun, Deng, Wang, Kong, Fu, Che, Liao, Li, Geng, Mao and Li. This is an open-access article distributed under the terms of the Creative Commons Attribution License (CC BY). The use, distribution or reproduction in other forums is permitted, provided the original author(s) and the copyright owner(s) are credited and that the original publication in this journal is cited, in accordance with accepted academic practice. No use, distribution or reproduction is permitted which does not comply with these terms.

frontiers | Frontiers in Plant Science

REVIEW
published: 25 April 2022
doi: 10.3389/fpls.2022.887723

Biotechnological Road Map for Innovative Weed Management

Albert Chern Sun Wong[1], Karen Massel[1], Yasmine Lam[1], Jessica Hintzsche[1] and Bhagirath Singh Chauhan[2,3]*

[1]Centre for Crop Science, Queensland Alliance for Agriculture and Food Innovation, The University of Queensland, Brisbane, QLD, Australia, [2]Centre for Crop Science, Queensland Alliance for Agriculture and Food Innovation, The University of Queensland, Gatton, QLD, Australia, [3]School of Agriculture and Food Sciences, The University of Queensland, Gatton, QLD, Australia

In most agriculture farmlands, weed management is predominantly reliant on integrated weed management (IWM) strategies, such as herbicide application. However, the overuse and misuse of herbicides, coupled with the lack of novel active ingredients, has resulted in the uptrend of herbicide-resistant weeds globally. Moreover, weedy traits that contribute to weed seed bank persistence further exacerbate the challenges in weed management. Despite ongoing efforts in identifying and improving current weed management processes, the pressing need for novel control techniques in agricultural weed management should not be overlooked. The advent of CRISPR/Cas9 gene-editing systems, coupled with the recent advances in "omics" and cheaper sequencing technologies, has brought into focus the potential of managing weeds in farmlands through direct genetic control approaches, but could be achieved stably or transiently. These approaches encompass a range of technologies that could potentially manipulate expression of key genes in weeds to reduce its fitness and competitiveness, or, by altering the crop to improve its competitiveness or herbicide tolerance. The push for reducing or circumventing the use of chemicals in farmlands has provided an added incentive to develop practical and feasible molecular approaches for weed management, although there are significant technical, practical, and regulatory challenges for utilizing these prospective molecular technologies in weed management.

Keywords: weed, CRISPR, genomics, biotechnology, herbicide, transient, RNAi, gene drive

OPEN ACCESS

Edited by:
Goetz Hensel,
Heinrich Heine University Düsseldorf, Germany

Reviewed by:
Chandrima Shyam,
Kansas State University, United States
Ilias Travlos,
Agricultural University of Athens, Greece

****Correspondence:***
Albert Chern Sun Wong
albertchernsun.wong@uq.edu.au

Specialty section:
This article was submitted to Plant Biotechnology, a section of the journal Frontiers in Plant Science

Received: *01 March 2022*
Accepted: *07 April 2022*
Published: *25 April 2022*

Citation:
Wong ACS, Massel K, Lam Y, Hintzsche J and Chauhan BS (2022) Biotechnological Road Map for Innovative Weed Management. Front. Plant Sci. 13:887723. doi: 10.3389/fpls.2022.887723

INTRODUCTION

The world population is projected to increase from the current average of 7.7 billion people in 2018–2020 to 8.5 billion people in 2030 (OECD/FAO, 2021). Population growth is one of the key drivers affecting global agricultural commodities for food and non-food demand. One of the most significant challenges facing crop improvement programs globally is the capacity to adequately match crop production with demand, thereby ensuring food security. Global crop production is encumbered by various abiotic and biotic stresses which are further exacerbated by climate change. It is evident that innovative approaches and technologies are urgently needed to address these issues, ensuring global crop production can meet the expected world population increase in the coming years.

Numerous initiatives spearheaded by various research institutes, private companies, and philanthropic organizations to tackle both abiotic and biotic stresses are currently underway. Many of these initiatives involve the use of recent advances in genome editing to improve crop resilience and adaptability to various environments, improve yields in suboptimal conditions, and increase crops' resistance to pathogens and insect pests. To date, several promising findings, such as the alterations of plant architecture, increased drought adaptation capabilities, increased salt tolerance, and increased pest and disease resistance have been reported (Wang et al., 2014; Yin and Qiu, 2019; Zhang et al., 2019; Tyagi et al., 2020; Zeng et al., 2020; Massel et al., 2021). A recent report on the transgenic expression of the human RNA demethylase *FTO* (fat mass and obesity associated) gene in rice and potato have resulted in an astonishingly ~50% increase in yield (Yu et al., 2021), although the approach involved would be considered as genetically modified (GM) and will fall under GM regulations.

Many molecular strategies for crop improvements have been largely focused on the improvement of crop resilience, adaptability, and yield, such as improving resistance to pathogens and insect pests. However, an equally pressing issue in farming is the control of weeds in agricultural lands. Weeds are a detrimental threat to global crop production in both developing and developed countries (Chauhan, 2020). Overall, among the biotic factors causing crop losses, weeds contribute to the highest potential yield loss to crops, followed by animal pests (insects, mites, nematodes, birds, rodents, etc.) and pathogens (fungi, viruses, bacteria, etc., Oerke, 2006). Annual crop losses and cost of weeds have been estimated to be at AUD 3.3 billion in Australia and USD 33 billion in the United States (Pimentel et al., 2005; Lewellyn et al., 2016).

Some molecular approaches have been implemented in conjunction with herbicide application to reduce the proliferation of weeds in agricultural lands. One such approach is the development of herbicide-resistant crops, such as the well-known Roundup Ready® crops (Padgette et al., 1995, 1996; Barry et al., 1997). The development of glyphosate-resistant crops enables the application of glyphosate, a non-selective herbicide, to eliminate unwanted weeds in the field at various application timings, thus enhancing the level of weed control. However, the emergence of herbicide-resistant GM crops has also contributed to the lack of novel herbicides discovery as it encourages the use of existing herbicides (Duke, 2012). Other factors such as the banning of currently used herbicides, high cost of new active ingredients discovery and marketing further discourage the development of novel herbicides (Duke, 2012; Székács, 2021). Nevertheless, ongoing research for novel mode-of-action herbicides is crucial as it provides alternative tools to combat and circumvent current trends of herbicide-resistant weeds. For example, in the lysine biosynthesis pathway which remains largely unexplored for herbicide development, novel inhibitors that target dihydrodipicolinate synthase (DHDPS), which catalyzes the first and rate-limiting step in lysine biosynthesis has been reported (Da Costa et al., 2021).

Gene discovery, "omics," and genome editing technologies currently applied in crop research can be potentially applied to weeds as tools for weed management. However, unlike in crop improvement, the utilization of molecular technologies to control weeds poses many challenges. These challenges include concerns surrounding the use and regulation of GM technologies in managing weeds and non-crop plant species in the wild, and the potential ecological risks posed by the intentional release of GM plant materials (Neve, 2018; Westwood et al., 2018; Barrett et al., 2019). Aside from GM methods, transient technologies relying on the non-transformative applications of RNA interference (RNAi) mechanism are also potential molecular approaches to control weeds instead of heavy reliance on herbicides. To date, significant advances in this technology have been made in crop pest and disease management (Cagliari et al., 2019).

The ongoing challenges in controlling weed-related damage to agriculture production have highlighted the need for new avenues to control weeds, other than relying on the conventional use of herbicides. Weed control technology must continuously improve to stay ahead of weed adaptation and evolution, and molecular approaches could potentially be explored as tools to control weeds. This review discusses the current challenges in managing herbicide resistance in weeds, and the molecular approaches that could be integrated into current strategies and aid in future weed management. Molecular approaches, including CRISPR/Cas9, gene drives and RNAi technology, are discussed in this review, along with a proposed list of potential gene targets for future molecular research on weed management.

CHALLENGES IN WEED MANAGEMENT

Weed management is challenging due to the diversity of weed and crop species and the various agricultural climates that these crops can be sown. There is no "one size fits all" model for any cropping system. The application of mechanical or chemical control methods alone has failed to lead to a sufficient suppression of weeds. However, integrated weed management (IWM) approaches, which encompasses coordinated application of various mechanical, chemical, and biological control methods, can help reduce weed seed bank and provide environmental and economic benefits in the long run (Harker and O'Donovan, 2013; Knezevic et al., 2017; Jabran and Chauhan, 2018; Alagbo et al., 2022). Despite the usefulness of IWM, such strategies need to be heavily researched to determine the appropriate cultural, physical, and chemical methods that would be the most beneficial for the agroecological zone. Additionally, the change in the global climate has rendered some tried and true practices ineffective, leaving the door open to innovation in IWM.

Climate change has raised complications in a number of different agricultural systems, and many of the challenges with weed management will be intensified which have been summarized in Ramesh et al. (2017). Firstly, with the expected reduction in rainfall in already dry regions, the resilience of crops will be encumbered. In this scenario, weeds have mechanisms to allow them to combat such stressors and out-compete the struggling crops, while also having extended

periods of growth beyond their usual growing season (Peters and Gerowitt, 2014; Ramesh et al., 2017). This is also partially linked to their ability to quickly accumulate mutations to be better adapted to rapidly changing climate scenarios, in contrast to many crops which rely on breeding programs to introgress desired traits in a relatively slow manner. Focusing more on the management side, climate change is expected to result in the need for new weed management strategies that will need to be rapidly implemented to be an effective combatant to the rapid climate variance. The change in climate will also result in the increased instability of current herbicides. For example, suddenly warmer regions will need to implement herbicides with higher heat tolerances or spray strategies will need to be altered to navigate new patterns of rainfall. Thus, from the examples highlighted above, the potential to further agitate weed management systems due to climate change can be seen. In addition to the compounding effects of climate change on weed management, the following review highlights some of the traits that allow for weeds to be so hardy, in addition to the already known complications prominent within weed management.

Herbicide Resistance in Weeds

The increased occurrence of various herbicide-resistant weeds in agricultural lands is one of the major issues faced in weed management. Human interventions and farming practices, such as the massive adoption of herbicide-based technologies to control weeds over large farmlands, have contributed to the evolution of herbicide resistance in many weeds (Cardina et al., 2002; Roux and Reboud, 2007). This is especially the case with continuous and non-judicious use of herbicides with the same mode of action. Biological factors that include the genetics, life cycle, and ecology of weeds also play a part in the evolution of their herbicide resistance mechanisms. Furthermore, no new mode of action herbicide has been released in the market for more than 30 years (Duke, 2012), which adds further pressure in controlling the increased number of herbicide-resistant weeds globally. Although herbicides with new modes of action, such as cinmethylin (Campe et al., 2018), tetflupyrolimet (Dayan, 2019; Dayan et al., 2019), and cyclopyrimorate (Shino et al., 2021) have been developed, weed control cannot be heavily dependent on utilizing novel herbicides as weeds can also develop resistance. From 1957 to 2020, the global reported number of unique cases of herbicide-resistant weeds has increased from 2 to 507 (Heap, 2022). In general, herbicide resistance mechanisms can be categorized into two broad types: (1) target-site resistance, and (2) non-target site resistance.

Target-site resistance typically involves specific site mutations in the target enzyme, which prevents herbicide from binding to the target enzyme. Mutations could occur in the binding sites within the enzyme, or on other parts of the enzyme which could alter the conformation of the enzyme in ways that the herbicide could no longer inhibit the activity of the enzyme. Other forms of target-site resistance include target gene amplification (the increase in target gene copies) and the increase in target gene expression. These resistance mechanisms aim to increase the production capacity and abundance of the target enzyme, in which higher doses of a herbicide would be required to fully inhibit the target enzyme. For example, gene amplification of the herbicide target gene 5-enolpyruvylshikimate-3-phosphate synthase (EPSPS) has been reported in weed species, such as *Amaranthus palmeri* (Gaines et al., 2010), *Chloris truncata* (Ngo et al., 2018), and *Hordeum glaucum* (Adu-Yeboah et al., 2020), whereas ACCase gene amplification has been reported in *Digitaria sanguinalis* (Laforest et al., 2017).

Non-target site resistance stems from the physiological characteristics of the plant and how it absorbs, metabolizes, and/or sequesters the herbicide (Jugulam and Shyam, 2019). As opposed to target-site resistance mechanisms, non-target site resistance is significantly more challenging to identify, as reducing the concentration of the herbicides entering and remaining in the plant systems usually involve multiple gene families controlling key processes such as metabolism, translocation, and sequestration of the herbicide molecules. Cases of weeds that have evolved non-target site resistance against major herbicide groups have been summarized in recent literature (Gaines et al., 2020; Perotti et al., 2020). For example, enhanced metabolism of the herbicide molecules is associated with the proteins, such as cytochrome P-450 monooxygenases (P450s), glutathione-S-transferases (GSTs) and/or glycosyl-transferases (GTs), which are involved in the various phases of herbicide detoxification (Gaines et al., 2020; Perotti et al., 2020). P450s form one of the largest gene families in plants and are vital to plant development in defense, having roles in the synthesis of hormones, lipids, primary and secondary metabolites, and metabolisms of various compounds (Mizutani, 2012; Xu et al., 2015). However, in terms of herbicide metabolism, they participate in the first phase by modifying the chemical functional groups of the herbicide molecules, enabling the conjugation of the herbicide molecules *via* GSTs or GTs to thiols groups or glucose (Cummins et al., 2013; Chronopoulou et al., 2017). Conjugated herbicide molecules are then transported to vacuoles *via* transporter proteins, such as the ATP-binding cassette (ABC) proteins (Martinoia et al., 1993; Theodoulou, 2000; Conte and Lloyd, 2011), and cation amino acid transporter (CAT; Su et al., 2004; Jóri et al., 2007), for compartmentalization and degradation.

Another example of non-target site resistance is through reducing translocation of the herbicide, so once the herbicide enters the source leaves they are prevented from reaching the growing and meristematic tissues *via* the phloem and/or xylem. Reduced translocation can be due to sequestration, which traps the herbicide molecules within the source tissues, or altered activity of transporter proteins, which either prevent or limit the entrance of the herbicide molecules into the phloem and/or xylem (Délye, 2013). Reduced translocation of glyphosate (Ge et al., 2011, 2012; Moretti and Hanson, 2017), paraquat (Yu et al., 2004, 2010; Brunharo and Hanson, 2017; Moretti and Hanson, 2017), and 2,4-D (Riar et al., 2011; Goggin et al., 2016) have been reported in different weed species.

Weed Seed Bank Persistence

Most weed species are known to be hardy and persistent in nature, producing thousands of seeds that can withstand various adverse environmental conditions, while staying dormant in

the soil for long periods (Manalil and Chauhan, 2021; Chauhan and Manalil, 2022). When optimal germination conditions are met, the seeds will germinate and compete with the crops sown on the same area of land. This makes weed management challenging, such as the application of selective herbicides when both the weeds and the crop in the farmland belong to the same group of flowering plants (e.g., monocot weed species growing within cereal crops). Consistent application of the range of control methods in IWM can be a long-term solution for minimizing weed seed bank, although only a limited number of studies on weed seed bank corresponding to management are available (Sosnoskie et al., 2009; Schwartz et al., 2015). Additionally, in agricultural farmlands, weed seed bank can contain seeds of multiple different weed species. Every weed species has their own biology, life cycle, and ecology, which in turn would require different IWM approaches.

Seed dormancy is the main contributor to a persistent weed seed bank globally and is a trait with high plasticity in weed species, thus, making weed control difficult to achieve as it adjusts the weed population to a cropping system (Baskin and Baskin, 2006; Schwartz-Lazaro and Copes, 2019). Dormancy can be categorized into two types: (1) primary dormancy, where dormancy is induced during seed development and prior to dispersion from the mother plant, and (2) secondary dormancy, when the dispersed seeds are met with suboptimal environmental conditions for germination (Carmona, 1992; Vivian et al., 2008). While seed dormancy is also a heritable genetic trait, it is complex to study due to the trait's genetic and environmental (G × E) interactions (Foley and Fennimore, 1998). Nevertheless, recent genetic and molecular studies on seed dormancy using model plant species have provided important genomic information to aid the understanding of seed dormancy in weeds (Gu et al., 2018; Pipatpongpinyo et al., 2020), and genes that are involved in the regulation of seed dormancy have been extensively reviewed (Graeber et al., 2012; Nonogaki, 2014; Klupczyńska and Pawłowski, 2021).

Lack of Genomic Resources in Weeds

Major obstacles in implementing molecular approaches for weed management include the lack of genomic resources on many major weeds, which encompasses the lack of genomic and molecular studies on weeds relative to many crop plants. Tools from genomics and molecular biology should be utilized to obtain genomic information on weeds, which can aid in the investigation of herbicide resistance mechanisms.

Initiatives such as the International Weed Genomics Consortium[1] have begun to fully sequence several major weed species in recent years, such as *Lolium rigidum* and *Conyza sumatrensis* (Manning, 2021). This initiative and future works in addressing greater availability of genomic resources of various major weed species would be beneficial not only for the development of molecular approaches for diagnostic and weed management, but also for a better understanding of weed biology, weedy traits, and the adaptive evolution of herbicide resistance (Ravet et al., 2018). Genomic resources of these major weed species could also be important in revealing potential genetic resources that could be utilized for future crop breeding for the integration of beneficial traits from weed species into crops. Harnessing the genetic information of weed species also enables a better understanding of weeds' biotic and abiotic tolerance. As most weeds are extremely tolerant to various harsh environments, generating and studying the genomic resources of these weeds could also aid in the understanding of stress tolerance and possibly be applied to related crops. Other genomic information such as population genetics can also potentially contribute to management decisions, such as the choice of herbicides and herbicide rotation (Perotti et al., 2020).

POTENTIAL MOLECULAR APPROACHES TARGETING WEEDS TO CONTROL FITNESS

In the current context of agriculture, the goal of studying weed biology and physiology is to understand the habitat, life cycle, propagation, and proliferation patterns of weeds, while applying these to reduce their fitness and colonization in agricultural farmlands. Herbicide application and other management-based approaches are means to reduce the fitness of the weed population in agricultural lands. Long-term objectives of weed management would be to reduce the global weed seed banks, effectively controlling the weed populations rather than treating the "symptom" of managing weeds as they appear. Numerous genetic approaches could be implemented which could be used to improve weed management in the future (**Figure 1**). These strategies combine genomics and biotechnological tools and could be implemented in either the crop or weed species depending on the desired outcome.

Genomics Tools

The increasing level of "omics" data available in weed species enables researchers to gain better insights into weedy characteristics such as dormancy, invasiveness, and herbicide tolerance/susceptibility mechanisms. In the case of glyphosate resistance in *Ipomoea purpurea*, using targeted exome re-sequencing, Van Etten et al. (2020) found no mutations in the expected glyphosate target protein of EPSPS, but instead found selective sweeps in other genes involved in herbicide detoxification which varied by population. Therefore, although the physiological mechanism is the same for glyphosate resistance in this weed, varied populations of divergent mechanisms for herbicide detoxification are present. Understanding the evolved herbicide resistance tactics of weeds can provide prospective genes and gene networks that could be manipulated in a diverse range of crops for alternative herbicide tolerance mechanisms.

Advances in genomics tools and resources for weeds will be crucial for the development of various molecular approaches for weed management. Cumulative efforts in building genomic resources for weeds will form the basis for the development

[1]https://www.weedgenomics.org/

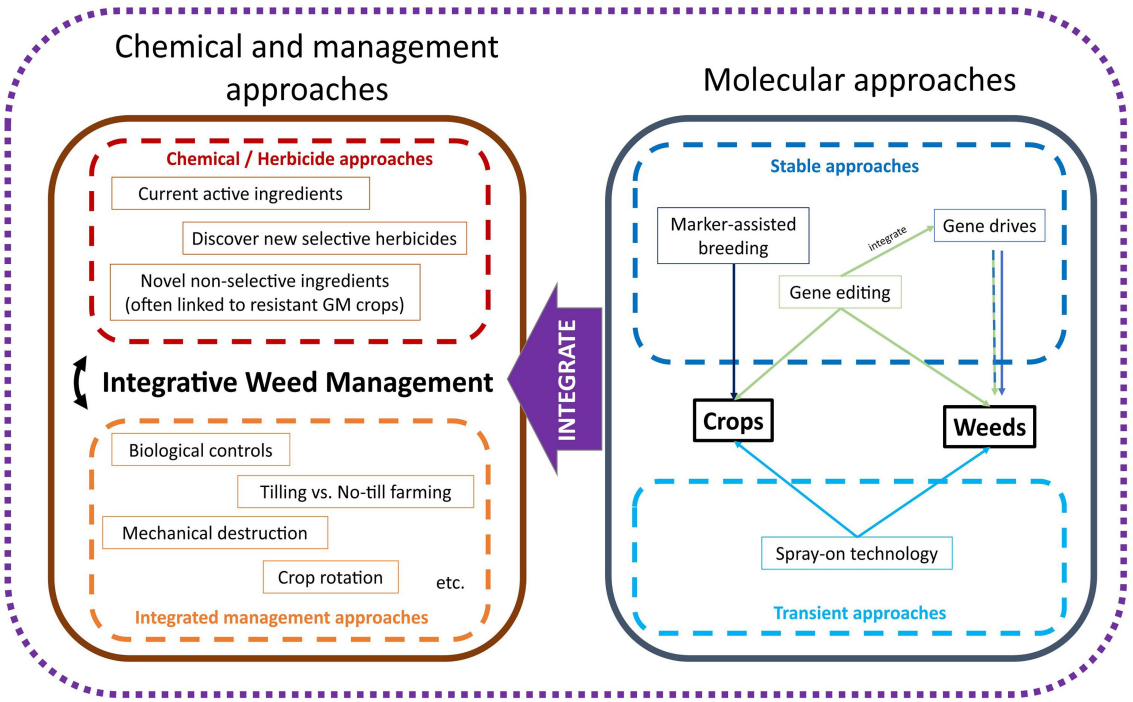


FIGURE 1 | A conceptual framework for innovative weed management. Conventional approaches using chemicals and farm management are often applied together and can be improved or integrated with biotechnological approaches for future weed management. Biotechnological weed management can be applied to crops or weeds *via* stable and transient approaches.

of plant transformation and gene editing protocols for gene function studies. It can also help scientists to better understand complex traits such as abiotic stresses, and various non-target site resistance mechanisms employed by weeds (Ravet et al., 2018). However, the development of genomic tools and "omics" database for weeds poses several challenges. These include the complexities in establishing the understanding of underlying biology across the large diversity of weed species and the diverse nature of weed-living systems (Martin et al., 2019; Patterson et al., 2019). Furthermore, unlike reference model plant species and other well-studied crop species, obtaining the desired genotypes (e.g., highly homogenous lines) for the development of genomic reference materials is encumbered by the maintenance of large genetic diversity in weeds (Basu et al., 2004; Stewart et al., 2009; Vigueira et al., 2013).

Marker-assisted crop breeding has led to enormous genetic gains for numerous traits such as disease resistance and yields, and have the potential to be applied for weed management strategies. Researchers can use Genome-Wide Association Studies (GWAS) to associate mutations in genetic elements to key traits for improved weed management, such as herbicide tolerance or those that allow crops to outcompete weeds. This strategy has been successfully applied to crop species such as wheat (Shi et al., 2020; Xu et al., 2020), cotton (Thyssen et al., 2014, 2018), sorghum (Adhikari et al., 2020), and fababean (Abou-Khater et al., 2022) for varied natural herbicide tolerance.

Similarly, novel genetic variation can be induced using chemical mutagenesis to create mutant populations, in turn producing new allelic variants and/or discovering new modes of action for weed control. Implementation of this method can be seen where imidazolidinone tolerance in wheat (Newhouse et al., 1992) and chickpea (Croser et al., 2021) was produced using ethyl methanesulfonate (EMS) mutant population. *Leucaena leucocephala* is another example of the implementation of chemical mutagenesis for weed management. Normally a pasture crop in Northern Australia, *Leucaena leucocephala* is known to be a rampant weed in other regions. In an attempt to combat this weed, a mutagenized population was created to develop various sterile alternatives, including cytoplasmic male sterile and a triploid variety (Mcmillan et al., 2019). Although EMS mutagenesis can achieve a non-GM outcome in an elite crop variety and provide a rapid strategy to market, the effects of this approach on agronomic/quality traits will need further evaluation.

CRISPR/Cas9

The CRISPR/Cas9 approach has been one of the most used technologies for genetic modification of crops and other organisms. It is a flexible and versatile option for highly targeted modification of genomes, mostly applied to disrupt gene function (Zhang et al., 2018). First, it creates highly targeted Double-Stranded Breaks (DSB) within the host genome with the introduction of two CRISPR components: a guide RNA (gRNA) and a CRISPR Associated Nuclease (Cas). The Cas protein contains two nuclease domains which each cut one strand of the DNA, targeted to the specific location in the genome

through the small non-coding gRNA. Targeting potential of the gRNA limited to regions directly upstream of a Cas-dependent Protospacer Adjacent Motif (PAM), which for the most common Cas9 from *Streptococcus pyogenes* is 5′-NGG-3′. Together, these components facilitate targeted DSBs, forcing the plant to repair the break by Non-Homologous End Joining (NHEJ) or Homology-Directed Repair (HDR). The first and most predominant in plants, NHEJ, fixes the break by ligating the broken ends together, but often does so erroneously. If targeted to the coding region of a gene, a frameshift mutation will lead to a gene knockout. The randomness of NHEJ repair means the outcomes are often viewed synonymously with mutagenesis or natural mutation, allowing gene-edited products to avoid the regulatory constraints of being classified as genetically modified.

The application of CRISPR/Cas9 in crop improvement has been extensively reviewed (Chen et al., 2019; Massel et al., 2021). Modified versions of the Cas9 proteins have also resulted in newer technologies such as base editing and prime editing for precise genome editing (Molla et al., 2021). The CRISPR/Cas9 approach is certainly a promising tool that could be utilized and adapted for weed management in two ways. The first would be to modify the genomes of the crop to boost its performance and outcompete weeds, through mechanisms such as increased herbicide tolerance, improved early vigor, or through allelopathic means to reduce weed establishment. Alternatively, one could implement gene editing strategies to the weed itself to alter its development or herbicide tolerance.

The delivery of the CRISPR/Cas9 constructs often requires the establishment of efficient transformation systems for many of these major weed species. Plant transformation systems are expensive to develop, time-consuming, and often genotype-specific. Developing plant transformation systems for the appropriate weeds would be highly challenging. In addition to optimizing plant transformation systems for these weed species, the delivery of the CRISPR/Cas9 constructs editing targeted genes in specific weed species, and the propagation of weed species carrying these constructs will be difficult from a regulatory standpoint. Although GM regulation could be avoided if the CRISPR/Cas9 editing components could be segregated out from the transgenic population prior to releasing into the wild for propagation, the regulations are highly complex and vary globally. Nevertheless, the rapid advancement of CRISPR/Cas9 technology could be useful for designing synthetic gene drives that could potentially be used for population and fitness control in weeds.

Gene Drive

Gene drive refers to the process which sequences of DNA are biasedly inherited in their favor and circumventing Mendelians inheritance, which results in a preferential increase of a specific genotype (Burt and Trivers, 2006; National Academies of Sciences, Engineering, and Medicine, 2016; Alphey et al., 2020). They are able to spread through populations, even when they impose a fitness cost on their host (Lindholm et al., 2016). Gene drives exist in nature through a variety of mechanisms, such as meiotic drives, transposable elements, and homing endonuclease genes (HEGs). HEGs were first suggested as tools that can be used for generating synthetic gene drives (Burt, 2003), and were first used in gene-drive systems in strains of *Drosophila* (Rong and Golic, 2003; Chan et al., 2013) or anopheline mosquitoes (Windbichler et al., 2011).

The idea of using gene drives for weed management is not new, as it has been discussed in several studies (Neve, 2018; Westwood et al., 2018; Barrett et al., 2019). Unlike the implementation of gene drives in controlling insect populations, the utilization of gene drives to control weeds faces significant challenges caused by the diversity of weed biology, and technical difficulties in developing efficient gene drive that can work in plants. Gene drives enable the spread of specific alleles only over generations; thus, the utilization of gene drives will be most effective in organisms that can reproduce quickly or that are highly dispersed. Unfortunately, not all weed species can be selected for genetic management *via* gene drive, due to different life-history factors. This includes modes of reproduction (sexual, asexual, or hermaphrodite), modes of crossing (inbreeding or outcrossing), modes of seed/pollen dispersal, seed dormancy, and genetic architecture such as polyploidy.

An efficient gene drive would require good cutting specificities so that the intended genetic change can be accurately inherited onto the progeny. The subsequent discovery of targeted genome editing tools, such as CRISPR/Cas9, have further improved cutting specificities and efficiencies of gene drive systems. CRISPR/Cas9-based gene drives have been successfully demonstrated in bacteria (Valderrama et al., 2019), yeast (Dicarlo et al., 2015), insects (Gantz and Bier, 2015; Gantz et al., 2015; Hammond et al., 2016; Kyrou et al., 2018), mice (Grunwald et al., 2019), and most recently in *Arabidopsis* (Zhang et al., 2021). Furthermore, a successful CRISPR/Cas9-based gene drive requires an efficient HDR pathway, instead of the NHEJ pathway (Gantz and Bier, 2015). In plants, HDR can be difficult to achieve as NHEJ is predominantly used to repair double-strand breaks (Puchta, 2004; Huang and Puchta, 2019). However, it has been shown that factors such as the amount of donor template, the concentration of Cas9 protein in the cell, and the timing of generating double-stranded breaks determine HDR efficiency in plants (Čermák et al., 2015; Gil-Humanes et al., 2017; Miki et al., 2018; Chen et al., 2019; Peng et al., 2020). The regulatory context will determine how this technology is able to be deployed in different jurisdictions and the extent to which societies (and markets) accept the use of gene drives, as HDR gene editing is often viewed as a GM outcome and subject to strict regulations.

By overcoming the biology and technical challenges of developing gene drive systems for weed management, gene drives can be used to (1) suppress the weed population, or (2) sensitize the weed population. Suppressing mechanisms refer to proliferating the mutation of crucial genes that will reduce the fitness of the weed population, thereby reducing their capability to compete with crops. The sensitizing approach refers to specifically reintroducing the herbicide susceptibility back into the resistant weed population.

Transient Technology

Transient technology allows the user to temporarily manipulate the gene expression of the plant without making any stable changes to the genomic DNA. This means that outcomes are not subjected to strict GM regulations, significantly less development time is required, and do not rely on having tissue culture systems in place to modify the genome. Further, these systems can often be applied to weeds or crops that are already growing to modify traits on-the-spot, rather than requiring a gene drive system to spread the desired changes throughout the population.

The utilization of a double-stranded RNA (dsRNA) spray packaging has been shown to improve a range of management options for diseases and insects across a range of plant species (Mitter et al., 2017). This approach packages a dsRNA capable of targeting and downregulating the expression of key genes in the host plant involved in disease/pest growth. There is enormous potential for a similar approach to be applied to control weeds. One option is to use RNAi to target herbicide-resistant weeds, reducing the expression of their tolerance mechanism so previously developed herbicides will continue to work. Alternatively, this system could be adapted to target key genes that are solely found within weed species without impacting their expression in crops, whereby reducing the gene expression may reduce the competitiveness of the weed (e.g., development issues, loss of flowering, and reduced seed set).

Spray-on technologies have been rapidly advancing, where systems have been developed for transient expression of genes (or RNAi machinery) through packaging into viral vectors. Torti et al. (2021) demonstrated that target genes controlling growth and other physiological changes can be modified *via* the RNAi approach, and this may be applied to weed management. It is possible that a spray-on strategy could be used to specifically target either the crop or weed species using promoters that would only drive expression of genes in either plant. In terms of herbicide efficiency, one could imagine a scenario where a farmer could boost herbicide tolerance in the crop species without creating a stable genetic alteration that would not express in the weed species. Similarly, the weeds could be specifically targeted with an RNAi vector to silence key endogenous genes which would complement or replace the use of herbicides. Furthermore, the genes are non-transmissible to the next generation so different herbicide treatments could be applied over the years to reduce the emergence of herbicide-resistant weed populations (Mitter et al., 2017; Cagliari et al., 2019). Transient silencing/overexpression approaches are not expected to be regulated as GM products, thus they could be developed and released to potentially complement or replace current weed management strategies.

POTENTIAL GENE TARGETS FOR REDUCING WEED FITNESS

Regardless of the challenges in implementing molecular approaches in weed management, either *via* genome editing approaches, or the dsRNA spray for transient editing, numerous prospective genes could be targeted for knockout and knockdown in weed species to reduce fitness, or conversely, genes targeted in the crop to improve fitness. Much of the challenge for spray-on technologies will be to ensure the transient alterations to gene expression are solely found in either the weed or crop species. As for the utilization of gene drives to release into the cropping environment, it will rely heavily on the successful creation of transgenic weeds carrying the gene drive, and the capability to drive the intended mutation into the weed population across several generations.

Cytochrome P450 Family and Herbicide Target Genes

There is a wide range of potential gene targets that could be targeted by the abovementioned molecular approaches. Genes that will lead to various downstream phenotypic effects that reduce the plant's survival and fitness when perturbed are often desirable targets for these approaches. For example, to improve herbicide efficiencies, one could consider altering genes within the cytochrome P450 family. These proteins have been shown to be upregulated in response to herbicide application (Pasquer et al., 2006; Hirose et al., 2007; Lu et al., 2015), which antagonizes the application of other herbicides, such as ACCases and acetolactate synthase (ALS) inhibitors (Peterson et al., 2016). Therefore, reducing the expression of P450s could potentially make the plant more susceptible to the herbicide, if the knockdown/out of this gene was not lethal.

However, although gene members of the cytochrome P450 family and other gene families (such as glutathione-S-transferases and glycosyl-transferases) involved in non-target site resistance are obvious targets for genetic manipulation, these gene families are often large and diverse (Martin et al., 2019), which makes targeting these genes specifically almost impractical. Thus, genetic resources from "omics" studies could also aid in revealing conditions and genetic elements that could be involved in the regulatory network of these superfamilies conferring herbicide resistance. For example, further understanding of how P450s are induced by herbicide application can be useful in designing vectors to exploit this mechanism. Hirose et al. (2007) has reported that the promoter of CYP72A21 in rice is activated when 2,4-D was applied, leading to increased CYP72A21 expression. One could consider altering the promoter region *via* gene editing to deactivate or suppress its sensitivity to 2,4-D application, which may avoid any constraints if a complete knockout is lethal. Thus, through targeting genes such as P450s, herbicide efficiency could be boosted by increasing the susceptibility in weed species.

Plant Growth Regulator Genes

Two options for improving weed management are to reduce the competitiveness of the weed species or to improve the early vigor of the crop plant. Therefore, genes that are involved in primary functions of growth and development could be targeted for either trait. In terms of reducing weeds' fitness and competitiveness, knockdown of these genes in weeds would be particularly useful in increasing their susceptibility to various biotic and abiotic stresses. For example, members of the

phenylalanine ammonia-lyase (PAL) gene family could be targeted in the weed species. These genes are involved in the first step of the phenylpropanoid biosynthesis pathway, which leads to the synthesis of precursors of various primary and secondary metabolites important for growth and responses to various biotic and abiotic stresses, such as UV radiation, temperature, and pathogen infection (Edwards et al., 1985; Dixon and Paiva, 1995; Huang et al., 2010; Vogt, 2010; Kim and Hwang, 2014; Feng et al., 2022). Additionally, molecular components (e.g., transcription factors, hormone receptors, and transporters) that interact with plant hormones to regulate plant development could be selected as potential targets for reducing weed competitiveness. However, developing molecular tools targeting these components can be highly challenging due to the complex network of interactions between the molecular components and plant hormones (Domagalska and Leyser, 2011; Vanstraelen and Benková, 2012; Gallavotti, 2013; Schaller et al., 2015; Waldie and Leyser, 2018). Provided that challenges on developing genomic tools and resources for weeds can be overcome, the testing of gene drive systems and spray-on transient technologies targeting plant growth regulator genes in weeds could potentially complement many current weed management strategies.

Alternatively, improving early vigor of the crop plant may lead to improved growth which in turn, leads to suppression of weed growth (De Vida et al., 2006). Although in some instances, researchers have been searching for plants that can maintain high yields despite weed competition, this strategy further contributes to the ongoing weed seed bank issues. Therefore, weed-suppressive strategies and control methods employed in IWM are preferred. Additionally, there have been a few studies searching for QTLs for weed competitive traits in crops (Coleman et al., 2001; Bharamappanavara et al., 2020; Dimaano et al., 2020). Although many of these studies have not mentioned specific genes from fine mapping, it is likely that genes involved in growth and development like maturity genes, tillering genes, and leaf development genes will be strong candidates for improvement.

Sex Determining and Flowering Time Genes

Plants possess diverse sexual systems that include obligate selfing, outcrossing, and apomixis. Different sexual systems are determined by their underlying genetics of temporal and spatial development of reproductive systems, resulting in sexual systems such as hermaphroditism, dioecism, monoecism and so on (Bawa and Beach, 1981; Charlesworth, 2002). Studies of the genetic basis of sex determining genes influencing floral and reproductive organs development in the genus *Silene* (Monéger, 2007; Bernasconi et al., 2009; Charlesworth, 2013), and the weed species of *Amaranthus tuberculatus* and *Amaranthus palmeri* (Montgomery et al., 2019, 2021), have provided gene targets that could potentially be tested for gene drive development and spray-on transient technology. Perturbing sex determining genes, including male-sterility and female-sterility factors, could potentially create an imbalance of sexes within the weed population, thus potentially causing the weed population to collapse. Interestingly, a flowering time gene, *FLOWERING LOCUS T* (*FT*) homolog is reported to be in the male-specific Y (MSY) region in the dioecious weed species of *Amaranthus tuberculatus* and *Amaranthus palmeri* (Montgomery et al., 2021), suggesting that perturbing the expression of this *FT* homolog could potentially alter the flowering time and affect fitness.

Flowering time genes have been extensively characterized in various plants, and the perturbation of these genes, such as *CONSTANS* (*CO*) and *FT*, result in abnormal timing of flowering and floral development (Koornneef et al., 1991; Putterill et al., 1995; Araki et al., 1998; Kobayashi et al., 1999; Kim et al., 2013). Disrupting the genetic sequence and expression of *CO* and *FT* homologs in weeds using gene drive and transient technology could potentially generate offspring with abnormal flowering time and floral development. This could directly affect the competitiveness of weeds in farmlands. However, it is important to note that the homologs of *CO*, *FT*, and their counterparts with similar amino acid sequences such as *CO*-like and *FT*-like genes in different plant species can possess various levels of functional redundancy (Yano et al., 2000; Izawa et al., 2002; Hayama and Coupland, 2004; Yoo et al., 2004; Hanzawa et al., 2005; Faure et al., 2007; Wong et al., 2014; Wolabu et al., 2016). Therefore, in-depth functional characterization of these genes in various weeds species would be required to test the feasibility of selecting flowering time genes as targets for molecular weed management.

Seed Dormancy

Targeting seed dormancy genes is another obvious choice to inhibit seed fitness. In plants, there are varied combinations of seed dormancy genes that coordinate the control and longevity (Li and Foley, 1997; Nonogaki, 2014; Pipatpongpinyo et al., 2020). Oftentimes, these genes include transcription factors that induce flavonoid biosynthesis, production and accumulation of ABA, and gibberellic acid biosynthesis (Finch-Savage and Leubner-Metzger, 2006; Debeaujon et al., 2007). By implementing CRISPR/Cas9 targeting seed dormancy genes and incorporating into gene drives, it could potentially reduce the capability of the seed to germinate in the environment. This would work similarly to the "terminator technology" or genetic use restriction technology (GURT) to maintain the intellectual property of genetically modified materials (Visser et al., 2001; Lombardo, 2014). In this technology, there is a genetic switch that once released would mean the next generation of seeds are non-viable.

Seed Shattering

Seed shattering is a key weedy trait that differentiates domesticated and wild plants (Dong and Wang, 2015). In crops, the retainment of inflorescence/pods is a staple of domestication which allows farmers to harvest the crops rather than the natural shedding of mature grains from the crops. The loss of the seed shattering trait would be important to reduce the spread of weeds across agricultural lands. A common mechanism in seed shattering in both monocots and dicots is the formation of the abscission layer in the inflorescence/pods *via* cell wall thickening and lignification (Harlan and deWet, 1965; Elgersma et al., 1988; Fuller and Allaby, 2009; Seymour et al., 2013; Dong and

Wang, 2015). This mechanism and subsequent physiological processes leading to seed shattering are controlled by a complex network of plant signaling components involving plant hormones (Vivian-Smith and Koltunow, 1999). On the gene level, it has been reported that the loss-of-function mutation in the major seed shattering gene in sorghum (*Sh1*) and its ortholog in rice was selected for their non-shattering phenotypes (Lin et al., 2012; Lv et al., 2018; Li et al., 2019). Konishi et al. (2006) has reported that the non-shattering trait in domesticated rice can be caused by a single nucleotide change in the *qSH1* gene. As such, CRISPR/Cas9 or base editing could potentially be applied in a variety of weed species to re-create the single nucleotide polymorphism (SNP) in the homologous regulatory region of the *qSH1* gene in rice to emulate loss of shattering.

Root Exudate Profile Modification

Natural phenomenon such as allelopathy may give insight into alternative methods for weed control. In these cases, plants are in direct chemical-mediated competition with each other, and there is a potential to exploit these natural systems to reduce weed seed banks. The alteration of the root exudate profiles in crops *via* molecular approaches to boost crop competitiveness and decrease weed fitness presents a relatively unexplored area of research for weed management. One example where this has already been achieved is in the competition of sorghum and the parasitic plant *Striga hermonthica* (Bellis et al., 2020), which is a major concern when growing this staple food throughout Africa (Ejeta and Gressel, 2007). Bellis et al. (2020) used CRISPR/Cas9 to edit a *Striga*-susceptible sorghum variety to generate a loss-of-function mutation in the *LOW GERMINATION STIMULANT 1* (*LGS1*) gene, which is believed to alter the stereochemistry of strigolactones in the root exudates, which in turn affect the fitness of the parasitic weed. Similarly, Bari et al. (2021) demonstrated CRISPR/Cas9 editing on the strigolactone biosynthetic gene, *More Axillary Growth 1* (*MAX1*), in tomato to confer resistance against root parasitic weed *Phelipanche aegyptiaca*.

Crop allelopathy and other allelopathy applications, such as straw mulching, can be effectively used to control weeds in the field (Iqbal et al., 2007; Schulz et al., 2013; Andrew et al., 2015). Identified allelochemicals include many plant secondary metabolites and plant growth regulators (Cheng and Cheng, 2015). As such, the molecular approaches discussed in this review could potentially be employed to target biosynthesis and regulatory genes of these allelochemical compounds, with the possibility to customize crop root exudate profiles that can exert negative effects on the growth of neighboring weed species. Successful implementation of this approach would be akin to the engineered crop producing its own "herbicide" to control weeds.

CONCLUSION AND FUTURE DIRECTIONS

Research efforts in weed science have been mainly focused on chemical weed control and herbicide resistance. Due to the lack of economic value in studying weeds (aside from studying how we can effectively kill them in farmlands) as compared to food and industrial crops, there is a general lack of weed genomic resources available, which could potentially be tapped for various purposes. The availability of weed genomic resources could aid in the further understanding of weeds' resilience and their stress tolerance, their evolution and adaptation to various climates, and discovery of potentially untapped useful bioproducts. The advancement of biotechnological tools and their uses in weed species would directly benefit other applications. For example, we could improve our understanding of the underlying genetics of weed species and use this knowledge to boost weed growth in harsh environments for bioremediation purposes in contaminated mining sites.

Although many of the molecular approaches discussed in this review possess several technical and regulatory challenges of their own, their potential usefulness in weed management in reducing or circumventing the use of chemicals in farmlands brings many benefits. However, several roadblocks need to be addressed. Apart from the investment required for establishing transformation systems in weeds, good scientific education for the public on the use of these technologies are also required for the successful adoption of these technologies in weed management. Also, concerns regarding the use and release of gene drives into weed population, such as the unintentional transmission of genetic materials to closely related non-weed species, and the possible outcome of population collapse or extinction in weed species and the effect on the ecological scale would also need to be addressed.

AUTHOR CONTRIBUTIONS

AW and BC developed the concept for the review. AW and KM wrote the manuscript. YL, JH, and BC provided substantial additions and revised the manuscript. AW performed the submission of the article. All authors contributed to the article and approved the submitted version.

ACKNOWLEDGMENTS

We thank the GRDC (Grains Research and Development Corporation), Australia for financial support.

REFERENCES

Abou-Khater, L., Maalouf, F., Jighly, A., Alsamman, A. M., Rubiales, D., Rispail, N., et al. (2022). Genomic regions associated with herbicide tolerance in a worldwide faba bean (*Vicia faba* L.) collection. *Sci. Rep.* 12:158. doi: 10.1038/s41598-021-03861-0

Adhikari, P., Goodrich, E., Fernandes, S. B., Lipka, A. E., Tranel, P., Brown, P., et al. (2020). Genetic variation associated with PPO-inhibiting herbicide tolerance in sorghum. *PLoS One* 15:e0233254. doi: 10.1371/journal.pone.0233254

Adu-Yeboah, P., Malone, J. M., Fleet, B., Gill, G., and Preston, C. (2020). EPSPS gene amplification confers resistance to glyphosate resistant populations of Hordeum glaucum Stued (northern barley grass) in South Australia. *Pest Manag. Sci.* 76, 1214–1221. doi: 10.1002/ps.5671

Alagbo, O., Akinyemiju, O., and Chauhan, B. (2022). Weed management in rainfed upland rice fields under varied agro-ecologies in Nigeria. *Rice Sci.* 29:2.

Alphey, L. S., Crisanti, A., Randazzo, F., and Akbari, O. S. (2020). Standardizing the definition of gene drive. *Proc. Natl. Acad. Sci. U. S. A.* 117, 30864–30867. doi: 10.1073/pnas.2020417117

Andrew, I., Storkey, J., and Sparkes, D. (2015). A review of the potential for competitive cereal cultivars as a tool in integrated weed management. *Weed Res.* 55, 239–248. doi: 10.1111/wre.12137

Araki, T., Kobayashi, Y., Kaya, H., and Iwabuchi, M. (1998). The flowering-time geneFT and regulation of flowering in *Arabidopsis*. *J. Plant Res.* 111, 277–281. doi: 10.1007/BF02512184

Bari, V. K., Nassar, J. A., and Aly, R. (2021). CRISPR/Cas9 mediated mutagenesis of MORE AXILLARY GROWTH 1 in tomato confers resistance to root parasitic weed Phelipanche aegyptiaca. *Sci. Rep.* 11:3905. doi: 10.1038/s41598-021-82897-8

Barrett, L. G., Legros, M., Kumaran, N., Glassop, D., Raghu, S., and Gardiner, D. M. (2019). Gene drives in plants: opportunities and challenges for weed control and engineered resilience. *Proc. R. Soc. B Biol. Sci.* 286:20191515. doi: 10.1098/rspb.2019.1515

Barry, G. F., Kishore, G. M., Padgette, S. R., and Stallings, W. C. (1997). Glyphosate-tolerant 5-enolpyruvylshikimate-3-phosphate synthases. US Patent. 5633435.

Baskin, C. C., and Baskin, J. M. (2006). The natural history of soil seed banks of arable land. *Weed Sci.* 54, 549–557. doi: 10.1614/WS-05-034R.1

Basu, C., Halfhill, M. D., Mueller, T. C., and Stewart, C. N. (2004). Weed genomics: new tools to understand weed biology. *Trends Plant Sci.* 9, 391–398. doi: 10.1016/j.tplants.2004.06.003

Bawa, K. S., and Beach, J. H. (1981). Evolution of sexual systems in flowering plants. *Annal. Miss. Bot. Gard.* 68, 254–274. doi: 10.2307/2398798

Bellis, E. S., Kelly, E. A., Lorts, C. M., Gao, H., Deleo, V. L., Rouhan, G., et al. (2020). Genomics of sorghum local adaptation to a parasitic plant. *Proc. Natl. Acad. Sci. U. S. A.* 117, 4243–4251. doi: 10.1073/pnas.1908707117

Bernasconi, G., Antonovics, J., Biere, A., Charlesworth, D., Delph, L. F., Filatov, D., et al. (2009). Silene as a model system in ecology and evolution. *Heredity* 103, 5–14. doi: 10.1038/hdy.2009.34

Bharamappanavara, M., Siddaiah, A. M., Ponnuvel, S., Ramappa, L., Patil, B., Appaiah, M., et al. (2020). Mapping QTL hotspots associated with weed competitive traits in backcross population derived from *Oryza sativa* L. and *O. glaberrima* Steud. *Sci. Rep.* 10:22103. doi: 10.1038/s41598-020-78675-7

Brunharo, C. A. C. G., and Hanson, B. D. (2017). Vacuolar sequestration of paraquat is involved in the resistance mechanism in *Lolium perenne* L. spp. multiflorum. *Front. Plant Sci.* 8:1485. doi: 10.3389/fpls.2017.01485

Burt, A. (2003). Site-specific selfish genes as tools for the control and genetic engineering of natural populations. *Proc. R. Soc. Lond. Ser. B Biol. Sci.* 270, 921–928. doi: 10.1098/rspb.2002.2319

Burt, A., and Trivers, R. (2006). *Genes in Conflict: The Biology of Selfish Genetic Elements*. Cambridge, MA: The Belknap Press of Harvard University Press.

Cagliari, D., Dias, N. P., Galdeano, D. M., Dos Santos, E. A., Smagghe, G., and Zotti, M. J. (2019). Management of pest insects and plant diseases by non-transformative RNAi. *Front. Plant Sci.* 10:1319. doi: 10.3389/fpls.2019.01319

Campe, R., Hollenbach, E., Kämmerer, L., Hendriks, J., Höffken, H. W., Kraus, H., et al. (2018). A new herbicidal site of action: cinmethylin binds to acyl-ACP thioesterase and inhibits plant fatty acid biosynthesis. *Pestic. Biochem. Physiol.* 148, 116–125. doi: 10.1016/j.pestbp.2018.04.006

Cardina, J., Herms, C. P., and Doohan, D. J. (2002). Crop rotation and tillage system effects on weed seedbanks. *Weed Sci.* 50, 448–460. doi: 10.1614/0043-1745(2002)050[0448:CRATSE]2.0.CO;2

Carmona, R. (1992). Problematic and management of weed seed banks in agricultural soils. *Plant. Daninha* 10, 5–16.

Čermák, T., Baltes, N. J., Čegan, R., Zhang, Y., and Voytas, D. F. (2015). High-frequency, precise modification of the tomato genome. *Genome Biol.* 16:232. doi: 10.1186/s13059-015-0796-9

Chan, Y.-S., Huen, D. S., Glauert, R., Whiteway, E., and Russell, S. (2013). Optimising homing endonuclease gene drive performance in a semi-refractory species: the *Drosophila melanogaster* experience. *PLoS One* 8:e54130. doi: 10.1371/journal.pone.0054130

Charlesworth, D. (2002). Plant sex determination and sex chromosomes. *Heredity* 88, 94–101. doi: 10.1038/sj.hdy.6800016

Charlesworth, D. (2013). Plant sex chromosome evolution. *J. Exp. Bot.* 64, 405–420. doi: 10.1093/jxb/ers322

Chauhan, B. S. (2020). Grand challenges in weed management. *Front. Agron.* 1:3. doi: 10.3389/fagro.2019.00003

Chauhan, B. S., and Manalil, S. (2022). Seedbank persistence of four summer grass weed species in the northeast cropping region of Australia. *PLoS One* 17:e0262288. doi: 10.1371/journal.pone.0262288

Chen, K., Wang, Y., Zhang, R., Zhang, H., and Gao, C. (2019). CRISPR/Cas genome editing and precision plant breeding in agriculture. *Annu. Rev. Plant Biol.* 70, 667–697. doi: 10.1146/annurev-arplant-050718-100049

Cheng, F., and Cheng, Z. (2015). Research progress on the use of plant allelopathy in agriculture and the physiological and ecological mechanisms of allelopathy. *Front. Plant Sci.* 6:1020. doi: 10.3389/fpls.2015.01020

Chronopoulou, E., Georgakis, N., Nianiou-Obeidat, I., Madesis, P., Perperopoulou, F., Pouliou, F., et al. (2017). "Plant glutathione transferases in abiotic stress response and herbicide resistance," in *Glutathione in Plant Growth, Development, and Stress Tolerance*. eds. M. A. Hossain, M. G. Mostofa, P. Diaz-Vivancos, D. J. Burritt, M. Fujita and L.-S. P. Tran (Cham: Springer International Publishing).

Coleman, R. K., Gill, G. S., and Rebetzke, G. J. (2001). Identification of quantitative trait loci for traits conferring weed competitiveness in wheat (*Triticum aestivum* L.). *Aust. J. Agric. Res.* 52, 1235–1246. doi: 10.1071/AR01055

Conte, S. S., and Lloyd, A. M. (2011). Exploring multiple drug and herbicide resistance in plants--spotlight on transporter proteins. *Plant Sci.* 180, 196–203. doi: 10.1016/j.plantsci.2010.10.015

Croser, J., Mao, D., Dron, N., Michelmore, S., Mcmurray, L., Preston, C., et al. (2021). Evidence for the application of emerging technologies to accelerate crop improvement—a collaborative pipeline to introgress herbicide tolerance into chickpea. *Front. Plant Sci.* 12:779122. doi: 10.3389/fpls.2021.779122

Cummins, I., Wortley, D. J., Sabbadin, F., He, Z., Coxon, C. R., Straker, H. E., et al. (2013). Key role for a glutathione transferase in multiple-herbicide resistance in grass weeds. *Proc. Natl. Acad. Sci. U. S. A.* 110, 5812–5817. doi: 10.1073/pnas.1221179110

Da Costa, T. P. S., Hall, C. J., Panjikar, S., Wyllie, J. A., Christoff, R. M., Bayat, S., et al. (2021). Towards novel herbicide modes of action by inhibiting lysine biosynthesis in plants. *Elife* 10:e69444. doi: 10.7554/eLife.69444

Dayan, F. E. (2019). Current status and future prospects in herbicide discovery. *Plants* 8:341. doi: 10.3390/plants8090341

Dayan, F. E., Haesaert, G., Van Leeuwen, T., Holden-Dye, L., Crossthwaite, A., and Nauen, R. (2019). Pesticides modes of action and resistance: a perspective from the 2019 IUPAC congress. *Outlooks Pest Manag.* 30, 157–163. doi: 10.1564/v30_aug_04

De Vida, F. B. P., Laca, E. A., Mackill, D. J., Fernández, G. M., and Fischer, A. J. (2006). Relating rice traits to weed competitiveness and yield: a path analysis. *Weed Sci.* 54, 1122–1131. doi: 10.1614/WS-06-042R.1

Debeaujon, I., Lepiniec, L., Pourcel, L., and Routaboul, J.-M. (2007). "Seed coat development and dormancy," in *Annual Plant Reviews, Seed Development, Dormancy and Germination*. eds. K. Bradford and H. Nonogaki (UK: Blackwell Publishing Ltd).

Délye, C. (2013). Unravelling the genetic bases of non-target-site-based resistance (NTSR) to herbicides: a major challenge for weed science in the forthcoming decade. *Pest Manag. Sci.* 69, 176–187. doi: 10.1002/ps.3318

Dicarlo, J. E., Chavez, A., Dietz, S. L., Esvelt, K. M., and Church, G. M. (2015). Safeguarding CRISPR-Cas9 gene drives in yeast. *Nat. Biotechnol.* 33, 1250–1255. doi: 10.1038/nbt.3412

Dimaano, N. G. B., Ali, J., Mahender, A., Sta Cruz, P. C., Baltazar, A. M., Diaz, M. G. Q., et al. (2020). Identification of quantitative trait loci governing early germination and seedling vigor traits related to weed competitive ability in rice. *Euphytica* 216:159. doi: 10.1007/s10681-020-02694-8

Dixon, R. A., and Paiva, N. L. (1995). Stress-induced phenylpropanoid metabolism. *Plant Cell* 7, 1085–1097. doi: 10.1105/tpc.7.7.1085

Domagalska, M. A., and Leyser, O. (2011). Signal integration in the control of shoot branching. *Nat. Rev. Mol. Cell Biol.* 12, 211–221. doi: 10.1038/nrm3088

Dong, Y., and Wang, Y.-Z. (2015). Seed shattering: from models to crops. *Front. Plant Sci.* 6:476. doi: 10.3389/fpls.2015.00476

Duke, S. O. (2012). Why have no new herbicide modes of action appeared in recent years? *Pest Manag. Sci.* 68, 505–512. doi: 10.1002/ps.2333

Edwards, K., Cramer, C. L., Bolwell, G. P., Dixon, R. A., Schuch, W., and Lamb, C. J. (1985). Rapid transient induction of phenylalanine ammonia-

lyase mRNA in elicitor-treated bean cells. *Proc. Natl. Acad. Sci. U. S. A.* 82, 6731–6735. doi: 10.1073/pnas.82.20.6731

Ejeta, G., and Gressel, J. (2007). *Integrating New Technologies for Striga Control: Towards Ending the Witch-Hunt*. Singapore: World Scientific Publishing Co Pte Ltd.

Elgersma, A., Leeuwangh, J., and Wilms, H. J. (1988). Abscission and seed shattering in perennial ryegrass (*Lolium perenne* L.). *Euphytica* 39, 51–57. doi: 10.1007/BF00043367

Faure, S., Higgins, J., Turner, A., and Laurie, D. A. (2007). The FLOWERING LOCUS T-like gene family in barley (Hordeum vulgare). *Genetics* 176, 599–609. doi: 10.1534/genetics.106.069500

Feng, Y., Huang, Q., Zhang, R., Li, J., Luo, K., and Chen, Y. (2022). Molecular characterisation of PAL gene family reveals their role in abiotic stress response in lucerne (*Medicago sativa*). *Crop Past. Sci.* 73:1558. doi: 10.1071/CP21558

Finch-Savage, W. E., and Leubner-Metzger, G. (2006). Seed dormancy and the control of germination. *New Phytol.* 171, 501–523. doi: 10.1111/j.1469-8137.2006.01787.x

Foley, M. E., and Fennimore, S. A. (1998). Genetic basis for seed dormancy. *Seed Sci. Res.* 8, 173–182.

Fuller, D. Q., and Allaby, R. (2009). "Seed dispersal and crop domestication: shattering, germination and seasonality in evolution under cultivation," in *Annual Plant Reviews Volume 38: Fruit Development and Seed Dispersal*. (UK: Blackwell Publishing Ltd).

Gaines, T. A., Duke, S. O., Morran, S., Rigon, C. A. G., Tranel, P. J., Küpper, A., et al. (2020). Mechanisms of evolved herbicide resistance. *J. Biol. Chem.* 295, 10307–10330. doi: 10.1074/jbc.REV120.013572

Gaines, T. A., Zhang, W., Wang, D., Bukun, B., Chisholm, S. T., Shaner, D. L., et al. (2010). Gene amplification confers glyphosate resistance in *Amaranthus palmeri*. *Proc. Natl. Acad. Sci. U. S. A.* 107, 1029–1034. doi: 10.1073/pnas.0906649107

Gallavotti, A. (2013). The role of auxin in shaping shoot architecture. *J. Exp. Bot.* 64, 2593–2608. doi: 10.1093/jxb/ert141

Gantz, V. M., and Bier, E. (2015). Genome editing. The mutagenic chain reaction: a method for converting heterozygous to homozygous mutations. *Science* 348, 442–444. doi: 10.1126/science.aaa5945

Gantz, V. M., Jasinskiene, N., Tatarenkova, O., Fazekas, A., Macias, V. M., Bier, E., et al. (2015). Highly efficient Cas9-mediated gene drive for population modification of the malaria vector mosquito *Anopheles stephensi*. *Proc. Natl. Acad. Sci. U. S. A.* 112, E6736–E6743. doi: 10.1073/pnas.1521077112

Ge, X., D'avignon, D. A., Ackerman, J. J. H., Collavo, A., Sattin, M., Ostrander, E. L., et al. (2012). Vacuolar glyphosate-sequestration correlates with glyphosate resistance in ryegrass (Lolium spp.) from Australia, South America, and Europe: a 31P NMR investigation. *J. Agric. Food Chem.* 60, 1243–1250. doi: 10.1021/jf203472s

Ge, X., D'avignon, D. A., Ackerman, J. J., Duncan, B., Spaur, M. B., and Sammons, R. D. (2011). Glyphosate-resistant horseweed made sensitive to glyphosate: low-temperature suppression of glyphosate vacuolar sequestration revealed by 31P NMR. *Pest Manag. Sci.* 67, 1215–1221. doi: 10.1002/ps.2169

Gil-Humanes, J., Wang, Y., Liang, Z., Shan, Q., Ozuna, C. V., Sánchez-León, S., et al. (2017). High-efficiency gene targeting in hexaploid wheat using DNA replicons and CRISPR/Cas9. *Plant J.* 89, 1251–1262. doi: 10.1111/tpj.13446

Goggin, D. E., Cawthray, G. R., and Powles, S. B. (2016). 2,4-D resistance in wild radish: reduced herbicide translocation via inhibition of cellular transport. *J. Exp. Bot.* 67, 3223–3235. doi: 10.1093/jxb/erw120

Graeber, K., Nakabayashi, K., Miatton, E., Leubner-Metzger, G., and Soppe, W. J. (2012). Molecular mechanisms of seed dormancy. *Plant Cell Environ.* 35, 1769–1786. doi: 10.1111/j.1365-3040.2012.02542.x

Grunwald, H. A., Gantz, V. M., Poplawski, G., Xu, X. S., Bier, E., and Cooper, K. L. (2019). Super-Mendelian inheritance mediated by CRISPR-Cas9 in the female mouse germline. *Nature* 566, 105–109. doi: 10.1038/s41586-019-0875-2

Gu, X.-Y., Pipatpongpinyo, W., Zhang, L., Zhou, Y., Ye, H., and Feng, J. (2018). Two contrasting patterns and underlying genes for coadaptation of seed dormancy and flowering time in rice. *Sci. Rep.* 8:16813. doi: 10.1038/s41598-018-34850-5

Hammond, A., Galizi, R., Kyrou, K., Simoni, A., Siniscalchi, C., Katsanos, D., et al. (2016). A CRISPR-Cas9 gene drive system targeting female reproduction in the malaria mosquito vector Anopheles gambiae. *Nat. Biotechnol.* 34, 78–83. doi: 10.1038/nbt.3439

Hanzawa, Y., Money, T., and Bradley, D. (2005). A single amino acid converts a repressor to an activator of flowering. *Proc. Natl. Acad. Sci. U. S. A.* 102, 7748–7753. doi: 10.1073/pnas.0500932102

Harker, K. N., and O'donovan, J. T. (2013). Recent weed control, weed management, and integrated weed management. *Weed Technol.* 27, 1–11. doi: 10.1614/WT-D-12-00109.1

Harlan, J. R., and Dewet, J. M. (1965). Some thoughts about weeds. *Econ. Bot.* 19, 16–24. doi: 10.1007/BF02971181

Hayama, R., and Coupland, G. (2004). The molecular basis of diversity in the photoperiodic flowering responses of *Arabidopsis* and rice. *Plant Physiol.* 135, 677–684. doi: 10.1104/pp.104.042614

Heap, I. (2022). The International Herbicide-Resistant Weed Database [Online]. Available at: https://www.weedscience.org/Pages/ChronologicalIncrease.aspx (Accessed February 3, 2022).

Hirose, S., Kawahigashi, H., Tagiri, A., Imaishi, H., Ohkawa, H., and Ohkawa, Y. (2007). Tissue-specific expression of rice CYP72A21 induced by auxins and herbicides. *Plant Biotechnol. Rep.* 1, 27–36. doi: 10.1007/s11816-006-0003-2

Huang, J., Gu, M., Lai, Z., Fan, B., Shi, K., Zhou, Y.-H., et al. (2010). Functional analysis of the *Arabidopsis* PAL gene family in plant growth, development, and response to environmental stress. *Plant Physiol.* 153, 1526–1538. doi: 10.1104/pp.110.157370

Huang, T.-K., and Puchta, H. (2019). CRISPR/Cas-mediated gene targeting in plants: finally a turn for the better for homologous recombination. *Plant Cell Rep.* 38, 443–453. doi: 10.1007/s00299-019-02379-0

Iqbal, J., Cheema, Z., and An, M. (2007). Intercropping of field crops in cotton for the management of purple nutsedge (*Cyperus rotundus* L.). *Plant Soil* 300, 163–171. doi: 10.1007/s11104-007-9400-8

Izawa, T., Oikawa, T., Sugiyama, N., Tanisaka, T., Yano, M., and Shimamoto, K. (2002). Phytochrome mediates the external light signal to repress FT orthologs in photoperiodic flowering of rice. *Genes Dev.* 16, 2006–2020. doi: 10.1101/gad.999202

Jabran, K., and Chauhan, B. S. (eds.) (2018). "Overview and significance of non-chemical weed control," in *Non-Chemical Weed Control* (London, United Kingdom: Academic Press).

Jóri, B., Soós, V., Szegő, D., Páldi, E., Szigeti, Z., Rácz, I., et al. (2007). Role of transporters in paraquat resistance of horseweed *Conyza canadensis* (L.) Cronq. *Pestic. Biochem. Physiol.* 88, 57–65. doi: 10.1016/j.pestbp.2006.08.013

Jugulam, M., and Shyam, C. (2019). Non-target-site resistance to herbicides: recent developments. *Plants* 8:417. doi: 10.3390/plants8100417

Kim, D. S., and Hwang, B. K. (2014). An important role of the pepper phenylalanine ammonia-lyase gene (PAL1) in salicylic acid-dependent signalling of the defence response to microbial pathogens. *J. Exp. Bot.* 65, 2295–2306. doi: 10.1093/jxb/eru109

Kim, W., Park, T. I., Yoo, S. J., Jun, A. R., and Ahn, J. H. (2013). Generation and analysis of a complete mutant set for the *Arabidopsis* FT/TFL1 family shows specific effects on thermo-sensitive flowering regulation. *J. Exp. Bot.* 64, 1715–1729. doi: 10.1093/jxb/ert036

Klupczyńska, E. A., and Pawłowski, T. A. (2021). Regulation of seed dormancy and germination mechanisms in a changing environment. *Int. J. Mol. Sci.* 22:1357. doi: 10.3390/ijms22031357

Knezevic, S. Z., Jhala, A., and Datta, A. (2017). "Integrated weed management," in *Encyclopedia of Applied Plant Sciences*. eds. B. Thomas, B. G. Murray and D. J. Murphy (Oxford: Academic Press).

Kobayashi, Y., Kaya, H., Goto, K., Iwabuchi, M., and Araki, T. (1999). A pair of related genes with antagonistic roles in mediating flowering signals. *Science* 286, 1960–1962. doi: 10.1126/science.286.5446.1960

Konishi, S., Izawa, T., Lin, S. Y., Ebana, K., Fukuta, Y., Sasaki, T., et al. (2006). An SNP caused loss of seed shattering during rice domestication. *Science* 312, 1392–1396. doi: 10.1126/science.1126410

Koornneef, M., Hanhart, C. J., and Van Der Veen, J. H. (1991). A genetic and physiological analysis of late flowering mutants in *Arabidopsis thaliana*. *Mol. Gen. Genet.* 229, 57–66. doi: 10.1007/BF00264213

Kyrou, K., Hammond, A. M., Galizi, R., Kranjc, N., Burt, A., Beaghton, A. K., et al. (2018). A CRISPR-Cas9 gene drive targeting doublesex causes complete population suppression in caged Anopheles gambiae mosquitoes. *Nat. Biotechnol.* 36, 1062–1066. doi: 10.1038/nbt.4245

Laforest, M., Soufiane, B., Simard, M.-J., Obeid, K., Page, E., and Nurse, R. E. (2017). Acetyl-CoA carboxylase overexpression in herbicide-resistant large crabgrass (*Digitaria sanguinalis*). *Pest Manag. Sci.* 73, 2227–2235. doi: 10.1002/ps.4675

Lewellyn, R. S., Ronning, D., Ouzman, J., Walker, S., Mayfield, A., and Clarke, M. (2016). Impact of weeds on Australian grain production: the cost of weeds to Australian grain growers and the adoption of weed management and tillage practices. Report for GRDC. CSIRO, Australia.

Li, B., and Foley, M. E. (1997). Genetic and molecular control of seed dormancy. *Trends Plant Sci.* 2, 384–389. doi: 10.1016/S1360-1385(97)90053-4

Li, F., Numa, H., Hara, N., Sentoku, N., Ishii, T., Fukuta, Y., et al. (2019). Identification of a locus for seed shattering in rice (*Oryza sativa* L.) by combining bulked segregant analysis with whole-genome sequencing. *Mol. Breed.* 39, 1–14. doi: 10.1007/s11032-019-0941-3

Lin, Z., Li, X., Shannon, L. M., Yeh, C.-T., Wang, M. L., Bai, G., et al. (2012). Parallel domestication of the Shattering1 genes in cereals. *Nat. Genet.* 44, 720–724. doi: 10.1038/ng.2281

Lindholm, A. K., Dyer, K. A., Firman, R. C., Fishman, L., Forstmeier, W., Holman, L., et al. (2016). The ecology and evolutionary dynamics of meiotic drive. *Trends Ecol. Evol.* 31, 315–326. doi: 10.1016/j.tree.2016.02.001

Lombardo, L. (2014). Genetic use restriction technologies: a review. *Plant Biotechnol. J.* 12, 995–1005. doi: 10.1111/pbi.12242

Lu, H.-P., Edwards, M., Wang, Q.-Z., Zhao, H.-J., Fu, H.-W., Huang, J.-Z., et al. (2015). Expression of cytochrome P450 CYP81A6 in rice: tissue specificity, protein subcellular localization, and response to herbicide application. *J. Zhejiang Univ. Sci. B* 16, 113–122. doi: 10.1631/jzus.B1400168

Lv, S., Wu, W., Wang, M., Meyer, R. S., Ndjiondjop, M.-N., Tan, L., et al. (2018). Genetic control of seed shattering during African rice domestication. *Nat. Plants* 4, 331–337. doi: 10.1038/s41477-018-0164-3

Manalil, S., and Chauhan, B. S. (2021). Seedbank persistence and emergence pattern of Argemone mexicana, Rapistrum rugosum and Sonchus oleraceus in the eastern grain region of Australia. *Sci. Rep.* 11:18095. doi: 10.1038/s41598-021-97614-8

Manning, A. (2021). International Weed Genomics Consortium—Collaborative Effort to Combat Crop-Threatening Weeds Headed by CSU Scientists. Available at: https://agsci.source.colostate.edu/international-effort-to-combat-crop-threatening-weeds-headed-by-csu-scientists/ (Accessed October 22, 2021).

Martin, S. L., Parent, J.-S., Laforest, M., Page, E., Kreiner, J. M., and James, T. (2019). Population genomic approaches for weed science. *Plants* 8:354. doi: 10.3390/plants8090354

Martinoia, E., Grill, E., Tommasini, R., Kreuz, K., and Amrhein, N. (1993). ATP-dependent glutathione S-conjugate 'export' pump in the vacuolar membrane of plants. *Nature* 364, 247–249. doi: 10.1038/364247a0

Massel, K., Lam, Y., Wong, A. C. S., Hickey, L. T., Borrell, A. K., and Godwin, I. D. (2021). Hotter, drier, CRISPR: the latest edit on climate change. *Theor. Appl. Genet.* 134, 1691–1709. doi: 10.1007/s00122-020-03764-0

Mcmillan, H. E., Liu, G., Shelton, H. M., Dalzell, S. A., Godwin, I. D., Gamage, H., et al. (2019). Sterile leucaena becomes a reality? *Trop. Grasslands-Forrajes Trop.* 7, 74–79. doi: 10.17138/tgft(7)74-79

Miki, D., Zhang, W., Zeng, W., Feng, Z., and Zhu, J.-K. (2018). CRISPR/Cas9-mediated gene targeting in *Arabidopsis* using sequential transformation. *Nat. Commun.* 9:1967. doi: 10.1038/s41467-018-04416-0

Mitter, N., Worrall, E. A., Robinson, K. E., Li, P., Jain, R. G., Taochy, C., et al. (2017). Clay nanosheets for topical delivery of RNAi for sustained protection against plant viruses. *Nat. Plants* 3:16207. doi: 10.1038/nplants.2016.207

Mizutani, M. (2012). Impacts of diversification of cytochrome P450 on plant metabolism. *Biol. Pharm. Bull.* 35, 824–832. doi: 10.1248/bpb.35.824

Molla, K. A., Sretenovic, S., Bansal, K. C., and Qi, Y. (2021). Precise plant genome editing using base editors and prime editors. *Nat. Plants* 7, 1166–1187. doi: 10.1038/s41477-021-00991-1

Monéger, F. (2007). Sex determination in plants. *Plant Signal. Behav.* 2, 178–179. doi: 10.4161/psb.2.3.3728

Montgomery, J. S., Giacomini, D. A., Weigel, D., and Tranel, P. J. (2021). Male-specific Y-chromosomal regions in waterhemp (*Amaranthus tuberculatus*) and Palmer amaranth (*Amaranthus palmeri*). *New Phytol.* 229, 3522–3533. doi: 10.1111/nph.17108

Montgomery, J. S., Sadeque, A., Giacomini, D. A., Brown, P. J., and Tranel, P. J. (2019). Sex-specific markers for waterhemp (*Amaranthus tuberculatus*) and Palmer amaranth (*Amaranthus palmeri*). *Weed Sci.* 67, 412–418. doi: 10.1017/wsc.2019.27

Moretti, M. L., and Hanson, B. D. (2017). Reduced translocation is involved in resistance to glyphosate and paraquat in Conyza bonariensis and Conyza canadensis from California. *Weed Res.* 57, 25–34. doi: 10.1111/wre.12230

National Academies of Sciences, Engineering, and Medicine (2016). *Gene Drives on the Horizon: Advancing Science, Navigating Uncertainty, and Aligning Research With Public Values*, Washington, DC: The National Academies Press.

Neve, P. (2018). Gene drive systems: do they have a place in agricultural weed management? *Pest Manag. Sci.* 74, 2671–2679. doi: 10.1002/ps.5137

Newhouse, K. E., Smith, W. A., Starrett, M. A., Schaefer, T. J., and Singh, B. K. (1992). Tolerance to imidazolinone herbicides in wheat. *Plant Physiol.* 100, 882–886. doi: 10.1104/pp.100.2.882

Ngo, T. D., Malone, J. M., Boutsalis, P., Gill, G., and Preston, C. (2018). EPSPS gene amplification conferring resistance to glyphosate in windmill grass (*Chloris truncata*) in Australia. *Pest Manag. Sci.* 74, 1101–1108. doi: 10.1002/ps.4573

Nonogaki, H. (2014). Seed dormancy and germination—emerging mechanisms and new hypotheses. *Front. Plant Sci.* 5:223. doi: 10.3389/fpls.2014.00233

OECD/FAO (2021). *Agricultural and Food Markets: Trends and Prospects. OECD-FAO Agricultural Outlook 2021–2030*. Paris: OECD Publishing.

Oerke, E. C. (2006). Crop losses to pests. *J. Agric. Sci.* 144, 31–43. doi: 10.1017/S0021859605005708

Padgette, S. R., Kolacz, K. H., Delannay, X., Re, D. B., Lavallee, B. J., Tinius, C. N., et al. (1995). Development, identification, and characterization of a glyphosate-tolerant soybean line. *Crop Sci.* 35, 1451–1461. doi: 10.2135/cropsci1995.0011183X003500050032x

Padgette, S., Re, D., Barry, G., Eichholtz, D., Delannay, X., Fuchs, R., et al. (1996). "New weed control opportunities: development of soybeans with a roundup ready gene," in *Herbicide Resistant Crops: Agricultural, Economic, Environmental, Regulatory, and Technological Aspects*. ed. D. Stephen (Boca Raton, FL: CRC Press).

Pasquer, F., Ochsner, U., Zarn, J., and Keller, B. (2006). Common and distinct gene expression patterns induced by the herbicides 2,4-dichlorophenoxyacetic acid, cinidon-ethyl and tribenuron-methyl in wheat. *Pest Manag. Sci.* 62, 1155–1167. doi: 10.1002/ps.1291

Patterson, E. L., Saski, C., Küpper, A., Beffa, R., and Gaines, T. A. (2019). Omics potential in herbicide-resistant weed management. *Plants* 8:607. doi: 10.3390/plants8120607

Peng, F., Zhang, W., Zeng, W., Zhu, J.-K., and Miki, D. (2020). Gene targeting in *Arabidopsis* via an all-in-one strategy that uses a translational enhancer to aid Cas9 expression. *Plant Biotechnol. J.* 18, 892–894. doi: 10.1111/pbi.13265

Perotti, V. E., Larran, A. S., Palmieri, V. E., Martinatto, A. K., and Permingeat, H. R. (2020). Herbicide resistant weeds: a call to integrate conventional agricultural practices, molecular biology knowledge and new technologies. *Plant Sci.* 290:110255. doi: 10.1016/j.plantsci.2019.110255

Peters, K. J., and Gerowitt, B. (2014). Important maize weeds profit in growth and reproduction from climate change conditions represented by higher temperatures and reduced humidity. *J. Appl. Bot. Food Qual.* 87, 234–242. doi: 10.5073/JABFQ.2014.087.033

Peterson, M. A., Mcmaster, S. A., Riechers, D. E., Skelton, J., and Stahlman, P. W. (2016). 2,4-D past, present, and future: a review. *Weed Technol.* 30, 303–345. doi: 10.1614/WT-D-15-00131.1

Pimentel, D., Zuniga, R., and Morrison, D. (2005). Update on the environmental and economic costs associated with alien-invasive species in the United States. *Ecol. Econ.* 52, 273–288. doi: 10.1016/j.ecolecon.2004.10.002

Pipatpongpinyo, W., Korkmaz, U., Wu, H., Kena, A., Ye, H., Feng, J., et al. (2020). Assembling seed dormancy genes into a system identified their effects on seedbank longevity in weedy rice. *Heredity* 124, 135–145. doi: 10.1038/s41437-019-0253-8

Puchta, H. (2004). The repair of double-strand breaks in plants: mechanisms and consequences for genome evolution. *J. Exp. Bot.* 56, 1–14. doi: 10.1093/jxb/eri025

Putterill, J., Robson, F., Lee, K., Simon, R., and Coupland, G. (1995). The CONSTANS gene of *Arabidopsis* promotes flowering and encodes a protein showing similarities to zinc finger transcription factors. *Cell* 80, 847–857. doi: 10.1016/0092-8674(95)90288-0

Ramesh, K., Matloob, A., Aslam, F., Florentine, S. K., and Chauhan, B. S. (2017). Weeds in a changing climate: vulnerabilities, consequences, and

implications for future weed management. *Front. Plant Sci.* 8:95. doi: 10.3389/fpls.2017.00095

Ravet, K., Patterson, E. L., Krähmer, H., Hamouzová, K., Fan, L., Jasieniuk, M., et al. (2018). The power and potential of genomics in weed biology and management. *Pest Manag. Sci.* 74, 2216–2225. doi: 10.1002/ps.5048

Riar, D. S., Burke, I. C., Yenish, J. P., Bell, J., and Gill, K. (2011). Inheritance and physiological basis for 2,4-D resistance in prickly lettuce (*Lactuca serriola* L.). *J. Agric. Food Chem.* 59, 9417–9423. doi: 10.1021/jf2019616

Rong, Y. S., and Golic, K. G. (2003). The homologous chromosome is an effective template for the repair of mitotic DNA double-strand breaks in *Drosophila*. *Genetics* 165, 1831–1842. doi: 10.1093/genetics/165.4.1831

Roux, F., and Reboud, X. (2007). Herbicide resistance dynamics in a spatially heterogeneous environment. *Crop Prot.* 26, 335–341. doi: 10.1016/j.cropro.2005.08.020

Schaller, G. E., Bishopp, A., and Kieber, J. J. (2015). The Yin-Yang of hormones cytokinin and auxin interactions in plant development. *Plant Cell* 27, 44–63. doi: 10.1105/tpc.114.133595

Schulz, M., Marocco, A., Tabaglio, V., Macias, F. A., and Molinillo, J. M. (2013). Benzoxazinoids in rye allelopathy-from discovery to application in sustainable weed control and organic farming. *J. Chem. Ecol.* 39, 154–174. doi: 10.1007/s10886-013-0235-x

Schwartz, L. M., Gibson, D. J., Gage, K. L., Matthews, J. L., Jordan, D. L., Owen, M. D., et al. (2015). Seedbank and field emergence of weeds in glyphosate-resistant cropping systems in the United States. *Weed Sci.* 63, 425–439. doi: 10.1614/WS-D-14-00089.1

Schwartz-Lazaro, L. M., and Copes, J. T. (2019). A review of the soil seedbank from a weed scientists perspective. *Agronomy* 9:369. doi: 10.3390/agronomy9070369

Seymour, G. B., Østergaard, L., Chapman, N. H., Knapp, S., and Martin, C. (2013). Fruit development and ripening. *Annu. Rev. Plant Biol.* 64, 219–241. doi: 10.1146/annurev-arplant-050312-120057

Shi, C., Zheng, Y., Geng, J., Liu, C., Pei, H., Ren, Y., et al. (2020). Identification of herbicide resistance loci using a genome-wide association study and linkage mapping in Chinese common wheat. *Crop J.* 8, 666–675. doi: 10.1016/j.cj.2020.02.004

Shino, M., Hamada, T., Shigematsu, Y., Hirase, K., Banba, S., Tsukamoto, Y., et al. (2021). "Chapter 30—discovery and mode of action of cyclopyrimorate: a new paddy rice herbicide," in *Recent Highlights in the Discovery and Optimization of Crop Protection Products*. eds. P. Maienfisch and S. Mangelinckx (London, United Kingdom: Academic Press).

Sosnoskie, L. M., Herms, C. P., Cardina, J., and Webster, T. M. (2009). Seedbank and emerged weed communities following adoption of glyphosate-resistant crops in a long-term tillage and rotation study. *Weed Sci.* 57, 261–270. doi: 10.1614/WS-08-147.1

Stewart, C. N., Tranel, P. J., Horvath, D. P., Anderson, J. V., Rieseberg, L. H., Westwood, J. H., et al. (2009). Evolution of weediness and invasiveness: charting the course for weed genomics. *Weed Sci.* 57, 451–462. doi: 10.1614/WS-09-011.1

Su, Y. H., Frommer, W. B., and Ludewig, U. (2004). Molecular and functional characterization of a family of amino acid transporters from *Arabidopsis*. *Plant Physiol.* 136, 3104–3113. doi: 10.1104/pp.104.045278

Székács, A. (2021). "3—Herbicide mode of action," in *Herbicides*. eds. R. Mesnage and J. G. Zaller (Amsterdam, Netherlands: Elsevier). doi: 10.1016/B978-0-12-823674-1.00008-0

Theodoulou, F. L. (2000). Plant ABC transporters. *Biochim. Biophys. Acta* 1465, 79–103. doi: 10.1016/s0005-2736(00)00132-2

Thyssen, G., Mccarty, J. C., Li, P., Jenkins, J. N., and Fang, D. D. (2014). Genetic mapping of non-target-site resistance to a sulfonylurea herbicide (Envoke®) in upland cotton (*Gossypium hirsutum* L.). *Mol. Breed.* 33, 341–348. doi: 10.1007/s11032-013-9953-6

Thyssen, G. N., Naoumkina, M., Mccarty, J. C., Jenkins, J. N., Florane, C., Li, P., et al. (2018). The P450 gene CYP749A16 is required for tolerance to the sulfonylurea herbicide trifloxysulfuron sodium in cotton (*Gossypium hirsutum* L.). *BMC Plant Biol.* 18:186. doi: 10.1186/s12870-018-1414-2

Torti, S., Schlesier, R., Thümmler, A., Bartels, D., Römer, P., Koch, B., et al. (2021). Transient reprogramming of crop plants for agronomic performance. *Nat. Plants* 7, 159–171. doi: 10.1038/s41477-021-00851-y

Tyagi, S., Kesiraju, K., Saakre, M., Rathinam, M., Raman, V., Pattanayak, D., et al. (2020). Genome editing for resistance to insect pests: an emerging tool for crop improvement. *ACS Omega* 5, 20674–20683. doi: 10.1021/acsomega.0c01435

Valderrama, J. A., Kulkarni, S. S., Nizet, V., and Bier, E. (2019). A bacterial gene-drive system efficiently edits and inactivates a high copy number antibiotic resistance locus. *Nat. Commun.* 10:5726. doi: 10.1038/s41467-019-13649-6

Van Etten, M., Lee, K. M., Chang, S. M., and Baucom, R. S. (2020). Parallel and nonparallel genomic responses contribute to herbicide resistance in Ipomoea purpurea, a common agricultural weed. *PLoS Genet.* 16:e1008593. doi: 10.1371/journal.pgen.1008593

Vanstraelen, M., and Benková, E. (2012). Hormonal interactions in the regulation of plant development. *Annu. Rev. Cell Dev. Biol.* 28, 463–487. doi: 10.1146/annurev-cellbio-101011-155741

Vigueira, C. C., Olsen, K. M., and Caicedo, A. L. (2013). The red queen in the corn: agricultural weeds as models of rapid adaptive evolution. *Heredity* 110, 303–311. doi: 10.1038/hdy.2012.104

Visser, B., Van Der Meer, I., Louwaars, N., Beekwilder, J., and Eaton, D. (2001). The impact of 'terminator' technology. *Biotechnol. Dev. Monit.* 48, 9–12.

Vivian, R., Silva, A. A., Gimenes, M., Fagan, E. B., Ruiz, S. T., and Labonia, Y. (2008). Weed seed dormancy as a survival mechanism—brief review. *Planta Daninha* 26, 695–706. doi: 10.1590/S0100-83582008000300026

Vivian-Smith, A., and Koltunow, A. M. (1999). Genetic analysis of growth-regulator-induced parthenocarpy in *Arabidopsis*. *Plant Physiol.* 121, 437–452. doi: 10.1104/pp.121.2.437

Vogt, T. (2010). Phenylpropanoid biosynthesis. *Mol. Plant* 3, 2–20. doi: 10.1093/mp/ssp106

Waldie, T., and Leyser, O. (2018). Cytokinin targets auxin transport to promote shoot branching. *Plant Physiol.* 177, 803–818. doi: 10.1104/pp.17.01691

Wang, Y., Cheng, X., Shan, Q., Zhang, Y., Liu, J., Gao, C., et al. (2014). Simultaneous editing of three homoeoalleles in hexaploid bread wheat confers heritable resistance to powdery mildew. *Nat. Biotechnol.* 32, 947–951. doi: 10.1038/nbt.2969

Westwood, J. H., Charudattan, R., Duke, S. O., Fennimore, S. A., Marrone, P., Slaughter, D. C., et al. (2018). Weed management in 2050: perspectives on the future of weed science. *Weed Sci.* 66, 275–285. doi: 10.1017/wsc.2017.78

Windbichler, N., Menichelli, M., Papathanos, P. A., Thyme, S. B., Li, H., Ulge, U. Y., et al. (2011). A synthetic homing endonuclease-based gene drive system in the human malaria mosquito. *Nature* 473, 212–215. doi: 10.1038/nature09937

Wolabu, T. W., Zhang, F., Niu, L., Kalve, S., Bhatnagar-Mathur, P., Muszynski, M. G., et al. (2016). Three FLOWERING LOCUS T-like genes function as potential florigens and mediate photoperiod response in sorghum. *New Phytol.* 210, 946–959. doi: 10.1111/nph.13834

Wong, A. C., Hecht, V. F., Picard, K., Diwadkar, P., Laurie, R. E., Wen, J., et al. (2014). Isolation and functional analysis of CONSTANS-LIKE genes suggests that a central role for CONSTANS in flowering time control is not evolutionarily conserved in *Medicago truncatula*. *Front. Plant Sci.* 5:486. doi: 10.3389/fpls.2014.00486

Xu, L., Liu, H., Kilian, A., Bhoite, R., Liu, G., Si, P., et al. (2020). QTL mapping using a high-density genetic map to identify candidate genes associated with metribuzin tolerance in hexaploid wheat (*Triticum aestivum* L.). *Front. Plant Sci.* 11:573439. doi: 10.3389/fpls.2020.573439

Xu, J., Wang, X.-Y., and Guo, W.-Z. (2015). The cytochrome P450 superfamily: key players in plant development and defense. *J. Integr. Agric.* 14, 1673–1686. doi: 10.1016/S2095-3119(14)60980-1

Yano, M., Katayose, Y., Ashikari, M., Yamanouchi, U., Monna, L., Fuse, T., et al. (2000). Hd1, a major photoperiod sensitivity quantitative trait locus in rice, is closely related to the *Arabidopsis* flowering time gene CONSTANS. *Plant Cell* 12, 2473–2484. doi: 10.1105/tpc.12.12.2473

Yin, K., and Qiu, J.-L. (2019). Genome editing for plant disease resistance: applications and perspectives. *Philos. Trans. R. Soc. B Biol. Sci.* 374:20180322. doi: 10.1098/rstb.2018.0322

Yoo, S. Y., Kardailsky, I., Lee, J. S., Weigel, D., and Ahn, J. H. (2004). Acceleration of flowering by overexpression of MFT (MOTHER OF FT AND TFL1). *Mol. Cell* 17, 95–101.

Yu, Q., Cairns, A., and Powles, S. B. (2004). Paraquat resistance in a population of Lolium rigidum. *Funct. Plant Biol.* 31, 247–254. doi: 10.1071/FP03234

Yu, Q., Huang, S., and Powles, S. (2010). Direct measurement of paraquat in leaf protoplasts indicates vacuolar paraquat sequestration as a resistance mechanism in *Lolium rigidum*. *Pestic. Biochem. Physiol.* 98, 104–109. doi: 10.1016/j.pestbp.2010.05.007

Yu, Q., Liu, S., Yu, L., Xiao, Y., Zhang, S., Wang, X., et al. (2021). RNA demethylation increases the yield and biomass of rice and potato plants in field trials. *Nat. Biotechnol.* 39, 1581–1588. doi: 10.1038/s41587-021-00982-9

Zeng, Y., Wen, J., Zhao, W., Wang, Q., and Huang, W. (2020). Rational improvement of rice yield and cold tolerance by editing the three genes OsPIN5b, GS3, and OsMYB30 with the CRISPR–Cas9 system. *Front. Plant Sci.* 10:1663. doi: 10.3389/fpls.2019.01663

Zhang, A., Liu, Y., Wang, F., Li, T., Chen, Z., Kong, D., et al. (2019). Enhanced rice salinity tolerance via CRISPR/Cas9-targeted mutagenesis of the OsRR22 gene. *Mol. Breed.* 39:47. doi: 10.1007/s11032-019-0954-y

Zhang, Y., Massel, K., Godwin, I. D., and Gao, C. (2018). Applications and potential of genome editing in crop improvement. *Genome Biol.* 19:210. doi: 10.1186/s13059-018-1586-y

Zhang, T., Mudgett, M., Rambabu, R., Abramson, B., Dai, X., Michael, T. P., et al. (2021). Selective inheritance of target genes from only one parent of sexually reproduced F1 progeny in *Arabidopsis*. *Nat. Commun.* 12:3854. doi: 10.1038/s41467-021-24195-5

Conflict of Interest: The authors declare that the research was conducted in the absence of any commercial or financial relationships that could be construed as a potential conflict of interest.

Publisher's Note: All claims expressed in this article are solely those of the authors and do not necessarily represent those of their affiliated organizations, or those of the publisher, the editors and the reviewers. Any product that may be evaluated in this article, or claim that may be made by its manufacturer, is not guaranteed or endorsed by the publisher.

Copyright © 2022 Wong, Massel, Lam, Hintzsche and Chauhan. This is an open-access article distributed under the terms of the Creative Commons Attribution License (CC BY). The use, distribution or reproduction in other forums is permitted, provided the original author(s) and the copyright owner(s) are credited and that the original publication in this journal is cited, in accordance with accepted academic practice. No use, distribution or reproduction is permitted which does not comply with these terms.

frontiers | Frontiers in Plant Science

REVIEW
published: 29 April 2022
doi: 10.3389/fpls.2022.837563

A Walk Through the Maze of Secondary Metabolism in Orchids: A Transcriptomic Approach

*Devina Ghai[1], Arshpreet Kaur[1], Parvinderdeep S. Kahlon[2], Sandip V. Pawar[3] and Jaspreet K. Sembi[1]**

[1]Department of Botany, Panjab University, Chandigarh, India, [2]Chair of Phytopathology, TUM School of Life Sciences, Technical University of Munich, Freising, Germany, [3]University Institute of Pharmaceutical Sciences, Panjab University, Chandigarh, India

Orchids have a huge reservoir of secondary metabolites making these plants of immense therapeutic importance. Their potential as curatives has been realized since times immemorial and are extensively studied for their medicinal properties. Secondary metabolism is under stringent genetic control in plants and several molecular factors are involved in regulating the production of the metabolites. However, due to the complex molecular networks, a complete understanding of the specific molecular cues is lacking. High-throughput omics technologies have the potential to fill up this lacuna. The present study deals with comparative analysis of high-throughput transcript data involving gene identification, functional annotation, and differential expression in more than 30 orchid transcriptome data sets, with a focus to elucidate the role of various factors in alkaloid and flavonoid biosynthesis. Comprehensive analysis of the mevalonate (MVA) pathway, methyl-D-erythritol 4-phosphate (MEP) pathway, and phenylpropanoid pathway provide specific insights to the potential gene targets for drug discovery. It is envisaged that a positive stimulation of these pathways through regulation of pivotal genes and alteration of specific gene expression, could facilitate the production of secondary metabolites and enable efficient tapping of the therapeutic potential of orchids. This further would lay the foundation for developing strategies for genetic and epigenetic improvement of these plants for development of therapeutic products.

Keywords: secondary metabolism, transcriptome, orchids, alkaloids, flavonoids

OPEN ACCESS

Edited by:
Manoj K. Sharma, Jawaharlal Nehru University, India

Reviewed by:
Pardeep Kumar Bhardwaj, Institute of Bio-Resources and Sustainable Development (IBSD), India
Paromik Bhattacharyya, Institute of Himalayan Bioresource Technology (CSIR), India

****Correspondence:***
Jaspreet K. Sembi
jaspreet.sembi@pu.ac.in

Specialty section:
This article was submitted to Plant Biotechnology, a section of the journal Frontiers in Plant Science

Received: *16 December 2021*
Accepted: *11 April 2022*
Published: *29 April 2022*

Citation:
Ghai D, Kaur A, Kahlon PS, Pawar SV and Sembi JK (2022) A Walk Through the Maze of Secondary Metabolism in Orchids: A Transcriptomic Approach. Front. Plant Sci. 13:837563. doi: 10.3389/fpls.2022.837563

INTRODUCTION

Orchids are members of one of the most advanced plant families, the Orchidaceae with their unique morphology (labellum, gynostemium), functional characteristics, and ecological adaptations (mycorrhizal association, and velamen) that are not found in model plants. Though popular as affluent ornamentals, orchids were first discovered for their therapeutic properties. The restorative properties of orchids have been well documented since times immemorial, Theophrastus in his book named "*Enquiry into Plants*" reported the use of orchids as therapeutics. These plants have also found reference in Indian and Chinese traditional pharmacopeia. In Indian Ayurvedic system of medicine, "*Ashtavarga*" is an important formulation, consisting of eight herbs, out of which four are orchids, that is, *Habenaria edgeworthii* (vriddhi), *Habenaria*

intermedia (riddhi), *Malaxis acuminata* (jeevaka), and *Malaxis muscifera* (rishibhak). Similarly, in Chinese medicine, *Anoectochilus roxburghii* has been promoted as "*King medicine*" to treat snake bites, lung and liver disease, and hypertension (He et al., 2006). "*Shi-Hu*," an orchid-based therapeutic formulation, prepared from *Dendrobium nobile* and allied species, is prized as a tonic because of its efficiency in treating lung, kidney, and stomach diseases, hyperglycemia, and diabetes (Bulpitt et al., 2007). "*Tian-Ma*" derived from tubers of *Gastrodia elata* is effectively used in the treatment of headaches, migraines, epilepsy, high blood pressure, rheumatism, fever, and nervous problems (Kong et al., 2003). In addition to their use as therapeutics, these plants have also been widely used as tonics and restoratives. The most important example is *Dactylorhiza hatagirea* which is used as an aphrodisiac (Lawler, 1984). Several orchids, such as Shwethuli (*Zeuxine strateumatica*) and Salabmisri (*Eulophia dabia*), *Vanda testacea*, and *Rhynchostylis retusa*, are used as aphrodisiacs, blood purifiers, general restorative tonics, and for treating rheumatism, piles, bronchitis, and inflammations (Chauhan, 1990; Vij et al., 2013; Hossain et al., 2020; **Figure 1**). These healing and restorative properties are due to the presence of a rich diversity of phytochemicals which are bioactive and are responsible for the pharmacognostic potential of these plants (Teoh, 2016).



FIGURE 1 | Some therapeutically important orchid species. **(A)**, *Eulophia dabia* (D.Don) Hochr.; **(B)**, *Zeuxine strateumatica* (L.) Schltr.; **(C)**, *Dactylorhiza hatagirea* (D.Don) Soó; **(D)**, *Malaxis muscifera* (Lindl.) Kuntze; **(E)**, *Habenaria intermedia* D.Don; **(F)**, *Habenaria pectinata* D.Don; **(G)**, *Vanda testacea* (Lindl.) Rchb.f.; **(H)**, *Platanthera edgeworthii* (Hook.f. ex Collett) R.K.Gupta; **(I)**, *Crepidium acuminatum* (D.Don) Szlach.

The integration of traditional knowledge with modern research can pave a way as promising leads for the discovery of novel drugs with greater therapeutic potential than synthetic medicine offering new horizons in the field of therapeutics and drug discovery. However, the studies in this direction are not commensurate with the immense potential of these plants. This is mainly due to lack of complete understanding of the spectrum of molecular networks of secondary metabolism. Even though there have been a number of studies on the phytochemical profiling and the biological activity, there is limited information about the regulating molecular cues and the alternate biosynthetic routes which are utilized in these plants as a survival strategy in harsh and dynamic climatic conditions. Various omics approaches can be instrumental to understand and elucidate these complex mazes and help in utilization of these plants as therapeutics to their fullest potential.

Recent times have revolutionized the process of deciphering the genetic identity of the germplasm by using minimal amount of tissues to generate humongous volume of data using transcriptomic approach. Genome editing with the help of transcriptomic sequencing provide extra choices for genetic improvement in orchids. For techniques like CRISPR/Cas9, the sequence of the genome of the host can ascertain the specific and accurate target sites to increase the efficiency of the genome editing process (Kui et al., 2017) and can be highly beneficial for overall improvement of the germplasm. Transcriptomic sequencing has also helped in increasing the pace for the development of Simple Sequence Repeats (SSR), which are the microsatellite markers with random tandem repeats of 2–6 nucleotides. These markers are widely used because of their reproducibility, co-dominant nature, extreme polymorphism, simplicity, abundance, and easy amplification. The development of SSR markers in these medicinally important orchids can help in germplasm breeding, marker-assisted selection, parentage analysis, and genetic diversity studies. The SSR markers identified can help in evaluating and understanding genetic relationships quantitatively and qualitatively (Li et al., 2014) and help in constructing genetic maps of these plants which will further help in taxonomy, genetics, and genomic studies.

The reference genome of many medicinal non-model plants is not available. Transcriptomic approach provides an alternative way for collecting high-throughput data for gene identification, expression analysis, and putative functional characterization using metabolic profiling data (Góngora-Castillo and Buell, 2013). Whole transcriptome shotgun sequencing (WTSS) makes it possible to probe the genes of various metabolite biosynthesis processes and the relationship between the genes and plant metabolites. Another approach, termed as the Phytochemical genomics approach, involves sequence data sets combined with metabolomic data sets to elucidate the complete profile of secondary metabolites. In Digital gene expression analysis, differential expression of genes which are involved in secondary metabolism is studied to decipher the genetic variability and help in the drug discovery. The development of single-cell transcriptomics will aid in identifying networks and pathways and further facilitate drug discovery and development. The

present study is an exhaustive review of the omics research on secondary metabolism in orchids, primarily focusing on the use of transcriptomic data for the analysis of genes and pathways associated with the synthesis of secondary metabolites and could be further be used for establishing the therapeutic potential of the orchids.

ESTABLISHMENT OF ORCHIDS AS THERAPEUTIC AGENTS

The therapeutic potential of orchids has been reported since times immemorial. In 1579, Langham (1579) reported the antipyretic and anti-diarrheal properties of orchids. A Caribbean folklore mentions the use of *Vanilla claviculata* for treating wounds and syphilis (Griffith, 1847) while the flowers of *Vanilla griffithii* (Burkill, 1935) and leaf paste of *Vanda roxburghii* were used in treating fever (Chawla et al., 1992). *Dendrobium huoshanense* stems are reported to be beneficial for the eye, stomach, and liver ailments (Hsieh et al., 2008; Luo et al., 2008) while those of *Dendrobium monoliforme* are reported to be antipyretic (Zhao et al., 2003). Oil-based extracts of stems and leaves of *Anoectochilus formosanus* are effective for the treatment of hypertension, impotency, liver spleen disorders, and chest and abdominal pains (Satish et al., 2003). Leaf decoction of *Dendrobium candidum* is used for treating diabetes (Wu et al., 2004). Traditional usage of orchids as restoratives and tonics have been widely and commonly reported. The tubers of *Dactylorhiza hatagirea* have been used for the preparation of "*Salep*" which possess healing qualities (Lawler, 1984). Similar preparations like "*dbang lag*" have been used to provide sustenance for Tibetan monks practicing in remote caves (Teoh, 2019). Such studies coupled with ethnobotanical knowledge formed basis of many systematic reviews on utilization of orchids as therapeutic agents (Lawler, 1984).

Due to the significant role of orchids in the traditional medicine system, it has become imperative that these traditional remedies should be utilized for the discovery of new therapeutics. A plethora of studies has been reported ever since, to investigate the role of orchids as promising source of bioactive agents. A number of reports on the antioxidant and anti-inflammatory potential of various orchids like *Phalaenopsis* hybrids (Minh et al., 2016) and *Dendrobium officinale* (Zhang et al., 2017) have come up. Cytotoxic and apoptotic effects have also been reported in *Dendrobium crepidatum* and *D. chrysanthum* (Prasad and Koch, 2016). Antimicrobial activity has also been documented in *Dendrobium monoliforme* (Paudel et al., 2018). Antihyperglycemic (*Dactylorhiza hatagirea*; Choukarya et al., 2019), anti-diabetic and hepatoprotective activity (*Calanthe fimbriata*; Peng et al., 2019) have been reported.

To provide a sound scientific scaffolding for development of potential therapeutic products, efforts have been also directed to isolate and profile the phytochemicals from plant extracts. Various classes of secondary metabolites have been isolated from different plant parts and evaluated for biological activity. Phenanthrenes, like denbinobin, from *Dendrobium nobile*, showed potential cytotoxic activity (Lee et al., 1995), prevented metastatic gastric cancer, and showed potent therapeutic activity against hepatic fibrosis (Yang et al., 2007; Song et al., 2012). Similarly, kinsenoside from *Anoectochilus roxburghii* showed antihyperglycemic activity (Zhang et al., 2007). Cymbidine A from *Cymbidium goeringii* is responsible for the hypotensive and diuretic activity (Watanabe et al., 2007). Flavones C-glycosides and anthocyanins from red *Phalaenopsis* hybrids exhibited antioxidant activity (Kuo et al., 2010). Polysaccharides from *Dendrobium officinale* (Liu et al., 2011) and *Gastrodia elata* (Bao et al., 2017) have exhibited immune-enhancing potential. Galactoxyloglucan (GXG), a purified polysaccharide from *Dendrobium huoshanense*, improved insulin sensitivity, thus preventing hyperglycemia (Wang et al., 2019). Role of flavonoids especially rutin, in imparting antioxidant potential have also been highlighted in *Dendrobium officinale* (Zhang et al., 2017). Flavonoids of *Dactylorhiza hatagirea* also exhibited antihyperglycemic activity (Choukarya et al., 2019). Sesquiterpenoids from *Dendrobium nobile* exhibited neuroprotective activity (Ma et al., 2019b), while bibenzyl compounds from *Dendrobium officinale* showed cytotoxic activity (Ren et al., 2020). A group of compounds (phenanthrenes, bibenzyls, glucosyloxybenzyl succinate derivatives, flavonoids, lignans, terpenoids, etc.) isolated from *Pleione,* showed anti-tumor, anti-neurodegenerative, and anti-inflammatory biological activities (Wu et al., 2019). Despite a large number of reports on the phytochemical profiling in orchids, the studies are not commensurate with the immense potential of orchids as therapeutic agents. Omics techniques offer a great opportunity to provide an alternate and efficient method to study and characterize specific phytochemicals. Transcriptomic approaches can generate insights to the secondary metabolite biosynthetic pathways and can aid in functional characterization of their key regulatory genes.

TRANSCRIPTOMIC DATASETS IN ORCHIDS

Undeterred by the peculiarity in their unique characteristics, orchids are depreciated with respect to understanding their molecular complexities. A complete understanding of the spectrum of the molecular networks by isolated analyses of gene families is not plausible due to the limited availability of orchid genomes. On the other hand, transcriptome-wide analyses can help resolve complex metabolic pathways which are at play in these plants. Transcriptome is a complete set of mRNA and non-coding RNA produced by a cell or organism at a particular point of time. It generates large-scale transcripts that could help in analyzing different gene families all at once and could also guide toward understanding cross-links in mechanisms involved. The analysis begins with the collection of the desired tissue and subsequent isolation of RNA from the collected sample. The isolated RNA is used for the synthesis of complementary DNA which is eventually utilized for the construction of libraries after sequencing. There are large numbers of sequencing techniques that are prevalent nowadays, such as Roche/454, Illumina, Applied Biosystems SOLiD, and

Helicos HeliScope (Magi et al., 2010). Even though these techniques produce abundant short reads at a much higher throughput than any Sanger sequencer but data presented after such analysis is a set of short reads composed of several hundred base pairs. The reads, thus, obtained are curated as raw reads. These read are first filtered and adjusted based on the quality control measures. Then the filtered reads are first either reconstructed using *de novo* assembly in absence of reference genome or assembled by alignment to the reference genome (Wolf, 2013). The assembly of the reads can be performed with tools like Trinity (Grabherr et al., 2011), Velvet (Zerbino and Birney, 2008), SPAdes (Bankevich et al., 2012), or SOAPdenovo-Trans (Xie et al., 2014). The assembled reads form contigs or singletons; both of these are part of unigenes. The functional annotation of the unigenes or transcripts is completed using various databases, such as NCBI,[1] KEGG,[2] and SwissProt.[3] Additionally, the number of reads for a transcript provides the level of its abundance, thus serving as the starting point for biological inference of spatiotemporal gene expression (Wolf, 2013; Ma et al., 2019a). Transcriptome helps in identification of transcripts involved in primary and secondary metabolism and their splice variants (Wang et al., 2009). Comparing the levels of differentially expressed genes at different developmental stages or environmental conditions, provide insights into the physiological status of the tissue at a specific time. These data sets also contain information of small RNAs, long non-coding RNAs, and molecular repeats etc., and provide a tentative framework for functional assertion for putative annotations. These data can serve as an important lead for modern pharmaceutical industry toward development of herbal-based medicines.

High-throughput transcriptomic approaches produce extensive data sets that can be applied to identify candidate key genes in specific physiological processes using co-expression networks analysis (Carrera et al., 2009; Windram et al., 2014). On the other hand, targeted sequencing using degenerate primers proves to be economical and enables exhaustive analysis of specific genes. Specific genes exhibiting significant sequence similarity with gens involved in similar biological processes can be amplified by degenerate primers in related organisms (Wei et al., 2003). Functional validation of putative genes using metabolic profiling of flavonoids using gene-insertion mutants and transgenic plants with overexpressing genes could be used to understand the role genes in secondary metabolism. Further, recombinant proteins and *in vitro* biochemical assays could be used to decipher catalytic activity of the proteins. This "reverse genetics" approach for gene identification is very promising where bioinformatic prediction of candidate genes preceded the experimental analysis.

There have been a limited number of transcriptome-wide studies in orchids to explore and elucidate different aspects of orchid development (**Table 1**), however, the efforts are not in line with the immense advantage of using transcriptomic techniques to decipher various molecular networks. The therapeutic potential of orchids is closely associated with the intricate maze of secondary metabolism pathways and their by-products is mainly responsible for their diverse therapeutic properties. These pathways are, in turn, under strict control of an array of molecular factors which regulate the synthesis of phytochemicals. A large number of gene families are specifically associated with various biosynthetic pathways. Transcriptomic data emerging from various studies conducted in orchids have been tabulated in **Table 1** and it is evident that Illumina sequencing was the most commonly used sequencing method and Trinity was the most common assembler software used. A maximum number of final reads were obtained in *Dendrobium officinale* (81,284,898; Yuan et al., 2020) and highest number of unigenes were identified in *Dendrobium huoshanense* (499,190, Zhou et al., 2020). A huge variation was noticed in the total number of unigenes as reported in different plant parts using different techniques. In *Dendrobium officinale*, the range in the number of unigenes was observed from 2,99,107 (Shen et al., 2017) to 23,131 (Adejobi et al., 2021) as reported from various tissues. Similarly, in *Dendrobium catenatum*, 23,139 unigenes were reported from stem tissue (Lei et al., 2018) and the number drastically increased to 478,361 in *Dendrobium huoshanense* when roots and leaves were also included for analysis (Yuan et al., 2018). This can be attributed to specific gene expression in tissues at various stages of growth and development and environmental conditions. In *Phalaenopsis amabilis*, a comparative number of unigenes were reported, 37,723 and 34,020, from petals and labellum, respectively (Yang et al., 2014), indicating that a similar genetic profile can be seen in tissues at comparable physiological stages. In *Anoectochilus roxburghii*, 186,865 unigenes were reported from root, stem, and leaves (Chen et al., 2020). Interestingly, different techniques and platforms used for sequencing analysis can also play a role in this variation. Root, stem, and leaf tissues of *Dendrobium huoshanense* reported 4,99,190 unigenes when the Illumina HiSeq2000 platform was used (Zhou et al., 2020) while 4,78,361 unigenes were identified when Illumina Hiseq 2500 platform was used (Yuan et al., 2018). Hence, it can be concluded that a lot of variation is observed in the transcriptomic data, and hence, the analysis needs to be supported with substantial functional studies.

FUNCTIONAL ANNOTATION OF SECONDARY METABOLISM SPECIFIC GENES

Transcriptomic data can provide a basic lead for functional studies if a unified, systematic, and statistically significant approach is adopted for its assembly and characterization. To scrutinize the functionality of the unigenes identified from the transcriptomic data set, their assessment was carried out against different databases like KEGG, Swissprot, and non-redundant database (Nr; **Table 2**). The highest similarity of the unigenes was found against the Nr database except in

[1]https://www.ncbi.nlm.nih.gov/
[2]https://www.genome.jp/kegg/
[3]https://www.expasy.org/resources/uniprotkb-swiss-prot

TABLE 1 | Enumeration of transcriptomic data in orchids.

Plant name	Sequencing platform	Assembly	Plant part	Raw reads	Final reads	Total unigenes	References
Anoectochilus roxburghii	Illumina HiSeq X Ten	Trinity	Roots, Stems, and Leaves	–	–	186,865	Chen et al., 2020
	Illumina HiSeq 2000	Trinity v.2.0.6 software	Non-mycorrhizal plant (NM)	NM 61,226,728 60,542,772 67,559,786	NM 61,071,914 60,425,910 67,410,292	–	Zhang et al., 2020a
			Mycorrhizal plant (M)	M 55,632,192 65,007,376 67,125,158	M 55,492,010 64,859,884 66,965,132		
Bletilla striata	Illumina Hiseq4000	Trinity	Leaves, tubers and roots	–	–	42,974 genes	Ma et al., 2021
Bletilla striata (*Thunb.*) *Reichb.f.* varieties	Illumina HiSeq 2000 platform	Trinity	Pseudobulbs	270,734,628	–	291,021	Chen et al., 2021
Calanthe tsoongiana	Illumina HiSeq X Ten	Trinity	Four transitional stages from seed to seedling	592,645,857	577,527,375	73,528	Jiang et al., 2021a
Cymbidium goeringii	Illumina HiSeq™ 2000 platform	Trinity	Floral bud, Half-flowering, Full flowering stage	161,763,530	159,616,374	85,868	Ramya et al., 2019
Cymbidium kanran	Illumina HiSeq™ 2,500	Trinity	Buds and flowers	–	–	181,335 transcripts and 74,713 unigenes	Zhou et al., 2021
Cymbidium longibracteatum	Illumina HiSeq 2000 platform	Trinity	Yellow leaves (YL)	YL 39,557,830	YL 5,685,015,511	116,422	Jiang et al., 2018
			Green leaves (GL)	GL 38,536,724	GL 5,503,245,825		
Cymbidium tortisepalum var. *longibracteatum* cultivars	Illumina HiSeq 2000 platform	Trinity	Green Rhizome (GR)	–	GR 39,557,830 27,672,832 33,858,264 29,254,152	134,527	Jiang et al., 2021b
			Yellow Rhizome (YR)		YR 38,536,724 33,875,625 30,554,768 26,698,355		
Dactylorhiza hatagirea	Illumina GA IIx platform	SOAP denovo-Trans	Leaves (L) Shoots (S) Tubers (T)	L 22,009,740 S 21,263,988 T 25,884,232	L 15,917,274 S 15,456,424 T 17,788,506	37,371	Dhiman et al., 2019
Dendrobium catenatum	Illumina HiSeqTM 4000	–	Stems	–	–	23,139	Lei et al., 2018
Dendrobium huoshanense	Illumina HiSeq 2000 platform	Trinity	Roots, Stems, and Leaves	476,746,678	444,999,698	499,190	Zhou et al., 2020
	Illumina HiSeq 2500 platform	Trinity	Roots, Stems, and Leaves	736,904,076	716,634,006	478,361	Yuan et al., 2018
Dendrobium Nestor (*Dendrobium parishii* × *D. anosmum*)	Illumina HiSeq™ 4000 platform	Trinity	Flower bud stage (F)	F 50,047,108	F 47,538,849	161,228	Cui et al., 2021
			Half bloom stage (H)	H 48,759,280	H 47,538,849		
			Full bloom stage (B)	B 51,171,054	B 48,879,555		
Dendrobium nobile	Illumina HiSeq 4000 platform	Trinity	Stems	43,01,49,656	41,48,90,782	207,283	Li et al., 2017

(Continued)

TABLE 1 | Continued

Plant name	Sequencing platform	Assembly	Plant part	Raw reads		Final reads		Total unigenes	References
Dendrobium officinale	HiSeqTM 2500 Illumina	–	Roots Control (CK)	CK	83, 206, 690	CK	81,284,898	23,131	Adejobi et al., 2021
			MeJa treated (MeJa)	MeJa	82,623,796	MeJa	81,047,188		
	Illumina	–	Leaves	–		–		–	Zhang et al., 2021b
	BGISEQ-500	Trinity	Protocorm like bodies and Leaves	–		–		157, 901	Wang et al., 2020
	Illumina HiSeq 4000 platform	–	Roots, Stems, and Leaves	771,499,974		747,574,430		24,927	Yuan et al., 2020
	Illumina HiSeq 4000	Trinity 2.4.0	Leaves	–		269,267,462		60,597	Chen et al., 2019
	Illumina HiSeq 2500 platform	Trinity	Roots (R)	R	54,469,054, 71,462,678	R	54,433,348, 71,35,890	299,107	Shen et al., 2017
			Stems (S)	S	50,076,260, 64,920,086	S	50,076,260, 64,826,004		
			Leaves (L)	L	73,647,052, 53,904,216	L	73,534,024, 53,862,708		
			Flowers (F)	F	38,776,952, 38,669,310	F	38,736,660, 38,602,508		
	454 GS FLX Titanium platform	–	Stems	553,084		518,223		36,407	Guo et al., 2013
	Illumina HiSeq 4,000	–	Flowers of two cultivars Wanhu No.5 and Wanhu No.6	–		–		25,484 genes	Li et al., 2021a
Dendrobium sinense	–	–	Leaves and Pseudobulbs	568,756,484		563,154,602		72,797	Zhang et al., 2021a
Gastrodia elata hybrid (*Gastrodia elata Bl.f.elata* × *Gastrodia elata Bl.f.pilifera*)	Illumina HiSeq™ 2000	Trinity	Tuber	20,611,556		20,237,474		34,323	Wang et al., 2020
Gastrodia elata	BGISEQ-500 platform	Trinity	tuber, stem and flowers	–		–		113,067	Shan et al., 2021
Ophrys exaltata, O. sphegodes and *O. garganica*	454 and Solexa, Sanger sequencing	–	–	–		–		121,917 transcript	Sedeek et al., 2013
Paphiopedilum armeniacum	Illumina HiSeq4000	Trinity v2.4.0	Capsules	–		–		183,737	Fang et al., 2020
Paphiopedilum hirsutissimum	Illumina HiSeq™ 2000	Trinity (version: v2.9.0)	Flowers	–		18,236,750–21,697,775		28,805–34,806	Li et al., 2021b
Phalaenopsis amabilis white cultivar (Baiyuzan)	Illumina HiSeq 2500 platform	Trinity	Petals of White (WP) cultivar	WP	50,282,202 47,998,340 53,788,240	WP	19,744,124 28,758,568 36,877,122	114,293	Meng et al., 2019
Purple cultivar (Baolonghuanghou)			Petals of Purple (PP) cultivar	PP	49,944,218 50,589,170 41,232,748	PP	49,091,862 49,558,168 40,475,996		
Phalaenopsis amabilis	Illumina HiSeq 2000 system	Trinity	Petals (P) Labellum (L)	–		P L	10, 734, 813 16, 224, 038	37, 723 34,020	Yang et al., 2014

(Continued)

TABLE 1 | Continued

Plant name	Sequencing platform	Assembly	Plant part	Raw reads	Final reads	Total unigenes	References
Red *Phalaenopsis* Dtps. Jiuhbao Red Rose Yellow *Phalaenopsis* Dtps.	Illumina HiSeq™ 2000	Trinity software (version trinityrnaseq_r2012-03-17)	Red Flower bud (RB) Yellow Flower bud (YB)	–	RB 8,889,080 YB 10,734,813	51,771	Gao et al., 2016
Fuller's Sunset *Phalaenopsis* hybrid: Konggangjinli	Illumina HiSeq2000	Trinity	Leaf	118,996,000	79,434,350	21, 348 genes 31,708 isogenes	Xu et al., 2015
Pleione limprichtii	Illumina HiSeqTM 4,000	Trinity	Flower petals and Lips	–	–	80,525	Zhang et al., 2020b
Vanda "Tan Chay Yan"	MiSeq Desktop Sequencer (Illumina)	CLC Genomic Workbench software Version 6.0	Tepals	4,955,918	4,826,959	–	Mohd-Hairul et al., 2020
Vanilla planifolia	454/Illumina	Velvet and Oases	Pods, Leaves, Stems and Roots	–	1,678,293	301,459 contigs	Rao et al., 2014

TABLE 2 | Functional Annotation using KEGG, SwissProt, and non-redundant (Nr) database.

Plant name	KEGG	SwissProt	Nr database	References
Anoectochilus roxburghii	66,542 unigenes	59,736 unigenes	87,781 unigenes	Chen et al., 2020
Calanthe tsoongiana	9,946 unigenes	25,124 unigenes	35,368 unigenes	Jiang et al., 2021a
Cymbidium goeringii	33,417 unigenes	36,911 unigenes	54,640 unigenes	Ramya et al., 2019
Cymbidium longibracteatum	10,723 unigenes	21,297 unigenes	33,487 unigenes	Jiang et al., 2018
Cymbidium tortisepalum var. *longibracteatum*	44,141	44,577	70,576	Jiang et al., 2021b
Dactylorhiza hatagirea	9,130 transcripts	–	21,695 transcripts	Dhiman et al., 2019
Dendrobium catenatum	4,203 unigenes	–	–	Lei et al., 2018
Dendrobium huoshanense	112,603 unigenes	225,268 unigenes	140,919 unigenes	Zhou et al., 2020
	108,417 unigenes	101,132 unigenes	196,739 unigenes	Yuan et al., 2018
Dendrobium nobile	18,911 unigenes	48,431 unigenes	56,378 unigenes	Li et al., 2017
Dendrobium officinale	71,648 unigenes	62,695 unigenes	99,474 unigenes	Wang et al., 2021
	12,877 genes	18,804 genes	29,229 genes	Chen et al., 2019
	65,286 unigenes	38,765 unigenes	70,146 unigenes	Shen et al., 2017
	20,274 unigenes	13,418 unigenes	22,752 unigenes	Guo et al., 2013
Gastrodia elata hybrid (*Gastrodia elata Bl.f.elata* × *Gastrodia elata Bl.f.pilifera*)	8,364 unigenes	19,028 unigenes	24,230 unigenes	Wang et al., 2020
Gastrodia elata	56,585	52,164	71,069	Shan et al., 2021
Ophrys exaltata, O. sphegodes and *O. garganica*	7,394 transcripts	–	–	Sedeek et al., 2013
Paphiopedilum armeniacum	12,141 unigenes	44,893 unigenes	89,289 unigenes	Fang et al., 2020
Phalaenopsis amabilis white cultivar (Baiyuzan) and purple cultivar (Baolonghuanghou)	16,777 unigenes	–	48,071 unigenes	Meng et al., 2019
Red *Phalaenopsis* Yellow *Phalaenopsis*	5,446 unigenes	19,446 unigenes	27,084 unigenes	Gao et al., 2016
Phalaenopsis hybrid: Konggangjinli	14,099 unigenes	–	–	Xu et al., 2015
Pleione limprichtii	11,067 unigenes	21,177 unigenes	33,459 unigenes	Zhang et al., 2020b
Vanilla planifolia	–	–	130,550 unigenes	Rao et al., 2014

the case of *Dendrobium huoshanense* where the SwissProt similarity of unigenes was the highest (Zhou et al., 2020). Out of 186,865 unigenes identified in *Anoectochilus roxburghii,* approximately 35, 32, and 47% were annotated using KEGG, SwissProt, and Nr database (Chen et al., 2020). However, only 9,946 out of 73,528 unigenes were annotated by KEGG in *Calanthe tsoongiana* (Jiang et al., 2021a). In *Dendrobium officinale*, the unigenes characterized using SwissProt varied from 13,418 (Guo et al., 2013) to 62,695 unigenes (Wang et al., 2021). The variation could be due to the use of different platforms used for sequencing or assembly and due to the type of tissue used in different studies.

The annotation of genes or transcripts obtained using various servers helped in the characterization of genes based on their functional roles. The KEGG analysis of different studies in association with pathways of secondary metabolism has been summarized in **Table 3**. KEGG analysis of stem, leaves, and roots revealed the presence of cyanoamino acid metabolism, phenylpropanoid biosynthesis, diterpenoid biosynthesis, flavonoid and flavonol biosynthesis, steroid biosynthesis, and isoflavonoid biosynthesis pathways in *Anoectochilus roxburghii* (Chen et al., 2020). 65,286 unigenes in *Dendrobium officinale* (Shen et al., 2017), 10,723 unigenes in *Cymbidium longibracteatum* (Jiang et al., 2018), and 9,130 unigenes in *Dactylorhiza hatagirea* (Dhiman et al., 2019) were annotated by KEGG analysis. Differential gene expression (DEG) of the different colored buds of *Phalaenopsis* sp. suggested that most DEGs were of phenylpropanoid biosynthesis which suggests the role of anthocyanins for variable colors (Gao et al., 2016). The number of unigenes annotated to phenylpropanoid varies from 49 unigenes in *Phalaenopsis* sp. (Gao et al., 2016) to 466 in *Cymbidium goeringii* (Ramya et al., 2019). In a transcriptomic study of *Pleione limprichtii*, 11,067 genes were mapped to 131 KEGG pathways and 1,294 unigenes were associated with secondary metabolite synthesis (Zhang et al., 2020b).

Even though large numbers of secondary metabolites are produced by plants, only a selected compounds have important medicinal properties. These secondary metabolites can be grouped into various classes like alkaloids, terpenoids, polyphenols, phenanthrene, bibenzyl derivatives, etc. Therapeutic effects of different alkaloids especially terpenoid alkaloids have been widely reported in orchids (Sut et al., 2017; Gantait et al., 2021; Ghai et al., 2021). These terpenes alkaloids are formed through the mevalonate (MVA) pathway and methyl-D-erythritol 4-phosphate (MEP) pathway (**Figure 2**). MVA pathway initiates with acetyl-CoA as a precursor. Acetyl-CoA undergoes a series of catalyzation reactions to produce isopentyl pyrophosphate (IPP) and dimethylallyl pyrophosphate (DMAPP). These IPP units are further processed to form sesquiterpenes. Meanwhile, the MEP pathway begins with the condensation of pyruvate and D-glyceraldehyde-3-phosphate by 1-Deoxy-D-xylulose-5-phosphate synthase (DXS). The regulatory mechanisms and biochemistry of the mevalonate (MVA) and methyl-D-erythritol 4-phosphate (MEP) pathway are well characterized. In MVA, 3-hydroxy-3-methylglutaryl coenzyme A reductase (HMGR) lays an important role in controlling the metabolic flux. The regulation of mevalonate kinase (MK) is regulated by feedback mechanism at both transcriptional and post-translational levels (Hinson et al., 1997). The isopentyl pyrophosphate (IPP) units are isomerized into dimethylallyl pyrophosphate (DMAPP) by IPP isomerase which is the initiating molecule in terpenoid biosynthesis. The enzyme, 1-deoxy-D-xylulose-5-phosphate synthase (DXS), is key player in controlling influx into the MEP pathway through decarboxylation reaction and is regulated by feedback mechanism through IPP and DMAPP (Banerjee et al., 2013). This can be corroborated by the higher expression of DXS and the terpenoid levels in the inflorescences in *Arabidopsis* (Carretero-Paulet et al., 2002). This process proceeds to form IPP and DMAPP *via* multistep reactions catalyzed by a series of enzymes. The MEP and MVA pathways are both linked by an intermediary precursor isopentenyl pyrophosphate. Subsequently, the pathways result in the formation of monoterpenoids, diterpenoids, carotenoids, sesquiterpenoids, and some other metabolites. Sesquiterpene alkaloids are the most abundant types of alkaloids of *Dendrobium* (Chen et al., 2019). Hsiao et al. (2011) reported the identification of 50 unigenes of the MEP and MVA pathways in *Phalaenopsis* while in *Cymbidium goeringii*, 32 unigenes of MVA and 38 unigenes of MEP pathway were identified (Ramya et al., 2019). Forty-six unigenes in *Dendrobium huoshanense* (Yuan et al., 2018) and 36 in *Dendrobium officinale* (Shen et al., 2017) related to the MEP and MVA pathway were identified. According to Li et al. (2017), isoprene units obtained through the MEP pathway were responsible for the biosynthesis of dendrobine in *Dendrobium nobile*. The expression of *acetyl-CoA acetyltransferase* (*AACT*), *mevalonate diphosphosphate decarboxylase* (*MVD*), *phosphomevalonate kinase* (*PMK*), and *Alpha-humulene synthase* (*TPS21*) changes upon inoculation of the orchid with MF23 (*Mycena* sp.) which results in induction of pathway leading to dendrobine biosynthesis (Li et al., 2017). Besides fungal stimulation, methyl jasmonate (MeJA) treatment of *D. officinale* also results in increased expression of genes associated with MEP and MVA pathway (Chen et al., 2019). Toh et al. (2017) also studied the fragrant sites in *Vanda* Mimi Palmer which indirectly points toward the sites of high monoterpenoid production. Higher expression of *3-hydroxy-3-methylglutaryl coenzyme A reductase* (*HMGR*) and *1-deoxyxylulose-5-phosphate synthetase* (*DXS*) was observed in root than in leaf but *DXS* and *1-deoxy-D-xylulose-5-phosphate reductoisomerase* (*DXR*) were abundant mainly in stems of *Dendrobium huoshanense* (Yuan et al., 2018). Yuan et al. (2018) suggested stem-specific accumulation of alkaloids in *D. huoshanense* but leaf-specific accumulation is observed in *D. officinale* (Shen et al., 2017). A series of enzymes associated with strictosidine were also identified in a study on *Dendrobium officinale* (Shen et al., 2017). Accumulation of dendrobine, a sesquiterpene alkaloid, was consistently more when the expression of *PMK* and *MVD* was high but got reduced as the expression of the aforementioned genes decreased in MF23 infected *Dendrobium nobile* orchid plant (Li et al., 2017). In the same study, the dendrobine pathway was negatively correlated with the expression of *TPS21* but no relation with genes of MEP was observed (Li et al., 2017). Secologanin synthase (SCS) which is essential for the synthesis of secologanin has also been reported to be involved in alkaloid biosynthesis (Guo et al., 2013). Different terpenes are synthesized from isopentenyl diphosphate through two pathways mevalonate pathway and methylerythritol phosphate pathway. Hsiao et al. (2006) analyzed transcriptomes of *Phalaenopsis bellina* and *Phalaenopsis equestris* where genes related to the DXP-geraniol linalool pathway were identified by data mining. In another study, regulation of monoterpene biosynthesis by PbbHLH4 in *Phalaenopsis* orchid was provided (Chuang et al., 2018). Terpene synthases (TPSs) are responsible for the structure diversity of terpene while cytochromes P450 (CYPs) further modifies the products from TPSs which provide further diversification of terpenes (Tsai et al., 2017). In

TABLE 3 | KEGG pathway analysis of secondary metabolism.

Plant name (*Reference*)	Unigenes/transcripts	Secondary metabolism		
		Pathway	Unigenes/transcripts	
Anoectochilus roxburghii (Chen et al., 2020)	66,542 unigenes	Biosynthesis of other secondary metabolites	Root Stem Leaf	3,369 unigenes 3,302 unigenes 3,280 unigenes
Calanthe tsoongiana (Jiang et al., 2021a)	9,946 unigenes in 25 pathways	Biosynthesis of other secondary metabolites	290 unigenes	
Cymbidium goeringii (Ramya et al., 2019)	33,417 unigenes	Anthocyanin biosynthesis Indole alkaloid biosynthesis Isoflavonoid biosynthesis Tropane, piperidine and pyridine alkaloid biosynthesis Isoquinoline alkaloid biosynthesis Monoterpenoid biosynthesis Sesquiterpenoid and triterpenoid biosynthesis Flavone and flavonol biosynthesis Diterpenoid biosynthesis Terpenoid backbone biosynthesis Flavonoid biosynthesis Phenylpropanoid biosynthesis Biosynthesis of secondary metabolites	9 unigenes 21 unigenes 36 unigenes 50 unigenes 51 unigenes 56 unigenes 75 unigenes 134 unigenes 172 unigenes 197 unigenes 236 unigenes 466 unigenes 3,197 unigenes	
Dendrobium catenatum (Lei et al., 2018)	4,203 unigenes	Flavonoid biosynthesis	31 unigenes	
Dendrobium huoshanense (Zhou et al., 2020)	112,603 unigenes annotated in 131 pathways	Biosynthesis of other secondary metabolites	2,237 unigenes	
(Yuan et al., 2018)	108,417 unigenes annotated to 33 pathways	Biosynthesis of other secondary metabolites	1,298 unigenes	
Dendrobium nobile (Li et al., 2017)	18,911 unigenes assigned to 131 pathways	Biosynthesis of other secondary metabolites	507 genes	
Dendrobium officinale (Chen et al., 2019)	12,877 genes grouped into 19 secondary level pathways	Biosynthesis of other secondary metabolites	716 genes	
Dendrobium officinale (Guo et al., 2013)	20,274 unigenes	Biosynthesis of other secondary metabolites	5 unigenes	
Gastrodia elata hybrid (*Gastrodia elata Bl.f.elata* × *Gastrodia elata Bl.f.pilifera*) (Wang et al., 2020)	8,364 unigenes	Phenylpropanoid biosynthesis Flavonoid biosynthesis Flavone and flavonol biosynthesis Tropane, piperidine and pyridine alkaloid biosynthesis Isoquinoline alkaloid biosynthesis Anthocyanin biosynthesis	92 unigenes 39 unigenes 18 unigenes 13 unigenes 8 unigenes 1 unigene	
Ophrys exaltata *O. sphegodes* *O. garganica* (Sedeek et al., 2013)	7,394 transcripts	Biosynthesis of other secondary metabolites	252 transcripts	
Phalaenopsis amabilis white cultivar (Baiyuzan) *Phalaenopsis amabilis* purple cultivar (Baolonghuanghou) (Meng et al., 2019)	16,777 unigenes assigned to 129 pathways	Phenylpropanoid synthesis Flavonoid synthesis Flavone and flavonol synthesis Anthocyanin synthesis Biosynthesis of other secondary metabolites	168 genes 39 genes 19 genes 7 genes 328 genes	
Red *Phalaenopsis* Dtps. Jiuhbao Red Rose Yellow *Phalaenopsis* Dtps. Fuller's Sunset (Gao et al., 2016)	5,446 unigenes	Phenylpropanoid biosynthesis Flavonoid biosynthesis Indole alkaloid biosynthesis Flavone and Flavonol biosynthesis Isoquinoline alkaloid biosynthesis	49 genes 21 genes 1 gene 13 genes 11 genes	

(Continued)

TABLE 3 | Continued

Plant name (*Reference*)	Unigenes/transcripts	Secondary metabolism	
		Pathway	**Unigenes/transcripts**
Phalaenopsis hybrid: Konggangjinli (Xu et al., 2015)	14,099 unigenes assigned to 123 pathways	Biosynthesis of secondary metabolites	791 unigenes
		Terpenoid backbone biosynthesis	55 unigenes
		Indole alkaloid biosynthesis	1 unigene
		Monoterpenoid biosynthesis	1 unigene
		Diterpenoid biosynthesis	20 unigenes
		Sesquiterpenoid and triterpenoid biosynthesis	4 unigenes
		Phenylpropanoid biosynthesis	75 unigenes
		Flavonoid biosynthesis	34 unigenes
		Flavone and flavonol biosynthesis	15 unigenes
		Isoquinoline alkaloid biosynthesis	9 unigenes
		Tropane, piperidine and pyridine alkaloid biosynthesis	20 unigenes
Pleione limprichtii (Zhang et al, 2020b)	11,067 unigenes mapped onto 131 pathways	Biosynthesis of secondary metabolites	1,294 unigenes
		Phenylpropanoid biosynthesis	167 unigenes
		Terpenoid backbone biosynthesis	53 unigenes
		Flavonoid biosynthesis	36 unigenes
		Diterpenoid biosynthesis	35 unigenes
		Isoquinoline alkaloid biosynthesis	28 unigenes
		Tropane, piperidine and pyridine alkaloid biosynthesis	24 unigenes
		Flavone and flavonol biosynthesis	7 unigenes
		Sesquiterpenoid and triterpenoid biosynthesis	5 unigenes
		Anthocyanin biosynthesis	1 unigene

D. huoshanense, 229 unigenes of the P450 superfamily were identified (Yuan et al., 2018) but in *D. officinale*, 236 unigenes associated with P450 were mined (Shen et al., 2017). Strictosidine synthase had higher expression levels in protocorm like bodies (PLBs) than in leaves suggesting the higher content of total alkaloid is related to the higher amount of precursor strictosidine produced in *D. officinale* (Wang et al., 2021). The positive stimulation of either MEP or MVA pathway could eventually lead to an increase in the production of alkaloids which could eventually increase the therapeutic potential of the orchid plant.

Besides alkaloids, the role of flavonoids as antioxidant, anti-cancer, and anti-aging agents has also been highlighted (Middleton et al., 2000). The flavonoids are compounds with bridged phenyl rings which are synthesized through the phenylpropanoid pathway. Flavonoid also provides resistance against disease and insects in plants and enable the plant for adapting to adverse environmental conditions with the help of increased production in secondary metabolites (Campos and Hamdan, 2000; Yuan et al., 2020). *Anoectochilus roxburghii* is rich in flavonoid compounds, such as dihydroquercetin, quercetin, kaempferol, and myricetin (Ye et al., 2017), which are responsible for the drug activity of this orchid plant (Chen et al., 2020). Lei et al. (2018) reported about C-glycosides type flavonoids are more abundant than O-glycosides in *Dendrobium*. The metabolic analysis of *Anoectochilus roxburghii* revealed an abundance of flavonoids in leaves than in roots or stems (Chen et al., 2020). The by-products of the shikimate pathway are the precursor for a large assortment of secondary metabolites (Tzin et al., 2012; Takayuki et al., 2013). It is a multistep process that starts with the condensation of phosphoenolpyruvate (PEP) and erythrose 4-phosphate (E4P; **Figure 3**). The intermediate chorismite after further processing leads to the independent formation of aromatic amino acids, tryptophan, tyrosine, phenylalanine. Phenylalanine is the precursor for the Phenylpropanoid pathway which ultimately results in the synthesis of flavonoids. PAL is the most important rate limiting fulcrum enzyme that links primary metabolism with secondary metabolism (Vogt, 2010; Fraser and Chapple, 2011). A positive correlation between the PAL enzyme activity and accumulation of phenylpropanoid compounds has been widely reported (Bate et al., 1994; Vogt, 2010). Carbon flux into different branches of flavonoid synthesis is regulated by flavonol synthase (FLS; Davies et al., 2003). In *Arabidopsis*, activity of hydroxycinnamoyl-CoA shikimate/quinate hydroxycinnamoyl transferase (HCT) led to maneuvering of the metabolic flux into flavonoids through Chalcone synthase (CHS) activity (Besseau et al., 2007). Additionally, there are several transcription factors that regulate the gene expression which ultimately controls the metabolic flux. The expression of regulatory molecules like MYB is inversely proportional to lignin production, thus facilitating the metabolic flux toward flavonoid production (Fornale et al., 2010). Similarly, elicitors like salicylic acid and methyl jasmonate positively diverts the metabolic flux toward increased production of secondary metabolites (Creelman and Mullet, 1997; Kessler and Baldwin, 2002). Phenylalanine is catalyzed by phenylalanine ammonia lyase (PAL) to form cinnamate which is converted to *p*-coumaroyl-CoA by trans-cinnamate 4-monooxygenase (C4H) and 4-coumaroyl-CoA

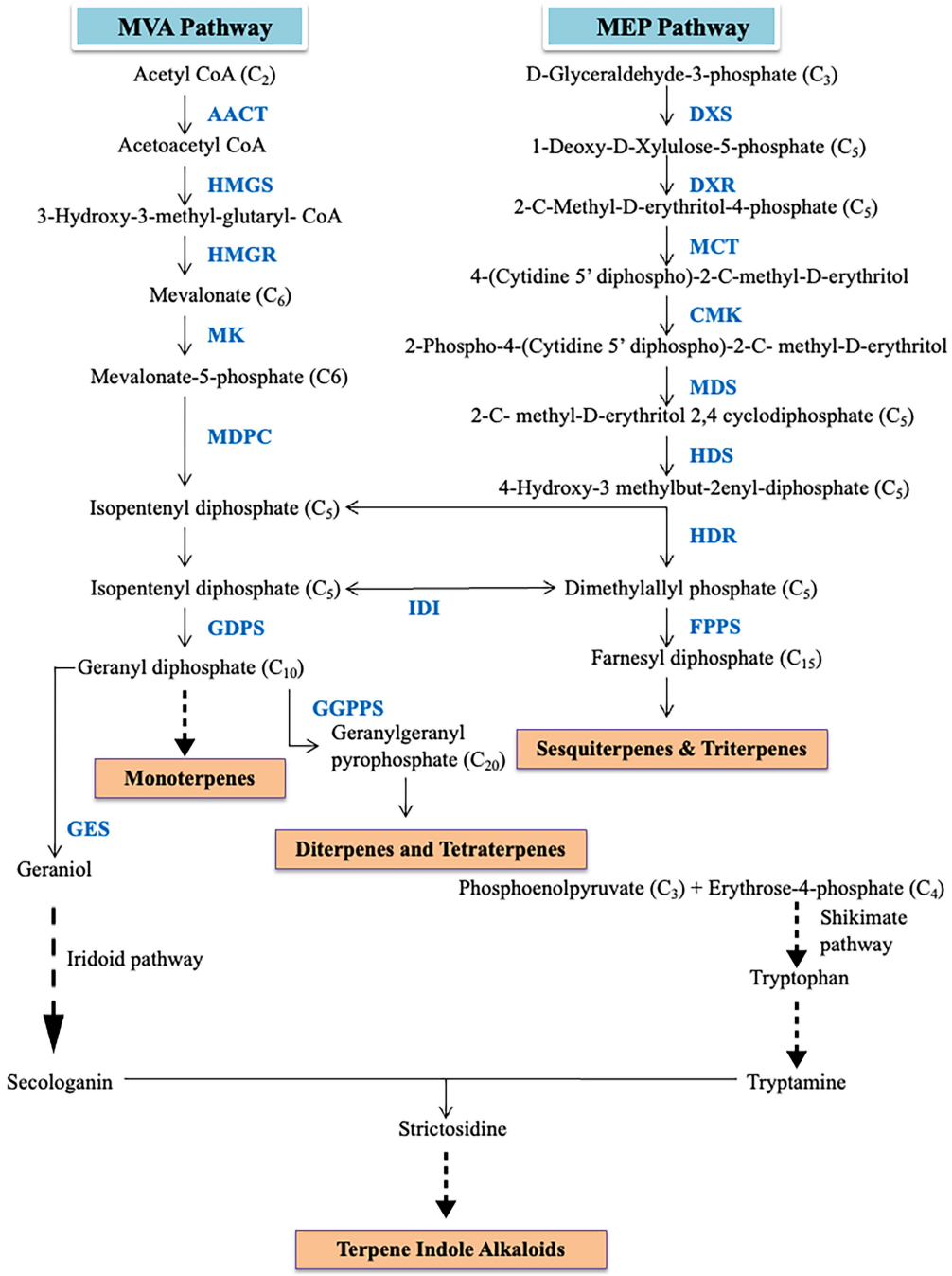


FIGURE 2 | Diagrammatic representation of methyl-D-erythritol 4-phosphate (MEP) and mevalonate (MVA) pathway.

synthase (4CL). *p*-coumaroyl-CoA is further processed by series of different enzymes to form flavonoids, flavonols, flavanones, and anthocyanins.

A total of 15 unigenes encoding seven enzymes of the flavonoid pathway were identified from *D. huoshanense* (Zhou et al., 2020) while 31 and 19 unigenes in *D. catenatum* (Lei et al., 2018) and *Pleione limprichtii* (Zhang et al., 2020b). In a study on *Anoectochilus roxburghii*, inoculation with *Ceratobasidium* sp. AR2 increases the flavonoid content of the plant by upregulating *PAL*, *chalcone synthase* (*CHS*), *4CL* and downregulating of *cinnamate 4-hydroxylase* (*C4H*), and *chalcone isomerase* (*CHI*) genes (Zhang et al., 2020a). In a new cultivar of *Cymbidium longibracteatum* with yellow leaves and tubers, seven unigenes related to flavonoid biosynthesis were upregulated (Jiang et al., 2018). Similarly, expression levels of *CHS*, *CHI*, *dihydroflavonol 4-reductase* (*DFR*), *anthocyanidin synthase*

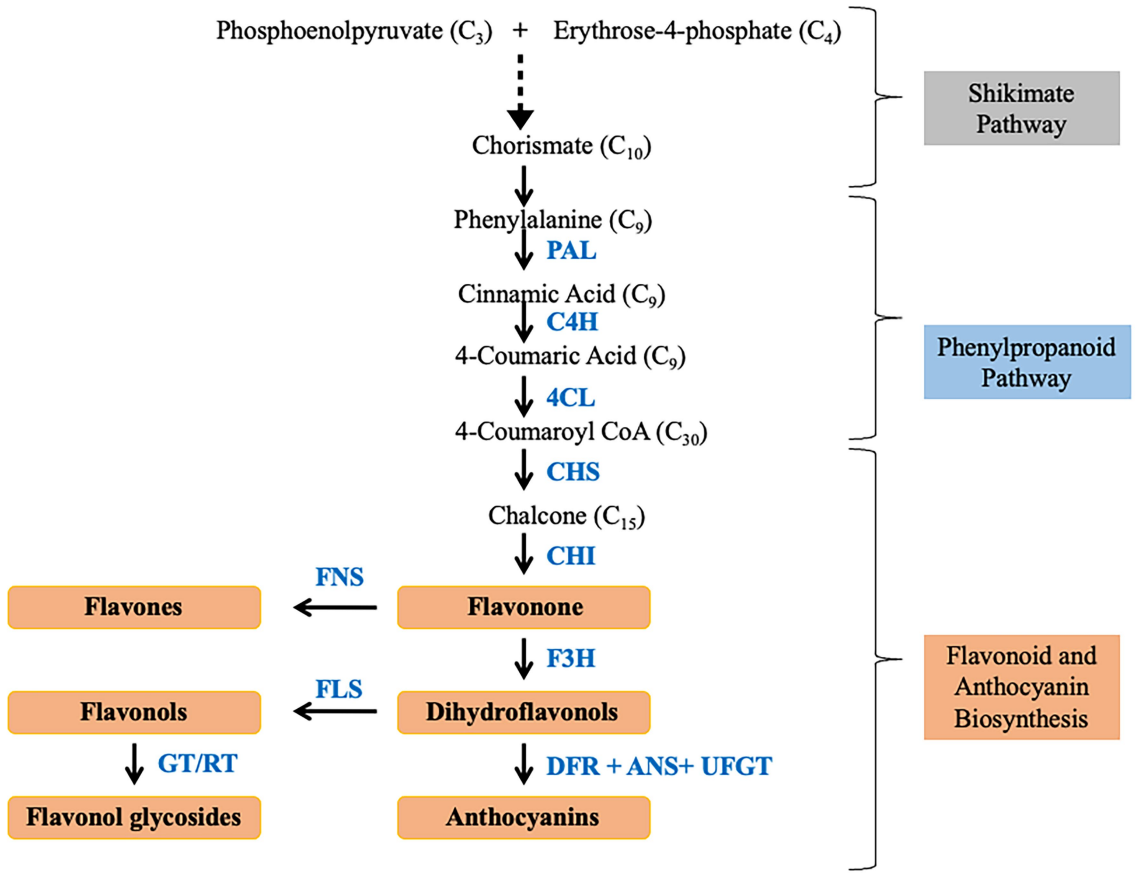


FIGURE 3 | Schematic flowchart depicting flavonoid and anthocyanin biosynthesis.

(*ANS1*), and *UDP-glucose: flavonoid-3-O-glucosyltransferase* (*UFGT*) were comparatively higher in red, corroborating with higher anthocyanin content in the red stems of *D. candidum* (Jia et al., 2021). Similarly, most of the genes involved in anthocyanin biosynthesis were upregulated during floral development of *Dendrobium* nestor (Cui et al., 2021). Expression of *PAL* and *HMG-CoA* reductase was upregulated in the abaxial surface of the tissue of *Vanda* Mimi Palmer (Toh et al., 2017). The rate of flavonoid production in plants was reported to be controlled by *CHS* with associated *CHI*. The higher expression levels of *CHS*, *CHI*, *flavonol synthase* (*FLS*), *DFR*, and *Anthocyanidin reductase* (*ANR*) in roots than in stems and leaves of *A. roxburghii* were reported as well (Chen et al., 2020). Upregulation of *LAR1*, *DFR3*, *flavanone 3-hydroxylase* (*F3H*), *CHS1*, *CHS2*, and *CHS3* in leaves facilitates the copious accumulation of flavonoids in leaves of *Dedrobium officinale* (Yuan et al., 2020). In the same study, *Dihydroflavonol reductase* (*DFR*), which is responsible for the conversion of flavonoids into anthocyanin biosynthesis, has higher expression in stems and leaves. MeJA treatment in *D. officinale* lead to the accumulation of bibenzyl (erianin and gigantol) increased due to upregulation of *PAL*, *4CL*, *C4H*, and *CYP450* (Adejobi et al., 2021). During explant browning in *Phalaenopsis* sp., higher expression of *PhPAL*, *PhCHS*, and *Ph4CL* was observed which suggest the role of anthocyanin in the early stages of tissue browning (Xu et al., 2015). Similarly, upregulated expression of *Pa4CL*, *PaANS*, *PaF3H*, and *PaDFR* was detected in purple petal cultivar of *Phalaenopsis amabilis* (Meng et al., 2019). The study on *Phalaenopsis* did not identify any DEGs related to *CHS*, *ANS*, *DFR*, and *flavonoid-3′-hydroxylase* (*F3′H*) in white petals which could be due to either technical limitations or due to absence of anthocyanin pathway (Yang et al., 2014). Similarly, no transcript of flavonoid-3′,5′-hydroxylase (*F3′5′H*) was identified from the transcriptome of *Ophrys* even though 61 transcripts of anthocyanins pathway were mined (Sedeek et al., 2013). Expression of *PlCHS*, *PlCHI*, and *PlFLS* was upregulated in white petals but colored petals had higher expression of *PlF3'H*, *PlDFR*, and *PlANS* in *Pleione limprichtii* (Zhang et al., 2020b). *PAL*, *4CL*, and *C4H* were upregulated in 8 and 10 weeks old seeds of *Vanilla planifolia* (Rao et al., 2014). Expression of *trans-resveratrol-di-O-methyltransferase-like* (*ROMT*) encoding gene, responsible for resveratrol biosynthesis, was high in tubers of *Dactylorhiza hatagirea* (Dhiman et al., 2019). It positively correlates with the fact that tubers of this plant are used as anti-inflammatory, anticarcinogenic, and as a cardioprotective agent. Higher expression of *ROMT* correlated with the abundant quantity of resveratrol and stilbenes (Dhiman et al., 2019). The role of caffeic acid, coumaric acid, and Caffeoyl

CoA in the synthesis of resveratrol and stilbenes has also been pointed out in the same study. Genes associated with flavonoid pathways were reported to be regulated by UDP-glycosyltransferase and cytochrome P450 (Liu et al., 2013). DcTT8, a bHLH transcription factor in *D. candidum*, regulated the anthocyanin production by binding to the promoter region of *DcF3′H* and *DcUFGT* (Jia et al., 2021). The above review asserts that transcriptomic approaches can serve as a boon for gene discovery, functional annotation, and expression profiling in non-model organisms.

CONCLUSION

Orchids grow in a variety of habits and habitats mainly owing to the presence of an array of unique secondary metabolites which help these plants sustain the stressful conditions. Therefore, these plants have emerged as important source for bioprospecting following traditional approaches. Omics technology, on the other hand, offer great potential for analysis of the complete metabolic pathways and provides detailed insights to gene function for drug discovery and other therapeutic interventions. The present study is a comprehensive analysis of transcriptomes more than 30 orchids mainly focusing on the alkaloids and flavonoids pathways. It can form the basis of an effective resource for the functional studies on tapping the immense potential of unique orchid secondary metabolites to facilitate development of novel therapeutic products from these plants.

AUTHOR CONTRIBUTIONS

JS conceptualized the work. DG and AK performed the analysis and prepared the original draft. PK, SP, and JS critically reviewed and edited the draft. All the authors have read and approved the final version.

ACKNOWLEDGMENTS

DG is grateful to Council of Scientific and Industrial Research for Senior Research Fellowship (File No. 09/135(0809)/2018-EMR-I). AK is thankful to Department of Science and Technology (DST) for INSPIRE Fellowship for Research Students (File No. DST/INSPIRE/03/2021/002638). JS is thankful for partial financial support received from Department of Science and Technology, Government of India under Promotion of University Research and Scientific Excellence (PURSE) grant scheme. Authors are thankful to Jagdeep Verma for the photographs of orchid plants.

REFERENCES

Adejobi, O. I. I., Guan, J., Yang, L., Hu, J. M., Yu, A., Muraguri, S., et al. (2021). Transcriptomic analyses shed light on critical genes associated with bibenzyl biosynthesis in *Dendrobium officinale*. *Plan. Theory* 10:633. doi: 10.3390/plants10040633

Banerjee, A., Wu, Y., Banerjee, R., Li, Y., Yan, H., and Sharkey, T. D. (2013). Feedback inhibition of deoxy-d-xylulose-5-phosphate synthase regulates the methylerythritol 4-phosphate pathway. *J. Biol. Chem.* 288, 16926–16936. doi: 10.1074/jbc.M113.464636

Bankevich, A., Nurk, S., Antipov, D., Gurevich, A. A., Dvorkin, M., Kulikov, A. S., et al. (2012). SPAdes: a new genome assembly algorithm and its applications to single-cell sequencing. *J. Comput. Biol.* 19, 455–477. doi: 10.1089/cmb.2012.0021

Bao, Q., Qian, L., Gong, C., and Shen, X. (2017). Immune-enhancing activity of polysaccharides from *Gastrodia elata*. *J. Food Process. Preserv.* 41:e13016. doi: 10.1111/jfpp.13016

Bate, N. J., Orr, J., Ni, W., Meromi, A., Nadler-Hassar, T., Doerner, P. W., et al. (1994). Quantitative relationship between phenylalanine ammonia-lyase levels and phenylpropanoid accumulation in transgenic tobacco identifies a rate-determining step in natural product synthesis. *Proc. Natl. Acad. Sci. U. S. A.* 91, 7608–7612. doi: 10.1073/pnas.91.16.7608

Besseau, S., Hoffmann, L., Geoffroy, P., Lapierre, C., Pollet, B., and Legrand, M. (2007). Flavonoid accumulation in *Arabidopsis* repressed in lignin synthesis affects auxin transport and plant growth. *Plant Cell* 19, 148–162. doi: 10.1105/tpc.106.044495

Bulpitt, C. J., Li, Y., Bulpitt, P. F., and Wang, J. J. (2007). The use of orchids in Chinese medicine. *J. R. Soc. Med.* 100, 558–563. doi: 10.1177/014107680710012014

Burkill, I. H. (1935). *A Dictionary of the Economic Products of the Malay Peninsula, Vol. II*. London: Crown Agents.

Campos, E. G., and Hamdan, F. F. (2000). Cloning of the chaperonin t-complex polypeptide 1 gene from *Schistosoma mansoni* and studies of its expression levels under heat shock and oxidative stress. *Parasitol. Res.* 86, 253–258. doi: 10.1007/s004360050039

Carrera, J., Rodrigo, G., Jaramillo, A., and Elena, S. F. (2009). Reverse-engineering the *Arabidopsis thaliana* transcriptional network under changing environmental conditions. *Genome Biol.* 10, R96–R15. doi: 10.1186/gb-2009-10-9-r96

Carretero-Paulet, L., Ahumada, I., Cunillera, N., Rodriguez-Concepcion, M., Ferrer, A., Boronat, A., et al. (2002). Expression and molecular analysis of the *Arabidopsis DXR* gene encoding 1-deoxy-D-xylulose 5-phosphate reductoisomerase, the first committed enzyme of the 2-C-methyl-D-erythritol 4-phosphate pathway. *Plant Physiol.* 129, 1581–1591. doi: 10.1104/pp.003798

Chauhan, N. S. (1990). Medicinal orchids of Himachal Pradesh. *J Orchid Soc. India.* 4, 99–105.

Chawla, A. S., Sharma, A. K., Handa, S. S., and Dhar, K. L. (1992). Chemical studies and anti-inflammatory activity of *Vanda roxburghii* roots. *Indian J. Pharm. Sci.* 54, 159–161.

Chen, Y., Pan, W., Jin, S., and Lin, S. (2020). Combined metabolomic and transcriptomic analysis reveals key candidate genes involved in the regulation of flavonoid accumulation in *Anoectochilus roxburghii*. *Process Biochem.* 91, 339–351. doi: 10.1016/j.procbio.2020.01.004

Chen, Y., Wang, Y., Lyu, P., Chen, L., Shen, C., and Sun, C. (2019). Comparative transcriptomic analysis reveal the regulation mechanism underlying MeJA-induced accumulation of alkaloids in *Dendrobium officinale*. *J. Plant Res.* 132, 419–429. doi: 10.1007/s10265-019-01099-6

Chen, J., Zhu, F., Liu, L., Yi, L., Dai, Y., Chen, S., et al. (2021). Integrative analyses of transcriptome and metabolome shed light on the regulation of secondary metabolites in pseudobulbs of two *Bletilla striata* (Thunb.) Reichb. f. varieties. *J. Appl. Res. Med. Aromat. Plants* 293:110738. doi: 10.1016/j.scienta.2021.110738

Choukarya, R., Choursia, A., and Rathi, J. (2019). In vivo and in vitro antidiabetic activity of hydroalcoholic extract of *Dactylorhiza hatagirea* roots: an evaluation of possible phytoconstituents. *J. Drug Deliv. Ther.* 9, 76–81. doi: 10.22270/jddt.v9i6-s.3752

Chuang, Y., Hung, Y., Tsai, W., Chen, W., and Chen, H. (2018). PbbHLH4 regulates floral monoterpene biosynthesis in *Phalaenopsis* orchids. *J. Exp. Bot.* 69, 4363–4377. doi: 10.1093/jxb/ery246

Creelman, R. A., and Mullet, J. E. (1997). Biosynthesis and action of jasmonates in plants. *Annu. Rev. Plant Biol.* 48, 355–381. doi: 10.1146/annurev.arplant.48.1.355

Cui, X., Deng, J., Huang, C., Tang, X., Li, X., Li, X., et al. (2021). Transcriptomic analysis of the anthocyanin biosynthetic pathway reveals the molecular mechanism associated with purple color formation in *Dendrobium* Nestor. *Life* 11:113. doi: 10.3390/life11020113

Davies, K. M., Schwinn, K. E., Deroles, S. C., Manson, D. G., Lewis, D. H., Bloor, S. J., et al. (2003). Enhancing anthocyanin production by altering competition for substrate between flavonol synthase and dihydroflavonol 4-reductase. *Euphytica* 131, 259–268. doi: 10.1023/A:1024018729349

Dhiman, N., Sharma, N. K., Thapa, P., Sharma, I., Swarnkar, M. K., Chawla, A., et al. (2019). De novo transcriptome provides insights into the growth behaviour and resveratrol and trans-stilbenes biosynthesis in *Dactylorhiza hatagirea*:– an endangered alpine terrestrial orchid of western Himalaya. *Sci. Rep.* 9, 13133–13113. doi: 10.1038/s41598-019-49446-w

Fang, L., Xu, X., Li, J., Zheng, F., Li, M., Yan, J., et al. (2020). Transcriptome analysis provides insights into the non-methylated lignin synthesis in *Paphiopedilum armeniacum* seed. *BMC Genomics* 21:524. doi: 10.1186/s12864-020-06931-1

Fornale, S., Shi, X., Chai, C., Encina, A., Irar, S., Capellades, M., et al. (2010). ZmMYB31 directly represses maize lignin genes and redirects the phenylpropanoid metabolic flux. *Plant J.* 64, 633–644. doi: 10.1111/j.1365-313X.2010.04363.x

Fraser, C. M., and Chapple, C. (2011). The phenylpropanoid pathway in *Arabidopsis*. *Arabidopsis Book* 9:e0152. doi: 10.1199/tab.0152

Gantait, S., Das, A., Mitra, M., and Chen, J. T. (2021). Secondary metabolites in orchids: biosynthesis, medicinal uses, and biotechnology. *S. Afr. J. Bot.* 139, 338–351. doi: 10.1016/j.sajb.2021.03.015

Gao, L. W., Jiang, D. H., Yang, Y. X., Li, Y. X., Sun, G. S., Ma, Z. H., et al. (2016). De novo sequencing and comparative analysis of two *Phalaenopsis* orchid tissue-specific transcriptomes. *Russ. J. Plant Physiol.* 63, 391–400. doi: 10.1134/S1021443716020072

Ghai, D., Verma, J., Kaur, A., Thakur, K., Pawar, S. V., and Sembi, J. K. (2021). "Bioprospection of orchids and appraisal of their therapeutic indications," in *Bioprospecting of Plant Biodiversity for Industrial Molecules*. eds. S. K. Upadhyay and S. P. Singh (Chichester, West Sussex, UK: John Wiley & Sons Ltd), 401–424.

Góngora-Castillo, E., and Buell, C. R. (2013). Bioinformatics challenges in de novo transcriptome assembly using short read sequences in the absence of a reference genome sequence. *Nat. Prod. Rep.* 30, 490–500. doi: 10.1039/c3np20099j

Grabherr, M. G., Haas, B. J., Yassour, M., Levin, J. Z., Thompson, D. A., Amit, I., et al. (2011). Trinity: reconstructing a full-length transcriptome without a genome from RNA-Seq data. *Nat. Biotechnol.* 29, 644–652. doi: 10.1038/nbt.1883

Griffith, R. E. (1847). *Medicinal Botany or Descriptions of the More Important Plants Used in Medicine With Their History, Properties and Mode of Administration*. Philadelphia: Lea and Blanchard.

Guo, X., Li, Y., Li, C., Luo, H., Wang, L., Qian, J., et al. (2013). Analysis of the *Dendrobium officinale* transcriptome reveals putative alkaloid biosynthetic genes and genetic markers. *Gene* 527, 131–138. doi: 10.1016/j.gene.2013.05.073

He, C., Wang, C., Guo, S., Yang, J., and Xiao, P. (2006). A novel flavonoid Glucoside from *Anoectochilus roxburghii* (Wall.) Lindl. *J. Integr. Plant Biol.* 48, 359–363. doi: 10.1111/j.1744-7909.2006.00179.x

Hinson, D. D., Chambliss, K. L., Toth, M. J., Tanaka, R. D., and Gibson, K. M. (1997). Post-translational regulation of mevalonate kinase by intermediates of the cholesterol and nonsterol isoprene biosynthetic pathways. *J. Lipid Res.* 38, 2216–2223. doi: 10.1016/S0022-2275(20)34935-X

Hossain, M. M., Akter, S., and Uddin, S. B. (2020). "Screening of bioactive phytochemicals in some indigenous epiphytic orchids of Bangladesh" in *Orchid Biology: Recent Trends and Challenges* (Singapore: Springer Nature), 481–506.

Hsiao, Y., Chen, Y., Huang, S., Pan, Z., Fu, C., Chen, W., et al. (2011). Gene discovery using next-generation pyrosequencing to develop ESTs for *Phalaenopsis* orchids. *BMC Genomics* 12:360. doi: 10.1186/1471-2164-12-360

Hsiao, Y., Tsai, W., Kuoh, C., Huang, T., Wang, H., Wu, T., et al. (2006). Comparison of transcripts in *Phalaenopsis bellina* and *Phalaenopsis equestris* (Orchidaceae) flowers to deduce monoterpene biosynthesis pathway. *BMC Plant Biol.* 6:14. doi: 10.1186/1471-2229-6-14

Hsieh, Y. S., Chien, C., Liao, S. K., Liao, S. F., Hung, W. T., Yang, W. B., et al. (2008). Structure and bioactivity of the polysaccharides in medicinal plant *Dendrobium huoshanense*. *Bioorg. Med. Chem.* 16, 6054–6068. doi: 10.1016/j.bmc.2008.04.042

Jia, N., Wang, J. J., Liu, J., Jiang, J., Sun, J., Yan, P., et al. (2021). DcTT8, a bHLH transcription factor, regulates anthocyanin biosynthesis in *Dendrobium candidum*. *Plant Physiol. Biochem.* 162, 603–612. doi: 10.1016/j.plaphy.2021.03.006

Jiang, Y., Liu, Y., Song, H., and He, J. (2021b). Integrated transcriptomics and metabolomics uncover the molecular basis of flavonoid accumulation in the rhizomes of two *Cymbidium tortisepalum* var. *longibracteatum* cultivars. *Sci. Hortic.* 293:110738. doi: 10.1016/j.scienta.2021.110738

Jiang, Y., Song, H. Y., He, J. R., Wang, Q., and Liu, J. (2018). Comparative transcriptome analysis provides global insight into gene expression differences between two orchid cultivars. *PLoS One* 13:e0200155. doi: 10.1371/journal.pone.0200155

Jiang, Y., Tian, M., Wang, C., and Zhang, Y. (2021a). Transcriptome sequencing and differential gene expression analysis reveal the mechanisms involved in seed germination and protocorm development of *Calanthe tsoongiana*. *Gene* 772:145355. doi: 10.1016/j.gene.2020.145355

Kessler, A., and Baldwin, I. T. (2002). Plant responses to insect herbivory: the emerging molecular analysis. *Annu. Rev. Plant Biol.* 53, 299–328. doi: 10.1146/annurev.arplant.53.100301.135207

Kong, J. M., Goh, N. K., Chia, L. S., and Chia, T. F. (2003). Recent advances in traditional plant drugs and orchids. *Acta Pharmacol. Sin.* 24, 7–21.

Kui, L., Chen, H., Zhang, W., He, S., Xiong, Z., Zhang, Y., et al. (2017). Building a genetic manipulation tool box for orchid biology: identification of constitutive promoters and application of CRISPR/Cas9 in the orchid, *Dendrobium officinale*. *Front. Plant Sci.* 7:2036. doi: 10.3389/fpls.2016.02036

Kuo, P. C., Chen, G. F., Yang, M. L., and Wu, T. S. (2010). High-performance liquid chromatography profiling of pigments from *Phalaenopsis* hybrids and their contribution to antioxidant and antityrosinase activities. *Acta Hortic.* 878, 89–95. doi: 10.17660/ActaHortic.2010.878.9

Langham, W. (1579). *The Garden of Health*. London. 123–126.

Lawler, L. (1984). "Ethnobotany of the Orchidaceae," in *Orchid Biology, Reviews & Perspectives III*. ed. J. Arditti (Ithaca: Cornell University), 27–149.

Lee, Y. H., Park, J. D., Baek, N. I., Kim, S. I., and Ahn, B. Z. (1995). In vitro and in vivo antitumoral phenanthrenes from the aerial parts of *Dendrobium nobile*. *Planta Med.* 61, 178–180. doi: 10.1055/s-2006-958043

Lei, Z., Zhou, C., Ji, X., Wei, G., Huang, Y., Yu, W., et al. (2018). Transcriptome analysis reveals genes involved in flavonoid biosynthesis and accumulation in *Dendrobium catenatum* from different locations. *Sci. Rep.* 8, 1–16. doi: 10.1038/s41598-018-24751-y

Li, Q., Ding, G., Li, B., and Guo, S. X. (2017). Transcriptome analysis of genes involved in dendrobine biosynthesis in *Dendrobium nobile* Lindl. Infected with mycorrhizal fungus MF23 (*Mycena* sp.). *Sci. Rep.* 7, 1–16. doi: 10.1038/s41598-017-00445-9

Li, N., Dong, Y., Lv, M., Qian, L., Sun, X., Liu, L., et al. (2021a). Combined analysis of volatile terpenoid metabolism and transcriptome reveals transcription factors related to terpene synthase in two cultivars of *Dendrobium officinale* flowers. *Front. Genet.* 12:661296. doi: 10.3389/fgene.2021.661296

Li, X., Fan, J., Luo, S., Yin, L., Liao, H., Cui, X., et al. (2021b). Comparative transcriptome analysis identified important genes and regulatory pathways for flower color variation in *Paphiopedilum hirsutissimum*. *BMC Plant Biol.* 21:495. doi: 10.1186/s12870-021-03256-3

Li, X., Jin, F., Jin, L., Jackson, A., Huang, C., Li, K., et al. (2014). Development of *Cymbidium ensifolium* genic-SSR markers and their utility in genetic diversity and population structure analysis in cymbidiums. *BMC Genet.* 15, 1–14. doi: 10.1186/s12863-014-0124-5

Liu, X. J., Lu, Y., Yuan, Y., Liu, S., Guan, C., Chen, S., et al. (2013). De novo transcriptome of *Brassica juncea* seed coat and identification of genes for the biosynthesis of flavonoids. *PLoS One* 8:e71110. doi: 10.1371/journal.pone.0071110

Liu, X. F., Zhu, J., Ge, S. Y., Xia, L. J., Yang, H. Y., Qian, Y. T., et al. (2011). Orally administered *Dendrobium officinale* and its polysaccharides enhance immune functions in BALB/c mice. *Nat. Prod. Commun.* 6, 867–870. PMID: 21815428

Luo, J. P., Deng, Y. Y., and Zha, X. Q. (2008). Mechanism of polysaccharides from *Dendrobium huoshanense* on streptozotocin-induced diabetic cataract. *Pharm. Biol.* 46, 243–249. doi: 10.1080/13880200701739397

Ma, X., Meng, Y., Wang, P., Tang, Z., Wang, H., and Tian, X. (2019a). Bioinformatics-assisted, integrated omics studies on medicinal plants. *Brief. Bioinform.* 21, 1857–1874. doi: 10.1093/bib/bbz132

Ma, C., Meng, C. W., Zhou, Q. M., Peng, C., Liu, F., Zhang, J. W., et al. (2019b). New sesquiterpenoids from the stems of *Dendrobium nobile* and their neuroprotective activities. *Fitoterapia* 138:104351. doi: 10.1016/j.fitote.2019.104351

Ma, X., Tang, K., Tang, Z., Dong, A., Meng, Y., and Wang, P. (2021). Organ-specific, integrated omics data-based study on the metabolic pathways of the medicinal plant *Bletilla striata* (Orchidaceae). *BMC Plant Biol.* 21:504. doi: 10.1186/s12870-021-03288-9

Magi, A., Benelli, M., Gozzini, A., Girolami, F., Torricelli, F., and Brandi, M. L. (2010). Bioinformatics for next generation sequencing data. *Genes* 1, 294–307. doi: 10.3390/genes1020294

Meng, X., Li, G., Gu, L., Sun, Y., Li, Z., Liu, J., et al. (2019). Comparative metabolomic and transcriptome analysis reveal distinct flavonoid biosynthesis regulation between petals of white and purple *Phalaenopsis amabilis*. *J. Plant Growth Regul.* 39, 823–840. doi: 10.1007/s00344-019-10025-y

Middleton, E. J., Kandaswami, C., and Theoharides, T. C. (2000). The effects of plant flavonoids on mammalian cells: implications for inflammation, heart disease, and cancer. *Pharmacol. Rev.* 52, 673–751. PMID: 11121513

Minh, T. N., do Khang, T., Tuyen, P. T., Minh, L. T., Anh, L. H., Quan, L. V., et al. (2016). Phenolic compounds and antioxidant activity of *Phalaenopsis* orchid hybrids. *Antioxidants* 5:31. doi: 10.3390/antiox5030031

Mohd-Hairul, A. R., Ong Abdullah, J., Song, A. A. L., Foo, H. L., Namasivayam, P., and Rahim, R. A. (2020). Volatile constituents and floral transcriptome analyses provide new insights into fragrance biosynthesis of *Vanda* 'Tan Chay Yan'. *Plant Biosyst.* 1–8. doi: 10.1080/11263504.2020.1829733 [Epub ahead of print].

Paudel, M. R., Rajbanshi, N., Sah, A. K., Acharya, S., and Pant, B. (2018). Antibacterial activity of selected *Dendrobium* species against clinically isolated multiple drug resistant bacteria. *Afr. J. Microbiol. Res.* 12, 426–432. doi: 10.5897/AJMR2018.8846

Peng, Y., Gao, Y., Zhang, X., Zhang, C., Wang, X., Zhang, H., et al. (2019). Antidiabetic and hepatoprotective activity of the roots of *Calanthe fimbriata* Franch. *Biomed. Pharmacother.* 111, 60–67. doi: 10.1016/j.biopha.2018.12.066

Prasad, R., and Koch, B. (2016). In vitro anticancer activities of Ethanolic extracts of *Dendrobium crepidatum* and *Dendrobium chrysanthum* against T-cell lymphoma. *J. Cytol. Histol.* 07:432. doi: 10.4172/2157-7099.1000432

Ramya, M., Park, P. H., Chuang, Y., Kwon, O. K., An, H. R., Park, P. M., et al. (2019). RNA sequencing analysis of *cymbidium goeringii* identifies floral scent biosynthesis related genes. *BMC Plant Biol.* 19:337. doi: 10.1186/s12870-019-1940-6

Rao, X., Krom, N., Tang, Y., Widiez, T., Havkin-Frenkel, D., Belanger, F. C., et al. (2014). A deep transcriptomic analysis of pod development in the vanilla orchid (*Vanilla planifolia*). *BMC Genomics* 15:964. doi: 10.1186/1471-2164-15-964

Ren, G., Deng, W. Z., Xie, Y. F., Wu, C. H., Li, W. Y., Xiao, C. Y., et al. (2020). Bibenzyl derivatives from leaves of *Dendrobium officinale*. *Nat. Prod. Commun.* 15, 1934578X2090867–1934578X2090865. doi: 10.1177/1934578X20908678

Satish, M. N., Abhay, P. S., Chen-Yue, L., Chao-Lin, K., and Hsin-Sheng, T. (2003). Studies on tissue culture of Chinese medicinal plant resources in Taiwan and their sustainable utilization. *Bot. Bull. Acad. Sin.* 44, 79–98.

Sedeek, K. E. M., Qi, W., Schauer, M. A., Gupta, A. K., Poveda, L., Xu, S., et al. (2013). Transcriptome and proteome data reveal candidate genes for pollinator attraction in sexually deceptive orchids. *PLoS One* 8:e64621. doi: 10.1371/journal.pone.0064621

Shan, T., Yin, M., Wu, J., Yu, H., Liu, M., Xu, R., et al. (2021). Comparative transcriptome analysis of tubers, stems, and flowers of *Gastrodia elata* Blume reveals potential genes involved in the biosynthesis of phenolics. *Fitoterapia* 153:104988. doi: 10.1016/j.fitote.2021.104988

Shen, C., Guo, H., Chen, H., Shi, Y., Meng, Y., Lu, J., et al. (2017). Identification and analysis of genes associated with the synthesis of bioactive constituents in *Dendrobium officinale* using RNASeq. *Sci. Rep.* 7:187. doi: 10.1038/s41598-017-00292-8

Song, J. I., Kang, Y. J., Yong, H., Kim, Y. C., and Moon, A. (2012). Denbinobin, a phenanthrene from *Dendrobium nobile*, inhibits invasion and induces apoptosis in SNU-484 human gastric cancer cells. *Oncol. Rep.* 27, 813–818. doi: 10.3892/or.2011.1551

Sut, S., Maggi, F., and Dall'Acqua, S. (2017). Bioactive secondary metabolites from orchids (Orchidaceae). *Chem. Biodivers.* 14:e1700172. doi: 10.1002/cbdv.201700172

Takayuki, T., Mutsumi, W., Rainer, H., and Fernie, A. R. (2013). Shikimate and phenylalanine biosynthesis in the green lineage. *Front. Plant Sci.* 4:62. doi: 10.3389/fpls.2013.00062

Teoh, E. S. (2016). *Medicinal Orchids of Asia*. Cham: Springer.

Teoh, E. S. (2019). *Orchids as Aphrodisiac, Medicine or Food*. Cham: Springer.

Toh, C., Mohd-Hairul, A. R., Ain, N. M., Namasivayam, P., Go, R., Abdullah, N. A. P., et al. (2017). Floral micromorphology and transcriptome analyses of a fragrant Vandaceous orchid, Vanda Mimi palmer, for its fragrance production sites. *BMC. Res. Notes* 10:554. doi: 10.1186/s13104-017-2872-6

Tsai, W. C., Dievart, A., Hsu, C. C., Hsiao, Y. Y., Chiou, S. Y., Huang, H., et al. (2017). Post genomics era for orchid research. *Bot. Stud.* 22, 1–22. doi: 10.3390/ijms22136947

Tzin, V., Malitsky, S., Zvi, M. M. B., Bedair, M., Sumner, L., Aharoni, A., et al. (2012). Expression of a bacterial feedback-insensitive 3-deoxy-d-arabinoheptulosonate 7-phosphate synthase of the shikimate pathway in *Arabidopsis* elucidates potential metabolic bottlenecks between primary and secondary metabolism. *New Phytol.* 194, 430–439. doi: 10.1111/j.1469-8137.2012.04052.x

Vij, S. P., Verma, J., and Kumar, S. C. (2013). *Orchids of Himachal Pradesh*. Bishen Singh Mahendra Pal Singh, Dehradun.

Vogt, T. (2010). Phenylpropanoid biosynthesis. *Mol. Plant* 3, 2–20. doi: 10.1093/mp/ssp106

Wang, Z., Gerstein, M., and Snyder, M. (2009). RNA-Seq: a revolutionary tool for transcriptomics. *Nat. Rev. Genet.* 10, 57–63. doi: 10.1038/nrg2484

Wang, Z., Jiang, W., Liu, Y., Meng, X., Su, X., Cao, M., et al. (2021). Putative genes in alkaloid biosynthesis identified in *Dendrobium officinale* by correlating the contents of major bioactive metabolites with genes expression between Protocorm-like bodies and leaves. *BMC Genomics* 22:579. doi: 10.1186/s12864-021-07887-6

Wang, H. Y., Li, Q. M., Yu, N. J., Chen, W. D., Zha, X. Q., Wu, D. L., et al. (2019). *Dendrobium huoshanense* polysaccharide regulates hepatic glucose homeostasis and pancreatic β-cell function in type 2 diabetic mice. *Carbohydr. Polym.* 211, 39–48. doi: 10.1016/j.carbpol.2019.01.101

Wang, Y., Shahid, M. Q., Ghouri, F., and Baloch, F. S. (2020). De novo assembly and annotation of the juvenile tuber transcriptome of a *Gastrodia elata* hybrid by RNA sequencing: detection of SSR markers. *Biochem. Genet.* 58, 914–934. doi: 10.1007/s10528-020-09983-w

Watanabe, K., Tanaka, R., Sakurai, H., Iguchi, K., Yamada, Y., Hsu, C. S., et al. (2007). Structure of Cymbidine A, a monomeric peptidoglycan-related compound with hypotensive and diuretic activities, isolated from a higher plant, *cymbidium goeringii* (Orchidaceae). *Chem. Pharm. Bull.* 55, 780–783. doi: 10.1248/cpb.55.780

Wei, X., Kuhn, D. N., and Narasimhan, G. (2003). "Degenerate primer design via clustering." in *Computational Systems Bioinformatics. CSB2003. Proceedings of the 2003 IEEE Bioinformatics Conference*, 75–83.

Windram, O., Penfold, C. A., and Denby, K. J. (2014). Network modeling to understand plant immunity. *Annu. Rev. Phytopathol.* 52, 93–111. doi: 10.1146/annurev-phyto-102313-050103

Wolf, J. B. W. (2013). Principles of transcriptome analysis and gene expression quantification: an RNA-seq tutorial. *Mol. Ecol. Resour.* 13, 559–572. doi: 10.1111/1755-0998.12109

Wu, X. Q., Li, W., Chen, J. X., Zhai, J. W., Xu, H. Y., Ni, L., et al. (2019). Chemical constituents and biological activity profiles on Pleione (Orchidaceae). *Molecules* 24:3195. doi: 10.3390/molecules24173195

Wu, H. S., Xu, J. H., Chen, L. Z., and Sun, J. J. (2004). Studies on anti-hyperglycemic effect and its mechanism of *Dendrobium candidum*. *Zhongguo ZhongYao Za Zhi* 29, 160–163.

Xie, Y., Wu, G., Tang, J., Luo, R., Patterson, J., Liu, S., et al. (2014). SOAPdenovo-trans: de novo transcriptome assembly with short RNA-Seq reads. *Bioinformatics* 30, 1660–1666. doi: 10.1093/bioinformatics/btu077

Xu, C., Zeng, B., Huang, J., Huang, W., and Liu, Y. (2015). Genome-wide transcriptome and expression profile analysis of *Phalaenopsis* during explant browning. *PLoS One* 10:e0123356. doi: 10.1371/journal.pone.0123356

Yang, H., Sung, S. H., and Kim, Y. C. (2007). Antifibrotic phenanthrenes of *Dendrobium nobile* stems. *J. Nat. Prod.* 70, 1925–1929. doi: 10.1021/np070423f

Yang, Y., Wang, J., Ma, Z., Sun, G., and Zhang, C. (2014). De novo sequencing and comparative transcriptome analysis of white petals and red labella in *Phalaenopsis* for discovery of genes related to flower color and floral differentiation. *Acta Soc. Bot. Pol.* 83, 191–199. doi: 10.5586/asbp.2014.023

Ye, S., Zhao, Q., and Zhang, A. (2017). *Anoectochilus roxburghii*: a review of its phytochemistry, pharmacology, and clinical applications. *J. Ethnopharmacol.* 209, 184–202. doi: 10.1016/j.jep.2017.07.032

Yuan, Y., Yu, M., Jia, Z., Song, X., Liang, Y., and Zhang, J. (2018). Analysis of *Dendrobium huoshanense* transcriptome unveils putative genes associated with active ingredients synthesis. *BMC Genomics* 19:978. doi: 10.1186/s12864-018-5305-6

Yuan, Y., Zhang, J., Liu, X., Meng, M., Wang, J., and Lin, J. (2020). Tissue-specific transcriptome for *Dendrobium officinale* reveals genes involved in flavonoid biosynthesis. *Genomics* 112, 1781–1794. doi: 10.1016/j.ygeno.2019.10.010

Zerbino, D. R., and Birney, E. (2008). Velvet: algorithms for de novo short read assembly using de Bruijn graphs. *Genome Res.* 18, 821–829. doi: 10.1101/gr.074492.107

Zhang, Y., Cai, J., Ruan, H., Pi, H., and Wu, J. (2007). Antihyperglycemic activity of kinsenoside, a high yielding constituent from *Anoectochilus roxburghii* in streptozotocin diabetic rats. *J. Ethnopharmacol.* 114, 141–145. doi: 10.1016/j.jep.2007.05.022

Zhang, C., Chen, J., Huang, W., Song, X., and Niu, J. (2021a). Transcriptomics and metabolomics reveal purine and phenylpropanoid metabolism response to drought stress in *Dendrobium sinense*, an endemic orchid species in Hainan Island. *Front. Physiol.* 12:692702. doi: 10.3389/fgene.2021.692702

Zhang, Y., Li, Y., Chen, X., Meng, Z., and Guo, S. (2020a). Combined metabolome and transcriptome analyses reveal the effects of mycorrhizal fungus *Ceratobasidium* sp. AR2 on the flavonoid accumulation in *Anoectochilus roxburghii* during different growth stages. *Int. J. Mol. Sci.* 21:564. doi: 10.3390/ijms21020564

Zhang, M., Yu, Z., Zeng, D., Si, C., Zhao, C., Wang, H., et al. (2021b). Transcriptome and metabolome reveal salt-stress responses of leaf tissues from *Dendrobium officinale*. *Biomol. Ther.* 11:736. doi: 10.3390/biom11050736

Zhang, Y., Zhang, L., Liu, J., Liang, J., Si, J., and Wu, S. (2017). *Dendrobium officinale* leaves as a new antioxidant source. *J. Funct. Foods* 37, 400–415. doi: 10.1016/j.jff.2017.08.006

Zhang, Y., Zhou, T., Dai, Z., Dai, X., Li, W., Cao, M., et al. (2020b). Comparative transcriptomics provides insight into floral color polymorphism in a *Pleione limprichtii* orchid population. *Int. J. Mol. Sci.* 21:247. doi: 10.3390/ijms21010247

Zhao, C., Liu, Q., Halaweish, F., Shao, B., Ye, Y., and Zhao, W. (2003). Copacamphane, picrotoxane, and alloaromadendrane sesquiterpene glycosides and phenolic glycosides from *Dendrobium moniliforme*. *J. Nat. Prod.* 66, 1140–1143. doi: 10.1021/np0301801

Zhou, P., Pu, T., Gui, C., Zhang, X., and Gong, L. (2020). Transcriptome analysis reveals biosynthesis of important bioactive constituents and mechanism of stem formation of *Dendrobium huoshanense*. *Sci. Rep.* 10:2857. doi: 10.1038/s41598-020-59737-2

Zhou, Z., Ying, Z., Wu, Z., Yang, Y., Fu, S., Xu, W., et al. (2021). Anthocyanin genes involved in the flower coloration mechanisms of *cymbidium kanran*. *Front. Plant Sci.* 12:737815. doi: 10.3389/fpls.2021.737815

Conflict of Interest: The authors declare that the research was conducted in the absence of any commercial or financial relationships that could be construed as a potential conflict of interest.

Publisher's Note: All claims expressed in this article are solely those of the authors and do not necessarily represent those of their affiliated organizations, or those of the publisher, the editors and the reviewers. Any product that may be evaluated in this article, or claim that may be made by its manufacturer, is not guaranteed or endorsed by the publisher.

Copyright © 2022 Ghai, Kaur, Kahlon, Pawar and Sembi. This is an open-access article distributed under the terms of the Creative Commons Attribution License (CC BY). The use, distribution or reproduction in other forums is permitted, provided the original author(s) and the copyright owner(s) are credited and that the original publication in this journal is cited, in accordance with accepted academic practice. No use, distribution or reproduction is permitted which does not comply with these terms.

frontiers | Frontiers in Plant Science

REVIEW
published: 29 April 2022
doi: 10.3389/fpls.2022.879366

Heat Stress-Mediated Constraints in Maize (*Zea mays*) Production: Challenges and Solutions

Ahmed H. El-Sappah[1,2,3†], Shabir A. Rather[4†], Shabir Hussain Wani[5], Ahmed S. Elrys[6], Muhammad Bilal[7], Qiulan Huang[3,8], Zahoor Ahmad Dar[9], Mohamed M. A. Elashtokhy[2], Nourhan Soaud[10], Monika Koul[11], Reyazul Rouf Mir[12], Kuan Yan[1,3], Jia Li[1,3†], Khaled A. El-Tarabily[13,14] and Manzar Abbas[1,3]**

[1] School of Agriculture, Forestry and Food Engineering, Yibin University, Yibin, China, [2] Department of Genetics, Faculty of Agriculture, Zagazig University, Zagazig, Egypt, [3] Key Laboratory of Sichuan Province for Refining Sichuan Tea, Yibin, China, [4] Center for Integrative Conservation, Xishuangbanna Tropical Botanical Garden, Chinese Academy of Sciences, Menglun, China, [5] Mountain Research Centre for Field Crops Khudwani Anantnag, SKUAST–Kashmir, Srinagar, India, [6] Department of Soil Science, Faculty of Agriculture, Zagazig University, Zagazig, Egypt, [7] School of Life Sciences and Food Engineering, Huaiyin Institute of Technology, Huaian, China, [8] College of Tea Science, Yibin University, Yibin, China, [9] Dryland Agriculture Research Station, SKUAST–Kashmir, Srinagar, India, [10] Department of Crop Science, Faculty of Agriculture, Zagazig University, Zagazig, Egypt, [11] Department of Botany, Hansraj College, University of Delhi, New Delhi, India, [12] Division of Genetics and Plant Breeding, Faculty of Agriculture (FoA), SKUAST–Kashmir, Sopore, India, [13] Department of Biology, College of Science, United Arab Emirates University, Al Ain, United Arab Emirates, [14] Harry Butler Institute, Murdoch University, Murdoch, WA, Australia

OPEN ACCESS

Edited by:
Ahmad M. Alqudah, Aarhus University, Denmark

Reviewed by:
Mona F. A. Dawood, Assiut University, Egypt
Piyoosh Kumar Babele, Rani Lakshmi Bai Central Agricultural University, India
Iqrar Ahmad Rana, University of Agriculture, Faisalabad, Pakistan

***Correspondence:**
Khaled A. El-Tarabily
ktaraily@uaeu.ac.ae
Manzar Abbas
abbas2472@hotmail.com

† These authors have contributed equally to this work

Specialty section:
This article was submitted to Plant Biotechnology, a section of the journal Frontiers in Plant Science

Received: *19 February 2022*
Accepted: *30 March 2022*
Published: *29 April 2022*

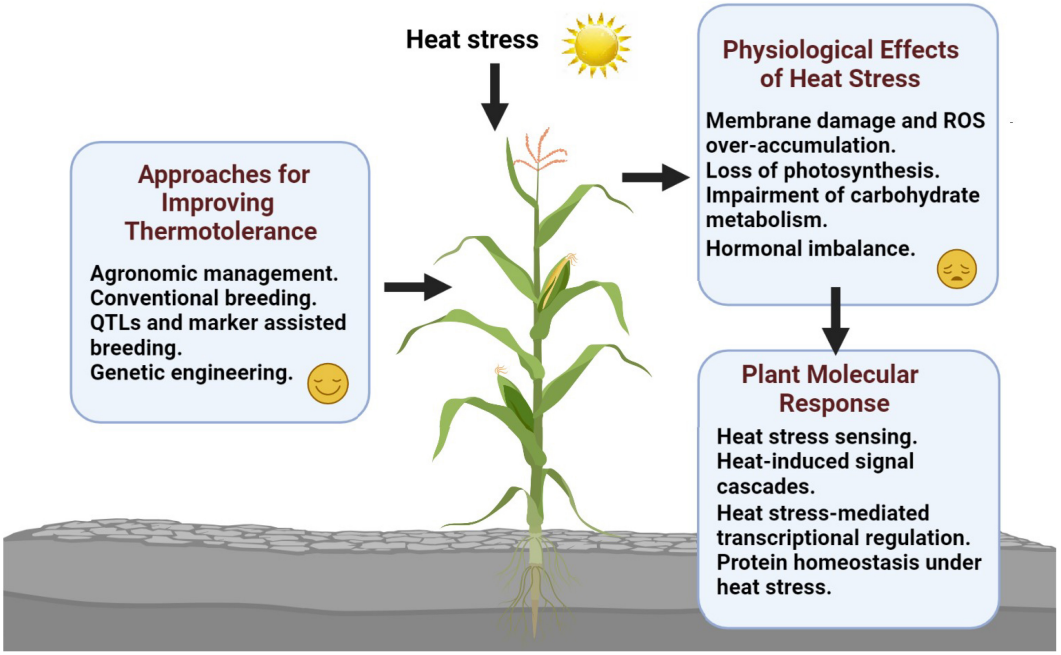
Citation:
El-Sappah AH, Rather SA, Wani SH, Elrys AS, Bilal M, Huang Q, Dar ZA, Elashtokhy MMA, Soaud N, Koul M, Mir RR, Yan K, Li J, El-Tarabily KA and Abbas M (2022) Heat Stress-Mediated Constraints in Maize (Zea mays) Production: Challenges and Solutions. Front. Plant Sci. 13:879366. doi: 10.3389/fpls.2022.879366

An increase in temperature and extreme heat stress is responsible for the global reduction in maize yield. Heat stress affects the integrity of the plasma membrane functioning of mitochondria and chloroplast, which further results in the over-accumulation of reactive oxygen species. The activation of a signal cascade subsequently induces the transcription of heat shock proteins. The denaturation and accumulation of misfolded or unfolded proteins generate cell toxicity, leading to death. Therefore, developing maize cultivars with significant heat tolerance is urgently required. Despite the explored molecular mechanism underlying heat stress response in some plant species, the precise genetic engineering of maize is required to develop high heat-tolerant varieties. Several agronomic management practices, such as soil and nutrient management, plantation rate, timing, crop rotation, and irrigation, are beneficial along with the advanced molecular strategies to counter the elevated heat stress experienced by maize. This review summarizes heat stress sensing, induction of signaling cascade, symptoms, heat stress-related genes, the molecular feature of maize response, and approaches used in developing heat-tolerant maize varieties.

Keywords: abiotic stress, gene signaling cascade, heat stress, molecular response, *Zea mays*

INTRODUCTION

Heat stress is the most devastating abiotic stress factor influencing seasonal growth and spatial variations in various crops (Sallam et al., 2018; Magaña Ugarte et al., 2019). Global warming caused by the increasing growth of the population and the accompanying industrial development has become a concern that cannot be overlooked (Baus, 2017). Also, the average rise in global temperature between 1900 and 2020 was 1.13°C, and it is expected to increase by 1.4–5.8°C in 2100



GRAPHICAL ABSTRACT | This review summarized heat stress-mediated morphological and physiological changes in maize and elucidated the molecular mechanisms responsible for maize response to heat stress. Furthermore, plausible approaches to dissecting the regulatory network associated with heat stress response and improving maize adaptation to global warming have been discussed. This figure was made using BioRender.

(**Figure 1**; Houghton et al., 2001). This gradual increase in global warming and heat waves have become a serious threat to crop productivity (Hoegh-Guldberg et al., 2019). Data published by the Food and Agriculture Organization has revealed the annual relative yield loss in major cereal crops (Faostat, 2019). Also, recent studies have shown that effective heat stress tolerance *via* genetic improvement is the only possible remedy; otherwise, every 1°C temperature rise will cause a 6.0% yield loss of wheat, 3.2% of rice, 7.4% of maize, and 3.1% of soybean (Zhao et al., 2017; Kraus et al., 2022). However, due to increasing population growth, crop yield ought to increase by 70% for sustaining food security to meet the demand of a projected 9 billion population rise in 2050 (Popp et al., 2013; Dawson et al., 2016).

Maize (*Zea mays*) is an important cereal crop that belongs to the Poaceae family (Li et al., 2022) and has ensured global food security with a worldwide production $\geq 1 \times 10^9$ t (10^{12} kg) since 2013 (Faostat, 2017). Maize was initially cultivated in tropical areas under rainfed conditions (Li J. et al., 2021; Maitra et al., 2021). However, there is an increased demand for maize due to its utilization of carbohydrates as biomass for ethanol fuel production, leaves and stem as livestock fodder, grains as raw material in the baking industry, and food and feed crop in many countries (Rooney et al., 2007; Parmar et al., 2017; Dar et al., 2021). Maize is a rich source of starch and calcium in addition to numerous essential minerals, vitamins, and fiber. However, it labors to some nutrients, such as vitamins B12 and C (McKevith, 2004). Iron absorption, particularly the non-heme iron present in maize, can be inhibited by some components of the diet being consumed, such as vegetables, coffee (e.g., polyphenols), tea (e.g., oxalates), milk (e.g., calcium), and eggs (e.g., phosvitin) (Ranum et al., 2014).

Elevated temperature accelerates crop growth but shortens its growing season (Mo et al., 2016; Hu et al., 2017; Ahmed et al., 2018; Ihsan et al., 2019). Additionally, maize growth requires an optimum daytime temperature range of 28–32°C, comparatively higher than the optimum temperature necessary for other cereal crops, such as wheat (*Triticum aestivum*) and rice (*Oryza sativa*) (Sánchez et al., 2014).

The global change resulting from harsh climatic conditions has negatively affected maize crop yields (Lobell et al., 2011; Ahmed et al., 2018; El-Sappah and Rather(eds)., 2022). Also, increased temperature stimulates the over-accumulation of phenolic compounds, resulting in cell necrosis, consequently contributing to maize yield loss (Tebaldi and Lobell, 2018). Furthermore, heat stress (>32°C) causes the deterioration of several metabolic processes in maize plants, including a severe break in photosynthesis, increased surface transpiration rate (Crafts-Brandner and Salvucci, 2002; Sharma et al., 2020), pollen-sterilization at anthesis (flowering stage) (Gourdji et al., 2013), kernels shortening at grain-filling stage (Singletary et al., 1994; Rezaei et al., 2015), cumulatively resulting in a significant yield loss.

The approval of multiple agronomic and breeding alternatives along with advanced genomic tools is inevitable to cope with the deleterious effects of extreme temperatures (Waqas et al., 2021). Several agronomic management practices, such as the management of soil and nutrients, crop rotation, plantation rate, timing, and irrigation, are beneficial for the development of heat

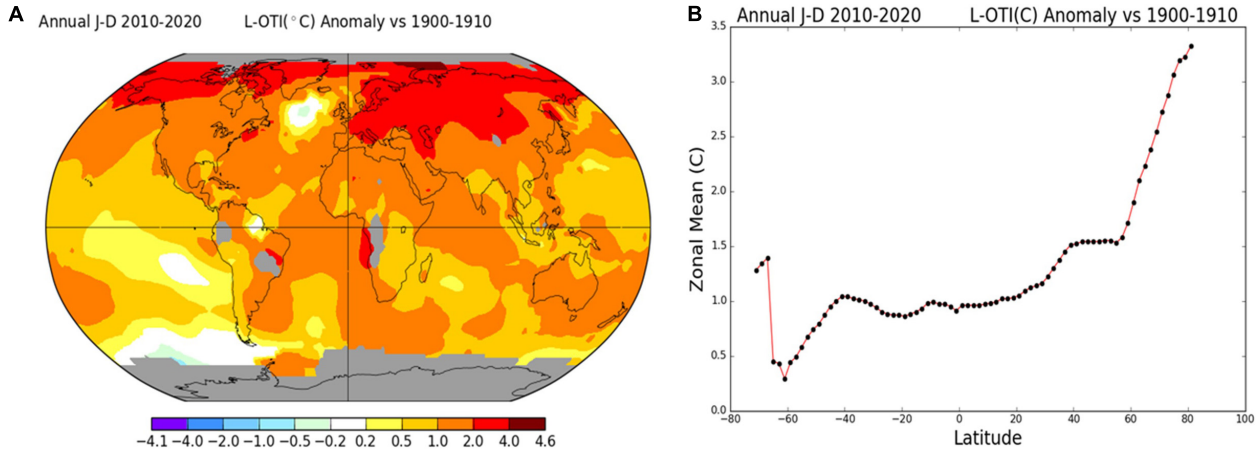


FIGURE 1 | (A) Map of annual mean temperature change (°C) during 1900–1910 and 2010–2020. **(B)** The zonal means plot. Air temperature data of the land surface was retrieved from GHCNv4 (GISS analysis based on global historical climatology network v4), and sea surface temperature data was retrieved from ERSST_v5 (NOAA/NCEI's extended reconstructed sea surface temperature v5). The number at the top right-hand corner of the map plot is an estimate (°C) of the global mean of the calculated area. The maps were made using GISS Surface Temperature Analysis software (https://data.giss.nasa.gov/gistemp/maps/index.html).

tolerance in maize (Sabagh et al., 2020). Genetically modified crops could also be a valuable resource for the development of novel traits that enhance the survival of plants under harsh conditions (Jha et al., 2020). In recent years, the rate of crop improvement has accelerated owing to the rapid progress in plant molecular biology. In several crops, different genetic approaches, including marker-assisted selection (MAS), map-based gene cloning, quantitative trait locus (QTL) mapping, and genome editing (such as RNA interference [RNAi] and CRISPR)/CRISPR-associated-9, Cas9), have been utilized for the selection and improvement of plant traits (Waqas et al., 2021).

This review summarized heat stress-mediated morphological and physiological changes in maize and elucidated the molecular mechanisms responsible for maize response to heat stress. We also discussed plausible approaches in dissecting the regulatory network associated with heat stress response and improving maize adaptation to global warming.

IMPACT OF HEAT STRESS ON DIFFERENT GROWTH STAGES

Vegetative Stage

Technically, the growth of stems, leaves, and roots, usually referred to as vegetative growth, is also known as germination, leaf, and tasseling (Dolatabadian et al., 2010). Heat stress affects the abovementioned growth stages (**Figure 2**) significantly. Also, the optimum soil temperature for maize seeds germination is 21°C, whereas <13°C causes a severe stoppage in germination and <10°C causes a total cessation (Kaspar and Bland, 1992; Towil, 2010; Sánchez et al., 2014). The germination rate of spring sowing of maize seeds cultivated in higher altitudes, such as North Europe and North America, is comparatively low due to low soil temperature (Paul et al., 1996). Early seed germination may expose the crop to freezing temperature, and early flowering leads to short crop duration leading to severe yield loss (Jagadish et al., 2016). However, late cultivation for optimum temperature conditions caused a severe loss in yield due to pest attacks (Rosenzweig et al., 2001). Therefore, only the day-neutral spring maize is favorably cultivated in higher altitudes (Colasanti and Muszynski, 2009).

Notably, the younger seedlings are less susceptible to high temperatures (Sánchez et al., 2014). The overall required temperature range for early maize seedling growth is 30–35°C, and the optimal temperature is around 20°C (Khaeim et al., 2022), 4–6°C higher than the suitable temperature for wheat and barley growth (Sánchez et al., 2014). Importantly, depending upon maize variety and below 20°C, every 0.5°C downfalls in daily temperature resulted in 10–20 days extended crop duration (Rahman et al., 2009). At an average daytime temperature of 15°C may take 200 days for the maturity of maize crop (Wilson et al., 1995).

Maize is susceptible to cold temperature but can recover from its effects if height is less than 15 cm when exposed to cold (Sakai and Larcher, 2012). Temperature below 10°C causes stunted root growth, whereas 17°C temperature results in 1.5 mm root growth per day, and temperature above 40°C inhibits root growth (Ryel et al., 2002). Maize seedlings can recover from constraints of drought stress because it is naturally resistant to drought (Daryanto et al., 2016). In conclusion, maize can recover from adverse climatic conditions if exposed at very early vegetative growth stages. The early cultivation of maize also facilitates the avoidance of pest attacks and the possible development of diseases (Bruns, 2003). So, early sowing of maize is highly recommended.

Reproductive Stage

The fruit setting stage is the reproductive stage that begins with vegetative growth termination and flowering initiation. The stage is susceptible to unexpected fluctuation in temperature, i.e., >32°C temperature, or frost causing severe yield loss (Silim et al., 2006; Siebers et al., 2017). Also, hailstorm adversely affects

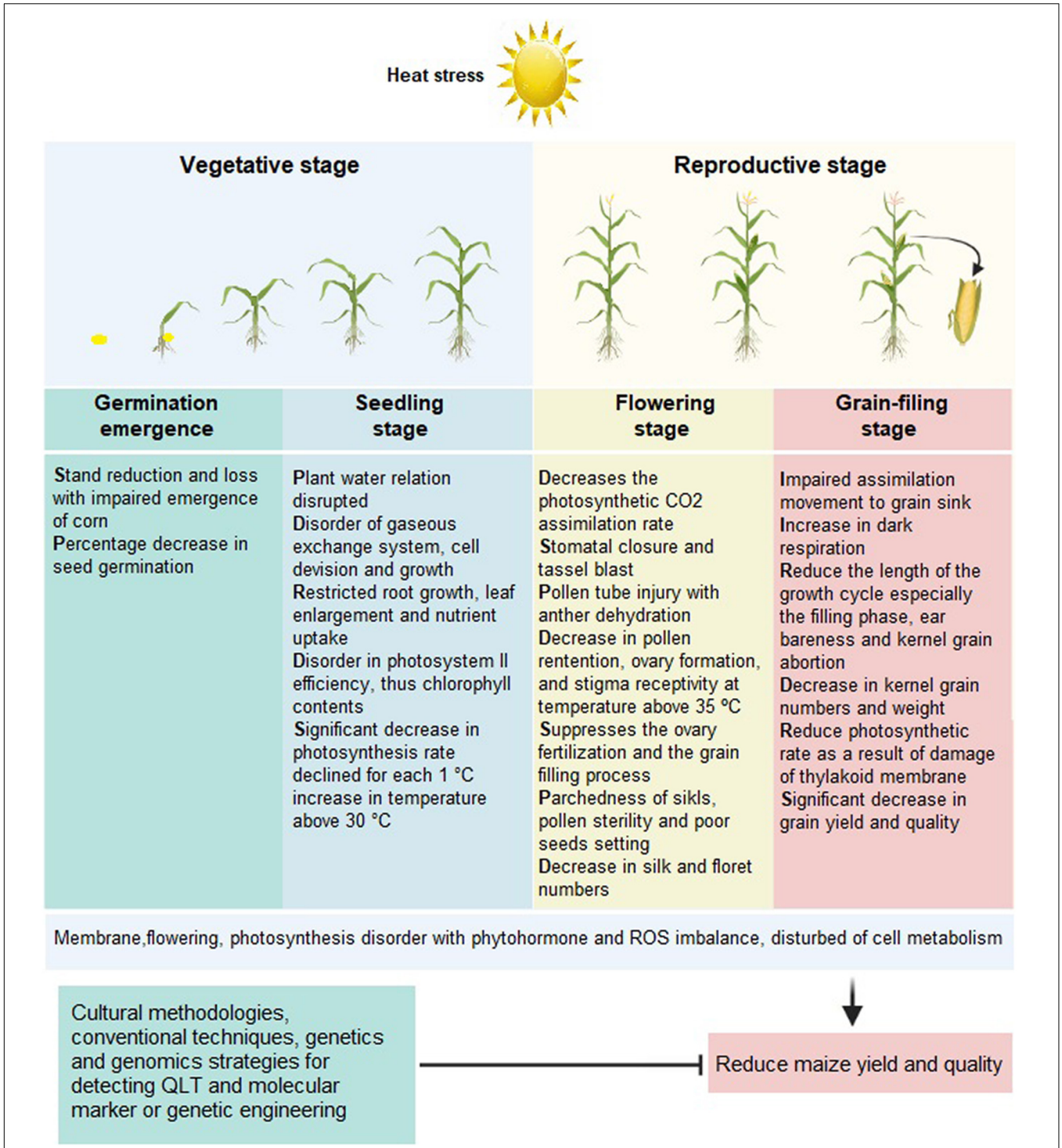


FIGURE 2 | Morphological and physiological characteristics of maize under heat stress. This figure was made using BioRender.

outcomes at the jointing and silking stage (Chen K. et al., 2018). Similarly, soil moisture contents before, during, and after silking result in a severe reduction in yield by 25, 21, and 50%, respectively (Pandey et al., 2000). The optimum temperature at tasseling is between 21 and 30°C (Kiniry and Bonhomme, 1991). Additionally, elevated temperature encourages respiration (Guo et al., 2019) and shortens grain-filling duration, contributing to a significant yield loss (Sánchez et al., 2014). Conversely, low-temperature extends the length of the grain-filling period, the appropriate phase change of photosynthesis to dry matter, and

grain filling, resulting in a higher yield (Dordas, 2009; Edreira et al., 2014; Chao et al., 2016). Overall, during pollination and grain filling, temperatures ≥35°C suppress fertilization in maize and decreases its yield by 101 kg/ha per day (Naveed et al., 2014; Dawood et al., 2020).

PHYSIOLOGICAL EFFECTS OF HEAT STRESS

Membrane Damage and Reactive Oxygen Species Over-Accumulation

Heat stress causes cell physiological changes, such as inactivating the photosystem II (PSII) reaction center and the denaturation of the lipid bilayer and embedded proteins in the thylakoid membrane, resulting in the damaging of the cell membrane (Yang et al., 1996; Nijabat et al., 2020). The damaged cell membrane has caused severe retardation of ion exchange, leakage of electrolytes, viscous cytosol due to water loss, toxic compounds production, and homeostasis disruption (Stanley and Parkin, 1991; Demidchik, 2015). Also, these changes have resulted in plant growth cessation through leaf wilt, reduced leaf area, and leaf abscission (Bartels and Sunkar, 2005; Mafakheri et al., 2010). Furthermore, the cell membrane stability varies with plant tissue age, growth stage, growing season, plant species, and heat intensity (Nijabat et al., 2020). Therefore, the plant's retention of its cell membrane stability and water contents under heat stress during the vegetative and reproductive growth period has generated higher yields (Khakwani et al., 2012).

Heat stress stimulates ROS biosynthesis that promotes membranous lipids peroxidation, leakage of cellular contents, protein degradation, enzymatic inactivation, bleaching of chlorophyll pigments, and DNA damage, consequently resulting in necrosis (He and Häder, 2002; Mujahid et al., 2007). Phospholipids-peroxidation causes the production of malondialdehyde (MDA) which causes damage to the cell membrane (Pamplona, 2008; Wadhwa et al., 2012). Additionally, ROS causes polyunsaturated fatty acid peroxidation, leading to chain breakage contributing to increased membrane permeability and fluidity (Catalá, 2009). Notably, the increased accumulation of H_2O_2 causes lipid peroxidation and membrane damage (Banerjee and Roychoudhury, 2018; Yadav et al., 2018). Heat stress-mediated genetic variations have been investigated in several cereal crops, including wheat, barley, rice, and maize (Kumari et al., 2009; Khajuria et al., 2016; Swapna and Shylaraj, 2017). Balanced redox reaction system activation via enzymatic antioxidants, such as superoxide dismutase, catalase, ascorbate peroxidase, glutathione reductase, and non-enzymatic antioxidants, such as NADH; NADPH; ascorbic acid, glutathione, and secondary metabolites play a crucial role in heat stress tolerance (Wahid et al., 2007; Foyer and Shigeoka, 2011).

Loss of Photosynthesis

Photosynthetic apparatus is highly vulnerable to damage when exposed to heat stress and intense light (Essemine et al., 2012; Li Y. T. et al., 2020). Therefore, heat stress causes a severe reduction in carbon assimilation, restricts electron transfer, aggravates oxidative damage and photoinhibition of PSII, resulting in significant yield loss (Elferjani and Soolanayakanahally, 2018; Li Y. T. et al., 2020). Heat stress also denatures vital enzymes associated with the Calvin cycle, such as rubisco, and reduces carbon assimilation in C3 plants (Dias and Brüggemann, 2010; Zhang et al., 2020a). However, C4 plants, such as maize, harbor the CO_2 concentration mechanism (Dai et al., 1993; Majeran and van Wijk, 2009), reducing the restriction of photosynthetic carbon assimilation *via* the Calvin cycle (von Caemmerer and Furbank, 2016). Furthermore, Phosphoenol pyruvate carboxylase is the highly thermostable initial enzyme involved in the C4 cycle (O'Leary et al., 2011), suggesting that other photosynthesis pathways contribute to declining photosynthetic carbon assimilation under heat stress in maize (Li Y. T. et al., 2020). Notably, the photosynthetic apparatus acclimatizes to heat stress by improving its antioxidant capacity and changing leaf structure and metabolism (Li Y. T. et al., 2020). However, shock heat stress during flowering causes irreparable yield loss by damaging the leaves, rendering them unable to sprout again due to the completion of vegetative growth (Li Y. T. et al., 2020).

Respiration plays a crucial role in photosynthesis, whereas its inhibition suppresses CO_2 fixation and photoinhibition (Gardeström and Igamberdiev, 2016). However, stomatal closure does not limit the exchange of gases like CO_2 but limits the transpiration rate through leaves. The CO_2 concentration mechanism of C4 plants, such as maize leaves, provides more robust resistance to stomatal restriction than in C3 plants (Markelz et al., 2011). Additionally, the blockage of respiratory electron transfer inhibits photorespiration resulting in PSII photoinhibition (Rochaix, 2011; Zhang et al., 2017). Transpiration through stomata is an important heat-dissipating mechanism, with their closure under heat stress resulting in severe loss in net photosynthetic rate (Pn) (Caine et al., 2019). The lower stomatal conductance (Gs) in maize leaves maintains water-use efficiency but damages photosynthetic apparatus under heat stress. Therefore, the lower Gs due to stomata closure indicates less heat dissipation *via* the transpiration mechanisms in the leaves of C4 plants, such as maize, compared to C3 plants (El-Sharkawy, 2007; Li Y. T. et al., 2020).

Photoinhibition of photosystems (PSI and PSII) in the chloroplast results from the degradation of the light receptors under heat stress contributing to the significant halt in photosynthesis (Zivcak et al., 2015). The oxygen-evolving complex (OEC) of PSII is highly sensitive to heat stress than of high-intensity light, whereas the D1 protein of PSII is more sensitive to high-intensity light instead of heat stress (Vass and Cser, 2009; Tóth et al., 2011). It is reported that heat stress significantly affects the acceptor site of PSII instead of PSI in maize leaves (Yan et al., 2013; Li Y. T. et al., 2020). Accordingly, OEC is the primary site in maize leaf cells affected by heat stress, whereas D1 is the primary site affected by high-intensity light. The over-accumulation of ROS is another cause of D1 protein denaturation (Kong et al., 2013). Therefore, overexpression of OEC and D1 protein and downregulation of ROS *via* genetic engineering

and breeding techniques will improve heat tolerance in maize (Li and Howell, 2021).

Imbalance/Deregulation in Primary and Secondary Metabolism

Traditionally, metabolites are divided into primary and secondary/specialized metabolites. Primary metabolites reinforce cell and secondary/specialized metabolites are concerned with an organism's interaction with its environment. Primary metabolism produces precursors for secondary metabolite biosynthesis and plays a direct and central role in plant growth, development, and reproduction. It also produces precursors for secondary metabolite biosynthesis (Medeiros et al., 2021). Secondary metabolites possess functional and chemical diversity (Erb and Kliebenstein, 2020). Thousands of metabolites serve as mediators for the various interactions between plant and the environment (Medeiros et al., 2021). During a stress response, plants fine-tune their metabolic production accordingly; however, the mechanisms, reasons, and regulations for this process are only partially understood.

Leaf metabolites were most affected by long-duration salt, heat, or drought stress treatments compared with the rest of the maize organs. The raffinose pathway metabolites (raffinose and galactinol) and some amino acids such as threonine, tryptophan, and histidine also stood out in the heat stress metabolome profile (Joshi et al., 2021). In the metabolic studies of Joshi et al. (2021), 2,549 genes were upregulated including galactinol synthase (*Zm00001d028931*), stachyose synthase (*Zm00001d039685*), and a putative inositol transporter (*Zm00001d018803*), while 2,587 genes were downregulated as a result of heat stress. Two stress-induced arginine decarboxylase paralogs exhibited a similar dichotomy with drought and heat, inducing *Zm00001d051194*. However, the responses from pairing drought and heat stressors contrasts with the pattern exhibited by the raffinose pathway genes described above where the effects of heat and salt were correlated (Joshi et al., 2021).

Heat stress adversely affects carbohydrate catabolism by denaturing relevant enzymes resulting in the over-accumulation of starch and sucrose (Ruan et al., 2010; Xalxo et al., 2020). Varied expression patterns of genes and proteins involved in carbohydrate metabolism were observed in *Arabidopsis* exposed to heat stress (Kaplan et al., 2004). In addition, heat stress causes over-accumulation of maltose, sucrose, and cell wall-specific monosaccharides (Lima et al., 2013; Sengupta et al., 2015). Additionally, the metabolic profiling of plants exposed to two abiotic stress factors, such as drought and heat, showed over-accumulation of glucose, fructose, sucrose, trehalose, maltose responsible for maintaining cell turgor pressure, stabilizing cell membranes and proteins (Rodziewicz et al., 2014; Kumar et al., 2021). During unfavorable conditions, plants digest starch molecules to get energy as a substitute for glucose; however, extended heat stress causes depletion of all carbohydrate reservoirs and causes plants starvation (Kaplan et al., 2004; Djanaguiraman et al., 2010).

Temperature significantly affects starch biosynthesis in maize kernels, which contributes to the total dry weight of grains (Keeling et al., 1994). Heat stress stimulates the production of osmolytes including fructose, mannose, sucrose, and proline, which plays a vital role in heat stress tolerance (Slama et al., 2015; Sharma et al., 2019). The grain-filling rate and duration are determined by the sucrose contents available in kernels and enzyme activity level (Singletary et al., 1994; Alam et al., 2021). Short interval time series analysis revealed that the "tipping point" for maize metabolome perturbation is lengthened at a >1 day of drought stress, including a combined effect of drought and heat stress (Bechtold et al., 2016). Generally, heat stress causes mechanical changes, whereas drought stress results in the disequilibrium of osmosis in plants cell (Haswell and Verslues, 2015). Therefore, abiotic stress-mediated changes in metabolic responses are probably attributed to adaptations to drought and heat stresses (Kaplan et al., 2004; Khan et al., 2015).

Osmolytes also contribute a crucial role in maintaining membrane structure (Sharma et al., 2019), alleviating proteins degradation, reducing ionic toxicity, protecting cell organelles, scavenging ROS, protecting antioxidant compounds, and maintaining redox equilibrium (Hasanuzzaman et al., 2020). Osmolytes, such as sucrose, fructose, and mannose, are resources of energy, nutrition, structural materials, signaling molecules, and crucially contribute to seed germination and the growth of plantlets (Osuna et al., 2015). Maize (*Zea mays* L.) seedlings exposed to heat stress displayed sudden degradation of glycan contents and upregulated fructose and mannose metabolism (Lieu et al., 2021). The expression of genes involved in fructose, mannose, and sucrose biosynthesis was also upregulated in 21-day-old maize seedlings exposed to heat stress (Stavridou et al., 2021).

The mitochondria and nuclear membrane structure were also disrupted by heat stress, more severe in the heat-sensitive hybrid (Török et al., 2014; Li Y. T. et al., 2020). Also, disruption of mitochondrial membrane structure decreases the efficiency of oxidative phosphorylation, requiring increased consumption of carbohydrates to supply sufficient ATP and further reducing light energy utilization (Li Y. T. et al., 2020). Additionally, many chloroplast proteins are encoded by the nuclear genome; hence, destruction of the nuclear envelope may inhibit the upregulation of photo-protection mechanisms, aggravating the photosynthetic mechanism damage and delaying photo inhibition repair and structural damage (Kumar and Kaushik, 2021). The less grouped PSII units are more sensitive to light, partly explaining the more severe PSII under heat stress (Strasser et al., 2004).

Hormonal Imbalance

Phytohormones, such as auxin/indole acetic acid (IAA), gibberellic acid (GA), abscisic acid (ABA), cytokinin (CTK), ethylene (ET), salicylic acid (SA), brassinosteroids (BRs), strigolactone (SL), and jasmonic acid (JA) importantly regulates cellular processes which are ubiquitous to plant growth under abiotic stress factors (Sharma et al., 2019). Heat stress causes over-accumulation of ABA and the downregulation of CTK, resulting in the improper development of maize kernels (Cheikh and Jones, 1994; Niu et al., 2021). The application of benzyladenine on maize seedlings maintains a proper balance between ABA and CTK, causing an increased heat tolerance

(Cheikh and Jones, 1994). Similarly, the treatment of maize seedlings with Ca^{2+} ions solution and ABA improves the antioxidant enzyme activity, reduces lipid peroxidation, and improves heat tolerance (Hossain et al., 2015; Yang et al., 2021). Similarly, SA, GA, and H_2S stimulate the biosynthesis of proline, betaine, and trehalose, contributing to the enhanced antioxidant activity in maize (Li, 2015; Li Z. G. et al., 2015; Zhou et al., 2018). Overexpression of *ZmbZIP4* induces longer primary roots, more lateral roots, and enhanced biosynthesis of ABA, which cumulatively results in enhanced abiotic stress tolerance (Ma et al., 2018).

MOLECULAR MECHANISMS OF PLANT RESPONSES TO HEAT STRESS

Heat Stress Sensing

Plant cells and organelles harbor an efficient heat sensing mechanism that subsequently stimulates a signaling cascade for rapid adaptive modifications (**Figure 3**; Nievola et al., 2017; Niu and Xiang, 2018). For example, calcium ions (Ca^{2+}) flow through their conducting channels, acting as messengers in a signaling cascade to sense and respond to heat stimuli (Jammes et al., 2011). The plasma membrane is also a primary heat-sensing organelle that contains three types of Ca^{2+} conducting channels, including voltage-dependent Ca^{2+}-permeable channels (VDCCs), voltage-independent Ca^{2+}-permeable channels (VICCs), depolarization-activated Ca^{2+}-permeable channels (DACCs), and hyperpolarization-activated Ca^{2+}-permeable channels (HACCs) (Horváth et al., 2012; Liu et al., 2018). These channels are also known as cyclic nucleotide-gated ion channels (CNGCs), naturally tetrameric cationic, and comprise six transmembrane domains (Urquhart et al., 2011). Notably these CNGCs can be genetically modified as homotetrameric or heterotetrameric to improve their ability to respond to diverse and variable intensities (Ketehouli et al., 2019; Tan et al., 2020).

In maize, 11 plasma membrane-localized CNGC genes were identified, contributing a major role in heat tolerance (Hao and Qiao, 2018). The downregulation of *AtCNGC2*, *AtCNGC6*, *PpCNGCb*, and *PpCNGC* resulted in an increased accumulation of the following heat shock proteins; *Hsp18.2*, *Hsp25.3,* and *Hsp70* (Gao et al., 2012; Finka and Goloubinoff, 2014). Glutamate heat receptor-like channels also stimulated the Ca^{2+} signaling cascade on exposure to heat stress, and the exogenous application of glutamate resulted in improved heat tolerance in maize (Li et al., 2019). Other calcium channel families have been identified as responsible for the heat tolerance capability in maize, such as downregulation of synaptotagmin A that caused the downregulation of HSPs (Yan et al., 2017; Bourgine and Guihur, 2021). Under heat stress, maize annexin, such as *AnxZm33* and *AnxZm35* expression stimulated HACCs in the roots and cytosol (Bassani et al., 2004; Nichols, 2005; Mortimer et al., 2008; He et al., 2019). Phosphoinositide-specific phospholipases C (PLCs) genes, such as *PLC3* and *PLC9* are plasma membrane-localized heat sensors that stimulate phosphoinositide-signaling mediated Ca^{2+} channels (Rupwate and Rajasekharan, 2012; Hayes et al., 2021). For example, *ZmPLC1* encodes a PI-PLC, which plays a major role in maize roots during drought stress (Zhai et al., 2013).

Additionally, heat stress alters the normal working of the chloroplasts and mitochondria membranes, resulting in the over-accumulation of ROS simultaneously stimulating the Ca^{2+} signaling pathway (Li B. et al., 2018; Navarro et al., 2021). ROS, including NADPH-oxidase (NOX) and respiratory burst oxidase homolog, also stimulate signaling cascade for heat tolerance (Sagi and Fluhr, 2006; Takemoto et al., 2007; Chapman et al., 2019). However, the over-accumulation of ROS stimulates a Ca^{2+} based signaling cascade in the cytosol, which then stimulates phosphorylation mediated calcium-dependent protein kinases (CDPKs), causing a direct activation of the respiratory burst oxidase homolog D (RBOHD) (Gao et al., 2014; Marcec et al., 2019). RTH5 family proteins comprise four transmembrane functional domains responsible for membrane embedding and two EF motifs, FAD and NAD, required for Ca^{2+}transport (Lin et al., 2009; Nestler et al., 2014). In maize, RTH5 protein encodes NOX, distributed among all eukaryotic species (Bedard et al., 2007).

Heat-Induced Signal Cascades

Heat-sensitive CNGC gene families comprise the cyclic nucleotide-binding domain and calmodulin-binding domain (CaMBD), facing toward cytosol (Gao et al., 2012; Duszyn et al., 2019). Ca^{2+} sensor-dependent transcription regulation depends upon calcineurin b-like protein (CBL), CDPK, and calmodulin (CaM) (Reddy et al., 2004, 2011; Hashimoto and Kudla, 2011). CDPKs can sense Ca^{2+} to assist their EF-hand domain and transduce Ca^{2+} signals *via* their protein kinase domain (Shi et al., 2018). In maize, 35 CDPKs were identified (Ma et al., 2013), and *ZmCDPK1* has been characterized in cold-stressed roots and leaves (Weckwerth et al., 2015). CaMs bind with the C-terminal of CNGC family genes to activate the heat shock signaling pathway (Hao and Qiao, 2018), as mitogen-activated protein kinase 6 and calmodulin-binding protein kinase 3 (CBK3) (Yan et al., 2017). In maize, the Ca^{2+}–CaM contributes to the activation of ABA-induced antioxidants and nitric oxide (NO) production (Hu et al., 2007; Sang et al., 2008).

Many TFs, such as bZIP, CAMTA, MYB, and WRKY, bind with CaM proteins due to various abiotic and biotic stresses effects (**Table 1**; Yang et al., 2013). Among all, the CAMTA-mediated transcriptional regulation network is dominant, contributing against the diverse environmental stresses, including heat stress, salinity, drought, heavy metals, and exogenous application of hormones (Pandey et al., 2013; Yang et al., 2013; Yue et al., 2015). Additionally, CAMTA genes also play a key role in the mutual induction of regulation in expressing different stress-responsive genes and hormones (Reddy et al., 2000; Yang and Poovaiah, 2002). For example, heat stress induces upregulation of multiple *ZmCAMTA* genes in maize plants (Atkinson et al., 2013). In maize, *ZmCAMTA1*, *ZmCAMTA2*, and *ZmCAMTA3* have been identified, and their expression was upregulated during heat stress (Yue et al., 2015).

Heat stress affects plasma membrane, mitochondria, endoplasmic reticulum, and chloroplasts, resulting in ROS over-accumulation, a critical secondary signaling messenger (Sewelam et al., 2014; Czarnocka and Karpińskiski, 2018).

TABLE 1 | Heat stress-related transcription factor (TF) families in maize.

Family	Gene	Function/stress	References
HSF	*ZmHsf-01*	Heat stress response The upregulation of *ZmHsf-01* is probably with H3K9 hyperacetylation in the promoter region after heat treatment	Lin et al., 2011; Kim et al., 2012; Zhang et al., 2020c
	ZmHsf-03	Heat stress response	Lin et al., 2011
	ZmHsf-04	Heat stress response	Lin et al., 2011
	ZmHsf05	Heat stress response	Jiang et al., 2017
	ZmHsf06	Heat stress response	Li H.-C. et al., 2015
	HSFA6b	Heat stress response Connects ABA signaling and ABA-mediated heat responses	Huang et al., 2016; Gao et al., 2019
	HSFA1	Stimulates immediate expression of different heat shock responsive transcription factors (TFs), including *DREB2A*, *HSFA2*, *HSFA7*, HSFBs, and multiprotein-bridging factor 1C (*MBF1C*)	Yan et al., 2020; Zhao J. et al., 2021
	Hsftf13	Responses to ABA And thermotolerance Activate the Hsp90 and other HSFs	Huang et al., 2016; Li Z. et al., 2020
	ZmHsf-11	Heat stress response	Lin et al., 2011
	ZmHsf-17	Heat stress response	Lin et al., 2011
	ZmHsf-23	Heat stress response	Lin et al., 2011
	ZmHsf-25	Heat stress response	Lin et al., 2011
DREB/CBF	*ZmDREB2A*	Salt, heat, drought, and cold	Qin et al., 2007
AP2/EREBP	*Zm00001d008546*	Heat stress response	Jagtap et al., 2020
MYB/MYC	*ZmMYB-R1*	Cold, salinity, drought, ABA, and heat	Liu et al., 2012
bZIP	*ZmbZIP60 (Zm00001d046718)*	Heat stress bzip28 and bzip60 double-mutant plants are sensitive to heat stress Activates the expression of a type-A HSF, Hsftf13, which, in turn, upregulates the expression of a constellation of HSP genes	Liu et al., 2012; Li Z. et al., 2020
	ZmbZIP17	Drought, ABA, heat, and salt	Jia et al., 2009
	ZmbZIP28	Encodes an ER membrane-associated bZIP transcription factor, contributes to the upregulation of heat-responsive genes and to heat tolerance *bZIP28* binds directly to the promoters of heat-responsive genes	Gao et al., 2008; Zhang et al., 2017
	ZmbZIP4	Heat, cold, salinity, and ABA Contributes to stress resistance in maize by regulating ABA synthesis and root development	Ma et al., 2018
NAC	*Zm00001d010227*	Drought and heat stress	Jagtap et al., 2020
GARP	*Zm00001d044785 (ZmGlk1)*	Heat stress The expression of *ZmGLK1* or *ZmG2* in rice leads to elevated levels of Chl, carotenoid, and xanthophyll cycle pigments and to increased levels of some PSII components	Jagtap et al., 2020; Yeh et al., 2021
WRKY	*ZmWRKY44*	Salt, heat, ABA, and H_2O_2 Have transcriptional activation functions	Kimotho et al., 2019
	ZmWRKY106	Drought, high temperature, ABA, and salt Play a role in the abiotic stress response by regulating stress-related genes through the ABA-signaling pathway Reactive oxygen species (ROS) scavenging	Wang et al., 2018a
	ZmWRKY40	Drought, salinity, heat, and ABA Regulating stress-responsive genes, such as *DREB2B* and *RD29A*	Wang et al., 2018b; Leng and Zhao, 2020
HSP	*ZmERD2*	Heat, salinity, cold, PEG, and dehydration	Song et al., 2016
	ZmERD3	mRNA accumulation	Song et al., 2018
NF-Y	*ZmNF-YA3*	Drought and heat *ZmNF-YA3* is directly bound to the promoter regions of two bHLH TFs (*bHLH92* and FMA) and one bZIP TF (*bZIP45*) involved in the ABA-related pathway	Su et al., 2018; Kimotho et al., 2019

TABLE 2 | Key genes related to heat stress mechanisms.

Genes	Gene description	Function	References
Zm00001d044732 ABA	ABA-induced protein	Acts as a signaling hormone in plants against abiotic stress, but its function in energy homeostasis under heat stress	Cheikh and Jones, 1994
Zm00001d045675 (*AS*)	Asparagine synthetase homolog 1	Elevated maximum daily temperature induces alternative splicing and the roles of SR (serine/arginine-rich) 45a	Li and Howell, 2021
Zm00001d047847 (SR45a)	Serine/arginine-rich splicing factor SR45a	Elevated maximum daily temperature induces alternative splicing and the roles of SR (serine/arginine-rich) 45a	Li and Howell, 2021
GRMZM2G388045 GAMETE EXPRESSED 1 (GEX1)	Encode GAMETE EXPRESSED 1 (GEX1)	Protective roles for reproductive stage under HS	Gao et al., 2019
GRMZM2G377194 CYCD5;1	Encode cyclin D5;1	Protective roles for reproductive stage under HS Increased seed set	Gao et al., 2019
GRMZM2G406715	Encodes a bZIP transcription factor		Gao et al., 2019
GRMZM2G062914 (MPK14)	Expresses a maize mitogen-activated protein kinase, MPK14.	Its Arabidopsis ortholog is *AtMPK1* can mediate and augment ABA signaling	Gao et al., 2019
GRMZM2G059225 (ARF)	Discolored-paralog3 putative ARF GTPase-activating domain protein with ankyrin repeat-containing protein	GTPase activator activity	Gao et al., 2019
Zm00001d028408 (*HSP26)*	Heat shock protein 18 (Heat shock protein 26)	Early heat stress marker gene	Nieto-Sotelo et al., 1990; Abou-Deif et al., 2019
Zm00001d006036 (ZmHSP70)	Heat shock 70 kDa protein	Heat stress response Induced by heat in diurnal temperature cycles	Rashed et al., 2021
Zm00001d003554 (ZmHSP22)	22.0 kDa class IV heat shock protein	Heat stress response Induced by heat in diurnal temperature cycles	Rashed et al., 2021
Zm00001d028557 (ZmHSP17.9)	17.9 kDa class I heat shock protein	Heat stress response Induced by heat in diurnal temperature cycles	Rashed et al., 2021
Zm00001d047542 (ZmHSP17.6)	17.6 kDa class II heat shock protein	Heat stress response Induced by heat in diurnal temperature cycles	Rashed et al., 2021
Hsp18.2	Heat shock protein 18.2	Heat stress response	Borghi, 2010
HSP90	Heat shock protein 90	Induced by heat in diurnal temperature cycles	Marrs et al., 1993
Zm00001d038806 (HSP101)	Heat shock protein 101	Induced by heat in diurnal temperature cycles Play essential roles in both induced and basal thermotolerance and primary root growth	Nieto-Sotelo et al., 2002
Zm00001d014090	Mitochondrial heat shock protein 60	Induced by heat in diurnal temperature cycles	Prasad et al., 1990

(Continued)

TABLE 2 | (Continued)

Genes	Gene description	Function	References
GRMZM2G409658	Encodes a Calcineurin b-like protein-interacting protein kinase (CIPK)	Involved in the stress response process Function in signal transduction	Gao et al., 2019
GRMZM2G116452	Encodes Peroxidase superfamily protein	Involved in the stress response process	Gao et al., 2019
GRMZM2G060349	Encodes a DNA mismatch repair protein, MutS2	Upregulated by high temperature Involved in the stress response process	Gao et al., 2019
GRMZM2G023081	Encodes a cysteine-rich domain-containing protein	Involved in the stress response process	Gao et al., 2019
GRMZM2G061515	Auxin-responsive GH3 family protein expresses an indole-3-acetic acid-amido synthetase	Involved in the stress response process Function in signal transduction Involved in maintaining auxin homeostasis *in vivo* through catalyzing excess IAA conjugation to amino acids	Ludwig-Müller, 2011
GRMZM2G377194	Encodes a D-type cyclin, CYCD5;1	Upregulated by high temperature	Gao et al., 2019
GRMZM2G026892	Encodes a cysteine-rich protein (CRP)	Lose its stability under HS, and thus mean that it is unable to protect the process of seed-set	Gao et al., 2019
GRMZM2G176605	Encodes an ankyrin repeat domain-containing protein	Both pollen tube growth and germination are damaged due to the downregulation of an ankyrin repeat-containing protein	Huang et al., 2006
ZmHSP17.0 and Zm00014a_022730 (ZmHSP17.8)	Heat shock protein 17.2 and Heat shock protein, respectively	Form dodecamers at temperatures lower than heat shock (HS) Protect cellular proteins from aggregation during times of heat stress	Klein et al., 2014
chloroplast sHSP26	Small heat shock protein, chloroplastic	Involved in maize heat tolerance	Hu et al., 2015
Zm00014a018076 ZmHSP16.9	Class I heat shock protein 1	Expressed in root, leaf, and stem tissues under 40°C treatment, which HS and exogenous H_2O_2 upregulate	Sun et al., 2012
Zm00001d028325	brs1;brassinosteroid synthesis1	Confers thermotolerance	Dhaubhadel et al., 1999
Zm00001d029149	Zinc finger protein CONSTANS-LIKE 13	Heat response gene	Jagtap et al., 2020
Zm00001d029892	Metalloendoproteinase 1-MMP	Heat response gene	Jagtap et al., 2020
Zm00001d033805	Glutamate decarboxylase 1 (GAD 1)	Heat response gene Ca2+/calmodulin has been shown to bind GAD and stimulate its activity	Sachs et al., 1996; Jagtap et al., 2020
Zm00001d002597	Rho GTPase-activating protein 3	Heat response gene	Jagtap et al., 2020
Zm00001d003643	L-Ascorbate peroxidase S chloroplastic/mitochondrial	Heat response gene	Jagtap et al., 2020

(Continued)

TABLE 2 | (Continued)

Genes	Gene description	Function	References
Zm00001d006036	Heat shock 70 kDa protein 9 mitochondrial	Heat response gene	Jagtap et al., 2020
Zm00001d041701	Acyl carrier protein 2 chloroplastic	Heat response gene	Jagtap et al., 2020
Zm00001d048592	rca2; RUBISCO activase2: encodes the beta form of RUBISCO activase	Heat response gene	Jagtap et al., 2020
Zm00001d051056	*S*-adenosylmethionine decarboxylase proenzyme	Heat response gene	Jagtap et al., 2020
Zm00001d017729	Serine/threonine-protein kinase MHK	Heat response gene	Jagtap et al., 2020
Zm00001d017992	Metalloendoproteinase 1	Heat response gene	Jagtap et al., 2020
Zm00001d037273	Peptide methionine sulfoxide reductase msrB	Heat response gene	Jagtap et al., 2020
Zm00001d037663	NADH-ubiquinone oxidoreductase 10.5 kDa subunit	Heat response gene	Jagtap et al., 2020
Zm00001d039188	Putative leucine-rich repeat receptor-like protein kinase family protein	Heat response gene	Jagtap et al., 2020
Zm00001d011760	DNAJ heat shock N-terminal domain-containing protein	Heat response gene DNAJ proteins are co-chaperones of the Hsp70 machine, which play a critical role by stimulating Hsp70 ATPase activity, thereby stabilizing its interaction with client proteins	Pegoraro et al., 2011; Jagtap et al., 2020
ZmNIP2-3	Aquaporin NOD26-like membrane integral protein	Heat response gene Differentially phosphorylated under heat stress Encode aquaporins involved in silicon transport	Brusamarello-Santos et al., 2012; Jagtap et al., 2020
Zm00001d045220	Late embryogenesis abundant protein group 2	Heat response gene The LEA proteins are a family of hydrophilic proteins presumed to play a protective role during exposure to different abiotic stresses	Amara et al., 2013; Jagtap et al., 2020
Zm00001d046363	*S*-adenosyl-L-methionine-dependent methyltransferases superfamily protein	Heat response gene	Jagtap et al., 2020
Zm00001d002262	Uncharacterized LOC100502514	High grain yield QTL is related to heat stress	Frey et al., 2016
Zm00001d005002	Carbohydrate transporter/sugar porter/transporter	High grain yield QTL is related to heat stress	Frey et al., 2016
Zm00001d004960	Uncharacterized LOC100281571	High grain yield QTL is related to heat stress	Frey et al., 2016
Zm00001d043407	Uncharacterized LOC100282523	High grain yield QTL is related to heat stress	Frey et al., 2016
Zm00001d013918	Thylakoid lumenal 17.4 kDa protein chloroplastic	High grain yield QTL is related to heat stress	Frey et al., 2016
Zm00001d047096	Beta-expansin 1a	High grain yield QTL is related to heat stress	Frey et al., 2016

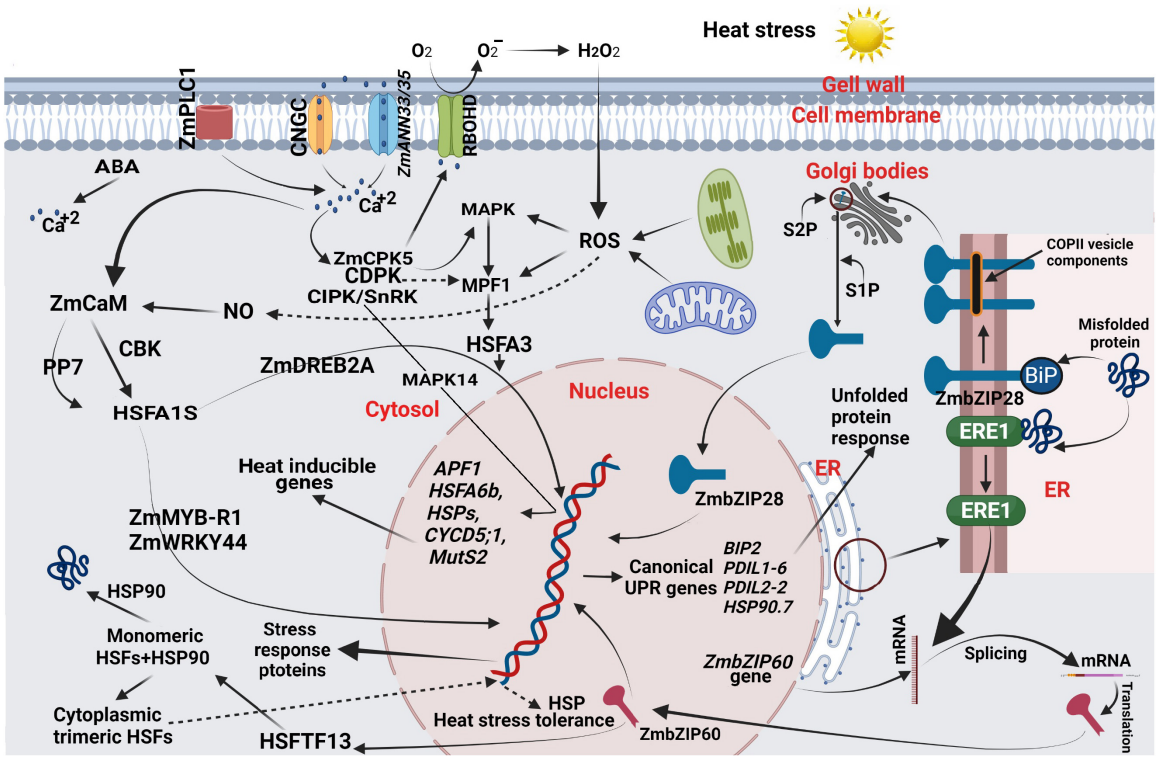


FIGURE 3 | A heat stresses responsive regulatory network in maize. Heat stress damages the cell membrane when exposed to heat stress and promotes the release of apoplastic Ca^{2+}. Heat stress disturbs the plasma membrane's fluidity and permeability, resulting in a loss in function of chloroplasts and mitochondria, higher cytosolic Ca^{2+}, ROS, NO, and over-accumulation of misfolded or unfolded proteins. Increased cytosolic Ca^{2+}, ROS, and NO are secondary messengers and stimulate downstream regulatory networks. Heat stress disrupts protein homeostasis, inducing unfolded-protein response (UPR) and signaling pathways mediated by IRE1-*ZmZIP60* and *ZmZIP28*. The *ZmZIP60* activates the expression of a type-A HSF and *HSFTF13*, which upregulates the expression of HSP genes, i.e., *Hsp90*. The Ca^{2+} signaling is essential in heat tolerance of seed-set in maize under field conditions, where calcium, a critical secondary messenger, converges signals transmitted from high temperature, membrane fluidity, calcium efflux, and ABA (among others), amplifying them through the activation downstream of genes, such as *HSFA6b*, *ABF1*, *CYCD5*;1, *MutS2*, and HSPs during reproductive stage via the MAPK pathway, and eventually enhance maize tolerance to heat stress for seed-set. This figure was made using BioRender.

When maize was exposed to high temperature, the related genes for protein processing in the endoplasmic reticulum (ER) pathway were significantly enriched, which mainly induced heat shock proteins expressions, such as *Hsp40*, *Hsp70*, *Hsp90*, *Hsp100* (**Table 2**), and small HSP (Qian et al., 2019). In response, heat stress response (HSR) genes, such as MYB, AP2/EREBP, NAC, BRs, HSPs, Rubisco, antioxidants (APX and Glutathione *S*-transferase), and kinases are activated to respond to ROS (Khan et al., 2019; Jagtap et al., 2020). ROS, such as H_2O_2 produced by RBOHD, acted as a signaling molecule that directly stimulates mitogen-activated protein kinases, such as MAPK3 and MAPK6, which activate Ca^{2+} or CDPK-mediated phosphorylation *HSFA2* and *HSFA4a* (Luna et al., 2011; Frederickson Matika and Loake, 2014). H_2O_2 also directly activates *HSFA1a*, *HSFA4a*, and *HSFA8* transcription factors, and NO signaling cascade, inducing the binding of heat shock element (HSE) with promoters of HSPs (Miller and Mittler, 2006; Li B. et al., 2018). Phytohormones, such as IAA, CKs, ABA, ET, GA, SA, BRs, and JA, contribute to the signal transduction pathways during heat stress (Eyidogan et al., 2012; Li N. et al., 2021). Several studies indicated calcineurin b-like protein-interacting protein kinase (CIPK) and named sucrose non-fermenting 1-related kinase (SnRK) family members as key players in pollen tube growth seed-set and abiotic stress by perceiving and mediating Ca^{2+} signaling (Yang et al., 2008; Zhou et al., 2015). The Ca^{2+} signaling plays an essential role in the heat tolerance of seed-set in maize under field conditions. In this, calcium, as the critical secondary messenger converges signals transmitted from high temperature, membrane fluidity, calcium efflux, and ABA (among others), amplifies them through activation downstream of genes, such as *HSFA6b*, *ABF1*, *CYCD5;1*, MutS2, and HSPs during reproductive stage via the MAPK pathway (**Figure 3** and **Tables 1**, **2**), and eventually enhancing maize tolerance to heat stress for seed-set (Gao et al., 2019).

Heat Stress-Mediated Transcriptional Regulation

Heat stress stimulates transcription of heat stress factors (HSFs) (**Table 1**) which subsequently results in overexpression of HSPs to mitigate the effect of heat stress (El-Sappah et al., 2012, 2017). However, only HSF or HSP overexpression has no significant role in heat tolerance, indicating that both gene families act synergistically (Wang et al., 2004).

Maize contains 25 HSFs, further divided into A, B, and C subclasses (Lin et al., 2011). Class A HSFs contribute to

transcriptional activation, whereas the rest two classes have no specific role in transcriptional activation due to the absence of specific protein motifs (Reddy et al., 2014; Haider et al., 2021). A master transcription activator *HSFA1* stimulates immediate expression of different heat shock responsive transcription factors (TFs), including dehydration responsive element binding protein 2A (*DREB2A*), *HSFA2*, *HSFA7*, HSFBs, and multiprotein-bridging factor 1C (*MBF1C*) (Yan et al., 2020; Zhao J. et al., 2021). Additionally, heat stress stimulates the transactivation of *HSFA1* upon the interaction between *Hsp70* and *Hsp90* (Ohama et al., 2017).

HSFA1 is comprised two alleles; *HSFA1a* and *HSFA1b* (El-Shershaby et al., 2019). *HSFA1* stimulates transcription of ERF/AP2 and *DREB2A* (Mizoi et al., 2012), *HSFA2* acts as a heat-inducible trans-activator of different genes (Chauhan et al., 2013), and *HSFA3* regulates the expression of *DREB2A* and *DREB2C* (Chen et al., 2010). *ZmHsf-6* belongs to class A1, *ZmHsf-1*, *ZmHsf-4*, *ZmHsf-5,* and *ZmHsf-17* belong to subclass A2, *ZmHsf-3*, *ZmHsf-11,* and *ZmHsf-25* belong to class B, all contributing key roles in heat tolerance in maize (**Table 1**; Lin et al., 2011; Zhang et al., 2020b; Jiang et al., 2021). The expression of *ZmHsf-6* was localized in pollens, and its expression was upregulated under heat stress (Jiang et al., 2021). Furthermore, *Hsp70-2* and *Hsp70-4* are downstream targets of *ZmHsf-6* and contribute significantly to abiotic stress response (Li H.-C. et al., 2015). The highest expression of *ZmHsf-1*, *ZmHsf-3,* and *ZmHsf-23* was observed in maize plants exposed to heat stress proving their significant role in maize during heat stress (**Tables 1**, **2**; Lin et al., 2011).

In maize, ZmAP2/ERF is the most prominent TFs family comprised of 292 potential members, out of which 153 belong to the ERF subfamily (Zhou et al., 2012). Also, *ZmDREB2A* plays an essential role in heat tolerance and during drought tolerance in maize plants (Qin et al., 2007) when subjected to heat stress, *DREB2A* regulates transcription of *HSFA3* by stimulating coactivation complex comprised of NUCLEAR FACTOR Y, SUBUNIT A2 (NF-YA2), DNA POLYMERASE II SUBUNIT B3-1 (DPB3-1)/NF-YC10, and NF-YB3 (Schramm et al., 2008). Additionally, heat stress causes the over-accumulation of secondary heat stress-responsive ROS, with *HSFA4a* and *HSFA8* acting as sensors (Cimini et al., 2019; Xu et al., 2021). The maize genome contains 72 MYB TFs, with only 46 playing a key role in abiotic stress response (Du et al., 2012; Chen Y. et al., 2018). Maize plants exposed to abiotic stress factors including heat, salinity, drought, cold, and ABA resulted in overexpression of *ZmMYB-R* (**Table 2**; Liu et al., 2012; Kimotho et al., 2019).

Protein Homeostasis Under Heat Stress

Heat stress interrupts the molecular mechanism of proper protein folding in the ER, which is toxic to ER (Howell, 2013; Fragkostefanakis et al., 2016). Unfolded-protein response (UPR) is an adaptive change in ER that avoids the toxic effect of misfolded proteins (**Figure 3**; Vitale and Boston, 2008); however, prolonged toxicity resulted in programmed cell death (Iurlaro and Muñoz-Pinedo, 2016). UPR also stimulates the signaling cascade to send an ER message to the nucleus to initiate the expression of toxicity-responsive genes (Neill et al., 2019). ER stress activates UPR *via* splicing of *ZmbZIP60* transcripts with the help of kinase (IRE1) and membrane-localized TFs, such as *ZmbZIP17* and a type II membrane protein *ZmbZIP28* (**Figure 3**; Nawkar et al., 2018; Pastor-Cantizano et al., 2020). Both signaling factors bind, producing heterodimers resulting from the upregulation of stress-responsive genes (Gayral et al., 2020). N-terminal domain of *bZIP28* transcription factor face toward cytosol, whereas C-terminal domain face toward the lumen of ER (Liu et al., 2007). From ER, *bZIP28* was first associated with Sar1 GTPase for packaging inside COPII vesicles and then exported to Golgi bodies for modifications by the Golgi site-1 and site-2 proteases (S1P and S2P) (Chung et al., 2018; Pastor-Cantizano et al., 2020). Under heat stress, the N-terminus of bZIP28 is cleaved by S2P, released inside the cytosol, and finally transported to the nucleus. Similarly, IRE1 activates the *bZIP60* transcription factor by splicing and transporting to the nucleus (Reimold et al., 2000; Huang et al., 2017).

The second abiotic stress signaling pathway initiated from ER is comprised of IRE1, a splicing protein, namely kinase/ribonuclease, which activates the *bZIP60* transcription factor *via* proteolysis (Kørner et al., 2015; Pastor-Cantizano et al., 2020). When maize seedlings are exposed to heat stress, the transcript of *ZmbZIP60* is activated by splicing and transferred to the nucleus to induce the expression of HSPs (Li Z. et al., 2018). Another ER-localized *ZmbZIP17* transcription factor is activated under heat and ABA stress and subsequently transported into the nucleus to transactivate HSPs with the help of UPR (Cacas, 2015). HSPs maintain cell metabolites stability under heat stress (Efeoğlu, 2009). Major HSPs which play a key role during heat tolerance in maize are *ZmHSP16.9*, *ZmsHSP17*, *ZmsHSP17.8*, *ZmsHSP26*, *ZmHSP68*, *ZmHSP70*, *ZmHSP90*, and *ZmHSP101* (**Tables 1**, **2**; Sun et al., 2012; Klein et al., 2014; Kumar et al., 2019; Zhao Y. et al., 2021). For example, when maize plants are exposed to heat stress at the reproductive stage, *ZmHSP101* is overexpressed in pollens to prevent their mortality, keep them viable and result in more grains (Gurley, 2000). Generally, transcriptome studies of four heat-tolerant and four heat-susceptible inbred lines, 607 heat-responsive genes, and 39 heat-tolerance genes were identified (Frey et al., 2015).

APPROACHES FOR IMPROVING THERMOTOLERANCE

Agronomic Management

Several agronomic management practices, such as soil and nutrients management, crop rotation, plantation rate, timing, and irrigation, are beneficial in heat tolerance in maize (Sabagh et al., 2020). For example, early sowing of longer season varieties can overcome heat stress in spring maize (Liu et al., 2013). Similarly, nighttime subsurface drip irrigation reduces the root-zone causes in soil temperature, resulting in improved growth and yield in maize (Dong et al., 2016). Additionally, optimized irrigation enhances water use efficiency and aids heat tolerance (Tao and Zhang, 2010). Maize crops exposed to drought and heat stresses during vegetative growth are likely to have shortened reproductive growth stage, resulting in yield loss; however, they can be managed by maintaining soil moisture contents at 65% *via* drip irrigation (Yuan et al., 2004).

Heat stress negatively affects the absorption of adequate concentrations of minerals and nutrients required for normal metabolic and physiological processes (Fahad et al., 2017). For example, nitrogen (N) and magnesium (Mg) are structural parts of chlorophyll, phosphorus (P) is a structural part of nucleic acids (DNA and RNA), and potassium is required for osmotic regulation and activation of enzymes (Waraich et al., 2012; Meena et al., 2020). Additionally, nitrogen plays a key role in utilizing absorbed light, carbon assimilation, and heat tolerance (Meena et al., 2019). Thus, nutrient management can mitigate physiological disorders of maize plants exposed to heat stress, such as applying potassium (K), improving membranes' stability, and maintaining turgor pressure in maize (Tao and Zhang, 2010). Specifically, nutrient management at the grain-filling stage contributes significantly to increased yield. Additionally, applying bioregulators, such as Putrescine and Thiourea, improved heat tolerance in maize seedlings (Yadav et al., 2017).

Exogenous application of plant growth regulators, such as ABA and $CaCl_2$, play a key role in heat tolerance in maize by improving the capability of PSII and stopping the ROS, respectively (Gong et al., 1997; Tao and Zhang, 2010). Artificial application of auxin also improves abiotic stresses, including drought, salinity, waterlogging, heat and cold stress, UV irradiation, and heavy metals tolerance (Vardhini and Anjum, 2015). Similarly, the CK application helps mitigate the denaturation of proteins metabolites due to over-accumulation of ROS and improves the rate of photosynthesis in maize (Zulfiqar and Ashraf, 2021). Additionally, the application of SA and ABA ameliorate the effects of abiotic stress factors, improve seedling growth, mitigate ROS, stimulate the cell-signaling pathway via biosynthesis of NO, resulting in enhanced plant growth and crop yield (Meena et al., 2015). Exogenous application of GA improves the growth and development of plants via mitigating adverse effects of abiotic stresses (Yamaguchi, 2008). The BRs are a newly discovered group of plant hormones with promising potential in abiotic stress tolerance, ROS tolerance, and heat stress tolerance (Arif et al., 2020).

Conventional Breeding

Availability of genetic variations in a population and relationship among traits is base for any successful plant breeding program (Lorenz et al., 2011; Aruah et al., 2012). The exact knowledge of genetic parameters, including population structure, heritability, and genotypic variance among the traits under selection pressure, helps develop efficient breeding lines (Farshadfar et al., 2013). In traditional breeding, selection procedures have been developed to identify and subsequently multiply maize verities with improved heat tolerance (Gong et al., 2015; Gedil and Menkir, 2019). Breeding heat-tolerant varieties is an effective strategy for improving heat tolerance in the spring maize grain-filling stage (Mishra et al., 2021). Many maize cultivars have been screened for canopy structure, flag leaf stomata, and rate of photosynthesis to obtain maximum yield and heat tolerance (Sah et al., 2020). The application of genetic markers accompanied by next-generation sequencing (NGS) has accelerated various development in breeding techniques (Le Nguyen et al., 2019).

Quantitative Trait Locus and Marker-Assisted Breeding

Conventional breeding has significantly improved the selection of heat-tolerant crop varieties (Fu et al., 2012; Bai et al., 2018). During heat stress at the reproductive stage, quantitative trait locus (QTLs) play a major role in pollen production and preservation, receptivity and pollen tube development, proper grain-filling, and post-anthesis leaf senescence (Tiwari and Yadav, 2019). Therefore, the number and origin of QTLs are pivotal to mitigating heat stress (Sharma et al., 2017). Also, the number of QTLs and their roles studied in heat stress-exposed maize seedlings were six during pollen heat tolerance (Tiwari and Yadav, 2019), 11 at two different loci (HSI_{DY} and HSI_{DYA}) during grain-filling located on chromosomes 2, 3, 5, and 9 (Frey et al., 2016) and six during heat susceptibility index (Van Inghelandt et al., 2019). Moreover, 6 and 5 QTLs have been detected associated with pollen tube growth and pollen germination, respectively, using a recombinant inbred population with 45 materials under abiotic stresses, including high temperature (Frova and Sari-Gorla, 1994; Frova et al., 1998). Therefore, these QTLs can be employed in conventional breeding to improve heat tolerance in maize cultivars (Frey et al., 2015). Previously explored maize QTLs can be assessed by exploring the following datasets; http://www.maizegdb.org and http://www.plantstress.com.

Quantitative trait locus are being widely employed in the introgression of favorable alleles in elite maize cultivars *via* backcrossing and confirmation in F1 (Frey et al., 2016; Cerrudo et al., 2018). Molecular markers including simple sequence repeats (SSR), single nucleotide polymorphisms (SNPs), random amplified polymorphic DNA (RAPD), and amplified fragment length polymorphism associated with heat tolerance are also employed in MAS (El-Sappah et al., 2019; Younis et al., 2020). The SNP and SSR are vast in identifying genotypes with maximum heat tolerance (Sabagh et al., 2020). Genome-wide association study (GWAS) is also a valuable tool in identifying novel QTLs responsible for heat tolerance to improve the genetic pool in maize breeding (Wen et al., 2014; Lafarge et al., 2017; Lin et al., 2020). GWAS is also helpful in revealing the linkage between SNPs and specific traits that confers heat tolerance at the flowering stage (Lafarge et al., 2017). GWAS was performed in sub-tropical maize, identifying significant SNPs and haplotype blocks associated with yield contributing traits that help select donor lines with favorable alleles for multiple characteristics, providing insights into heat stress tolerance genetics (Longmei et al., 2021; Seetharam et al., 2021).

Genetic and Metabolic Engineering

Recently, several gene families have been identified and subsequently characterized in maize involved in heat stress response, such as heat shock protein-70 and heat shock factor (Casaretto et al., 2016; Jagtap et al., 2020; Jiang et al., 2021). Additionally, transcriptomic profiling of maize seedlings exposed to heat stress showed several differentially expressed genes employed in developing improved heat-tolerant maize varieties using robust genome editing techniques, such as RNAi and CRISPR/Cas9 (El-Sappah et al., 2021; Razzaq et al., 2021;

Singh et al., 2021). Integration of robust genetic engineering techniques has accelerated conventional breeding of maize by reducing the time of variety development with the application of genetic markers in the early detection of desired traits in F1 (Ahmar et al., 2020). Furthermore, fast growth in NGS has enabled high throughput sequencing of desired traits which is cost-effective, time-saving, reproducible, impossible to achieve *via* conventional breeding (Kulski, 2016).

In maize, several genes have been identified to develop genetically modified (GMO) or transgenic verities with improved heat tolerance (Tiwari and Yadav, 2019; Malenica et al., 2021). For example, overexpression of *ZmVPP1* and *OsMYB55* resulted in increased heat and drought tolerance in maize (Casaretto et al., 2016; Wang et al., 2016). Furthermore, the HSFs gene family plays a pivotal role during heat stress (Haider et al., 2021). Up to 25 HSFs have been reported in several cereal crops, and their key role is confirmed in regulating Hsp genes (Guo et al., 2008). This discovery of identifying and characterizing HSFs and their role in regulating Hsp genes has provided a fundamental basis for the development of GM maize with the highest heat stress tolerance (Ahuja et al., 2010). Furthermore, the overexpression of chloroplast localized 6-phosphogluconate dehydrogenase (6PGDH) PGD3 displayed an over-accumulation of starch in maize endosperm under heat stress improved grain size and weight, whereas, *WPGD1* and *WPGD2* transgenes can increase the number of kernels to mitigate losses in high nighttime temperature conditions (Ribeiro et al., 2020). In the metabolic studies of Joshi et al. (2021), a total of 5,136 genes expression were affected in response to heat stress.

CONCLUSION

Plant growth, development, and productivity are significantly affected by abiotic or biotic stresses because the plants, as sessile organisms, cannot move to favorable environments. Globally, high temperature has become a significant stressor that has accelerated the increase in the air temperature in the recent decades. Maize is a C4 crop species that belongs to the Poaceae family and is moderately sensitive to abiotic stresses, such as temperature. Maize plants are considered to be heat tolerant, but an extended duration of a temperature $>35°C$ is deemed to be unfavorable for the development and growth of crops. In comparison, temperatures above 40°C, mainly during flowering and grain-filling season, will negatively affect the grain productivity of grain in these plants.

Heat stress may alter several physiological processes, namely membrane fluidity, net photosynthesis, respiration rate, hormone levels, osmolytes accumulation, and so on. High temperatures are related to several metabolic events at cellular and sub-cellular levels, leading to the production of ROS and oxidative stress. The anti-oxidative defense system is a prospective mechanism to protect them from ROS damage in plants. Finally, several agronomic management practices, such as the management of soil and nutrients, crop rotation, plantation rate, timing, and irrigation, are beneficial in developing heat tolerance in maize, along with advanced genomic tools. This review summarizes heat stress sensing, the induction of signaling cascade, symptoms, heat stress-related genes, molecular feature of maize response, and approaches to establishing heat-tolerant maize varieties.

FUTURE PERSPECTIVES

Environmental factors affecting maize growth and development include rainfall, light intensity, temperature (heat and cold), relative humidity, heavy metal stress, and wind speed. Drought and heat stress have severe implications for sustainable crop yield. Therefore, it is necessary to develop maize verities having maximum tolerance against drought and heat stress with breeding and genetic engineering. Although substantial efforts had been made to develop heat-tolerant maize verities *via* conventional breeding, it has limitations, such as being laborious, time-consuming, and the possibility of only intra-species gene transfer. However, modern genetic approaches, such as GWAS and genotyping by sequencing, have facilitated inter-species gene transfer to develop maize verities with the highest heat tolerance. Additionally, the complementation of conventional breeding with the development of modern and robust genetic engineering techniques, such as RNAi, CRISPR/Cas9, and TILLING, has accelerated the process of variety development.

AUTHOR CONTRIBUTIONS

AE-S, KE-T, JL, SAR, RRM, and MA: conceptualization. AE-S: writing original draft and collecting the data. AE-S and ASE: draw the figures. AE-S, KY, SHW, MB, QH, ZAD, MMAE, MK, RRM, JL, and KE-T: review, and editing of the manuscript. AE-S, KE-T, and MA: writing final copy. All authors contributed to the article and approved the submitted version.

ACKNOWLEDGMENTS

Many thanks to Prof. Dr. Wang Ling, the President of Yibin University, for her support. At the same time, thanks to Zhou Lei and Jiang Qianwen, the International Office Team, for their continuous help to achieve a suitable environment for research. KE-T would like to thank the library at Murdoch University, Australia, for the valuable online resources and comprehensive databases.

REFERENCES

Abou-Deif, M. H., Rashed, M. A.-S., Khalil, K. M., and Mahmoud, F. E.-S. (2019). Proteomic analysis of heat shock proteins in maize (*Zea mays* L.). *Bull. Natl. Res. Cent.* 43:199.

Ahmar, S., Gill, R. A., Jung, K.-H., Faheem, A., Qasim, M. U., Mubeen, M., et al. (2020). Conventional and molecular techniques from simple breeding to speed breeding in crop plants: recent advances and future outlook. *Int. J. Mol. Sci.* 21:2590. doi: 10.3390/ijms2107 2590

Ahmed, I., Ur Rahman, M. H., Ahmed, S., Hussain, J., Ullah, A., and Judge, J. (2018). Assessing the impact of climate variability on maize using simulation modeling under semi-arid environment of Punjab, Pakistan. *Environ. Sci. Pollut. Res.* 25, 28413–28430. doi: 10.1007/s11356-018-2884-3

Ahuja, I., De Vos, R. C., Bones, A. M., and Hall, R. D. (2010). Plant molecular stress responses face climate change. *Trends Plant Sci.* 15, 664–674. doi: 10.1016/j.tplants.2010.08.002

Alam, M. R., Nakasathien, S., Molla, M. S. H., Islam, M. A., Maniruzzaman, M., Ali, M. A., et al. (2021). Kernel water relations and kernel filling traits in maize (*Zea mays* L.) are influenced by water-deficit condition in a tropical environment. *Front. Plant Sci.* 12:717178. doi: 10.3389/fpls.2021.717178

Amara, I., Capellades, M., Ludevid, M. D., Pagès, M., and Goday, A. (2013). Enhanced water stress tolerance of transgenic maize plants over-expressing LEA Rab28 gene. *J. Plant Physiol.* 170, 864–873. doi: 10.1016/j.jplph.2013.01.004

Arif, Y., Singh, P., Siddiqui, H., Bajguz, A., and Hayat, S. (2020). Salinity induced physiological and biochemical changes in plants: an omic approach towards salt stress tolerance. *Plant Physiol. Biochem.* 156, 64–77. doi: 10.1016/j.plaphy.2020.08.042

Aruah, B. C., Uguru, M. I., and Oyiga, B. C. (2012). Genetic variability and inter-relationship among some Nigerian pumpkin accessions (*Cucurbita* spp.). *Int. J. Plant Breed.* 6, 34–41.

Atkinson, N. J., Lilley, C. J., and Urwin, P. E. (2013). Identification of genes involved in the response of Arabidopsis to simultaneous biotic and abiotic stresses. *Plant Physiol.* 162, 2028–2041. doi: 10.1104/pp.113.222372

Bai, S., Yu, H., Wang, B., and Li, J. (2018). Retrospective and perspective of rice breeding in China. *J. Genet. Genomics* 45, 603–612. doi: 10.1016/j.jgg.2018.10.002

Banerjee, A., and Roychoudhury, A. (2018). "Abiotic stress, generation of reactive oxygen species, and their consequences: an overview," in *Reactive Oxygen Species in Plants: Boon or Bane? Revisiting the Role of ROS*, eds V. P. Singh, S. Singh, D. Tripathi, S. Mohan Prasad, and D. K. Chauhan (Hoboken, NJ: John Wiley & Sons Ltd), 23–50. doi: 10.1002/9781119324928.ch2

Bartels, D., and Sunkar, R. (2005). Drought and salt tolerance in plants. *CRC Crit. Rev. Plant Sci.* 24, 1446–1452.

Bassani, M., Neumann, P. M., and Gepstein, S. (2004). Differential expression profiles of growth-related genes in the elongation zone of maize primary roots. *Plant Mol. Biol.* 56, 367–380. doi: 10.1007/s11103-004-3474-y

Baus, D. (2017). *Overpopulation and the Impact on the Environment*. Master thesis. New York, NY: City University of New York.

Bechtold, U., Penfold, C. A., Jenkins, D. J., Legaie, R., Moore, J. D., Lawson, T., et al. (2016). Time-series transcriptomics reveals that *AGAMOUS-LIKE22* affects primary metabolism and developmental processes in drought-stressed Arabidopsis. *Plant Cell* 28, 345–366. doi: 10.1105/tpc.15.00910

Bedard, K., Lardy, B., and Krause, K. H. (2007). NOX family NADPH oxidases: not just in mammals. *Biochimie* 89, 1107–1112. doi: 10.1016/j.biochi.2007.01.012

Borghi, L. (2010). Inducible gene expression systems for plants. *Plant Dev. Biol.* 655, 65–75. doi: 10.1007/978-1-60761-765-5_5

Bourgine, B., and Guihur, A. (2021). Heat shock signaling in land plants: from plasma membrane sensing to the transcription of small heat shock proteins. *Front. Plant Sci.* 12:710801. doi: 10.3389/fpls.2021.710801

Bruns, H. A. (2003). Controlling aflatoxin and fumonisin in maize by crop management. *J. Toxicol. Toxin Rev.* 22, 153–173. doi: 10.1081/txr-120024090

Brusamarello-Santos, L., Pacheco, F., Aljanabi, S., Monteiro, R., Cruz, L., Baura, V., et al. (2012). Differential gene expression of rice roots inoculated with the diazotroph *Herbaspirillum seropedicae*. *Plant Soil* 356, 113–125. doi: 10.1007/s11104-011-1044-z

Cacas, J.-L. (2015). "Out for a walk along the secretory pathway during programmed cell death," in *Plant Programmed Cell Death*, eds A. H. Gunawardena and P. F. McCabe (Powell, WY: Springer), 123–161. doi: 10.1007/978-3-319-21033-9_6

Caine, R. S., Yin, X., Sloan, J., Harrison, E. L., Mohammed, U., Fulton, T., et al. (2019). Rice with reduced stomatal density conserves water and has improved drought tolerance under future climate conditions. *New Phytol.* 221, 371–384. doi: 10.1111/nph.15344

Casaretto, J. A., El-Kereamy, A., Zeng, B., Stiegelmeyer, S. M., Chen, X., Bi, Y.-M., et al. (2016). Expression of OsMYB55 in maize activates stress-responsive genes and enhances heat and drought tolerance. *BMC Genomics* 17:312. doi: 10.1186/s12864-016-2659-5

Catalá, A. (2009). Lipid peroxidation of membrane phospholipids generates hydroxy-alkenals and oxidized phospholipids active in physiological and/or pathological conditions. *Chem. Phys. Lipids* 157, 1–11. doi: 10.1016/j.chemphyslip.2008.09.004

Cerrudo, D., Cao, S., Yuan, Y., Martinez, C., Suarez, E. A., Babu, R., et al. (2018). Genomic selection outperforms marker assisted selection for grain yield and physiological traits in a maize doubled haploid population across water treatments. *Front. Plant Sci.* 9:366. doi: 10.3389/fpls.2018.00366

Chao, L., Zou, J.-X., Peng, S., Peng, Y., Yuan, S.-F., Xia, W., et al. (2016). causes and impacts for heat stress in spring maize during grain filling in the North China plain â a review. *J. Integr. Agric.* 15, 2677–2687. doi: 10.1016/s2095-3119(16)61409-0

Chapman, J. M., Muhlemann, J. K., Gayomba, S. R., and Muday, G. K. (2019). RBOH-dependent ROS synthesis and ROS scavenging by plant specialized metabolites to modulate plant development and stress responses. *Chem. Res. Toxicol.* 32, 370–396. doi: 10.1021/acs.chemrestox.9b00028

Chauhan, H., Khurana, N., Agarwal, P., Khurana, J. P., and Khurana, P. (2013). A seed preferential heat shock transcription factor from wheat provides abiotic stress tolerance and yield enhancement in transgenic *Arabidopsis* under heat stress environment. *PLoS One* 8:e79577. doi: 10.1371/journal.pone.0079577

Cheikh, N., and Jones, R. J. (1994). Disruption of maize kernel growth and development by heat stress (role of cytokinin/abscisic acid balance). *Plant Physiol.* 106, 45–51. doi: 10.1104/pp.106.1.45

Chen, H., Hwang, J. E., Lim, C. J., Kim, D. Y., Lee, S. Y., and Lim, C. O. (2010). *Arabidopsis* DREB2C functions as a transcriptional activator of HsfA3 during the heat stress response. *Biochem. Biophys. Res. Commun.* 401, 238–244. doi: 10.1016/j.bbrc.2010.09.038

Chen, K., Ali, S., Chen, Y., Sohail, A., Jan, A., and Fahad, S. (2018). Effect of ridge-covering mulching materials on hormonal changes, antioxidative enzyme activities and production of maize in semi-arid regions of China. *Agric. Water Manag.* 204, 281–291. doi: 10.1016/j.agwat.2018.03.023

Chen, Y., Cao, Y., Wang, L., Li, L., Yang, J., and Zou, M. (2018). Identification of MYB transcription factor genes and their expression during abiotic stresses in maize. *Biol. Plant.* 62, 222–230. doi: 10.1007/s10535-017-0756-1

Chung, K. P., Zeng, Y., Li, Y., Ji, C., Xia, Y., and Jiang, L. (2018). Signal motif-dependent ER export of the Qc-SNARE BET12 interacts with MEMB12 and affects PR1 trafficking in *Arabidopsis*. *J. Cell Sci.* 131:jcs202838. doi: 10.1242/jcs.202838

Cimini, S., Gualtieri, C., Macovei, A., Balestrazzi, A., De Gara, L., and Locato, V. (2019). Redox balance-DDR-miRNA triangle: relevance in genome stability and stress responses in plants. *Front. Plant Sci.* 10:989. doi: 10.3389/fpls.2019.00989

Colasanti, J., and Muszynski, M. (2009). "The maize floral transition," in *Handbook of Maize: its Biology*, Vol. 1, eds S. C. Hake and J. L. Bennetzen (New York, NY: Springer Science), 41–55. doi: 10.1111/nph.16772

Crafts-Brandner, S. J., and Salvucci, M. E. (2002). Sensitivity of photosynthesis in a C4 plant, maize, to heat stress. *Plant Physiol.* 129, 1773–1780. doi: 10.1104/pp.002170

Czarnocka, W., and Karpińskiski, S. (2018). Friend or foe? Reactive oxygen species production, scavenging and signaling in plant response to environmental stresses. *Free Radic. Biol. Med.* 122, 4–20. doi: 10.1016/j.freeradbiomed.2018.01.011

Dai, Z., Ku, M. S., and Edwards, G. E. (1993). C4 photosynthesis (the CO2-concentrating mechanism and photorespiration). *Plant Physiol.* 103, 83–90. doi: 10.1104/pp.103.1.83

Dar, Z. A., Dar, S. A., Khan, J. A., Lone, A. A., Langyan, S., Lone, B. A., et al. (2021). Identification for surrogate drought tolerance in maize inbred lines utilizing high-throughput phenomics approach. *PLoS One* 16:e0254318. doi: 10.1371/journal.pone.0254318

Daryanto, S., Wang, L., and Jacinthe, P.-A. (2016). Global synthesis of drought effects on maize and wheat production. *PLoS One* 11:e0156362. doi: 10.1371/journal.pone.0156362

Dawood, M., Moursi, Y., Amro, A., Baenziger, P., and Sallam, A. (2020). Investigation of heat-induced changes in the grain yield and grains metabolites, with molecular insights on the candidate genes in barley. *Agronomy* 10:1730. doi: 10.3390/agronomy10111730

Dawson, T. P., Perryman, A. H., and Osborne, T. M. (2016). Modelling impacts of climate change on global food security. *Clim. Change* 134, 429–440. doi: 10.1007/s10584-014-1277-y

Demidchik, V. (2015). Mechanisms of oxidative stress in plants: from classical chemistry to cell biology. *Environ. Exp. Bot.* 109, 212–228. doi: 10.1016/j.envexpbot.2014.06.021

Dhaubhadel, S., Chaudhary, S., Dobinson, K. F., and Krishna, P. (1999). Treatment with 24-epibrassinolide, a brassinosteroid, increases the basic thermotolerance of *Brassica napus* and tomato seedlings. *Plant Mol. Biol.* 40, 333–342. doi: 10.1023/a:1006283015582

Dias, M., and Brüggemann, W. (2010). Limitations of photosynthesis in *Phaseolus vulgaris* under drought stress: gas exchange, chlorophyll fluorescence and Calvin cycle enzymes. *Photosynthetica* 48, 96–102. doi: 10.1007/s11099-010-0013-8

Djanaguiraman, M., Prasad, P. V., and Seppanen, M. (2010). Selenium protects sorghum leaves from oxidative damage under high temperature stress by enhancing antioxidant defense system. *Plant Physiol. Biochem.* 48, 999–1007. doi: 10.1016/j.plaphy.2010.09.009

Dolatabadian, A., Sanavy, S. A. M. M., and Asilan, K. S. (2010). Effect of ascorbic acid foliar application on yield, yield component and several morphological traits of grain corn under water deficit stress conditions. *Not. Sci. Biol.* 2, 45–50. doi: 10.15835/nsb234717

Dong, X., Xu, W., Zhang, Y., and Leskovar, D. I. (2016). Effect of irrigation timing on root zone soil temperature, root growth and grain yield and chemical composition in corn. *Agronomy* 6:34. doi: 10.3390/agronomy6020034

Dordas, C. (2009). Dry matter, nitrogen and phosphorus accumulation, partitioning and remobilization as affected by N and P fertilization and source–sink relations. *Eur. J. Agron.* 30, 129–139. doi: 10.1016/j.eja.2008.09.001

Du, H., Feng, B.-R., Yang, S.-S., Huang, Y.-B., and Tang, Y.-X. (2012). The R2R3-MYB transcription factor gene family in maize. *PLoS One* 7:e37463. doi: 10.1371/journal.pone.0037463

Duszyn, M., świeżawska, B., Szmidt-Jaworska, A., and Jaworski, K. (2019). Cyclic nucleotide gated channels (CNGCs) in plant signalling—current knowledge and perspectives. *J. Plant Physiol.* 241:153035. doi: 10.1016/j.jplph.2019.153035

Edreira, J. I. R., Mayer, L. I., and Otegui, M. E. (2014). Heat stress in temperate and tropical maize hybrids: kernel growth, water relations and assimilate availability for grain filling. *Field Crops Res.* 166, 162–172. doi: 10.1016/j.fcr.2014.06.018

Efeoğlu, B. (2009). Heat shock proteins and heat shock response in plants. *Gazi Univ. J. Sci.* 22, 67–75.

Elferjani, R., and Soolanayakanahally, R. (2018). Canola responses to drought, heat, and combined stress: shared and specific effects on carbon assimilation, seed yield, and oil composition. *Front. Plant Sci.* 9:1224. doi: 10.3389/fpls.2018.01224

El-Sappah, A., Shawky, A., Sayed-Ahmad, M., and Youssef, M. (2012). Nile tilapia as bio indicator to estimate the contamination of water using SDS-PAGE and RAPDPCR techniques. *Egypt. J. Genet. Cytol.* 41, 209–227. doi: 10.21608/ejgc.2012.10536

El-Sappah, A. H., Mm, H. I, El-Awady, H., Yan, S., Qi, S., Liu, J., et al. (2019). Tomato natural resistance genes in controlling the root-knot nematode. *Genes* 10:925. doi: 10.3390/genes10110925

El-Sappah, A. H., and Rather, S. A. (eds). (2022). "Genomics approaches to study abiotic stress tolerance in plants," in *Plant Abiotic Stress Physiology*, Vol. 2, (Burlington: Apple Academic Press), 25. doi: 10.1201/9781003180579-2

El-Sappah, A. H., Shawky, A., Sayed-Ahmad, M. S., and Youssef, M. (2017). Estimation of heat shock protein 70 (hsp 70) gene expression in nile tilapia (*Oreochromis niloticus*) using quantitative real-time PCR. *Zagazig J. Agric. Res.* 44, 1003–1015. doi: 10.21608/zjar.2017.52300

El-Sappah, A. H., Yan, K., Huang, Q., Islam, M. M., Li, Q., Wang, Y., et al. (2021). Comprehensive mechanism of gene silencing and its role in plant growth and development. *Front. Plant Sci.* 12:705249. doi: 10.3389/fpls.2021.705249

El-Sharkawy, M. A. (2007). Physiological characteristics of cassava tolerance to prolonged drought in the tropics: implications for breeding cultivars adapted to seasonally dry and semiarid environments. *Braz. J. Plant Physiol.* 19, 257–286. doi: 10.1590/s1677-04202007000400003

El-Shershaby, A., Ullrich, S., Simm, S., Scharf, K.-D., Schleiff, E., and Fragkostefanakis, S. (2019). Functional diversification of tomato HsfA1 factors is based on DNA binding domain properties. *Gene* 714:143985. doi: 10.1016/j.gene.2019.143985

Erb, M., and Kliebenstein, D. J. (2020). Plant secondary metabolites as defenses, regulators, and primary metabolites: the blurred functional trichotomy. *Plant Physiol.* 184, 39–52. doi: 10.1104/pp.20.00433

Essemine, J., Govindachary, S., Ammar, S., Bouzid, S., and Carpentier, R. (2012). Enhanced sensitivity of the photosynthetic apparatus to heat stress in digalactosyl-diacylglycerol deficient Arabidopsis. *Environ. Exp. Bot.* 80, 16–26. doi: 10.1016/j.envexpbot.2011.12.022

Eyidogan, F., Oz, M., Yucel, M., and Oktem, H. (2012). "Signal transduction of phytohormones under abiotic stresses," in *Phytohormones and Abiotic Stress Tolerance in Plants*, eds N. A. Khan, R. Nazar, N. Iqbal, and N. A. Anjum (Berlin: Springer), 1–48. doi: 10.1007/978-3-642-25829-9_1

Fahad, S., Bajwa, A. A., Nazir, U., Anjum, S. A., Farooq, A., Zohaib, A., et al. (2017). Crop production under drought and heat stress: plant responses and management options. *Front. Plant Sci.* 8:1147. doi: 10.3389/fpls.2017.01147

Faostat, F. (2017). Available Online at: http://www.fao.org/faostat/en/#data.QC [accessed January 2018].

Faostat, F. (2019). *Food and Agriculture Organization of the United Nations-Statistic Division*. Available Online at: https://www.fao.org/faostat/en/#data.QC

Farshadfar, E., Romena, H., and Safari, H. (2013). Evaluation of variability and genetic parameters in agro-physiological traits of wheat under rain-fed condition. *Int. J. Agric. Crop Sci.* 5, 1015–1021.

Finka, A., and Goloubinoff, P. (2014). The CNGCb and CNGCd genes from *Physcomitrella patens* moss encode for thermosensory calcium channels responding to fluidity changes in the plasma membrane. *Cell Stress Chaperones* 19, 83–90. doi: 10.1007/s12192-013-0436-9

Foyer, C. H., and Shigeoka, S. (2011). Understanding oxidative stress and antioxidant functions to enhance photosynthesis. *Plant Physiol.* 155, 93–100. doi: 10.1104/pp.110.166181

Fragkostefanakis, S., Mesihovic, A., Hu, Y., and Schleiff, E. (2016). Unfolded protein response in pollen development and heat stress tolerance. *Plant Reprod.* 29, 81–91. doi: 10.1007/s00497-016-0276-8

Frederickson Matika, D. E., and Loake, G. J. (2014). Redox regulation in plant immune function. *Antioxid. Redox Signal.* 21, 1373–1388. doi: 10.1089/ars.2013.5679

Frey, F. P., Presterl, T., Lecoq, P., Orlik, A., and Stich, B. (2016). First steps to understand heat tolerance of temperate maize at adult stage: identification of QTL across multiple environments with connected segregating populations. *Theor. Appl. Genet.* 129, 945–961. doi: 10.1007/s00122-016-2674-6

Frey, F. P., Urbany, C., Hüttel, B., Reinhardt, R., and Stich, B. (2015). Genome-wide expression profiling and phenotypic evaluation of European maize inbreds at seedling stage in response to heat stress. *BMC Genomics* 16:123. doi: 10.1186/s12864-015-1282-1

Frova, C., Caffulli, A., and Pallavera, E. (1998). Mapping quantitative trait loci for tolerance to abiotic stresses in maize. *J. Exp. Zool.* 282, 164–170. doi: 10.1002/(sici)1097-010x(199809/10)282:1/2<164::aid-jez18>3.0.co;2-u

Frova, C., and Sari-Gorla, M. (1994). Quantitative trait loci (QTLs) for pollen thermotolerance detected in maize. *Mol. Gen. Genet.* 245, 424–430. doi: 10.1007/BF00302254

Fu, J., Momcilovic, I., Prasad, P., Josipovic, S., and Ludwig, E. (2012). "Molecular bases and improvement of heat tolerance in crop plants," in *Heat Stress: Causes, Prevention and Treatments*, eds S. Josipovic and E. Ludwig (Hauppauge, NY: Nova Science Publishers), 185–214.

Gao, F., Han, X., Wu, J., Zheng, S., Shang, Z., Sun, D., et al. (2012). A heat-activated calcium-permeable channel–Arabidopsis cyclic nucleotide-gated ion channel 6–is involved in heat shock responses. *Plant J.* 70, 1056–1069. doi: 10.1111/j.1365-313X.2012.04969.x

Gao, H., Brandizzi, F., Benning, C., and Larkin, R. M. (2008). A membrane-tethered transcription factor defines a branch of the heat stress response in *Arabidopsis thaliana*. *Proc. Natl. Acad. Sci. U.S.A.* 105, 16398–16403. doi: 10.1073/pnas.0808463105

Gao, J., Wang, S., Zhou, Z., Wang, S., Dong, C., Mu, C., et al. (2019). Linkage mapping and genome-wide association reveal candidate genes conferring thermotolerance of seed-set in maize. *J. Exp. Bot.* 70, 4849–4864. doi: 10.1093/jxb/erz171

Gao, X., Cox, K. L. Jr., and He, P. (2014). Functions of calcium-dependent protein kinases in plant innate immunity. *Plants* 3, 160–176. doi: 10.3390/plants3010160

Gardeström, P., and Igamberdiev, A. U. (2016). The origin of cytosolic ATP in photosynthetic cells. *Physiol. Plant.* 157, 367–379. doi: 10.1111/ppl.12455

Gayral, M., Arias Gaguancela, O., Vasquez, E., Herath, V., Flores, F. J., Dickman, M. B., et al. (2020). Multiple ER-to-nucleus stress signaling pathways are activated during *Plantago asiatica* mosaic virus and *Turnip mosaic* virus

infection in *Arabidopsis thaliana*. *Plant J.* 103, 1233–1245. doi: 10.1111/tpj.14798

Gedil, M., and Menkir, A. (2019). An integrated molecular and conventional breeding scheme for enhancing genetic gain in maize in Africa. *Front. Plant Sci.* 10:1430. doi: 10.3389/fpls.2019.01430

Gong, F., Wu, X., Zhang, H., Chen, Y., and Wang, W. (2015). Making better maize plants for sustainable grain production in a changing climate. *Front. Plant Sci.* 6:835. doi: 10.3389/fpls.2015.00835

Gong, M., Li, Y.-J., Dai, X., Tian, M., and Li, Z.-G. (1997). Involvement of calcium and calmodulin in the acquisition of heat-shock induced thermotolerance in maize seedlings. *J. Plant Physiol.* 150, 615–621. doi: 10.1016/s0176-1617(97)80328-8

Gourdji, S. M., Sibley, A. M., and Lobell, D. B. (2013). Global crop exposure to critical high temperatures in the reproductive period: historical trends and future projections. *Environ. Res. Lett.* 8:024041. doi: 10.1088/1748-9326/8/2/024041

Guo, H., Li, S., Kang, S., Du, T., Tong, L., and Ding, R. (2019). Annual ecosystem respiration of maize was primarily driven by crop growth and soil water conditions. *Agric. Ecosyst. Environ.* 272, 254–265. doi: 10.1016/j.agee.2018.11.026

Guo, J., Wu, J., Ji, Q., Wang, C., Luo, L., Yuan, Y., et al. (2008). Genome-wide analysis of heat shock transcription factor families in rice and *Arabidopsis*. *J. Genet. Genomics* 35, 105–118. doi: 10.1016/S1673-8527(08)60016-8

Gurley, W. B. (2000). HSP101: a key component for the acquisition of thermotolerance in plants. *Plant Cell* 12, 457–460. doi: 10.1105/tpc.12.4.457

Haider, S., Rehman, S., Ahmad, Y., Raza, A., Tabassum, J., Javed, T., et al. (2021). In silico characterization and expression profiles of heat shock transcription factors (HSFs) in maize (*Zea mays* L.). *Agronomy* 11:2335. doi: 10.3390/agronomy11112335

Hao, L., and Qiao, X. (2018). Genome-wide identification and analysis of the CNGC gene family in maize. *PeerJ* 6:e5816. doi: 10.7717/peerj.5816

Hasanuzzaman, M., Bhuyan, M., Zulfiqar, F., Raza, A., Mohsin, S. M., Mahmud, J. A., et al. (2020). Reactive oxygen species and antioxidant defense in plants under abiotic stress: revisiting the crucial role of a universal defense regulator. *Antioxidants* 9:681. doi: 10.3390/antiox9080681

Hashimoto, K., and Kudla, J. (2011). Calcium decoding mechanisms in plants. *Biochimie* 93, 2054–2059. doi: 10.1016/j.biochi.2011.05.019

Haswell, E. S., and Verslues, P. E. (2015). The ongoing search for the molecular basis of plant osmosensing. *J. Gen. Physiol.* 145, 389–394. doi: 10.1085/jgp.201411295

Hayes, S., Schachtschabel, J., Mishkind, M., Munnik, T., and Arisz, S. A. (2021). Hot topic: thermosensing in plants. *Plant Cell Environ.* 44, 2018–2033. doi: 10.1111/pce.13979

He, F., Gao, C., Guo, G., Liu, J., Gao, Y., Pan, R., et al. (2019). Maize annexin genes ZmANN33 and ZmANN35 encode proteins that function in cell membrane recovery during seed germination. *J. Exp. Bot.* 70, 1183–1195. doi: 10.1093/jxb/ery452

He, Y.-Y., and Häder, D.-P. (2002). UV-B-induced formation of reactive oxygen species and oxidative damage of the cyanobacterium *Anabaena* sp.: protective effects of ascorbic acid and N-acetyl-L-cysteine. *J. Photochem. Photobiol. B Biol.* 66, 115–124. doi: 10.1016/s1011-1344(02)00231-2

Hoegh-Guldberg, O., Jacob, D., Taylor, M., Bolaños, T. G., Bindi, M., Brown, S., et al. (2019). The human imperative of stabilizing global climate change at 1.5°C. *Science* 365:eaaw6974. doi: 10.1126/science.aaw6974

Horváth, I., Glatz, A., Nakamoto, H., Mishkind, M. L., Munnik, T., Saidi, Y., et al. (2012). Heat shock response in photosynthetic organisms: membrane and lipid connections. *Prog. Lipid Res.* 51, 208–220. doi: 10.1016/j.plipres.2012.02.002

Hossain, M. A., Bhattacharjee, S., Armin, S. M., Qian, P., Xin, W., Li, H. Y., et al. (2015). Hydrogen peroxide priming modulates abiotic oxidative stress tolerance: insights from ROS detoxification and scavenging. *Front. Plant Sci.* 6:420. doi: 10.3389/fpls.2015.00420

Houghton, J. T., Ding, Y., Griggs, D. J., Noguer, M., Van Der Linden, P. J., Dai, X., et al. (2001). *Climate Change 2001: the Scientific Basis: Contribution of Working Group I to the Third Assessment Report of the Intergovernmental Panel on Climate Change*. Cambridge: Cambridge university press.

Howell, S. H. (2013). Endoplasmic reticulum stress responses in plants. *Annu. Rev. Plant Biol.* 64, 477–499. doi: 10.1146/annurev-arplant-050312-120053

Hu, X., Huang, Y., Sun, W., and Yu, L. (2017). Shifts in cultivar and planting date have regulated rice growth duration under climate warming in China since the early 1980s. *Agric. For. Meteorol.* 247, 34–41. doi: 10.1016/j.agrformet.2017.07.014

Hu, X., Jiang, M., Zhang, J., Zhang, A., Lin, F., and Tan, M. (2007). Calcium/calmodulin is required for abscisic acid-induced antioxidant defense and functions both upstream and downstream of H_2O_2 production in leaves of maize plants. *New Phytol.* 173, 27–38. doi: 10.1111/j.1469-8137.2006.01888.x

Hu, X., Yang, Y., Gong, F., Zhang, D., Zhang, L., Wu, L., et al. (2015). Protein sHSP26 improves chloroplast performance under heat stress by interacting with specific chloroplast proteins in maize (*Zea mays*). *J. Proteom.* 115, 81–92. doi: 10.1016/j.jprot.2014.12.009

Huang, H.-W., Zeng, X., Rhim, T., Ron, D., and Ryoo, H. D. (2017). The requirement of IRE1 and XBP1 in resolving physiological stress during *Drosophila* development. *J. Cell Sci.* 130, 3040–3049. doi: 10.1242/jcs.203612

Huang, J., Chen, F., Del Casino, C., Autino, A., Shen, M., Yuan, S., et al. (2006). An ankyrin repeat-containing protein, characterized as a ubiquitin ligase, is closely associated with membrane-enclosed organelles and required for pollen germination and pollen tube growth in lily. *Plant Physiol.* 140, 1374–1383. doi: 10.1104/pp.105.074922

Huang, Y.-C., Niu, C.-Y., Yang, C.-R., and Jinn, T.-L. (2016). The heat stress factor HSFA6b connects ABA signaling and ABA-mediated heat responses. *Plant Physiol.* 172, 1182–1199. doi: 10.1104/pp.16.00860

Ihsan, M. Z., Daur, I., Alghabari, F., Alzamanan, S., Rizwan, S., Ahmad, M., et al. (2019). Heat stress and plant development: role of sulphur metabolites and management strategies. *Acta Agric. Scand. B Soil Plant Sci.* 69, 332–342. doi: 10.1080/09064710.2019.1569715

Iurlaro, R., and Muñoz-Pinedo, C. (2016). Cell death induced by endoplasmic reticulum stress. *FEBS J.* 283, 2640–2652.

Jagadish, S., Bahuguna, R. N., Djanaguiraman, M., Gamuyao, R., Prasad, P., and Craufurd, P. Q. (2016). Implications of high temperature and elevated CO2 on flowering time in plants. *Front. Plant Sci.* 7:913. doi: 10.3389/fpls.2016.00913

Jagtap, A. B., Vikal, Y., and Johal, G. S. (2020). Genome-wide development and validation of cost-effective KASP marker assays for genetic dissection of heat stress tolerance in maize. *Int. J. Mol. Sci.* 21:7386. doi: 10.3390/ijms21197386

Jammes, F., Hu, H. C., Villiers, F., Bouten, R., and Kwak, J. M. (2011). Calcium-permeable channels in plant cells. *FEBS J.* 278, 4262–4276. doi: 10.1111/j.1742-4658.2011.08369.x

Jha, A. K., Chakraborty, S., Kumari, K., and Bauddh, K. (2020). "Ecological consequences of genetically modified crops on soil biodiversity," in *Ecological and Practical Applications for Sustainable Agriculture*, eds K. Bauddh, S. Kumar, R. Singh, and J. Korstad (Singapore: Springer), 89–106. doi: 10.1007/978-981-15-3372-3_5

Jia, Z., Lian, Y., Zhu, Y., He, J., Cao, Z., and Wang, G. (2009). Cloning and characterization of a putative transcription factor induced by abiotic stress in *Zea mays*. *Afr. J. Biotechnol.* 8, 6764–6771.

Jiang, L., Hu, W., Qian, Y., Ren, Q., and Zhang, J. (2021). Genome-wide identification, classification and expression analysis of the Hsf and Hsp70 gene families in maize. *Gene* 770:145348. doi: 10.1016/j.gene.2020.145348

Jiang, C., Zu, C., Lu, D., Zheng, Q., Shen, J., Wang, H., et al. (2017). Effect of exogenous selenium supply on photosynthesis, Na^+ accumulation and antioxidative capacity of maize (*Zea mays* L.) under salinity stress. *Sci. Rep.* 7:42039. doi: 10.1038/srep42039

Joshi, J., Hasnain, G., Logue, T., Lynch, M., Wu, S., Guan, J.-C., et al. (2021). A core metabolome response of maize leaves subjected to long-duration abiotic stresses. *Metabolites* 11:797. doi: 10.3390/metabo11110797

Kaplan, F., Kopka, J., Haskell, D. W., Zhao, W., Schiller, K. C., Gatzke, N., et al. (2004). Exploring the temperature-stress metabolome of Arabidopsis. *Plant Physiol.* 136, 4159–4168. doi: 10.1104/pp.104.052142

Kaspar, T., and Bland, W. L. (1992). Soil temperature and root growth. *Soil Sci.* 154, 290–299. doi: 10.1097/00010694-199210000-00005

Keeling, P., Banisadr, R., Barone, L., Wasserman, B., and Singletary, G. (1994). Effect of temperature on enzymes in the pathway of starch biosynthesis in developing wheat and maize grain. *Funct. Plant Biol.* 21, 807–827. doi: 10.1071/pp9940807

Ketehouli, T., Idrice Carther, K. F., Noman, M., Wang, F.-W., Li, X.-W., and Li, H.-Y. (2019). Adaptation of plants to salt stress: characterization of Na+ and

K+ transporters and role of CBL gene family in regulating salt stress response. *Agronomy* 9:687. doi: 10.3390/agronomy9110687

Khaeim, H., Kende, Z., Jolánkai, M., Kovács, G. P., Gyuricza, C., and Tarnawa, Á. (2022). Impact of temperature and water on seed germination and seedling growth of maize (*Zea mays* L.). *Agronomy* 12:397. doi: 10.3390/agronomy12020397

Khajuria, P., Singh, A. K., and Singh, R. (2016). Identification of heat stress tolerant genotypes in bread wheat. *Electron. J. Plant Breed.* 7, 1446–1452.

Khakwani, A. A., Dennett, M. D., Munir, M., and Baloch, M. S. (2012). Wheat yield response to physiological limitations under water stress condition. *J. Anim. Plant Sci.* 22, 773–780.

Khan, A., Ali, M., Khattak, A. M., Gai, W.-X., Zhang, H.-X., Wei, A.-M., et al. (2019). Heat shock proteins: dynamic biomolecules to counter plant biotic and abiotic stresses. *Int. J. Mol. Sci.* 20:5321. doi: 10.3390/ijms20215321

Khan, M. I. R., Fatma, M., Per, T. S., Anjum, N. A., and Khan, N. A. (2015). Salicylic acid-induced abiotic stress tolerance and underlying mechanisms in plants. *Front. Plant Sci.* 6:462. doi: 10.3389/fpls.2015.00462

Kim, J.-M., To, T. K., Ishida, J., Matsui, A., Kimura, H., and Seki, M. (2012). Transition of chromatin status during the process of recovery from drought stress in *Arabidopsis thaliana*. *Plant Cell Physiol.* 53, 847–856. doi: 10.1093/pcp/pcs053

Kimotho, R. N., Baillo, E. H., and Zhang, Z. (2019). Transcription factors involved in abiotic stress responses in maize (*Zea mays* L.) and their roles in enhanced productivity in the post genomics era. *PeerJ* 7:e7211. doi: 10.7717/peerj.7211

Kiniry, J., and Bonhomme, R. (1991). Predicting maize phenology. *Predict. Crop Phenol.* 11, 115–131.

Klein, R. D., Chidawanyika, T., Tims, H. S., Meulia, T., Bouchard, R. A., and Pett, V. B. (2014). Chaperone function of two small heat shock proteins from maize. *Plant Sci.* 221-222, 48–58. doi: 10.1016/j.plantsci.2014.01.012

Kong, L., Wang, F., Si, J., Feng, B., Zhang, B., Li, S., et al. (2013). Increasing in ROS levels and callose deposition in peduncle vascular bundles of wheat (*Triticum aestivum* L.) grown under nitrogen deficiency. *J. Plant Interact.* 8, 109–116. doi: 10.1080/17429145.2012.712723

Kørner, C. J., Du, X., Vollmer, M. E., and Pajerowska-Mukhtar, K. M. (2015). Endoplasmic reticulum stress signaling in plant immunity—at the crossroad of life and death. *Int. J. Mol. Sci.* 16, 26582–26598. doi: 10.3390/ijms161125964

Kraus, K., Hnilickova, H., Pecka, J., Lhotska, M., Bezdickova, A., Martinek, P., et al. (2022). The effect of the application of stimulants on the photosynthetic apparatus and the yield of winter wheat. *Agronomy* 12:78. doi: 10.3390/agronomy12010078

Kulski, J. K. (ed.) (2016). "Next-generation sequencing—an overview of the history, tools, and "Omic" applications," in *Next Generation Sequencing–Advances, Applications and Challenges*, (London: InTech), 3–60.

Kumar, A., and Kaushik, P. (2021). Heat stress and its impact on plant function: an update. *Preprints* 2021:2021080489.

Kumar, K., Singh, I., Aggarwal, C., Tewari, I., Jha, A. K., Yadava, P., et al. (2019). Expression profiling of heat shock protein genes in two contrasting maize inbred lines. *Int. J. Curr. Microbiol. Appl. Sci.* 8, 347–358. doi: 10.20546/ijcmas.2019.806.039

Kumar, M., Kumar Patel, M., Kumar, N., Bajpai, A. B., and Siddique, K. H. M. (2021). Metabolomics and molecular approaches reveal drought stress tolerance in plants. *Int. J. Mol. Sci.* 22:9108. doi: 10.3390/ijms22179108

Kumari, S., Sabharwal, V. P., Kushwaha, H. R., Sopory, S. K., Singla-Pareek, S. L., and Pareek, A. (2009). Transcriptome map for seedling stage specific salinity stress response indicates a specific set of genes as candidate for saline tolerance in *Oryza sativa* L. *Funct. Integr. Genomics* 9, 109–123. doi: 10.1007/s10142-008-0088-5

Lafarge, T., Bueno, C., Frouin, J., Jacquin, L., Courtois, B., and Ahmadi, N. (2017). Genome-wide association analysis for heat tolerance at flowering detected a large set of genes involved in adaptation to thermal and other stresses. *PLoS One* 12:e0171254. doi: 10.1371/journal.pone.0171254

Le Nguyen, K., Grondin, A., Courtois, B., and Gantet, P. (2019). Next-generation sequencing accelerates crop gene discovery. *Trends Plant Sci.* 24, 263–274. doi: 10.1016/j.tplants.2018.11.008

Leng, P., and Zhao, J. (2020). Transcription factors as molecular switches to regulate drought adaptation in maize. *Theor. Appl. Genet.* 133, 1455–1465. doi: 10.1007/s00122-019-03494-y

Li, B., Gao, K., Ren, H., and Tang, W. (2018). Molecular mechanisms governing plant responses to high temperatures. *J. Integr. Plant Biol.* 60, 757–779. doi: 10.1111/jipb.12701

Li, Z., Srivastava, R., Tang, J., Zheng, Z., and Howell, S. H. (2018). *Cis*-effects condition the induction of a major unfolded protein response factor, *ZmbZIP60*, in response to heat stress in maize. *Front. Plant Sci.* 9:833. doi: 10.3389/fpls.2018.00833

Li, H.-C., Zhang, H.-N., Li, G.-L., Liu, Z.-H., Zhang, Y.-M., Zhang, H.-M., et al. (2015). Expression of maize heat shock transcription factor gene ZmHsf06 enhances the thermotolerance and drought-stress tolerance of transgenic Arabidopsis. *Funct. Plant Biol.* 42, 1080–1091. doi: 10.1071/FP15080

Li, Z. G., Xie, L. R., and Li, X. J. (2015). Hydrogen sulfide acts as a downstream signal molecule in salicylic acid-induced heat tolerance in maize (*Zea mays* L.) seedlings. *J. Plant Physiol.* 177, 121–127. doi: 10.1016/j.jplph.2014.12.018

Li, J., Zhang, L., Elbaiomy, R. G., Chen, L., Wang, Z., Jiao, J., et al. (2022). Evolution analysis of *FRIZZY PANICLE* (*FZP*) orthologs explored the mutations in DNA coding sequences in the grass family (Poaceae). *PeerJ* 10:e12880. doi: 10.7717/peerj.12880

Li, J., Zhang, L., Yuan, Y., Wang, Q., Elbaiomy, R., Zhou, W., et al. (2021). In silico functional prediction and expression analysis of C2H2 zinc-finger family transcription factor revealed regulatory role of ZmZFP126 in maize growth. *Front. Genet.* 12:770427. doi: 10.3389/fgene.2021.770427

Li, N., Euring, D., Cha, J. Y., Lin, Z., Lu, M., Huang, L.-J., et al. (2021). Plant hormone-mediated regulation of heat tolerance in response to global climate change. *Front. Plant Sci.* 11:627969. doi: 10.3389/fpls.2020.627969

Li, Y. T., Xu, W. W., Ren, B. Z., Zhao, B., Zhang, J., Liu, P., et al. (2020). High temperature reduces photosynthesis in maize leaves by damaging chloroplast ultrastructure and photosystem II. *J. Agron. Crop Sci.* 206, 548–564. doi: 10.1111/jac.12401

Li, Z., Tang, J., Srivastava, R., Bassham, D. C., and Howell, S. H. (2020). The transcription factor bZIP60 links the unfolded protein response to the heat stress response in maize. *Plant Cell* 32, 3559–3575. doi: 10.1105/tpc.20.00260

Li, Z., and Howell, S. H. (2021). Heat stress responses and thermotolerance in maize. *Int. J. Mol. Sci.* 22:948. doi: 10.3390/ijms22020948

Li, Z. G. (2015). Synergistic effect of antioxidant system and osmolyte in hydrogen sulfide and salicylic acid crosstalk-induced heat tolerance in maize (*Zea mays* L.) seedlings. *Plant Signal. Behav.* 10:e1051278. doi: 10.1080/15592324.2015.1051278

Li, Z.-G., Ye, X.-Y., and Qiu, X.-M. (2019). Glutamate signaling enhances the heat tolerance of maize seedlings by plant glutamate receptor-like channels-mediated calcium signaling. *Protoplasma* 256, 1165–1169. doi: 10.1007/s00709-019-01351-9

Lieu, E. L., Kelekar, N., Bhalla, P., and Kim, J. (2021). Fructose and mannose in inborn errors of metabolism and cancer. *Metabolites* 11:479. doi: 10.3390/metabo11080479

Lima, R. B., Dos Santos, T. B., Vieira, L. G. E., Ferrarese, M. D. L. L., Ferrarese-Filho, O., Donatti, L., et al. (2013). Heat stress causes alterations in the cell-wall polymers and anatomy of coffee leaves (*Coffea arabica* L.). *Carbohydr. Polym.* 93, 135–143. doi: 10.1016/j.carbpol.2012.05.015

Lin, F., Ding, H., Wang, J., Zhang, H., Zhang, A., Zhang, Y., et al. (2009). Positive feedback regulation of maize NADPH oxidase by mitogen-activated protein kinase cascade in abscisic acid signalling. *J. Exp. Bot.* 60, 3221–3238. doi: 10.1093/jxb/erp157

Lin, F., Wani, S. H., Collins, P. J., Wen, Z., Li, W., Zhang, N., et al. (2020). QTL mapping and GWAS for identification of loci conferring partial resistance to Pythium sylvaticum in soybean(*Glycine max* (L.) Merr). *Mol. Breed.* 40:54.

Lin, Y.-X., Jiang, H.-Y., Chu, Z.-X., Tang, X.-L., Zhu, S.-W., and Cheng, B.-J. (2011). Genome-wide identification, classification and analysis of heat shock transcription factor family in maize. *BMC Genomics* 12:76. doi: 10.1186/1471-2164-12-76

Liu, J., Niu, Y., Zhang, J., Zhou, Y., Ma, Z., and Huang, X. (2018). Ca2+ channels and Ca2+ signals involved in abiotic stress responses in plant cells: recent advances. *Plant Cell Tissue Organ Cult.* 132, 413–424. doi: 10.1007/s11240-017-1350-0

Liu, J.-X., Srivastava, R., Che, P., and Howell, S. H. (2007). An endoplasmic reticulum stress response in *Arabidopsis* is mediated by proteolytic processing and nuclear relocation of a membrane-associated transcription factor, bZIP28. *Plant Cell* 19, 4111–4119. doi: 10.1105/tpc.106.050021

Liu, L., Hao, Z., Weng, J., Li, M., Zhang, D., Bai, L., et al. (2012). Identification of drought-responsive genes by cDNA-amplified fragment length polymorphism in maize. *Ann. Appl. Biol.* 161, 203–213. doi: 10.1111/j.1744-7348.2012.00565.x

Liu, Z., Hubbard, K. G., Lin, X., and Yang, X. (2013). Negative effects of climate warming on maize yield are reversed by the changing of sowing date and cultivar selection in Northeast China. *Glob. Change Biol.* 19, 3481–3492. doi: 10.1111/gcb.12324

Lobell, D. B., Bänziger, M., Magorokosho, C., and Vivek, B. (2011). Nonlinear heat effects on African maize as evidenced by historical yield trials. *Nat. Clim. Change* 1, 42–45. doi: 10.1038/nclimate1043

Longmei, N., Gill, G. K., Zaidi, P. H., Kumar, R., Nair, S. K., Hindu, V., et al. (2021). Genome wide association mapping for heat tolerance in sub-tropical maize. *BMC Genomics* 22:154. doi: 10.1186/s12864-021-07463-y

Lorenz, A. J., Chao, S., Asoro, F. G., Heffner, E. L., Hayashi, T., Iwata, H., et al. (2011). Genomic selection in plant breeding: knowledge and prospects. *Adv. Agron.* 110, 77–123.

Ludwig-Müller, J. (2011). Auxin conjugates: their role for plant development and in the evolution of land plants. *J. Exp. Bot.* 62, 1757–1773. doi: 10.1093/jxb/erq412

Luna, E., Pastor, V., Robert, J., Flors, V., Mauch-Mani, B., and Ton, J. (2011). Callose deposition: a multifaceted plant defense response. *Mol. Plant Microbe Interact.* 24, 183–193. doi: 10.1094/MPMI-07-10-0149

Ma, H., Liu, C., Li, Z., Ran, Q., Xie, G., Wang, B., et al. (2018). ZmbZIP4 contributes to stress resistance in maize by regulating ABA synthesis and root development. *Plant Physiol.* 178, 753–770. doi: 10.1104/pp.18.00436

Ma, P., Liu, J., Yang, X., and Ma, R. (2013). Genome-wide identification of the maize calcium-dependent protein kinase gene family. *Appl. Biochem. Biotechnol.* 169, 2111–2125. doi: 10.1007/s12010-013-0125-2

Mafakheri, A., Siosemardeh, A., Bahramnejad, B., Struik, P. C., and Sohrabi, Y. (2010). Effect of drought stress on yield, proline and chlorophyll contents in three chickpea cultivars. *Aust. J. Crop Sci.* 4, 580–585.

Magaña Ugarte, R., Escudero, A., and Gavilán, R. G. (2019). Metabolic and physiological responses of Mediterranean high-mountain and alpine plants to combined abiotic stresses. *Physiol. Plant.* 165, 403–412. doi: 10.1111/ppl.12898

Maitra, P., Al-Rashid, J., Barman, N. C., Khan, M., Morshed, N., Mandal, D., et al. (2021). Sand particle size and phosphorus amount affect *Rhizophagus irregularis* spore production using in vitro propagated spore as a starter inoculum in rhizosphere of maize (*Zea mays*) plantlets. *J. Fungi* 7:846. doi: 10.3390/jof7100846

Majeran, W., and van Wijk, K. J. (2009). Cell-type-specific differentiation of chloroplasts in C4 plants. *Trends Plant Sci.* 14, 100–109. doi: 10.1016/j.tplants.2008.11.006

Malenica, N., Duniæ, J. A., Vukadinoviæ, L., Cesar, V., and Šimiæ, D. (2021). Genetic approaches to enhance multiple stress tolerance in maize. *Genes* 12:1760. doi: 10.3390/genes12111760

Marcec, M. J., Gilroy, S., Poovaiah, B. W., and Tanaka, K. (2019). Mutual interplay of Ca2+ and ROS signaling in plant immune response. *Plant Sci.* 283, 343–354. doi: 10.1016/j.plantsci.2019.03.004

Markelz, R. C., Strellner, R. S., and Leakey, A. D. (2011). Impairment of C4 photosynthesis by drought is exacerbated by limiting nitrogen and ameliorated by elevated [CO2] in maize. *J. Exp. Bot.* 62, 3235–3246. doi: 10.1093/jxb/err056

Marrs, K. A., Casey, E. S., Capitant, S. A., Bouchard, R. A., Dietrich, P. S., Mettler, I. J., et al. (1993). Characterization of two maize HSP90 heat shock protein genes: expression during heat shock, embryogenesis, and pollen development. *Dev. Genet.* 14, 27–41. doi: 10.1002/dvg.1020140105

McKevith, B. (2004). Nutritional aspects of cereals. *Nutr. Bull.* 29, 111–142. doi: 10.1111/j.1467-3010.2004.00418.x

Medeiros, D. B., Brotman, Y., and Fernie, A. R. (2021). The utility of metabolomics as a tool to inform maize biology. *Plant Commun.* 2:100187. doi: 10.1016/j.xplc.2021.100187

Meena, A. K., Singh, D. K., Pandey, P. C., and Nanda, G. (2019). Dynamics of dry matter and nitrogen distribution in transplanted rice on mollisols. *J. Plant Nutr.* 42, 749–758. doi: 10.1080/01904167.2019.1567777

Meena, M. K., Ghawana, S., Dwivedi, V., Roy, A., and Chattopadhyay, D. (2015). Expression of chickpea CIPK25 enhances root growth and tolerance to dehydration and salt stress in transgenic tobacco. *Front. Plant Sci.* 6:683. doi: 10.3389/fpls.2015.00683

Meena, R. S., Lal, R., and Yadav, G. S. (2020). Long-term impact of topsoil depth and amendments on carbon and nitrogen budgets in the surface layer of an Alfisol in Central Ohio. *Catena* 194:104752. doi: 10.1016/j.catena.2020.104752

Miller, G., and Mittler, R. (2006). Could heat shock transcription factors function as hydrogen peroxide sensors in plants? *Ann. Bot.* 98, 279–288. doi: 10.1093/aob/mcl107

Mishra, V., Cruise, J. F., and Mecikalski, J. R. (2021). Assimilation of coupled microwave/thermal infrared soil moisture profiles into a crop model for robust maize yield estimates over Southeast United States. *Eur. J. Agron.* 123:126208. doi: 10.1016/j.eja.2020.126208

Mizoi, J., Shinozaki, K., and Yamaguchi-Shinozaki, K. (2012). AP2/ERF family transcription factors in plant abiotic stress responses. *Biochim. Biophys. Acta* 1819, 86–96. doi: 10.1016/j.bbagrm.2011.08.004

Mo, F., Sun, M., Liu, X.-Y., Wang, J.-Y., Zhang, X.-C., Ma, B., et al. (2016). Phenological responses of spring wheat and maize to changes in crop management and rising temperatures from 1992 to 2013 across the Loess Plateau. *Field Crops Res.* 196, 337–347. doi: 10.1016/j.fcr.2016.06.024

Mortimer, J. C., Laohavisit, A., Macpherson, N., Webb, A., Brownlee, C., Battey, N. H., et al. (2008). Annexins: multifunctional components of growth and adaptation. *J. Exp. Bot.* 59, 533–544. doi: 10.1093/jxb/erm344

Mujahid, A., Pumford, N. R., Bottje, W., Nakagawa, K., Miyazawa, T., Akiba, Y., et al. (2007). Mitochondrial oxidative damage in chicken skeletal muscle induced by acute heat stress. *J. Poult. Sci.* 44, 439–445. doi: 10.2141/jpsa.44.439

Navarro, J. A., Saiz-Bonilla, M., Sanchez-Navarro, J. A., and Pallas, V. (2021). The mitochondrial and chloroplast dual targeting of a multifunctional plant viral protein modulates chloroplast-to-nucleus communication, RNA silencing suppressor activity, encapsidation, pathogenesis and tissue tropism. *Plant J.* 108, 197–218. doi: 10.1111/tpj.15435

Naveed, S., Aslam, M., Maqbool, M., Bano, S., Zaman, Q., and Ahmad, R. (2014). Physiology of high temperature stress tolerance at reproductive stages in maize. *J. Anim. Plant Sci.* 24, 1141–1145.

Nawkar, G. M., Lee, E. S., Shelake, R. M., Park, J. H., Ryu, S. W., Kang, C. H., et al. (2018). Activation of the transducers of unfolded protein response in plants. *Front. Plant Sci.* 9:214. doi: 10.3389/fpls.2018.00214

Neill, E. M., Byrd, M. C., Billman, T., Brandizzi, F., and Stapleton, A. E. (2019). Plant growth regulators interact with elevated temperature to alter heat stress signaling via the Unfolded Protein Response in maize. *Sci. Rep.* 9:10392. doi: 10.1038/s41598-019-46839-9

Nestler, J., Liu, S., Wen, T.-J., Paschold, A., Marcon, C., Tang, H. M., et al. (2014). Roothairless5, which functions in maize (*Zea mays* L.) root hair initiation and elongation encodes a monocot-specific NADPH oxidase. *Plant J.* 79, 729–740. doi: 10.1111/tpj.12578

Nichols, C. (2005). *Functional Characterisation of Plant Annexins*. Ph.D. thesis. Cambridge: University of Cambridge.

Nieto-Sotelo, J., Martínez, L. M., Ponce, G., Cassab, G. I., Alagón, A., Meeley, R. B., et al. (2002). Maize HSP101 plays important roles in both induced and basal thermotolerance and primary root growth. *Plant Cell* 14, 1621–1633. doi: 10.1105/tpc.010487

Nieto-Sotelo, J., Vierling, E., and Ho, T.-H. D. (1990). Cloning, sequence analysis, and expression of a cDNA encoding a plastid-localized heat shock protein in maize. *Plant Physiol.* 93, 1321–1328. doi: 10.1104/pp.93.4.1321

Nievola, C. C., Carvalho, C. P., Carvalho, V., and Rodrigues, E. (2017). Rapid responses of plants to temperature changes. *Temperature* 4, 371–405. doi: 10.1080/23328940.2017.1377812

Nijabat, A., Bolton, A., Mahmood-Ur-Rehman, M., Shah, A. I., Hussain, R., Naveed, N. H., et al. (2020). Cell membrane stability and relative cell injury in response to heat stress during early and late seedling stages of diverse carrot (*Daucus carota* L.) germplasm. *Hortscience* 55, 1446–1452. doi: 10.21273/hortsci15058-20

Niu, S., Du, X., Wei, D., Liu, S., Tang, Q., Bian, D., et al. (2021). Heat stress after pollination reduces kernel number in maize by insufficient assimilates. *Front. Genet.* 12:728166. doi: 10.3389/fgene.2021.728166

Niu, Y., and Xiang, Y. (2018). An overview of biomembrane functions in plant responses to high-temperature stress. *Front. Plant Sci.* 9:915. doi: 10.3389/fpls.2018.00915

Ohama, N., Sato, H., Shinozaki, K., and Yamaguchi-Shinozaki, K. (2017). Transcriptional regulatory network of plant heat stress response. *Trends Plant Sci.* 22, 53–65. doi: 10.1016/j.tplants.2016.08.015

O'Leary, B., Park, J., and Plaxton, W. C. (2011). The remarkable diversity of plant PEPC (phosphoenolpyruvate carboxylase): recent insights into the physiological functions and post-translational controls of non-photosynthetic PEPCs. *Biochem. J.* 436, 15–34. doi: 10.1042/BJ20110078

Osuna, D., Prieto, P., and Aguilar, M. (2015). Control of seed germination and plant development by carbon and nitrogen availability. *Front. Plant Sci.* 6:1023. doi: 10.3389/fpls.2015.01023

Pamplona, R. (2008). Membrane phospholipids, lipoxidative damage and molecular integrity: a causal role in aging and longevity. *Biochim. Biophys. Acta* 1777, 1249–1262. doi: 10.1016/j.bbabio.2008.07.003

Pandey, N., Ranjan, A., Pant, P., Tripathi, R. K., Ateek, F., Pandey, H. P., et al. (2013). CAMTA 1 regulates drought responses in *Arabidopsis thaliana*. *BMC Genomics* 14:216. doi: 10.1186/1471-2164-14-216

Pandey, R., Maranville, J., and Admou, A. (2000). Deficit irrigation and nitrogen effects on maize in a Sahelian environment: I. Grain yield and yield components. *Agric. Water Manag.* 46, 15–27. doi: 10.1016/s0378-3774(00)00074-3

Parmar, A., Sturm, B., and Hensel, O. (2017). Crops that feed the world: production and improvement of cassava for food, feed, and industrial uses. *Food Secur.* 9, 907–927. doi: 10.1007/s12571-017-0717-8

Pastor-Cantizano, N., Ko, D. K., Angelos, E., Pu, Y., and Brandizzi, F. (2020). Functional diversification of ER stress responses in *Arabidopsis*. *Trends Biochem. Sci.* 45, 123–136. doi: 10.1016/j.tibs.2019.10.008

Paul, E. A., Paustian, K. H., Elliott, E., and Cole, C. V. (1996). *Soil Organic Matter in Temperate AgroecosystemsLong Term Experiments in North America*. Boca Raton, FL: CRC Press.

Pegoraro, C., Mertz, L. M., Da Maia, L. C., Rombaldi, C. V., and De Oliveira, A. C. (2011). Importance of heat shock proteins in maize. *J. Crop Sci. Biotechnol.* 14, 85–95.

Popp, J., Petö, K., and Nagy, J. (2013). Pesticide productivity and food security. A review. *Agron. Sustain. Dev.* 33, 243–255. doi: 10.1007/s13593-012-0105-x

Prasad, T., Hack, E., and Hallberg, R. (1990). Function of the maize mitochondrial chaperonin hsp60: specific association between hsp60 and newly synthesized F1-ATPase alpha subunits. *Mol. Cell. Biol.* 10, 3979–3986. doi: 10.1128/mcb.10.8.3979-3986.1990

Qian, Y., Ren, Q., Zhang, J., and Chen, L. (2019). Transcriptomic analysis of the maize (*Zea mays* L.) inbred line B73 response to heat stress at the seedling stage. *Gene* 692, 68–78. doi: 10.1016/j.gene.2018.12.062

Qin, F., Kakimoto, M., Sakuma, Y., Maruyama, K., Osakabe, Y., Tran, L. S. P., et al. (2007). Regulation and functional analysis of ZmDREB2A in response to drought and heat stresses in *Zea mays* L. *Plant J.* 50, 54–69. doi: 10.1111/j.1365-313X.2007.03034.x

Rahman, M. A., Chikushi, J., Yoshida, S., and Karim, A. (2009). Growth and yield components of wheat genotypes exposed to high temperature stress under control environment. *Bangladesh J. Agric. Res.* 34, 360–372. doi: 10.3329/bjar.v34i3.3961

Ranum, P., Peña-Rosas, J. P., and Garcia-Casal, M. N. (2014). Global maize production, utilization, and consumption. *Ann. N. Y. Acad. Sci.* 1312, 105–112. doi: 10.1111/nyas.12396

Rashed, M. A.-S., Abou-Deif, M. H., Khalil, K. M., and Mahmoud, F. E.-S. (2021). Expression levels of heat shock proteins through western blot and real-time polymerase chain reaction in maize. *Jordan J. Biol. Sci.* 14, 671–676. doi: 10.1007/s00726-010-0538-y

Razzaq, A., Kaur, P., Akhter, N., Wani, S. H., and Saleem, F. (2021). Next-generation breeding strategies for climate-ready crops. *Front. Plant Sci.* 12:620420. doi: 10.3389/fpls.2021.620420

Reddy, A., Reddy, V. S., and Golovkin, M. (2000). A calmodulin binding protein from *Arabidopsis* is induced by ethylene and contains a DNA-binding motif. *Biochem. Biophys. Res. Commun.* 279, 762–769. doi: 10.1006/bbrc.2000.4032

Reddy, A. S., Ben-Hur, A., and Day, I. S. (2011). Experimental and computational approaches for the study of calmodulin interactions. *Phytochemistry* 72, 1007–1019. doi: 10.1016/j.phytochem.2010.12.022

Reddy, P. S., Kavi Kishor, P. B., Seiler, C., Kuhlmann, M., Eschen-Lippold, L., Lee, J., et al. (2014). Unraveling regulation of the small heat shock proteins by the heat shock factor *HvHsfB2c* in barley: its implications in drought stress response and seed development. *PLoS One* 9:e89125. doi: 10.1371/journal.pone.0089125

Reddy, V. S., Day, I. S., Thomas, T., and Reddy, A. S. N. (2004). KIC, a novel Ca2+ binding protein with one EF-hand motif, interacts with a microtubule motor protein and regulates trichome morphogenesis. *Plant Cell* 16, 185–200. doi: 10.1105/tpc.016600

Reimold, A. M., Etkin, A., Clauss, I., Perkins, A., Friend, D. S., Zhang, J., et al. (2000). An essential role in liver development for transcription factor XBP-1. *Genes Dev.* 14, 152–157. doi: 10.1101/gad.14.2.152

Rezaei, E. E., Webber, H., Gaiser, T., Naab, J., and Ewert, F. (2015). Heat stress in cereals: mechanisms and modelling. *Eur. J. Agron.* 64, 98–113. doi: 10.1016/j.eja.2014.10.003

Ribeiro, C., Hennen-Bierwagen, T. A., Myers, A. M., Cline, K., and Settles, A. M. (2020). Engineering 6-phosphogluconate dehydrogenase to improve heat tolerance in maize seed development. *bioRxiv [Preprint]* doi: 10.1101/2020.05.21.108985

Rochaix, J.-D. (2011). Regulation of photosynthetic electron transport. *Biochim. Biophys. Acta* 1807, 375–383.

Rodziewicz, P., Swarcewicz, B., Chmielewska, K., Wojakowska, A., and Stobiecki, M. (2014). Influence of abiotic stresses on plant proteome and metabolome changes. *Acta Physiol. Plant.* 36, 1–19. doi: 10.1007/s11738-013-1402-y

Rooney, W. L., Blumenthal, J., Bean, B., and Mullet, J. E. (2007). Designing sorghum as a dedicated bioenergy feedstock. *Biofuels Bioprod. Biorefin.* 1, 147–157. doi: 10.1186/s13068-017-0892-z

Rosenzweig, C., Iglesius, A., Yang, X.-B., Epstein, P. R., and Chivian, E. (2001). Climate change and extreme weather events: implications for food production, plant diseases, and pests. *Glob. Change Hum. Health* 2, 90–104.

Ruan, Y.-L., Jin, Y., Yang, Y.-J., Li, G.-J., and Boyer, J. S. (2010). Sugar input, metabolism, and signaling mediated by invertase: roles in development, yield potential, and response to drought and heat. *Mol. Plant* 3, 942–955. doi: 10.1093/mp/ssq044

Rupwate, S. D., and Rajasekharan, R. (2012). Plant phosphoinositide-specific phospholipase C: an insight. *Plant Signal. Behav.* 7, 1281–1283. doi: 10.4161/psb.21436

Ryel, R., Caldwell, M., Yoder, C., Or, D., and Leffler, A. (2002). Hydraulic redistribution in a stand of *Artemisia tridentata*: evaluation of benefits to transpiration assessed with a simulation model. *Oecologia* 130, 173–184. doi: 10.1007/s004420100794

Sabagh, A. E., Hossain, A., Iqbal, M. A., Barutçular, C., Islam, M. S., Çiğ, F., et al. (2020). "Maize adaptability to heat stress under changing climate," in *Plant Stress Physiology*, ed. A. Hossain (London: IntechOpen).

Sachs, M. M., Subbaiah, C. C., and Saab, I. N. (1996). Anaerobic gene expression and flooding tolerance in maize. *J. Exp. Bot.* 47, 1–15. doi: 10.1104/pp.109.2.433

Sagi, M., and Fluhr, R. (2006). Production of reactive oxygen species by plant NADPH oxidases. *Plant Physiol.* 141, 336–340. doi: 10.1104/pp.106.078089

Sah, R., Chakraborty, M., Prasad, K., Pandit, M., Tudu, V., Chakravarty, M., et al. (2020). Impact of water deficit stress in maize: phenology and yield components. *Sci. Rep.* 10:2944. doi: 10.1038/s41598-020-59689-7

Sakai, A., and Larcher, W. (2012). *Frost Survival of Plants: Responses and Adaptation to Freezing Stress*. Berlin: Springer Science & Business Media.

Sallam, A., Amro, A., El-Akhdar, A., Dawood, M. F. A., Kumamaru, T., and Stephen Baenziger, P. (2018). Genetic diversity and genetic variation in morpho-physiological traits to improve heat tolerance in Spring barley. *Mol. Biol. Rep.* 45, 2441–2453. doi: 10.1007/s11033-018-4410-6

Sánchez, B., Rasmussen, A., and Porter, J. R. (2014). Temperatures and the growth and development of maize and rice: a review. *Glob. Change Biol.* 20, 408–417. doi: 10.1111/gcb.12389

Sang, J., Zhang, A., Lin, F., Tan, M., and Jiang, M. (2008). Cross-talk between calcium-calmodulin and nitric oxide in abscisic acid signaling in leaves of maize plants. *Cell Res.* 18, 577–588. doi: 10.1038/cr.2008.39

Schramm, F., Larkindale, J., Kiehlmann, E., Ganguli, A., Englich, G., Vierling, E., et al. (2008). A cascade of transcription factor DREB2A and heat stress transcription factor HsfA3 regulates the heat stress response of *Arabidopsis*. *Plant J.* 53, 264–274. doi: 10.1111/j.1365-313X.2007.03334.x

Seetharam, K., Kuchanur, P. H., Koirala, K., Tripathi, M. P., Patil, A., Sudarsanam, V., et al. (2021). Genomic regions associated with heat stress tolerance in tropical maize (*Zea mays* L.). *Sci. Rep.* 11:13730. doi: 10.1038/s41598-021-93061-7

Sengupta, S., Mukherjee, S., Basak, P., and Majumder, A. L. (2015). Significance of galactinol and raffinose family oligosaccharide synthesis in plants. *Front. Plant Sci.* 6:656. doi: 10.3389/fpls.2015.00656

Sewelam, N., Jaspert, N., Van Der Kelen, K., Tognetti, V. B., Schmitz, J., Frerigmann, H., et al. (2014). Spatial H2O2 signaling specificity: H2O2 from chloroplasts and peroxisomes modulates the plant transcriptome differentially. *Mol. Plant* 7, 1191–1210. doi: 10.1093/mp/ssu070

Sharma, A., Kumar, V., Shahzad, B., Ramakrishnan, M., Singh Sidhu, G. P., Bali, A. S., et al. (2020). Photosynthetic response of plants under different abiotic stresses: a review. *J. Plant Growth Regul.* 39, 509–531.

Sharma, A., Shahzad, B., Kumar, V., Kohli, S. K., Sidhu, G. P. S., Bali, A. S., et al. (2019). Phytohormones regulate accumulation of osmolytes under abiotic stress. *Biomolecules* 9:285. doi: 10.3390/biom9070285

Sharma, D. K., Torp, A. M., Rosenqvist, E., Ottosen, C.-O., and Andersen, S. B. (2017). QTLs and potential candidate genes for heat stress tolerance identified from the mapping populations specifically segregating for *Fv*/*Fm* in wheat. *Front. Plant Sci.* 8:1668. doi: 10.3389/fpls.2017.01668

Shi, S., Li, S., Asim, M., Mao, J., Xu, D., Ullah, Z., et al. (2018). The *Arabidopsis* calcium-dependent protein kinases (CDPKs) and their roles in plant growth regulation and abiotic stress responses. *Int. J. Mol. Sci.* 19:1900. doi: 10.3390/ijms19071900

Siebers, M. H., Slattery, R. A., Yendrek, C. R., Locke, A. M., Drag, D., Ainsworth, E. A., et al. (2017). Simulated heat waves during maize reproductive stages alter reproductive growth but have no lasting effect when applied during vegetative stages. *Agric. Ecosyst. Environ.* 240, 162–170. doi: 10.1016/j.agee.2016.11.008

Silim, S., Coe, R., Omanga, P., and Gwata, E. (2006). The response of pigeonpea genotypes of different duration types to variation in temperature and photoperiod under field conditions in Kenya. *J. Food Agric. Environ.* 4, 209–214.

Singh, R., Gupta, R., Bhardwaj, R., and Singh, R. (2021). "CRISPR/CAS9 technologies to enhance tolerance to abiotic stress in crop plants," in *Environmental Stress Physiology of Plants and Crop Productivity*, eds T. Kaur and S. Arora (New York, NY: Bantam Books), 206. doi: 10.2174/9781681087900121010016

Singletary, G. W., Banisadr, R., and Keeling, P. L. (1994). Heat stress during grain filling in maize: effects on carbohydrate storage and metabolism. *Funct. Plant Biol.* 21, 829–841. doi: 10.1071/pp9940829

Slama, I., Abdelly, C., Bouchereau, A., Flowers, T., and Savouré, A. (2015). Diversity, distribution and roles of osmoprotective compounds accumulated in halophytes under abiotic stress. *Ann. Bot.* 115, 433–447. doi: 10.1093/aob/mcu239

Song, J., Weng, Q., Ma, H., Yuan, J., Wang, L., and Liu, Y. (2016). Cloning and expression analysis of the Hsp70 gene ZmERD2 in *Zea mays*. *Biotechnol. Biotechnol. Equip.* 30, 219–226. doi: 10.1080/13102818.2015.1131625

Song, X., Weng, Q., Zhao, Y., Ma, H., Song, J., Su, L., et al. (2018). Cloning and expression analysis of ZmERD3 gene from *Zea mays*. *Iran J. Biotechnol.* 16:e1593. doi: 10.21859/ijb.1593

Stanley, D. W., and Parkin, K. L. (1991). Biological membrane deterioration and associated quality losses in food tissues. *Crit. Rev. Food Sci. Nutr.* 30, 487–553. doi: 10.1080/10408399109527554

Stavridou, E., Voulgari, G., Michailidis, M., Kostas, S., Chronopoulou, E. G., Labrou, N. E., et al. (2021). Overexpression of a biotic stress-inducible *Pvgstu* gene activates early protective responses in tobacco under combined heat and drought. *Int. J. Mol. Sci.* 22:2352. doi: 10.3390/ijms22052352

Strasser, R. J., Tsimilli-Michael, M., and Srivastava, A. (2004). "Analysis of the chlorophyll a fluorescence transient," in *Chlorophyll a Fluorescence*, eds G. C. Papageorgiou and Govindjee (Dordrecht: Springer), 321–362. doi: 10.1007/978-1-4020-3218-9_12

Su, H., Cao, Y., Ku, L., Yao, W., Cao, Y., Ren, Z., et al. (2018). Dual functions of ZmNF-YA3 in photoperiod-dependent flowering and abiotic stress responses in maize. *J. Exp. Bot.* 69, 5177–5189. doi: 10.1093/jxb/ery299

Sun, L., Liu, Y., Kong, X., Zhang, D., Pan, J., Zhou, Y., et al. (2012). ZmHSP16. 9, a cytosolic class I small heat shock protein in maize (*Zea mays*), confers heat tolerance in transgenic tobacco. *Plant Cell Rep.* 31, 1473–1484. doi: 10.1007/s00299-012-1262-8

Swapna, S., and Shylaraj, K. S. (2017). Screening for osmotic stress responses in rice varieties under drought condition. *Rice Sci.* 24, 1446–1452.

Takemoto, D., Tanaka, A., and Scott, B. (2007). NADPH oxidases in fungi: diverse roles of reactive oxygen species in fungal cellular differentiation. *Fungal Genet. Biol.* 44, 1065–1076. doi: 10.1016/j.fgb.2007.04.011

Tan, Y.-Q., Yang, Y., Zhang, A., Fei, C.-F., Gu, L.-L., Sun, S.-J., et al. (2020). Three CNGC family members, CNGC5, CNGC6, and CNGC9, are required for constitutive growth of *Arabidopsis* root hairs as Ca2+-permeable channels. *Plant Commun.* 1:100001. doi: 10.1016/j.xplc.2019.100001

Tao, F., and Zhang, Z. (2010). Adaptation of maize production to climate change in North China Plain: quantify the relative contributions of adaptation options. *Eur. J. Agron.* 33, 103–116. doi: 10.1016/j.eja.2010.04.002

Tebaldi, C., and Lobell, D. (2018). Estimated impacts of emission reductions on wheat and maize crops. *Clim. Change* 146, 533–545. doi: 10.1007/s10584-015-1537-5

Tiwari, Y. K., and Yadav, S. K. (2019). High temperature stress tolerance in maize (*Zea mays* L.): physiological and molecular mechanisms. *J. Plant Biol.* 62, 93–102. doi: 10.1007/s12374-018-0350-x

Török, Z., Crul, T., Maresca, B., Schütz, G. J., Viana, F., Dindia, L., et al. (2014). Plasma membranes as heat stress sensors: from lipid-controlled molecular switches to therapeutic applications. *Biochim. Biophys. Acta* 1838, 1594–1618. doi: 10.1016/j.bbamem.2013.12.015

Tóth, S. Z., Nagy, V., Puthur, J. T., Kovács, L., and Garab, G. (2011). The physiological role of ascorbate as photosystem ii electron donor: protection against photoinactivation in heat-stressed leaves. *Plant Physiol.* 156, 382–392. doi: 10.1104/pp.110.171918

Towil, L. E. (2010). Long-term pollen storage. *Plant Breed. Rev.* 13, 179–207. doi: 10.1002/9780470650059.ch5

Urquhart, W., Chin, K., Ung, H., Moeder, W., and Yoshioka, K. (2011). The cyclic nucleotide-gated channels AtCNGC11 and 12 are involved in multiple Ca^{2+}-dependent physiological responses and act in a synergistic manner. *J. Exp. Bot.* 62, 3671–3682. doi: 10.1093/jxb/err074

Van Inghelandt, D., Frey, F. P., Ries, D., and Stich, B. (2019). QTL mapping and genome-wide prediction of heat tolerance in multiple connected populations of temperate maize. *Sci. Rep.* 9:14418. doi: 10.1038/s41598-019-50853-2

Vardhini, B. V., and Anjum, N. A. (2015). Brassinosteroids make plant life easier under abiotic stresses mainly by modulating major components of antioxidant defense system. *Front. Environ. Sci.* 2:67. doi: 10.3389/fenvs.2014.00067

Vass, I., and Cser, K. (2009). Janus-faced charge recombinations in photosystem II photoinhibition. *Trends Plant Sci.* 14, 200–205. doi: 10.1016/j.tplants.2009.01.009

Vitale, A., and Boston, R. S. (2008). Endoplasmic reticulum quality control and the unfolded protein response: insights from plants. *Traffic* 9, 1581–1588. doi: 10.1111/j.1600-0854.2008.00780.x

von Caemmerer, S., and Furbank, R. T. (2016). Strategies for improving C4 photosynthesis. *Curr. Opin. Plant Biol.* 31, 125–134. doi: 10.1016/j.pbi.2016.04.003

Wadhwa, N., Mathew, B. B., Jatawa, S., and Tiwari, A. (2012). Lipid peroxidation: mechanism, models and significance. *Int. J. Curr. Sci.* 3, 29–38.

Wahid, A., Gelani, S., Asharf, M., and Foolad, M. R. (2007). Heat tolerance in plants: an overview. *Environ. Exp. Bot.* 61, 199–223. doi: 10.1016/j.envexpbot.2007.05.011

Wang, C.-T., Ru, J.-N., Liu, Y.-W., Li, M., Zhao, D., Yang, J.-F., et al. (2018a). Maize WRKY transcription factor ZmWRKY106 confers drought and heat tolerance in transgenic plants. *Int. J. Mol. Sci.* 19:3046. doi: 10.3390/ijms19103046

Wang, C.-T., Ru, J.-N., Liu, Y.-W., Yang, J.-F., Li, M., Xu, Z.-S., et al. (2018b). The maize WRKY transcription factor ZmWRKY40 confers drought resistance in transgenic *Arabidopsis*. *Int. J. Mol. Sci.* 19:2580. doi: 10.3390/ijms19092580

Wang, W., Vinocur, B., Shoseyov, O., and Altman, A. (2004). Role of plant heat-shock proteins and molecular chaperones in the abiotic stress response. *Trends Plant Sci.* 9, 244–252. doi: 10.1016/j.tplants.2004.03.006

Wang, X., Wang, H., Liu, S., Ferjani, A., Li, J., Yan, J., et al. (2016). Genetic variation in ZmVPP1 contributes to drought tolerance in maize seedlings. *Nat. Genet.* 48, 1233–1241. doi: 10.1038/ng.3636

Waqas, M. A., Wang, X., Zafar, S. A., Noor, M. A., Hussain, H. A., Azher Nawaz, M., et al. (2021). Thermal stresses in maize: effects and management strategies. *Plants* 10:293. doi: 10.3390/plants10020293

Waraich, E., Ahmad, R., Halim, A., and Aziz, T. (2012). Alleviation of temperature stress by nutrient management in crop plants: a review. *J. Soil Sci. Plant Nutr.* 12, 221–244. doi: 10.4014/jmb.2105.05009

Weckwerth, P., Ehlert, B., and Romeis, T. (2015). ZmCPK1, a calcium-independent kinase member of the *Zea mays* CDPK gene family, functions as a negative

regulator in cold stress signalling. *Plant Cell Environ.* 38, 544–558. doi: 10.1111/pce.12414

Wen, W., Li, D., Li, X., Gao, Y., Li, W., Li, H., et al. (2014). Metabolome-based genome-wide association study of maize kernel leads to novel biochemical insights. *Nat. Commun.* 5:3438. doi: 10.1038/ncomms4438

Wilson, D., Muchow, R., and Murgatroyd, C. (1995). Model analysis of temperature and solar radiation limitations to maize potential productivity in a cool climate. *Field Crops Res.* 43, 1–18. doi: 10.1016/0378-4290(95)00037-q

Xalxo, R., Yadu, B., Chandra, J., Chandrakar, V., and Keshavkant, S. (2020). "Alteration in carbohydrate metabolism modulates thermotolerance of plant under heat stress," in *Heat Stress Tolerance in Plants: Physiological, Molecular and Genetic Perspectives*, eds S. H. Wani and V. Kumar (Hoboken, NJ: Wiley), 77–115. doi: 10.1016/j.jprot.2020.103968

Xu, Y., Chu, C., and Yao, S. (2021). The impact of high-temperature stress on rice: challenges and solutions. *Crop J.* 9, 963–976. doi: 10.3390/plants10010043

Yadav, S., Tiwari, Y. K., Singh, V., Patil, A. A., Shanker, A., Lakshmi, N. J., et al. (2018). Physiological and biochemical basis of extended and sudden heat stress tolerance in maize. *Proc. Natl. Acad. Sci. India Sect. B Biol. Sci.* 88, 249–263. doi: 10.1007/s40011-016-0752-9

Yadav, S., Vanaja, M., and Maheswari, M. (2017). Exogenous application of bio-regulators for alleviation of heat stress in seedlings of maize. *J. Agric. Res.* 2:000137.

Yamaguchi, S. (2008). Gibberellin metabolism and its regulation. *Annu. Rev. Plant Biol.* 59, 225–251. doi: 10.1146/annurev.arplant.59.032607.092804

Yan, K., Chen, P., Shao, H., Shao, C., Zhao, S., and Brestic, M. (2013). Dissection of photosynthetic electron transport process in sweet sorghum under heat stress. *PLoS One* 8:e62100. doi: 10.1371/journal.pone.0062100

Yan, Q., Huang, Q., Chen, J., Li, J., Liu, Z., Yang, Y., et al. (2017). *SYTA* has positive effects on the heat resistance of *Arabidopsis*. *Plant Growth Regul.* 81, 467–476. doi: 10.1007/s10725-016-0224-5

Yan, Q., Zong, X., Wu, F., Li, J., Ma, T., Zhao, Y., et al. (2020). Integrated analysis of co-expression, conserved genes and gene families reveal core regulatory network of heat stress response in *Cleistogenes songorica*, a xerophyte perennial desert plant. *BMC Genomics* 21:715. doi: 10.1186/s12864-020-07122-8

Yang, G., Rhodes, D., and Joly, R. J. (1996). Effects of high temperature on membrane stability and chlorophyll fluorescence in glycinebetaine-deficient and glycinebetaine-containing maize lines. *Funct. Plant Biol.* 23, 437–443. doi: 10.1071/pp9960437

Yang, L., Wang, Y., and Yang, K. (2021). *Klebsiella variicola* improves the antioxidant ability of maize seedlings under saline-alkali stress. *PeerJ* 9:e11963. doi: 10.7717/peerj.11963

Yang, T., Peng, H., Whitaker, B. D., and Jurick, W. M. (2013). Differential expression of calcium/calmodulin-regulated SlSRs in response to abiotic and biotic stresses in tomato fruit. *Physiol. Plant.* 148, 445–455. doi: 10.1111/ppl.12027

Yang, T., and Poovaiah, B. (2002). A calmodulin-binding/CGCG box DNA-binding protein family involved in multiple signaling pathways in plants. *J. Biol. Chem.* 277, 45049–45058. doi: 10.1074/jbc.M207941200

Yang, W., Kong, Z., Omo-Ikerodah, E., Xu, W., Li, Q., and Xue, Y. (2008). Calcineurin B-like interacting protein kinase OsCIPK23 functions in pollination and drought stress responses in rice (*Oryza sativa* L.). *J. Genet. Genomics* 35, 531–543, S1–S2. doi: 10.1016/S1673-8527(08)60073-9

Yeh, S.-Y., Lin, H.-H., Chang, Y.-M., Chang, Y.-L., Chang, C.-K., Huang, Y.-C., et al. (2021). Maize Golden2-like transcription factors boost rice chloroplast development, photosynthesis, and grain yield. *Plant Physiol.* 188, 442–459. doi: 10.1093/plphys/kiab511

Younis, A., Ramzan, F., Ramzan, Y., Zulfiqar, F., Ahsan, M., and Lim, K. B. (2020). Molecular markers improve abiotic stress tolerance in crops: a review. *Plants* 9:1374. doi: 10.3390/plants9101374

Yuan, B. Z., Sun, J., and Nishiyama, S. (2004). Effect of drip irrigation on strawberry growth and yield inside a plastic greenhouse. *Biosyst. Eng.* 87, 237–245. doi: 10.1016/j.biosystemseng.2003.10.014

Yue, R., Lu, C., Sun, T., Peng, T., Han, X., Qi, J., et al. (2015). Identification and expression profiling analysis of calmodulin-binding transcription activator genes in maize (*Zea mays* L.) under abiotic and biotic stresses. *Front. Plant Sci.* 6:576. doi: 10.3389/fpls.2015.00576

Zhai, S., Gao, Q., Liu, X., Sui, Z., and Zhang, J. (2013). Overexpression of a *Zea mays* phospholipase C1 gene enhances drought tolerance in tobacco in part by maintaining stability in the membrane lipid composition. *Plant Cell Tissue Organ Cult.* 115, 253–262. doi: 10.1007/s11240-013-0358-3

Zhang, D., Li, Q., Yamori, W., and Wei, M. (2020a). *The Rate-Limiting Step for Photosynthetic CO2 Utilization Under Varying Atmospheric Evaporative Demand in Solanum lycopersicum (Tomato)*. Durham, NC: Research Square Company.

Zhang, H., Li, G., Fu, C., Duan, S., Hu, D., and Guo, X. (2020b). Genome-wide identification, transcriptome analysis and alternative splicing events of Hsf family genes in maize. *Sci. Rep.* 10:8073. doi: 10.1038/s41598-020-65068-z

Zhang, H., Li, G., Hu, D., Zhang, Y., Zhang, Y., Shao, H., et al. (2020c). Functional characterization of maize heat shock transcription factor gene ZmHsf01 in thermotolerance. *PeerJ* 8:e8926. doi: 10.7717/peerj.8926

Zhang, S.-S., Yang, H., Ding, L., Song, Z.-T., Ma, H., Chang, F., et al. (2017). Tissue-specific transcriptomics reveals an important role of the unfolded protein response in maintaining fertility upon heat stress in Arabidopsis. *Plant Cell* 29, 1007–1023. doi: 10.1105/tpc.16.00916

Zhao, C., Liu, B., Piao, S., Wang, X., Lobell, D. B., Huang, Y., et al. (2017). Temperature increase reduces global yields of major crops in four independent estimates. *Proc. Natl. Acad. Sci. U.S.A.* 114, 9326–9331. doi: 10.1073/pnas.1701762114

Zhao, J., Lu, Z., Wang, L., and Jin, B. (2021). Plant responses to heat stress: physiology, transcription, noncoding RNAs, and epigenetics. *Int. J. Mol. Sci.* 22:117. doi: 10.3390/ijms22010117

Zhao, Y., Du, H., Wang, Y., Wang, H., Yang, S., Li, C., et al. (2021). The calcium-dependent protein kinase ZmCDPK7 functions in heat-stress tolerance in maize. *J. Integr. Plant Biol.* 63, 510–527. doi: 10.1111/jipb.13056

Zhou, L., Lan, W., Chen, B., Fang, W., and Luan, S. (2015). A calcium sensor-regulated protein kinase, CALCINEURIN B-LIKE PROTEIN-INTERACTING PROTEIN KINASE19, is required for pollen tube growth and polarity. *Plant Physiol.* 167, 1351–1360. doi: 10.1104/pp.114.256065

Zhou, M.-L., Tang, Y.-X., and Wu, Y.-M. (2012). Genome-wide analysis of AP2/ERF transcription factor family in *Zea mays*. *Curr. Bioinformatics* 7, 324–332. doi: 10.2174/157489312802460776

Zhou, Z. H., Wang, Y., Ye, X. Y., and Li, Z. G. (2018). Signaling molecule hydrogen sulfide improves seed germination and seedling growth of maize (*Zea mays* L.) under high temperature by inducing antioxidant system and osmolyte biosynthesis. *Front. Plant Sci.* 9:1288. doi: 10.3389/fpls.2018.01288

Zivcak, M., Brestic, M., Kunderlikova, K., Sytar, O., and Allakhverdiev, S. I. (2015). Repetitive light pulse-induced photoinhibition of photosystem I severely affects CO 2 assimilation and photoprotection in wheat leaves. *Photosynth. Res.* 126, 449–463. doi: 10.1007/s11120-015-0121-1

Zulfiqar, F., and Ashraf, M. (2021). Bioregulators: unlocking their potential role in regulation of the plant oxidative defense system. *Plant Mol. Biol.* 105, 11–41. doi: 10.1007/s11103-020-01077-w

Conflict of Interest: The authors declare that the research was conducted in the absence of any commercial or financial relationships that could be construed as a potential conflict of interest.

Publisher's Note: All claims expressed in this article are solely those of the authors and do not necessarily represent those of their affiliated organizations, or those of the publisher, the editors and the reviewers. Any product that may be evaluated in this article, or claim that may be made by its manufacturer, is not guaranteed or endorsed by the publisher.

Copyright © 2022 El-Sappah, Rather, Wani, Elrys, Bilal, Huang, Dar, Elashtokhy, Soaud, Koul, Mir, Yan, Li, El-Tarabily and Abbas. This is an open-access article distributed under the terms of the Creative Commons Attribution License (CC BY). The use, distribution or reproduction in other forums is permitted, provided the original author(s) and the copyright owner(s) are credited and that the original publication in this journal is cited, in accordance with accepted academic practice. No use, distribution or reproduction is permitted which does not comply with these terms.

frontiers | Frontiers in Plant Science

REVIEW
published: 29 April 2022
doi: 10.3389/fpls.2022.882835

Glyco-Engineering Plants to Produce Helminth Glycoproteins as Prospective Biopharmaceuticals: Recent Advances, Challenges and Future Prospects

Alex van der Kaaij, Kim van Noort, Pieter Nibbering, Ruud H. P. Wilbers and Arjen Schots*

Laboratory of Nematology, Plant Sciences Group, Wageningen University and Research, Wageningen, Netherlands

Glycoproteins are the dominant category among approved biopharmaceuticals, indicating their importance as therapeutic proteins. Glycoproteins are decorated with carbohydrate structures (or glycans) in a process called glycosylation. Glycosylation is a post-translational modification that is present in all kingdoms of life, albeit with differences in core modifications, terminal glycan structures, and incorporation of different sugar residues. Glycans play pivotal roles in many biological processes and can impact the efficacy of therapeutic glycoproteins. The majority of biopharmaceuticals are based on human glycoproteins, but non-human glycoproteins, originating from for instance parasitic worms (helminths), form an untapped pool of potential therapeutics for immune-related diseases and vaccine candidates. The production of sufficient quantities of correctly glycosylated putative therapeutic helminth proteins is often challenging and requires extensive engineering of the glycosylation pathway. Therefore, a flexible glycoprotein production system is required that allows straightforward introduction of heterologous glycosylation machinery composed of glycosyltransferases and glycosidases to obtain desired glycan structures. The glycome of plants creates an ideal starting point for *N*- and *O*-glyco-engineering of helminth glycans. Plants are also tolerant toward the introduction of heterologous glycosylation enzymes as well as the obtained glycans. Thus, a potent production platform emerges that enables the production of recombinant helminth proteins with unusual glycans. In this review, we discuss recent advances in plant glyco-engineering of potentially therapeutic helminth glycoproteins, challenges and their future prospects.

Keywords: glycan, glycosylation, glycoprotein, biopharmaceutical, helminth, plant made pharmaceutical

OPEN ACCESS

Edited by:
Ralf Alexander Wilhelm, Julius Kühn-Institute, Germany

Reviewed by:
Stephanie Archer-Hartmann, University of Georgia, United States
Juliana Parsons, University of Freiburg, Germany

****Correspondence:***
Alex van der Kaaij
alex.vanderkaaij@wur.nl

Specialty section:
This article was submitted to Plant Biotechnology, a section of the journal Frontiers in Plant Science

Received: *24 February 2022*
Accepted: *28 March 2022*
Published: *29 April 2022*

Citation:
van der Kaaij A, van Noort K, Nibbering P, Wilbers RHP and Schots A (2022) Glyco-Engineering Plants to Produce Helminth Glycoproteins as Prospective Biopharmaceuticals: Recent Advances, Challenges and Future Prospects. Front. Plant Sci. 13:882835. doi: 10.3389/fpls.2022.882835

PHARMACEUTICAL PROTEIN PRODUCTION IN PLANTS

In plant molecular farming, valuable small molecules and proteins are produced in plants often with the aim to ultimately use these compounds as drugs. Plant molecular farming emerged around 1990 after the first expression of antibodies and albumin in plants (Hiatt et al., 1989; Sijmons et al., 1990; Stieger et al., 1991). Afterward, proof-of-concept studies have confirmed the potential for plant-produced biopharmaceuticals as a substitute of or supplement to

conventional drugs (Schillberg and Finnern, 2021). Plant-produced biopharmaceutical proteins include a wide variety of proteins such as antibodies, vaccines, cytokines and enzymes. Currently, two plant-produced pharmaceuticals have received market approval. Carrot-cell-suspension-produced glucocerebrosidase has been approved to be used in enzyme replacement therapy for the lysosomal storage disorder Gaucher disease (Zimran et al., 2011; Grabowski et al., 2014) and recently a plant-based SARS-CoV2 vaccine has been approved in Canada (Health Canada Medicago Covifenz COVID-19 Vaccine, 2022). Many other plant-based biopharmaceuticals are currently in clinical trials, including vaccines for influenza (Ward et al., 2020) and *Bacillus anthracis* (Paolino et al., 2022). As the field of plant molecular farming continues to develop and reaches maturity, an increasing number of biopharmaceuticals will enter clinical trials and possibly reach market approval.

The majority of biopharmaceutical proteins are glycosylated (Walsh, 2018), a process where carbohydrate structures (glycans) are covalently attached to a protein backbone. Glycans can be crucial for the function of these proteins and a plethora of biological processes. On protein level, glycans can be important for protein folding and glycan dependent quality control, localization, protection against degradation, solubility and activity (Moremen et al., 2012; Hebert et al., 2014; Strasser et al., 2021). In addition, glycans can play a role in protein-protein interactions, interactions with cells and tissues, and immunogenicity (Varki and Gagneux, 2015). For this reason, heterologous production of complex glycoproteins is often performed in eukaryotic expression systems that naturally glycosylate proteins. Two main types of glycosylation exist: *N*-glycosylation and *O*-glycosylation. Initial *N*-glycosylation steps occur in the endoplasmic reticulum and are highly conserved among eukaryotes (Strasser, 2018), whereas glycans are modified with kingdom-specific glycan structures in the Golgi (Strasser, 2016). In contrast, *O*-glycosylation is not that highly conserved between eukaryotes. Various types of *O*-glycosylation exist in different species, and are predominantly initiated in either the ER or Golgi depending on the type of *O*-glycan. Common steps in the glycosylation machinery of plants that affect the production of heterologous glycoproteins are illustrated in **Figure 1**.

Notwithstanding their different glycosylation pattern, plants have shown to be well suited for the production of human glycoproteins over the last two decades (Bosch et al., 2013; Schoberer and Strasser, 2018). More recently, glycoproteins from parasitic worms have been reconstituted in plants (Wilbers et al., 2017). The glycome of plants is limited (with the exception of *O*-glycans on cell wall glycoproteins) and this allows production of heterologous proteins with a more homogenous glycan composition. It is also striking that plants tolerate the presence of engineered exogenous *N*- and *O*-glycans on their proteins by not showing an aberrant phenotype. These two properties make plants a suitable platform for the heterologous production of glycoproteins through adaptation of their glycosylation machinery, referred to as glyco-engineering (Montero-Morales and Steinkellner, 2018). Plant-production of glycoproteins is scalable from cell suspension cultures in flasks to GMP bioreactors, or entire plants in greenhouses (Lobato Gómez et al., 2021). Moreover, protein production in plants is rapid and flexible when using transient expression with agrobacterial or viral vectors (Kapila et al., 1997; Lobato Gómez et al., 2021). Plant expression systems also guarantee the absence of mammalian pathogens and oncogenic sequences (Fischer and Emans, 2000). These advantages and recent admission of the plant-based SARS-CoV2 vaccine, show that plant-based production systems are now a scalable, economically viable and safe option to produce biopharmaceuticals that depend on a specific glycan composition.

For many years the plant glyco-engineering field has focused mainly on the production of biopharmaceutical glycoproteins with a humanized glycan composition. Non-human glycoproteins, with native glycosylation patterns, have been largely ignored but form an untapped pool of potential biopharmaceuticals. The prime example of non-human glycoproteins with putative therapeutic applications are those produced by helminths (parasitic worms). Helminth glycoproteins show potential as therapeutics against immune-related disease (including allergies and autoimmune diseases) and are highly promising anti-helminth vaccine candidates (Bunte et al., 2022). Anti-helminth vaccines are direly needed since a quarter of the world population is infected with parasitic worms (Hotez et al., 2008; WHO, 2022). In addition, helminth infections in livestock cause a lot of distress by affecting animal well-being and lead to a loss in livestock productivity (Charlier et al., 2016). Once infected, anthelmintic drugs can be administered to reduce (chronic) infections of helminths in both humans and livestock. However, excessive usage, notably in animal husbandry, has led to anthelmintic drug resistance (James et al., 2009). Therefore, vaccines as alternative control measure are required to protect humans and livestock (Hotez et al., 2016; Claerebout and Geldhof, 2020). Currently, the only source to obtain helminth antigens is from the parasite itself, which requires the sacrifice of deliberately infected animals. Previous attempts to produce recombinant helminth vaccines, in for instance *E. coli* and yeast, have not met desired protection levels, possibly due to their non-native glycan composition (Geldhof et al., 2007; Meyvis et al., 2008). In addition, several helminth glycoproteins that are investigated for their therapeutic potential rely on their glycan composition for their activity (Ryan et al., 2020; Bunte et al., 2022).

This review focuses on recent developments in glyco-engineering and possibilities to further improve glyco-engineering strategies in plants with special emphasis on glycoproteins from helminths. First, the wide diversity of helminth *N*- and *O*-glycans will be described. Second, reconstitution of various helminth glycoforms by using different glyco-engineering strategies in plants will be described. Finally, a perspective will be given on applications and possible future directions to produce non-human glycoproteins with tailor-made glycans.

DIVERSITY OF HELMINTH GLYCANS

During an infection, helminths secrete immunomodulatory products, such as small molecules, RNA species, glycolipids and

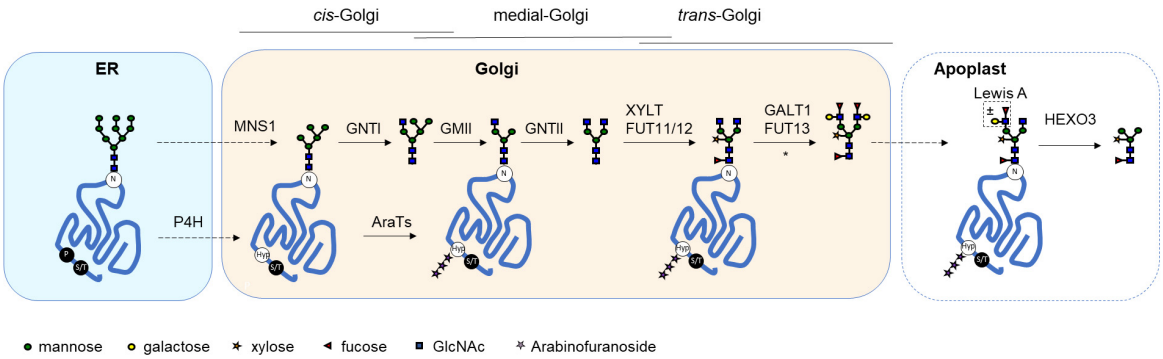


FIGURE 1 | Glycosylation pathways in plants. A schematic overview of successive glycan modifying steps in the plant secretory pathway. Glycoproteins receive an *N*-glycan in the endoplasmic reticulum (ER) on an asparagine residue (N) within the consensus sequence (*N*-X-S/T), where X can be any amino acid except proline. After ER quality control, the correctly folded protein passes through the Golgi compartment. Within the Golgi immature high mannose-type *N*-glycans are modified in a tightly regulated process. First, Golgi α-mannosidase I (MNS1) trims down the *N*-glycan to a Man5 structure. In subsequent steps a diantennary *N*-glycan is synthesized, which in plants is substituted with core α1,3-fucose and β1,2-xylose. In some cases [as indicated by an asterisk (*)], this *N*-glycan is further extended with Lewis A motifs. Once secreted into the extracellular space (or apoplast) a terminal GlcNAc glycan structure can be trimmed down to a paucimannosidic glycan by the β-hexosaminidase HEXO3. Classical *O*-glycan synthesis in plants is initiated by the hydroxylation of proline residues by prolyl-4-hydroxylases (P4H) in the ER and/or Golgi. These hydroxyproline residues (Hyp) can then be substituted with extensin-like *O*-glycans (substitution with arabinofuranoside by AraTs) or more complex arabinogalactan *O*-glycans, recently reviewed in Petersen et al. (2021). In contrast to animals, serine (S) and threonine (T) residues are not substituted with *O*-glycans in plants. GnTI, *N*-acetyl-glucosaminyltransferase I; GMII, Golgi-α-mannosidase II; GnTII, *N*-acetyl-glucosaminyltransferase II; XYLT, β1,2-xylosyltransferase; FUT11/12, Core α1,3-fucosyltransferase; GALT1, β1,3-galactosyltransferase; FUT13, α1,4-fucosyltransferase.

glycoproteins, to evade the host immune system and facilitate chronic infection (Bunte et al., 2022). The interplay between helminth secretory products and the host is partially mediated *via* glycan-dependent mechanisms (Bunte et al., 2022). Helminth glycoproteins can be decorated by a myriad of different *N*- and *O*-glycans as illustrated in **Figure 2**. The composition of these glycans differs between helminth species that belong to the distinct phyla Platyhelminthes (cestodes and trematodes) or Nematoda (nematodes). Furthermore, the glycan composition can differ between developmental stages and sexes within a single species (Smit et al., 2015; Hokke and van Diepen, 2017).

Mannosidic-Type *N*-Glycans

All helminth species possess glycoproteins with mannosidic glycans. However, the abundance and diversity of the mannosidic glycans is species-dependent (Hokke and van Diepen, 2017). Mannosidic *N*-glycans can range from high-mannose type (Man7-9) to Man5 and paucimannosidic *N*-glycans (Man3). In addition, Man5 or Man3 *N*-glycans can carry a single branched GlcNAc residue with or without further branch extensions (hybrid or single-branched *N*-glycans, respectively). Several helminth species, like the trematode *Fasciola hepatica* and nematode *Haemonchus contortus*, contain even shorter *N*-glycans, where additional mannoses are trimmed from the Man3 structure resulting in Man2 glycan structures (Paschinger and Wilson, 2015; Garcia-Campos et al., 2016; Ravidà et al., 2016).

N-Glycan Core Modifications

Various *N*-glycan core modifications have been observed in helminth species and in different developmental stages of a single species (Hokke and van Diepen, 2017). The main modification of the core is fucosylation. In early developmental stages of the trematode *Schistosoma mansoni*, *N*-glycans have an α1,3-fucose on their core. In later stages a core α1,6-fucose was found in the presence or absence of core α1,3-fucose. More densely fucosylated *N*-glycan cores were observed in adults of the nematode *H. contortus*. A trifucosylated core, with an α1,3-fucose attached to the distal core *N*-acetyl-glucosamine (GlcNAc) and two core fucoses (α1,3 and α1,6) attached to the proximal core GlcNAc, is the dominant glycan species on the H11 glycoprotein of *H. contortus* (Haslam et al., 1996). Additionally, galactosylation of the distal core α1,3-fucose and proximal core α1,6-fucose has been observed in *H. contortus* (Haslam et al., 1996; Hokke and van Diepen, 2017). *N*-glycan core xylosylation is uncommon in helminths, but has been observed in *S. mansoni* larval stages during the first three to 6 days after infection of humans, and in mature eggs and miracidia (Smit et al., 2015).

Branching and Elongation of *N*-Glycans

The degree of *N*-glycan branching is also highly variable between different helminth species and between different developmental stages (Smit et al., 2015; Hokke and van Diepen, 2017). Complex tri- or tetra-antennary *N*-glycans are often extended with β1,4-linked galactose or *N*-acetyl-galactosamine (GalNAc) as part of a LacNAc (LN) or LacdiNAc (LDN) motif (**Figure 2**), respectively (Haslam et al., 2000; Smit et al., 2015). In several helminth species these LN and LDN motifs are further substituted with α1,3-fucose linked to a GlcNAc (part of a Lewis X or LD*N*-F motif) and is frequently found in the antennae of *N*-glycans. Additional α1,2-fucoses can be attached to the α1,3-linked fucoses in the antennae to form difucosylated glycan structures, as found on the *N*-glycans of SmVAL-9 (Yoshino et al., 2014). Another terminal glycan structure, but less common, is a fucosylated terminal poly GlcNAc structure, which has been described for

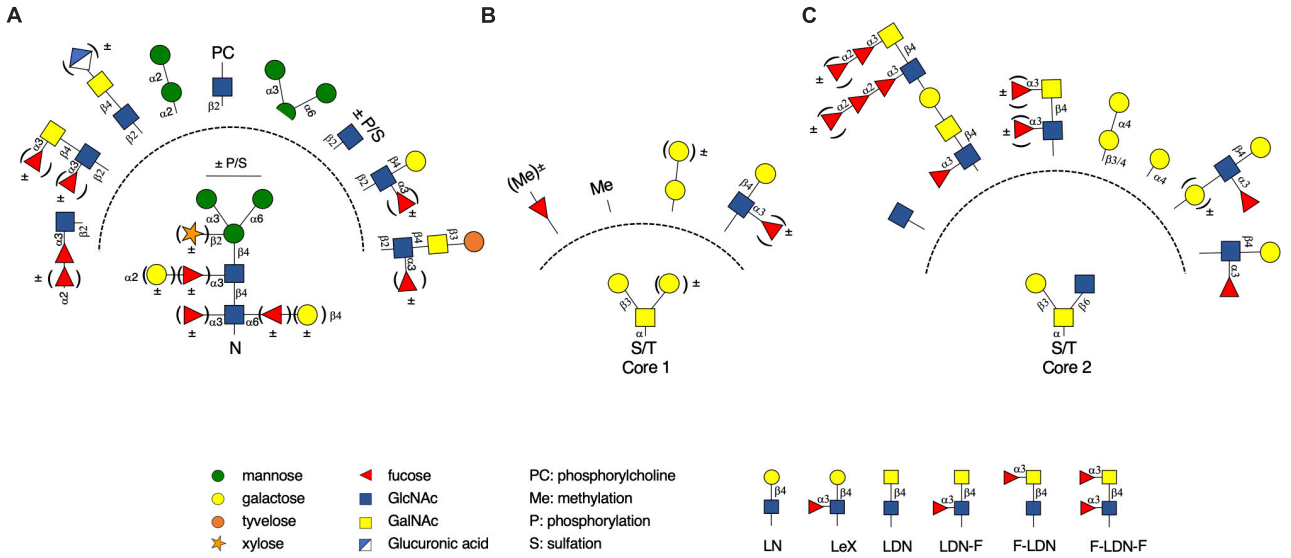


FIGURE 2 | Diversity of helminth glycans. **(A)** A selection of *N*-glycan motifs found on different helminth glycoproteins. Besides immature mannosidic glycans, helminth *N*-glycans can be substituted with different core residues or are extended with different glycan motifs in their antenna. Some modifications are shared with animals, whereas other modifications are quite unusual. **(B,C)** A selection of *O*-glycan motifs found on different helminth glycoproteins, which are divided between typical core 1 **(B)** and core 2 **(C)** *O*-glycans. The linkage between different monosaccharides has been indicated where possible.

Dirofilaria immitis (Martini et al., 2019). In contrast to human *N*-glycans extension of antennary galactose with sialic acid is never observed in helminths.

Unusual *N*-Glycan (Non-)carbohydrate Moieties

Within the helminth glycome there are several unusual modifications found on *N*-glycans. The non-carbohydrate moiety phosphorylcholine (PC) was attached to antennary GlcNAc residues or distal core GlcNAc of *N*-glycans in several helminth species (Pöltl et al., 2007; Paschinger et al., 2012). PC can also be attached to GalNAc combined in a LDN(-F) motif, although this is less common (Wilson and Paschinger, 2016; Martini et al., 2019). PC is found in parasitic nematodes and cestodes, as well as in free-living nematodes such as *Caenorhabditis elegans* (Lochnit et al., 2000; Hokke and van Diepen, 2017). LDN motifs can also be extended with the unusual sugar moiety glucuronic acid that has been found on *N*-glycans of *Dirofilaria immitis* (Martini et al., 2019). Glucuronic acid is even found on antennae that are already modified with PC (Martini et al., 2019). Another rare sugar is tyvelose, which is found on *N*-glycans in *Trichinella spiralis* as an extension of LDN*N*-F (Reason et al., 1994). Besides these uncommon moieties as part of helminth *N*-glycans other post-glycosylation modifications such as methylation, sulfation or phosphorylation were found on different helminth glycans (Ravidà et al., 2016; Jiménez-Castells et al., 2017).

O-Glycans

Helminth glycoproteins can also harbor *O*-glycans and most of them are initiated by the addition of GalNAc (*O*-GalNAc glycans). *O*-glycosylation in helminths shows resemblance with mammalian *O*-GalNAc glycosylation but lacks variants that are capped with sialic acid. The structures encountered are similar to mammalian core 1 and core 2 *O*-glycan structures (**Figure 2**; Casaravilla et al., 2003; Hokke and van Diepen, 2017). Both cores can be elongated with a wide variety of glycan motifs, but the observed extensions can differ between core 1 and core 2 *O*-glycans (Hokke and van Diepen, 2017). Core 1 *O*-glycans can be elongated with poly-galactose (mainly α1-4 linked), Lewis X or a single fucose moiety as found in *Echinococcus multilocularis*, *S. mansoni* and *Toxocara canis*, respectively. Core 2 *O*-glycans can be elongated with terminal poly-galactose, Lewis X, F-LDN or LDN-F. Poly-fucosylated versions of LDN with α1,2-linked fucose (di-fucosylated and/or tri-fucosylated motifs) are found in *S. mansoni* (Smit et al., 2015). The possible combinations of core structures, elongations and terminal structures result in an array of different *O*-glycans (Talabnin et al., 2013; Smit et al., 2015; Hewitson et al., 2016). For several helminth species unique *O*-GalNac cores have also been observed. For *S. mansoni*, a core 1 *O*-glycan with additional β1,6-linked galactose and other extensions have been observed in several life stages (Smit et al., 2015). *H. contortus* has a rare *O*-GalNAc glycan, which is substitute with α1,3-linked galactose (core 8) (van Stijn et al., 2010). Not all helminth *O*-glycans are GalNAc-based glycans. *O*-glycans have been detected in *S. mansoni* and *Heligmosomoides polygyrus* that were initiated with an uncharacterized hexose (Jang-Lee et al., 2007; Hewitson et al., 2016). These rare *O*-glycans were further extended with fucose or another hexose residue. Helminth *O*-glycans can also be modified with post-glycosylation modifications such as methylation. Methylated *O*-glycans have been found on common core 1 and core 2 *O*-glycans of helminths (Hokke and van Diepen, 2017). Although the knowledge on the helminth *O*-glycome is

relatively limited compared to the *N*-glycome, it is receiving more attention, possibly leading to the discovery of structures and post-glycosylation modifications previously unknown to the helminth *O*-glycome.

GLYCO-ENGINEERING HELMINTH GLYCANS IN PLANTS

The large variety in helminth *N*- and *O*-glycan composition largely affects glyco-engineering strategies in order to produce glycoproteins that could serve as immunomodulatory therapeutics or vaccine candidates. To study the effect of various glycoforms of these helminth proteins, a platform is needed that is capable of producing the desired glycoprotein with a defined glycan composition. A combination of strategies can be used to ultimately obtain a tailor-made glycoprotein that is identical to the native helminth glycoprotein, but can be different for each target species. In plants, this combination of strategies can include avoiding the addition of undesired plant glycan motifs (core α1,3-fucose, β1,2-xylose and/or Lewis A), addition of desired sugar residues by exogenous glycosyltransferases, and avoiding processing of glycans by endogenous glycosidases (**Figure 3**). Furthermore, it is important that newly introduced glycosyltransferases localize to the proper Golgi compartment. The localization of these enzymes to distinct Golgi compartments is determined by the cytoplasmic, transmembrane, and stem region (CTS region) of glycosyltransferases (Grabenhorst and Conradt, 1999; Sasai et al., 2001). If the localization is incorrect, glycosyltransferases are unable to function properly or the glycan is modified "too early," which could interfere with subsequent modifications (Wilbers et al., 2017; Kallolimath et al., 2018). However, the latter option can also be exploited to alter the glycan in such a way that it is no longer recognized as substrate for glycosyltransferases later in the Golgi. This makes it possible to synthesize for instance mono-antennary or hybrid *N*-glycans (**Figure 3**). Similarly, processing of glycans by endogenous glycosidases should in most cases be avoided, but sometimes the action of glycosidases could be beneficial to fine-tune a specific glycan composition (**Figure 3**).

Mannosidic Type *N*-Glycans

To mimic the high-mannose type *N*-glycans (Man7-9) as found on many helminth glycoproteins, a strategy is needed that prevents maturation of these high-mannose *N*-glycans. The best known method to achieve this, is the addition of an ER retention signal, such as the C-terminal H/KDEL peptide sequence (Napier et al., 1992; Schouten et al., 1996). Retention of the glycoprotein in the late ER prevents the glycan from being modified by Golgi mannosidases. Alternatively, kifunensine (KIF), an α-mannosidase I inhibitor, has been used as a hydroponic treatment to increase the fraction of Man9 structures in *N. benthamiana* leaves (Krahn et al., 2017; Roychowdhury et al., 2018). Another inhibitor, swainsonine, has been used as additive in transgenic rice cultures to generate Man5 *N*-glycans by inhibition of α-mannosidase II (Choi et al., 2018). Man5 structures can also be created through the use of a *N*-acetyl-glucosaminyltransferase (GnT) I RNAi line of *N. benthamiana*, but this strategy also seemed to result in shorter Man3 and Man4 structures (Uthailak et al., 2021). Engineering toward specific mannosidic glycans remains challenging, as the necessary glyco-engineering strategies have not yet been developed or require additional optimization.

N-Glycan Core Fucosylation and Xylosylation

Native plant *N*-glycans carry core a α1,3-fucose and β1,2-xylose, which are not always present on helminth *N*-glycans. Therefore, the inhibition of plant core α1,3-fucosyl- and β1,2-xylosyltransferases to prevent their addition to *N*-glycans is a prevalent achievement. Targeted interruption of core FucTs and XylTs has also been accomplished through RNA interference (RNAi) in a variety of plant species (Cox et al., 2006; Sourrouille et al., 2008; Strasser et al., 2008; Shin et al., 2011). For *N. benthamiana* this resulted in the ΔXT/FT RNAi line, which lacked plant-native *N*-glycan core modifications on the majority of the produced *N*-glycans (Strasser et al., 2008). The inability of RNAi to completely inactivate core FucT and/or XylT genes was later overcome through CRISPR/Cas9 technology in *Nicotiana benthamiana* (Jansing et al., 2019). Specific helminths, such as *S. mansoni,* do synthesize *N*-glycans that carry core α1,3-fucose with or without β1,2-xylose. The generation of individual knock-out plant lines for either core FucT or XylT genes by Jansing et al. (2019) may prove useful to obtain *N*-glycans that lack either α1,3-fucose or β1,2-xylose. Taken together, plant lines obtained through the different approaches may all be suitable for glyco-engineering of helminth *N*-glycans.

To synthesize core α1,6-fucosylated *N*-glycans in plants a core α1,6-fucosyltransferase (FucT) should be introduced, such as FucT8 from *Drosophila melanogaster*, *Homo sapiens* or *Mus musculus* (DmFucT8, HsFucT8, or MmFucT8, respectively) (Castilho et al., 2011a; Wilbers et al., 2016). In some cases, core α1,3-fucosylation is also desired. When using plants deficient in FucT and XylT activity, reintroduction of core α1,3-fucose is required, which can be achieved by co-expression of an α1,3-FucT from *S. mansoni* (SmFucTC) or a hybrid *Zea mays* core α1,3-FucT with the CTS domain of *A. thaliana* FucT11 (Castilho et al., 2015; van Noort et al., 2020). An aspect that needs attention is glycosyltransferase inhibition that may occur upon simultaneous introduction of multiple FucTs. A strict order of fucosylation is observed for synthesis of double fucosylated *N*-glycan proximal cores of for instance *S. mansoni*, with α1,6-fucosylation preceding α1,3-fucosylation (Paschinger et al., 2005, 2019). Therefore, aberrant Golgi localization of transiently introduced (hybrid) FucTs should be carefully monitored to avoid disruption of the activity of introduced FucTs (van Noort et al., 2020).

Introduction of Galactose-Extended *N*-Glycans

In plants, the only galactosylated native *N*-glycan structure is a Lewis A structure. Plants have shown to display the Lewis A glycan motifs on endogenous glycoproteins (Fitchette-Lainé et al., 1997; Strasser et al., 2007b) and in some

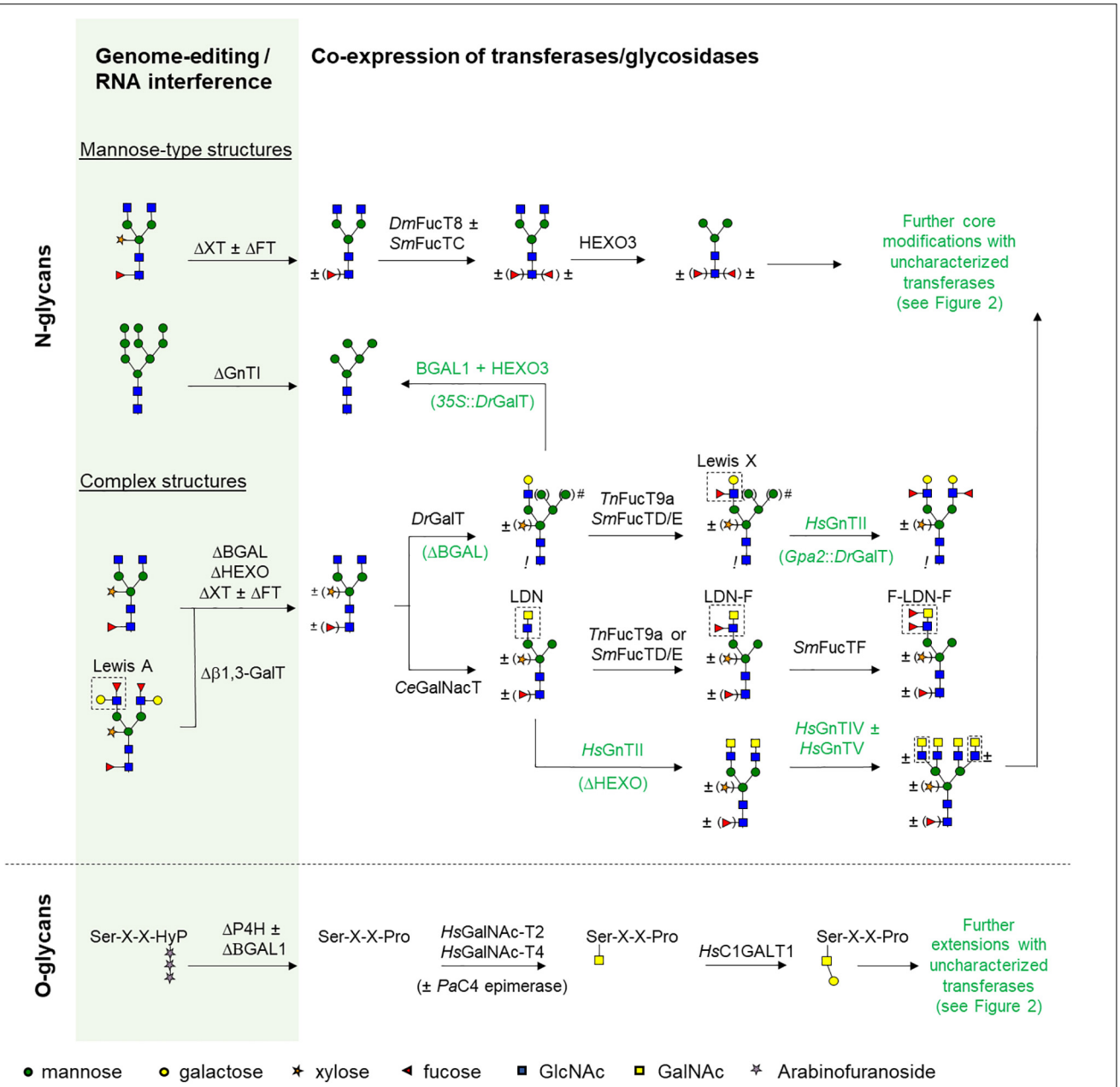


FIGURE 3 | Strategies to engineer helminth glycans. Schematic presentation of glycan engineering strategies for the synthesis of helminth *N*- and *O*-linked glycans in plants. In the green column plant wild-type glycan structures are depicted. To optimize the plant glycosylation pathway for "helminthisation" several genes need to be silenced by RNA interference or knocked out by genome editing techniques and these are indicated with Δ. From these different starting points glyco-engineering strategies have been illustrated to synthesize different mannosidic *N*-glycan structures, more complex structures with different antennary glycan motifs, and initiation of core 1 *O*-glycans. After choosing an appropriate plant line as starting point (either wild-type, RNAi line or genome edited), glyco-engineering commences by co-expression of different glycosyltransferases and/or glycosidases. The origin of each enzyme is given with two letter abbreviations for species names (Ce, *Caenorhabditis elegans*; Dm, *Drosophila melanogaster*; Dr, *Danio rerio*; Hs, *Homo sapiens*; Pa, *Pseudomonas aeruginosa;* Sm, *Schistosoma mansoni*; Tn, *Tetraodon nigriviridus*). No origin is given for plant endogenous enzymes. Enzymes: BGAL, β-galactosidase; HEXO, β-hexosaminidase; GnT, *N*-acetyl-glucosaminyltransferase; GalT, galactosyltransferase; GalNAcT, *N*-acetyl-galactosaminyl-transferase; FT, fucosyltransferase 11/12; FucT, fucosyltransferase; XT, xylosyltransferase. Other abbreviations or symbols: Asn, asparagine; Ser, serine; Thr, threonine; Pro, proline; Hyp, hydroxyproline; X, any amino acid; #, promoter strength for DrGalT determines the glycan composition, where control of expression with a dual 35S promoter results in hybrid glycans, but controlled expression with a weaker *Gpa2* resistance gene promoter results in single-branched glycans. !: core a1,3-fucose is absent upon over-expression of DrGalT.

cases on recombinant glycoproteins (Weise et al., 2007; Castilho et al., 2011b; Wilbers et al., 2016). The presence of Lewis A shows that plants have the machinery to add β1,3-galactose to glycans. Interestingly, β1,3-galactose is always seen in combination with α1,4-fucose in the Lewis A motif. The presence of plant Lewis A epitopes on recombinant glycoproteins can be completely abolished by the disruption of β1,3-galactosyltransferase 1 as has been demonstrated in moss (Parsons et al., 2012).

In contrast to any β1,3-galactose-extended glycans, helminth glycoproteins carry *N*-glycans that are extended with antennary β1,4-linked galactose (LN). The synthesis of L*N*-carrying *N*-glycans has been achieved in *N. tabacum* upon c*o*-expression of a hybrid β1,4-galactosyltransferase 1 (sialGalT) of *Danio rerio* or *H. sapiens* (Anusiem and Beetlestone, 1976; Hesselink et al., 2014). The original CTS domain of GalT was replaced with the CTS domain of *Rattus norvegicus* α2,6-sialyltransferase (sial). The sial-CTS domain translocates GalT to the *trans*-Golgi, as earlier addition of galactose can significantly hinder the activity of endogenous *N*-acetyl-glucosaminyltransferase II (GnTII), mannosidase II (α-Man II) and xylosyltransferase (XylT), leading to the synthesis of hybrid *N*-glycans (Johnson and Chrispeels, 1987; Bakker et al., 2001; Wilbers et al., 2017). In addition to localization, promotor strength can be exploited to avoid interference with the activity of certain glycosyltransferases to achieve the synthesis of a specific glycan (Wilbers et al., 2017; Kallolimath et al., 2018). For example, strong expression of sialGalT under control of a 35S promoter allows for the synthesis of hybrid *N*-glycans, whereas sialDrGalT expression under the control of the weaker Gpa2 promoter allows synthesis of single branched non-hybrid *N*-glycans (**Figure 3**).

Galactose-extended *N*-glycans are sometimes fucosylated (Lewis X), as is seen for *N*-glycans on omega-1 and IPSE/alpha-1 from *S. mansoni* (Wuhrer et al., 2006; Meevissen et al., 2010). Synthesis of Lewis X was achieved upon c*o*-expression of sialDrGalT and a hybrid α1,3-FucT9a (sialFucT9a) from *Tetraodon nigriviridus* (Rouwendal et al., 2009; Wilbers et al., 2017). More recently, the fucosyltransferases FucTD and FucTE from the parasite *S. mansoni* were identified as enzymes able to synthesize Lewis X, where SmFucTD and SmFucTE were most efficient (van Noort et al., 2020). The presence of predominantly monoantennary Lewis X-carrying *N*-glycans upon engineering suggests that introduction of a sialGalT still interferes with endogenous GnTII activity (Wilbers et al., 2017; van Noort et al., 2020).

While the synthesis of Lewis X is efficient, the synthesis of LN is not always efficient and depends on the protein under investigation (Strasser et al., 2009; Kriechbaum et al., 2020). For this reason, it was postulated that endogenous plant β-galactosidases (BGALs) along the secretory pathway could interfere with the synthesis of galactose-extended *N*-glycans. Recently, BGAL1 from *N. benthamiana* (homologous to BGAL8 from *A. thaliana*) has been characterized as an apoplast localized β-galactosidase and the major contributor to degalactosylation of both *N*- and *O*-linked glycans (including endogenous Lewis A). Impairment of NbBGAL1, through RNAi and CRISPR, resulted in a significant increase in galactosylation on various glycoproteins (Kriechbaum et al., 2020). Due to the redundancy of substrate specificity of the BGAL enzyme family and the number of β-galactosidases detected in apoplast fluid, it is likely that residual β-galactosidase activity may still lower the level of galactosylation (Dean et al., 2007; Buscaill et al., 2019). Therefore, additional research into remaining β-galactosidases and their ability to cleave *N*- and *O*-glycans is required to optimize glyco-engineering strategies for galactose containing *N*-glycans.

Introduction of GalNAc-Extended *N*-Glycans

Helminth *N*-glycans often contain GalNAc as is seen in LDN and fucosylated LDN (**Figure 2**). Engineering of LDN carrying *N*-glycans requires the addition of a GalNAc on a terminal GlcNAc residue. Recently, LDN was synthesized on the *N*-glycans of *S. mansoni* kappa-5 in *N. benthamiana* by introduction of a *N*-acetyl-galactosaminyltransferase from *C. elegans* (CeGalNAcT) (Wilbers et al., 2017). GalNAc is never observed in plant glycans, and it was initially expected that incorporation of this sugar into *N*-glycans would require synthesis of UDP-GalNAc as substrate and facilitate its transport into the Golgi. However, it was observed that c*o*-expression of a C4 epimerase to enhance substrate availability as well as c*o*-expression of UDP-GalNAc transporters for improved Golgi localization was not required (Wilbers et al., 2017). This shows that, even though GalNAc is not native to plant *N*-glycans, UDP-GalNAc is present within the correct Golgi compartment.

The LDN motif can be further modified by expression of a α1,3-fucosyltransferase (α1,3-FucT; e.g., sialTnFucT9a, SmFucTD or SmFucTE) to yield a LD*N*-F motif (Wilbers et al., 2017; van Noort et al., 2020). Moreover, the glycan motif F-LD*N*-F could be synthesized upon c*o*-expression of these enzymes with SmFucTF. The possibility to synthesize fucosylated LDN with SmFucTD, SmFucTE and SmFucTF is a promising finding for the production of (fucosylated) LDN carrying helminth glycoproteins, such as kappa-5. From *S. mansoni.*

Similar to the synthesis of galactose-extended *N*-glycans, it seems that fucosylation of LDN, to obtain LD*N*-F, enhances the extension of *N*-glycans with GalNAc (Wilbers et al., 2017). Plant-native β-hexosaminidases (HEXOs) activity may limit the generation of LDN glycan motifs on kappa-5 in GalNAcT-expressing *Nicotiana benthamiana* (Alvisi et al., 2021). HEXOs are hydrolytic enzymes that are able to remove terminal GlcNAc and GalNAc residues from complex *N*-glycans, thereby generating typical plant paucimannosidic *N*-glycans (Shin et al., 2017; Alvisi et al., 2021). Plants harbor several HEXO homologs (HEXO1, HEXO2 and HEXO3) that differ by their substrate specificity and sub-cellular localization. HEXO1 and HEXO3 of *A. thaliana* and *N. benthamiana* are involved in the processing of plant *N*-glycans to paucimannosidic *N*-glycans, where HEXO1 is active in the vacuole and HEXO3 in the apoplast (Strasser et al., 2007a; Shin et al., 2017). *N*-glycans with non-endogenous GalNAc extended *N*-glycans can be processed by HEXO3 in the apoplast of *N. benthamiana*. In addition, HEXO2 was characterized as a membrane-bound enzyme specifically cleaving GalNAc residues from *N*-glycans (Alvisi et al., 2021). Unfortunately, targeted transient RNAi was not sufficient to improve LDN synthesis in plants (Alvisi et al., 2021). Future

efforts should now focus on the generation of a NbHEXO knock-out plants to accelerate helminthisation of *N*-glycans in a plant expression system.

Introduction of *N*-Glycan Branching

In contrast to plants, various helminth glycoproteins carry additional branches on their *N*-glycan structures. This was observed on tri- and tetra-antennary LDN(-F) carrying *N*-glycans of *S. mansoni* kappa-5, the tetra-antennary PC-glycans on ES-62 from *Acanthocheilonema viteae* and the tri- and tetra-antennary *N*-glycans with tyvelose of *T. spiralis* (Reason et al., 1994; Harnett et al., 2005; Meevissen et al., 2011). Plants can only synthesize up to two branches on their *N*-glycans, as plants lack *N*-acetylglucosaminyltransferases (GnT) IV and V (Sheshukova et al., 2016). Currently, the synthesis of *N*-glycans with LN, Lewis X, LDN and (F-)LDN(-F) is predominantly mono-antennary (Wilbers et al., 2017; van Noort et al., 2020). Co-expression of exogenous GnTII from *A. thaliana* (AtGnTII) or *H. sapiens* (HsGnTII) could increase the occurrence of di-antennary *N*-glycans structures (Schneider et al., 2014; Dicker et al., 2016). In order to synthesize tri- or tetra-antennary *N*-glycans additional exogenous transferases are required, such as GnTIV and GnTV. Castilho and colleagues demonstrated that co-expression of GnTIV and GnTV from *H. sapiens* allows synthesis of tetra-antennary *N*-glycans (Castilho et al., 2011b). This strategy may also be used to produce helminth glycoproteins with tri- and tetra-antennary carrying *N*-glycans. A potential challenge for increasing the number of branches, is the possible activity of β-hexosaminidases on the initial GlcNAc, and possibly GalNAc extension, of each branch.

Engineering Helminth *O*-Glycans

Helminth glycoproteins also have been shown to carry complex *O*-glycans (Hokke and van Diepen, 2017). The synthesis of *O*-glycans on helminth glycoproteins produced in plants is a next challenge that will allow the study of the role of these proteins in parasitism and their effectiveness as biopharmaceuticals. Just as with *N*-glycans, glyco-engineering of helminth *O*-glycans shows resemblance with humanization of the plant production platform. Most helminth *O*-glycans are initiated with *O*-GalNAc. *O*-GalNAc glycans are absent in plants, which allows for a bottom-up approach for the synthesis of such glycans. Two simultaneous, but independent studies have shown that *O*-GalNAc glycans can be synthesized, either by expression of GalNAcT2 and C1GalT1 leading to mucin core 1 *O*-GalNAc glycans (Castilho et al., 2012) or the combination of GalNAcT2, GalNAcT4and a GlcNAc C4-epimerase leading to *O*-GalNAc glycans (Yang et al., 2012). The synthesis of *O*-GalNAc glycans was possible despite hypothesized interference of prolyl-4-hydroxylases (P4H) and subsequent plant-native *O*-glycosylation in *N. benthamiana* (Montero-Morales and Steinkellner, 2018). Plant native *O*-glycans could pose an issue in terms of immunogenicity when using plant-based pharmaceuticals (Yates et al., 1996; Leonard et al., 2005). In addition, plant native *O*-glycans could sterically hinder the synthesis of helminth *O*-glycans. A P4H1 knock-out in *Physcomitrella patens* prevents proline conversion into hydroxyproline (Hyp) on recombinant EPO (Parsons et al., 2013). In *N. benthamiana*, P4H1, P4H4, P4H9 and P4H10 have recently been identified as enzymes capable of forming hydroxyproline on recombinant proteins (Mócsai et al., 2021). Unfortunately, transient RNAi of these genes in *N. benthamiana* was insufficient to reduce P4H activity completely, due to redundancy within the substrate specificity of the P4H genes. However, it remains unknown to what extent plant-native glycosylation interferes with the substrate specificity of *O*-GalNAc glycans. It is anticipated that the effect of galactosidases and possibly hexosaminidases could be a bigger issue for the synthesis of mucin-type *O*-GalNAc glycans. BGAL1 from *N. benthamiana* has been shown to remove the terminal galactose from core 1 *O*-GalNAc glycans (Kriechbaum et al., 2020), whereas β-hexosaminidases can cleave off HexNAc residues in an elongated *O*-GalNAc glycan (Cheng et al., 2013). Therefore, more research is required into enzymes involved in *O*-glycan synthesis and hydrolysis, as this might be required for efficient production of native helminth *O*-glycosylated proteins.

PERSPECTIVE

Over the last two decades, "humanization" of the plant glycosylation pathway has shown that plants can efficiently produce various glycoproteins with engineered human *N*-glycans. But next to the focus on "humanization" of glycans, plants can be exploited to produce many other glycoproteins with tailor-made glycans. Enlarging the plant glyco-engineering toolbox for the synthesis of non-human glycans will fuel research to the function of specific glycan structures or glycoproteins with potential novel applications. In case of helminths, we described the possibilities to synthesize specific helminth *N*-glycans, which we refer to as "helminthisation" (Wilbers et al., 2017). Helminthisation of the plant glycosylation pathway will allow investigation into the function of specific glycan motifs and glycosyltransferases in parasite biology, development, and immunomodulation. Ultimately, the production of specific helminth glycan structures or helminth glycoproteins with a native glycan composition in plants can be used for development of vaccines, diagnostic tools, and novel biopharmaceuticals for the treatment of allergies and autoimmune diseases (Bunte et al., 2022).

Besides helminths, the search for useful glycoproteins can even be extended to other kingdoms. This includes potentially biologically active glycoproteins from marine animals or insects, which might have interesting applications as therapeutics (Caldwell and Pagett, 2010; Hykollari et al., 2018). Other possibilities include bio-glycoprotein adhesives (Lutz et al., 2022), hydrogels (Böni et al., 2018; Zhong et al., 2018) and cryoprotectants (Tas et al., 2021; Dou et al., 2022). These various glycoproteins have specific glycosylation patterns that can be difficult to reconstitute in conventional expression systems and production of such glycoproteins could benefit from plant-based expression systems.

Plants offer a highly versatile and flexible expression system in terms of glyco-engineering, where glycans can be modified by introducing glycosyltransferases and/or glycosidases in a modular fashion (**Figure 3**). In addition, the choice

of promoter strength can further increase the flexibility of the platform. For instance, we described that over-expression of β1,4-galactosyltransferases interferes with plant endogenous glycosyltransferases, but this offers opportunities to engineer hybrid or single-branched glycan structures as found in several helminth species. Although several helminth glycan motifs can be efficiently engineered in plants, other helminth glycan modifications cannot be synthesized yet in plants. In addition, little progress has been made on engineering the *O*-glycans observed in helminths, except for the initiation of core 1 *O*-glycans. For several helminth glycan modifications, the relevant glycosyltransferases, enzymes involved in substrate synthesis, and/or nucleotide transporters are currently still unknown. But, with the availability of many parasite genome sequences, plants offer an excellent platform for the functional characterization of novel parasite genes that are involved in the biosynthesis of helminth glycans, as was illustrated for fucosyltransferases of *S. mansoni* (van Noort et al., 2020).

Other techniques that greatly enhance the versatility of a plant-based glyco-engineering platform is the use of RNAi or genome editing techniques to counteract undesired glycan modifications by plant endogenous enzymes. With an expanding glyco-engineering toolbox, more and more enzymes are also being identified that should be targeted. The presence of recently identified glycosidases along the secretory pathway, such as BGAL1 and HEXOs (HEXO2 and HEXO3) in *N. benthamiana* (Kriechbaum et al., 2020; Alvisi et al., 2021), could pose a major hurdle for engineering helminth glycans that carry galactose- or GalNAc-extended glycans, respectively. With current developments in genome editing techniques in plants, the activity of these enzymes could easily be disrupted, but care should be taken with knocking out multiple of these genes at once. Some of these targets might be involved in vital biological processes in the plant, such as the synthesis or remodeling of endogenous *O*-glycans of cell wall glycoproteins (Petersen et al., 2021; Strasser et al., 2021), whereas others play a role in processing non-endogenous glycans and putatively play a role in plant defense responses of the plant (Buscaill et al., 2019; Alvisi et al., 2021).

Taken together, efforts to improve plants as production platform for glycoproteins with a defined glycan composition, offers possibilities to open-up new fields of research. Increased knowledge on engineering of the plant glycosylation pathways could assist other fields of research ranging from animal parasitology and immunology to plant sciences.

AUTHOR CONTRIBUTIONS

All authors listed have made a substantial, direct, and intellectual contribution to the work, and approved it for publication.

FUNDING

This work was supported by a grant from the center for unusual collaboration (an alliance between Eindhoven University of Technology, Utrecht University, the University Medical Center Utrecht and Wageningen University and Research) and by the TTW Veni Grant 16740 from Netherlands Organization for Scientific Research.

ACKNOWLEDGMENTS

We would like to thank Nick Bovee and Joep Debets for their input in the initial phase of writing this manuscript.

REFERENCES

Alvisi, N., van Noort, K., Dwiani, S., Geschiere, N., Sukarta, O., Varossieau, K., et al. (2021). β-Hexosaminidases Along the Secretory Pathway of Nicotiana benthamiana Have Distinct Specificities Toward Engineered Helminth *N*-Glycans on Recombinant Glycoproteins. *Front. Plant Sci.* 12:638454. doi: 10.3389/fpls.2021.638454

Anusiem, A. C. I., and Beetlestone, J. G. (1976). Cooperative ligand binding by ferrihemoglobin: an experimental artifact? *Biopolymers* 15, 403–414. doi: 10.1002/bip.1976.360150216

Bakker, H., Bardor, M., Molthoff, J. W., Gomord, V., Elbers, I., Stevens, L. H., et al. (2001). Galactose-extended glycans of antibodies produced by transgenic plants. *Proc. Natl. Acad. Sci. U.S.A.* 98, 2899–2904. doi: 10.1073/pnas.031419998

Böni, L. J., Zurflüh, R., Baumgartner, M. E., Windhab, E. J., Fischer, P., Kuster, S., et al. (2018). Effect of ionic strength and seawater cations on hagfish slime formation. *Sci. Rep.* 8:9867. doi: 10.1038/s41598-018-27975-0

Bosch, D., Castilho, A., Loos, A., Schots, A., and Steinkellner, H. (2013). *N*-glycosylation of plant-produced recombinant proteins. *Curr. Pharm. Des.* 19, 5503–5512. doi: 10.2174/1381612811319310006

Bunte, M. J. M., Schots, A., Kammenga, J. E., and Wilbers, R. H. P. (2022). Helminth Glycans at the Host-Parasite Interface and Their Potential for Developing Novel Therapeutics. *Front. Mol. Biosci.* 8:1358. doi: 10.3389/fmolb.2021.807821

Buscaill, P., Chandrasekar, B., Sanguankiattichai, N., Kourelis, J., Kaschani, F., Thomas, E. L., et al. (2019). Glycosidase and glycan polymorphism control hydrolytic release of immunogenic flagellin peptides. *Science* 364, eaav0748. doi: 10.1126/science.aav0748

Caldwell, G. S., and Pagett, H. E. (2010). Marine glycobiology: current status and future perspectives. *Mar. Biotechnol.* 12, 241–252. doi: 10.1007/s10126-010-9263-5

Casaravilla, C., Freire, T., Malgor, R., Medeiros, A., Osinaga, E., and Carmona, C. (2003). Mucin-type *O*-glycosylation in helminth parasites from major taxonomic groups: evidence for widespread distribution of the Tn antigen (GalNAc-Ser/Thr) and identification of UDP-GalNAc:polypeptide *N*-acetylgalactosaminyltransferase activity. *J. Parasitol.* 89, 709–714. doi: 10.1645/GE-2970

Castilho, A., Bohorova, N., Grass, J., Bohorov, O., Zeitlin, L., Whaley, K., et al. (2011a). Rapid high yield production of different glycoforms of ebola virus monoclonal antibody. *PLoS One* 6:e26040. doi: 10.1371/journal.pone.0026040

Castilho, A., Gattinger, P., Grass, J., Jez, J., Pabst, M., Altmann, F., et al. (2011b). *N*-Glycosylation engineering of plants for the biosynthesis of glycoproteins with bisected and branched complex *N*-glycans. *Glycobiology* 21, 813–823. doi: 10.1093/glycob/cwr009

Castilho, A., Gruber, C., Thader, A., Oostenbrink, C., Pechlaner, M., Steinkellner, H., et al. (2015). Processing of complex *N*-glycans in IgG Fc-region is affected by core fucosylation. *MAbs* 7, 863–870. doi: 10.1080/19420862.2015.1053683

Castilho, A., Neumann, L., Daskalova, S., Mason, H. S., Steinkellner, H., Altmann, F., et al. (2012). Engineering of sialylated mucin-type *O*-glycosylation in plants. *J. Biol. Chem.* 287, 36518–36526. doi: 10.1074/jbc.M112.402685

Charlier, J., De Waele, V., Ducheyne, E., Van Der Voort, M., Vande Velde, F., and Claerebout, E. (2016). Decision making on helminths in cattle: diagnostics, economics and human behaviour. *Ir. Vet. J.* 69:14. doi: 10.1186/s13620-016-0073-6

Cheng, P. F., Snovida, S., Ho, M. Y., Cheng, C. W., Wu, A. M., and Khoo, K. H. (2013). Increasing the depth of mass spectrometry-based glycomic coverage by additional dimensions of sulfoglycomics and target analysis of permethylated glycans. *Anal. Bioanal. Chem.* 405, 6683–6695. doi: 10.1007/s00216-013-7128-2

Choi, H. Y., Park, H., Hong, J. K., Kim, S. D., Kwon, J. Y., You, S. K., et al. (2018). *N*-glycan Remodeling Using Mannosidase Inhibitors to Increase High-mannose Glycans on Acid α-Glucosidase in Transgenic Rice Cell Cultures. *Sci. Rep.* 8:16130. doi: 10.1038/s41598-018-34438-z

Claerebout, E., and Geldhof, P. (2020). Helminth Vaccines in Ruminants: from Development to Application. *Vet. Clin. North Am. Food Anim. Pract.* 36, 159–171. doi: 10.1016/j.cvfa.2019.10.001

Cox, K. M., Sterling, J. D., Regan, J. T., Gasdaska, J. R., Frantz, K. K., Peele, C. G., et al. (2006). Glycan optimization of a human monoclonal antibody in the aquatic plant Lemna minor. *Nat. Biotechnol.* 24, 1591–1597. doi: 10.1038/nbt1260

Dean, G. H., Zheng, H., Tewari, J., Huang, J., Young, D. S., Yeen, T. H., et al. (2007). The Arabidopsis MUM2 gene encodes a β-galactosidase required for the production of seed coat mucilage with correct hydration properties. *Plant Cell* 19, 4007–4021. doi: 10.1105/tpc.107.050609

Dicker, M., Tschofen, M., Maresch, D., König, J., Juarez, P., Orzaez, D., et al. (2016). Transient glyco-engineering to produce recombinant IgA1 with defined *N*-and *O*-glycans in plants. *Front. Plant Sci.* 7:18. doi: 10.3389/fpls.2016.00018

Dou, M., Lu, C., and Rao, W. (2022). Bioinspired materials and technology for advanced cryopreservation. *Trends Biotechnol.* 40, 93–106. doi: 10.1016/j.tibtech.2021.06.004

Fischer, R., and Emans, N. (2000). Molecular farming of pharmaceutical proteins. *Transgenic Res.* 9, 279–299. doi: 10.1023/a:1008975123362

Fitchette-Lainé, A. C., Gomord, V., Cabanes, M., Michalski, J. C., Macary, M., Saint, et al. (1997). *N*-glycans harboring the Lewis a epitope are expressed at the surface of plant cells. *Plant J.* 12, 1411–1417. doi: 10.1046/j.1365-313x.1997.12061411.x

Garcia-Campos, A., Ravidà, A., Nguyen, D. L., Cwiklinski, K., Dalton, J. P., Hokke, C. H., et al. (2016). Tegument Glycoproteins and Cathepsins of Newly Excysted Juvenile Fasciola hepatica Carry Mannosidic and Paucimannosidic *N*-glycans. *PLoS Negl. Trop. Dis.* 10:e0004688. doi: 10.1371/journal.pntd.0004688

Geldhof, P., De Maere, V., Vercruysse, J., and Claerebout, E. (2007). Recombinant expression systems: the obstacle to helminth vaccines? *Trends Parasitol.* 23, 527–532. doi: 10.1016/j.pt.2007.08.012

Grabenhorst, E., and Conradt, H. S. (1999). The cytoplasmic, transmembrane, and stem regions of glycosyltransferases specify their in vivo functional sublocalization and stability in the Golgi. *J. Biol. Chem.* 274, 36107–36116. doi: 10.1074/jbc.274.51.36107

Grabowski, G. A., Golembo, M., and Shaaltiel, Y. (2014). Taliglucerase alfa: an enzyme replacement therapy using plant cell expression technology. *Mol. Genet. Metab.* 112, 1–8. doi: 10.1016/j.ymgme.2014.02.011

Harnett, W., Harnett, M., and Byron, O. (2005). Structural / Functional Aspects of ES-62 - A Secreted Immunomodulatory Phosphorylcholine-Containing Filarial Nematode Glycoprotein. *Curr. Protein Pept. Sci.* 4, 59–71. doi: 10.2174/1389203033380368

Haslam, S. M., Coles, G. C., Morris, H. R., and Dell, A. (2000). Structural characterization of the *N*-glycans of Dictyocaulus viviparus: discovery of the Lewis x structure in a nematode. *Glycobiology* 10, 223–229. doi: 10.1093/glycob/10.2.223

Haslam, S. M., Coles, G. C., Munn, E. A., Smith, T. S., Smith, H. F., Morris, H. R., et al. (1996). Haemonchus contortus glycoproteins contain *N*-linked oligosaccharides with novel highly fucosylated core structures. *J. Biol. Chem.* 271, 30561–30570. doi: 10.1074/jbc.271.48.30561

Health Canada Medicago Covifenz COVID-19 Vaccine (2022). Available online at: https://www.canada.ca/en/health-canada/services/drugs-health-products/covid19-industry/drugs-vaccines-treatments/vaccines/medicago.html [Accessed on March 23, 2022].

Hebert, D. N., Lamriben, L., Powers, E. T., and Kelly, J. W. (2014). The intrinsic and extrinsic effects of *N*-linked glycans on glycoproteostasis. *Nat. Chem. Biol.* 10, 902–910. doi: 10.1038/nchembio.1651

Hesselink, T., Rouwendal, G. J. A., Henquet, M. G. L., Florack, D. E. A., Helsper, J. P. F. G., and Bosch, D. (2014). Expression of natural human β1,4-GalT1 variants and of non-mammalian homologues in plants leads to differences in galactosylation of *N*-glycans. *Transgenic Res.* 23, 717–728. doi: 10.1007/s11248-014-9806-z

Hewitson, J. P., Nguyen, D. L., van Diepen, A., Smit, C. H., Koeleman, C. A., McSorley, H. J., et al. (2016). Novel *O*-linked methylated glycan antigens decorate secreted immunodominant glycoproteins from the intestinal nematode Heligmosomoides polygyrus. *Int. J. Parasitol.* 46, 157–170. doi: 10.1016/j.ijpara.2015.10.004

Hiatt, A., Caffferkey, R., and Bowdish, K. (1989). Production of antibodies in transgenic plants. *Nature* 342, 76–78. doi: 10.1038/342076a0

Hokke, C. H., and van Diepen, A. (2017). Helminth glycomics – glycan repertoires and host-parasite interactions. *Mol. Biochem. Parasitol.* 215, 47–57. doi: 10.1016/j.molbiopara.2016.12.001

Hotez, P. J., Bottazzi, M. E., and Strych, U. (2016). New vaccines for the world's poorest people. *Annu. Rev. Med.* 67, 405–417. doi: 10.1146/annurev-med-051214-024241

Hotez, P. J., Brindley, P. J., Bethony, J. M., King, C. H., Pearce, E. J., and Jacobson, J. (2008). Helminth infections: the great neglected tropical diseases. *J. Clin. Invest.* 118, 1311–1321. doi: 10.1172/JCI34261

Hykollari, A., Malzl, D., Eckmair, B., Vanbeselaere, J., Scheidl, P., Jin, C., et al. (2018). Isomeric separation and recognition of anionic and zwitterionic n-glycans from royal jelly glycoproteins. *Mol. Cell. Proteomics* 17, 2177–2196. doi: 10.1074/MCP.RA117.000462

James, C. E., Hudson, A. L., and Davey, M. W. (2009). Drug resistance mechanisms in helminths: is it survival of the fittest? *Trends Parasitol.* 25, 328–335. doi: 10.1016/j.pt.2009.04.004

Jang-Lee, J., Curwen, R. S., Ashton, P. D., Tissot, B., Mathieson, W., Panico, M., et al. (2007). Glycomics Analysis of Schistosoma mansoni Egg and Cercarial Secretions. *Mol. Cell. Proteomics* 6, 1485–1499. doi: 10.1074/mcp.M700004-MCP200

Jansing, J., Sack, M., Augustine, S. M., Fischer, R., and Bortesi, L. (2019). CRISPR/Cas9-mediated knockout of six glycosyltransferase genes in Nicotiana benthamiana for the production of recombinant proteins lacking β-1,2-xylose and core α-1,3-fucose. *Plant Biotechnol. J.* 17, 350–361. doi: 10.1111/pbi.12981

Jiménez-Castells, C., Vanbeselaere, J., Kohlhuber, S., Ruttkowski, B., Joachim, A., and Paschinger, K. (2017). Gender and developmental specific *N*-glycomes of the porcine parasite Oesophagostomum dentatum. *Biochim. Biophys. Acta Gen. Subj.* 1861, 418–430. doi: 10.1016/j.bbagen.2016.10.011

Johnson, K. D., and Chrispeels, M. J. (1987). Substrate Specificities of N -Acetylglucosaminyl-. *Plant Physiol.* 84, 1301–1308. doi: 10.1104/pp.84.4.1301

Kallolimath, S., Gruber, C., Steinkellner, H., and Castilho, A. (2018). Promoter Choice Impacts the Efficiency of Plant Glyco-Engineering. *Biotechnol. J.* 13:1700380. doi: 10.1002/biot.201700380

Kapila, J., De Rycke, R., Montagu, M., Van, and Angenon, G. (1997). Corrigendum to 'An Agrobacterium-mediated transient gene expression system for intact leaves' [Plant Sci. 122 (1997) 101–108]. *Plant Sci.* 124:227. doi: 10.1016/S0168-9452(97)04651-7

Krahn, N., Spearman, M., Meier, M., Dorion-Thibaudeau, J., McDougall, M., Patel, T. R., et al. (2017). Inhibition of glycosylation on a camelid antibody uniquely affects its FcγRI binding activity. *Eur. J. Pharm. Sci.* 96, 428–439. doi: 10.1016/j.ejps.2016.09.040

Kriechbaum, R., Ziaee, E., Grünwald-Gruber, C., Buscaill, P., van der Hoorn, R. A. L., and Castilho, A. (2020). BGAL1 depletion boosts the level of β-galactosylation of *N*- and *O*-glycans in N. benthamiana. *Plant Biotechnol. J.* 18, 1537–1549. doi: 10.1111/pbi.13316

Leonard, R., Petersen, B. O., Himly, M., Kaar, W., Wopfner, N., Kolarich, D., et al. (2005). Two novel types of *O*-glycans on the mugwort pollen allergen Art v 1 and their role in antibody binding. *J. Biol. Chem.* 280, 7932–7940. doi: 10.1074/jbc.M410407200

Lobato Gómez, M., Huang, X., Alvarez, D., He, W., Baysal, C., Zhu, C., et al. (2021). Contributions of the international plant science community to the fight against human infectious diseases – part 1: epidemic and pandemic diseases. *Plant Biotechnol. J.* 19, 1901–1920. doi: 10.1111/pbi.13657

Lochnit, G., Dennis, R. D., and Geyer, R. (2000). Phosphorylcholine Substituents in Nematodes: structures, Occurrence and Biological Implications. *Biol. Chem.* 381, 839–847. doi: 10.1515/BC.2000.106

Lutz, T. M., Kimna, C., Casini, A., and Lieleg, O. (2022). Bi*o*-based and bi*o*-inspired adhesives from animals and plants for biomedical applications. *Mater. Today Bio*. 13:100203. doi: 10.1016/j.mtbio.2022.100203

Martini, F., Eckmair, B., Štefaniæ, S., Jin, C., Garg, M., Yan, S., et al. (2019). Highly modified and immunoactive *N*-glycans of the canine heartworm. *Nat. Commun.* 10:75. doi: 10.1038/s41467-018-07948-7

Meevissen, M. H. J., Balog, C. I. A., Koeleman, C. A. M., Doenhoff, M. J., Schramm, G., Haas, H., et al. (2011). Targeted Glycoproteomic Analysis Reveals That Kappa-5 is a Major. *Mol. Cell. Proteomics* 10, M110.005710. doi: 10.1074/mcp.M110.005710

Meevissen, M. H. J., Wuhrer, M., Doenhoff, M. J., Schramm, G., Haas, H., Deelder, A. M., et al. (2010). Structural characterization of glycans on omega-1, a major schistosoma mansoni egg glycoprotein that drives Th2 responses. *J. Proteome Res.* 9, 2630–2642. doi: 10.1021/pr100081c

Meyvis, Y., Callewaert, N., Gevaert, K., Timmerman, E., Van Durme, J., Schymkowitz, J., et al. (2008). Hybrid *N*-glycans on the host protective activation-associated secreted proteins of Ostertagia ostertagi and their importance in immunogenicity. *Mol. Biochem. Parasitol.* 161, 67–71. doi: 10.1016/j.molbiopara.2008.05.004

Mócsai, R., Göritzer, K., Stenitzer, D., Maresch, D., Strasser, R., and Altmann, F. (2021). Prolyl Hydroxylase Paralogs in Nicotiana benthamiana Show High Similarity With Regard to Substrate Specificity. *Front. Plant Sci.* 12:302. doi: 10.3389/fpls.2021.636597

Montero-Morales, L., and Steinkellner, H. (2018). Advanced Plant-Based Glycan Engineering. *Front. Bioeng. Biotechnol.* 6:81. doi: 10.3389/fbioe.2018.00081

Moremen, K. W., Tiemeyer, M., and Nairn, A. V. (2012). Vertebrate protein glycosylation: diversity, synthesis and function. *Nat. Rev. Mol. Cell Biol.* 13, 448–462. doi: 10.1038/nrm3383

Napier, R. M., Fowke, L. C., Hawes, C., Lewis, M., and Pelham, H. R. (1992). Immunological evidence that plants use both HDEL and KDEL for targeting proteins to the endoplasmic reticulum. *J. Cell Sci.* 102, 261–271. doi: 10.1242/jcs.102.2.261

Paolino, K. M., Regules, J. A., Moon, J. E., Ruck, R. C., Bennett, J. W., Remich, S. A., et al. (2022). Safety and immunogenicity of a plant-derived recombinant protective antigen (rPA)-based vaccine against Bacillus anthracis: a Phase 1 dose-escalation study in healthy adults. *Vaccine* 40, 1864–1871. doi: 10.1016/J.VACCINE.2022.01.047

Parsons, J., Altmann, F., Arrenberg, C. K., Koprivova, A., Beike, A. K., Stemmer, C., et al. (2012). Moss-based production of asialo-erythropoietin devoid of Lewis A and other plant-typical carbohydrate determinants. *Plant Biotechnol. J.* 10, 851–861. doi: 10.1111/j.1467-7652.2012.00704.x

Parsons, J., Altmann, F., Graf, M., Stadlmann, J., Reski, R., and Decker, E. L. (2013). A gene responsible for prolyl-hydroxylation of moss-produced recombinant human erythropoietin. *Sci. Rep.* 3:3019. doi: 10.1038/srep03019

Paschinger, K., Gonzalez-Sapienza, G. G., and Wilson, I. B. H. (2012). Mass spectrometric analysis of the immunodominant glycan epitope of Echinococcus granulosus antigen Ag5. *Int. J. Parasitol.* 42, 279–285. doi: 10.1016/j.ijpara.2012.01.002

Paschinger, K., Staudacher, E., Stemmer, U., Fabini, G., and Wilson, I. B. H. (2005). Fucosyltransferase substrate specificity and the order of fucosylation in invertebrates. *Glycobiology* 15, 463–474. doi: 10.1093/glycob/cwi028

Paschinger, K., and Wilson, I. B. H. (2015). Two types of galactosylated fucose motifs are present on *N*-glycans of Haemonchus contortus. *Glycobiology* 25, 585–590. doi: 10.1093/glycob/cwv015

Paschinger, K., Yan, S., and Wilson, I. B. H. (2019). *N*-glycomic complexity in anatomical simplicity: caenorhabditis elegans as a non-model nematode? *Front. Mol. Biosci.* 6:9. doi: 10.3389/fmolb.2019.00009

Petersen, B. L., MacAlister, C. A., and Ulvskov, P. (2021). Plant Protein *O*-Arabinosylation. *Front. Plant Sci.* 12:400. doi: 10.3389/fpls.2021.645219

Pöltl, G., Kerner, D., Paschinger, K., and Wilson, I. B. H. (2007). *N*-Glycans of the porcine nematode parasite Ascaris suum are modified with phosphorylcholine and core fucose residues. *FEBS J.* 274, 714–726. doi: 10.1111/j.1742-4658.2006.05615.x

Ravidà, A., Aldridge, A. M., Driessen, N. N., Heus, F. A. H., Hokke, C. H., and O'Neill, S. M. (2016). Fasciola hepatica Surface Coat Glycoproteins Contain Mannosylated and Phosphorylated *N*-glycans and Exhibit Immune Modulatory Properties Independent of the Mannose Receptor. *PLoS Negl. Trop Dis*.10, e0004601. doi: 10.1371/journal.pntd.0004601

Reason, A. J., Ellis, L. A., Appleton, J. A., Wisnewski, N., Grieve, R. B., Mcneil, M., et al. (1994). Novel tyvelose-containing tri- and tetra-antennary *N*-glycans in the immunodominant antigens of the intracellular parasite Trichinella spiralis. *Glycobiology* 4, 593–603. doi: 10.1093/glycob/4.5.593

Rouwendal, G. J. A., Florack, D. E. A., Hesselink, T., Cordewener, J. H., Helsper, J. P. F. G., and Bosch, D. (2009). Synthesis of Lewis X epitopes on plant *N*-glycans. *Carbohydr. Res.* 344, 1487–1493. doi: 10.1016/j.carres.2009.05.003

Roychowdhury, S., Oh, Y. J., Kajiura, H., Hamorsky, K. T., Fujiyama, K., and Matoba, N. (2018). Hydroponic Treatment of Nicotiana benthamiana with Kifunensine Modifies the *N*-glycans of Recombinant Glycoprotein Antigens to Predominantly Man9 High-Mannose Type upon Transient Overexpression. *Front. Plant Sci.* 9:62. doi: 10.3389/fpls.2018.00062

Ryan, S. M., Eichenberger, R. M., Ruscher, R., Giacomin, P. R., and Loukas, A. (2020). Harnessing helminth-driven immunoregulation in the search for novel therapeutic modalities. *PLoS Pathog.* 16:e1008508. doi: 10.1371/journal.ppat.1008508

Sasai, K., Ikeda, Y., Tsuda, T., Ihara, H., Korekane, H., Shiota, K., et al. (2001). The Critical Role of the Stem Region as a Functional Domain Responsible for the Oligomerization and Golgi Localization of *N*-Acetylglucosaminyltransferase V. *J. Biol. Chem.* 276, 759–765. doi: 10.1074/jbc.M00497 2200

Schillberg, S., and Finnern, R. (2021). Plant molecular farming for the production of valuable proteins Critical evaluation of achievements and future challenges. *J. Plant Physiol.* 258–259, 153359. doi: 10.1016/j.jplph.2020.153359

Schneider, J. D., Castilho, A., Neumann, L., Altmann, F., Loos, A., Kannan, L., et al. (2014). Expression of human butyrylcholinesterase with an engineered glycosylation profile resembling the plasma-derived orthologue. *Biotechnol. J.* 9, 501–510. doi: 10.1002/biot.201300229

Schoberer, J., and Strasser, R. (2018). Plant glyco-biotechnology. *Semin. Cell Dev. Biol.* 80, 133–141. doi: 10.1016/j.semcdb.2017.07.005

Schouten, A., Roosien, J., van Engelen, F. A., de Jong, G. A., Borst-Vrenssen, A. W., Zilverentant, J. F., et al. (1996). The C-terminal KDEL sequence increases the expression level of a single-chain antibody designed to be targeted to both the cytosol and the secretory pathway in transgenic tobacco. *Plant Mol. Biol.* 30, 781–793. doi: 10.1007/BF00019011

Sheshukova, E. V., Komarova, T. V., and Dorokhov, Y. L. (2016). Plant factories for the production of monoclonal antibodies. *Biochem.* 81, 1118–1135. doi: 10.1134/S0006297916100102

Shin, Y. J., Castilho, A., Dicker, M., Sádio, F., Vavra, U., Grünwald-Gruber, C., et al. (2017). Reduced paucimannosidic N -glycan formation by suppression of a specific β-hexosaminidase from Nicotiana benthamiana. *Plant Biotechnol. J.* 15, 197–206. doi: 10.1111/pbi.12602

Shin, Y. J., Chong, Y. J., Yang, M. S., and Kwon, T. H. (2011). Production of recombinant human granulocyte macrophage-colony stimulating factor in rice cell suspension culture with a human-like *N*-glycan structure. *Plant Biotechnol. J.* 9, 1109–1119. doi: 10.1111/j.1467-7652.2011.00636.x

Sijmons, P. C., Dekker, B. M. M., Schrammeijer, B., Verwoerd, T. C., van den Elzen, P. J. M., and Hoekema, A. (1990). Production of Correctly Processed Human Serum Albumin in Transgenic Plants. *Nat. Biotechnol.* 8, 217–221. doi: 10.1038/nbt0390-217

Smit, C. H., van Diepen, A., Nguyen, D. L., Wuhrer, M., Hoffmann, K. F., Deelder, A. M., et al. (2015). Glycomic Analysis of Life Stages of the Human Parasite Schistosoma mansoni Reveals Developmental Expression Profiles of Functional and Antigenic Glycan Motifs. *Mol. Cell. Proteomics* 14, 1750–1769. doi: 10.1074/mcp.M115.048280

Sourrouille, C., Marquet-Blouin, E., D'Aoust, M. A., Kiefer-Meyer, M. C., Seveno, M., Pagny-Salehabadi, S., et al. (2008). Down-regulated expression of plant-specific glycoepitopes in alfalfa. *Plant Biotechnol. J.* 6, 702–721. doi: 10.1111/j.1467-7652.2008.00353.x

Stieger, M., Neuhaus, G., Momma, T., Schell, J., and Kreuzaler, F. (1991). Self assembly of immunoglobulins in the cytoplasm of the alga Acetabularia mediterranea. *Plant Sci.* 73, 181–190. doi: 10.1016/0168-9452(91)90027-6

Strasser, R. (2016). Plant protein glycosylation. *Glycobiology* 26, 926–939. doi: 10.1093/GLYCOB/CWW023

Strasser, R. (2018). Protein Quality Control in the Endoplasmic Reticulum of Plants. *Annu. Rev. Plant Biol.* 69, 147–172. doi: 10.1146/annurev-arplant-042817-040331

Strasser, R., Bondili, J. S., Schoberer, J., Svoboda, B., Liebminger, E., Gloössl, J., et al. (2007a). Enzymatic Properties and Subcellular Localization of Arabidopsis β-*N*-Acetylhexosaminidases. *Plant Physiol.* 145, 5–16. doi: 10.1104/pp.107.101162

Strasser, R., Bondili, J. S., Vavra, U., Schoberer, J., Svoboda, B., Glössl, J., et al. (2007b). A unique β1,3-galactosyltransferase is indispensable for the biosynthesis of *N*-glycans containing Lewis a structures in Arabidopsis thaliana. *Plant Cell* 19, 2278–2292. doi: 10.1105/tpc.107.052985

Strasser, R., Castilho, A., Stadlmann, J., Kunert, R., Quendler, H., Gattinger, P., et al. (2009). Improved virus neutralization by plant-produced anti-HIV antibodies with a homogeneous β1,4-galactosylated *N*-glycan profile. *J. Biol. Chem.* 284, 20479–20485. doi: 10.1074/JBC.M109.014126/ATTACHMENT/B190FAD2-31FF-409C-BA56-C0FB4EFA985A/MMC1.PDF

Strasser, R., Seifert, G., Doblin, M. S., Johnson, K. L., Ruprecht, C., Pfrengle, F., et al. (2021). Cracking the "Sugar Code": a Snapshot of *N*- and *O*-Glycosylation Pathways and Functions in Plants Cells. *Front. Plant Sci.* 12:157. doi: 10.3389/fpls.2021.640919

Strasser, R., Stadlmann, J., Schähs, M., Stiegler, G., Quendler, H., Mach, L., et al. (2008). Generation of glyco-engineered Nicotiana benthamiana for the production of monoclonal antibodies with a homogeneous human-like *N*-glycan structure. *Plant Biotechnol. J.* 6, 392–402. doi: 10.1111/j.1467-7652.2008.00330.x

Talabnin, K., Aoki, K., Saichua, P., Wongkham, S., Kaewkes, S., Boons, G. J., et al. (2013). Stage-specific expression and antigenicity of glycoprotein glycans isolated from the human liver fluke, Opisthorchis viverrini. *Int. J. Parasitol.* 43, 37–50. doi: 10.1016/j.ijpara.2012.10.013

Tas, R. P., Sampaio Pinto, V., Wennekes, T., Laake, L. W., and Voets, I. K. (2021). From the freezer to the clinic. *EMBO Rep.* 22:e52162. doi: 10.15252/embr.202052162

Uthailak, N., Kajiura, H., Misaki, R., and Fujiyama, K. (2021). Transient Production of Human β-Glucocerebrosidase With Mannosidic-Type *N*-Glycan Structure in Glycoengineered Nicotiana benthamiana Plants. *Front. Plant Sci.* 12:1039. doi: 10.3389/fpls.2021.683762

van Noort, K., Nguyen, D.-L., Kriechbaumer, V., Hawes, C., Hokke, C. H., Schots, A., et al. (2020). Functional characterization of Schistosoma mansoni fucosyltransferases in Nicotiana benthamiana plants. *Sci. Rep.* 10:18528. doi: 10.1038/s41598-020-74485-z

van Stijn, C. M. W., van den Broek, M., Vervelde, L., Alvarez, R. A., Cummings, R. D., Tefsen, B., et al. (2010). Vaccination-induced IgG response to Galα1–3GalNAc glycan epitopes in lambs protected against Haemonchus contortus challenge infection. *Int. J. Parasitol.* 40, 215–222. doi: 10.1016/j.ijpara.2009.07.009

Varki, A., and Gagneux, P. (2015). "Biological Functions of Glycans," in *Essentials of Glycobiology*, 3rd Edn, eds A. Varki, R. D. Cummings, J. D. Esko, P. Stanley, G. W. Hart, M. Aebi, et al. (Cold Spring Harbor, (NY): Cold Spring Harbor Laboratory Press).

Walsh, G. (2018). Biopharmaceutical benchmarks 2018. *Nat. Biotechnol.* 36, 1136–1145. doi: 10.1038/nbt.4305

Ward, B. J., Makarkov, A., Séguin, A., Pillet, S., Trépanier, S., Dhaliwall, J., et al. (2020). Efficacy, immunogenicity, and safety of a plant-derived, quadrivalent, virus-like particle influenza vaccine in adults (18–64 years) and older adults (=65 years): two multicentre, randomised phase 3 trials. *Lancet* 396, 1491–1503. doi: 10.1016/S0140-6736(20)32014-6

Weise, A., Altmann, F., Rodriguez-Franco, M., Sjoberg, E. R., Bäumer, W., Launhardt, H., et al. (2007). High-level expression of secreted complex glycosylated recombinant human erythropoietin in the *Physcomitrella* Δ-fuc-t Δ-xyl-t mutant. *Plant Biotechnol. J.* 5, 389–401. doi: 10.1111/j.1467-7652.2007.00248.x

WHO (2022). *Soil Transmitted Helminth Infections*. Available online at: https://www.who.int/news-room/fact-sheets/detail/soil-transmitted-helminth-infections [Accessed on Feb 14, 2022]

Wilbers, R. H. P., Westerhof, L. B., Reuter, L. J., Castilho, A., van Raaij, D. R., Nguyen, D.-L., et al. (2016). The *N*-glycan on Asn54 affects the atypical *N*-glycan composition of plant-produced interleukin-22, but does not influence its activity. *Plant Biotechnol. J.* 14, 670–681. doi: 10.1111/pbi.12414

Wilbers, R. H. P., Westerhof, L. B., van Noort, K., Obieglo, K., Driessen, N. N., Everts, B., et al. (2017). Production and glyco-engineering of immunomodulatory helminth glycoproteins in plants. *Sci. Rep.* 7:45910. doi: 10.1038/srep45910

Wilson, I. B. H., and Paschinger, K. (2016). Sweet secrets of a therapeutic worm: mass-spectrometric *N*-glycomic analysis of Trichuris suis. *Anal. Bioanal. Chem.* 408, 461–471. doi: 10.1007/s00216-015-9154-8

Wuhrer, M., Balog, C. I. A., Catalina, M. I., Jones, F. M., Schramm, G., Haas, H., et al. (2006). IPSE/alpha-1, a major secretory glycoprotein antigen from schistosome eggs, expresses the Lewis X motif on core-difucosylated *N*-glycans. *FEBS J.* 273, 2276–2292. doi: 10.1111/j.1742-4658.2006.05242.x

Yang, Z., Drew, D. P., Jørgensen, B., Mandel, U., Bach, S. S., Ulvskov, P., et al. (2012). Engineering mammalian mucin-type *O*-glycosylation in plants. *J. Biol. Chem.* 287, 11911–11923. doi: 10.1074/jbc.M111.312918

Yates, E. A., Valdor, J.-F., Haslam, S. M., Morris, H. R., Dell, A., Mackie, W., et al. (1996). Characterization of carbohydrate structural features recognized by anti-arabinogalactan-protein monoclonal antibodies. *Glycobiology* 6, 131–139. doi: 10.1093/glycob/6.2.131

Yoshino, T. P., Brown, M., Wu, X.-J., Jackson, C. J., Ocadiz-Ruiz, R., Chalmers, I. W., et al. (2014). Excreted/secreted Schistosoma mansoni venom allergen-like 9 (SmVAL9) modulates host extracellular matrix remodelling gene expression. *Int. J. Parasitol.* 44, 551–563. doi: 10.1016/j.ijpara.2014.04.002

Zhong, T., Min, L., Wang, Z., Zhang, F., and Zuo, B. (2018). Controlled self-assembly of glycoprotein complex in snail mucus from lubricating liquid to elastic fiber. *RSC Adv.* 8, 13806–13812. doi: 10.1039/C8RA01439F

Zimran, A., Brill-Almon, E., Chertkoff, R., Petakov, M., Blanco-Favela, F., Muñoz, E. T., et al. (2011). Pivotal trial with plant cell–expressed recombinant glucocerebrosidase, taliglucerase alfa, a novel enzyme replacement therapy for Gaucher disease. *Blood* 118, 5767–5773. doi: 10.1182/blood-2011-07-366955

Conflict of Interest: The authors declare that the research was conducted in the absence of any commercial or financial relationships that could be construed as a potential conflict of interest.

Publisher's Note: All claims expressed in this article are solely those of the authors and do not necessarily represent those of their affiliated organizations, or those of the publisher, the editors and the reviewers. Any product that may be evaluated in this article, or claim that may be made by its manufacturer, is not guaranteed or endorsed by the publisher.

Copyright © 2022 van der Kaaij, van Noort, Nibbering, Wilbers and Schots. This is an open-access article distributed under the terms of the Creative Commons Attribution License (CC BY). The use, distribution or reproduction in other forums is permitted, provided the original author(s) and the copyright owner(s) are credited and that the original publication in this journal is cited, in accordance with accepted academic practice. No use, distribution or reproduction is permitted which does not comply with these terms.

frontiers | Frontiers in Plant Science

REVIEW
published: 09 May 2022
doi: 10.3389/fpls.2022.888425

Molecular Determinants of *in vitro* Plant Regeneration: Prospects for Enhanced Manipulation of Lettuce (*Lactuca sativa* L.)

Tawni Bull[1,2] *and Richard Michelmore*[1,3]*

[1] The Genome Center, University of California, Davis, Davis, CA, United States, [2] Graduate Group in Horticulture and Agronomy, University of California, Davis, Davis, CA, United States, [3] Department of Plant Sciences, University of California, Davis, Davis, CA, United States

In vitro plant regeneration involves dedifferentiation and molecular reprogramming of cells in order to regenerate whole organs. Plant regeneration can occur via two pathways, *de novo* organogenesis and somatic embryogenesis. Both pathways involve intricate molecular mechanisms and crosstalk between auxin and cytokinin signaling. Molecular determinants of both pathways have been studied in detail in model species, but little is known about the molecular mechanisms controlling *de novo* shoot organogenesis in lettuce. This review provides a synopsis of our current knowledge on molecular determinants of *de novo* organogenesis and somatic embryogenesis with an emphasis on the former as well as provides insights into applying this information for enhanced *in vitro* regeneration in non-model species such as lettuce (*Lactuca sativa* L.).

Keywords: regeneration, organogenesis, lettuce, somatic embryogenesis, WUSCHEL, *Lactuca sativa* (L.)

OPEN ACCESS

Edited by:
Goetz Hensel,
Heinrich Heine University Düsseldorf, Germany

Reviewed by:
Tatjana Cosic,
University of Belgrade, Serbia
Mohsen Hesami,
University of Guelph, Canada

***Correspondence:**
Richard Michelmore
rwmichelmore@ucdavis.edu

Specialty section:
This article was submitted to Plant Biotechnology, a section of the journal Frontiers in Plant Science

Received: *02 March 2022*
Accepted: *31 March 2022*
Published: *09 May 2022*

Citation:
Bull T and Michelmore R (2022) Molecular Determinants of in vitro Plant Regeneration: Prospects for Enhanced Manipulation of Lettuce (Lactuca sativa L.). Front. Plant Sci. 13:888425. doi: 10.3389/fpls.2022.888425

INTRODUCTION

Plants have evolved a remarkable ability to regenerate tissues from differentiated organs, which involves the conversion of one cell type to others. Such plasticity provides the ability to regenerate whole organs and plants via dedifferentiation of cells and reprogramming of cell fates. There are three main types of regeneration: (1) Tissue regeneration, (2) *de novo* organogenesis, and (3) somatic embryogenesis (Xu and Huang, 2014; Sugimoto et al., 2019). Bryophytes have high capacity for tissue regeneration; for example, *Marchantia* spp. are capable of regenerating new meristems within their thallus (Yasui et al., 2019). However, vascular plants follow different regeneration pathways, which include *de novo* organogenesis or somatic embryogenesis (**Figure 1**). *De novo* organogenesis involves the regeneration of whole organs that did not previously exist. There are two types of *de novo* organogenesis: direct and indirect regeneration. Direct regeneration involves the development of organs directly from explants, whereas indirect regeneration involves an intermediate undifferentiated callus phase. For example, some plants, such as *Jatropha curcas* and succulents of the Cactaceae and Crassulaceae families (Preece, 2003; Severino et al., 2011), are capable of direct regeneration of new roots and shoots from stem cuttings. In contrast, many plants, such as lettuce, exhibit indirect organogenesis and regenerate shoots from calli (Michelmore and Eash, 1985). Somatic embryogenesis involves the regeneration of embryo or embryo-like structures from somatic cells, which can develop into a whole plant. In all forms of

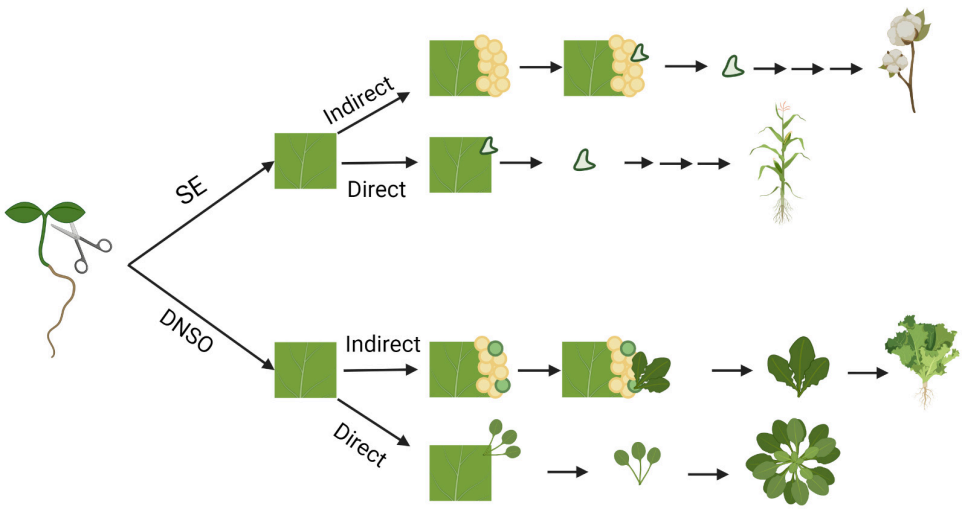


FIGURE 1 | Pathways of *in vitro* regeneration of vascular plants. Somatic embryogenesis (SE) and *de novo* shoot organogenesis (DNSO) can occur directly on the explant or indirectly with the formation of pluripotent callus as an intermediate step. Species that are capable of regeneration for each pathway are represented from top to bottom: cotton, maize, *Arabidopsis*, and lettuce. Figure created using BioRender (https://biorender.com/).

regeneration, cells must undergo dedifferentiation or transdifferentiation (reprogramming) into a more totipotent cell, ultimately changing the fate of the progenitor cell.

Plant tissue culture and totipotency were first proposed by Haberlandt in 1902 (Krikorian and Berquam, 1969; Thorpe, 2007), who attempted to culture isolated photosynthetic leaf cells. Although this proved unsuccessful, it was the start of many decades of work on developing and improving plant tissue culture methods for multiple plant species. These failed experiments led to the development of root cultures using root tip cells in tomato and bud cultures. In 1904, embryo culture was first successful when embryos of crucifers (Brassicaceae) were isolated aseptically and grown in culture (Norstog, 1979). The first "true" plant tissue cultures were obtained on Knop's medium from cambial tissues of sycamore maple (*Acer psuedoplatanus*) by Gautheret in 1934. This approach was optimized by additions of auxin, indole acetic acid (IAA), and B vitamins. This resulted in tissues that could be grown indefinitely in culture and the regeneration of both roots and shoots (Gautheret, 1934, 1935, 1939). The previous studies, however, used explant tissues that already contained meristematic cells. It was not until 1948 that methods were developed to induce roots and shoots from non-meristematic explants (Skoog and Tsui, 1948). This drastically increased the number of species that could be studied using *in vitro* culture systems (Miller et al., 1955; Skoog and Miller, 1957), and led to the recognition of the importance of exogenous ratios of cytokinin and auxin in culture medium. The differing ratios were shown to affect cell fate transition to either rooting or shooting from callus cells (Skoog and Miller, 1957), where high ratios of auxin to cytokinin promoted root regeneration, low ratios of auxin to cytokinin promoted shoot regeneration, and intermediate levels promoted proliferation of callus tissues. From the early to mid-1900s, research helped develop common plant tissue culture methods and media still used today (van Overbeek et al., 1941; Gautheret, 1942, 1955; Nobe'court, 1955). The earliest plant tissue culture media were based on nutrient necessities of whole plants, with the most common being Knop's solution (Loomis and Schull, 1937). Numerous studies were conducted to optimize culture medium and in 1962, Murashige and Skoog reported a medium (MS salts) containing salt concentrations 25 times higher than those in Knop's solution; in particular this resulted in much higher concentrations of NO3− and NH4+. The development of MS salts is still considered to be a major breakthrough in tissue culture because MS salts are still commonly used in plant tissue culture. The combination of exogenous plant hormones and appropriate salts allowed the study of basic plant biology questions about cell behavior, genetic improvement, disease biology, germplasm conservation, and clonal propagation.

Plant tissue culture to achieve *in vitro* regeneration was originally used to answer fundamental questions in plant biology but has since evolved to be foundational for genetic improvement, micropropagation, genetic engineering, and biotechnology (Michelmore et al., 1987; Zhang et al., 2006; Loberant and Altman, 2010; Xu and Huang, 2014; Chokheli et al., 2020). However, *in vitro* regeneration is not possible for all plant species and regeneration is very genotype dependent. Therefore, studying the molecular determinants of plant regeneration and exploiting these signaling pathways for improved *in vitro* regeneration of those recalcitrant genotypes and species is important. This review provides a synopsis of our current understanding of the pathways involved in *de novo* organogenesis and somatic embryogenesis. We focus on what is known of the molecular determinants of indirect *de novo* shoot organogenesis, which is the mode of regeneration in lettuce (*Lactuca sativa* L.). Finally, we describe future directions for improvement of *in vitro* regeneration of lettuce and other Compositae species.

MOLECULAR DETERMINANTS OF REGENERATION

Recently, many advances have been made toward understanding the cellular and molecular mechanisms that underlie plant regeneration (Xu and Huang, 2014; Ikeuchi et al., 2016; Sugimoto et al., 2019). Each of the regeneration processes described above have been studied in detail in model plants such as *Arabidopsis thaliana*. Each process entails a complex of molecular players involved in signaling and developmental pathways that regulate the dedifferentiation (somatic embryogenesis) or reprogramming (*de novo* organogenesis) of cells.

Organogenic Callus Formation

Callus formation is the first step in indirect organogenesis. Based on morphology, calli are thought to be the result of the dedifferentiation of cells to form totipotent cells. Callus can originate from the initiation of multiple pathways that contain some overlap in gene expression (Fehér, 2019) and can be auxin or wound induced (Fehér, 2019). In *Arabidopsis*, auxin induced calli resemble pluripotent cells similar to root tip cells at the molecular level and originate from pluripotent pericycle cells located adjacent to xylem poles (Atta et al., 2009; Sugimoto et al., 2010; Fehér, 2019). Root cell-like, auxin-induced callus follows a similar pathway as lateral root formation. In contrast, wound-induced callus does not involve players of lateral root formation, but rather occurs via upregulation of cytokinin signaling (Iwase et al., 2011a,b; Ikeuchi et al., 2017). Due to the similarity of gene expression patterns during callus formation with other developmental pathways some consider it a form of transdifferentiation rather than dedifferentiation (Fehér, 2019).

Many genes and transcription factors that are involved in lateral root development are also critical players in auxin-induced callus formation (**Figure 2**). For example, the *LATERAL ORGAN BOUNDARIES* (*LBD*) family of genes, such as *LBD16*, *17*, *18*, and *29*, are critical to both lateral root formation and callus production (Fan et al., 2012; Feng et al., 2012; Xu et al., 2012; Lee H. W. et al., 2019). Ectopic expression of *LBD* genes led to the spontaneous formation of callus without exogenous applications of auxin and cytokinin, and repression of *LBD16* showed inhibited callus formation (Fan et al., 2012). In lateral root formation, *LBD16* and *LBD29* are positively regulated by AUXIN RESPONSE FACTOR7 (ARF7) and ARF19, which provides evidence that *ARFs* are also involved in callus formation (Okushima et al., 2007). Furthermore, JUMONJI C DOMAIN CONTAINING PROTEIN 30 (JMJ30) interacts with ARF7 and ARF19 and directly binds to cis elements of *LBD16* and *LBD29*, promoting their expression (Lee et al., 2018). Other key players in both lateral root and callus formation are *ABERRANT LATERAL ROOT FORMATION 4* (*ALF4*) and *SOLITARY ROOT/IAA14* (*SLR/IAA14*). *ALF4* is involved in the earliest divisions of pericycle cells during lateral root formation. In *alf4* mutants, callus-forming capability was lost in multiple tissues (DiDonato et al., 2004; Sugimoto et al., 2010). It was later shown that *ALF4* is targeted for downregulation by CALLUS FORMATION RELATED-1 (CRF-1), which encodes an enzyme involved in very long chain fatty acid (VLCFA) biosynthesis (Shang et al., 2016). Another molecule involved in VLCFA biosynthesis is the AP2 transcription factor, PUCHI, which is also a key regulator controlling cell proliferation in lateral root primordia; *puchi-1* mutants resulted in both defective and disorganized lateral root and callus formation further indicating a link between these pathways (Trinh et al., 2019). SLR is a member of the auxin signaling protein family Aux/IAA, and *slr-1* mutants in *A. thaliana* were defective in both lateral root and callus formation (Fukaki et al., 2002; Shang et al., 2016). The functions of these genes and transcription factors provides evidence that callus formation and lateral root development have similar underlying mechanisms. In addition, callus formation can be initiated via a wound-induced signaling pathway and activation of a cytokinin response. Transcription factors involved during wound-induced callus formation include APETALA2/Ethylene Responsive Factor (AP2/ERF)-type transcription factors, WOUND-INDUCED DEDIFFERENTIATION1 (WIND1), and homologs (Iwase et al., 2011a,b, 2013). In Arabidopsis, expression of *WIND1* and homologs are upregulated upon wounding and promote pluripotent callus formation at cut sites (Iwase et al., 2011a,b). Expression of *Arabidopsis WIND1* was also shown to induce callus formation in other species such as rapeseed, tomato, and tobacco (Iwase et al., 2013). A transcriptome analysis showed WIND1 activates over 2,000 genes involved in multiple pathways including wound-induced cellular reprogramming and vascular formation (Iwase et al., 2021).

Among the genes upregulated by WIND1 are those encoding for other AP2/ERF-type transcription factors including *PLETHORA* (PLT) genes (Kareem et al., 2015; Iwase et al., 2021). *PLT* genes work through the auxin signaling pathway, are often transcribed in response to auxin accumulation, and are activated downstream of *ARF7* and *ARF19* (Aida et al., 2004; Hofhuis et al., 2013). *PLT3*, PLT5, and PLT7 upregulate *PLT1* and *PLT2*, which are important players in the regulation of lateral root formation, root apical meristem maintenance (RAM), and callus pluripotency (Xu et al., 2006; Durgaprasad et al., 2019). In *Arabidopsis, PLT1* is also upregulated by JANUS through the recruitment of RNA Polymerase II to the root meristem (Xiong et al., 2020). In addition to root meristem maintenance, PLT proteins play important roles in conjunction with *BABYBOOM/PLT4* (*BBM/PLT4*) in early embryogenesis (described further in section "Somatic Embryogenesis"), and activate regeneration responses in shoot organs by regulating the shoot promoting factors *CUPPED-SHAPED COTYLEDON1 (CUC1)* and *CUC2* (Radhakrishnan et al., 2020). PLT-CUC2 together work through the auxin biosynthesis pathway and are essential for proper distribution and repolarization of auxin through PIN-FORMED (PIN) proteins (described further in section "*De novo* Root Organogenesis") (Kareem et al., 2015; Shimotohno et al., 2018; Radhakrishnan et al., 2020).

Callus formation also involves epigenetic regulators. One regulator, HISTONE ACETYLTRANSFERASE OF THE GNAT/MYST SUPERFAMILY 1 (HAG1), also known as A. thaliana GENERAL CONTROL NON-REPRESSED 5

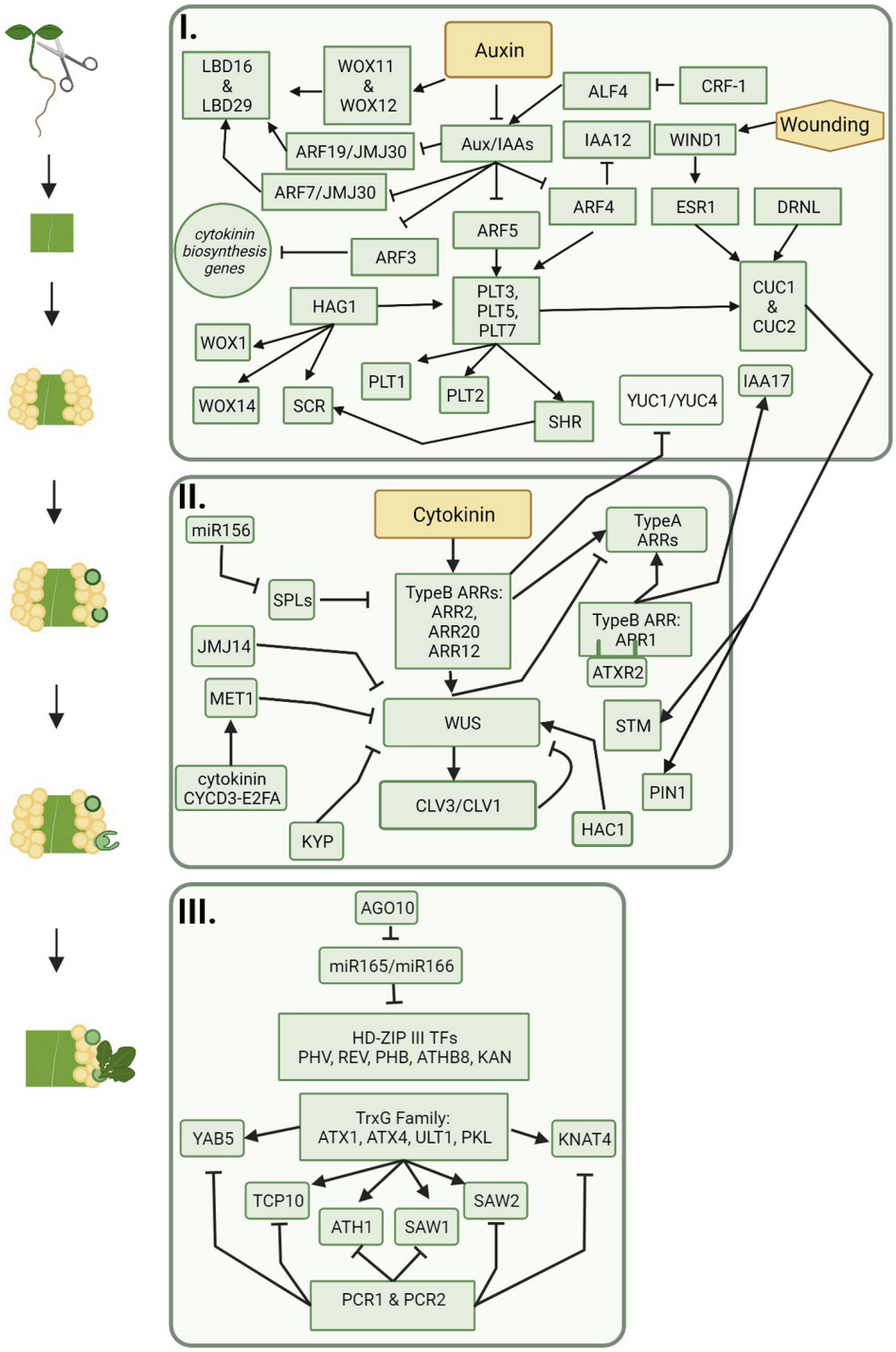


FIGURE 2 | The progression of molecular players during indirect *de novo* shoot organogenesis. Callus is formed on auxin rich medium and includes signaling pathways represented in box one. Shoot promersitems and meristematic centers are formed on cytokinin rich medium and include signaling pathways represented in box two. Shoot regeneration follows meristem formation and is represented by the signaling pathways included in box three. Figure created using BioRender (https://biorender.com/).

(AtGCN5), acts upstream of *PLT1* and *PLT2* (Kornet and Scheres, 2009; Kim et al., 2018). HAG1 also epigenetically upregulates root meristem genes *WUSHCEL RELATED HOMEOBOX 5* (*WOX5*), *WOX14*, and *SCARECROW* (*SCR)* by acetylating the N terminus of histone 3. HAG1 is further involved in determining the root–shoot axis in embryo development and is a regulator

of floral meristem activity (Kim et al., 2018). The RAM gene, *ROOT CLAVATA-HOMOLOG 1* (*RCH1*), is also highly expressed in callus (Sugimoto et al., 2010), providing further evidence of homologies between lateral root development and callus formation. Although initiation of callus can follow multiple pathways, this provides further evidence that each pathway contains overlapping players.

De novo Root Organogenesis

De novo root organogenesis is the process by which adventitious roots are formed from detached plant tissues such as leaves and stems. Multiple studies have investigated the regeneration of the RAM in *A. thaliana* (Tian et al., 2002; Casamitjana-Martínez et al., 2003; Galinha et al., 2007; de Smet et al., 2008; Müller and Sheen, 2008; Perilli et al., 2012). The quiescent center (QC) is the site of stem cell maintenance of the RAM that is regenerated after QC ablation or entire removal of the root tip; polar transportation of auxin driven by PIN-FORMED (PIN) proteins results in auxin accumulation in cells adjacent to the damaged QC cells, which drives the reprogramming to new QC cells (van den Berg et al., 1997; Wildwater et al., 2005).

One of the key molecular players in root organogenesis is auxin. In *Arabidopsis,* auxin accumulates at cut sites, which induces expression of the homeobox transcription factors WOX11 and WOX12 (Liu et al., 2014). WOX11 and WOX12 directly upregulate *WOX5*, *LBD16*, and *LBD29*, marking the first step in cell differentiation and the formation of root meristems (Goh et al., 2012; Liu et al., 2014; Hu and Xu, 2016). Auxin accumulation at wound sites in *Arabidopsis* drives the expression of *PLT* genes (as seen in callus formation), which will in turn upregulate *SHORT ROOT* (*SHR*) (Kareem et al., 2015). The SHR proteins will localize to the nucleus, inducing the expression of *SCR*; SHR and SCR are both involved in QC identity and radial patterning (van den Berg et al., 1997; Wildwater et al., 2005). SCR and PLT work together with plant-specific teosinte-branched cycloidea PNCP (TCP) in PLT-TCP-SCR complexes to promote the organization of PIN proteins and expression of *WOX5* in new meristem QC cells (Xu et al., 2006; Shimotohno et al., 2018). Root primordia formation is inhibited in *shr, plt1,* and *plt2* mutants, indicating that these genes play an important role during root formation from root founder cells (Bustillo-Avendaño et al., 2018).

De novo Shoot Organogenesis

Shoot organogenesis may occur with direct regeneration of a shoot from an explant or indirect regeneration from a callus (**Figure 1**). Because a callus seems to resemble root tip cells rather than shoot cells at the molecular level, callus cells must undergo changes in gene expression that push the cells toward shoot development rather than root development. Shoot regeneration has been studied extensively in plants; however, while many genes and hormones have been identified as important players in the process (**Figure 2**), the detailed molecular interactions and pathways are unclear (reviewed in Xu et al., 2006; Su and Zhang, 2014; Xu and Huang, 2014; Ikeuchi et al., 2016; Lardon and Geelen, 2020).

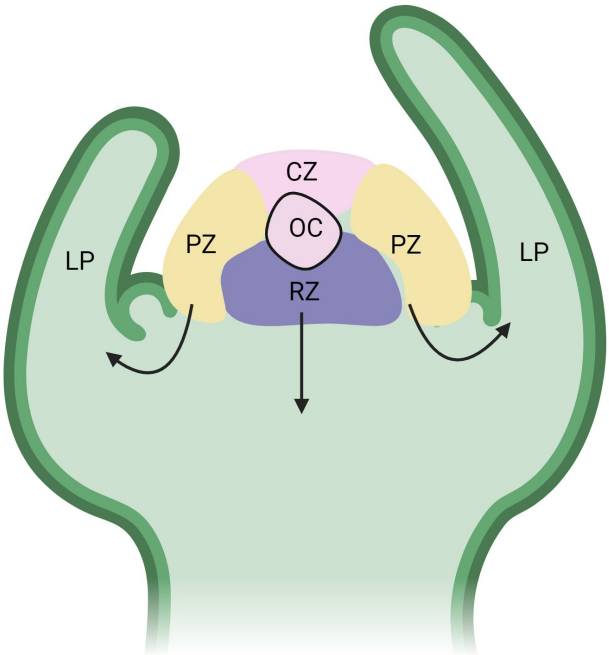


FIGURE 3 | Functional domains of the shoot apical meristem (SAM). The organizing center (OC) is part of the central zone (CZ), which consists of a stem cell pool that replenishes cells to the peripheral zone (PZ) and rib zone (RB). The black arrows represent the direction of differentiating cells from the PZ to form leaf primordia (LP) and the RZ to form the stem. WUS expression is high in the OC and is regulated by CLV3/CLV1 from the CZ in a negative feedback loop. Figure created using BioRender (https://biorender.com/).

Regeneration of shoots from callus requires the formation of a primary meristem or a shoot apical meristem (SAM) (**Figure 3**). Similar to the RAM, the SAM contains a population of pluripotent stem cells that give rise to all aboveground organs of a plant. The undifferentiated state of the organizing center (OC), which is similar to the RAM QC, and surrounding stem cells is maintained by a feedback mechanism between WUSHEL (WUS) and the signaling peptide CLAVATA3 (CLV3) (Sarkar et al., 2007). Leaves and other lateral organs arise from the peripheral regions of the SAM and the stem arises from the basal cells, called the rib zone. The SAM also contains the central zone, which consists of a stem cell pool that will replenish cells in the peripheral and rib zones that have further differentiated (Bowman and Eshed, 2000; Kwiatkowska, 2004). Unlike auxin accumulation in the RAM, the SAM contains high levels of cytokinins. Organization of auxin and cytokinin in cells help promote differentiation of pluripotent cells to either shoot or root cells.

Shoot regeneration from callus occurs in four stages: (1) Formation of a pluripotent callus, (2) shoot promeristem formation, (3) shoot progenitor development, and (4) shoot regeneration (Shin et al., 2020). The development of a pluripotent callus cell mass (section "Synopsis of Studies on the Regeneration of Lettuce") that highly expresses the No Apical Meristem/*A. thaliana* activating factor (NAC) transcription

factor genes, *CUC1* and *CUC2* (Gordon et al., 2007), transitions into promeristems composed of a primary meristem of actively dividing cells. Within the callus *CUC2* expression marks pre-meristematic regions by promoting cell proliferation and leading to the localized upregulation of a key shoot meristem regulator, *SHOOT MERSITEMLESS* (STM), and *PIN1*. As seen in *de novo* root organogenesis, PIN1 proteins polarly localize, denoting areas of cellular reprogramming toward promeristematic cells (Gordon et al., 2007). Both STM and PIN1 aid in the development of radial patterning as STM marks the promeristem and PIN1 marks primordia (Gordon et al., 2007). Because PIN1 proteins are important players in both promeristem formation and root *de novo* organogenesis, this suggests that auxin transport is important for both shoot and root meristem patterning.

Proper regulation and distribution of *CUC1, CUC2,* and *WUS* are critical for shoot progenitor cells. These NAC transcription factors are subject to upstream regulation during shoot promeristem formation. AP2/ERF-type transcription factors, ENHANCER OF SHOOT REGENERATION 1 (ESR1)/DORNROSCHEN (DRN) and ESR2/DRN-LIKE (DRNL) participate in upstream regulation of *CUC* genes by actively binding to the promoter and inducing expression (Banno et al., 2001; Kirch et al., 2003; Ikeda et al., 2006). Mutants of *esr1, esr2,* and *esr1 esr2* show a reduction in shoot regeneration. This is likely due to improper regulation of *CUC1* and *CUC2* (Matsuo et al., 2011). WIND1 also upregulates *ESR1* by directly binding to the vascular-responsive motifs in the *ESR1* promoter (Iwase et al., 2017), suggesting that WIND1 is important in multiple plant regeneration processes. PLT5 and PLT7, which are induced during callus production, also influence the expression of *CUC1* and *CUC2* (Kareem et al., 2015). This further suggests that the molecular players and pathways involved in shoot regeneration are intertwined.

WUSCHEL (WUS) is a key regulator of the SAM and is upregulated during shoot regeneration. Expression of *WUS* is an important part of the conversion of a promeristem to a shoot progenitor as it represses cell division, cell elongation, and auxin-induced expression. This directs cell fate toward shoot development rather than root development. Ectopic expression of *AtWUS* results in *de novo* meristem formation and organogenesis in multiple plant species including *Arabidopsis* (Gallois et al., 2002; Negin et al., 2017), rice (Victorathisayam and Sridevi, 2020), and cotton (Bouchabké-Coussa et al., 2013). *WUS* expression is restricted to high cytokinin domains, while *CUC2* expression tends to be restricted to low cytokinin and high auxin domains. This is consistent with high expression of *CUC2* during induction of callus on media using higher concentrations of auxin (Daimon et al., 2003; Kareem et al., 2015). Regulation of *WUS* is subject to epigenetic regulation. METHYLTRANSFERASE1 (MET1), KRYPTONITE (KYP), histone acetyl transferase1 (HAC1), and JMJ14 are all required for proper expression of *WUS*, SAM organization, and shoot development (Li et al., 2011; Ishihara et al., 2019). *MET1* is induced by the cytokinin-CYCD3-E2FA module, which represses *WUS* expression, allowing cells to retain callus identity rather than transitioning to shoot cells. However, in later stages of *de novo* shoot organogenesis, *MET1* is spatially regulated, allowing for an increase in *WUS* expression in the inner cell layers of the callus (Liu et al., 2018). Previously, it was thought that *WUS* expression in the inner callus cell layers is directly activated by the cytokinin-responsive Type B ARABIDOPSIS RESPONSE REGULATORS (ARRS), ARR1, ARR2, ARR10, and ARR12 (Dai et al., 2017). However, a recent study showed that ARR1 is a strong inhibitor of callus formation and shoot regeneration. This occurs through indirect repression of *CLV3* by competitive binding with ARR12 (Liu et al., 2020). ARR1 also indirectly represses *WUS* by inducing expression of the auxin response repressor gene *INDOLE-3-ACETIC ACID INDUCIBLE17* (*IAA17*) (Liu et al., 2020). In addition, Type-B ARRs negatively regulate the expression of the auxin biosynthetic genes *YUCCA1* (*YUC1*) and *YUC4* (Meng et al., 2017). This results in indirect upregulation of *WUS* expression. Although it has been known for decades that auxin and cytokinin signaling is important for plant regeneration, these findings further untangle the underlying mechanisms of the signaling pathways.

Eukaryotic stem cells tend to have open chromatin states, while differentiated cells tend to have closed chromatin states (Shchuka et al., 2015). Epigenetic controls include Trithorax group (trxG) and Polycomb Group (PcG) proteins. The *A. thaliana* trxG, ATXR2, interacts with ARR1 and methylates the Type A ARRs, *ARR5* and *ARR7*, marking them for increased transcription. This leads to a repression of cytokinin signaling and a reduction in *de novo* shoot organogenesis (Lee et al., 2021). PcG protein complexes, specifically POLYCOMB REPRESSIVE COMPLEX1 (PRC1) and PRC2, are chromatin modifiers and bind to Polycomb Response Elements (PRE) to keep genes transcriptionally repressed in order to fine-tune the balance between cell proliferation and cell differentiation (Köhler and Hennig, 2010). PRC2 suppresses leaf identity via H3K27me3 of leaf identity genes. PRC2 is also involved in callus formation as PRC2 mutants *curly leaf swinger (clf swn)* and *embryonic flower2 (emf2)* are incapable of developing callus from leaf and cotyledon explants but retained the ability to form callus in root explants (He et al., 2012). This suggests PCR2 represses leaf identify genes, allowing for the transition to root-like callus cells. Other instances of epigenetic regulation during the early stages of regeneration include gene priming by LYSINE-SPECIFIC DEMETHYLASE 1-LIKE 3 (LDL3), which involves the elimination of methylation of lysine 4 on histone 3 (H3K4me2) during callus formation. This indirectly promotes the expression of genes that are involved in shoot progenitor development (Ishihara et al., 2019).

Regulatory microRNA, miR156, plays a role in activating cytokinin signaling by targeting *SQUAMOSA PROMOTER BINDING PROTEIN-LIKE* (*SPL*). *SPL* genes control transitions in shoot development—juvenile-to-adult and vegetative-to-reproductive—by binding to and regulating Type-B ARRs, decreasing shoot regenerative capacity with age (Xu et al., 2015, 2016). miRNA156 expression is higher in younger tissues, which partially explains why younger explant tissue (i.e., cotyledons) is more amenable to *in vitro* regeneration, when compared to more mature tissue types. Type B ARRs and WUS also regulate the Type A ARRs, *ARR7* and *ARR15*, which negatively regulate cytokinin signaling (Buechel et al., 2010).

After proper development of shoot progenitor cells, activation of leaf identity genes will lead to the development of leaf tissues

and leaf emergence. Two important players involved in shoot regeneration are miR165 and miR166, both of which target HD-ZIP III transcription factor genes *PHABULOSA* (*PHB*), *PHAVOLUTA* (*PHV*), *REVOLUTA* (*REV*), *KANADI* (*KAN*), and *ARABIDOPSIS THALIANA HOMEOBOX GENE 8* (*ATHB8*) (Shin et al., 2020). *PHB, PHV, REV,* and *KAN* function in radial leaf patterning (abaxial vs. adaxial), and *phb*, *phv*, *rev*, and *kan* mutants show a transition of abaxial leaf fates into adaxial leaf fates as well as altered auxin gradients (McConnell et al., 2001; Emery et al., 2003; Zhou et al., 2019). *ATHB8* and *SHR* expression activate simultaneously and lead to leaf vein precursor cells (Gardiner et al., 2010). An RNA-induced silencing complex, ARGONAUTE10 (AGO10), helps sequester and repress the activity of miR165 and miR166. This indirectly promotes the activity of these leaf identity genes. Interestingly, accumulation of miR165/166 in overexpressing *Arabidopsis* mutants resulting in less HD-ZIP III transcription factor activity in shoot progenitor cells, increased the overall shoot regeneration (Xue et al., 2017). This suggests that leaf identity genes work to suppress *in vitro* transition from meristematic cells into shoot cells. In addition, *AGO10* is repressed by LBD12, resulting in reduced apical meristem size (Ma et al., 2017). Leaf identity genes are also subject to epigenetic regulation. TrxG proteins, ATX1, ATX4, ULTRAPETALA1 (ULT1), and PICKLE (PKL), act as antagonists of PCR1 and PCR2 to activate transcription of leaf identity genes, which will aid in the development of leaves from shoot progenitor cells (Köhler and Hennig, 2010). In *A. thaliana*, ATX4 protein trimethylates histone 3 (H3K4me3) to increase the expression of the shoot identity genes *ARABIDOPSIS THALIANA HOMEOBOX GENE 1* (*ATH1*), *KNOTTED1-LIKE HOMEOBOX (KNOX) GENE 4* (*KNAT4*), *SAWTOOTH 1* (*SAW1*), *SAW2*, *TCP FAMILY TRANSCRIPTION FACTOR 10* (*TCP10*), and *YABBY 5* (*YAB5*) (Lee K. et al., 2019).

As elaborated above, *de novo* shoot regeneration is controlled by a complex network of genetic and epigenetic factors. Although we are gaining a more detailed understanding of the molecular players involved in this network via forward and reverse genetic approaches, there is clearly more information to discover involving interactions between these genetic, epigenetic, and hormone signaling pathways.

Embryogenic Callus Formation

Formation of embryogenic callus results from acquisition of a new cell fate through expression of embryonic regulators. Similar to organogenic calli, embryogenic calli have been observed to originate from cells surrounding vascular tissue (pre-procambial cells) (de Almeida et al., 2012). Endogenous application of plant growth regulators such as auxin and cytokinin have been shown to induce proliferation of embryonic tissues in some species, such as soybean and cotton (Raza et al., 2020; Elhiti and Stasolla, 2022). This is similar to auxin-induced callus formation suggesting upregulation of *ARFs* such as *ARF7* and *ARF19* are also requirements for the formation of embryonic callus. Furthermore, *LEAFY COTYLEDON1* (*LEC1*) and *LEC2* genes are major embryonic regulators that control embryo maturation and development (Gaj et al., 2005). *LEC1* overexpression induced embryogenic callus formation in *Arabidopsis*; however, *lec1* and *lec2* mutants resulted in the development of fewer somatic embryos via only indirect somatic embryogenesis (Gaj et al., 2005). This suggests that *LEC1* is sufficient, but not necessary to the formation of embryogenic callus. Overexpression of the MADS-box transcription factor, AGAMOUS-LIKE 15 (AGL15), induced embryogenic callus-like structures on SAMs and extended embryonic development from callus in *Arabidopsis* (Harding et al., 2003). Expression of specific genes and presence of proteins have been observed in embryogenic callus, but not observed in non-embryogenic callus. The MADS-box gene, *CUS1*, whose amino acid sequence is highly similar to Arabidopsis AGL1 and AGL5 amino acid sequences, was detected in embryogenic callus during somatic embryogenesis in cucumber (Filipecki et al., 1997). Additionally, in sugar cane, unique proteins were identified during embryonic callus formation including proteins related to metabolic activity and stress (Schuabb Heringer et al., 2015). Induction of somatic embryogenesis and formation of proembyrogenic masses on calli (section "Somatic Embryogenesis") involves different molecular players than formation of promeristems during organogenesis, but differences between embryogenic calli and organogenic calli formation, if any, are still not well characterized.

Somatic Embryogenesis

A second type of *in vitro* regeneration is somatic embryogenesis. Somatic embryogenesis results when a differentiated somatic cell undergoes molecular changes and genetic/epigenetic reprogramming resulting in the formation of a bipolar somatic embryo. In tissue culture, somatic embryogenesis can be induced in response to the addition of exogenous plant growth regulators or the introduction of stressful conditions. Similar to *de novo* organogenesis, somatic embryogenesis may originate directly at wound sites of explants or indirectly from embryogenic callus (Quiroz-Figueroa et al., 2006). Species tend to regenerate either through *de novo* organogenesis (e.g., tomato, lettuce, pepper) or somatic embryogenesis (e.g., cotton, wheat, rice) but rarely both (e.g., chickpea, purple coneflower) (Ozias-akins and Vasil, 1982; Michelmore et al., 1987; Rueb et al., 1994; Murthy et al., 1996; Choffe et al., 2000; Leelavathi et al., 2004; Heidmann et al., 2011; Sun et al., 2015).

Regulators and genetic determinants of embryo initiation are not well understood, although auxin signaling and accumulation are thought to play a major role. In tissue culture, addition of auxin is used to induce somatic embryogenesis by exposure of explants to high levels of auxin immediately followed by a transfer to auxin-free medium (Méndez-Hernández et al., 2019). This allows for the formation of auxin gradients within the developing embryos—areas of high auxin promote *WUS* expression, which denote areas of future SAM development as mentioned previously (Ikeuchi et al., 2016). In *Arabidopsis,* several *ARFs* are both up and downregulated during the first steps of somatic embryogenesis, and multiple *arf* mutants showed inhibited somatic embryogenesis (Wójcikowska and Gaj, 2017). *SOMATIC EMBRYOGENESIS RECEPTOR-LIKE KINASES* (SERKs), specifically *SERK1* in *Arabidopsis*, are upregulated in embryonic callus and are continually expressed from megasporogenesis until the heart stage of the embryonic

development (Hecht et al., 2001). Other genes, such as auxin-responsive gene *EgIAA9* from *Elaeis guineensis*, have been shown to be upregulated during somatic embryogenesis initiation (Ooi et al., 2012).

The transcription factor BABY BOOM (BBM) and the LEC1-AB13-FUS3-LEC2 (LAFL) complex are master regulators of somatic embryogenesis (Horstman et al., 2017; Jones et al., 2019). *BBM* encodes an AINTEGUMENTA-LIKE (AIL) AP2/ERF and directly regulates all LAFL genes. *LAFL* genes are also regulated by a BBM-like protein, PLT2 (Horstman et al., 2017). The *LAFL* gene group consists of the *LEC* transcription factor genes, including *LEC1*, *LEC2*, and *FUSCA3* (*FUS3*), and the ABA signaling transcription factor, ABSCISIC ACID INSENSITIVE 3 (ABI3). Somatic embryogenesis events are shown to significantly decrease in *lec* mutants (Gaj et al., 2005), and the overexpression of *LEC2* led to an increase in the expression of auxin biosynthesis genes *IAA30*, *YUC2*, *YUC4*, and *YUC10* (Stone et al., 2008; Junker et al., 2012), suggesting that *LEC* genes and the LAFL complex help promote auxin activity. LEC2 also induces the expression of *LEC1*, *LEAFY COTYLEDON 1-LIKE (L1L)*, *ABI3*, and *FUS3*. Another transcription factor, AGL15, has been shown to directly regulate *LAFL* (Zheng et al., 2009) and promote the expression of the AP2/ERF gene *At5g61590* (Zheng et al., 2013). *At5g61590* is a relative of the *Medicago truncatula SOMATIC EMBRYO-RELATED FACTOR 1* (*MtSERF1*), which is essential for somatic embryogenesis (Mantiri et al., 2008). Recently, another MADS-box transcription factor, AGL18, was identified as an active regulator in somatic embryogenesis in *Arabidopsis* (Paul et al., 2022). Overexpression of *AGL18* resulted in an increase in somatic embryogenesis, while a decrease was observed in *agl18* mutants; *agl15 agl18* double mutants resulted in even less frequent development of somatic embryos. While the functions of AGL15 and AGL18 transcription factors were relatively redundant, different gene targets for each transcription factor were present and an AGL15/AGL18 regulatory loop was identified. This provides evidence that AGL18 may act in conjunction with AGL15 during somatic embryogenesis. Along with *BBM*, *LAFL*, and *AGL15*, the ectopic expression of *WUS*, *PLT4*/*BBM*, *PLT5*/*EMBRYMAKER*, *MYB118*, and *RWP-RK DOMAIN-CONTAINING4* (*RKD4*)/*GROUNDED* (*GRD*) leads to the induction of somatic embryogenesis in *Arabidopsis* (Lotan et al., 1998; Boutilier et al., 2002; Harding et al., 2003; Gallois et al., 2004; Waki et al., 2011).

The master regulators work with other transcription factors to balance auxin, gibberellin (GA), and abscisic acid (ABA) signaling. In particular, the balance of GA and ABA has a major role in controlling cell identity in the developing embryo. Embryonic cells have been shown to have a higher ratio of GA to ABA than somatic cells (Yamaguchi et al., 2001; Mitchum et al., 2006; Hu et al., 2008). The LAFL transcription factors, LEC1, LEC2, FUS3, and AGL15, downregulate GA biosynthesis genes (Curaba et al., 2004; Zheng et al., 2009), while FUS3 positively regulates the ABA pathway (Gazzarrini et al., 2004). LEC1 and LEC2 promote the expression of auxin biosynthesis genes (Braybrook et al., 2006; Junker et al., 2012), and AGL15 negatively regulates the auxin response genes, *ARF6*, *ARF8*, and *TRANSPORT INHIBITOR RESPONSE1* (*TIR1*) (Zheng et al., 2016). LEC1 and AGL15 positively regulate *ABI3*. Generally, these transcription factors work to negatively regulate GA biosynthesis and positively regulate ABA and auxin biosynthesis, transitioning cells from embryonic cells (high GA/ABA ratios) into differentiated somatic cells (low GA/ABA ratios). MYB-family transcription factors, MYB118 and MYB115, also play important roles in somatic embryogenesis. These transcription factors promote the expression of *LEC1*; overexpression of both resulted in the formation of somatic embryos on root explants (Wang et al., 2008). The micro RNA miR396 is associated with somatic embryogenesis induction and helps control *PLT1* and *PLT2* (Szczygieł-Sommer and Gaj, 2019). Other evidence suggests that AGL15 forms protein complexes with SOMATIC EMBRYOGENESIS RECEPTOR-LIKE KINASES (SERKs), which are induced in response to auxin (Zheng et al., 2009). Ethylene has also been shown to impact somatic embryogenesis because interactions between ETHYLENE RESPONSE FACTOR 002 (ERF022) and LEC2, and the involvement of other AP2/ERF transcription factors have been observed (Zheng et al., 2013; Xu and Huang, 2014; Horstman et al., 2017). Reprogramming of somatic cells to form embryos and then back to differentiated somatic cells requires multiple hormone signaling pathways to work together.

Genomic DNA methylation patterns change during development. In mature tissues, *LEC1*, *LEC2*, and *AGL15* are hypermethylated in somatic cells, while hypomethylation has been seen of similar genes (e.g., *SERKs*, *LEC2*, *WUS)* in embryonic calli (Fraga et al., 2012). This suggests that somatic embryogenesis and genes involved in embryonic cell to somatic cell transition is subject to epigenetic regulation as the repression of embryonic genes leads to the development of mature and differentiated tissues. There is conflicting evidence for the role of DNA methylation in somatic embryogenesis. In some studies, the demethylation agent 5-azacitidine strongly inhibited embryogenesis in *Medicago truncatula* and *Arabidopsis* (Santos and Fevereiro, 2002; Grzybkowska et al., 2018), while in other plants, such as in *Coco nucifera* and *Acca sellowiana*, its application increased embryogenesis (Fraga et al., 2012; Osorio-Montalvo et al., 2020). This suggests that differential DNA methylation is required for successful somatic embryogenesis but its effects are highly genotype and species dependent.

Two critical regulatory epigenetic pathways, PcG and PKL, are involved in the epigenetic regulation of genes during somatic embryogenesis. As in shoot organogenesis, the PRC2-mediated H3K27 methylation, part of the PcG pathway, is involved in the repression of *LEC1*, *LEC2*, and *FUS3*, aiding in the transition from embryonic to somatic cells (Makarevich et al., 2006). The Repressive LEC2 Element (RLE) in the *LEC2* promoter recruits PCR2 for methylation and repression of *LEC2* in somatic cells (Berger et al., 2011). Evidence supporting this includes an increase in somatic embryogenesis of *Arabidopsis* in vegetative tissue depleted of PRC2 (Mozgová et al., 2017). PRC2 has also been shown to negatively regulate other important regulators of plant regeneration including WOX5, WOX11, WUS, and STM. PKL encodes for a chromatin remodeling factor, which serves to rearrange nucleosome positions in order to regulate gene expression. Multiple studies have demonstrated that *pkl* mutants

show an increase in the ectopic expression of *LEC1*, *LEC2*, and *FUS3*, resulting in embryonic traits in somatic tissues (Ogas et al., 1997; Henderson et al., 2004). This suggests that PKL plays a role in negatively regulating embryonic genes in somatic tissues. However, the specific molecular mechanism by which PKL works is still unclear.

Small Signaling Peptides in Plant Regeneration

Signaling peptides are important players in plant development. One family of signaling peptides, CLAVATA/ENDOSPERM SURROUNDING REGION (CLE), has central roles in modulating stem cell differentiation during plant growth and development (Katsir et al., 2011). These peptides are post-translationally processed and contain a signal peptide targeting the protein for secretion, where it is used for cell-to-cell communication (Yamaguchi et al., 2016). In *A. thaliana*, there are 32 CLE peptides including CLV1, CLV2, and CLV3. CLV3 is secreted from cells and interacts with CLV1, a leucine-rich repeat receptor kinase, to maintain stem cell populations in the apical meristem (Clark et al., 1995; Hirakawa et al., 2008). In *clv1* and *clv3* mutants, plants develop enlarged shoot and floral apical meristems, suggesting improper signaling disruption to maintenance of stem cell populations (Clark et al., 1995). *WUS* promotes cell proliferation and division and upregulates *CLV1-CLV3*. This results in the downregulation of *WUS* by CLV1-CLV3 in a negative feedback loop. This feedback mechanism produces and maintains a constant stem cell pool (Mayer et al., 1998; Brand et al., 2000). Manipulating either WUS, CLV1, and/or CLV3 could lead to larger stem cell pools and greater potential for cell division. This in conjunction with downstream molecular players, such as *CUC* genes, *PLT* genes, or *SPL*, and could potentially lead to more and faster plant regeneration. However, this would require careful orchestration of the key regulators.

Growth Regulating Factors as Agents for Increased Regeneration

Growth Regulating Factors (GRF) are a transcription factor family that regulates many aspects of plant growth and development including leaf, stem, root, seed development, flowering, regulation of stress, and plant longevity. The first GRF, Os-*GRF1*, was identified two decades ago during a differential expression study of responses of deep-water rice to GA (van der Knaap et al., 2000). GRFs have now been identified in many plant species, where typically 8–20 different GRF genes are present in each genome (Omidbakhshfard et al., 2015). GRFs form complexes with their cofactor, GRF-interacting Factors (GIF), and will bind to *cis*-regulatory elements of different developmental genes in plants (Kim, 2019). For example, *AtGRF7* binds to the promoter of the AP2/ERF gene *Dehydration responsive element binding protein2A* (*DREB2A*) and represses gene expression in leaf veins (Kim et al., 2012). In *Arabidopsis, GRFs* have been shown to be expressed in leaf and root tissue where prolific cell growth is occurring and tend to decrease with plant age (Kim et al., 2003; Lee et al., 2009; Hewezi et al., 2012; Szczygieł-Sommer and Gaj, 2019).

GRF proteins are post-transcriptionally regulated by miR396 throughout the course of plant development; miR396 recognizes and binds to GRF, resulting in degradation or translational arrest. Expression of miR396 occurs at low levels in leaf primordia that gradually increase throughout organ development and maturity (Rodriguez et al., 2010). Expression of *AtGRF2* is restricted to specific portions of the leaf during development through antagonistic expression of *miR396* (Rodriguez et al., 2010). In rice, *miR396* mutants resulted in an upregulation of multiple *GRF* genes, in particular *GRF3*. These mutants also produced plants with longer leaves and shorter internodes (Miao et al., 2020). Because of their involvement in organ development, GRF and miR396 are potential targets for increasing *in vitro* regeneration.

GRFs regulate players important for *in vitro* regeneration. GRF proteins from rice, OsGRF3 and OSGRF10 repress promoter activity of a KNOX gene, *Oskn2* (Kuijt et al., 2014). In the same study, barley GRF, BGRF1, repressed *Hooded/Bkn3*, a barley KNOX gene, and overexpression of *OsGRF10*, *AtGRF4*, *AtGRF5*, and *AtGRF6* repressed activity of *KNAT2* in *Arabidopsis*. In addition, overexpression of *OsGRF3* and *OsGRF10* induced root and shoot formation on primary tillers of rice (Kuijt et al., 2014). Because regulation of *KNOX* genes is necessary for cell identity transitions from meristem cells to mature organ cells (Hake et al., 1995, 2004; Tsuda et al., 2011), the reported functions of these GRFs demonstrate the potential importance of GRFs in both organogenesis and somatic embryogenesis. An RNA-seq study in rice showed upregulation of *OsGRF6* resulted in an increase in expression of the auxin biosynthesis gene, *OsYUCCA-like*, and signaling genes, *OsARF2*, *OsARF7*, *OsARF11* (Gao et al., 2015). In addition, altered expression of *GRF* and *GIF* affect root growth through regulation of *PLT1*, *PLT2*, and *SCR* (Ercoli et al., 2018). In Arabidopsis, the double mutant *gif1/an3 gif2* and the triple mutant *gif1/an3 gif2 gif3* both showed the formation of a disorganized QC and larger RAM, while overexpression of *GRF3* with a mutated miRNA binding site (*rGRF3*) resulted in smaller meristems (Ercoli et al., 2018). These studies provide evidence that GRFs and GIFs are upstream regulators of molecular determinants involved in callus formation and shoot meristem identity, giving altered expression of GRFs and GIFs the potential to increase regeneration in plants.

GRFs and GIFs have now been shown to enhance regeneration capacity and rates in plants. Ectopic expression of *AtGRF5* and orthologs increased callus production in canola and shoot organogenesis in sugar beet, soybean, and sunflower; also, ectopic expression of the maize *GRF5* ortholog increased formation of embryogenic calli indicating that GRFs regulate multiple *in vitro* regeneration pathways (Kong et al., 2020). In addition, transformation with a chimeric *GRF-GIF* gene fusion can increase the rate and number of regenerates in wheat, rice, and citrus (Debernardi et al., 2020). Independent transformations and co-transformations of multiple wheat *GRF*s fused with *GIF*s were studied including *GRF4*, *GRF5*, *GIF1*, *GIF2*, and *GIF3*; the chimeric transgene composed of a fusion between GRF4 and GIF1 (GRF4-GIF1) resulted in the highest frequency of regeneration in wheat among all combinations of GRFs and GIFs tested. In addition to increased regeneration, shoot regeneration and transgenesis in wheat was successful without the use of

cytokinins in the culture medium. Furthermore, regeneration could be induced from leaf explants rather than immature embryos. The efficacy of chimeric transgene was also tested in the dicotyledonous species, *Citrus*, using the *Citrus* and *Vitis* GRF4 and GIF1 homologs (Debernardi et al., 2020). Furthermore, the use of the microRNA insensitive *rGRF4-GIF* resulted in greater stimulation of regeneration in wheat, rice, and *Citrus*. This is a major breakthrough and will be exploited for the regeneration of recalcitrant species and cultivars, leading to a likelihood of higher transformation rates.

PROSPECTS FOR ENHANCED REGENERATION IN LETTUCE

Synopsis of Studies on the Regeneration of Lettuce

Lettuce, *Lactuca sativa* L. (Compositae), is a dicotyledonous plant that can be regenerated by indirect *de novo* shoot organogenesis (**Figure 4**) and was a model for early studies of regeneration (reviewed in Michelmore and Eash, 1985). Some genotypes regenerate readily on a variety of media formulations and growth regulators; however, some lettuce genotypes are recalcitrant to regeneration. Lettuce is also amenable to *Agrobacterium*-mediated transformation (Michelmore et al., 1987). Protocols for high efficiency, genotype-independent regeneration of lettuce are required in order to fully benefit from biotechnological approaches, including genome editing, for crop improvement. Given differences in regeneration rates of different genotypes and the wealth of knowledge from model species described above, top-down and bottom-up approaches to the molecular basis of regeneration in lettuce could lead to protocols for enhanced regeneration of multiple genotypes.

Lettuce regeneration has been studied for many decades. Lettuce was among the first plants to be tested for regeneration. The first studies on *in vitro* regeneration of lettuce failed to produce shoots from leaves of *L. sativa* and *L. canadensis* (LaRue, 1933, 1936). Later, regeneration of lettuce shoots was successful with the addition of adenine and kinetin to the growth medium (Doerschug and Miller, 1967). In this study, the regenerative capability of hypocotyl, cotyledon, and mature leaf explants was tested on the same base medium with different combinations of IAA, kinetin, and adenine, and cotyledons were shown to be the most effective explant source for shoot regeneration. In the same study, kinetin was effective at promoting the transition from callus formation to shoot regeneration (Doerschug and Miller, 1967). This suggested that in lettuce, as shown in other plant species, high levels of cytokinin promotes the formation of shoot meristems that results from the transition of cell fate from root-like callus cells to shoot cells. Later studies focused on the optimization of factors influencing lettuce regeneration, including media formulations, plant growth regulator use, light requirements, temperature, explant type, and genotype (Doerschug and Miller, 1967; Kadkade and Seibert, 1977; Koevary, 1978; Sasaki, 1979, 1982; Alconero, 1983; Webb et al., 1984; Michelmore and Eash, 1985). Light intensity and photoperiod were shown to be also important for lettuce regeneration; cotyledon explants developed well-formed shoots with a 16-h photoperiod but significantly fewer shoots formed in the dark; additionally, the presence of red light doubled the number of buds and shoots (Kadkade and Seibert, 1977). In aggregate, callus formation occurred on all lettuce cultivars studied when using both auxins and cytokinins in the culture medium, although there were differences between genotypes. Shoot regeneration was elicited when the medium contained cytokinins with little or no auxins. Although mature leaves and hypocotyls showed regenerative capabilities, cotyledons were the most amenable explant source for regeneration.

Indirect *de novo* shoot organogenesis in lettuce involves cell divisions of spongy, palisade, and epidermal cells. A cytohistological study of adventitious bud formation from cotyledon explants revealed initial divisions of spongy and palisade cells followed by divisions of epidermal cells to form tetrads (Nuti Ronchi and Gregorini, 1970). Callus was formed from the division of mesophyll cells and inward proliferation of epidermal cells. Subsequently, adventitious buds arose from one or two epidermal cells, which led to the formation and organization of shoot apical meristems. This study provided the timeline and steps that occur during organogenesis; however, the tools were not available to study the underlying genetic and molecular constituents responsible for the changes in cell anatomy and transition of cell fate, particularly epidermal cells to meristematic centers.

Like most plant species, regenerative capacity is highly dependent on genotype and there is considerable variation in regenerative capacity among lettuce cultivars (Michelmore et al., 1987; Curtis et al., 1994; Ampomah-Dwamena et al., 1997; Mohebodini et al., 2011). There is no significant correlation to regeneration efficiency and morphological group (i.e., crisphead, butterhead, cos, and leaf). In a side-by-side study, highly regenerating genotypes included Bambino (crisphead), Iceberg (crisphead), Cobham Green (butterhead), Sweet Butter (butterhead), Simpson Elite (leaf), Rosalita (cos), and Paris White (cos); recalcitrant genotypes included Oak Leaf (leaf), Royal Oak Leaf (leaf), Sangria (crisphead), and Mainspring (butterhead) (Ampomah-Dwamena et al., 1997). Generation of stable transgenics of lettuce relies on *Agrobacterium*-mediated transformation and *in vitro* regeneration. Therefore, it is important to understand and identify the genetic and molecular players to increase regeneration in order to manipulate recalcitrant lettuce varieties.

Known Molecular Determinants for Regeneration in Lettuce

There have been few studies on the molecular determinants of regeneration in lettuce. A dominant mutation of the ethylene receptor ETR1-1 was shown to inhibit shoot regeneration in lettuce (Kim and Botella, 2004). Lettuce cultivars LEI26 and Seagreen were transformed using *Agrobacterium*-mediated transformation for the introduction of GUS under the control of the CaMV 35S constitutive promoter and the mutated ethylene receptor *etr1-1* under the control of a leaf senescence-specific

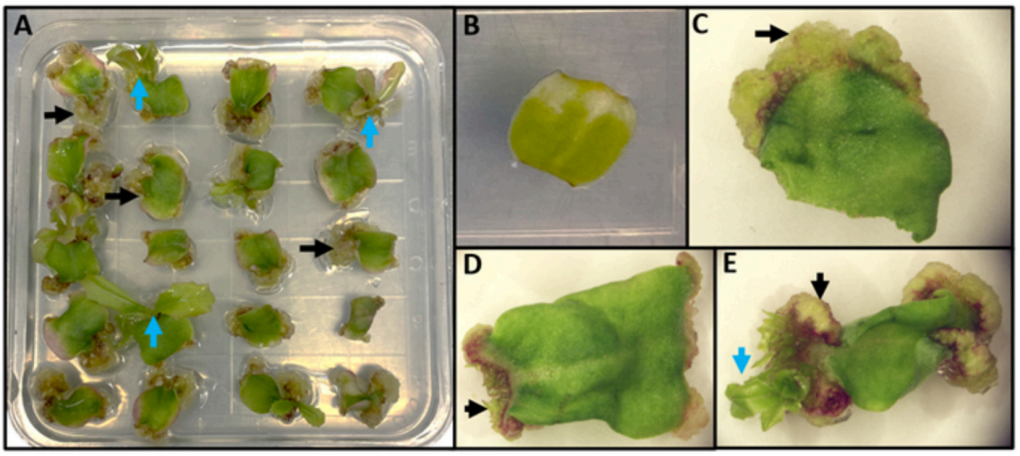


FIGURE 4 | Representation of indirect *de novo* shoot organogenesis in lettuce. **(A)** A plate of 20 explants undergoing indirect *de novo* shoot regeneration. Black arrows represent friable callus formation at the wounded end of explants; blue arrows represent shoot regeneration from calli. **(B)** An explant before callus formation. **(C)** An explant during callus formation (black arrow). **(D)** First organized growth from callus (black arrow). **(E)** Indirect shoot regeneration (blue arrow) from callus (black arrow).

promoter, *sag12*. Transformations with 35S:GUS showed high regenerative potential with 85% of explants developing shoots, while the introduction of *sag12:etr1-1* significantly reduced regenerative potential with only 2.86% of explants producing shoots. Explants transformed with *sag:etr1-1* also stimulated root formation directly from cotyledon explants without the formation of callus (Kim and Botella, 2004). This suggests that ethylene responses are important in *in vitro* lettuce regeneration in which inhibiting ethylene receptors promotes root formation and inhibits callus and shoot formation. This is consistent with observations of other ethylene response factors during *in vitro* regeneration, such as the early expression of AP2/ERF transcription factors during callus formation and the involvement of ERF022 activity during somatic embryogenesis (Iwase et al., 2011a,b; Zheng et al., 2013; Xu and Huang, 2014; Horstman et al., 2017).

Data is limited for lettuce on the effects of the pathways and molecular determinants described in other species. A recent study examined the chronological expression of homeobox genes during *in vitro* regeneration of lettuce (Farina et al., 2021). Gene expression profiles of lettuce homologs to the homeobox WOX family transcription factor genes *WUS* (*LsWUS1L* and *LsWUS2L*) and the KNOTTED1-LIKE homeobox family transcription factor gene *ST-M* (*LsSTM*), were examined in cotyledon explants over 12 days on inductive medium. A time course analysis showed a steady increase of expression of *LsWUS1*; in early days of culture, increased expression of *LsWUS2L* correlated with the formation of poorly vacuolated cells with large nuclei in the explants. Expression of *LsSTM1L* also drastically increased in early days of culture, followed by a later decrease, suggesting that it helps recruit proteins and regulates expression of genes needed for the initiation of regeneration in lettuce (Farina et al., 2021). This parallels patterns of *WUS* and *STM* expression observed early in plant regeneration, specifically during the formation of shoot promeristems and meristematic centers from callus in *Arabidopsis* (Daimon et al., 2003; Zhang et al., 2017). This is also consistent with the essential role WUS plays in maintaining the stem cell pool that is critical for proper SAM function (Sarkar et al., 2007). The CCAAT-binding transcription factors, *LEC1* and *LEC2*, play a major role in development and maturation of embryos (see sections "Embryogenic Callus Formation and Somatic Embryogenesis"). Nothing has been reported for homologs of *LEC1* and *LEC2* in lettuce. It would be interesting to overexpress homologs of these transcription factors in lettuce to determine if this results in enhanced regeneration as in *Arabidopsis*, tobacco, and cassava (Gaj et al., 2005; Guo et al., 2013; Brand et al., 2019). Similarly, over-expression of *CUC1* and *CUC2* as well as *PLT* genes (see sections "Organogenic Callus Formation, *De novo* Root Organogenesis, and *De novo* Shoot Organogenesis") may also result in enhanced regeneration of lettuce as in Arabidopsis (Ikeda et al., 2006; Matsuo et al., 2009; Kareem et al., 2015).

MADS-Box Genes in Lettuce

MADS-box transcription factors, particularly AGL15 and AGL18, are major molecular players involved in *in vitro* regeneration (see sections "Embryogenic Callus Formation and Somatic Embryogenesis"). There are at least 82 MADS-box encoding genes in lettuce (Ning et al., 2019), most of which have been studied in relation to flowering time and floral development (reviewed in Han et al., 2021). Of these 82 genes, 23 encoded for M-type genes of the type 1 lineage and 59 floral genes of the type II lineage containing a MIKC domain. Within the type II MADs-box genes, 10 belonged to the *AGL15* subfamily which contained homologs of Arabidopsis and tomato *AGL15* genes. Currently, no work has been reported on the role of lettuce MADs-box genes during *in vitro* regeneration. The 10 genes identified in the *AGL15* subfamily should be characterized for their roles in regeneration in lettuce; it should be tested

whether over expression of ALG15 results in increased somatic embryogenesis as in *Arabidopsis* (Paul et al., 2022).

Growth Regulating Factors in Lettuce

There are 15 *GRF* genes in lettuce and their chromosomal locations, gene structure, conserved motifs, and expression patterns have been characterized (Zhang et al., 2021). One *GRF* gene was studied in detail. *LsaGRF5* showed low expression in leaves and roots with high expression in reproductive buds, suggesting an important function in flower development. The GRF regulator, *miR396a*, had high expression in mature flowers and stems and low expression in reproductive buds. These data suggest that high levels of *LsaGRF5* expression in young tissues is coincident with actively dividing cells; as the cells and tissues mature, *LsaGRF5* becomes downregulated by *miR396a*; this is similar to what is observed in other species (see section "Growth Regulating Factors as Agents for Increased Regeneration"). Furthermore, overexpression of *LsaGRF5* resulted in larger leaf size, while overexpression of miR396a resulted in smaller leaf size (Zhang et al., 2021). However, none of the 15 *GRF* genes have been characterized for their effects on regeneration in lettuce. Given the success of GRF or GRF-GIF fusions with other species (see section "Growth Regulating Factors as Agents for Increased Regeneration"), it is likely that similar enhanced rates of regeneration and transformation will be reported soon.

CONCLUSION AND FUTURE PERSPECTIVES

The underlying processes of plant regeneration all involve cell fate transition by reprogramming gene expression. The several pathways involved in plant development and regeneration are complex. Although each pathway has unique molecular players, many of the key regulators overlap and have important functions in each. Auxin and cytokinin signaling pathways play a major role in regulating multiple regenerative pathways and accompany the genome-wide switch in gene expression profile during the early stages of regeneration. Other phytohormones, such as GA, ABA, and ethylene, also contribute to plant regeneration and cell fate transition.

Many of the players and regulators important for *in vitro* regeneration have been studied in model species, such as *Arabidopsis,* but have not been functionally characterized in non-model species such as lettuce. The complete genome sequence of *L. sativa* (Reyes-Chin-Wo et al., 2017) has provided useful genic targets for modification by genome editing. Currently, genome editing of lettuce requires *Agrobacterium*-mediated transformation, which requires *in vitro* regeneration; therefore, studying molecular determinants and understanding pathways controlling regeneration in lettuce has great value. Identifying orthologs of genes discussed in this review and then characterizing them in other systems, such as lettuce, will help form a more generalized understanding of *in vitro* regeneration in plants. Further studies on identification of recalcitrant varieties, quantitative trait locus analyses on varieties with varying regenerative capabilities, and expression profiles during *in vitro* regeneration could provide insight into other genes regulated during *in vitro* regeneration of lettuce. Understanding these pathways in lettuce will allow for a better understanding of the pathways in other important crops, particularly within the Compositae family such as sunflower, artichoke, safflower, and many ornamentals.

AUTHOR CONTRIBUTIONS

RM and TB conceived the idea for the manuscript. TB conducted the literature review and drafted the manuscript and figures. Both authors reviewed the final manuscript and approved submission.

FUNDING

This work was supported the USDA NIFA Specialty Crop Research Initiative (SCRI) (Grant Nos. 2015-51181-24283 and 2021-51181-35903) to RM.

ACKNOWLEDGMENTS

We would like to thank Allen Van Deynze for providing input and Elizabeth Georgian for assistance in editing this manuscript.

REFERENCES

Aida, M., Beis, D., Heidstra, R., Willemsen, V., Blilou, I., Galinha, C., et al. (2004). The PLETHORA genes mediate patterning of the *Arabidopsis* root stem cell niche. *Cell* 119, 109–120. doi: 10.1016/j.cell.2004.09.018

Alconero, R. (1983). Regeneration of plants from cell suspensions of *Lactuca saligna*, *Lactuca sativa*, and *Lactuca serriola*. *HortScience* 18, 305–307.

Ampomah-Dwamena, C., Conner, A. J., and Fautrier, A. G. (1997). Genotypic response of lettuce cotyledons to regeneration in vitro. *Sci. Horticult.* 71, 137–145. doi: 10.1016/s0304-4238(97)00098-8

Atta, R., Laurens, L., Boucheron-Dubuisson, E., Guivarc'h, A., Carnero, E., Giraudat-Pautot, V., et al. (2009). Pluripotency of *Arabidopsis* xylem pericycle underlies shoot regeneration from root and hypocotyl explants grown in vitro. *Plant J.* 57, 626–644. doi: 10.1111/j.1365-313X.2008.03715.x

Banno, H., Ikeda, Y., Niu, Q.-W., and Chua, N.-H. (2001). Overexpression of *Arabidopsis* ESR1 induces initiation of shoot regeneration. *Plant Cell* 13:2609. doi: 10.1105/tpc.010234

Berger, N., Dubreucq, B., Roudier, F., Dubos, C., and Lepiniec, L. (2011). Transcriptional regulation of *Arabidopsis* LEAFY COTYLEDON2 Involves RLE, a cis-element that regulates trimethylation of histone H3 at lysine-27. *Plant Cell* 23:4065. doi: 10.1105/tpc.111.087866

Bouchabké-Coussa, O., Obellianne, M., Linderme, D., Montes, E., Maia-Grondard, A., Vilaine, F., et al. (2013). Wuschel overexpression promotes somatic embryogenesis and induces organogenesis in cotton (*Gossypium hirsutum* L.) tissues cultured in vitro. *Plant Cell Rep.* 32, 675–686. doi: 10.1007/s00299-013-1402-9

Boutilier, K., Offringa, R., Sharma, V. K., Kieft, H., Ouellet, T., Zhang, L., et al. (2002). Ectopic expression of BABY BOOM triggers a conversion from

vegetative to embryonic growth. *Plant Cell* 14, 1737–1749. doi: 10.1105/tpc.001941

Bowman, J. L., and Eshed, Y. (2000). Formation and maintenance of the shoot apical meristem. *Trends Plant Sci.* 5, 110–115. doi: 10.1016/s1360-1385(00)01569-7

Brand, A., Quimbaya, M., Tohme, J., and Chavarriaga-Aguirre, P. (2019). *Arabidopsis* LEC1 and LEC2 orthologous genes are key regulators of somatic embryogenesis in cassava. *Front. Plant Sci.* 10:673. doi: 10.3389/fpls.2019.00673

Brand, U., Fletcher, J. C., Hobe, M., Meyerowitz, E. M., and Simon, R. (2000). Dependence of stem cell fate in *Arabidopsis* on a feedback loop regulated by CLV3 activity. *Science* 289, 617–619. doi: 10.1126/science.289.5479.617

Braybrook, S. A., Stone, S. L., Park, S., Bui, A. Q., Le, B. H., Fischer, R. L., et al. (2006). Genes directly regulated by LEAFY COTYLEDON2 provide insight into the control of embryo maturation and somatic embryogenesis. *Proc. Natl. Acad. Sci. U.S.A.* 103, 3468–3473. doi: 10.1073/pnas.0511331103

Buechel, S., Leibfried, A., To, J. P. C., Zhao, Z., Andersen, S. U., Kieber, J. J., et al. (2010). Role of A-type ARABIDOPSIS RESPONSE REGULATORS in meristem maintenance and regeneration. *Eur. J. Cell Biol.* 89, 279–284. doi: 10.1016/j.ejcb.2009.11.016

Bustillo-Avendaño, E., Ibáñez, S., Sanz, O., Sousa Barros, J. A., Gude, I., Perianez-Rodriguez, J., et al. (2018). Regulation of hormonal control, cell reprogramming, and patterning during de novo root organogenesis. *Plant Physiol.* 176, 1709–1727. doi: 10.1104/pp.17.00980

Casamitjana-Martínez, E., Hofhuis, H. F., Xu, J., Liu, C. M., Heidstra, R., and Scheres, B. (2003). Root-specific CLE19 overexpression and the so1l/2 suppressors implicate a CLV-like pathway in the control of *Arabidopsis* root meristem maintenance. *Curr. Biol.* 13, 1435–1441. doi: 10.1016/s0960-9822(03)00533-5

Choffe, K. L., Victor, J. M. R., Murch, S. J., and Saxena, P. K. (2000). In vitro regeneration of *Echinacea purpurea* L.: direct somatic embryogenesis and indirect shoot organogenesis in petiole culture. In Vitro Cell. *Dev. Biol. Plant* 36, 30–36. doi: 10.1007/s11627-000-0008-4

Chokheli, V. A., Dmitriev, P. A., Rajput, V. D., Bakulin, S. D., Azarov, A. S., Varduni, T. V., et al. (2020). Recent development in micropropagation techniques for rare plant species. *Plants* 9:1733. doi: 10.3390/plants9121733

Clark, S. E., Running, M. P., and Meyerowitz, E. M. (1995). CLAVATA3 is a specific regulator of shoot and floral meristem development affecting the same processes as CLAVATA1. *Development* 121, 2057–2067. doi: 10.1242/dev.121.7.2057

Curaba, J., Moritz, T., Blervaque, R., Parcy, F., Raz, V., Herzog, M., et al. (2004). AtGA3ox2, a key gene responsible for bioactive gibberellin biosynthesis, is regulated during embryogenesis by LEAFY COTYLEDON2 and FUSCA3 in *Arabidopsis*. *Plant Physiol.* 136, 3660. doi: 10.1104/pp.104.047266

Curtis, I. S., Power, J. B., Blackhall, N. W., de Laat, A. M. M., and Davey, M. R. (1994). Genotype-independent transformation of lettuce using *Agrobacterium tumefaciens*. *J. Exp. Bot.* 45, 1441–1449. doi: 10.1093/jxb/45.10.1441

Dai, X., Liu, Z., Qiao, M., Li, J., Li, S., and Xiang, F. (2017). ARR12 promotes de novo shoot regeneration in *Arabidopsis thaliana* via activation of WUSCHEL expression. *J. Integr. Plant Biol.* 59, 747–758. doi: 10.1111/jipb.12567

Daimon, Y., Takabe, K., and Tasaka, M. (2003). The CUP-SHAPED COTYLEDON genes promote adventitious shoot formation on calli. *Plant Cell Physiol.* 44, 113–121. doi: 10.1093/pcp/pcg038

de Almeida, M., Vieira De Almeida, C., Mendes, E., Gilvano, G., Brondani, E., and Fiori De Abreu-Tarazi, M. (2012). Pre-procambial cells are niches for pluripotent and totipotent stem-like cells for organogenesis and somatic embryogenesis in the peach palm: a histological study. *Plant Cell Rep.* 31, 1495–1515. doi: 10.1007/s00299-012-1264-6

de Smet, I., Vassileva, V., de Rybel, B., Levesque, M. P., Grunewald, W., van Damme, D., et al. (2008). Receptor-like kinase ACR4 restricts formative cell divisions in the *Arabidopsis* root. *Science* 322, 594–597. doi: 10.1126/science.1160158

Debernardi, J. M., Tricoli, D. M., Ercoli, M. F., Hayta, S., Ronald, P., Palatnik, J. F., et al. (2020). A GRF–GIF chimeric protein improves the regeneration efficiency of transgenic plants. *Nat. Biotechnol.* 38, 1274–1279. doi: 10.1038/s41587-020-0703-0

DiDonato, R. J., Arbuckle, E., Buker, S., Sheets, J., Tobar, J., Totong, R., et al. (2004). *Arabidopsis* ALF4 encodes a nuclear-localized protein required for lateral root formation. *Plant J.* 37, 340–353. doi: 10.1046/j.1365-313x.2003.01964.x

Doerschug, M. R., and Miller, C. O. (1967). Chemical control of adventitious organ formation in *Lactuca sativa* explants. *Am. J. Bot.* 54, 410–413. doi: 10.1002/j.1537-2197.1967.tb10658.x

Durgaprasad, K., Roy, M. V., Venugopal M, A., Kareem, A., Raj, K., Willemsen, V., et al. (2019). Gradient expression of transcription factor imposes a boundary on organ regeneration potential in plants. *Cell Rep.* 29, 453–463.e3. doi: 10.1016/j.celrep.2019.08.099

Elhiti, M., and Stasolla, C. (2022). Transduction of signals during somatic embryogenesis. *Plants* 11:178. doi: 10.3390/plants11020178

Emery, J. F., Floyd, S. K., Alvarez, J., Eshed, Y., Hawker, N. P., Izhaki, A., et al. (2003). Radial patterning of *Arabidopsis* shoots by class III HD-ZIP and KANADI genes. *Curr. Biol.* 13, 1768–1774. doi: 10.1016/j.cub.2003.09.035

Ercoli, M. F., Ferela, A., Debernardi, J. M., Perrone, A. P., Rodriguez, R. E., and Palatnik, J. F. (2018). GIF transcriptional coregulators control root meristem homeostasis. *Plant Cell* 30, 347–359. doi: 10.1105/tpc.17.00856

Fan, M., Xu, C., Xu, K., and Hu, Y. (2012). LATERAL ORGAN BOUNDARIES DOMAIN transcription factors direct callus formation in *Arabidopsis* regeneration. *Cell Res.* 22, 1169–1180. doi: 10.1038/cr.2012.63

Farina, P., Fambrini, M., Pugliesi, C., and Viviani, A. (2021). Expression of homeobox genes during in vitro culture of *Lactuca sativa*. *Plant Biosyst.* 155, 609–621. doi: 10.1080/11263504.2020.1762793

Fehér, A. (2019). Callus, dedifferentiation, totipotency, somatic embryogenesis: what these terms mean in the era of molecular plant biology? *Front. Plant Sci.* 10:536. doi: 10.3389/fpls.2019.00536

Feng, Z., Zhu, J., Du, X., and Cui, X. (2012). Effects of three auxin-inducible LBD members on lateral root formation in *Arabidopsis thaliana*. *Planta* 236, 1227–1237. doi: 10.1007/s00425-012-1673-3

Filipecki, M. K., Sommer, H., and Malepszy, S. (1997). The MADS-box gene CUS1 is expressed during cucumber somatic embryogenesis. *Plant Sci.* 125, 63–74. doi: 10.1016/s0168-9452(97)00056-3

Fraga, H. P. F., Vieira, L. N., Caprestano, C. A., Steinmacher, D. A., Micke, G. A., Spudeit, D. A., et al. (2012). 5-Azacytidine combined with 2,4-D improves somatic embryogenesis of *Acca sellowiana* (O. Berg) Burret by means of changes in global DNA methylation levels. *Plant Cell Rep.* 31, 2165–2176. doi: 10.1007/s00299-012-1327-8

Fukaki, H., Tameda, S., Masuda, H., and Tasaka, M. (2002). Lateral root formation is blocked by a gain-of-function mutation in the SOLITARY-ROOT/IAA14 gene of *Arabidopsis*. *Plant J.* 29, 153–168. doi: 10.1046/j.0960-7412.2001.01201.x

Gaj, M. D., Zhang, S., Harada, J. J., and Lemaux, P. G. (2005). Leafy cotyledon genes are essential for induction of somatic embryogenesis of *Arabidopsis*. *Planta* 222, 977–988. doi: 10.1007/s00425-005-0041-y

Galinha, C., Hofhuis, H., Luijten, M., Willemsen, V., Blilou, I., Heidstra, R., et al. (2007). PLETHORA proteins as dose-dependent master regulators of *Arabidopsis* root development. *Nature* 449, 1053–1057. doi: 10.1038/nature06206

Gallois, J.-L., Nora, F. R., Mizukami, Y., and Sablowski, R. (2004). WUSCHEL induces shoot stem cell activity and developmental plasticity in the root meristem. *Genes Dev.* 18, 375–380. doi: 10.1101/gad.291204

Gallois, J.-L., Woodward, C., Reddy, G. V., and Sablowski, R. (2002). Combined SHOOT MERISTEMLESS and WUSCHEL trigger ectopic organogenesis in *Arabidopsis*. *Development* 129, 3207–3217. doi: 10.1242/dev.129.13.3207

Gao, F., Wang, K., Liu, Y., Chen, Y., Chen, P., Shi, Z., et al. (2015). Blocking miR396 increases rice yield by shaping inflorescence architecture. *Nat. Plants* 2:15196. doi: 10.1038/nplants.2015.196

Gardiner, J., Donner, T. J., and Scarpella, E. (2010). Simultaneous activation of SHR and ATHB8 expression defines switch to preprocambial cell state in *Arabidopsis* leaf development. *Dev. Dyn.* 240, 261–270. doi: 10.1002/dvdy.22516

Gautheret, R. J. (1934). Culture du tissus cambial. *Comptes Rendus Hebdomadaires Se'ances de l'Acad. Sci.* 15, 2195–2196.

Gautheret, R. J. (1935). *Recherches sur la Culture des Tissus Végétaux*. Paris: Thèse Sc, 279.

Gautheret, R. J. (1939). Sur la possibilite' de re'aliser la culture inde'finie des tissus de tubercules de carotte. *Comptes Rendus Hebdomadaires Se'ances de l'Acad. Sci.* 208, 118–120.

Gautheret, R. J. (1942). He'te'ro-auxines et cultures de tissus ve'ge'taux. *Bull. Soc. Chimie Biol.* 24, 13–21.

Gautheret, R. J. (1955). Sur la variabilite' des proprie'te's physiologiques des cultures de tissues ve'ge'taux. *Rev. Gen. Bot.* 65, 5–112.

Gazzarrini, S., Tsuchiya, Y., Lumba, S., Okamoto, M., and McCourt, P. (2004). The transcription factor FUSCA3 controls developmental timing in *Arabidopsis* through the hormones gibberellin and abscisic acid. *Dev. Cell* 7, 373–385. doi: 10.1016/j.devcel.2004.06.017

Goh, T., Joi, S., Mimura, T., and Fukaki, H. (2012). The establishment of asymmetry in *Arabidopsis* lateral root founder cells is regulated by LBD16/ASL18 and related LBD/ASL proteins. *Development* 139, 883–893. doi: 10.1242/dev.071928

Gordon, S. P., Heisler, M. G., Reddy, G. V., Ohno, C., Das, P., and Meyerowitz, E. M. (2007). Pattern formation during de novo assembly of the *Arabidopsis* shoot meristem. *Development* 134, 3539–3548. doi: 10.1242/dev.010298

Grzybkowska, D., Morończyk, J., Wójcikowska, B., and Gaj, M. D. (2018). Azacitidine (5-AzaC)-treatment and mutations in DNA methylase genes affect embryogenic response and expression of the genes that are involved in somatic embryogenesis in *Arabidopsis*. *Plant Growth Regul.* 85, 243–256. doi: 10.1007/s10725-018-0389-1

Guo, F., Liu, C., Xia, H., Bi, Y., and Zhao, C. (2013). Induced expression of AtLEC1 and AtLEC2 differentially promotes somatic embryogenesis in transgenic tobacco plants. *PLoS One* 8:e71714. doi: 10.1371/journal.pone.0071714

Hake, S., Char, B. R., Chuck, G., Foster, T., Long, J., and Jackson, D. (1995). Homeobox genes in the functioning of plant meristems. *Philos. Trans. R. Soc. B* 350, 45–51. doi: 10.1098/rstb.1995.0136

Hake, S., Smith, H. M. S., Holtan, H., Magnani, E., Mele, G., and Ramirez, J. (2004). The role of KNOX genes in plant development. *Annu. Rev. Cell Dev. Biol.* 20, 125–151. doi: 10.1146/annurev.cellbio.20.031803.093824

Han, R., Truco, M. J., Lavelle, D. O., and Michelmore, R. W. (2021). A composite analysis of flowering time regulation in lettuce. *Front. Plant Sci.* 12:632708. doi: 10.3389/fpls.2021.632708

Harding, E. W., Tang, W., Nichols, K. W., Fernandez, D. E., and Perry, S. E. (2003). Expression and maintenance of embryogenic potential is enhanced through constitutive expression of AGAMOUS-like 15. *Plant Physiol.* 133:653. doi: 10.1104/pp.103.023499

He, C., Chen, X., Huang, H., and Xu, L. (2012). Reprogramming of H3K27me3 Is critical for acquisition of pluripotency from cultured *Arabidopsis* tissues. *PLoS Genet.* 8:e1002911. doi: 10.1371/journal.pgen.1002911

Hecht, V., Vielle-Calzada, J.-P., Hartog, M. V., Schmidt, E. D. L., Boutilier, K., Grossniklaus, U., et al. (2001). The *Arabidopsis* SOMATIC EMBRYOGENESIS RECEPTOR KINASE 1 gene is expressed in developing ovules and embryos and enhances embryogenic competence in culture 1. *Plant Physiol.* 127, 803–816. doi: 10.1104/pp.010324

Heidmann, I., de Lange, B., Lambalk, J., Angenent, G. C., and Boutilier, K. (2011). Efficient sweet pepper transformation mediated by the BABY BOOM transcription factor. *Plant Cell Reports* 30, 1107–1115. doi: 10.1007/s00299-011-1018-x

Henderson, J. T., Li, H. C., Rider, S. D., Mordhorst, A. P., Romero-Severson, J., Cheng, J. C., et al. (2004). PICKLE Acts throughout the plant to repress expression of embryonic traits and may play a role in gibberellin-dependent responses. *Plant Physiol.* 134, 995–1005. doi: 10.1104/pp.103.030148

Hewezi, T., Maier, T. R., Nettleton, D., and Baum, T. J. (2012). The Arabidopsis MicroRNA396-GRF1/GRF3 regulatory module acts as a developmental regulator in the reprogramming of root cells during cyst nematode infection. *Plant Physiol.* 159, 321–335. doi: 10.1104/pp.112.193649

Hirakawa, Y., Shinohara, H., Kondo, Y., Inoue, A., Nakanomyo, I., Ogawa, M., et al. (2008). Non-cell-autonomous control of vascular stem cell fate by a CLE peptide/receptor system. *Proc. Natl. Acad. Sci. U.S.A.* 105, 15208–15213. doi: 10.1073/pnas.0808444105

Hofhuis, H., Laskowski, M., Du, Y., Prasad, K., Grigg, S., Pinon, V., et al. (2013). Phyllotaxis and rhizotaxis in arabidopsis are modified by three PLETHORA transcription factors. *Curr. Biol.* 23, 956–962. doi: 10.1016/j.cub.2013.04.048

Horstman, A., Li, M., Heidmann, I., Weemen, M., Chen, B., Muino, J. M., et al. (2017). The BABY BOOM transcription factor activates the LEC1-ABI3-FUS3-LEC2 network to induce somatic embryogenesis. *Plant Physiol.* 175, 848–857. doi: 10.1104/pp.17.00232

Hu, J., Mitchum, M. G., Barnaby, N., Ayele, B. T., Ogawa, M., Nam, E., et al. (2008). Potential sites of bioactive gibberellin production during reproductive growth in *Arabidopsis*. *Plant Cell* 20, 320–336. doi: 10.1105/tpc.107.057752

Hu, X., and Xu, L. (2016). Transcription factors WOX11/12 directly activate WOX5/7 to promote root primordia initiation and organogenesis 1. *Plant Physiol.* 172, 2363–2373. doi: 10.1104/pp.16.01067

Ikeda, Y., Banno, H., Niu, Q.-W., Howell, S. H., and Chua, N.-H. (2006). The ENHANCER OF SHOOT REGENERATION 2 gene in *Arabidopsis* regulates CUP-SHAPED COTYLEDON 1 at the transcriptional level and controls cotyledon development. *Plant Cell Physiol.* 47, 1443–1456. doi: 10.1093/pcp/pcl023

Ikeuchi, M., Iwase, A., Rymen, B., Lambolez, A., Kojima, M., Takebayashi, Y., et al. (2017). Wounding triggers callus formation via dynamic hormonal and transcriptional changes. *Plant Physiol.* 175, 1158–1174. doi: 10.1104/pp.17.01035

Ikeuchi, M., Ogawa, Y., Iwase, A., and Sugimoto, K. (2016). Plant regeneration: cellular origins and molecular mechanisms. *Development* 143, 1442–1451. doi: 10.1242/dev.134668

Ishihara, H., Sugimoto, K., Tarr, P. T., Temman, H., Kadokura, S., Inui, Y., et al. (2019). Primed histone demethylation regulates shoot regenerative competency. *Nat. Commun.* 10, 1–15. doi: 10.1038/s41467-019-09386-5

Iwase, A., Harashima, H., Ikeuchi, M., Rymen, B., Ohnuma, M., Komaki, S., et al. (2017). WIND1 promotes shoot regeneration through transcriptional activation of ENHANCER OF SHOOT REGENERATION1 in *Arabidopsis*. *Plant Cell* 29, 54–69. doi: 10.1105/tpc.16.00623

Iwase, A., Kondo, Y., Laohavisit, A., Takebayashi, A., Ikeuchi, M., Matsuoka, K., et al. (2021). WIND transcription factors orchestrate wound-induced callus formation, vascular reconnection and defense response in *Arabidopsis*. *New Phytol.* 232, 734–752. doi: 10.1111/nph.17594

Iwase, A., Mitsuda, N., Ikeuchi, M., Ohnuma, M., Koizuka, C., Kawamoto, K., et al. (2013). *Arabidopsis* WIND1 induces callus formation in rapeseed, tomato, and tobacco. *Plant Signal. Behav.* 8:e27432. doi: 10.4161/psb.27432

Iwase, A., Mitsuda, N., Koyama, T., Hiratsu, K., Kojima, M., Arai, T., et al. (2011a). The AP2/ERF transcription factor WIND1 controls cell dedifferentiation in *Arabidopsis*. *Curr. Biol.* 21, 508–514. doi: 10.1016/j.cub.2011.02.020

Iwase, A., Ohme-Takagi, M., and Sugimoto, K. (2011b). WIND1: A key molecular switch for plant cell dedifferentiation. *Plant Signal. Behav.* 6, 1943–1945. doi: 10.4161/psb.6.12.18266

Jones, T., Lowe, K., Hoerster, G., Anand, A., Wu, E., Wang, N., et al. (2019). Maize transformation using the morphogenic genes. *Methods Mol. Biol.* 1864, 81–93. doi: 10.1007/978-1-4939-8778-8_6

Junker, A., Mönke, G., Rutten, T., Keilwagen, J., Seifert, M., Thi, T. M. N., et al. (2012). Elongation-related functions of LEAFY COTYLEDON1 during the development of *Arabidopsis thaliana*. *Plant J.* 71, 427–442. doi: 10.1111/j.1365-313X.2012.04999.x

Kadkade, P., and Seibert, M. (1977). Phytochrome-regulated organogenesis in lettuce tissue culture. *Nature* 270, 49–50. doi: 10.1038/270049a0

Kareem, A., Durgaprasad, K., Sugimoto, K., Du, Y., Pulianmackal, A. J., Trivedi, Z. B., et al. (2015). PLETHORA genes control regeneration by a two-step mechanism. *Curr. Biol.* 25, 1017–1030. doi: 10.1016/j.cub.2015.02.022

Katsir, L., Davies, K. A., Bergmann, D. C., and Laux, T. (2011). Peptide signaling in plant development. *Curr. Biol.* 21, R356–R364.

Kim, J., Yang, W., Forner, J., Lohmann, J. U., Noh, B., and Noh, Y. (2018). Epigenetic reprogramming by histone acetyltransferase HAG1/AtGCN5 is required for pluripotency acquisition in Arabidopsis. *EMBO J.* 37:e98726. doi: 10.15252/embj.201798726

Kim, J. H. (2019). Biological roles and an evolutionary sketch of the GRF-GIF transcriptional complex in plants. *BMB Rep.* 52:227. doi: 10.5483/BMBRep.2019.52.4.051

Kim, J. H., and Botella, J. R. (2004). Etr1-1 gene expression alters regeneration patterns in transgenic lettuce stimulating root formation. *Plant Cell* 78, 69–73. doi: 10.1023/b:ticu.0000020396.64257.c1

Kim, J. H., Choi, D., and Kende, H. (2003). The AtGRF family of putative transcription factors is involved in leaf and cotyledon growth in *Arabidopsis*. *Plant J.* 36, 94–104. doi: 10.1046/j.1365-313x.2003.01862.x

Kim, J.-S., Mizoi, J., Kidokoro, S., Maruyama, K., Nakajima, J., Nakashima, K., et al. (2012). *Arabidopsis* GROWTH-REGULATING FACTOR7 functions as a transcriptional repressor of abscisic acid-and osmotic stress-responsive

genes. including DREB2A W. *Plant Cell* 24, 3393–3405. doi: 10.1105/tpc.112.100933

Kirch, T., Simon, R., Grünewald, M., and Werr, W. (2003). The DORNRÖSCHEN/ENHANCER OF SHOOT REGENERATION1 gene of *Arabidopsis* acts in the control of meristem cell fate and lateral organ development. *Plant Cell* 15:694. doi: 10.1105/tpc.009480

Koevary, K. (1978). Tissue culture propagation of head lettuce. *HortScience* 12, 459–460.

Köhler, C., and Hennig, L. (2010). Regulation of cell identity by plant polycomb and trithorax group proteins. *Curr. Opin. Genet. Dev.* 20, 541–547. doi: 10.1016/j.gde.2010.04.015

Kong, J., Martin-Ortigosa, S., Finer, J., Orchard, N., Gunadi, A., Batts, L. A., et al. (2020). Overexpression of the transcription factor GROWTH-REGULATING FACTOR5 improves transformation of dicot and monocot species. *Front. Plant Sci.* 11:572319. doi: 10.3389/fpls.2020.572319

Kornet, N., and Scheres, B. (2009). Members of the GCN5 histone acetyltransferase complex regulate PLETHORA-mediated root stem cell niche maintenance and transit amplifying cell proliferation in *Arabidopsis*. *Plant Cell* 21, 1070–1079. doi: 10.1105/tpc.108.065300

Krikorian, A. D., and Berquam, D. L. (1969). Plant cell and tissue cultures: the role of HABERLANDT 1. *Bot. Rev.* 35, 59–67.

Kuijt, S. J. H., Greco, R., Agalou, A., Shao, J., 't Hoen, C. C. J., Övernäs, E., et al. (2014). Interaction between the GROWTH-REGULATING FACTOR and KNOTTED1-LIKE HOMEOBOX families of transcription factors. *Plant Physiol.* 164, 1952–1966. doi: 10.1104/pp.113.222836

Kwiatkowska, D. (2004). Structural integration at the shoot apical meristem: models, measurements, and experiments. *Am. J. Bot.* 91, 1277–1293. doi: 10.3732/ajb.91.9.1277

Lardon, R., and Geelen, D. (2020). Natural variation in plant pluripotency and regeneration. *Plants* 9, 1–28. doi: 10.3390/plants9101261

LaRue, C. D. (1933). Regeneration in mutilated seedlings. *Proc. Natl. Acad. Sci. U.S.A.* 19, 53–63. doi: 10.1073/pnas.19.1.53

LaRue, C. D. (1936). Tissue culture of spermatophytes. *Proc. Natl. Acad. Sci. U.S.A.* 22, 201–209. doi: 10.1073/pnas.22.4.201

Lee, B. H., Ko, J. H., Lee, S., Lee, Y., Pak, J. H., and Kim, J. H. (2009). The *Arabidopsis* GRF-INTERACTING FACTOR gene family performs an overlapping function in determining organ size as well as multiple developmental properties. *Plant Physiol.* 151, 655–668. doi: 10.1104/pp.109.141838

Lee, H. W., Cho, C., Pandey, S. K., Park, Y., Kim, M. J., and Kim, J. (2019). LBD16 and LBD18 acting downstream of ARF7 and ARF19 are involved in adventitious root formation in *Arabidopsis*. *BMC Plant Biol.* 19:46. doi: 10.1186/s12870-019-1659-4

Lee, K., Park, O. S., Choi, C. Y., and Seo, P. J. (2019). ARABIDOPSIS TRITHORAX 4 facilitates shoot identity establishment during the plant regeneration process. *Plant Cell Physiol.* 60, 826–834. doi: 10.1093/pcp/pcy248

Lee, K., Park, O. S., Go, J. Y., Yu, J., Han, J. H., Kim, J., et al. (2021). *Arabidopsis* ATXR2 represses de novo shoot organogenesis in the transition from callus to shoot formation. *Cell Rep.* 37:109980. doi: 10.1016/j.celrep.2021.109980

Lee, K., Park, O. S., and Seo, P. J. (2018). JMJ30-mediated demethylation of H3K9me3 drives tissue identity changes to promote callus formation in *Arabidopsis*. *Plant J.* 95, 961–975. doi: 10.1111/tpj.14002

Leelavathi, S., Sunnichan, V. G., Kumira, R., Vijaykanth, G. P., Bhatnagar, R. K., and Reddy, V. S. (2004). A simple and rapid Agrobacterium-mediated transformation protocol for cotton (*Gossypium hirsutum* L.): *Embryogenic calli* as a source to generate large numbers of transgenic plants. *Plant Cell Rep.* 22, 465–447. doi: 10.1007/s00299-003-0710-x

Li, W., Liu, H., Cheng, Z. J., Su, Y. H., Han, H. N., Zhang, Y., et al. (2011). DNA methylation and histone modifications regulate de novo shoot regeneration in *Arabidopsis* by modulating WUSCHEL expression and auxin signaling. *PLoS Genet.* 7:e1002243. doi: 10.1371/journal.pgen.1002243

Liu, H., Zhang, H., Dong, Y. X., Hao, Y. J., and Zhang, X. S. (2018). DNA METHYLTRANSFERASE1-mediated shoot regeneration is regulated by cytokinin-induced cell cycle in *Arabidopsis*. *New Phytol.* 217, 219–232. doi: 10.1111/nph.14814

Liu, J., Sheng, L., Xu, Y., Li, J., Yang, Z., Huang, H., et al. (2014). WOX11 and 12 are involved in the first-step cell fate transition during de novo root organogenesis in *Arabidopsis*. *Plant Cell* 26, 1081–1093. doi: 10.1105/tpc.114.122887

Liu, Z., Dai, X., Li, J., Liu, N., Liu, X., Li, S., et al. (2020). The type-B cytokinin response regulator ARR1 inhibits shoot regeneration in an ARR12-dependent manner in *Arabidopsis*. *Plant Cell* 32, 2271–2291. doi: 10.1105/tpc.19.00022

Loberant, B., and Altman, A. (2010). "Micropropagation of plants," in *Encyclopedia of Industrial Biotechnology: Bioprocess, Bioseparation, and Cell Technology*, ed. M. C. Flickinger (Hoboken, NJ: John Wiley & Sons, Inc.), 1–17. doi: 10.1007/s11120-017-0473-9

Loomis, W. G., and Schull, C. A. (1937). *Methods in Plant Physiology*. New York, NY: McGraw-Hull, 58.

Lotan, T., Ohto, M. A., Matsudaira Yee, K., West, M. A. L., Lo, R., Kwong, R. W., et al. (1998). *Arabidopsis* LEAFY COTYLEDON1 Is sufficient to induce embryo development in vegetative cells. *Cell* 93, 1195–1205. doi: 10.1016/s0092-8674(00)81463-4

Ma, W., Wu, F., Sheng, P., Wang, X., Zhang, Z., Zhou, K., et al. (2017). The LBD12-1 transcription factor suppresses apical meristem size by repressing argonaute 10 expression. *Plant Physiol.* 173:801. doi: 10.1104/pp.16.01699

Makarevich, G., Leroy, O., Akinci, U., Schubert, D., Clarenz, O., Goodrich, J., et al. (2006). Different Polycomb group complexes regulate common target genes in *Arabidopsis*. *EMBO Rep.* 7, 947–952. doi: 10.1038/sj.embor.7400760

Mantiri, F. R., Kurdyukov, S., Lohar, D. P., Sharopova, N., Saeed, N. A., Wang, X. D., et al. (2008). The transcription factor MtSERF1 of the ERF subfamily identified by transcriptional profiling is required for somatic embryogenesis induced by auxin plus cytokinin in *Medicago truncatula*. *Plant Physiol.* 146, 1622–1636. doi: 10.1104/pp.107.110379

Matsuo, N., Makino, M., and Banno, H. (2011). Arabidopsis ENHANCER OF SHOOT REGENERATION (ESR)1 and ESR2 regulate in vitro shoot regeneration and their expressions are differentially regulated. *Plant Sci.* 181, 39–46. doi: 10.1016/j.plantsci.2011.03.007

Matsuo, N., Mase, H., Makino, M., Takahashi, H., and Banno, H. (2009). Identification of ENHANCER OF SHOOT REGENERATION 1-upregulated genes during in vitro shoot regeneration. *Plant Biotechnol.* 26, 385–393. doi: 10.5511/plantbiotechnology.26.385

Mayer, K. F. X., Schoof, H., Haecker, A., Lenhard, M., Jürgens, G., and Laux, T. (1998). Role of WUSCHEL in regulating stem cell fate in the arabidopsis shoot meristem. *Cell* 95, 805–815. doi: 10.1016/s0092-8674(00)81703-1

McConnell, J. R., Emery, J., Eshed, Y., Bao, N., Bowman, J., and Barton, M. K. (2001). Role of PHABULOSA and PHAVOLUTA in determining radial patterning in shoots. *Nature* 411, 709–713. doi: 10.1038/35079635

Méndez-Hernández, H. A., Ledezma-Rodríguez, M., Avilez-Montalvo, R. N., Juárez-Gómez, Y. L., Skeete, A., Avilez-Montalvo, J., et al. (2019). Signaling overview of plant somatic embryogenesis. *Front. Plant Sci.* 10:77. doi: 10.3389/fpls.2019.00077

Meng, W. J., Cheng, Z. J., Sang, Y. L., Zhang, M. M., Rong, X. F., Wang, Z. W., et al. (2017). Type-B ARABIDOPSIS RESPONSE REGULATORs specify the shoot stem cell niche by dual regulation of WUSCHEL. *Plant Cell* 29, 1357–1372. doi: 10.1105/tpc.16.00640

Miao, C., Wang, D., He, R., Liu, S., and Zhu, J. K. (2020). Mutations in MIR396e and MIR396f increase grain size and modulate shoot architecture in rice. *Plant Biotechnol. J.* 18, 491–501. doi: 10.1111/pbi.13214

Michelmore, R., Marsh, E., Seely, S., and Landry, B. (1987). Transformation of lettuce (*Lactuca sativa*) mediated by *Agrobacterium tumefaciens*. *Plant Cell Rep.* 6, 439–442.

Michelmore, R. W., and Eash, J. A. (1985). "Lettuce," in *The Handbook of Plant Cell Culture*, Vol. 4, eds D. A. Evans, W. R. Sharp, and P. V. Ammirato (New York, NY: Macmillan) 512–551.

Miller, C., Skoog, F., von Saltza, M. H., and Strong, F. M. (1955). Kinetin, a cell division factor from desoxyribonucleic acid. *J. Am. Chem. Soc.* 77:1392. doi: 10.1021/ja01610a105

Mitchum, M. G., Yamaguchi, S., Hanada, A., Kuwahara, A., Yoshioka, Y., Kato, T., et al. (2006). Distinct and overlapping roles of two gibberellin 3-oxidases in *Arabidopsis* development. *Plant J.* 45, 804–818. doi: 10.1111/j.1365-313X.2005.02642.x

Mohebodini, M., Javaran, M. J., and Alizadeh, H. (2011). Effects of genotype, explant age and growth regulators on callus induction and direct shoot

regeneration of Lettuce (*Lactuca sativa* L.). *Aust. J. Crop Sci.* 5, 92–95. doi: 10.33899/rjs.2012.44416

Mozgová, I., Muñoz-Viana, R., and Hennig, L. (2017). PRC2 represses hormone-induced somatic embryogenesis in vegetative tissue of A*rabidopsis thaliana*. *PLoS Genet.* 13:e1006562. doi: 10.1371/journal.pgen.1006562

Müller, B., and Sheen, J. (2008). Cytokinin and auxin interaction in root stem-cell specification during early embryogenesis. *Nature* 453, 1094–1097. doi: 10.1038/nature06943

Murthy, B. N. S., Victor, J., Singh, R. P., Fletcher, R. A., and Praveen, K. S. (1996). In vitro regeneration of chickpea (*Cicer arietinum* L.): stimulation of direct organogenesis and somatic embryogenesis by thidiazuron. *Plant Growth Regul.* 19, 233–240. doi: 10.1007/bf00037796

Negin, B., Shemer, O., Sorek, Y., and Williams, L. E. (2017). Shoot stem cell specification in roots by the WUSCHEL transcription factor. *PLoS One* 12:e0176093. doi: 10.1371/journal.pone.0176093

Ning, K., Han, Y., Chen, Z., Luo, C., Wang, S., Zhang, W., et al. (2019). Genome-wide analysis of MADS-box family genes during flower development in lettuce. *Plant Cell Environ.* 42, 1868–1881. doi: 10.1111/pce.13523

Nobe'court, P. (1955). Variations de la morphologie et de la structure de cultures de tissues ve'ge'taux. *Berichte Schweizerische Bot. Gesellschaft* 65, 475–480.

Norstog, K. (1979). "Embryo culture as a tool in the study of comparative and developmental morphology," in *Plant Cell and Tissue Culture*, eds W. R. Sharp, P. O. Larsen, E. F. Paddock, and V. Raghavan (Columbus, OH: Ohio State Univ. Press), 179–202. doi: 10.1016/0145-305x(87)90019-x

Nuti Ronchi, V., and Gregorini, G. (1970). Histological study of adventitious bud formation on *Lactuca sativa* cotyledons cultured in vitro. *Giornale Bot. Italiano* 104, 443–455. doi: 10.1080/11263507009426517

Ogas, J., Cheng, J. C., Sung, Z. R., and Somerville, C. (1997). Cellular differentiation regulated by gibberellin in the *Arabidopsis thaliana* pickle mutant. *Science* 277, 91–94. doi: 10.1126/science.277.5322.91

Okushima, Y., Fukaki, H., Onoda, M., Theologis, A., and Tasaka, M. (2007). ARF7 and ARF19 regulate lateral root formation via direct activation of LBD/ASL genes in *Arabidopsis*. *Plant Cell* 19, 118–130. doi: 10.1105/tpc.106.047761

Omidbakhshfard, M. A., Proost, S., Fujikura, U., and Mueller-Roeber, B. (2015). Growth-Regulating Factors (GRFs): a small transcription factor family with important functions in plant biology. *Mol. Plant* 8, 998–1010. doi: 10.1016/j.molp.2015.01.013

Ooi, S. E., Choo, C. N., Ishak, Z., and Ong-Abdullah, M. (2012). A candidate auxin-responsive expression marker gene, EgIAA9, for somatic embryogenesis in oil palm (*Elaeis guineensis* Jacq.). *Plant Cell Tissue Organ Cult.* 110, 201–212. doi: 10.1007/s11240-012-0143-8

Osorio-Montalvo, P., De-la-Peña, C., Oropeza, C., Nic-Can, G., Córdova-Lara, I., Castillo-Castro, E., et al. (2020). A peak in global DNA methylation is a key step to initiate the somatic embryogenesis of coconut palm (*Cocos nucifera* L). *Plant Cell Rep.* 39, 1345–1357. doi: 10.1007/s00299-020-02568-2

Ozias-akins, P., and Vasil, I. K. (1982). Plant Regeneration from Cultured Immature embryos and inflorescences *Triticum aestivum* L. (Wheat): evidence for somatic embryogenesis. *Protoplasma* 110, 95–105. doi: 10.1007/bf01281535

Paul, P., Joshi, S., Tian, R., Diogo Junior, R., Chakrabarti, M., and Perry, S. E. (2022). The MADS-domain factor AGAMOUS-Like18 promotes somatic embryogenesis. *Plant Physiol.* 188, 1617–1631. doi: 10.1093/plphys/kiab553

Perilli, S., di Mambro, R., and Sabatini, S. (2012). Growth and development of the root apical meristem. *Curr. Opin. Plant Biol.* 15, 17–23. doi: 10.1016/j.pbi.2011.10.006

Preece, J. E. (2003). A century of progress with vegetative plant propagation. *Hortscience* 38, 1015–1025. doi: 10.1094/PDIS-07-14-0679-FE

Quiroz-Figueroa, F. R., Rojas-Herrera, R., Galaz-Avalos, R. M., and Loyola-Vargas, V. M. (2006). Embryo production through somatic embryogenesis can be used to study cell differentiation in plants. *Plant Cell Tissue Organ Cult.* 86, 285–301. doi: 10.1007/s11240-006-9139-6

Radhakrishnan, D., Shanmukhan, A. P., Kareem, A., Aiyaz, M., Varapparambathu, V., Toms, A., et al. (2020). A coherent feed-forward loop drives vascular regeneration in damaged aerial organs of plants growing in a normal developmental context. *Development (Cambridge)* 147:dev185710. doi: 10.1242/dev.185710

Raza, G., Singh, M. B., and Bhalla, P. L. (2020). Somatic embryogenesis and plant regeneration from commercial *Soybean cultivars*. *Plants* 9:38. doi: 10.3390/plants9010038

Reyes-Chin-Wo, S., Wang, Z., Yang, X., Kozik, A., Arikit, S., Song, C., et al. (2017). Genome assembly with in vitro proximity ligation data and whole-genome triplication in lettuce. *Nat. Commun.* 8, 1–11. doi: 10.1038/ncomms14953

Rodriguez, R. E., Mecchia, M. A., Debernardi, J. M., Schommer, C., Weigel, D., and Palatnik, J. F. (2010). Control of cell proliferation in *Arabidopsis thaliana* by microRNA miR396. *Development* 137, 103–112. doi: 10.1242/dev.043067

Rueb, S., Leneman, M., Schilperoort, R. A., and Hensgens, L. A. M. (1994). Efficient plant regeneration through somatic embryogenesis from callus induced on mature rice embryos (*Oryza sativa* L.). *Plant Cell Tissue Organ Cult.* 36, 259–264. doi: 10.1007/bf00037729

Santos, D., and Fevereiro, P. (2002). Loss of DNA methylation affects somatic embryogenesis in *Medicago truncatula*. *Plant Cell Tissue Organ Cult.* 70, 155–161.

Sarkar, A. K., Luijten, M., Miyashima, S., Lenhard, M., Hashimoto, T., Nakajima, K., et al. (2007). Conserved factors regulate signaling in *Arabidopsis thaliana* shoot and root stem cell organizers. *Nature* 446, 811–814. doi: 10.1038/nature05703

Sasaki, H. (1979). Physiological and morphological studies on development of vegetable crops VI. Effect of several auxins, cytokinins and cytokinin-ribosides on the adventitious bud formation of lettuce hypocotyl tissue cultured in vitro. *Physiol. Morphol. Stud. Dev. Veg. Crops* 48, 67–72.

Sasaki, H. (1982). Effect of temperature and light on adventitious bud formation of lettuce hypocotyl tissue cultured in vitro. *J. Jpn Soc. Horticult.* 51, 187–194. doi: 10.2503/jjshs.51.187

Schuabb Heringer, A., Barroso, T., Ferreira Macedo, A., Santa-Catarina, C., Martins, G. H., Souza, F., et al. (2015). Label-free quantitative proteomics of embryogenic and non-embryogenic callus during sugarcane somatic embryogenesis. *PLoS One* 10:e0127803. doi: 10.1371/journal.pone.0127803

Severino, L. S., Lima, R. L. S., Lucena, A. M. A., Freire, M. A. O., Sampaio, L. R., Veras, R. P., et al. (2011). Propagation by stem cuttings and root system structure of *Jatropha curcas*. *Biomass Bioenergy* 35, 3160–3166. doi: 10.1016/j.biombioe.2011.04.031

Shang, B., Xu, C., Zhang, X., Cao, H., Xin, W., and Hu, Y. (2016). Very-long-chain fatty acids restrict regeneration capacity by confining pericycle competence for callus formation in *Arabidopsis*. *Proc. Natl. Acad. Sci. U.S.A.* 113, 5101–5106. doi: 10.1073/pnas.1522466113

Shchuka, V. M., Malek-Gilani, N., Singh, G., Langroudi, L., Dhaliwal, N. K., Moorthy, S. D., et al. (2015). Chromatin dynamics in lineage commitment and cellular reprogramming. *Genes* 6, 641–661. doi: 10.3390/genes6030641

Shimotohno, A., Heidstra, R., Blilou, I., and Scheres, B. (2018). Root stem cell niche organizer specification by molecular convergence of PLETHORA and SCARECROW transcription factor modules. *Genes Dev.* 32, 1085–1100. doi: 10.1101/gad.314096.118

Shin, J., Bae, S., and Seo, P. J. (2020). De novo shoot organogenesis during plant regeneration. *J. Exp. Bot.* 71, 63–72. doi: 10.1093/jxb/erz395

Skoog, F., and Miller, C. O. (1957). Chemical regulation of growth and organ formation in plant tissue cultures in vitro. *Symp. Soc. Exp. Biol.* 11, 118–131.

Skoog, F., and Tsui, C. (1948). Chemical control of growth and bud formation in tobacco stem segments and callus cultured in vitro. *Am. J. Bot.* 35, 782–787. doi: 10.1002/j.1537-2197.1948.tb08148.x

Stone, S. L., Braybrook, S. A., Paula, S. L., Kwong, L. W., Meuser, J., Pelletier, J., et al. (2008). Arabidopsis LEAFY COTYLEDON2 induces maturation traits and auxin activity: implications for somatic embryogenesis. *Proc. Natl. Acad. Sci. U.S.A.* 105, 3151–3156. doi: 10.1073/pnas.0712364105

Su, Y. H., and Zhang, X. S. (2014). The hormonal control of regeneration in plants. *Curr. Top. Dev. Biol.* 108, 35–69. doi: 10.1016/B978-0-12-391498-9.00010-3

Sugimoto, K., Jiao, Y., and Meyerowitz, E. M. (2010). *Arabidopsis* regeneration from multiple tissues occurs via a root development pathway. *Dev. Cell* 18, 463–471. doi: 10.1016/j.devcel.2010.02.004

Sugimoto, K., Temman, H., Kadokura, S., and Matsunaga, S. (2019). To regenerate or not to regenerate: factors that drive plant regeneration. *Curr. Opin. Plant Biol.* 47, 138–150. doi: 10.1016/j.pbi.2018.12.002

Sun, S., Kang, X. P., Xing, X. J., Xu, X. Y., Cheng, J., Zheng, S. W., et al. (2015). Agrobacterium-mediated transformation of tomato (*Lycopersicon esculentum* L. cv. Hezuo 908) with improved efficiency. *Biotechnol. Biotechnol. Equip.* 29, 861–868. doi: 10.1080/13102818.2015.1056753

Szczygieł-Sommer, A., and Gaj, M. D. (2019). The miR396–GRF regulatory module controls the embryogenic response in *Arabidopsis* via an auxin-related pathway. *Int. J. Mol. Sci.* 20:5221. doi: 10.3390/ijms20205221

Thorpe, T. A. (2007). History of plant tissue culture. *Mol. Biotechnol.* 37, 169–180.

Tian, Q., Uhlir, N. J., and Reed, J. W. (2002). *Arabidopsis* SHY2/IAA3 inhibits auxin-regulated gene expression. *Plant Cell* 14, 301–319. doi: 10.1105/tpc.010283

Trinh, D. C., Lavenus, J., Goh, T., Boutté, Y., Drogue, Q., Vaissayre, V., et al. (2019). PUCHI regulates very long chain fatty acid biosynthesis during lateral root and callus formation. *Proc. Natl. Acad. Sci. U.S.A.* 116, 14325–14330. doi: 10.1073/pnas.1906300116

Tsuda, K., Ito, Y., Sato, Y., and Kurata, N. (2011). Positive autoregulation of a KNOX gene is essential for shoot apical meristem maintenance in rice. *Plant Cell* 23, 4368–4381. doi: 10.1105/tpc.111.090050

van den Berg, C., Willemsen, V., Hendriks, G., Weisbeek, P., and Scheres, B. (1997). Short-range control of cell differentiation in the *Arabidopsis* root meristem. *Nature* 390, 287–289. doi: 10.1038/36856

van der Knaap, E., Kim, J. H., and Kende, H. (2000). A novel gibberellin-induced gene from rice and its potential regulatory role in stem growth. *Plant Physiol.* 122:695. doi: 10.1104/pp.122.3.695

van Overbeek, J., Conklin, M. E., and Blakeslee, A. F. (1941). Factors in coconut milk essential for growth and development of very young *Datura embryos*. *Science* 94, 350–351. doi: 10.1126/science.94.2441.350

Victorathisayam, T., and Sridevi, G. (2020). Ectopic expression of WUSCHEL (AtWUS) gene alters plant growth and development in. *Rice Plant* 8, 43–53. doi: 10.11648/j.plant.20200803.11

Waki, T., Hiki, T., Watanabe, R., Hashimoto, T., and Nakajima, K. (2011). The *Arabidopsis* RWP-RK Protein RKD4 triggers gene expression and pattern formation in early embryogenesis. *Curr. Biol.* 21, 1277–1281. doi: 10.1016/j.cub.2011.07.001

Wang, X., Niu, Q. W., Teng, C., Li, C., Mu, J., Chua, N. H., et al. (2008). Overexpression of PGA37/MYB118 and MYB115 promotes vegetative-to-embryonic transition in *Arabidopsis*. *Cell Res.* 19, 224–235. doi: 10.1038/cr.2008.276

Webb, D. T., Torres, L. D., and Fobert, P. (1984). Interactions of growth regulators, explant age, and culture environment controlling organogenesis from lettuce cotyledons in vitro. *Can. J. Bot.* 62, 586–590. doi: 10.1139/b84-088

Wildwater, M., Campilho, A., Perez-Perez, J. M., Heidstra, R., Blilou, I., Korthout, H., et al. (2005). The RETINOBLASTOMA-RELATED gene regulates stem cell maintenance in *Arabidopsis* roots. *Cell* 123, 1337–1349. doi: 10.1016/j.cell.2005.09.042

Wójcikowska, B., and Gaj, M. D. (2017). Expression profiling of AUXIN RESPONSE FACTOR genes during somatic embryogenesis induction in *Arabidopsis*. *Plant Cell Rep.* 36, 843–858. doi: 10.1007/s00299-017-2114-3

Xiong, F., Zhang, B.-K., Liu, H.-H., Wei, G., Wu, J.-H., Wu, Y.-N., et al. (2020). Transcriptional regulation of PLETHORA1 in the root meristem through an importin and its two antagonistic cargos. *Plant Cell* 32, 3812–3824. doi: 10.1105/tpc.20.00108

Xu, J., Hofhuis, H., Heidstra, R., Sauer, M., Friml, J., and Scheres, B. (2006). A molecular framework for plant regeneration. *Science* 311, 385–388. doi: 10.1126/science.1121790

Xu, K., Liu, J., Fan, M., Xin, W., Hu, Y., and Xu, C. (2012). A genome-wide transcriptome profiling reveals the early molecular events during callus initiation in Arabidopsis multiple organs | Elsevier Enhanced Reader. *Genomics* 100, 116–124. doi: 10.1016/j.ygeno.2012.05.013

Xu, L., and Huang, H. (2014). Genetic and epigenetic controls of plant regeneration. *Curr. Top. Dev. Biol.* 108, 1–33. doi: 10.1016/B978-0-12-391498-9.00009-7

Xu, M., Hu, T., Zhao, J., Park, M.-Y., Earley, K. W., Wu, G., et al. (2016). Developmental functions of miR156-regulated SQUAMOSA PROMOTER BINDING PROTEIN-LIKE (SPL) genes in *Arabidopsis thaliana*. *PLoS Genet.* 12:e1006263. doi: 10.1371/journal.pgen.1006263

Xu, Z., Zhang, C., Ge, X., Wang, N., Zhou, K., Yang, X., et al. (2015). Construction of a high-density linkage map and mapping quantitative trait loci for somatic embryogenesis using leaf petioles as explants in upland cotton (*Gossypium hirsutum* L.). *Plant Cell Rep.* 34, 1177–1187. doi: 10.1007/s00299-015-1776-y

Xue, T., Dai, X., Wang, R., Wang, J., Liu, Z., and Xiang, F. (2017). ARGONAUTE10 inhibits in vitro shoot regeneration via repression of miR165/166 in *Arabidopsis thaliana*. *Plant Cell Physiol.* 58, 1789–1800. doi: 10.1093/pcp/pcx117

Yamaguchi, S., Kamiya, Y., and Sun, T. P. (2001). Distinct cell-specific expression patterns of early and late gibberellin biosynthetic genes during *Arabidopsis* seed germination. *Plant J.* 28, 443–453. doi: 10.1046/j.1365-313x.2001.01168.x

Yamaguchi, Y. L., Ishida, T., and Sawa, S. (2016). CLE peptides and their signaling pathways in plant development. *J. Exp. Bot.* 67, 4813–4826.

Yasui, Y., Tsukamoto, S., Sugaya, T., Nishihama, R., Wang, Q., Kato, H., et al. (2019). GEMMA CUP_ASSOCIATED MYB1, an ortholog of axillary meristem regulators is essential in vegetative reproduction in *Marchantia polyphorma*. *Curr. Biol.* 29, 3986–3995. doi: 10.1016/j.cub.2019.10.004

Zhang, B., Tong, Y., Luo, K., Zhai, Z., Liu, X., Shi, Z., et al. (2021). Identification of GROWTH-REGULATING FACTOR transcription factors in lettuce (*Lactuca sativa*) genome and functional analysis of LsaGRF5 in leaf size regulation. *BMC Plant Biol.* 21:485. doi: 10.1186/s12870-021-03261-6

Zhang, X., Henriques, R., Lin, S.-S., Niu, Q.-W., and Chua, N.-H. (2006). Agrobacterium-mediated transformation of *Arabidopsis thaliana* using the floral dip method. *Nat Protoc.* 1, 641–646. doi: 10.1038/nprot.2006.97

Zhang, Y., Jiao, Y., Jiao, H., Zhao, H., and Zhu, Y. (2017). Two-step functional innovation of the stem-cell factors WUS/WOX5 during plant evolution. *Mol. Biol. Evol.* 34, 640–653. doi: 10.1093/molbev/msw263

Zheng, Q., Zheng, Y., Ji, H., Burnie, W., and Perry, S. E. (2016). Gene Regulation by the AGL15 transcription factor reveals hormone interactions in somatic embryogenesis. *Plant Physiol.* 172, 2374–2387. doi: 10.1104/pp.16.00564

Zheng, Q., Zheng, Y., and Perry, S. E. (2013). AGAMOUS-Like15 promotes somatic embryogenesis in *Arabidopsis* and soybean in part by the control of ethylene biosynthesis and response. *Plant Physiol.* 161, 2113–2127. doi: 10.1104/pp.113.216275

Zheng, Y., Ren, N., Wang, H., Stromberg, A. J., and Perry, S. E. (2009). Global identification of targets of the *Arabidopsis* MADS domain protein AGAMOUS-Like15. *Plant Cell* 21, 2563–2577. doi: 10.1105/tpc.109.068890

Zhou, C., Han, L., Zhao, Y., Wang, H., Nakashima, J., Tong, J., et al. (2019). Transforming compound leaf patterning by manipulating REVOLUTA in *Medicago truncatula*. *Plant J.* 100, 562–571. doi: 10.1111/tpj.14469

Conflict of Interest: The authors declare that the research was conducted in the absence of any commercial or financial relationships that could be construed as a potential conflict of interest.

Publisher's Note: All claims expressed in this article are solely those of the authors and do not necessarily represent those of their affiliated organizations, or those of the publisher, the editors and the reviewers. Any product that may be evaluated in this article, or claim that may be made by its manufacturer, is not guaranteed or endorsed by the publisher.

Copyright © 2022 Bull and Michelmore. This is an open-access article distributed under the terms of the Creative Commons Attribution License (CC BY). The use, distribution or reproduction in other forums is permitted, provided the original author(s) and the copyright owner(s) are credited and that the original publication in this journal is cited, in accordance with accepted academic practice. No use, distribution or reproduction is permitted which does not comply with these terms.

frontiers | Frontiers in Plant Science

ORIGINAL RESEARCH
published: 13 May 2022
doi: 10.3389/fpls.2022.912293

Successful Production and Ligninolytic Activity of a Bacterial Laccase, Lac51, Made in *Nicotiana benthamiana via* Transient Expression

*André van Eerde[1], Anikó Várnai[2], Yanliang Wang[1], Lisa Paruch[1], John-Kristian Jameson[2], Fen Qiao[3], Hans Geir Eiken[1], Hang Su[1], Vincent G. H. Eijsink[2] and Jihong Liu Clarke[1]**

[1]NIBIO - Norwegian Institute of Bioeconomy Research, Ås, Norway, [2]Faculty of Chemistry, Biotechnology and Food Science, Norwegian University of Life Sciences (NMBU), Ås, Norway, [3]Institute of Plant Protection, Chinese Academy of Agricultural Sciences, Haidian, China

OPEN ACCESS

Edited by:
Junhua Peng,
Huazhi Bio-Tech Co., Ltd., China

Reviewed by:
Valentina Perna,
Technical University of Denmark, Denmark
Jianguo Su,
Huazhong Agricultural University, China
Chao Ran,
Feed Research Institute (CAAS), China

***Correspondence:**
Jihong Liu Clarke
jihong.liu-clarke@nibio.no

Specialty section:
This article was submitted to Plant Biotechnology, a section of the journal Frontiers in Plant Science

Received: *05 April 2022*
Accepted: *27 April 2022*
Published: *13 May 2022*

Citation:
van Eerde A, Várnai A, Wang Y, Paruch L, Jameson J-K, Qiao F, Eiken HG, Su H, Eijsink VGH and Clarke JL (2022) Successful Production and Ligninolytic Activity of a Bacterial Laccase, Lac51, Made in Nicotiana benthamiana via Transient Expression. Front. Plant Sci. 13:912293. doi: 10.3389/fpls.2022.912293

Giant panda could have bamboo as their exclusive diet for about 2 million years because of the contribution of numerous enzymes produced by their gut bacteria, for instance laccases. Laccases are blue multi-copper oxidases that catalyze the oxidation of a broad spectrum of phenolic and aromatic compounds with water as the only byproduct. As a "green enzyme," laccases have potential in industrial applications, for example, when dealing with degradation of recalcitrant biopolymers, such as lignin. In the current study, a bacterial laccase, Lac51, originating from *Pseudomonas putida* and identified in the gut microbiome of the giant panda's gut was transiently expressed in the non-food plant *Nicotiana benthamiana* and characterized. Our results show that recombinant Lac51 exhibits bacterial laccase properties, with optimal pH and temperature at 7–8 and 40°C, respectively, when using syringaldazine as substrate. Moreover, we demonstrate the functional capability of the plant expressed Lac51 to oxidize lignin using selected lignin monomers that serve as substrates of Lac51. In summary, our study demonstrates the potential of green and non-food plants as a viable enzyme production platform for bacterial laccases. This result enriches our understanding of plant-made enzymes, as, to our knowledge, Lac51 is the first functional recombinant laccase produced in plants.

Keywords: bacterial laccase, lignin degrading enzymes, transient expression, tobacco, plant biotechnology

INTRODUCTION

Laccases (EC 1.10.3.2, benzenediol:oxygen oxidoreductases) are a group of blue multi-copper oxidoreductases which are able to catalyze the oxidation of phenols and aromatic biopolymers (e.g., lignin) using molecular oxygen. Laccases, e.g., Lac51, a bacterial laccase originating from the gut microbe *Pseudomonas putida*, are also proposed to play important roles in helping giant panda (*Ailuropoda melanoleuca*) to subsist on bamboo as their almost exclusive diet, by

facilitating the oxidation of lignin moieties, thereby aiding the digestion of bamboo (Zhu et al., 2011; Fang et al., 2012).

Being versatile and eco-friendly enzymes (i.e., not producing toxic peroxide intermediates), laccases have received much attention from scientists and industry. They have been widely applied in food, pulp and paper processing, textile industries, and bioremediation (Chauhan et al., 2017; Yang et al., 2017). Besides, there is a growing interest in their potential utilization for treatment of recalcitrant biomass, such as lignocellulose materials.

In nature, laccases are widely distributed among plants, fungi, bacteria, and insects (Ausec et al., 2011). The most intensively studied ligninolytic laccases and the most applied industrial laccases are from fungi, especially the white-rot basidiomycetes (Martinez et al., 2017). Fungal laccases have a high redox potential and have been used in varying industrial applications, such as food processing, beverage stabilization, and pulp bleaching (Martinez et al., 2017). Unfortunately, fungal laccases are sensitive to temperature and alkaline conditions, which limits their use in industrial applications, where harsh conditions are normally applied in processes such as biomass pretreatment and pulp and paper bleaching (Martinez et al., 2017). In such processes, bacterial laccases could become an alternative as most of them exhibit better tolerance to a broad pH range and high thermostability. For example, the well-known CotA laccase, a coat protein of *Bacillus subtilis*, displays high thermostability with a half-life of inactivation at 80°C of about 4 h (Martins et al., 2002). Furthermore, a laccase isolated from γ-proteobacterium JB works optimally at 55°C and is highly alkali-tolerant, being stable in the pH range 4–10 (Singh et al., 2007).

Owing to their advantageous physiochemical properties, bacterial laccases may become attractive biocatalysts for diverse industrial applications, including lignin processing. Lignin degradation is an important step to facilitate the ability of downstream oxidases to act on the lignin, thus creating access to plant carbohydrates. To achieve lignin degradation, low-molecular-weight small molecules (e.g., ABTS, HBT, and syringaldazine) could act as redox shuttles between the laccase and the lignin (Chen et al., 2012). By using low-molecular-weight redox mediators, such as 2, 2′-azino-bis (3-ethylbenzothazoline-6-sulfonate) (ABTS) and 1-hydroxybenzotriazole (HBT), the range of substrates a laccase can catalyze can be greatly expanded (Chauhan et al., 2017). Actinomycetes, particularly *Streptomyces* species which carry small two-domain laccases have been shown to have high lignin-degrading capacity when supplied with redox mediators (Majumdar et al., 2014). In addition, a *Comamonas* sp. B-9 isolated from eroded bamboo slips exhibits high lignin-degrading activity when grown on kraft lignin as carbon source, which has been attributed to secreted enzymes that include laccases (Chen et al., 2012).

Heterologous expression of bacterial laccases has mostly been done using *Escherichia coli* as the production host (Martins et al., 2002; Suzuki et al., 2003; Wu et al., 2010; Fang et al., 2012). This approach may suffer from low yields or formation of inclusion bodies, complicating downstream purification (Suzuki et al., 2003). Plants have been used for heterologous production of various industrial enzymes (Kwon et al., 2018) due to the low-cost and flexible production scalability. Indeed, plants have been exploited for expression of different laccases derived from plants and fungi (Hood et al., 2003; Wang et al., 2004; Sonoki et al., 2005; Ligaba-Osena et al., 2017; Preethi et al., 2020), but hardly for laccases of bacterial origin.

In this study, we aimed at transiently expressing a bacterial laccase, denoted as Lac51 and originating from a gut microbe of the giant panda (Fang et al., 2012), using the plant *Nicotiana benthamiana*, and to investigate the enzymatic properties of the plant-derived Lac51. Next to assessing substrate oxidation, an LC–MS–MS method was used to investigate the fate of substrates 2,6-dimethoxyphenol (2,6-DMP) and 3,4-dihydroxybenzaldehyde (3,4-DHBA) upon oxidation by plant-produced Lac51, thus generating insight into product formation by this laccase. The functional capability of the enzyme to modify lignin was assessed using selected lignin monomers.

MATERIALS AND METHODS

Lac51 Gene Synthesis

The *lac51* gene (GenBank accession number JN867369.1) from *Pseudomonas putida* (strain L, GenBank accession number AY450556.1; Fang et al., 2012) was chemically synthesized without its native signal peptide by GeneArt (New York, United States) after codon optimization for expression in *Nicotiana benthamiana*. The original TAT signal peptide at the N-terminus was replaced with the plant-derived signal peptide of Barley α-amylase (GenBank accession number CAX51374) linked with a His_6-tag on the N-terminal end of *lac51*.

Construction of the Lac51 Plant Expression Vector

The *lac51* coding region was inserted into the plant transient expression vector pEAQ-*HT*-DEST1 (Sainsbury et al., 2009), as shown in **Figure 1**, using a Gateway cloning system provided by Life Technologies (BP&LR Clonase II kit, donor vector pDONR™/Zeo, Invitrogen, United States). The Gateway cloning BP and LR reactions (Karimi et al., 2002) were conducted based on the manufacturer's protocol, as described previously (Dobrica et al., 2017). Like the *lac51* gene expression vector, a vector containing the red fluorescent protein (*rfp*) reporter gene was constructed.

Agrobacterium-Mediated Transient Expression in *Nicotiana benthamiana*

The plant expression vectors pEAQ-*HT*-DEST1/RFP and pEAQ-*HT*-DEST1/Lac51 were introduced into ElectroMAX™ *Agrobacterium tumefaciens* LBA4404 cells (Invitrogen, United States) by electroporation using a BTX ECM 630 electroporator (BTX-Division of Harvard Apparatus, United States), with the parameters 2.0 kV, 200 Ω, and 25 μF, as described by Clarke et al. (2008). *Agrobacterium* LBA4404 harboring the expression vectors was cultured on LB medium supplemented with 50 mg L^{-1} kanamycin and incubated at 28°C for 72 h. The transformed clones were verified by colony PCR using the gene-specific-attB1/attB2 primer pair (attB1_lac51PSP 5′-GGGGACAAGTTTG

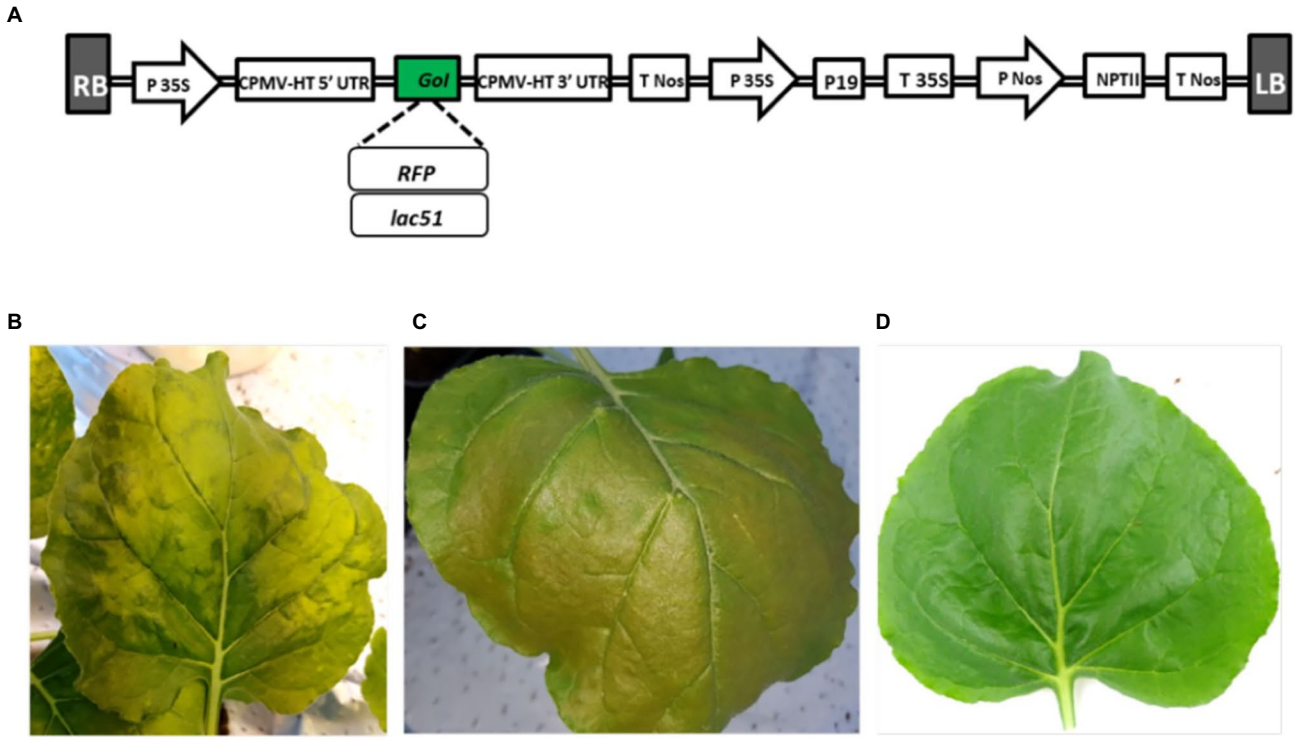


FIGURE 1 | Expression of Lac51. **(A)** Schematic illustration of *lac51* and red fluorescent protein (*RFP*) gene expression vectors. The Lac51-encoding gene was introduced into the pEAQ-HT-DEST1 vector using Gateway cloning technology. RB and LB, right and left borders; CPMV-HT 5′ UTR and 3′ UTR, 5′ and 3′ untranslated regions derived from Cowpea mosaic virus (CPMV); P 35S and T 35S, 35S promoter and terminator; P Nos and T Nos, nopaline synthase promoter and terminator; P19, suppressor of gene silencing; NPTII, neomycin phosphotransferase II gene conferring kanamycin resistance. **(B–D)** Phenotype of *Nicotiana benthamiana* leaves expressing *lac51* **(B)** and the *rfp* reporter gene **(C)**, where the latter gives a distinguishable red color, at 5 dpi, as compared to a leaf infiltrated only with buffer as control **(D)**.

TACAAAAAAGCAGGCTAT GGCTAACAAG CACCTGAG-3′; attB2_lac51PSP 5′-GGGGACC ACTTTGTACAAG AAAGCTGG GTCTACTTCA CCTCAATAGCAG-3′).

For transient expression of the *lac51* and *rfp* genes, *Agrobacterium* cells harboring pEAQ-*HT*-DEST1/RFP or pEAQ-*HT*-DEST1/Lac51 were cultured and prepared as described earlier (Clarke et al., 2017; Dobrica et al., 2017) and infused into *N. benthamiana*, using an in-house vacuum-based agroinfiltration protocol as described previously (Sainsbury et al., 2009). Around 4–6--week-old tobacco plants grown in the growth chamber under a photoperiod of 16 h light and 8 h dark with a temperature of 22°C were subjected to agroinfiltration, using a 2 ml syringe without needle on the underside of the leaves, basically as described by Dobrica et al. (2017). After the agroinfiltration, the *N. benthamiana* plants were grown further in a greenhouse maintaining the growth conditions and harvested after n—days (representing dpi n—m).

Protein Extraction, Western Blot, and Purification

Protein extraction and Western blot analysis were done as before (Gottschamel and Lössl, 2016), with the following modifications. Briefly, for total protein analysis, frozen and grinded leaf samples were homogenized in pre-cold extraction buffer [0.7 M Sucrose, 0.5 M Tris–HCl pH 9.4, 50 mM EDTA, 0.1 M KCl, 2% β-mercaptoethanol (β-ME), 1x Complete protease inhibitor (CPI; Roche, Switzerland)]. After addition of an equal volume of phenol, mixing and incubation on a shaker for 10 min, and centrifugation at 5,500 *g* for 10 min at 4°C, the upper green phase was recovered and re-extracted with cold extraction buffer, mixed and incubated on a shaker for 10 min, and centrifuged at 5,500 *g* for 10 min at 4°C. The upper green phase was collected, and proteins were precipitated by overnight incubation with four volumes of 0.1 M NH_4-acetate in methanol at −20°C. The pellet was recovered after centrifugation at 10,000 *g* for 10 min at 4°C, washed with 0.1 M NH_4-acetate in methanol, air-dried, and dissolved in 1% SDS. The total soluble proteins were obtained by incubating the grinded leaf materials. After incubation for 15 min on ice, the supernatant was retained after centrifugation at 20,000 *g* for 30 min at 4°C. The protein concentration was determined with the Bradford assay (BioRad, United States) using bovine serum albumin (BSA) as standard.

For Western blot analysis, denatured protein samples were separated by electrophoresis in 4–12% SDS-polyacrylamide gels (Invitrogen, United States) and transferred to nitrocellulose membranes (Invitrogen, United States). The membranes were incubated with TBS-T solution (20 mM Tris–HCl pH 7.6, 137 mM NaCl, 0.1% Tween-20) containing 5% BSA as blocking

buffer and subsequently treated with the primary and secondary antibodies diluted in TBS-T solution with 1% BSA. The recombinant proteins were detected with 1:5,000 diluted polyclonal anti-polyHistidine antibody produced in mouse, 1:20,000 diluted anti-AP-conjugated mouse IgG secondary antibody (Promega, United States) and a colorimetric reaction using the AP color development kit (Bio-Rad, United States). Protein samples prepared from tobacco leaves infiltrated with buffer were used as negative control.

For purification, powdered Lac51-containing leaf material was mixed with extraction buffer (0.15 M sodium phosphate buffer pH 8.0, 0.3 M KCl, 20 mM β-ME), filtered through Miracloth (Merck, Darmstadt, Germany) and centrifuged at 25,000 *g*, Lac51 was captured from the resulting supernatant by affinity chromatography using Ni^{2+}-NTA beads (Qiagen, Hilden, Germany), washed with wash buffer (0.1 M sodium phosphate buffer pH 8.0, 0.3 M KCl, 10 mM imidazole), and eluted with elution buffer (0.1 M sodium phosphate buffer pH 8.0, 0.3 M KCl, 0.3 M imidazole). The eluted protein was concentrated using a 30 kDa MWCO Macrosep ultrafiltration device (Pall, Port Washington, United States) and buffer was exchanged to 0.05 M sodium phosphate buffer pH 8.0, 0.1 M KCl.

Enzyme Activity Determination Assays

Laccase activity was assessed with 2,2′-azino-bis (3-ethylbenzothiazoline-6-sulphonic acid; ABTS, Roche diagnostic, Mannheim, Germany) and syringaldazine (Thermo Scientific, Rockford, United States) as model substrates. As a reference, *Tv*Lac from *Trametes versicolor* (Sigma Aldrich, Saint Louis, MO, United States) was used. Enzymatic reactions were set up in 96-well plates with 200 µl total reaction volumes containing 0.1 mM substrate (ABTS or syringaldazine) in 50 mM Na-acetate buffer pH 5.0. The plate was incubated in an Eppendorf Thermomixer C (Eppendorf AG, Hamburg, Germany) at 37°C and 400 rpm and scanned with a Synergy H4 Hybrid plate reader (BioTek, Winooski, VT, United States) at 0.5, 5, 10, 20, and 30 min. Reactions were scanned at 350 and 740 nm for detecting ABTS and the ABTS radical, respectively, and at 530 nm for detecting the oxidized form of syringaldazine. In addition, the full spectrum of the final reactions, from 300 nm to 800 nm, was recorded after 31 min (see **Supplementary Figure S1**).

Determination of pH and Temperature Optima of the Plant Produced Lac51

To evaluate the biochemical activity of Lac51 in different conditions, syringaldazine was used as substrate. The assay system contained Cu^{2+}-saturated Lac51, 50 mM Na-acetate pH 5.0, and 30 µM syringaldazine in a final volume of 0.1 ml. The absorbance was measured at 530 nm for over 30 min at 37°C. The effect of pH on laccase activity was determined using the following buffers: 50 mM Na-acetate buffer (pH 3.0–5.0), 50 mM K_2HPO_4-KH_2PO_4 buffer (pH 6.0–8.0), and 50 mM Tris–HCl buffer (pH 7.0–9.0). The effect of temperature was measured from 25 to 50°C in 50 mM Tris–HCl (pH 7.0).

Enzymatic Reaction With Lignin Monomers

Seven phenolic compounds were tested as potential substrates of Lac51: 2,6-DMP, 3,4-dimethoxybenzalcohol (3,4-DMBA), 3,4-dihydroxybenzaldehyde (3,4-DHBA), 4-methoxybenzylalcohol (4-MBA), gallic acid (GA), vanillin (V), and guaiacol (G), all purchased from Sigma Aldrich (Saint Louis, MO, United States). Enzymatic reactions were carried out in 2-ml Eppendorf tubes with 0.2 ml of total volume. The reactions contained 3 mM substrate and Lac51 or *Tv*Lac in 10 mM BisTris-HCl buffer pH 6.5. The reactions were incubated in an Eppendorf Thermomixer C (Eppendorf AG) at 37°C and 800 rpm for 24 h. After 24 h, the reactions were filtered through a 96-well filter plate equipped with 0.45-µm filter membrane (Merck Millipore Ltd., Tullagreen Carrigtwohill, Ireland) and analyzed with high performance liquid chromatography (HPLC) using a Dionex Ultimate 3000 (Dionex, Sunnyvale, United States) equipped with an Agilent Eclipse Plus C18 RRND 1.8 µm, 2.1 × 50 mm column equilibrated at 30°C and coupled to a Dionex Ultimate 3000 RS VWD UV detector and an LTQ Velos Pro Mass Spectrometer detector (Thermo Scientific, Rockford, United States). The equipment used was as follows: Column: Agilent Eclipse Plus C18 RRND 1.8 µm, 2.1 × 50 mm column; column temperature: 30°C; flow rate: 0.4 ml/min; detection: UV coupled to MS with direct flow; UV–Vis recorded at 315, 450, and 600 nm; MS scan in the *m/z* range 85–1,200. Initially, the column was conditioned with a mixture of 5% eluent B (100% ACN with 0.1% TFA) and 95% eluent A (100% H_2O with 0.1% TFA) for 0.5 min, followed by a linear gradient increasing eluent B from 5 to 95% over 9.5 min. The concentration of eluent B was kept at 95% for 5 min, then increased linearly to 100% over 1 min. Next, the concentration of eluent B was set back to 5% with a linear gradient over 0.5 min. The chromatographic profile ended with reconditioning the column at 5% eluent B for 9 min before the next injection.

RESULTS

Expression and Purification of Lac51 in *Nicotiana benthamiana*

The *lac51-* and *rfp*-expressing vectors (**Figure 1A**) were constructed and successfully introduced in *N. benthamiana* plants (leaves) using vacuum infiltration. Five days after infiltration (dpi), phenotypical alterations (**Figures 1B,C**) could be found when compared with the wild-type control (infiltrated with buffer; **Figure 1D**). To identify the optimal harvest time, material from *lac51*-expressing plant leaves was harvested at different days post infiltration (5, 7, 9, and 12) for analysis of Lac51 accumulation. Total proteins were isolated and subjected to Western blot analysis (**Figure 2**), which showed accumulation of Lac51, peaking at 7 dpi (**Figure 2A**). After 7 dpi, the amount of target protein declined rapidly, potentially indicating protein instability. Then, Lac51 was extracted and purified from leaves

harvested at 7 dpi, using Ni-affinity chromatography and subsequently used for activity assays.

Lac51 Enzyme Activity on Model Substrates

Expression of an active Lac51 protein in *N. benthamiana* was confirmed with the model substrate syringaldazine, using *Tv*Lac (*Trametes versicolor* laccase) as positive control. Lac51 was able to oxidize syringaldazine to its quinone form (indicated by an increase in absorbance at 530 nm), and in the first 10 min of the incubation, the activity of Lac51 was comparable with that of *Tv*Lac (**Figure 3**). However, while *Tv*Lac remained active up to 30 min (i.e., throughout the course of the reaction), the increase in the signal at 530 nm stopped after 10 min in reactions with Lac51, indicating inactivation of the enzyme.

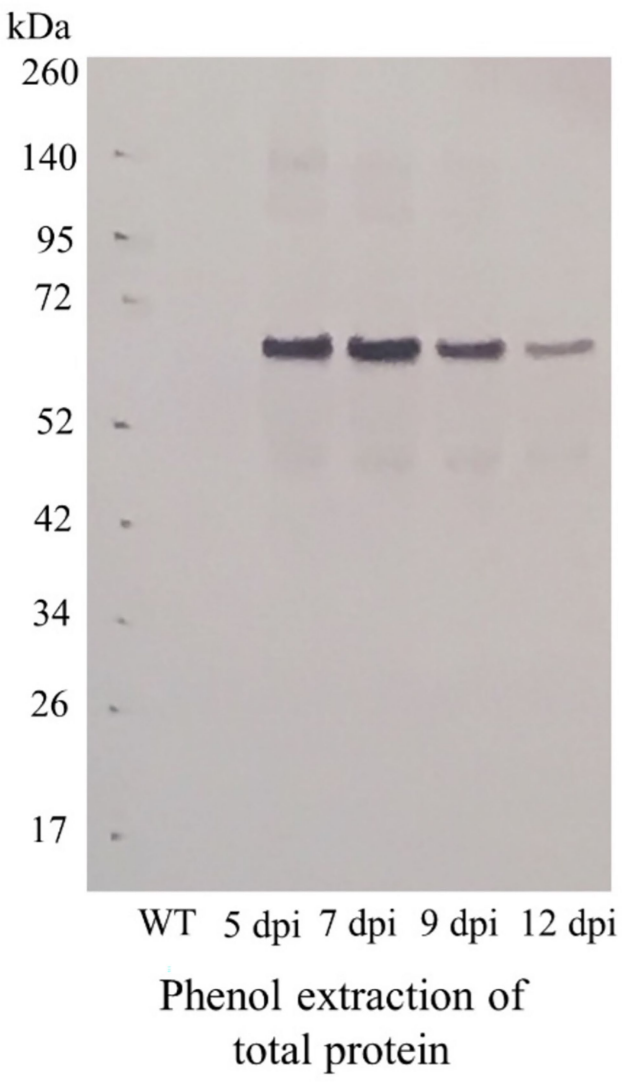


FIGURE 2 | Accumulation of Lac51 protein in *Nicotiana benthamiana* leaves. Immunoblot analysis of total protein extracts from *N. benthamiana* leaves infiltrated with the *lac51* construct, harvested 5, 7, 9, and 12 days after infiltration (dpi) or non-infiltrated leaves (WT).

Lac51 was also incubated with ABTS (**Figure 4**), which is regarded as one of the most sensitive substrates for detecting laccase activity (Li et al., 2008). Accordingly, the control laccase *Tv*Lac generated ABTS radicals at a constant rate (**Figure 4B**), which coincided with a decrease in the ABTS concentration (**Figure 4A**; **Supplementary Figure S1**). On the other hand, incubating ABTS with Lac51 led to only a small decrease in the concentration of the substrate within the initial 5 min, after which the ABTS concentration remained constant throughout the reaction (**Figure 4A**). In addition, Lac51 generated no detectable amounts of ABTS radicals (**Figure 4B**). It is noteworthy that the ligninolytic activity of two enzymes is best compared based on substrate consumption because laccases catalyze radical reactions and generate a broad range of products, some of which may be polymeric and, hence, insoluble in the reaction medium.

Determination of pH and Temperature Optima of Lac51 Using Syringaldazine

As Lac51 showed measurable activity on syringaldazine, we used syringaldazine as a substrate and measured the rate of substrate consumption in the pH range of 3.0–9.0 and temperature range of 25–50°C. The optimal pH for the oxidation of syringaldazine was found to be 7.0, and the optimal temperature at pH 7.0 was found to be 40°C, as shown in **Figure 5**.

Enzyme Activity on Lignin Monomers

Lac51 and the positive control *Tv*Lac were tested for activity on seven lignin monomers. Spectrophotometric analysis revealed that Lac51 was active on three (2,6-DMP, 3,4-DHBA, and GA), while *Tv*Lac was active on five of these seven substrates [2,6-DMP, 3,4-DHBA, GA, vanillin (V), and guaiacol (G); **Table 1**]. After 24 h incubation, Lac51 oxidized 13% of 2,6-DMP, 41% of 3,4-DHBA and 19% of GA (**Figure 6**). *Tv*Lac, on the other hand, reacted more readily with these substrates, oxidizing completely 2,6-DMP and 3,4-DHBA, and leaving only 2% of GA behind in the reaction after 24 h. The action of both enzymes led to formation of insoluble residues in the reactions with 2,6-DMP and GA, presumably through polymerization of the lignin monomers.

Formation of soluble laccase reaction products was confirmed with LC-UV/MS^2 analysis (**Supplementary Figure S2**; **Table 2**; **Supplementary Table S1**). The product profiles of the two enzymes, judged from both UV (**Supplementary Figure S2**) and MS profiles (**Table 2**; **Supplementary Table S1**) differed on all three substrates, which in part may be due to the differences in the extent of substrate conversion and/or polymerization. When subjecting the compounds detected by MS to MS^2 fragmentation (**Supplementary Table S1**), we could identify signals corresponding to the oxidized dimer of 2,6-DMP (with *m/z* value 305.00 in **Table 2**). In the reaction of 2,6-DMP with *Tv*Lac (which led to complete conversion of the substrate, **Figure 6**), products accumulated mostly in the insoluble fraction, leaving virtually no low-molecular-weight components in

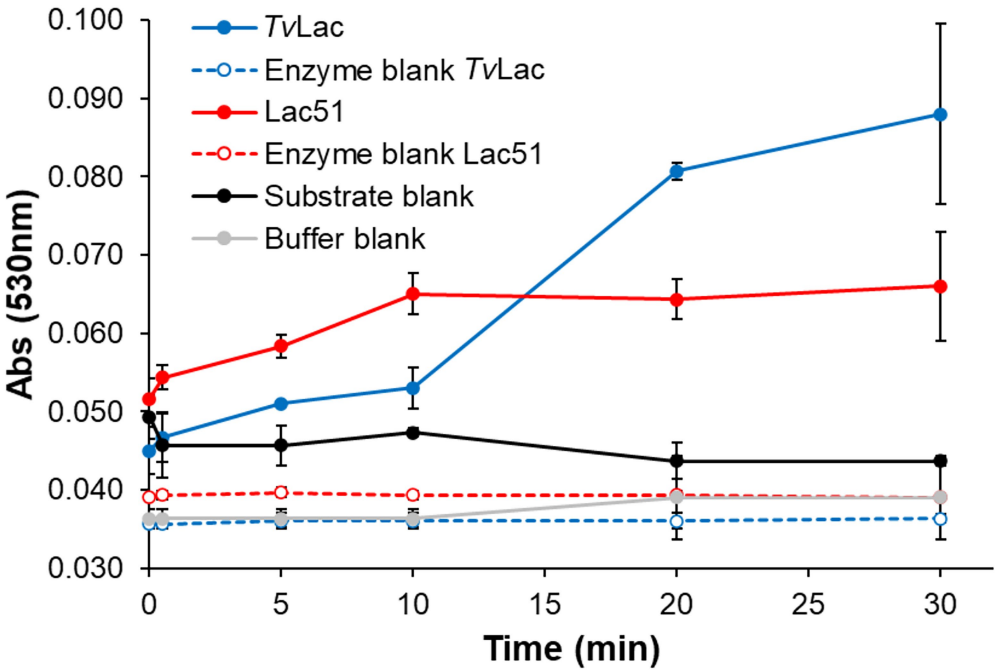


FIGURE 3 | Laccase activity with syringaldazine. Syringaldazine (0.1 mM) was incubated with 0.4 μM Lac51 (red) or 0.2 μM *Tv*Lac (blue) in 50 mM Na-acetate buffer pH 5.0 at 37°C. The reaction was followed by detecting the formation of syringaldazine quinone at 530 nm. Substrate (black line) and enzyme blanks (dashed lines) were prepared by omitting enzymes and substrate, respectively; the buffer blank (gray line) lacked both enzyme and substrate. Error bars indicate SD of triplicates.

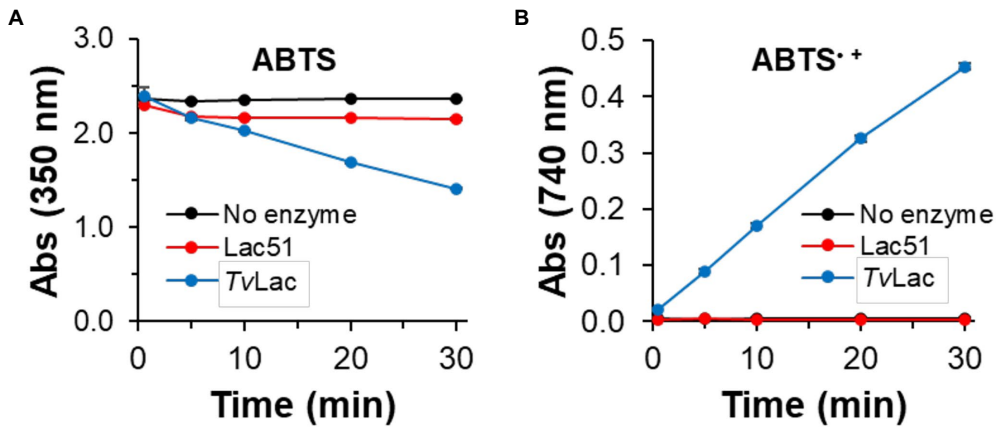


FIGURE 4 | Laccase activity using ABTS. ABTS (0.1 mM) was incubated with 0.4 μM Lac51 (red) or 0.4 μM *Tv*Lac (blue) in 50 mM Na-acetate buffer pH 5.0 at 37°C. The reaction was followed by detecting **(A)** the consumption of ABTS at 350 nm and **(B)** the formation of $ABTS^{\bullet+}$ radical cations at 740 nm. Error bars indicate SD of triplicates.

solution, apart from small amounts of the oxidized dimer (**Supplementary Figure S2A**; **Table 2**). As insoluble polymer was also observed when treating 2,6-DMP with Lac51, albeit in a smaller amount than with *Tv*Lac, it is likely that the peaks observed in the reaction with Lac51 are the intermediate oligomeric products that are polymerized further to form the insoluble residue. Notably, the concentration of the oxidized dimer of 2,6-DMP (at 6.67 min in **Supplementary Figure S2A**) corresponded to the extent of substrate conversion by the two enzymes on 2,6-DMP (**Figure 6**).

DISCUSSION

In the current study, we assessed transient expression of a bacterial laccase, Lac51, originating from *Pseudomonas putida*

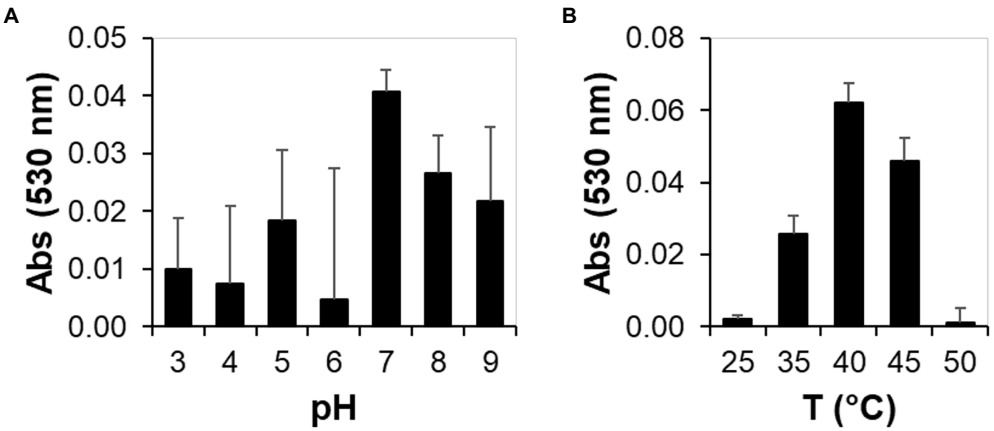


FIGURE 5 | Biochemical activity of plant expressed Lac51 toward syringaldazine under different pH and temperature conditions. Syringaldazine assay was performed in different conditions containing 0.4 μM Cu^{2+}-saturated Lac51, 50 mM Na-acetate, and 30 μM syringaldazine in a final volume of 0.1 ml with different pH **(A)** and temperature **(B)**. The absorbance was measured at 530 nm for over 30 min at 37°C.

TABLE 1 | Activity profile of Lac51 and *Tv*Lac on lignin monomers.

Enzyme	2,6-DMP	3,4-DMBA	3,4-DHBA	4-MBA	GA	V	G
Lac 51	+	–	+	–	+	–	–
*Tv*Lac	+	–	+	–	+	+	+

Lignin monomers (3 mM) were incubated with Lac51 or TvLac in 10 mM BisTris-HCl buffer pH 6.5 at 37°C. The substrates are abbreviated as follows: 2,6-dimethoxyphenol (2,6-DMP); 3,4-dimethoxybenzalcohol (3,4-DMBA); 3,4-dihydroxybenzaldehyde (3,4-DHBA); 4-methoxybenzylalcohol (4-MBA); gallic acid (GA); vanillin (V); and guaiacol (G). A '+' sign indicates modification of the substrate by the laccase. A "-" sign indicates negative modification of the substrate by the laccase.

and identified in the giant panda's gut, in the non-food plant *N. benthamiana* using a vacuum infiltration-based system, providing a low-cost alternative to bacterial and eukaryotic expression hosts. Plants or plant cells/tissues have been used to express valuable recombinant proteins, including vaccines, enzymes, and biopharmaceuticals in molecular farming and have been established as an economically viable (and scalable) alternative to mainstream production systems (Clarke et al., 2013; Bock, 2015; Buyel et al., 2017). In general, nuclear or transient expression is preferred for expression of eukaryotic proteins, mostly when post-translational modification (e.g., glycosylation) of the target protein is a requirement for protein functionality or stability, whereas plastid expression is often the more common choice for expression of bacterial proteins (Xu et al., 2012). Plants have also been exploited for expression of different plant cell wall-active enzymes, including laccases derived from plants and fungi (Hood et al., 2003; Wang et al., 2004; Sonoki et al., 2005), but not laccases of bacterial origin (Preethi et al., 2020). Plant genetic engineering technologies have expanded the diversity of well-established plant-based bioproduction platforms (Paul and Ma, 2011; Xu et al., 2012) and also expressing systems, while stable transgenic lines display high yield of the final product and transient expressing plants exhibit fast processes (Gecchele et al., 2015).

In this work, the recombinant His_6-tagged Lac51 was successfully cloned and transiently expressed in *N. benthamiana*, and the plant-derived Lac51 was shown to be produced in a catalytically active form. Notably, protein instability affected Lac51 accumulation over time, showing the impact of harvest time on the protein yield. Overexpression of plant cell wall-degrading enzymes especially in plant chloroplasts, which is often used for bacterial enzymes, can be a severe physiological burden for the host plant and limit plant growth (Oey et al., 2009). Apart from minor alterations in the leaf tissue (as compared to the RFP control), this was not the case during transient expression of Lac51 (**Figure 1**). The present results show the capability and potential of plant produced enzymes, that, however, still needs further research.

The catalytic activity of the plant produced Lac51 was compared to that of a commercially available fungal laccase *Tv*Lac from *Trametes versicolor* (this study) and to literature data for a recombinant Lac51 expressed in *Escherichia coli* [an earlier study by Fang et al. (2012)]. In general, the plant-expressed Lac51 was found to have similar substrate specificity as well as similar pH (7–8) and temperature (40–45°C) optima on syringaldazine compared to the *E. coli*-expressed variant (Fang et al., 2012). Differences in apparent operational stability may be attributed to differences in reaction conditions, the reaction time in particular [5 min vs. 30 min in Fang et al. (2012) and this study, respectively]. When comparing the (plant expressed) bacterial Lac51 to the fungal *Tv*Lac (this study), there were clear differences

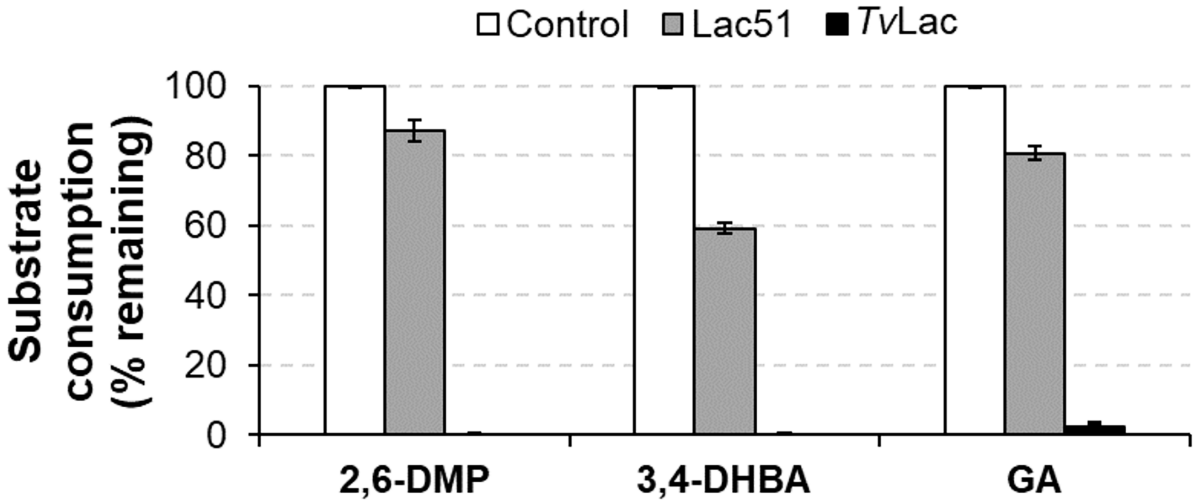


FIGURE 6 | Activity of Lac51 and *Tv*Lac on 2,6-dimethoxyphenol (2,6-DMP), 3,4-dihydroxybenzaldehyde (3,4-DHBA), and gallic acid (GA). Lignin monomers (3 mM) were incubated with 2 μM Lac51 or *Tv*Lac in 10 mM BisTris-HCl buffer pH 6.5 at 37°C for 24 h. The reaction was followed by detecting the consumption of substrate at 315 nm for 2,6-DMP and GA and at 450 nm for 3,4-DHBA. The control reactions contained the substrates without enzyme. Reactions were run in triplicate; error bars represent SDs.

TABLE 2 | Reaction products of Lac51 and *Tv*Lac with lignin monomers identified with LC-UV/MS.

		Compounds identified		
Substrate	**Enzyme**	**Retention time (min)**	***m/z* (H^+) Positive mode**	**Compound type**
2,6-DMP	No enzyme	5.47	155.00	Monomer
		5.49, 6.67	305.00	Oxidized dimer
		5.49[a], 6.67[a], 7.75[a]	307.09	
	Lac51	5.47[a]	155.00	Monomer
		5.54[a]	374.00	
		5.49, 6.67	305.00	Oxidized dimer
		5.49[a], 6.67[a], 7.75[a]	307.09	
		–[b]	–[b]	Insoluble polymer
	*Tv*Lac	5.49, 6.27[a]	305.00	Oxidized dimer
		–[b]	–[b]	Insoluble polymer
3,4-DHBA	No enzyme	2.47	138.92	Monomer
	Lac51	2.47	138.92	Monomer
		4.71	257.09	
		5.04[a]	275.09	
		8.11[a]	451.09	
	*Tv*Lac	1.66[a]	468.09	
		2.18[a]	472.92	
		4.32[a]	466.09	
		4.71	257.09	
		5.04[a]	275.09	
		8.11[a]	451.09	
GA	No enzyme	0.82	170.92	Monomer
	*Tv*Lac	–[b]	–[b]	Insoluble polymer
	Lac51	–[b]	–[b]	Insoluble polymer

Lignin monomers 2,6-DMP, 3,4-DHBA or GA (3 mM) were incubated with Lac51 or TvLac in 10 mM BisTris-HCl buffer pH 6.5 at 37°C for 24 h. For the UV chromatograms, see ***Supplementary Figure S2****.*

[a]*Products with no UV absorbance in* ***Supplementary Figure S2****.*

[b]*Insoluble polymeric products were not detected with LC–MS as they were filtered out of solution before loading the sample on the column.*

in substrate specificity and operational stability between the two enzymes under the tested conditions. In general, *Tv*Lac acted more readily with the tested substrates (**Figures 4**, **6**) and retained its activity over a longer time period (**Figure 3**). The differences in operational stability (**Figure 3**) and possible mode of action (see **Figure 4**) indicate that laccases need to be selected carefully for targeted applications.

In summary, we transiently expressed a bacterial laccase originating from a giant panda gut microbe, denoted as Lac51, which is the first functional recombinant laccase produced in plants. The plant-expressed Lac51 showed enzymatic properties and lignin degradation potential similar to the *E. coli*-expressed variant reported earlier (Fang et al., 2012). Thus, our study demonstrates successful production of a catalytically active bacterial laccase and further shows the potential of green and non-food plants e.g., *N. benthamiana* as an economical enzyme production platform for the future production of bacterial enzymes.

DATA AVAILABILITY STATEMENT

The original contributions presented in the study are included in the article/**Supplementary Material**, further inquiries can be directed to the corresponding author.

AUTHOR CONTRIBUTIONS

AE, AV, HE, VE, and JC conceived and designed the study. LP, YW, and FQ carried out vector design, sequencing and participated in agroinfiltration. YW and AE performed

protein purification and analysis, J-KJ analyzed enzyme properties. AE, YW, AV, HS, and JC drafted the manuscript. All authors contributed to the article and approved the submitted version.

FUNDING

This work was supported by the NIBIO core funding "ArcGene" project 11145 and the Research Council of Norway, through grants 243974 (Bioboost) and 270038 (NorBioLab).

ACKNOWLEDGMENTS

The authors thank Hege S. Steen, Sissel Haugslien, and Inger Heldal for their technical support to this study.

SUPPLEMENTARY MATERIAL

The Supplementary Material for this article can be found online at: https://www.frontiersin.org/articles/10.3389/fpls.2022.912293/full#supplementary-material

REFERENCES

Ausec, L., Zakrzewski, M., Goesmann, A., Schluüter, A., and Mandic-Mulec, I. (2011). Bioinformatic analysis reveals high diversity of bacterial genes for laccase-like enzymes. *PLoS One* 6:e25724. doi: 10.1371/journal.pone.0025724

Bock, R. (2015). Engineering plastid genomes: methods, tools, and applications in basic research and biotechnology. *Annu. Rev. Plant Biol.* 66, 211–241. doi: 10.1146/annurev-arplant-050213-040212

Buyel, J. F., Twyman, R. M., and Fischer, R. (2017). Very-large-scale production of antibodies in plants: the biologization of manufacturing. *Biotechnol. Adv.* 35, 458–465. doi: 10.1016/j.biotechadv.2017.03.011

Chauhan, P. S., Goradia, B., and Saxena, A. (2017). Bacterial laccase: recent update on production, properties and industrial applications. *3 Biotech* 7:323. doi: 10.1007/s13205-017-0955-7

Chen, Y. H., Chai, L. Y., Zhu, Y. H., Yang, Z. H., Zheng, Y., and Zhang, H. (2012). Biodegradation of kraft lignin by a bacterial strain *Comamonas* sp. B-9 isolated from eroded bamboo slips. *J. Appl. Microbiol.* 112, 900–906. doi: 10.1111/j.1365-2672.2012.05275.x

Clarke, J. L., Paruch, L., Dobrica, M.-O., Caras, I., Tucureanu, C., Onu, A., et al. (2017). Lettuce-produced hepatitis C virus E1E2 heterodimer triggers immune responses in mice and antibody production after oral vaccination. *Plant Biotechnol. J.* 15, 1611–1621. doi: 10.1111/pbi.12743

Clarke, J. L., Spetz, C., Haugslien, S., Xing, S., Dees, M. W., Moe, R., et al. (2008). *Agrobacterium tumefaciens*-mediated transformation of poinsettia, *Euphorbia pulcherrima*, with virus-derived hairpin RNA constructs confers resistance to *Poinsettia mosaic virus*. *Plant Cell Rep.* 27, 1027–1038. doi: 10.1007/s00299-008-0526-9

Clarke, J. L., Waheed, M. T., and Lössl, A. G. (2013). How can plant genetic engineering contribute to cost-effective fish vaccine development for promoting sustainable aquaculture? *Plant Mol. Biol.* 83, 33–40. doi: 10.1007/s11103-013-0081-9

Dobrica, M. O., Lazar, C., Paruch, L., Skomedal, H., Steen, H., Haugslien, S., et al. (2017). A novel chimeric hepatitis B virus S/preS1 antigen produced in mammalian and plant cells elicits stronger humoral and cellular immune response than the standard vaccine-constituent, S protein. *Antivir. Res.* 144, 256–265. doi: 10.1016/j.antiviral.2017.06.017

Fang, W., Fang, Z., Zhou, P., Chang, F., Hong, Y., Zhang, X., et al. (2012). Evidence for lignin oxidation by the giant panda fecal microbiome. *PLoS One* 7:e50312. doi: 10.1371/journal.pone.0050312

Gecchele, E., Merlin, M., Brozzetti, A., Falorni, A., Pezzotti, M., and Avesani, L. (2015). A comparative analysis of recombinant protein expression in different biofactories: bacteria, insect cells and plant systems. *J. Vis. Exp.* 97:e52459. doi: 10.3791/52459

Gottschamel, J., and Lössl, A. (2016). Erratum to: chloroplast-based expression of recombinant proteins by gateway cloning technology. *Methods Mol. Biol.* 1385:E1. doi: 10.1007/978-1-4939-3289-4_20

Hood, E. E., Bailey, M. R., Beifuss, K., Magallanes-Lundback, M., Horn, M. E., Callaway, E., et al. (2003). Criteria for high-level expression of a fungal laccase gene in transgenic maize. *Plant Biotechnol. J.* 1, 129–140. doi: 10.1046/j.1467-7652.2003.00014.x

Karimi, M., Inze, D., and Depicker, A. (2002). GATEWAYTM vectors for *Agrobacterium*-mediated plant transformation. *Trends Plant Sci.* 7, 193–195. doi: 10.1016/s1360-1385(02)02251-3

Kwon, K. C., Sherman, A., Chang, W. J., Kamesh, A., Biswas, M., Herzog, R. W., et al. (2018). Expression and assembly of largest foreign protein in chloroplasts: oral delivery of human FVIII made in lettuce chloroplasts robustly suppresses inhibitor formation in *haemophilia A* mice. *Plant Biotechnol. J.* 16, 1148–1160. doi: 10.1111/pbi.12859

Li, A., Zhu, Y., Xu, L., Zhu, W., and Tian, X. (2008). Comparative study on the determination of assay for laccase of *Trametes* sp. *Afr. J. Biochem. Res.* 2, 181–183. doi: 10.5897/AJBR.9000064

Ligaba-Osena, A., Hankoua, B., DiMarco, K., Pace, R., Crocker, M., McAtee, J., et al. (2017). Reducing biomass recalcitrance by heterologous expression of a bacterial peroxidase in tobacco (*Nicotiana benthamiana*). *Sci. Rep.* 7:17104. doi: 10.1038/s41598-017-16909-x

Majumdar, S., Lukk, T., Solbiati, J. O., Bauer, S., Nair, S. K., Cronan, J. E., et al. (2014). Roles of small laccases from Streptomyces in lignin degradation. *Biochemistry* 53, 4047–4058. doi: 10.1021/bi500285t

Martinez, A. T., Ruiz-Duenas, F. J., Camarero, S., Serrano, A., Linde, D., Lund, H., et al. (2017). Oxidoreductases on their way to industrial biotransformations. *Biotechnol. Adv.* 35, 815–831. doi: 10.1016/j.biotechadv.2017.06.003

Martins, L. O., Soares, C. M., Pereira, M. M., Teixeira, M., Costa, T., Jones, G. H., et al. (2002). Molecular and biochemical characterization of a highly stable bacterial laccase that occurs as a structural component of the *Bacillus subtilis* endospore coat. *J. Biol. Chem.* 277, 18849–18859. doi: 10.1074/jbc.M200827200

Oey, M., Lohse, M., Kreikemeyer, B., and Bock, R. (2009). Exhaustion of the chloroplast protein synthesis capacity by massive expression of a highly stable protein antibiotic. *Plant J.* 57, 436–445. doi: 10.1111/j.1365-313X.2008.03702.x

Paul, M., and Ma, J. K. C. (2011). Plant-made pharmaceuticals: leading products and production platforms. *Biotechnol. Appl. Biochem.* 58, 58–67. doi: 10.1002/bab.6

Preethi, P. S., Gomathi, A., Srinivasan, R., Kumar, J. G. S. P., Murugesan, K., and Kodiveri, M. G. (2020). "Laccase: recombinant expression, engineering and its promising applications," in *Microbial Enzymes: Roles and Applications in Industries. Microorganisms for Sustainability*, *Vol. 11* (Singapore: Springer).

Sainsbury, F., Thuenemann, E. C., and Lomonossoff, G. P. (2009). pEAQ: versatile expression vectors for easy and quick transient expression of heterologous proteins in plants. *Plant Biotechnol. J.* 7, 682–693. doi: 10.1111/j.1467-7652.2009.00434.x

Singh, G., Capalash, N., Goel, R., and Sharma, P. (2007). A pH-stable laccase from alkali-tolerant γ-proteobacterium JB: purification, characterization and indigo carmine degradation. *Enzym. Microb. Technol.* 41, 794–799. doi: 10.1016/j.enzmictec.2007.07.001

Sonoki, T., Kajita, S., Ikeda, S., Uesugi, M., Tatsumi, K., Katayama, Y., et al. (2005). Transgenic tobacco expressing fungal laccase promotes the detoxification of environmental pollutants. *Appl. Microbiol. Biotechnol.* 67, 138–142. doi: 10.1007/s00253-004-1770-8

Suzuki, T., Endo, K., Ito, M., Tsujibo, H., Miyamoto, K., and Inamori, Y. (2003). A thermostable laccase from *Streptomyces lavendulae* REN-7: purification, characterization, nucleotide sequence, and expression. *Biosci. Biotechnol. Biochem.* 67, 2167–2175. doi: 10.1271/bbb.67.2167

Wang, G., Li, Q., Luo, B., and Chen, X. (2004). Ex planta phytoremediation of trichlorophenol and phenolic allelo chemicals via an engineered secretory laccase. *Nat. Biotechnol.* 22, 893–897. doi: 10.1038/nbt982

Wu, J., Kim, K. S., Lee, J. H., and Lee, Y. C. (2010). Cloning, expression in *Escherichia coli*, and enzymatic properties of laccase from *Aeromonas hydrophila* WL-11. *J. Environ. Sci.* 22, 635–640. doi: 10.1016/S1001-0742(09)60156-X

Xu, J., Dolan, M. C., Medrano, G., Cramer, C. L., and Weathers, P. J. (2012). Green factory: plants as bioproduction platforms for recombinant proteins. *Biotechnol. Adv.* 30, 1171–1184. doi: 10.1016/j.biotechadv.2011.08.020

Yang, J., Li, W., Ng, T. B., Deng, X., Lin, J., and Ye, X. (2017). Laccases: production, expression regulation, and applications in pharmaceutical biodegradation. *Front. Microbiol.* 8:832. doi: 10.3389/fmicb.2017.00832

Zhu, L., Wu, Q., Dai, J., Zhang, S., and Wei, F. (2011). Evidence of cellulose metabolism by the giant panda gut microbiome. *Proc. Natl. Acad. Sci. U. S. A.* 108, 17714–17719. doi: 10.1073/pnas.1017956108

Conflict of Interest: The authors declare that the research was conducted in the absence of any commercial or financial relationships that could be construed as a potential conflict of interest.

Publisher's Note: All claims expressed in this article are solely those of the authors and do not necessarily represent those of their affiliated organizations, or those of the publisher, the editors and the reviewers. Any product that may be evaluated in this article, or claim that may be made by its manufacturer, is not guaranteed or endorsed by the publisher.

Copyright © 2022 van Eerde, Várnai, Wang, Paruch, Jameson, Qiao, Eiken, Su, Eijsink and Clarke. This is an open-access article distributed under the terms of the Creative Commons Attribution License (CC BY). The use, distribution or reproduction in other forums is permitted, provided the original author(s) and the copyright owner(s) are credited and that the original publication in this journal is cited, in accordance with accepted academic practice. No use, distribution or reproduction is permitted which does not comply with these terms.

frontiers | Frontiers in Plant Science

ORIGINAL RESEARCH
published: 19 May 2022
doi: 10.3389/fpls.2022.878733

Eradication of *Potato Virus S*, *Potato Virus A*, and *Potato Virus M* From Infected *in vitro*-Grown Potato Shoots Using *in vitro* Therapies

Jean Carlos Bettoni[1]‡, Liya Mathew[1‡], Ranjith Pathirana[1†], Claudia Wiedow[1], Donald A. Hunter[1], Andrew McLachlan[1], Subuhi Khan[2], Joe Tang[2] and Jayanthi Nadarajan[1]*

[1]The New Zealand Institute for Plant and Food Research Limited, Food Industry Science Centre, Palmerston North, New Zealand, [2]Plant Health and Environment Laboratory, Ministry for Primary Industries, Auckland, New Zealand

OPEN ACCESS

Edited by:
Walter Chitarra, Council for Agricultural and Economics Research (CREA), Italy

Reviewed by:
Giorgio Gambino, Institute for Sustainable Plant Protection (CNR), Italy
Svetlana Kushnarenko, Institute of Plant Biology and Biotechnology, Kazakhstan

***Correspondence:**
Jean Carlos Bettoni
Jean.Bettoni@plantandfood.co.nz

†Present address:
Ranjith Pathirana, Plant & Food Research Australia Pty Ltd., Waite Institute, Urrbrae, SA, Australia

‡These authors share first authorship

Specialty section:
This article was submitted to Plant Biotechnology, a section of the journal Frontiers in Plant Science

Received: 18 February 2022
Accepted: 19 April 2022
Published: 19 May 2022

Citation:
Bettoni JC, Mathew L, Pathirana R, Wiedow C, Hunter DA, McLachlan A, Khan S, Tang J and Nadarajan J (2022) Eradication of Potato Virus S, Potato Virus A, and Potato Virus M From Infected in vitro-Grown Potato Shoots Using in vitro Therapies. Front. Plant Sci. 13:878733. doi: 10.3389/fpls.2022.878733

Certain viruses dramatically affect yield and quality of potatoes and have proved difficult to eradicate with current approaches. Here, we describe a reliable and efficient virus eradication method that is high throughput and more efficacious at producing virus-free potato plants than current reported methods. Thermotherapy, chemotherapy, and cryotherapy treatments were tested alone and in combination for ability to eradicate single and mixed *Potato virus S* (PVS), *Potato virus A* (PVA), and *Potato virus M* (PVM) infections from three potato cultivars. Chemotherapy treatments were undertaken on *in vitro* shoot segments for four weeks in culture medium supplemented with 100 mg L^{-1} ribavirin. Thermotherapy on *in vitro* shoot segments was applied for two weeks at 40°C (day) and 28°C (night) with a 16 h photoperiod. Plant vitrification solution 2 (PVS2) and cryotherapy treatments included a shoot tip preculture followed by exposure to PVS2 either without or with liquid nitrogen (LN, cryotherapy) treatment. The virus status of control and recovered plants following therapies was assessed in post-regeneration culture after 3 months and then retested in plants after they had been growing in a greenhouse for a further 3 months. Microtuber production was investigated using *in vitro* virus-free and virus-infected segments. We found that thermotherapy and cryotherapy (60 min PVS2 + LN) used alone were not effective in virus eradication, while chemotherapy was better but with variable efficacy (20–100%). The most effective result (70–100% virus eradication) was obtained by combining chemotherapy with cryotherapy, or by consecutive chemotherapy, combined chemotherapy and thermotherapy, then cryotherapy treatments irrespective of cultivar. Regrowth following the two best virus eradication treatments was similar ranging from 8.6 to 29% across the three cultivars. The importance of virus removal on yield was reflected in "Dunluce" free of PVS having higher numbers of microtubers and in "V500' free of PVS and PVA having a greater proportion of microtubers > 5 mm. Our improved procedure has potential for producing virus-free planting material for the potato industry. It could also underpin the global exchange of virus-free germplasm for conservation and breeding programs.

Keywords: cryotherapy, thermotherapy, chemotherapy, high-health plants, shoot tips, cryopreservation, microtubers, *Solanum tuberosum*

INTRODUCTION

Potato (*Solanum tuberosum*) is the world's third most important food crop after rice and wheat, and is the staple food of 1.3 billion people (Devaux et al., 2021). In 2019, the planted area of potatoes, globally, reached 17.3 million hectares, producing of over 370 million tons of which 45% was produced in China (25%), India (14%), and Russia (6%; FAOSTAT-Food and Agriculture Organization of the United Nations, 2021). In New Zealand, potato is a valuable commodity crop with 497,634 MT produced from 9,775 ha: in 2020, this production was valued at NZ$ 1.1 billion, including a significant export value close to NZ$ 106 million (Potatoes NZ, 2021). At the New Zealand Institute for Plant and Food Research Ltd. (PFR), we maintain field collections covering both old and new cultivars that have been used in breeding programs. A subset of these are held in tissue culture and a cryopreservation program to secure the collection is underway (Pathirana et al., 2019), with over 300 lines already secured.

High-quality seed potato is crucial for successful potato cultivation (Onofre et al., 2021). Viral diseases are one of the primary reason for degeneration of seed potatoes and thus constitute a major constraint for sustainable potato production (Awasthi and Verma, 2017; Priegnitz et al., 2019; Wasilewska-Nascimento et al., 2020). Vegetative propagation of potato results in virus transmission from generation to generation, with virus titers accumulating as a result of repeated propagation and infection events (Thomas-Sharma et al., 2016; Priegnitz et al., 2020). As well as inducing increased susceptibility to other pathogens, viral diseases cause economic losses due to their negative impacts on yield and tuber quality (Lin et al., 2014; Adolf et al., 2020).

Although around 57 viruses have been identified as infecting cultivated potatoes, only a few are reported to have a major economic impact. *Potato virus M* (PVM; *Carlavirus*), *Potato virus A* (PVA; *Potyvirus*), and *Potato virus S* (PVS; *Carlavirus*) are typically the most significant viral pathogens (either as single or as mixed infections) associated with substantial production losses (Wang et al., 2011; Fletcher, 2012; Kreuze et al., 2020). These virus species are disseminated through tubers and by aphids in a non-persistent manner. PVS and PVA are also transmitted by contact (Valkonen, 2007; Fuentes et al., 2021). Plants infected by PVM and PVS may not always show symptoms depending on the cultivar and virus isolates (Kreuze et al., 2020; Bradshaw, 2021). Furthermore, mixed infection can increase symptom severity and virus accumulation (Nyalugwe et al., 2012; Moreno and López-Moya, 2020).

Production of virus-free plants is necessary for successful management of viral diseases and for sustainable breeding activities including preservation of potato germplasm and global exchange of genetic resources (Naik and Khurana, 2003; Volmer et al., 2017; Ellis et al., 2020). Besides complete eradication, there are no effective measures for controlling viruses once the plants are infected (Nazarov et al., 2020; Rubio et al., 2020). Therefore, there is a need to develop efficient methods to eradicate virus species to ensure production and supply of high-healthy planting material for the potato industry. Various *in vitro*-based techniques have been used to eradicate viruses in potato plants. For example, meristem culture used either alone (Quazi and Martin, 1978; Wang et al., 2006; Zhang et al., 2019) or in combination with thermotherapy (Wang et al., 2006; AlMaarri et al., 2012; Waswa et al., 2017), chemotherapy (AlMaarri et al., 2012), and electrotherapy (AlMaarri et al., 2012). In meristem culture-based methods, the size of the explant affects the efficacy of virus eradication; it is usually necessary to excise shoot tips of 0.2 mm containing an apical dome with one or two leaf primordia (Wang et al., 2006; Zhang et al., 2019). Excision of such small shoot tips is laborious, time-consuming, and a highly skilled task: results can also be variable in terms of shoot regrowth and the frequency of virus eradication (Bettoni et al., 2016; Magyar-Tábori et al., 2021). The inability to guarantee complete removal of viral particles, especially in mixed infections, remains a limitation for these meristem culture-based methods (Faccioli and Marani, 1998; Zhang et al., 2019). Application of shoot tip cryotherapy as a novel method for plant virus eradication has also been tested in potato with mixed results (Wang et al., 2006; Jianming et al., 2012; Yi et al., 2014; Li et al., 2016, 2018a; Zhang et al., 2019). For example, *Potato leafroll virus* (PLRV) and *Potato virus Y* (PVY) have been successfully eliminated with high efficacy using cryogenic treatments (Wang et al., 2006; Yi et al., 2014; Zhang et al., 2019); however, this method completely failed in producing PVM- and PVS-free potato plants when they presented as a mixed infection (Li et al., 2018a; Zhang et al., 2019).

Improved potato virus eradication has been achieved by combining two or more *in vitro*-based techniques. Combining chemotherapy with thermotherapy (Fletcher et al., 1988; Fang et al., 2005; Dhital et al., 2007; Nasir et al., 2010; Antonova et al., 2017) and meristem culture (Zhang et al., 2019) or chemotherapy with cryotherapy (Kushnarenko et al., 2017) were shown to provide more effective virus eradication than just a single technique. However, the efficacy of these methods varied according to the virus species, their infection level (single or mixed, virus titer) and cultivars used, as well as the virus-host combination (Antonova et al., 2017; Waswa et al., 2017; Gong et al., 2019). Furthermore, duration and temperature of the thermotherapy treatment, types, and concentrations of antiviral agents used in chemotherapy, as well as the size of the excised shoot tip can affect the success of virus eradication (AlMaarri et al., 2012; Kushnarenko et al., 2017; Waswa et al., 2017; Magyar-Tábori et al., 2021). Therefore, standardization of the virus eradication methodology is important, especially when the plants have mixed infections.

Herein, we investigated the effect of chemotherapy, thermotherapy, and cryotherapy on eradication of PVM, PVA, and PVS from *in vitro* cultured shoots of three potato cultivars. More specifically, we combined several of these methods to develop a novel technology that is high throughput, easier,

and more effective in eradicating virus. We believe that this technology can be easily adopted and transferred between laboratories, facilitating delivery of healthy propagating material to growers for commercial production and for germplasm conservation and plant exchange. Data demonstrating the positive effect that removal of these viruses has on microtuber yield are also presented.

MATERIALS AND METHODS

Plant Material and Explant Preparation for *in vitro* Therapies

Tissue-cultured plants of three potato (*Solanum tuberosum* L.) cultivars "Dunluce," "Tahi," and "V500" were obtained from the Lincoln site of PFR and used in this study. Infected *in vitro* stock plants with PVM, PVA, and PVS were previously identified and confirmed using the reverse-transcription polymerase chain reaction (RT-qPCR) method (see below) prior to the experiments outlined here. Virus-infected cultures ("Dunluce" with PVS, "Tahi" with PVA and PVS, and "V500" with PVM and PVS) were multiplied and maintained in an actively growing state on basal medium (BM) composed of half-strength Murashige and Skoog (1962; MS) macronutrients, full-strength MS micronutrients, and Linsmaier and Skoog (1965; LS) vitamins supplemented with 30 g L^{-1} sucrose and 7.5 g L^{-1} agar. For all experiments, the pH of culture media was adjusted to 6 prior to autoclaving at 121°C for 20 min. Cultures were incubated in a growth room maintained at 24°C with a 16 h photoperiod at a photosynthetic flux density of 40 µmol s^{-1} m^{-2} provided by cool-white fluorescent tubes (hereafter called standard conditions). Subculture into fresh BM was performed every 4 weeks throughout the experiment.

The explants used for *in vitro* therapies were nodal sections (1 cm in length) obtained from 3-week-old *in vitro* stock plants and placed on 90 × 15 mm disposable polystyrene Petri plates containing 25 ml of BM at a density of 30 to 40 nodal sections per plate. The nodal sections were cultured under standard conditions to provide uniform explant material for the therapies. The apical shoot tips (1 mm) for cryotherapy were excised from the nodal sections after 1 week, and the shoots (1.5 cm) for chemotherapy/thermotherapy experiments were excised from the nodal sections after 2 weeks. **Figure 1** shows the workflow for this study.

In vitro Therapies for Virus Eradication

Control Shoot Tips (SP)

Uniform apical shoot tips (1 mm length) were excised from 1-week-old shoots and cultured on recovery medium (RM) consisting of MS macro and micro elements, LS vitamins, 25 g L^{-1} sucrose, 0.05 mg L^{-1} indole-3-acetic acid, 0.05 mg L^{-1} gibberellic acid, 0.3 mg L^{-1} zeatin, and 6 g L^{-1} agar at pH 5.7; (Kim et al., 2006 with modifications) and incubated in the dark at 24°C for 1 week before transfer to standard conditions.

Plant Vitrification Solution 2 Treatment (PVS2)

Uniform apical shoot tips (1 mm length) were excised from 1-week-old shoots and transferred to liquid preculture medium 1 (half-strength MS macronutrients, MS micronutrients, and LS vitamins containing 0.3 M sucrose) and maintained for 24 h on a shaker (50 rpm) in darkness at 24°C. They were then transferred to liquid preculture medium 2 (same salts as preculture medium 1 but with 0.7 M sucrose) and maintained under the same conditions for another 16 h. Precultured shoot tips were treated with plant vitrification solution 2 (PVS2) [filter-sterilized MS, 0.4 M sucrose, 30% (w/v) glycerol, 15% (w/v) ethylene glycol (EG), and 15% (w/v) dimethyl sulfoxide (DMSO), pH 5.8] (Sakai et al., 1990) at 22°C for 60 min (PVS2 treatment).

Following PVS2 treatment, the shoot tips were washed with unloading solution (filter-sterilized half-strength MS macronutrients, MS micronutrients + 1.2 M sucrose at pH 5.8) pre-warmed to 40°C and maintained in the solution for 20 min at room temperature (22°C). Thereafter, for recovery, shoot tips were transferred to an intermediate recovery medium (half-strength MS macronutrients, MS micronutrients supplemented with 0.6 M sucrose, and 7.5 g L^{-1} agar) overnight in the dark and then transferred to RM. Cultures were maintained 1 week in the dark at 24°C, before being transferred to standard conditions.

Additionally, the survival, shoot regrowth, and virus eradication efficiency from shoot tips after treatment with one of seven PVS2 exposure periods between 5 and 135 min in "Dunluce" and after short, medium, and long PVS2 exposure periods (5, 60, and 135 min, respectively) in "Tahi" and "V500" were assessed.

Cryotherapy

For cryotherapy (Cryo), similar steps to those described in "PVS2" were followed, and 2 minutes before the end of PVS2 incubations, PVS2-treated shoot tips were placed into a thin layer of PVS2 on sterile aluminum foil strips (~6 × 25 mm) and then plunged into LN. After 1 hour of LN exposure, the aluminum foil strips with shoot tips were thawed quickly by inverting the strips into unloading solution and recovered as described in "PVS2" above.

Thermotherapy (T)

Apical shoot segments (1–1.5 cm in length) were excised from 2-week-old shoots and placed in 98 × 60 mm disposable polystyrene clear tissue culture vessels with 50 ml BM at a density of 15 nodal sections per culture vessel. After 2 days of culture under standard conditions, the culture vessels containing shoot segments were moved into a growth chamber with 40% relative humidity at a photosynthetic photon flux density of 70 µmol s^{-1} m^{-2} provided by cool-white fluorescent tubes. The shoots were grown in an alternating temperature regime of 28°C for 8 h in darkness and 40°C for 16 h with light for 2 weeks. Apical shoot tips (1 mm length) were excised from heat-treated shoots and cultured on RM in the dark at 24°C for 1 week before transfer to standard conditions.

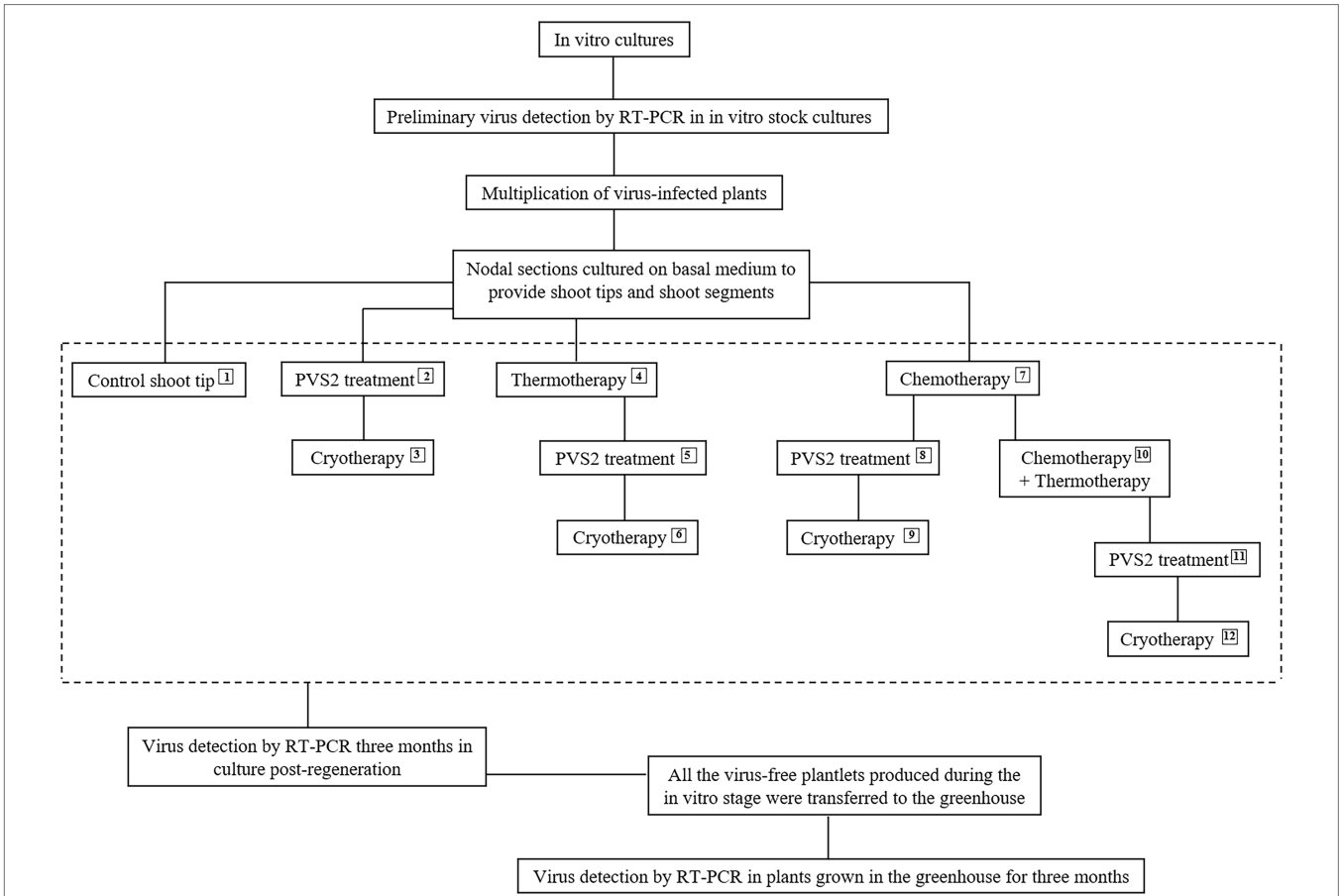


FIGURE 1 | Flowchart depicting the 12 *in vitro* therapies used for eradicating *Potato virus S*, *Potato virus A,* and *Potato virus M* from infected *in vitro*-grown potato shoots. Plant vitrification solution 2 (PVS2) and cryotherapy treatments were performed on 1 mm apical shoot tips and thermotherapy and chemotherapy on 1–1.5 cm apical shoot segments.

Thermotherapy + PVS2 (T + PVS2)

Apical shoot segments (1–1.5 cm in length) were subjected to thermotherapy, as described in "Thermotherapy", after which apical shoot tips (1 mm length) were excised and subjected to PVS2 treatment (PVS2) as described in "PVS2".

Thermotherapy + Cryotherapy (T + Cryo)

Apical shoot segments (1–1.5 cm in length) were subjected to thermotherapy, as described in "Thermotherapy", after which apical shoot tips (1 mm length) were excised and subjected to cryotherapy (Cryo) as described in "Cryotherapy".

Chemotherapy (C)

Apical shoot segments (1–1.5 cm in length) were excised from 2-week-old shoots and placed in 98 × 60 mm disposable polystyrene clear tissue culture vessels containing 50 ml BM supplemented with 100 mg L^{-1} ribavirin (Duchefa®, Haarlen, Netherlands) at a density of 15 nodal sections per culture vessel. Ribavirin was filter-sterilized and added to the medium after autoclaving. The cultures were maintained under standard conditions. After 4 weeks of ribavirin treatment, apical shoot tips (1 mm length) were excised and placed on RM and incubated in the dark at 24°C for 1 week before transfer to standard conditions.

Chemotherapy + PVS2 (C + PVS2)

Apical shoot segments (1–1.5 cm in length) were cultured on BM supplemented with 100 mg L^{-1} ribavirin for 4 weeks under standard conditions, as described in "Chemotherapy", after which apical shoot tips (1 mm length) were excised and subjected to PVS2 treatment (PVS2) as described in "PVS2".

Chemotherapy + Cryotherapy (C + Cryo)

Apical shoot segments (1–1.5 cm in length) were cultured on BM supplemented with 100 mg L^{-1} ribavirin for 4 weeks under standard conditions, as described in "Chemotherapy", after which apical shoot tips (1 mm length) were excised and subjected to cryotherapy (Cryo) as described in "Cryotherapy".

Chemotherapy Followed by Combined Chemotherapy and Thermotherapy [C + (C + T)]

Apical shoot segments (1–1.5 cm in length) were cultured on BM supplemented with 100 mg L^{-1} ribavirin for 2 weeks

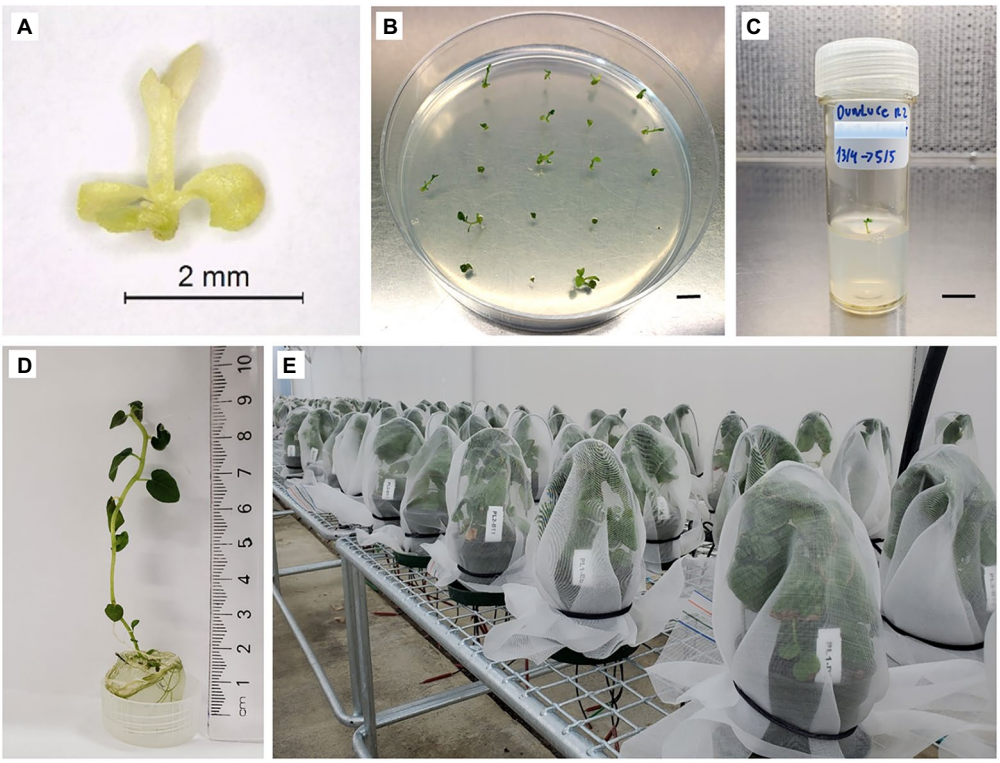


FIGURE 2 | Shoot tip recovery process in potato "Dunluce" following a combined chemotherapy + cryotherapy treatment. **(A)** Shoot tip 1 week after combined chemotherapy + cryotherapy and **(B)** 3 weeks recovery from cryoexposure. **(C)** Shoot transferred to vial and **(D)** grown for 3 months. **(E)** Plants after 3 months of growth in the greenhouse. Bars = B 0.6 cm, C 0.7 cm.

under standard conditions, as described in "Chemotherapy", after which the tissue culture vessel containing the shoots in ribavirin medium was transferred to thermotherapy conditions as described in "Thermotherapy" for additional 2 weeks, followed by apical shoot tip isolation (1 mm length) and recovery process as described in "Thermotherapy".

Chemotherapy Followed by Combined Chemotherapy and Thermotherapy, Then PVS2 [C + (C + T) + PVS2]

Apical shoot segments (1–1.5 cm in length) were treated as described in "Chemotherapy Followed by Combined Chemotherapy and Thermotherapy [C + (C + T)]" above, after which apical shoot tips (1 mm length) were excised and subjected to PVS2 treatment (PVS2), as described in "PVS2".

Chemotherapy Followed by Combined Chemotherapy and Thermotherapy, Then Cryotherapy [C + (C + T) + Cryo]

Apical shoot segments (1–1.5 cm in length) were treated as described in "Chemotherapy Followed by Combined Chemotherapy and Thermotherapy [C + (C + T)]", after which apical shoot tips (1 mm length) were excised and subjected to cryotherapy (Cryo), as described in "Cryotherapy".

Shoot Tip Recovery

Shoot tip survival (shoot tips that exhibited growth of a green cell mass or leaf tissue; **Figure 2A**) and regrowth (shoot tips exhibiting organized shoots with a new leaf emerging; **Figure 2B**) were recorded 3–6 weeks post-culture on RM. Regenerated shoots with approx. 1 cm of growth were transferred to individual vials (30 ml capacity) with 10 ml of BM and grown under standard conditions (**Figures 2B,C**).

Virus Detection

The virus status of plant materials was tested using RT-qPCR. Primers and probes (**Table 1**) were purchased from Integrated DNA Technologie.[1] The potato mitochondrial NADH dehydrogenase subunit 5 (*nad5*) gene transcript (Khan et al., 2015) and the plant nuclear gene transcript exocyst complex component (*sec3*) were used as the plant positive controls for cDNA synthesis. RT-qPCR was performed on nucleic acids isolated from young leaves of tissue-cultured plantlets and greenhouse-grown plants by the commercial company SlipStream Automation[2] using their standard in-house CTAB- and plate-based extraction and cDNA

[1]https://sg.idtdna.com
[2]https://www.slipstream-automation.co.nz

TABLE 1 | Primers and probes used for detection of PVS, PVA, PVM, plant mitochondrial gene transcript NADH dehydrogenase subunit 5 (*nad5*), and plant nuclear gene transcript exocyst complex component (*sec3*).

Primer/probe	Sequence	Amplicon size (bp)	References
NAD5-TM-F	GCTTCTTGGGGCTTCTTGTT		Khan et al. (2015) (modified from Menzel et al., 2002)
NAD5-TM-R	CCAGTCACCAACATTGGCATAA	176	Khan et al. (2015) (modified from Menzel et al., 2002)
NAD5-P	/56-FAM/AGGATCCGC/ZEN/ATAGCCCTCGATTTATGTG/3IABkFQ/		Botermans et al. (2013)
sec3_F	GCTTGCACACGCCATATCAAT		Tang et al. (2017)
sec3_R	TGGATTTTACCACCTTCCGCA		Tang et al. (2017)
PVS-F	TTGACACATTCGATTATGTGAC		This study
PVS-R	GTGATTGCGCACAATCTCAGC		
PVS-P1*	FAM-ATGGCAATTGACAAGTCGAACAGAAATG-BHQ-1		
PVS-P2*	FAM-AGGAGACGATAGCTCATAACGCTCACAA-BHQ-1		
PVA-F	TGTCGATTTAGGTACTGCTGGGAC		Agindotan et al. (2007)
PVA-R	TGCTTTGGTTTGTAAGATAGCAAGTG		
PVA-P	FAM-CACTACCAATGCTCAAAGGTAAGAGTGTCG-BHQ-1		
PVM-F	AGGTGTCACAGGTGCTATCGC		This study
PVM-R	TCACCTCGGTTACTCCTTCATC		
PVM-P	6FAM-CGCCACGCGCACATTGTA-MGBNFQ		

**PVS-P1 and PVS-P2 probes are used to detect all PVS strains.*
PVM, Potato virus M, PVA, Potato virus A, PVS, Potato virus S, and bp, base pairs.

synthesis methodology. cDNA generated using SuperScriptIV[3] from the RNA was diluted 5-fold with TE buffer (pH 8.0) for use in PCR. PCRs for PVS, PVA, PVM, and *nad5* were performed in 5.5 µl volumes containing 0.9 x Roche Lightcycler 480 Master Mix,[4] 680 nM primers, 227 nM probe, and 2 µl diluted cDNA. Prior to amplification, cDNA was denatured at 95°C for 4 min and then cycled 40 times with 95°C/15 s and 60°C/45 s. Samples were scored with the LightCycler 480 software release 1.5.1.62 SP2 using the "Abs Quant/Fit Points" analysis with the Noise Band fixed at a fluorescence value of 3, 1.5, and 3 for PVA, PVM, and PVS, respectively. Samples with viral Ct values greater than 35 were interpreted as absent for virus. PCRs for *sec3* were performed in 7 µl reactions using 1 x Roche Lightcycler 480 Master Mix, 3.12 mM Mg^{2+}, 400 nM primers, and 2 µl cDNA. Prior to amplification, the cDNA was denatured at 95°C for 10 min and then cycled 45 times with 95°C/15 s, 60°C/15 s, and 72°C/30s. Following PCR, melt curve analysis was performed at 95°C/60s and 40°C/60s, followed by heating to 65°C and then to 95°C with continuous data acquisition at 25 acquisitions per degree Celsius. Results were scored with LightCycler 480 software release 1.5.1.62 SP2 using the "Abs Quant/Fit Points" analysis with the Noise Band fixed at a fluorescence value of 5.

Plantlet material was confirmed to have single or mixed virus infections prior to therapies by RT-qPCR. RT-qPCR-based diagnostic of stock plants revealed the presence of single virus infection of PVS for the cultivar "Dunluce," PVS and PVA for "Tahi," and PVS and PVM for "V500." The presence of viruses in potato cultivars that underwent the *in vitro* therapies and controls were assessed at two different stages: firstly of cultures post-regeneration, 3 months after therapy treatments (**Figure 2D**), and secondly on all samples with initial negative test results after growing plants on the greenhouse for a further 3 months (**Figure 2E**).

In vitro Rooting, Acclimatization, and Plant Maintenance in the Greenhouse

One apical shoot segment (1.5 cm in length), containing two to three fully expanded *in vitro* leaves, from each virus-free plant was cultured in an individual vial (30 ml capacity) on BM under standard conditions for 2 weeks to initiate rooting. The rooted plantlets were then transferred to individual 12-cm diameter pots (800 ml capacity) containing a commercial substrate Daltons® potting mix (Daltons, Matamata, New Zealand) in an insect-proof greenhouse at 22 ± 2°C with a 12–14 h photoperiod under natural light. Plants were individually covered with insect-proof net to prevent possible virus-cross contamination (**Figure 2E**). After 3 months of growth (September to November), leaves were collected for further confirmation of the sanitary status by RT-qPCR.

Assessment of the Impact of Virus Infection on Microtuber Production

In vitro microtubers were induced using the method of Wakasa et al. (2020) with modifications as follows. Apical shoot segments (1 cm length) containing a single leaf and one to two axillary buds were obtained from 3-week-old *in vitro* virus-free and virus-infected stock plants. Five shoot segments were placed into 100 ml liquid BM in a 500-mL Erlenmeyer flask and were cultured on a shaker (75 rpm) under standard conditions for 2 weeks (**Figures 3A–D**). The BM was then discarded and replaced with liquid microtuber production medium (MPM; Li et al., 2013; Zhang et al., 2019) and grown in the dark at 24°C. The MPM is composed of BM supplemented with 60 g L^{-1} sucrose and 4 mg L^{-1} kinetin. Data on the number of microtubers produced per vessel and the size of microtubers (diameter) were recorded after 2 weeks of culture in liquid MPM (**Figures 3E,F**).

[3]ThermoFisher.com
[4]https://lifescience.roche.com/

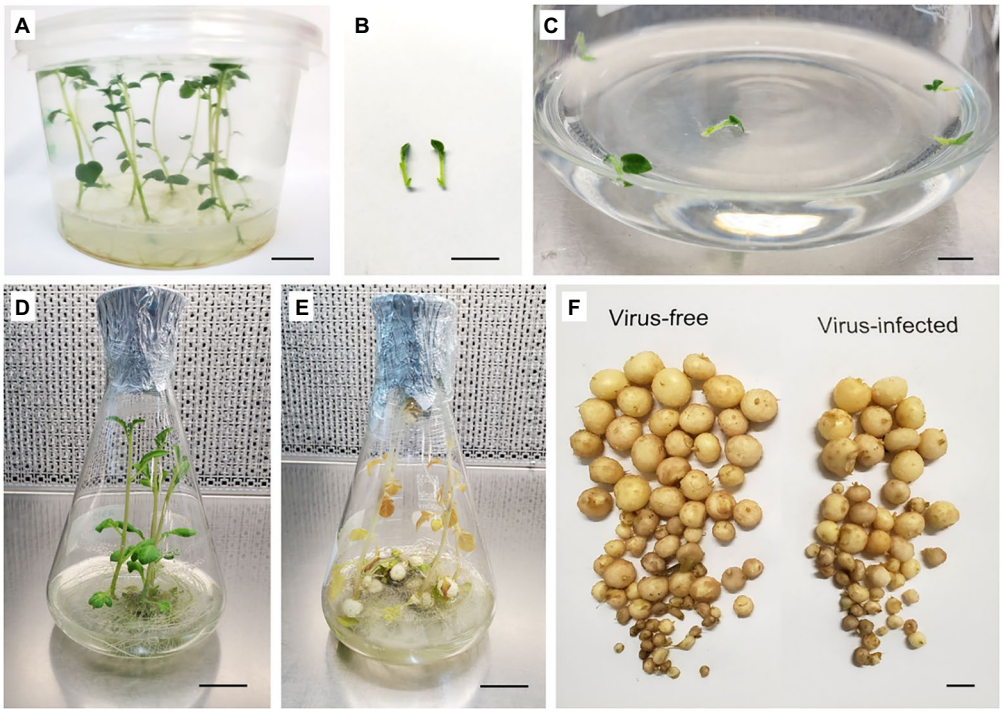


FIGURE 3 | Microtuber production in *in vitro* cultures of potato cultivar "Dunluce." **(A)** 3-week-old *in vitro* stock plants. **(B)** Shoot segments (1 cm) used as the explant source for microtuber production. **(C)** Shoot segments after initiation and **(D)** growth after 14 days of liquid culture at 24°C with a photoperiod of 16 h light day^{-1}. **(E)** Cultures after 14 days in microtuber production medium at 24°C in the dark. **(F)** Microtubers produced on shoots derived from virus-free (left) and *Potato Virus S*-infected (right) *in vitro* plants of "Dunluce" potato. Bars = A, B, C, and F 1 cm; D and E 2.3 cm.

Data Analysis

A minimum of 20 shoot tips were used per replicate with three replicates per treatment in a randomized block design. Shoot tip survival and regrowth results were both analyzed using binomial generalized linear models (GLM) with logit link (logistic regression). For each treatment, the results were presented as the number of samples, the percentage success, and a 95% confidence interval for the percentage. Confidence limits for the predicted treatment means were calculated from the logistic regression results except for those means of 100% for which the confidence limits were replaced by limits calculated using the Wilson Score method (Agresti and Coull, 1998; **Supplementary Tables 1–5**). Comparisons between treatment means were made using pairwise contrasts.

The numbers of microtubers produced per vessel from virus-free and virus-infected sources were compared using one-way ANOVA separately for each cultivar., and the proportions of microtubers in each size class (<5 mm, 5–10 mm, >10 mm) were analyzed using a binomial GLM with a logit link separately for each cultivar and size class (**Supplementary Tables 6, 7**). All analyses were performed using Genstat 19th edition (VSN International, Hemel Hempstead, United Kingdom). Frequency of virus eradication was calculated as the percentage of virus-free plants over the total number of plants used for virus detection. Up to 10 plantlets recovered from *in vitro* therapies and controls were randomly selected from the population and virus tested using RT-qPCR. The total number of plantlets used for virus testing varied depending on the number of samples obtained in each treatment.

RESULTS

Effects of the *in vitro* Therapies on Shoot Tip Viability and Virus Eradication

All the shoot tips in the controls survived and at least 96.8% regenerated shoots (**Table 2**). All the regenerated plants from the virus-infected positive controls remained virus-infected (**Tables 3**). After 2 weeks of thermotherapy alone or thermotherapy in combinations with chemotherapy, shoots developed a yellowish coloring at the tip. Despite this possible sign of stress, there was no significant impact on shoot tip regrowth of cultivar "Dunluce"; however, shoot tip regrowth of cultivars "Tahi" and 'V500" was reduced compared to the control (**Table 2**). For "V500," all the thermo- and chemo-treated shoot tips survived, but only a proportion produced viable plants (50.8 and 48.3%, respectively) with most shoot tips having yellowish growth that failed to develop (**Table 2**; **Supplementary Tables 1, 2**).

The effectiveness of virus eradication differed among the virus species: PVA was more readily eradicated than PVS and PVM, regardless of the method used (**Table 3**). Cryotherapy resulted in regrowth ranging from 42.2 to 55.4% across the

TABLE 2 | Survival and regrowth levels (%) of shoot tips excised from *in vitro*-grown potato cultivars "Dunluce," "Tahi," and "V500" following each treatment of virus eradication.

Treatment	"Dunluce"			"Tahi"			"V500"		
	N	Survival (%)	Regrowth (%)	*N*	Survival (%)	Regrowth (%)	*N*	Survival (%)	Regrowth (%)
ST (control)	62	100 a	96.8 a	61	100 a	98.4 a	60	100 a	100 a
PVS2	61	98.4 ab	73.8 b	63	100 a	58.7 d	65	96.9 ab	58.5 b
Cryo	74	94.6 bc	55.4 c	70	77.1 c	44.3 de	64	93.8 bc	42.2 bcde
T	62	100 a	93.5 a	60	98.3 ab	80 bc	61	100 a	50.8 bc
T + PVS2	72	95.8 abc	47.2 c	72	94.4 b	43.1 de	63	87.3 cd	33.3 def
T + Cryo	78	67.9 ef	12.8 e	63	76.2 c	11.1 g	76	80.3 d	23.7 f
C	60	98.3 ab	90 a	60	100 a	80 bc	60	100 a	48.3 bcd
C + PVS2	67	88.1 cd	56.7 c	67	92.5 b	40.3 e	70	95.7 abc	41.4 cde
C + Cryo	80	55 f	28.8 d	70	58.6 d	8.6 g	76	80.3 d	19.7 f
C + (C + T)	61	98.4 ab	88.5 a	60	100 a	81.7 b	60	100 a	41.7 bcde
[C + (C + T)] + PVS2	66	78.8 de	48.5 c	64	93.8 b	65.6 cd	60	100 a	45 bcde
[C + (C + T)] + Cryo	75	58.7 f	10.7 e	74	56.8 d	17.6 fg	69	63.8 e	29 f

N, number of shoot tips used for each treatment; ST, shoot tip; Cryo, cryotherapy (liquid nitrogen treatment); PVS2, plant vitrification solution 2 (without liquid nitrogen exposure); T, thermotherapy; and C, chemotherapy. Different letters in the same column indicate significant differences at $p < 0.05$ according to pairwise contrasts.

TABLE 3 | Effect of virus eradication treatments on percentage of potato plants from cultivars "Dunluce," "Tahi," and "V500" that were virus-free in a single or mix-infection.

Treatment	"Dunluce"	"Tahi"			"V500"		
	Virus-free plants (%)	Virus-free plants (%)			Virus-free plants (%)		
	PVS	PVS	PVA	PVS- and PVA-free	PVS	PVM	PVS- and PVM-free
ST (control)	0 (0/10)	0 (0/10)	0 (0/10)	0 (0/10)	0 (0/10)	0 (0/10)	0 (0/10)
PVS2	0 (0/10)	0 (0/10)	0 (0/10)	0 (0/10)	0 (0/10)	0 (0/10)	0 (0/10)
Cryo	0 (0/10)	0 (0/10)	20 (2/10)	0 (0/10)	0 (0/10)	0 (0/10)	0 (0/10)
T	0 (0/10)	0 (0/10)	70 (7/10)	0 (0/10)	30 (3/10)	20 (2/10)*	20 (2/10)*
T + PVS2	20 (2/10)	20 (2/10)	70 (7/10)	20 (2/10)	20 (2/10)	0 (0/10)	0 (0/10)
T + Cryo	70 (7/10)	29 (2/7)	100 (7/7)	29 (2/7)	30 (3/10)	20 (2/10)	20 (2/10)
C	20 (2/10)	50 (5/10)	100 (10/10)	50 (5/10)	40 (4/10)	30 (3/10)*	30 (3/10)*
C + PVS2	40 (4/10)	60 (6/10)	60 (6/10)	60 (6/10)	40 (4/10)	20 (2/10)	20 (2/10)
C + Cryo	90 (9/10)	100 (6/6)	100 (6/6)	100 (10/10)	70 (7/10)	70 (7/10)	70 (7/10)
C + (C + T)	50 (5/10)	60 (6/10)	100 (10/10)	60 (6/10)	60 (6/10)	50 (5/10)	40 (4/10)
C + (C + T) + PVS2	80 (8/10)	60 (6/10)	100 (10/10)	60 (6/10)	40 (4/10)	50 (5/10)	40 (4/10)
[C + (C + T)] + Cryo	100 (8/8)	70 (7/10)	100 (10/10)	70 (7/10)	100 (10/10)	70 (7/10)	70 (7/10)
Plants grown *in vitro* for three months that tested negative	45	40	75	44	43	33	31
Plants tested negative at first test, grown in the greenhouse for three months, and retested negative	45	40	75	44	43	31	29

**Plants grown in vitro were PVM-free, but one of these plants within the corresponding treatments tested positive for PVM later in plants grown in the greenhouse.*
ST, shoot tip; Cryo, cryotherapy (liquid nitrogen treatment); PVS2, plant vitrification solution 2 (without liquid nitrogen exposure); +LN, liquid nitrogen treatment; T, thermotherapy; C, chemotherapy; PVM, Potato virus M; PVA, Potato virus A; and PVS, Potato virus S. Different letters in the same column indicate significant differences at $p < 0.05$ according to pairwise contrasts. Virus status of potato cultivars that underwent the in vitro therapies were assayed in in vitro plants have been grown for 3 months and confirmed again after grown the plants in greenhouse for 3 months. Numbers in parentheses are the number of plantlets showing a negative reaction for the virus/total samples analyzed by reverse-transcription PCR.

three potato cultivars, however failed to eradicate PVS and PVM (**Tables 2, 3**). PVS2 treatment alone was not sufficient to eradicate any of the viruses. Shoot tips from "Tahi" recovered from cryotherapy were 20% PVA-free but still infected with PVS (**Table 3**).

Thermotherapy alone did not produce any virus-free plants in "Dunluce" and "Tahi"; meanwhile, in cultivar "V500," one in 10 plants was free of PVS and PVM. Interestingly, two out of 10 thermotherapy-derived "V500" plants were free of PVM after 3 months in tissue culture but one subsequently tested positive for PVM after further plant growth in the greenhouse (**Table 3**).

Chemo-treated shoot tips produced similar rates of survival (about 100%) across the three potato cultivars with shoot

regrowth varying from 48.3 to 90%, the lowest of which was for "V500" and the highest for "Dunluce" (**Table 2**). Chemotherapy alone was not always able to eradicate viruses; it was more efficient at eliminating PVA than PVS or PVM. After chemotherapy, "Tahi" initially infected with PVS and PVA had around 50% of plants free of virus. This compared to only 20% of plants free of virus for both "Dunluce" (which was only infected with PVS) and "V500" (which had a mixed infection of PVS and PVM). As noted for thermotherapy, three out of 10 "V500" plants submitted to chemotherapy were PVM-free after 3 months of *in vitro* culture post-regeneration. However, one of the progeny from this sample tested positive for PVM later in the greenhouse (**Table 3**).

Improvements on virus eradication were achieved through consecutive chemotherapy followed by combined chemotherapy and thermotherapy [C + (C + T)] treatments, with 50% of the evaluated "Dunluce" plants being free of PVS, 60% of the "Tahi" plants being free of PVS and PVA in mixed infection, and 40% of the "V500" plants being free of PVS and PVM in mixed infection (**Table 3**).

Thermotherapy or chemotherapy treatments followed by cryotherapy and the combination of all treatments affected shoot tip survival and regrowth in all three potato cultivars assessed (**Table 2**). When thermotherapy was combined with cryotherapy, the regrowth varied from 11.1% ("Tahi") to 23.7% ("V500"). Chemotherapy in combination with cryotherapy resulted in a particularly low regrowth of 8.6% in "Tahi." In general, shoot tips from treatments combined with either PVS2 (PVS2-treated shoot tips without LN exposure) or/and cryotherapy (PVS2 + LN exposure) treatments had the lowest regrowth (**Table 2**). Although regrowth was lower in shoot tips recovered after combining chemotherapy with cryotherapy, this method resulted in the highest frequencies of virus eradication in both single and mixed infections. All the "Tahi" plants recovered after chemotherapy combined with cryotherapy were free from both PVS and PVA, while nine out of 10 "Dunluce" plants evaluated were free from PVS and seven out of 10 "V500" plants were free from both PVS and PVM (**Table 3**).

The efficiency of virus eradication using thermotherapy followed by cryotherapy differed between virus species and cultivar. While 70% of the "Dunluce" plants evaluated were PVS-free, only 29% of the "Tahi" plants evaluated were free from both PVS and PVA, and 20% of the "V500" plants were free of PVS and PVM (**Table 3**).

Shoots exposed to chemotherapy followed by combined chemotherapy plus thermotherapy; then, cryotherapy {[C + (C + T)] + Cryo} had significantly decreased regrowth compared to the control or to shoots received individual treatments (**Table 2**). Although the shoot tip survival was relatively high (58.7–63.8%), most of the shoot tips produced just leaves with no evidence of a continued growth or turned into callus and failed to regenerate. The combination of all treatments resulted in shoot regrowth of 10.7–29% across the three potato cultivars with virus eradication rates of 70–100% (**Table 3**).

TABLE 4 | Effect of seven plant vitrification solution 2 (PVS2) exposure durations without (–LN) and with freezing in liquid nitrogen (+LN) on the survival and regrowth of shoot tips excised from *in vitro*-grown potato "Dunluce" infected with *Potato virus S*.

LN	PVS2 time (min)	Survival (%)	Regrowth (%)	*N*
–LN	5	100 a	96.8 a	63
	15	100 a	91.8 a	61
	60	98.4 ab	73.8 b	61
	90	96.7 abc	73.3 b	60
	105	91.8 bc	70.5 bc	61
	120	91.8 bc	55.7 cd	61
	135	47.5 e	9.8 f	61
+LN	5	78.8 d	22.7 e	66
	15	100 a	78.5 b	65
	60	94.6 bc	55.4 cd	74
	90	98.6 ab	56.5 cd	69
	105	89.1 cd	45.3 d	64
	120	90.5 cd	41.9 d	74
	135	41.7 e	3.3 f	60

–LN, cryotherapy procedure followed without liquid nitrogen exposure; +LN, liquid nitrogen treatment; PVS2, plant vitrification solution 2; and N, number of shoot tips used for each treatment. Different letters in the same column indicate significant differences at $p < 0.05$ according to pairwise contrasts.

Virus-free plants, at low frequencies, could be found in shoots subjected to thermo- or/and chemo-therapy followed by PVS2 exposure for 60 min without freezing in LN (PVS2 treatment). However, the efficiency of virus eradication was much higher when shoot tips were thermo- or/and chemo-treated followed by LN exposure (Cryo; **Table 3**).

Effect of PVS2 Exposure Duration on Shoot Tip Viability and Virus Eradication

Survival and regrowth of shoot tips decreased as durations of PVS2 treatment increased, for all three cultivars. Extended PVS2 exposure duration of 135 min resulted in the least shoot tip survival and regrowth, even without LN exposure (**Tables 4, 5; Supplementary Tables 3–5**).

Shoot tip survival of "Dunluce" was between 48 to 100% and 42 to 100% across the seven PVS2 exposure times for non-LN (without freezing in LN) treated and LN-treated (Cryo) explants, respectively (**Table 4**). Regrowth percentages in non-LN-treated shoot tips decreased from 97 to 3.3% as the PVS2 exposure time increased. In LN-treated shoot tips (Cryo), the maximum regrowth was 79% after 15 min of PVS2 exposure. Shoot tips exposed to PVS2 for a duration shorter or longer than 15 min showed reduced viability (**Table 4**). Although the regrowth of "Dunluce" shoot tips was high when incubated at the optimized PVS2 treatment duration (15 min) and exposed to LN, all recovered plants were infected with virus. Likewise, all shoot tips exposed to PVS2 without freezing in LN, were virus-infected regardless of the PVS2 exposure time. While the optimized vitrification solution exposure duration followed by LN treatment failed to eradicate PVS, one out of two plants tested free of this virus when a longer PVS2 exposure (135 min) was followed by LN treatment (**Table 6**). Longer PVS2 exposure followed by LN treatment (Cryo) resulted in regrowth of only two of out 60 treated shoot tips. The PVS was not able to

TABLE 5 | Effect of three plant vitrification solution 2 (PVS2) exposure durations without (–LN) and with freezing in liquid nitrogen (+LN) on survival and regrowth of shoot tips excised from *in vitro*-grown potato cultivars "Tahi" (infected with *Potato virus S* and *Potato virus A*) and "V500" (infected with *Potato virus S* and *Potato virus M*).

LN	"Tahi"				"V500"			
	PVS2 time (min)	Survival (%)	Regrowth (%)	*N*	PVS2 time (min)	Survival (%)	Regrowth (%)	*N*
–LN	5	100 a	100 a	60	5	100 a	96.7 a	61
	60	100 a	58.7 b	63	60	96.9 ab	58.5 b	65
	135	42.2 c	10.9 d	64	135	56.7 c	23.3 c	60
+LN	5	87.7 b	29.2 c	65	5	88.5 b	16.4 c	61
	60	77.1 b	44.3 bc	70	60	93.8 b	42.2 b	64
	135	41.3 c	3.2 d	63	135	46.0 c	4.8 d	63

–LN, cryotherapy procedure followed without liquid nitrogen exposure; +LN, liquid nitrogen treatment; PVS2, plant vitrification solution 2; and N, number of shoot tips used for each treatment. Different letters in the same column indicate significant differences at $p < 0.05$ according to pairwise contrasts.

be eradicated when shoot tips of cultivar "Dunluce" were exposed to PVS2 for a duration shorter than 135 min prior to LN treatment (**Table 5**).

There were no significant differences in regrowth between shoot tips of "V500" and "Tahi" that were immersed in LN and those without LN immersion (PVS2 treatment) for the PVS2 exposure durations of 60 and 135 min (**Table 5**). Shoot regrowth was higher in explants that were exposed to PVS2 for 5 min without freezing in LN (97–100%) than those that were immersed in LN (16–29%; **Supplementary Tables 4, 5**). All the shoot tips that were exposed to PVS2 without LN treatment remained virus-infected. As observed in "Dunluce," all the shoot tips of "Tahi" and "V500" that were exposed to PVS2 without LN treatment remained virus-infected. Only the shoot tips that were exposed to PVS2 for 135 min and immersed in LN produced virus-free plants (**Table 6**). Although one plant from each cultivar was free of mixed virus infection, only two and three out of 63 treated shoot tips of "Tahi" and "V500" were recovered after cryotherapy, respectively. Shoot tips exposed to PVS2 for a duration shorter than 135 min followed by LN treatment failed to eradicate mixed infections of PVS plus PVA and PVS plus PVM in "V500" and "Tahi" cultivars, respectively. For "Tahi," although both plants recovered from shoot tips exposed to 135 min in PVS2 and immersed in LN were free of PVA, only one of those was also free of PVS (**Table 6**).

All regenerated potato plantlets were successfully rooted *in vitro* and survived the acclimatization process. No visible morphological difference was apparent in the plants following 3 months' growth in the greenhouse. Except for two "V500" plants, all the plants that were virus-free at the *in vitro* stage were found to have a virus-free status after 3 months in the greenhouse. The two "V500" plants (from mixed-infected with PVS and PVM) tested positive for PVM; one was derived from thermotherapy alone and the other from chemotherapy alone (**Table 3**).

Comparative Assessment of Microtuber Production in the Virus-Free and Virus-Infected Potato Plants

Each of the three potato cultivars consistently produced 7–19 microtubers of varied size per vessel (**Figure 4**). Single infection of PVS in "Dunluce" had a negative impact on microtuber production *in vitro*: the number of microtubers per vessel was significantly lower in PVS-infected plantlets (12.6) than in PVS-free plantlets (19.4; **Figures 3, 4** and **Supplementary Table 6**). Although there were no significant differences in the number of microtubers per vessel and proportions of microtubers in each size class between virus-free and virus-infected "V500" and "Tahi," there was a tendency for higher proportions of large microtubers (>10 mm) to be produced in virus-free plantlets (**Supplementary Table 7**). A minimal increment of 5% in larger sized microtubers (>10 mm) was achieved when virus-free shoots were used as the source of material for microtuber production. Cultivar "V500" produced almost twice the percentage of small-sized microtubers from virus-infected (38.3%) material compared with virus-free (20.3%) material (**Figure 4**).

DISCUSSION

Potato is highly susceptible to virus infections and viruses have long affected global potato production (Kreuze et al., 2020). Thus, considerable effort has been made to establish robust systems for obtaining and maintaining virus-free potato plants. The cultivation of virus-resistant plants might be a desirable and sustainable strategy to overcome this problem (Farnham and Baulcombe, 2006; Valkonen, 2008; Orbegozo et al., 2016). However, virus resistance is not easily achievable for most crops and viruses, and mutations in the viral genome or even mixed infection can overcome this resistance (García-Cano et al., 2006; Tian and Valkonen, 2013; Rubio et al., 2020). Therefore, the development of technologies to produce virus-free propagation material followed by the ongoing planting of high-healthy plants is still the most effective strategy for managing viruses in commercial production systems (Gong et al., 2019; Magyar-Tábori et al., 2021).

In this study, we combined several virus eradication methods (thermotherapy, chemotherapy, and cryotherapy) to efficiently eradicate single and mixed PVS, PVA, and PVM infection from virus-infected *in vitro* cultures of potato cultivars "Dunluce," "Tahi," and "V500". We found that the combination of chemotherapy and cryotherapy (C + Cryo), or chemotherapy

treatment prior to combining chemotherapy treatment with thermotherapy followed by cryotherapy {[C + (C + T)] + Cryo} resulted in high efficiency of PVS, PVA, and PVM eradication; 70–100% across the three potato cultivars tested. Though the regrowth percentage was low in shoots exposed to chemotherapy followed by cryotherapy (8.6–28.8%), high levels of virus-free plants were obtained. Indeed, plants of "Tahi" were 100% free from PVS and PVA, "Dunluce" were 90% PVS-free, and "V500" were 70% free from mixed infection of PVS and PVM. The combination of all treatments resulted in similar shoot regrowth (10.7–29%) across the three cultivars with virus eradication rates of between 70 and 100%: with rates for "Tahi" (mixed-infected with PVS and PVA) being lower than "V500" (mixed-infected with PVS and PVM) which was lower than "Dunluce" (PVS-infected). Although the efficacy of these two treatments in eradicating viruses was similar, incorporating thermotherapy was more time-consuming and required a temperature-controlled growth chamber; therefore, our study shows that the combination of chemotherapy and cryotherapy is a more appropriate strategy for eradication of PVS, PVM, and PVA from infected *in vitro* potato plants.

In this study, isolating and regrowing plants from 1 mm shoot tips (without any virus eradication treatment) completely failed to eradicate single infections of PVS, mixed infections of PVS and PVA, and PVS and PVM from infected *in vitro* potato shoots. In shoot tip culture, the size of excised shoot tip affects to the success of virus eradication (Bettoni et al., 2021a); our results confirm that the 1 mm shoot tips were not a suitable explant size for virus eradication. In addition, the virus location in the infected shoot tips may be a bottleneck to achieving efficient virus eradication by shoot tip culture (Wang et al., 2021). Previously, PLRV, PVY, PVS, and *Potato virus X* (PVX) have been eradicated by 0.2 mm shoot tip culture from *in vitro* diseased shoots (Wang et al., 2006; AlMaarri et al., 2012; Jianming et al., 2012; Zhang et al., 2019). Although 0.2 mm shoot tip culture could eradicate virus species, a proportion of recovered plants were still virus-infected, with eradication efficiency being related to the specific interaction between virus species and potato genotype. Improved virus eradication using shoot tip culture has been achieved when it is combined with thermotherapy (Waswa et al., 2017). High temperature treatments can prevent virus movement toward meristematic cells by inhibiting viral replication and degrading RNA and therefore, decreasing the viral particle load in infected shoot tips (Wang et al., 2008; Wang et al., 2018a). Wang et al. (2006) found that PLRV and PVY eradication frequencies increased from 56 to 90% and 62 to 93%, respectively, when 0.2 mm shoot tips were excised from shoots heat-treated at 36°C for 4 weeks, compared to shoot tips not subjected to heat treatment (thermotherapy). We found that thermotherapy involving alternating temperature of 28°C (8 h in dark) and 40°C (16 h in light) for 2 weeks followed by the excision of 1 mm shoot tips resulted in very low efficiency of virus eradication in "V500," which was mixed-infected with PVS and PVM, and failed to eradicate either the single infection of PVS from "Dunluce" or the mixed infection of PVS and PVA from "Tahi." Although 70% of "Tahi" shoots were free of PVA following this thermotherapy regime, none of the recovered plants were free of PVS. In general, prolonged heat treatment associated with high temperatures can increase the frequency of virus eradication, but at the same time reduces the viability of the treated explants, as host plants are often sensitive to these conditions (Zhao et al., 2018; Wang et al., 2018a; Farhadi-Tooli et al., 2022).

The combination of chemotherapy and cryotherapy reported here involved treatment of the shoots in medium containing 100 mg L^{-1} ribavirin for 4 weeks, followed by cryotherapy. Previously, Kushnarenko et al. (2017) have combined chemotherapy and cryotherapy procedures to eradicate virus species from *in vitro* shoots of potato. In their study, PVM and PVS were successfully eradicated from potato cultivars "Tamyr" and "Nartau" after three subcultures (45 days each; total of 135 days) on medium with 100 mg L^{-1} ribavirin followed by cryotherapy. In our study, in addition to PVM and PVS, we also successfully eradicated PVA by combining chemotherapy and cryotherapy. Since our procedure did not require such a

TABLE 6 | Effect of plant vitrification solution 2 (PVS2) exposure duration of 5, 60, and 135 min without (–LN) and with freezing in liquid nitrogen (+LN) on shoot regrowth level and percentage of potato plants from cultivars "Dunluce," "Tahi," and "V500" that were virus-free in a single or mix-infection.

LN	PVS2 time (min)	"Dunluce"		"Tahi"				"V500"			
		Shoot regrowth (%)	PVS- free plants (%)	Shoot regrowth (%)	Virus-free plants (%)			Shoot regrowth (%)	Virus-free plants (%)		
					PVS	PVA	PVS- and PVA-free		PVS	PVM	PVS- and PVM-free
–LN	5	96.8 a	0 (0/10)	100 a	0 (0/10)	0 (0/10)	0 (0/10)	96.7 a	0 (0/10)	0 (0/10)	0 (0/10)
	60	73.8 b	0 (0/10)	58.7 b	0 (0/10)	0 (0/10)	0 (0/10)	58.5 b	0 (0/10)	0 (0/10)	0 (0/10)
	135	9.8 f	0 (0/6)	10.9 d	0 (0/10)	0 (0/10)	0 (0/10)	23.3 c	0 (0/10)	0 (0/10)	0 (0/10)
+LN	5	22.7 e	0 (0/10)	29.2 c	0 (0/10)	0 (0/10)	0 (0/10)	16.4 c	0 (0/10)	0 (0/10)	0 (0/10)
	60	55.4 cd	0 (0/10)	44.3 bc	0 (0/10)	20 (2/10)	0 (0/10)	42.2 b	0 (0/10)	0 (0/10)	0 (0/10)
	135	3.3 f	50 (1/2)	3.2 d	50 (1/2)	100 (2/2)	50 (1/2)	4.8 d	33 (1/3)	33 (1/3)	33 (1/3)

–LN, cryotherapy procedure followed without liquid nitrogen exposure; +LN, liquid nitrogen treatment; PVS2, plant vitrification solution 2; PVM, Potato virus M; PVA, Potato virus A; and PVS, Potato virus S. Numbers in parentheses are the number of plantlets showing a negative reaction for the virus/total samples analyzed by reverse-transcription PCR. Different letters in the same column of shoot regrowth indicate significant differences at $P < 0.05$ according to pairwise contrasts.

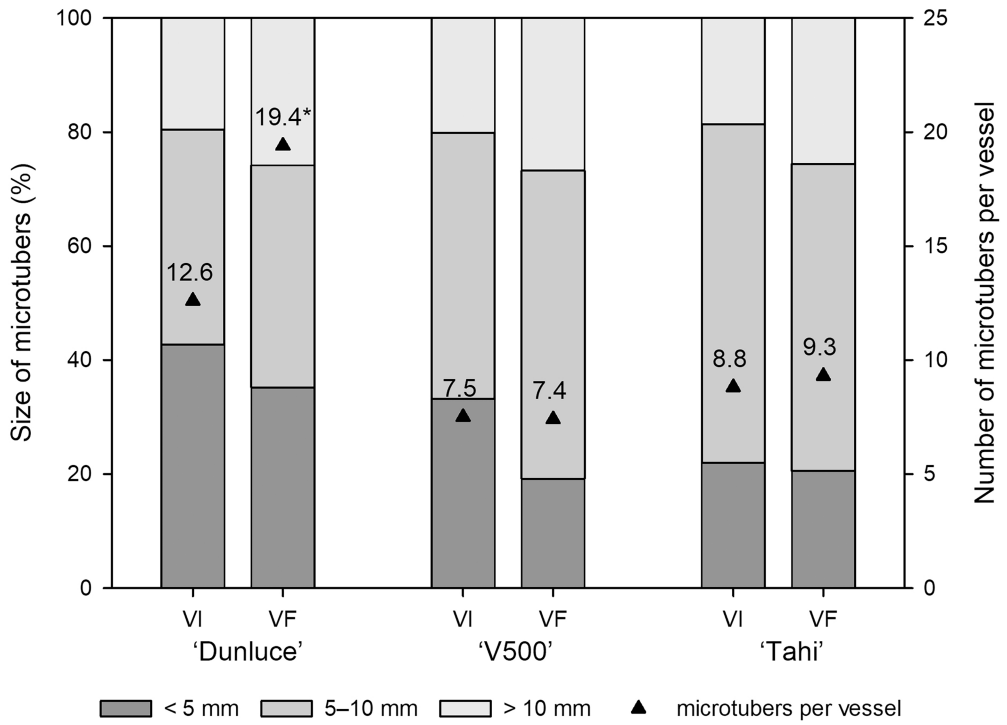


FIGURE 4 | Effect of virus infection on proportion of microtuber size produced in potato cultivars "Dunluce" (infected with *Potato virus S*), "V500" (infected with *Potato virus S* and *Potato virus M*), and "Tahi" (infected with *Potato virus S* and *Potato virus A*) after 2 weeks in microtuber production media. *VI virus-infected plants; VF virus-free plants.* * indicates significant differences at $p < 0.05$ in microtuber numbers according to analysis of variance.

long period of culture on ribavirin, it could provide a higher throughput and more cost effective technique, as well as reducing the potential for somaclonal variation through reducing the number of culture steps. In our study, 1-mm apical shoot tips were excised from plants treated with ribavirin for 4 weeks, then subjected to droplet-vitrification cryotherapy using 60 min PVS2 exposure at 22°C; in contrast, Kushnarenko et al. (2017) used slightly larger shoot tips (1.5–2.0 mm), a different cryotherapy technique (vitrification) and shorter PVS2 exposure (30 min). These differences might explain why a longer ribavirin treatment was necessary for the eradication of PVM and PVS in the study of Kushnarenko et al. (2017). We note that chemotherapy treatment alone could eliminate viruses from all three cultivars but with low efficacy; this could be significantly improved by combining chemotherapy with cryotherapy, specifically from 20 to 90% in "Dunluce," 50 to 100% in "Tahi," and 20 to 70% in "V500."

In recent years, shoot tip cryotherapy has proven to be an effective method to eradicate viruses from *in vitro* infected plants in multiple species of economic importance (Cui et al., 2015; Pathirana et al., 2015; Bettoni et al., 2018, 2019a, 2021a; Bi et al., 2018; Souza et al., 2020; Farhadi-Tooli et al., 2022; Wang et al., 2022a). Cryotherapy makes use of LN exposure (−196°C) to selectively destroy vacuolated and differentiated cells that are known to harbor viruses within shoot tips (Wang et al., 2009; Wang and Valkonen, 2009). In this study, cryotherapy (60 min PVS2 exposure + LN) alone failed to eradicate virus in "Dunluce" singly infected with PVS or mixed infections of PVS and PVA in "Tahi," and PVS and PVM in "V500." Similarly, Kushnarenko et al. (2017) found that cryotherapy alone did not produce any potato plants free from mixed infection of PVS and PVM. Working on six PVS-infected potato cultivars, Zhang et al. (2019) found that successful PVS eradication using cryotherapy was cultivar dependent. About 17% of the "Iverpotet/Smaragd" cryo-recovered plants were PVS-free, while all of the other potato cultivars were still PVS infected after cryotherapy. Li et al. (2018a) also reported that cryotherapy alone completely failed to generate PVS and *Potato spindle tuber viroid* (PSTVd)-free plants from *in vitro* infected potato "Zihuabai" shoots. In our study, although cryotherapy resulted in low efficiency (20%) of PVA eradication in "Tahi," the cryo-recovered plants were still PVS-infected. Recent research has shown that not all viruses can be eradicated using shoot tip cryotherapy, particularly in those that are able to infect regions within the meristem (Wang et al., 2008, 2018b, 2022a; Li et al., 2016, 2018a; Zhao et al., 2018; Mathew et al., 2021). The ongoing presence of PVS and PVM after cryotherapy might be because these viruses can be located very close to the meristem; hence, it is possible for a small portion of the infected cells to remain alive following cryo-treatment, meaning the regenerated plants will remain virus-infected.

Even though cryotherapy techniques are based on cryopreservation, unlike cryopreservation, cryotherapy protocols should seek to eliminate the maximum portion of differentiated

and infected cells, particularly in plant species infected with viruses that are difficult to eradicate such as PVS and PVM. This is a balancing act: a strategy to improve virus eradication could be to use either shorter or longer PVS2 exposure durations than the optimal, but this may result in fewer cells from which to recover plants after LN exposure (Bi et al., 2018; Bettoni et al., 2019a, 2021b; Souza et al., 2020; Wang et al., 2022b). Working on *Vitis vinifera* Cabernet Sauvignon, Bi et al. (2018) found that *Grapevine leafroll-associated virus-3* (GLRaV-3) was eradicated from diseased shoot tips independent of PVS2 exposure duration (50–100 min). Although, there was no influence of PVS2 exposure duration on GLRaV-3 eradication, it was evident that the long exposure to PVS2 (100 min) significantly reduced the percentage of cells surviving in the apical dome and leaf primordia. GLRaV-3 is a phloem-limited virus and, therefore, it might explain why Bi et al. (2018) did not observe any difference in virus eradication across the range of PVS2 times, even though longer PVS2 exposure duration of 100 min resulted in fewer cells that recover after LN exposure. In our study, the viability of shoot tips and the ability of cryotherapy to produce virus-free plants was directly associated with duration of exposure to PVS2. Extended PVS2 exposure durations of 135 min at room temperature followed by LN treatment resulted in very low shoot tip regrowth of 3.2–4.8% across the three potato cultivars; however, one out of 60 cryo-treated shoot tips from each cultivar did regenerate a virus-free plant irrespective of whether there was a single or mixed infection of PVS, PVM, and PVA. In vitrification-based methods, tolerance to freezing in LN is achieved through an osmotic process when shoot tips are placed in highly concentrated vitrification solutions (Volk et al., 2006). In addition to any LN effect, the long PVS2 exposure duration of 135 min used in this study might have selectively weakened and killed cells that harbored viruses through osmotic and chemical stress and therefore, influenced the production of virus-free plants after cryotherapy. It is worth noting that although cryotherapy alone (135 min PVS2 + LN) was able to produce at least one virus-free plant in each potato cultivar, when combined with chemotherapy it resulted in higher shoot regrowth and virus eradication frequencies.

Results obtained in the present study clearly demonstrate that PVS, PVA, and PVM in single or mixed infection negatively affect microtuber production of *in vitro* cultures of "Dunluce," "Tahi," and "V500." This finding is consistent with results reported by Li et al. (2013, 2018b) and Zhang et al. (2019). Li et al. (2013) and Zhang et al. (2019) also noted that the co-infections of PLRV + PVY and PLRV + PVS and the triple infection of PVY and PVX + PVS could lead to negative effects on vegetative growth of potato *in vitro*. Negative effects on tuber yield of single or mixed infections of PVX + PVS have also been reported in greenhouse- and field-grown potato plants (Wright, 1977; Nyalugwe et al., 2012; Gong et al., 2019). Negative effects of virus infection on tuber yield of field-grown potato plants have been well documented and have long been a constraint for sustainable potato production (Brunt, 2011; Wang et al., 2011). This highlights the need to produce healthy and virus-free seed potatoes to support the potato industry.

To guard against possible false negatives, the virus status of plants that underwent *in vitro* therapies should be assessed for a second time after the plants have grown in the greenhouse: one should not rely just on the test result for *in vitro* plants. Virus titer may have been reduced and virus particles may occur in tissues that are not sampled for virus testing at the *in vitro* stage in some treatments, resulting in false negative, as we have shown in two "V500" plants (PVM-infected) derived from thermotherapy and chemotherapy treatments in this research and previously in raspberry and apple plants infected with *Raspberry bushy dwarf virus* and *Apple hammerhead viroid*, subjected to chemotherapy treatment (Mathew et al., 2021), and combined thermotherapy with cryotherapy (Bettoni et al., 2022), respectively. Therefore, repeat virus testing on progenies growing in the greenhouse and later in the field is recommended as standard best practice to confirm virus-free status of the plant materials.

In addition to presenting a protocol for virus eradication, we also identified an effective droplet-vitrification cryopreservation method to preserve potato shoot tips for long-term storage, using *in vitro* plants as source materials. Nodal sections from this material were placed on BM medium for 1 week to generate shoots from which uniform 1 mm apical shoots could be excised. Shoot tips were precultured on media enriched with sucrose, followed by PVS2 treatment for 15 min at 22°C prior to LN exposure. Shoot tips were warmed in unloading solution and placed on intermediate recovery medium overnight and, finally, transferred to recovery medium. This method resulted in high regrowth (79%) in potato cultivar "Dunluce." Availability of a simple and efficient cryopreservation protocol that results in high levels of viability (≥ 40% after LN exposure), such as the one presented here, may facilitate the technology transfer between laboratories and the implementation of cryopreserved base collections (Volk et al., 2016; Bettoni et al., 2019b, 2021b).

Our study identified procedures that resulted in high frequencies of eradication of PVS, PVA, and PVM viruses from infected potato cultivars. The consistency of the results across three cultivars with single or mixed infections suggests that these procedures have great potential to assist the production and supply of virus-free planting materials for the potato industry. Furthermore, it might also be a valuable tool to support the global exchange of germplasm underpinning breeding activities.

DATA AVAILABILITY STATEMENT

The datasets presented in the study are either included in the article or in the **Supplementary Material**: further inquiries can be directed to the corresponding author.

AUTHOR CONTRIBUTIONS

JB, LM, RP, CW, DH, and JN conceived and designed the research and internal/external liaison with partners and

service providers for contracts and IP rights protection. JB and LM planned and performed the experiments. JB, LM, and CW collected plant material for diagnosis. JB collected and interpreted the data, conducted the microtuber experiment, acclimatized and managed the plants in the greenhouse, prepared tables and figures, and wrote the original manuscript. DH wrote the diagnosis protocol. AM conducted the statistical analysis and helped prepare the figures. SK and JT developed the primers for virus diagnosis. All authors contributed to the article and approved the submitted version.

FUNDING

This research was funded by the New Zealand Institute for Plant and Food Research Limited SSIF funding (1972—"Breeding Technology Development").

ACKNOWLEDGMENTS

The authors wish to thank Pam Fletcher and Samantha Baldwin for providing virus-infected potato tissue cultures, Andrew Mullan and Belinda Diepenheim for tissue culture media preparation, Julie Ryan and Ian King for technical assistance in the greenhouse, Juliana Souza for technical help with acclimatization of potato plants, Benjamin Franzmayr of Slipstream Automation for RT-qPCR analysis, and Keith Funnell and Mary Christey for providing internal review of the manuscript.

SUPPLEMENTARY MATERIAL

The Supplementary Material for this article can be found online at: https://www.frontiersin.org/articles/10.3389/fpls.2022.878733/full#supplementary-material

REFERENCES

Adolf, B., Andrade-Piedra, J., Molina, F. R., Przetakiewicz, J., Hausladen, H., Kromann, P., et al. (2020). "Fungal, oomycete, plasmodiophorid diseases of potato," in *The Potato Crop*. eds. H. Campos and O. Ortiz (Cham: Springer), 307–350.

Agindotan, B. O., Shiel, P. J., and Berger, P. H. (2007). Simultaneous detection of potato viruses, PLRV, PVA, PVX and PVY from dormant potato tubers by TaqMan® real-time RT-PCR. *J. Virol. Methods* 142, 1–9. doi: 10.1016/j.jviromet.2006.12.012

Agresti, A., and Coull, B. A. (1998). Approximate is better than "exact" for interval estimation of binomial proportions. *Am. Stat.* 52, 119–126. doi: 10.2307/2685469

AlMaarri, K., Massa, R., and AlBiski, F. (2012). Evaluation of some therapies and meristem culture to eliminate potato Y potyvirus from infected potato plants. *Plant Biotechnol.* 29, 237–243. doi: 10.5511/plantbiotechnology.12.0215a

Antonova, O. Y., Apalikova, O. V., Ukhatova, Y. V., Krylova, E. A., Shuvalov, O. Y., Shuvalova, A. R., et al. (2017). Eradication of viruses in microplants of three cultivated potato species (*Solanun tuberosum* L., *S. phureja* Juz. & bulk., *S. stenotomum* Juz. & Buk.) using combined thermos-chemotherapy method. *Agric. Biol.* 52, 95–104. doi: 10.15389/agrobiology.2017.1.95eng

Awasthi, L. P., and Verma, H. N. (2017). Current status of viral diseases of potato and their eco-friendly management – a critical review. *Virol. Res. Rev.* 1, 1–16. doi: 10.15761/VRR.1000122

Bettoni, J. C., Bonnart, R., and Volk, G. M. (2021b). Challenges in implementing plant shoot tip cryopreservation technologies. *Plant Cell Tissue Organ. Cult.* 144, 21–34. doi: 10.1007/s11240-020-01846-x

Bettoni, J. C., Costa, M. D., Gardin, J. P. P., Kretzschmar, A. A., and Pathirana, R. (2016). Cryotherapy: a new technique to obtain grapevine plants free of viruses. *Rev. Bras. Frutic.* 38:e-833. doi: 10.1590/0100-29452016833

Bettoni, J. C., Costa, M. D., Souza, J. A., Volk, G. M., Nickel, O., da Silva, F. N., et al. (2018). Cryotherapy by encapsulation-dehydration is effective for in vitro eradication of latent viruses from 'Marubakaido' apple rootstock. *J. Biotechnol.* 269, 1–7. doi: 10.1016/j.jbiotec.2018.01.014

Bettoni, J. C., Fazio, G., Costa, L. C., Hurtado-Gonzales, O. P., Rwahnih, M. A., Nedrow, A., et al. (2022). Thermotherapy followed by shoot tip cryotherapy eradicates latent viruses and apple hammerhead viroid from in vitro apple rootstocks. *Plan. Theory* 11:582. doi: 10.3390/plants11050582

Bettoni, J. C., Kretzschmar, A. A., Bonnart, R., Shepherd, A., and Volk, G. M. (2019b). Cryopreservation of 12 *Vitis* species using apical shoot tips derived from plants grown in vitro. *HortSciece* 54, 976–981. doi: 10.21273/HORTSCI13958-19

Bettoni, J. C., Marković, Z., Bi, W., Volk, G. M., Matsumoto, T., and Wang, Q.-C. (2021a). Grapevine shoot tip cryopreservation and cryotherapy: secure storage of disease-free plants. *Plants* 10:2190. doi: 10.3390/plants10102190

Bettoni, J. C., Souza, J. A., Volk, G. M., Costa, M. D., da Silva, F. N., and Kretzschmar, A. A. (2019a). Eradication of latent viruses from apple cultivar 'Monalisa' shoot tips using droplet-vitrification cryotherapy. *Sci. Hortic.* 250, 12–18. doi: 10.1016/j.scienta.2019.02.033

Bi, W. L., Hao, X.-Y., Cui, Z.-H., Pathirana, R., Volk, G. M., and Wang, Q.-C. (2018). Shoot tip cryotherapy for efficient eradication of grapevine leafroll-associated virus-3 from diseased grapevine in vitro plants. *Ann. Appl. Biol.* 173, 261–270. doi: 10.1111/aab.12459

Botermans, M., Van de Vossenberg, B., Verhoeven, J. T. J., Roenhorst, J., Hooftman, M., Dekter, R., et al. (2013). Development and validation of a real-time RT-PCR assay for generic detection of pospiviroids. *J. Virol. Methods* 187, 43–50. doi: 10.1016/j.jviromet.2012.09.004

Bradshaw, J. E. (2021). "Improving resistance to diseases and pests: a dynamic situation," in *Potato Breeding: Theory and Practice*. ed. J. E. Bradshaw (Cham: Springer Nature), 247–337. doi: 10.1007/978-3-030-64414-7_5

Brunt, A. A. (2011). "The main viruses infecting potato crops," in *Virus and virus-like diseases of potatoes and production of seed-potatoes*. eds. G. Loebenstein, P. H. Berger, A. Brunt and R. H. Lawson (Dordrecht: Kluwer), 65–67. doi: 10.1007/978-94-007-0842-6_5

Cui, Z. H., Li, B. Q., Bi, W. L., and Wang, Q. C. (2015). Plant pathogen eradication by cryotherapy of shoot tips: development, achievements and prospective. *Acta Hortic.* 1083, 35–41. doi: 10.17660/ActaHortic.2015.1083.2

Devaux, A., Goffart, J. P., Kromann, P., Andrade-Piedra, J., Polar, V., and Hareau, G. (2021). The potato of the future: opportunities and challenges in sustainable Agri-food systems. *Potato Res.* 64, 681–720. doi: 10.1007/s11540-021-09501-4

Dhital, S. P., Sakha, B. M., and Lim, H. T. (2007). Utilization of shoot cuttings for elimination of PLRV and PVY by thermotherapy and chemotherapy from potato (*Solanum tuberosum* L.). *Nepal J. Sci. Technol.* 7, 1–6. doi: 10.3126/njst.v7i0.528

Ellis, D., Salas, A., Chavez, O., Gomez, R., and Anglin, N. (2020). "Ex situ conservation of potato [*Solanum* section Petota (Solanaceae)] genetic resources in genebanks," in *The Potato Crop*. eds. H. Campos and O. Ortiz (Cham: Springer), 109–138.

Faccioli, G., and Marani, F. (1998). "Virus elimination by meristem tip culture and tip micrografting," in *Plant Virus Diseases Control*. eds. A. Hadidi, A. R. K. Khetarpal and H. Koganezawa (St. Paul, MN: APS Press), 346–380.

Fang, Y. L., Dhital, S. P., Li, K. H., Khu, D. M., Kim, H. Y., and Lim, H. T. (2005). Utilization of single nodal cuttings and therapies for eradication of double-infected potato viruses (PLRV and PVY) from *in vitro* plantlets of potato (*Solanum tuberosum*). *J. Kor. Soc. Hortic. Sci.* 46, 119–125.

FAOSTAT-Food and Agriculture Organization of the United Nations (2021). Crops and livestock products. Available at: http://www.fao.org/faostat/en/#data/QCL. (Accessed September 02, 2021).

Farhadi-Tooli, S., Ghanbari, A., Kermani, M. J., Zeinalabedini, M., Bettoni, J. C., Naji, A. M., et al. (2022). Droplet-vitrification cryotherapy and thermotherapy as efficient tools for the eradication of apple chlorotic leaf spot virus and apple stem grooving virus from virus-infected quince in vitro cultures. *Eur. J. Plant Pathol.* 162, 31–43. doi: 10.1007/s10658-021-02400-x

Farnham, G., and Baulcombe, D. C. (2006). Artificial evolution extends the spectrum of viruses that are targeted by a disease–resistance gene from potato. *Proc. Natl. Acad. Sci. U. S. A.* 103, 18828–18833. doi: 10.1073/pnas.0605777103

Fletcher, J. D. (2012). A virus survey of New Zealand fresh, process and seed potato crops during 2010-11. *N. Z. Plant Prot.* 65, 197–203. doi: 10.30843/nzpp.2012.65.5366

Fletcher, P. J., Fletcher, J. D., and Cross, R. J. (1988). Potato germplasm: *in vitro* storage and virus reduction. *N. Z. J. Crop. Hortic. Sci.* 26, 249–252. doi: 10.1080/01140671.1998.9514060

Fuentes, S., Gibbs, A. J., Adams, I. P., Wilson, C., Botermans, M., Fox, A., et al. (2021). Potato virus A isolates from three continents: their biological properties, phylogenetics, and prehistory. *Phytopathology* 111, 217–226. doi: 10.1094/PHYTO-08-20-0354-FI

García-Cano, E., Resende, R. O., Fernández-Muñoz, R., and Moriones, E. (2006). Synergistic interaction between tomato chlorosis virus and tomato spotted wilt virus results in breakdown of resistance in tomato. *Phytopathology* 96, 1263–1269. doi: 10.1094/PHYTO-96-1263

Gong, H., Igiraneza, C., and Dusengemungu, L. (2019). Major in vitro techniques for potato virus elimination and post eradication detection methods. A review. *Am. J. Potato Res.* 96, 379–389. doi: 10.1007/s12230-019-09720-z

Jianming, B., Xiaoling, C., Xinxiong, L., Huachun, G., Xia, X., and Zhie, Z. (2012). Can cryopreservation eliminate the potato virus X (PVX) and potato spindle tuber viroid (PSTVd)? *Biosci. Meth.* 3, 34–40. doi: 10.5376/bm.2012.03.0005

Khan, S., Mackay, J., Liefting, L., and Ward, L. (2015). Development of a duplex one-step RT-qPCR assay for the simultaneous detection of apple scar skin viroid and plant RNA internal control. *J. Virol. Methods* 221, 100–105. doi: 10.1016/j.jviromet.2015.04.032

Kim, H. H., Yoon, J. W., Park, Y. E., Cho, E. F., Sohn, J. K., Kim, T. S., et al. (2006). Cryopreservation of potato cultivated varieties and wild species: critical factors in droplet vitrification. *Cryo Lett.* 27, 223–234.

Kreuze, J. F., Souza-Dias, J. A. C., Jeevalatha, A., Figueira, A. R., Valkonen, J. P. T., and Jones, R. A. C. (2020). "Viral diseases in potato," in *The Potato Crop*. eds. H. Campos and O. Ortiz (Cham: Springer), 389–430.

Kushnarenko, S., Romadanova, N., Aralbayeva, M., Zholamanova, S., Alexandrova, A., and Karpova, O. (2017). Combined ribavirin treatment and cryotherapy for efficient *potato virus M* and *potato virus S* eradication in potato (*Solanum tuberosum* L.) in vitro shoots. In vitro cell. *Dev. Biol. Plant* 53, 425–432. doi: 10.1007/s11627-017-9839-0

Li, J. W., Chen, H. Y., Li, J., Zhang, Z., Blystad, D. R., and Wang, Q. C. (2018b). Growth, microtuber production and physiological metabolism in virus-free and virus-infected potato in vitro plantlets grown under NaCl-induced salt stress. *Eur. J. Plant Pathol.* 152, 417–432. doi: 10.1007/s10658-018-1485-9

Li, B. Q., Feng, C. H., Hu, L. Y., Wang, M. R., and Wang, Q. C. (2016). Shoot tip culture and cryopreservation for eradication of apple stem pitting virus (ASPV) and apple stem grooving virus (ASGV) from apple rootstocks 'M9' and 'M26'. *Ann. Appl. Biol.* 168, 142–150. doi: 10.1111/aab.12250

Li, J. W., Wang, M. R., Chen, H. Y., Zhao, L., Cui, Z. H., Zhang, Z., et al. (2018a). Long-term preservation of potato leafroll virus, potato virus S, and potato spindle tuber viroid in cryopreserved shoot tips. *Appl. Microbiol. Biotechnol.* 102, 10743–10754. doi: 10.1007/s00253-018-9405-7

Li, J. W., Wang, B., Song, X. M., Wang, R. R., Chen, L., Zhang, H., et al. (2013). *Potato leafroll virus* (PLRV) and *potato virus Y* (PVY) influence vegetative growth, physiological metabolism, and microtuber production of in vitro-grown shoots of potato (*Solanum tuberosum* L.). *Plant. Cell. Tiss. Org.* 114, 313–324. doi: 10.1007/s11240-013-0327-x

Lin, Y. H., Johnson, D. A., and Pappu, H. R. (2014). Effect of potato virus S infection on late blight resistance in potato. *Am. J. Potato Res.* 91, 642–648. doi: 10.1007/s12230-014-9394-8

Linsmaier, E. M., and Skoog, F. (1965). Organic growth factor requirements of tobacco tissue cultures. *Physiol. Plant.* 18, 100–127. doi: 10.1111/j.1399-3054.1965.tb06874.x

Magyar-Tábori, K., Mendler-Drienyovszki, N., Hanász, A., Zsombik, L., and Dobránszki, J. (2021). Phytotoxicity and other adverse effects on the in vitro shoot cultures caused by virus elimination treatments: reasons and solutions. *Plan. Theory* 10:670. doi: 10.3390/plants10040670

Mathew, L., Tiffin, H., Erridge, Z., McLachlan, A., Hunter, D., and Pathirana, R. (2021). Efficiency of eradication of raspberry bushy dwarf virus from infected raspberry (*Rubus idaeus*) by in vitro chemotherapy, thermotherapy and cryotherapy and their combinations. *Plant Cell Tissue Organ Cult.* 144, 133–141. doi: 10.1007/s11240-020-01829-y

Menzel, W., Jelkmann, W., and Maiss, E. (2002). Detection of four apple viruses by multiplex RT-PCR assays with coamplification of plant mRNA as internal control. *J. Virol. Methods* 99, 81–92. doi: 10.1016/s0166-0934(01)00381-0

Moreno, A. B., and López-Moya, J. J. (2020). When viruses play team sports: mixed infections in plants. *Phytopathology* 110, 29–48. doi: 10.1094/PHYTO-07-19-0250-FI

Murashige, T., and Skoog, F. (1962). A revised medium for rapid growth and bio assays with tobacco tissue cultures. *Physiol. Planta.* 15, 473–497. doi: 10.1111/j.1399-3054.1962.tb08052.x

Naik, P. S., and Khurana, S. P. (2003). Micropropagation in potato seed production: need to revise seed certification standards. *J. Indian Potato Assoc.* 30, 267–273.

Nasir, I. A., Tabassum, B., Latif, Z., Javed, M. A., Haider, M. S., Javed, M. A., et al. (2010). Strategies to control potato virus Y under in vitro conditions. *Pak. J. Phytopathol.* 22, 63–70.

Nazarov, P. A., Baleev, D. N., Ivanova, M. I., Sokolova, L. M., and Karakozova, M. V. (2020). Infectious plant diseases: etiology, current status, problems and prospects in plant protection. *Acta Nat.* 12, 46–59. doi: 10.32607/actanaturae.11026

Nyalugwe, E. P., Wilson, C. R., Coutts, B. A., and Jones, R. A. C. (2012). Biological properties of potato virus X in potato: effects of mixed infection with potato virus S and resistance phenotypes in cultivars from three continents. *Plant Dis.* 96, 43–54. doi: 10.1094/PDIS-04-11-0305

Onofre, K. F. A., Forbes, G. A., Andrade-Piedra, J. L., Buddenhagen, C. E., Fulton, J. C., Gatto, M., et al. (2021). An integrated seed health strategy and phytosanitary risk assessment: potato in the republic of Georgia. *Agric. Syst.* 191:103144. doi: 10.1016/j.agsy.2021.103144

Orbegozo, J., Solorzano, D., Cuellar, W. J., Bartolini, I., Roman, L. M., Ghislain, M., et al. (2016). Marker-free PLRV resistant potato mediated by Cre-*lox*P excision and RNAi. *Transgenic Res.* 25, 813–828. doi: 10.1007/s11248-016-9976-y

Pathirana, R., Mathew, L., Jibran, R., Hunter, D. A., and Morgan, E. R. (2019). Cryopreservation and cryotherapy research on horticultural crops in New Zealand. *Acta Hortc.* 1234, 29–36. doi: 10.17660/ActaHortic.2019.1234.4

Pathirana, R., McLachlan, A., Hedderley, D., Carra, A., Carimi, F., and Panis, B. (2015). Removal of leafroll viruses from infected grapevine plants by droplet vitrification. *Acta Hortic.* 1083, 491–498. doi: 10.17660/ActaHortic.2015.1083.64

Potatoes NZ. (2021). AGM papers and annual report 2021. Annual reports - Potatoes New Zealand. Available at: info@potatoesnz.co.nz. (Accessed September 02, 2021).

Priegnitz, U., Lommen, W. J. M., van der Vlugt, R. A. A., and Struik, P. C. (2019). Impact of positive selection on incidence of different viruses during multiple generations of potato seed tubers in Uganda. *Potato Res.* 62, 1–30. doi: 10.1007/s11540-018-9394-z

Priegnitz, U., Lommen, W. J. M., van der Vlugt, R. A. A., and Struik, P. C. (2020). Potato yield and yield components as affected by positive selection during several generations of seed multiplication in southwestern Uganda. *Potato Res.* 63, 507–543. doi: 10.1007/s11540-020-09455-z

Quazi, M. H., and Martin, S. D. (1978). Pathogen-free potato plants regenerated from meristem-tip cultures. *N. Z. J. Exp. Agric.* 6, 305–307. doi: 10.1080/03015521.1978.10426293

Rubio, L., Galipienso, L., and Ferriol, I. (2020). Detection of plant viruses and disease management: relevance of genetic diversity and evolution. *Front. Plant Sci.* 11:1092. doi: 10.3389/fpls.2020.01092

Sakai, A., Kobayashi, S., and Oiyama, I. (1990). Cryopreservation of nucellar cells of navel orange (*Citrus sinensis* Osb. Var. *brasiliensis* Tanaka) by vitrification. *Plant Cell Rep.* 9, 30–33. doi: 10.1007/BF00232130

Souza, J. A., Bogo, A., Bettoni, J. C., Dalla Costa, M., da Silva, F. N., Casa, R. T., et al. (2020). Droplet-vitrification cryotherapy for eradication of apple stem

grooving virus and apple stem pitting virus from "Marubakaido" apple rootstock. *Trop. Plant Pathol.* 45, 148–152. doi: 10.1007/s40858-019-00321-z

Tang, X., Zhang, N., Si, H., and Calderón-Urrea, A. (2017). Selection and validation of reference genes for RT-qPCR analysis in potato under abiotic stress. *Plant Methods* 13:85. doi: 10.1186/s13007-017-0238-7

Thomas-Sharma, S., Abdurahman, A., Ali, S., Andrade-Piedra, J. L., Bao, S., Charkowski, A. O., et al. (2016). Seed degeneration in potato: the need for an integrated seed health strategy to mitigate the problem in developing countries. *Plant Pathol.* 65, 3–16. doi: 10.1111/ppa.12439

Tian, Y.-P., and Valkonen, J. P. T. (2013). Genetic determinants of *potato virus Y* required to overcome or trigger hypersensitive resistance to PVY strain group O controlled by the gene Ny in potato. *Mol. Plant-Microbe Interact.* 26, 297–305. doi: 10.1094/MPMI-09-12-0219-R

Valkonen, J. P. T. (2007). "Potato viruses: economical losses and biotechnological potential," in *Potato Biology and Biotechnology: Advances and Perspectives*. eds. D. Vreugdenhil, J. Bradshaw, C. Gebhardt, F. Govers, D. K. L. MacKerron, M. A. Taylor, et al. (Netherlands: Elsevier Science), 619–641.

Valkonen, J. P. T. (2008). Novel resistances to four potyviruses in tuber-bearing potato species, and temperature-sensitive expression of hypersensitive resistance to potato virus Y. *Ann. Appl. Biol.* 130, 91–104. doi: 10.1111/j.1744-7348.1997.tb05785.x

Volk, G. M., Harris, J. L., and Rotindo, K. E. (2006). Survival of mint shoot tips after exposure to cryoprotectant solution components. *Cryobiology* 52, 305–308. doi: 10.1016/j.cryobiol.2005.11.003

Volk, G. M., Henk, A. D., Jenderek, M., and Richards, C. M. (2016). Probabilistic Viability Calculations for cryopreserving vegetatively propagated collections in genebanks. *Genet. Resources Crop Evol.* 64, 1613–1622. doi: 10.1007/s10722-016-0460-6

Volmer, R., Villagaray, R., Cárdenas, J., Castro, M., Chávez, O., Anglin, N., et al. (2017). A large-scale viability assessment of the potato cryobanks at the international potato center (CIP). In vitro cell. *Dev. Biol. Plant* 53, 309–317. doi: 10.1007/s11627-017-9846-1

Wakasa, T., Kasai, A., Yamazaki, M., Tabei, Y., Tsuyama, M., Igarashi, T., et al. (2020). Rapid analysis of *GBSS1* and *Vinv* genes expressed in potato tubers using microtubers produced in liquid culture medium. *Plant Cell Rep.* 39, 1415–1424. doi: 10.1007/s00299-020-02572-6

Wang, M. R., Bi, W. L., Bettoni, J. C., Zhang, D., Volk, G. M., and Wang, Q. C. (2022b). Shoot tip cryotherapy for plant pathogen eradication. *Plant Pathol.* 1–14. doi: 10.1111/ppa.13565

Wang, Q., Cuellar, W. J., Rajamaki, M. L., Hirata, Y., and Valkonen, J. P. T. (2008). Combined thermotherapy and cryotherapy for efficient virus eradication: relation of virus distribution, subcellular changes, cell survival and viral RNA degradation in shoot tips. *Mol. Plant Pathol.* 9, 237–250. doi: 10.1111/j.1364-3703.2007.00456.x

Wang, M. R., Cui, Z. H., Li, J. W., Hao, X. Y., Zhao, L., and Wang, Q. C. (2018a). In vitro thermotherapy-based methods for plant virus eradication. *Plant Methods* 14:87. doi: 10.1186/s13007-018-0355-y

Wang, M. R., Hamborg, Z., Blystad, D. R., and Wang, Q. C. (2021). Combining thermotherapy with meristem culture for improved eradication of onion yellow dwarf virus and shallot latent virus from infected in vitro-cultured shallot shoots. *Ann. Appl. Biol.* 178, 442–449. doi: 10.1111/aab.12646

Wang, M. R., Hamborg, Z., Ma, X. Y., Blystad, D. R., and Wang, Q. C. (2022a). Double-edged effects of the cryogenic technique for virus eradication and preservation in shallot shoot tips. *Plant Pathol.* 71, 494–504. doi: 10.1111/ppa.13466

Wang, Q., Liu, Y., Xie, Y., and You, M. (2006). Cryotherapy of potato shoot tips for efficient elimination of *potato leafroll virus* (PLRV) and *potato virus Y* (PVY). *Potato Res.* 49, 119–129. doi: 10.1007/s11540-006-9011-4

Wang, B., Ma, Y., Zhang, Z., Wu, Z., Wu, Y., Wang, Q., et al. (2011). Potato viruses in China. *Crop Prot.* 30, 1117–1123. doi: 10.1016/j.cropro.2011.04.001

Wang, Q. C., Panis, B., Engelmann, F., Lambardi, M., and Valkonen, J. P. T. (2009). Cryotherapy of shoot tips: a technique for pathogen eradication to produce healthy planting materials and prepare healthy plant genetic resources for cryopreservation. *Ann. Appl. Biol.* 154, 351–363. doi: 10.1111/j.1744-7348.2008.00308.x

Wang, Q. C., and Valkonen, J. P. T. (2009). Cryotherapy of shoot tips: novel pathogen eradication method. *Trends Plant Sci.* 14, 119–122. doi: 10.1016/j.tplants.2008.11.010

Wang, M. R., Yang, W., Zhao, L., Li, J. W., Liu, K., Yu, J. W., et al. (2018b). Cryopreservation of virus: a novel biotechnology for long-term preservation of virus in shoot tips. *Plant Methods* 14:47. doi: 10.1186/s13007-018-0312-9

Wasilewska-Nascimento, B., Boguszewska-Mańkowska, D., and Zarzyńska, K. (2020). Challenges in the production of high-quality seed potatoes (*Solanum tuberosum* L.) in the tropics and subtropics. *Agron.* 10:260. doi: 10.3390/agronomy10020260

Waswa, M., Kakuhenzire, R., and Ochwo-ssemakula, M. (2017). Effect of thermotherapy duration, virus type and cultivar interactions on elimination of potato viruses X and S in infected seed stocks. *African J. Plant Sci.* 11, 61–70. doi: 10.5897/AJPS2016.1497

Wright, N. S. (1977). The effect of separate infections by potato viruses X and S on netted gem potato. *Am. Potato J.* 54, 147–149. doi: 10.1007/BF02852870

Yi, J. Y., Lee, G. A., Jeong, J. W., Lee, S. Y., and Lee, Y. G. (2014). Eliminating potato virus Y (PVY) and potato leaf roll virus (PLRV) using cryotherapy of in vitro-grown potato shoot tips. *Korean J. Crop Sci.* 59, 498–504. doi: 10.7740/KJCS.2014.59.4.498

Zhang, Z., Wang, Q. C., Spetz, C., and Blystay, D. R. (2019). In vitro therapies for virus elimination of potato-valuable germplasm in Norway. *Sci. Hortic.* 249, 7–14. doi: 10.1016/j.scienta.2019.01.027

Zhao, L., Wang, W. R., Cui, Z. H., Chen, L., Volk, G. M., and Wang, Q. C. (2018). Combining thermotherapy with cryotherapy for efficient eradication of *apple stem grooving virus* from infected in-vitro-cultured apple shoots. *Plant Dis.* 102, 1574–1580. doi: 10.1094/PDIS-11-17-1753-RE

Conflict of Interest: JB LM, RP, CW, DH, AM, and JN were employed by The New Zealand Institute for Plant and Food Research Limited.

The remaining authors declare that the research was conducted in the absence of any commercial or financial relationships that could be construed as a potential conflict of interest.

Publisher's Note: All claims expressed in this article are solely those of the authors and do not necessarily represent those of their affiliated organizations, or those of the publisher, the editors and the reviewers. Any product that may be evaluated in this article, or claim that may be made by its manufacturer, is not guaranteed or endorsed by the publisher.

Copyright © 2022 Bettoni, Mathew, Pathirana, Wiedow, Hunter, McLachlan, Khan, Tang and Nadarajan. This is an open-access article distributed under the terms of the Creative Commons Attribution License (CC BY). The use, distribution or reproduction in other forums is permitted, provided the original author(s) and the copyright owner(s) are credited and that the original publication in this journal is cited, in accordance with accepted academic practice. No use, distribution or reproduction is permitted which does not comply with these terms.

frontiers | Frontiers in Plant Science

ORIGINAL RESEARCH
published: 20 May 2022
doi: 10.3389/fpls.2022.881244

Genomics-Assisted Improvement of Super High-Yield Hybrid Rice Variety "Super 1000" for Resistance to Bacterial Blight and Blast Diseases

Zhizhou He[1,2†], Yeyun Xin[3†], Chunlian Wang[4†], Hanshu Yang[3], Zhi Xu[1], Jihua Cheng[1], Zhouwei Li[1], Changrong Ye[1], Hexing Yin[1], Zhenyu Xie[2], Nan Jiang[5], Jing Huang[3], Jinhua Xiao[1], Bingchuan Tian[1], Yan Liang[6], Kaijun Zhao[4*] and Junhua Peng[1*]*

[1] Huazhi Bio-Tech Co., Ltd., Changsha, China, [2] Tropical Crops Genetic Resources Institute, Chinese Academy of Tropical Agricultural Sciences, Haikou, China, [3] China National Hybrid Rice Research and Development Center, Changsha, China, [4] National Key Facility for Crop Gene Resources and Genetic Improvement (NFCRI), Institute of Crop Science, Chinese Academy of Agriculture Sciences (CAAS), Beijing, China, [5] Key Laboratory of Southern Rice Innovation and Improvement, Ministry of Agriculture and Rural Affairs, Hunan Engineering Laboratory of Disease and Pest Resistant Rice Breeding, Yuan Longping High-Tech Agriculture Company Ltd., Changsha, China, [6] State Key Laboratory of Rice Biology, China National Rice Research Institute, Hangzhou, China

OPEN ACCESS

Edited by:
Xiaojie Wang,
Northwest A&F University, China

Reviewed by:
Romesh Kumar Salgotra,
Sher-e-Kashmir University of Agricultural Sciences and Technology of Jammu, India
Yan Li,
Sichuan Agricultural University, China

***Correspondence:**
Junhua Peng
junhuapeng2022@outlook.com
Kaijun Zhao
zhaokaijun@caas.cn
Yan Liang
liangyan01@caas.cn

[†] These authors have contributed equally to this work and share first authorship

Specialty section:
This article was submitted to Crop and Product Physiology, a section of the journal Frontiers in Plant Science

Received: 24 February 2022
Accepted: 19 April 2022
Published: 20 May 2022

Citation:
He Z, Xin Y, Wang C, Yang H, Xu Z, Cheng J, Li Z, Ye C, Yin H, Xie Z, Jiang N, Huang J, Xiao J, Tian B, Liang Y, Zhao K and Peng J (2022) Genomics-Assisted Improvement of Super High-Yield Hybrid Rice Variety "Super 1000" for Resistance to Bacterial Blight and Blast Diseases. Front. Plant Sci. 13:881244. doi: 10.3389/fpls.2022.881244

The two-line rice hybrid "Super 1000" (GX24S × R900) represents a major landmark achievement of breeding for super-hybrid rice in China. However, both male parent R900 and hybrid "Super 1000" have an obvious defect of high susceptibility to rice bacterial blight (BB) and blast. Thus, improving disease resistance and maintaining the original high-yield capacity are essential for the sustainable application of "Super 1000." In this study, the application of closely linked single-nucleotide polymorphism (SNP) markers for foreground selection of dominant resistance gene loci together with genome-wide SNP markers for the background selection rapidly improved the disease resistance of R900 without disturbing its high-yield capacity. A series of improved R900 lines (iR900, in BC_2Fn and BC_3Fn generations) were developed to stack resistance genes (*Xa23+Pi9*, *Xa23+Pi1+Pi2/9*) by marker-assisted backcrossing and field selection for phenotypes, and further crossed with the female line GX24S to obtain improved hybrid variety Super 1000 (iS1000). The genetic backgrounds of iS1000 and "Super 1000" were profiled by using a 56 K SNP-Chip, and results showed that they shared 98.76% of similarity. Meanwhile, evaluation of the field disease resistance showed that the iR900 lines and iS1000 hybrids possess significantly enhanced resistance to both BB and rice blast. Resistance spectrum assays revealed that the iR900 lines and their derived hybrids exhibited high-level resistance to 28 *Xoo* strains tested, and enhanced resistance to leaf blast at the seedling stage when infected with 38 *Magnaporthe oryzae* isolates. Between 2019 and 2020, the multi-location field trials across the middle and lower reaches of the Yangtze River were launched and showed that the iS1000 slightly out-yielded than the original variety. In a large-scale demonstration site (6.73 ha, Yunnan, China), the iS1000 achieved 17.06 t/hm^2 of yield in 2019. Moreover, the high similarity was observed in main

agronomic traits and grain quality when comparing the improved lines/hybrids to original ones (iR900 vs. R900, iS1000 vs. S1000). This work presented a typical genomics-assisted breeding strategy and practice, which involves in directional introgression and rapid stack of multiple disease resistance genes, endowing the super-high-yield hybrid rice variety with holistic disease resistance but without yield penalty.

Keywords: hybrid rice, Super 1000, R900, bacterial blight and blast resistance, genomics-assisted selection

INTRODUCTION

Hybrid rice with high yield has greatly contributed to the increase in food production over the past half-century (Ma and Yuan, 2015). To better harness the yield potential, China has launched the "super-hybrid rice breeding program" in 1996. Since 2001, several pioneer hybrid rice combinations have been developed, and these super-hybrids roughly yielded 8.3 t/ha in commercial production. In 2014, a super-hybrid rice variety "Y Liangyou 900" marked a milestone with a yield of 15.4 t/ha (Yuan, 2018). Recently, another super-hybrid rice variety "Super 1000" constantly yielded 16 t/ha, and set the world record of rice yield (17.28 t/ha) in Yunnan province of China in 2018 (He et al., 2020). Efforts have still been made for a sustainable increase in rice yield. However, a foreseeable challenge is that the high yield potential of hybrid rice varieties is frequently threatened by various stresses. Therefore, it is imperative to rapidly develop stress-resilient rice varieties to ensure food security (Springer and Schmitz, 2017).

Rice bacterial blight (BB) and rice blast caused by *Xanthomonas oryzae* pv. *Oryzae (Xoo)* and *Magnaporthe oryzae*, respectively, are the two most prevalent and destructive diseases in global rice production (Wing et al., 2018; Raina et al., 2019; Samal et al., 2019). The rice blast affects crops in more than 80 countries, and can lead to yield losses by as high as 50% (Dayton, 2014). Similarly, rice BB affects millions of hectares of rice annually, with an estimated crop loss of as high as 75% (Zhao and Zhang, 2021). Super-high-yield hybrid rice breeding has made great progress in boosting rice yield in China, but its production is seriously threatened by rice blast and BB attributed to extensive use of a few non-resistant parents over the past years. Tremendous efforts have been devoted to characterizing the genetic diversity of rice germplasm resources to discover resistance genes. To date, at least 17 genes for BB resistance (Xu et al., 2022) and 25 genes for rice blast resistance have been cloned and are available for breeding purposes (Wing et al., 2018). Among these genes, the BB resistance gene *Xa23* is a new executor R gene located on the long arm of rice chromosome 11, and confers a dominant and extremely broad-spectrum of resistance against BB at all growth stages. The BB resistance gene *Xa23* is not expressed under normal conditions but can be activated immediately in the face of *Xoo*'s attack, and trigger the strong hypersensitive response at the infection site, thereby limiting the expansion of the pathogen, resulting in a high-level BB resistance (Wang et al., 2015).

For rice blast, the resistance gene *Pi2* confers dominant and broad-spectrum resistance to diverse *M. oryzae* isolates, and was mapped on the short arm close to the centromere of chromosome 6, at a locus carrying at least six RB resistance genes (*Pi2, Pi9*, *Pigm*, *Piz-t*, *Piz*, and *Pi50*; Liu et al., 2002; Hayashi et al., 2004; Deng et al., 2006; Zhu et al., 2012). In addition, *Pi1* is an allele at the *Pik* locus located at the end of the long arm of rice chromosome 11, and also confers dominant and durable resistance to a broad spectrum of rice blast isolates (Yu et al., 1996; Hua et al., 2012). Among those resistance genes, *Xa23*, *Pi1*, *Pi2/Pi9* have been widely used in the marker-assisted hybrid rice breeding programs due to their dominant effect and broad-spectrum resistance.

The development of rice varieties with durable and broad-spectrum resistance is an effective, economical, and environmentally sound way to prevent diseases (Wang and Valent, 2017). However, the conventional breeding approach takes many years to incorporate resistance into a susceptible (S) rice variety. Furthermore, resistance genes are sometimes associated with yield penalty because of linkage drag or unknown genetic background effects (Deng et al., 2017; Nelson et al., 2018). Genomic breeding technology is now widely applied to improve breeding efficiency by using foreground and background selection with the assistance of molecular markers (Bailey-Serres et al., 2019). Foreground selection enables the precise selection of individuals carrying the desirable target genes with the help of the marker information during the breeding process (Bai et al., 2006). The background selection devotes to accelerate the genomic recovery of the recipient parent genotype (RPG) by the assistance of markers across the whole genome (Hillel et al., 1990; Hospital et al., 1992; Xu et al., 2012). Computer simulations demonstrated that use of molecular markers for the background selection can accelerate recovery of the RPG by two or three generations (Tanksley et al., 1989). Large numbers of informative markers are available for use in the background selections, and these include single-nucleotide polymorphisms (SNP) that can be assayed in high-throughput genotyping arrays (Bevan et al., 2017). A lot of high-throughput genotyping platforms are established in recent years, and SNP markers are more efficient in terms of time and cost compared with other markers when a large number of markers are required for the background selection (Zhang et al., 2017; Wing et al., 2018). Breeders can use genome-wide markers to eliminate 70–80% of individuals in breeding generations without having to invest in laborious field testing (McCouch et al., 2013). Further, the combination of conventional breeding and genomic technologies, including foreground, background, and phenotypic selections, provides powerful options for increasing environmental resilience and productivity (Jez Joseph et al., 2016). The selection of plant traits

by using these tools can significantly accelerate market entry of new varieties.

The hybrid rice restorer line R900 is a major innovative achievement of super-high-yield rice breeding because "Super 1000," a combination derived from R900, has set the high-yield records in many places in recent years. However, R900 and "Super 1000" are highly susceptible (HS) to BB and rice blast, which not only exposed a production risk but also limited their application in a large scale. We here demonstrate genomics-assisted rapid and directional improvement of R900 and the derived hybrid variety Super 1000 for broad-spectrum resistance to both BB and rice blast.

MATERIALS AND METHODS

Plant Materials

Plant materials used in this study include Super 1000 (a two-line-hybrid rice combination with super-high yield in China), R900 (the restorer line of Super 1000), GX24S (the PTGMS line of Super 1000), and resistance gene donors (HZ02455 containing *Xa23* + *Pi9* and HZ02411 containing *Pi1* + *Pi2*). The rice varieties JG30 and CO39 were used as S controls, while CBB23 and Gumei4 were used as resistant (R) controls.

Population Development and Breeding Selection Procedure

The improved R900 (iR900) lines and improved Super 1000 (iS1000) hybrids were developed by marker-assisted backcrossing as described in **Figure 1**. The hybrid rice restorer line R900 was crossed with resistance donors and the F_1 plants were backcrossed with the recurrent parent R900. In each backcross generation, all individual plants were genotyped for foreground selection, and the plants containing the target genes were genotyped for the background selection. To pyramid the three resistance genes, double-cross F_1 population was generated for marker-assisted selection. Finally, a series of improved lines iR900-1 (*Xa23* + *Pi9*), iR900-2 (*Xa23* + *Pi1* + *Pi2*), and iR900-3 (*Xa23* + *Pi1* + *Pi9*) were developed. These improved lines were then crossed with GX24S, the PTGMS line of Super 1000, to obtain the iS1000 hybrids iS1000-1 (*Xa23* + *Pi9*), iS1000-2 (*Xa23* + *Pi1* + *Pi2*), and iS1000-3 (*Xa23* + *Pi1* + *Pi9*) for disease-resistance and agronomic evaluations.

Genomics-Assisted Foreground and Background Selection

Closely linked SNP markers, which are located upstream and downstream of the target genes (*Xa23*, *Pi1*, *Pi2/Pi9*), were used to track the target genes for foreground selection. By screening the whole genome SNP markers of recipient parent and donor parents, a total of 120 polymorphic SNP markers evenly distributed on each chromosome were selected for the background selection.

The fresh young leaves of 3-leaf seedlings were collected and placed in a 96-well plate, DNA was extracted by using Cetyltrimethylammonium Bromide (CTAB) method (Doyle and Doyle, 1987) on the TECAN Freedom EVO platform (Lifescience). Kompetitive allele-specific PCR (KASP) primers for each SNP were designed using BatchPrimer 3 (You et al., 2008). Genotyping was carried out on the Douglas Array Type and Nexar ultra-high-throughput genotyping platform (Douglas) following the user's manuals.

The background recovery rate was calculated as in the following:

$$\text{Background recovery rate} = (a^*2 + b)/[(a + b + c)\times 2]\times 100$$

Where *a* is the number of homozygous genotype loci identical to the donor (for example, AA), *b* is the number of heterozygous genotype loci (Aa), and *c* is the number of homozygous genotype loci (aa) identical to the receptor.

Genetic Background Recovery Profiling by RICE 56K Gene Chip

The DNA samples were prepared using CTAB method for genotyping with a high-density Affymetrix 56 K SNP Chip. The rice 56K SNP chip contains 56,897 SNP markers selected from the dataset of whole-genome resequencing of 3,024 rice core germplasm from 89 countries or regions around the world (Li et al., 2014). The DNA amplification, fragmentation, chip hybridization, DNA ligation, and signal amplification were performed using the Affymetrix Axiom® 2.0 Assay Manual Target Prep Protocol QRC. Staining and scanning were performed on the GeneTitan® Multi-Channel Instrument (ThermoFisher) according to the manufacturer's procedure. Monomorphic markers, and/or showing unclear SNPs were excluded from the analysis. The filtered genotypic data was used for the background analysis.

Evaluation of BB Resistance

The hybrid rice restorer line R900 and the iR900-1(harboring *Xa23*), Super 1000 (S1000), and the iS1000-1 (harboring *Xa23*) were planted in the field (Sanya, Hainan), during the dry season in 2019–2020 for BB resistance evaluation. The *indica* rice variety JG30 and its near-isogenic R line CBB23 (harboring *Xa23*) are used as S and R controls, respectively. Twenty-eight *Xoo* strains (**Table 1**) from different countries used in this study are stocks in Kaijun Zhao's laboratory. The *Xoo* cells were cultured in a PPS medium [ferv-filtering juice of 300-g potato, 5-g peptone, 15-g sucrose, 2-g $Na_2HPO_4{\cdot}12H_2O$, and 0.5g Ca $(NO_3)_2{\cdot}4H_2O$] at 28°C for 48 h. The bacterial inoculum was prepared by suspending bacterial culture in sterile, distilled water at an optical density of 1.0 (OD600). The bacterial suspensions were used for inoculation on fully expanded rice leaves at the booting stage. For each rice genotype, three plants were inoculated by the leaf-clipping method (Kauffman et al., 1973). For each plant, 3–5 fully expanded leaves were inoculated. The disease symptom was scored by lesion length (cm) and photographs were taken 2 weeks post-inoculation. The leaves with lesion length shorter than 1.0, 1.1–2.5, and longer than 2.5 were classified as highly resistant (HR), R and S, respectively.

Evaluation of Rice Blast Resistance

R900 and iR900-1 (harboring *Pi9*), iR900-2 (harboring *Pi1* and *Pi2*), iR900-3 (harboring *Pi1* and *Pi9*), were planted in the State

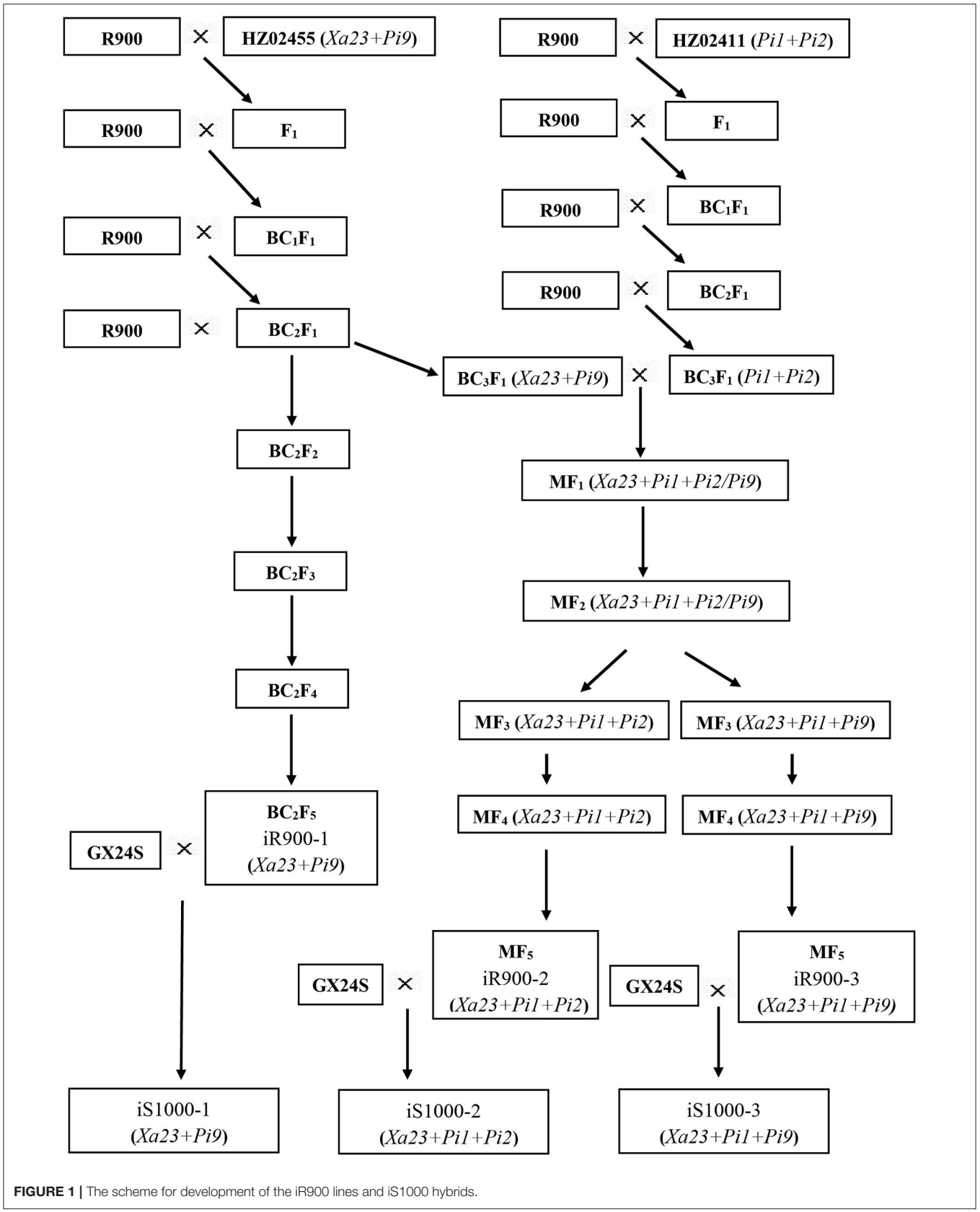


FIGURE 1 | The scheme for development of the iR900 lines and iS1000 hybrids.

TABLE 1 | Resistance assessment of rice genotypes against 28 *Xoo* strains[a].

Xoo strain	Origin of *Xoo* strain	Rice genotype					
		JG30	R900	S1000	iR900-1	iS1000-1	CBB23
HLJ-72	China	6.47	6.93	7.53	2.00	0.10	0.67
HB17	China	7.20	5.93	5.50	1.47	0.47	1.27
NX42	China	10.07	5.90	6.57	3.87	0.90	1.17
ZHE173	China	3.97	5.50	2.20	1.10	0.40	0.83
GD1358	China	8.10	6.87	4.27	2.43	0.50	0.87
LN57	China	7.33	5.77	6.20	1.53	0.37	0.83
JS49-6	China	4.63	6.37	6.73	2.50	0.53	1.50
PXO61	Philippines	6.10	4.17	4.40	0.67	0.10	0.50
PXO86	Philippines	4.00	5.70	2.93	1.93	0.73	0.67
PXO71	Philippines	6.10	5.03	4.23	1.33	2.30	0.67
PXO112	Philippines	7.00	7.10	8.47	0.97	0.25	0.53
PXO99	Philippines	8.00	6.80	7.27	1.03	0.10	0.10
PXO280	Philippines	7.10	3.00	4.40	0.23	0.25	0.53
PXO339	Philippines	4.80	2.93	3.50	1.63	0.10	0.40
PXO341	Philippines	11.43	2.87	6.17	2.17	0.45	0.43
T7174	Japan	8.50	10.80	12.10	0.10	0.10	0.10
T7147	Japan	4.93	3.23	3.63	0.80	0.10	1.17
T7133	Japan	4.97	4.87	4.87	2.73	2.33	0.47
KXO19	Korea	12.80	6.13	7.60	2.50	0.10	0.30
KXO85	Korea	10.17	8.03	8.20	1.80	0.17	0.90
KXO576	Korea	8.13	5.17	3.23	0.40	0.30	0.10
PP8511	Bangladesh	7.20	4.47	8.37	1.33	0.45	0.83
GX15-4	China	11.77	7.47	7.57	1.80	0.40	0.80
YUN17-3	China	10.90	10.53	9.03	2.00	0.60	0.77
YUN17-8	China	10.73	9.50	11.87	2.57	0.83	0.67
YUN18-2-2	China	11.17	5.57	4.63	2.30	0.97	2.43
YUN18-16	China	9.57	8.80	6.30	0.93	1.10	0.80
LN44	China	11.37	8.77	7.43	1.73	3.33	1.97
Mean (cm)		8.02aA	6.22bA	6.26bA	1.64cB	0.65cB	0.80cB

[a] *The inoculation assays were performed during 2019-2020 in Sanya Experimental Station of CAAS, Hainan Province, China. The data in the table is mean BB lesion length (cm). Lesion length for each rice line against each Xoo strain was the mean of three leaves, measured at 14 days after inoculation. For the mean lesion length of 28 Xoo strains (last row in the table), the values followed by a common letter are not significantly different as determined by the least-significant difference (LSD) test at $p < 0.01$ (small letter) or $p < 0.001$ (capital letter), respectively.*

Key Laboratory of Rice Biology, China National Rice Research Institute (Hangzhou, Zhejiang) during 2019–2020 for blast resistance evaluation at seedling stage by spraying inoculation (Yu et al., 2013). The *indica* rice variety CO39 was used as the S control. For each rice genotype, at least 15 plants at the 3–4-leaf stage were inoculated by spraying spores of *M. Oryzae*. The disease levels are scored following a standard 0–9 rating evaluation system (IRRI, 1996; Latif et al., 2011), wherein scores 0–1, 2, 3, 4-6, 7, and 8–9 represent HR, R, moderately resistant (MR), moderately susceptible (MS), S, and HS, respectively. A total of 38 *M. Oryzae* isolates (**Table 2**) were used for spraying inoculation, and disease evaluation was performed in triplicates.

Leaf and neck blast resistances were evaluated under natural blast nurseries of two locations (Changsha and Jiangyong, Hunan) in 2020 and 2021. Eighteen plants were planted in the disease nursery for R900, the iR900 lines, Super 1000, and the iS1000 hybrids. The HS cultivar CO39 was sown on the plot borders. The field screening of resistance was performed by using a randomized block design with three replications. Additionally, the seedling was assessed for blast resistance by artificial inoculation with a mix of four representative isolates collected from Qionglai and Pujiang of Sichuan Province, Jiangyong and Changsha of Hunan Province, following the method described by Liu et al. (2019) with a minor modification,

TABLE 2 | The detailed information of the *M. Oryzae* isolates and the disease reaction evaluated using a 0–9 rating system.

Isolate code	Place of origin	Rice genotype				
		CO39	R900	R900-*Pi9*	R900-*Pi1* + *Pi9*	R900-*Pi1* + *Pi2*
19-765-1-4	Zhejiang, China	7	5	1	1	3
16-755-1-4	Zhejiang, China	9	0	0	7	0
19-763-7-2	Zhejiang, China	7	7	1	1	3
19-763-7-1	Zhejiang, China	9	1	1	3	3
19-765-1-3	Zhejiang, China	9	0	0	0	3
19-765-1-2	Zhejiang, China	9	5	7	5	3
16-755-2-4	Zhejiang, China	7	0	0	0	3
18-550-2-12	Hunan, China	0	1	3	0	1
2016CH2	Hunan, China	0	0	5	0	0
2016CH48	Hunan, China	5	7	0	5	5
2016CH47	Hunan, China	0	3	3	5	0
2016CH1	Hunan, China	9	0	0	0	0
2016CH50	Hunan, China	9	0	7	3	5
2016CH51	Hunan, China	9	5	5	0	0
2016CH52	Hunan, China	9	1	3	3	1
20-767	Zhejiang, China	9	0	3	1	3
2016CH49	Hunan, China	9	9	7	5	5
2016CH8	Hunan, China	9	3	5	5	5
2016CH7	Hunan, China	7	5	3	0	0
2016GD-1	Guangdong, China	5	3	3	3	1
2016CH-5	Hunan, China	9	3	3	0	3
2016ZY10	Unknown	3	9	7	9	9
2016ZY-1	Unknown	9	5	3	3	5
2016CH6	Hunan, China	9	9	5	7	3
2016GD2	Guangdong, China	9	5	0	3	3
18-162-7-1	Jiangxi, China	9	0	7	3	5
18-162-1-2	Jiangxi, China	0	0	0	0	0
195-2-2	Unknown	5	1	0	1	0
Z36-2	Unknown	7	9	0	1	0
RB10	Guangdong, China	9	9	5	3	3
18-162-5-1	Jiangxi, China	7	0	0	0	0
Z36-1	Unknown	7	0	0	0	0
18-162-5-4	Jiangxi, China	0	7	9	5	5
P06-6	Philippines	9	7	9	5	3
WJ2359	Wujin, China	9	5	7	5	7
2016ZY-7	Unknown	7	5	1	3	5
2016ZY-7	Unknown	9	0	0	0	0
RB14	Unknown	7	5	9	3	5

conidia were suspended to a concentration of 1×10^5 spores per ml in 0.1% (w/v) TWEEN-20. A volume of 4 ml suspension was sprayed on 14-day-old rice seedlings. Inoculated plants were kept in a growth chamber at 28°C with 90% humidity and in the dark for the first 24 h, followed by a 14/10-h light/dark cycle. The disease symptom was assessed 1 week after inoculation according to the evaluation system above (IRRI, 1996; Latif et al., 2011).

Evaluation of Yield, Main Agronomic Traits, and Grain Quality of the iR900 Lines and iS1000 Hybrids

The iR900-1 lines (containing resistance genes *Xa23* + *Pi9*) and the recurrent parent R900 were planted with one replication in the summer season in 2019, at Changsha, Hunan Province. Each plot comprised of five rows with eight plants per row at a planting density of 20 cm between plants and rows. Based on field observation, the five best-improved lines were selected. Ten plants with days to heading recorded in the middle of the central rows in each plot were sampled for measurements of agronomic traits, including plant height, panicle number, panicle length, spikelets per panicle, filled-grain percentage, 1,000-grain weight, and yield per plant. The agronomic traits were measured according to the standard evaluation system for rice (IRRI, 1996).

The iS1000 containing *Xa23* + *Pi9* (iS1000-1) and the original Super 1000 (S1000) were planted in the summer season in 2019 at seven locations as described in He et al. (2020). A large-scale (6.73 ha) field demonstration under super-high-yielding cultivation practices were also performed for the iS1000-1 in Yunnan Province in 2019, The yield was evaluated by an expert group in accordance with the yield measurement method for super-rice of the Ministry of Agriculture and Rural Affairs of China. The iS1000-2 containing *Xa23* + *Pi1* + *Pi2*, iS1000-3 containing *Xa23* + *Pi1* + *Pi9,* and the original Super 1000 were planted in the summer season in 2020 at five locations in the middle and lower reaches of the Yangtze River using the method described by the China National Crop Variety Approval Committee. Yield per plot, seven main agronomic traits, and five grain quality traits were analyzed. To compare yield and yield components under the disease-stressed environment, another trial was conducted for the iS1000-2 and the original Super 1000 in the occurrence of natural blast epidemic and artificially BB-inoculated in Changsha, Hunan Province. Yield per plot and four yield component traits were investigated. The *t*-test was performed to examine the statistical significance of differences in yield and agronomic traits by using Microsoft Office Excel software.

RESULTS

Development of the iR900 Lines and iS1000 Hybrid Containing *Xa23* and *Pi9* Genes

All the foreground and the background SNP markers were used to genotype R900, HZ02455 (donor of *Xa23* + *Pi9*), and the F_1 plants to confirm the polymorphism of the markers. The F_1 plants were then backcrossed with R900. A total of 368 BC_1F_1 plants were genotyped using the foreground markers, and 93 plants with genes *Xa23* and *Pi9* were selected for the background examination using 115 SNP markers. The background analysis revealed that the background recovery rate ranged from 63.9 to 82.6% in these 93 individuals. Three plants with the highest background recovery rate were selected to further backcross with R900 to develop the BC_2F_1 population. For the BC_2F_1, a total of 550 plants were genotyped using the foreground markers, and 142 plants with genes *Xa23* and *Pi9* were selected for the background examination using 60 SNP markers. The background analysis revealed that the background recovery rate ranged from 83.3 to 96.1%. Three plants with the highest background recovery rate were selected to further backcross with R900. In the BC_3F_1 population, a total of 92 plants were genotyped using the foreground markers, and 19 plants with genes *Xa23* and *Pi9* were selected for the background examination using 16 SNP markers. The background analysis revealed that the background recovery rate ranged from 95.9 to 99.0%. In parallel, the BC_2F_1 plant selected was also selfed to get BC_2F_2. In the BC_2F_2 population, 207 plants with genes *Xa23* and *Pi9* were genotyped for background selection using 32 SNP markers. The background analysis revealed that the background recovery rate ranged from 93.9 to 98.8%. Among them, the plants with the highest background recovery rate, homozygous genotypes of *Xa23* and *Pi9* genes, and maximum phenotypic similarity to R900 were selected for continuous self-pollination till BC_2F_5. The best plants (iR900-1) from the BC_2F_5 population were crossed with the sterile line GX24S to produce an improved "Super 1000" combination (iS1000-1) which contains *Xa23* + *Pi9* genes (**Figure 1**).

The best line selected from BC_2F_3 of the iR900 lines and its corresponding hybrid combination iSuper 1000 containing *Xa23* + *Pi9* genes were genotyped using the high-density 56K SNP chip to analyze the genetic background. It was found that the background recovery rate between the iR900-1 and R900 is 96.8% (**Figure 2**), and the genetic similarity between the improved Super 1000 (iS1000-1) and Super 1000 is 98.8% (**Figure 3**), slightly higher than that between the R900 and iR900 as expected.

Development of the iR900 Lines and iS1000 Hybrid Containing Genes *Xa23* + *Pi1* + *Pi2*/*Pi9*

The F_1 plants derived from the cross between R900 and HZ02411 (*Pi1* and *Pi2* donor) were genotyped using foreground SNP markers, and 10 F_1 plants with target genes were backcrossed with R900. In the BC_1F_1 population, a total of 768 plants were genotyped using the foreground markers, and 186 plants with *Pi1* and *Pi2* genes were selected for the background genotyping using 111 SNP markers. The background analysis revealed that the background recovery rate ranged from 72.0 to 90.4%. Three plants with the highest background recovery rate were selected to backcross with R900. In the BC_2F_1 population, a total of 620 plants were genotyped using the foreground markers, and 145 plants with genes *Pi1* and *Pi2* were selected for the background genotyping using 32 SNP markers. The background recovery rate ranged from 87.9 to 95.4%, and two plants with the highest background recovery rate were selected to backcross with R900. In the BC_3F_1 population, a total of 94 plants were genotyped using foreground markers, and 21 plants with genes *Pi1* and *Pi2* were selected for the background genotyping using 11 SNP markers. The background analysis revealed that the background recovery rate ranged from 97.1 to 98.6%. To pyramid the genes *Xa23* + *Pi1* + *Pi2*/*Pi9* in the R900 genetic background, the best plants with *Xa23* and *Pi9* genes from the BC_3F_1 population of R900/HZ02455 were crossed with the best plants with genes *Pi1* and *Pi2* from BC_3F_1 population of R900/HZ02411 to produce

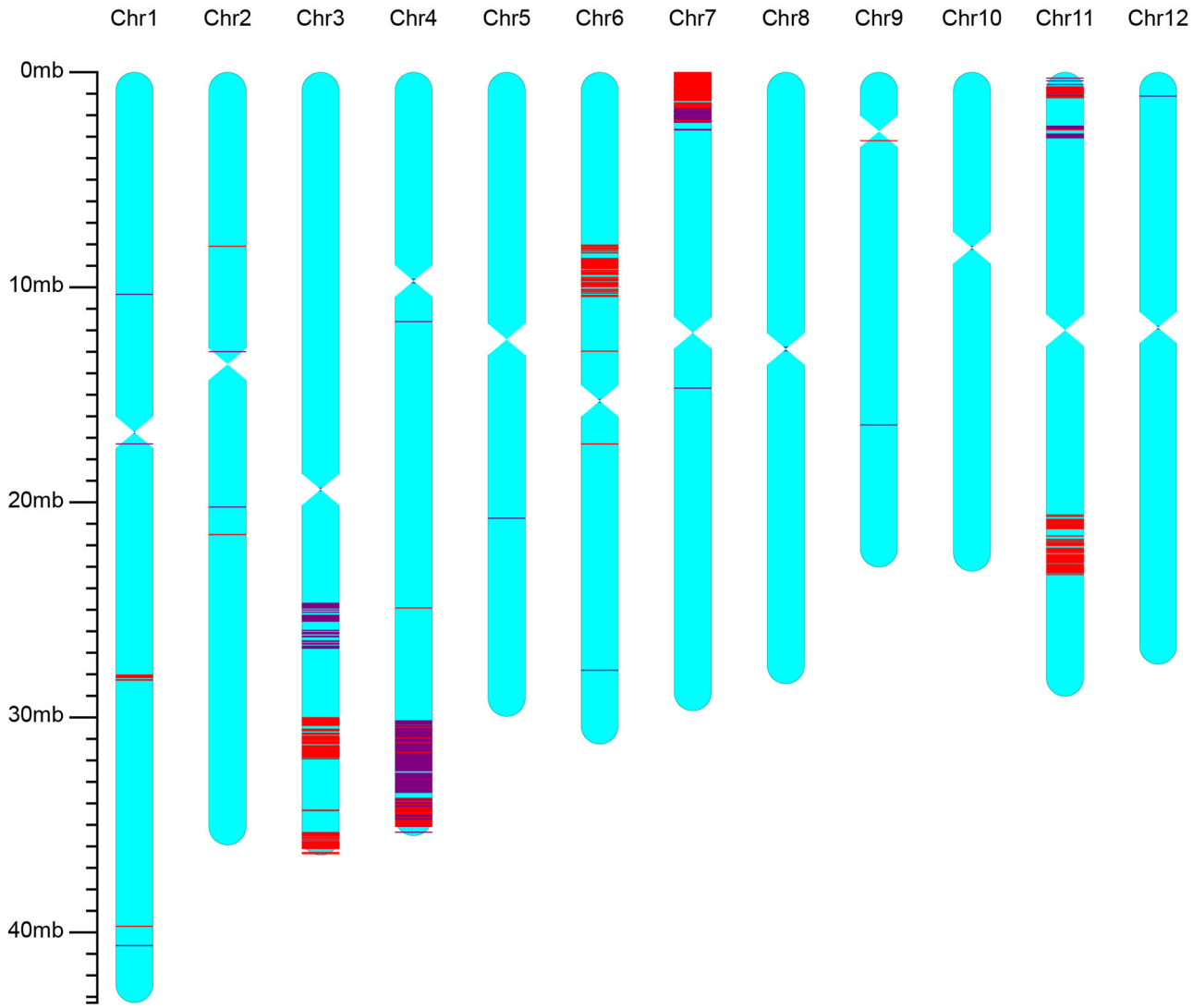


FIGURE 2 | Genetic background of the iR900 line containing genes *Xa23* + *Pi9* revealed by using the rice 56K SNP chip. The red lines indicate the SNP loci with homozygous genotypes of the donor parent; the purple lines indicate the SNP loci with heterozygous genotypes.

multi-cross F_1 (MF_1) seeds. Based on the foreground selection of 72 MF_1 plants, plants with *Xa23*+*Pi1*+*Pi2/Pi9* were selfed to generate MF_2 seeds. Among 3,098 MF_2 plants subjected to foreground screening, the plants with *Xa23* + *Pi1* + *Pi2/Pi9* and similar or superior agronomic traits to R900 were selfed to generate MF_3 seeds. According to the foreground and field screening of the desired target traits and comprehensive agronomic traits, plants with homozygous genotypes of genes *Xa23* + *Pi1* + *Pi2* and *Xa23* + *Pi1* + *Pi9* and superior agronomic traits were selfed till MF_5. The best plant in the MF_5 population was crossed with the sterile line GX24S to produce two types of improved "Super 1000" hybrid combinations which contain genes *Xa23* + *Pi1* + *Pi2* (iS1000-2) and *Xa23* + *Pi1* + *Pi9* (iS1000-3) (**Figure 1**).

Phenotypes of iR900-1 Line and iS1000-1 Hybrid for BB Resistance

A set of 28 individual *Xoo* strains were used to infect plant leaves for each of the genotypes to be examined. The degree of BB resistance is indexed by lesion length on leaves post-inoculation, and the shorter lesion length indicates higher resistance. The resistance assays showed that both R900 and S1000 are HS to BB. As showed in **Table 1** and **Figure 4**, the lesion lengths of the recurrent parent R900 ranged from 2.87 cm (against PXO341) to 10.8 cm (against T7174) with the mean length of 6.22 cm (**Table 1**). Similarly, the lesion lengths of the hybrid Super 1000 (S1000) ranged from 2.2 cm (against ZHE173) to 12.1 cm (against T7174) with a mean length of 6.26 cm (**Table 1**). In contrast, the mean lesion lengths of the

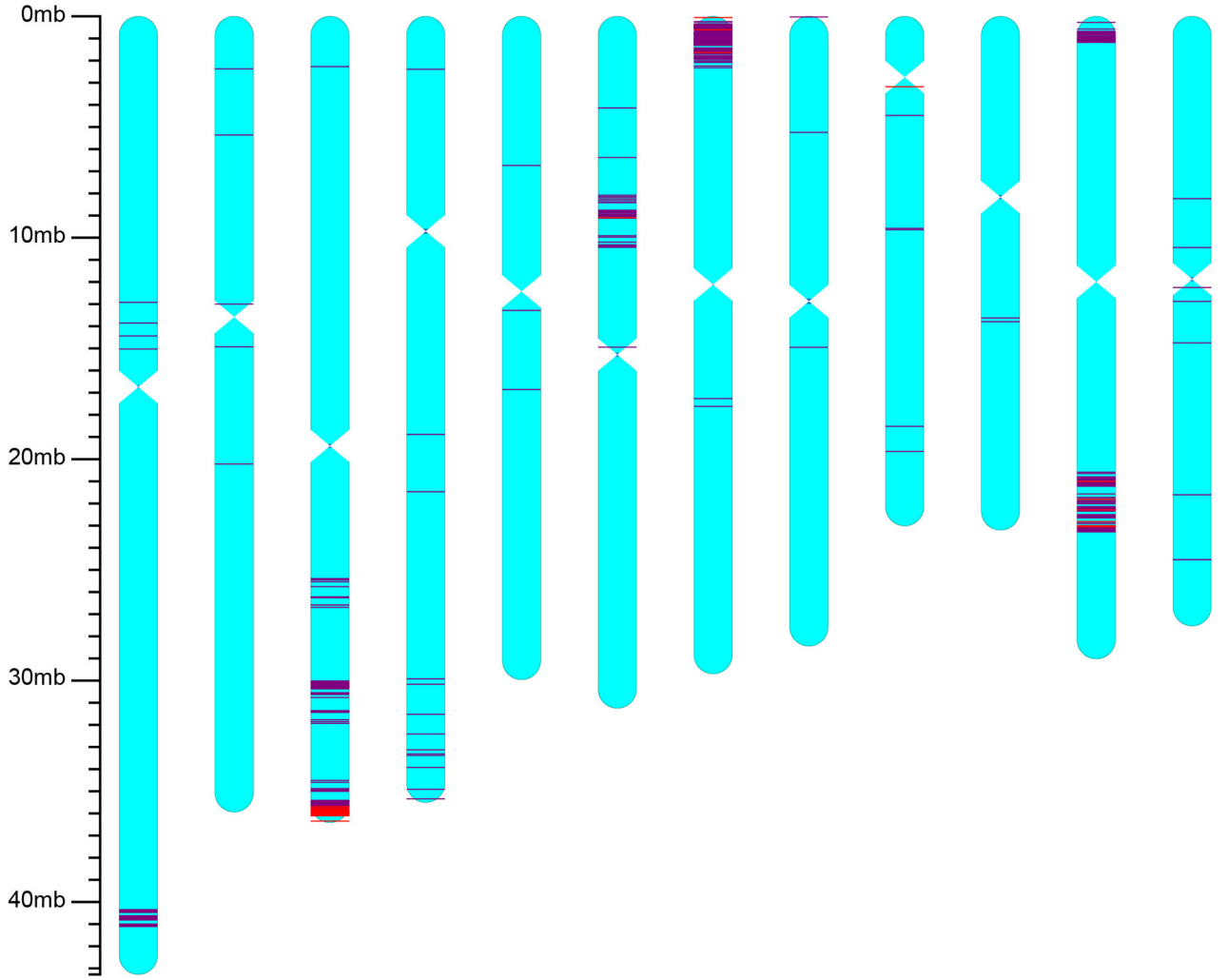


FIGURE 3 | Genetic background of the iS1000 containing genes *Xa23* + *Pi9* revealed by using rice 56K SNP chip. The red lines indicate the SNP loci with homozygous genotypes of the donor parent, the purple lines indicate the SNP loci with heterozygous genotypes.

S control (JG30) and the R control (CBB23) are 8.02 and 0.80 cm, respectively (**Table 1**). These data also indicated that a specific rice genotype responds differently to different *Xoo* strains (**Table 1**).

As showed in **Table 1** and **Figure 4**, weak symptom was found on the leaves of iR900-1 and iS1000-1 post-inoculation. The *Xoo* strains led to 1.64 cm (0.40–3.87 cm) of lesions in length for iR900-1, and 0.65 cm (0.10–0.90 cm) of lesions in length for iS1000-1 (**Table 1**, **Figure 4**), indicating that the resistance level of both iR900-1 and iS1000-1 is comparable to the R control CBB23 (**Table 1**, **Figure 4**). These results clearly demonstrated that introducing the *Xa23* gene enhanced the BB resistance remarkably in both parent iR900-1 and hybrid iS1000-1.

Phenotypes of the iR900 Lines and iS1000 Hybrids for Rice Blast Resistance

The blast resistance reaction was evaluated at 7–10 days after spraying inoculation, using a 0–9 rating system (**Table 2**). The phenotypic results for infection of 38 *M. Oryzae* isolates were calculated for resistance frequency and a higher frequency represents a broader resistance spectrum. As showed in **Figure 5**, the resistance frequency of iR900-2 carrying *Pi1* + *Pi2*, and iR900-3 carrying *Pi1* + *Pi9* were 71.05%, which is clearly higher than that of R900 (52.63%), while the resistance frequency of S control CO39 is dramatically low (15.79%). These results verify that blast resistance is occurring in those lines with R genes. It is worth to note that the line iR900-1 carrying *Pi9* did not perform an improved resistance spectrum (resistance frequency: 53.33%)



FIGURE 4 | Assessment of BB resistance of 6 rice genotypes. The disease reactions of the rice genotypes, including S (JG30) and R (CBB23) checks, to the representative *Xoo* strain PXO99 inoculated using the leaf-clipping method. The R and S lesions 14 days after inoculation are shown by representative leaves.

compared to R900 (resistance frequency: 52.63%), which may suggest that pyramiding of *Pi9* and *Pi1* is required for a broader blast resistance spectrum.

Blast resistance was also evaluated on rice panicle neck under field conditions (Changsha, Hunan) in 2020 and 2021. Panicle neck blast evaluation showed that the recurrent parent R900 was HS with 60% infection rate in Changsha, while the iR900 lines presented much higher resistance with 10–20% infection rate in the same nursery (**Table 3**). The iR900 lines with two R genes exhibited better panicle neck blast resistance than the line with only one R gene. For the hybrid combinations, Super 1000 was HS to blast in the 2 years at two locations, with leaf blast score ranging from 6 to 7 and panicle neck blast infection rate from 80 to 90% (**Table 3**). In contrast, the iS1000 hybrids exhibited resistance to blast with the highest score of 2 for leaf blast and 10% of the infection rate for panicle neck blast infection. The iS1000 with R genes *Pi1* + *Pi2* exhibited slightly better panicle neck blast resistance than the hybrid with R genes *Pi1* + *Pi9* in Changsha nursery in 2020 (**Table 3**).

Further, the seedling leaf blast resistance was tested by spray inoculation with a mix of four representative isolates. The checks CO39 and Gumei4 showed HS and HR to seedling leaf blast, with a score of 9 and 0, respectively (**Figure 6**). The original R900 and Super 1000 showed a resistance score of 6 (S) and 7 (S), while the iR900-2 and iS1000-2 presented a resistance score of 1 (R) and 2 (R) (**Figure 6**). In short, resistance to rice blast was effectively enhanced in the iR900 and its derived Super 1000 hybrid variety.

Performance of Yield, Agronomic and Grain Quality Traits of the iR900 Lines and the iS1000 Hybrids

Five of the iR900-1 lines were evaluated for key agronomic traits as compared to the original R900. In general, no significant difference was observed between the iR900 lines and the original R900 for most of the agronomic traits (**Table 4**). Nevertheless, some differences were still detected for a few traits, including spikelet fertility, yield per plant, etc. For example, the spikelet fertility of the iR900-1-3 and iR900-1-4 was higher than that of the original R900 by 10 and 8.8%, respectively, and the yield per plant of the iR900-1-4

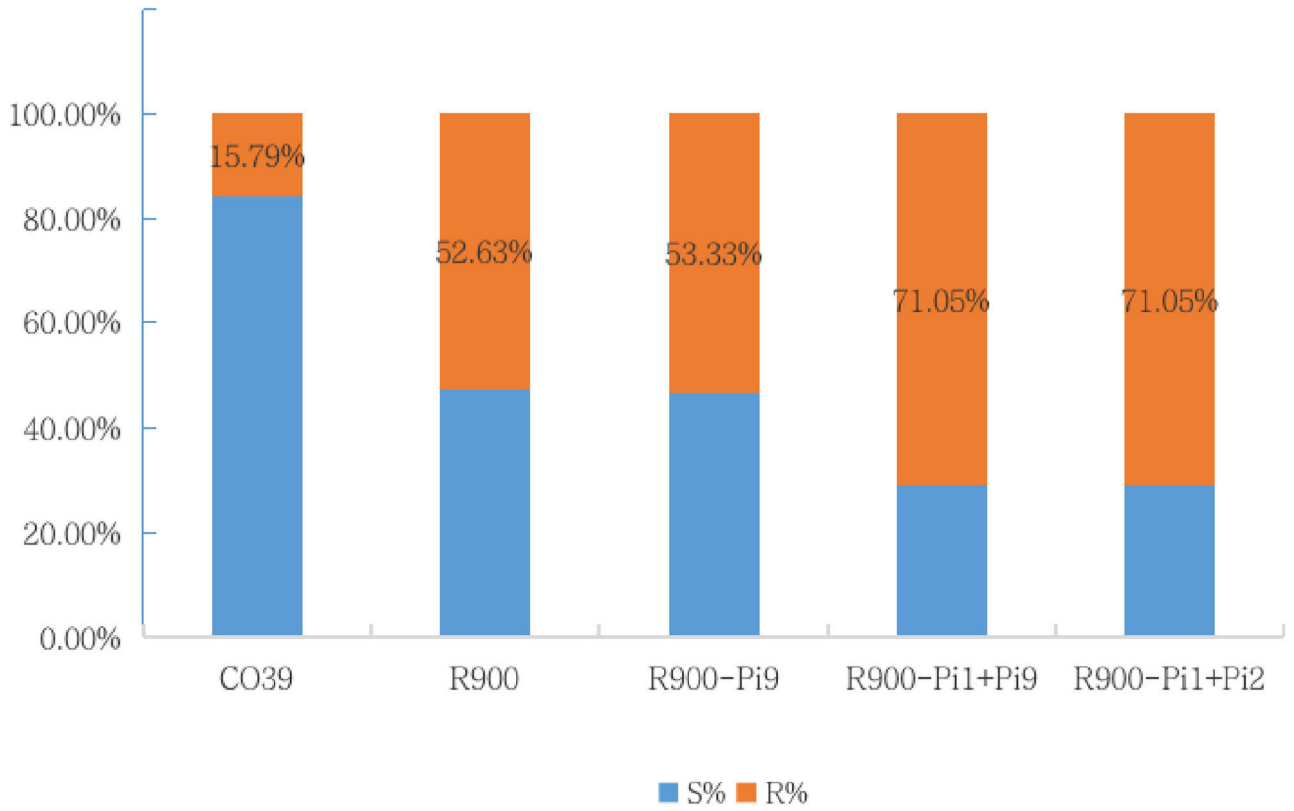


FIGURE 5 | The resistance frequency/spectrum of five genotypes based on the disease reaction phenotype of spraying inoculation and disease evaluation at seedling stage.

TABLE 3 | Performance of leaf and panicle neck blast resistances of the iR900 and iS1000 hybrids in natural blast nurseries.

Location	Year	Line and hybrid	Leaf blast score	Panicle neck blast infection rate (%)
Changsha, Hunan, China	2020	R900	-	60.0
		iR900-1 (*Xa23* + *Pi9*)	-	20.0
		iR900-2 (*Xa23*+*Pi1*+*Pi2*)	-	10.0
		iR900-3 (*Xa23*+*Pi1*+*Pi9*)	-	10.0
		S1000	-	80.0
		iS1000-2 (*Xa23*+*Pi1*+*Pi2*)	-	6.7
		iS1000-3 (*Xa23*+*Pi1*+*Pi9*)	-	10.0
Jiangyong, Hunan, China	2020	S1000	-	86.6
		iS1000-2 (*Xa23*+*Pi1*+*Pi2*)	-	0
		iS1000-3 (*Xa23*+*Pi1*+*Pi9*)	-	0
Changsha, Hunan, China	2021	S1000	7	90.0
		iS1000-2 (*Xa23*+*Pi1*+*Pi2*)	0	8.3
Jiangyong, Hunan, China	2021	S1000	6	81.6
		iS1000-2 (*Xa23*+*Pi1*+*Pi2*)	2	1.4

and iR900-1-5 was higher than that of the original R900 by 7.5 and 5.1 g, respectively. Furthermore, the panicle number of the iR900-1-4 outnumbered that of the original R900 by 0.9 per plant, and the 1,000-grain weight of the iR900-1-5 exceeded that of the original R900 by 2.3 g (**Table 4**). These results indicated that the main agronomic traits of the five

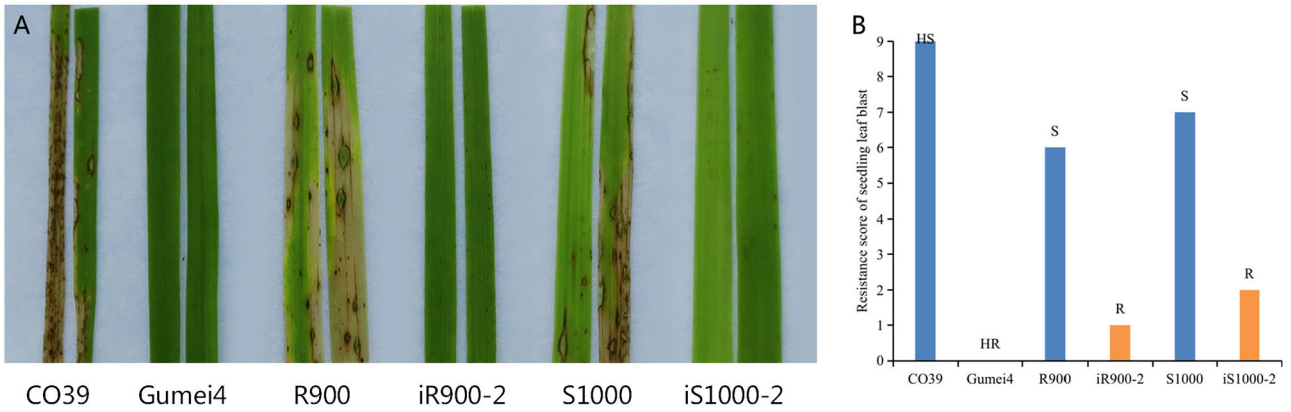


FIGURE 6 | Evaluation of seedling blast resistance of six rice genotypes. **(A)** Disease reactions of the rice genotypes, including the S (CO39) and R (Gumei4) checks, to a mix of four isolates by using spraying inoculation. **(B)** Resistance score and resistance level. HR, highly resistant; R, resistant; MR, moderately resistant; S, susceptible; HS, highly susceptible.

TABLE 4 | The performance of yield and main agronomic traits of the iR900 lines containing genes *Xa23*+ *Pi9*.

Line	Trait[a]							
	Yield (g/plant)	DTH(d)	PH (cm)	PN	PL (cm)	NGP	FGP (%)	GW (g)
R900	23.1	98.7	108.6	3.8	24.7	358.2	71.9	24.0
iR900-1-1	26.0	98.3	109.5	4.5	24.2	315.9	74.8	25.5
iR900-1-2	27.0	99.6	107.2	4.6	23.4	338.0	73.4	24.0
iR900-1-3	27.8	100.2	108.2	3.9	23.7	348.6	81.9**	24.8
iR900-1-4	30.6*	99.3	111.0	4.7*	23.1	331.6	80.7**	24.7
iR900-1-5	28.2*	99.5	108.4	4.2	24.8	331.8	77.5	26.3**

[a]*DTH, days to heading; PH, plant height (cm); PN, panicle number/plant; PL, panicle length (cm); NGP, number of grains/panicle; FGP, filled-grain percentage (%); GW, 1,000-grain weight (g).*

*, ** *Significant difference with R900 at the 5 and 1% probability level, respectively.*

selected lines are essentially identical, but the yield per plant and filled-grain percentage were superior to that of the recurrent parent, R900.

Large-scale multi-site field trials were launched in 2 consecutive years (2019 and 2020) to compare the iS1000-1 and the original Super 1000 for yield and some key agronomic traits. It was found that no significant difference was observed for yield and all of the tested agronomic traits in 2019 (He et al., 2020). The results in 2020 showed that the average yields of the two iS1000 hybrids were 9.9 t/ha and 9.6 t/ha which was higher than that of the original Super 1000 by 4.2 and 1.1%, respectively. We investigated seven agronomic traits (days to maturity, plant height, spikelets/panicle, filled-grain percentage, and 1,000-grain weight) and data were collected from five locations. Non-significant differences were found between the iS1000 hybrids and the original Super 1000 for the traits observed (**Table 5**).

To profile grain quality, rice grains from three sites were collected and characterized for five important rice quality characteristics (milling rice percentage, grain length/width ratio, chalky rice percentage, gel consistency, and amylose content). It was shown that these traits were statistically identical between the iS1000 hybrid combinations and the original Super 1000 (**Table 5**).

Furthermore, yield potential was explored in a large-scale field demo trial with and without biotic stress for the improved and original Super 1000. The yield of a large-scale (6.73 ha) field demonstration (Yunnan, China) in 2019 showed that the iS1000 with resistance achieved a super-high yield of 17.1 t/hm^2, which nearly reached a yield record of the original Super 1000 set in 2018.

Under the biotic stress conditions, the iS1000 also performed a constant high yield compared to the original Super 1000. Both original and two improved varieties were planted in Changsha for natural blast infection and BB inoculation. Under the serious blast outbreak conditions and BB stresses, the original Super 1000 had a yield loss of 26.6 and 31% compared with the two iS1000 hybrids, respectively. The yield components data showed that the filled-grain percentage of the original Super 1000 was declined by 24 and 18.2% compared with two iS1000 hybrids, which illustrated that the yield losses were caused by rice blast and BB epidemics (**Table 6**). In summary, all these results approved that the iR900 lines and the derived iS1000 hybrids maintained

TABLE 5 | The performance of yield, main agronomic, and grain quality traits of the iS1000 hybrids.

Hybrid	Trait[a]												
	Yield (t/hm^2)	DTH	PH (cm)	PN	PL (cm)	NGP	FGP (%)	GW (g)	MRP (%)	L/W	CRP (%)	GC (mm)	AC (%)
S1000	9.5	89	120.1	9.1	24.1	272.6	83.1	23.5	70.3	2.7	11.6	86.6	25.7
iS1000-2	9.9	88.6	121.2	10.2	24.2	275.8	83.4	23.5	70.4	2.7	12.9	88.3	26.9
iS1000-3	9.6	89.2	120.8	9.1	24.6	283.5	84	23.8	70.8	2.8	10.5	88.3	25.7

[a] *DTH, days to heading; PH, plant height (cm); PN, panicle number; PL, panicle length (cm); NGP, number of grains per panicle; FGP, filled-grain percentage (%); GW, 1,000-grain weight (g); MRP, milling rice percentage (%); L/W, grain length-width ratio; CRP, chalky rice percentage (%); GC, gel consistency (mm); AC, amylose content (%).*

TABLE 6 | Comparison of yield and yield components between the iS1000 and the original Super 1000 under disease stresses.

Variety and environment	Trait[a]				
	Yield (t/hm^2)	PN	NGP	FGP (%)	GW (g)
S1000 under blast epidemic	7.6	8.9	262.8	60.9	23.1
iS1000-2 under blast epidemic	10.3	9.5	249.8	84.9	25.3
S1000 under BB artificial inoculation	5.9	7.2	261.1	47.7	23.6
iS1000-2 under BB artificial inoculation	8.6	7.2	280.9	65.9	24.2

[a] *PN, panicle number; NGP, number of grains per panicle; FGP, filled-grain percentage (%); GW, 1,000-grain weight (g).*

the key agronomic traits, some selected lines and their hybrids even performed higher yields to that of the non-improvement checks, the original R900 and Super 1000.

DISCUSSION

Fast Improvement Achieved by Genome-Wide Marker-Assisted Selections

Conventional breeding, an experience-based approach has played a great role to develop elite rice varieties in the past (Wing et al., 2018), but usually has a long breeding cycle and low efficiency. In general, it takes 8–10 years for a whole breeding cycle (Gao, 2021) and has considerable uncertainty for predicting results of the selected lines (Bevan et al., 2017). Alternatively, genomics technology based on genome information has been widely applied to improve breeding efficiency that is demonstrated in case of precise incorporation of target gene into elite varieties by the marker-assisted foreground and background selection. In this decade, the high-throughput and affordable genotyping platforms have enabled practical breeding to be performed in a rapid and precise manner that takes full advantage of genomic information (Herzog and Frisch, 2011; Springer and Schmitz, 2017; Wei et al., 2021). In this study, four dominant major resistance genes were introduced into the background of a super-hybrid-rice restorer line R900 by genomics-assisted selection. Two tightly linked SNP markers for each target gene and 120 polymorphic background SNP markers were applied for the genomic marker-assisted selections. In BC_1F_1 populations, the background recovery rate of the plants with target genes were 82.6 and 90.4%, much higher than the expected average of 75% in the first backcross generation. With backcross advanced to BC_3F_1, the background recovery rate of the target plants ranged from 95.9 to 99.0%, and the genetic background of recurrent parent R900 was rapidly recovered in the iR900 lines. In the recent reports, the background selection was mostly based on a few SSR markers which had low resolution and inadequate whole-genome coverage (Priyadarshi et al., 2018; Yang et al., 2019; Ramalingam et al., 2020). The SNP array with abundant markers is an efficient tool for the background analysis, which was almost 300 times more cost-effective in relative to SSR markers (Khanna et al., 2015). The analysis by high-density rice 56K SNP chip revealed that the selected line from BC_2F_3 of the iR900 has a background recovery rate of 96.8% to the recurrent parent R900. Therefore, genome-wide marker-assisted background selections can be performed to significantly reduce backcross generations in crop improvement (Hospital and Charcosset, 1997; Frisch et al., 1999; Frisch and Melchinger, 2001).

Stacking Genes to Improve BB and Blast Resistance

The iR900 lines and the iS1000 hybrids with R genes clearly showed enhanced resistance against BB and rice blast diseases. The improved lines of R900 and the derived Super 1000 hybrid containing *Xa23* are HR to the 28 tested *Xoo* strains. These results implied that the *Xa23* gene has a dominant effect because both iR900 lines (*Xa23/Xa23*) and iS1000 hybrids (*Xa23/xa23*) can exhibit broad-spectrum resistance to BB isolates worldwide. It is known that the *Xa23* gene expresses in a dominant manner and confers strong resistance to BB with the broadest resistance spectrum that has been widely utilized in breeding programs (Zhou et al., 2009; Huang et al., 2012; Jiang et al., 2015). However, the other resistance genes, such as *Xa7* and *Xa21,* can be overcome in the recent years by the new virulent BB strains

due to pathogenic variation and evolution (Zhang, 2009; Chen et al., 2011; Wang et al., 2014).

For resistance to blast at the seedling stage, the iR900 lines containing *Pi1* + *Pi2/Pi9* exhibited resistance to 71.05% of 38 *M. Oryzae* isolates under artificial inoculation, showing an obviously increased resistance frequency/spectrum compared with that of the original R900 (**Figure 5**). Furthermore, the field trial also showed that the iR900 lines presented a significantly increased resistance level for panicle neck blast, conferring the highest grade of resistance to leaf blast (score = 2) and lowest 10% of infection rate (10%) for panicle neck blast in the iS1000. These results revealed that it is feasible to stack multiple resistance genes for broad-spectrum resistance and increased resistance levels. It is more usual to use a single R gene in breeding for resistance. For instance, the *Pi9* gene was HR to 43 *M. oryzae* isolates from 13 countries (Liu et al., 2002); therefore, it has been widely employed in rice breeding programs (Ni et al., 2015; Luo et al., 2017). However, we found that integration of the *Pi9* gene alone into R900 is not applicable to broaden resistance spectrum and increase resistance level to blast. First, iR900-*Pi9* showed resistance to only 53.3% of the 38 *M. Oryzae* isolates tested, almost comparable to that of the recurrent parent R900. Second, both iR900-*Pi9* and iS1000-*Pi9* showed rather a high percentage of blast infection on panicle neck in the field nurseries, 20 and 95.6%, respectively (He et al., 2020), implying that a single *Pi9* gene is not effective for blast control in the background of R900 and its hybrid Super 1000. Owing to the dynamic and evolving nature of host-pathogen interactions, single-gene resistance is often easily overcome by evolving pathogen populations after a few years of cultivation. Resistance breeding is therefore an ongoing process, and resistance must be managed strategically (Nelson et al., 2018). While incorporating resistance gene into breeding strategies might improve the durability of resistance, there is an exigency for pyramiding multiple genes for attaining durable resistance (Hittalmani et al., 2000; Singh et al., 2012). As the results showed in our study, the resistance spectrum to blast is remarkably broadened by a combination of *Pi9* and *Pi1* (from 53.3 to 71.05%). In the field nursery, the iR900 lines with two blast genes also presented better panicle neck blast resistance than the single gene *Pi9* (**Table 3**). The stacking of several resistance genes with different recognition spectra and environmental optima into a single background is thus a credible strategy for achieving more durable disease resistance (Bailey-Serres et al., 2019).

Improvement of Disease Resistance Without Yield Penalty

Crops' defense activation usually causes growth inhibition and yield reduction, which are referred to as trade-offs between growth and defense (Nelson et al., 2018). The genomics-assisted breeding strategy involves precise target genes identification and whole genomic background selection is helpful to avoid these problems. In our study, we developed large populations in BC_1F_1 and BC_2F_1 generations, more than 100 SNP markers covering the whole rice genome were used to analyze the genetic background. In the BC_2F_1 population, the highest background recovery rate reached over 95%. The field trial showed that the main agronomic traits of the selected lines of the iR900 are essentially identical to the recurrent parent R900. The multi-site trials also showed that non-significant differences were found between the iS1000 hybrids and the original Super 1000. Given the potential trade-offs between resistance and yield, comprehensive traits should be considered when selecting final target plants after the molecular marker-based foreground and background selection (Nelson et al., 2018). The success of integrating phenotypic selection along with the background selection in the breeding programs for selecting superior recombinants has been demonstrated earlier by Ellur et al. (2016). The results in this study also indicate that a wise strategy to overcome linkage drag in breeding for resistance is to use commercial variety harboring resistance genes as a donor rather than the wild and landraces with the resistance genes. It is expected that favorable genes are accumulated in the improved donor and subsequently transfer of these genes would help in further improving the background of the pyramided lines (Pradhan et al., 2016).

CONCLUSION

Significant resistance was achieved for overcoming BB and rice blast diseases in the improved parental R900 lines (iR900) and the corresponding hybrids, the improved Super 1000 hybrids (iS1000). In addition to improved disease resistance, field trials and large-scale demonstrations on multi-locations showed that iS1000 hybrids maintain super-high yield and exhibit identical agronomic traits to the original "Super 1000," indicating a successful practice for trait improvement with genomics-assisted breeding. The present study also implies that it is feasible to conduct genetic improvement for other crops using a similar approach.

DATA AVAILABILITY STATEMENT

The original contributions presented in the study are included in the article/supplementary material, further inquiries can be directed to the corresponding authors.

AUTHOR CONTRIBUTIONS

ZH, JP, and YX designed the research. ZH, CW, ZXu, JC, CY, and YL drafted the manuscript. ZH, CW, HY, ZXu, JC, ZL, CY, HY, ZXi, NJ, JH, and YL performed the experiments and data analysis. ZH, JP, KZ, YX, ZXu, JC, CY, NJ, JX, BT, and YL revised and finalized the manuscript. All authors read and approved the final manuscript.

FUNDING

This work was supported by the program Super Hybrid Rice Innovation Team, the National Natural Science Foundation of China (U20A2035, 32072412), the Central Public-interest Scientific Institution Basal Research Fund for Chinese Academy of Tropical Agricultural Sciences (No. 1630032019037), and the Hainan Yazhou Bay Seed Laboratory (B21HJ0218).

ACKNOWLEDGMENTS

We are grateful to Prof. Longping Yuan, who first proposed this project and generously provided the seeds of R900 for improvement. We thank him for his insightful suggestions and field guidance on this project. We would also like to thank our colleagues in Huazhi Bio-Tech Co., Ltd., who assisted with genotyping, disease evaluation, grain quality analysis, and multi-location field trials.

REFERENCES

Bai, J., Zhang, Q., and Jia, X. (2006). Comparison of different foreground and background selection methods in marker-assisted introgression. *Acta Genet. Sin.* 33, 1073–1080. doi: 10.1016/S0379-4172(06)60144-3

Bailey-Serres, J., Parker, J. E., Ainsworth, E. A., Oldroyd, G. E. D., and Schroeder, J. I. (2019). Genetic strategies for improving crop yields. *Nature* 575, 109–118. doi: 10.1038/s41586-019-1679-0

Bevan, M. W., Uauy, C., Wulff, B. B. H., Zhou, J., Krasileva, K., and Clark, M. D. (2017). Genomic innovation for crop improvement. *Nature* 543, 346–354. doi: 10.1038/nature22011

Chen, S., Liu, X., Zeng, L., Ouyang, D., Yang, J., and Zhu, X. (2011). Genetic analysis and molecular mapping of a novel recessive gene *xa34(t)* for resistance against *Xanthomonas oryzae* pv. oryzae. *Theor. Appl. Genet.* 122, 1331–1338. doi: 10.1007/s00122-011-1534-7

Dayton, L. (2014). Agribiotechnology: blue-sky rice. *Nature* 514, S52–S54. doi: 10.1038/514S52a

Deng, Y., Zhai, K., Xie, Z., Yang, D., Zhu, X., Liu, J., et al. (2017). Epigenetic regulation of antagonistic receptors confers rice blast resistance with yield balance. *Science* 355, 962–965. doi: 10.1126/science.aai8898

Deng, Y., Zhu, X., Shen, Y., and He, Z. (2006). Genetic characterization and fine mapping of the blast resistance locus Pigm(t) tightly linked to *Pi2* and *Pi9* in a broad-spectrum resistant Chinese variety. *Theor. Appl. Genet.* 113, 705–713. doi: 10.1007/s00122-006-0338-7

Doyle, J. J., and Doyle, J. L. (1987). A rapid DNA isolation procedure for small quantities of fresh leaf tissue. *Phytochem Bull.* 9, 11–15.

Ellur, R. K., Khanna, A., Gopala Krishnan, S., Bhowmick, P. K., Vinod, K. K., Nagarajan, M., et al. (2016). Marker-aided incorporation of *Xa38*, a novel bacterial blight resistance gene, in PB1121 and comparison of its resistance spectrum with *xa13* + *Xa21*. *Sci. Rep.* 6:29188. doi: 10.1038/srep29188

Frisch, M., Bohn, M., and Melchinger, A. E. (1999). Comparison of selection strategies for marker-assisted backcrossing of a gene. *Crop Sci.* 39, 1295–1301. doi: 10.2135/cropsci1999.3951295x

Frisch, M., and Melchinger, A. E. (2001). Marker-assisted backcrossing for simultaneous introgression of two genes. *Crop Sci.* 41, 1716–1725. doi: 10.2135/cropsci2001.1716

Gao, C. (2021). Genome engineering for crop improvement and future agriculture. *Cell* 184, 1621–1635. doi: 10.1016/j.cell.2021.01.005

Hayashi, K., Hashimoto, N., Daigen, M., and Ashikawa, I. (2004). Development of PCR-based SNP markers for rice blast resistance genes at the Piz locus. *Theor. Appl. Genet.* 108, 1212–1220. doi: 10.1007/s00122-003-1553-0

He, Z., Xin, Y., Jiang, N., Liang, Y., Huang, J., Yang, H., et al. (2020). Evaluation of resistance, yield and major agronomic traits in the directionally-improved Super 1000. *Hybrid rice* 35, 94–99. doi: 10.16267/j.cnki.1005-3956.20200330.108

Herzog, E., and Frisch, M. (2011). Selection strategies for marker-assisted backcrossing with high-throughput marker systems. *Theor. Appl. Genet.* 123, 251–260. doi: 10.1007/s00122-011-1581-0

Hillel, J., Schaap, T., Haberfeld, A., Jeffreys, A. J., Plotzky, Y., Cahaner, A., et al. (1990). DNA fingerprints applied to gene introgression in breeding programs. *Genetics* 124, 783–789. doi: 10.1093/genetics/124.3.783

Hittalmani, S., Parco, A., Mew, T. V., Zeigler, R. S., and Huang, N. (2000). Fine mapping and DNA marker-assisted pyramiding of the three major genes for blast resistance in rice. *Theor. Appl. Genet.* 100, 1121–1128. doi: 10.1007/s001220051395

Hospital, F., and Charcosset, A. (1997). Marker-assisted introgression of quantitative trait loci. *Genetics* 147, 1469–1485. doi: 10.1093/genetics/147.3.1469

Hospital, F., Chevalet, C., and Mulsant, P. (1992). Using markers in gene introgression breeding programs. *Genetics* 132, 1199–1210. doi: 10.1093/genetics/132.4.1199

Hua, L., Wu, J., Chen, C., Wu, W., He, X., Lin, F., et al. (2012). The isolation of *Pi1*, an allele at the *Pik* locus which confers broad spectrum resistance to rice blast. *Theor. Appl. Genet.* 125, 1047–1055. doi: 10.1007/s00122-012-1894-7

Huang, B., Xu, J. Y., Hou, M. S., Ali, J., and Mou, T. M. (2012). Introgression of bacterial blight resistance genes *Xa7, Xa21, Xa22* and *Xa23* into hybrid rice restorer lines by molecular marker-assisted selection. *Euphytica* 187, 449–459. doi: 10.1007/s10681-012-0758-1

IRRI (1996). *Standard Evaluation System for Rice*. The Philippines: IRRI.

Jez Joseph, M., Lee Soon, G., and Sherp Ashley, M. (2016). The next green movement: plant biology for the environment and sustainability. *Science* 353, 1241–1244. doi: 10.1126/science.aag1698

Jiang, J., Yang, D., Ali, J., and Mou, T. (2015). Molecular marker-assisted pyramiding of broad-spectrum disease resistance genes, *Pi2* and *Xa23*, into GZ63-4S, an elite thermo-sensitive genic male-sterile line in rice. *Mol. Breed.* 35:83. doi: 10.1007/s11032-015-0282-9

Kauffman, H. E., Reddy, A. P. K., Hsieh, S. P. Y., and Merca, S. D. J. P. (1973). An improved technique for evaluating resistance of rice varieties to *Xanthomonas oryzae*. *Plant Dis. Rep.* 57, 537–541.

Khanna, A., Sharma, V., Ellur, R. K., Shikari, A. B., Gopala Krishnan, S., Singh, U. D., et al. (2015). Development and evaluation of near-isogenic lines for major blast resistance gene(s) in Basmati rice. *Theor. Appl. Genet.* 128, 1243–1259. doi: 10.1007/s00122-015-2502-4

Latif, M. A., Badsha, M. A. H., Tajul, M. I., Kabir, M. S., Rafii, M. Y., Mia, M. A. T. J. S. R., et al. (2011). Identification of genotypes resistant to blast, bacterial leaf blight, sheath blight and tungro and efficacy of seed treating fungicides against blast disease of rice. *Sci Res Essays.* 6, 2804–2811. doi: 10.5897/SRE11.315

Li, J., Wang, J., and Zeigler, R. S. (2014). The 3,000 rice genomes project: new opportunities and challenges for future rice research. *Giga Sci.* 3:8. doi: 10.1186/2047-217X-3-8

Liu, G., Lu, G., Zeng, L., and Wang, G. L. (2002). Two broad-spectrum blast resistance genes, *Pi9(t)* and *Pi2(t)*, are physically linked on rice chromosome 6. *Mol. Genet. Genom.* 267, 472–480. doi: 10.1007/s00438-002-0677-2

Liu, M., Zhang, S., Hu, J., Sun, W., Padilla, J., He, Y., et al. (2019). Phosphorylation-guarded light-harvesting complex II contributes to broad-spectrum blast resistance in rice. *Proc. Natl. Acad. Sci. U. S. A.* 116, 17572–17577. doi: 10.1073/pnas.1905123116

Luo, W., Huang, M., Guo, T., Xiao, W., Wang, J., Yang, G., et al. (2017). Marker-assisted selection for rice blast resistance genes Pi2 and Pi9 through high-resolution melting of a gene-targeted amplicon. *Plant Breed* 136, 67–73. doi: 10.1111/pbr.12447

Ma, G., and Yuan, L. (2015). Hybrid rice achievements, development and prospect in China. *J. Integr. Agric.* 14, 197–205. doi: 10.1016/S2095-3119(14)60922-9

McCouch, S., Baute, G. J., Bradeen, J., Bramel, P., Bretting, P. K., Buckler, E., et al. (2013). Feeding the future. *Nature* 499, 23–24. doi: 10.1038/499023a

Nelson, R., Wiesner-Hanks, T., Wisser, R., and Balint-Kurti, P. (2018). Navigating complexity to breed disease-resistant crops. *Nat. Rev. Genet.* 19, 21–33. doi: 10.1038/nrg.2017.82

Ni, D., Song, F., Ni, J., Zhang, A., Wang, C., Zhao, K., et al. (2015). Marker-assisted selection of two-line hybrid rice for disease resistance to rice blast and bacterial blight. *Field Crops Res.* 184, 1–8. doi: 10.1016/j.fcr.2015.07.018

Pradhan, S. K., Nayak, D. K., Pandit, E., Behera, L., Anandan, A., Mukherjee, A. K., et al. (2016). Incorporation of bacterial blight resistance genes into lowland rice cultivar through marker-assisted backcross breeding. *Phytopathology* 106, 710–718. doi: 10.1094/PHYTO-09-15-0226-R

Priyadarshi, R., Arremsetty, H. P. S., Singh, A. K., Khandekar, D., Ulaganathan, K., Shenoy, V., et al. (2018). Marker-assisted improvement of the elite maintainer

line of rice, IR 58025B for wide compatibility (*S5(n)*) gene. *Front. Plant Sci.* 9:1051. doi: 10.3389/fpls.2018.01051

Raina, M., Salgotra, R. K., Pandotra, P., Rathour, R., and Singh, K. (2019). Genetic enhancement for semi-dwarf and bacterial blight resistance with enhanced grain quality characteristics in traditional Basmati rice through marker-assisted selection. *C. R. Biol.* 342, 142–153. doi: 10.1016/j.crvi.2019.04.004

Ramalingam, J., Raveendra, C., Savitha, P., Vidya, V., Chaithra, T. L., Velprabakaran, S., et al. (2020). Gene pyramiding for achieving enhanced resistance to bacterial blight, blast, and sheath blight diseases in rice. *Front. Plant Sci.* 11:591457. doi: 10.3389/fpls.2020.591457

Samal, P., Pote, T. D., Krishnan, S. G., Singh, A. K., Salgotra, R. K., and Rathour, R. (2019). Integrating marker-assisted selection and doubled haploidy for rapid introgression of semi-dwarfing and blast resistance genes into a Basmati rice variety "Ranbir Basmati". *Euphytica* 215:149. doi: 10.1007/s10681-019-2473-7

Singh, V. K., Singh, A., Singh, S. P., Ellur, R. K., Choudhary, V., Sarkel, S., et al. (2012). Incorporation of blast resistance into "PRR78", an elite Basmati rice restorer line, through marker assisted backcross breeding. *Field Crops Res.* 128, 8–16. doi: 10.1016/j.fcr.2011.12.003

Springer, N. M., and Schmitz, R. J. (2017). Exploiting induced and natural epigenetic variation for crop improvement. *Nat. Rev. Genet.* 18, 563–575. doi: 10.1038/nrg.2017.45

Tanksley, S. D., Young, N. D., Paterson, A. H., and Bonierbale, M. W. (1989). RFLP mapping in plant breeding: new tools for an old science. *Nat. Biotechnol.* 7, 257–264. doi: 10.1038/nbt0389-257

Wang, C., Fan, Y., Zheng, C., Qin, T., Zhang, X., and Zhao, K. (2014). High-resolution genetic mapping of rice bacterial blight resistance gene *Xa23*. *Mol. Genet. Genomics* 289, 745–753. doi: 10.1007/s00438-014-0848-y

Wang, C., Zhang, X., Fan, Y., Gao, Y., Zhu, Q., Zheng, C., et al. (2015). XA23 is an executor r protein and confers broad-spectrum disease resistance in rice. *Mol. Plant.* 8, 290–302. doi: 10.1016/j.molp.2014.10.010

Wang, G., and Valent, B. (2017). Durable resistance to rice blast. *Science* 355, 906–907. doi: 10.1126/science.aam9517

Wei, X., Qiu, J., Yong, K., Fan, J., Zhang, Q., Hua, H., et al. (2021). A quantitative genomics map of rice provides genetic insights and guides breeding. *Nat. Genet.* 53, 243–253. doi: 10.1038/s41588-020-00769-9

Wing, R. A., Purugganan, M. D., and Zhang, Q. (2018). The rice genome revolution: from an ancient grain to Green Super Rice. *Nat. Rev. Genet.* 19, 505–517. doi: 10.1038/s41576-018-0024-z

Xu, Y., Lu, Y., Xie, C., Gao, S., Wan, J., and Prasanna, B. M. (2012). Whole-genome strategies for marker-assisted plant breeding. *Mol. Breed.* 29, 833–854. doi: 10.1007/s11032-012-9699-6

Xu, Z., Xu, X., Wang, Y., Liu, L., Li, Y., Yang, Y., et al. (2022). A varied Avr*Xa23*-like TALE enables the bacterial blight pathogen to avoid being trapped by *Xa23* resistance gene in rice. *J. Adv. Res.* 1:7. doi: 10.1016/j.jare.2022.01.007

Yang, D., Tang, J., Yang, D., Chen, Y., Ali, J., and Mou, T. (2019). Improving rice blast resistance of Feng39S through molecular marker-assisted backcrossing. *Rice* 12:70. doi: 10.1186/s12284-019-0329-3

You, F. M., Huo, N., Gu, Y. Q., Luo, M.-C., Ma, Y., Hane, D., et al. (2008). BatchPrimer3: a high throughput web application for PCR and sequencing primer design. *BMC Bioinformat.* 9:253. doi: 10.1186/1471-2105-9-253

Yu, M., Dai, Z., Pan, C., Chen, X., Yu, L., Zhang, X., et al. (2013). Resistance spectrum difference between two broad-spectrum blast resistance genes, *Pigm* and *Pi2* , and their interaction effect on *Pi1*. *Acta Agronom. Sin.* 39:1927. doi: 10.3724/SP.J.1006.2013.01927

Yu, Z. H., Mackill, D. J., Bonman, J. M., McCouch, S. R., Guiderdoni, E., Notteghem, J. L., et al. (1996). Molecular mapping of genes for resistance to rice blast (*Pyricularia grisea* Sacc.). *Theor. Appl. Genet.* 93, 859–863. doi: 10.1007/BF00224086

Yuan, L. (2018). Progress in breeding of super hybrid rice. *J. Agric.* 8, 71–73.

Zhang, Q. (2009). Genetics and improvement of bacterial blight resistance of hybrid rice in China. *Rice Sci.* 16, 83–92. doi: 10.1016/S1672-6308(08)60062-1

Zhang, X. W., He, Z. Z., Jiang, N., Deng, H. F., and Li, J. M. (2017). High-throughput genotyping techniques and their applications in rice. *Biotechnol. Bull.* 33, 67–73. doi: 10.13560/j.cnki.biotech.bull.1985.2017-0467

Zhao, K., and Zhang, Q. (2021). A climate-resilient R gene in rice traps two pathogen effectors for broad and durable resistance to bacterial blight. *Mol. Plant.* 14, 366–368. doi: 10.1016/j.molp.2021.01.018

Zhou, Y., Xu, J., Zhou, S., Yu, J., Xie, X., Xu, M., et al. (2009). Pyramiding *Xa23* and *Rxo1* for resistance to two bacterial diseases into an elite indica rice variety using molecular approaches. *Mol. Breed.* 23, 279–287. doi: 10.1007/s11032-008-9232-0

Zhu, X., Chen, S., Yang, J., Zhou, S., Zeng, L., Han, J., et al. (2012). The identification of *Pi50(t)*, a new member of the rice blast resistance *Pi2/Pi9* multigene family. *Theor. Appl. Genet.* 124, 1295–1304. doi: 10.1007/s00122-012-1787-9

Conflict of Interest: ZH, ZXu, JC, ZL, CY, HY, JX, BT, and JP were employed by Huazhi Bio-Tech Co., Ltd., Changsha, China. NJ was employed by Key Laboratory of Southern Rice Innovation and Improvement, Ministry of Agriculture and Rural Affairs, Hunan Engineering Laboratory of Disease and Pest Resistant Rice Breeding, Yuan Longping High-Tech Agriculture Company Ltd., Changsha, China.

The remaining authors declare that the research was conducted in the absence of any commercial or financial relationships that could be construed as a potential conflict of interest.

Publisher's Note: All claims expressed in this article are solely those of the authors and do not necessarily represent those of their affiliated organizations, or those of the publisher, the editors and the reviewers. Any product that may be evaluated in this article, or claim that may be made by its manufacturer, is not guaranteed or endorsed by the publisher.

Copyright © 2022 He, Xin, Wang, Yang, Xu, Cheng, Li, Ye, Yin, Xie, Jiang, Huang, Xiao, Tian, Liang, Zhao and Peng. This is an open-access article distributed under the terms of the Creative Commons Attribution License (CC BY). The use, distribution or reproduction in other forums is permitted, provided the original author(s) and the copyright owner(s) are credited and that the original publication in this journal is cited, in accordance with accepted academic practice. No use, distribution or reproduction is permitted which does not comply with these terms.

frontiers | Frontiers in Plant Science

MINI REVIEW
published: 26 May 2022
doi: 10.3389/fpls.2022.904829

Clustered Regularly Interspaced Short Palindromic Repeats-Associated Protein System for Resistance Against Plant Viruses: Applications and Perspectives

Fredy D. A. Silva and Elizabeth P. B. Fontes**

Department of Biochemistry and Molecular Biology/Bioagro, National Institute of Science and Technology in Plant-Pest Interactions, Universidade Federal de Viçosa, Viçosa, Brazil

OPEN ACCESS

Edited by:
Peng Zhang,
Center for Excellence in Molecular Plant Sciences (CAS), China

Reviewed by:
Rahul Mahadev Shelake,
Gyeongsang National University, South Korea

***Correspondence:**
Fredy D. A. Silva
fredy.silva@ufv.br
Elizabeth P. B. Fontes
bbfontes@ufv.br

Specialty section:
This article was submitted to Plant Biotechnology, a section of the journal Frontiers in Plant Science

Received: *25 March 2022*
Accepted: *03 May 2022*
Published: *26 May 2022*

Citation:
Silva FDA and Fontes EPB (2022) Clustered Regularly Interspaced Short Palindromic Repeats-Associated Protein System for Resistance Against Plant Viruses: Applications and Perspectives. Front. Plant Sci. 13:904829. doi: 10.3389/fpls.2022.904829

Different genome editing approaches have been used to engineer resistance against plant viruses. The clustered regularly interspaced short palindromic repeats (CRISPR)/CRISPR-associated protein (Cas; CRISPR/Cas) systems to create pinpoint genetic mutations have emerged as a powerful tool for molecular engineering of plant immunity and increasing resistance against plant viruses. This review presents (i) recent advances in engineering resistance against plant viruses by CRISPR/Cas and (ii) an overview of the potential host factors as targets for the CRISPR/Cas system-mediated broad-range resistance and immunity. Applications, challenges, and perspectives in enabling the CRISPR/Cas system for crop protection are also outlined.

Keywords: CRISPR/Cas, genome editing, resistance to viruses, susceptibility genes, virus-host interactions, plant antiviral immunity

INTRODUCTION

The agronomic impact caused by phytopathogens imposes severe yield losses on many important crops worldwide. Agricultural productivity reduction is a recurrent problem due to diseases caused by phytopathogens; viruses are among the principal constraints to crop productivity in a world impacted by accelerated climate change (Savary et al., 2019; Amari et al., 2021). Advances in plant genome editing technology have achieved remarkable breakthroughs in many fields and have been used in plant biotechnology as a tool to improve several traits in an unprecedented way. Part of this progress results from the use of clustered regularly interspaced short palindromic repeats (CRISPR) and CRISPR-associated genes (Cas), CRISPR/Cas system as a tool for genome editing, modulating gene regulation, epigenetic editing, and chromatin engineering (Cong et al., 2013; Doudna and Charpentier, 2014; Adli, 2018; Melo et al., 2021). CRISPR/Cas systems have provided the means to engineer different aspects of the molecular biology's central dogma (CD) involved in gene regulation, which will undoubtedly accelerate

crop improvement (Pramanik et al., 2021a). CRISPR/Cas current applications include gene discovery, introgression, generation of biotic/abiotic stress-resistant crops, plant cell factories, and delayed senescence (Pramanik et al., 2021a). CRISPR/Cas systems have also enhanced the plant immunity and resistance against phytopathogenic viruses by targeting viral genome sequences or host recessive genes in the plant genome (Borrelli et al., 2018; Zahir and Mahfouz, 2021). The first strategy relies on the CRISPR/Cas system harboring sequences that target specific regions of viral genomes. The genome of most plant virus families is composed of RNA; however, some families comprise DNA virus species (Sastry et al., 2019). Based on the genome nature, the plant viruses are classified into 26 families encompassing six different groups: (+) sense ssRNA viruses, (−) sense ssRNA viruses, (+/−) sense ssRNA viruses, dsRNA viruses, (+) sense ssDNA viruses, and (+/−) sense ssDNA viruses. Some economically relevant plant viruses include species from the *Virgaviridae*, *Tospoviridae*, *Geminiviridae*, *Bromoviridae*, and *Potyviridae* families, such as *Tobacco mosaic virus (TMV)*, *Tomato spotted wilt virus (TSWV)*, *Tomato yellow leaf curl virus (TYLCV)*, *Cucumber mosaic virus (CMV)*, *Potato virus Y (PVY)*, *African cassava mosaic virus (ACMV)*, *Plum pox virus (PPV)*, *Brome mosaic virus (BMV)*, and *Bean golden mosaic virus* (BGMV; Rybicki, 2015; Silva et al., 2017). *Geminiviridae* is one large family of plant viruses divided into nine genera bearing agronomic interest because geminivirus species can infect several mono- and dicotyledonous plants, including maize, tomato, potato, cucumber, cassava, pepper, bean, and cotton (Mansoor et al., 2006; Sastry et al., 2019).

Several strategies have been used to control plant viruses. Approaches may be based on traditional techniques, including prophylaxis to prevent virus spread. Other strategies use chemicals to control virus dispersion by natural insect vectors or the removal of infected plants. Additionally, the genomic-assisted selection of resistant cultivars obtained by plant breeding has been used with success (Pérez-de-Castro et al., 2012). More recently, crop transgenic lines expressing small interference RNAs (siRNAs) and RNA interference (RNAi) targeted to viral sequences have been extensively used to obtain resistance (Loriato et al., 2020; Rubio et al., 2020). Successful RNAi-based transgenic plant immunity strategies include the engineered resistance against TYLCV and BGMV (Aragão and Faria, 2009; Leibman et al., 2015). Nevertheless, the emergence of the CRISPR technology with customizable specificities of the RNA-guided nucleases (RGNs), like Cas9, has made targeted genome editing the mainstream method employed by plant virologists to obtain resistance to viruses in several crops (Ali et al., 2015). In addition to simplicity, versatility, and rapid nature, the CRISPR/Cas technology has efficiently modified several viral genomes and endogenous genes in a large variety of crop hosts. CRISPR/Cas-meditated genome interference systems have generated resistance in plants against several viruses, including bean yellow dwarf virus (BeYDV; Baltes et al., 2015), beet severe curly top virus (BSCTV; Ji et al., 2015), tomato yellow leaf curl virus (TYLCV; Tashkandi et al., 2018), African cassava mosaic virus (ACMV; Mehta et al., 2019), cotton leaf curl Multan virus (CLCuMuV; Yin et al., 2019), chili leaf curl virus (ChiLCV; Roy et al., 2019), cauliflower mosaic virus (CaMV; Liu et al., 2018), and cucumber mosaic virus (CMV; Zhang et al., 2018). Although the potential of this strategy is unquestionable, limitations due to off-target editing effects, the rapid evolution of mutants resulting from the mutagenic nature of the CRISPR/Cas system, and the possibility of generating viral escapes in a short time are under constant debate (Mehta et al., 2019). To overcome these issues, new recently discovered CRISPR/Cas systems and multiple gRNAs targeted to different sites have been employed (Shafiq et al., 2021; Zahir and Mahfouz, 2021). In addition, the recessive resistance mediated by potential host susceptibility factors has been considered a promising alternative for applying the CRISPR/Cas system toward broad-range resistance and immunity. This review describes briefly some genome editing tools employed as antiviral strategies and primarily advances in CRISPR/Cas-mediated resistance against plant viruses by targeting viral genomes and/or host susceptibility/recessive resistant genes.

MOLECULAR EDITING TOOLS TO IMPROVE PLANT IMMUNITY AGAINST VIRUSES

Different molecular approaches have been employed to improve plant immunity against viruses. Among those, the nucleases zinc-finger nucleases (ZFNs) and transcription activator-like effector nucleases (TALENs) have taken a prominent place as genome editing techniques (Bibikova et al., 2003; Cheng et al., 2015). ZFNs are fusion proteins of zinc-finger transcriptional activators and *Fok1* endonuclease, whereas, in TALENs, the *Fok1* endonuclease is linked to a bacterial TALE protein. Both designed endonucleases are well-characterized tools for targeting effectors to a specific genome region; they require a specific amino acid sequence (a zinc-finger or TALE motif) that recognizes a DNA sequence of the genome. However, some drawbacks make the use of ZFNs and TALENs limited. Because ZFNs require an amino acid sequence to specify the target site, there is a need for multiple designs to recognize different regions in the genome. Likewise, a single TALE motif recognizes one nucleotide, and hence an array of TALENs is required to associate with longer DNA sequences (Becker and Boch, 2021). Furthermore, in both approaches, the target specificity derives from protein-DNA association; thereby, they can only edit targeted DNA viruses, not being used to edit several plant RNA virus genomes. In addition, replication is partially inhibited for some plant viruses because they can only target a single site (Zahir and Mahfouz, 2021).

The CRISPR/Cas system is not limited as ZFNs and TALENs. Due to the feasibility of its mechanism, CRISPR/Cas has become an alternative tool for controlling viral infections by directly editing viral genomes or host factors. CRISPR/Cas was first described as an immune system of archaea and bacteria for defense against viruses by specific interaction of short-viral sequences based on complementarity (Labrie et al., 2010). The system consists of an RNA sequence complementary to the

target sequence known as the spacer or CRISPR RNA (crRNA), and a scaffold sequence followed by the CAS protein known as the trans-activating crRNA (tracrRNA; Deltcheva et al., 2011; Gardiner et al., 2022). The most used system is the CRISPR/Cas9 (**Figure 1**). The mechanism requires a single guide (sg) RNA containing a fusion of 20 nucleotide spacer and scaffold sequence that directs the Cas9 endonuclease to a specific region of the genomic DNA. Additionally, a short NGG sequence and a protospacer adjacent motif (PAM) are required. Cas9 promotes a double-strand break that will be repaired by the host cell resulting in an insertion or deletion that can potentially disrupt the open reading frame of the targeted gene (Doudna and Charpentier, 2014; Jiang and Doudna, 2017).

A recently developed system, the PAMless SpCas9 variant with relaxed nucleotide preference, has overcome these sequence limitations by increasing the number of possible CRISPR/Cas targets (Walton et al., 2020; Ren et al., 2021). Advantages and applications of the CRISPR/Cas systems include (i) improvement of plant immunity by targeting RNA or DNA viral genome with single or multiplex targets (Hussain et al., 2018), (ii) engineering recessive resistance by editing CRISPR/Cas-targeted host-factors required for viral replication or movement

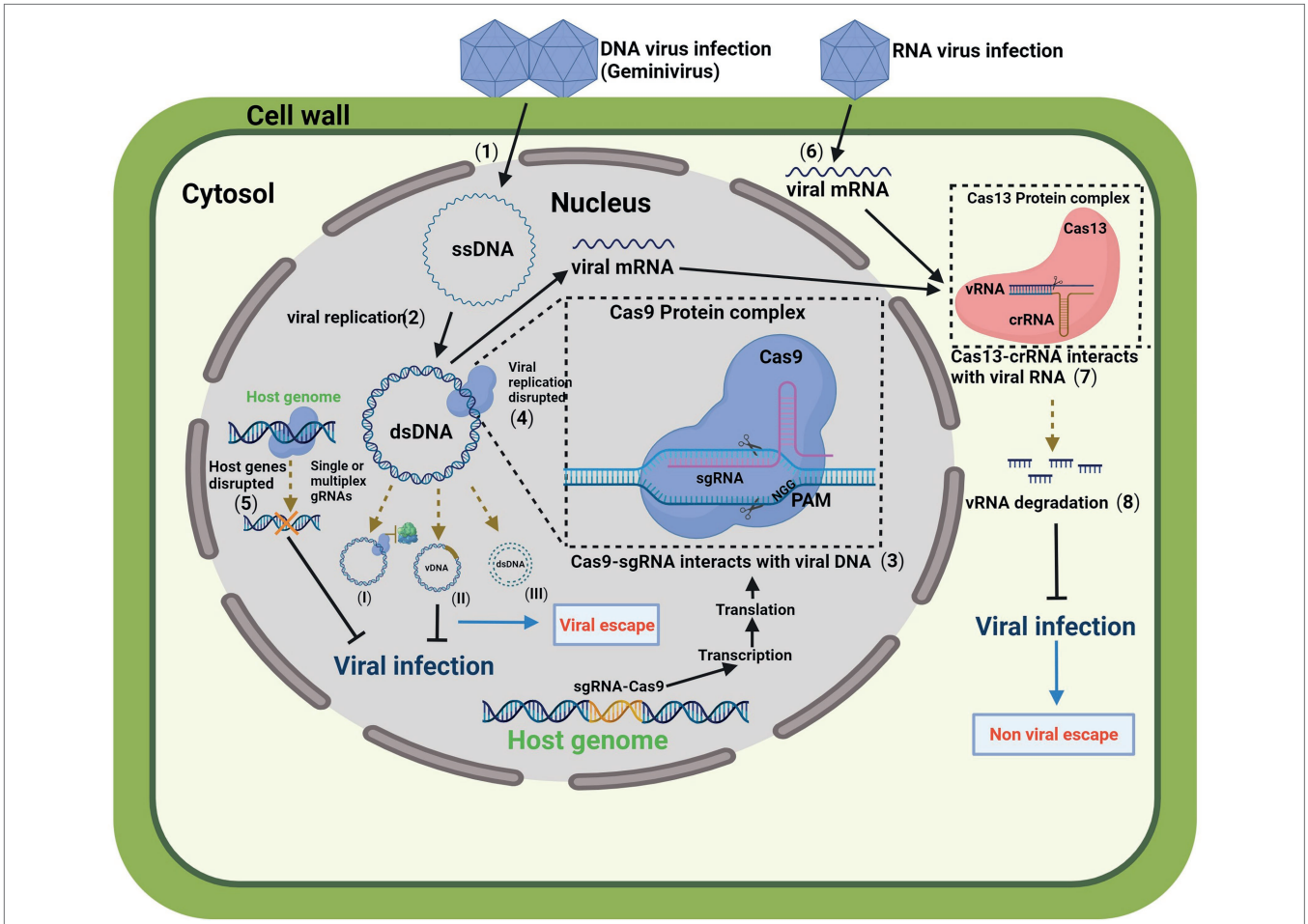


FIGURE 1 | A schematic model for engineering resistance to plant viruses provided by the clustered regularly interspaced short palindromic repeats (CRISPR)/CRISPR-associated protein (CRISPR/Cas) systems. Plant genome transformed with CRISPR/Cas9 system expresses a functional Cas9 protein complex Cas9/gRNA. After Geminivirus infection (1), the viral single-stranded DNA (ssDNA) is delivered into the cytoplasm and translocated to the nucleus. The host nuclear machinery assists the complementary strand synthesis resulting in the viral replication to double-stranded DNA (dsDNA) (2), producing multiple viral copies. The Cas9 protein complex Cas9/gRNA binds to the viral genome (3), which is assisted by a short sequence of 20 nucleotides that directs the Cas9 endonuclease to a specific region of the genomic DNA where it acts as a molecular scissor. A protospacer adjacent motif (PAM) is required. The action of Cas9 results in a double-strand break, and virus replication is disrupted by preventing access to replication proteins (4; I), introducing pinpoint mutations in the viral genome (II), or disrupting the genome by cleavage of dsDNA (III). The CRISPR/Cas system mutagenic property may generate some viral variants. Alternatively, the Cas9 protein complex with multiple gRNAs can target plant host factors to disrupt genes important for viral replication or movement (5). Combining multiplex CRISPR/Cas systems, such as Cas13 and Cas9, is a possible alternative to avoid viral escapes and targeting RNA viruses. After RNA virus infection (6), the viral mRNA interacts with CRISPR/Cas13 system through a short CRISPR RNA (crRNA; 7). The Cas13-crRNA complex is RNA-guided RNA-targeted, and the cleavage of the vRNA induces vRNA degradation (8) and disrupts viral infection. The figure was created with BioRender.com. Cas, CRISPR-associated; CRISPR, clustered regulatory interspaced short palindromic repeats; dsDNA, double-stranded DNA; ssDNA, single-stranded DNA; sgRNA, single guide RNA; vDNA, viral DNA; CRNA, CRISPR RNA; ssRNA, single-stranded RNA; tracrRNA, trans-activating crRNA; and PAM, protospacer adjacent motif.

(Cao et al., 2020), (iii) recovery of plants with viral symptoms after infection, as a diagnostic system in plants, and (iv) also the generation of edited non-transgenic crops (Aman et al., 2020).

CRISPR/Cas-MEDIATED VIRUS GENOME EDITING TO CONTROL INFECTION IN PLANTS

Plant viruses are the most diverse phytopathogens globally, impacting cultivated crops. Due to the simplicity of their genome, composed mainly of RNA, plant viruses evolve rapidly. The CRISPR/Cas system can mediate genome interference in DNA or RNA genomes, providing an efficient strategy to control plants viruses (Aman et al., 2020). Accordingly, the CRISPR/Cas9 system has generated plant immunity against viruses in several crops, including beans, tomato, cassava, cotton, chili, wheat, cucumber, and soybean. *Nicotiana benthamiana* plants expressing Cas9-sgRNA to the targeted bean yellow dwarf virus (BeYDV) genome displayed reduced virus load and symptoms (Baltes et al., 2015). Likewise, tomato plants expressing Cas9-sgRNA targeting TYLCV coat protein (CP) or replicase (Rep) sequences were resistant to TYLCV (Tashkandi et al., 2018). Recently, the use of the CRISPR/Cas9 system with multiple sgRNAs, which target essential conserved regions for replication of viral genomes, has improved the resistance of plants against several viruses, including cotton leaf curl Multan virus (CLCuMuV; Yin et al., 2019), wheat dwarf virus (WDV; Kis et al., 2019), and soybean mosaic virus (SMV; Zhang et al., 2020). Likewise, the expression of Cas9-sgRNA targeting ACMV transcription activator (AC2) and replication enhancer (AC3) sequences generated moderate resistance to the begomovirus in cassava (Mehta et al., 2019). Limitations of the CRISPR/Cas9 systems targeting viral genomes include the possibility of generating viral escapes and variants capable of replication (Mehta et al., 2019; Aman et al., 2020). In addition to CRISPR/Cas9, other CRISPR/Cas variants, including Cas3, Cas9, Cas12, Cas13, and Cas14, have potentially been deployed to improve plant immunity (**Figure 1**). For example, CRISPR/Cas3 system can be used as multiplex targets for double-stranded DNA viruses (dsDNA) or RNA viruses using multiplex sites (Aman et al., 2020). In another study, plants have been engineered using the CRISPR/Cas13 system that targeted TMV and turnip mosaic virus (TuMV) genomes, enhancing plant immunity against these plant RNA viruses (Aman et al., 2018). Furthermore, CRISPR/Cas13 was able to protect potato plants from potato virus Y (PVY; Zhan et al., 2019).

The CRISPR/Cas12 is another system used for resistance to viruses. CRISPR/Cas12 can target both dsDNA and ssDNA viruses (Aman et al., 2020). Applications of CRISPR/Cas12a system include the detection of plant viruses in different crops such as apples and tomato (Cho et al., 2016; Aman et al., 2020; Mahas et al., 2021). The technology has advanced with engineered Cas nucleases to improve their efficiency and precision for the next generation CRISPR editing technologies. The engineered nuclease CRISPR-MAD7 system, a Class 2 type V-A CRISPR-Cas (Cas12a/Cpf1) with low homology to canonical Cas12a nucleases, is a typical example of these new nucleases (Liu et al., 2020). CRISPR/Cas14a is a compact nuclease isolated from archaea, which can be targeted to a single-stranded DNA (ssDNA) genome. The sequence-independence and unrestricted cleavage mechanism make CRISPR/Cas14a a potential tool for engineering resistance against plant ssDNA viruses (Khan et al., 2019). Finally, an alternative strategy employs a combination of CRISPR/Cas systems (Cas3, Cas9, Cas12, Cas13, and Cas14) as a multiplex to enhance plant immunity. These advances in molecular technologies make CRISPR/Cas a powerful tool for improving plant immunity against viruses.

CRISPR/Cas SYSTEMS-MEDIATED HOST GENOME EDITING TO IMPROVE PLANT IMMUNITY AGAINST PLANT VIRUSES

Plant viruses are obligate intracellular parasites that require the host cellular machinery to translate their viral genome, replicate, and spread to neighbor cells (Kumar, 2019). Many plant host factors are crucial for viral infections and have been extensively studied as potential targets for controlling plant diseases. Indeed, recessive resistance can be achieved either by silencing a negative regulator of plant defense or a host gene essential for infection. For resistance to viruses, the latter has predominated and been identified as loss-of-susceptibility mutants. The first identified natural recessive resistant genes against RNA viruses mapped to mutations in eukaryotic translation initiation factors *eIF4E* and *eIF4G* genes (Calil and Fontes, 2017). Due to its simplicity and accuracy, the CRISPR/Cas systems have been used as a powerful tool to mediate host genome editing and improve plant immunity against plant viruses in several crops (**Table 1**). CRISPR/Cas9 sgRNA targeting N′ and C′ termini of eukaryotic translation initiation factor *eIF4E* gene has induced broad-spectrum resistance against the potyviruses zucchini yellow mosaic virus (ZYMV) in cucumber, papaya ringspot mosaic virus-W (PRSV-W) in papaya, and immunity to ipomovirus cucumber vein yellowing virus (CVYV; Chandrasekaran et al., 2016). Due to the physiological importance of translation, the induction of specific pinpoint mutations using CRISPR/Cas is a strategy to avoid deleterious effects by mutating translation initiation genes. Sequence-specific mutations of *eIF(iso)4E* from *Arabidopsis thaliana* by CRISPR/Cas9 provided resistance to TuMV (Pyott et al., 2016). CRISPR/Cas9 editing *eIF4G* in rice has induced resistance to rice tungro spherical virus (RTSV; Macovei et al., 2018). The CRISPR/nCas9 cytidine deaminase system introduced a single mutation in the *eIF4E1* generating resistant plants to clover yellow vein virus (ClYVV; Bastet et al., 2019). Simultaneous CRISPR/Cas9-mediated editions of eIF4E isoforms nCBP-1 and nCBP-2 reduced cassava brown streak virus (CBSV) symptoms and severity (Gomez et al., 2019). In addition to translation initiation factors as targets for CRISPR/Cas-mediated resistance to RNA viruses, the nuclear protein coilin, and

TABLE 1 | Summary of CRISPR/Cas system mediating resistance to plant virus by targeting host factors.

CRISPR/Cas system	Plant species	Target host factor	Genus/Plant virus	References
CRISPR/Cas9	Cucumber (*Cucumis sativus* L.)	Host factor eukaryotic translation initiation factor 4E (eIF4E)	*Potyvirus/Cucumber vein yellow virus* (CuVYV)	Chandrasekaran et al., 2016
CRISPR/Cas9	Cucumber (*Cucumis sativus* L.)	Host factor eukaryotic translation initiation factor 4E (eIF4E)	*Potyvirus/Zucchini yellow mosaic virus* (ZYMV)	Chandrasekaran et al., 2016
CRISPR/Cas9	Cucumber (*Cucumis sativus* L.)	Host factor eukaryotic translation initiation factor 4E (eIF4E)	*Potyvirus/Papaya ring spot virus-W* (PRSV-W)	Chandrasekaran et al., 2016
CRISPR/Cas9	*Arabidopsis thalaiana*	Host factor eukaryotic translation initiation factor eIF(iso)4E	*Potyvirus/Turnip mosaic virus* (TuMV)	Pyott et al., 2016
CRISPR/Cas9	Rice (*Oriza sativa*)	Host factor eukaryotic translation initiation factor eIF4G	*Tungrovirus/Rice tungo spherical virus* (RTSV)	Macovei et al., 2018
CRISPR/nCas9 cytidine deaminase	*Arabidopsis thaliana*	Substitutions encoded by a *Pisum sativum* eIF4E virus-resistance allele into the *Arabidopsis thaliana* eIF4E1	*Potyvirus/Clover yellow vein virus* (RTSV)	Bastet et al., 2019
CRISPR/Cas9	Cassava (*Manihot esculenta* Crantz)	Simultaneous editions of IF4E isoforms nCBP-1 and nCBP-2	*Ipomovirus/Cassava brown streak virus* (CBSV)	Gomez et al., 2019
CRISPR/Cas9	Potato (*Solanum tuberosum*)	Nuclear Coilin	*Potyvirus/Potato virus Y* (PVY)	Makhotenko et al., 2019
CRISPR/Cas9	Soya bean [*Glycine max* (L.) Merr.]	Multiple targets of isoflavanoids pathway flavone-3-hydrolases (*GmF3H1*, *GmF3H2*) flavone synthase II (*GmFNSII-1*)	*Potyvirus/Soya bean mosaic virus* (SMV)	Zhang et al., 2020
CRISPR/Cas9	Tomato (*Solanum lycopersum*)	Susceptibility (*S*-gene) factor	*Begomovirus/Tomato yellow leaf curl virus* (TYLCV)	Pramanik et al., 2021b

flavanone-3-hydroxylase (*F3H*)/flavone synthase II (*FNSII*) genes have also been used as targets for resistance to RNA virus of the *Potyviridae* family. Editing coilin by the CRISPR/Cas9 system increased the resistance of edited potato lines to PVY (Makhotenko et al., 2019). Also, the CRISPR/Cas9 mediated multiplex gene-editing technology has been employed to target flavone-3-hydroxylases [*Glycine max* (Gm)*F3H1* and *GmF3H2*] and flavone synthase II (*GmFNSII-1*) genes as a metabolic engineering approach that resulted in increased isoflavone content and enhanced resistance of edited soybean plants to soybean mosaic virus (SMV; Zhang et al., 2020).

Despite these reports, the application of CRISPR/Cas for host genome editing in plant immunity has been limited because of the restricted repertoire of characterized naturally loss-of-susceptibility mutants or recessive-resistant genes. In the lack of known recessive resistant genes, a loss-of-function mutation in susceptibility genes, which will not cause deleterious effects on plant growth and productivity, can be an alternative target for CRISPR/Cas-mediated host immunity. In fact, the inactivation of a necessary host factor for infection is supposed to account for recessively inherited disease resistance to plant viruses. For the ssDNA bipartite begomoviruses, two susceptibility genes, the endosomal NSP-interacting syntaxin-6 domain-containing protein (NISP), and NSP-interacting GTPase (NIG), which are involved in the intracellular traffic of viral DNA, may be targets for enhancing resistance in crops (Carvalho et al., 2008; Gouveia-Mageste et al., 2021). Silencing of *NISP* enhanced resistance to cabbage leaf curl virus (CabLCV) in Arabidopsis without yield penalty, an essential property for considering susceptibility genes as targets for engineering recessive resistance. Accordingly, the silenced lines display lower DNA viral load and attenuated symptoms and are phenotypically indistinguishable from the control lines under normal conditions (Gouveia-Mageste et al., 2021). Likewise, CRISPR/Cas9 sgRNA has been employed to target the susceptibility gene (S-gene) *SlPelo* for the monopartite begomovirus TYLCV inducing resistance in edited tomato plants against the virus (Pramanik et al., 2021b). Silencing the S-gene suppressed viral DNA accumulation and restricted the systemic spread of TYLCV to non-inoculated leaves (Pramanik et al., 2021b). Collectively, these results demonstrate the potential of CRISPR/Cas systems to generate host-mediated immunity to DNA and RNA viruses by targeting susceptibility genes or resistant recessive genes. The efficiency of the CRISPR/Cas systems in introducing mutagenesis in multiple target sites offers a precise genome editing technology for engineering a variety of transgene-free resistant crops.

CONCLUSION AND FUTURE PERSPECTIVES

Clustered regularly interspaced short palindromic repeats/Cas systems have a central role in plant biotechnology as an accurate molecular tool for editing genomes, rapidly improving desired traits, creating new plant varieties, and enhancing plant immunity against phytopathogens. The use of CRISPR/Cas systems is suitable for mediating viral genome editing while maintaining the biological functions of cells. Additionally, CRISPR/Cas systems have the potential to edit host factors, improving plant immunity against plant viruses. Nevertheless, a drawback in CRISPR/Cas-mediated host genome editing to enhance plant immunity is the limited repertoire of well-characterized recessive resistant genes or host susceptibility genes in which mutations are not likely to cause host growth defects. A better understanding

of the host-virus interactome will expand the use of CRISPR/Cas for editing host susceptibility genes, which may be more efficient targets for durable resistance against viruses.

Meanwhile, advances in the next generation CRISPR editing technology variants, such as the CRISPR-MAD7 system and engineered nucleases Cas12a, increase the accuracy, range of possibilities, and applications. Engineered Cas MAD7-RR, MAD7-RVR, and M-AFID (MAD7-APOBEC fusion-induced deletion) increase the targeting range of MAD7 by creating predictable deletions from 5′-deaminated Cs to the MAD7-cleavage site. This new CRISPR-MAD7 system has an efficiency of up to 65.6%, as demonstrated in mutant rice and wheat plants (Lin et al., 2021). MAD7 can expand the CRISPR toolbox for genome engineering due to its highly efficient target to gene disruption and insertions, different protospacer adjacent motifs, and small-guide RNA requirements (Liu et al., 2020). Other advances in CRISPR/Cas systems have improved precision and provided multiple edited sites in viral genomes toward reaching a lower risk of generating viral escapes or new variants. Using new CRISPR/Cas systems (Cas3, Cas12, Cas13, and Cas14) as multiplex sgRNAs targeting different sites is a new and more efficient strategy to improve broad-spectrum resistance, prevent viral infections, and control disease in the field.

AUTHOR CONTRIBUTIONS

FDAS and EPBF wrote the drafts with input from both authors. All authors contributed to the article and approved the submitted version.

FUNDING

This work was partially supported by the Council for Advanced Professional Training (CAPES)—88887.511855/2020-00, National Council for Scientific and Technological Development (CNPq)—441955/2019-3, and Fapemig.

REFERENCES

Adli, M. (2018). The CRISPR tool kit for genome editing and beyond. *Nat. Commun.* 9:1911. doi: 10.1038/s41467-018-04252-2

Ali, Z., Abulfaraj, A., Idris, A., Ali, S., Tashkandi, M., and Mahfouz, M. M. (2015). CRISPR/Cas9-mediated viral interference in plants. *Genome Biol.* 16:238. doi: 10.1186/s13059-015-0799-6

Aman, R., Ali, Z., Butt, H., Mahas, A., Aljedaani, F., Khan, M. Z., et al. (2018). RNA virus interference via CRISPR/Cas13a system in plants. *Genome Biol.* 19:1. doi: 10.1186/s13059-017-1381-1

Aman, R., Mahas, A., and Mahfouz, M. (2020). Nucleic acid detection using CRISPR/Cas biosensing technologies. *ACS Synth. Biol.* 9, 1226–1233. doi: 10.1021/acssynbio.9b00507

Amari, K., Huang, C., and Heinlein, M. (2021). Potential impact of global warming on virus propagation in infected plants and agricultural productivity. *Front. Plant Sci.* 12:649768. doi: 10.3389/fpls.2021.649768

Aragão, F., and Faria, J. (2009). First transgenic geminivirus-resistant plant in the field. *Nat. Biotechnol.* 27, 1086–1088. doi: 10.1038/nbt1209-1086

Baltes, N., Hummel, A., Konecna, E., Cegan, R., Burns, A. N., Bisaro, D. M., et al. (2015). Conferring resistance to geminiviruses with the CRISPR–Cas prokaryotic immune system. *Nat. Plants* 1:15145. doi: 10.1038/nplants.2015.145

Bastet, A., Zafirov, D., Giovinazzo, N., Guyon-Debast, A., Nogué, F., Robaglia, C., et al. (2019). Mimicking natural polymorphism in *eIF4E* by CRISPR-Cas9 base editing is associated with resistance to potyviruses. *Plant Biotechnol. J.* 17, 1736–1750. doi: 10.1111/pbi.13096

Becker, S., and Boch, J. (2021). TALE and TALEN genome editing technologies. *Gene Genome* 2:100007. doi: 10.1016/j.ggedit.2021.100007

Bibikova, M., Beumer, K., Trautman, J. K., and Carroll, D. (2003). Enhancing gene targeting with designed zinc-finger nucleases. *Science* 300:764. doi: 10.1126/science.1079512

Borrelli, V. M. G., Brambilla, V., Rogowsky, P., Marocco, A., and Lanubile, A. (2018). The enhancement of plant disease resistance using CRISPR/Cas9 technology. *Front. Plant Sci.* 9:1245. doi: 10.3389/fpls.2018.01245

Calil, I. P., and Fontes, E. P. B. (2017). Plant immunity against viruses: antiviral immune receptors in focus. *Ann. Bot.* 119, 711–723. doi: 10.1093/aob/mcw200

Cao, Y., Zhou, H., Zhou, X., and Li, F. (2020). Control of plant viruses by CRISPR/Cas system-mediated adaptive immunity. *Front. Microbiol.* 11:593700. doi: 10.3389/fmicb.2020.593700

Carvalho, C. M., Fontenelle, M. R., Florentino, L. H., Santos, A. A., Zerbini, F. M., and Fontes, E. P. B. (2008). A novel nucleocytoplasmic traffic GTPase was identified as a functional target of the bipartite geminivirus nuclear shuttle protein. *Plant J.* 55, 869–880. doi: 10.1111/j.1365-313X.2008.03556.x

Chandrasekaran, J., Brumin, M., Wolf, D., Leibman, D., Klap, C., Pearlsman, M., et al. (2016). Development of broad virus resistance in non-transgenic cucumber using CRISPR/Cas9 technology. *Mol. Plant Pathol.* 17, 1140–1153. doi: 10.1111/mpp.12375

Cheng, X., Li, F., Cai, J., Chen, W., Zhao, N., Sun, Y., et al. (2015). Artificial TALE as a convenient protein platform for engineering broad-Spectrum resistance to Begomoviruses. *Viruses* 7, 4772–4782. doi: 10.3390/v7082843

Cho, I. S., Igori, D., Lim, S., Choi, G. S., Hammond, J., Lim, H. S., et al. (2016). Deep sequencing analysis of apple infecting viruses in Korea. *Plant Pathol. J.* 32, 441–451. doi: 10.5423/PPJ.OA.04.2016.0104

Cong, L., Ran, F. A., Cox, D., Lin, S., Barretto, R., Habib, N., et al. (2013). Multiplex genome engineering using CRISPR/Cas systems. *Science* 339, 819–823. doi: 10.1126/science.1231143

Deltcheva, E., Chylinski, K., Sharma, C. M., Gonzales, K., Chao, Y., Pirzada, Z. A., et al. (2011). CRISPR RNA maturation by trans-encoded small RNA and host factor RNase III. *Nature* 471, 602–607. doi: 10.1038/nature09886

Doudna, J. A., and Charpentier, E. (2014). Genome editing. The new frontier of genome engineering with CRISPR-Cas9. *Science* 346:1258096. doi: 10.1126/science.1258096

Gardiner, J., Ghoshal, B., Wang, M., and Jacobsen, S. E. (2022). CRISPR-Cas mediating transcriptional control and epi-mutagenesis. *Plant Physiol.* 188, 1811–1824. doi: 10.1093/plphys/kiac033

Gomez, M. A., Lin, Z. D., Moll, T., Chauhan, R. D., Hayden, L., Renninger, K., et al. (2019). Simultaneous CRISPR/Cas9-mediated editing of cassava *eIF4E* isoforms *nCBP-1* and *nCBP-2* reduces cassava brown streak disease symptom severity and incidence. *Plant Biotechnol. J.* 17, 421–434. doi: 10.1111/pbi.12987

Gouveia-Mageste, B. C., Martins, L. G. C., Dal-Bianco, M., Machado, J. P. B., Silva, J. C. F., Kim, A. Y., et al. (2021). A plant-specific syntaxin-6 protein contributes to the intracytoplasmic route for the begomovirus CabLCV. *Plant Physiol.* 187, 158–173. doi: 10.1093/plphys/kiab252

Hussain, B., Lucas, S. J., and Budak, H. (2018). CRISPR/Cas9 in plants: at play in the genome and at work for crop improvement. *Brief. Funct. Genom.* 17, 319–328. doi: 10.1093/bfgp/ely016

Ji, X., Zhang, H., Zhang, Y., Wang, Y., and Gao, C. (2015). Establishing a CRISPR-Cas-like immune system conferring DNA virus resistance in plants. *Nat. Plants* 1:15144. doi: 10.1038/nplants.2015.144

Jiang, F., and Doudna, J. A. (2017). CRISPR–Cas9 structures and mechanisms. *Annu. Rev. Biophys.* 46, 505–529. doi: 10.1146/annurev-biophys-062215-010822

Khan, M. Z., Haider, S., Mansoor, S., and Amin, I. (2019). Targeting plant ssDNA viruses with engineered miniature CRISPR-Cas14a. *Trends Biotechnol.* 37, 800–804. doi: 10.1016/j.tibtech.2019.03.015

Kis, A., Hamar, E., Tholt, G., Ban, R., and Havelda, Z. (2019). Creating highly efficient resistance against wheat dwarf virus in barley by employing CRISPR/Cas9 system. *Plant Biotechnol. J.* 17, 1004–1006. doi: 10.1111/pbi.13077

Kumar, R. V. (2019). Plant antiviral immunity against Geminiviruses and viral counter-defense for survival. *Front. Microbiol.* 10:1460. doi: 10.3389/fmicb.2019.01460

Labrie, S., Samson, J., and Moineau, S. (2010). Bacteriophage resistance mechanisms. *Nat. Rev. Microbiol.* 8, 317–327. doi: 10.1038/nrmicro2315

Leibman, D., Prakash, S., Wolf, D., Zelcer, A., Anfoka, G., Haviv, S., et al. (2015). Immunity to tomato yellow leaf curl virus in transgenic tomato is associated with accumulation of transgene small RNA. *Arch. Virol.* 160, 2727–2739. doi: 10.1007/s00705-015-2551-7

Lin, Q., Zhu, Z., Liu, G., Sun, C., Lin, D., Xue, C., et al. (2021). Genome editing in plants with MAD7 nuclease. *J. Genet. Genomics* 48, 444–451. doi: 10.1016/j.jgg.2021.04.003

Liu, Z., Schiel, J. A., Maksimova, E., Strezoska, Z., Zhao, G., Anderson, E. M., et al. (2020). ErCas12a CRISPR-MAD7 for model generation in human cells, mice, and rats. *CRISPR J.* 3, 97–108. doi: 10.1089/crispr.2019.0068

Liu, H., Soyars, C. L., Li, J., Fei, Q., He, G., Peterson, B. A., et al. (2018). CRISPR/Cas9-mediated resistance to cauliflower mosaic virus. *Plant direct.* 2:e00047. doi: 10.1002/pld3.47

Loriato, V. A. P., Martins, L. G. C., Euclydes, N. C., Reis, P. A. B., Duarte, C. E. M., and Fontes, E. P. B. (2020). Engineering resistance against geminiviruses: a review of suppressed natural defenses and the use of RNAi and the CRISPR/Cas system. *Plant Sci.* 292:110410. doi: 10.1016/j.plantsci.2020.110410

Macovei, A., Sevilla, N. R., Cantos, C., Jonson, G. B., Slamet-Loedin, I., Čermák, T., et al. (2018). Novel alleles of rice *eIF4G* generated by CRISPR/Cas9-targeted mutagenesis confer resistance to *Rice tungro spherical virus*. *Plant Biotechnol. J.* 16, 1918–1927. doi: 10.1111/pbi.12927

Mahas, A., Hassan, N., Aman, R., Marsic, T., Wang, Q., Ali, Z., et al. (2021). LAMP-Coupled CRISPR-Cas12a Module for Rapid and Sensitive Detection of Plant DNA Viruses. *Viruses* 13:466. doi: 10.3390/v13030466

Makhotenko, A. V., Khromov, A. V., Snigir, E. A., Makarova, S. S., Makarov, V. V., Suprunova, T. P., et al. (2019). Functional analysis of Coilin in virus resistance and stress tolerance of potato Solanum tuberosum using CRISPR-Cas9 editing. *Dokl. Biochem. Biophys.* 484, 88–91. doi: 10.1134/S1607672919010241

Mansoor, S., Amin, I., Hussain, M., Zafar, Y., and Briddon, R. W. (2006). Engineering novel traits in plants through RNA interference. *Trends Plant Sci.* 11, 559–565. doi: 10.1016/j.tplants.2006.09.010

Mehta, D., Stürchler, A., Anjanappa, R. B., Zaidi, S. S. A., Hoffmann, M. H., Gruissem, W., et al. (2019). Linking CRISPR-Cas9 interference in cassava to the evolution of editing-resistant geminiviruses. *Genome Biol.* 20:80. doi: 10.1186/s13059-019-1678-3

Melo, B. P., Lourenço-Tessutti, I. T., Fraga, O. T., Pinheiro, L. B., de Jesus Lins, C. B., Morgante, C. V., et al. (2021). Contrasting roles of GmNAC065 and GmNAC085 in natural senescence, plant development, multiple stresses and cell death responses. *Sci Rep.* 11:11178. doi: 10.1038/s41598-021-90767-6

Pérez-de-Castro, A. M., Vilanova, S., Cañizares, J., Pascual, L., Blanca, J. M., Díez, M. J., et al. (2012). Application of genomic tools in plant breeding. *Curr. Genom.* 13, 179–195. doi: 10.2174/138920212800543084

Pramanik, D., Shelake, R. M., Kim, M. J., and Kim, J. Y. (2021a). CRISPR-mediated engineering across the central dogma in plant biology for basic research and crop improvement. *Mol. Plant* 14, 127–150. doi: 10.1016/j.molp.2020.11.002

Pramanik, D., Shelake, R. M., Park, J., Kim, M. J., Hwang, I., Park, Y., et al. (2021b). CRISPR/Cas9-mediated generation of pathogen-resistant tomato against *tomato yellow leaf curl virus* and powdery mildew. *Int. J. Mol. Sci.* 22:1878. doi: 10.3390/ijms22041878

Pyott, D. E., Sheehan, E., and Molnar, A. (2016). Engineering of CRISPR/Cas9-mediated potyvirus resistance in transgene-free *Arabidopsis* plants. *Mol. Plant Pathol.* 17, 1276–1288. doi: 10.1111/mpp.12417

Ren, Q., Sretenovic, S., Liu, S., Tang, X., Huang, L., He, Y., et al. (2021). PAM-less plant genome editing using a CRISPR–SpRY toolbox. *Nat. Plants* 7, 25–33. doi: 10.1038/s41477-020-00827-4

Roy, A., Zhai, Y., Ortiz, J., Neff, M., Mandal, B., Mukherjee, S. K., et al. (2019). Multiplexed editing of a begomovirus genome restricts escape mutant formation and disease development. *PLoS One* 14:e0223765. doi: 10.1371/journal.pone.0223765

Rubio, L., Galipienso, L., and Ferriol, I. (2020). Detection of plant viruses and disease management: relevance of genetic diversity and evolution. *Front. Plant Sci.* 11:1092. doi: 10.3389/fpls.2020.01092

Rybicki, E. P. (2015). A top ten list for economically important plant viruses. *Arch. Virol.* 160, 17–20. doi: 10.1007/s00705-014-2295-9

Sastry, K. S., Mandal, B., Hammond, J., Scott, S. W., and Briddon, R. W. (2019). *Encyclopedia of Plant Viruses and Viroids*. New Delhi: Springer Nature.

Savary, S., Willocquet, L., Pethybridge, S. J., Esker, P., McRoberts, N., and Nelson, A. (2019). The global burden of pathogens and pests on major food crops. *Nat. Ecol. Evol.* 3, 430–439. doi: 10.1038/s41559-018-0793-y

Shafiq, S. M., Naeem, S. M., Zafar, I., Amir, R., and Al-Sadi, A. M. (2021). Next-generation sequencing and the CRISPR-Cas nexus: A molecular plant virology perspective. *Front. Microbiol.* 11:609376. doi: 10.3389/fmicb.2020.609376

Silva, J. C. F., Carvalho, T. F. M., Basso, M. F., Deguchi, M., Pereira, W. A., Sobrinho, R. R., et al. (2017). Geminivirus data warehouse: a database enriched with machine learning approaches. *BMC Bioinformatics* 18:240. doi: 10.1186/s12859-017-1646-4

Tashkandi, M., Ali, Z., Aljedaani, F., Shami, A., and Mahfouz, M. M. (2018). Engineering resistance against *tomato yellow leaf curl virus* via the CRISPR/Cas9 system in tomato. *Plant Signal. Behav.* 13:e1525996. doi: 10.1080/15592324.2018.1525996

Walton, R. T., Christie, K. A., Whittaker, M. N., and Kleinstiver, B. P. (2020). Unconstrained genome targeting with near-PAMless engineered CRISPR-Cas9 variants. *Science* 368, 290–296. doi: 10.1126/science.aba8853

Yin, K., Han, T., Xie, K., Zhao, J., Song, J., and Liu, Y. (2019). Engineer complete resistance to *cotton leaf curl Multan virus* by the CRISPR/Cas9 system in *Nicotiana benthamiana*. *Phytopathol. Res.* 1:9. doi: 10.1186/s42483-019-0017-7

Zahir, A., and Mahfouz, M. M. (2021). CRISPR/Cas systems versus plant viruses: engineering plant immunity and beyond. *Plant Physiol.* 186, 1770–1785. doi: 10.1093/plphys/kiab220

Zhan, X., Zhang, F., Zhong, Z., Chen, R., Wang, Y., Chang, L., et al. (2019). Generation of virus-resistant potato plants by RNA genome targeting. *Plant Biotechnol. J.* 17, 1814–1822. doi: 10.1111/pbi.13102

Zhang, P., Du, H., Wang, J., Pu, Y., Yang, C., Yan, R., et al. (2020). Multiplex CRISPR/Cas9-mediated metabolic engineering increases soya bean isoflavone content and resistance to soya bean mosaic virus. *Plant Biotechnol. J.* 18, 1384–1395. doi: 10.1111/pbi.13302

Zhang, T., Zheng, Q., Yi, X., An, H., Zhao, Y., Ma, S., et al. (2018). Establishing RNA virus resistance in plants by harnessing CRISPR immune system. *Plant Biotechnol. J.* 16, 1415–1423. doi: 10.1111/pbi.12881

Conflict of Interest: The authors declare that the research was conducted in the absence of any commercial or financial relationships that could be construed as a potential conflict of interest.

Publisher's Note: All claims expressed in this article are solely those of the authors and do not necessarily represent those of their affiliated organizations, or those of the publisher, the editors and the reviewers. Any product that may be evaluated in this article, or claim that may be made by its manufacturer, is not guaranteed or endorsed by the publisher.

Copyright © 2022 Silva and Fontes. This is an open-access article distributed under the terms of the Creative Commons Attribution License (CC BY). The use, distribution or reproduction in other forums is permitted, provided the original author(s) and the copyright owner(s) are credited and that the original publication in this journal is cited, in accordance with accepted academic practice. No use, distribution or reproduction is permitted which does not comply with these terms.

frontiers | Frontiers in Plant Science

PERSPECTIVE
published: 27 May 2022
doi: 10.3389/fpls.2022.889995

Gene Editing to Accelerate Crop Breeding

*Kanwarpal S. Dhugga**

International Center for Maize and Wheat Improvement (CIMMYT), El Batan, Mexico

Recent advances in biotechnology have helped increase tissue transformation efficiency and the frequency and specificity of gene editing to an extent that introducing allelic variants directly in elite varieties has become possible. In comparison to the conventional approach of crossing an elite recipient line with an exotic donor parent to introduce the trait of interest followed by repeated backcrossing, direct introduction of major-effect allelic variants into elite varieties saves time and resources, and eliminates yield drag resulting from the residual donor genes at the end of backcrossing.

Keywords: accelerated breeding, backcrossing, disease resistance, gene editing, grain biofortification, maize lethal necrosis, rust resistance, SDN-1 -2 and -3

INTRODUCTION

Forward breeding, which entails selection of recombinants with improved performance in appropriate environments, has been the driving force behind increasing crop yields over time. Discovery of heterosis, a term used to describe the improved performance of a hybrid as compared to its inbred parents, qualitatively increased the rate of yield improvement in the early phase of hybrid breeding (Sivasankar et al., 2012). Biotic and abiotic stresses drag yield down and contribute to the gap between the potential and the harvested grain yield (Duvick, 2005).

Indispensable as forward breeding is to crop improvement, particularly for complex traits and in stressful environments, it is a resource-intensive and time-consuming process. Even for simple traits inherited by single genes, several backcrosses (BC) are required to reconstitute the genome of the recipient parent. Another drawback of introgressing a trait through the conventional approach is the yield drag, a term used to refer to the reduction in grain yield from the unwanted genes from the donor parent that persist even after repeated backcrossing. Since these genes have not previously been subjected to selection for agronomic performance, they tend to reduce harvestable yield of the converted variety.

The number of genes from the donor parent that would still persist after m backcrosses, assuming no selection and no suppression of recombination, is $n^*d^*(1/2)^m$ where d is the fraction of loci that differ between the donor and the elite line and n is the total number of genes in the crop species. As an example, bread wheat has ~110 K genes (Consortium et al., 2018). If a wild, donor accession differs from the recurrent parent at 30% of the loci, after four backcrosses more than a thousand genes from the donor parent would continue to be present in the converted variety.

In crosses between widely divergent lines, limited recombination could limit the proportion of the genomic segments of the donor parent that are introduced into the recurrent parent's genome but could also pose a challenge in reducing the size of the introgressed donor segment, increasing the chances of linkage drag (Hao et al., 2020).

Markers could assist in reducing, but not eliminating, the donor parent genomic segments at BC1 stage. Breeding programs operating with limited resources would

OPEN ACCESS

Edited by:
James Lloyd,
Stellenbosch University, South Africa

Reviewed by:
Jitesh Kumar,
University of Minnesota Twin Cities, United States

***Correspondence:**
Kanwarpal S. Dhugga
k.dhugga@cgiar.org

Specialty section:
This article was submitted to Plant Biotechnology, a section of the journal Frontiers in Plant Science

Received: *04 March 2022*
Accepted: *09 May 2022*
Published: *27 May 2022*

Citation:
Dhugga KS (2022) Gene Editing to Accelerate Crop Breeding. Front. Plant Sci. 13:889995. doi: 10.3389/fpls.2022.889995

find it challenging to employ markers at this step. The choice, nevertheless, between introducing a gene variant into an elite variety without any accompanying donor genes using modern technology vs. forward breeding is obvious.

Speed breeding offers an alternative to reduce time in advancing generations in a controlled environment (Watson et al., 2018). It is not easily suited, however, for crops with large plants, like maize, pearl millet, and sorghum.

In the subsequent sections, I present the advantages gene editing has over conventional or speed breeding for at least the simply inherited traits.

GENE EDITING CAN REDUCE THE TIME TO PRODUCT DEVELOPMENT AND ELIMINATE YIELD DRAG

Genetic engineering to introduce traits for which sufficient natural variation was not available proved to be effective in combating insect pests and weeds (Rafalski, 2017). However, the benefits of the GM crops have mostly been realized by the farmers of the developed countries (Klümper and Qaim, 2014). The cost of the seed and consumer resistance against the GM crops have kept them out of the developing countries, particularly Africa (Rafalski, 2017).

Modern technologies have made it possible to accelerate improvement of genetically simple traits, which are controlled or influenced by single or a few genes, without the concerns associated with the GM crops.

The field of gene editing has progressed through several phases starting with oligo-mediated editing in the 1980s (Carroll, 2017). The main hurdle in its adoption was the low frequency of the edited events (Zhu et al., 1999, 2000). A relatively new technique, clustered regularly interspersed short palindromic repeats (CRISPR) and CRISPR-associated protein 9 (Cas9), referred to as CRISPR-Cas9, has revolutionized the field of gene editing because of its ease of use, specificity, and a high success rate (Svitashev et al., 2015).

CRISPR-Cas9-mediated gene editing has been used to mutate genes either through the spontaneous non-homologous end-joining (NHEJ) after the double-strand break at the precise site targeted by the guide-RNA or through gene deletion by using two guide-RNA molecules simultaneously. This has been referred to as site-directed nuclease scenario-1 (SDN1) (Podevin et al., 2013; Savitashev et al., 2015). The other two scenarios, SDN2 and SDN3, entail template-mediated nucleotide changes and insertion of a gene or a DNA fragment into the genome, respectively.

Myriad examples of gene editing using the CRISPR-Cas system in crop plants are listed in recent reviews (Schenke and Cai, 2020; Tiwari et al., 2021). Most of what I discuss in the subsequent sections is related to accelerating varietal improvement by directly introducing high-value traits into elite lines (Gao et al., 2020).

To demonstrate the effect of a gene variant via gene editing, experimental lines, which are older accessions, have been used in a great majority of published reports in crop plants, obviously because it is difficult to transform elite varieties directly (Schenke and Cai, 2020; Tiwari et al., 2021). To transfer the newly created trait from an experimental line into elite varieties requires crossing and backcrossing, which negates the advantage of gene editing with regard to shortening the time to product development as well as in eliminating yield drag.

Editing a gene directly in elite varieties eliminates the need for backcrossing (**Figure 1**). After self-pollinating or outcrossing the edited plants to the non-edited plants of the same genetic makeup accompanied by simultaneous screening for any unintended changes in the genome with highly sensitive molecular tools ensures no elements of the vector backbone remain in the edited plants (Zastrow-Hayes et al., 2015). According to my colleagues in industry, commercialization of the same trait advanced through conventional breeding as generated by gene editing reduced the time to market the improved variety by approximately two-thirds in the latter case (**Figure 1**). Savings in field resources, which constitute one of the most expensive components of varietal development, is proportional to the time saved; only 2–3 instead of 5–6 generations are needed for the gene edited plants to commercialize as compared to forward breeding.

BOTTLENECKS IN GENE EDITING IN ELITE VARIETIES ARE BEING OVERCOME

The hurdle of transforming elite varieties directly has recently been overcome by including cell morphogenesis genes in the transformation vector (Lowe et al., 2016, 2018a,b; Debernardi et al., 2020). In maize, inclusion of cell morphogenesis genes in the transformation vector and finetuning their expression made it possible to transform elite varieties directly with very high efficiency (Lowe et al., 2016, 2018a). Similarly, transformation efficiency was significantly improved in wheat by including a growth regulating factor and its cofactor in the transformation vector (Debernardi et al., 2020). A previously published and most commonly used protocol worked inconsistently in different laboratories (Ishida et al., 2015). The recent advances in high efficiency transformation have paved the way to edit genes directly in elite lines, at least in major crops.

Under a partnership with Corteva Agriscience, we at CIMMYT have successfully transformed elite lines of tropical maize with nearly perfect efficiency. This has opened the door to use gene editing approaches directly in the commercial lines.

NO DEARTH OF TRAITS IN CROP PLANTS THAT CAN BE IMPROVED BY GENE EDITING

Disease resistance and grain biofortification are two of the areas where gene editing can help expedite crop improvement. Some other traits specific to different crops are also amenable to improvement by gene editing.

Rancidity in pearl millet flour, which is caused by oxidation of unsaturated fatty acids released by lipases, limits its shelf

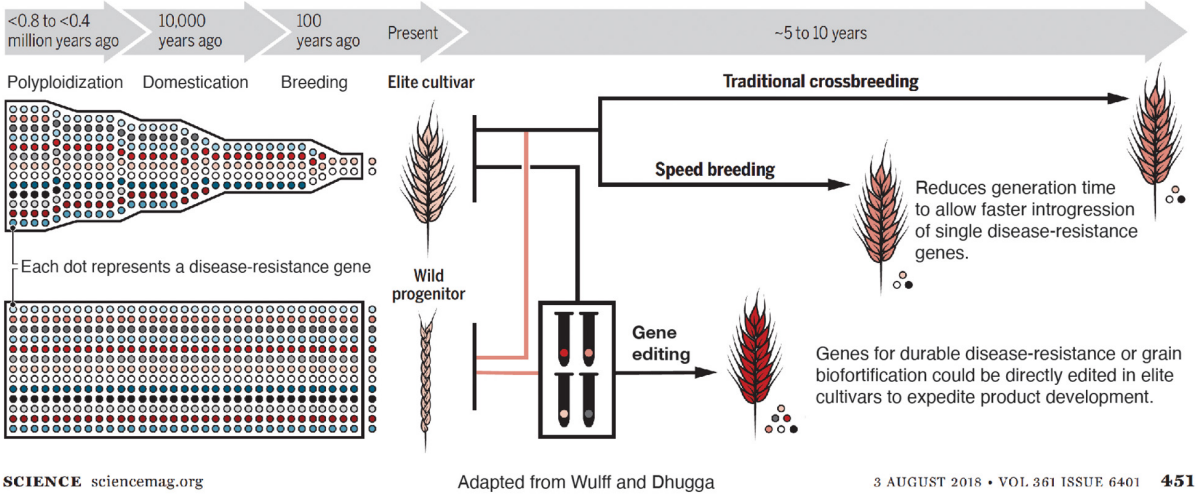


FIGURE 1 | Introducing disease resistance into wheat. Genetic diversity for disease resistance in wheat has been lost through bottlenecks imposed by polyploidization, domestication, and breeding. Resistance genes from wild relatives can be incorporated into elite cultivars by crossbreeding, which is sped up by speed breeding, and further accelerated by gene editing directly in elite lines (from Wulff and Dhugga, 2018). Reprinted with permission from AAAS.

life (Goyal and Chugh, 2017). It could potentially be reduced by addressing a few qualitative steps in fatty acid formation and triglyceride hydrolysis. Suppressing a *fatty acid desaturase* (*FAD2*), which converts oleic to linoleic acid, specifically in the seed substantially increased the proportion of oleic acid in the oil (Damude and Kinney, 2008). As mutants in the *FAD2* had pleiotropic effects, this gene might prove to be a challenge in reducing rancidity through a knockout in pearl millet. An alternative could be to replace the native promoter of *FAD2* with the one that is not expressed, or is expressed at a low level, in the seed but is expressed normally in other tissues (Shi et al., 2017). Lipases, which release fatty acids from triglycerides upon grinding of the grains into flour, offer an alternative target to reduce rancidity in pearl millet (Goyal and Chugh, 2017).

Striga is an obligate root parasitic weed that affects maize and sorghum production in semiarid tropics in Asia and Africa, particularly in nitrogen-poor soils. Its seeds germinate only when they sense a signal secreted by the host roots (Gobena et al., 2017). Mutation in a single gene involved in the formation of a specific type of strigolactone significantly improved Striga resistance in sorghum (Gobena et al., 2017). Instead of backcrossing this mutant gene into other elite varieties, it could be directly created by gene editing.

Rusts affect wheat crop more than any other disease. Approximately one-fifth of the wheat crop is lost to diseases every year (Oerke, 2006). Resistance against fungal diseases in wheat like powdery mildew and rusts can be significantly improved by editing single or a few genes. Once disease resistance breaks down, new genes for resistance must be introduced. The source of disease resistance genes is generally found in wild or genetically divergent accessions (Wulff and Dhugga, 2018).

Host resistance, which is attributed to resistant (R) genes, results from a hypersensitive response of the host, which kills the cells around the infected cell and thus limits the spread of the pathogen (Gill et al., 2015). These genes are generally involved in cell signaling. This type of resistance tends to break down with time, however, requiring the introduction of new sources of resistance, again necessitating backcrossing to the recipient line. Non-host resistance, in contrast, involves metabolic or transport proteins. It allows the pathogen to grow at a slow rate but without significantly affecting grain yield. It is also referred to as durable resistance or adult plant resistance (APR). Further, the APR genes confer resistance against a broad spectrum of fungal pathogens (Moore et al., 2015). Because of its durability, CIMMYT breeders prefer APR to host resistance and have integrated it into their breeding program.

Three APR loci, Lr34, Lr46, and Lr67 are known in wheat and genes for two (Lr34 and Lr67) have been isolated. Whereas Lr34 encodes an ATP-binding cassette (ABC) transporter, Lr67 encodes a hexose transporter (Krattinger et al., 2009; Moore et al., 2015). Just to highlight the durability of resistance conferred by these genes, Lr34 has not broken down for over the 100 years it has been available to the breeders and thus farmers (Moore et al., 2015). In both Lr34 and Lr67, mutations occur in the transmembrane domains of the respective proteins they encode, apparently making the proteins non-functional. Loss of function of the mutated protein has been demonstrated for Lr67 in a heterologous system but not for the Lr34 protein, apparently because its substrate is not known (Krattinger et al., 2009; Moore et al., 2015). ABC family of transporters facilitates the transport of a wide variety of substrates and is also referred to as multidrug resistance (MDR) protein family in bacteria. However, like Lr67,

the causal mutations occur in two of the transmembrane domains in Lr34 as well, one of which, a tyrosine to histidine change, is expected to attenuate, if not destroy, its function.

These non-functional transporters, although might normally be involved in the transport of plant metabolites, likely confer resistance against the fungal pathogens by blocking the transport of toxins or effectors that kill the plant cells. The mutations are partially dominant, which can be explained by the dimerization of the encoded proteins. Assuming the mutant and the wildtype alleles express at the same level in a heterozygote, three-fourths of the dimers would be expected to be defective. Many transporters are known to function as dimers (Feng and Frommer, 2015).

At least for Lr67, as the mutant protein that confers resistance is non-functional, an exact replication of the mutation in the elite lines is not necessary. Simple inactivation via an SDN1 knockout should phenocopy the spontaneous mutant (Moore et al., 2015). Same logic could be applied to Lr34.

Although homeoalleles for each of the isolated APR genes are present, genetic alteration of a single homeolog confers resistance (Krattinger et al., 2009; Moore et al., 2015). With gene editing, it is possible to knockout all three homeoalleles and then test them individually and in combinations to determine whether they further augment resistance. If so, it will help expand the repertory of the tools to improve disease resistance. Since the mutations will be in the same exact genetic background, constituting these combinations and testing them for rust resistance would be straightforward.

Another target for SDN1 editing in wheat is resistance against powdery mildew, which is controlled by Mildew Locus O (MLO), a dominant suppressor of resistance. All three homeoalleles must be knocked out to confer resistance (Acevedo-Garcia et al., 2017; Li et al., 2022). Li et al. (2022) in fact succeeded in generating mutations in all three loci in elite lines directly, a feat that can be reproduced in other susceptible commercial varieties.

Resistance against Fusarium head blight in wheat could be directly introduced into elite varieties by knocking out a histidine-rich calcium-binding protein (Su et al., 2019).

Maize lethal necrosis (MLN), a viral disease that swept through Kenya starting a decade ago and spread to the neighboring countries, devastated crop production (Boddupalli et al., 2020). CIMMYT identified a strong QTL that provides qualitative resistance against MLN (Murithi et al., 2021). The QTL, which was completely recessive, was present in an exotic line, which is unrelated to the African germplasm. The strength of this QTL is displayed in **Figure 2** where the same inbred line with or without the QTL was inoculated with MLN. As forward breeding to introgress this QTL continues, we have also fine mapped it and are in the process of identifying the causal gene through gene editing. Once identified, this gene could be directly knocked out in the susceptible elite lines, which could be turned around in 2–3 years instead of 7–8 years it takes to introgress with backcrossing.

Editing herbicide tolerance into varieties directly could help reduce drudgery for women in Africa where they have to manually remove weeds from the crops (Savitashev et al., 2015; Sun et al., 2016). Affordability of herbicides by the smallholder farmers remains a question mark, however, so the penetration of this trait remains uncertain.

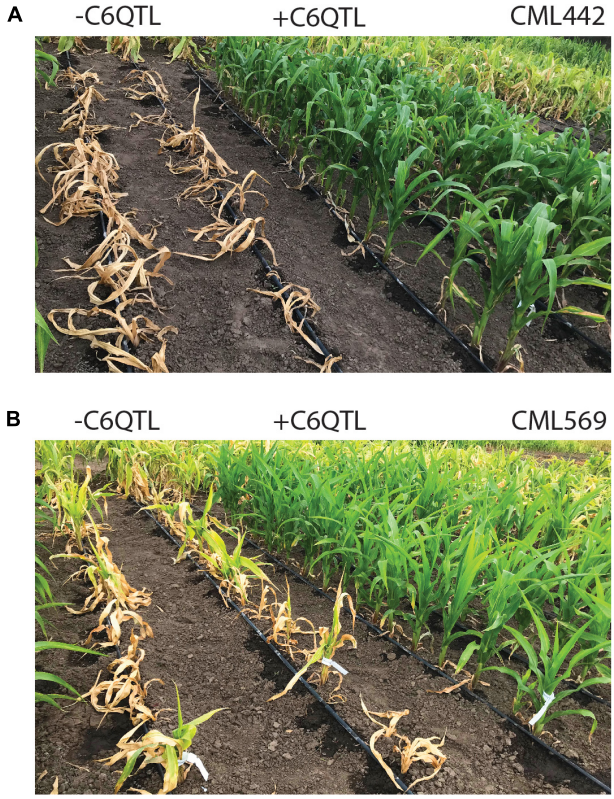


FIGURE 2 | A large-effect QTL provides strong protection against maize lethal necrosis (MLN). Inbred line CML442 **(A)** and CML569 **(B)** after inoculation with the MLN viruses without (left) or with (right) the C6QTL from the inbred donor line KS23-6 after four backcrosses to the recurrent parent. The lines were screened for MLN in Naivasha, Kenya. Picture credit: Michael Olsen.

Grain biofortification is critical for proper development of the children in developing countries where a lack of micronutrients and vitamins can cause developmental defects (Wen et al., 2022). Phytic acid chelates divalent cations and keeps them from being absorbed in the digestive system. A twofold variation of grain phytic acid in a breeding population suggested it was possible to improve divalent cation availability within the existing range of genetic variability (Wen et al., 2022). Shukla et al. (2009) demonstrated that it was possible to reduce grain phytic acid in maize by gene editing, targeting the enzyme that phosphorylates inositol. The same approach could be used to reduce phytic acid in already released commercial varieties, particularly targeted for increased iron and zinc contents (Wen et al., 2022). Similarly, provitamin-A in the grains of maize and other cereals could be improved by knocking out the genes that divert the substrate to other reactions as well as the ones that oxidize beta-carotene (Sestili et al., 2019).

Dough from wheat flour turns dark because of polyphenol oxidase (PPO) activity. Similarly, peeled potatoes turn brown if left exposed to air. Gene editing has been used to knock out a PPO gene in potato, which reduced browning

(González et al., 2020). We are using a similar approach in wheat to prolong dough longevity.

PROSPECTS OF GENE EDITING IN CROP IMPROVEMENT: SDN1, SDN2, OR SDN3

Homology directed repair (SDN2), promoter swapping, and allele replacement or insertion (SDN3) have been successfully demonstrated in crop plants (Savitashev et al., 2015; Shi et al., 2017). Low frequency of the edited events, which would be lower still in crops where transformation is a challenge, and extensive screening required to identify the targeted changes would limit the use of these approaches to high-value traits, however (Zhu et al., 1999, 2000; Shukla et al., 2009). An example of the large-effect, high-value QTL is displayed in **Figure 2**. These were the hurdles that kept the prior gene editing technologies from wide adoption (Zhu et al., 1999, 2000; Shukla et al., 2009; Carroll, 2017). Further, SDN3-derived events would invite increased regulatory scrutiny (Podevin et al., 2013). As has been the case thus far, gene editing via SDN1 would most likely continue to dominate trait improvement in commercial germplasm followed by limited use of SDN2 and SDN3 in that order for the traits that justify investment of additional resources.

Editing of genes with major effect directly in elite varieties, mostly with SDN1, is already underway and will help expedite crop improvement going forward. There is no dearth of high-value traits controlled by single genes the desired variants of which can be reproduced using SDN1, thus eliminating the pleiotropic effects associated with the residual donor genes that cannot be completely removed by conventional plant breeding.

DATA AVAILABILITY STATEMENT

The original contributions presented in the study are included in the article further inquiries can be directed to the corresponding author.

AUTHOR CONTRIBUTIONS

The author confirms being the sole contributor of this work and has approved it for publication.

FUNDING

Research in KSD laboratory on maize lethal necrosis is supported by a grant from the Bill and Melinda Gates Foundation (BMGF) (OPP1193833).

REFERENCES

Acevedo-Garcia, J., Spencer, D., Thieron, H., Reinstädler, A., Hammond-Kosack, K., Phillips, A. L., et al. (2017). mlo-based powdery mildew resistance in hexaploid bread wheat generated by a non-transgenic TILLING approach. *Plant Biotechnol. J.* 15, 367–378. doi: 10.1111/pbi.12631

Boddupalli, P., Suresh, L., Mwatuni, F., Beyene, Y., Makumbi, D., Gowda, M., et al. (2020). Maize Lethal Necrosis (MLN): efforts toward containing the spread and impact of a devastating transboundary disease in sub-Saharan Africa. *Virus Res.* 282:197943. doi: 10.1016/j.virusres.2020.197943

Carroll, D. (2017). Genome editing: past, present, and future. *Yale J. Biol. Med.* 90, 653–659.

Consortium, I. W. G. S., Appels, R., Eversole, K., Stein, N., Feuillet, C., Keller, B., et al. (2018). Shifting the limits in wheat research and breeding using a fully annotated reference genome. *Science* 361:eaar7191. doi: 10.1126/science.aar7191

Damude, H. G., and Kinney, A. J. (2008). Enhancing plant seed oils for human nutrition. *Plant Physiol.* 147, 962–968. doi: 10.1104/pp.108.121681

Debernardi, J. M., Tricoli, D. M., Ercoli, M. F., Hayta, S., Ronald, P., Palatnik, J. F., et al. (2020). A GRF–GIF chimeric protein improves the regeneration efficiency of transgenic plants. *Nat. Biotechnol.* 38, 1274–1279. doi: 10.1038/s41587-020-0703-0

Duvick, D. N. (2005). The contribution of breeding to yield advances in maize (Zea mays L.). *Adv. Agronomy* 86:83.

Feng, L., and Frommer, W. B. (2015). Structure and function of SemiSWEET and SWEET sugar transporters. *Trends Biochem. Sci.* 40, 480–486. doi: 10.1016/j.tibs.2015.05.005

Gao, H., Gadlage, M. J., Lafitte, H. R., Lenderts, B., Yang, M., Schroder, M., et al. (2020). Superior field performance of waxy corn engineered using CRISPR–Cas9. *Nat. Biotechnol.* 38, 579–581. doi: 10.1038/s41587-020-0444-0

Gill, U. S., Lee, S., and Mysore, K. S. (2015). Host versus nonhost resistance: distinct wars with similar arsenals. *Phytopathology* 105, 580–587. doi: 10.1094/PHYTO-11-14-0298-RVW

Gobena, D., Shimels, M., Rich, P. J., Ruyter-Spira, C., Bouwmeester, H., Kanuganti, S., et al. (2017). Mutation in sorghum LOW GERMINATION STIMULANT 1 alters strigolactones and causes Striga resistance. *Proc. Natl. Acad. Sci.* 114, 4471–4476. doi: 10.1073/pnas.1618965114

González, M. N., Massa, G. A., Andersson, M., Turesson, H., Olsson, N., Fält, A.-S., et al. (2020). Reduced enzymatic browning in potato tubers by specific editing of a polyphenol oxidase gene via ribonucleoprotein complexes delivery of the CRISPR/Cas9 system. *Front. Plant Sci.* 10:1649. doi: 10.3389/fpls.2019.01649

Goyal, P., and Chugh, L. (2017). Shelf life determinants and enzyme activities of pearl millet: a comparison of changes in stored flour of hybrids, CMS lines, inbreds and composites. *J. Food Sci. Technol.* 54, 3161–3169. doi: 10.1007/s13197-017-2752-z

Hao, M., Zhang, L., Ning, S., Huang, L., Yuan, Z., Wu, B., et al. (2020). The resurgence of introgression breeding, as exemplified in wheat improvement. *Front. Plant Sci.* 11:252. doi: 10.3389/fpls.2020.00252

Ishida, Y., Tsunashima, M., Hiei, Y., and Komari, T. (2015). "Transformation using immature embryos," in *Agrobacterium Protocols*, ed. K. Wang (New York, NY: Springer Science+Business Media), 189–198.

Klümper, W., and Qaim, M. (2014). A meta-analysis of the impacts of genetically modified crops. *PloS One* 9:e111629. doi: 10.1371/journal.pone.0111629

Krattinger, S. G., Lagudah, E. S., Spielmeyer, W., Singh, R. P., Huerta-Espino, J., McFadden, H., et al. (2009). A putative ABC transporter confers durable resistance to multiple fungal pathogens in wheat. *Science* 323, 1360–1363. doi: 10.1126/science.1166453

Li, S., Lin, D., Zhang, Y., Deng, M., Chen, Y., Lv, B., et al. (2022). Genome-edited powdery mildew resistance in wheat without growth penalties. *Nature* 2022, 1–6. doi: 10.1038/s41586-022-04395-9

Lowe, K., Hoerster, G., Anand, A., Wang, N., McBride, K., and Gordon-Kamm, B. (2018a). Genotype independent transformation in maize via direct somatic embryogenesis. *In Vitro Cell. Dev. Biol. Anim.* 54, S16–S16. doi: 10.1007/s11627-018-9905-2

Lowe, K., La Rota, M., Hoerster, G., Hastings, C., Wang, N., Chamberlin, M., et al. (2018b). Rapid genotype "independent" Zea mays L. (maize) transformation via direct somatic embryogenesis. *In Vitro Cell. Dev. Biol. Plant* 54, 240–252.

Lowe, K., Wu, E., Wang, N., Hoerster, G., Hastings, C., Cho, M. J., et al. (2016). Morphogenic regulators baby boom and wuschel improve monocot transformation. *Plant Cell* 28, 1998–2015. doi: 10.1105/tpc.16.00124

Moore, J. W., Herrera-Foessel, S., Lan, C., Schnippenkoetter, W., Ayliffe, M., Huerta-Espino, J., et al. (2015). A recently evolved hexose transporter variant confers resistance to multiple pathogens in wheat. *Nat. Genet.* 47, 1494–1498. doi: 10.1038/ng.3439

Murithi, A., Olsen, M. S., Kwemoi, D. B., Veronica, O., Ertiro, B. T., Beyene, Y., et al. (2021). Discovery and Validation of a Recessively Inherited Major-Effect QTL Conferring Resistance to Maize Lethal Necrosis (MLN) Disease. *Front. Genet.* 12:767883. doi: 10.3389/fgene.2021.767883

Oerke, E. C. (2006). Crop losses to pests. *J. Agric. Sci.* 144, 31–43.

Podevin, N., Davies, H. V., Hartung, F., Nogue, F., and Casacuberta, J. M. (2013). Site-directed nucleases: a paradigm shift in predictable, knowledge-based plant breeding. *Trends Biotechnol.* 31, 375–383. doi: 10.1016/j.tibtech.2013.03.004

Rafalski, J. A. (2017). Biotechnology and bioeconomy of complex traits in crop plants. *Biotechnologia* 98, 67–71. doi: 10.1111/gcbb.12610

Savitashev, S., Young, J., Schwartz, C., Gao, H., Falco, S. C., and Cigan, A. M. (2015). Targeted mutagenesis, precise gene editing and site-specific gene insertion in maize using Cal9 and guide RNA. *Plant Physiol.* 169, 931–945. doi: 10.1104/pp.15.00793

Schenke, D., and Cai, D. (2020). Applications of CRISPR/Cas to improve crop disease resistance: beyond inactivation of susceptibility factors. *Iscience* 23:101478. doi: 10.1016/j.isci.2020.101478

Sestili, F., Garcia-Molina, M. D., Gambacorta, G., Beleggia, R., Botticella, E., De Vita, P., et al. (2019). Provitamin a biofortification of durum wheat through a TILLING approach. *Int. J. Mol. Sci.* 20:5703. doi: 10.3390/ijms20225703

Shi, J. R., Gao, H. R., Wang, H. Y., Lafitte, H. R., Archibald, R. L., Yang, M. Z., et al. (2017). ARGOS8 variants generated by CRISPR-Cas9 improve maize grain yield under field drought stress conditions. *Plant Biotechnol. J.* 15, 207–216. doi: 10.1111/pbi.12603

Shukla, V. K., Doyon, Y., Miller, J. C., DeKelver, R. C., Moehle, E. A., Worden, S. E., et al. (2009). Precise genome modification in the crop species Zea mays using zinc-finger nucleases. *Nature* 459, 437–U156. doi: 10.1038/nature07992

Sivasankar, S., Collinson, S., Gupta, R., and Dhugga, K. S. (2012). "Maize," in *Hadnbook of Bioenergy Crop Plants*, eds C. Kole, C. P. Joshi, and D. R. Shonnard (Boca Raton, FL: CRC Press), 405–432.

Su, Z., Bernardo, A., Tian, B., Chen, H., Wang, S., Ma, H., et al. (2019). A deletion mutation in TaHRC confers Fhb1 resistance to Fusarium head blight in wheat. *Nat. Genet.* 51, 1099–1105. doi: 10.1038/s41588-019-0425-8

Sun, Y., Zhang, X., Wu, C., He, Y., Ma, Y., Hou, H., et al. (2016). Engineering herbicide-resistant rice plants through CRISPR/Cas9-mediated homologous recombination of acetolactate synthase. *Mol. Plant* 9, 628–631. doi: 10.1016/j.molp.2016.01.001

Svitashev, S., Young, J. K., Schwartz, C., Gao, H., Falco, S. C., and Cigan, A. M. (2015). Targeted mutagenesis, precise gene editing, and site-specific gene insertion in maize using Cas9 and guide RNA. *Plant Physiol.* 169, 931–945.

Tiwari, M., Kumar Trivedi, P., and Pandey, A. (2021). Emerging tools and paradigm shift of gene editing in cereals, fruits, and horticultural crops for enhancing nutritional value and food security. *Food Energy Secur.* 10:e258.

Watson, A., Ghosh, S., Williams, M. J., Cuddy, W. S., Simmonds, J., Rey, M.-D., et al. (2018). Speed breeding is a powerful tool to accelerate crop research and breeding. *Nat. Plants* 4, 23–29. doi: 10.1038/s41477-017-0083-8

Wen, Z., Juliana, P., Dhugga, H., Velazquez, M., Lopez, U., Perez, A., et al. (2022). Genome-wide association study of phytic acid in wheat grain unravels markers for improving biofortification. *Front. Plant Sci.* 13:830147. doi: 10.3389/fpls.2022.830147

Wulff, B. B. H., and Dhugga, K. S. (2018). Wheat—the cereal abandoned by GM: genetic modification of wheat for disease resistance could help stabilize food production. *Science* 361, 451–452. doi: 10.1126/science.aat5119

Zastrow-Hayes, G. M., Lin, H. N., Sigmund, A. L., Hoffman, J. L., Alarcon, C. M., Hayes, K. R., et al. (2015). Southern-by-sequencing: a robust screening approach for molecular characterization of genetically modified crops. *Plant Genome* 8:37. doi: 10.3835/plantgenome2014.3808.0037

Zhu, T., Mettenburg, K., Peterson, D. J., Tagliani, L., and Baszczynski, C. L. (2000). Engineering herbicide-resistant maize using chimeric RNA/DNA oligonucleotides. *Nat. Biotechnol.* 18, 555–558. doi: 10.1038/75435

Zhu, T., Peterson, D. J., Tagliani, L., Clair, G. S., Baszczynski, C. L., and Bowen, B. (1999). Targeted manipulation of maize genes in vivo using chimeric RNA/DNA oligonucleotides. *Proc. Natl. Acad. Sci.* 96, 8768–8773. doi: 10.1073/pnas.96.15.8768

Conflict of Interest: The author declares that the research was conducted in the absence of any commercial or financial relationships that could be construed as a potential conflict of interest.

Publisher's Note: All claims expressed in this article are solely those of the authors and do not necessarily represent those of their affiliated organizations, or those of the publisher, the editors and the reviewers. Any product that may be evaluated in this article, or claim that may be made by its manufacturer, is not guaranteed or endorsed by the publisher.

Copyright © 2022 Dhugga. This is an open-access article distributed under the terms of the Creative Commons Attribution License (CC BY). The use, distribution or reproduction in other forums is permitted, provided the original author(s) and the copyright owner(s) are credited and that the original publication in this journal is cited, in accordance with accepted academic practice. No use, distribution or reproduction is permitted which does not comply with these terms.

frontiers | Frontiers in Plant Science

ORIGINAL RESEARCH
published: 31 May 2022
doi: 10.3389/fpls.2022.922694

Production of Recombinant Active Human TGFβ1 in *Nicotiana benthamiana*

*Aditya Prakash Soni[1], Juhee Lee[1,2], Kunyoo Shin[1,2], Hisashi Koiwa[3,4] and Inhwan Hwang[1]**

[1] Department of Life Science, Pohang University of Science and Technology, Pohang, South Korea, [2] Department of Biological Sciences, College of Natural Science, Seoul National University, Seoul, South Korea, [3] Molecular and Environmental Plant Sciences, Texas A&M University, College Station, TX, United States, [4] Vegetable and Fruit Development Center, Department of Horticultural Sciences, Texas A&M University, College Station, TX, United States

The production of recombinant proteins in plant systems is receiving wider attention. Indeed, various plant-produced pharmaceuticals have been shown to be biologically active. However, the production of human growth factors and cytokines in heterologous systems is still challenging because they often act as complex forms, such as homo- or hetero-dimers, and their production is tightly regulated *in vivo*. In this study, we demonstrated that the mature form of human TGFβ1 produced and purified from *Nicotiana benthamiana* shows biological activity in animal cells. To produce the mature form of TGFβ1, various recombinant genes containing the mature form of TGFβ1 were generated and produced in *N. benthamiana*. Of these, a recombinant construct, *BiP:M:CBM3:LAP[C33S]:EK:TGFβ1*, was expressed at a high level in *N. benthamiana*. Recombinant proteins were one-step purified using cellulose-binding module 3 (CBM3) as an affinity tag and microcrystalline cellulose (MCC) beads as a matrix. The TGFβ1 recombinant protein bound on MCC beads was proteolytically processed with enterokinase to separate mature TGFβ1. The mature TGFβ1 still associated with Latency Associated Protein, [LAP(C33S)] that had been immobilized on MCC beads was released by HCl treatment. Purified TGFβ1 activated TGFβ1-mediated signaling in the A549 cell line, thereby inducing phosphorylation of SMAD-2, the expression of *ZEB-2* and *SNAIL1*, and the formation of a filopodia-like structure. Based on these results, we propose that active mature TGFβ1, one of the most challenging growth factors to produce in heterologous systems, can be produced from plants at a high degree of purity *via* a few steps.

Keywords: recombinant proteins, human growth factors, LAP-TGFβ1, human TGFβ1, *Nicotiana benthamiana*, CBM3, acid activation

OPEN ACCESS

Edited by:
Nobuyuki Matoba,
University of Louisville, United States

Reviewed by:
Ann Meyers,
University of Cape Town, South Africa
Kouki Matsuo,
National Institute of Advanced Industrial Science and Technology (AIST), Japan

***Correspondence:**
Inhwan Hwang
ihhwang@postech.ac.kr

Specialty section:
This article was submitted to Plant Biotechnology, a section of the journal Frontiers in Plant Science

Received: *18 April 2022*
Accepted: *11 May 2022*
Published: *31 May 2022*

Citation:
Soni AP, Lee J, Shin K, Koiwa H and Hwang I (2022) Production of Recombinant Active Human TGFβ1 in Nicotiana benthamiana. Front. Plant Sci. 13:922694. doi: 10.3389/fpls.2022.922694

INTRODUCTION

Plants have gained significant attention as hosts for recombinant protein production systems, with potential advantages, such as low maintenance cost, easy scalability, and no human pathogen contamination (Schillberg et al., 2003; Holtz et al., 2015). Various technologies have been developed to realize the potential of plants in the production of recombinant proteins. Of these, the most

crucial is the expression vector. Various types of expression vectors have been developed that can give up to 800 mg/kg fresh weight (Maclean et al., 2007) when used in transient expression in *Nicotiana benthamiana* (Regnard et al., 2010; Werner et al., 2011). Additionally, various domains that contribute to the increase in gene expression and/or protein translation have been identified, including the M domain (Kang et al., 2018), matrix attachment regions (MARs) (Zhao et al., 2017), and various 5′ and 3′ untranslated regions (Kim Y. et al., 2014; Diamos et al., 2016).

Various recombinant proteins have been produced in plants. These include hepatitis B surface antigen (Mason et al., 1992), hemagglutinin (D'Aoust et al., 2008), consensus domain III of dengue virus E glycoprotein, cEDIII (Kim et al., 2015), and Zika virus antibodies, c2A10G6 (Diamos et al., 2020), CHKV mab (Hurtado et al., 2019), human epidermal growth factor (Wirth et al., 2004), human basic fibroblast growth factor (An et al., 2013), human growth hormone (Xu et al., 2010), human FGF (Wang et al., 2015), human interleukin 6 (Islam et al., 2018b), and E2 protein of classical swine fever virus as a vaccine (Sohn et al., 2018; Park et al., 2020).

Transforming growth factor beta (TGFβ) is a signaling molecule with crucial roles during early development and the regulation of immune responses in mammals (Wu and Hill, 2009). In animal cells, TGFβ1 is translated as a pre-pro-form that undergoes multiple proteolytic processing to produce active mature TGFβ1. During the processing of TGFβ1 to the active mature form, post-translational modification is one of the most crucial requirements to attain proper folding and trafficking to the plasma membrane. The pro-form of TGFβ1, LAPTGFβ1, is glycosylated at three residues (the amino acid positions of 82, 136, and 176). Among these, Asn82 and Asn136 are necessary for the proper secretion of LAPTGFβ1 (Sha et al., 1989; Brunner et al., 1992). Studies on the molecular events in the processing of the precursor showed that proteolytic processing occurs twice to produce the mature form. After synthesis, the first proteolytic cleavage occurs between Gly29 and Leu30 of pre-pro-TGFβ1, thereby yielding pro-TGFβ1 (amino acids 30 to 390). Proteolytic processing of the pro-TGFβ1 occurs at a cluster of basic amino acid residues (R-H-R-R) immediately preceding Ala279 to yield the mature TGFβ1. The processing site conforms to a consensus cleavage motif for the mammalian convertase furin. Despite the cleavage, TGFβ1 dimers remain attached to the LAP domain non-covalently even after secretion and only get released upon activation (Khalil, 1999). This tight regulation prevents undesired interaction with ubiquitous receptors at the cell surface. These complicated processing steps render the production of active TGFβ1 as a recombinant protein highly difficult. In the recombinant TGFβ1 protein production system without Latent TGFβ1-binding protein (LTBP), C33 has the capability to form an intramolecular disulfide bond with a cysteine residue in mature TGFβ1 (Gentry et al., 1987), which then inhibits the release of mature TGFβ1 dimers from the LAP without activation. When the C33S mutation was introduced into LAP mature TGFβ1 was more easily released from LAP-TGFβ1 (pro-TGFβ1) (Brunner et al., 1992).

In this study, we investigated whether we can produce and purify transforming growth factor-beta 1 (TGFβ1) in *N. benthamiana*. TGFβ1 also plays a very important role in wound healing, one of the most complicated processes that require complex coordination among cells, starting with the influx of inflammatory cells, epithelial to mesenchymal cells trans-differentiation, and extracellular matrix formation. The topical application of TGFβ has been shown to improve healing (Clark, 1996). In a canine model, TGFβ1 and TGFβ2 have been shown to enhance bone formation (Ruskin et al., 2000; Sumner et al., 2001). Because of its clinical importance, there is a high demand for recombinant TGFβ1. Indeed, in *E. coli*, the mature form of TGFβ1 was produced as an inclusion body. Subsequently, active TGFβ1 was produced from the inclusion bodies by several cycles of denaturation and renaturation steps (Kim Y.V. et al., 2014). Recently, active human TGFβ1 has been successfully produced and purified from CHO cells at a yield of 30 mg per liter (Zou and Sun, 2004). In addition, an attempt was made to produce TGFβ1 in *N. benthamiana*. The Latency Associated Protein (LAP) domain together with the mature TGFβ1, LAPTGFβ1, was expressed and processed into a biologically active form through in-planta cleavage by co-expression of protease, *furin*, a convertase (Wilbers et al., 2016). However, in this case, the expression level was too low to purify active TGFβ1, although the acid-treated total soluble protein showed a certain degree of activity.

Here, to produce active mature TGFβ1, we designed a recombinant gene consisting of various domains, such as the LAP domain of TGFβ1 for proper folding and dimerization (Gray and Mason, 1990), the CBM3 domain for protein purification, and the M domain to increase the expression level. Moreover, we showed that mature TGFβ1 can be released from full-length recombinant TGFβ1 *via* proteolytic processing and activated by HCl treatment. Finally, we demonstrated that plant-produced mature TGFβ1 can activate TGFβ1-mediated signaling in animal cells.

RESULTS

Design of the TGFβ1 Recombinant Gene Construct and Its Expression in *Nicotiana benthamiana*

To produce recombinant TGFβ1 in plants, we first determined whether the mature form of TGFβ1 could be expressed in a soluble form. In *E. coli*, the mature form of TGFβ1 is expressed as an insoluble inclusion body (Tuan et al., 1996; Kim Y.V. et al., 2014). Active TGFβ1 was produced from the inclusion body *via* complicated processes involving solubilization using 8 M urea and refolding using the glutathione redox system. We generated an ER-targeted N-terminal His-tagged mature TGFβ1 construct by including BiP leader sequence from

Arabidopsis BiP1 giving rise to *BiP:6xHis:TGFβ1* (**Figure 1A**) and expressed it in *N. benthamiana* using *Agrobacterium*-mediated infiltration. Total soluble protein extracts and insoluble pellet fractions were prepared from infiltrated leaves at 5 DPI and analyzed by SDS/PAGE and Western blotting using an anti-TGFβ1 antibody. BiP:6xHis:TGFβ1 (12.5 kD) was largely detected in the pellet fraction, with a minor proportion in the soluble protein extracts (**Figure 1B**), indicating that mature TGFβ1 is produced as insoluble aggregates in plants, as reported in *E. coli*. To improve the solubility of mature TGFβ1 in plants, we generated another recombinant construct of TGFβ1, *BiP:6xHis:LAP[C33S]TGFβ1*, by including the Latency Associated Protein (LAP) domain of TGFβ1. It is known that LAP-TGFβ1 is hydrophilic, whereas mature TGFβ1 is extremely hydrophobic. In addition, we introduced the C33S mutation in the LAP domain, since the mutation causes an increase in the expression level and also makes it easy to release TGFβ1 in animal cells (Zou and Sun, 2004).

BiP:6xHis:LAP[C33S]TGFβ1 was transiently expressed in the ER of leaf cells in *N. benthamiana*. Total soluble protein extracts and insoluble pellet fractions were analyzed by SDS/PAGE and Western blotting using the anti-TGFβ1 antibody. BiP:6xHis:LAP[C33S]TGFβ1 was largely present in the soluble fraction (**Figure 1C**), indicating that LAP[C33S] increases the solubility of the recombinant TGFβ 1 protein.

The results showing that BiP:6xHis:LAP[C33S]TGFβ1 could be expressed as soluble protein in *N. benthamiana* prompted us to further modify the TGFβ1 recombinant gene in two directions: one to improve the expression level of the recombinant *TGFβ1* gene and the other to incorporate an affinity tag for purification of the recombinant proteins. We explored the M domain to improve the expression level and the CBM3 domain, a cellulose binding domain, as an affinity tag for purification. Many CBDs have been identified from different fungal and bacterial proteins (Ong et al., 1989; Linder and Teeri, 1996). The M domain is a fragment (231 to 290 aa positions) of a human protein tyrosine phosphatase, receptor type C (CD45). It contains multiple N-glycosylation sites and, has been shown to enhance protein expression levels up to sevenfold when fused to a target protein (Kang et al., 2018). We fused the M and CBM3 domains sequentially to the C-terminus of the BiP leader sequence, followed by *LAP[C33S]TGFβ1* to yield *BiP:M:CBM3:LAP[C33S]TGFβ1* (called *BMC:LAP[C33S]TGFβ1* hereafter). The M domain is used to increase the expression level of fusion proteins (Kang et al., 2018). Initial attempts for Ni^{2+}-NTA-based purification were not successful in terms of recovery and purity of the recombinant protein. Thus, the CBM3 tag was selected as an affinity tag because it specifically binds to MCC beads with high affinity (Hong et al., 2007; Islam et al., 2018b). We expressed *BMC:LAP[C33S]TGFβ1* in *N. benthamiana via Agrobacterium*-mediated infiltration, and its expression was analyzed by SDS/PAGE and Western blotting using anti-TGFβ1. The expression level of M domain-containing *BMC:LAP[C33S]TGFβ1* was higher than that of *BiP:6xHis:LAP[C33S]TGFβ1* (**Figure 1D**). A band at 50 kDa corresponded to BiP:6xHis:LAP[C33S]TGFβ1 full-length protein while in the case of BMC:LAP[C33S]TGFβ1, the full length appeared to be subjected to proteolysis and the 50 kDa band was produced that contained the C-terminal LAP[C33S]TGFβ 1 region.

TGFβ1 Recombinant Proteins Can Be Purified Using Microcrystalline Cellulose Beads

Next, TGFβ1 recombinant proteins were purified. To do this, we tested whether BMC:LAP[C33S]TGFβ1 can be purified using microcrystalline cellulose (MCC) beads, a cheap and natural resource that has been used for the purification of recombinant proteins in previous studies (Islam et al., 2018b). CBM3 strongly binds to MCC beads (Kumari et al., 2020), whereas no proteins from *N. benthamiana* leaf tissues were detected in the MCC bead-bound fraction. Thus, MCC beads can be used to purify CBM3-containing recombinant proteins expressed in *N. benthamiana*. However, CBM3-containing MCS-hIL6 cannot be eluted (Islam et al., 2018b). Thus, the target proteins can be released by proteolytic processing of recombinant proteins bound to MCC beads. In fact, in the case of TGFβ1, furin-mediated proteolysis is responsible for the release of mature TGFβ1 from the LAP domain.

To purify TGFβ1 recombinant proteins using MCC beads, total protein extracts were prepared from *N. benthamiana* leaf tissues harvested at 7 DPI and mixed with MCC beads. The MCC beads were washed extensively to remove loosely bound non-specific proteins. To analyze the purification of TGFβ1 recombinant proteins, proteins were released from MCC beads by boiling. The released proteins were analyzed by SDS/PAGE and Western blotting using an anti-TGFβ1 antibody. BMC:LAP[C33S]TGFβ1 was purified to a high degree (**Figure 2**) and detected as a single band by anti-TGFβ1 in both the total soluble extracts and the MCC-bound fraction. Anti-TGFβ1 did not detect any band in the unbound and washing fractions, indicating that BMC:LAP[C33S]TGFβ1 strongly binds to MCC beads.

Substitution of Furin With Enterokinase Leads to Efficient Processing of TGFβ1 Recombinant Protein for the Release of Mature TGFβ1

Next, we examined whether mature TGFβ1 could be released from the full-length BMC:LAP[C33S]TGFβ1 recombinant protein. We used the convertase furin, which is responsible for the processing of mature TGFβ1 from the LAP domain (Dubois et al., 2001). A furin cleavage site consisting of RHRR residues is located between LAP and TGFβ1 in the native sequence. To enhance furin cleavage efficiency, we explored a different furin cleavage site by changing the sequence of the cleavage site from RHRR to RERRRKKR to yield *BMC:LAP[C33S]:F2:TGFβ1*. To test the cleavage of TGFβ1 recombinant proteins by furin, we generated an ER-targeted furin construct, *BiP:furin*$_{26-595}$*:6xHis:HDEL*. The *furin* construct was co-expressed together with *BMC:LAP[C33S]TGFβ1* or *BMC:LAP[C33S]:F2:TGFβ1* in *N. benthamiana*. To examine

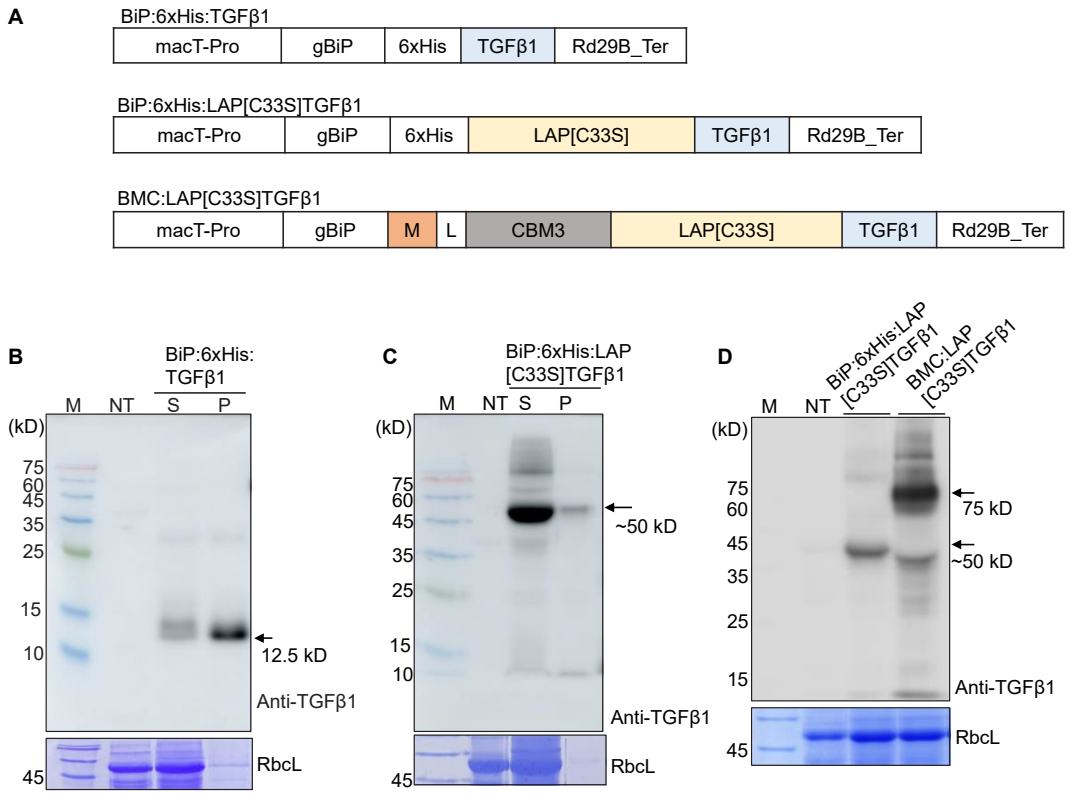


FIGURE 1 | Design and expression of various *TGFβ1* recombinant constructs to produce soluble proteins at high levels in *Nicotiana benthamiana*. **(A)** Schematic presentation of the constructs. LAP[C33S]TGFβ1, pro-TGFβ1; gBiP, genomic DNA fragment encoding the ER targeting signal (aa residues from 1 to 23) of Arabidopsis BiP1 (BAA13947); macT-pro and Rd29B_Ter, the promoter and terminator of Arabidopsis *Rd29B*, respectively; 6xHis, His tag; M, a highly N-glycosylated region (amino acid positions 231–290) of human protein tyrosine phosphatase, receptor type C (CD45); CBM3, cellulose-binding module 3 from *Clostridium thermocellum* cellulosomal scaffoldin subunit A; L, linker sequence (GGGGSGGGGS). **(B–D)** Western blot analysis of TGFβ1 recombinant proteins. The indicated constructs were transiently expressed in *N. benthamiana* by *Agrobacterium*-mediated infiltration. Total protein extracts from *N. bethamiana* leaf tissues were separated by SDS/PAGE and analyzed by Western blotting using an anti-TGFβ1 antibody. The gel was stained with Coomassie brilliant blue (CBB) to obtain the large subunit of the Rubisco complex (RbcL) band, which was used as a loading control. M, molecular weight standard; NT, non-transformed wild-type; S, total soluble protein; P, insoluble pellet fraction; arrow, recombinant protein.

the release of mature TGFβ1 from BMC:LAP[C33S]TGFβ1 and BMC:LAP[C33S]:F2:TGFβ1 by BiP:furin$_{26-595}$:6xHis:HDEL, total protein extracts from *N. benthamiana* leaf tissues at 3, 5, and 7 DPI were separated by SDS/PAGE and analyzed by Western blotting using the anti-TGFβ1 antibody. Even in the presence of BiP:furin$_{26-595}$:6xHis:HDEL, the TGFβ1 recombinant protein was largely intact, as in the case without co-expression of *BiP:furin$_{26-595}$:6xHis:HDEL* (**Supplementary Figure 1**), indicating that furin does not efficiently process both of the TGFβ1 recombinant proteins in *N. benthamiana*. The expression of *BiP:furin$_{26-595}$:6xHis:HDEL* was confirmed by Western blot analysis using an anti-His antibody. A possible explanation might be improper or partial activation of furin. In mammalian cells, furin undergoes two-step cleavage, first in the ER and another at the trans-Golgi network. In our current study, furin was localized to the ER by using the ER retention motif HDEL, which might have caused a problem in the activation of furin in *N. benthamiana*.

Next, as an alternative approach, we examined whether another protease, enterokinase (EK), could replace furin for the release of mature TGFβ1 from the full-length TGFβ1 recombinant protein. EK is a serine protease. The recombinant catalytic subunit is widely used for the cleavage of recombinant proteins that contain a recognition sequence, DDDDK (Gasparian et al., 2011). We replaced the furin cleavage site (RRHR) with an EK site (DDDDK) to yield construct *BMC:LAP[C33S]:EK:TGFβ1* (**Supplementary Figure 2**). We first compared the expression levels of *BMC:LAP[C33S]:EK:TGFβ1* and *BMC:LAP[C33S]TGFβ1* in *N. benthamiana*. Total soluble protein extracts from the leaves of *N. benthamiana* transformed with *BMC:LAP[C33S]TGFβ1* and *BMC:LAP[C33S]:EK:TGFβ1* at 3, 5, and 7 DPI were separated by SDS/PAGE and analyzed by anti-TGFβ1 antibody. The replacement of the furin cleavage site with an EK site did not affect the expression level of the *TGFβ1* recombinant gene (**Supplementary Figures 2B,C**). Next, we examined whether full-length TGFβ1 recombinant proteins could be cleaved by an enterokinase light chain. For this, we first purified BMC:LAP[C33S]:EK:TGFβ1 using MCC beads. The MCC beads bound with recombinant protein BMC:LAP[C33S]:EK:TGFβ1 were incubated with EK. Proteins

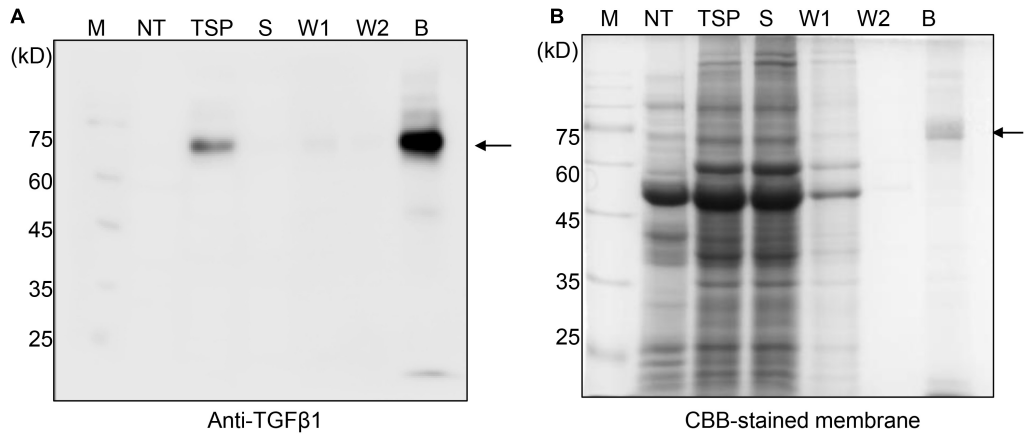


FIGURE 2 | BMC:LAP[C33S]TGFβ1 shows strong and specific binding to MCC beads. **(A,B)** SDS/PAGE and Western blot analyses. Total soluble protein (TSP) extracts were incubated with MCC beads for 2 h at 4°C. The supernatant was collected as the unbound fraction (S) after centrifugation. The pellet containing MCC beads was collected separately and washed four times (W1–W4; only W1 and W2 were used for analysis). Proteins bound to the MCC beads were released by boiling them in SDS sample buffer. Protein samples were separated by SDS/PAGE and analyzed by Western blotting using anti-TGFβ1 antibodies **(A)** or CBB staining of the gel **(B)**. M, molecular weight standard; NT, non-transformed wild-type *N. benthamiana*; B, proteins bound to MCC beads; Arrow, BMC:LAP[C33S]TGFβ1.

in the digestion buffer and proteins bound to MCC beads were separately collected and analyzed by SDS/PAGE and Western blotting using an anti-TGFβ1 antibody. A protein band at 12.5 kD corresponding to monomeric mature TGFβ1 was detected only with EK (**Figure 3**). Moreover, BMC:LAP[C33S]:EK:TGFβ1 was cleaved by EK with over 90% efficiency, as calculated based on western blot band intensity, indicating that the recombinant proteins of TGFβ1 were correctly and efficiently processed by EK. However, the 12.5 kD band was detected in proteins from the MCC bead fraction but not in the EK buffer fraction, indicating that the mature form of TGFβ1 was not released from the LAP domain, consistent with earlier results showing that mature TGFβ1 is tightly associated with LAP after cleavage.

Mature TGFβ1 Is Released From LAP *via* Activation With HCl Treatment

It is well-known that mature TGFβ1 is tightly associated with the LAP domain after cleavage by Furin in mammalian cells to regulate the availability of active TGFβ1 (Khalil, 1999). We asked how mature TGFβ1 could be released from the LAP after cleavage. Another question was how mature TGFβ1 could be activated after release from the LAP domain. In fact, the release and activation of TGFβ1 from LAP has been a real challenge, which makes the production of active TGFβ1 as a recombinant protein very difficult. Concerning the activation of TGFβ1, TGFβs are secreted in a biologically latent form, either smaller L-TGFβ or large LL-TGFβ, and none of them can interact with TGFβ receptors (Miyazono et al., 1991; Bonewald, 1999). Latent TGFβs can be activated *in vitro* by physiochemical factors, such as a low pH of 2 or a high pH of 8, a high temperature of 100°C, urea, detergents, such as SDS, and chaotropic agents (Brown et al., 1990). In addition, a few proteases, such as plasmin, calpain, neuraminidase, cathepsins B and D, and thrombospondin-1, activate latent TGFβ1 (TSP-1) (Miyazono et al., 1991; Schultz-Cherry et al., 1995; Khalil, 1999). A previous study showed that

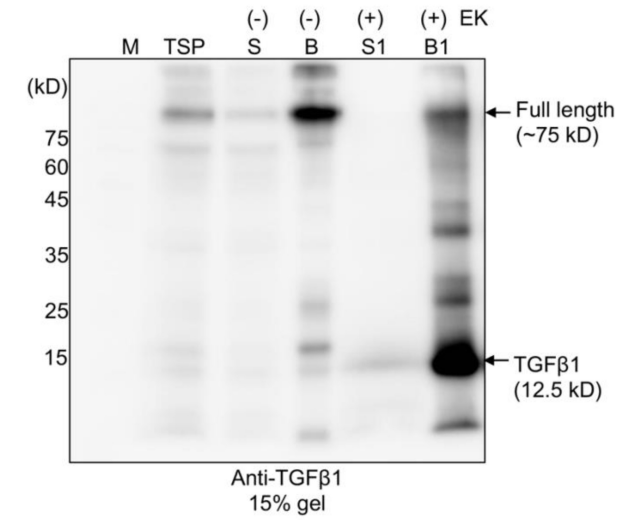


FIGURE 3 | The full-length TGFβ1 recombinant protein is efficiently processed by enterokinase, but the mature form remains associated with the LAP domain. Full-length TGFβ1 recombinant proteins were purified using MCC beads and subsequently incubated with (+) or without (-) enterokinase at 25°C for 16 h. The incubation solutions (S and S1) and MCC beads (B and B1) were collected separately. The MCC beads were washed with 40 mM Tris-Cl (pH 7.4) to remove enterokinases. Proteins still bound to the MCC beads were released by boiling them in SDS/PAGE sample buffer. All protein samples were separated by SDS/PAGE and analyzed by Western blotting using an anti-TGFβ1 antibody. TSP, total soluble protein.

latent TGFβ1 is converted to the active form upon treatment with a low pH of 3.7 at 37°C in a time-dependent manner, yielding a significant portion or the maximum with incubation for only 15 min or 120 min, respectively (Nocera and Chu, 1995). The released TGFβ1 remained relatively stable for 24 h at the pH and temperature mentioned above. We examined whether mature

TGFβ1 could be released from LAP at a low pH. Full-length recombinant proteins of TGFβ1 bound onto MCC beads were treated with EK, and the MCC beads were washed four times with 40 mM Tris-Cl (pH 7.4) buffer to remove EK and other non-specific proteins released from MCC beads. Subsequently, the MCC beads were incubated in an activation buffer with a pH of approximately 1.5–2 for 30 min at 25°C. Proteins released into the incubation solution were collected separately. Proteins bound to MCC beads were also collected by boiling the MCC beads in the SDS/PAGE sample buffer. These proteins were separated by SDS/PAGE and analyzed by Western blotting using an anti-TGFβ1 antibody. A major portion of mature TGFβ1 was detected in the solution fraction (**Figure 4**, lane S2), indicating that low pH treatment leads to the release of mature TGFβ1 from the LAP domain. A previous study suggested that a low pH causes denaturation of LAP but not TGFβ (Lawrence, 1995), thereby disturbing the interaction between them.

Next, we examined whether the mature TGFβ1 released by low pH treatment could yield the dimer form of mature TGFβ1. Proteins were separated by non-reducing tricin/PAGE without denaturation using DTT and analyzed by Western blotting using anti-TGFβ1 antibodies. As a control, commercial TGFβ1 was included in the analysis. Mature TGFβ1 was detected at 25 kD, corresponding to the dimer position (**Figure 5** and **Supplementary Figure 3**), indicating that mature TGFβ1 exists as a dimer.

Contaminating Proteins in Mature TGFβ1 Preparation Are Removed by a Second Microcrystalline Cellulose Bead Binding

The mature TGFβ1 preparation obtained by HCl treatment was contaminated with the uncleaved full-length TGFβ1 recombinant proteins together with a few degradation products. We wanted to further purify mature TGFβ1 to a higher degree of purity. CBM3 is known to bind tightly to MCC beads. However, the HCl treatment caused the release of the full-length recombinant proteins together with the degradation products. Since these contaminating proteins still contained CBM3, we asked whether they could again bind to MCC beads under mild pH conditions. For this, the pH of the mature TGFβ1 preparation obtained from MCC beads was adjusted to a pH of 4 by adding 40 mM Tris-base (pH ∼11), mixed with MCC beads, and incubated for 2 h. The mixture was separated into supernatant and MCC bead fractions. Proteins in the MCC beads were obtained by boiling them in SDS/PAGE sample buffer. These protein samples were separated by SDS/PAGE and analyzed by Western blotting using an anti-TGFβ1 antibody. In this rebinding process, the majority of contaminating proteins were detected in the MCC bead fraction (S2-B fraction), and TGFβ1 was largely detected in the supernatant fraction (S2-S fraction) (**Figures 6A,B**), indicating that the majority of contaminating proteins could be eliminated by rebinding to MCC beads. However, some of the mature TGFβ1 protein was lost during this purification step (S2-B fraction).

Endotoxin-free recombinant proteins are one of the most critical advantages of using plants as hosts for recombinant protein production. Lipopolysaccharides (LPS) have always been an important concern when recombinant proteins are produced in *E. coli*. To deliver the recombinant gene into plant cells, we used *Agrobacterium*-mediated transformation. Thus, we examined the level of endotoxins, if any, in purified mature TGFβ1. Purified mature TGFβ1 preparation contained <0.013 EU/μg (<0.0013 ng/μg) endotoxin (**Supplementary Figure 4**), which is much lower than the acceptable limit of endotoxins in recombinant proteins, <1 EU/μg (<1 ng/μg) (Magnusdottir et al., 2013; Nomura et al., 2017).

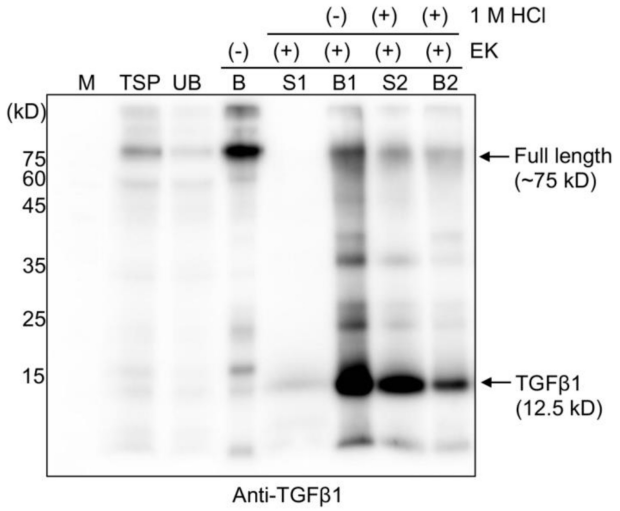


FIGURE 4 | HCl treatment releases mature TGFβ1 from the LAP domain after enterokinase cleavage. Total soluble protein (TSP) extracts were mixed with MCC beads for 2 h at 4°C. The supernatant and MCC beads were separated into unbound (UB) and MCC bead-bound (B) fractions. The MCC bead fraction was washed four times with washing buffer (40 mM Tris-Cl, pH 7.4, 0.05% Triton X-100). Subsequently, MCC beads were suspended in EK buffer (50 mM Tris-Cl, pH 7.4, 150 mM NaCl, 2 mM $CaCl_2$, and 0.5% Triton X-100) and incubated with EK at 25°C for 16 h. The supernatant (S1) and MCC beads (B1) were collected separately. The MCC beads (B1) carrying the complex of mature TGFβ1 and BMC-LAP were mixed with activation buffer (40 mM Tri-Cl, pH 7.4, and 150 mM NaCl), and 1 M HCl was added at 1/20th the volume (V/V) of activation buffer to give 50 mM HCl as the final concentration and incubated in a shaker at 25°C for 30 min. The supernatant (S2) and MCC beads (B2) were collected separately. Proteins bound to the MCC beads were recovered by boiling them in SDS/PAGE sample buffer. Proteins were separated by 15% SDS/PAGE and analyzed by Western blotting using an anti-TGFβ1 antibody. M, molecular weight standard; arrows, the position of full-length or cleaved TGFβ1.

Plant-Produced Mature TGFβ1 Activates Downstream Signaling and Induces Filopodia-Like Structures in the A549 Cell Line

We next examined whether plant-produced mature TGFβ1 was biologically active. TGFβ1 facilitates the oligomerization of Ser/Thr receptor kinases and phosphorylates cytoplasmic signaling molecules SMAD2 and SMAD3 (Schmierer and Hill, 2007). The very first step in TGFβ1 signaling is the binding of the ligand to dimers of receptor TβRII, which leads to

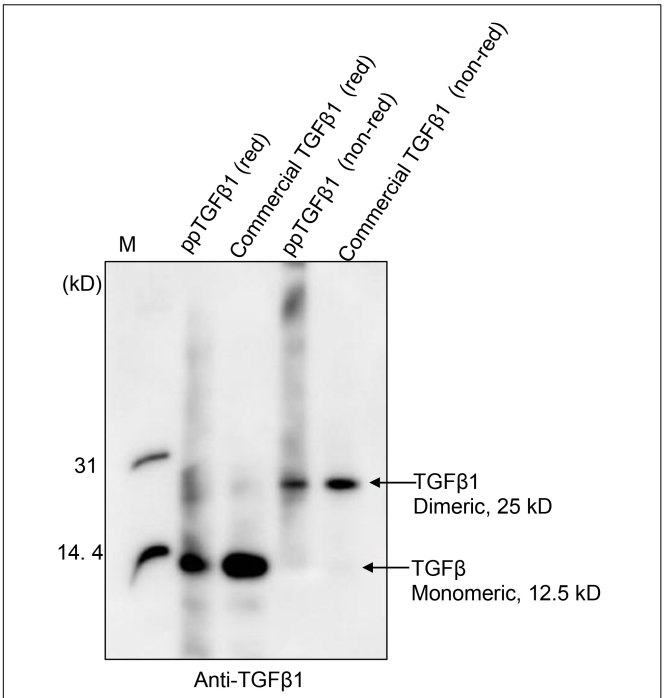


FIGURE 5 | Mature TGFβ1 is released as dimers from the full-length TGFβ1 recombinant protein *via* EK-mediated proteolytic cleavage, followed by acid activation. The mature TGFβ1 released from the full-length TGFβ1 recombinant proteins by HCl treatment was separated by 10% Tricin/PAGE under reducing or non-reducing conditions and analyzed by Western blotting using an anti-TGFβ1 antibody. Commercial mature TGFβ1 (50 ng) produced in HEK293 cells was included as a positive control.

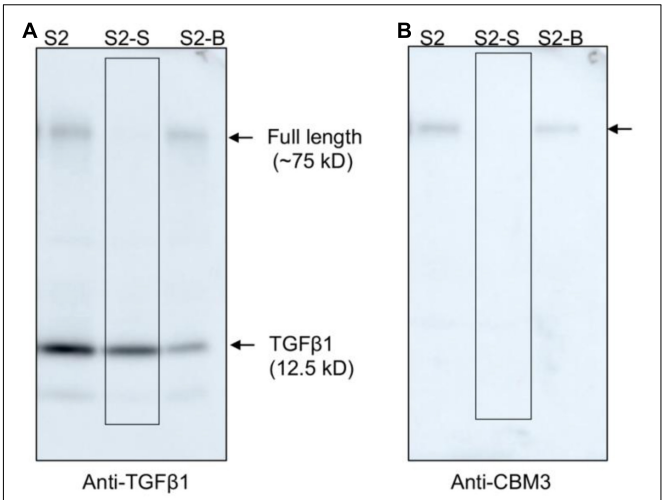


FIGURE 6 | Full-length TGFβ1 recombinant proteins and other contaminating proteins can be removed from mature TGFβ1 by rebinding to MCC beads. The pH of the mature TGFβ1 preparation (S2) obtained after HCl treatment was adjusted by adding 40 mM Tris base (pH ∼11.0) until the pH reached 4.0. Subsequently, the mature TGFβ1 preparation was mixed with MCC beads and incubated on a twister at 4°C for 2 h. The mixture was centrifuged at 2,000 × g for 5 min, and the supernatant (S2-S) and MCC beads (S2-B) were recovered separately. Proteins bound to MCC beads were recovered by boiling them in SDS sample buffer. Protein samples were separated by SDS/PAGE and analyzed by Western blotting using anti-TGFβ1 **(A)** and anti-CBM3 **(B)** antibodies. Arrows, the position of full-length or mature TGFβ1.

oligomerization with TβRI to yield a heterotetrameric complex (Wrana et al., 1992). This interaction leads to a cascade of events and phosphorylates SMAD2 and SMAD3 proteins (Albers et al., 2018). We compared the activity of plant-produced TGFβ1 (ppTGFβ1) with commercial recombinant TGFβ1 produced in HEK293 cells. Human lung cancer cell A549 was cultured with or without ppTGFβ1 or commercial TGFβ1 (10 ng/ml) for 48 h. We measured the phosphorylated SMAD2 (p-SMAD2) levels. Upon treatment with commercial TGFβ1, the p-SMAD2 level dramatically increased in the A549 cell line. The ppTGFβ1 treatment also increased the p-SMAD2 level to a level higher than that with commercial TGFβ1 (**Figure 7A**), indicating that ppTGFβ1 is as active as commercial TGFβ1. To support this finding, we examined the activation of downstream genes. It is well-known that the epithelial–mesenchymal transition (EMT) pathway is upregulated upon TGFβ1 treatment (Liu et al., 2013). Two genes, *SNAIL1* and *ZEB2*, are known as TGFβ1 downstream signaling genes. qRT-PCR revealed that treatment with both commercial TGFβ1 and ppTGFβ1 rapidly enhanced *SNAIL1* transcript levels in A549 cells to the same degree (**Figure 7B**). Consistent with this, the transcript level of zinc-finger E-box-binding 2 (*ZEB2*), a transcription factor activated by SNAIL1, also increased upon treatment with both commercial TGFβ1 and ppTGFβ1 to the same degree. Finally, we examined the morphological changes in A549 cells. Actin reorganization is a prominent morphological alteration induced by TGFβ1, leading to lamellipodia/filopodia formation. In the absence of TGFβ1, the A549 cells showed regular shapes. However, treatment with both commercial TGFβ1 and ppTGFβ1 induced EMT-like elongated structures and filopodia formation (**Figure 7C**). These results confirm that ppTGFβ1 is as active as commercial TGFβ 1.

DISCUSSION

In this study, we developed an efficient purification and one-pot activation method to produce active human TGFβ1 in *N. benthamiana*. Often, the production of recombinant proteins includes many rounds of purifications and downstream processing that can lead to not only an increased production cost but also a loss of yield. Our approach did not include tedious and complicated steps of refolding after purification, as in *E. coli*. To our knowledge, this is the first time that active dimeric TGFβ1 has been produced and purified in plants without the refolding process.

Recombinant human TGFβ1 was produced in heterologous systems, such as *E. coli* and HEK293 cell lines. In *E. coli*, the mature form of TGFβ1 was expressed. However, it was expressed as an inclusion body in *E. coli*, which requires multiple rounds of denaturation and a refolding process to yield active mature TGFβ1. In contrast, active TGFβ1 was successfully produced in CHO cells without the refolding process (Zou and Sun, 2004). In their study, LAP[C33S]TGFβ1 was expressed as a secretory protein using the leader sequence of rat serum albumin, one of

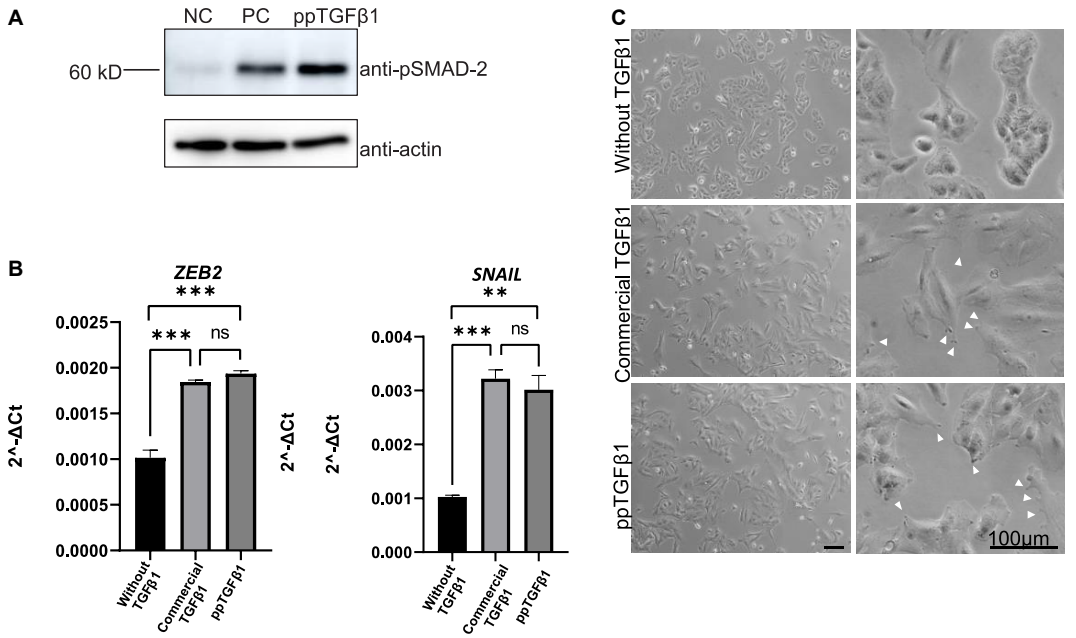


FIGURE 7 | The mature TGFβ1 produced in plants activates the downstream signaling of TGFβ1 in the A549 cell line. **(A)** Phosphorylation of SMAD2. Total proteins were prepared from the A-546 cell line and treated with plant-produced TGFβ1 (ppTGFβ1) or commercial TGFβ1 (PC) at a concentration of 10 ng/ml concentration for 48 h. Proteins were separated by SDS/PAGE and analyzed with Western blotting using anti-pSMAD or anti-actin antibodies. NC, negative control (4 mM HCl). **(B)** qRT-PCR analysis of upregulated EMT pathway-specific genes. Total RNA was prepared from the A-546 cell line treated as in panel **(A)**. qRT-PCR was performed using primers for *ZEB2*- or *SNAIL*-specific primers. *GAPDH* was used as an internal control. qRT-PCR was performed with three independent biological samples, and statistical analysis was performed using an unpaired *t*-test (GraphPad Prism 9). The values are the means with standard deviations ($n = 3$). **(C)** Microscopic image of the A-546 cells. The cells were treated as in panel **(A)**. Images of cells were taken 48 h after treatment with plant-produced TGFβ1 or commercial TGFβ1. Arrows, filopodia. Scale bar = 100 μm. $^{**}P < 0.05$ and $^{***}P < 0.001$.

the most abundantly secreted proteins in cells, to enhance the targeting of recombinant protein to the ER. The secreted protein was purified by Ni^{2+}-NTA affinity purification followed by low pH (pH 3.0) activation, thereby releasing TGFβ1 from its LAP domain. Finally, TGFβ1 was further purified by size-exclusion chromatography at a yield of approximately 20 mg/l.

In a previous study, an attempt was made to produce TGFβ1 in plants. When LAPTGFβ1, the pro-form of TGFβ1, was co-expressed with *furin*, active TGFβ1 was produced (Wilbers et al., 2016). However, the expression level was too low for the purification of mature TGFβ1. The activity was tested using acid-activated total soluble protein and ELISA. In this study, we also used the pro-form of TGFβ1, LAP[C33S]TGFβ1, to produce TGFβ1 in *N. benthamiana*. In the production of recombinant proteins in heterologous systems, one of most important aspects is the expression level. We used the M domain to increase the expression level of TGFβ1. The M domain has been shown to increase the protein expression level when the fusion protein is targeted at the ER (Kang et al., 2018). In addition, the stability of recombinant proteins is crucial to achieving a high yield. In plants, the ER is the best place to produce recombinant proteins because it provides a suitable environment for correct folding and post-translational modification and is the place with the least risk of proteolytic degradation (Schouten et al., 1996). Often, an ER retention motif is added to the C-terminus for ER accumulation. However, it has been shown that the addition of extra amino acid residues to the C-terminus of TGFβ1 hampers biological activity (Wakefield et al., 1991). Thus, we did not add the ER retention motif to the C-terminus of the TGFβ1 recombinant protein. This could be a limiting factor in increasing the expression level. In plants, another member of the TGFβ family, TGFβ3, was successfully produced in *N. tabacum* (Gisby et al., 2011). To produce TGFβ3 at a high level in plants, the authors integrated the gene encoding the mature form of TGFβ3 into the chloroplast genome. Indeed, this approach is one of the most powerful ways to increase expression levels in plants. However, the mature form of TGFβ3 was produced as an inclusion body, which necessitates denaturation and refolding, as in the case of TGFβ1 in *E. coli*.

Another important step in the production of recombinant proteins is protein purification from the total protein extracts of plant leaf tissues. Indeed, it has been estimated that the purification steps account for 70–80% of the production costs (Raven et al., 2014). Various fusion tags have been introduced to improve protein purification, recovery, and solubility (Loughran and Walls, 2017). Recently, cellulose-binding module 3 (CBM3) has been used as an affinity purification tag due to its high selectivity and tight binding to cellulose, which is an inexpensive material (Wan et al., 2011; You and Zhang, 2013; Islam et al., 2018b). The binding affinity between CBM3 and MCC beads is extremely high and can only be disrupted by strong denaturants (Sarikaya et al., 2003; Andrade et al., 2010). We included CBM3 as an affinity tag for protein purification of the

TGFβ1 recombinant protein. Indeed, BMC:LAP[C33S]TGFβ1 tightly bound to MCC beads. Moreover, the recombinant protein BMC:LAP[C33S]:EK:TGFβ1 bound to the MCC beads was efficiently cleaved by EK. In this process, furin, an endogenous processing enzyme, was less efficient in processing BMC:LAP[C33S]TGFβ1 bound to MCC beads. However, the mature form of TGFβ1 was not released from MCC beads even after EK treatment. One possibility is that mature TGFβ1 may be tightly associated with LAP[C33S] as reported previously (Khalil, 1999). This behavior of mature TGFβ1 is advantageous in purifying mature TGFβ1 after EK cleavage. MCC beads can be washed to remove EK after the cleavage reaction.

The release of active mature TGFβ1 from LAP is tightly controlled in cells and induced by signaling *in vivo* (Shi et al., 2011). Thus, in the production of TGFβ1 as a recombinant protein, the release and activation of TGFβ1 from the LAP domain is challenging. Various treatments, including high salt (1 M NaCl), urea (1–4 M), detergent (0.5% SDS), DTT, and low pH buffers (glycine pH 3.0), did not induce the release of mature TGFβ1 from the LAP domain (del Amo-Maestro et al., 2019). We found that treatment with a high concentration of HCl successfully released mature TGFβ1 from the LAP domain in dimeric form after EK cleavage. The release of TGFβ1 was specific to a high concentration of HCl but not to other acidic conditions, such as 0.2 M glycine (pH 2.0). This raises the possibility that an acidic pH, together with Cl^-, but not acidic conditions *per se*, plays a role in the release of mature TGFβ1 from the LAP domain. However, this needs to be further investigated.

Recently, recombinant TGFβ1 was produced in mammalian cells such as CHO cells. However, in general, recombinant protein production in animal cells requires a highly sophisticated facility that should be run under aseptic conditions. Also, the running cost is high, which leads to a high price of the final product. In contrast, plants as a bio-factory give great freedom to such situations. The facility and running cost are thought to be much lower than those for animal cells. An additional advantage is that recombinant proteins produced in plants are free from animal pathogens. In this study, we explore this possibility using TGFβ1, one of the challenging targets in recombinant protein production. The pure TGFβ1 that could be obtained in our current study was up to 1 mg/kg of fresh weight. In the case of the CHO cells, the amount of protein produced was up to 30 mg/L. The yield *per se* appears to be lower in *N. benthamiana* than in CHO cells. However, considering the high running cost and expansive facility, for the production of recombinant TGFβ1, we believe that the plant system may still be competitive to the CHO system. In addition, there are still rooms to enhance the expression level of recombinant TGFβ1 using strong expression vectors such as virus-based expression vectors. As the current study employed simple and inexpensive steps for purification, it would definitely reduce the overall cost of the final product once higher expression is achieved. We demonstrate that dimeric active TGFβ1 can be produced in plants and purified using cheap MCC beads to a high degree of purity without using time-consuming and costly processes, such as denaturation and refolding *in vitro*. The purity of the final TGFβ1 product can be further improved by additional steps involving size exclusion, ion exchange, or hydrophobic interaction chromatography. In conclusion, this plant-based system is a low-cost production system for dimeric active TGFβ1 that can be used for pharmaceutical purposes.

MATERIALS AND METHODS

Recombinant Gene Constructs

Codon-optimized *LAPTGFβ1* (without signal peptide, GenBank NM_000660) was chemically synthesized (Bioneer Corp., Daejeon, South Korea). *TGFβ1* was amplified with PCR from *LAPTGFβ1* using *Bam*HI_6xHis_TGFβ1 forward primer and *Xho*I_LAP_TG_R2 reverse primer (**Supplementary Table 1**). The PCR product was digested by *Bam*HI and *Xho*I restriction endonucleases and ligated to *pTEX1-BiP:HA:mCor1:LysM:His:HDEL* (Song et al., 2021) to generate *pTEX1-BiP-6xHis-TGFβ1*. The *M* domain and *CBM3* were amplified with PCR from *1300-BMC-SazCA* (Kumari et al., 2020). *Bam*HI and *Spe*I restriction sites were introduced in the *M* domain by overhang PCR using primers MF and MR (**Supplementary Table 1**). To introduce an *Spe*I site to the 5' end, and *Xma*I and *Xho*I sites to the 3' end of *CBM3*, PCR was carried out using primers CBM_F and CBM_R (**Supplementary Table 1**).

The PCR product *Bam*HI-M-*Spe*I was digested with *Bam*HI and *Spe*I restriction endonucleases and ligated to *pTEX1-BiP:HA:mCor1:LysM:His:HDEL* (Song et al., 2021) to generate *pTEX1-BM*. The PCR product, *Spe*I-CBM3-*Xma*I-*Xho*I, was digested with *Spe*I and *Xho*I restriction endonucleases and ligated to *pTEX1-BM* digested by *Spe*I and *Xho*I to produce another intermediate vector, *pTEX1-BMC*. Chemically synthesized *LAPTGFβ1* was digested by *Xma*I and *Xho*I restriction endonucleases and ligated to *pTEX1-BMC* digested with the same restriction endonucleases to yield *pTEX1-BMC:LAPTGFβ*. [C33S] mutation in the LAP domain was introduced by overhang PCR using forward primer *Xma*I_GG_LAPC33S and reverse primer *Xho*I_LAP TG_R2. The PCR product was digested with *Xma*I and *Xho*I restriction endonucleases and ligated to *pTEX1-BMC:LAPTGFβ1*, digested with the same restriction endonucleases to yield *pTEX1-BMC:LAP[C33S]TGFβ1*. To replace the furin cleavage site with an enterokinase cleavage site (DDDDK), overlap PCR was performed using four primers, *Xma*I_LAP-TG_F1, Fu: EK_OL_R1, Fu: EK _OL_F2, *Xho*I_LAP_TG_R2 (**Supplementary Table 1**), and the PCR product was digested with the *Xma*I and *Xho*I restriction endonucleases and ligated to *pTEX1-BMC:LAP[C33S]TGFβ1* digested with the same restriction endonucleases to yield *pTEX1-BMC:LAP[C33S]:EK:TGFβ*.

Plant Growth Conditions

Wild-type *Nicotiana benthamiana* plants were grown in a controlled greenhouse. The temperature and relative humidity were controlled at 24°C and 40–65%, respectively. The photoperiod was adapted to a long-day photoperiod (14 h light and 10 h dark; light intensity, 130–150 $\mu E/m^2$) for 5–7 weeks. Five- to seven-week-old plants were used for agro-infiltration.

Transient Expression of Recombinant *TGFβ1* in *Nicotiana benthamiana*

All expression vectors were transformed into *Agrobacterium tumefaciens* strain EHA105 by electroporation and plated on an LB-agar plate containing 50 mg/ml kanamycin and 50 mg/ml rifampicin. A single colony was used to inoculate in 5 ml LB medium and cultured overnight. A 5 ml culture was added to 50 ml LB medium containing suitable antibiotics. Cells were pelleted by centrifugation at 3,500 × g for 10 min and resuspended in infiltration buffer (10 mM MES, 10 mM $MgSO_4$, 200 μM acetosyringone, pH 5.6) at 0.8 OD_{600}. The cell suspension was maintained at room temperature for 2–4 h before infiltration. Leaves of 5–7-week-old plants were infiltrated on the abaxial side using a 1 ml syringe without a needle or by vacuum infiltration. Infiltrated plants were returned to the greenhouse for further growth of 3–7 days.

Leaf samples were harvested, ground in liquid nitrogen using a mortar and pestle to give fine powder and mixed with 5 volumes (w/v) of protein extraction buffer (50 mM Tris-Cl, pH 7.4, 300 mM NaCl, 1 mM DTT, 0.1% [v/v] Triton X-100, and 1X protease inhibitor cocktail). The total soluble protein was recovered after centrifugation at 13,000 × g for 15 min. Protein concentrations were measured using the Bradford protein method (Bio-Rad, Hercules, CA, United States).

SDS-PAGE and Western Blot Analysis

Protein samples were separated using 10–15% SDS/PAGE. Gels were stained with 0.25% CBB R-250 (AMRESCO, cat. no: 6104-59-2) in a staining solution containing 45% methanol and 10% glacial acetic acid or analyzed by Western blotting with suitable antibodies.

For Western blot analysis, membranes were blocked with 5% fat-free skim milk in TBST buffer (20 mM Tris-Cl, pH 7.5, 150 mM NaCl, 0.1% Tween-20) for 2 h and incubated with rabbit anti-TGFβ1 (Abcam, ab179695), rabbit anti-CBM3 (Bio app., South Korea), anti-phospho-SMAD2 (AB3849-I Merck, Rahway, New Jersey, United States), or anti-actin-clone C4 (Merck, Rahway, New Jersey, United States) antibodies as the primary antibody at a dilution of 1:1,000–1:5,000 in TBST with 5% non-fat dry milk overnight followed by washing and incubation with respective secondary antibodies at a dilution of 1:5,000–1:10,000 in TBST at room temperature for 2 h. Immunoblot images were captured using an Amersham Imager 680 (GE Healthcare, Chicago, IL, United States).

Protein Purification Using Microcrystalline Cellulose Beads and Microcrystalline Cellulose Bead-Bound Cleavage of Full-Length TGFβ1 Recombinant Proteins by Enterokinase

To purify BMC:LAP[C33S]:EK:TGFβ1, total soluble protein (TSP) extracts were mixed with an MCC bead (Sigma Aldrich, Burlington, MA, United States) slurry in batch. First, the MCC bead slurry was prepared by mixing MCC bead powder with autoclaved distilled water at a 1:1 (w/v) ratio. The MCC beads were washed five times to remove very fine particles. Finally, an equal volume of sterile water was added to the MCC beads, and the MCC bead slurry was maintained at 4°C for future use. TSP extracts (150 ml) from 30 g FW leaf tissues were mixed with 8 ml MCC slurry and incubated at 4°C for 2 h with gentle shaking. After the binding of proteins to MCC beads, samples were centrifuged at 2,000 × g for 2 min, and the supernatant and MCC beads were separately collected for unbound proteins and MCC bead-bound proteins, respectively. The recovered beads were washed five times with 10 bead volumes of 40 mM Tris-HCl buffer (pH 7.4, 0.05% Triton X-100) to remove loosely bound proteins. MCC bead-bound proteins were released by boiling them in SDS/PAGE sample buffer, and the purity of MCC bead-purified TGFβ1 recombinant proteins was examined by SDS/PAGE and Western blot analysis.

To remove the N-terminal region from the mature TGFβ1, MCC beads bound with BMC:LAP[C33S]:EK:TGFβ1 recombinant proteins were first washed with enterokinase (EK) buffer (50 mM Tris-HCl, pH 7.4, 150 mM NaCl, 2 mM $CaCl_2$, and 0.5% Triton X-100) and then divided into two 50 ml conical tubes at equal volumes. EK (30 units in 4 ml EK cleavage buffer) was added to the MCC beads bound with TGFβ1 recombinant proteins, and the mixture was incubated at 25°C in a shaking incubator for 16 h.

Release and Activation of Mature TGFβ1 From the LAP Domain and Purification of Mature TGFβ1

After EK-mediated proteolytic cleavage of BMC:LAP[C33S]:EK:TGFβ1, MCC beads were centrifuged at 3,000 × g for 5 min, and the pelleted MCC beads were collected and washed twice with 5 ml of 40 mM Tris-HCl (pH 7.4). For the release and activation of mature TGFβ1, TGFβ1/BMC:LAP[C33S]-bound MCC beads were suspended in 5 ml activation buffer (40 mM Tri-HCl pH 7.4, and 150 mM NaCl). After gentle mixing, 1 M HCl at 1/20th the volume of activation buffer was added to TGFβ1/BMC:LAP[C33S]-bound MCC beads to give a final HCl concentration of 50 mM. The mixture was incubated at 25°C for 30 min with gentle mixing. The mature form of TGFβ1 was recovered in the supernatant after centrifugation at 3,000 × g at 4°C for 5 min. To recover any remaining mature TGFβ1 from MCC beads, 2 ml activation buffer and 100 μl of 1 M HCl were added to the MCC beads, gently mixed for 1 min, and the supernatant was collected after centrifugation. The pH of the pooled supernatant was increased to 4.0 by adding 40 mM Tris base (pH ∼11.0). The concentration of NaCl was readjusted to get final concentration 150 mM.

To further purify the mature TGFβ1, the supernatant was mixed again with 1 ml of the MCC bead slurry and incubated for 2 h. The mature TGFβ1 was recovered from the supernatant after centrifugation at 3,000 × g for 5 min. Purified TGFβ1 was extensively dialyzed against 4 mM HCl and subjected to centrifugation at 14,000 × g for 20 min, and the supernatant containing mature TGFβ1 was recovered. The dialyzed protein was concentrated using a Millipore 10 K centrifugal filter

(Millipore, Burlington, MA, United States), and BSA was added to a 0.1% final concentration. The protein sample was filter-sterilized and stored at –80°C.

Endotoxin Level Determination

The endotoxin level in purified mature TGFβ1 (ppTGFβ1) was determined using a Toxisensor Chromogenic LAL Endotoxin Assay Kit (GenScript, Cat no. L00350C, NJ, United States) according to the manufacturer's protocol.

Biological Activity of Plant-Produced Mature TGFβ1

Animal cell line A549 was purchased from the Korean Cell Line Bank (KCLB). Cells were seeded in 6-well plates (2.0×10^5) and cultured in RPMI 1640 medium (Welgene, Gyeongsan-si, South Korea) supplemented with 10% fetal bovine serum (FBS) (Merck, Darmstadt, Germany), 100 IU/mL penicillin, and 100 μg/mL streptomycin (Welgene, Gyeongsan-si, South Korea). After 24 h of incubation, the cells were treated with 10 ng/ml commercial mature TGFβ1 (Abcam, Cambridge, United Kingdom), 10 ng/ml ppTGFβ1, or 4 mM HCl as a negative control and incubated at 37°C in 5% CO_2 for 48 h.

Real-Time Quantitative PCR

The cells were detached by scrapers and collected. Total RNA was prepared using the RNeasy Mini Kit (Qiagen, Hilden, Germany) and purified using the Qiagen RNeasy Mini Kit. RNA concentration and purity were determined using a NanoDrop One spectrophotometer (Thermo Fisher Scientific, Waltham, MA, United States). cDNA was prepared from 2 μg total RNA using a high-capacity cDNA Reverse Transcription Kit (Applied biosystems, Waltham, MA, United States) with oligo-dT as the primer, according to the manufacturer's instructions. Quantitative RT-PCR was performed using SYBR Green Supermix and a one-step cycler (Applied biosystems, Waltham, MA, United States). Gene expression was normalized to the housekeeping gene *GAPDH*. The following primer pairs were used for qRT-PCR: *ZEB2* (sense, 5′- GGC GCA AAC AAG CCA ATC CCA -3′; antisense, 5′- TTC ACT GGA CCA TCT ACA GAG GCT T -3′); *SNAIL* (sense, 5′- ACC CCA CAT CCT TCT CAC TG -3′; antisense, 5′- TAC AAA AAC CCA CGC AGA CA -3′). The 20 μl PCR mixture contained 200 ng template, 0.5 μM each of the forward and reverse primers, and 1 × SYBR master mix. The PCR conditions were as follows: initial denaturation at 95°C for 10 min, followed by 40 cycles of 95°C for 15 s and 60°C for 1 min. To confirm specific amplification, a melting curve was generated by heating at 95°C for 15 s, then at 60°C for 1 min, and increasing the temperature by 0.3°C every 15 s up to 95°C. Statistical analysis was performed using an unpaired *t*-test (GraphPad Prism 9).

DATA AVAILABILITY STATEMENT

The original contributions presented in the study are included in the article/**Supplementary Material**, further inquiries can be directed to the corresponding author.

AUTHOR CONTRIBUTIONS

IH and AS contributed to conceptualizing this study and wrote the manuscript. AS made the construct designs and performed the required experiments. JL and KS contributed to determining the biological activity of ppTGFβ1. HK contributed to designing a few of the experiments. All authors contributed to the article and approved the submitted version.

FUNDING

This work was carried out with the support of "Cooperative Research Program for Agriculture Science and Technology Development (Project No. PJ015701012021)," Rural Development Administration, South Korea and also a grant from the Korea Health Technology R&D Project through the Korea Health Industry Development Institute (KHIDI), funded by the Ministry of Health (HV20C0156), South Korea.

SUPPLEMENTARY MATERIAL

The Supplementary Material for this article can be found online at: https://www.frontiersin.org/articles/10.3389/fpls.2022.922694/full#supplementary-material

Supplementary Figure 1 | Furin does not cleave the furin cleavage site located between mature TGFβ1 and LAP in the full-length TGFβ1 recombinant protein *in vivo*. **(A)** Schematic presentation of the constructs. The native and modified furin cleavage sites (RHRR and RERRRKKR in *BMC:LAP[C33S]TGFβ1* and *BMC:LAP[C33S]:F2:TGFβ1*, respectively) are indicated in the TGFβ1 recombinant constructs. For the Furin construct, the furin gene encoding amino acid positions from 26 to 595 was fused to the leader sequence of *Arabidopsis* BiP. His tag and ER retention signal HDEL were also added to the C-terminus of furin. **(B)** Failure of the full-length TGFβ1 recombinant protein by furin. *BiP:furin*$_{26-595}$*:6xHis:HDEL* was co-expressed with two TGFβ1 recombinant constructs in *N. benthamiana*. Total soluble protein samples prepared at 3, 5, and 7 DPI were separated on 15% SDS/PAGE and analyzed by Western blotting using anti-TGFβ1 or anti-His antibodies. Arrows, full-length recombinant protein or cleaved TGFβ1.

Supplementary Figure 2 | Replacement of the furin cleavage site for efficient proteolytic cleavage. **(A)** Schematic presentation of the constructs containing either the furin cleavage sequence (RHRR) or the enterokinase cleavage sequence (DDDDK). **(B,C)** The expression level of *BMC:LAP[C33S]TGFβ1* and *BMC:LAP[C33S]:EK:TGFβ1*. Total protein extracts from leaf tissues of *N. benthamiana* harvested at 3, 5, and 7 DPI were analyzed by SDS/PAGE and Western blotting using anti-TGFβ1 antibody. M, molecular weight standard; NT, non-transformed wild-type; Arrow, full-length recombinant protein.

Supplementary Figure 3 | Treatment with HCl, but not with other acids, releases dimeric TGFβ1 after proteolytic cleavage. After EK-mediated cleavage, MCC beads bound with the TGFβ1/BMC:LAP complex were treated with various acids for 30 min at 25°C. The supernatants from the MCC beads were separated on 10% Tricin-PAGE and analyzed by Western blotting using anti-TGFβ1 antibodies. Only HCl treatment released the dimers of TGFβ1. In contrast, the citrate buffer largely produced monomers of TGFβ1. M, molecular weight standard; HCl, 1 M HCl; CB, 30 mM citrate buffer; Gly, 200 mM glycine pH 2.

Supplementary Figure 4 | Plant-produced and purified mature TGFβ1 contains an extremely low level of endotoxin. The amount of endotoxin was measured by a chromogenic LAL-assay. **(A)** The standard curve was generated using a commercial *E. coli* endotoxin standard. **(B)** Varying amounts (1–4 μg) of purified ppTGFβ1 were used to determine the endotoxin level. The values are means with standard deviations ($n = 3$).

REFERENCES

Albers, R. E., Selesniemi, K., Natale, D. R. C., and Brown, T. L. (2018). TGF-β induces Smad2 phosphorylation, ARE induction, and trophoblast differentiation. *Int. J. Stem Cells* 11, 111–120. doi: 10.15283/ijsc17069

An, N., Ou, J., Jiang, D., Zhang, L., Liu, J., Fu, K., et al. (2013). Expression of a functional recombinant human basic fibroblast growth factor from transgenic rice seeds. *Int. J. Mol. Sci.* 14, 3556–3567. doi: 10.3390/ijms14023556

Andrade, F. K., Moreira, S. M. G., Domingues, L., and Gama, F. M. P. (2010). Improving the affinity of fibroblasts for bacterial cellulose using carbohydrate-binding modules fused to RGD. *J. Biomed. Mater. Res. Part A* 92A, 9–17. doi: 10.1002/jbm.a.32284

Bonewald, L. F. (1999). Regulation and regulatory activities of transforming growth factor β. *Crit. Rev. Eukaryot. Gene Exp.* 9, 33–44.

Brown, P. D., Wakefiel, L. M., Levinson, A. D., and Sporn, M. B. (1990). Physicochemical activation of recombinant latent transforming growth factor-beta's 1, 2, and 3. *Growth Fact.* 3, 35–43. doi: 10.3109/08977199009037500

Brunner, A. M., Lioubin, M. N., Marquardt, H., Malacko, A. R., Wang, W. C., Shapiro, R. A., et al. (1992). Site-directed mutagenesis of glycosylation sites in the transforming growth factor-beta 1 (TGF beta 1) and TGF beta 2 (414) precursors and of cysteine residues within mature TGF beta 1: effects on secretion and bioactivity. *Mol. Endocrinol.* 6, 1691–1700.

Clark, R. A. F. (1996). *The Molecular and Cellular Biology of Wound Repair*. New York, NY: Plenum Press.

D'Aoust, M.-A., Lavoie, P.-O., Couture, M. M.-J., Trépanier, S., Guay, J.-M., Dargis, M., et al. (2008). Influenza virus-like particles produced by transient expression in *Nicotiana benthamiana* induce a protective immune response against a lethal viral challenge in mice. *Plant Biotechnol. J.* 6, 930–940. doi: 10.1111/j.1467-7652.2008.00384.x

del Amo-Maestro, L., Marino-Puertas, L., Goulas, T., and Gomis-Rüth, F. X. (2019). Recombinant production, purification, crystallization, and structure analysis of human transforming growth factor β2 in a new conformation. *Sci. Rep.* 9:86660. doi: 10.1038/s41598-019-44943-4

Diamos, A. G., Hunter, J. G. L., Pardhe, M. D., Rosenthal, S. H., Sun, H., Foster, B. C., et al. (2020). High level production of monoclonal antibodies using an optimized plant expression system. *Front. Bioeng. Biotechnol.* 7:472. doi: 10.3389/fbioe.2019.00472

Diamos, A. G., Rosenthal, S. H., and Mason, H. S. (2016). 5′ and 3′ untranslated regions strongly enhance performance of geminiviral replicons in *Nicotiana benthamiana* leaves. *Front. Plant Sci.* 7:200. doi: 10.3389/fpls.2016.00200

Dubois, C. M., Blanchette, F., Laprise, M.-H., Leduc, R., Grondin, F., and Seidah, N. G. (2001). Evidence that furin is an authentic transforming growth factor-β1-converting enzyme. *Am. J. Pathol.* 158, 305–316. doi: 10.1016/s0002-9440(10)63970-3

Gasparian, M. E., Bychkov, M. L., Dolgikh, D. A., and Kirpichnikov, M. P. (2011). Strategy for improvement of enteropeptidase efficiency in tag removal processes. *Protein Exp. Purif.* 79, 191–196. doi: 10.1016/j.pep.2011.04.005

Gentry, L. E., Webb, N. R., Lim, G. J., Brunner, A. M., Ranchalis, J. E., Twardzik, D. R., et al. (1987). Type 1 transforming growth factor beta: amplified expression and secretion of mature and precursor polypeptides in Chinese hamster ovary cells. *Mol. Cell. Biol.* 7, 3418–3427. doi: 10.1128/mcb.7.10.3418-3427.1987

Gisby, M. F., Mellors, P., Madesis, P., Ellin, M., Laverty, H., O'Kane, S., et al. (2011). A synthetic gene increases TGFβ3 accumulation by 75-fold in tobacco chloroplasts enabling rapid purification and folding into a biologically active molecule. *Plant Biotechnol. J.* 9, 618–628. doi: 10.1111/j.1467-7652.2011.00619.x

Gray, A. M., and Mason, A. J. (1990). Requirement for activin a and transforming growth factor–β1 pro-regions in homodimer assembly. *Science* 247, 1328–1330. doi: 10.1126/science.2315700

Holtz, B. R., Berquist, B. R., Bennett, L. D., Kommineni, V. J. M., Munigunti, R. K., White, E. L., et al. (2015). Commercial-scale biotherapeutics manufacturing facility for plant-made pharmaceuticals. *Plant Biotechnol. J.* 13, 1180–1190. doi: 10.1111/pbi.12469

Hong, J., Ye, X., and Zhang, Y.-H. P. (2007). Quantitative determination of cellulose accessibility to cellulase based on adsorption of a nonhydrolytic fusion protein containing CBM and GFP with its applications. *Langmuir* 23, 12535–12540. doi: 10.1021/la7025686

Hurtado, J., Acharya, D., Lai, H., Sun, H., Kallolimath, S., Steinkellner, H., et al. (2019). In vitro and in vivo efficacy of anti-chikungunya virus monoclonal antibodies produced in wild-type and glycoengineered Nicotiana benthamiana plants. *Plant Biotechnol. J.* 18, 266–273. doi: 10.1111/pbi.13194

Islam, M. R., Kwak, J., Lee, J., Hong, S., Khan, M. R. I., Lee, Y., et al. (2018b). Cost-effective production of tag-less recombinant protein in *Nicotiana benthamiana*. *Plant Biotechnol. J.* 17, 1094–1105.

Kang, H., Park, Y., Lee, Y., Yoo, Y.-J., and Hwang, I. (2018). The fusion of a highly N-glycosylated polypeptide increases the expression of ER-localized proteins in plants. *Sci. Rep.* 8:4612. doi: 10.1038/s41598-018-22860-2

Khalil, N. (1999). TGF-β: from latent to active. *Microbes Infect.* 1, 1255–1263.

Kim, M.-Y., Jang, Y.-S., Yang, M.-S., and Kim, T.-G. (2015). High expression of consensus dengue virus envelope glycoprotein domain III using a viral expression system in tobacco. *Plant Cell Tissue Organ Cult.* 122, 445–451.

Kim, Y., Lee, G., Jeon, E., Sohn, E., Lee, Y., Kang, H., et al. (2014). The immediate upstream region of the 5′-UTR from the AUG start codon has a pronounced effect on the translational efficiency in *Arabidopsis thaliana*. *Nucleic Acids Res.* 42, 485–498. doi: 10.1093/nar/gkt864

Kim, Y. V., Gasparian, M. E., Bocharov, E. V., Chertkova, R. V., Tkach, E. N., Dolgikh, D. A., et al. (2014). New strategy for high-level expression and purification of biologically active monomeric TGF-β1/C77S in *Escherichia coli*. *Mol. Biotechnol.* 57, 160–171.

Kumari, M., Lee, J., Lee, D. W., and Hwang, I. (2020). High-level production in a plant system of a thermostable carbonic anhydrase and its immobilization on microcrystalline cellulose beads for CO2 capture. *Plant Cell Rep.* 39, 1317–1329. doi: 10.1007/s00299-020-02566-4

Lawrence, D. A. (1995). Transforming growth factor-beta: an overview. *Kidney Int. Suppl.* 49, S19–S23.

Linder, M., and Teeri, T. T. (1996). The cellulose-binding domain of the major cellobiohydrolase of *Trichoderma reesei* exhibits true reversibility and a high exchange rate on crystalline cellulose. *Proc. Natl. Acad. Sci.* 93, 12251–12255. doi: 10.1073/pnas.93.22.12251

Liu, J., Hu, G., Chen, D., Gong, A.-Y., Soori, G. S., Dobleman, T. J., et al. (2013). Suppression of SCARA5 by Snail1 is essential for EMT-associated cell migration of A549 cells. *Oncogenesis* 2:e73. doi: 10.1038/oncsis.2013.37

Loughran, S. T., and Walls, D. (2017). Tagging recombinant proteins to enhance solubility and aid purification. *Protein Chromatogr.* 681, 131–156.

Maclean, J., Koekemoer, M., Olivier, A. J., Stewart, D., Hitzeroth, I. I, Rademacher, T., et al. (2007). Optimization of human papillomavirus type 16 (HPV-16) L1 expression in plants: comparison of the suitability of different HPV-16 L1 gene variants and different cell-compartment localization. *J. Gen. Virol.* 88, 1460–1469. doi: 10.1099/vir.0.82718-0

Magnusdottir, A., Vidarsson, H., Björnsson, J. M., and Örvar, B. L. (2013). Barley grains for the production of endotoxin-free growth factors. *Trends Biotechnol.* 31, 572–580. doi: 10.1016/j.tibtech.2013.06.002

Mason, H. S., Lam, D. M., and Arntzen, C. J. (1992). Expression of hepatitis B surface antigen in transgenic plants. *Proc. Natl. Acad. Sci.* 89, 11745–11749.

Miyazono, K., Olofsson, A., Colosetti, P., and Heldin, C. H. (1991). A role of the latent TGF-beta 1-binding protein in the assembly and secretion of TGF-beta 1. *EMBO J.* 10, 1091–1101. doi: 10.1002/j.1460-2075.1991.tb08049.x

Nocera, M., and Chu, T. M. (1995). Characterization of latent transforming growth factor-β from human seminal plasma. *Am. J. Reprod. Immunol.* 33, 282–291.

Nomura, Y., Fukui, C., Morishita, Y., and Haishima, Y. (2017). A biological study establishing the endotoxin limit for in vitro proliferation of human mesenchymal stem cells. *Regen. Ther.* 7, 45–51. doi: 10.1016/j.reth.2017.08.004

Ong, E., Greenwood, J. M., Gilkes, N. R., Kilburn, D. G., Miller, R. C. Jr., and Warren, R. A. J. (1989). The cellulose-binding domains of cellulases: tools for biotechnology. *Trends Biotechnol.* 7, 239–243.

Park, Y., Lee, S., Kang, H., Park, M., Min, K., Kim, N. H., et al. (2020). A classical swine fever virus E2 fusion protein produced in plants elicits a neutralizing humoral immune response in mice and pigs. *Biotechnol. Lett.* 42, 1247–1261. doi: 10.1007/s10529-020-02892-3

Raven, N., Rasche, S., Kuehn, C., Anderlei, T., Klöckner, W., Schuster, F., et al. (2014). Scaled-up manufacturing of recombinant antibodies produced by plant cells in a 200-L orbitally-shaken disposable bioreactor. *Biotechnol. Bioeng.* 112, 308–321. doi: 10.1002/bit.25352

Regnard, G. L., Halley-Stott, R. P., Tanzer, F. L., Hitzeroth, I. I., and Rybicki, E. P. (2010). High-level protein expression in plants through the use of a novel

autonomously replicating geminivirus shuttle vector. *Plant Biotechnol. J.* 8, 38–46. doi: 10.1111/j.1467-7652.2009.00462.x

Ruskin, J. D., Hardwick, R., Buser, D., Dahlin, C., and Schenk, R. K. (2000). Alveolar ridge repair in a canine model using rhTGF-β1with barrier membranes. *Clin. Oral Implants Res.* 11, 107–115.

Sarikaya, M., Tamerler, C., Jen, A. K.-Y., Schulten, K., and Baneyx, F. (2003). Molecular biomimetics: nanotechnology through biology. *Nat. Mater.* 2, 577–585. doi: 10.1038/nmat964

Schillberg, S., Fischer, R., and Emans, N. (2003). Molecular farming of recombinant antibodies in plants. *Cell. Mol. Life Sci.* 60, 433–445.

Schmierer, B., and Hill, C. S. (2007). TGFβ–SMAD signal transduction: molecular specificity and functional flexibility. *Nat. Rev. Mol. Cell Biol.* 8, 970–982. doi: 10.1038/nrm2297

Schouten, A., Roosien, J., van Engelen, F. A., de Jong, G. A., Borst-Vrenssen, A. W., Zilverentant, J. F., et al. (1996). The C-terminal KDEL sequence increases the expression level of a single-chain antibody designed to be targeted to both the cytosol and the secretory pathway in transgenic tobacco. *Plant Mol. Biol.* 30, 781–793. doi: 10.1007/BF00019011

Schultz-Cherry, S., Chen, H., Mosher, D. F., Misenheimer, T. M., Krutzsch, H. C., Roberts, D. D., et al. (1995). Regulation of transforming growth factor-β activation by discrete sequences of thrombospondin 1. *J. Biol. Chem.* 270, 7304–7310. doi: 10.1074/jbc.270.13.7304

Sha, X., Brunner, A. M., Purchio, A. F., and Gentry, L. E. (1989). Transforming growth factor β1: importance of glycosylation and acidic proteases for processing and secretion. *Mol. Endocrinol.* 3, 1090–1098. doi: 10.1210/mend-3-7-1090

Shi, M., Zhu, J., Wang, R., Chen, X., Mi, L., Walz, T., et al. (2011). Latent TGF-β structure and activation. *Nature* 474, 343–349.

Sohn, E., Lee, Y., Park, N., Park, M., Kim, N., Park, S., et al. (2018). Development of plant-produced E2 protein for use as a green vaccine against classical swine fever virus. *J. Plant Biol.* 61, 241–252. doi: 10.1007/s12374-018-0133-4

Song, S.-J., Shin, G.-I., Noh, J., Lee, J., Kim, D.-H., Ryu, G., et al. (2021). Plant-based, adjuvant-free, potent multivalent vaccines for avian influenza virus via *Lactococcus* surface display. *J. Integr. Plant Biol.* 63, 1505–1520. doi: 10.1111/jipb.13141

Sumner, D. R., Turner, T. M., Urban, R. M., Leven, R. M., Hawkins, M., Nichols, E. H., et al. (2001). Locally delivered rhTGF-β2 enhances bone ingrowth and bone regeneration at local and remote sites of skeletal injury. *J. Orthop. Res.* 19, 85–94. doi: 10.1016/S0736-0266(00)00015-2

Tuan, T.-L., Cheung, D. T., Wu, L.-T., Yee, A., Gabriel, S., Han, B., et al. (1996). Engineering, expression and renaturation of targeted TGF-beta fusion proteins. *Connect. Tissue Res.* 34, 1–9. doi: 10.3109/03008209609028888

Wakefield, L. M., Kondaiah, P., Hollands, R. S., Winokur, T. S., and Sporn, M. B. (1991). Addition of a C-terminal extension sequence to transforming growth factor-pl interferes with biosynthetic processing and abolishes biological activity. *Growth Fact.* 5, 243–253. doi: 10.3109/08977199109000288

Wan, W., Wang, D., Gao, X., and Hong, J. (2011). Expression of family 3 cellulose-binding module (CBM3) as an affinity tag for recombinant proteins in yeast. *Appl. Microbiol. Biotechnol.* 91, 789–798. doi: 10.1007/s00253-011-3373-5

Wang, Y.-P., Wei, Z.-Y., Zhong, X.-F., Lin, C.-J., Cai, Y.-H., Ma, J., et al. (2015). Stable expression of basic fibroblast growth factor in chloroplasts of tobacco. *Int. J. Mol. Sci.* 17:19. doi: 10.3390/ijms17010019

Werner, S., Breus, O., Symonenko, Y., Marillonnet, S., and Gleba, Y. (2011). High-level recombinant protein expression in transgenic plants by using a double-inducible viral vector. *Proc. Natl. Acad. Sci.* 108, 14061–14066. doi: 10.1073/pnas.1102928108

Wilbers, R. H. P., Westerhof, L. B., Raaij, D. R., Adrichem, M., Prakasa, A. D., Lozano-Torres, J. L., et al. (2016). Co-expression of the protease furin in *Nicotiana benthamiana* leads to efficient processing of latent transforming growth factor−β1 into a biologically active protein. *Plant Biotechnol. J.* 14, 1695–1704. doi: 10.1111/pbi.12530

Wirth, S., Calamante, G., Mentaberry, A., Bussmann, L., Lattanzi, M., Barañao, L., et al. (2004). Expression of active human epidermal growth factor (hEGF) in tobacco plants by integrative and non-integrative systems. *Mol. Breed.* 13, 23–35.

Wrana, J. L., Attisano, L., Cárcamo, J., Zentella, A., Doody, J., Laiho, M., et al. (1992). TGFβ signals through a heteromeric protein kinase receptor complex. *Cell* 71, 1003–1014.

Wu, M. Y., and Hill, C. S. (2009). TGF-β superfamily signaling in embryonic development and homeostasis. *Dev. Cell* 16, 329–343. doi: 10.1016/j.devcel.2009.02.012

Xu, J., Okada, S., Tan, L., Goodrum, K. J., Kopchick, J. J., and Kieliszewski, M. J. (2010). Human growth hormone expressed in tobacco cells as an arabinogalactan-protein fusion glycoprotein has a prolonged serum life. *Transgenic Res.* 19, 849–867. doi: 10.1007/s11248-010-9367-8

You, C., and Zhang, Y.-H. P. (2013). Self-assembly of synthetic metabolons through synthetic protein scaffolds: one-step purification, co-immobilization, and substrate channeling. *ACS Synth. Biol.* 2, 102–110. doi: 10.1021/sb300068g

Zhao, C.-P., Guo, X., Chen, S.-J., Li, C.-Z., Yang, Y., Zhang, J.-H., et al. (2017). Matrix attachment region combinations increase transgene expression in transfected Chinese hamster ovary cells. *Sci. Rep.* 7:42805. doi: 10.1038/srep42805

Zou, Z., and Sun, P. D. (2004). Overexpression of human transforming growth factor-β1 using a recombinant CHO cell expression system. *Protein Exp. Purif.* 37, 265–272. doi: 10.1016/j.pep.2003.06.001

Conflict of Interest: The authors declare that the research was conducted in the absence of any commercial or financial relationships that could be construed as a potential conflict of interest.

Publisher's Note: All claims expressed in this article are solely those of the authors and do not necessarily represent those of their affiliated organizations, or those of the publisher, the editors and the reviewers. Any product that may be evaluated in this article, or claim that may be made by its manufacturer, is not guaranteed or endorsed by the publisher.

Copyright © 2022 Soni, Lee, Shin, Koiwa and Hwang. This is an open-access article distributed under the terms of the Creative Commons Attribution License (CC BY). The use, distribution or reproduction in other forums is permitted, provided the original author(s) and the copyright owner(s) are credited and that the original publication in this journal is cited, in accordance with accepted academic practice. No use, distribution or reproduction is permitted which does not comply with these terms.

frontiers | Frontiers in Plant Science

ORIGINAL RESEARCH
published: 02 June 2022
doi: 10.3389/fpls.2022.905264

Nested miRNA Secondary Structure Is a Unique Determinant of miR159 Efficacy in *Arabidopsis*

Muhammad Imran[1†], Tengfei Liu[1†], Zheng Wang[2†], Min Wang[1], Shulin Liu[1], Xinyan Gao[1,3], Anning Wang[1,3], Songfeng Liu[1,3], Zhixi Tian[1,3] and Min Zhang[1]*

[1]State Key Laboratory of Plant Cell and Chromosome Engineering, Institute of Genetics and Developmental Biology, Innovative Academy for Seed Design, Chinese Academy of Sciences, Beijing, China, [2]Beijing Vegetable Research Center (BVRC), Beijing Academy of Agriculture and Forestry Sciences (BAAFS), Beijing, China, [3]University of Chinese Academy of Sciences, Beijing, China

MicroRNAs (miRNAs) are 20- to 24-nucleotide small RNAs, and whenever a pri-miRNA precursor includes another miRNA precursor, and both of these precursors may generate independent non overlapping mature miRNAs, we called them nested miRNAs. However, the functional and regulatory roles of nested miRNA structures in plants are still unknown. In this study, the *Arabidopsis* nested miR159a structure, which consists of two nested miRNAs, miR159a.1, and miR159a.2, was used as a model to determine miRNA-mediated gene silencing in plants. Complementation analysis of nested miR159a structures revealed that the miR159a structure can differentially complement the *mir159ab* phenotype, and a duplex nested structure in the tail end region of the pre-miR159a fold back may have a possible dominant function, indicating the importance of the flanking sequence of the stem in the cleavage of the mature miRNA. Furthermore, continuously higher expression of the miR159a.2 duplex in the severe leaf curl phenotype indicates that miR159a.2 is functional in *Arabidopsis* and suggests that in plants, a miRNA precursor may encode multiple regulatory small RNAs. Taken together, our study demonstrates that the nested miR159a structure regulated by duplex mutations of miR159a has a unique pattern and provides novel insight into silencing efficacy of *Arabidopsis* miR159a.

Keywords: *Arabidopsis thaliana*, pri-miR159a, nested miRNA structure, efficacy, duplex mutation

OPEN ACCESS

Edited by:
Joydeep Banerjee,
Indian Institute of Technology Kharagpur, India

Reviewed by:
Adinpunya Mitra,
Indian Institute of Technology Kharagpur, India
Nithya Kutty,
MIT World Peace University, India

***Correspondence:**
Min Zhang
zhangmin@genetics.ac.cn

†These authors have contributed equally to this work

Specialty section:
This article was submitted to Plant Biotechnology, a section of the journal Frontiers in Plant Science

Received: *26 March 2022*
Accepted: *09 May 2022*
Published: *02 June 2022*

Citation:
Imran M, Liu T, Wang Z, Wang M, Liu S, Gao X, Wang A, Liu S, Tian Z and Zhang M (2022) Nested miRNA Secondary Structure Is a Unique Determinant of miR159 Efficacy in Arabidopsis. Front. Plant Sci. 13:905264. doi: 10.3389/fpls.2022.905264

INTRODUCTION

MicroRNAs (miRNAs) are 20- to 24-nucleotide (nt) small RNAs that guide target mRNAs at the posttranscriptional level in both animals and plants (Jones-Rhoades et al., 2006). MiRNAs are also referred to as master regulators of gene expression in plants because they are active in several important developmental activities (Palatnik et al., 2003; Chen, 2012) and stress responses (Chiou et al., 2006; Sunkar et al., 2007). There are two separate stages in the plant miRNA pathway. First is the production stage, in which the microRNA is processed from a double-stranded RNA precursor transcript (Pegler et al., 2019). Second is the action stage, in which the mature microRNA guides an effector complex to directly suppress the expression of target genes that are highly complementary to microRNA target sequences (Schwab et al., 2005;

Liu et al., 2014). It is obvious that both stages play an important role in the function of microRNAs. A number of studies have been performed on the action stage of the miRNA pathway, and many miRNA target mRNAs have been identified (Mallory et al., 2004; Schwab et al., 2005; Addo-Quaye et al., 2008). The microRNA production stage is complex and refers to many factors that take part in the progression to liberated mature microRNA. In addition to these factors related to microRNA production, a recent study proved that the secondary structure of pri-miRNAs has significant implications for miRNA processing (Starega-Roslan et al., 2011). For instance, pri-miR172a required an ~15-nucleotide fragment in the lower stem for processing (Mateos et al., 2010; Werner et al., 2010), while the upper stem area had only a minor effect. The efficiency and precision of miR171a and miR390a processing were aided by a bulge adjacent to a cleavage site in the lower stem of pri-miR171a and an area 4–6 nucleotides below the miR390a/miR390a* duplex (Cuperus et al., 2010; Song et al., 2010). In contrast, the conserved upper stem of pri-miR319, which includes a terminal loop, is critical for sequential cleavage for miR319 production, while the lower stem portion of pri-miR319 is unnecessary (Bologna et al., 2009). Similarly, other factor influencing the regulatory efficiency include miRNA precursors that produces fold back hairpin structures. A miRNA precursor is generally expected to produce one miRNA-miRNA* duplex (Bartel, 2004; Kim, 2005; Winter et al., 2009). Indeed, Zhang et al. reported that 19 miRNA precursors in Arabidopsis that can yield multiple distinct miRNA-like RNAs in addition to miRNAs and miRNA*s (Zhang et al., 2010). Therefore, functionally testing of these possible factors on miRNA-target interactions would be interesting.

Arabidopsis miR159 has been extensively examined as a framework for miRNA-mediated gene silencing in plants (Vella et al., 2004; Allen et al., 2010). *MIR159* is tightly involved in plant development and highly conserved in many plant species, including angiosperms, mosses, and lycopods (Rhoades et al., 2002; Li et al., 2014). Bioinformatics analysis predicted more than 20 targets potentially regulated by the deeply conserved miR159 family in *Arabidopsis*, including eight MYB genes. However, a genetic study showed that only *MYB33* and *MYB65* were functionally targeted by miR159, and *mir159ab* developmental abnormalities were reversed in a *myb33mir159ab* quadruple mutant (Allen et al., 2007). This limited functional precision, as established by genetics, has been discovered in other plant miRNA systems (such as the miR319 pathway), implying that additional factors are required for functional miRNA-target interactions (Seitz, 2009). However, one untested hypothesis is that whether nested miR159a.1 and miR159a.2 are sensitive to miR159 regulation in *Arabidopsis*. Recently, two reports efficiently advanced silencing efficacy. First, Zheng et al. reported that *MYB33/65* contains a distinctive RNA secondary structure (i.e., stem-loops overlapping the miR159 binding site) that is a sensitive target of miR159 (Zheng et al., 2017), which underpins the narrow functional specificity of Arabidopsis miR159. Second, Li et al. demonstrated that factors beyond complementarity (e.g., miR159:*MYB33* transcript stoichiometry and mutation of the miR159 binding site in *MYB33*) govern the efficacy of the miR159-*MYB33* silencing outcome (Li et al., 2014). This research contributes to the increasing evidence that sequence complementarity alone may not guarantee good miRNA silencing in plants and that other aspects may be functional.

In our deep-sequencing-based study of small RNAs we identified that many miRNA precursors (including *MIR159* precursors) were completely included in another miRNA precursor, and we called them nested miRNA structures (Liu et al., 2016). Previous research showed that the *MIR159* precursor is exceptionally long, and other tiny RNAs generated from it have been identified in *Arabidopsis* by large-scale sequencing (Fahlgren et al., 2007) and genome-scale analyses (Zhang et al., 2010; Li et al., 2011). In *Arabidopsis*, the miR159 family is encoded by three genes, *MIR159a*, *MIR159b*, *MIR159c*, and miR159a, and miR159b is highly expressed compared miR159c. miR159a and miR159b have redundant functions, and neither single mutant displayed any phenotype. The double mutant *mir159ab* has pleiotropic morphological defects, including altered growth habits, curled leaves, small siliques, and small seeds (Allen et al., 2007; Allen et al., 2010; Alonso-Peral et al., 2012; Allen et al., 2013; Li et al., 2014). Furthermore, two members, *ath-MIR159a* and *ath-MIR159b*, consist of sibling mature miRNAs, and another member, *ath-MIR159c*, does not consist of other mature miRNAs inside canonical miR159. Therefore, we used *ath-MIR159a* as a model to investigate the regulatory relationship of nested structures and miR159 functions. In this study, by carrying out in planta miR159 efficacy assays, to uncover the regulatory role of nested structure we hypothesized that (1) distant miR159a.1 regulate miR159a.2; (2) nested miR159a.2 regulate miR159a.1; (3) miR159a.1 or miR159a.2 itself regulated. To test these hypothesis, we restructured the *MIR159* precursors and analysed the effect of nested structure on miR159a function.

MATERIALS AND METHODS

Plant Materials and Growth Conditions

Arabidopsis thaliana wild-type Columbia-0 (Col-0) and *mir159ab* mutant plants were grown in the greenhouse of the Institute of Genetics and Developmental Biology, Chinese Academy of Sciences. Seeds of the *mir159ab* mutant were provided by Professor Anthony A. Millar (Research School of Biology, Australian National University, Australia). Plants were grown in growth rooms with 16 h light and 8 h dark at 22°C. Size parameters were measured with ImageJ software.[1]

Generation of Constructs Carrying Nested miR159a Structure Variants

For complementation of *mir159ab*, the various nested miR159a structure constructs *mir159a.1-solo*, *mir159a.1-rep*, *mir159a.2-solo*,

[1]http://rsb.info.nih.gov/ij/

mir159a.2-rep, *mir159a.12-invert*, *mir159a.123-mix*, *mir159a.12-mix*, *mir159a.13-mix*, *mir159a.23-mix*, *mir159a.21-mix*, and *mir159a.ns* containing a 186-bp genomic fragment of miR159a with respective duplex mutations were synthesized and cloned into the pUC57 vector by Integrated DNA Technologies, Beijing China. Synthesized fragments were sequenced to verify their integrity and then cloned into the pMDC99 vector (Invitrogen). To combine the promoter of miR159a, the 1.5 kb promoter region was amplified and cloned into the pMDC99 vector. Restriction enzyme digestion and sequencing were used to validate the entry vectors, which were then recombined into the destination vector pMDC99 through Gateway LR reaction (Curtis and Grossniklaus, 2003). Primers specific for each construct were designed by Primer Premier 5.0 (PREMIER Biosoft Palo Alto CA United States) and are listed in **Supplementary Table S1**.

Transformation of *Arabidopsis*

All vectors were transformed into *Agrobacterium tumefaciens* strain GV3101 by electroporation (Hellens et al., 2000) and then transformed into the *Arabidopsis mir159ab* double mutant by using the floral dip method (Steven and Andrew, 1998). *A. tumefaciens* cells containing nested miRNA variants were harvested by centrifugation at 5000 × *g* for 8 min and resuspended in 5% sucrose solution to a final OD of 0.5. The shoot apex of *mir159ab* plants were dipped into a bacterial suspension supplemented with 0.05% Silwet (Silwet L-77, Sigma). Seeds were grown on agar plates containing Murashige and Skoog basal medium and antibiotics to pick transformants. Transformants were identified and transplanted into the soil after 7–10 days of growth.

Quantitative Real-Time Polymerase Chain Reaction (qRTPCR) Assay

Total RNA was isolated from plants at different growth stages with TRIzol reagent (Invitrogen, United States), and the integrity of purified RNA was then examined by agarose gel electrophoresis and quantified with a Nanodrop 2000 spectrophotometer (Thermo Fisher Scientific, Waltham, MA, United States). For quantitative detection of the genes, cDNA was first synthesized using M-MLV (Promega, United States) and detected with TransStart Tip Green qPCR SuperMix (Trans Gen Biotech, China). For comparison of sibling mature miRNA, total RNA was purified with the miRcute miRNA purification kit (Tiangen Biotech, China) and reverse transcribed to cDNA with a miRcute Plus miRNA first-strand cDNA synthesis kit (Tiangen). A minute Plus miRNA qPCR kit (SYBR Green) was used for qRT-PCR by following the manufacturer's protocol in a total volume of 20 µl. All qRT-PCRs (for both reference and genes of interest) were carried out on a Rotor-Gene Q Real-time PCR machine in triplicate under the following cycling conditions: 1 cycle of 95°C/5 min, 45 cycles of 95°C/15 s, and 60°C/15 s, and fluorescence was analysed at 72°C/20 s. A 55°C–99°C melting cycle was then carried out. *CYCLOPHILIN* (*At2g29960*) was used to normalize mRNA levels, and all sibling mature miR159 levels were normalized to U-6. The value for each gene represents the average of triplicate assays. The $2^{-\Delta Ct}$ method for relative quantification of gene expression was used to determine the level of miRNA expression.

Statistical Analysis

The one-way ANOVA with the SPSS 11.5 package for Windows (SPSS, Inc., Chicago, IL, United States) was used for statistical analysis in this work. The Student's *t*-test was used to examine the differences between the different groups of data. Results with a corresponding probability value of $p < 0.05$ and $p < 0.01$ were considered to be statistically significant and very significant, respectively.

RESULTS

Effects of Nested pri-miR159a Structure Regulation

The processing of miRNA precursors results in the release of a double-stranded miRNA/miRNA* duplex. When a pri-miRNA precursor includes another miRNA precursor and both of these precursors may generate independent non overlapping mature miRNAs, we designated them nested miRNAs. In our deep-sequencing-based study of small RNAs, we identified that many miRNA precursors were completely included in another miRNA precursor (Liu et al., 2016). Among these miRNA precursors, *Phaseolus vulgaris* miR159a precursor encodes a second miR159a.2 (*Glycine max* precursor) and both have distinct accumulation pattern, independent of miR159 activity and does not preserve a direct relationship under different growth conditions, which suggests that pvumiR159a precursor can potentially introduce two distinct miRNAs expressed from same precursor (Contreras-Cubas et al., 2012) Furthermore, the *Arabidopsis* miR159a precursor is unusually long (**Figure 1A**) and additional small RNAs originating from the precursors have been reported through large scale sequencing (Fahlgren et al., 2007) and genome-scale analyses (Zhang et al., 2010; Li et al., 2011), but its regulatory role is still hidden. Therefore, to understand the important role of *Arabidopsis* nested miR159a structure, (which consists of three nested miRNAs, miR159a.1, miR159a.2, and miR159a.3) we hypothesized that (1) distant miR159a.1 can regulate miR159a.2; (2) nested miR159a.2 can regulate miR159a.1; (3) miR159a.1 or miR159a.2 itself can regulate (**Figure 1B**). To test this hypothesis, we artificially designed five nested miR159a structural constructs through miRNA duplex mutation, and analysed the effects of each precursor miRNA (miR159a.1, miR159a.2, and miR159a.3). To investigate the regulatory role of miR159a.1 and miR159a.2, first we designed the repeat of miR159a.1 (miR159a.1-rep) and miR159a.2 (miR159a.2-rep) constructs independently to identify the distant effect and strength. Then, to check the structural position influence on regulation of miR159a.1 and miR159a.2, we exchanged the position between these two miRNAs. Further, to identify whether this stem core region is necessary for miR159a.1 and miR159a.2 regulations, we created a construct by removing the stem region. Notably, in all the above constructions, the miRNA secondary structures were kept almost similar to wild type except changes the positions of precursor miRNA. Finally, we completely

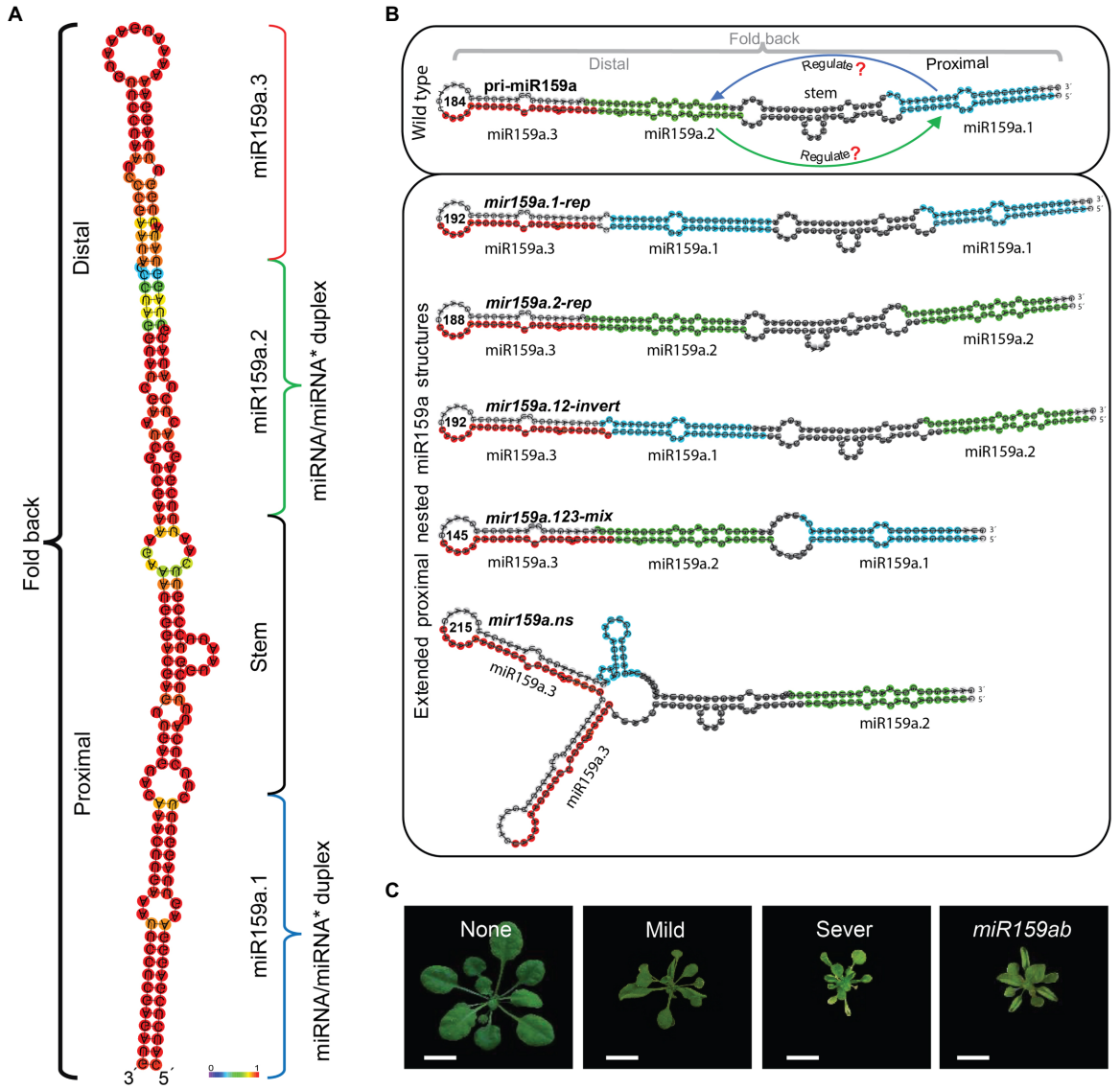


FIGURE 1 | Effects of nested pri-miR159a structure and phenotype classification. **(A)** The secondary structure of the miR159a was predicted with mfold 3.2. Fold back indicates the proximal and distal parts used for pri-miR159a duplex mutation. Blue, green, and red colour indicate the position of duplex miR159a.1 (containing sibling's miR159a.1–5 and miR159a. 1–3, that are located on 5 and 3 prime arm of miR159a secondary structure, respectively), miR159a.2 (Containing sibling's miR159a.2–5 and miR159a. 2–3, that are also located on 5 and 3 prime arm of miR159a secondary structure, respectively) and miR159a.3, respectively. **(B)** Modified secondary structural view for pri-miR159a (upper box) set with comparison to different artificially designed variants (lower box) for complementation test in the extended proximal region. Blue, green, red, and black region on miRNA secondary structure indicates, miR159a.1, miR159a.2, miR159a.3, and core stem region, respectively. The green and blue arrow indicates that miR159a.1 may regulate miR159a.2 and vice versa (upper box). Each nested variant is named according to the combination of miRNA duplex region. **(C)** Three-week-old primary transformants from each construct grown in parallel and categorized based on the presence and severity of upward leaf curl (none; indistinguishable from wild-type, mild; display of less leaf curliness, and severe; more leaves showing curliness).

destroyed the secondary structure of pri-miR159a by repeating the terminal loop sequence, miR159a.3 and also deleted some base pairs from miR159a.1 to validate role of the nested secondary structures in miRNA processing. In addition, except *mir159a.123-mix*, others construct had longer sequence length than the wild type pri-miR159a (184 nts; **Figure 1B**). By following this strategy, we performed the complementation test of these nested structures to recognize the value of each duplex miRNA.

As deregulated MYB33/65 activity by miR159 is tightly correlated with the extent of upward leaf curl (Allen et al., 2007), this trait was used to visually assess the strength of the complementation of the *mir159ab* phenotype by each construct and was categorized using three levels: none, mild, and severe (**Figure 1C**). Furthermore, rosette diameter, leaf area, lamina length, and lamina width in transgenic plants were examined. By using this strategy, we analysed nested miR159a structure regulation in *A. thaliana*.

Complementation Analysis in the Extended Proximal Fold Back for Nested pri-miR159a Structure Regulatory Footprints

Since all *mir159ab* defects are caused by the deregulation of the redundant GAMYB-like gene pair *MYB33*/*MYB65*, the *mir159ab* double mutant is an excellent method for investigating miRNA-mediated gene silencing (Allen et al., 2007), and these mutant phenotypes, including leaf curl and dwarfed stature, are easily scored. Therefore, by complementing *mir159ab* with different miR159a variants with modified miRNA duplex positions, their abundance, and deficiency, the impact of asymmetrical miRNA secondary structures on the silencing outcome of miR159 or their variants can be evaluated.

For the study of nested structure regulation in the extended fold back regions, we artificially designed a total of 5 constructs (**Figures 2A,B**) by repeating (*mir159a.1-rep*, *mir159a.2-rep*), inverting (*mir159a.12-invert*), and deleting (*mir159a.123-mix, mir159a.ns*) the miR159a duplex precursor. Among them, four constructs were symmetrical, and one had an asymmetrical structure in which the miR159a secondary structure was disrupted by repeating miR159a.3 and a terminal loop. All the constructs were named according to their structural changes as follows: (I) *mir159a.1-rep*, in which the miR159a.2 duplex region is replaced with an miR159a.1 duplex; (II) *mir159a.2-rep*, in which the mir159a.1 duplex region is replaced with an mir159a.2 duplex; (III) *mir159a.12-Invert*, in which the miR159a.1 and miR159a.2 duplex regions are mutually exchanged; (IV) *mir159a.123 mix*, in which the stem region between miR159a.1 and miR159a.2 was deleted and the remaining fold backs were mixed; (V) *mir159a-nested structure*, in which the miR159a secondary structure was disrupted completely as compared to miR159a (**Figure 2B**). The five miR159a variant constructs were individually transformed into *mir159ab,* and the phenotypes of multiple primary transformants were scored (**Figure 2C**). Leaf area, leaf length, and leaf width were measured at individual leaf positions of plants harvested 22 days after stratification (DAS), which is just before bolting occurs in both systems. Growth measurements were performed at this time point to decrease the potential influence of flowering time on leaf number and/or size (**Figure 2D**). From these data, we found that the *mir159a.1-rep* and *mir159a.123* mixed transgenic lines showed a rescued *mir159ab* phenotype. The lamina width was restored to the same level as that of the wild type, and rosette diameter, leaf area, and lamina length were also significantly increased compared to that of *mir159ab* (**Figure 2E**). Furthermore, the leaf area of 1st, 3rd, 5th, 7th 9th, and 11th leaves in transgenic plants was like that of wild-type and *mir159ab* plants, which also showed significant restoration in *mir159a.1-rep* and *mir159a.123-mix* transgenic plants but not others (**Figure 2F**). We further detected the expression level of *MIR159* and its response factors *MYB33* and *MYB65* (**Figure 3**). All 57 *mir159a.1-rep* T1 plants were fully complemented with thick and short wide leaves compared to those of the wild type (**Figures 2C,D**). Interestingly, the expression of miR159a.1–3 and miR159a.1–5 was not induced in the *miR159a.1-rep* transgenic plants, but the levels of *MYB33* and *MYB65* were still suppressed, which hinted that there was another pathway that was independent of the expression of miR159a.1 and related to the structure of the miR159 precursor, to regulate *MYB33* and *MYB65*. In contrast, all 48 *mir159a.2-rep* primary transformants showed the severe leaf curl phenotype with *mir159ab*, indicating that the introduction of miR159a.2 in place of miR159a.1 and keeping the position of miR159a.2 in the secondary structure made the *mir159ab* phenotype more serious. Mature RNA expression analysis showed that the miR159a.2–5 expression was induced six-fold possibly because of the structure with the double miR159a.2 duplex being transformed into the plant. However, the expression level of miR159a.1 in the *mir159a.2-rep* was not increased, and *MYB33* and *MYB65* were still expressed at a high level so that the phenotype was not rescued. Similarly, *mir159a.12-invert* could not rescue the phenotype, indicating that the miRNA structural position has a potential role in silencing efficacy. To further test whether the stem segment of the long miR159a precursor between the miR159a.1 and miR159a.2 duplex was necessary for its processing, we deleted the stem region of the miR159a precursor (**Figures 2C,D**). Surprisingly, all 23 *mir159a.123mix* primary transformants appeared similar to the wild type, but their leaves were wider than those of the wild type, and <16% of transgenic plants showed rounded leaves and the rescued phenotype, suggesting that individual absence of core stem does not prevent silencing altogether (**Figures 2C,D**). Furthermore, we irregularly disrupted the pri-miR159a secondary structure by repetition of miR159a.3 and the terminal loop and found that all 20 *mir159a.ns* primary transformants did not rescue the phenotype of the *mir159ab* mutant (**Figures 2C,D**), which showed a severe phenotype with male sterility characteristics. Taken together, these results indicate that the structure of the miR159 precursor plays an important role in miRNA function, including influencing the *MIR159* expression level and downstream response factor regulation. We also hypothesize that the miR159a.1 part and where it is in the structure may play more important roles according to the phenotype rescued only in *mir159a.1-rep* and *mir159a.123-mix* transgenic lines but not others. qRT-PCR was then performed on rosettes to measure the expression levels of sibling mature miRNAs in nested miR159a structure transgenic plants. We obtained the differential expression profiles of mature sibling miRNAs (**Figure 3A**). For instance, except for *mir159a.12invert*, mature complementary miR159a.1–5 and miR159a.1–3 expression was lower in both rescued and nonrescued transgenic plants than in wild-type plants. In contrast, the expression level of miR159a.2–5 was 2- to 10-fold higher in all non-rescued plants than in the wild type. miR159a.2–3 and miR159a.3 showed a similar expression pattern with 1-to-2-fold higher expression in *mir159a.12-invert* and *mir159a.ns* compared to the wild type (**Figure 3A**). Furthermore, as predicted, the *MYB33* transcript level was elevated 1- to 6-fold in mild- to severe-phenotype mutants, while low transcript levels were present in plants not expressing the phenotype. In addition, *MYB65* and *CP1* were dramatically suppressed with a similar pattern in the none phenotype group (**Figure 3B**).

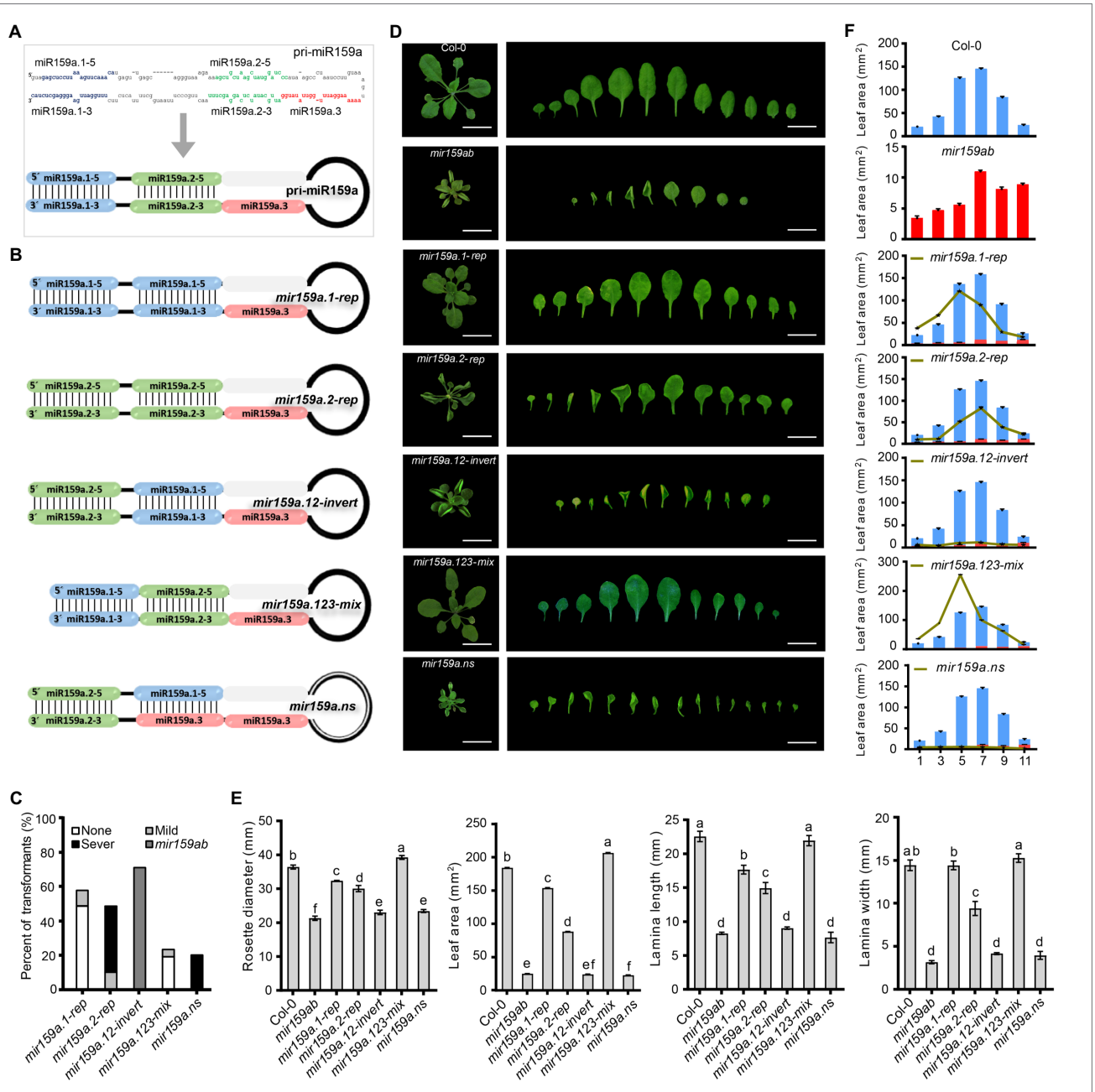


FIGURE 2 | Complementation assay in the extended proximal fold back of nested pri-miR159a structure. **(A)** Schematic showing the sequence and structure design for pri-miR159a. **(B)** Nested structural variant design in the extended proximal fold back of pri-miR159a-driven transgenic Arabidopsis. **(C)** Percentage of primary transformants showing no, mild, and severe leaf curl phenotypes. **(D)** Phenotypes of 22-day-old transgenic plants. Scale bar: 1 cm. **(E)** The size of a rosette, lamina length, lamina width, and leaf area of plants were evaluated. For measurement, the fourth true leaf of 28-day-old plants was collected. Data are presented as the mean ± SD (Standard deviation; $n > 10$) and statistically distinct genotypes were determined by one-way ANOVA with a *post-hoc* least significant difference (LSD) multiple comparisons within each group ($p < 0.05$, marked with different characters). **(F)** Leaf area of (1st, 3rd, 5th, 7th, 9th, and 11th) plants was evaluated. For measurement, 28-day-old plants were collected. Data are presented as the mean ± SD (Standard deviation; $n > 5$).

Minimum Sequence Length Required for Accurate Processing of Nested pri-miR159a Structures

The length of mature miRNAs generated from different miRNA genes may differ (Griffiths-Jones et al., 2007). The fast increasing interest in miRNA length diversity expands the miRNA universe and improves the regulatory potential of miRNAs (Chiang et al., 2010). Besides this, the secondary structure of the pri-miRNA has significant implications for miRNA processing (Starega-Roslan et al., 2011). For example, pri-miR172a required

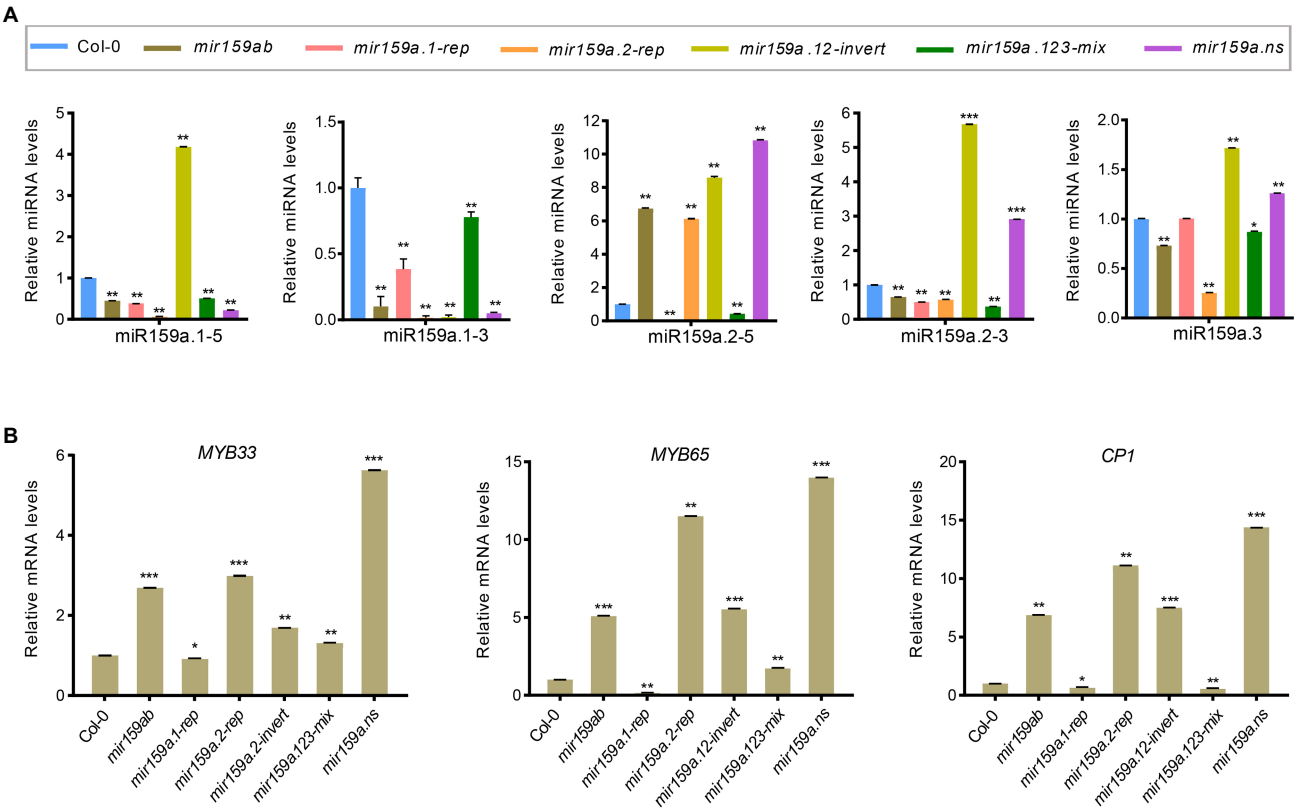


FIGURE 3 | Expression analysis of miR159a sibling's miRNA and MYB genes in the extended proximal nested transgenic plants. **(A)** The miRNA levels of miR159a siblings in the rosettes of *mir159ab* plants complemented by the nested miR159a variants in comparison with wild type and *mir159ab*. All miR159a siblings and mature miR159a levels were normalized to *U-6* and the relative expression in the wild type was set as 1. Measurements are the average of three technical replicates. Error bars represent the SEM (Standard error mean). Asterisks indicate statistically significant differences at $p < 0.05$ (*) and $p < 0.01$ (**) by Student's *t*-test. **(B)** The mRNA levels of *MYB33*, *MYB65,* and *CP1* were examined in Col-0, mir159ab and nested miR159a variants and were normalized to *CYCLOPHILIN*. The relative expression in the wild type was set as 1. Measurements are the average of three technical replicates. Error bars represent the SEM (Standard error mean). Asterisks indicate statistically significant differences at $p < 0.05$ (*) and $p < 0.01$ (**) by Student's *t*-test. *** mean $p < 0.001$.

an ~15-nucleotide fragment in the lower stem for processing (Mateos et al., 2010; Werner et al., 2010), whereas the upper stem region had only a modest influence. In contrast, the conserved upper stem of pri-miR319, which includes a terminal loop, is important for sequential cleavage for miR319 synthesis, but the lower stem section of pri-miR319 is superfluous (Bologna et al., 2009). Thus, the structural determinants that affect miRNA regulation differ based on the miRNA and miR159a has not yet been formally addressed. Thus, we further investigate the regulation of the nested structure with the minimum sequence length of the pri-miR159a fold back (if the miR159a.1 part is the key sequence) for accurate processing of miR159a, we further artificially designed six symmetrical constructs (**Figure 4**) by shortening the length of nucleotides ranging from 154 to 104 by mixing, replacing, inverting, and deleting the miR159a duplex region and designated them as (I) *mir159a.12-mix*, in which the miR159a.1 and miR159a.2-duplex regions were combined and miR159a.3 was deleted; (II) *mir159a.13-mix*, in which the miR159a.1 and miR159a.3-duplex regions were combined and the miR159a.2 duplex was deleted; (III) *mir159a.21-mix*, in which the miR159a.1 and miR159a.2-duplex regions were exchanged and miR159a.3 was deleted; (IV) *mir159a.23-mix*, in which the miR159a.1 duplex region was deleted only; (V) *mir159a.1-solo*, in which only the miR159a.1-duplex with a stem part was combined with a terminal loop; (VI) *mir159a.2-solo*, in which the only miR159a.2-duplex region was directly combined with the terminal loop region instead of the stem.

Complementation Analysis in the Concise Distal Fold Back for Accurate Processing of Nested pri-miR159a Structures

Similarly, in the second level of the nested structure, we shortened the sequence length by deleting the sibling mature miRNA duplex region, and we named them the concise distal pri-miR159a groups (e.g., *mir159a.13-mix*, *mir159a.23-mix*; **Figure 4**). These six miR159a constructs were individually transformed into *mir159ab,* and the phenotypes of multiple primary transformants were scored. As all 48 *mir159a.12-mix* T1 plants were fully complemented with a large petiole, their rosette leaf margins were slightly undulated compared to those

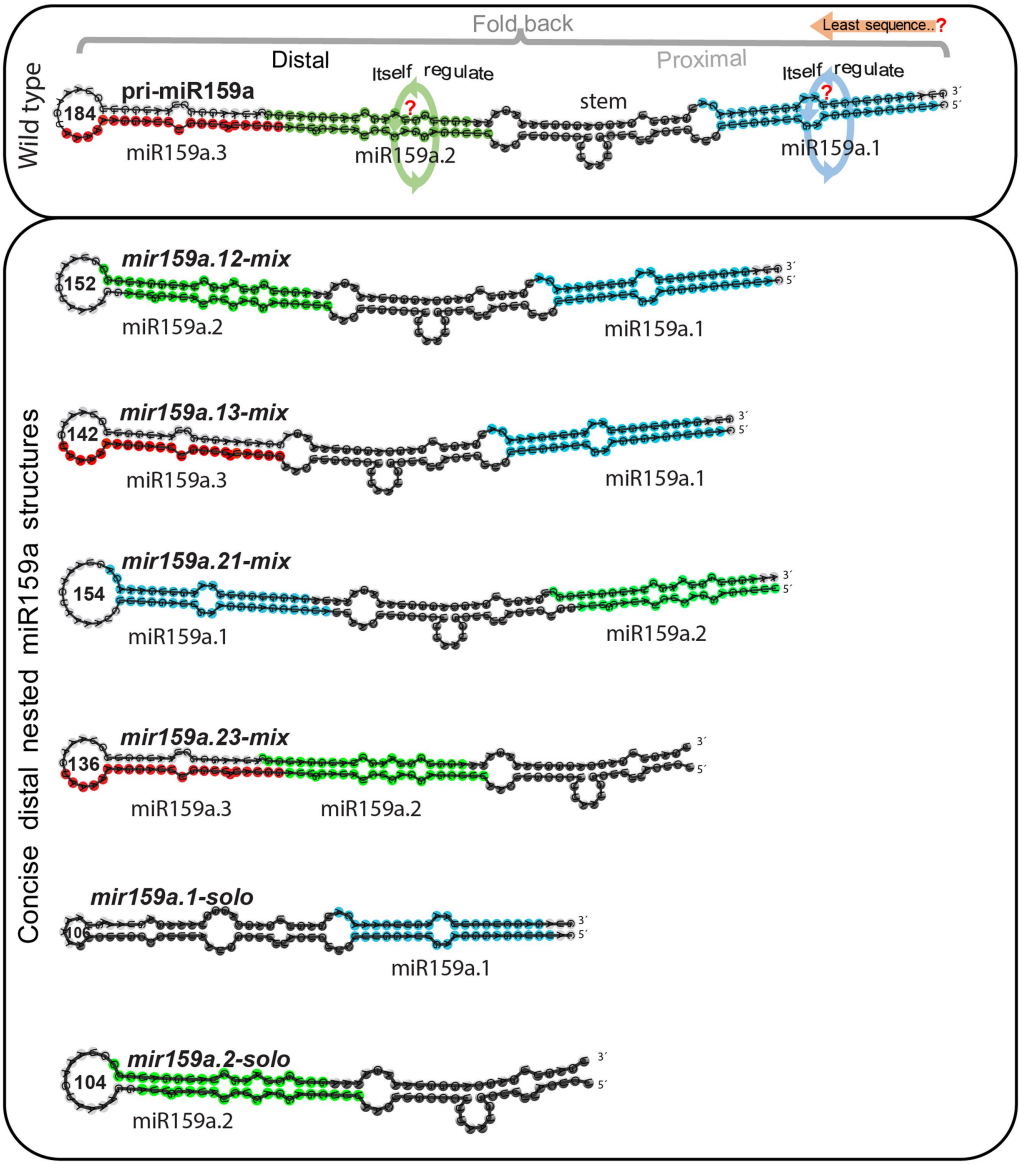


FIGURE 4 | Least sequence required for accurate processing of nested pri-miR159a structures. Schematic secondary structural view for pri-miR159a (upper box) set with comparison to different artificially designed variants containing least sequence (lower box) for complementation test in the concise distal region. Blue, green, red, and black region on miRNA secondary structure indicates, miR159a.1, miR159a.2, miR159a.3, and core stem region, respectively. The orange arrow indicates the minimum sequence requirement for nested miR159a structure regulation. While the green and blue circle with arrow indicates itself regulation of corresponding miRNAs (upper box). Each nested variant is named according to the combination of miRNA duplex region.

of the wild type (**Figures 5A–C**). Similarly, all 36 *mir159a.13-mix* primary transformants appeared like the wild type, but their leaves were longer than those of the wild type with little spiny (with sharp stiff points) rosette leaves (**Figures 5A–C**), suggesting that individual absence of the core stem and miR159a.2 does not prevent silencing alone. In contrast, all 16 and 42 primary transformants appeared mild from *mir159ab* (**Figures 5A–C**), indicating that the introduction of miR159a.2 in place of miR159a.1 and keeping the position of miR159a.2 in the secondary structure can prevent complementation of the *mir159ab* phenotype and act as a measure of silencing. Similarly, *mir159a.1-solo* and *mir159a.2-solo* analysis indicated that all 60 and 17 primary transformants did not rescue the phenotype of the *mir159ab* mutant (**Figures 5A–C**), indicating that the miRNA structural position has a potential role in silencing efficacy. The rosette diameter, lamina length, lamina width, and leaf area were also significantly restored to the wild-type values in *mir159a.12-mix* and *mir159a.13-mix* transgenic plants but not others (**Figures 5D,E**).

To investigate whether miRNA abundances are affected by structural determinants that are important for miR159a

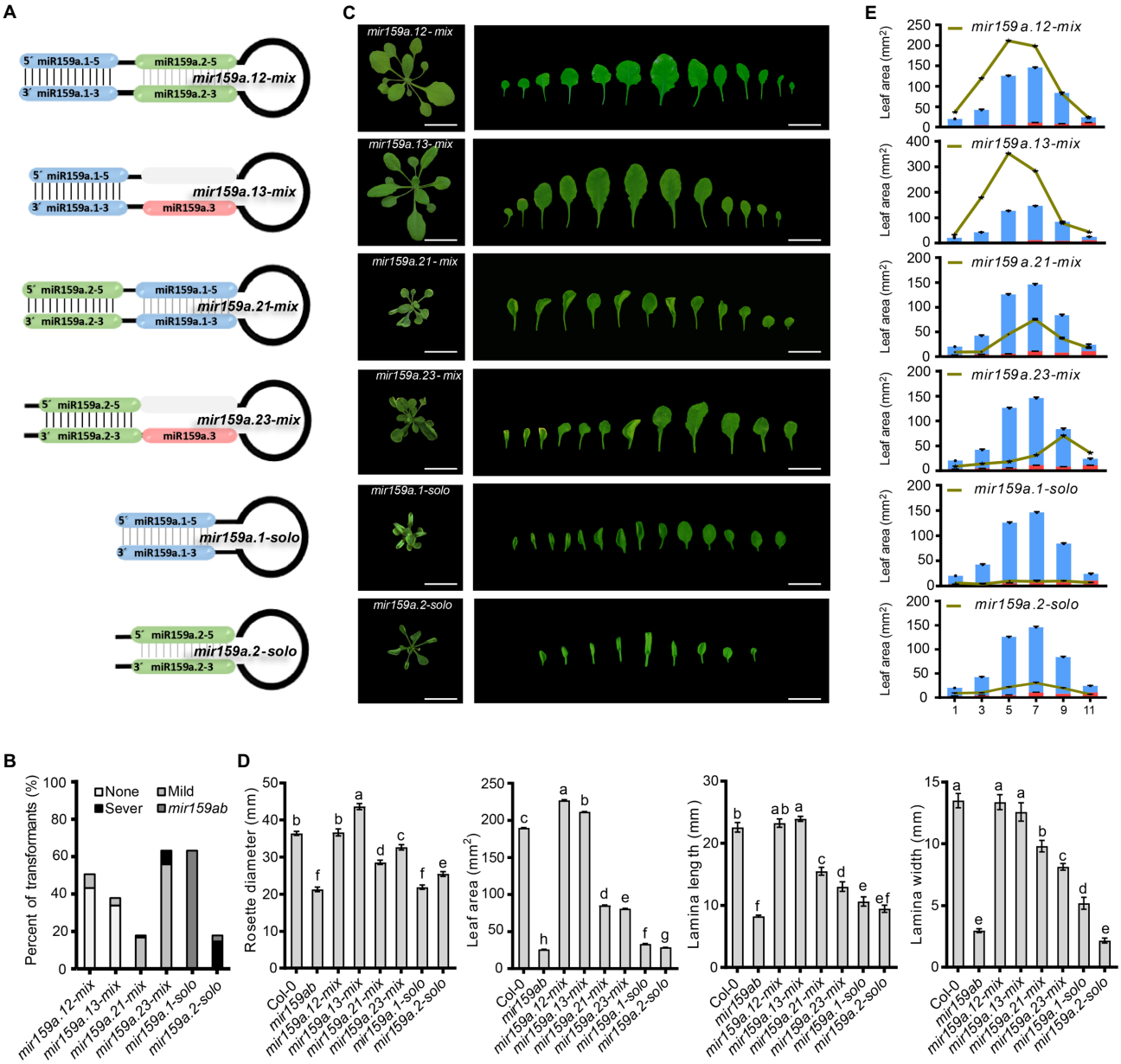


FIGURE 5 | Complementation assay in the concise distal fold back of nested pri-miR159a structure. **(A)** Schematic showing nested structure complementation in the concise distal fold back of pri-miR159a-driven transgenic *Arabidopsis*. **(B)** Percentage of primary transformants showing no, mild, and severe leaf curl phenotypes. **(C)** Phenotypes of 22-day-old transgenic plants. Scale bar: 1 cm. **(D)** The size of a rosette, lamina length, lamina width, and leaf area of plants were evaluated. For measurement, the fourth true leaf of 28-day-old plants was collected. Data are presented as the mean ± SD (Standard deviation; $n > 10$) and statistically distinct genotypes were determined by one-way ANOVA with a *post-hoc* least significant difference (LSD) multiple comparisons within each group ($p < 0.05$, marked with different characters). **(E)** Leaf area of (1st, 3rd, 5th, 7th, 9th, and 11th) plants was evaluated. For measurement, 28-day-old plants were collected. Data are presented as the mean ± SD (Standard deviation; $n > 5$).

processing in the nested concise fold, miRNA assays were performed to estimate sibling mature miR159 levels. Similar to the extended fold back, we also obtained the differential expression profiles of mature sibling miRNAs (**Figures 6A,B**). The same contradictory results showed that although the phenotype was rescued in *mir159a.12-mix* and *mir159a.13-mix* transgenic plants, the expression level of miR159a.1 was not increased, and the transcript levels of *MYB33*/*MYB65* and *CP1* were reduced compared to that of *mir159ab*. In contrast, miR159a.1–5 expression was higher in only *mir159a.1-solo*, but the phenotype was maintained, and the transcript levels of *MYB33*/*MYB65* and *CP1* were still high. These results suggested that there existed another way that self-supported the expression of miR159a.1 and was related to the structure

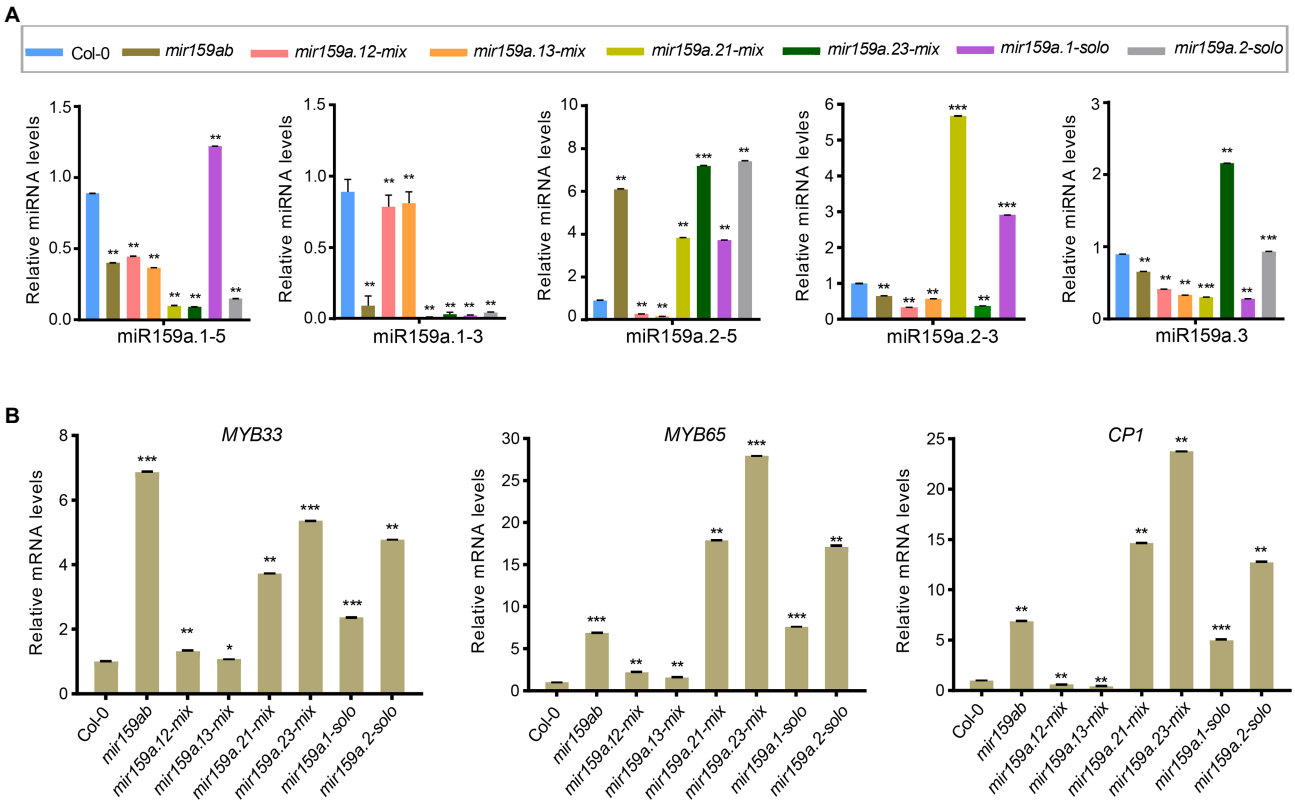


FIGURE 6 | Expression analysis of miR159a sibling's miRNA and MYB genes in the concise distal nested transgenic plants. **(A)** The miRNA levels of miR159a siblings in the rosettes of *mir159ab* plants complemented by the nested miR159a variants in comparison with wild type and *mir159ab*. All miR159a siblings and mature miR159a levels were normalized to *U-6* and the relative expression in the wild type was set as 1. Measurements are the average of three technical replicates. Error bars represent the SEM (Standard error mean). Asterisks indicate statistically significant differences at $p < 0.05$ (*) and $p < 0.01$ (**) by Student's *t*-test. **(B)** The mRNA levels of *MYB33*, *MYB65*, and *CP1* were examined in Col-0, *mir159ab* and nested miR159a variants and were normalized to *CYCLOPHILIN*. The relative expression in the wild type was set as 1. Measurements are the average of three technical replicates. Error bars represent the SEM (Standard error mean). Asterisks indicate statistically significant differences at $p < 0.05$ (*) and $p < 0.01$ (**) by Student's *t*-test. *** mean $p < 0.001$.

of the miR159 precursor to regulate the target mRNA (**Figures 6A,B**).

DISCUSSION

In plants, many miRNA-target relationships are ancient, and they appear to play fundamental roles in plant growth and development. Despite extensive analyses, there has been little investigation into the properties of structural determinants that govern their efficacy. Here, taking advantage of the miR159-MYB33/MYB65 module as a model system, we examined the new nested miR159 structure properties that control the efficacy of silencing by a highly conserved plant miRNA.

A previous study reported that RNA secondary structures are the major determinant of the silencing efficacy of miR159 in Arabidopsis and contribute to the narrow functional specificity of miR159 (Allen et al., 2007; Li et al., 2014; Zheng et al., 2017). To further narrow down this miR159 functional specificity, we functionally analysed the effect of nested miR159a secondary structures to identify structural determinants important for miR159 processing. Here, we introduced a series of nested structure duplex precursor mutations that either disrupted base pairing or closed unpaired bases in the foldback to identify structural features important for miRNA regulation.

In our study, we found that *mir159a.1-rep* and *mir159a.123-mix* from extended proximal parts (**Figure 2**) and *mir159a.12-mix* and *mir159a.13-mix* from concise distal parts (**Figure 5**) have a miR159a.1 duplex structure at the tail end of pri-miR159a (**Figure 7**) and rescued the phenotype with little differences in morphology. Additionally, the expression level of miR159a.1–3 was increased compared to that of *mir159ab*, whilethe transcript levels of *MYB33/MYB65* were almost similar/little higher compared to wild type Col-0. These results suggested that the miR159a.1 duplex present at the tail end region may result in an equal function in the regulation of plant development. However, we transformed the miR159a.1 duplex only from the concise distal part (*mir159a.1-solo*) and observed that the primary transformants did not show a rescued phenotype and that the majority showed severe morphology, that further suggests that a specific sequence length is required to work properly It has been reported that plants possess a wider range in the length

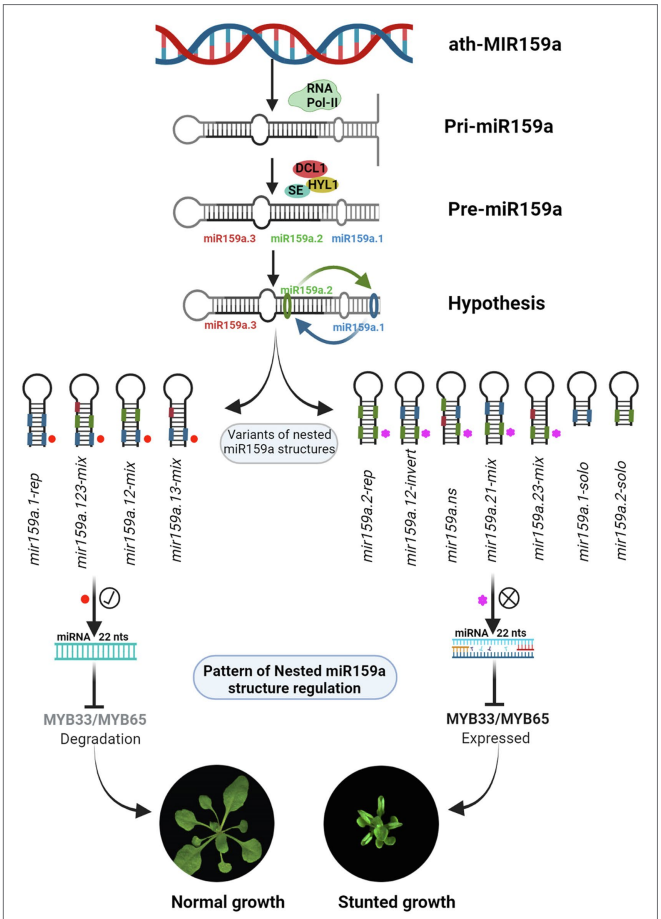


FIGURE 7 | The schematic representation of nested miR159a structure regulation in *Arabidopsis thaliana*.

of pri-miRNA than do animals, which indicates that the long stem region is important for miRNA cleavage (Bologna et al., 2013a), thus supported our results. In plants, the miRNA/miRNA* duplex is generated from two rounds of cleavage of the DCL1-HYL1-SE complex, and the first cleavage reaction at the lower-stem region is more important for the generation of the special duplex. In our study, the appropriate miR159a.1–3 was only expressed when the miR159a.1 duplex at the tail end of the pri-miR159a included the *mir159a.1-rep*, *mir159a.123-mix*, *mir159a.12-mix* or *mir159a.13-mix*, but the *mir159a.12-invert* constructs failed to rescue the phenotype of the mutants, which is consistent with the importance of the flanking sequence of the lower stem for the first cut of the DCL1-HYL1-SE complex (Bologna et al., 2013a). Furthermore, the results suggested that the upper stem is also necessary for the second cleavage reaction; nevertheless, the reaction was only dependent on the stem length rather than the specific sequence.

In contrast, the *mir159a.2-rep* from the extended proximal part (**Figure 2**), *mir159a.21-mix*, and *mir159a.23-mix* from the concise distal part (**Figure 5**) showed a miR159a.2 duplex structure at the tail end of the pri-miR159a fold back, and all the primary transformants did not rescue the phenotype and showed the mild phenotype with little differences in morphology (**Figure 7**). These results suggest that when a duplex nested structure is present on the tail end, part of the pri-miR159a may have a possible dominant function, but after a certain length of the sequence, it may not work properly. Finally, to confirm the effect of the miR159a secondary structure role in processing determinants, a *mir159a.ns* construct was designed with a disrupted miRNA secondary structure, and we observed that all the primary transformants did not rescue the phenotype and showed a severe phenotype and male sterility characteristics, suggests that an asymmetric duplex differed in unpaired nucleotides with protruding base moieties might alters the RISC programming (**Figure 5**). It has been reported that the AGO1-RISC activates the machinery involved in siRNA synthesis, and an asymmetric miRNA duplex changes the conformation of AGO1 (Manavella et al., 2012), which further support our result of nested duplex structure regulation. Furthermore, we found that the expression level of miR159a.2–3/2–5 was increased and that miR159a.1–3 was absent in transgenic plants, which suggested that miR159a.1 may play a negative role in regulating the expression of miR159a.2. Although the higher expressed miR159a.2 could not rescue the phenotype of the mutants, most of the transgenic lines showed a mild phenotype and the transcript levels of MYB33/MYB65 were significantly higher compared to wild type Col-0 indicating that miR159a.2 may function in some developmental process. It will be a challenge to determine the role of miR159a.2 in further studies. It is well known that pre-miR159 is processed through the non-conical pathway, and their biogenesis starts from loop to base, while in contrast, pri-miR172a processes from the base to the loop of the fold-back structure (Bologna et al., 2013b). Therefore, it is likely that two processing pathways for evolutionarily conserved miRNAs exist in plants. Similarly, these duplex nested structures may have more possible processing pathways, but further investigation is needed to confirm these results.

Overall, our results revealed the miRNA abundances in the nested MIRNA transformants with severe phenotypic defects were higher than those of miR159a in wild-type plants, and wild-type plants had approximately four-fold higher miR159 levels than the miR159a mutant in which *MYB33/65* was fully suppressed. This suggests that the silencing effectiveness of miR159a could be an order of magnitude greater than that of all of the other nested miRNAs studied. Furthermore, the continuously higher expression of the miR159a.2 duplex suggests that miR159a.2 is functional in *Arabidopsis* and that its accumulation is completely different from that of miR159a.1, implying that they may have regulatory roles that are independent of one another. This arrangement is conserved across plant populations, with some accumulating miR159.2 in visible quantities, inferring those similar processes could be at work in other plants.

CONCLUSION

In brief, these findings provide a clue to help decode the information embedded in the sequence of the pri-miRNA

duplex region in response to nested structure regulation of miRNAs.

DATA AVAILABILITY STATEMENT

The original contributions presented in the study are included in the article/**Supplementary Material**; further inquiries can be directed to the corresponding author.

AUTHOR CONTRIBUTIONS

ZT designed the experiments and managed the project. MI, TL, ZW, MW, SL, XG, AW, and SFL performed gene cloning and functional analysis. MI, MZ, and ZT wrote the manuscript. All authors contributed to the article and approved the submitted version.

FUNDING

This work was supported by grants from the National Key Research and Development Program of China (2021YFF1000101) and the International Partnership Program of Chinese Academy of Sciences (153E11KYSB20190045).

ACKNOWLEDGMENTS

We thank Anthony A. Millar (Australian National University, Australia) for generously providing the seeds of the *mir159ab* mutant.

SUPPLEMENTARY MATERIAL

The Supplementary Material for this article can be found online at: https://www.frontiersin.org/articles/10.3389/fpls.2022.905264/full#supplementary-material

REFERENCES

Addo-Quaye, C., Eshoo, T. W., Bartel, D. P., and Axtell, M. J. (2008). Endogenous siRNA and miRNA targets identified by sequencing of the *Arabidopsis* degradome. *Curr. Biol.* 18, 758–762. doi: 10.1016/j.cub.2008.04.042

Allen, R. S., Li, J., Alonso-Peral, M. M., White, R. G., Gubler, F., and Millar, A. A. (2010). MicroR159 regulation of most conserved targets in *Arabidopsis* has negligible phenotypic effects. *Silence* 1:18. doi: 10.1186/1758-907X-1-18

Allen, R. S., Li, J., Stahle, M. I., Dubroué, A., Gubler, F., and Millar, A. A. (2007). Genetic analysis reveals functional redundancy and the major target genes of the Arabidopsis miR159 family. *Proc. Natl. Acad. Sci. USA* 104, 16371–16376. doi: 10.1073/pnas.0707653104

Allen, R. S., Nakasugi, K., Doran, R. L., Millar, A. A., and Waterhouse, P. M. (2013). Facile mutant identification *via* a single parental backcross method and application of whole genome sequencing based mapping pipelines. *Front. Plant Sci.* 4:362. doi: 10.3389/fpls.2013.00362

Alonso-Peral, M. M., Sun, C., and Millar, A. A. (2012). MicroRNA159 can act as a switch or tuning microRNA independently of its abundance in Arabidopsis. *PLoS One* 7:e34751. doi: 10.1371/journal.pone.0034751

Bartel, D. P. (2004). MicroRNAs: genomics, biogenesis, mechanism, and function. *Cell* 116, 281–297. doi: 10.1016/S0092-8674(04)00045-5

Bologna, N. G., Mateos, J. L., Bresso, E. G., and Palatnik, J. F. (2009). A loop-to-base processing mechanism underlies the biogenesis of plant microRNAs miR319 and miR159. *EMBO J.* 28, 3646–3656. doi: 10.1038/emboj.2009.292

Bologna, N. G., Schapire, A. L., and Palatnik, J. F. (2013a). Processing of plant microRNA precursors. *Brief. Funct. Genomics* 12, 37–45. doi: 10.1093/bfgp/els050

Bologna, N. G., Schapire, A. L., Zhai, J., Chorostecki, U., Boisbouvier, J., Meyers, B. C., et al. (2013b). Multiple RNA recognition patterns during microRNA biogenesis in plants. *Genome Res.* 23, 1675–1689. doi: 10.1101/gr.153387.112

Chen, X. (2012). Small RNAs in development–insights from plants. *Curr. Opin. Genet. Dev.* 22, 361–367. doi: 10.1016/j.gde.2012.04.004

Chiang, H. R., Schoenfeld, L. W., Ruby, J. G., Auyeung, V. C., Spies, N., Baek, D., et al. (2010). Mammalian microRNAs: experimental evaluation of novel and previously annotated genes. *Genes Dev.* 24, 992–1009. doi: 10.1101/gad.1884710

Chiou, T.-J., Aung, K., Lin, S.-I., Wu, C.-C., Chiang, S.-F., and Su, C.-L. (2006). Regulation of phosphate homeostasis by microRNA in Arabidopsis. *Plant Cell* 18, 412–421. doi: 10.1105/tpc.105.038943

Contreras-Cubas, C., Rabanal, F. A., Arenas-Huertero, C., Ortiz, M. A., Covarrubias, A. A., and Reyes, J. L. (2012). The *Phaseolus vulgaris* miR159a precursor encodes a second differentially expressed microRNA. *Plant Mol. Biol.* 80, 103–115. doi: 10.1007/s11103-011-9847-0

Cuperus, J. T., Montgomery, T. A., Fahlgren, N., Burke, R. T., Townsend, T., Sullivan, C. M., et al. (2010). Identification of MIR390a precursor processing-defective mutants in Arabidopsis by direct genome sequencing. *Proc. Natl. Acad. Sci. U. S. A.* 107, 466–471. doi: 10.1073/pnas.0913203107

Curtis, M. D., and Grossniklaus, U. (2003). A gateway cloning vector set for high-throughput functional analysis of genes in planta. *Plant Physiol.* 133, 462–469. doi: 10.1104/pp.103.027979

Fahlgren, N., Howell, M. D., Kasschau, K. D., Chapman, E. J., Sullivan, C. M., Cumbie, J. S., et al. (2007). High-throughput sequencing of Arabidopsis microRNAs: evidence for frequent birth and death of MIRNA genes. *PLoS One* 2:e219. doi: 10.1371/journal.pone.0000219

Griffiths-Jones, S., Saini, H. K., Van Dongen, S., and Enright, A. J. (2007). miRBase: tools for microRNA genomics. *Nucleic Acids Res.* 36, D154–D158. doi: 10.1093/nar/gkm952

Hellens, R., Mullineaux, P., and Klee, H. (2000). Technical focus: a guide to Agrobacterium binary Ti vectors. *Trends Plant Sci.* 5, 446–451. doi: 10.1016/S1360-1385(00)01740-4

Jones-Rhoades, M. J., Bartel, D. P., and Bartel, B. (2006). MicroRNAs and their regulatory roles in plants. *Annu. Rev. Plant Biol.* 57, 19–53. doi: 10.1146/

Kim, V. N. (2005). MicroRNA biogenesis: coordinated cropping and dicing. *Nat. Rev. Mol. Cell Biol.* 6, 376–385.

Li, Y., Li, C., Ding, G., and Jin, Y. (2011). Evolution of MIR159/319 microRNA genes and their post-transcriptional regulatory link to siRNA pathways. *BMC Evol. Biol.* 11, 1–18. doi: 10.1186/1471-2148-11-122

Li, J., Reichel, M., and Millar, A. A. (2014). Determinants beyond both complementarity and cleavage govern microR159 efficacy in Arabidopsis. *PLoS Genet.* 10:e1004232. doi: 10.1371/journal.pgen.1004232

Liu, T., Fang, C., Ma, Y., Shen, Y., Li, C., Li, Q., et al. (2016). Global investigation of the co-evolution of MIRNA genes and micro RNA targets during soybean domestication. *Plant J.* 85, 396–409. doi: 10.1111/tpj.13113

Liu, Q., Wang, F., and Axtell, M. J. (2014). Analysis of complementarity requirements for plant microRNA targeting using a *Nicotiana benthamiana* quantitative transient assay. *Plant Cell* 26, 741–753. doi: 10.1105/tpc.113.120972

Mallory, A. C., Reinhart, B. J., Jones-Rhoades, M. W., Tang, G., Zamore, P. D., Barton, M. K., et al. (2004). MicroRNA control of PHABULOSA in leaf development: importance of pairing to the microRNA 5′ region. *EMBO J.* 23, 3356–3364. doi: 10.1038/sj.emboj.7600340

Manavella, P. A., Koenig, D., and Weigel, D. (2012). Plant secondary siRNA production determined by microRNA-duplex structure. *Proc. Natl. Acad. Sci. U. S. A.* 109, 2461–2466. doi: 10.1073/pnas.1200169109

Mateos, J. L., Bologna, N. G., Chorostecki, U., and Palatnik, J. F. (2010). Identification of microRNA processing determinants by random mutagenesis of Arabidopsis MIR172a precursor. *Curr. Biol.* 20, 49–54. doi: 10.1016/j.cub.2009.10.072

Palatnik, J. F., Allen, E., Wu, X., Schommer, C., Schwab, R., Carrington, J. C., et al. (2003). Control of leaf morphogenesis by microRNAs. *Nature* 425, 257–263. doi: 10.1038/nature01958

Pegler, J. L., Grof, C. P., and Eamens, A. L. (2019). The plant microRNA pathway: The production and action stages. *Plant MicroRNAs*, 15–39. doi: 10.1007/978-1-4939-9042-9_2

Rhoades, M. W., Reinhart, B. J., Lim, L. P., Burge, C. B., Bartel, B., and Bartel, D. P. (2002). Prediction of plant microRNA targets. *Cell* 110, 513–520. doi: 10.1016/S0092-8674(02)00863-2

Schwab, R., Palatnik, J. F., Riester, M., Schommer, C., Schmid, M., and Weigel, D. (2005). Specific effects of microRNAs on the plant transcriptome. *Dev. Cell* 8, 517–527. doi: 10.1016/j.devcel.2005.01.018

Seitz, H. (2009). Redefining microRNA targets. *Curr. Biol.* 19, 870–873. doi: 10.1016/j.cub.2009.03.059

Song, L., Axtell, M. J., and Fedoroff, N. V. (2010). RNA secondary structural determinants of miRNA precursor processing in *Arabidopsis*. *Curr. Biol.* 20, 37–41. doi: 10.1016/j.cub.2009.10.076

Starega-Roslan, J., Krol, J., Koscianska, E., Kozlowski, P., Szlachcic, W. J., Sobczak, K., et al. (2011). Structural basis of microRNA length variety. *Nucleic Acids Res.* 39, 257–268. doi: 10.1093/nar/gkq727

Steven, J. C., and Andrew, F. B. (1998). Floral dip: a simplified method for Agrobacterium-mediated transformation of *Arabidopsis thaliana*. *Plant J.* 16, 735–743. doi: 10.1046/j.1365-313x.1998.00343.x

Sunkar, R., Chinnusamy, V., Zhu, J., and Zhu, J.-K. (2007). Small RNAs as big players in plant abiotic stress responses and nutrient deprivation. *Trends Plant Sci.* 12, 301–309. doi: 10.1016/j.tplants.2007.05.001

Vella, M. C., Choi, E.-Y., Lin, S.-Y., Reinert, K., and Slack, F. J. (2004). The *C. elegans* microRNA let-7 binds to imperfect let-7 complementary sites from the lin-41 3′ UTR. *Genes Dev.* 18, 132–137. doi: 10.1101/gad.1165404

Werner, S., Wollmann, H., Schneeberger, K., and Weigel, D. (2010). Structure determinants for accurate processing of miR172a in *Arabidopsis thaliana*. *Curr. Biol.* 20, 42–48. doi: 10.1016/j.cub.2009.10.073

Winter, J., Jung, S., Keller, S., Gregory, R. I., and Diederichs, S. (2009). Many roads to maturity: microRNA biogenesis pathways and their regulation. *Nat. Cell Biol.* 11, 228–234. doi: 10.1038/ncb0309-228

Zhang, W., Gao, S., Zhou, X., Xia, J., Chellappan, P., Zhou, X., et al. (2010). Multiple distinct small RNAs originate from the same microRNA precursors. *Genome Biol.* 11, R81–R18. doi: 10.1186/gb-2010-11-8-r81

Zheng, Z., Reichel, M., Deveson, I., Wong, G., Li, J., and Millar, A. A. (2017). Target RNA secondary structure is a major determinant of miR159 efficacy. *Plant Physiol.* 174, 1764–1778. doi: 10.1104/pp.16.01898

Conflict of Interest: The authors declare that the research was conducted in the absence of any commercial or financial relationships that could be construed as a potential conflict of interest.

Publisher's Note: All claims expressed in this article are solely those of the authors and do not necessarily represent those of their affiliated organizations, or those of the publisher, the editors and the reviewers. Any product that may be evaluated in this article, or claim that may be made by its manufacturer, is not guaranteed or endorsed by the publisher.

Copyright © 2022 Imran, Liu, Wang, Wang, Liu, Gao, Wang, Liu, Tian and Zhang. This is an open-access article distributed under the terms of the Creative Commons Attribution License (CC BY). The use, distribution or reproduction in other forums is permitted, provided the original author(s) and the copyright owner(s) are credited and that the original publication in this journal is cited, in accordance with accepted academic practice. No use, distribution or reproduction is permitted which does not comply with these terms.

frontiers | Frontiers in Plant Science

ORIGINAL RESEARCH
published: 06 June 2022
doi: 10.3389/fpls.2022.893495

Identification of Reference Genes for Reverse Transcription-Quantitative PCR Analysis of Ginger Under Abiotic Stress and for Postharvest Biology Studies

Gang Li[1†], Jiawei Ma[1†], Junliang Yin[1], Fengling Guo[2], Keyong Xi[1], Peihua Yang[1], Xiaodong Cai[1], Qie Jia[1], Lu Li[3], Yiqing Liu[1] and Yongxing Zhu[1*]*

[1] College of Horticulture and Gardening, Spice Crops Research Institute, Yangtze University, Jingzhou, China, [2] Institute of Economic Crops, Hubei Academy of Agricultural Sciences, Wuhan, China, [3] School of Environmental Science and Engineering, Suzhou University of Science and Technology, Suzhou, China

OPEN ACCESS

Edited by:
Peng Zhang,
Center for Excellence in Molecular Plant Sciences (CAS), China

Reviewed by:
Suresh Kumar,
Indian Agricultural Research Institute (ICAR), India
Youxiong Que,
Fujian Agriculture and Forestry University, China

***Correspondence:**
Yongxing Zhu
xbnlzyx@163.com
Yiqing Liu
Liung906@163.com

[†] These authors have contributed equally to this work

Specialty section:
This article was submitted to Plant Biotechnology, a section of the journal Frontiers in Plant Science

Received: *10 March 2022*
Accepted: *27 April 2022*
Published: *06 June 2022*

Citation:
Li G, Ma J, Yin J, Guo F, Xi K, Yang P, Cai X, Jia Q, Li L, Liu Y and Zhu Y (2022) Identification of Reference Genes for Reverse Transcription-Quantitative PCR Analysis of Ginger Under Abiotic Stress and for Postharvest Biology Studies. Front. Plant Sci. 13:893495. doi: 10.3389/fpls.2022.893495

Gene expression analysis largely improves our understanding of the molecular basis underpinning various plant biological processes. Stable reference genes play a foundational role during the normalization of gene expression levels. However, until now, there have been few reference genes suitable for ginger reverse transcription-quantitative PCR (RT-qPCR) research. In this study, 29 candidate reference genes with stable expression patterns across multiple ginger tissues and 13 commonly used reference genes were selected to design RT-qPCR primers. After amplification specificity validation, 32 candidates were selected and further evaluated by RT-qPCR using samples from various organs subjected to NaCl, drought, heat, waterlogging, and chilling stress. Four strategies, including delta-CT, BestKeeper, geNorm, and NormFinder, were used to rank the stability of reference genes, and the ranks produced by these four strategies were comprehensively evaluated by RefFinder to determine the final rank. Overall, the top three stability reference genes indicated by RefFinder were *RBP* > *ATPase* > *40S_S3*. Their expression pattern correlation analysis showed that the coefficients among each pair of *RBP*, *ATPase*, and *40S_S3* were larger than 0.96, revealing consistent and stable expression patterns under various treatments. Then, the expression of three *pathogenesis-related* (*PR*) genes and seven *MYB* genes in rhizomes during postharvest storage and subjected to pathogen infection was normalized by *RBP*, *ATPase*, *40S_S3*, *RBP* and *ATPase*, *ATPase* and *40S-S3*, and *RBP* and *40S-S3*. The results showed that *PR* and *MYB* genes were induced by postharvest deterioration and pathogen infection. The correlation coefficients of *RBP/ATPase*, *RBP/40S_S3*, *ATPase/40S_S3*, *RBP* and *ATPase/ATPase* and *40S-S3*, *RBP* and *ATPase/RBP* and *40S-S3*, and *ATPase* and *40S-S3/RBP* and *40S-S3* were 0.99, 0.96, 0.99, 0.99, 1.00, and 1.00, respectively, which confirmed the stability of these three reference genes in postharvest biology studies of ginger. In summary, this study identified appropriate reference genes for RT-qPCR in ginger and facilitated gene expression studies under biotic and abiotic stress conditions.

Keywords: ***Zingiber officinale*** **Roscoe, RT-qPCR, reference gene, internal control, RefFinder**

INTRODUCTION

Gene expression analysis is an important approach for improving our understanding of the molecular basis underpinning various plant biological processes (Zhu et al., 2019a). RT-qPCR is one of the most frequently used methods for studying gene expression patterns because of its higher sensitivity, accuracy, and reproducibility (Yin et al., 2021). However, due to differences in sample collection, total RNA extraction, mRNA reverse transcription, and PCR procedures, many RT-qPCR experiments are difficult to repeat (Bustin et al., 2009; Kozera and Rapacz, 2013). To eliminate the influence of these adverse factors, some stable expression genes, commonly called reference genes, are used as internal controls to normalize the expression of target genes, which is considered one of the most efficient approaches to correct biases in RT-qPCR studies (Mughal et al., 2018). Reference genes are applied to normalize or quantify gene expression in RT-qPCR analyses. Their expressions are generally expected to remain stable under various experimental treatments, during different growth stages, and in different organs. Therefore, they can be used to correct non-specific variations, such as differences in the quality of extracted RNA and the amount of extracted RNA, the efficiency of cDNA synthesis, and the overall transcriptional activity of the analyzed samples (Kumar, 2014).

Ginger (*Zingiber officinale* Roscoe) contains many bioactive constituents and has been widely used in food, as spices, as flavoring agents, and as medicine (Cheng et al., 2021). Therefore, it has been cultivated in many tropical and subtropical countries, where it has become one of the most economically significant vegetables in the Zingiberaceae family (Yin et al., 2020a). Due to ginger's economic importance, many studies have been conducted to determine the expression patterns of genes associated with growth and development, abiotic and biotic stress responses, and the quality and quantity of ginger (Peng et al., 2022). Genes, including *TUB2* and *ACT11*, have been used as the internal reference genes in RT-qPCR analysis (Li et al., 2020). Based on previous reports, Lv et al. (2020) selected 14 candidate reference genes and identified *28S* and *COX* as the most stable reference genes in ginger. These 14 candidate reference genes were orthologs of the most commonly used reference genes in other plants, such as a guar (Jaiswal et al., 2019). A suitable reference gene must be expressed steadily in different tissues across all developmental stages and under a wide variety of experimental conditions (Mughal et al., 2018; Yin et al., 2021). However, several reports demonstrate that these commonly used reference genes can lead to inadequate normalization of genes. They may not be expressed constitutively and stably in different tissues or under different conditions in all plant species (Hong et al., 2008; Reddy et al., 2016). Therefore, there is an essential need for system identification and validation of alternative reference genes in ginger to accurately normalize gene expression research. Furthermore, reference genes suitable for gene expression analysis of ginger during postharvest storage are still lacking, which largely constraints research on ginger postharvest biology.

Because of its high resolution, sensitivity, and vast dataset, high-throughput deep RNA-seq has been widely used to decipher molecular biological changes and regulations in plants exposed to a variety of treatments in various tissues (Zhu et al., 2019b; Yin et al., 2021). In recent years, sequence information and the corresponding expression profiling produced by RNA-seq have been employed to identify new reference genes in several plant species, such as grape (González-Agüero et al., 2013), alligator weed (Yin et al., 2021), soybean (Yim et al., 2015), and *Lycoris aurea* (Ma et al., 2016). Most recently, we reported a high-quality, chromosome-scale reference genome of the ginger cultivar "Zhugen," which laid the foundation for identifying appropriate RT-qPCR reference genes and can be used as an excellent resource for further research on ginger gene expression research (Li et al., 2021).

In this study, we used comprehensive expression profiling results from large-scale RNA-seq data to identify the most stably expressed genes from a variety of ginger tissues subjected to different treatments. Meanwhile, the expression levels of the selected genes under various treatments were further determined using RT-qPCR. Then, the expression stability of selected genes was first ranked by the four algorithms (geNorm, delta-CT, BestKeeper, and NormFinder) and finally ranked by RefFinder by comprehensively considering the ranks produced by the four algorithms. Moreover, the expression patterns of genes related to the postharvest storage of ginger, such as three *pathogenesis-related* (*PR*) genes and seven *MYB* genes, were analyzed as a case study to investigate the application of these newly developed reference genes in postharvest biology studies. This study lays the foundation for further gene expression analyses of ginger in future research.

MATERIALS AND METHODS

Ginger Growth and Treatment

A pot culture experiment was performed in the greenhouse of Yangtze University (Jingzhou, Hubei Province, China, 112.026207°E, 30.361273°N). Three *Zingiber officinale* cultivars "Shandongdajiang," "Yunnanluopingxiaohuangjiang," and "Fengtoujiang," which were collected from the North, Southwest, and Central China regions, were sown in 40 silica sand-filled pots (diameter: 20 cm, height: 25 cm). For greenhouse cultivation, the temperature was set to 28/25°C with a photoperiod of 14 h light/10 h dark. After 90 days of planting, healthy seedlings of uniform size (approximately 50 cm in height) were divided into five groups and subsequently subjected to different treatments: (a) water (control), (b) NaCl (2%, w/v), (c) drought (40% FC, field capacity), (d) waterlogging (the pots were submerged 1∼2 cm under the water surface), (e) chilling (10°C), and (f) heat stress (ginger seedlings were treated with 40°C/32°C day/night temperature in a growth chamber) (Yin et al., 2020b). For each treatment, at least 30 seedlings were used per test. After 5 days of treatment, the roots, rhizomes, and leaves were collected and immediately frozen in liquid nitrogen, followed by storage at a temperature of −80°C until further use.

RNA Isolation and cDNA Synthesis

Total RNA was isolated from samples using the TRIzol reagent (Invitrogen, Carlsbad, CA, United States). The concentration and purity of RNA were evaluated using the NanoDrop Spectrophotometer (NanoDrop Technologies, Wilmington, DE, United States), and their integrity and quality were also analyzed by performing 1.5% (w/v) agarose gel electrophoresis. The cDNA was synthesized using the RevertAid First Strand cDNA Synthesis Kit with oligo-dT and 1 μg of total RNA (Thermo Scientific, Waltham, MA, United States) in a PTC-200 Thermal Cycler (MJ Research Corp., Ltd., Waltham, MA, United States) (Zhu et al., 2020).

Selection Candidate Reference Genes

In our previous study, Illumina RNA-seq data (accession number PRJNA592215) of four samples collected from the red stem inner portion, green stem, young yellow rhizome, and red stem surface section with three biological replications were produced and used to profile the expression patterns of ginger genes. The Fragments per Kilobase per Million Reads (FPKM), mean values (MV), and standard deviation (SD) of the individual genes were calculated according to 12 data sets. In order to select the considerably high and stable expression candidates, genes with MV values greater than 50 were selected. Then, according to the SD, these selected genes were ranked from the least to the highest SD. Furthermore, based on the functional annotations, 29 candidates with known functions were selected from the top 500 genes. The gene sequences of 13 commonly used reference genes, including *PP2A2* (AT1G10430), *TUBA4* (AT1G50010), *LOS1* (AT1G56070), *UBC35* (AT1G78870), *SAM-Mtase* (AT2G32170), *ACT1* (AT2G37620), *ACT2* (AT3G18780), *TPL40B* (AT3G52590), *UBC10* (AT4G05320), *UBC9* (AT4G27960), *TUBB8* (AT5G23860), *Clathrin* (AT5G46630), and *EF1α* (AT5G60390), were collected and used as a query to perform BLASTn against ginger transcripts with *E*-value < 1e-10 (Vandesompele et al., 2002; Jain et al., 2006; Hong et al., 2008; Kozera and Rapacz, 2013). The best hits were manually extracted, and their expression profiles were also analyzed. The heatmap was illustrated using the R package "ggplot" with the command "pheatmap [log2 (data), color = col, cluster_cols = FALSE, cluster_rows = T)," and box plots were produced using the R function with the command "boxplot (log(data), col = 'green,' pars = list (pch = NA, ylab = 'Average $\log_2$(FPKM),' xlab = 'Gene')]" (Yin et al., 2021). To further evaluate the expression stability of the 29 selected genes, dot plots were drawn according to the reported method by Yin et al. (2021). Specifically, indicators including coefficient of maximum fold change (MFC, maximum FPKM value/minimum FPKM value) and variation (CV, SD of FPKM/average of FPKM) were calculated and used to produce the dot plot.

Designing and Specificity Confirmation of Reverse Transcription-Quantitative PCR Primers

Primer Premier 5.0 (PREMIER Biosoft International, Palo Alto, CA, United States) was used to design the gene-specific primers, and exon–exon fragments were specifically targeted while designing the RT-qPCR primers to avoid any possible mismatches and amplification of genomic DNA (Gou et al., 2020). To validate the specificity of primers, a reaction mixture with a total volume of 20 μL was used to perform PCR amplification in an MJ Research PTC-200 thermal cycler. The 20 μL reaction mixture contains 10 μL 2 × Taq Master Mix (Vazyme, Nanjing, China), 3–5 μL DNA template (400 mg L^{-1}), 1 μL each of forward and reverse primers (synthesized by GenScript, Shanghai, China), and 5 μL ddH_2O. The reaction program was set as follows: (1) denaturation at 94°C for 5 min; (2) then denaturation at 94°C for 30 s, annealing at 58°C for 30 s, and extensions at 72°C for 30 s, repeated for 35 cycles; (3) following a final extension at 72°C for 10 min (Yin et al., 2018). Then, 8 μL PCR amplification products were verified by electrophoresis on a 1.5% agarose gel and visualized using the Gel Doc XR system (Bio-Rad, Hercules, CA, United States).

Reverse Transcription-Quantitative PCR and Data Analysis

RNA samples from ginger cv. "Fengtoujiang" were used to evaluate reference gene stability. RT-qPCR was conducted using SYBR Green Master Mix (Vazyme, Nanjing, China) with the cDNA as a template on a CFX 96 Real-Time PCR system (Bio-Rad, Hercules, CA, United States). The volume of the reaction mixture was 20 μL, which contained 0.4 μL of each of the forward and reverse primers (10 μM), 2.0 μL of diluted cDNA, 10 μL of SYBR Green I Master, and the addition of PCR-grade water up to 20 μL. The RT-qPCR reaction program was set as follows: (1) denaturation at 95°C for 30 s; (2) then denaturation at 95°C for 10 s, annealing at 60°C for 30 s, repeated for 40 cycles; and (3) a melting curve protocol (65–95°C with fluorescence measured every 0.5°C). Three biological replications were adopted for each sample. For RT-qPCR results, RefFinder[1] was used to evaluate the stability of reference genes under various stresses (NaCl, drought, waterlogging, chilling, and heat) in ginger. Then, samples from cultivars "Shandongdajiang" and "Yunnanluopingxiaohuangjiang" were used to evaluate the stability of the top four stable reference genes. The pairs.panels function in the R package "psych" was used to perform the correlation analysis of the RT-qPCR results of the top four stable reference genes using three ginger cultivars. The standard curve was generated using a set of 10-fold dilutions of cDNA in a RT-qPCR assay according to the equation $E = [10^{-(1/\text{slope})} - 1] \times 100\%$. Then, based on the slope of the standard curve, the regression coefficient (R^2) and the RT-qPCR efficiency (E) of primers were calculated (Yin et al., 2021). While preparing and performing RT-qPCR, the Minimum Information for Publication of Quantitative Real-Time PCR Experiments (MIQE) guidelines were followed (Bustin et al., 2009).

Validation of Candidate References

In order to verify the stability of the top three stable reference genes, two sets of samples were prepared. Uniform sized-young ginger rhizomes (cv. "Shandongdajiang" and

[1]http://blooge.cn/RefFinder/

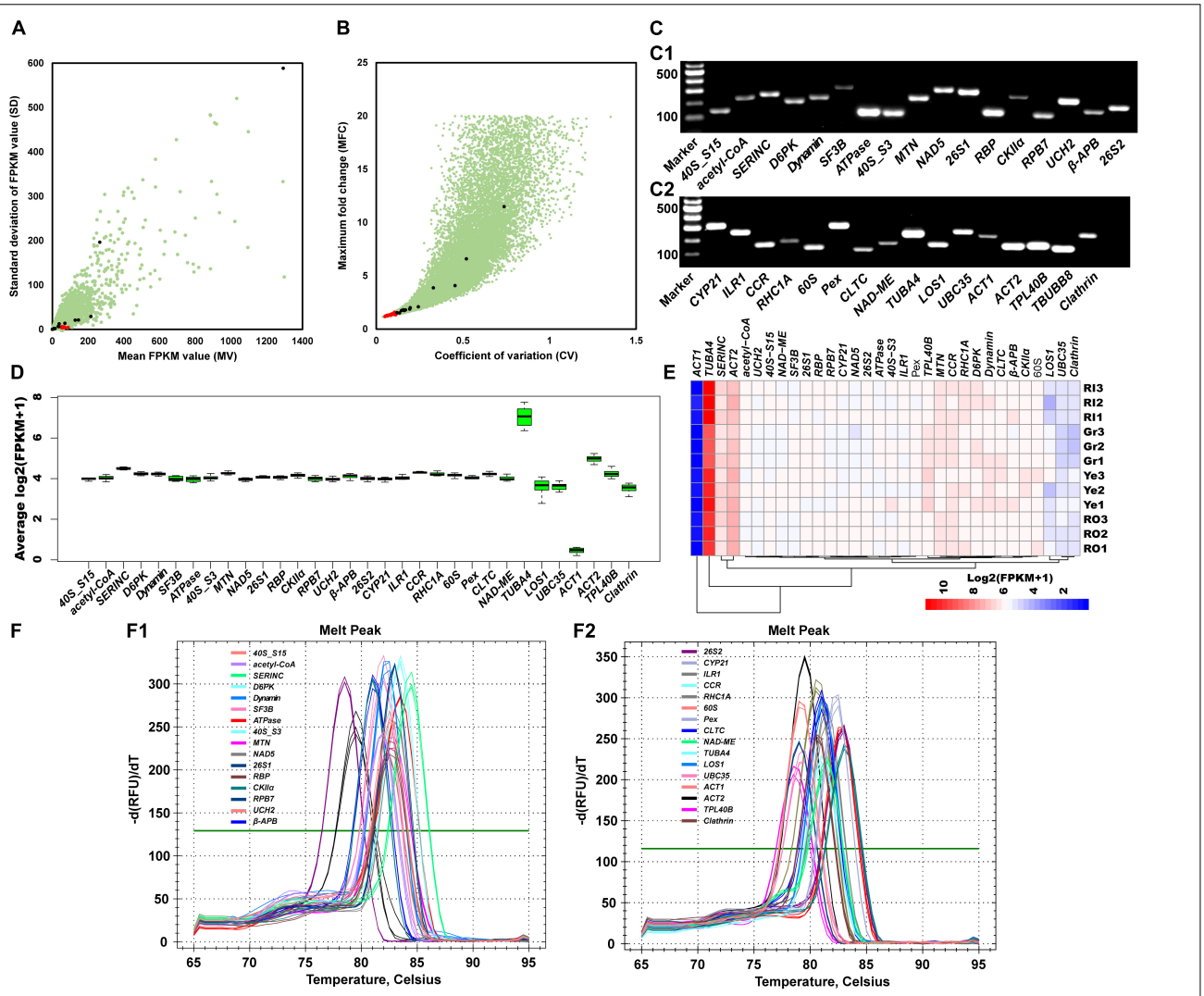


FIGURE 1 | Selection of candidate reference genes. **(A)** SD (standard deviation of FPKM value), MV (mean value of FPKM) values, and **(B)** MFC (maximum fold change) and CV (coefficient of variation) values are used to indicate the expression stability of 32 selected candidate reference genes. Red dots represent the 29 selected stable expression genes, black dots represent the 13 commonly used reference genes, and green dots represent the other genes. **(C)** Primers' specificity is confirmed by resolving PCR products on an agarose gel. Marker, Marker I. The other lanes belong to the PCR products of candidate reference genes. **(D)** Expression stability overview of 32 selected candidate genes. Box and whisker plot graphs show $\log_2$(FPKM + 1) values of each selected gene under different treatments in multiple tissues. Black boxes and lines represent the 25th and 75th percentiles and medians, respectively. Whisker caps represent the maximum and minimum values. **(E)** Gene expression levels under different conditions. RI, Gr, Ye, and RO represent ginger samples collected from the inner red stem part, the green stem, the young yellow rhizome, and the red stem surface part. **(F)** Melting peak and melting curve of 32 primers of corresponding candidates to confirm the specificity.

"Yunnanluopingxiaohuangjiang") with no visible injuries or vascular discolorations were selected for further analysis. For postharvest dehydration stress treatment, about 50 ginger rhizomes (cv. "Shandongdajiang") were held in a growth chamber with 22 ± 2°C and 65% relative humidity conditions. Ginger rhizome samples were collected after 0, 7, 14, 21, and 28 days of postharvest dehydration stress.

Fusarium solani strain was isolated from the surface of naturally decaying ginger rhizomes (cv. "Yunnanluopingxiaohuangjiang") and was cultured [potato dextrose agar (PDA)] at 28°C. A spore suspension (1×10^8 spores mL^{-1}) was prepared by washing 5-day-old sporulating cultures with sterile distilled water. For *F. solani* infection treatment, the different samples were treated as follows: ginger rhizomes were wounded with a sterilized borer (1.0 cm deep × 0.2 cm wide) at three points around the equator of each rhizome. Each wound was treated with 50 μL of spore suspension. The control rhizomes were wounded and treated with 50 μl sterile water. All treated rhizomes were incubated separately in a plastic box covered with preservative film at 28°C and 90 ± 5% relative humidity for 7 days. Rhizome tissues with a depth of 1.5 cm were collected at the cross area of healthy tissues and disease lesions using a sterilized cork borer. A sample annulus of 1.5–2.0 cm

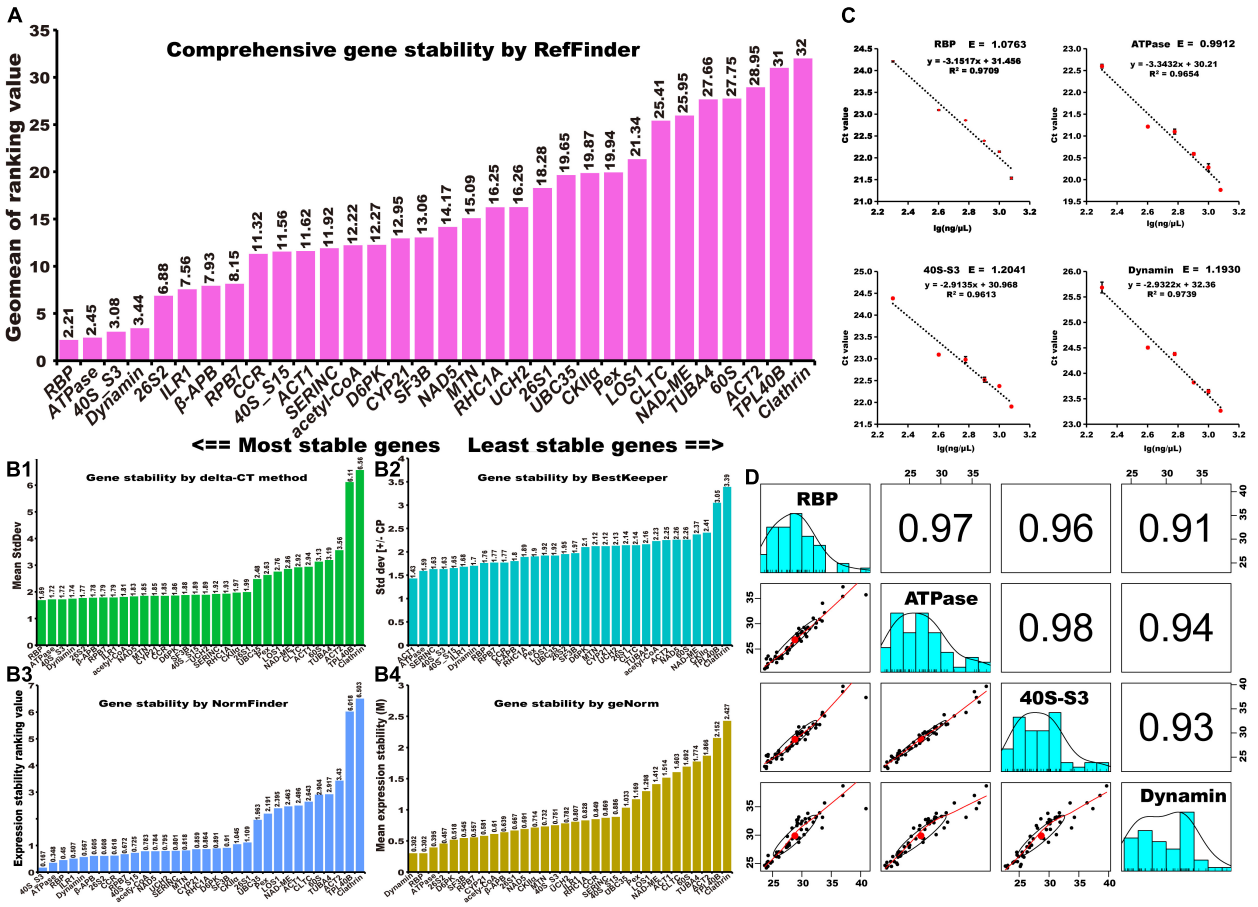


FIGURE 2 | Identification of stable reference genes. Stability rankings of candidate reference genes across samples using five calculation methods: **(A)** RefFinder, **(B1)** delta-CT, **(B2)** BestKeeper, **(B3)** NormFinder, and **(B4)** geNorm. **(C)** The PCR regression coefficient, R^2, and PCR amplification efficiency, E, of *RBP*, *ATPase*, *40S-S3*, and *Dynamin*. **(D)** The stability of *RBP*, *ATPase*, and *40S-S3* was pairwise compared by surveying their expression levels in multiple tissues of three ginger cultivars under five kinds of stress treatments.

around the wound was collected after 7 days of treatment. All samples were frozen in liquid nitrogen immediately and stored at −80°C. The relative expression of investigated genes was calculated with the $2^{-\Delta\Delta Cq}$ method (Pfaffl, 2001). For the quantification of double reference genes, ΔΔCq was calculated as [((Cqgene – Cqreference1)experiment – (Cqgene – Cqreference1)control)/2 + ((Cqgene – Cqreference2)experiment – (Cqgene – Cqreference2)control)/2 (Gou et al., 2020)].

RESULTS

Selection of Candidate Reference Genes

To select suitable candidate reference genes, a set of RNA-seq data was used to determine the expression levels of ginger genes. Gene expression levels were normalized to FPKM values. Then, the FPKM values were used to calculate the mean FPKM (MV) and standard deviation of the FPKM (SD) values. Genes were then ranked from the smallest to the largest according to SD, and 29 genes with MV greater than 50 were selected (**Figure 1A** and **Supplementary Table 1**). To estimate their expression stability, the maximum fold change of FPKM (MFC) and coefficient of variation (CV; SD of FPKM/average of FPKM) values were calculated. As shown in **Supplementary Table 1**, the MFC and CV values of these 29 selected candidates were less than 1.5 and 0.1, respectively (**Figure 1B** and **Supplementary Table 2**). Accordingly, the MV, SD, MFC, and CV values revealed that 29 candidate genes were suitable. Meanwhile, commonly used reference genes in *Arabidopsis* were used to perform BLAST to search for homolog genes in ginger, resulting in the identification of another 13 candidate reference genes (**Figure 1A** and **Supplementary Table 3**).

Then, 42 pairs of primers with a fragment size of PCR products between 100 and 301 bp were designed according to the sequences of the candidate reference genes (**Supplementary Table 4**). Their specificity was further checked by PCR amplification and 1.5% (w/v) agarose gel electrophoresis (**Figure 1C**). As a result, 10 pairs were filtered out due to low specificity (**Figure 1C**), and 32 pairs of primers (*40S_S15*, *acetyl-CoA*, *SERINC*, *D6PK*, *Dynamin*, *SF3B*, *ATPase*, *40S_S3*, *MTN*, *NAD5*, *26S1*, *RBP*, *CKIIα*, *RPB7*, *UCH2*, β-*APB*, *26S2*, *CYP21*,

TABLE 1 | Detailed primer information for *RBP*, *ATPase*, and *40S_S3*.

Primer_ID	Primer sequences (5′-3′)	Length (bp)	Tm (°C)	Amplicon length (bp)
RBP-F	CCTATGAAGCGTAGAAACACAAG	23	60	123
RBP-R	GGAAGGACAACATCCCAAATC	21		
ATPase-F	CGTGGGAGATGCTGGAG	17	60	119
ATPase-R	GGATGATGCCGACAATGAG	19		
40S_S3-F	GGACGGAGTGTTCTTTGC	18	60	113
40S_S3-R	GGATAATGATCTCGGTTCG	19		

ILR1, *CCR*, *RHC1A*, *60S*, *Pex*, *CLTC*, *NAD-ME*, *TUBA4*, *LOS1*, *UBC35*, *ACT1*, *ACT2*, *TPL40B*, and *Clathrin*) were retained for further stability validation. RNA-seq profiling data were further analyzed to illustrate the gene's expression stability. As shown in the boxplot (**Figure 1D**) and heatmap (**Figure 1E**), the expression levels of these 32 candidate genes were fairly stable and consistent under different treatments and among different organs. Candidates that were homologous to commonly used reference genes, such as *TUBA4*, *UBC35*, *ACT1*, and *ACT2*, were less stable than candidates selected based on MV and SD values (**Figure 1D**). Melting curve analysis showed that a single peak was observed in each pair of primers (**Figure 1F**). In summary, these results demonstrate that the selected candidate reference genes are stable and that the primers are specific for amplification.

Identification of Stable Reference Genes

Reference genes should be stably expressed in different periods, treatments, and organs (Mughal et al., 2018). To estimate the expression stability of 32 selected reference genes in ginger, their expression was evaluated using RT-qPCR with different cv. "Fengtoujiang" tissues (leaf, rhizomes, and roots) subjected to different treatments (drought, heat, NaCl, waterlogging, and chilling stress) (**Supplementary Table 5**). Five software tools, namely RefFinder, BestKeeper, NormFinder, geNorm, and delta-CT, were used to identify suitable reference genes. The expression stability of the selected genes was first ranked by the four algorithms of delta-CT, BestKeeper, NormFinder and geNorm (**Figures 2B1–B4**). As a comprehensive tool, RefFinder can be used to produce the final overall ranking of candidate references according to the geometric mean of the weights of each candidate, calculated by the delta-CT, BestKeeper, geNorm, and NormFinder methods. The top four stability reference genes given by RefFinder were *RBP* > *ATPase* > *40S_S3* > *Dynamin* (**Figure 2A**).

Then, the PCR efficiencies of *RBP*, *ATPase*, *40S_S3*, and *Dynamin* were calculated. As can be seen in **Figure 2C**, the amplification efficiency (E) of each primer pair varied between 99.1% for *ATPase* and 120.4% for *40S_S3*. The regression coefficient (R^2) ranged from 0.961 (*40S_S3*) to 0.974 (*Dynamin*). To further validate the stability of *RBP*, *ATPase*, *40S_S3*, and *Dynamin*, their expression levels in the roots, rhizomes, and leaf tissues of another two ginger cultivars, "Shandongdajiang" and "Yunnanluopingxiaohuangjiang," under different stress conditions were determined by RT-qPCR (**Supplementary Table 6**). Then, the Cq values generated from the three cultivars were collected to perform a correlation analysis (**Figure 2D**). The results showed that, without *Dynamin*, the relative coefficient between each pair of *RBP*, *ATPase*, and *40S_S3* was larger than 0.96, suggesting that *RBP*, *ATPase*, and *40S_S3* are favorable reference genes for RT-qPCR studies for ginger. Primer information for *RBP*, *ATPase*, and *40S_S3* is listed in **Table 1**.

Application of Reference Genes in the Postharvest Study of Ginger

As shown in **Figure 3A**, the rhizome gradually deteriorated during the 28 days of postharvest storage. The expression levels of three *pathogenesis-related* (*PR*) genes, *NbRbohA*, *WRKY7*, and *WRKY8*, were determined by *RBP*, *ATPase*, and *40S-S3*, respectively (**Figure 3B**). Generally, the expression patterns of the three *PR* genes determined by the three reference genes were similar. The expression of *NbRbohA* normalized by *RBP* was slightly increased on days 7 and 14 of storage but significantly increased on days 21 and 28, whereas its expression levels normalized by *ATPase* and *40S-S3* were slightly decreased on days 7 and 14 but significantly increased on days 21 and 28. The expression of *WRKY7* and *WRKY8* normalized by *ATPase* and *40S-S3* showed similar trends. Their expression decreased on days 7 and 14 but increased on days 21 and 28. The expression of *WRKY7* normalized by *RBP* decreased on day 7 but increased after 14 days of treatment. The expression of *WRKY8* normalized by *RBP* increased throughout treatment.

MYB genes are functionally associated with lignin synthesis and many other growth processes (Chen et al., 2021). The RT-qPCR analysis revealed that the expression of seven *MYB* genes in postharvest storage samples, and *F. solani* inoculation samples showed similar trends when normalized by *RBP*, *ATPase*, and *40S-S3*. In postharvest storage samples, *Myb52.2*, *Myb91.1*, and *Myb40.1* were upregulated after 7 days of storage, with *Myb52.2* being the largest upregulated gene. The other four genes, *Myb54.1*, *Myb29.1*, *Myb24.5*, and *Myb09.1*, were normally expressed after 7 days of storage in the ginger rhizome (**Figure 3C**). Meanwhile, the expression of seven *MYB* genes in ginger under *F. solani* inoculation rhizome for 7 days was analyzed (**Figure 3D**), and the results showed that, besides *Myb54.1*, the other six genes *Myb29.1*, *Myb24.5*, *Myb09.1*, *Myb52.2*, *Myb91.1*, and *Myb40.1* were upregulated, especially for *Myb24.5* and *Myb29.1*, which were the top two sharply upregulated *MYB* genes (**Figure 3E**).

To further validate the stability of *RBP*, *ATPase*, and *40S_S3* during their application to postharvest storage studies, *PR* and *MYB* gene expression levels in ginger rhizomes determined by RT-qPCR were used to perform correlation analysis (**Figure 3F**). The results showed that the relative coefficients between each pair of *RBP*, *ATPase*, and *40S_S3* were greater than 0.96, which further confirmed that *RBP*, *ATPase*, and *40S_S3* are favorable RT-qPCR reference genes for postharvest biology studies in ginger rhizomes.

Furthermore, the expression levels of *PR* and *MYB* genes were further analyzed with double reference genes, including *RBP* and *ATPase*, *ATPase* and *40S-S3*, and *RBP* and *40S-S3*. The results showed that the expression patterns of these genes

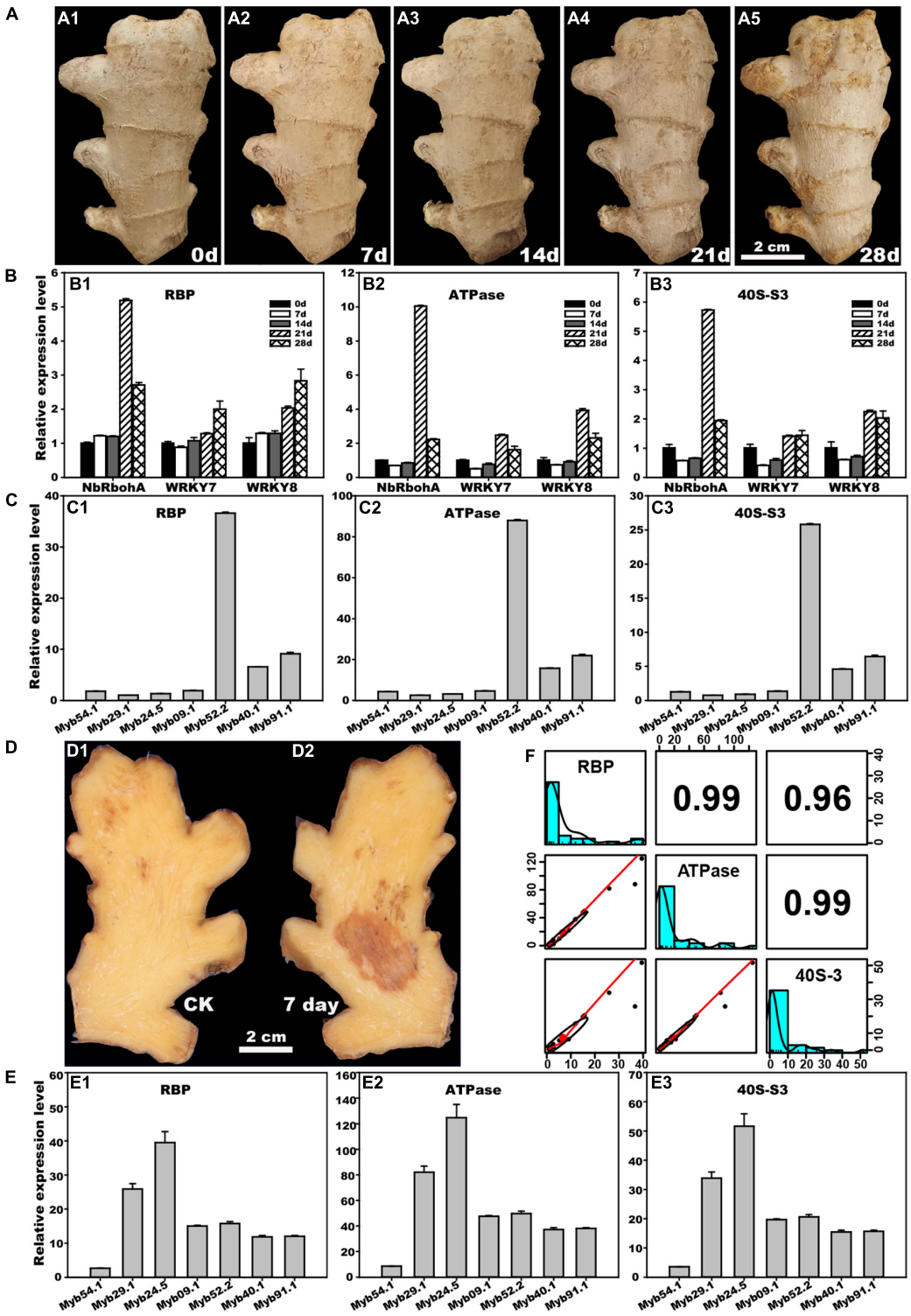


FIGURE 3 | Application of stability reference genes *RBP*, *ATPase*, and *40S-S3* to postharvest ginger. **(A)** Natural deterioration of ginger rhizome during 0 to 28 days postharvest storage. **(B)** Changes in relative expression levels of three *pathogenesis-related* genes during rhizome postharvest storage determined by *RBP*, *ATPase*, and *40S-S3*. **(C)** Changes in the relative expression level of seven flavonoid-related *MYB* genes during rhizome 7 days natural postharvest storage determined by *RBP*, *ATPase*, and *40S-S3*. **(D)** Disease lesion of the rhizome after inoculation by *Fusarium solani* for 7 days. **(E)** Changes in the relative expression level of seven flavonoid-related *MYB* genes after rhizome inoculation by *F. solani* for 7 days determined by *RBP*, *ATPase*, and *40S-S3*. **(F)** Validation stability by correlation analysis of the relative expression levels of three *pathogenesis-related* and seven flavonoid-related genes determined by *RBP*, *ATPase*, and *40S-S3* above.

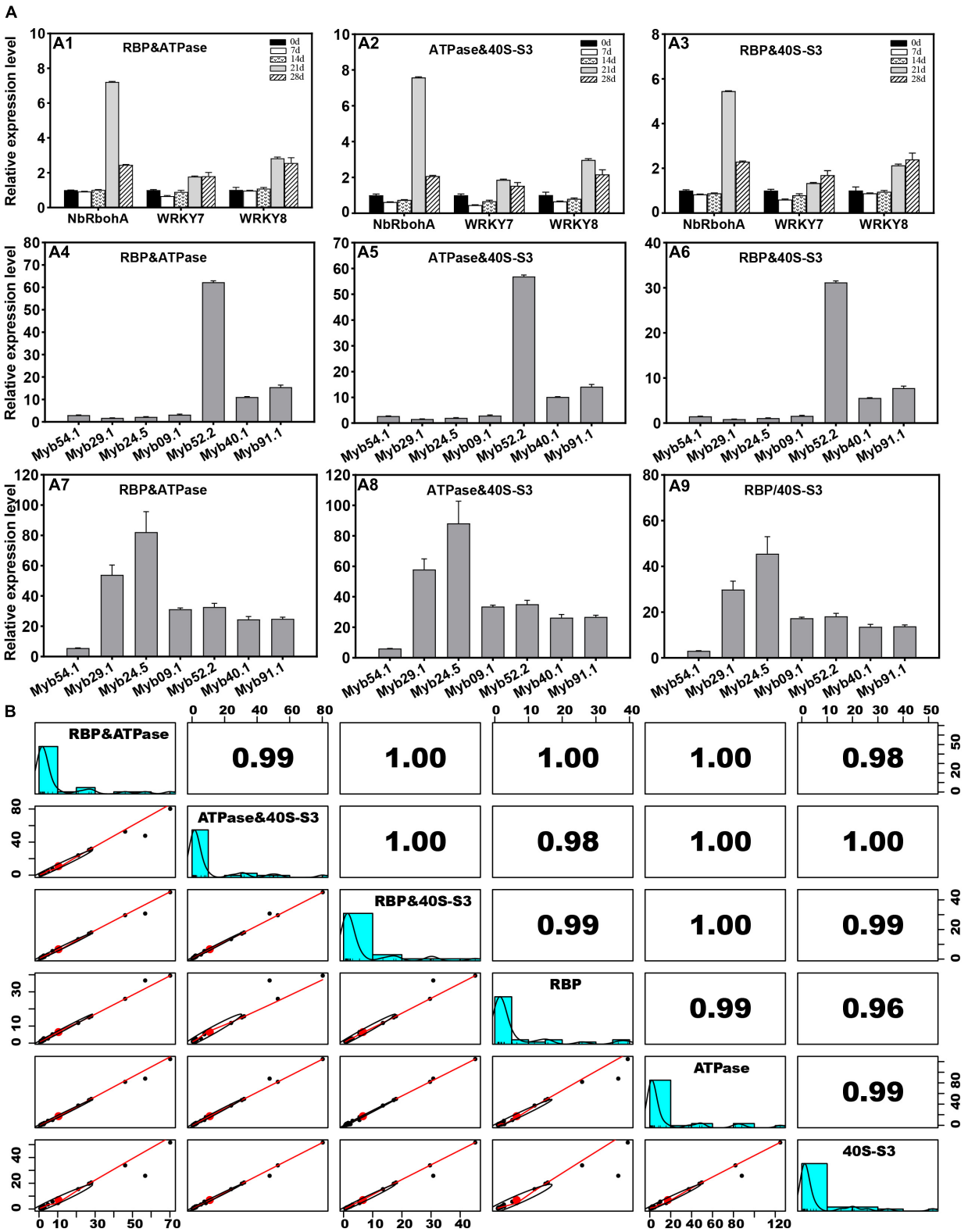


FIGURE 4 | Estimation of the stability of the double reference gene method. **(A)** The expression levels of *PR* and *MYB* genes are determined by reference gene pairs of *RBP* and *ATPase*, *ATPase* and *40S-S3*, or *RBP* and *40S-S3*. **(B)** Correlation analysis of expression levels determined by two and single reference genes.

standardized by double reference genes were consistent with those calculated by a single reference gene (**Figures 4A1–A9**). The results showed that the relative coefficient between each pair of *RBP* and *ATPase*, *ATPase* and *40S-S3*, and *RBP* and *40S-S3* was greater than 0.96 (**Figure 4B**). The relative coefficient between *RBP* and *ATPase* and *ATPase* and *40S-S3* was 0.99. The relative coefficient between *RBP* and *ATPase* and *RBP* and *40S-S3* was 1.00. The relative coefficient between *ATPase* and *40S-S3* and *RBP* and *40S-S3* was 1.00.

DISCUSSION

There are many constraints in the ginger planting process, such as heat, chilling, drought, waterlogging, and salt stress, and the rhizome deteriorates after harvest due to dehydration, pathogen invasion, and senescence (Lv et al., 2020). Quantification of the expression patterns of key genes by RT-qPCR is an important and commonly used approach for deciphering the response mechanism of ginger under different conditions (Fan et al., 2013; Zhu et al., 2019a). Apparently, ideal reference genes are crucial to the reliability and accuracy of the RT-qPCR analysis (Mughal et al., 2018). Until now, evaluation and validation of reference genes have been performed in many plants, but limited information is available on stable reference gene development for ginger. Furthermore, there is still no report about using RNA-seq datasets to facilitate the development of stable expression reference genes in ginger.

RNA-Seq Data Boosted the Selection of Candidate Stable Reference Genes

In recent years, expression information and assembling sequences produced by RNA-seq have been used to identify novel and stable reference genes for several plant species (Leebens-Mack et al., 2019; Yin et al., 2021). Previously, we produced a set of transcriptome data and determined the expression levels of ginger genes in various tissues. In this study, the expression profiling data were used to develop appropriate internal reference genes for the quantification of genes in ginger, with specific attention to the application of reference genes in studies associated with stress and rhizome postharvest storage.

Suitable reference genes must meet three main criteria, as proposed by Mughal et al. (2018): (1) The genes must be above the basal cell background (moderate to a high level of expression); (2) the genes must exhibit expression in different developmental stages, various physiological states, and multiple tissues; and (3) the gene expression levels show low variation among different tissues and developmental, physiological, and environmental conditions. Accordingly, to select suitable candidate reference genes, the expression levels of ginger genes determined by RNA-seq were normalized to FPKM values, which were then used to calculate the SD (FPKM standard deviation) and MV (FPKM mean value) values. Genes were further ranked from smallest to largest according to the SD value, and 29 candidates with MV values greater than 50 were selected from the top-ranking genes (**Figure 1A** and **Supplementary Table 1**). Meanwhile, MFC (FPKM maximum fold change) and CV (coefficient of variation, SD of FPKM/average of FPKM) values were also reported as crucial indicators for estimating the expression stability of candidates. Thus, the MFC and CV values of the candidates were further calculated; the results showed that the MFC and CV of these 29 selected candidates were smaller than 1.5 and 0.1, respectively (**Figure 1B** and **Supplementary Table 2**). The SD, MV, MFC, and CV indicators suggested that these 29 selected candidate genes were suitable for subsequent reference primer development.

Interestingly, those commonly used reference genes, such as *Actin*, *Tubulin*, *EF1α*, and *Ubiquitin* (Yin et al., 2021), were not found in the 29 candidates. By querying commonly used reference genes in *Arabidopsis* against the ginger genome, 13 ginger homologs were manually identified and used as candidate references (**Supplementary Table 3**). According to SD, MV, MFC, and CV values (**Figures 1A,B,D,E**), the expression patterns of these 13 candidates varied across different tissues and environmental conditions, implying that the candidates lacked stability and were not suitable for use as references. Similar to these results, previous studies also reported that these commonly used reference genes were not always stably and constitutively expressed in different tissues, treatments, and species (Hong et al., 2008; Reddy et al., 2016). For example, Reddy et al. (2016) reported that the newly developed reference genes performed significantly better than the traditionally used reference genes, such as *Actin* and *EF1α*. Hong et al. (2008) found that the most commonly used reference gene, *Actin,* was inappropriate for use as a reference gene in *Brachypodium distachyon,* as some variations of the transcript levels were detected in different plant tissues and under different growth conditions. However, to compare the stability of newly selected candidates with that of traditionally used reference genes, we retained the 13 candidates and conducted further primer design and stability assessments.

RBP, *ATPase*, and *40S_S3* Were Validated to Be the Most Stable Reference Genes

Reference genes should be stably expressed in different periods, treatments, and tissues (Yin et al., 2021). To validate the expression stability and screen the best ones for gene expression normalization in ginger, we then evaluated the expression levels of 32 candidate reference genes in different samples using RT-qPCR (**Supplementary Table 5**). To improve the reliability of the assessment of reference genes, we used four algorithms (BestKeeper, NormFinder, geNorm, and delta-CT) and a combination of the four statistical methods called RefFinder in the present study to identify stable reference genes. However, the ranking orders of the 32 candidate reference genes determined by the five algorithms showed some differences, mainly because of the different statistical strategies. Ranking order differences have also been found in several other studies. For example, Duan et al. (2017) found that, due to differences among the algorithms, the most unstable genes identified by the four algorithms were mostly the same, whereas the ranking order of the most stable genes was different. Similarly, in this study, *Clathrin*

and *TPL40B* were indicated to be the most unstable genes in the four algorithms (BestKeeper, NormFinder, geNorm, and delta-CT), while the order of stable genes was slightly different. RefFinder is a comprehensive tool that can be used to produce a final overall ranking of candidate reference genes according to the geometric mean of the weights of every gene generated by the NormFinder, BestKeeper, geNorm, and delta-CT programs (Xie et al., 2012). Thus, RefFinder was used to produce the final ranking order, and the final top four stability reference genes ranked by RefFinder were *RBP* > *ATPase* > *40S_S3* > *Dynamin* (**Figure 2A**).

Similar to previous studies (Hong et al., 2008; Reddy et al., 2016), in this study, we also found that our newly developed reference genes performed better than the traditionally used reference genes. Comprehensive ranking using RefFinder showed that *RBP*, *ATPase*, *40S_S3*, and *Dynamin* were ranked as the top four stable genes, while traditional references, such as *ACT2*, *TUB4*, *UBC35*, and *LOS1*, were ranked as the most unstable genes in the sample sets. Traditional reference genes are widely used in plant molecular biology studies, but the stability of these genes needs to be verified in more plant species, in different tissues, and under various conditions. Based on this study and many other studies, RNA-seq data should be used to develop novel reference genes. Moreover, at least two reference genes are highly recommended because only one may lead to relatively large errors (Kozera and Rapacz, 2013; Mughal et al., 2018).

PCR efficiency analysis of *RBP*, *ATPase*, *40S_S3*, and *Dynamin* confirmed that the corresponding primers had high amplification efficiency and were suitable for RT-qPCR analysis (**Figure 2C**). Furthermore, the stability of *RBP*, *ATPase*, *40S_S3*, and *Dynamin* was confirmed using two more ginger cultivars subjected to different stress conditions (**Supplementary Table 6**). Correlation analysis of Cq values obtained from three cultivars showed that, besides *Dynamin*, the relative coefficient between each pair of *RBP*, *ATPase*, and *40S_S3* was larger than 0.96. These results revealed that the relative expression levels determined by *RBP*, *ATPase*, and *40S_S3* are fairly similar, and they are the optimal reference genes for ginger gene expression analysis in different cultivars, tissues, and experimental conditions.

RBP, *ATPase*, and *40S_S3* Performed Well in Postharvest Ginger Genes' Quantification

The rhizome is an economically crucial part of ginger and usually goes through one or more years of storage. During postharvest storage, microorganisms are important causal agents of spoilage. *MYB* transcription factors (TFs) participate in many developmental and physiological processes, including modulating lignin biosynthesis and plant resistance against pathogens (Zhang et al., 2019; Chen et al., 2021). To further test the stability and possible usage of selected reference genes in the postharvest biology study of ginger rhizomes, *RBP*, *ATPase*, and *40S-S3* were used to normalize the expression patterns of three *pathogenesis-related* (*PR*) genes (including two PTI-related genes, *WRKY7* and *WRKY8*, and one reactive oxygen-related gene, *NbRbohA*) and seven *MYBs* (Yin et al., 2020c; Chen et al., 2021). Ginger rhizomes gradually deteriorated during 28 days of postharvest storage, which may be due to microbial infection. Gene expression analysis of three *PR* genes, *NbRbohA*, *WRKY7*, and *WRKY8*, showed similar expression patterns at different time points during storage when standardized by three reference genes (*RBP*, *ATPase*, and *40S-S3*). Similarly, seven *MYB* genes that were potentially functionally associated with lignin synthesis were upregulated in *F. solani*-inoculated rhizomes, regardless of which reference genes (*RBP*, *ATPase*, or *40S-S3*) were used (**Figure 3E**). Similarly, the stability of *RBP*, *ATPase*, and *40S_S3* was tested using postharvest storage samples, and the results showed that seven *MYB* genes had similar expression trends, regardless of which reference genes (*RBP*, *ATPase*, and *40S-S3*) were used. For further validation, correlation analysis was performed using the expression data of three *PR* and seven *MYB* genes determined by *RBP*, *ATPase*, and *40S_S3* (**Figure 3F**). The pairwise coefficients of *RBP* and *ATPase*, *RBP* and *40S_S3*, and *ATPase* and *40S_S3* were 0.99, 0.96, and 0.99, respectively, which confirmed the stability of the three selected reference genes in the postharvest biology study of ginger rhizomes. Moreover, as recommended by Kozera and Rapacz (2013), at least two reference genes should be used during gene quantification studies because using one could result in significant biases. For example, Derveaux et al. (2010) indicated that three-fold bias was detected in 25% of the analyzed results or even six-fold bias in 10% of the quantification results. Thus, in this study, the expression patterns of 10 selected genes were further analyzed with double reference genes, including *RBP* and *ATPase*, *ATPase* and *40S-S3*, and *RBP* and *40S-S3*. As shown in **Figure 4A**, the expression patterns determined by double reference genes showed a similar tendency as those determined by single reference genes, i.e., *RBP*, *ATPase*, and *40S-S3* (**Figures 3B,C,E**). Furthermore, the correlation analysis of expression levels determined by reference gene pairs of *RBP* and *ATPase*, *ATPase* and *40S-S3*, or *RBP* and *40S-S3* reached 0.99 (**Figure 4B**). Accordingly, based on our results, each pair of *RBP*, *ATPase*, and *40S-S3* is suitable for double reference genes for the RT-qPCR study of ginger, especially for the determination of the expression pattern of genes functionally associated with ginger postharvest biological responses.

CONCLUSION

In this study, three stably expressing genes, *RBP*, *ATPase*, and *40S_S3*, were identified as suitable for the accurate normalization of target gene expression in ginger across all experimental subsets. *RBP*, *ATPase*, and *40S_S3* were also recommended for application to gene expression analyses in postharvest biology studies of ginger rhizomes. Our results support the importance of using high-throughput transcriptomic data to select new reference genes in RT-qPCR experiments, as traditionally used reference genes did not show stable enough expressions in ginger. Our identification of optimal reference genes could make an important contribution to qPCR-based gene expression analysis for ginger functional genomics.

DATA AVAILABILITY STATEMENT

The datasets presented in this study can be found in online repositories. The names of the repository/repositories and accession number(s) can be found in the article/ **Supplementary Material**.

AUTHOR CONTRIBUTIONS

GL, JY, and YZ designed the experiments. GL, JM, KX, and PY conducted the experiments and analyzed the data with supervision by FG, XC, QJ, and LL. JY wrote the manuscript. All authors read and approved the manuscript.

FUNDING

This work was supported by the Natural Science Foundation of Hubei Province (2021CBF512) and Scientific Research Program of the Hubei Provincial Department of Education (No. D20201301).

SUPPLEMENTARY MATERIAL

The Supplementary Material for this article can be found online at: https://www.frontiersin.org/articles/10.3389/fpls.2022.893495/full#supplementary-material

Supplementary Table 1 | FPKM candidate.

Supplementary Table 2 | Blast candidate.

Supplementary Table 3 | FPKM annotation candidate.

Supplementary Table 4 | Candidate primer information.

Supplementary Table 5 | Fengtoujiang Cq values.

Supplementary Table 6 | Other cultivars Cq values.

Supplementary Table 7 | *PR* and *MYB* primer information.

Supplementary Table 8 | *PR* and *MYB* Cq values.

REFERENCES

Bustin, S. A., Benes, V., Garson, J. A., Hellemans, J., Huggett, J., Kubista, M., et al. (2009). The MIQE guidelines: minimum information for publication of quantitative real-time PCR experiments. *Clin. Chem.* 55, 611–622. doi: 10.1373/clinchem.2008.112797

Chen, L., Wu, F., and Zhang, J. (2021). Nac and myb families and lignin biosynthesis-related members identification and expression analysis in melilotus albus. *Plants* 10:303. doi: 10.3390/plants10020303

Cheng, S. P., Jia, K. H., Liu, H., Zhang, R. G., Li, Z. C., Zhou, S. S., et al. (2021). Haplotype-resolved genome assembly and allele-specific gene expression in cultivated ginger. *Hortic. Res.* 8:188. doi: 10.1038/s41438-021-00599-8

Derveaux, S., Vandesompele, J., and Hellemans, J. (2010). How to do successful gene expression analysis using real-time PCR. *Methods* 50, 227–230. doi: 10.1016/j.ymeth.2009.11.001

Duan, M., Wang, J., Zhang, X., Yang, H., Wang, H., Qiu, Y., et al. (2017). Identification of optimal reference genes for expression analysis in radish (*Raphanus sativus* L.) and its relatives based on expression stability. *Front. Plant Sci.* 8:1605. doi: 10.3389/fpls.2017.01605

Fan, C., Ma, J., Guo, Q., Li, X., Wang, H., and Lu, M. (2013). Selection of reference genes for quantitative real-time PCR in bamboo (*phyllostachys edulis*). *PLoS One* 8:e56573. doi: 10.1371/journal.pone.0056573

González-Agüero, M., García-Rojas, M., Di Genova, A., Correa, J., Maass, A., Orellana, A., et al. (2013). Identification of two putative reference genes from grapevine suitable for gene expression analysis in berry and related tissues derived from RNA-seq data. *BMC Genomics* 14:878. doi: 10.1186/1471-2164-14-878

Gou, T., Yang, L., Hu, W., Chen, X., Zhu, Y., Guo, J., et al. (2020). Silicon improves the growth of cucumber under excess nitrate stress by enhancing nitrogen assimilation and chlorophyll synthesis. *Plant Physiol. Biochem* 152, 53–61. doi: 10.1016/j.plaphy.2020.04.031

Hong, S. Y., Seo, P. J., Yang, M. S., Xiang, F., and Park, C. M. (2008). Exploring valid reference genes for gene expression studies in *Brachypodium distachyon* by real-time PCR. *BMC Plant Biol.* 8:112. doi: 10.1186/1471-2229-8-112

Jain, M., Nijhawan, A., Tyagi, A. K., and Khurana, J. P. (2006). Validation of housekeeping genes as internal control for studying gene expression in rice by quantitative real-time PCR. *Biochem. Biophys. Res. Commun.* 345, 646–651. doi: 10.1016/j.bbrc.2006.04.140

Jaiswal, P. S., Kaur, N., and Randhawa, G. S. (2019). Identification of reference genes for qRT-PCR gene expression studies during seed development and under abiotic stresses in cyamopsis tetragonoloba. *Crop Sci.* 59, 252–265. doi: 10.2135/cropsci2018.05.0313

Kozera, B., and Rapacz, M. (2013). Reference genes in real-time PCR. *J. Appl. Genet* 54, 391–406. doi: 10.1007/s13353-013-0173-x

Kumar, R. (2014). Role of microRNAs in biotic and abiotic stress responses in crop plants. *Appl. Biochem. Biotechnol.* 174, 93–115. doi: 10.1007/s12010-014-0914-2

Leebens-Mack, J. H., Barker, M. S., Carpenter, E. J., Deyholos, M. K., Gitzendanner, M. A., Graham, S. W., et al. (2019). One thousand plant transcriptomes and the phylogenomics of green plants. *Nature* 574, 679–685. doi: 10.1038/s41586-019-1693-2

Li, H. L., Wu, L., Dong, Z., Jiang, Y., Jiang, S., Xing, H., et al. (2021). Haplotype-resolved genome of diploid ginger (*Zingiber officinale*) and its unique gingerol biosynthetic pathway. *Hortic. Res.* 8:189. doi: 10.1038/s41438-021-00627-7

Li, H., Wu, L., Tang, N., Liu, R., Jin, Z., Liu, Y., et al. (2020). Analysis of transcriptome and phytohormone profiles reveal novel insight into ginger (*Zingiber officinale Rose*) in response to postharvest dehydration stress. *Postharvest Biol. Technol.* 161:111087. doi: 10.1016/j.postharvbio.2019.111087

Lv, Y., Li, Y., Liu, X., and Xu, K. (2020). Identification of ginger (*Zingiber officinale Roscoe*) reference genes for gene expression analysis. *Front. Genet* 11:586098. doi: 10.3389/fgene.2020.586098

Ma, R., Xu, S., Zhao, Y., Xia, B., and Wang, R. (2016). Selection and validation of appropriate reference genes for quantitative real-time PCR analysis of gene expression in lycoris aurea. *Front. Plant Sci.* 7:536. doi: 10.3389/fpls.2016.00536

Mughal, B. B., Leemans, M., Spirhanzlova, P., Demeneix, B., and Fini, J. B. (2018). Reference gene identification and validation for quantitative real-time PCR studies in developing xenopus laevis. *Sci. Rep.* 8:496. doi: 10.1038/s41598-017-18684-1

Peng, H., Hu, H., Xi, K., Zhu, X., Zhou, J., Yin, J., et al. (2022). Silicon nanoparticles enhance ginger rhizomes tolerance to postharvest deterioration and resistance to *Fusarium solani*. *Front. Plant Sci.* 13:816143. doi: 10.3389/fpls.2022.816143

Pfaffl, M. W. (2001). A new mathematical model for relative quantification in real-time RT-PCR. *Nucleic Acids Res.* 29, 45e–445e. doi: 10.1093/nar/29.9.e45

Reddy, D. S., Bhatnagar-Mathur, P., Reddy, P. S., Sri Cindhuri, K., Sivaji Ganesh, A., and Kumar Sharma, K. (2016). Identification and validation of reference genes and their impact on normalized gene expression studies across cultivated and wild Cicer species. *PLoS One* 11:e148451. doi: 10.1371/journal.pone.0148451

Vandesompele, J., De Preter, K., Pattyn, F., Poppe, B., Van Roy, N., De Paepe, A., et al. (2002). Accurate normalization of real-time quantitative RT-PCR data by geometric averaging of multiple internal control genes. *Genome Biol* 3:RESEARCH0034. doi: 10.1186/gb-2002-3-7-research0034

Xie, F., Xiao, P., Chen, D., Xu, L., and Zhang, B. (2012). miRDeepFinder: a miRNA analysis tool for deep sequencing of plant small RNAs. *Plant Mol. Biol.* 80, 75–84. doi: 10.1007/s11103-012-9885-2

Yim, A. K., Wong, J. W., Ku, Y. S., Qin, H., Chan, T. F., and Lam, H. M. (2015). Using RNA-Seq data to evaluate reference genes suitable for gene expression studies in soybean. *PLoS One* 10:e0136343. doi: 10.1371/journal.pone.0136343

Yin, F., Liu, X., Cao, B., and Xu, K. (2020a). Low pH altered salt stress in antioxidant metabolism and nitrogen assimilation in ginger (*Zingiber officinale*) seedlings. *Plant Physiol.* 168, 648–659. doi: 10.1111/ppl.13011

Yin, J., Hou, L., Jiang, X., Yang, J., He, Y., Zhou, X., et al. (2021). Identification and validation of reference genes for quantitative real-time PCR studies in alligatorweed (*Alternanthera philoxeroides*). *Weed Sci.* 69, 404–411. doi: 10.1017/wsc.2021.32

Yin, J., Liu, M., Ma, D., Wu, J., Li, S., Zhu, Y., et al. (2018). Identification of circular RNAs and their targets during tomato fruit ripening. *Postharvest Biol. Technol.* 136, 90–98. doi: 10.1016/j.postharvbio.2017.10.013

Yin, J., Tian, J., Li, G., Zhu, Y., Zhou, X., He, Y., et al. (2020b). Carbohydrate, phytohormone, and associated transcriptome changes during storage root formation in alligatorweed (*Alternanthera philoxeroides*). *Weed Sci.* 68, 382–395. doi: 10.1017/wsc.2020.37

Yin, J., Wang, L., Zhao, J., Li, Y., Huang, R., Jiang, X., et al. (2020c). Genome-wide characterization of the C2H2 zinc-finger genes in *Cucumis sativus* and functional analyses of four CsZFPs in response to stresses. *BMC Plant Biol.* 20:359. doi: 10.1186/s12870-020-02575-1

Zhang, Y. L., Zhang, C. L., Wang, G. L., Wang, Y. X., Qi, C. H., Zhao, Q., et al. (2019). The R2R3 MYB transcription factor MdMYB30 modulates plant resistance against pathogens by regulating cuticular wax biosynthesis. *BMC Plant Biol.* 19:362. doi: 10.1186/s12870-019-1918-4

Zhu, Y. X., Gong, H. J., and Yin, J. L. (2019a). Role of silicon in mediating salt tolerance in plants: a review. *Plants* 8:147. doi: 10.3390/plants8060147

Zhu, Y. X., Jia, J. H., Yang, L., Xia, Y. C., Zhang, H. L., Jia, J. B., et al. (2019b). Identification of cucumber circular RNAs responsive to salt stress. *BMC Plant Biol.* 19:164. doi: 10.1186/s12870-019-1712-3

Zhu, Y., Jiang, X., Zhang, J., He, Y., Zhu, X., Zhou, X., et al. (2020). Silicon confers cucumber resistance to salinity stress through regulation of proline and cytokinins. *Plant Physiol Biochem* 156, 209–220. doi: 10.1016/j.plaphy.2020.09.014

Conflict of Interest: The authors declare that the research was conducted in the absence of any commercial or financial relationships that could be construed as a potential conflict of interest.

Publisher's Note: All claims expressed in this article are solely those of the authors and do not necessarily represent those of their affiliated organizations, or those of the publisher, the editors and the reviewers. Any product that may be evaluated in this article, or claim that may be made by its manufacturer, is not guaranteed or endorsed by the publisher.

Copyright © 2022 Li, Ma, Yin, Guo, Xi, Yang, Cai, Jia, Li, Liu and Zhu. This is an open-access article distributed under the terms of the Creative Commons Attribution License (CC BY). The use, distribution or reproduction in other forums is permitted, provided the original author(s) and the copyright owner(s) are credited and that the original publication in this journal is cited, in accordance with accepted academic practice. No use, distribution or reproduction is permitted which does not comply with these terms.

frontiers | Frontiers in Plant Science

ORIGINAL RESEARCH
published: 14 June 2022
doi: 10.3389/fpls.2022.917770

Differential Gene Expression and Withanolides Biosynthesis During *in vitro* and *ex vitro* Growth of *Withania somnifera* (L.) Dunal

*Sachin Ashok Thorat[1], Arya Kaniyassery[1], Poornima Poojari[1], Melissa Rangel[2], Shashikala Tantry[1], Kodsara Ramachandra Kiran[1], Manjunath B. Joshi[3], Padmalatha S. Rai[4], Anna-Maria Botha[5] and Annamalai Muthusamy[1]**

[1] Department of Plant Sciences, Manipal School of Life Sciences, Manipal Academy of Higher Education (MAHE), Manipal, India, [2] Manipal School of Life Sciences, Manipal Academy of Higher Education (MAHE), Manipal, India, [3] Department of Ageing Research, Manipal School of Life Sciences, Manipal Academy of Higher Education (MAHE), Manipal, India, [4] Department of Biotechnology, Manipal School of Life Sciences, Manipal Academy of Higher Education (MAHE), Manipal, India, [5] Department of Genetics, Faculty of Agriculture, University of Stellenbosch, Stellenbosch, South Africa

Ashwagandha (*Withania somnifera* L. Dunal) is a medicinally important plant with withanolides as its major bioactive compounds, abundant in the roots and leaves. We examined the influence of plant growth regulators (PGRs) on direct organogenesis, adventitious root development, withanolide biosynthetic pathway gene expression, withanolide contents, and metabolites during vegetative and reproductive growth phases under *in vitro* and *ex vitro* conditions. The highest shooting responses were observed with 6-benzylaminopurine (BAP) (2.0 mg L^{-1}) + Kinetin (KIN) (1.5 mg L^{-1}) supplementation. Furthermore, BAP (2.0 mg L^{-1}) + KIN (1.5 mg L^{-1}) + gibberellic acid (GA_3) (0.5 mg L^{-1}) exhibited better elongation responses with *in vitro* flowering. Half-strength MS medium with indole-3-butyric acid (IBA) (1.5 mg L^{-1}) exhibited the highest rooting responses and IBA (1.0 mg L^{-1}) with highest fruits, and overall biomass. Higher contents of withaferin A (WFA) [~8.2 mg g^{-1} dry weight (DW)] were detected in the reproductive phase, whereas substantially lower WFA contents (~1.10 mg g^{-1} DW) were detected in the vegetative phase. Cycloartenol synthase (*CAS*) ($P = 0.0025$), sterol methyltransferase (*SMT*) ($P = 0.0059$), and 1-deoxy-D-xylulose-5-phosphate reductase (*DXR*) ($P = 0.0375$) genes resulted in a significant fold change in expression during the reproductive phase. The liquid chromatography-mass spectrometry (LC-MS) analysis revealed metabolites that were common (177) and distinct in reproductive (218) and vegetative (167) phases. Adventitious roots cultured using varying concentrations of indole-3-acetic acid (IAA) (0.5 mg L^{-1}) + IBA (1.0 mg L^{-1}) + GA_3 (0.2 mg L^{-1}) exhibited the highest biomass, and IAA (0.5 mg L^{-1}) + IBA (1.0 mg L^{-1}) exhibited the highest withanolides content. Overall, our findings demonstrate the peculiarity of withanolide biosynthesis during distinct growth phases, which is relevant for the large-scale production of withanolides.

Keywords: adventitious roots, differential gene expression, *in vitro*, *ex vitro*, metabolites, organogenesis, *Withania somnifera*, withanolide

Abbreviations: BAP, 6-benzylaminopurine; KIN, Kinetin; IBA, indole-3-butyric acid; IAA, indole-3-acetic acid; GA_3, gibberellic acid; WFA, withaferin A; WA, withanolide A; WN, withanone; WB, withanolide B; WD, withanolide D; FW, fresh-weight; DW, dry-weight; PGRs, plant growth regulators.

OPEN ACCESS

Edited by:
Ramamoorthy Siva, VIT University, India

Reviewed by:
Muthu Thiruvengadam, Konkuk University, South Korea
Manickavasagam Markandan, Bharathidasan University, India

***Correspondence:**
Annamalai Muthusamy
a.msamy@manipal.edu

Specialty section:
This article was submitted to Plant Biotechnology, a section of the journal Frontiers in Plant Science

Received: *12 April 2022*
Accepted: *12 May 2022*
Published: *14 June 2022*

Citation:
Thorat SA, Kaniyassery A, Poojari P, Rangel M, Tantry S, Kiran KR, Joshi MB, Rai PS, Botha A-M and Muthusamy A (2022) Differential Gene Expression and Withanolides Biosynthesis During in vitro and ex vitro Growth of Withania somnifera (L.) Dunal. Front. Plant Sci. 13:917770. doi: 10.3389/fpls.2022.917770

INTRODUCTION

Withania somnifera (L.) Dunal, widely known as Ashwagandha, Indian Ginseng, or Winter Cherry, belongs to the Solanaceae family. It is an essential aromatic medicinal plant regularly used in traditional medicine (Singh et al., 2015). The plant possesses multipotential therapeutic properties, and in India, it is used in various Ayurvedic formulations (Shasmita et al., 2018). Studies have shown that the plant is effective for the treatment of various ailments and diseases, such as cancer, asthma, aging, and neurological and inflammatory disorders, due to its anti-cancer, anti-stress, anti-inflammatory, antianxiety, anticonvulsant, adaptogenic, immunomodulatory, endocrine, and cardiovascular activities (Kulkarni and Dhir, 2008; Dar et al., 2015; Singh et al., 2015; Gurav et al., 2020). Its multiple pharmaceutical properties are due to secondary metabolites known as withanolides, withaferin A (WFA), withanolide A (WA), withanolide D (WD), and withanone (WN) (Chatterjee et al., 2010). Recently, this plant has been reported for its potential effectiveness in treating and managing COVID-19 symptoms (Chikhale et al., 2021; Saggam et al., 2021). In addition, *in silico* studies on WN and withanoside V have shown a possible antiviral role in inhibiting the activity of a protease (M^{pro}) from SARS-CoV-2 (Kumar et al., 2020).

Withanolides are comprised of thirty carbon compounds known as triterpenoids synthesized from isoprene units through a withanolide biosynthetic pathway. Furthermore, it has divided into two classical pathways, namely, cytosolic mevalonic acid (MVA) and plastidial methylerythritol phosphate (MEP) pathways. Important genes involved in this pathway, such as 3-hydroxy-3-methylglutaryl-coenzyme A reductase (*HMGR*), convert hydroxymethylglutaryl coenzyme A into mevalonate, marking the first step of MVA pathway in the cytosol. In contrast, 1-deoxy-D-xylulose-5-phosphate reductase (*DXR*) gene converts 1-deoxy-d-xylulose-5-phosphate into 2-*o*-methyl-d-erythritol-4-phosphate, marking the first step of the MEP pathway in the plastid. Cycloartenol synthase (*CAS*) and sterol methyltransferase (*SMT*) genes are intermediates in synthesizing 24-methylenecycloartenol and subsequently forming various withanolides (Dhar et al., 2015).

Due to extensive uses in medicinal formulations, the demand for dried plant material for withanolide production has increased worldwide (Sathiyabama and Parthasarathy, 2018). Withanolide biosynthesis is a plant tissue-specific process and depends on the growing conditions in the natural habitat. The traditional cultivation of *W. somnifera* in field conditions is laborious and time-consuming, and the product yield is also affected by a range of biotic and abiotic factors. Thus, these factors influence the biosynthesis of withanolides and their purity, further complicates the analysis of phytochemical composition. This results in an inadequate yield of products that cannot meet the demands in the current international market (Sangwan et al., 2004; Sivanandhan et al., 2012). In contrast, plant biotechnological tools, such as *in vitro* culture propagation, show higher growth rates under optimal growth conditions. This facilitates fast cell proliferation, leading to a significant growth irrespective of seasonal variations. Collectively, *in vitro* culture methods assist in producing callus and plantlets in a controlled environment and can be upscaled to large-scale bioreactors without interferences from biotic and abiotic factors (Rao and Ravishankar, 2002; Verpoorte et al., 2002).

Currently, biotechnological tools are widely used for the conservation, *in vivo* and *in vitro* breeding, selection, and genetic and metabolic engineering of *W. somnifera* genotypes. Plant tissue culture has also shown a great potential for the rapid production of phytomedicines (Singh et al., 2016). Several conventional and molecular experiments have been performed in *W. somnifera* for crop improvement, but none of them have used novel bioactive molecules to enhance growth and metabolite production in *W. somnifera* (Poornima et al., 2019; Sharma et al., 2020; Srivastava and Sangwan, 2020; Thorat et al., 2021). Although several studies are available on the *in vitro* regeneration and the quantification of withanolides, withanolide biosynthetic pathway gene expression, distribution of metabolites during the vegetative and reproductive phases, and adventitious root formation have not been reported. Therefore, this study has evaluated the influence of different combinations of plant growth regulators (PGRs) on multiple shoot initiation, direct organogenesis, plantlet regeneration, *in vitro* and *ex vitro* flowering, and adventitious root formation. Furthermore, we have also looked at withanolide contents, metabolite profile, and differential gene expression of the withanolide biosynthetic pathway during the vegetative and reproductive phases.

MATERIALS AND METHODS

In vitro Seed Germination, Multiple Shoot Induction, and Regeneration

The seeds of Ashwagandha var. Jawahar Asgandh-20 were procured from ICAR-Directorate of Medicinal and Aromatic Plants Research, Anand, Gujarat. The seeds were washed under running water for 30 min, treated with 2% Tween 20 for 15 min, and rinsed with distilled water. Then, surface decontamination was achieved using aqueous 0.1% mercuric chloride (w/v), and later seeds were rinsed five times with autoclaved distilled water. The seeds were inoculated aseptically onto half-strength MS (Murashige and Skoog, 1962) and fortified with 0.25 mg L^{-1} gibberellic acid (GA_3). Then, the seeds were incubated in the dark for 48 h and then exposed to 40 μmol m^{-2} s^{-1} cool-white, fluorescent light with a 16-h photoperiod for germination. The shoot tips, as well as nodal segments, were taken from 3-week-old *in vitro* grown seedlings and inoculated onto MS media with different concentrations of 6-benzylaminopurine (BAP) (0.5, 1.0, 1.5, 2.0, 2.5, and 3.0 mg L^{-1}) and Kinetin (KIN) (0.5, 1.0, 1.5, 2.0, 2.5, and 3.0 mg L^{-1}) individually, and later well responded to KIN (1.5 mg L^{-1}) + BAP (0.5–3.0 mg L^{-1}) in various combinations. However, MS without BAP and KIN was eliminated because several studies have demonstrated that it is ineffective on multiple shoot induction and regeneration. After 20 days, the number of shoots >2 cm were counted and noted. The growing shoots were subcultured on the same medium supplemented with GA_3 for multiplication and elongation. After 40 days, shoots with a minimum height of

2.5 cm were transplanted onto half-strength MS media fortified with different indole-3-butyric acid (IBA) concentrations (0.0, 0.5, 1.0, 1.5, and 2.0 mg L^{-1}). The well-rooted plantlets were hardened on a sterile mix of soil, coir, and sand in a 1:1:1 ratio and maintained in the plant tissue culture room for 10 days. Furthermore, the plantlets were transferred to plastic pots in the same combination of soil without sterilization in the greenhouse for acclimatization.

In vitro and *ex vitro* Flowering and Fruit Set

During the induction and development of shoots and roots, the interesting phase of *in vitro* flowering was also observed and noted. Plantlets showed continuously developing flowers *ex vitro* and set fruits. All the *in vitro* and *ex vitro* flowers and fruits were carefully counted from all the treatment groups. In addition, the seeds were collected during *in vitro* and *ex vitro* flowering and assessed for their viability and germination patterns.

Adventitious Root Culture

Leaf segments (5 mm × 5 mm) along the midrib were excised from 35-day-old *in vitro* seedlings and inoculated onto MS media. The initiation of adventitious roots was observed at the leaf midrib after 30 days of culture. Root segments (around 1.0 cm long), including the root tip, were inoculated on liquid MS media for proliferation. MS media with 0.5 mg L^{-1} indole-3-acetic acid (IAA) in a combination with different IBA (1.0 and 2.0 mg L^{-1}) concentrations and without PGRs were used for liquid media. Furthermore, these two combinations were analyzed with and without 0.20 mg L^{-1} GA_3. The adventitious roots were inoculated in 25 ml liquid MS media and incubated for a 16-h light and 8-h dark photoperiod for 1 week, followed by complete darkness, in an incubation shaker at room temperature (25 ± 2°C) at 80 rpm. The root cultures were maintained in three replicates in conical flasks for each combination of PGRs.

Expression of Genes Involved in the Withanolide Biosynthetic Pathway

The expression levels of withanolide biosynthetic pathway genes, such as *CAS*, *DXR*, 3-hydroxy-3-methylglutaryl-coenzyme A reductase (*HMGR*), and *SMT*, were examined for a comparative analysis of vegetative and reproductive phase plants. Briefly, 100 mg of leaf tissue from vegetative and reproductive phase plants was powdered using liquid nitrogen, and total RNA was extracted using TRI Reagent® (MRC #TR118) according to the manufacturer's instructions. Furthermore, the concentration and purity of the RNA were quantified using Nanodrop ND-100 Spectrophotometer (Thermo Scientific, MA, United States). Then, isolated RNAs (2 μg) were treated with DNase I to eliminate DNA contamination using DNa-free™ Kit (Invitrogen™ #AM1906). Later, cDNA was synthesized using a High-Capacity cDNA Reverse Transcription Kit (Applied Biosystems™ #4368814) as directed by the manufacturer's protocol. The quantitative real-time expression of genes was performed with QuantStudio 6 Pro Real-Time PCR systems (Applied Biosystems™, United States) using PowerUp™ SYBR™ Green Master Mix (Applied Biosystems™ #A25741).

The abundance of transcripts in the samples was determined by the relative quantification of mRNA using the comparative cycle threshold (*Ct*) method. Furthermore, the *ACTIN* gene was used as constitutively expressed control to normalize the quantity of template cDNA. The quantitative relative expression of mRNA was determined by the $2^{-\Delta\Delta CT}$ method (Kiran et al., 2020). The primers' list and their sequences are depicted in **Supplementary Table 1**.

Extraction and Quantitative Analysis of Withanolides

The hardened plantlets were used for the extraction of withanolides. The plantlets and adventitious roots were harvested, washed thoroughly, and dried at 40°C in a hot air oven for 3 days, and 1 g of plant materials (roots, shoots, and leaves) was grounded into a fine powder with the help of a mortar and pestle. Analytical grades, namely WFA, WA, withanolide B (WB), and WN, were purchased from Natural Remedies Pvt Ltd. (Bangalore, India) and used as standards. The fine powder was extracted thrice with 25% methanol in a shaker incubator at 37°C and filtered with Whatman filter paper at every 2 h interval, followed by depigmentation and defatting with an equal volume of n-hexane three times; finally, the methanol: water phase was separated and defatted with an equal volume of chloroform for three times; chloroform phase was separated and evaporated till dryness at 40°C in a vacuum concentrator (Eppendorf®) and stored at −20°C till HPLC analysis (Sangwan et al., 2008).

The samples were re-dissolved in a known volume of methanol and filtered through a 0.2-μm syringe filter (Minisart, Sartorius Stedim Biotech) for HPLC analysis. The withanolides were quantitatively analyzed using Waters Alliance HPLC 2695 with Separation Module System consisting of Dual λ Absorbance Detector 2487 and Phenomenex Luna-C18 column (250 mm × 4.6 mm) and monitored using the Empower 2Pro software. A binary gradient of water (solvent A) and methanol (solvent B), both containing 0.1% formic acid (FA), was used. Gradient system was carried out at 25°C and was initially at 60 A/40 B and gradually changed to 40 A/60 B in 12.0 min duration, maintained for the next 2.0 min, then changed to 25 A/75 B at 14 min, and then to 5 A/95 B at 16.0 min at a flow rate of 1.0 ml min^{-1}. The compounds were detected, and peaks were assigned by running the four commercial withanolide standards of known concentration and consequent comparison of retention times. The calibration curve was generated with respective standards. The WFA, WA, WB, and WN contents were identified by comparing retention time with standards, and the concentration was calculated using a regression equation obtained from a calibration curve using the Empower 2 pro software.

Liquid Chromatography–Mass Spectrometry Analysis

Whole plant samples were dried in a hot air oven at 40°C for 3 days. Later, 100 mg of each representative sample (whole

plant) from vegetative and reproductive phases was pooled and grounded to a fine powder using liquid nitrogen in a pre-chilled mortar and pestle. Total metabolites were extracted using 1 ml of chilled acidified methanol comprising 99.875% of methanol and 0.125% of FA. Then, the extract was passed through a 0.2-μm syringe filter (Minisart, Sartorius Stedim Biotech) and stored at −20°C. Furthermore, the extract was filtered with a 0.2-μm syringe filter (Minisart, Sartorius Stedim Biotech) and stored at −20°C. The untargeted metabolite profiling of *W. somnifera* was achieved using Agilent 6530 Accurate-Mass Q-TOF liquid chromatography-mass spectrometry (LC-MS) HPLC ESI system (Agilent Technologies, Santa Clara, CA, United States). The metabolites separation was performed using a 250 mm × 4.6 mm C18 column (Phenomenex-Luna) with mobile phases consisting of solvent A (0.1% FA in Milli-Q water) and solvent B (0.1% FA in acetonitrile). The injection volume of 8 μl was used with a 0.5-ml min^{-1} flow rate and 70 min run time through positive ESI mode in triplicates through gradient method and with maintained ion range (Kiran et al., 2021; Swathy et al., 2021). Metabolites were identified using the Plantcyc online database based on their *m/z* values, and each compound was represented by its molecular formula, retention time, and mass error ($\leq \pm$ 30 ppm).

Statistical Analysis

All the tissue culture experiments were conducted in triplicates with 10 explants in each group, and values in the table were expressed as mean ± standard error (SE). The cultures were subcultured every 15 days, observed periodically for the percentage of responses in each stage, and noted. The values of the experiments were subjected to statistical analysis with analysis of variance (ANOVA) and compared using Duncan's multiple range tests (Gomez and Gomez, 1984). The gene expression significance values were analyzed using multiple *t*-test, and all the graphical figures were made using the GraphPad 8 Prism software.

RESULTS

Multiple Shoot Initiation From Shoot Tip Explants

Shoot tip explants inoculated on MS basal medium supplemented with different PGRs, either alone or in combination with varying concentrations of BAP and KIN (0.5–3.0 mg L^{-1}), had shown a differential response in multiple shoot initiation, shoot length, and days required for shoot initiation (**Table 1**). The maximum number of shoots (9.0) was noted on the BAP (2.0 mg L^{-1}) + KIN (1.5 mg L^{-1}), followed by BAP (1.0 mg L^{-1}) + KIN (1.5 mg L^{-1}) and BAP (1.5 mg L^{-1}) + KIN (1.5 mg L^{-1}), and the lowest was noted on BAP (3.0 mg L^{-1}). The minimum number of days (30.0) required for shoot initiation was noted on BAP (2.0 mg L^{-1}) and KIN (1.5 mg L^{-1}) followed by BAP (2.0 mg L^{-1}) + KIN (1.5 mg L^{-1}), whereas the delayed (42.0 days) shoot initiation was noted on BAP (3.0 mg L^{-1}) + KIN (1.5 mg L^{-1}). The maximum shoot length (5.36 ± 0.40 cm) was noted in BAP (2.0 mg L^{-1}) + KIN (1.5 mg L^{-1}), followed by KIN (2.0 mg L^{-1}) and BAP (1.0 mg L^{-1}) + KIN (1.5 mg L^{-1}) (**Figures 1A–D**).

Multiple Shoot Initiation From Nodal Explants

Nodal explants were inoculated on MS basal medium supplemented with different PGRs, either alone or in combination with varying concentrations of BAP and KIN (0.5–3.0 mg L^{-1}), showing multiple shoot initiations with shoot lengths and times required for shoot initiation at varied frequencies (**Table 2**). The maximum number of shoots (23.0) was noted with BAP (2.0 mg L^{-1}) + KIN (2.0 mg L^{-1}), followed by BAP (2.0 mg L^{-1}), BAP (2.5 mg L^{-1}), and BAP (2.5 mg L^{-1}) + KIN (1.5 mg L^{-1}), and the lowest was noted with KIN (0.5 mg L^{-1}). Among different PGRs, early shoot initiation (28.0 days) was noted on MS fortified with BAP (2.0 mg L^{-1}), followed by BAP (2.0 mg L^{-1}) + KIN (1.5 mg L^{-1}) and KIN (2.0 mg L^{-1}), whereas the delayed (42.0 days) shoot initiation was noted with BAP (3.0 mg L^{-1}) + KIN (1.5 mg L^{-1}). The maximum shoot length (6.03 cm) was noted in BAP (2.0 mg L^{-1}), followed by BAP (2.0 mg L^{-1}) + KIN (1.5 mg L^{-1}) (**Table 2** and **Figures 2A,B**).

Multiplication and Elongation of Shoots and *in vitro* Flowering

Multiple shoots from the shoot tip and nodal explants were transferred to MS medium supplemented with different PGRs + GA_3 or in combination. They displayed the effects on

TABLE 1 | *In vitro* responses of shoot tip explants of *Withania somnifera* to different concentrations of PGRs.

Concentrations of PGRs (mgL^{-1})	Number of shoots/explant	Days to initiation of multiple shoots	Length of shoots (cm)
BAP			
0.5	3.0 ± 0.57b	37.0 ± 3.51ab	2.60 ± 0.10e
1.0	3.0 ± 0.57b	34.0 ± 2.64c	2.93 ± 0.30d
1.5	4.0 ± 0.57a	33.0 ± 2.51cd	3.50 ± 0.30b
2.0	4.0 ± 1.15a	30.0 ± 1.52e	3.86 ± 0.30a
2.5	3.0 ± 1.0b	34.0 ± 2.64c	3.40 ± 0.10bc
3.0	2.0 ± 0.57c	38.0 ± 2.51ab	3.20 ± 0.20c
KIN			
0.5	4.0 ± 1.0b	34.0 ± 2.51c	3.70 ± 0.30d
1.0	5.0 ± 0.57a	39.0 ± 1.52a	4.0 ± 0.20c
1.5	5.0 ± 1.0a	30.0 ± 1.52e	4.26 ± 0.25b
2.0	4.0 ± 1.15b	33.0 ± 3.0cd	4.76 ± 0.25a
2.5	4.0 ± 0.57b	37.0 ± 3.51b	4.0 ± 0.20c
3.0	3.0 ± 0.57c	37.0 ± 3.51b	3.86 ± 0.20cd
BAP and KIN			
0.5 + 1.5	5.0 ± 0.57d	37.0 ± 1.52bc	4.03 ± 0.15de
1.0 + 1.5	7.0 ± 0.57b	38.0 ± 3.05b	4.43 ± 0.20b
1.5 + 1.5	7.0 ± 0.57b	37.0 ± 2.0bc	4.4 ± 0.26bc
2.0 + 1.5	9.0 ± 0.57a	32.0 ± 2.0d	5.36 ± 0.40a
2.5 + 1.5	6.0 ± 0.57c	38.0 ± 2.64b	4.06 ± 0.20d
3.0 + 1.5	5.0 ± 0.57d	42.0 ± 1.52a	3.83 ± 0.15e

Mean values within a column having same alphabet are not significantly different ($p < 0.05$) according to Duncan's multiple range test (DMRT). Data are the mean and standard deviation for n = 3 independent experiments.

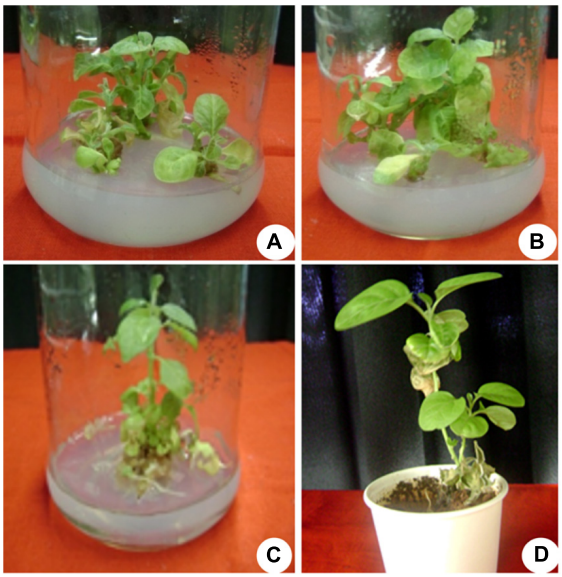


FIGURE 1 | The *in vitro* culture of *Withania somnifera*. **(A)** Shoot multiplication (scale = 2.5 cm), **(B)** shoot elongation (scale = 3.6 cm), **(C)** shoot elongation and rooting (scale = 5.8 cm), and **(D)** hardening of plantlets (scale = 7.7 cm).

elongation, shoot length, number of leaves, and flowers at a varied frequency (**Table 3**). The highest percentage of shoot elongation (82.0%) was noted on the BAP (2.0 mg L^{-1}) + KIN (1.5 mg L^{-1}) + GA_3 (0.5 mg L^{-1}), followed by BAP (1.5 mg L^{-1}) + KIN (1.5 mg L^{-1}) + GA_3 (0.5 mg L^{-1}) and KIN (2.0 mg L^{-1}) + GA_3 (0.5 mg L^{-1}) (**Figures 1B**, **2C**). Maximum shoot length (6.56 cm) with a maximum number of leaves (12.0) was noted on BAP (2.0 mg L^{-1}) + KIN (1.5 mg L^{-1}) + GA_3 (0.5 mg L^{-1}), followed by KIN (2.0 mg L^{-1}) + GA_3 (0.5 mg L^{-1}) and BAP (2.0 mg L^{-1}) + GA_3 (0.5 mg L^{-1}). A maximum number of flowers *in vitro* (7.0) was noted on BAP (2.0 mg L^{-1}) + KIN (1.5 mg L^{-1}) + GA_3 (0.5 mg L^{-1}) and BAP (2.0 mg L^{-1}) + GA_3 (0.5 mg L^{-1}), respectively, followed by BAP (1.5 mg L^{-1}) + KIN (1.5 mg L^{-1}) + GA_3 (0.5 mg L^{-1}) and BAP (1.5 mg L^{-1}) + GA_3 (0.5 mg L^{-1}) (**Table 3** and **Figures 3A–F**).

Induction of Roots, *in vitro* Flowering, and Fruit Set

The elongated shoots (4–6 cm) were transferred to a half-strength MS medium or supplemented with varying concentrations of IBA (0.5–2.0 mg L^{-1}) for root induction. Data on the percentage of rooting, number of *in vitro* flowers, number of fruits, number of roots, fresh weight (FW) and dry weight (DW), and percentage of hardening were recorded (**Table 4**). The maximum rooting percentage (84.0%) was noted for IBA (1.5 mg L^{-1}), followed by IBA (1.0 mg L^{-1}), IBA (2.0 mg L^{-1}), and IBA (0.5 mg L^{-1}). A maximum number of flowers (18.0) was noted on IBA (1.0 mg L^{-1}) during the rooting of shoots, followed by IBA (1.5 mg L^{-1}), IBA (0.5 mg L^{-1}), and IBA (2.0 mg L^{-1}) (**Figures 1C**, **2D,E**). The maximum number of fruits (13.0), highest root length (6.90 cm), FW (4.63 g), and DW (0.43 g) were noted on IBA (1.0 mg L^{-1}), followed by IBA (1.5 mg L^{-1}). The plantlet with developed roots was removed carefully from culture vessels, gently washed under tap water, transferred to a plastic cup containing sterile soil, and hardened in the tissue culture room at 25 ± 2.0°C with a photoperiod of 16 h light and 8 h dark. The maximum percentage of hardening (82.66%) was noted on IBA (1.0 mg L^{-1}), followed by IBA (1.5 mg L^{-1}) (**Figures 1D**, **2F**). Furthermore, continuous *ex vitro* flowering and fruit setting were observed (**Figures 4A–F**). The ripe fruits were collected and shade-dried, and seeds were collected from fruits and stored at room temperature. Seeds showed a substantial germination percentage under *in vitro* and *ex vitro* conditions.

Adventitious Root Initiation and Culture

The adventitious root was induced from leaf segments (5 mm) of *in vitro* grown seedlings on MS medium supplemented with different PGRs either alone or in combination with GA_3 (0.20 mg L^{-1}) (**Table 5**). Among all combinations, the IAA (0.5 mg L^{-1}) + IBA (1.0 mg L^{-1}) + GA3 (0.2 mg L^{-1}) and IAA (0.5 mg L^{-1}) + IBA (2.0 mg L^{-1}) + GA_3 (0.2 mg L^{-1}) exhibited a higher growth with maximum FW (2.56 g) and DW (0.81 ± 1.11), respectively, followed by IAA (0.5 mg L^{-1}) + IBA (2.0 mg L^{-1}) and IAA (0.5 mg L^{-1}) + IBA (1.0 mg L^{-1}) (**Figures 5A–H**).

TABLE 2 | *In vitro* responses of nodal explants of *Withania somnifera* to different concentrations of PGRs.

Concentrations of PGRs (mgL^{-1})	Number of shoots per explant	Days for initiation of multiple shoots	Length of the shoots (cm)
BAP			
0.5	10.0 ± 1.15d	34.0 ± 2.64bc	3.03 ± 0.20de
1.0	10.0 ± 1.15d	33.0 ± 2.51c	3.56 ± 0.32d
1.5	13.0 ± 1.0c	32.0 ± 1.15cd	4.13 ± 0.25c
2.0	18.0 ± 2.51a	28.0 ± 1.52e	6.03 ± 0.20a
2.5	17.0 ± 1.52ab	36.0 ± 2.08b	5.13 ± 0.35b
3.0	10.0 ± 2.0d	40.0 ± 2.08a	4.06 ± 0.3cd
KIN			
0.5	8.0 ± 1.52de	38.0 ± 3.05ab	4.13 ± 0.30de
1.0	12.0 ± 1.15c	38.0 ± 1.15ab	4.40 ± 0.30d
1.5	14.0 ± 2.0b	36.0 ± 2.08b	4.96 ± 0.20b
2.0	16.0 ± 2.0a	30.0 ± 3.05c	5.56 ± 0.25a
2.5	12.0 ± 1.52c	36.0 ± 2.64b	4.73 ± 0.11bc
3.0	9.0 ± 2.08d	40.0 ± 1.52a	3.96 ± 0.15e
BAP and KIN			
0.5 + 1.5	11.0 ± 20d	39.0 ± 2.08b	4.66 ± 0.15bc
1.0 + 1.5	14.0 ± 1.52c	38.0 ± 1.52bc	4.96 ± 0.15b
1.5 + 1.5	15.0 ± 1.52bc	35.0 ± 3.21cd	4.96 ± 0.20b
2.0 + 1.5	23.0 ± 2.51a	30.0 ± 1.15e	5.80 ± 0.30a
2.5 + 1.5	17.0 ± 1.52b	37.0 ± 2.08c	4.43 ± 0.25c
3.0 + 1.5	14.0 ± 1.52c	42.0 ± 1.52a	4.23 ± 0.11cd

Mean values within a column having same alphabet are not significantly different ($p < 0.05$) according to Duncan's multiple range test (DMRT). Data are the mean and standard deviation for n = 3 independent experiments.

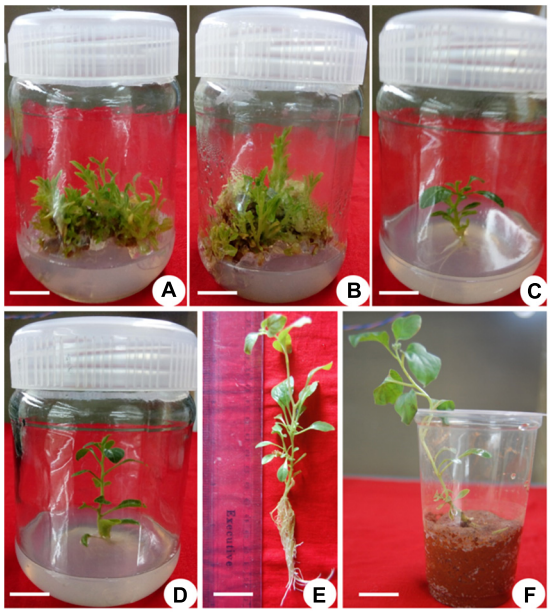


FIGURE 2 | Multiple shoot induction in *Withania somnifera*. **(A)** Induction of multiple shoots from nodal explant with 6-benzylaminopurine (BAP) and Kinetin (KIN) (scale bar = 0.5–1.3 cm), **(B)** multiplication of shoots with BAP and TDZ (scale bar = 1.00–3.05 cm), **(C)** elongation of shoots using BAP and KIN (scale bar = 2–5.3 cm), **(D)** induction of roots from elongated shoots [indole-3-butyric acid (IBA) 0.3 mg/L] (scale bar = 6.5 cm), **(E)** well-developed plantlets (scale bar = 18 cm), and **(F)** hardening of plantlets at 25 ± 2 °C.

Expression of Withanolide Biosynthetic Pathway Genes

The investigation revealed an increased fold change in the expression of all genes in the reproductive phase when compared to that of genes in the vegetative phase. The maximal level of fold change expression was observed in the *HMGR* gene, followed by *SMT* and *CAS*, and a minimal level of fold change expression was observed in the *DXR* gene. Reproductive phase plants revealed a higher expression of withanolide biosynthetic pathway genes, which was confirmed by a significantly higher expression of *HMGR* (3.88-fold) followed by that of *SMT* (2.63-fold, $P = 0.0059$), *CAS* (2.58-fold, $P = 0.0025$), and *DXR* (2.24-fold, $P = 0.0375$) in comparison with their levels in the vegetative phase (**Figure 6**).

Quantitative Analysis of Withanolides

Withanolide contents were quantified from the *ex vitro* grown plantlets (in vegetative and reproductive phases) and adventitious roots. The standard curves for WFA, WA, WB, and WN were plotted with different dilutions (0.001–1.0 mg L^{-1}) and were found to be linear. The regression coefficients were recorded at 1.0, 0.9994, 1.0, and 0.9996 for WFA, WA, WB, and WN, respectively, and calculated from the calibration curve and the peak area determined by the concentration. The standards of WFA, WA, WB, and WN were eluted at the retention times of 6.43, 7.9, 11.56, and 8.38 min, respectively. The quantitative analysis of withanolide contents from the shoot and root tissues of *ex vitro* reproductive phase plantlets revealed that the maximum amount of withanolides was recorded for WFA (8.199 mg g^{-1} DW), followed by WA (0.352 mg g^{-1} DW) and WN (0.813 mg g^{-1} DW) in shoots. Furthermore, a substantially lower amount of WA (1.349 mg g^{-1} DW), WFA (0.33 mg g^{-1} DW), and WN (0.067 mg g^{-1} DW) was observed (**Figure 7A**). However, lower amounts of WFA (1.091 mg g^{-1} DW), WA (0.025 mg g^{-1} DW), and WN (0.0015 mg g^{-1} DW) were noted in shoots, and similarly, WFA (0.053 mg g^{-1} DW), WA (0.006 mg g^{-1} DW), WN (0.003 mg g^{-1} DW), and WB (0.044 mg g^{-1} DW) were noted in vegetative phase roots (**Figure 7B**). In addition, differential amounts of WA and WN contents were noted with different concentrations of IBA in the adventitious root culture. Maximum WA (0.077 mg g^{-1} DW) and WN (0.080 mg g^{-1} DW) contents were recorded with IAA (0.5 mg L^{-1}) + IBA (1.0 mg L^{-1}), followed by IAA (0.5 mg L^{-1}) + IBA (2.0 mg L^{-1}) + GA_3 (0.2 mg L^{-1}). The lowest amount of WA and WN content was recorded with IAA (0.5 mg L^{-1}) + IBA (1.0 mg L^{-1}) + GA_3 (0.2 mg L^{-1}) (**Figure 8**).

Liquid Chromatography-Mass Spectrometry Characterization and Identification of Metabolites

Metabolites from the vegetative and reproductive phases of *W. somnifera* were identified by liquid chromatography–mass spectrometry analysis. Metabolites that were common and distinct in the vegetative and reproductive phases were

TABLE 3 | Effects of BAP, KIN, and GA_3 on percentage of elongation, length of shoots, and number of leaves and flowers in *Withania somnifera*.

PGRs (mgL^{-1})	Percentage of elongation	Length of shoots (cm)	Number of leaves	Number of flowers
BAP + GA_3				
0.5 + 0.5	59.66 ± 4.50e	4.0 ± 0.20de	6.0 ± 1.15c	3.0 ± 0.57e
1.0 + 0.5	64.33 ± 3.21cd	5.56 ± 0.32b	7.0 ± 1.15b	5.0 ± 0.57c
1.5 + 0.5	70.0 ± 2.0b	5.23 ± 0.15bc	7.0 ± 0.57b	6.0 ± 0.57b
2.0 + 0.5	73.0 ± 3.0a	6.36 ± 0.37a	10.0 ± 1.52a	7.0 ± 1.15a
2.5 + 0.5	65.33 ± 1.52c	5.13 ± 0.65c	7.0 ± 0.57b	4.0 ± 1.15d
3.0 + 0.5	59.66 ± 1.52e	4.36 ± 0.35d	6.0 ± 0.57c	3.0 ± 0.57e
KIN + GA_3				
0.5 + 0.5	61.0 ± 3.60d	4.46 ± 0.30de	6.0 ± 0.57d	2.0 ± 0.57d
1.0 + 0.5	66.66 ± 3.05c	5.06 ± 0.85c	7.0 ± 0.57c	4.0 ± 1.52b
1.5 + 0.5	74.33 ± 2.08ab	5.63 ± 0.37b	7.0 ± 0.57c	4.0 ± 0.57b
2.0 + 0.5	76.33 ± 2.08a	6.46 ± 0.15a	10.0 ± 1.15a	5.0 ± 0.57a
2.5 + 0.5	64.0 ± 4.0cd	5.36 ± 0.58bc	8.0 ± 1.52b	4.0 ± 0.57b
3.0 + 0.5	61.66 ± 3.51d	4.63 ± 0.47d	6.0 ± 0.57d	3.0 ± 0.57c
BAP + KIN + GA_3				
0.5 + 1.5 + 0.5	70.33 ± 2.51cd	5.06 ± 0.25de	7.0 ± 0.57c	4.0 ± 0.57d
1.0 + 1.5 + 0.5	73.33 ± 3.05c	5.60 ± 0.20c	8.0 ± 1.15bc	5.0 ± 1.15c
1.5 + 1.5 + 0.5	77.33 ± 2.08b	5.96 ± 0.20b	9.0 ± 0.57b	6.0 ± 1.52b
2.0 + 1.5 + 0.5	82.0 ± 2.64a	6.56 ± 0.20a	12.0 ± 1.15a	7.0 ± 1.52a
2.5 + 1.5 + 0.5	67.66 ± 2.51d	5.23 ± 0.45d	8.0 ± 0.57bc	4.0 ± 0.57d
3.0 + 1.5 + 0.5	62.66 ± 3.05e	5.23 ± 0.11d	7.0 ± 0.57c	4.0 ± 1.15d

Mean values within a column having same alphabet are not significantly different ($p < 0.05$) according to Duncan's multiple range test (DMRT). Data are the mean and standard deviation for n = 3 independent experiments.

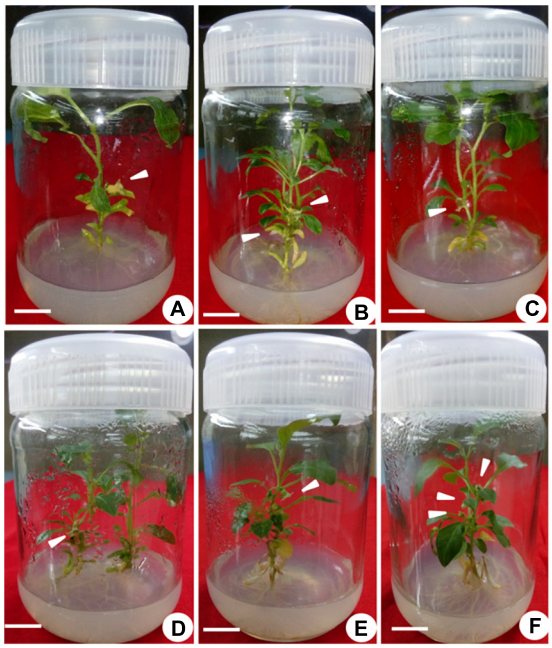


FIGURE 3 | *In vitro* flowering of *Withania somnifera*. **(A)** *In vitro* flower formation from second node (scale bar = 0.7 cm), **(B)** first and second nodes (scale bar = 0.6 and 0.5 cm); **(C,D)** second node (scale bar = 0.6 and 0.4 cm), **(E)** sixth node (scale bar = 0.5 cm), and **(F)** third, fourth, and fifth nodes (scale bar = 0.4, 0.3, and 0.7 cm).

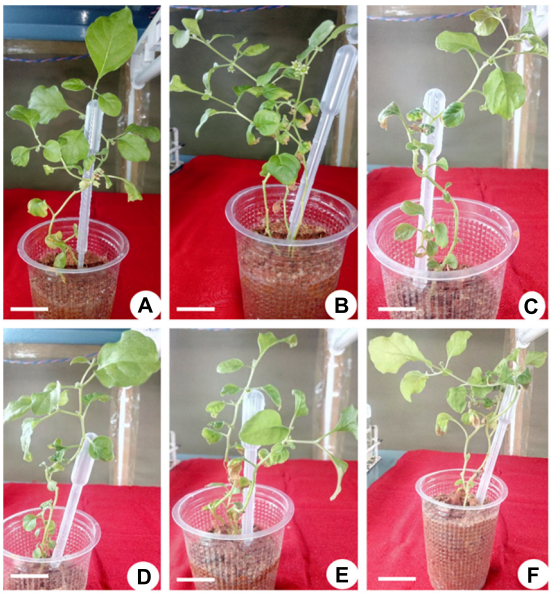


FIGURE 4 | *Ex vitro* flowering in 30-day-old plantlets of *Withania somnifera*. Flower formation from **(A)** 6th node (scale bar = 13.7 cm), **(B)** 7th node (scale bar = 14.4 cm), **(C)** 11th node (scale bar = 17.5 cm), **(D)** 10th node (scale bar = 12.8 cm), **(E)** 10th node (scale bar = 12.5 cm), and **(F)** 12th node (scale bar = 17.6 cm).

characterized separately after the identification. The untargeted qualitative analysis of individual metabolites was performed with a positive ionization mode. Overall, around 786 hits were observed in the vegetative and reproductive phases together. Among them, 177 were found to be common in both phases, 218 were distinctly found in the vegetative phase, and 167 were in the reproductive phase (**Figure 9**). Furthermore, all hits were individually searched in the plantcyc database for metabolite identification. The identified metabolites were 47 common (**Supplementary Table 2**), 28 distinctly vegetative (**Supplementary Table 3**), and 28 distinctly reproductive (**Supplementary Table 4**) metabolites.

DISCUSSION

Multiple Shoot Initiation From Shoot Tip and Nodal Explants

Our results indicated that the effect of BAP or KIN alone or in combination coincides with previously reported shoot multiplication in *W. somnifera* in MS medium fortified with IBA and 2,4-D, using a shoot tip explant (Sen and Sharma, 1991) and the apical bud (Sivanesan, 2007). Similarly, multiple shoots were recorded with BAP and KIN using auxiliary buds (Siddique et al., 2004; Saritha and Naidu, 2007), multiple shoot regeneration was investigated with BAP, 2,4-D, and naphthalene acetic acid (NAA) using the shoot/shoot tip (Ghimire et al., 2010; Joshi and Padhya, 2010; Kanungo and Sahoo, 2011; Supe et al., 2011;

TABLE 4 | Effect of different combinations of IBA on *in vitro* flowering and rooting responses in *Withania somnifera*.

MS + IBA (mgL^{-1})	Percentage rooting	Number of flowers	Number of fruits	Root length (cm)	Number of roots	Growth (g)		Percentage of hardening
						FW	DW	
1/2 MS	15.66 ± 6.02d	5.0 ± 0.57d	4.0 ± 1.15c	4.20 ± 0.40cd	7.0 ± 1.52e	1.52 ± 0.38de	0.19 ± 0.01d	54.33 ± 4.04d
1/2 MS + 0.5	36.66 ± 6.11c	10.0 ± 3.05c	6.0 ± 2.51bc	5.76 ± 0.45b	11.0 ± 2.08c	2.14 ± 0.15d	0.24 ± 0.03cd	67.0 ± 3.10c
1/2 MS + 1.0	56.33 ± 6.50b	18.0 ± 1.52a	13.0 ± 2.51a	6.90 ± 0.36a	17.0 ± 1.52a	4.63 ± 0.17a	0.43 ± 0.01a	82.66 ± 4.16a
1/2 MS + 1.5	84.0 ± 3.60a	14.0 ± 1.52b	8.0 ± 0.57b	5.76 ± 0.25b	15.0 ± 2.08ab	3.59 ± 0.34b	0.38 ± 0.03ab	80.33 ± 2.51ab
1/2 MS + 2.0	56.33 ± 3.21b	10.0 ± 1.52c	6.0 ± 20bc	4.76 ± 0.25c	10.0 ± 1.52cd	3.0 ± 0.11bc	0.29 ± 0.02c	79.66 ± 1.52b

Mean values within a column having same alphabet are not significantly different ($p < 0.05$) according to Duncan's multiple range test (DMRT). Data are the mean and standard deviation for n = 3 independent experiments.

TABLE 5 | Responses of adventitious root formation from leaf culture.

Plant growth regulators (mgL^{-1})			Level of growth	Weight (g)	
IAA	**IBA**	**GA_3**		**Fresh weight**	**Dry weight**
0.5	1	–	+	1.63 ± 0.15c	0.24 ± 0.02bc
0.5	2	–	++	1.96 ± 0.15b	0.19 ± 0.0d
0.5	1	0.20	+++	2.56 ± 0.20a	0.24 ± 0.01bc
0.5	2	0.20	+++	2.26 ± 0.15ab	0.81 ± 1.11a

The experiment was performed in triplicate with 3 explants each. +- less growth, ++ - moderate growth, +++- higher growth. Mean values within a column having the same alphabet are not significantly different ($p < 0.05$) according to Duncan's multiple range test (DMRT). Data are the mean and standard deviation for n = 3 independent experiments.

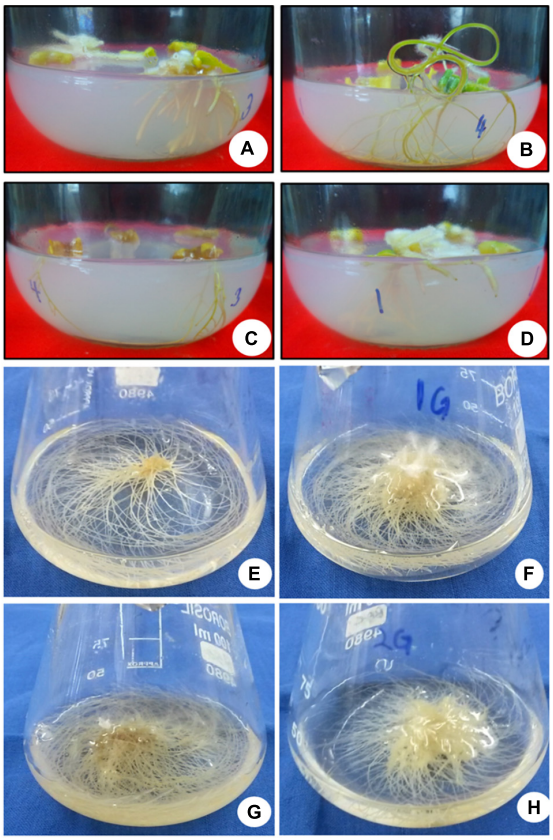


FIGURE 5 | Induction and culture of adventitious roots. **(A)** Profuse growth of thick ramified roots after 25 days, **(B)** active root growth observed at 25 days, **(C)** thin, brittle roots, turned brown after 30 days, **(D)** thick roots, showing a hint of callogenesis at midrib after 40 days, **(E)** adventitious roots in MS basal media, **(F)** roots in MS + 0.5 mg L^{-1} indole-3-acetic acid (IAA) + 1.0 mg L^{-1} IBA, **(G)** MS + 0.5 mg L^{-1} IAA + 1.0 m gL^{-1} IBA + 0.20 mg L^{-1} gibberellic acid (GA_3), and **(H)** MS media + 0.5 mg L^{-1} IAA + 2.0 mg L^{-1} IBA.

Chakraborty et al., 2013), and 100% of the shooting was observed in the presence of a combination of BAP and KIN (Mir et al., 2014). In addition, multiple shoots were observed using axillary buds with BAP and NAA (Saritha and Naidu, 2007), BAP and KIN (Sabir et al., 2008), and axillary buds with BA (Fatima and Anis, 2012). The lower concentration of BAP required a longer time for breaking the bud, whereas a moderate concentration showed the maximum shoot length, number of shoots, and early bud breakage compared to the higher concentration of BAP. BAP is known for promoting cell differentiation and facilitates shoot organogenesis, whereas KIN is effective in bud breaking and rejuvenation and is known to induce a synergetic effect with other cytokinins (Shyamali and Kazumi, 2007).

Similar to shoot tip explants, nodal explants also responded differentially to various concentrations of PGRs. Our results corroborated with shoot multiplication from nodal explants of *Withania* using BA, IAA, and adenine sulfate (Sivanandhan et al., 2015), the development of multiple shoots with BAP and IAA (Sivanesan and Murugesan, 2008), and the proliferation of axillary shoots with thidiazuron (TDZ) (Fatima and Anis, 2011). Furthermore, multiple shoot formation was reported upon supplementation with BAP, NAA, and $ZnSO_4$ (Fatima et al., 2011; Fatima and Anis, 2012); BAP, IAA, and spermidine (Sivanandhan et al., 2011); BAP, IAA, and L-glutamine (Sivanandhan et al., 2015), BAP and MS–B5 (Kannan and Anbazhakan, 2016), and using BAP and TDZ (Kulkarni et al., 2000).

Multiplication and Elongation of Shoots, *in vitro* Flowering, and Adventitious Roots

This study showed a prominent percentage of elongation with BAP (2.0 mg L^{-1}) and KIN (2.0 mg L^{-1}) + GA_3 (0.5 mg L^{-1}), which was comparable with the results of Logesh et al. (2010). Our observations are in conformity with those of BAP, IAA, and GA_3 combination treatment in numerous *W. somnifera* explants, such as the nodal explant (Sivanesan and Murugesan, 2008), leaf (Kumar et al., 2011), and epicotyl (Udayakumar et al., 2013). Remarkably, we have observed *in vitro* flower formation during root initiation, which is supported by the stimulatory effect of BAP and KIN with GA_3 on *in vitro* flowering and fruiting phenomena with KIN and IAA (Saritha and Naidu, 2007), and the *in vitro* flowering with BA and IAA in *W. somnifera* (Sivanandhan et al., 2015). Flowering under *in vitro* conditions is a unique process, resulting in an addition to the other two existing reports in *W. somnifera*. This technique of rapid *in vitro* flower generation is very useful to develop seeds prior to their natural maturity; thus, it reduces the duration of the breeding cycle. *In vitro* developed seeds are important for studying genetic analysis and molecular marker technology. Furthermore, similar reports of *in vitro* flowering were described in *Swertia chirayita* (Sharma et al., 2014) with IBA, and *Andrographis lineata* (Mohammed et al., 2016) with BA and NAA.

Previously, cytokinin-induced *in vitro* flowering was reported in *Anethum graveolens* (Jana and Shekhawat, 2011), *Swertia chirayita* (Sharma et al., 2014), and *Guizotia abyssinica* (Baghel and Bansal, 2014). The impact of the synergistic effect of endogenous auxin and cytokinin facilitates *in vitro* flowering at the species level in *Micrococca mercurialis* (Jeyachandran and Bastin, 2013), *Withania* (Saritha and Naidu, 2007), *Ocimum basilicum* (Sudhakaran and Sivasankari, 2002),

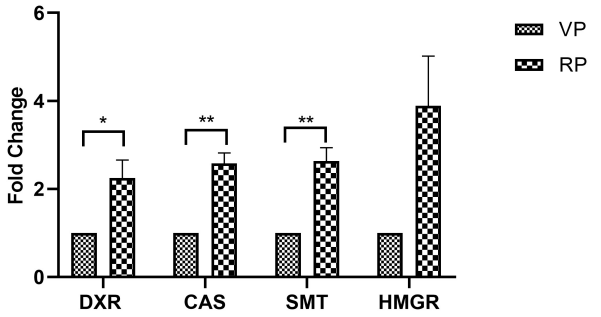


FIGURE 6 | Expression of selected withanolide biosynthetic pathway genes analyzed by qRT-PCR in the leaves of *Withania somnifera* from vegetative (VP) and reproductive (RP) growth phases. The data were represented as mean ± SEM of fold change with respect to VP phase (n = 3) and multiple t-test were performed. Significant difference at $^{*}P > 0.05$; $^{**}P > 0.01$.

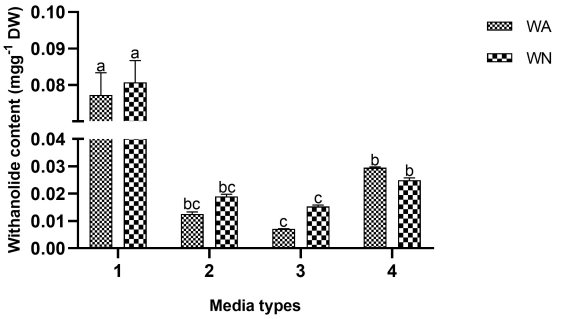


FIGURE 8 | Withanolide A and withanone content (mg g^{-1} DW) from root cultures of *Withania somnifera*. (1) MS + 0.5 mg L^{-1} IAA + 1.0 mg L^{-1} IBA, (2) MS + 0.5 mg L^{-1} IAA + 2 mg L^{-1} IBA, (3) MS + 0.5 mg L^{-1} IAA + 2 mg L^{-1} IBA + 0.2 mg L^{-1} GA_3, and (4) MS + 0.5 mg L^{-1} IAA + 1 mg L^{-1} IBA + 0.2 mg L^{-1} GA_3. Mean values within a column having the same alphabet are not significantly different (p = 0.05) according to DMRT (n = 3).

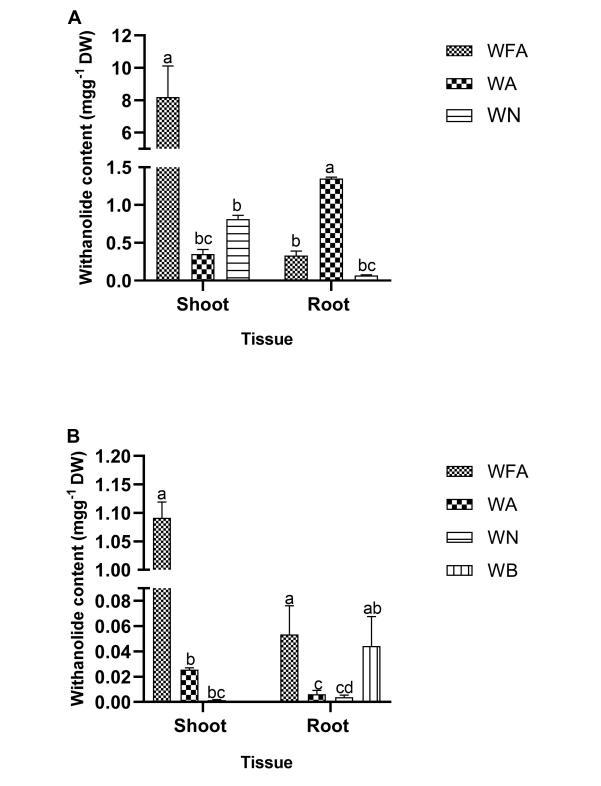


FIGURE 7 | Withanolide content (mg g^{-1} DW) of *Withania somnifera*. **(A)** RP and **(B)** VP. Mean values within a column having the same alphabet are not significantly different (p = 0.05) according to Duncan's multiple range test (DMRT) (n = 3).

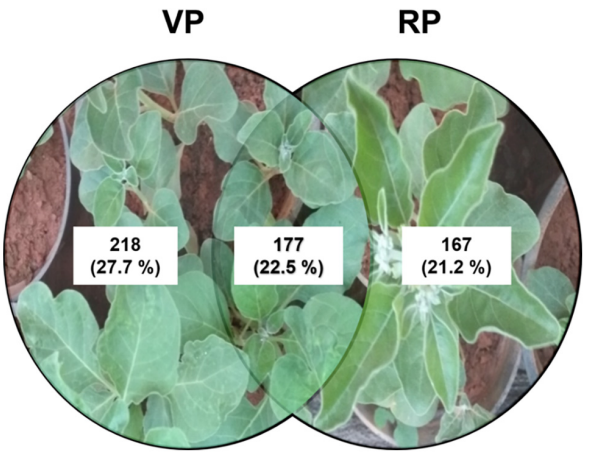


FIGURE 9 | Comparative analysis and distribution of untargeted LC-MS hits of metabolites from VP and RP from whole plant extract of *Withania somnifera*. The hits were noted and analyzed for its distribution in distinct growth phases.

Kniphofia leucocephala (Taylor et al., 2005), and *Vitex negundo* (Thiruvengadam and Jayabalan, 2001). Hence, the addition of cytokinin hormone induces the development of *in vitro* flowering in various plants under *in vitro* conditions, similar to this study.

Our results on the rooting responses (root length, number of roots, and FW and DW) of the *in vitro* shoot with IBA showed similarity with the maximum rooting percentage in the presence of IBA (Sivanesan, 2007). Moreover, IBA also showed a positive effect in this study as well as on the *in vitro* flowering and fruiting of *Brassica campestris* (Verma and Singh, 2007), *Anthemis xylopoda* (Erdag and Emek, 2009), *Heliotropium indicum* (Bagadekar and Jayaraj, 2011), *Ceropegia pusilla* (Kalimuthu and Prabakaran, 2013), and *Brachystelma glabrum* (Lakshmi et al., 2017).

The results on adventitious root formation corroborated those of Wadegaonkar et al. (2006), who used an amalgamation of IAA and IBA for adventitious root initiation and the production of withanolides. Rangaraju et al. (2019) reported that IBA alone induced the highest adventitious root formation in different *W. somnifera* varieties. Similarly, the development of adventitious roots (using a suspension culture) and the effective accumulation of biomass were noted in *Panax notoginseng* (Gao et al., 2005) and *Echinacea purpurea* (Wu et al., 2007). Recently, an adventitious root culture was established using a B5 medium fortified with

3 mM NO_3 and 2.5 mM phosphate, and a significant fold increase in calycosin-7-O-β-D-glucoside and antioxidant activity was recorded in *Astragalus membranaceus* (Jin et al., 2020). The development of adventitious roots from medicinal and aromatic plants has been practiced as an alternate technique for the large-scale production of bioactive compounds, especially for plants that usually reserve their medicinal compounds in their roots. In addition, for the prevention of extensive plant collection from forest areas, several rare endangered threatened (RET) species have been protected (Jiang et al., 2017).

Expression of Withanolide Biosynthetic Pathway Genes

During stress conditions, withanolide biosynthesis is maintained through the upregulated expression of withanolide biosynthetic pathway genes, such as *CAS*, *SMT*, *DXR*, *HMGR*, and others (Singh et al., 2018), which act both as precursors and intermediates for withanolide biosynthesis. In this study, *HMGR* exhibited the highest fold change difference with respect to the vegetative phase, followed by a significant fold change difference in *SMT*, *CAS*, and *DXR* expression. Similar results were observed with the overexpression of *CAS* (3.08-fold) in the hairy root culture of *W. somnifera*, which enhanced withanolide production compared to the control groups (Saxena et al., 2017). *CAS* regulates the synthesis of cycloartenol from the precursor squalene 2,3-epoxidases, while the increased expression of *DXR* and *HMGR* promotes the production of withanolide contents in leaf tissues during drought stress conditions (Singh et al., 2014; Singh et al., 2018). *DXR* and *HMGR* are the precursors in the MEP and MVA pathways in withanolide biosynthesis, respectively. *DXR* and *HMGR* along with other genes were differentially expressed during withanolide biosynthesis when key genes were silenced through tobacco rattle virus (TRV) (Agarwal et al., 2018).

Quantitative Analysis of Withanolides

The increased biosynthesis of WFA was recorded in the shoots trailed by WN and WA, whereas WA was higher in the roots, followed by WFA and WN in the reproductive phase than the vegetative phase plants. There were almost ten times increase in WFA, WA, and WN from the reproductive phase plants compared to vegetative phase plants. This might be due to the twofold increased expression of withanolide biosynthetic genes during the reproductive phase. Our results conform with those of Chatterjee et al. (2010), Dhar et al. (2013), and Singh et al. (2015) with a higher amount of WFA being recorded in leaves, followed by that of WN, whereas WA was higher in the roots, followed by WFA and WN. Subsequently, a higher amount of WFA was quantified *in vitro* flowers than *in vivo* fruits (Sivanandhan et al., 2015). There are several kinds of withanolides reported from different *W. somnifera* sections (Dhar et al., 2015). This study also showed a higher amount of WFA, WA, and WN in *in vitro* regenerated plants by using BAP and KIN in combination, which is similar to the results from Sabir et al. (2008). In contrast, a higher amount of WA was noted in shoots regenerated using BAP and KIN. Furthermore, a significantly higher accumulation of withanolide contents in the reproductive phase of the plants was directly proportional to the increased expression of withanolide biosynthetic pathway genes. The influence of GA_3 on withanolide contents in adventitious roots was studied and found to be decreasing significantly than IAA/IBA treatment. Similar observations were reported by Senthil et al. (2015) where the IBA and IAA induced the highest amount of WFA and WA from the roots. In contrast, Praveen and Murthy (2010) showed the maximum amount of WA (8.8 mg g^{-1} DW) in roots with IBA supplementation (0.5 mg L^{-1}).

Liquid Chromatography-Mass Spectrometry Characterization and Identification of Metabolites

LC-MS analysis in different phases (i.e., vegetative and reproductive) identified untargeted metabolites that were later segregated as common and distinct to these two growth phases. In addition, identifying metabolites from different growth stages in *W. somnifera* can be employed to understand plant developmental processes linked to withanolide biosynthesis in leaves and roots. Common metabolites from vegetative and reproductive phases, such as L-methionine, L-tryptophan, and isatin, were identified. Metabolites, such as anthranilate, cycloglutamate, gibberellin, and others, were the characteristics of the vegetative phase. Furthermore, carnitine, amphetamine, hypusine, and other metabolites were the characteristics of the reproductive phase. Similar reports are available for *Brassica rapa* (Zou et al., 2021) and *Silybum marianum* (Khan et al., 2015) plants.

Development of Adventitious Roots

Biomass and ginsenoside production was affected by the inoculum density of adventitious roots (Jeong et al., 2009). Here, adventitious roots were initiated in a solid medium and established using suspension culture. Our results align with the development of adventitious roots from ginseng in suspension cultures and the biosynthesis of ginsenosides (Yu et al., 2000). Similarly, adventitious root cultures were established for anthocyanin production from *Raphanus sativus* using MS medium (Betsui et al., 2004). Tropane alkaloid production was also observed in adventitious root culture development on Gamborg's B5 medium (Min et al., 2007). Moreover, a full-strength MS medium was used to establish adventitious roots to determine biomass accumulation and production of withanolides. Similarly, Yamamoto and Kamura (1997) reported that a method for culturing adventitious roots, saikosaponin production in *Bupleurum falcatum*, and adventitious root cultures for biomass production in *Panax ginseng* were also studied (Yu et al., 2000). Furthermore, Wu et al. (2006, 2007) achieved the *in vitro* production of adventitious roots with a half-strength MS medium.

CONCLUSION

Medicinal plants have recently gained major attention for their use in healthcare industries due to the trend of phytotherapeutics. Among various medicinal plants, *W. somnifera* has received increasing importance for its broad pharmacological properties against various diseases, including COVID-19. The present

investigation demonstrates the influence of various PGRs on shoots and nodal explants and found that a combination of BAP and KIN enhanced shoot multiplication and growth characteristics. The obtained results showed *in vitro* flowering, increased expression of withanolide biosynthetic pathway genes and withanolide contents during the reproductive phase, and adventitious root cultures for the first time. In addition, we revealed that various metabolites present during the vegetative and reproductive phases by LC-MS analysis. These findings will improve our understanding of the withanolide biosynthetic pathway during different growth phases. In addition, *in vitro* tissue culture propagation using various PGRs provides excellent tools for propagating plants for scientific use and enhances the quantity of its commercial secondary metabolites. Our results are useful for rapid multiplication and isolation of medicinally important withanolides on industrial scales for drug research and as subsequent therapeutics in treating various chronic diseases.

DATA AVAILABILITY STATEMENT

The original contributions presented in this study are included in the article/**Supplementary Material**, further inquiries can be directed to the corresponding author/s.

AUTHOR CONTRIBUTIONS

AM, PR, and A-MB: conceptualization, funding acquisition, and supervision. SAT, PP, MR, AK, ST, and AM: performing the experiments. SAT, AK, PP, MR, KK, and AM: data analysis. AM, SAT, AK, and KK: writing the original draft. AM, SAT, AK, PR, MJ, and A-MB: review and editing with contributions of all authors. All authors contributed to the article and approved the submitted version.

ACKNOWLEDGMENTS

We thank the Manipal Academy of Higher Education (MAHE), Manipal, Karnataka, India, TIFAC-CORE and FIST, DST, New Delhi, and K-FIST, VGST, Govt. of Karnataka, for the facilities. We are grateful to K. Satyamoorthy, Director, Manipal School of Life Sciences, MAHE for their encouragement and support. We are thankful to MAHE for the T.M.A. Pai Ph.D. scholarship to SAT, AK, and KK. We are indebted to the International Cooperation Division, Department of Science and Technology (DST), Govt. of India, New Delhi, for the financial assistance through the Indo-South Africa Joint Collaborative Project (DST/INT/South Africa/P-10/2016 dated 15 September 2016) to AM and as Women Scientist [Ref. No. SR/WOS-A/LS-564/2011 (G) dated 26 July 2012], DST, New Delhi, to PP. We would like to thank M. Radhakrishna Rao for his suggestions.

SUPPLEMENTARY MATERIAL

The Supplementary Material for this article can be found online at: https://www.frontiersin.org/articles/10.3389/fpls.2022.917770/full#supplementary-material

REFERENCES

Agarwal, A. V., Singh, D., Dhar, Y. V., Michael, R., Gupta, P., Chandra, D., et al. (2018). Virus-induced silencing of key genes leads to differential impact on withanolide biosynthesis in the medicinal plant, *Withania somnifera*. *Plant Cell Physiol.* 59, 262–274. doi: 10.1093/pcp/pcx179

Bagadekar, A. N., and Jayaraj, M. (2011). *In vitro* flowering of *Heliotropium indicum* L. – an important medicinal herb. *Asian J. Exp. Biol. Sci.* 2, 90–95.

Baghel, S., and Bansal, Y. K. (2014). Synergistic effect of BAP and GA_3 on *in vitro* flowering of *Guizotia abyssinica* Cass. A multipurpose oil crop. *Physiol. Mol. Biol. Plants* 20, 241–247. doi: 10.1007/s12298-014-0229-3

Betsui, F., Tanaka-Nishikawa, N., and Shimomura, K. (2004). Anthocyanin production in adventitious root cultures of *Raphanus sativus* L. cv. Peking Koushin. *Plant Biotechnol.* 21, 387–391. doi: 10.5511/plantbiotechnology

Chakraborty, N., Banerjee, D., Ghosh, M., Pradhan, P., Gupta, N. S., Acharya, K., et al. (2013). Influence of plant growth regulators on callus mediated regeneration and secondary metabolites synthesis in *Withania somnifera* (L.) Dunal. *Physiol. Mol. Biol. Plants* 19, 117–125. doi: 10.1007/s12298-012-0146-2

Chatterjee, S., Srivastava, S., Khalid, A., Singh, N., Sangwan, R. S., Sidhu, O. P., et al. (2010). Comprehensive metabolic fingerprinting of *Withania somnifera* leaf and root extracts. *Phytochemistry* 71, 1085–1094. doi: 10.1016/j.phytochem.2010.04.001

Chikhale, R. V., Gurav, S. S., Patil, R. B., Sinha, S. K., Prasad, S. K., Shakya, A., et al. (2021). SARS-CoV-2 host entry and replication inhibitors from Indian ginseng: an in-silico approach. *J. Biomol. Struct. Dyn.* 39, 4510–4521. doi: 10.1080/07391102.2020.1778539

Dar, N. J., Hamid, A., and Ahmad, M. (2015). Pharmacologic overview of *Withania somnifera*, the Indian ginseng. *Cell. Mol. Life Sci.* 72, 4445–4460. doi: 10.1007/s00018-015-2012-1

Dhar, N., Rana, S., Bhat, W. W., Razdan, S., Pandith, S. A., Khan, S., et al. (2013). Dynamics of withanolide biosynthesis in relation to temporal expression pattern of metabolic genes in *Withania somnifera* (L.) Dunal: a comparative study in two morpho-chemo variants. *Mol. Biol. Rep*. 40, 7007–7016. doi: 10.1007/s11033-013-2820-z

Dhar, N., Razdan, S., Rana, S., Bhat, W. W., Vishwakarma, R., and Lattoo, S. K. (2015). A decade of molecular understanding of withanolide biosynthesis and in vitro studies in *Withania somnifera* (L.) Dunal: prospects and perspectives for pathway engineering. *Front. Plant Sci.* 6:1031. doi: 10.3389/fpls.2015.01031

Erdag, B. B., and Emek, Y. C. (2009). Adventitious shoot regeneration and *in vitro* flowering of *Anthemis xylopoda* O. Schwarz, a critically endangered Turkish endemic. *Turk. J. Biol.* 33, 319–326. doi: 10.3906/biy-0810-2

Fatima, N., Ahmad, N., and Anis, M. (2011). Enhanced *in vitro* regeneration and change in photosynthetic pigments, biomass and proline content in *Withania somnifera* L. (Dunal) induced by copper and zinc ions. *Plant Physiol. Biochem.* 49, 1465–1471. doi: 10.1016/j.plaphy.2011.08.011

Fatima, N., and Anis, M. (2011). Thidiazuron induced high frequency axillary shoot multiplication in *Withania somnifera* L. Dunal. *J. Med. Plant Res.* 5, 6681–6687. doi: 10.5897/JMPR11.622

Fatima, N., and Anis, M. (2012). Role of growth regulators on in vitro regeneration and histological analysis in Indian ginseng (*Withania somnifera* L.) Dunal. *Physiol. Mol. Biol. Plants* 18, 59–67. doi: 10.1007/s12298-011-0099-x

Gao, X., Zhu, C., Jia, W., Gao, W., Qiu, M., Zhang, Y., et al. (2005). Induction and characterization of adventitious roots directly from the explants of *Panax notoginseng*. *Biotechnol. Lett.* 27, 1771–1775. doi: 10.1007/s10529-005-3553-4

Ghimire, B. K., Seong, E. S., Kim, E. H., Lamsal, K., Yu, C. Y., and Chung, I. M. (2010). Direct shoot organogenesis from petiole and leaf discs of *Withania somnifera* (L.) Dunal. *Afr. J. Biotechnol.* 9, 7453–7461. doi: 10.5897/AJB10.1250

Gomez, K. A., and Gomez, A. A. (1984). *Statistical Procedures for Agricultural Research*. Hoboken, NJ: John Wiley & Sons.

Gurav, N. S., Gurav, S. S., and Sakharwade, S. N. (2020). Studies on *Ashwagandha Ghrita* with reference to murcchana process and storage conditions. *J. Ayurveda Integr. Med.* 11, 243–249. doi: 10.1016/j.jaim.2019.10.004

Jana, S., and Shekhawat, G. S. (2011). Plant growth regulators, adenine sulfate and carbohydrates regulate organogenesis and in vitro flowering of *Anethum graveolens*. *Acta Physiol. Plant.* 33, 305–311. doi: 10.1007/s11738-010-0548-0

Jeong, C. S., Murthy, H. N., Hahn, E. J., Lee, H. L., and Paek, K. Y. (2009). Inoculum size and auxin concentration influence the growth of adventitious roots and accumulation of ginsenosides in suspension cultures of ginseng (*Panax ginseng* CA Meyer). *Acta Physiol. Plant.* 31, 219–222. doi: 10.1007/s11738-008-0206-y

Jeyachandran, R., and Bastin, M. (2013). An efficient protocol for in vitro flowering and fruiting in *Micrococca mercurialis* (L.) Benth. *Int. J. Nat. Appl. Sci.* 2, 18–22.

Jiang, X. L., Piao, X. C., Gao, R., Jin, M. Y., Jiang, J., Jin, X. H., et al. (2017). Improvement of bioactive compound accumulation in adventitious root cultures of an endangered plant species, *Oplopanax elatus*. *Acta Physiol. Plant.* 39:226. doi: 10.1007/s11738-017-2525-3

Jin, H., Yu, Y., Hu, S., Quan, X., and Wu, S. (2020). Effect of nitrogen concentration, source, and phosphate concentration on accumulation of biomass and calycosin-7-O-β-D-glucoside in *Astragalus membranaceus* adventitious roots. *In Vitro Cell. Dev. Biol. Plant* 56, 407–414. doi: 10.1007/s11627-020-10072-1

Joshi, A. G., and Padhya, M. A. (2010). Shoot regeneration from leaf explants of *Withania somnifera* (L.) Dunal. *Not. Sci. Biol.* 2, 63–65. doi: 10.15835/nsb213609

Kalimuthu, K., and Prabakaran, R. (2013). *In vitro* flowering from nodal explants of *Ceropegia pusilla* Wight and Arn. *Int. J. Bot. Res.* 3, 35–42.

Kannan, T. M., and Anbazhakan, S. (2016). Direct regeneration of *Withania somnifera* (L.) Dunal–a medicinal plant. *World Sci. News* 32, 73–83.

Kanungo, S., and Sahoo, S. L. (2011). Direct organogenesis of *Withania somnifera* L. from apical bud. *Int. Res. J. Biotechnol.* 2, 58–61.

Khan, M. A., Abbasi, B. H., Ali, H., Ali, M., Adil, M., and Hussain, I. (2015). Temporal variations in metabolite profiles at different growth phases during somatic embryogenesis of *Silybum marianum* L. *PCTOC* 1201, 127–139. doi: 10.1007/s11240-014-0587-0

Kiran, K. R., Deepika, V. B., Swathy, P. S., Prasad, K., Kabekkodu, S. P., Murali, T. S., et al. (2020). ROS-dependent DNA damage and repair during germination of NaCl primed seeds. *J. Photochem. Photobiol. B Biol.* 213:112050. doi: 10.1016/j.jphotobiol.2020.112050

Kiran, K. R., Swathy, P. S., Paul, B., Prasada, K. S., Rao, M. R., Joshi, M. B., et al. (2021). Untargeted metabolomics and DNA barcoding for discrimination of Phyllanthus species. *J. Ethnopharmacol.* 273:113928. doi: 10.1016/j.jep.2021.113928

Kulkarni, A. A., Thengane, S. R., and Krishnamurthy, K. V. (2000). Direct shoot regeneration from node, internode, hypocotyl and embryo explants of *Withania somnifera*. *PCTOC* 62, 203–209. doi: 10.1023/A:1006413523677

Kulkarni, S. K., and Dhir, A. (2008). *Withania somnifera*: an Indian ginseng. *Prog. Neuro Psychopharmacol. Biol. Psychiatry* 32, 1093–1105. doi: 10.1016/j.pnpbp.2007.09.011

Kumar, O. A., Jyothirmayee, G., and Tata, S. S. (2011). In vitro plant regeneration from leaf explants of *Withania somnifera* (L) Dunal (Ashwaganda)-an important medicinal plant. *Res. Biotechnol.* 2, 34–39.

Kumar, V., Dhanjal, J. K., Kaul, S. C., Wadhwa, R., and Sundar, D. (2020). Withanone and caffeic acid phenethyl ester are predicted to interact with main protease (M^{pro}) of SARS-CoV-2 and inhibit its activity. *J. Biomol. Struct. Dyn.* 39, 3842–3854. doi: 10.1080/07391102.2020.1772108

Lakshmi, S. R., Parthibhan, S., Sherif, N. A., Kumar, T. S., and Rao, M. V. (2017). Micropropagation, *in vitro* flowering, and tuberization in *Brachystelma glabrum* Hook. f., an endemic species. *In Vitro Cell. Dev. Biol. Plant* 53, 64–72.

Logesh, P., Settu, A., Thangavel, K., and Ganapathi, A. (2010). Direct in vitro regeneration of *Withania somnifera* (L.) Dunal through leaf disc culture. *Int. J. Biol. Technol.* 1, 1–4.

Min, J. Y., Jung, H. Y., Kang, S. M., Kim, Y. D., Kang, Y. M., Park, D. J., et al. (2007). Production of tropane alkaloids by small scale bubble column bioreactor cultures of *Scopolia parviflora* adventitious roots. *Bioresour. Technol.* 98, 1748–1753. doi: 10.1016/j.biortech.2006.07.033

Mir, B. A., Mir, S. A., and Koul, S. (2014). In vitro propagation and withaferin A production in *Withania ashwagandha*, a rare medicinal plant of India. *Physiol. Mol. Biol. Plants* 20, 357–364. doi: 10.1007/s12298-014-0243-5

Mohammed, A., Chiruvella, K. K., and Ghanta, R. G. (2016). In vitro plant regeneration, flowering and fruiting from nodal explants of *Andrographis lineata* nees (Acanthaceae). *J. Crop Sci. Biotechnol.* 19, 195–202. doi: 10.1007/s12892-016-0003-x

Murashige, T., and Skoog, F. (1962). A revised medium for rapid growth and bio assays with tobacco tissue cultures. *Physiol. Plant.* 15, 473–497. doi: 10.1111/j.1399-3054.1962.tb08052.x

Poornima, P., Kiran, K. R., Swathy, P. S., and Muthusamy, A. (2019). "*Withania somnifera* (L.) Dunal – an overview of bioactive molecules, medicinal properties and enhancement of bioactive molecules through breeding strategies," in *In vitro Plant Breeding Towards Novel Agronomic Traits – Biotic and Abiotic Stress Tolerance*, eds M. Kumar, A. Muthusamy, V. Kumar, and N. Bhalla-Sarin (Singapore: Springer), 1–25. doi: 10.1007/978-981-32-9824-8_1

Praveen, N., and Murthy, H. N. (2010). Production of withanolide-A from adventitious root cultures of *Withania somnifera*. *Acta Physiol. Plant.* 32, 1017–1022. doi: 10.1007/s11738-010-0489-7

Rangaraju, S., Lokesha, A. N., and Aswath, C. R. (2019). Improved production of withanolides in adventitious root cultures of *Withania somnifera* by suspension culture method. *Biosci. Biotechnol. Res. Commun.* 12, 73–79. doi: 10.21786/bbrc/12.1/10

Rao, S. R., and Ravishankar, G. A. (2002). Plant cell cultures: chemical factories of secondary metabolites. *Biotechnol. Adv.* 20, 101–153. doi: 10.1016/S0734-9750(02)00007-1

Sabir, F., Sangwan, N. S., Chaurasiya, N. D., Misra, L. N., and Sangwan, R. S. (2008). In vitro withanolide production by *Withania somnifera* L. cultures. *Z. Naturforsch. C.* 63, 409–412.

Saggam, A., Limgaokar, K., Borse, S., Chavan-Gautam, P., Dixit, S., Tillu, G., et al. (2021). *Withania somnifera* (L.) Dunal: opportunity for clinical repurposing in COVID-19 management. *Front. Pharmacol.* 12:623795. doi: 10.3389/fphar.2021.623795

Sangwan, R. S., Chaurasiya, N. D., Lal, P., Misra, L., Tuli, R., and Sangwan, N. S. (2008). Withanolide A is inherently de novo biosynthesized in roots of the medicinal plant ashwagandha (*Withania somnifera*). *Physiol. Plant.* 133, 278–287. doi: 10.1111/j.1399-3054.2008.01076.x

Sangwan, R. S., Chaurasiya, N. D., Misra, L. N., Lal, P., Uniyal, G. C., Sharma, R., et al. (2004). Phytochemical variability in commercial herbal products and preparations of *Withania somnifera* (Ashwagandha). *Curr. Sci.* 86, 461–465.

Saritha, K. V., and Naidu, C. V. (2007). In vitro flowering of *Withania somnifera* Dunal.—an important antitumor medicinal plant. *Plant Sci.* 172, 847–851. doi: 10.1016/j.plantsci.2006.12.016

Sathiyabama, M., and Parthasarathy, R. (2018). Withanolide production by fungal endophyte isolated from *Withania somnifera*. *Nat. Prod. Res.* 32, 1573–1577. doi: 10.1080/14786419.2017.1389934

Saxena, P., Ahlawat, S., Ali, A., Khan, S., and Abdin, M. Z. (2017). Gene expression analysis of the withanolide biosynthetic pathway in hairy root cultures of *Withania somnifera* elicited with methyl jasmonate and the fungus *Piriformospora indica*. *Symbiosis* 71, 143–154. doi: 10.1007/s13199-016-0416-9

Sen, J., and Sharma, A. K. (1991). Micropropagation of *Withania somnifera* from germinating seeds and shoot tips. *PCTOC* 26, 71–73. doi: 10.1007/BF00036108

Senthil, K., Thirugnanasambantham, P., Oh, T. J., Kim, S. H., and Choi, H. K. (2015). Free radical scavenging activity and comparative metabolic profiling of in vitro cultured and field grown *Withania somnifera* roots. *PLoS One* 10:e0123360. doi: 10.1371/journal.pone.0123360

Sharma, A., Rana, S., Rather, G. A., Misra, P., Dhar, M. K., and Lattoo, S. K. (2020). Characterization and overexpression of sterol Δ22-desaturase, a key enzyme modulates the biosyntheses of stigmasterol and withanolides in *Withania somnifera* (L.) Dunal. *Plant Sci.* 301:110642. doi: 10.1016/j.plantsci.2020.110642

Sharma, V., Kamal, B., Srivastava, N., Dobriyal, A. K., and Jadon, V. S. (2014). *In Vitro* flower induction from shoots regenerated from cultured axillary buds of endangered medicinal herb *Swertia chirayita* H. Karst. *Biotechnol. Res. Int.* 2014:264690. doi: 10.1155/2014/264690

Shasmita, Rai, M. K., and Naik, S. K. (2018). Exploring plant tissue culture in *Withania somnifera* (L.) Dunal: in vitro propagation and secondary metabolite production. *Crit. Rev. Biotechnol.* 38, 836–850. doi: 10.1080/07388551.2017.1416453

Shyamali, S., and Kazumi, H. (2007). "Advances in plant ethylene research," in *Proceedings of the 7th International Symposium on the Plant Hormone Ethylene* (Dordrecht: Springer), 153–155. doi: 10.1007/978-1-4020-6014-4

Siddique, N. A., Bari, M. A., Shahnewaz, S., Rahman, M. H., Hasan, M. R., Khan, M. S. I., et al. (2004). Plant regeneration of *Withania somnifera* (L.) Dunal (Ashwagandha) from nodal segments derived callus an endangered medicinal plant in Bangladesh. *J. Biol. Sci.* 4, 219–223. doi: 10.3923/jbs.2004.219.223

Singh, P., Guleri, R., and Pati, P. K. (2016). "In vitro propagation of *Withania somnifera* (L.) Dunal," in *Protocols for In Vitro Cultures and Secondary Metabolite Analysis of Aromatic and Medicinal Plants*, 2nd Edn. ed. S. Jain (New York, NY: Humana Press), 201–213. doi: 10.1007/978-1-4939-3332-7_14

Singh, P., Guleri, R., Singh, V., Kaur, G., Kataria, H., Singh, B., et al. (2015). Biotechnological interventions in *Withania somnifera* (L.) Dunal. *Biotechnol. Genet. Eng. Rev.* 31, 1–20. doi: 10.1080/02648725.2015.1020467

Singh, R., Gupta, P., Khan, F., Singh, S. K., Mishra, T., Kumar, A., et al. (2018). Modulations in primary and secondary metabolic pathways and adjustment in physiological behaviour of *Withania somnifera* under drought stress. *Plant Sci.* 272, 42–54. doi: 10.1016/j.plantsci.2018.03.029

Singh, S., Pal, S., Shanker, K., Chanotiya, C. S., Gupta, M. M., Dwivedi, U. N., et al. (2014). Sterol partitioning by HMGR and DXR for routing intermediates toward withanolide biosynthesis. *Physiol. Plant* 152, 617–633. doi: 10.1111/ppl.12213

Sivanandhan, G., Arun, M., Mayavan, S., Rajesh, M., Jeyaraj, M., Dev, G. K., et al. (2012). Optimization of elicitation conditions with methyl jasmonate and salicylic acid to improve the productivity of withanolides in the adventitious root culture of *Withania somnifera* (L.) Dunal. *Appl. Biochem. Biotechnol.* 168, 681–696. doi: 10.1007/s12010-012-9809-2

Sivanandhan, G., Mariashibu, T. S., Arun, M., Rajesh, M., Kasthurirengan, S., Selvaraj, N., et al. (2011). The effect of polyamines on the efficiency of multiplication and rooting of *Withania somnifera* (L.) Dunal and content of some withanolides in obtained plants. *Acta. Physiol. Plant.* 33, 2279–2288. doi: 10.1007/s11738-011-0768-y

Sivanandhan, G., Selvaraj, N., Ganapathi, A., and Manickavasagam, M. (2015). Effect of nitrogen and carbon sources on in vitro shoot multiplication, root induction and withanolides content in *Withania somnifera* (L.) Dunal. *Acta Physiol. Plant.* 37, 1–12. doi: 10.1007/s11738-014-1758-7

Sivanesan, I. (2007). Direct regeneration from apical bud explants of *Withania somnifera* Dunal. *Indian J. Biotechnol.* 6, 125–127.

Sivanesan, I., and Murugesan, K. (2008). An efficient regeneration from nodal explants of *Withania somnifera* Dunal. *Asian J. Plant Sci.* 7, 551–556. doi: 10.3923/ajps.2008.551.556

Srivastava, Y., and Sangwan, N. S. (2020). "Improving medicinal crops through phytochemical perspective: *Withania somnifera* (Ashwagandha)," in *Advancement in Crop Improvement Techniques*, eds N. Tuteja, R. Tuteja, N. Passricha, and S. K. Saifi (Duxford: Woodhead Publishing), 275–295. doi: 10.1016/B978-0-12-818581-0.00017-6

Sudhakaran, S., and Sivasankari, V. (2002). In vitro flowering response of *Ocimum basilicum* L. *J. Plant Biotechnol.* 4, 179–181.

Supe, U., Dhote, F., and Roymon, M. G. (2011). A review on micro propagation of *Withania somnifera*–a medicinal plant. *J. Agric. Sci. Technol.* 7, 1475–1483.

Swathy, P. S., Kiran, K. R., Joshi, M. B., Mahato, K. K., and Muthusamy, A. (2021). He–Ne laser accelerates seed germination by modulating growth hormones and reprogramming metabolism in brinjal. *Sci. Rep.* 11:7948. doi: 10.1038/s41598-021-86984-8

Taylor, N. J., Light, M. E., and Van Staden, J. (2005). In vitro flowering of *Kniphofia leucocephala*: influence of cytokinins. *PCTOC* 83, 327–333. doi: 10.1023/B:GROW.0000014889.16196.f7

Thiruvengadam, M., and Jayabalan, N. (2001). In vitro flowering of *Vitex negundo* L., a medicinal plant. *Plant Cell Biotechnol. Mol. Biol.* 2, 67–70.

Thorat, S. A., Poornima, P., Arya, K., Kiran, K. R., Satyamoorthy, K., Mahato, K. K., et al. (2021). Red laser-mediated alterations in seed germination, growth, pigments and withanolide content of ashwagandha [*Withania somnifera* (L.) Dunal]. *J. Photochem. Photobiol. B Biol.* 216:112144. doi: 10.1016/j.jphotobiol.2021.112144

Udayakumar, R., Choi, C. W., Kim, K. T., Kim, S. C., Kasthurirengan, S., Mariashibu, T. S., et al. (2013). In vitro plant regeneration from epicotyl explant of *Withania somnifera* (L.) Dunal. *J. Med. Plant Res.* 7, 43–52. doi: 10.5897/JMPR12.087

Verma, R., and Singh, R. R. (2007). Regeneration and *in vitro* flowering in *Brassica campestris* L. var. *Bhavani*. *Our Nat.* 5, 21–24. doi: 10.3126/on.v5i1.793

Verpoorte, R., Contin, A., and Memelink, J. (2002). Biotechnology for the production of plant secondary metabolites. *Phytochem. Rev.* 1, 13–25. doi: 10.1023/A:1015871916833

Wadegaonkar, P. A., Bhagwat, K. A., and Rai, M. K. (2006). Direct rhizogenesis and establishment of fast growing normal root organ culture of *Withania somnifera* Dunal. *PCTOC* 84, 223–225. doi: 10.1007/s11240-005-9011-0

Wu, C. H., Dewir, Y. H., Hahn, E. J., and Paek, K. Y. (2006). Optimization of culturing conditions for the production of biomass and phenolics from adventitious roots of *Echinacea angustifolia*. *J. Plant Biol.* 49, 193–199. doi: 10.1007/BF03030532

Wu, C. H., Murthy, H. N., Hahn, E. J., and Paek, K. Y. (2007). Large-scale cultivation of adventitious roots of *Echinacea purpurea* in airlift bioreactors for the production of chichoric acid, chlorogenic acid and caftaric acid. *Biotechnol. Lett.* 29, 1179–1182. doi: 10.1007/s10529-007-9399-1

Yamamoto, O., and Kamura, K. (1997). Production of saikosaponin in cultured roots of *Bupleurum falcatum* L. *Plant Tiss. Cult. Biotechnol.* 3, 138–147.

Yu, K. W., Hahn, E. J., and Paek, K. Y. (2000). Production of adventitious ginseng roots using bioreactors. *Korean J. Plant Tiss. Cult.* 27, 309–315.

Zou, L., Tan, W. K., Du, Y., Lee, H. W., Liang, X., Lei, J., et al. (2021). Nutritional metabolites in *Brassica rapa* subsp. *chinensis* var. *parachinensis* (choy sum) at three different growth stages: microgreen, seedling and adult plant. *Food Chem.* 357:129535. doi: 10.1016/j.foodchem.2021.129535

Conflict of Interest: The authors declare that the research was conducted in the absence of any commercial or financial relationships that could be construed as a potential conflict of interest.

Publisher's Note: All claims expressed in this article are solely those of the authors and do not necessarily represent those of their affiliated organizations, or those of the publisher, the editors and the reviewers. Any product that may be evaluated in this article, or claim that may be made by its manufacturer, is not guaranteed or endorsed by the publisher.

Copyright © 2022 Thorat, Kaniyassery, Poojari, Rangel, Tantry, Kiran, Joshi, Rai, Botha and Muthusamy. This is an open-access article distributed under the terms of the Creative Commons Attribution License (CC BY). The use, distribution or reproduction in other forums is permitted, provided the original author(s) and the copyright owner(s) are credited and that the original publication in this journal is cited, in accordance with accepted academic practice. No use, distribution or reproduction is permitted which does not comply with these terms.

frontiers | Frontiers in Plant Science

TYPE Original Research
PUBLISHED 25 July 2022
DOI 10.3389/fpls.2022.916550

Check for updates

OPEN ACCESS

EDITED BY
Peng Zhang,
Center for Excellence in Molecular Plant Sciences (CAS), China

REVIEWED BY
Florencia Díaz-Viraqué,
Institut Pasteur de Montevideo, Uruguay
Jia-Ming Song,
Guangxi University, China

*CORRESPONDENCE
Yanping Lan
lanyanping2000@126.com

SPECIALTY SECTION
This article was submitted to Plant Biotechnology, a section of the journal Frontiers in Plant Science

RECEIVED 09 April 2022
ACCEPTED 05 July 2022
PUBLISHED 25 July 2022

CITATION
Hu G, Cheng L, Cheng Y, Mao W, Qiao Y and Lan Y (2022) Pan-genome analysis of three main Chinese chestnut varieties.
Front. Plant Sci. 13:916550.
doi: 10.3389/fpls.2022.916550

COPYRIGHT
© 2022 Hu, Cheng, Cheng, Mao, Qiao and Lan. This is an open-access article distributed under the terms of the Creative Commons Attribution License (CC BY). The use, distribution or reproduction in other forums is permitted, provided the original author(s) and the copyright owner(s) are credited and that the original publication in this journal is cited, in accordance with accepted academic practice. No use, distribution or reproduction is permitted which does not comply with these terms.

Pan-genome analysis of three main Chinese chestnut varieties

Guanglong Hu, Lili Cheng, Yunhe Cheng, Weitao Mao, Yanjie Qiao and Yanping Lan*

Engineering & Technology Research Center for Chestnut of National Forestry and Grassland Administration, Key Laboratory of Biology and Genetic Improvement of Horticultural Crops (North China) of Ministry of Agriculture, Beijing Engineering Research Center for Deciduous Fruit Trees, Institute of Forestry and Pomology, Beijing Academy of Agriculture and Forestry Sciences, Beijing, China

Chinese chestnut (*Castanea mollissima* Blume) is one of the earliest domesticated plants of high nutritional and ecological value, yet mechanisms of *C. mollissima* underlying its growth and development are poorly understood. Although individual chestnut species differ greatly, the molecular basis of the formation of their characteristic traits remains unknown. Though the draft genomes of chestnut have been previously released, the pan-genome of different variety needs to be studied. We report the genome sequence of three cultivated varieties of chestnut herein, namely Hei-Shan-Zhai-7 (H7, drought-resistant variety), Yan-Hong (YH, easy-pruning variety), and Yan-Shan-Zao-Sheng (ZS, early-maturing variety), to expedite convenience and efficiency in its genetics-based breeding. We obtained three chromosome-level chestnut genome assemblies through a combination of Oxford Nanopore technology, Illumina HiSeq X, and Hi-C mapping. The final genome assemblies are 671.99Mb (YH), 790.99Mb (ZS), and 678.90Mb (H7), across 12 chromosomes, with scaffold N50 sizes of 50.50Mb (YH), 65.05Mb (ZS), and 52.16Mb (H7). Through the identification of homologous genes and the cluster analysis of gene families, we found that H7, YH and ZS had 159, 131, and 91 unique gene families, respectively, and there were 13,248 single-copy direct homologous genes in the three chestnut varieties. For the convenience of research, the chestnut genome database[1] was constructed. Based on the results of gene family identification, the presence/absence variations (PAVs) information of the three sample genes was calculated, and a total of 2,364, 2,232, and 1,475 unique genes were identified in H7, YH and ZS, respectively. Our results suggest that the *GBSS II-b* gene family underwent expansion in chestnut (relative to nearest source species). Overall, we developed high-quality and well-annotated genome sequences of three *C. mollissima* varieties, which will facilitate clarifying the molecular mechanisms underlying important traits, and shortening the breeding process.

KEYWORDS

***Castanea mollissima*, *de novo* assembly, pan-genome, waxy gene, Nanopore sequencing, genome database**

1 http://www.chestnutgenome.cn/#/map

Introduction

In 2020, at least 720 million people (≥9.9% of the global population) faced hunger, this represents an increase over previous years, and the greatest percentage of the total population since 2010 (FAO, IFAD, UNICEF, WFP, and WHO, 2021). Because of the ongoing climate change as well as the increasing global population and the COVID19 pandemic, the number of people facing hunger is expected to rise significantly. To alleviate global hunger, more attention needs to be given to non-staple food crops (Chapman et al., 2022). Historically, chestnuts was promoted to fight hunger (Gabriele et al., 2020). The XVIIIth century is considered by many as the worst century of hunger, because of which the chestnut tree tirelessly renewed its aid and continued to feed mountain residents (Adua, 1999).

Chinese chestnut (*C. mollissima* Blume; Fagaceae) has been cultivated for more than 6,000 years in the Banpo Ruins of Xi'an, China, according to archeological findings (Hao and Zhang, 2014). Chestnut is an important tree species currently cultivated in eastern Asia, both for its ecological and economic advantages. China is considered a gene center for the genus *Castanea* (Vavilov, 1952; Zhang et al., 2015). The chestnut is a traditional nut and also a popular food around the world (Guo et al., 2019). China is one of the top producers of chestnuts (Wang et al., 2020b). Over 300 cultivars have been selected for nut production (Li et al., 2009) Many characteristics of the chestnut plant affect its growth and development which in turn affects the development of the chestnut industry.

Presently, most of the chestnut varieties sold in the market are mid- and late-maturing, which cannot adequately meet the diversified needs of the market. Early-maturing chestnut varieties could be put on the market earlier, which would greatly improve the overall value of the nut (Cao, 2015) However, only a few early maturing cultivars are available in the market, which have the disadvantages of not being drought tolerant and not easily pruned. Breeding Early-maturing cultivars that are drought-resistant and easy-pruning is a priority for chestnut breeding (Ren and Jia, 2014; Zhao and Zhang, 2015). Fortunately we have bred three main cultivation varieties namely Hei-Shan-Zhai-7 (drought-resistant variety; Huang et al., 2009), Yan-Hong (easy-pruning variety; Gao et al., 1980), and Yan-Shan-Zao-Sheng (early-maturing variety; Cheng et al., 2013). If more varieties with early maturity, drought resistance and easy-pruning characteristics are sequenced, it will expedite clarifying the molecular mechanisms underlying these traits and shortening the breeding process.

Starch is one of the most important components of a chestnut, and accounts for 50–80% of its dry matter content (Liu et al., 2015). Chestnut starch is considered as a potentially functional component of dietary fiber, which may be sources of resistant starch, thus improving health (Liu et al., 2022). Given the rapid development of starch-based foods, chestnut starch shows increasing application potential. There have been numerous studies on chestnut as a new source of starch (Liu et al., 2015, 2019). The characteristics of chestnut starch vary greatly with the variety and its geographical distribution (Long et al., 2018). Waxiness is one of the most important edible qualities of chestnuts; however, this trait also varies greatly with the genotype and production area. The proportion of amylopectin and amylose in chestnut kernel starch varies among cultivars (Liang, 2011). However, there are few reports on waxy genes in chestnut due to the lack of genome sequence information.

There has been a rapid increase in the number of pan-genome studies on plants. The first published plant pan-genome was based on a comparison of whole-genome assemblies of seven wild soybean (*Glycine soja*) accessions (Li et al., 2014). Simultaneously, another study examined the pan-genome of rice (*Oryza sativa*), based on three divergent accessions (Schatz et al., 2014). In recent years, there has been a surge in plant genome sequencing projects and in the comparison of multiple related individuals. The high degree of genomic variation observed among individuals belonging to the same species led to the realization that single reference genomes do not represent the diversity within a species, which in turn led to the expansion of the pan-genome concept. Pan-genomes represent the genomic diversity of a species, and include core genes (i.e., genes found in all individuals) as well as variable genes (i.e., genes absent in some individuals). Genes involved in biotic and abiotic stress responses are commonly enriched within the variable gene groups. The growth of pan-genomics in plants and exploration of gene presence/absence variations (PAVs) can support plant breeding and evolutionary studies (Bayer et al., 2020).

Although the genome sequence of Chinese chestnut has been reported previously (LaBonte et al., 2018; Xing et al., 2019; Sun et al., 2020; Wang et al., 2020a), higher quality genome assembly and pan-genome analysis are required. In the present study, we generated high-quality chromosome-level reference genome assemblies of three *C. mollissima* varieties, namely Hei-Shan-Zhai-7 (drought-resistant variety), Yan-Hong (easy-pruning variety), and Yan-Shan-Zao-Sheng (early-maturing variety), using Oxford Nanopore Technology (ONT) and Illumina HiSeq X sequencing and Hi-C mapping, subsequently, we performed a pan-genome analysis and constructed a chestnut genome database. These results will help reveal differences in the traits of the three varieties and will support breeding programs aimed at the genetic improvement of chestnuts.

Materials and methods

Sampling collection and sequencing

Three chestnut including Hei-Shan-Zhai-7 (H7), Yan-Hong (YH), and Yan-Shan-Zao-Sheng (ZS) were used in this study. Healthy leaves were collected from the tress of all three varieties

growing in Shachang Village (40.3875°N, 117.0275°E), Miyun District, Beijing, China. The freshly harvested samples were immediately frozen in liquid nitrogen. High-quality and high-molecular-weight genomic DNA was extracted from the frozen leaves using the cetyltrimethylammonium bromide (CTAB) method (Yan et al., 2018). The quality and concentration of the extracted genomic DNA were examined by 1% agarose gel electrophoresis and with a Qubit fluorimeter (Invitrogen, Carlsbad, CA, United States). This high-quality DNA was used for subsequent Nanopore and Illumina sequencing.

Library construction and genome sequencing

Approximately 15 μg of genomic DNA was subjected to size selection using the BluePippin system (Sage Science, Beverly, MA, United States), and the size-selected 30–80-kb fragments were processed using the Ligation Sequencing Kit 1D (SQK-LSK109), according to the manufacturer's instructions, to generate ONT long-reads. Briefly, DNA fragments were repaired using the NEBNext FFPE Repair Mix (New England Biolabs, Ipswich, MA, United States). After end reparation and 3′-adenylation with the NEBNext End Repair/dA-Tailing Module reagents, ONT sequencing adapters were ligated to the fragments using the NEBNext Quick Ligation Module (E6056). The final library was sequenced on three different R9.4 flow cells using the PromethION DNA sequencer (Oxford Nanopore, Oxford, United Kingdom) for 48 h. The MinKNOW software (version 2.0) was used to conduct base calling from the raw signal data and to convert the fast5 files into fastq files. The resultant raw data were then filtered to remove reads less than 5 kb in size (short reads) and those containing low-quality bases and adapter sequences.

Illumina sequencing

Paired-end (PE) libraries, with 300-bp insert size, were constructed according to the Illumina standard protocol (San Diego, CA, United States), and subjected to PE (2 × 150 bp) sequencing on the Illumina HiSeq X Ten platform (Illumina, San Diego, CA, United States). Reads with low-quality bases, adapter sequences, and duplicated sequences were discarded, and the resultant clean reads were used for all subsequent analyses.

Genome assembly

Canu (version 1.5; Koren et al., 2017) was used to perform the initial read correction, and genome assembly was constructed using Wtdbg.[2] The consensus assembly was generated using two rounds of Racon (version 1.32; Robert et al., 2017) and three rounds of Pilon (version 1.21; Walker et al., 2017), which polished the Illumina reads using default settings.

Hi-C library construction and sequencing

We constructed Hi-C fragment libraries as described previously. (Rao et al., 2014). Briefly, the leaf tissues were fixed in formaldehyde, and then treated with *Hin*dIII restriction endonuclease to digest all DNA. The 5′ overhang of each fragment was repaired, labeled with biotinylated nucleotides, and ligated in a small volume. After reversing the crosslinks, the ligated DNA was purified and sheared to a length of 300–700 bp. The DNA fragments exhibiting interaction were captured with streptavidin beads and prepared for Illumina sequencing. The final Hi-C libraries were sequenced on the Illumina HiSeq X Ten platform (Illumina, San Diego, CA, United States) to obtain 2 × 150 bp PE reads. The quality of the Hi-C data was assessed through a two-step process. First, an insert fragment frequency plot was constructed to detect the quality of the Illumina sequencing. Then, BWA-MEM (version 0.7.10-r789; Li and Durbin, 2009) was used to align the clean PE reads to the construct the genome assembly draft. Finally, Hi-C-Pro (version 2.10.0; Servant et al., 2015) was used to find all valid reads from unique mapped read pairs.

Chromosomal-level genome assembly using Hi-C data

To correct contig error, a preassembly was generated by breaking the contigs into segments with an average length of 500 kb and then mapping the Hi-C data to these segments using BWA-MEM (version 0.7.10-r789; Li and Durbin, 2009). The corrected Hi-C contigs and valid reads were used to perform chromosomal-level genome assembly using LACHESIS (Burton et al., 2013) with the following parameters:

CLUSTER_MIN_RE_SITES = 22;CLUSTER_MAX_LINK_DENSITY = 2;CLUSTER_NONINFORMATIVE_RATIO = 2;ORDER_MIN_N_RES_IN_TRUNK = 10;ORDER_MIN_N_RES_IN_SHREDS = 10.

A genome-wide Hi-C heatmap was generated for each varieties using ggplot2 in the R package to evaluate the quality of the chromosomal-level genome assembly.

Assessment of the genome assemblies

The Illumina reads were first aligned to the filefish assembly using BWA-MEM (version 0.7.10-r789; Li and Durbin, 2009) to assess genome assembly completeness and accuracy. Subsequently, CEGMA (version 2.5; Parra et al., 2007) was used to find core eukaryotic genes (CEGs) in the genome, with the identity parameter set to >70%. Finally, the completeness of the genome

2 https://github.com/ruanjue/wtdbg

assembly was evaluated using benchmarking sets of universal single-copy orthologs (BUSCO; version 2.0; Simão et al., 2015).

Repeat annotation, gene prediction, and gene annotation

Because of the relatively low conservation of interspecies repeat sequences, a specific repeat sequence database needs to be constructed to predict species-specific repeat sequences. LTR-FINDER (version 1.05; Xu and Wang, 2007) and RepeatScout (version 1.0.5; Bai, 2007) were used to identify repetitive sequences in the chestnut genome sequences assembled in this study. Then, a repeat sequence database was constructed based on the principles of structural and *de novo* repeat prediction. These predicted repeats were classified using PASTEClassifer (version 1.0; Claire et al., 2017), and then merged with the Repbase database (version 19.06; Jurka et al., 2005) to create the final repeat database. Finally, RepeatMasker (version 4.0.6; Tarailo Graovac and Chen, 2009) was used to detect all repetitive sequences in the chestnut genome from that database with the following parameters: "-nolow -no_is -norna -engine wublast."

The genomic structure of the three Chinese chestnut varieties was determined using three approaches: *ab initio* prediction, homologous sequence search, and unigene predictions. The *ab initio* prediction was performed with Genscan (Burge and Karlin, 1997), Augustus (version 2.4; Stanke and Waack, 2003), GlimmerHMM (version 3.0.4; Majoros et al., 2004), GeneID (version 1.4; Blanco et al., 2007), and SNAP (version 2006-07-28; Korf, 2004). To predict genes in chestnut varieties based on homology, GeMoMa (version 1.3.1; Keilwagen et al., 2016; Jens et al., 2018) was used to search the genomes of *Arabidopsis thaliana*, *O. sativa*, *Quercus robur*, and *Fraxinus excelsior*. Then, based on these referenced transcripts, the chestnut genome assemblies were screened using Hisat (version 2.0.4; Kim et al., 2015), Stringtie (version 1.2.3; Pertea et al., 2015), TransDecoder (version 2.0),[3] and GeneMarkS-T (version 5.1; Tang et al., 2015). PASA (version 2.0.2; Campbell et al., 2006) was used to predict unigene sequences, without reference assembly, based on transcriptome data. Finally, the results obtained using the above methods were integrated by EVM (version 1.1.1; Haas et al., 2008), and modified with PASA (version 2.0.2; Campbell et al., 2006).

The predicted gene sequences were then compared with non-redundant (NR) protein sequences at the National Center for Biotechnology Information (NCBI; Marchler et al., 2011), euKaryotic Orthologous Groups of proteins (KOG; Koonin et al., 2004), Gene Ontology (GO; Dimmer et al., 2012), Kyoto encyclopedia of genes and genomes (KEGG; Kanehisa and Goto, 2000), and TrEMBL (Boeckmann et al., 2003) functional databases using BLAST (version 2.2.31; Altschul et al., 1990) with an e-value cutoff of 1E−5. Non-coding RNA, microRNA, and ribosomal RNA (rRNA) sequences were predicted by genome-wide alignment using BLAST (version 2.2.31; Altschul et al., 1990) based on the Rfam database (version 1.3.1; Griffiths et al., 2005). Transfer RNAs (tRNAs) were identified using tRNAscan-SE (version 1.3.1; Lowe and Eddy, 1997).

Comparative genomics

To resolve the phylogenetic position of the *C. mollissima* varieties (YH, H7, and ZS), OrthoMCL (version 2.0.9; Li et al., 2003) was first used to detect orthologous groups by retrieving the protein data of 10 plant species: Chinese chestnut (*C. mollissima*; Xing et al., 2019), summer squash (*Cucurbita pepo*; Montero et al., 2018), wild pear (*Pyrus betulifolia*; Dong et al., 2020), mulberry (*Morus notabilis*; He et al., 2013), peach (*Prunus persica*; Verde et al., 2013), oak (*Q. robur*; Plomion et al., 2018), indica rice (*O. sativa* subsp. *indica*; Du et al., 2017), mei (*Prunus mume*; Zhang et al., 2012), horsetail she-oak (*Casuarina equisetifolia*; Ye et al., 2019), and apple (*Malus domestica*; Zhang et al., 2019). Then using the single-copy protein sequences of *C. mollissima* (H7, YH, and ZS) and nine other chestnut species, an evolutionary tree was constructed using PHYML (version 3.0; Stéphane et al., 2010). The divergence time among species was estimated using the MCMCTree program of the PAML (version 4.0) package (Yang, 2007), and gene families that underwent expansion or contraction were identified using CAFÉ (version 4.0; de Bie et al., 2006). Collinearity analysis with the genome of *Q. robur* (parameter: -l 10,000, other parameters are default), and visualization of differences in size among the three genomes, the MUMmer software (Kurtz et al., 2004) was used to identify similar regions.

Pan-genome of three varieties of Chinese chestnut

Pan-genome enables the exploration of genetic variation and diversity among species, which is essential to fully understand the genetic control of phenotypes (Lu et al., 2015). Blastp (version 2.7.1; Jacob et al., 2008) was used to compare all protein sequences of the three chestnuts, with the following parameter: "-evalue 1e-5." Then, OrthoMCL (version 2.0.9) was used to identify homologous genes according to the comparison results. Finally, OrthoMCL (McL-14-137) was used to cluster the gene families, with the following parameters: "-I 1.5" and "-TE 20."

Construction of the chestnut genome database

The Chestnut Genome Database was set up using Tomcat and MySQL. The backend was designed and implemented using the SpringBoot + MyBatis framework, with CentOS as the server. Data were visualized using an open source ECharts

3 http://transdecoder.github.io

package. The genomic data of four chestnut varieties, H7, YH, ZS, and N11-1(Wang et al., 2020a), have been included in this database.

Characterization of waxy genes (*GBSS II*) in *Castanea mollissima*

The reference genome sequences and gene structure annotation information of *C. mollissima* varieties were downloaded from the Chestnut Genome Database (See Footnote 1). All protein sequences encoded by the waxy gene family were downloaded from the SwissProt database. With-evaluate is set to 1e-5, then blastp is used to search all possible waxy homology in *C. mollissima* (Altschul et al., 1990). We have also employed the HMMER web server (Finn et al., 2011). All public available waxy protein sequences were aligned using the MUSCLE software (Edgar, 2004) with default parameters. The Hidden Markov Model (HMM) model was constructed with the alignment results. Waxy genes sequences identified using BLAST and HMM method were then combined for further motif and domain analyses. The MEME software (Timothy et al., 2015) was employed to identify conserved motifs. Phylogenetic trees were constructed using IQtree (Lam-Tung et al., 2015). Conserved domains were predicted on the NCBI CDD database (Marchler-Bauer et al., 2015); All abovementioned results were visualized using TBtools software (Chen et al., 2020). With the help of TBtools, we have found two waxy genes were mis-assembled as one. Gene structure prediction and curation were conducted using the Fgenesh (Solovyev et al., 2006) software. With the high-quality waxy gene structure annotation, the gene position, exon number, and open reading frame (ORF) length were summarized using the GXF Stat function of the TBtools software. The subcellular localization of the GBSS protein family members was predicted using the CellO (Yu et al., 2006) software.

Data availability statement

The sequencing datasets and genome assemblies have been deposited in public repositories. The Illumina genome sequencing data were deposited in the NCBI Sequence Read Archive under the accession numbers SRR16288271 (Hei-Shan-Zhai-7), SRR16288268 (Yan-Hong) and SRR16288265 (Yan-Shan-Zao-Sheng). The Nanopore genome sequencing data were deposited in the NCBI Sequence Read Archive under the accession numbers SRR16288270 (Hei-Shan-Zhai-7), SRR16288267 (Yan-Hong) and SRR16288264 (Yan-Shan-Zao-Sheng). The Hi-C sequencing data were deposited in the NCBI Sequence Read Archive under the accession numbers SRR16288269 (Hei-Shan-Zhai-7), SRR16288266 (Yan-Hong) and SRR16288263 (Yan-Shan-Zao-Sheng). The URL links of accession numbers are listed in Supplementary Table S17.

Results and discussion

Genome assembly

Based on the distribution of 21-mers among the Illumina HiSeq reads. The genomes of *C. mollissima* were estimated to be 664.89 Mb (YH), 628.90 Mb (H7) and752.70 Mb (ZS), with approximately 0.98% (YH), 1.05% (H7) and 0.60% (ZS) heterozygosity. The k-mer distribution curve peaked at a depth of 57 (zs), 51 (YH) and 58 (H7), with a k-mer number of 34,316,017,419(YH), 36,619,119,572 (H7) and 43,087,876,811 (ZS; Supplementary Figure S1).

Three varieties of Chinese chestnut (YH, H7, and ZS) were sequenced using PromethION DNA sequencer. Overall, approximately 95.01, 99.22, and 83.62 Gb of clean data at a total sequencing depth of approximately 104×, 126×, and 122× were obtained for YH, H7, and ZS, respectively.

Nanopore's third-generation data were corrected to obtain high-accuracy data. Canu (version 1.5; Koren et al., 2017) was used to perform the initial read correction, and genome assembly was constructed using Wtdbg. The consensus assembly was generated using two rounds of Racon (version 1.32; Robert et al., 2017) and three rounds of Pilon (version 1.21; Walker et al., 2017), which polished the Illumina reads using default settings. The total lengths of the genome sequences were determined to be 679.87 Mb with a contig N50 of 3.65 Mb (YH), 790.99 Mb with a contig N50 of 2.17 Mb (ZS), and 687.24 Mb with a contig N50 of 3.39 Mb (H7; Table 1).

Hi-C libraries were sequenced on the Illumina sequencing platform using the Sequencing By Synthesis (SBS) technology, generating 325,605,014 (YH), 295,593,125 (ZS), and 284,973,447 (H7) reads.

To evaluate the quality of the Hi-C data, we plotted the frequencies of insert fragment length (Supplementary Figure S2). The fragment length distribution curve of all three varieties showed a peak at approximately 300 bp, which is consistent with the target size, and the peak type was narrow. Approximately 84.24% (YH), 90.36% (ZS), and 89.98% (H7) of the Hi-C read pairs could be successfully mapped on to the genome, and 62.01% (YH), 59.63% (ZS), and 56.15% (H7) of the read pairs could be uniquely mapped.

Our analyses showed 201,899,176 (YH), 176,262,008 (ZS), and 160,005,850 (H7) read pairs were uniquely correlated with the genome, respectively. Among these, 104,212,288 (YH),

TABLE 1 Summary of three *C. mollissima* genomes assembly.

Parameter	YH	H7	ZS
No. of contigs	1,514	1,460	827
Contig length (bp)	679,866,993	687,236,598	790,986,026
N50 (bp)	3,649,215	3,389,933	2,174,699
N90 (bp)	330,218	448,929	436,758
Contig max (bp)	24,666,180	21,536,999	14,385,919

129,536,245 (ZS), and 152,766,648 (H7) pairs were valid Hi-C data, thus accounting for 51.62, 73.49, and 95.48% of the uniquely correlated data, respectively, as detected by Hi-C-Pro in the Hi-C dataset (Supplementary Tables S1–S3). Overall, our evaluation indicates that the quality of Hi-C data of all three varieties is high. Among the three varieties, the quality of Hi-C data showed the following order: H7 > ZS > YH. Only valid read pairs were used for subsequent analyses.

Prior to constructing the chromosomal-level genome assembly, the initial Hi-C data-based assembly was corrected using BWA-MEM. Contigs were broken into 50-kb fragments, and sequences that could not be located on the original assembly were reassembled using Hi-C as candidate error regions. Then, to complete error correction of the initial assemblies, the locations of low Hi-C coverage depths in these regions were identified as error points. After correction, the genome was assembled using LACHESIS. After the Hi-C assembly and manual adjustment, genome sequence lengths of the three chestnut varieties, 671.99 Mb (YH), 790.99 Mb (ZS), and 678.90 Mb (H7), were located on 12 chromosomes, accounting for 98.84, 100, and 98.79% of the genome sequence length, respectively (Supplementary Tables S4–S6).

A total of 995 (64.57%) sequences mapped to YH, 1014 (100%) to ZS, and 927 (62.76%) to H7. Finally, the genomes of YH, ZS, and H7 assembled by Hi-C were analyzed, and the contig N50 and scaffold N50 values were determined as follows: 3.61 and 50.50 Mb, respectively, for YH; 1.69 and 65.05 Mb, respectively, for ZS; and 3.18 and 52.16 Mb, respectively, for H7 (Supplementary Tables S7–S9).

To better compare the quality of the three chromosome-level genome assemblies, we generated a genome-wide Hi-C heat map for each variety. All heat maps showed a distinction among the 12 chromosome groups. Within each group, the intensity of the interaction was the strongest along the diagonal (i.e., between adjacent sequences on the chromosome), while that between distant sequences was weak. This agrees with the principles of Hi-C auxiliary genome assembly, and shows that our genome assembly is high quality (Figure 1).

Completeness of the assembled genome

The three short sequences of Chinese chestnut genome obtained using the Illumina HiSeq platform were compared with the reference genome using the BWA software, and over 98.15% of the clean reads could be mapped to contigs. The CEGMA database, which contains 458 conserved core eukaryotic genes (CEGs), was used to assess the integrity of the final genome assembly (Table 2).

Finally, 90.00% (YH), 95.00% (ZS), and 90.97% (H7) of complete BUSCOs were found in the assemblies (Table 3). This indicates that all three genome assemblies are relatively complete and of high quality.

Evaluation of genome collinearity

C. mollissima and *Q. robur* are two related Fagaceae species that carry an identical number of chromosomes and exhibit high genome sequence similarity. Therefore, we compared the genomes of these two species to verify the accuracy of the three *C. mollissima* genome sequences. The results revealed high degree of synteny between homologous chromosomes of the two species, and further confirmed the reliability of our new genome assemblies (Figure 2).

Repeat annotation, gene prediction, and gene annotation

In YH, ZS, and H7 genomes, 437.75, 423.16, and 442.76 Mb repeat sequences were discovered, accounting for 64.38, 53.49, and 64.43% of the assembled *C. mollissima* genomes, respectively. The predominant repeat types were Gypsy, Copia, Lard, Line, and unknown (Supplementary Tables S10–S12).

Using a combination of *ab initio*-, homology-, and RNA-seq-based methods, a total of 31,792, 32,012, and 32,411 protein-coding genes were predicted in YH, ZS, and H7 genomes, respectively, with an average gene length of 4,523.08, 5,229.36, and 4,525.15 bp, respectively (Supplementary Table S13).

The non-coding RNA prediction identified 136 miRNAs, 483 rRNAs, and 641 tRNAs in YH; 152 miRNAs, 383 rRNAs, and 659 tRNAs in ZS; and 152 miRNAs, 571 rRNAs, and 740 tRNAs in H7 (Supplementary Table S14).

Next, we examined pseudogenes, which are similar to functional genes in terms of their nucleotide sequence but have evolved a novel function because of a mutation, such as insertion or deletion. Based on GeneWise, a total of 1921, 2,199, and 2009 pseudogenes were identified in YH, ZS, and H7 genomes, respectively, with an average length of 2903.33, 3940.76, and 2682.38 bp, respectively. Finally, 91.50% (YH), 97.43% (ZS), and 91.74% (H7) of the genes were successfully annotated based on existing databases; the functional classifications of these genes are summarized in Supplementary Table S15.

Comparative genome analysis

Genome sequences of the three Chinese chestnut varieties were compared with those of nine related plant species using OrthoMCL. A total of 20,622, 21,053, and 19,756 gene families and 77, 41, and 102 unique gene families were discovered in YH, ZS, and H7, respectively (Supplementary Table S16).

Compared with other plant species, Chinese chestnut varieties contain fewer unigene families. To further understand the evolutionary relationship between Chinese chestnut and other related plant species, PHYML was used with a combination

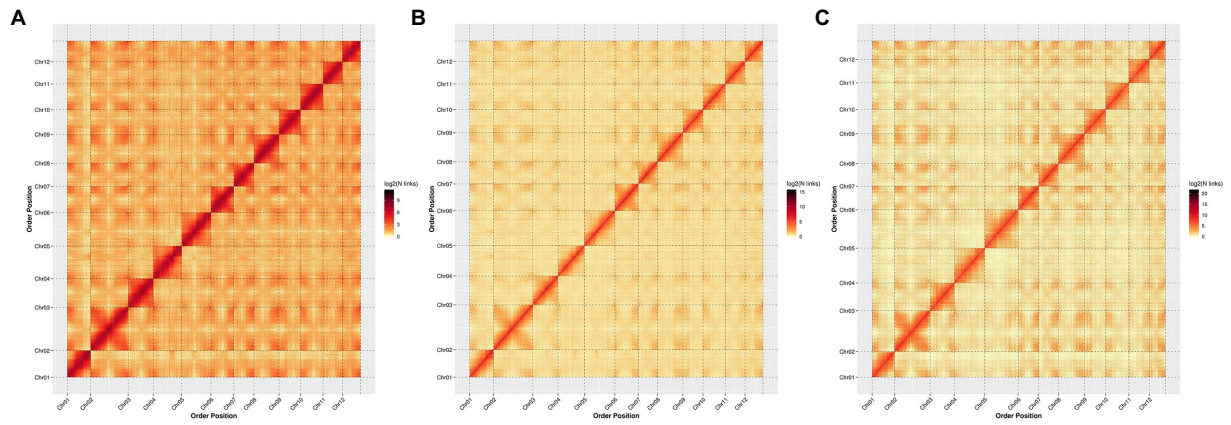


FIGURE 1
Hi-C interaction heat maps showing interactions among 12 chromosomes of each Chinese chestnut variety with the bin size of 10 kb resolution, using ggplot2 in the R package to evaluate the quality of the chromosomal-level genome assembly. **(A)**: YH; **(B)**: H7; and **(C)**: ZS.

TABLE 2 Assessment of the integrity of core genes in the three Chinese chestnut varieties.

Variety	No. of 458 CEGs present in the assembly	Percentage of 458 CEGs present in the assembly	No. of 248 highly conserved CEGs present	Percentage of 248 highly conserved CEGs present
YH	422	92.14%	204	82.26%
ZS	438	95.63%	214	86.29%
H7	426	93.01%	202	81.45%

dataset of the protein sequences of single-copy genes of Chinese chestnut and nine other species, and a phylogenetic tree was constructed using the maximum likelihood method. The results supported the hypothesis that Chinese chestnut and oak are sister groups (Figure 3).

Pan-genome analysis of three Chinese chestnut varieties

Alignment analysis by MUMmer software revealed that all 12 chromosomes in ZS were larger than those in the other two cultivars, especially chromosomes 2, 4, 5, and 8, and some fragments from YH and H7 together formed the chromosomal segments of ZS (Supplementary Figure S2).

Through the identification of homologous genes and cluster analysis of gene families, we found 159, 131, and 91 unique gene families in H7, YH, and ZS genomes, respectively, and a total of 13,248 single-copy direct homologous genes in the three chestnut varieties. Based on the results of gene family identification, the number of PAVs in the three genomes was calculated, and a total of 2,364, 2,232, and 1,475 unique genes were identified in H7, YH, and ZS genomes, respectively (Figure 4; Supplementary Table S18).

Castanea mollissima waxy gene (*GBSS II*) family analysis

Four *GBSS II* gene family members were identified in *C. mollissima* genomes, based on the original annotation, but were later confirmed as three genes based on manual correction after motif and domain analyses. The nucleotide sequences of waxy genes and the corresponding amino acid sequences are shown in Supplementary material chestnut-waxy-gene.pdf. To view the corrected gene structure annotation, see Supplementary material FixWaxy.gff3.

Did the waxy (*GBSS II*) gene family undergo expansion in chestnut? To answer this question, we conducted phylogenetic analyses of all GBSS proteins and related family members (Supplementary material chestnut-waxy-gene.pdf). The phylogenetic tree showed a clear GBSS clade. Based on the results of evolutionary analysis, we concluded the following: (1) GBSS I family exists only in monocotyledons; (2) GBSS II family exists in both monocotyledons and dicotyledons; (3) GBSS II in dicotyledons can be divided into two branches, and most species have only one GBSS II-b member in each branch; and (4) GBSS II-b branch in chestnut contains one more member than that in the nearest near source species (Figure 5). Gene structure annotation information in IGV revealed the proximity of the two *GBSS II* genes on chromosome 8 within a 14-kb region (Supplementary material chestnut-waxy-gene.pdf), indicating that the *GBSS II* gene family underwent tandem duplication in chestnut.

Database construction

The recent increase in genome resources has produced a wealth of data for in-depth analyses of the biology and evolution of *Castanea* plants, but obtaining and using these resources remains difficult. Therefore, we constructed the Chestnut

TABLE 3 Assessment of BUSCO notations in the *C. mollissima* genomes.

	YH	ZS	H7
Complete BUSCOs (C)	1,296 (90.00%)	1,368 (95.00%)	1,310 (90.97%)
Complete and single-copy BUSCOs (S)	1,244 (86.39%)	1,257 (87.29%)	1,262 (87.64%)
Complete and duplicated BUSCOs (D)	52 (3.61%)	111 (7.71%)	48 (3.33%)
Fragmented BUSCOs (F)	27 (1.88%)	25 (1.74%)	28 (1.94%)
Missing BUSCOs (M)	117 (8.12%)	47 (3.26%)	102 (7.08%)
Total Lineage BUSCOs	1,440	1,440	1,440

Genome Database (See Footnote 1). The genomic data of four chestnut varieties, H7, YH, ZS, and N11-1 (Wang et al., 2020a), have been included in this database. This database provides tools for browsing genomes (JBrowse), searching sequence databases (BLAST), and designing primers, combined with GO annotation and KEGG annotation. To better serve the research community, we continue to update our database and develop new tools (Figure 6).

Discussion

The number of people facing hunger is expected to increase significantly due to continued climate change and the COVID-19 pandemic. In 2020, at least 720million people (≥ 9.9% of the global population) will face hunger; It is the largest percentage of the total population since 2010 (FAO, IFAD, UNICEF, WFP, and WHO, 2021). In order to alleviate global hunger, more attention needs to be paid to non-staple food crops (Chapman et al., 2022). Chestnut, as a tree species that has been used to fight against hunger in history (Gabriele et al., 2020), should be paid more attention and studied.

Genome size variation

Genome size variation is a fundamental biological characteristic; however, its evolutionary causes and consequences are the topic of ongoing debate (Blommaert, 2020). There are few examples of intraspecific genome size variation and its phenotypic effects. Causes and consequences of genome size variation are particularly well understood in maize, with a recent study finding that genome size was selected for *via* its effects on flowering time at different altitudinal clines, which is consistent with the nucleotypic hypothesis (Bilinski et al., 2018).

In this study, based on the distribution of 21-mers among the Illumina HiSeq reads. The genomes of *C. mollissima* were estimated to be 664.89 Mb (YH), 628.90 Mb (H7) and 752.70 Mb (ZS), with approximately 0.98% (YH), 1.05% (H7) and 0.60% (ZS) heterozygosity. The k-mer distribution curve peaked at a depth of 57 (zs), 51 (YH) and 58 (H7), with a k-mer number of 34,316,017,419 (YH), 36,619,119,572 (H7) and 43,087,876,811 (ZS; Supplementary Figure S1). The total lengths of the genome sequences were determined to be 679.87 Mb with a contig N50 of 3.65 Mb (YH), 790.99 Mb with a contig N50 of 2.17 Mb (ZS), and 687.24 Mb with a contig N50 of 3.39 Mb (H7). After the Hi-C assembly and manual adjustment, genome sequence lengths of the three chestnut varieties, 671.99 Mb (YH), 790.99 Mb (ZS), and 678.90 Mb (H7), were located on 12 chromosomes, accounting for 98.84, 100, and 98.79% of the genome sequence length, respectively. Alignment analysis by MUMmer software revealed that all 12 chromosomes in ZS were larger than those in the other two cultivars, especially chromosomes 2, 4, 5, and 8, and some fragments from YH and H7 together formed the chromosomal segments of ZS (Supplementary Figure S2). The genome of early maturing variety ZS is significantly larger by approximately 100 MB than that of the other two varieties (YH and H7). The fruits of ZS matured one month earlier than the other two. Although genome size was found to be related with flowering time in maize (Bilinski et al., 2018), there is no direct evidence that genome size is related with fruit maturity in chestnut. Through more traditional evolutionary experiments and new techniques, it becomes more clear to understand the basis of intraspecific genome size variation and its potential direct phenotypic effects, as well as the possible causes of intraspecific genome size variation (Blommaert, 2020).

Database construction and waxy gene (*GBSS II*) family analysis

After the completion of the genome sequencing, an urgent issue is to share the genome data with the research community immediately, which expands the impact of these valuable sequence data and promotes collaboration. However, among the hundreds of sequenced angiosperm genomes, only a few of them have a well-constructed customized database to host its various genome information. A good genome database should meet two criteria: (i) integration of various types of genomic data, and (ii) providing genome analysis tools (Chen et al., 2018). The recent increase in genome resources has produced a wealth of data for in-depth analyses of the biology and evolution of *Castanea* plants, but obtaining and using these resources remains difficult. Therefore, we constructed the Chestnut Genome Database (See Footnote 1). The genomic data of four chestnut varieties, H7, YH,

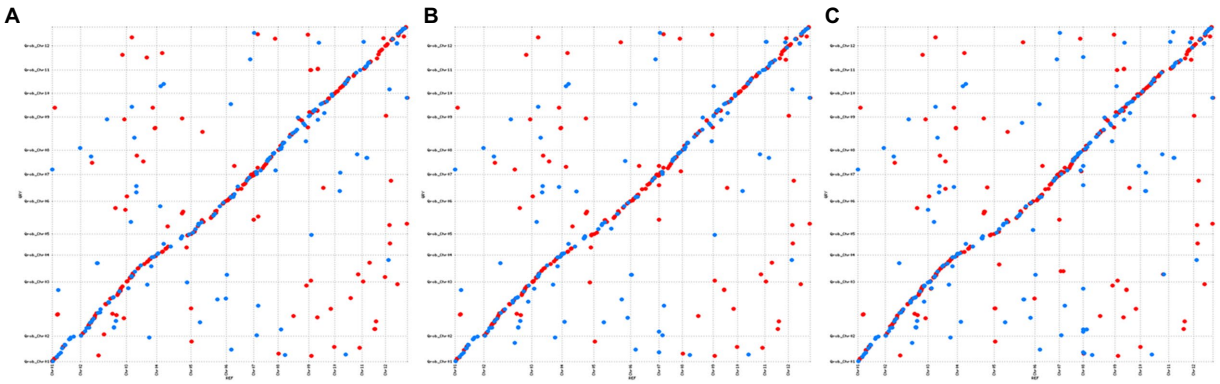


FIGURE 2
Analysis of collinearity between *C. mollissima and Q. robur* genomes using the MUMmer software. **(A)**: YH; **(B)**: H7; and **(C)**: ZS.

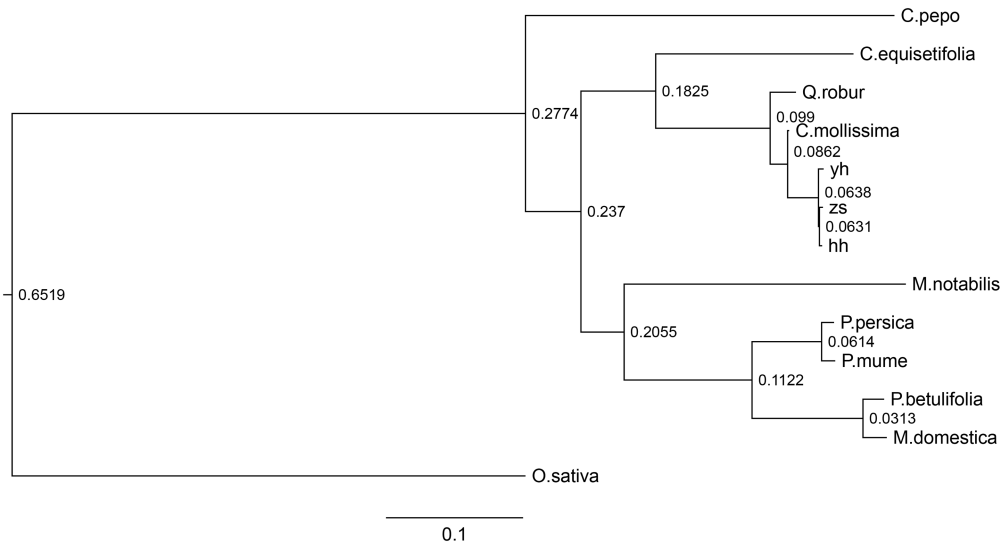


FIGURE 3
Analysis of evolutionary relationships among Chinese chestnut and nine other species. The phylogenetic tree was constructed by PHYML software using the single-copy protein sequences.

ZS, and N11-1 (Wang et al., 2020a), have been included in this database. This database provides tools for browsing genomes (JBrowse), searching sequence databases (BLAST), and designing primers, combined with GO annotation and KEGG annotation. For an example, we took full advantage of the convenience provided by this database in the waxy gene (*GBSS II*) family analysis.

Starch is one of the most important components of a chestnut, and accounts for 50–80% of its dry matter content (Liu et al., 2015). Chestnut starch is considered as a potentially functional component of dietary fiber, which may be sources of resistant starch, thus improving health (Liu et al., 2022). Chestnut starch has unique physicochemical properties, such as high swelling power, freeze–thaw stability, pasting viscosity, and low gelatinization temperature (Liu et al., 2015, 2019). The characteristics of chestnut starch vary greatly with the variety and its geographical distribution (Long et al., 2018). Waxiness is one of the most important edible qualities of chestnuts; however, this trait also varies greatly with the genotype and production area. Chestnut kernel starch consists mainly of two fractions, amylose and amylopectin. The proportion of amylopectin and amylose in chestnut kernel starch varies among cultivars; the percentage of amylopectin relative to the total starch in a chestnut ranges from 67 to 82%, and the proportion of amylopectin in chestnut kernel starch is approximately 2–5 times that of amylose (Liang, 2011). However, there are few reports on waxy genes in chestnut. Did the waxy (*GBSS II*) gene family undergo expansion in chestnut? To answer this question, we conducted phylogenetic analyses of all GBSS proteins and related family members. Our results suggested expansion of the *GBSS II*-b gene family member in chestnut (relative to the nearest source species). To elucidate

the waxiness of Chinese chestnut, it is necessary to combine genome, transcriptome and metabolome studies (Zhang et al., 2015; Chen et al., 2017; Liu et al., 2020). The study of waxy genes in chestnut has enlightenment for the study of other starchy plants.

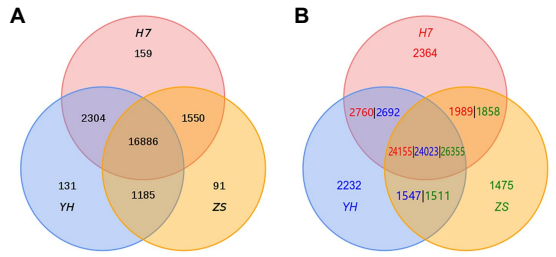


FIGURE 4
Venn diagram of the number of homologous gene families in H7, YH, and ZS genomes **(A)** and the number of homologous genes in H7, YH, and ZS genomes **(B)**, results from PAV analysis.

Pan-genome analysis and strategy for pyramiding breeding

The high degree of genomic variation observed among individuals belonging to the same species led to the realization that single reference genome do not represent the diversity within a species (Bayer et al., 2020). China is considered a gene center for the genus *Castanea* (Vavilov, 1952; Zhang et al., 2015). Over 300 cultivars have been selected for nut production, which are widely distributed in areas 370–2,800 m above the sea level in China (Li et al., 2009). Obviously, single reference genome cannot meet the needs of Chinese chestnut industry research and development. The resources of crop pan-genomes rather than single reference genomes will accelerate molecular breeding (Golicz et al., 2016a,b; Bayer et al., 2020; Jensen et al., 2020; Murukarthick et al., 2021). However, for some species, pan-genome-assisted breeding efforts remain limited due to the small size of the research communities (Rafael et al., 2021). At present, there are few reports about pan-genome in the study of nut crop. We have overcome various

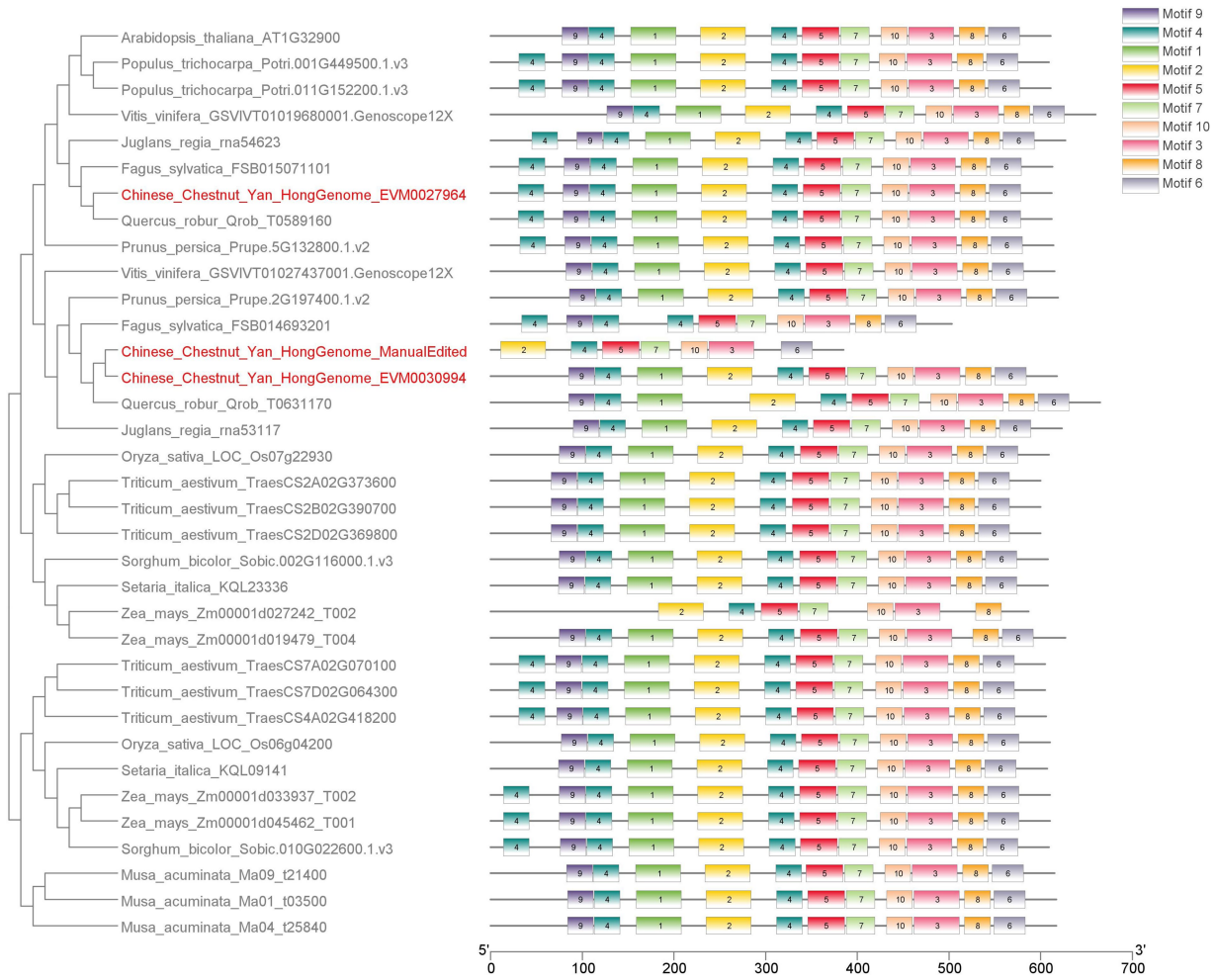


FIGURE 5
Evolution tree and motifs analysis of Chestnut GBSS II family members and 32 orther species. Phylogenetic trees were constructed using IQtree software.

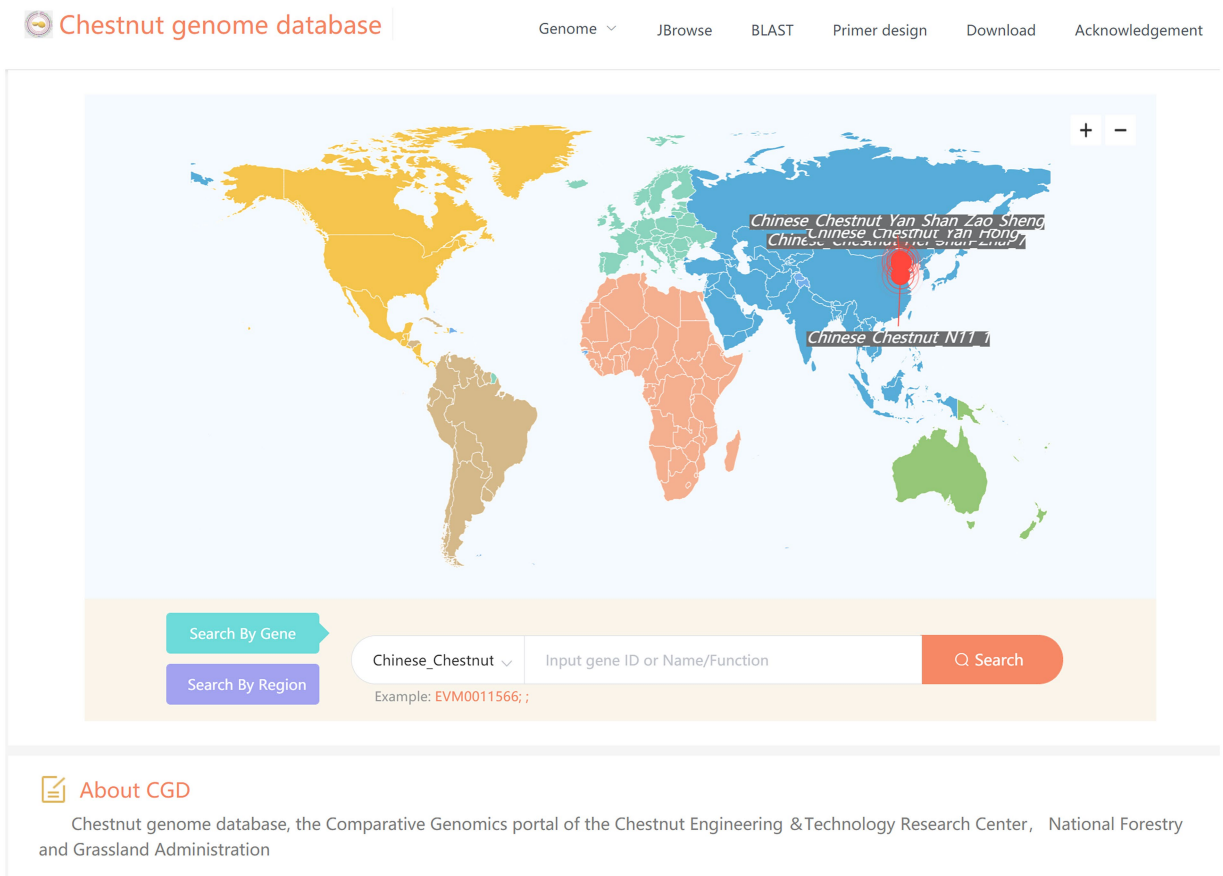


FIGURE 6
The user interface of Chestnut Genome Database for browsing genomes, searching for homologous sequences and designing primers.

difficulties and carried out pan-genome analysis in chestnut research for the first time.

A pan-genome project should select genotypes that have played an important role in breeding and genetics (Yu et al., 2008; Jain et al., 2019; Schreiber et al., 2020) to maximize the benefits for the research and breeding community. In the present study, we selected three main varieties, namely Hei-Shan-Zhai-7 (drought-resistant variety), Yan-Hong (easy-pruning variety), and Yan-Shan-Zao-Sheng (early-maturing variety), using Oxford Nanopore Technology (ONT) and Illumina HiSeq X sequencing and Hi-C mapping, performing a pan-genome analysis.

Early-maturing chestnut varieties could be put on the market earlier, which would greatly improve the overall value of the nut; chestnut orchards are mostly in mountainous areas with poor irrigation conditions; labor shortage and aging phenomenon in chestnut planting industry are serious (Ren and Jia, 2014; Zhao and Zhang, 2015), therefore, pyramiding breeding of early-maturing cultivars that are drought-resistant and easy-pruning is a priority for chestnut industry. Although several early maturing varieties (e.g., ZS) have been developed, however, genes responsible for early maturity in chestnut have not been investigated to date. Chinese chestnut is a monoecious plant, and having too many male flowers on an individual plant results in the overconsumption of nutrients and water (Feng, 1995). The mutant varieties (e.g., H7) with extremely short catkins has a significantly reduced number of flowers in the male inflorescence, which saves nutrition and water and improves drought resistance (Feng et al., 2011). Other studies have found genes that play important roles in flower development (Dong et al., 2017; Tian et al., 2018; Chen et al., 2019). We have acquired an invention patent- "open pollination" molecular chestnut breeding system (Hu et al., 2017) based on the character of extremely short catkins in H7. However, there is no short-catkin variety bred by molecular marker assisted selection. Only a few varieties (e.g., YH) can keep the number of fruiting branches after extensive cutting back pruning (Fan et al., 2009), the molecular mechanism still unknown.

In this study, based on the results of gene family identification, the number of PAVs in the three genomes was calculated, and a total of 2,364, 2,232, and 1,475 unique genes were identified in H7, YH, and ZS genomes, respectively (Figure 4; Supplementary Table S18). Based on the pan-genome analysis results, we have formulated the following strategy for pyramiding breeding. According to the

pan-genomic research results, combined with the "open pollination" molecular breeding system of Chinese chestnut, which saves time and effort, H7, YH and ZS are crossed with each other, and the hybrid fruit is directly optimized. The hybrid fruits containing at least two cultivars' unique genes will be selected, and the hybrid fruits without unique gene will be discarded. This strategy should accelerate the pyramiding breeding process of early-maturing, drought-resistant and easy-pruning cultivars.

Conclusion

In this study, we constructed high-quality chromosome-level genome assemblies of three *C. mollissima* varieties using a combination of ONT sequencing, Illumina HiSeq X sequencing, and Hi-C mapping. We constructed the chestnut genome database which provides tools for browsing genomes (JBrowse), searching sequence databases (BLAST), and designing primers. Through the identification of homologous genes and the cluster analysis of gene families, we found that H7, YH and ZS had 159,131and 91 unique gene families, respectively. The Presence/Absence variations (PAVs) information of the three sample genes was calculated, and there were 2,364, 2,232, and 1,475 unique genes in H7, YH and ZS, respectively. Our results suggested expansion of the *GBSS II-b* gene family member in chestnut (relative to the nearest source species). The pan-genome analysis of three main chestnut varieties will provide a solid foundation for future trait improvement, seedling breeding, conservation, and phylogenetic research.

Data availability statement

The datasets presented in this study can be found in online repositories. The names of the repository/repositories and accession number(s) can be found in the article/Supplementary material.

Author contributions

GH conducted the experiments, analyzed the data, and prepared the manuscript. LC, YC, WM, YQ, and YL performed the collection and processing of samples and analyzed the data. YL coordinated the experiments. All authors contributed to the article and approved the submitted version.

Funding

This work was financially supported by the National Basic Research Program of China (Grant no. 2013FY111700-2), the China National Key R&D Program (Grant no. 2018YFD1000605), the Special Fund for the Construction of Scientific and Technological Innovation Capability (Grant nos. KJCX20200114 and PT2022-07), Presidential Foundation of Institute of Forestry and Pomology (Grant no. LGY201901) and the Youth Scientist Fund of Institute of Forestry and Pomology, Beijing Academy of Agriculture and Forestry Sciences (LGYJJ202007).

Acknowledgments

We thank Guiyang Watch Biotechnology for their advice on gene family data analyses.

Conflict of interest

The authors declare that the research was conducted in the absence of any commercial or financial relationships that could be construed as a potential conflict of interest.

Publisher's note

All claims expressed in this article are solely those of the authors and do not necessarily represent those of their affiliated organizations, or those of the publisher, the editors and the reviewers. Any product that may be evaluated in this article, or claim that may be made by its manufacturer, is not guaranteed or endorsed by the publisher.

Supplementary material

The Supplementary Material for this article can be found online at: https://www.frontiersin.org/articles/10.3389/fpls.2022.916550/full#supplementary-material

References

Adua, M. (1999). The sweet chestnut throughout history from the Miocene to the third millennium. *Acta Hortic.* 29–36. doi: 10.17660/ActaHortic.1999.494.2

Altschul, S. F., Gish, W., Miller, W., Myers, E. W., and Lipman, D. J. (1990). Basic local alignment search tool. *J. Mol. Biol.* 215, 403–410.

Bai, F. (2007). Jones NC, Pevzner PA. De novo identification of repeat families in large genomes. Master's Thesis, Xi'an University of Electronic Science and technology.

Bayer, P. E., Golicz, A. A., Scheben, A., Batley, J., and Edwards, D. (2020). Plant pan-Genomes are the new Reference. *Nature plants* 6, 914–920. doi: 10.1038/s41477-020-0733-0

Bilinski, P., Albert, P. S., Berg, J. J., Birchler, J. A., Grote, M. N., Lorant, A., et al. (2018). Parallel altitudinal clines reveal trends in adaptive evolution of genome size in *Zea mays*. *PLoS Genet.* 14:e1007162. doi: 10.1371/journal.pgen.1007162

Blanco, E., Parra, G., and Guigó, R. (2007). Using geneid to identify genes. *Curr. Protocols Bioinform.* 4:e56. doi: 10.1002/0471250953.bi0403s18

Blommaert, J. (2020). Genome size evolution: towards new model systems for old questions. *Proceed. Royal Soc. B-Biol. Sci.* 287:20201441. doi: 10.1098/rspb.2020.1441

Boeckmann, B., Bairoch, A., Apweiler, R., Blatter, M. C., Estreicher, A., Gasteiger, E., et al. (2003). The SWISS-PROT protein knowledgebase and its

supplement TrEMBL in 2003. *Nucleic Acids Res.* 31, 365–370. doi: 10.1093/nar/gkg095

Burge, C., and Karlin, S. (1997). Prediction of complete gene structures in human genomic DNA. *J. Mol. Biol.* 268, 78–94. doi: 10.1006/jmbi.1997.0951

Burton, J. N., Adey, A., Patwardhan, R. P., Qiu, R., Kitzman, J. O., and Shendure, J. (2013). Chromosome-scale scaffolding of de novo genome assemblies based on chromatin interactions. *Nat. Biotechnol.* 31, 1119–1125. doi: 10.1038/nbt.2727

Campbell, M., Haas, B., Hamilton, J., Mount, S., and Buell, C. R. (2006). Comprehensive analysis of alternative splicing in rice and comparative analyses with Arabidopsis. *BMC Genomics* 7:327. doi: 10.1186/1471-2164-7-327

Cao, Q. (2015). Technical countermeasures for improving economic benefit of Yanshan chestnut. *China Fruits*, 56–58. doi: 10.16626/j.cnki.issn1000-8047.2015.02.027

Chapman, M. A., He, Y., and Zhou, M. (2022). Beyond a reference genome: pangenomes and population genomics of underutilised and orphan crops for future food and nutrition security. *New Phytol.* 234, 1583–1597. doi: 10.1111/nph.18021

Chen, C., Chen, H., Zhang, Y., Thomas, H. R., Frank, M. H., He, Y., et al. (2020). TBtools: An integrative toolkit developed for interactive analyses of big biological data. *Mol. Plant* 13, 1194–1202. doi: 10.1016/j.molp.2020.06.009

Chen, F., Dong, W., Zhang, J., Guo, X., Chen, J., Wang, Z., et al. (2018). The sequenced angiosperm genomes and genome databases. *Front. Plant Sci.* 9:418. doi: 10.3389/fpls.2018.00418

Chen, G., Li, J., Liu, Y., Zhang, Q., Gao, Y., Fang, K., et al. (2019). Roles of the GA-mediated SPL gene family and miR156 in the floral development of Chinese chestnut (*Castanea mollissima*). *Int. J. Mol. Sci.* 20:1577. doi: 10.3390/ijms20071577

Chen, L., Lu, D., Wang, T., Li, Z., Zhao, Y., Jiang, Y., et al. (2017). Identification and expression analysis of starch branching enzymes involved in starch synthesis during the development of chestnut (*Castanea mollissima* Blume) cotyledons. *PLoS One* 12:792. doi: 10.1371/journal.pone.0177792

Cheng, L., Hu, G., and Huang, W. (2013). "A brief introduction to a new variety of early maturing Chestnut 'Yanshan Zaosheng", in The 8th National Symposium on dry fruit production and scientific research progress, 94–95.

Claire, H., Sandie, A., Mark, M., Timothée, C., Olivier, I., Véronique, J., et al. (2017). PASTEC: an automatic transposable element classification tool. *PLoS One* 9:e91929. doi: 10.1371/journal.pone.0091929

de Bie, T., Cristianini, N., Demuth, J. P., and Hahn, M. W. (2006). CAFE: a computational tool for the study of gene family evolution. *Bioinformatics* 22, 1269–1271. doi: 10.1093/bioinformatics/btl097

Dimmer, E. C., Huntley, R. P., Alam, F. Y., Sawford, T., O'Donovan, C., Martin, M. J., et al. (2012). The UniProt-GO annotation database in 2011. *Nucleic Acids Res.* 40, D565–D570. doi: 10.1093/nar/gkr1048

Dong, B., Deng, Y., Wang, H., Gao, R., Stephen, G. U. K., Chen, S., et al. (2017). Gibberellic acid signaling is required to induce flowering of chrysanthemums grown under Both short and Long days. *Int. J. Mol. Sci.* 18:1259. doi: 10.3390/ijms18061259

Dong, X., Wang, Z., Tian, L., Zhang, Y., Qi, D., Huo, H., et al. (2020). De novo assembly of a wild pear (Pyrus betuleafolia) genome. *Plant Biotechnol. J.* 18, 581–595. doi: 10.1111/pbi.13226

Du, H., Yu, Y., Ma, Y., Gao, Q., Cao, Y., Chen, Z., et al. (2017). Sequencing and de novo assembly of a near complete indica rice genome. *Nat. Commun.* 8:15324. doi: 10.1038/ncomms15324

Edgar, R. C. (2004). MUSCLE: multiple sequence alignment with high accuracy and high throughput. *Nucleic Acids Res.* 32, 1792–1797. doi: 10.1093/nar/gkh340

Fan, C., Zhang, D., Jia, A., and Wang, Z. (2009). Problem and Resolventing method on thick planting orchard in *Castanea mollissima* Blume (Chinese chestnut) in Jixian County. *Tianjin Agri. Sci.* 15, 83–85. doi: 10.3969/j.issn.1006-6500.2009.05.025

FAO, IFAD, UNICEF, WFP, and WHO (2021). The state of food security and nutrition in the world 2021: transforming food systems for food security, improved nutrition and affordable healthy diets for all. Food and Agriculture Org.

Feng, Z. Q. (1995). Study of reason on thinning catkins in Chinese chestnut. Chinese Fruit

Feng, Y.-Q., Shen, Y.-Y., Qin, L., Cao, Q.-Q., and Han, Z.-H. (2011). Short catkin 1, a novel mutant of *Castanea mollissima*, is associated with programmed cell death during chestnut staminate flower differentiation. *Sci. Hortic.* 130, 431–435. doi: 10.1016/j.scienta.2011.07.014

Finn, R. D., Clements, J., and Eddy, S. R. (2011). HMMER web server: interactive sequence similarity searching. *Nucleic Acids Res.* 39, W29–W37. doi: 10.1093/nar/gkr367

Gabriele, B., Alberto, A., Giancarlo, B., and Jose, C.L. (2020). *The Chestnut Handbook: Crop & Forest Management*. Florida: CRC Press.

Gao, X., Lan, W., and He, X. (1980). New varieties of Beijing Chestnut. *China Fruits*, 49–51+69.

Golicz, A. A., Batley, J., and Edwards, D. (2016a). Towards plant Pangenomics. *Plant Biotechnol. J.* 14, 1099–1105. doi: 10.1111/pbi.12499

Golicz, A. A., Bayer, P. E., Barker, G. C., Edger, P. P., Kim, H., Martinez, P. A., et al. (2016b). The pangenome of an agronomically important crop plant *Brassica oleracea*. *Nat. Commun.* 7:13390. doi: 10.1038/ncomms13390

Griffiths, J. S., Moxon, S., Marshall, M., Khanna, A., Eddy, S. R., and Bateman, A. (2005). Rfam: annotating non-coding RNAs in complete genomes. *Nucleic Acids Res.* 33, D121–D124. doi: 10.1093/nar/gki081

Guo, J., Kong, L., Du, B., and Xu, B. (2019). Morphological and physicochemical characterization of starches isolated from chestnuts cultivated in different regions of China. *Int. J. Biol. Macromol.* 130, 357–368. doi: 10.1016/j.ijbiomac.2019.02.126

Haas, B. J., Salzberg, S. L., Zhu, W., Pertea, M., Allen, J. E., Orvis, J., et al. (2008). Automated eukaryotic gene structure annotation using EVidenceModeler and the program to assemble spliced alignments. *Genome Biol.* 9:R7. doi: 10.1186/gb-2008-9-1-r7

Hao, F., and Zhang, F. (2014). Textual research on the cultivation history of *Castanea mollissima* in China. *Ancient Mod. Agri.* 40–48. doi: 10.3969/j.issn.1672-2787.2014.03.006

He, N., Zhang, C., Qi, X., Zhao, S., Tao, Y., Yang, G., et al. (2013). Draft genome sequence of the mulberry tree Morus notabilis. *Nat. Commun.* 4:2445. doi: 10.1038/ncomms3445

Hu, G., Huang, W., Cheng, L., Zhang, J., Lan, Y., and Cao, Q. (2017). Molecular breeding method of short male inflorescence chestnut varieties. CN201510568054.2.2017.

Huang, W., Zhou, Z., Cheng, L., Chen, S., and He, X. (2009). A new variety of Chinese chestnut 'Heishanzhai 7'. *Forestry Sci.* 45, 177–183. doi: 10.11707/j.1001-7488.20090632

Jacob, A., Lancaster, J., Buhler, J., Harris, B., and Chamberlain, R. D. (2008). Mercury BLASTP: accelerating protein sequence alignment. *ACM* 1, 1–44. doi: 10.1145/1371579.1371581

Jain, R., Jenkins, J., Shu, S., Chern, M., Martin, J. A., Copetti, D., et al. (2019). Genome sequence of the model rice variety Kitaake X. *BMC Genomics* 20, 905. doi: 10.1186/s12864-019-6262-4

Jens, K., Frank, H., Michael, P., Sven, O. T., and Jan, G. (2018). Combining RNA-seq data and homology-based gene prediction for plants, animals and fungi. *BMC Bioinformatics* 19, 1–12. doi: 10.1186/s12859-018-2203-5

Jensen, S. E., Charles, J. R., Muleta, K., Bradbury, P. J., Casstevens, T., Deshpande, S. P., et al. (2020). Biotechnology-plant genomics; findings on plant genomics reported by investigators at Cornell University (A Sorghum practical haplotype graph facilitates genome-wide imputation and cost-effective genomic prediction). Biotech Week.

Jurka, J., Kapitonov, V. V., Pavlicek, A., Klonowski, P., Kohany, O., and Walichiewicz, J. (2005). Repbase update, a database of eukaryotic repetitive elements. *Cytogenet. Genome Res.* 110, 462–467. doi: 10.1159/000084979

Kanehisa, M., and Goto, S. (2000). KEGG: Kyoto encyclopedia of genes and genomes. *Nucleic Acids Res.* 28, 27–30. doi: 10.1093/nar/28.1.27

Keilwagen, J., Wenk, M., Erickson, J. L., Schattat, M. H., Grau, J., and Hartung, F. (2016). Using intron position conservation for homology-based gene prediction. *Nucleic Acids Res.* 44:e89. doi: 10.1093/nar/gkw092

Kim, D., Langmead, B., and Salzberg, S. L. (2015). HISAT: a fast spliced aligner with low memory requirements. *Nat. Methods* 12, 357–360. doi: 10.1038/nmeth.3317

Koonin, E. V., Fedorova, N. D., Jackson, J. D., Jacobs, A. R., Krylov, D. M., Makarova, K. S., et al. (2004). A comprehensive evolutionary classification of proteins encoded in complete eukaryotic genomes. *Genome Biol.* 5:R7. doi: 10.1186/gb-2004-5-2-r7

Koren, S., Walenz, B.P., Berlin, K., Miller, J.R., and Bergman, N.H. (2017). Biotechnology-genomics; Reports from National Human Genome Research Institute highlight recent findings in genomics (Canu: scalable and accurate long-read assembly via adaptive k-mer weighting and repeat separation) biotech Business Week.

Korf, I. (2004). Gene finding in novel genomes. *BMC Bioinformatics* 5:59. doi: 10.1186/1471-2105-5-59

Kurtz, S., Phillippy, A., Delcher, A. L., Smoot, M., Shumway, M., Antonescu, C., et al. (2004). Versatile and open software for comparing large genomes. *Genome Biol.* 5:R12. doi: 10.1186/gb-2004-5-2-r12

LaBonte, N. R., Zhao, P., and Woeste, K. (2018). Signatures of selection in the genomes of Chinese chestnut (*Castanea mollissima* Blume): The roots of nut tree domestication. *Front. Plant Sci.* 9:810. doi: 10.3389/fpls.2018.00810

Lam-Tung, N., Schmidt, H. A., Arndt, V. H., and Quang, M. B. (2015). IQ-TREE: A fast and effective stochastic algorithm for estimating maximum-likelihood phylogenies. *Mol. Biol. Evol.* 32, 268–274. doi: 10.1093/molbev/msu300

Li, G., Ai, C., Zhang, L., Wei, H., and Liu, Q. (2009). Chestnut genebank in China national clonal plant germplasm repository. *Acta Hortic.*, 25, 199–206. doi: 10.1093/bioinformatics/btp324

Li, H., and Durbin, R. (2009). Fast and accurate short read alignment with burrows-wheeler transform. *Bioinformatics* 25, 1754–1760. doi: 10.1093/bioinformatics/btp324

Li, L., Stoeckert, C. J., and Roos, D. S. (2003). OrthoMCL: identification of ortholog groups for eukaryotic genomes. *Genome Res.* 13, 2178–2189. doi: 10.1101/gr.1224503

Li, Y., Zhou, G., Ma, J., Jiang, W., Jin, L., Zhang, Z., et al. (2014). De novo assembly of soybean wild relatives for pan-genome analysis of diversity and agronomic traits. *Nat. Biotechnol.* 32, 1045–1052. doi: 10.1038/nbt.2979.

Liang, L. (2011). Study on the Material basis of Waxy Texture of Chestnut. Doctoral Thesis, Beijing Forestry University.

Liu, B., Lin, R., Jiang, Y., Jiang, S., Xiong, Y., Lian, H., et al. (2020). Transcriptome analysis and identification of genes associated with starch metabolism in Castanea henryi seed (Fagaceae). *Int. J. Mol. Sci.* 21:1431. doi: 10.3390/ijms21041431

Liu, T., Ma, M., Guo, K., Hu, G., Zhang, L., and Wei, C. (2019). Structural, thermal, and hydrolysis properties of large and small granules from C-type starches of four Chinese chestnut varieties. *Int. J. Biol. Macromol.* 137, 712–720. doi: 10.1016/j.ijbiomac.2019.07.023

Liu, C., Wang, S., Chang, X., and Wang, S. (2015). Structural and functional properties of starches from Chinese chestnuts. *Food Hydrocoll.* 43, 568–576. doi: 10.1016/j.foodhyd.2014.07.014

Liu, W., Zhang, Y., Wang, R., Li, J., Pan, W., Zhang, X., et al. (2022). Chestnut starch modification with dry heat treatment and addition of xanthan gum: Gelatinization, structural and functional properties. *Food Hydrocoll.* 124:107205. doi: 10.1016/j.foodhyd.2021.107205

Long, Z., Tianxiang, L., Guanglong, H., Ke, G., and Cunxu, W. (2018). Comparison of physicochemical properties of starches from nine Chinese chestnut varieties. *Molecules* 23:3248. doi: 10.3390/molecules23123248

Lowe, T. M., and Eddy, S. R. (1997). tRNAscan-SE: a program for improved detection of transfer RNA genes in genomic sequence. *Nucleic Acids Res.* 25, 955–964. doi: 10.1093/nar/25.5.955

Lu, F., Romay, M. C., Glaubitz, J. C., Bradbury, P. J., Elshire, R. J., Wang, T., et al. (2015). High-resolution genetic mapping of maize pan-genome sequence anchors. *Nat. Commun.* 6, 6914. doi: 10.1038/ncomms7914

Majoros, W. H., Pertea, M., and Salzberg, S. L. (2004). TigrScan and GlimmerHMM: two open source ab initio eukaryotic gene-finders. *Bioinformatics* 20, 2878–2879. doi: 10.1093/bioinformatics/bth315

Marchler, B. A., Lu, S., Anderson, J. B., Chitsaz, F., Derbyshire, M. K., DeWeese, S. C., et al. (2011). CDD: a conserved domain database for the functional annotation of proteins. *Nucleic Acids Res.* 39, D225–D229. doi: 10.1093/nar/gkq1189

Marchler-Bauer, A., Derbyshire, M. K., Gonzales, N. R., Lu, S., Chitsaz, F., Geer, L. Y., et al. (2015). CDD: NCBI's conserved domain database. *Nucleic Acids Res.* 43, D222–D226. doi: 10.1093/nar/gku1221

Montero, P. J., Blanca, J., Bombarely, A., Ziarsolo, P., Esteras, C., Martí, G. C., et al. (2018). De novo assembly of the zucchini genome reveals a whole-genome duplication associated with the origin of the Cucurbita genus. *Plant Biotechnol. J.* 16, 1161–1171. doi: 10.1111/pbi.12860

Murukarthick, J., Mona, S., Nils, S., and Martin, M. (2021). Building pan-genome infrastructures for crop plants and their use in association genetics. *DNA Res.* 28:dsaa030. doi: 10.1093/DNARES/DSAA030

Parra, G., Bradnam, K., and Korf, I. (2007). CEGMA: a pipeline to accurately annotate core genes in eukaryotic genomes. *Bioinformatics* 23, 1061–1067. doi: 10.1093/bioinformatics/btm071

Pertea, M., Pertea, G. M., Antonescu, C. M., Chang, T. C., Mendell, J. T., and Salzberg, S. L. (2015). StringTie enables improved reconstruction of a transcriptome from RNA-seq reads. *Nat. Biotechnol.* 33, 290–295. doi: 10.1038/nbt.3122

Plomion, C., Aury, J. M., Amselem, J., Leroy, T., Murat, F., Duplessis, S., et al. (2018). Oak genome reveals facets of long lifespan. *Nature plants.* 4, 440–452. doi: 10.1038/s41477-018-0172-3

Rafael, D. C., Yinjie, Q., Shujun, O., Mathew, B. H., and Candice, N. H. (2021). How the pan-genome is changing crop genomics and improvement. *Genome Biol.* 22, 1–9. doi: 10.1186/S13059-020-02224-8

Rao, S. S. P., Huntley, M. H., Durand, N. C., Stamenova, E. K., Bochkov, I. D., Robinson, J. T., et al. (2014). A 3D map of the human genome at Kilobase resolution reveals principles of chromatin looping. *Cell* 159, 1665–1680. doi: 10.1016/j.cell.2014.11.021

Ren, S., and Jia, Y. (2014). There are problems in the development of the chestnut industry in Zunhua, Hebei and countermeasures. *Pract. Techn. Inform. Fruit Trees*, 34–35.

Robert, V., Ivan, S., Niranjan, N., and Mile, Š. (2017). Fast and accurate de novo genome assembly from long uncorrected reads. *Genome Res.* 27, 737–746. doi: 10.1101/gr.214270.116

Schatz, M. C., Maron, L. G., Stein, J. C., Wences, A., Gurtowski, J., Biggers, E., et al. (2014). Whole genome de novo assemblies of three divergent strains of rice, *Oryza sativa*, document novel gene space of aus and indica. *Genome Biol.* 15:506. doi: 10.1186/s13059-014-0506-z

Schreiber, M., Mascher, M., Wright, J., Padmarasu, S., Himmelbach, A., Heavens, D., et al. (2020). A genome assembly of the barley 'Transformation Reference'. *Cult. Golden Promise.* 10, 1823–1827. doi: 10.1534/g3.119.401010

Servant, N., Varoquaux, N., Lajoie, B. R., Viara, E., Chen, C., Vert, J. P., et al. (2015). HiC-pro: an optimized and flexible pipeline for hi-C data processing. *Genome Biol.* 16:259. doi: 10.1186/s13059-015-0831-x

Simão, F. A., Waterhouse, R. M., Ioannidis, P., Kriventseva, E. V., and Zdobnov, E. M. (2015). BUSCO: assessing genome assembly and annotation completeness with single-copy orthologs. *Bioinformatics* 31, 3210–3212. doi: 10.1093/bioinformatics/btv351

Solovyev, V., Kosarev, P., Seledsov, I., and Vorobyev, D. (2006). Automatic annotation of eukaryotic genes, pseudogenes and promoters. *Genome Biol.* 7, S10–S1012. doi: 10.1186/gb-2006-7-s1-s10

Stanke, M., and Waack, S. (2003). Gene prediction with a hidden Markov model and a new intron submodel. *Bioinformatics* 19, ii215–ii225. doi: 10.1093/bioinformatics/btg1080

Stéphane, G., Jean-François, D., Vincent, L., Maria, A., Wim, H., and Olivier, G. (2010). New algorithms and methods to estimate maximum-likelihood phylogenies: assessing the performance of PhyML 3.0. *Syst. Biol.* 59, 307–321. doi: 10.1093/sysbio/syq010

Sun, Y., Lu, Z., Zhu, X., and Ma, H. (2020). Genomic basis of homoploid hybrid speciation within chestnut trees. *Nat. Commun.* 11:3375. doi: 10.1038/s41467-020-17111-w

Tang, S., Lomsadze, A., and Borodovsky, M. (2015). Identification of protein coding regions in RNA transcripts. *Nucleic Acids Res.* 43:e78. doi: 10.1093/nar/gkv227

Tarailo Graovac, M., and Chen, N. (2009). Using RepeatMasker to identify repetitive elements in genomic sequences. Current protocols in bioinformatics Chapter 4, Unit 4.10.

Tian, J., Zhao, X., Xie, L., Quan, J., Yao, L., Wang, G., et al. (2018). Research advances and molecular mechanism on SPL transcription factors in regulating plant flower development. *J. Nanjing For. Univ.* 42, 159–166. doi: 10.3969/j.issn.1000-2006.201708015

Timothy, B., James, J., and Charles, G. (2015). The MEME suite. *Nucleic Acids Res.* 43, W39–W49. doi: 10.1093/nar/gkv416

Vavilov, N. I. (1952). The origin, variation, immunity and breeding of cultivated plants. *Notes Queries* 197:462

Verde, I., Abbott, A. G., Scalabrin, S., Jung, S., Shu, S., Marroni, F., et al. (2013). The high-quality draft genome of peach (*Prunus persica*) identifies unique patterns of genetic diversity, domestication and genome evolution. *Nat. Genet.* 45, 487–494. doi: 10.1038/ng.2586

Walker, B. J., Abeel, T., Shea, T., Priest, M., Abouelliel, A., Sakthikumar, S., et al. (2017). Pilon: an integrated tool for comprehensive microbial variant detection and genome assembly improvement. *PLoS One* 9:e112963. doi: 10.1371/journal.pone.0112963

Wang, J., Tian, S., Sun, X., Cheng, X., Duan, N., Tao, J., et al. (2020a). Construction of Pseudomolecules for the Chinese chestnut (*Castanea mollissima*) Genome. *G3* 10, 3565–3574. doi: 10.1534/g3.120.401532

Wang, M., Wu, Y., Liu, Y., and Ouyang, J. (2020b). Effect of Ultrasonic and Microwave Dual-Treatment on the Physicochemical Properties of Chestnut Starch. *Polymers* 12:1718. doi: 10.1534/g3.120.401532

Xing, Y., Liu, Y., Zhang, Q., Nie, X., Sun, Y., Zhang, Z., et al. (2019). Hybrid de novo genome assembly of Chinese chestnut (*Castanea mollissima*). *GigaScience* 8:giz112. doi: 10.1093/gigascience/giz112

Xu, Z., and Wang, H. (2007). LTR_FINDER: an efficient tool for the prediction of full-length LTR retrotransposons. *Nucleic Acids Res.* 35, W265–W268. doi: 10.1093/nar/gkm286

Yan, J., Ma, C., Bo, C., Fan, X., Li, Z., Yang, Y., et al. (2018). A Modified CTAB Method for Genomic DNA Extraction from Apple Fruit. *Molec. Plant Breeding* 9, 3610–3615. doi: 10.13271/j.mpb.015.003610

Yang, Z. (2007). PAML 4: phylogenetic analysis by maximum likelihood. *Mol. Biol. Evol.* 24, 1586–1591. doi: 10.1093/molbev/msm088

Ye, G., Zhang, H., Chen, B., Nie, S., Liu, H., Gao, W., et al. (2019). De novo genome assembly of the stress tolerant forest species *Casuarina equisetifolia* provides insight into secondary growth. *Plant J Cell Molec. Biol.* 97, 779–794. doi: 10.1111/tpj.14159

Yu, C.-S., Chen, Y.-C., Lu, C.-H., and Hwang, J.-K. (2006). Prediction of protein subcellular localization. *Proteins-Structure Fun. Bioinform.* 64, 643–651. doi: 10.1002/prot.21018

Yu, J., Holland, J. B., McMulle, N. M. D., and Buckler, E. S. (2008). Genetic design and statistical power of nested association mapping in maize. *Genetics* 178, 539–551. doi: 10.1534/genetics.107.074245

Zhang, Q., Chen, W., Sun, L., Zhao, F., Huang, B., Yang, W., et al. (2012). The genome of *Prunus mume*. *Nat. Commun.* 3:1318. doi: 10.1038/ncomms2290

Zhang, L., Hu, J., Han, X., Li, J., Gao, Y., Richards, C. M., et al. (2019). A high-quality apple genome assembly reveals the association of a retrotransposon and red fruit colour. *Nat. Commun.* 10, 1494. doi: 10.1038/s41467-019-09518-x

Zhang, L., Lin, Q., Feng, Y., Fan, X., Zou, F., Yuan, D.-Y., et al. (2015). Transcriptomic identification and expression of starch and sucrose metabolism genes in the seeds of Chinese chestnut (*Castanea mollissima*). *J. Agric. Food Chem.* 63, 929–942. doi: 10.1021/jf505247d

Zhao, Y., and Zhang, J. (2015). Problems and countermeasures facing the sustainable and healthy development of Jingdong's chestnut industry: taking the Xinglong County production area as an example. *Technol. Outlook* 25, 213–214. doi: 10.3969/j.issn.1672-8289.2015.29.196

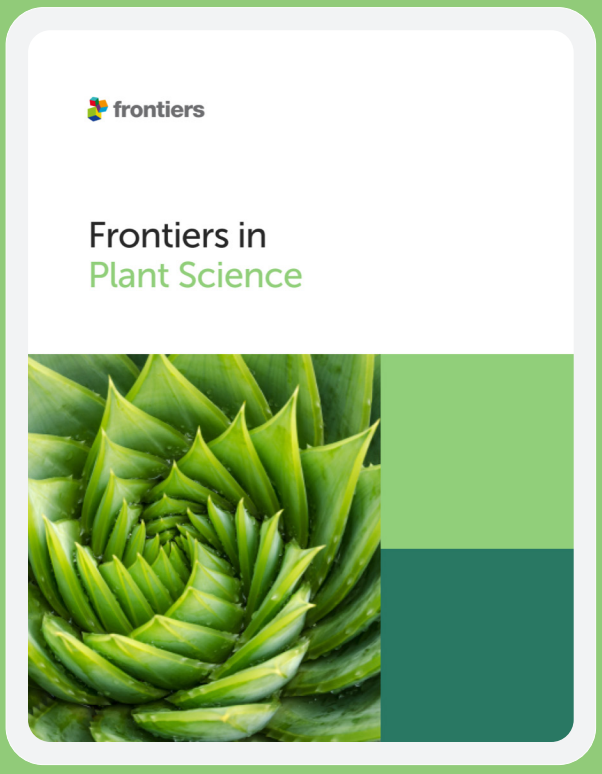
Frontiers in Plant Science

Cultivates the science of plant biology and its applications

The most cited plant science journal, which advances our understanding of plant biology for sustainable food security, functional ecosystems and human health.

Discover the latest Research Topics

See more →



Frontiers

Avenue du Tribunal-Fédéral 34
1005 Lausanne, Switzerland
frontiersin.org

Contact us

+41 (0)21 510 17 00
frontiersin.org/about/contact